

# MECHANICAL ENGINEERS' HANDBOOK

Materials and Engineering  
Mechanics » Volume  
**1**

**MYER KUTZ** EDITOR

FOURTH EDITION

WILEY



# **Mechanical Engineers' Handbook**





**Mechanical Engineers' Handbook**  
**Fourth Edition**

**Materials and Engineering**  
**Mechanics**

**Edited by**  
**Myer Kutz**

**WILEY**

Cover image: © denisovd / Thinkstock  
Cover design: Wiley

This book is printed on acid-free paper.  
Copyright © 2015

Published by John Wiley & Sons, Inc., Hoboken, New Jersey  
Published simultaneously in Canada

No part of this publication may be reproduced, stored in a retrieval system, or transmitted in any form or by any means, electronic, mechanical, photocopying, recording, scanning, or otherwise, except as permitted under Section 107 or 108 of the 1976 United States Copyright Act, without either the prior written permission of the Publisher, or authorization through payment of the appropriate per-copy fee to the Copyright Clearance Center, 222 Rosewood Drive, Danvers, MA 01923, (978) 750-8400, fax (978) 646-8600, or on the web at [www.copyright.com](http://www.copyright.com). Requests to the Publisher for permission should be addressed to the Permissions Department, John Wiley & Sons, Inc., 111 River Street, Hoboken, NJ 07030, (201) 748-6011, fax (201) 748-6008, or online at [www.wiley.com/go/permissions](http://www.wiley.com/go/permissions).

**Limit of Liability/Disclaimer of Warranty:** While the publisher and author have used their best efforts in preparing this book, they make no representations or warranties with the respect to the accuracy or completeness of the contents of this book and specifically disclaim any implied warranties of merchantability or fitness for a particular purpose. No warranty may be created or extended by sales representatives or written sales materials. The advice and strategies contained herein may not be suitable for your situation. You should consult with a professional where appropriate. Neither the publisher nor the author shall be liable for damages arising herefrom.

For general information about our other products and services, please contact our Customer Care Department within the United States at (800) 762-2974, outside the United States at (317) 572-3993 or fax (317) 572-4002.

Wiley publishes in a variety of print and electronic formats and by print-on-demand. Some material included with standard print versions of this book may not be included in e-books or in print-on-demand. If this book refers to media such as a CD or DVD that is not included in the version you purchased, you may download this material at <http://booksupport.wiley.com>. For more information about Wiley products, visit [www.wiley.com](http://www.wiley.com).

***Library of Congress Cataloging-in-Publication Data:***

Mechanical engineers handbook : materials and engineering mechanics / edited by Myer Kutz. –  
Fourth edition.

1 online resource.

Includes index.

Description based on print version record and CIP data provided by publisher; resource not viewed.

ISBN 978-1-118-90748-1 (ePub) – ISBN 978-1-118-90775-7 (Adobe PDF) – ISBN 978-1-118-11899-3  
(4-volume set) – ISBN 978-1-118-11282-3 (cloth : volume 1 : acid-free paper) 1. Mechanical  
engineering—Handbooks, manuals, etc. I. Kutz, Myer, editor of compilation.

TJ151

621-dc23

2014005952

Printed in the United States of America

10 9 8 7 6 5 4 3 2 1

*To Sol, Dorothy, and Jeanne, in Blessed Memory*



# Contents

---

Preface	ix
Vision for the Fourth Edition	xi
Contributors	xiii

## **PART 1 MATERIALS**

---

**1**

1. Carbon and Alloy Steels	3
<i>Bruce L. Bramfitt</i>	
2. Stainless Steels	39
<i>James Kelly</i>	
3. Aluminum Alloys	61
<i>J. G. Kaufman</i>	
4. Copper and Copper Alloys	117
<i>Konrad J. A. Kundig and Robert D. Weed</i>	
5. A Guide to Engineering Selection of Titanium Alloys for Design	229
<i>Matthew J. Donachie</i>	
6. Nickel and Its Alloys	267
<i>Gaylord D. Smith and Brian A. Baker</i>	
7. Magnesium and Its Alloys	289
<i>Robert E. Brown</i>	
8. A Guide to Engineering Selection of Superalloys for Design	299
<i>Matthew J. Donachie, John Marcin, and Stephen J. Donachie (deceased)</i>	
9. Thermoplastics, Thermosets, and Elastomers—Descriptions and Properties	353
<i>Edward N. Peters</i>	
10. Composite Materials	401
<i>Carl Zweben</i>	
11. Smart Materials	439
<i>James A. Harvey</i>	
12. Overview of Ceramic Materials, Design, and Application	453
<i>R. Nathan Katz</i>	
13. Electronic Materials and Packaging	475
<i>Warren C. Fackler</i>	
14. Sources of Material Data	515
<i>J. G. Kaufman</i>	
15. Quantitative Methods of Materials Selection	531
<i>Mahmoud M. Farag</i>	

**PART 2 ENGINEERING MECHANICS****553**

- 
16. Stress Analysis 555  
*Franklin E. Fisher*
  17. Force Measurement 623  
*Patrick Collins*
  18. Resistive Strain Measurement Devices 659  
*Mark Tuttle*
  19. An Introduction to the Finite-Element Method 681  
*Tarek I. Zohdi*
  20. Failure Models: Performance and Service Requirements for Metals 703  
*J. A. Collins, G.P. Potirniche, and S. R. Daniewicz*
  21. Failure Analysis of Plastics 771  
*Vishu Shah*
  22. Failure Modes: Performance and Service Requirements for Ceramics 789  
*Dietrich Munz*
  23. Viscosity Measurement 809  
*Ann M. Anderson, Bradford A. Bruno, and Lilla Safford Smith*
  24. Tribology Measurements 837  
*Prasanta Sahoo*
  25. Vibration and Shock 861  
*Singiresu S. Rao*
  26. Acoustics 885  
*Jonathan D. Blotter, Scott D. Sommerfeldt, and Kent L. Gee*
  27. Acoustical Measurements 953  
*Brian E. Anderson, Jonathan D. Blotter, Kent L. Gee, and Scott D. Sommerfeldt*
- Index 997

# Preface

---

The first volume of the fourth edition of the *Mechanical Engineers' Handbook* is comprised of two major parts. The first part, Materials, has 15 chapters. All of them appeared in the third edition; 10 have been updated for this new edition. They cover metals, plastics, composites, ceramics, smart materials, and electronic materials and packaging. The metals covered are carbon, alloy, and stainless steels; aluminum and aluminum alloys; copper and copper alloys; titanium alloys; nickel and its alloys; magnesium and its alloys; and superalloys. The intent in all of the materials chapters is to provide readers with expert advice on how particular materials are typically used and what criteria make them suitable for specific purposes. This part of Volume I concludes with a chapter on sources of materials data, the intent being to provide readers with guidance on finding reliable information on materials properties, in addition to those that can be found in this volume, and a chapter on analytical methods of materials selection, which is intended to give readers techniques for specifying which materials might be suitable for particular applications.

The second part of Volume 1, Engineering Mechanics, has 12 chapters, half of them new to the handbook. They cover a broad range of topics, including the fundamentals of stress analysis (this chapter, in the handbook since the first edition in 1986, has been updated for the first time), force measurement (new), strain measurement (new), the finite-element method, viscosity measurement (new), tribology measurements (new), vibration and shock (updated from the third edition), acoustics (new), and acoustics measurements (new). There is a three-chapter section on methodologies that engineers use to predict failures with three major classes of materials—metals, plastics, and ceramics (all three chapters have been updated). I have removed the chapter on lubrication of machine elements, which had been unchanged since the first edition in 1986. I was unable through the years and handbook editions to get anyone to update the chapter. The material is too old by now and many of the references can no longer be accessed (some of the organizations that developed referenced materials have simply disappeared). The chapters on viscosity and tribology measurements serve as replacements. The chapters on acoustics and acoustics measurements replace the chapter, Noise Measurements and Control, which had been unchanged since the first edition.

Chapters from the mechanical design section, formerly in this volume, have been moved to Volumes 2 and 3, with the exception of the chapter on electronic materials and packaging. Prefaces to those volumes provide further details on the move.

Contributors of the chapters in Volume 1 include professors, engineers working in industry, and consultants, mainly from North America, but also from Egypt, the Netherlands, the United Kingdom, Germany, and India. I would like to thank all of them for the considerable time and effort they put into preparing their chapters.





# Vision for the Fourth Edition

---

Basic engineering disciplines are not static, no matter how old and well established they are. The field of mechanical engineering is no exception. Movement within this broadly based discipline is multidimensional. Even the classic subjects, on which the discipline was founded, such as mechanics of materials and heat transfer, keep evolving. Mechanical engineers continue to be heavily involved with disciplines allied to mechanical engineering, such as industrial and manufacturing engineering, which are also constantly evolving. Advances in other major disciplines, such as electrical and electronics engineering, have significant impact on the work of mechanical engineers. New subject areas, such as neural networks, suddenly become all the rage.

In response to this exciting, dynamic atmosphere, the Mechanical Engineers' Handbook expanded dramatically, from one to four volumes for the third edition, published in November 2005. It not only incorporated updates and revisions to chapters in the second edition, published seven years earlier, but also added 24 chapters on entirely new subjects, with updates and revisions to chapters in the Handbook of Materials Selection, published in 2002, as well as to chapters in Instrumentation and Control, edited by Chester Nachtigal and published in 1990, but never updated by him.

The fourth edition retains the four-volume format, but there are several additional major changes. The second part of Volume I is now devoted entirely to topics in engineering mechanics, with the addition of five practical chapters on measurements from the Handbook of Measurement in Science and Engineering, published in 2013, and a chapter from the fifth edition of Eshbach's Handbook of Engineering Fundamentals, published in 2009. Chapters on mechanical design have been moved from Volume I to Volumes II and III. They have been augmented with four chapters (updated as needed) from Environmentally Conscious Mechanical Design, published in 2007. These chapters, together with five chapters (updated as needed, three from Environmentally Conscious Manufacturing, published in 2007, and two from Environmentally Conscious Materials Handling, published in 2009) in the beefed-up manufacturing section of Volume III, give the handbook greater and practical emphasis on the vital issue of sustainability.

Prefaces to the handbook's individual volumes provide further details on chapter additions, updates and replacements. The four volumes of the fourth edition are arranged as follows:

Volume 1: Materials and Engineering Mechanics—27 chapters

Part 1. Materials—15 chapters

Part 2. Engineering Mechanics—12 chapters

Volume 2: Design, Instrumentation and Controls—25 chapters

Part 1. Mechanical Design—14 chapters

Part 2. Instrumentation, Systems, Controls and MEMS —11 chapters

Volume 3: Manufacturing and Management—28 chapters

Part 1. Manufacturing—16 chapters

Part 2. Management, Finance, Quality, Law, and Research—12 chapters

Volume 4: Energy and Power—35 chapters

Part 1: Energy—16 chapters

Part 2: Power—19 chapters

The mechanical engineering literature is extensive and has been so for a considerable period of time. Many textbooks, reference works, and manuals as well as a substantial number of journals exist. Numerous commercial publishers and professional societies, particularly in the United States and Europe, distribute these materials. The literature grows continuously, as applied mechanical engineering research finds new ways of designing, controlling, measuring, making, and maintaining things, as well as monitoring and evaluating technologies, infrastructures, and systems.

Most professional-level mechanical engineering publications tend to be specialized, directed to the specific needs of particular groups of practitioners. Overall, however, the mechanical engineering audience is broad and multidisciplinary. Practitioners work in a variety of organizations, including institutions of higher learning, design, manufacturing, and consulting firms, as well as federal, state, and local government agencies. A rationale for a general mechanical engineering handbook is that every practitioner, researcher, and bureaucrat cannot be an expert on every topic, especially in so broad and multidisciplinary a field, and may need an authoritative professional summary of a subject with which he or she is not intimately familiar.

Starting with the first edition, published in 1986, my intention has always been that the Mechanical Engineers' Handbook stand at the intersection of textbooks, research papers, and design manuals. For example, I want the handbook to help young engineers move from the college classroom to the professional office and laboratory where they may have to deal with issues and problems in areas they have not studied extensively in school.

With this fourth edition, I have continued to produce a practical reference for the mechanical engineer who is seeking to answer a question, solve a problem, reduce a cost, or improve a system or facility. The handbook is not a research monograph. Its chapters offer design techniques, illustrate successful applications, or provide guidelines to improving performance, life expectancy, effectiveness, or usefulness of parts, assemblies, and systems. The purpose is to show readers what options are available in a particular situation and which option they might choose to solve problems at hand.

The aim of this handbook is to serve as a source of practical advice to readers. I hope that the handbook will be the first information resource a practicing engineer consults when faced with a new problem or opportunity—even before turning to other print sources, even officially sanctioned ones, or to sites on the Internet. In each chapter, the reader should feel that he or she is in the hands of an experienced consultant who is providing sensible advice that can lead to beneficial action and results.

Can a single handbook, even spread out over four volumes, cover this broad, interdisciplinary field? I have designed the Mechanical Engineers' Handbook as if it were serving as a core for an Internet-based information source. Many chapters in the handbook point readers to information sources on the Web dealing with the subjects addressed. Furthermore, where appropriate, enough analytical techniques and data are provided to allow the reader to employ a preliminary approach to solving problems.

The contributors have written, to the extent their backgrounds and capabilities make possible, in a style that reflects practical discussion informed by real-world experience. I would like readers to feel that they are in the presence of experienced teachers and consultants who know about the multiplicity of technical issues that impinge on any topic within mechanical engineering. At the same time, the level is such that students and recent graduates can find the handbook as accessible as experienced engineers.

# Contributors

---

Ann M. Anderson  
Union College  
Schenectady, New York

Brian E. Anderson  
Brigham Young University  
Provo, Utah

Brian A. Baker  
Special Metals Corporation  
Huntington, West Virginia

Jonathan D. Blotter  
Brigham Young University  
Provo, Utah

Bruce L. Bramfitt  
International Steel Group, Inc.  
Bethlehem, Pennsylvania

Robert E. Brown  
Magnesium Monthly Review  
Prattville, Alabama

Bradford A. Bruno  
Union College  
Schenectady, New York

Patrick Collins  
Mecmesin Ltd.  
Slinfold, United Kingdom

J. A. Collins  
The Ohio State University  
Columbus, Ohio

S. R. Daniewicz  
Mississippi State University  
Starkville, Mississippi

Matthew J. Donachie  
Rensselaer at Hartford  
Hartford, Connecticut

Stephen J. Donachie (Deceased)  
Special Metals Corporation  
Huntington, West Virginia

Warren C. Fackler  
Telesis Systems  
Cedar Rapids, Iowa

Mahmoud M. Farag  
The American University in Cairo  
Cairo, Egypt

Franklin E. Fisher  
Loyola Marymount University  
Los Angeles, California  
and  
Raytheon Company  
El Segundo, California

Kent L. Gee  
Brigham Young University  
Provo, Utah

James A. Harvey  
Under The Bridge Consulting, Inc.  
Corvallis, Oregon

R. Nathan Katz  
Worcester Polytechnic Institute  
Worcester, Massachusetts

J. G. Kaufman  
Kaufman Associates  
Lewes, Delaware

James Kelly  
Rochester, Michigan

Konrad J. A. Kundig  
Metallurgical Consultant  
Tucson, Arizona

John Marcin  
Rensselaer at Hartford  
Hartford, Connecticut

**xiv** Contributors

Dietrich Munz  
University of Karlsruhe  
Karlsruhe, Germany

Edward N. Peters  
SABIC  
Selkirk, New York

G. P. Potirniche  
University of Idaho  
Moscow, Idaho

Singiresu S. Rao  
University of Miami  
Coral Gables, Florida

Prasanta Sahoo  
Jadavpur University  
Kolkata, India

Vishu Shah  
Consultek Consulting Group  
Diamond Bar, California

Gaylord D. Smith  
Special Metals Corporation  
Huntington, West Virginia

Lilla Safford Smith  
Union College  
Schenectady, New York

Scott D. Sommerfeldt  
Brigham Young University  
Provo, Utah

Mark Tuttle  
University of Washington  
Seattle, Washington

Robert D. Weed  
Copper Development Association  
New York, New York

Tarek I. Zohdi  
University of California  
Berkeley, California

Carl Zweben  
Zweben Consulting  
Devon, Pennsylvania

**PART 1**

---

**MATERIALS**





# CHAPTER 1

---

## CARBON AND ALLOY STEELS

**Bruce L. Bramfitt**  
Research Laboratories  
International Steel Group, Inc.  
Bethlehem, Pennsylvania

<b>1 INTRODUCTION</b>	<b>3</b>	<b>6 CLASSIFICATION AND SPECIFICATIONS OF STEELS</b>	<b>26</b>
<b>2 STEEL MANUFACTURE</b>	<b>4</b>	6.1 Carbon Steels	27
<b>3 DEVELOPMENT OF STEEL PROPERTIES</b>	<b>5</b>	6.2 Alloy Steels	28
<b>4 ROLE OF ALLOYING ELEMENTS IN STEEL</b>	<b>18</b>	<b>7 SUMMARY</b>	<b>36</b>
<b>5 HEAT TREATMENT OF STEEL</b>	<b>24</b>	<b>BIBLIOGRAPHY</b>	<b>36</b>

### 1 INTRODUCTION

Steel is the most common and widely used metallic material in today's society. It can be cast or wrought into numerous forms and can be produced with tensile strengths exceeding 5 GPa. A prime example of the versatility of steel is in the automobile where it is the material of choice and accounts for over 60% of the weight of the vehicle. Steel is highly formable as seen in the contours of the automobile outerbody. Steel is strong and is used in the body frame, motor brackets, driveshaft, and door impact beams of the vehicle. Steel is corrosion resistant when coated with the various zinc-based coatings available today. Steel is dent resistant when compared with other materials and provides exceptional energy absorption in a vehicle collision. Steel is recycled and easily separated from other materials by a magnet. Steel is inexpensive compared with other competing materials such as aluminum and various polymeric materials.

In the past, steel has been described as an alloy of iron and carbon. Today, this description is no longer applicable since in some very important steels, e.g., interstitial-free (IF) steels and type 409 ferritic stainless steels, carbon is considered an impurity and is present in quantities of only a few parts per million. By definition, steel must be at least 50% iron and must contain one or more alloying elements. These elements generally include carbon, manganese, silicon, nickel, chromium, molybdenum, vanadium, titanium, niobium, and aluminum. Each chemical element has a specific role to play in the steelmaking process or in achieving particular properties or characteristics, e.g., strength, hardness, corrosion resistance, magnetic permeability, and machinability.

## 4 Carbon and Alloy Steels

### 2 STEEL MANUFACTURE

In most of the world, steel is manufactured by integrated steel facilities that produce steel from basic raw materials, i.e., iron ore, coke, and limestone. However, the fastest growing segment of the steel industry is the “minimill” that melts steel scrap as the raw material. Both types of facilities produce a wide variety of steel forms, including sheet, plate, structural, railroad rail, and bar products.

**Ironmaking.** When making steel from iron ore, a blast furnace chemically reduces the ore (iron oxide) with carbon in the form of coke. Coke is a spongelike carbon mass that is produced from coal by heating the coal to expel the organic matter and gases. Limestone (calcium carbonate) is added as a flux for easier melting and slag formation. The slag, which floats atop the molten iron, absorbs many of the unwanted impurities. The blast furnace is essentially a tall hollow cylindrical structure with a steel outer shell lined on the inside with special refractory and graphite brick. The crushed or pelletized ore, coke, and limestone are added as layers through an opening at the top of the furnace, and chemical reduction takes place with the aid of a blast of preheated air entering near the bottom of the furnace (an area called the bosh). The air is blown into the furnace through a number of water-cooled copper nozzles called tuyeres. The reduced liquid iron fills the bottom of the furnace and is tapped from the furnace at specified intervals of time. The product of the furnace is called pig iron because in the early days the molten iron was drawn from the furnace and cast directly into branched mold configurations on the cast house floor. The central branch of iron leading from the furnace was called the “sow” and the side branches were called “pigs.” Today the vast majority of pig iron is poured directly from the furnace into a refractory-lined vessel (submarine car) and transported in liquid form to a basic oxygen furnace (BOF) for refinement into steel.

**Steelmaking.** In the BOF, liquid pig iron comprises the main charge. Steel scrap is added to dilute the carbon and other impurities in the pig iron. Oxygen gas is blown into the vessel by means of a top lance submerged below the liquid surface. The oxygen interacts with the molten pig iron to oxidize undesirable elements. These elements include excess carbon (because of the coke used in the blast furnace, pig iron contains over 2% carbon), manganese, and silicon from the ore and limestone and other impurities like sulfur and phosphorus. While in the BOF, the liquid metal is chemically analyzed to determine the level of carbon and impurity removal. When ready, the BOF is tilted and the liquid steel is poured into a refractory-lined ladle. While in the ladle, certain alloying elements can be added to the steel to produce the desired chemical composition. This process takes place in a ladle treatment station or ladle furnace where the steel is maintained at a particular temperature by external heat from electrodes in the lid placed on the ladle. After the desired chemical composition is achieved, the ladle can be placed in a vacuum chamber to remove undesirable gases such as hydrogen and oxygen. This process is called degassing and is used for higher quality steel products such as railroad rail, sheet, plate, bar, and forged products. Stainless steel grades are usually produced in an induction or electric arc furnace, sometimes under vacuum. To refine stainless steel, the argon–oxygen decarburization (AOD) process is used. In the AOD, an argon–oxygen gas mixture is injected through the molten steel to remove carbon without a substantial loss of chromium (the main element in stainless steel).

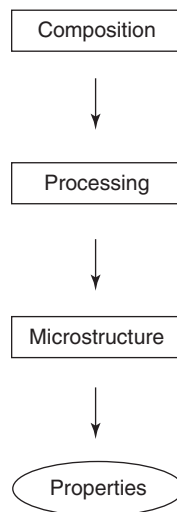
**Continuous Casting.** Today, most steel is cast into solid form in a continuous-casting (also called strand casting) machine. Here, the liquid begins solidification in a water-cooled copper mold while the steel billet, slab, or bloom is withdrawn from the bottom of the mold. The partially solidified shape is continuously withdrawn from the machine and cut to length for

further processing. The continuous-casting process can proceed for days or weeks as ladle after ladle of molten steel feeds the casting machine. Some steels are not continuously cast but are poured into individual cast iron molds to form an ingot that is later reduced in size by forging or a rolling process to some other shape. Since the continuous-casting process offers substantial economic and quality advantages over ingot casting, most steel in the world is produced by continuous casting.

**Rolling/Forging.** Once cast into billet, slab, or bloom form, the steel is hot rolled through a series of rolling mills or squeezed/hammered by forging to produce the final shape. To form hot-rolled sheet, a 50–300-mm-thick slab is reduced to final thickness, e.g., 2 mm, in one or more roughing stands followed by a series of six or seven finishing stands. To obtain thinner steel sheet, e.g., 0.5 mm, the hot-rolled sheet must be pickled in acid to remove the iron oxide scale and further cold rolled in a series of rolling stands called a tandem mill. Because the cold-rolling process produces a hard sheet with little ductility, it is annealed either by batch annealing or continuous annealing. New casting technology is emerging where thin sheets (under 1 mm) can be directly cast from the liquid through water-cooled, rotating rolls that act as a mold as in continuous casting. This new process eliminates many of the steps in conventional hot-rolled sheet processing. Plate steels are produced by hot rolling a slab in a reversing roughing mill and a reversing finishing mill. Steel for railway rails is hot rolled from a bloom in a blooming mill, a roughing mill, and one or more finishing mills. Steel bars are produced from a heated billet that is hot rolled in a series of roughing and finishing mills. Forged steels are produced from an ingot that is heated to forging temperature and squeezed or hammered in a hydraulic press or drop forge. The processing sequence in all these deformation processes can vary depending on the design, layout, and age of the steel plant.

### 3 DEVELOPMENT OF STEEL PROPERTIES

In order to produce a steel product with the desired properties, basic metallurgical principles are used to control three things:



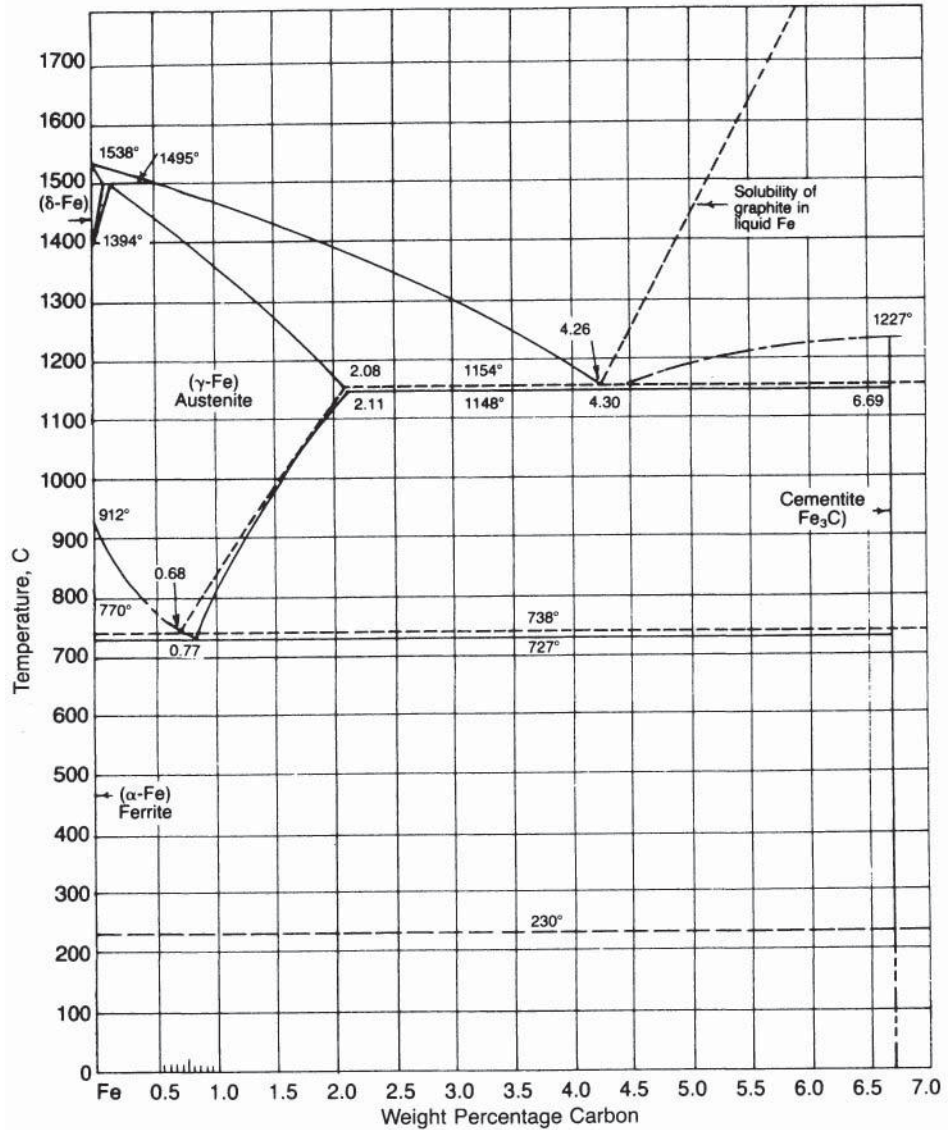
This means that the steel composition and processing route must be closely controlled in order to produce the proper microstructure. The final microstructure is of utmost importance in determining the properties of the steel product. This section will explore how various microstructures are developed and the unique characteristics of each microstructural component in steel. The next section will discuss how alloy composition also plays a major role.

**Iron–Carbon Equilibrium Diagram.** Since most steels contain carbon, the basic principles of microstructural development can be explained by the iron–carbon equilibrium diagram. This diagram, shown in Fig. 1, is essentially a map of the phases that exist in iron at various carbon contents and temperatures under equilibrium conditions. Iron is an interesting chemical element in that it undergoes three phase changes when heated from room temperature to liquid. For example, from room temperature to 912°C pure iron exists as ferrite (also called alpha iron), from 912 to 1394°C it exists as austenite (gamma iron), from 1394 to 1538°C it exists as ferrite again (delta iron), and above 1538°C it is liquid. In other words, upon heating, iron undergoes allotropic-phase transformations from ferrite to austenite at 912°C, austenite to ferrite at 1394°C, and ferrite to liquid at 1538°C. Each transformation undergoes a change in crystal structure or arrangement of the iron atoms in the crystal lattice. It must be remembered that all chemical elements in their solid form have specific arrangements of atoms that are essentially the basic building blocks in producing the element in the form that we physically observe. These atomic arrangements form a latticework containing billions of atoms all aligned in a systematic way. Some of these lattices have a cubic arrangement, with an atom at each corner of the cube and another atom at the cube center. This arrangement is called body-centered-cubic (bcc). Others have an atom at each corner of the cube and atoms at the center of each face of the cube. This is called face-centered-cubic (fcc). Other arrangements are hexagonal, some are tetragonal, etc. As an example, pure iron as ferrite has a bcc arrangement. Austenite has a fcc arrangement. Upon heating, bcc ferrite will transform to fcc austenite at 912°C. These arrangements or crystal structures impart different properties to steel. For example, a bcc ferritic stainless steel will have properties much different from a fcc austenitic stainless steel, as described later in this chapter.

Since pure iron is very soft and of low strength, it is of little interest commercially. Therefore, carbon and other alloying elements are added to enhance properties. Adding carbon to pure iron has a profound effect on ferrite and austenite, discussed above. One way to understand the effect of carbon is to examine the iron–carbon diagram (Fig. 1). This is a binary (two-element) diagram of temperature and composition (carbon content) constructed under near-equilibrium conditions. In this diagram, as carbon is added to iron, the ferrite- and austenite-phase fields expand and contract depending upon the carbon level and temperature. Also, there are fields consisting of two phases, e.g., ferrite plus austenite.

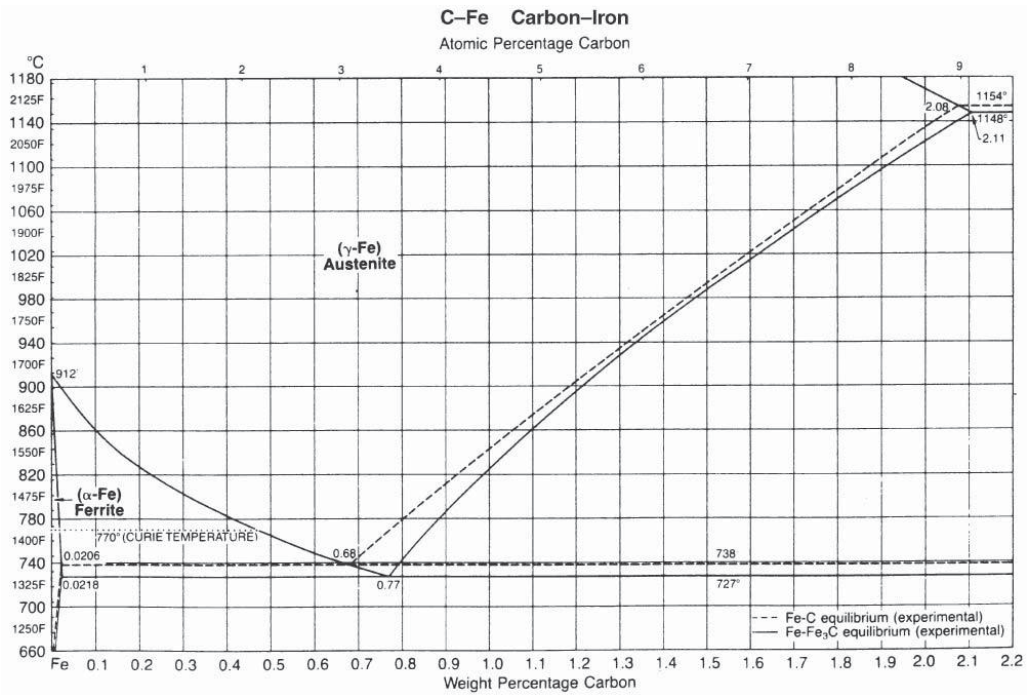
Since carbon has a small atomic diameter when compared with iron, it is called an interstitial element because it can fill the interstices between the iron atoms in the cubic lattice. Nitrogen is another interstitial element. On the other hand, elements such as manganese, silicon, nickel, chromium, and molybdenum have atomic diameters similar to iron and are called substitutional alloying elements. These substitutional elements can thus replace iron atoms at the cube corners, faces, or center positions. There are many binary-phase diagrams (Fe–Mn, Fe–Cr, Fe–Mo, etc.) and tertiary-phase diagrams (Fe–C–Mn, Fe–C–Cr, etc.) showing the effect of interstitial and substitutional elements on the phase fields of ferrite and austenite. These diagrams are found in the handbooks listed at the end of the chapter.

Being an interstitial or a substitutional element is important in the development of steel properties. Interstitial elements such as carbon can move easily about the crystal lattice whereas a substitutional element such as manganese is much more difficult to move. The movement of



**Figure 1** Iron–carbon binary-phase diagram. (Source: *Steels: Heat Treatment and Processing Principles*, ASM International, Materials Park, OH, 1990, p. 2.) Reprinted with permission of ASM International.

elements in a crystal lattice is called diffusion. Diffusion is a controlling factor in the development of microstructure. Another factor is solubility, which is a measure of how much of a particular element can be accommodated by the crystal lattice before it is rejected. In metals, when two or more elements are soluble in the crystal lattice, a solid solution is created (somewhat analogous to a liquid solution of sugar in hot coffee). For example, when added to iron, carbon has very limited solubility in ferrite but is about 100 times more soluble in austenite, as seen in the iron–carbon diagram in Fig. 2 (a limited version of the diagram in Fig. 1). The maximum solubility of carbon in ferrite is about 0.022% C at 727°C while the maximum

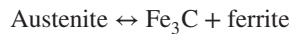


**Figure 2** Expanded portion of iron-carbon binary-phase diagram in Fig. 1. (Source: *Steels: Heat Treatment and Processing Principles*, ASM International, Materials Park, OH, 1990, p. 18.) Reprinted with permission of ASM International.



solubility of carbon in austenite is 100 times more, 2.11% C at 1148°C. At room temperature the solubility of carbon in iron is only about 0.005%. Any amount of carbon in excess of the solubility limit is rejected from solid solution and is usually combined with iron to form an iron carbide compound called cementite. This hard and brittle compound has the chemical formula  $\text{Fe}_3\text{C}$  and a carbon content of 6.7%. This is illustrated in the following two examples. The first example is a microstructure of a very low carbon steel (0.002% C), shown in Fig. 3a. The microstructure consists of only ferrite grains (crystals) and grain boundaries. The second example is a microstructure of a low-carbon steel containing 0.02% C, in Fig. 3b. In this microstructure, cementite can be seen as particles at the ferrite grain boundaries. The excess carbon rejected from the solid solution of ferrite formed this cementite. As the carbon content in steel is increased, another form of cementite appears as a constituent called pearlite, which can be found in most carbon steels. Examples of pearlite in low-carbon (0.08% C) and medium-carbon (0.20% C) steels are seen in Figs. 4a and 4b. Pearlite has a lamellar (parallel-plate) microstructure, as shown at higher magnification in Fig. 5, and consists of layers of ferrite and cementite. Thus, in these examples, in increasing the carbon level from 0.002–0.02 to 0.08–0.20%, the excess carbon is manifested as a carbide phase in two different forms, cementite particles and cementite in pearlite. Both forms increase the hardness and strength of iron. However, there is a trade-off; cementite also decreases ductility and toughness.

Pearlite forms on cooling austenite through a eutectoid reaction as seen below:

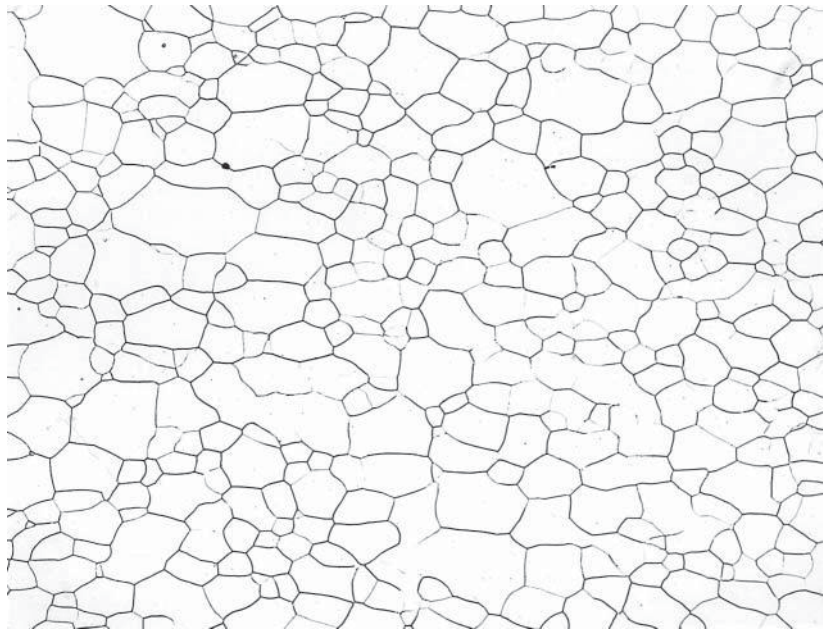


A *eutectoid* reaction occurs when a solid phase or constituent reacts to form two different solid constituents on cooling (a *eutectic* reaction occurs when a liquid phase reacts to form two solid phases). The eutectoid reaction is reversible on heating. In steel, the eutectoid reaction (under equilibrium conditions) takes place at 727°C and can be seen on the iron–carbon diagram (Fig. 1) as the “V” at the bottom left side of the diagram. A fully pearlitic microstructure forms at 0.77% C at the eutectoid temperature of 727°C (the horizontal line on the left side of the iron–carbon diagram). Steels with less than 0.77% C are called *hypo*eutectoid steels and consist of mixtures of ferrite and pearlite with the amount of pearlite increasing as the carbon content increases. The ferrite phase is called a *pro*eutectoid phase because it forms prior to the eutectoid transformation that occurs at 727°C. A typical example of proeutectoid ferrite is shown in Fig. 6. In this photomicrograph, the ferrite (the white-appearing constituent) formed on the prior austenite grain boundaries of hypoeutectoid steel with 0.60% C. The remaining constituent (dark appearing) is pearlite. Steels between 0.77% C and about 2% C are called *hyper*eutectoid steels and consist of pearlite with proeutectoid cementite. Cementite forms a continuous carbide network at the boundaries of the prior austenite grains. Because there is a carbide network, hypereutectoid steels are characterized as steels with little or no ductility and very poor toughness. This means that in the commercial world the vast majority of carbon steels are hypoeutectoid steels.

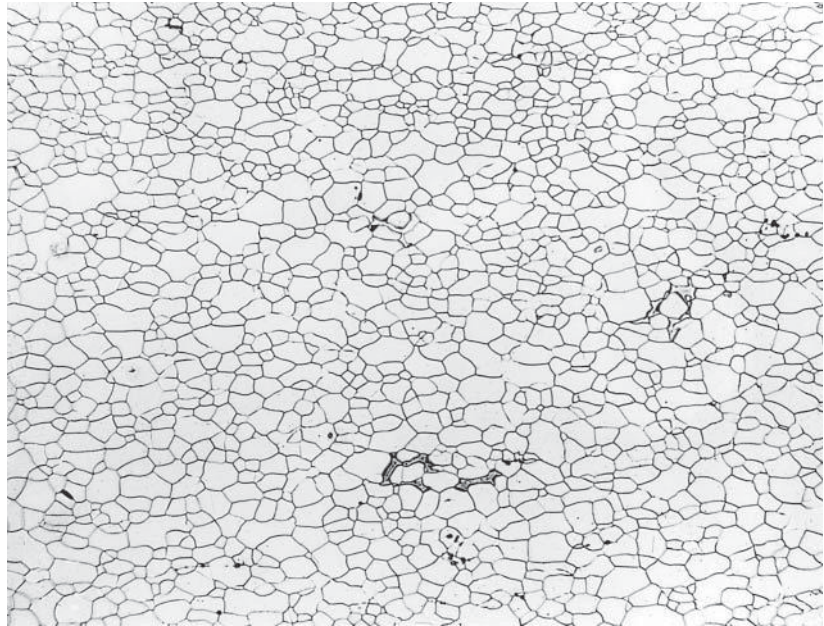
Thus, according to the iron–carbon diagram, steels that are processed under equilibrium or near-equilibrium conditions can form (a) pure ferrite at very low carbon levels generally under 0.005% C, (b) ferrite plus cementite particles at slightly higher carbon levels between 0.005% C and 0.022% C, (c) ferrite plus pearlite mixtures between 0.022% C and 0.77% C, (d) 100% pearlite at 0.77% C, and (e) mixtures of pearlite plus cementite networks between 0.77% C and 2% C. The higher the percentage of cementite, the higher the hardness and strength and lower the ductility and toughness of the steel.

**Departure from Equilibrium (Real World).** Industrial processes do not occur at equilibrium, and only those processes that take place at extremely slow heating and cooling rates can be considered near equilibrium, and these processes are quite rare. Therefore, under real



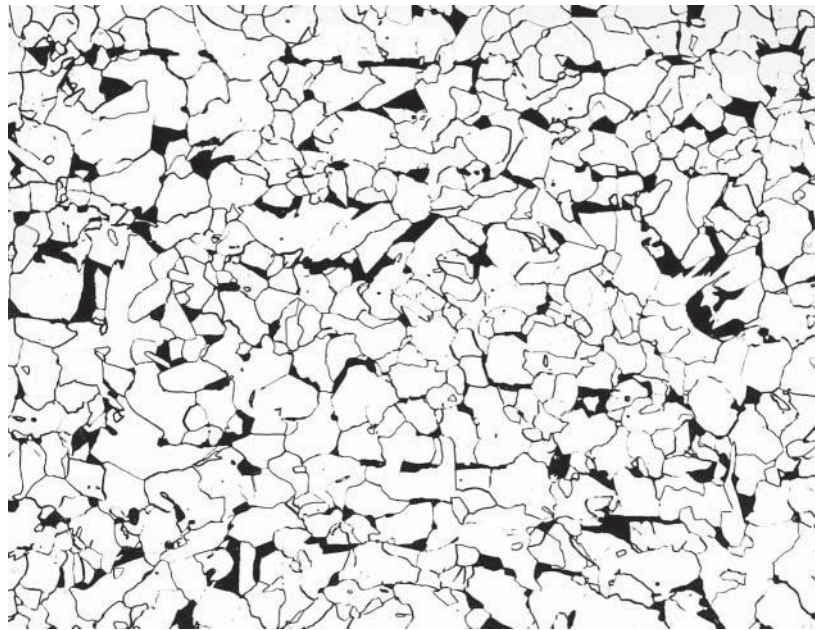


(a)

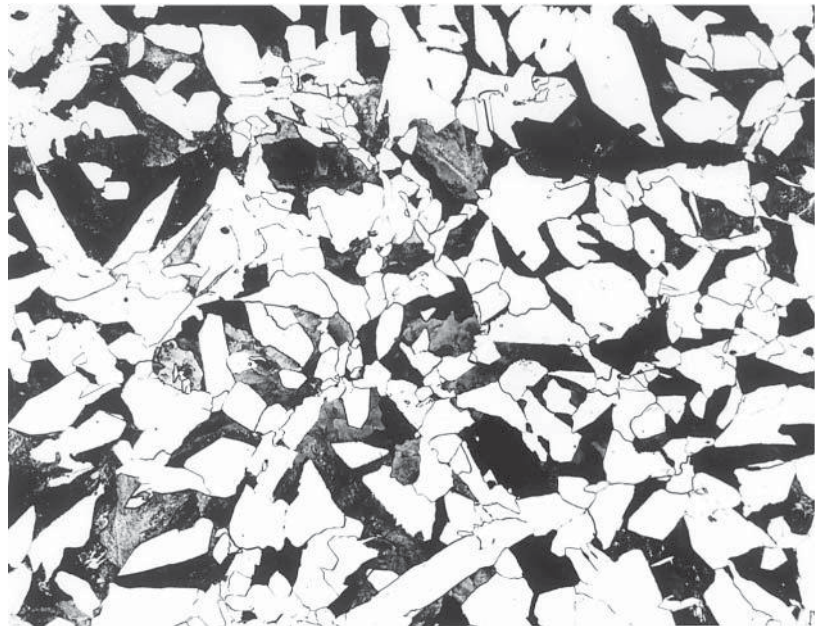


(b)

**Figure 3** (a) Photomicrograph of a very low carbon steel showing ferrite grains and (b) photomicrograph of a low-carbon steel showing ferrite grains with some cementite on the ferrite grain boundaries. (a) 500X and (b) 200X. Marshall's etch.



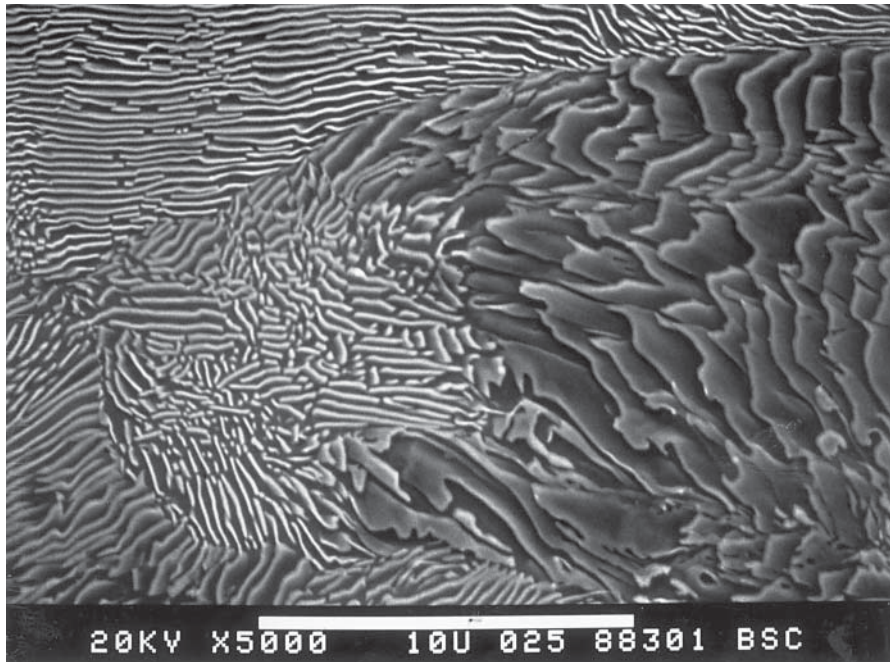
(a)



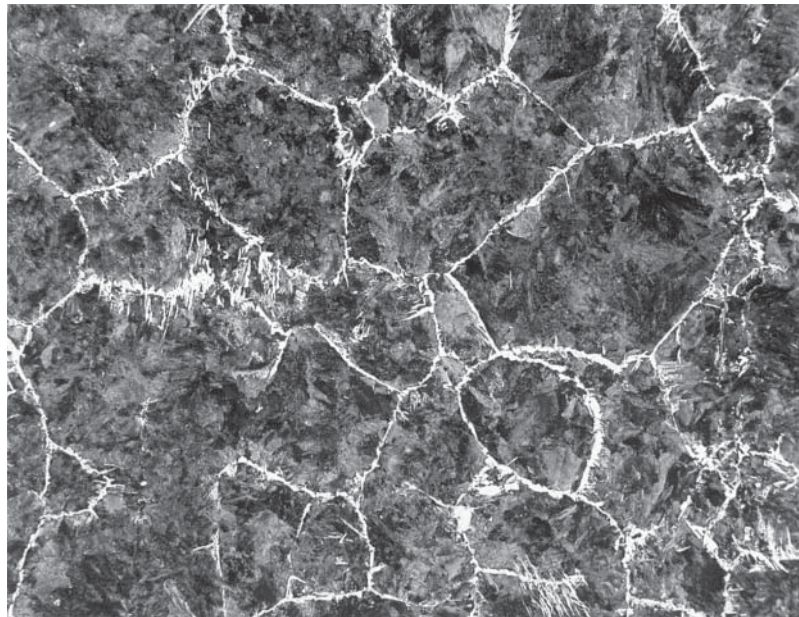
(b)

**Figure 4** (a) Photomicrograph of an SAE/AISI 1008 steel showing ferrite grains and pearlite (dark) and (b) photomicrograph of an SAE/AISI 1020 steel showing ferrite grains with an increased amount of pearlite. (a) and (b) both 200X, 4% picral + 2% nital etch.





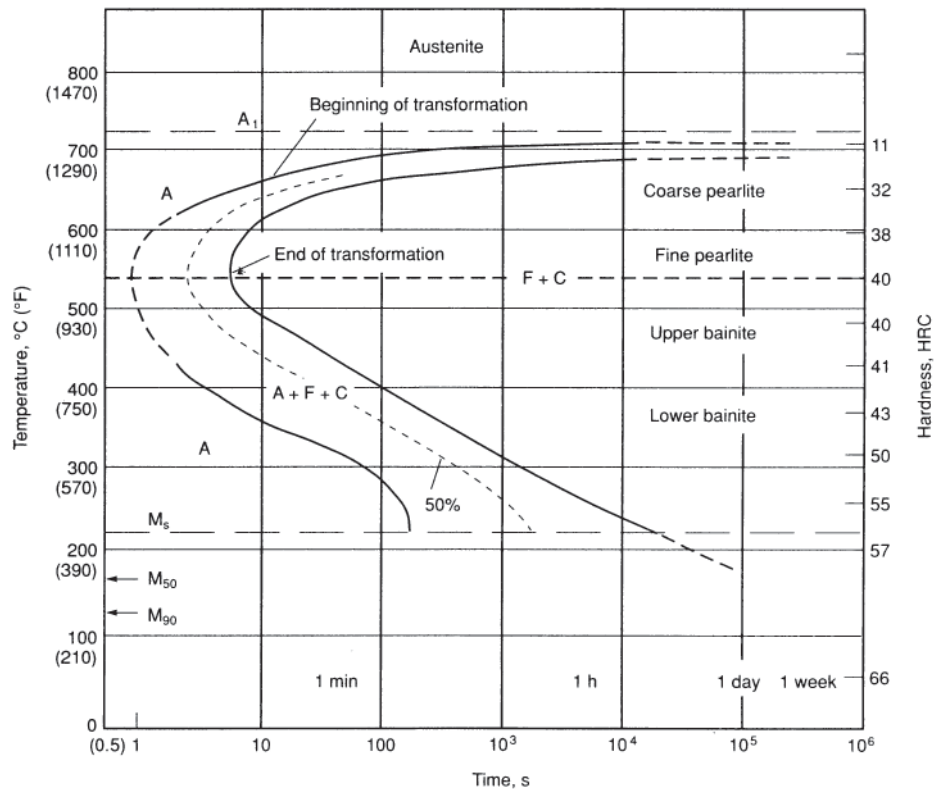
**Figure 5** Scanning electron micrograph of pearlite showing the platelike morphology of the cementite. 5000X. 4% picral etch.



**Figure 6** Photomicrograph of a medium-carbon hypoeutectoid steel showing a pearlite matrix and proeutectoid ferrite nucleating on the original (prior) austenite grain boundaries. 200X. 4% picral + 2% nital etch.

conditions, the iron–carbon diagram can only be used as a rough guideline since the equilibrium transformation temperatures shift to lower temperatures on cooling and to higher temperatures on heating. If steels are cooled at very fast rates, e.g., quenching in water, the iron–carbon diagram can no longer be used since there is a major departure from equilibrium. In fact, during the quenching of steel, new constituents form that are not associated with the iron–carbon diagram. Therefore, at fast cooling rates the concept of time–temperature transformation (TTT) diagrams must be considered. These diagrams are constructed under isothermal (constant) temperature (called IT diagrams) or continuous-cooling conditions (called CT diagrams). It is important to know how these diagrams are constructed so that we can understand the development of nonequilibrium microstructures, which are so important in carbon and alloy steels.

**Isothermal Transformation Diagram.** This diagram is formed by quenching very thin specimens of steel in salt baths set at various temperatures. For example, thin specimens of 0.79% C steel can be quenched into seven different liquid salt baths set at 650, 600, 550, 500, 450, 400, and 200°C. The specimens are held for various times at each temperature, then pulled from the bath and quickly quenched in cold water. The result will be a diagram called an isothermal transformation (IT) diagram, as shown in Fig. 7. The diagram is



**Figure 7** Isothermal transformation diagram of SAE/AISI 1080 steel showing the beginning and end of transformation curves with temperature and time. (Source: *ASM Handbook*, Vol. 1, *Properties and Selection: Irons, Steels, and High-Performance Alloys*, ASM International, Materials Park, OH, 1990, p. 128.) Reprinted with permission of ASM International.

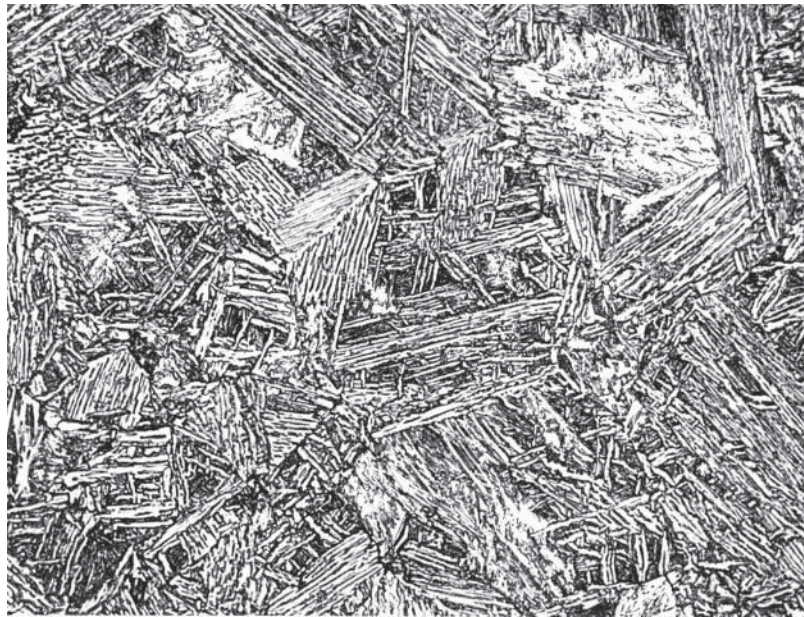
essentially a map showing where various constituents form. For example, at 650°C, austenite (A) begins to transform to pearlite if held in the bath for 10 s. The curve drawn through this point is the pearlite transformation start temperature and is labeled the beginning of transformation in Fig. 7. At about 100 s the pearlite transformation is finished. The second curve represents the pearlite transformation finish temperature and is labeled the end of transformation in Fig. 7. In this steel, pearlite forms at all temperatures along the start of the transformation curve from 727°C (the equilibrium temperature of the iron–carbon diagram) to 540°C (the “nose” of the curve). At the higher transformation temperatures, the pearlite interlamellar spacing (the spacing between cementite plates) is very coarse and decreases in spacing as the temperature is decreased, i.e., the nose of the IT diagram is approached. This is an important concept since a steel with a coarse pearlite interlamellar spacing is softer and of lower strength than a steel with a fine pearlite interlamellar spacing. Commercially, rail steels are produced with a pearlitic microstructure, and it has been found that the finer the interlamellar spacing, the harder the rail and the better the wear resistance. This means that rails will last longer in track if produced with the finest spacing allowable. Most rail producers employ an accelerated cooling process called head hardening to obtain the necessary conditions to achieve the finest pearlite spacing in the rail head (the point of wheel contact).

If the specimens are quenched to 450°C and held for various times, pearlite does not form. In fact, pearlite does not isothermally transform at transformation temperatures (in this case, salt pot temperatures) below the nose of the diagram in Fig. 7. The new constituent is called bainite, which consists of ferrite laths with small cementite particles (also called precipitates). An example of the microstructure of bainite is shown in Fig. 8. This form of bainite is called upper bainite because it is formed in the upper portion below the nose of the IT diagram (between about 540 and 400°C). Lower bainite, a finer ferrite–carbide microstructure, forms at lower temperatures (between 400 and about 250°C). Bainite is an important constituent in tough, high-strength, low-alloy steel.

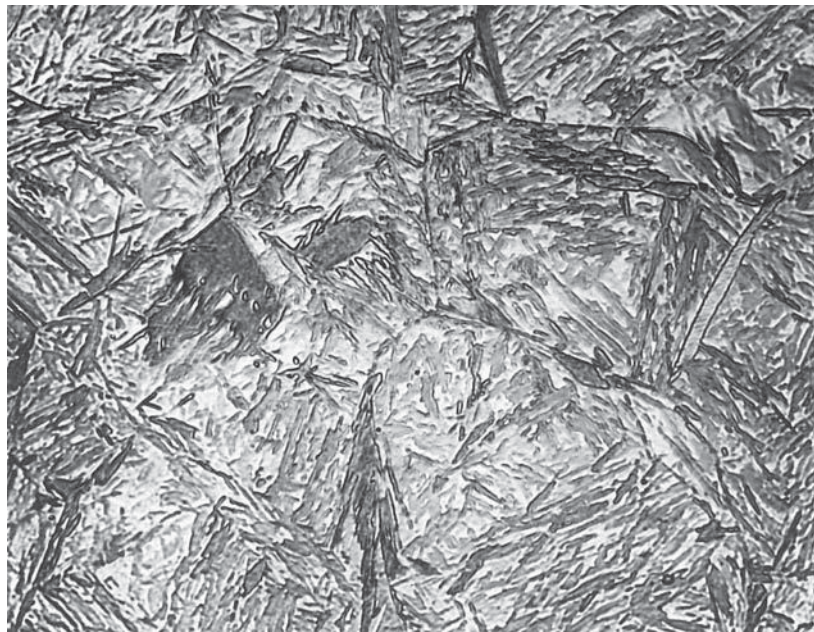
If specimens are quenched into a salt bath at 200°C, a new constituent called martensite will form. The start of the martensitic transformation is shown in Fig. 7 as  $M_s$  (at 220°C). Martensite is a form of ferrite that is supersaturated with carbon. In other words, because of the very fast cooling rate, the carbon atoms do not have time to diffuse from their interstitial positions in the bcc lattice to form cementite particles. An example of martensite is shown in Fig. 9. Steel products produced with an as-quenched martensitic microstructure are very hard and brittle, e.g., a razor blade. Most martensitic products are tempered by heating to temperatures between about 350 and 650°C. The tempering process allows some of the carbon to diffuse and form as a carbide phase from the supersaturated iron lattice. This softens the steel and provides some ductility. The degree of softening is determined by the tempering temperature and the time at the tempering temperature. The higher the temperature and the longer the time, the softer the steel. Most steels with martensite are used in the quenched and tempered condition.

**Continuous-Cooling Transformation Diagram.** The other more useful form of a time—temperature transformation diagram is the continuous-cooling transformation (CT) diagram. This differs from the IT diagram in that it is constructed by cooling small specimens at various cooling rates and measuring the temperatures at which transformations start and finish using a device called a dilatometer (a machine that measures dilation). Each phase transformation undergoes a distinct volume change (positive on cooling and negative on heating) that can be measured by a sensitive length-measuring device in the dilatometer. A CT diagram has





**Figure 8** Photomicrograph of a low-alloy steel showing a bainitic microstructure. 500X. 4% picral + 2% nital etch.



**Figure 9** Photomicrograph of a low-alloy steel showing a martensitic microstructure. 1000X. 4% picral + HCl and 10% sodium metabisulfate etch.

similar features to the IT diagram shown in Fig. 7 but is produced by continuous cooling rather than isothermal conditions. A continuous-cooling diagram is applicable for most industrial processes and should be used in lieu of an IT diagram. A CT diagram can also be constructed by quenching one end of a Jominy bar described below.

**Hardenability Concept.** In thick products, e.g., large-diameter bars, thick plates, and heavy forgings, the through-thickness properties are achieved through hardenability. Hardenability is the ability to induce depth of hardness in a steel product. The hardness level is obtained by controlling the amount of martensite in the microstructure. To increase the depth of hardness, certain alloying elements are added to the steel for increased hardenability. Elements, such as nickel, chromium, and molybdenum, shift the pearlite nose of the IT and CT diagrams to the right (longer times). With the nose out of the way on cooling, martensite can be formed over a wider range of cooling rates when compared with a steel without alloying elements.

There is a fairly simple test to measure the hardenability of steel called the Jominy test. A 25.4-mm-diameter and 102-mm-long bar is austenitized to 845°C for 1 h and then water quenched at one end of the bar. The quenching takes place in a specially designed fixture where the bar is suspended in the vertical position and water is directed against the machined bottom end face of the bar. After quenching, parallel flats 0.38 mm deep are machined on opposite sides of the bar. Hardness is measured at 1.6-mm ( $\frac{1}{16}$ -in.) intervals from the quenched end. The hardness is plotted against depth from the quenched end to produce a hardenability curve or band. A hardenability band for medium-carbon Society of Automotive Engineers/American Iron and Steel Institute (SAE/AISI) 1045 steel is shown in Fig. 10a. The two curves that form the band represent the maximum and minimum hardness values from many Jominy tests. To illustrate the concept of hardenability, compare the hardenability band for SAE/AISI 1045 steel to low-alloy SAE/AISI 4145 steel in Fig. 10b. These steels are similar except that the low-alloy steel has chromium and molybdenum additions as shown below:

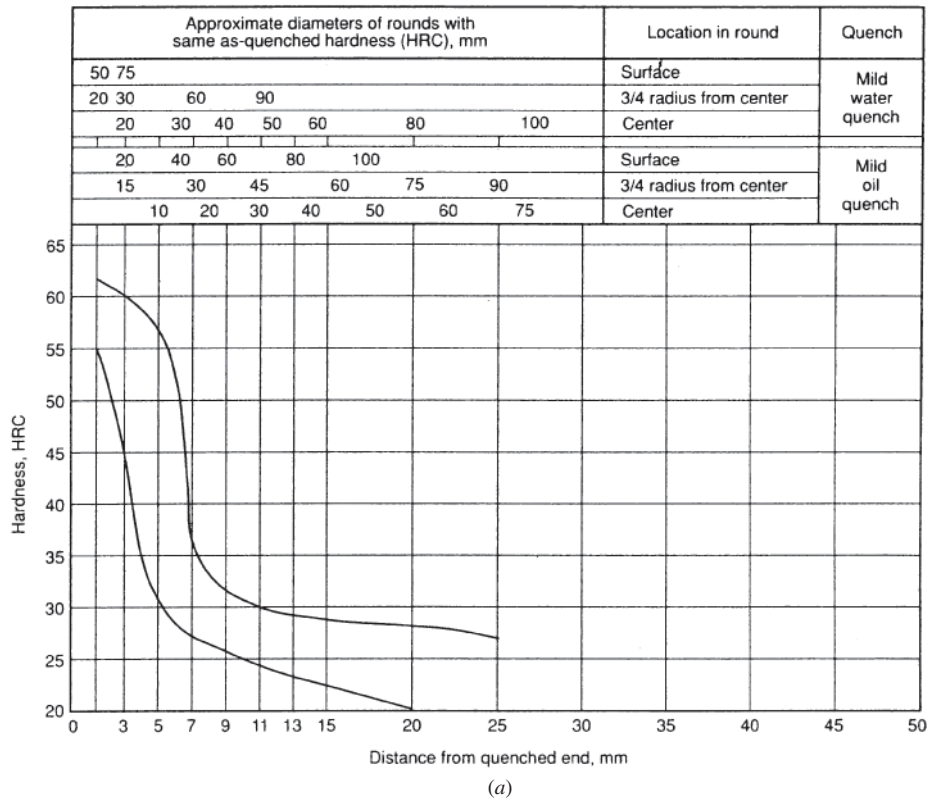
C	Mn	Si	Cr	Mo
0.42/0.51	0.50/1.00	0.15/0.35	—	—
0.42/0.49	0.65/1.10	0.15/0.35	0.75/1.20	0.15/0.25

As can be seen from the hardenability bands, the higher manganese, chromium, and molybdenum additions in the SAE/AISI 4145 steel produced a much greater depth of hardness than the plain-carbon steel. For example, a hardness of HRC 45 (Rockwell *C* scale) was achieved at a depth of only 3–6.5 mm in the SAE/AISI 1045 steel compared with a hardness of HRC 45 at a depth of 21–50 mm in the SAE/AISI 4145 steel. This low-alloy steel has many times the depth of hardness or hardenability of the plain-carbon steel. This means that a hardness of HRC 45 can be achieved in the center of a 100-mm-diameter bar of SAE/AISI 4145 steel compared to a 10-mm-diameter bar of SAE/AISI 1045 steel (both water quenched). The depth of hardness is produced by forming martensite near the quenched end of the bar with mixtures of martensite and bainite further in from the end and eventually bainite at the maximum depth of hardness. Hardenability is important since hardness is roughly proportional to tensile strength. To convert hardness to an approximate tensile strength, the conversion table in the American Society for Testing and Materials (ASTM) E140 can be used. A portion of this table is given below:



Hardness			
Rockwell C Scale	Vickers	Brinell 3000-kg Load	Approximate Tensile Strength (MPa)
60	697	(654)	—
55	595	560	2075
50	513	481	1760
45	446	421	1480
40	392	371	1250
35	345	327	1080
30	302	286	950
25	266	253	840

Heat-treating temperatures recommended by SAE  
 Normalize (for forged or rolled specimens only): 870 °C (1600 °F)  
 Austenitize: 845 °C (1550 °F)



**Figure 10** Hardenability curves for (a) SAE/AISI 1045 and (b) SAE/AISI 4145 showing depth of hardness with distance from the quenched end of a Jominy bar. (Source: ASM Handbook, Vol. 1, *Properties and Selection: Irons, Steels, and High-Performance Alloys*, ASM International, Materials Park, OH, 1997, p. 487.) Reprinted with permission of ASM International.

Heat-treating temperatures recommended by SAE  
 Normalize (for forged or rolled specimens only): 870 °C (1600 °F)  
 Austenitize: 845 °C (1550 °F)

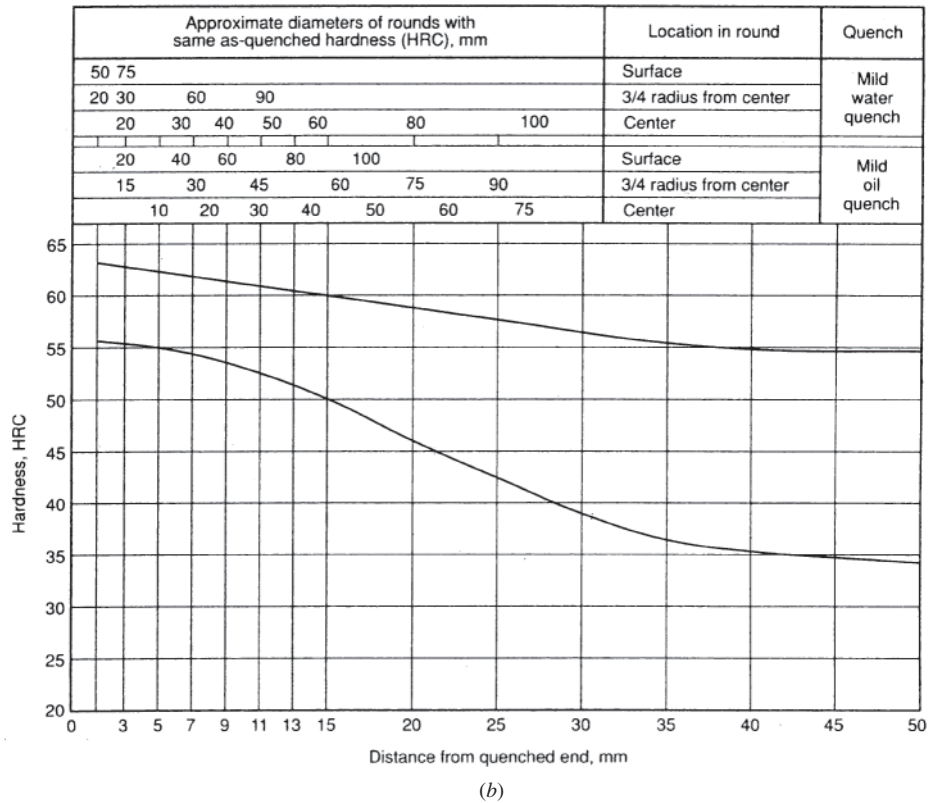
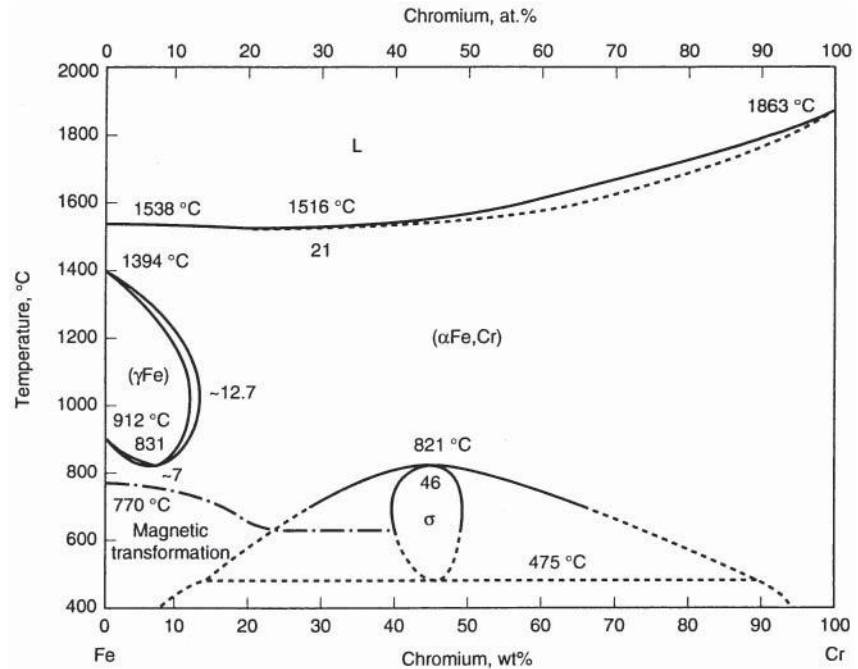


Figure 10 (Continued)

This table also lists Vickers and Brinell hardness values, which are different types of hardness tests. It can be seen that a hardness of HRC 45 converts to an approximate tensile strength of 1480 MPa.

#### 4 ROLE OF ALLOYING ELEMENTS IN STEEL

In the hardenability concept described in the previous section, alloying elements have a profound effect on depth of hardness. Alloying elements also change the characteristics of the iron-carbon diagram. For example, in the iron-carbon diagram (see Fig. 1) austenite cannot exist below the eutectoid temperature of 727°C. However, there are steels where austenite is the stable phase at room temperature, e.g., austenitic stainless steels and austenitic manganese steels. This can only be achieved through alloying. There are, however, special conditions where small amounts of austenite can be retained at room temperature during rapid quenching of low-alloy steel. When this occurs, the austenite is too rich in alloying elements to transform at room temperature and is thus retained as small regions in a martensitic microstructure.



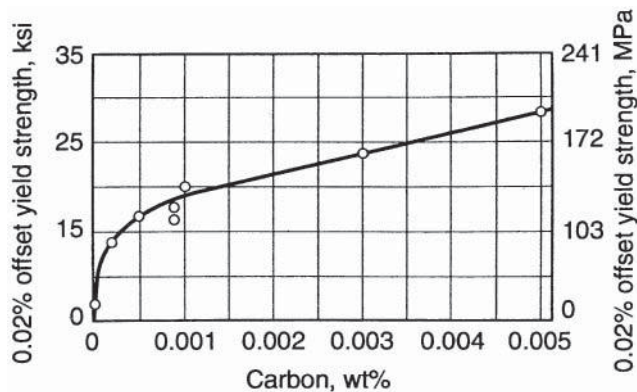
**Figure 11** Iron–chromium equilibrium-phase diagram. (Source: *ASM Handbook*, Vol. 20, *Materials Selection and Design*, ASM International, Materials Park, OH, 1997, p. 365.) Reprinted with permission of ASM International.

Because of this, it is called retained austenite. The retained austenite can be transformed through tempering the steel.

In austenitic stainless steels, when nickel is added with chromium, the austenite-phase field is expanded, allowing austenite to be stable at room temperature. The popular SAE/AISI 304 austenitic stainless steel contains 18% Cr and 8% Ni. Austenitic manganese steel (Hadfield steel) contains 12% Mn with 1% C. The Mn and C allow austenite to be stable at room temperature. Because of this ability, nickel and manganese are, therefore, called austenite stabilizers. Other elements are ferrite stabilizers, e.g., chromium, silicon, and molybdenum. A ferrite-stabilizing element expands the ferrite-phase field, and the austenite-phase field is restricted within what is called a gamma loop (gamma,  $\gamma$ , is the symbol for austenite). A gamma loop can be seen in the iron–chromium equilibrium diagram in Fig. 11. The gamma loop is shown at the left side of the diagram. According to this diagram, iron–chromium alloys with 12.7% Cr or higher, the transformation from austenite ( $\gamma$ ) to ferrite ( $\alpha$ ) does not occur and ferrite exists from room temperature to melting. Iron–chromium alloys make up an important class of stainless steels called ferritic and martensitic stainless steels.

Each particular alloying element has an influence on the structure and properties of steel. The following elements are important alloying elements in steel:

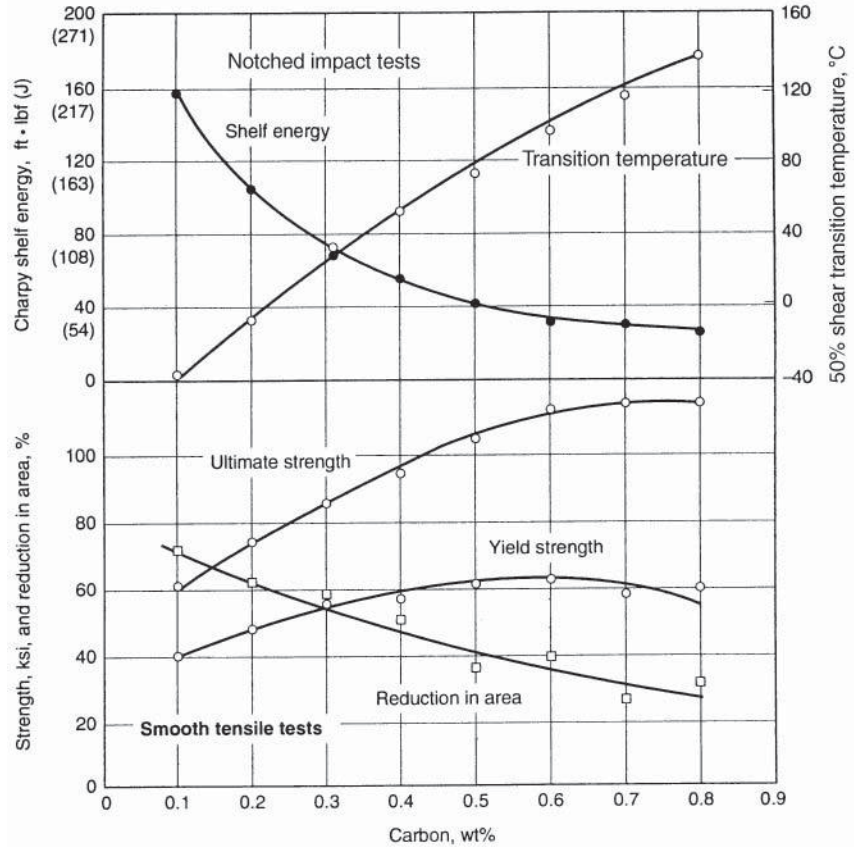
**Carbon.** Carbon is the most common alloying element in steel. It is inexpensive and has a strong influence on hardness and strength. It is the basic and essential alloying element in all plain-carbon, low-alloy, and tool steels. Carbon is an interstitial element that occupies sites between the larger iron atoms in the bcc and fcc lattices. The influence of carbon on the strength of iron can be seen in Fig. 12. Carbon can increase yield strength of pure iron (0% C) with a strength of about 28–190 MPa. At 0.005% C, the



**Figure 12** Effect of carbon in solid solution on the yield strength of iron. (Source: *ASM Handbook*, Vol. 20, *Materials Selection and Design*, ASM International, Materials Park, OH, 1997, p. 367.) Reprinted with permission of ASM International.

maximum solubility of carbon at room temperature the sevenfold increase in strength is due to interstitial solid-solution strengthening. Any excess carbon, above 0.005% C, will form an iron carbide compound called cementite ( $\text{Fe}_3\text{C}$ ). Cementite can exist as a particle, as a component of lamellar pearlite, or as a proeutectoid network on prior austenite grain boundaries in hypereutectoid steel. Thus, carbon in the form of cementite has a further influence on the strength of steel, as seen in Fig. 13. In this plot, the steels between 0.1% C and 0.8% C contain about 10–100% pearlite. Yield strength peaks at about 425 MPa at 0.6% C whereas tensile strength (ultimate strength) increases to 790 MPa at 0.8% C. These properties are for carbon steels in the air-cooled condition. In a 0.8% C steel, a further increase in strength can be achieved if faster cooling rates are used to produce a finer pearlite interlamellar spacing. In a fully pearlitic, head-hardened rail steel (accelerated cooled), the yield strength can increase to 860 MPa and tensile strength to 1070 MPa. Carbon also has a negative effect on properties, as seen in Fig. 13. For example, the percent reduction in area (as well as total elongation not shown) decreases with increasing carbon. The percent reduction in area is a measure of the cross-sectional area change in a tensile specimen before and after fracture. Notch toughness also decreases with carbon content, as seen in the decrease in upper shelf energy and the increase in transition temperature. Shelf energy is the upper portion or upper shelf of a curve of absorbed energy plotted from a Charpy test.

**Manganese.** Manganese is also an essential element in all carbon, low-alloy, and alloy steels. Manganese has several roles as an alloying element. One role is to assure that all residual sulfur is combined to form manganese sulfide ( $\text{MnS}$ ). Manganese is generally added to steel with a minimum manganese–sulfur ratio of 20:1. Without manganese the sulfur would combine with iron and form iron sulfide ( $\text{FeS}$ ), which is a brittle compound that lowers toughness and ductility and causes a phenomenon called hot shortness. Hot shortness is a condition where a compound (such as  $\text{FeS}$ ) or insoluble element (such as copper) in steel has a low melting point and thus forms an unacceptable cracklike surface condition during hot rolling. Another role of manganese is in strengthening steel. Manganese is a substitutional element and can replace iron atoms in the bcc or fcc lattice. Each 0.1% Mn added to iron will increase the yield strength by about 3 MPa. Manganese also lowers the eutectoid transformation temperature and lowers the eutectoid carbon content. In large amounts (12% or higher), manganese is



**Figure 13** Effect of carbon on the tensile and notched impact properties of ferrite-pearlite steels. (Source: *ASM Handbook*, Vol. 20, *Materials Selection and Design*, ASM International, Materials Park, OH, 1997, p. 367.) Reprinted with permission of ASM International.

an austenite stabilizer in alloy steels and forms a special class of steels called austenitic manganese steels (also called Hadfield manganese steels). These steels are used in applications requiring excellent wear resistance, e.g., in rock crushers and in railway track connections where two rails meet or cross.

**Silicon.** Silicon is added to many carbon and low-alloy steels as a deoxidizer, i.e., it removes dissolved oxygen from molten steel during the steel-refining process. Oxygen is an undesirable element in steel because it forms oxide inclusions, which can degrade ductility, toughness, and fatigue resistance. Silicon has a moderate effect on strengthening steel but is usually not added for strengthening. Each 0.1% Si increases the yield strength of iron by about 8 MPa. It is a ferrite stabilizer and is found in some stainless steels. Silicon is also added to steel for enhanced electrical properties, e.g., iron-silicon transformer steels at 3.25% Si. These carbon-free steels have high magnetic permeability and low core loss.

**Phosphorus.** Phosphorus is considered a tramp or residual element in steel and is carefully restricted to levels generally below 0.02%. However, like carbon, phosphorus is an interstitial element that can substantially strengthen iron. For this reason, phosphorus

is added to a special class of steels called rephosphorized steels for strength. Rephosphorized steels also have enhanced machinability.

*Sulfur.* Sulfur is also considered a tramp element in steel and is usually restricted to below about 0.02%. Although an element with a small atomic diameter, sulfur is not considered an interstitial alloying element because it is insoluble in iron. However, as in the case of phosphorus, sulfur is added to a special class of steels called resulfurized steels that have improved machinability. These steels are called free-machining steels.

*Copper.* In most steels copper is considered a tramp (residual) element and is restricted to levels below 0.04%. Copper, having a much lower melting point than iron, can create a detrimental steel surface condition known as hot shortness. Although not generally added to steel, there is a very special class of steels that contain high levels of copper to take advantage of the precipitation of copper particles during aging (a tempering process). These copper particles increase strength and hardness. Copper is also added to low-alloy steels for atmospheric corrosion protection (these steels are called weathering steels). One problem with copper in steel is that it cannot be oxidized and removed during steel refining. Thus, over time, the copper level of steel produced from steel scrap is slowly increasing.

*Nickel.* Nickel is an important element because of its positive effect on hardenability. Many important low-alloy steels contain nickel for this reason. Nickel, being a substitutional element in the iron lattice, has a small effect on increasing yield strength. Nickel, being an austenite stabilizer, is also a vital element in austenitic stainless steels. Nickel is also important in steels for cryogenic applications and storage tanks for liquefied hydrocarbon gases. Nickel does not form a carbide and remains in solid solution.

*Chromium.* Like nickel, chromium has a positive effect on hardenability and is an important alloying element in many low-alloy steels. For corrosion resistance, chromium is present in all stainless steels as a solid-solution element. In addition to hardenability and solid-solution effects, chromium forms several important chromium carbides that are necessary for wear resistance in many tool steels and steels used for rolls in hot- and cold-rolling mills.

*Molybdenum.* Molybdenum is a potent hardenability element and is found in many low-alloy steels. Molybdenum, like chromium, forms several types of carbides that are important for wear-resistant applications, e.g., tool steels. Molybdenum is added to minimize temper embrittlement in low-alloy steels. Temper embrittlement occurs when low-alloy steels are tempered in the temperature range of 260–370°C. The embrittlement is caused by tramp elements such as phosphorus that accumulate at the prior austenite grain boundaries and thus weaken the boundaries. Adding molybdenum prevents the accumulation of these undesirable elements at the boundaries. Molybdenum also enhances the creep strength of low-alloy steels at elevated temperatures and is used in rotors and other parts of generators in electric power plants. Creep is an undesirable process that allows steel to slowly elongate or creep under load. Eventually the component will fail.

*Vanadium.* Although vanadium is a potent hardenability element, its most useful role is in the formation of a vanadium nitride and vanadium carbide (it can also be in a combined form of vanadium carbonitride). A very important role of vanadium is in microalloyed steels, also called high-strength, low-alloy (HSLA) steels. These steels are strengthened by precipitation of vanadium nitrides and vanadium carbides (vanadium carbonitrides). The formation of vanadium carbide is important for wear resistance. Vanadium carbide is much harder than iron carbide, chromium carbide, and



molybdenum carbide. Vanadium is thus important in high-speed tool steels, which are used as drill bits that retain their hardness as the tool heats by friction.

*Tungsten.* Tungsten is not an addition to low-alloy steels but is a vital alloying element in high-speed tool steels where it forms hard tungsten carbide particles.

*Aluminum.* Aluminum is employed as a deoxidizer in steel and is generally used in conjunction with silicon (also a deoxidizer). A deoxidizer removes undesirable oxygen from molten steel. Once removed, the steel is called “killed.” Aluminum–silicon deoxidized (killed) steels are known as fine-grain steels. Another important role of aluminum is the formation of aluminum nitride (AlN) precipitate. Many steels depend upon the formation of AlN, especially steels used for sheet-forming applications requiring a high degree of formability such as parts that require deep drawing. These steels are called drawing-quality special-killed (DQSK) steels. The AlN precipitates help in the formation of an optimum crystallographic texture (preferred orientation) in low-carbon sheet steels for these deep-drawing applications. When aluminum combines with nitrogen to form AlN, the dissolved interstitial nitrogen is lowered. Lower interstitial nitrogen (interstitial nitrogen is also called free nitrogen) provides improved ductility. Aluminum can also substitute for silicon in electrical steels for laminations in electric motors and transformer cores.

*Titanium.* Titanium is a strong deoxidizer but is usually not used solely for that purpose. Titanium is important in microalloyed steels (HSLA steels) because of the formation of titanium nitride (TiN) precipitates. Titanium nitrides pin grain boundary movement in austenite and thus provide grain refinement. Another role of titanium is in steels containing boron where a titanium addition extracts nitrogen from liquid steel so that boron, a strong nitride former, remains in elemental form to enhance hardenability. Because of its affinity for both carbon and nitrogen, titanium is important in IF steels. Interstitial-free steels are an important class of steels with exceptional formability. Titanium, being a strong carbide former, is used as a carbide stabilizer in austenitic stainless steels (AISI type 321), ferritic stainless steels (AISI types 409, 439, and 444), and precipitation-hardening stainless steels (AISI types 600 and 635).

*Niobium (Columbium).* Niobium is also important in microalloyed (HSLA) steels for its precipitation strengthening through the formation of niobium carbonitrides. Some microalloyed steels employ both vanadium and niobium. Because of its affinity for both carbon and nitrogen, niobium is an element found in some IF steels. Niobium is also added as a carbide stabilizer (prevents carbides from dissolving and re-forming in undesirable locations) in some austenitic stainless steels (AISI types 347, 348, and 384), ferritic stainless steels (AISI types 436 and 444), and precipitation-hardening stainless steels (AISI type 630).

*Tantalum.* Because of its affinity for carbon, tantalum, like niobium, is added as a carbide stabilizer to some austenitic stainless steels (AISI types 347 and 348).

*Boron.* On a weight percent basis, boron is the most powerful hardenability element in steel. A minute quantity of boron, e.g., 0.003%, is sufficient to provide ample hardenability in a low-alloy steel. However, boron is a strong nitride former and can only achieve its hardenability capability if in elemental form. Thus, boron must be protected from forming nitrides by adding a sufficient amount of titanium to first combine with the nitrogen in the steel.

*Calcium.* Calcium is a strong deoxidizer in steel but is not used for that purpose. In an aluminum-deoxidized (killed) steel, calcium combines with sulfur to form calcium sulfide particles. This form of sulfide remains as spherical particles as compared with manganese sulfide, which is soft and elongates into stringers upon hot rolling.

Thus, steels properly treated with calcium do not have the characteristics associated with MnS stringers, i.e., property directionality or anisotropy.

*Zirconium.* Although expensive and rarely added to steel, zirconium acts like titanium in forming zirconium nitride particulates.

*Nitrogen.* Nitrogen is added to some steels, e.g., steels containing vanadium, to provide sufficient nitrogen for nitride formation. This is important in microalloyed steels containing vanadium. Nitrogen, being an interstitial element like carbon, strengthens ferrite. A number of austenitic stainless steels contain nitrogen for strengthening (AISI types 201, 202, 205, 304N, 304LN, 316N, and 316LN).

*Lead.* Lead is added to steel for enhanced machinability. Being insoluble in iron, lead particles are distributed through the steel and provide both lubrication and chip-breaking ability during machining. However, leaded steels are being discontinued around the world because of the environmental health problems associated with lead.

*Selenium.* Selenium is added to some austenitic stainless steels (AISI type 303Se), ferritic stainless steels (AISI type 430Se), and martensitic stainless steels (AISI type 416Se) for improved machined surfaces.

*Rare Earth Elements.* The rare earth elements cerium and lanthanum are added to steel for sulfide shape control, i.e., the sulfides become rounded instead of stringers. It is usually added in the form of mish metal (a metallic mixture of the rare earth elements).

*Residual Elements.* Tin, antimony, arsenic, and copper are considered residual elements in steel. They are also called tramp elements. These elements are not intentionally added to steel but remain in steel because they are difficult to remove during steelmaking and refining. Steels made by electric furnace melting employing scrap as a raw material contain higher levels of residual elements than steels made in an integrated steelmaking facility (blast furnace–BOF route). Some electric furnace melting shops use direct-reduced iron pellets to dilute the effect of these residuals.

*Hydrogen.* Hydrogen gas is also a residual element in steel and can be very deleterious. Hydrogen is soluble in liquid steel and somewhat soluble in austenite. However, it is very insoluble in ferrite and is rejected as atomic hydrogen ( $H^+$ ). If trapped inside the steel, usually in products such as thick plates, heavy forgings, or railroad rails, hydrogen will accumulate on the surfaces of manganese sulfide inclusions. When this accumulation takes place, molecular hydrogen ( $H_2$ ) can form and develop sufficient pressure to create internal cracks. As the cracks grow, they form what is termed hydrogen flakes and the product must be scrapped. However, if the product is slow cooled from the rolling temperature, the atomic hydrogen has sufficient time to diffuse from the product, thus avoiding hydrogen damage. Also, most modern steelmakers use degassing to remove hydrogen from liquid steel.

## 5 HEAT TREATMENT OF STEEL

One of the very important characteristics of steel is the ability to alter the microstructure through heat treatment. As seen in the previous sections, many different microstructural constituents can be produced. Each constituent imparts a particular set of properties to the final product. For example, by quenching a steel in water, the steel becomes very hard but brittle through the formation of martensite. By tempering the quenched steel, some ductility can be restored with some sacrifice in hardness and strength. Also, superior wear properties can be obtained in fully pearlitic microstructures, particularly if an accelerated cooling process is employed to develop a fine interlamellar spacing. Complex parts can be designed by taking advantage of the

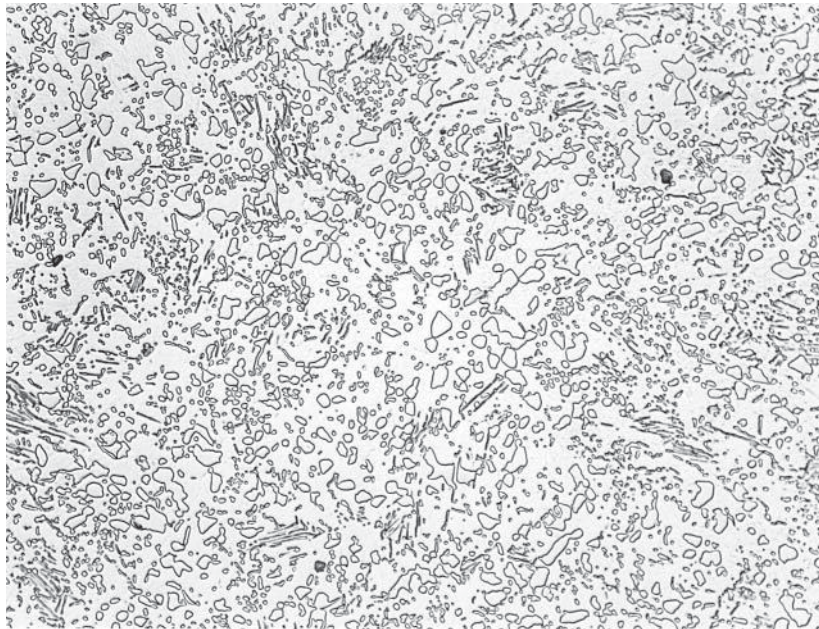


formability and ductility of ferritic sheet steel through cold rolling and annealing. The amount of pearlite in ferritic steel can be adjusted by carbon content and cooling rate to produce a wide range of hardness and strength. In quenched and tempered steels, a bainitic microstructure has a unique combination of high strength and toughness. Thus steel, more than any other metallic material, can be manipulated through heat treatment to provide a multiplicity of microstructures and final properties. The common types of heat treatment are listed below:

*Annealing (Full Annealing).* One of the most common heat treatments for steel is annealing. It is used to soften steel and to improve ductility. In this process, the steel is heated into the lower regions of the austenite-phase field and slow cooled to room temperature. The resulting microstructure consists of coarse ferrite or coarse ferrite plus pearlite, depending upon carbon and alloy content of the steel.

*Normalizing.* Steel is normalized by heating into the austenite-phase field at temperatures somewhat higher than those used by annealing followed by air cooling. Many steels are normalized to establish a uniform ferrite plus pearlite microstructure and a uniform grain size.

*Spheroidizing.* To produce a steel in its softest possible condition, it is usually spheroidized by heating just above or just below the eutectoid temperature of  $727^{\circ}\text{C}$  and holding at that temperature for an extended time. This process breaks down lamellar pearlite into small spheroids of cementite in a continuous matrix of ferrite, as seen in Fig. 14. To obtain a very uniform dispersion of cementite spheroids, the starting microstructure is usually martensite. This is because carbon is more uniformly distributed in martensite than in lamellar pearlite. The cementite lamella must first dissolve and then redistribute the carbon as spheroids whereas the cementite spheroids can form directly from martensite.



**Figure 14** Photomicrograph of a medium-carbon steel in the spheroidized condition. 500X. 4% picral + 2% nital etch.

*Process Annealing (Recrystallization Annealing).* Process annealing takes place at temperatures just below the eutectoid temperature of  $727^{\circ}\text{C}$ . This treatment is applied to low-carbon, cold-rolled sheet steels to restore ductility. In aluminum-killed steels, the recrystallized ferrite will have an ideal crystallographic texture (preferred orientation) for deep drawing into complex shapes such as oil filter cans and compressor housings. Crystallographic texture is produced by developing a preferred orientation of the ferrite grains, i.e., the crystal axes of the ferrite grains are oriented in a preferred rather than random orientation.

*Stress Relieving.* Steel products with residual stresses can be heated to temperatures approaching the eutectoid transformation temperature of  $727^{\circ}\text{C}$  to relieve the stress.

*Quenching.* To produce the higher strength constituents of bainite and martensite, the steel must be heated into the austenite-phase field and rapidly cooled by quenching in oil or water. High-strength, low-alloy steels are produced by this process followed by tempering. It must be noted that employing microalloying additions such as Nb, V, and Ti can also produce HSLA steels. These microalloyed steels obtain their strength by thermomechanical treatment rather than heat treatment.

*Tempering.* When quenched steels (martensitic steel) are tempered by heating to temperatures approaching the eutectoid temperature of  $727^{\circ}\text{C}$ , the dissolved carbon in the martensite forms cementite particles, and the steels become more ductile. Quenching and tempering are used in a variety of steel products to obtain desired combinations of strength and toughness.

## 6 CLASSIFICATION AND SPECIFICATIONS OF STEELS

Since there are literally thousands of different steels, it is difficult to classify them in a simple straightforward manner. However, some guidelines can be used. For example, steels are generally classified as carbon steel or alloy steel. A classification system was developed by the SAE as early as 1911 to describe these carbon and alloy steels. The AISI collaborated with SAE to refine the compositional ranges of the classification that are used today. Recently, a Unified Numbering System (UNS) was established that incorporates the SAE/AISI number.

Many steel products are purchased by specifications describing specific compositional, dimensional, and property requirements. Specification organizations such as ASTM have developed numerous specifications for steel products and the testing of steel products. Some specific product user groups in the United States have developed their own specifications, e.g., the American Bureau of Ships (ABS) for ship plate and other marine products, Aerospace Materials Specifications (AMS) for aerospace applications, the American Railway Engineering and Maintenance of Way Association (AREMA) for rail and rail products, the SAE for automotive applications, and the American Society of Mechanical Engineers (ASME) for steels produced to boiler code specifications. In Japan, there are standards developed by the Japanese Industrial Standards (JIS) Committee of the Ministry of International Trade and Industry. In the United Kingdom, there are the British Standards (BS) developed by the British Standards Institute. In Europe, Germany has the Deutsches Institut für Normung (DIN) standards, France the Association Francaise de Normalisation (AFNOR) standards, and Italy the Ente Nazionale Italiano di Unificazione (UNI) standards.

Specifications can be as simple as a hardness requirement, i.e., ASTM A1 for rail steel to elaborate compositional and property requirements as in ASTM A808, "High-strength low-alloy carbon–manganese–niobium–vanadium steel of structural quality with improved notch toughness." Describing specific specifications is beyond the scope of this handbook, but many of the key sources can be found in the Bibliography at the end of this chapter.

## 6.1 Carbon Steels

Carbon steels (also called plain-carbon steels) constitute a family of iron–carbon–manganese alloys. In the SAE/AISI system, the carbon steels are classified as follows:

Nonresulfurized carbon steels	10xx series
Resulfurized steels	11xx series
Rephosphorized and resulfurized steels	12xx series
High-manganese carbon steels	15xx series

A four-digit SAE/AISI number is used to classify the carbon steels with the first two digits being the series code and the last two digits being the nominal carbon content in points of carbon (1 point = 0.01% C). For example, SAE/AISI 1020 steel is a carbon steel containing 0.20% C (actually 0.18–0.22% C). The chemical composition limits for the above SAE/AISI 10xx series of carbon steels for semifinished products, forgings, hot- and cold-finished bars, wire, rods, and tubing are listed in *SAE Materials Standards Manual* (SAE HS-30, 1996). There are slight compositional variations for structural shapes, plates, strip, sheet, and welded tubing (see SAE specification J403). The *SAE Manual* gives the SAE/AISI number along with the UNS number. The carbon level spans the range from under 0.06% C to 1.03% C.

Because of the wide range in carbon content, the SAE/AISI 10xx carbon steels are the most commonly used steels in today's marketplace. All SAE/AISI 10xx series carbon steels contain manganese at levels between 0.25 and 1.00%. For a century, manganese has been an important alloying element in steel because it combines with the impurity sulfur to form manganese sulfide (MnS). MnS is much less detrimental than iron sulfide (FeS), which would form without manganese present. Manganese sulfides are usually present in plain and low-alloy steels as somewhat innocuous inclusions. The manganese that does not combine with sulfur strengthens the steel. However, with the development of steelmaking practices to produce very low sulfur steel, manganese is becoming less important in this role.

The SAE/AISI 11xx series of resulfurized steels contain between 0.08 and 0.33% sulfur. Although in most steel sulfur is considered an undesirable impurity and is restricted to less than 0.05%, in the SAE/AISI 11xx and 12xx series of steels, sulfur is added to form excess manganese sulfide inclusions. These are the free-machining steels that have improved machinability over lower sulfur steels due to enhanced chip breaking and lubrication created by the MnS inclusions.

The SAE/AISI 12xx series are also free-machining steels and contain both sulfur (0.16–0.35%) and phosphorus (0.04–0.12%). The SAE/AISI 15xx series contain higher manganese levels (up to 1.65%) than the SAE/AISI 10xx series of carbon steels.

Typical mechanical properties of selected SAE/AISI 10xx and 11xx series of carbon steels are listed in the first part of the table on pp. 20–23, Section 4, of the *ASM Metals Handbook*, Desktop Edition, 1985, for four different processing conditions (as rolled, normalized, annealed, and quenched and tempered). These properties are average properties obtained from many sources, and thus this table should only be used as a guideline. The as-rolled condition represents steel before any heat treatment was applied. Many applications utilize steel in the as-rolled condition. As can be seen from the aforementioned ASM table, yield and tensile strength are greater for steel in the normalized condition. This is because normalizing develops a finer ferrite grain size. Yield and tensile strength are lowest for steels in the annealed condition. This is due to a coarser grain size developed by the slow cooling rate from the annealing temperature. In general, as yield and tensile strength increase, the percent elongation decreases. For example, in the ASM table, annealed SAE/AISI 1080 steel has a tensile strength of 615 MPa and a total elongation of 24.7% compared with the same steel in the normalized condition, with a tensile strength of 1010 MPa and a total elongation of 10%. This relationship holds for most steel.

### *Special Low-Carbon Steels*

These are the steels that are not classified in the aforementioned SAE table or listed in the aforementioned ASM table. As mentioned earlier, carbon is not always beneficial in steels. These are special steels with carbon contents below the lower level of the SAE/AISI 10xx steels. There are a number of steels that are produced with very low carbon levels (less than 0.002% C), and all the remaining free carbon in the steel is tied up as carbides. These steels are known as IF steels, which means that the interstitial elements of carbon and nitrogen are no longer present in elemental form in the iron lattice but are combined with elements such as titanium or niobium as carbides and nitrides (carbonitrides). Interstitial-free steels are required for exceptional formability, especially in applications requiring deep drawability. Drawability is a property that allows the steel to be uniformly stretched (or drawn) in thickness in a closed die without localized thinning and necking (cracking or breaking). An example of a deep-drawn part would be a compressor housing for a refrigerator. With proper heat treatment, IF steels develop a preferred crystallographic orientation that favors a high plastic anisotropy ratio, or  $r$  value. High- $r$ -value steels have excellent deep-drawing ability and these steels can form difficult parts. Another type of low-carbon steel is a special class called DQSK steel. This type of aluminum-treated steel also has a preferred orientation and high  $r$  value. The preferred orientation is produced by hot rolling the steel on a hot strip mill followed by rapid cooling. The rapid cooling keeps the aluminum and interstitial elements from forming aluminum nitride particles (i.e., the Al and N atoms are in solid solution in the iron lattice). After rolling, the steel is annealed to allow aluminum nitride to precipitate. The aluminum nitride plays an important role in the development of the optimum crystallographic texture. The DQSK steel is used in deep-drawing applications that are not as demanding as those requiring IF steel.

A new family of steels called bake-hardening steels also have a low, but controlled carbon content. These steels gain strength during the paint–bake cycle of automotive production. Controlled amounts of both carbon and nitrogen combine with carbonitride-forming elements such as titanium and niobium during the baking cycle (generally 175°C for 30 min). The precipitation of these carbonitrides during the paint–bake cycle strengthens the steel by a process called aging.

Enameling steel is produced with as little carbon as possible because during the enameling process carbon in the form of carbides can react with the frit (the particles of glasslike material that melts to produce the enamel coating) to cause defects in the coating. Thus, steels to be used for enameling are generally decarburized in a special reducing atmosphere during batch annealing. In this process, the carbon dissipates from the steel. After decarburization, the sheet steel is essentially pure iron. Enamel coatings are used for many household appliances such as washers and dryers, stovetops, ovens, and refrigerators. Also, steel tanks in most hot-water heaters have a glass (or enameled) inside coating.

Electrical steels and motor lamination steels are also produced with as low a carbon content as possible. Dissolved carbon and carbides in these steels are avoided because the magnetic properties are degraded. The carbides, if present in the steel, inhibit the movement of the magnetic domains and lower the electrical efficiency. These steels are used in applications employing alternating current (AC) in transformers and electric motors. Most electric motors for appliances and other applications have sheet steel stacked in layers (called laminations) that are wound in copper wire. Electrical steels used for transformers contain silicon, which is added to enhance the development of a specific crystallographic orientation that favors electrical efficiency.

## 6.2 Alloy Steels

Alloy steels are alloys of iron with the addition of one or more of the following elements: carbon, manganese, silicon, nickel, chromium, molybdenum, and vanadium. The alloy steels

cover a wide range of steels, including low-alloy steels, stainless steels, heat-resistant steels, and tool steels. Some alloy steels, such as austenitic stainless steels, do not contain intentional additions of carbon. Silicon, when required, is added as a deoxidizer to the molten steel. Nickel provides strength and assists in hardening the steel by quenching and tempering heat treatment. This latter effect is called hardenability, which has been described earlier. Chromium is found in stainless steels for corrosion resistance. Chromium and molybdenum also assist in hardenability of the low-alloy steels. Vanadium strengthens the steel by forming precipitates of vanadium carbonitride. Vanadium is also a potent hardenability element.

### ***Low-Alloy Steels***

There is an SAE/AISI four-digit classification system for the low-alloy steels. As in the carbon steels, the first two digits are for the alloy class and the last two (or three) digits are for the carbon content. Because of the various combinations of elements, the system is more extensive than that used for the carbon steels. The general SAE/AISI classification system for low-alloy steels is as follows:

Manganese steels	13xx series
Nickel steels	23xx, 25xx series
Nickel–chromium steels	31xx, 32xx, 33xx, and 34xx series
Molybdenum steels	40xx, 44xx series
Chromium–molybdenum steels	41xx series
Nickel–chromium–molybdenum steels	43xx and 47xx series 81xx, 86xx, 87xx, and 88xx series 93xx, 94xx, 97xx, and 98xx series
Nickel–molybdenum steels	46xx and 48xx series
Chromium steels	50xx and 51xx series 50xxx, 51xxx, and 52xxx series
Chromium–vanadium steels	61xx series
Tungsten–chromium steels	71xxx, 72xx series
Silicon–manganese steels	92xx series
Boron steels	xxBxx series
Leaded steels	xxLxx series

The boron-containing steels are low-alloy steels with boron added in the amount of 0.0005–0.003%. Boron is a strong hardenability element. The leaded steels contain 0.15–0.35% lead for improved machinability (however, lead is no longer favored as an alloying addition because of health concerns).

A table in the aforementioned SAE HS-30 lists the composition limits of most of the families of the SAE/AISI low-alloy steels listed above. These steels are supplied in the form of bar, plate, and forged products and are usually heat treated to obtain specific mechanical properties, especially high strength and toughness. Mechanical properties of selected SAE/AISI low-alloy steels in the as-rolled, annealed, normalized, and quenched and tempered conditions are listed in the aforementioned ASM table. These properties are average properties and should only be used as a guideline. For example, SAE/AISI 4340 steel is usually heat treated by heating the component to 950–1000°C followed by quenching in oil. The component is then tempered at a temperature between 205 and 650°C. According to the aforementioned ASM table, this nickel–chromium–molybdenum steel in the quenched and tempered condition (tempered at 205°C) can achieve a yield strength of 1675 MPa and a tensile strength of 1875 MPa. Quenched and tempered low-alloy steels are used in a large number of applications requiring high strength and good toughness. Note that in the annealed condition SAE/AISI 4340 steel has a yield strength of only 745 MPa.



### ***Other Low-Alloy Steels***

There are a number of important steels that do not fit into the SAE/AISI classification system described above. Such classes are the microalloyed steels also called HSLA steels, dual-phase steels, trip steels, and high-performance steels.

*Microalloyed (High-Strength, Low-Alloy) Steels.* Microalloying is a term applied to steels that contain small additions of alloying elements that retard austenite recrystallization and pin austenite grain boundary movement by the formation of small carbide and/or nitride precipitates. These elements include vanadium, niobium, and titanium. These HSLA steels are produced for a variety of plates, structural shapes, bars, and sheet applications with yield strength varying from 290 to 690 MPa. These steels are covered under numerous SAE and ASTM specifications. The SAE high-strength, low-alloy steels are covered under specifications J410, J1392, and J1442 and the ASTM high-strength, low-alloy steels are covered under various specifications, including A242, A440, A441, A572, A588, A606, A607, A618, A633, A656, A690, A709, A714, A715, A808, A812, A841, A860, and A871. These HSLA steels have found wide application in areas such as bridge construction (structural beams), off-shore oil and natural gas platforms, ship hull and deck plate, and electrical transmission towers and poles. In the automobile, HSLA steels are used for safety (ultra-high-strength impact door beams and energy-absorbing bumper assemblies) and for increasing fuel economy through thinner (lighter weight) chassis structural sections. Microalloyed HSLA steels are also employed in large-diameter gas transmission pipelines.

*Dual-Phase Steels.* A relatively recent development, dual-phase steels are produced by rapidly cooling a medium-carbon steel, containing vanadium or molybdenum, from the two-phase ferrite plus austenite region. The austenite transforms into islands of martensite (stabilized at room temperature by the V and Mo additions) in a ferrite matrix. Depending upon the alloy content, the martensite islands can also contain austenite that is retained below the transformation temperature (called retained austenite). Thus, dual-phase steel may contain both martensite and austenite as a second phase (called MA constituent). The unique characteristic of dual-phase steels is the continuous yielding behavior during deformation; i.e., there is a lack of a yield point during deformation. This provides increased uniform elongation and work hardening so that those components or parts produced from dual-phase steel actually gain strength during the forming operation. Dual-phase steels are being applied in applications such as automobile wheel rims and wheel disks. Because of their energy-absorbing characteristics, dual-phase steels are being used in critical locations of the automobile for safety to protect the occupants in the event of a crash.

*Trip Steels.* Similar to dual-phase steels, trip steels have emerged as an energy-absorbing high-strength steel for the automobile. The term “trip” is derived from the mechanism of transformation induced plasticity. These steels contain a high percentage of retained austenite (10–15%). The austenite transforms to martensite during the forming of the part, thus providing enhanced formability or transforms upon impact in a crash.

*High-Performance Steels.* There are a number of high-performance steels that are used in critical applications. These low-alloy steels, such as HY80 and HY100, are used in applications requiring high strength and excellent toughness. The “80” and “100” in the codes represent the minimum yield strength in ksi units. Another family of low-alloy steels is used in heat exchangers, high-temperature piping, and boiler applications. These steels, like 2 $\frac{1}{4}$ % Cr–1% Mo, find wide use in these applications. Other high-performance steels are the Ni–Cr–Mo steels used as rotors for large

steam generators and motors in electric power plants. These steels must withstand temperatures of superheated steam and must maintain high strength, superior toughness, as well as high fatigue strength and creep resistance. The Ni–Cr–Mo–V steels are also used in pressure vessels in nuclear reactors.

### **Higher Alloy Steels**

There is a distinction between the low-alloy steels described above and the higher alloy steels (usually containing over 8% alloying elements). The higher alloy steels include stainless steels, tool steels, heat-resistant steels, wear-resistant steels, and ultrahigh-strength steels.

*Stainless Steels.* Stainless steels are corrosion-resistant steels that contain at least 10.5% chromium. Chromium is unique in that it forms a passive layer on the steel surface that provides protection from corrosion. There are basically five types of stainless steels: austenitic, ferritic, duplex, martensitic, and precipitation-hardening steels. These five types of stainless steel have a somewhat simplified classification system as follows:

Austenitic stainless steels with low nickel	2xx series
Austenitic stainless steels	3xx series
Ferritic stainless steels	4xx series
Duplex stainless steel	29
Martensitic stainless steels	4xx series
Precipitation-strengthening stainless steels	6xx (xx-x PH)

The classification system is different for the stainless steels than the system for SAE/AISI low-alloy steels in that the last two digits (xx) do not represent the carbon content and have no particular compositional meaning. Unfortunately, the classification system has some confusion with the ferritic and martensitic stainless steels both of the 4xx series. The 2xx series of austenitic stainless steels were developed during the 1950s when nickel became scarce. In these steels, manganese and nitrogen were substituted for the lower nickel level in order to maintain strength. Each type of stainless steel is expanded upon below:

**AUSTENITIC STAINLESS STEELS.** Austenitic stainless steels have sufficient alloying to stabilize austenite at room temperature. These steels, being austenitic, are nonmagnetic. Austenitic stainless steels have excellent low-temperature toughness, weldability, and corrosion resistance. On the other hand, they have relatively low yield strength and can only be strengthened by cold working the steel, by precipitation hardening, or by interstitial or substitutional solid-solution strengthening.

The table on pp. 15.1–15.4 of the *ASM Metals Handbook*, Desktop Edition, 1985, lists the composition limits of the austenitic stainless steels. In general, the 3xx series are iron–chromium–nickel alloys that contain 16–26% chromium and 6–22% nickel. The popular type 304 austenitic stainless steel contains 18–20% Cr and 8–12% Ni and is often referred to as “18–8” stainless steel for the chromium and nickel content. There are many compositional variations of austenitic stainless steels. The following list summarizes these variations:

201	Low nickel replaced with manganese and nitrogen
202	Higher Mn than 201
205	Higher Mn and N than 202
301	Lower Ni and Cr to increase work-hardening ability
302	General-purpose 18–8 stainless steel
302B	Scaling resistance improved with Si

303	Enhanced machinability with a S addition
303Se	Improved machined surfaces with a selenium addition
304	Popular 18–8 stainless steel, lower C than 302
304L	Low-carbon 304 for improved corrosion resistance
304LN	Low-carbon 304 with nitrogen added for strength
304H	Higher carbon 304
304Cu	Copper added for improved cold working
304N	Nitrogen added for strength
305	Higher Ni for reduced work hardening
308	Higher Cr and Ni for weldability
309	High Cr and Ni for heat resistance
309S	Lower carbon 309
309Cb	Niobium (columbium) added
310	Higher Cr and Ni than 309 for improved heat resistance
310S	Lower carbon 310
310Cb	Niobium (columbium) added
314	Higher Si for improved heat resistance
316	Mo added for improved corrosion resistance
316F	Higher S and P for machinability
316L	Lower C for improved corrosion resistance and weldability
316LN	Lower C and higher nitrogen (for strength)
316H	Higher carbon 316
316N	Nitrogen added for strength
316Ti	Titanium added
316Cb	Niobium (columbium) added
317	Higher Cr and Mo for improved corrosion resistance
317L	Low-carbon 317 for improved weldability
321	Titanium added to minimize Cr carbide precipitation
330	High Ni to minimize carburization and improve thermal shock
347	Nb and Ta added to minimize Cr carbide precipitation
347H	Higher carbon 347
348	Ta and Co added for restricted nuclear applications
348H	Higher carbon 348
384	Higher Ni for decreased work hardening

The limiting of carbon is important in austenitic stainless steels. When heated, carbon forms chromium carbide that precipitates on the austenite grain boundaries and produces a condition known as sensitization. Because the chromium is tied up as carbide, the chromium adjacent to the boundaries will be depleted in chromium and corrosion can take place. Sensitization is reversible by heating the steel to temperatures between 1040 and 1150°C followed by rapid cooling to room temperature. The high temperature dissolves the carbides and the rapid cooling prevents reprecipitation of the carbides. More on austenitic stainless steel can be found in Chapter 2.

**FERRITIC STAINLESS STEELS.** The ferritic stainless steels are basically iron–chromium alloys with chromium ranging from 10.5 to 27%. The compositional limits for the ferritic stainless steels are listed in the aforementioned ASM table. Nickel is absent in ferritic stainless steels except for minor amounts, i.e., less than 1%, in some alloys. These steels have a microstructure of ferrite at room temperature and are magnetic. Type 409 stainless steel with the lowest chromium level (10.5–11.75%) is the least expensive of the ferritic stainless steel series and is used for automotive exhaust systems because it far outlasts carbon steel in that application. There are fewer variations of



ferritic stainless steels than austenitic stainless steels. The ferritic stainless steels are listed below:

405	Low Cr with Al added
409	Low Cr, for automotive exhaust applications
429	Slightly less Cr, better weldability
430	General-purpose ferritic stainless steel
430F	Free machining with higher S and P
430Se	Selenium added for improved machined surfaces
434	Mo added for improved corrosion resistance
436	Mo, Nb, and Ta added for corrosion and heat resistance
439	Low C, Ti added to minimize sensitization
442	Higher Cr for improved oxide scaling resistance
444	Low C, Mo for corrosion resistance, Ti and Nb for sensitization
446	Highest Cr for improved scaling resistance

Ferritic stainless steels are described in more detail in Chapter 2.

**DUPLEX STAINLESS STEELS.** Type 329 is an iron–chromium alloy with 2.5–5% nickel and 1–2% molybdenum that has a mixed (duplex) microstructure of approximately equal percentages of ferrite and austenite. There are many more duplex stainless steels that have priority compositions and trade names (see Bibliography at the end of chapter). The corrosion characteristics of these duplex stainless steels are similar to austenitic stainless steels. However, they have higher strength and better resistance to stress–corrosion cracking than austenitic stainless steels. Duplex stainless steels are discussed in Chapter 2.

**MARTENSITIC STAINLESS STEELS.** To produce martensite in a stainless steel, the alloy must be transformed from the austenite-phase field. According to the equilibrium-phase diagram, this means that they have restricted chromium levels within the range required to form the gamma loop where austenite exists (see Fig. 11). The gamma loop is the region between 800 and 1400°C and 0 and 12.7% Cr in Fig. 11. Since austenite only exists in this restricted region, the steel must be heated within this temperature range and quenched to room temperature to form martensite. Martensitic stainless steels contain added carbon, which expands the gamma loop to allow higher chromium contents to be used. Because they can be heat treated, the martensitic stainless steels generally have higher strength than the austenitic and ferritic stainless steels. The martensitic stainless steels are listed below:

403	Select quality for highly stressed parts
410	General-purpose martensitic stainless steel
414	Ni added for improved corrosion
416	Higher P and S for improved machinability
416Se	Se added for improved machined surfaces
420	Higher C for increased strength
420F	Free machining with higher P and S
422	Mo, V, and W added for increased strength and toughness
431	Higher Cr, Ni added for improved corrosion resistance
440A	Highest Cr, C added for increased hardness
440B	Highest Cr, more C added for increased hardness/toughness
440C	Highest Cr, highest C for increased hardness/toughness
501	Low Cr, Mo added
502	Low C, Mo added

The compositional ranges for the martensitic stainless steels are shown in the aforementioned ASM table. Martensitic stainless steels are discussed in the next chapter.

**PRECIPITATION-HARDENING STAINLESS STEELS.** The precipitation-hardening stainless steels are iron–chromium–nickel alloys that develop high strength and toughness through additions of Al, Ti, Nb, V, and/or N, which form precipitates during an aging heat treatment. The base microstructures of precipitation-hardening stainless steels can be either martensitic or austenitic depending upon composition and processing. Some selected grades are listed below:

600	Austenitic grade with Mo, Al, Ti, V, and B added
630	Martensitic grade with Cu and Nb added
631	Austenitic grade with Al added
633	Austenitic grade with Mo and N added
635	Martensitic grade with Al and Ti added

The compositional ranges of the precipitation-hardening stainless steels are listed in the aforementioned ASM table.

**OTHER STAINLESS STEELS.** There are many stainless steels that do not fall within the AISI classification system. These steels have proprietary compositions and trade names. Details of many of these steels can be found in Chapter 2 and in the Bibliography at the end of this chapter.

**Tool Steels.** Tool steels are alloy steels that are used to cut or machine other materials. Tool steels contain various levels of Cr, Ni, Mo, W, V, and Co. The categories of tool steels are:

M series	Molybdenum high-speed steels
T series	Tungsten high-speed steels
Cr series	Chromium hot-work steels
H series	Molybdenum hot-work steels
A series	Air-hardening medium-alloy cold-work steels
D series	High-carbon high-chromium cold-work steels
O series	Oil-hardening cold-work steels
S series	Shock-resistant steels
L series	Low-alloy special-purpose tool steels
P series	Low-carbon mold steels
W series	Water-hardening tool steels

The compositional ranges of the various tool steels are listed in the table on pp. 758–759 of the *ASM Metals Handbook*, Vol. 20, 10th Edition, 1997. The high-speed steels are used in high-speed cutting tools such as drill bits. The hot-work tool steels are used in operations that utilize dies for punching, shearing, and forming materials at elevated temperatures, and the cold-work steels are used in similar operations at room temperature.

**Heat-Resistant Steels.** The upper temperature limit for use of carbon steels is about 370°C because of excessive oxidation and loss of strength. However, there are a number of alloy steels, called heat-resistant steels, that can be used at temperatures of 540–650°C. These steels include some of the ferritic stainless steels (405, 406, 409, 430, 434, and 439), quenched and tempered martensitic stainless steels (403, 410, 416, 422, and 431), precipitation-hardening martensitic stainless steels (15-5 PH,

17-4 PH, and PH 13-8 Mo), precipitation-hardening semiaustenitic stainless steels (AM-350, AM-355, 17-7 PH, and PH 15-7 Mo), and austenitic stainless steels (404, 309, 310, 316, 317, 321, 347, 202, and 216). In addition to the stainless steels, there are a number of proprietary alloys containing various levels of Cr, Ni, Mo, Nb, Ti, Cu, Al, Mn, V, N, or Si. The properties that are important to heat-resistant steels are creep and stress rupture. Creep is time-dependent strain occurring under stress. In more common terms creep is elongation or sagging of a part over time at elevated temperature. Stress rupture is a measure of the elevated temperature durability of material. These steels are generally specified under the ASME Boiler and Pressure Vessel Code.

*Wear-Resistant Steels (Austenitic Manganese Steels).* An important series of alloy steels are the austenitic manganese steels that contain 1.2% carbon and a minimum of 11% manganese. These steels, invented by Sir Robert Hadfield in 1882, are wear resistant and tough. Because they are difficult to hot work, these steels are usually cast into the final product form. The chemical compositional ranges for some selected austenitic manganese steels (ASTM A128) are listed below:

Grade	C	Mn	Cr	Mo	Ni	Si
A	1.55–1.35	11 (min)	—	—	—	1 (max)
B1	0.9–1.05	11.5–14	—	—	—	1 (max)
C	1.05–1.35	11.5–14	1.5–2.5	—	—	1 (max)
D	0.7–1.3	11.5–14	—	—	3–4	1 (max)
E1	0.7–1.3	11.5–14	—	0.9–1.2	—	1 (max)

The carbon addition is necessary to maintain an austenitic microstructure at room temperature. All grades must be heat treated by solution annealing at 1010–1090°C for 1–2 h per 25 mm of thickness followed by rapid water quenching. Because these alloys work harden during use, they are used in applications involving earthmoving (bucket blades), mining and quarrying (rock crushers), and railway trackwork (frogs, switches, and crossings).

### ***Ultrahigh-Strength Steel***

**MARAGING STEEL.** Another important series of alloy steels are the maraging steels. They are considered ultrahigh-strength steels because they can be heat treated to yield strength levels as high as 2.5 GPa. They also have excellent ductility and toughness. There are basically four grades that are produced to strength levels between 1.4 and 2.5 GPa.

Grade	Ni	Co	Mo	Ti	Al
18Ni (200)	18	8.5	3.3	0.2	0.1
18Ni (250)	18	8.5	5.0	0.4	0.1
18Ni (300)	18	9.0	5.0	0.7	0.1
18Ni (350)	18	12.5	4.2	1.6	0.1

The numbers in parentheses represent the nominal yield strength level in ksi. All maraging steels must be heat treated to achieve the desired properties. The heat treatment cycle for the 18Ni (200), 18Ni (250), and 18Ni (300) grades requires a solution

treatment at 820°C for 1 h per 25 mm of thickness, cooling to room temperature, and an aging treatment at 480°C for 4 h. The 18Ni (350) grade has an extended aging time of 12 h. The heat treatment develops a martensitic microstructure on cooling from austenite at 820°C. The aging step precipitates intermetallic compounds, e.g., Ni<sub>3</sub>Mo, that strengthen the martensitic matrix. Maraging steels can be machined before the aging treatment and have good weldability and excellent fracture toughness. They have found applications in missile and aircraft parts that require exceptional performance.

**MUSIC WIRE.** One of the strongest steel products commercially available is music wire. These wires can achieve levels of tensile strength approaching 5 GPa. The steel is basically SAE/AISI 1080. To obtain the ultrahigh-strength levels, rods of SAE/AISI 1080 are isothermally transformed to fine pearlite in a process known as patenting. The rods are then cold drawn to wire using large reductions in wire diameter through each die. The cold reduction forces the ferrite and cementite in the microstructure to align in a preferred orientation or fiber texture. The wires are used in musical instruments where they can be stretched under high tension to achieve certain musical notes. Ultrahigh-strength wires are also used to strengthen the rubber in automobile tires.

## 7 SUMMARY

Steel is one of the most versatile materials in today's society. It can be produced with a wide range of properties and is used in millions of applications. For example, stainless steels are used for their corrosion resistance, interstitial-free steels are used for their excellent formability characteristics, iron–silicon alloys are used for their electrical properties, austenitic manganese steels are used for their wear and abrasion resistance, microalloyed steels are used for their high strength, patented and cold-drawn eutectoid steel wires are used for their ultrahigh strength, dual-phase and trip steels are used for their energy absorption capability in a vehicle collision, and tool steels are used for their outstanding ability to cut and machine other materials. No other material can span such a range of properties and characteristics.

## BIBLIOGRAPHY

### Handbooks

- ASM Metals Handbook, Properties and Selection: Irons, Steels and High Performance Alloys*, Vol. 1, 10th ed., ASM International, Materials Park, OH, 1990.
- ASM Metals Handbook, Materials Selection and Design*, Vol. 20, 10th ed., ASM International, Materials Park, OH, 1997.
- ASM Metals Handbook*, Desk Edition, 2nd ed., ASM International, Materials Park, OH, 1998.
- ASM Specialty Handbook*®—*Stainless Steels*, ASM International, Materials Park, OH, 1994.
- ASM Specialty Handbook*®—*Carbon and Alloy Steels*, ASM International, Materials Park, OH, 1996.
- Engineering Properties of Steel*, ASM International, Materials Park, OH, 1982.
- Stahlschlüssel (Key to Steel)*, 18th ed., Verlag Stahlschlüssel Wegst GMBH, Marburg, 1998.
- Worldwide Guide to Equivalent Irons and Steels*, 4th ed., ASM International, Materials Park, OH, 2000.

### General References

- J. Beddoes and J. G. Parr, *Introduction to Stainless Steels*, 3rd ed., ASM International, Materials Park, OH, 1999.
- C. R. Brooks, *Principles of the Heat Treatment of Plain Carbon and Low Alloy Steels*, ASM International, Materials Park, OH, 1996.

- G. Krauss, *Steels—Heat Treatment and Processing Principles*, ASM International, Materials Park, OH, 1990.
- R. Honeycombe and H. K. D. H. Bhadeshia, *Steels: Microstructures and Properties*, 2nd ed., Wiley, New York, 1996.
- G. Roberts, G. Krauss, and R. Kennedy, *Tool Steels*, 10th ed., ASM International, Materials Park, OH, 1998.

### Specifications on Steel Products

- Annual Book of ASTM Standards*, Vol. 01.01, Steel—Piping, Tubing, Fittings, ASTM, West Conshohocken, PA.
- Annual Book of ASTM Standards*, Vol. 01.02, Ferrous Castings, Ferroalloys, Shipbuilding, ASTM, West Conshohocken, PA.
- Annual Book of ASTM Standards*, Vol. 01.03, Steel—Plate, Sheet, Strip, Wire, ASTM, West Conshohocken, PA.
- Annual Book of ASTM Standards*, Vol. 01.04, Steel—Structural, Reinforcing, Pressure Vessel, Railway, ASTM, West Conshohocken, PA.
- Annual Book of ASTM Standards*, Vol. 01.05, Steel—Bars, Forgings, Bearing, Chain, Springs, ASTM, West Conshohocken, PA.
- Annual Book of ASTM Standards*, Vol. 01.06, Coated Steel Products, ASTM, West Conshohocken, PA.
- SAE Materials Standards Manual*, SAE HS-30, Society of Automotive Engineers, Warrendale, PA, 2000.



# CHAPTER 2

---

## STAINLESS STEELS

**James Kelly**  
Rochester, Michigan

<b>1</b>	<b>EFFECT OF ALLOYING ELEMENTS</b>	<b>40</b>	<b>7</b>	<b>AGE-HARDENING MARTENSITIC STAINLESS STEELS</b>	<b>50</b>
<b>2</b>	<b>SOME FORMS OF CORROSION</b>	<b>43</b>	<b>8</b>	<b>DUPLEX STAINLESS STEELS</b>	<b>50</b>
	2.1 General Corrosion	43	<b>9</b>	<b>AUSTENITIC STAINLESS AND NICKEL ALLOYS</b>	<b>51</b>
	2.2 Stress Corrosion Cracking	43	<b>10</b>	<b>WELDING</b>	<b>53</b>
	2.3 Pitting Corrosion	44		10.1 Carbon versus Stainless Steel	53
	2.4 Crevice Corrosion	45		10.2 Austenitic Alloys	55
	2.5 Intergranular Corrosion	46		10.3 Duplex Stainless Steels	56
	2.6 Galvanic Corrosion	46		10.4 High-Molybdenum Alloys	56
<b>3</b>	<b>AOD, DUAL CERTIFICATION, AND CHEMISTRY CONTROL</b>	<b>47</b>		<b>WEBSITES</b>	<b>58</b>
<b>4</b>	<b>AVAILABILITY</b>	<b>49</b>		<b>REFERENCES</b>	<b>58</b>
<b>5</b>	<b>FERRITIC STAINLESS STEEL</b>	<b>49</b>		<b>TRADEMARKS</b>	<b>59</b>
<b>6</b>	<b>MARTENSITIC STAINLESS STEELS</b>	<b>50</b>			

Stainless steels are those alloys of iron and chromium, with or without other elements, containing at least 11% chromium. This is the minimum amount of chromium necessary to form a stable, passive chromium oxide film. It is this film which is the basis for the corrosion resistance of all stainless- and most nickel-based corrosion-resistant alloys.

There are six basic classifications of stainless steels: ferritic, martensitic, martensitic age hardening, duplex austenitic–ferritic, and austenitic. The most commonly produced of these are the ferritics 409 for automotive applications and 430 for corrosion-resistant/decorative uses, the martensitic grade 410, and the age-hardening martensitic 17-4PH<sup>®</sup>. The most popular of the austenitic–ferritic duplex grades is alloy 2205, with pitting corrosion resistance generally superior to 316L. For seawater applications the “superduplex” alloys, such as 255, SAF<sup>®</sup> 2507, and ZERON<sup>®</sup> 100, are required. The most broadly used austenitic stainless grades are 304L and 316L. A number of “superaustenitics” contain about 6–7% molybdenum, with moderate nickel, 18–25%. A nitrogen addition is required to maintain the austenitic structure. Of the higher nickel grades 20Cb-3<sup>®</sup> stainless is used for sulfuric acid and general chemical processing. The most commonly used of the very high nickel alloys is C-276. The austenitic stainless steels form a continuum with the nickel-based heat- and corrosion-resistant alloys. They are distinguished on the basis of nickel content by commercial definitions.

There is no recognized metallurgical definition of where one ends and the other begins.

## 1 EFFECT OF ALLOYING ELEMENTS

The corrosion behavior of the alloying elements in pure form influences the corrosion properties of the stainless or nickel grades containing them.

Chromium is the first example, with outstanding corrosion resistance in the passive state. In solutions of neutral pH, dissolved oxygen from the air is sufficient to maintain passivity. But in low-pH solutions, stronger oxidizing agents must be present, and halogen or sulfuric acids absent, in order to stabilize the passive condition. Chromium metal is not resistant to corrosion by reducing acids.<sup>1</sup>

Some examples from Uhlig<sup>1</sup> of the corrosion resistance of electrodeposited chromium are as follows:

Acid or Salt	Concentration %	Temperature		Corrosion Rate	
		°C	°F	mm/yr	mils/yr
Acetic	10	58	136	0.39	15
Ferric chloride	10	58	136	0.41 <sup>a</sup>	16 <sup>a</sup>
Formic	10	58	136	30	1,200
Hydrobromic	10	58	136	4.7	186
Hydrofluoric	10	12	54	25	1,000
Perchloric	10	58	136	0.86	42
Phosphoric	10	58	136	0.28	34
Sulfuric	10	12	54	0.86	11
Sulfuric	10	58	136	250	10,000
Sulfuric	100	12	34	0.76	30
Sulfuric	100	58	136	1.8	69

<sup>a</sup>Pitting occurred; this number does not reflect uniform corrosion.

There are three points to be made from these data. First, chromium as an alloying element is not particularly effective in promoting resistance to reducing or halogen acids. Second, in solutions of some halogen salts the passive layer was maintained by oxygen dissolved in the solution. Third, sulfuric acid behaves as a reducing acid in lower concentrations but as an oxidizing acid in concentrated form. When selecting alloys to resist sulfuric acid, one must bear this in mind.

Stainless steels containing only chromium and iron, specifically the ferritic and martensitic stainless steels, likewise have poor resistance to sulfuric acid solutions but may resist nitric acid. These chromium–iron alloys are not resistant to corrosion by halogen acids or by chloride salts. Those ferritic alloys which do have good to excellent chloride pitting resistance, such as E-Brite<sup>®</sup> and AL29-4C<sup>®</sup>, gain that resistance by the addition of 1 and 4% Mo, respectively.

Austenitic nickel alloys with resistance to concentrated (oxidizing) sulfuric acid require high chromium, such as the ThyssenKrupp VDM alloy 33, or silicon, as in the stainless grades A610, A611, and Sandvik<sup>®</sup> SX.

There are a few highly corrosion resistant nickel alloys with little or no chromium, including the various Ni–Mo “B” grades and the 67Ni–31Cu alloy 400. Excellent in reducing environments, they have almost no tolerance to oxidizing compounds in the environment. A newly developed nickel–molybdenum alloy, B-10, includes 8% Cr in its composition for limited resistance to low levels of oxidizers.

Molybdenum, in contrast to chromium, has very low resistance to oxidizing solutions but does resist reducing and halogen acids. Oxidizing acids such as nitric, aqua regia, and



concentrated sulfuric acids readily dissolve molybdenum metal. Hydrofluoric acid does not affect Mo, and hot (110°C) hydrochloric acid attacks molybdenum metal only slowly.<sup>1</sup> In both stainless steels and nickel-based alloys, molybdenum as an alloying element is required for resistance to halogen acids and to pitting by acid or oxidizing chlorides. The amount used ranges from 2% in 316L stainless up to 24–30% in alloys B through B-10. As an alloying addition, molybdenum improves the stability of the passive layer in the presence of halogens.

Tungsten at the 2–4% level is used, along with molybdenum, to improve chloride pitting corrosion resistance. Nickel metal in general is attacked by oxidizing solutions, while reducing solutions are less aggressive. Some examples<sup>1</sup> follow:

Acid	Notes	Concentration %	Temperature		Corrosion Rate	
			°C	°F	mm/yr	mils/yr
Hydrochloric	Air saturated	10	30	86	2	80
	N <sub>2</sub> saturated	10	30	86	0.25	10
Sulfuric	Aeration by convection	10	77	170	0.31	12.1
Sulfuric	Air saturated	10	82	180	4	160

Nickel metal is strongly attacked by phosphoric acid solutions containing ferric (oxidizing) salts, whereas it resists phosphoric acid solutions that are free of oxidizing compounds. Nickel metal resists neutral chloride solutions, such as sodium chloride, but is attacked by acid or oxidizing chloride salts. Alloys for use in reducing acids invariably have a considerable nickel content, ranging from as little as 8% in 304L to as much as 71% in alloy B-2.

Copper is generally resistant to reducing acid solutions containing only low levels of oxygen but is readily attacked by oxidizing acids. These include nitric, sulfurous, and concentrated sulfuric as well as solutions containing oxidizing salts, such as ferric chloride. Copper in solution tends to reduce the corrosion rate of stainless alloys in (reducing) sulfuric acid. Those alloys intended for use in environments containing much sulfuric acid invariably have some copper as an alloy addition. These include 904L, 20Cb-3<sup>®</sup>, 825, Nicrofer<sup>®</sup> 3127 hMo (alloy 31), and the Hastelloy alloys G, G-3, and G-30.

Additions of some 4 or 5% silicon increase corrosion resistance to oxidizing environments. The silicon is primarily used in alloys meant to withstand concentrated, hence oxidizing, sulfuric acid. Such alloys in current production include A610, A611, Sandvik SX<sup>®</sup>, and Haynes D-205<sup>TM</sup>. The use of silicon as an alloying element for corrosion resistance dates back to before World War I. Although not a stainless, one of the oldest and most generally corrosion resistant alloys ever developed is the 14.5% silicon cast iron, Duriron<sup>®</sup>. A silicon oxide film is believed to be responsible for this grade's useful resistance to environments ranging from oxidizing to reducing. This includes seawater and organic and many inorganic acids, though not halogen acids. The addition of 3% molybdenum provides resistance to hot hydrochloric acid. Lack of strength and ductility limits the cast iron's range of use.

When one speaks about the effect of this or that pure chemical on an alloy, one must emphasize that real industrial environments are complex mixtures of chemicals. These mixtures may behave in surprising ways, quite unlike what one might expect from the behavior of alloys in pure, laboratory-controlled environments. Corrosion rates depend not only upon the concentrations of various chemicals but also on the temperature. The temperature of liquid inside a vessel is one point that can be measured, but the temperature at the surface of submerged heating coils in that vessel is another and higher value. Likewise, the concentration of, say, an acid in the vessel is not the same as the concentration at the point where that acid is introduced to the mixture.

The most commonly used corrosion-resistant alloys are the stainless steels 304 (18% Cr–8% Ni, commonly known as 18-8 stainless steel) and 316 (17% Cr–11% Ni–2% Mo). The more corrosion resistant nickel alloys, such as C-276, have much higher levels of nickel, 57%, and molybdenum, 15.5%. Commercially pure nickel, and nickel–copper alloys are used for special environments.

Oxidizing and reducing environments are defined chemically with respect to whether hydrogen is oxidized or reduced under the environment in question. In an oxidizing environment, hydrogen will only be present chemically combined with some other element, for example with oxygen to form  $H_2O$ . In a reducing environment that  $H^+$  will be reduced to hydrogen gas,  $H_2$ .

Common oxidizing chemicals are nitric acid,  $HNO_3$ , and certain salts such as ferric chloride,  $FeCl_3$ , and cupric chloride,  $CuCl_2$ . The ferric and cupric ions are at a relatively high valences, +3 and +2, respectively, and readily accept electrons from, or oxidize, other materials to get their own valences reduced to a more stable level. Sulfuric acid,  $H_2SO_4$ , is normally a reducing acid. At high concentrations, above about 95%, sulfuric acid changes its character and becomes an oxidizing acid. Of course, dissolved oxygen contributes to the oxidizing character of an environment. To some extent so does dissolved elemental sulfur.

To resist oxidizing conditions, an alloy must contain some amount of chromium. In an oxidizing acid, simple materials such as 304 (18% Cr–8% Ni) or 310 (25% Cr–20% Ni) are often used. An unusually high level of chromium, 33%, is present in a Nicrofer<sup>®</sup> 3033 (UNS R20033, W.Nr. 1.4591), designed for oxidizing acids, specifically hot concentrated sulfuric. In any of these alloys the nickel content is necessary to make a stable austenitic alloy, but it does not contribute specifically to oxidizing acid resistance. Small additions of molybdenum or copper may be tolerated in these alloys to enhance resistance to chlorides or dilute sulfuric acid. But neither Mo nor Cu is helpful in resisting strongly oxidizing chemicals.

A common and severe test for resistance to oxidizing acids is boiling 65% nitric acid. The test, ASTM A 262 C, is run for five periods of 48 h each, specimens are weighed after each test period, and the results are averaged. This test is a good measure of resistance to intergranular corrosion in a sensitized alloy as well as to general corrosion in nitric acid. Test results<sup>2</sup> show 2205 at 0.13–0.20 mm/yr, which is good in spite of 3% Mo, and 304 at 0.23 mm/yr. Other molybdenum-bearing grades do not fare so well: 316L (2% Mo) at 0.87 mm/yr after only 24 h, AL-6XN<sup>®</sup> (6.3% Mo) at 0.74 mm/yr, 625 (9% Mo) at 0.76 mm/yr, and C-276 (15.5% Mo) at 0.74 mm/yr. These results do not mean that one cannot successfully use a higher Mo alloy in the presence of any nitric acid at all. They do indicate that high-molybdenum alloys may not behave at all well in hot, concentrated oxidizing industrial environments.

One cannot readily find boiling 65% nitric acid data for the 66% Ni–31% Cu alloy 400 (Monel<sup>®</sup> 400) or for the assorted B alloys—B, B-2, B-3, or B-4. Their corrosion rates in nitric acid are simply too high for the test to have any practical value. Alloys 400, B, and B-2 have no deliberate chromium addition, B-3 and B-4 only about 1.3% Cr. These grades may have excellent resistance to various reducing environments, but because there is essentially no chromium present, they will literally dissolve in nitric acid. Likewise, they are attacked by ferric, cupric, and chlorate ions and even dissolved oxygen in HCl.

The common “reducing” acids are sulfuric for concentrations under about 95%, phosphoric ( $H_3PO_4$ ), and hydrochloric. Of these by far the most corrosive is HCl, phosphoric being the less troublesome. Because reducing industrial environments usually also contain some oxidizing salts or oxygen from the air, most alloys used to withstand reducing chemical environments must contain some chromium, at least 15%. The alloy additions used to resist the reducing components of the environment are nickel, Ni, molybdenum, Mo, and copper, Cu. In sulfuric acid some amount of copper is usually used, such as in 20Cb-3<sup>®</sup> stainless, 904L, or 825. Even copper salts in the acid will reduce corrosion attack on stainless. 20Cb-3 uses carefully balanced proportions of Cu and Mo to resist sulfuric acid corrosion.

## 2 SOME FORMS OF CORROSION

### 2.1 General Corrosion

This is the most common form of corrosion, accounting for the greatest tonnage loss of metal. It is characterized by relatively uniform attack of the entire area exposed to the corrosive environment. Rusting steel exposed to the weather is a common example. Since the attack is linear with time, the life of equipment subject to general corrosion is reasonably predictable. Localized corrosion modes, such as pitting and crevice and stress corrosion, are more difficult to predict and tend to cause premature equipment failures.

Uniform corrosion rates may be stated as an average metal thickness loss with time, mils per year, or millimeters per year. A convenient rating for metals subject to uniform attack based on corrosion rates is as follows:

**Excellent**—rate less than 5 mils/yr (0.13 mm/yr). Metals suitable for making critical parts.

**Satisfactory**—rate 5–50 mils/yr (0.13–1.3 mm/yr). Metals generally suitable for noncritical parts where a higher rate of attack can be tolerated.

**Unsatisfactory**—rates over 50 mils/yr (1.3 mm/yr). Metals usually not acceptable in the environment.

An approximate ranking of alloys by increasing resistance to general corrosion would be 304L, 316L, 2205, 20Cb-3/825, AL-6XN, 625, and C-276. Alloy selection does depend upon the exact corrosive environment in question. An example is hot concentrated caustic, where commercially pure nickel or the 76% nickel alloy 600 is used.

Alloy 33 may be required for mixtures of caustic with oxidizing chemicals. For sulfuric acid alloy 20Cb-3 or 825 is usually chosen; however, if chlorides are present in the acid, one of the 6% molybdenum grades such as AL-6XN would be preferred. AL-6XN is used for organic acids, such as naphthenic acid in refinery service. For nitric acid service chromium is beneficial, but molybdenum is not. Alloys commonly selected include 304L or a low-carbon version of 310 stainless.

### 2.2 Stress Corrosion Cracking

For just about every alloy, there is some chemical environment that, combined with stress, will cause cracking. For brass that environment is ammonia or other nitrogen compounds. The source of stress is usually residual forming and welding stresses, which may reach the yield point of the material. Operating stress is rarely the issue.

For austenitic stainless steels chlorides are the major cause of stress corrosion cracking (SCC). An example is hot potable water under heat transfer conditions which permit chlorides to concentrate locally. Susceptible alloys include 304L, 316L, 321, and 347. Some 95% of 316L chemical plant equipment failures may be attributed to chloride SCC. The chlorides concentrate from trace amounts present in steam for heating or the cooling water in heat exchangers as well as from the product.

Chloride SCC occurs most quickly in austenitic stainless steels with about 8–10% nickel, alloys with much lower or much higher nickel content being less susceptible. As thermal stress relief is rarely practical with stainless fabrications, the metallurgical solution is a change in alloy. Nickel-free ferritic steels, such as E-BRITE, are highly resistant to chloride SCC but impractical to fabricate into a vessel.

The traditional solution in North America has been to go to a higher nickel alloy. Alloys with about 30% or more nickel are generally considered to be good engineering solutions to most chloride SCC problems, although they will crack under very severe conditions. 20Cb-3

at about 34% and 825 at 40% nickel have long been chosen for this service. Likewise the fine-grained Incoloy<sup>®</sup> 800, UNS N08800, 31% nickel, had been used in years past. However, this low-carbon, fine-grained version of 800 is now rarely available. Regardless of what it is called, “800” today usually is 800HT<sup>®</sup>, UNS N08811, a higher carbon, coarse-grained version. This grade is designed to maximize creep rupture strength for high-temperature applications.

Since the mid-1980s the 6% molybdenum superaustenitics have become available. Grades such as 254 SMO<sup>®</sup> with only 18% nickel or AL-6XN at 24% nickel have been used effectively to resist chloride SCC. The material cost of the “6-moly” grades is between that of 316L stainless and nickel alloy C-276. Although lower in nickel, the molybdenum content does tend to decrease susceptibility of austenitic stainless steel to chloride SCC.<sup>3</sup>

For greater resistance to both corrosion and chloride SCC the most used grade has been C-276, at 57% nickel, 15.5% Mo. There are now a number of alloys in this class, including C-22, Inconel<sup>®</sup> 686, C-2000, 59, and a new Japanese grade, MAT 21. These very high nickel alloys can easily reach five times or more the cost of 316L stainless steel. They are metallurgically excellent solutions to chloride SCC, particularly in severe environments. However, they are expensive choices for service conditions under which 316L lasted a few years before cracking. There is a less expensive choice, one that has long been used in Europe—a duplex stainless steel—that is, a stainless which is about half austenite and half ferrite. Duplex stainless steel is a practical solution to most 304L or 316L SCC failures. The most commonly available duplex in North America is 2205, at a cost comparable to that of 316L.

Other forms of SCC in stainless steels include caustic cracking and polythionic acid SCC. Caustic may crack carbon as well as stainless steel. High-nickel alloys such as alloy 600 or, better, commercially pure nickel (UNS N02201) is used for hot concentrated caustic.

Polythionic acid stress corrosion cracking (PASCC) is caused by sulfur compounds in the environment and most often encountered in refineries. Any stainless or nickel alloy that has been sensitized can be subject to PASCC. High-nickel alloys do not help; even 600 alloy will crack when sensitized.<sup>4</sup> To resist this form of SCC, the alloy must contain a strong carbide-forming element, or “stabilizing” element, such as columbium or titanium. Examples are 321, 347, 20Cb-3, 825, and 625. In addition the alloy must be given a stabilizing anneal so that the carbon is effectively combined with the Cb or Ti.

Normally, 304H or 316H would be quite sensitive to polythionic acid stress cracking, as these higher carbon, solution-annealed alloys readily sensitize. The matter has been addressed at one refinery by fabricating the equipment from one of these H-grade stainless steels, then stabilize annealing the completed fabrication. A temperature of about 1650°F (900°C) for a minimum of 1 h is used. This does precipitate carbides at the grain boundaries, but the temperature is high enough to permit chromium to diffuse back into the Cr-depleted grain boundary zone. In addition, this treatment relieves over half of the residual fabricating stress, thus reducing susceptibility to chloride SCC as well.

### 2.3 Pitting Corrosion

Pitting is an extremely localized form of corrosion that results in holes in the metal. Although total metal loss may be small, the equipment may be rendered useless because of perforation. Pitting usually requires a long initiation period before attack is visible. Once a pit has begun, the attack continues at an accelerating rate. Pits tend to grow in a manner that undermines or undercuts the surface. Typically a very small hole is seen on the surface. Poking at this hole with a sharp instrument may reveal a rather cavernous hole under what had looked like solid metal. In effect, a pit may be considered a self-formed crevice. Pitting attack increases with temperature.

Chloride solutions are the most common cause of pitting attack on stainless steels and nickel alloys. The alloying additions molybdenum, nitrogen, and to some extent chromium all contribute to pitting resistance. A laboratory measure of resistance to pitting corrosion is the critical pitting temperature, or CPT, which is the highest temperature at which an alloy

resists pitting in a given environment. Alloy ranking with respect to chloride pitting resistance would be 304L (0%Mo, poor), followed by 316L (2% Mo), 20Cb-3/825 (3% Mo), 2205 (3% Mo– 0.16%N), AL-6XN (6.3%Mo–0.22%N), 625 (9% Mo), and C-276 (15.5% Mo). Alloys AL-6XN and higher have sufficient resistance to be used in hot seawater service. The lower molybdenum grades, even 2205, are usually unsuitable for use in seawater.

## 2.4 Crevice Corrosion

Crevice corrosion, more so than pitting, is the limiting condition which often prevents the use of conventional austenitic stainless in chloride environments. The attack usually occurs in small volumes of stagnant solution under gasket surfaces, lap joints, marine fouling, and solid deposits and in the crevices under bolt heads and the mating surfaces of male and female threads. The mechanism involves oxygen depletion in the crevice, followed by chloride ion concentration and increase in acidity (decrease in pH) within the crevice. In a neutral environment (pH 7) the chloride solution within the crevice may contain 3–10 times as much chloride as the bulk solution and have a pH of only 2–3.

Susceptibility to crevice corrosion increases rapidly with temperature. Molybdenum and nitrogen additions to nickel–chromium–iron alloys improve their resistance to crevice corrosion. Together with the use of appropriate materials, design practice to minimize crevices and maintenance procedures to keep surfaces clean are required to combat the problem.

The usual laboratory measure of resistance to crevice corrosion is the critical crevice corrosion temperature, or CCCT, which is the highest temperature at which an alloy resists crevice corrosion in a given environment. For a given environment the CCCT is usually significantly lower than the CPT. Crevice corrosion resistance as measured by the ferric chloride test relates, to a degree, to performance in seawater. Here are the results for a number of alloys<sup>2</sup>—temperature for initiation of crevice corrosion in 10% ferric chloride ( $\text{FeCl}_3 \bullet 6\text{H}_2\text{O}$ ) per ASTM G 48 Practice B, pitting resistance equivalent (PRE)  $N = \text{Cr} + 3.3\% \text{ Mo} + 30(\% \text{ N})$ :

Alloy	Mo %	Temperature		Pitting Resistance Equivalent		References
		°C	°F	<i>N</i>		
316L	2.1	–3	27	23		5
825	2.7	–3	27	30		5
317L	3.2	2	35	29		5
2205	3.1	20	68	38		5
317 LXN <sup>TM</sup>	4.4	20	68	34		5
28	3.5	24	75	38		6
904L	4.4	24	75	35		5
904L	4.4	25	77	35		7
G	6.5	30	86	43		5
28	3.5	35	95	39		7
2507	4.0	35	95	47		7
1925hMo	6.2	40	104	47		7
33	1.4	40	104	50		7
AL-6XN	6.2	43	110	48		5
27-7MO	7.3	45	113	57		8
625	9.0	45	113	51		5
625	9.0	55	131	51		6
31	6.5	55	131	54		6
G-30	5.5	50	122	48		7
C-276	15.4	55	130	66		5

Using the more aggressive acidified ferric chloride, G 48 Practice D, and a different formula for PRE,  $N = \%Cr + 1.5(\%Mo + \%W + \%Nb)$ , Special Metals Corp. got somewhat different results, as follows:

Alloy	Mo %	Temperature		Pitting Resistance Equivalent	References
		°C	°F	<i>N</i>	
825	2.7	5	41	27	16
625	9.0	35	95	41	16
686CPT	16.3	>85	>185	51	16
C-276	16	45	113	45	16
C-2000	16	85	185	47	16
59	16	85	185	47	16
22	13	85	185	47	16

Corrosion test results are sensitive to exactly what test is used. Furthermore, even with the same tests published corrosion data give different rates depending upon the source. One might consider that a factor of 2 difference in corrosion rates is unimportant while a factor of 10 is significant.

## 2.5 Intergranular Corrosion

Intergranular corrosion consists of localized attack along the grain boundaries of the metal. Sensitization to this attack in stainless or nickel alloys is caused by precipitation of chromium-rich carbides in the grain boundaries, at a temperature low enough that a chromium-depleted zone forms. This precipitation most commonly occurs from the heat of welding. It may also result from a slow cool after annealing or from prolonged exposure to intermediate temperatures, roughly 850–1470°F in service.

A most effective means of combating intergranular corrosion is to restrict the carbon content of the alloy. In the stainless “L” grades 0.03% maximum is considered sufficient. High chromium and molybdenum additions, as in AL-6XN, also reduce the chance of intergranular attack. Another approach is to add columbium or titanium to tie up the carbon, the same as is done to resist polythionic acid SCC. 20Cb-3 stainless takes both approaches, being melted to low carbon as well as having a columbium addition.

## 2.6 Galvanic Corrosion

An electrical potential, or voltage, difference usually exists between two different metals that are in electrical contact and immersed in a corrosive solution. This potential difference causes current to flow and the less noble, or more anodic, metal suffers increased corrosion rate. The severity of attack depends upon the relative voltage difference between the metals, the relative exposed areas of each, and the particular corrosive environment.

The most common example is the old-fashioned flashlight battery, or dry cell. It has a shell of zinc metal (less noble, or anodic) filled with a moist corrosive paste that conducts electricity. The center post is made of graphite, which is quite noble (cathodic, does not tend to corrode). The potential (voltage) difference between zinc and graphite is about 1½ V. When an electric connection is made in a flashlight, the zinc corrodes, giving up electrons, which flow through the lightbulb toward the graphite cathode, the positive pole. In this case, because generating electricity is the point, no one minds that the zinc corrodes and gets used up.



The ratio of cathodic (noble) to anodic areas is an important factor in galvanic corrosion. An undesirable situation is a large cathode connected to a small anode, or a less noble metal. This can develop high current density, hence severe corrosion, at the anode. In that common zinc dry cell the zinc anode has a much larger area than the graphite cathode, so it has some useful working life before corroding through the zinc case.

For example, a large area of stainless in contact with a small surface area of carbon steel is undesirable. The potential difference will tend to corrode the carbon steel, and the very large area of stainless will make that corrosion occur quickly. The reverse condition is preferred. That is, a small area of stainless (or more noble metal) may be coupled with a much larger area of carbon steel (anodic) without significant problems. “Significant” depends upon the application. In the past, when ferritic stainless trim was used on carbon steel automobile bodies, the steel would tend to corrode most severely underneath the trim. In part that was because of the crevice salt, but it was accentuated by the galvanic difference between ferritic stainless and carbon steel.

There is some potential difference among the various stainless and nickel alloys. In practice, galvanic corrosion is rarely a problem among these various alloys.

There is, however, a significant potential difference between copper and stainless alloys. So long as the stainless steel is passive (not actively corroding) it is more noble enough than copper to corrode the copper alloy. An example is when a heat exchanger with a Muntz metal (60% Cu–40% Zn) tubesheet is retubed with AL-6XN<sup>®</sup> alloy instead of the original copper–nickel tubes. The potential difference is enough to corrode the copper alloy tubesheet. One ought to either replace the tubesheet with stainless steel or retube using a copper-based alloy.

Graphite is at the noble end of the galvanic series. If graphite is in contact with stainless or nickel alloys in a corrosive environment, those alloys may corrode preferentially. Galvanic effects have a positive side and may be used to protect equipment from corrosion, a common example being a zinc coating on steel. The zinc corrodes preferentially and in doing so protects the steel from corrosion (rusting). Zinc or magnesium anodes are often connected to equipment from a chemical process to steel ship hulls to protect them from corrosion. Most stainless steels, and a few higher nickel alloys, are available with different levels of carbon. For resistance to intergranular corrosion, a low-carbon steel is preferred, usually 0.03% carbon maximum in stainless. Such a stainless is referred to as an “L” grade, e.g., 304L and 316L.

### 3 AOD, DUAL CERTIFICATION, AND CHEMISTRY CONTROL

With respect to aqueous corrosion resistance, the lower the carbon, the better. For high-temperature service the opposite is true, and some minimum amount of carbon is required for both tensile and creep rupture strength.

The argon–oxygen decarburization (AOD) process for refining stainless steel was introduced in the 1970s. This made profound changes in how existing grades were produced as well as permitted totally new grades to be developed. Three of these changes are worth discussing—carbon, sulfur, and precise control of chemistry.

Prior to the AOD, carbon could not be removed in the refining process without also removing chromium. Low-carbon grades could only be produced by starting with low-carbon raw materials, specifically low-carbon ferrochrome. The expense of low-carbon ferrochrome meant that the L grades were inherently more expensive. The AOD now permits refining carbon to very low levels, even with starting stock of higher carbon.

Industrywide specifications such as the ASTM were written prior to the introduction of this new melting process. For example, ASTM A 240 for 304 stainless, UNS S30400, calls out 0.08% carbon maximum, no minimum, and 30,000 psi minimum yield strength. Low-carbon 18-8, 304L, S30403 is limited to 0.03% carbon, with a consequent lower limit for yield strength, 25,000 psi minimum. In addition, there is a 304H, meant for high-temperature use, with carbon

specified as a range, 0.04–0.10%, and annealing and grain size requirements. This constitutes three separate grades. It is more economical if the mills can melt steel to only two, not three, different levels of carbon, and dual certify. Consider 304, UNS S30400. As the carbon is specified only as a maximum, it might be possible to melt 304 to 0.03 maximum carbon. Lower carbon would also result in lower than the 30,000 psi yield strength required. However, using the AOD it is now possible to add a very small, precisely controlled amount of nitrogen. This does not harm intergranular corrosion resistance but it does tend to increase room temperature tensile properties. With care in annealing practice, it is possible to produce 304 with low enough carbon to meet the 304L specification, yet with high enough yield strength to meet 304 requirements. As this metal meets all specified requirements of both 304L and 304, the mill test report will show both S30403 and S30400, i.e., dual certified.

S30403/S30400 is appropriate for corrosion service but not for high-temperature mechanical properties. For useful creep rupture strength some minimum amount of carbon is required, typically 0.04%. The situation was addressed a few years ago by adding a number of H grades to ASTM A 240, with controlled carbon for high-temperature strength. The stainless 304H, S30409, has carbon specified 0.04–0.10% for high-temperature strength. In addition, there are grain size and minimum annealing temperature requirements. The 304, S30400, has no requirement for minimum carbon, control of grain size, or annealing temperature. Therefore any 304H containing no more than 0.08% carbon will meet 304 requirements and may be dual certified with 304. One should note that dual-certified 304L/304 is suited only for aqueous corrosion service but would have rather low strength at high temperature. Likewise dual-certified 304/304H is meant for high-temperature service but may be unsatisfactory for welded construction in a wet corrosive environment. In practice, there is rather little actual S30400 produced as sheet or plate at this time. Most is dual certified, one way or another.

Like carbon, sulfur can now readily be refined to very low levels, typically less than 0.005%. Compare this with typical ASTM A 240 levels of 0.030% S maximum. Usually, stainless steel intended for plate is refined to a low-sulfur level to improve hot workability. The plate is generally formed and welded, with rather little machining by the customer. Low sulfur is quite detrimental to machinability. As bar products are commonly meant to be machined, most stainless bar actually must be resulfurized to some level, about 0.02%, for improved machinability. When plate is intended to be drilled for a tubesheet, machinability becomes important and a resulfurized grade, although still keeping sulfur within the old 0.030% maximum, may be chosen.

It is precise control of chemistry, in particular nitrogen, that has permitted development of the superaustenitic 6% molybdenum grades. The ability to closely control nitrogen as an alloying addition has improved the weldability of duplex stainless steels and made them a practical alternative to the austenitics. Whereas formerly the only duplex stainless used in North America was 3RE60 tubing, today several grades of duplex and superduplex stainless plate, pipe, and bar products are used in significant and growing amounts.

Chemistry control also means that the producer will minimize the use of expensive alloying elements. To remain competitive, mills now melt to the bottom end of the allowable range. One consequence for the user is that 316L stainless, specified as 2.00–3.00% molybdenum, now has a melt range of about 2.00–2.10% Mo. Through the 1970s the typical Mo level of 316L was about 2.3%. In addition, the average nickel content has dropped from just below 12% in the 1970s down to around 10.2% Ni as currently produced.

The result has occasionally been that 35-yr-old 316L equipment replaced in kind gave an unexpectedly short life span. In part, of course, this is due to increased corrosive conditions from recycling, rather than dumping, water.

## 4 AVAILABILITY

The metallurgical aspects of alloy selection are well covered in this and other works. Along with corrosion resistance, strength, and fabricability, one of the most important material properties is availability. On a large project most alloys can be made in all product forms, in full mill heat lots. A contemporary example is 317LMX<sup>®</sup>, used as flat-rolled product in mill heat lot quantities, for flue gas desulfurization scrubbers. This grade is rarely, if ever, carried in stock by mills or service centers.

Few mills produce all the forms, such as sheet, plate, bar, pipe, pipe fittings, and appropriate weld fillers, needed to fabricate a chemical process vessel. The minimum quantity a mill requires per product form is large, and lead times can be significant. This may limit flexibility in the event of error, last-minute design changes, or later maintenance needs.

Consider what alternate, if more expensive, grade may be used to fill in for unavailable product forms or sizes. For example, AL-6XN has occasionally been used to fill out a bill of materials specified 317LMX. The stainless grades 304L and 316L are used in such quantity that availability is unlikely to be an issue. The same may not be true for more highly alloyed or specialized materials.

## 5 FERRITIC STAINLESS STEEL

The ferritic grades listed below exhibit corrosion resistance over a very wide range. All are subject to severe embrittlement after prolonged exposure in the 700–1100°F (370–600°C) temperature range. Alloy 409 is weldable and is the alloy used for automotive exhaust systems and catalytic converter shells. It has some useful high-temperature oxidation resistance to about 1200°F (650°C). In plate gauges it may be welded with ERNiCr-3 for better toughness. Alloy 409 is not suited for decorative applications as it may rust from exposure to weather. Alloy 416 is free machining, available both as a ferritic and a martensitic version; 430 is commonly used for decorative purposes as well as food-handling equipment. U-3Cr12L is a weldable, fairly high strength stainless used for piping. E-BRITE has chloride pitting resistance equal or superior to 316L stainless and practical immunity to chloride SCC. E-BRITE is currently available only as tubing for heat exchangers. AL29-4C<sup>®</sup> is extremely resistant to chloride pitting and is used for heat exchanger applications, available only as tubing or thin strip.

Ferritic Alloys (%)

Alloy	UNS	Cr	Ni	Mo	Si	Mn	Cu	C	Fe	Other
409	S40900	11	—	—	0.4	0.3	—	0.015	87	—
U-3Cr12L <sup>®</sup>	S40977	11.5	0.5	—	0.4	0.3	—	0.02	87	0.03 max N
405	S40500	12	—	—	0.3	0.5	—	0.06	86	0.3Al
416	S41600	13	—	—	0.5	1	—	0.05	85	0.2S 0.04P
430	S43000	16.5	—	—	0.5	0.5	—	0.08	83	—
439	S43035	17.2	—	—	0.5	0.4	—	0.015	81	0.5Ti
E-Brite <sup>®</sup>	S44627	26	—	1	0.2	0.1	—	0.002	72	0.1Cb
AL29-4C <sup>®</sup>	S44735	29	—	4	0.35	0.3	—	0.02	66	0.5Ti

## 6 MARTENSITIC STAINLESS STEELS

The only one of these that is readily welded is 410S. The higher carbon 410 may require significant preheat and postweld anneal. Consider the nickel alloy filler ERNiCr-3 for maximum resistance to weldment cracking at a sacrifice in strength and hardness. The corrosion resistance of 410 depends upon the heat-treated condition. For maximum corrosion resistance temper either below 750°F (400°C) or above 1100°F (600°C). Both 410 and the martensitic 416 are used in sporting arms construction. The 440 series are used for cutting tools, 440A and B for pocket knives; 440C and 154CM have the best edge retention and are used for fine custom knives and surgical tools.

Martensitic Alloys (%)

Alloy	UNS	Cr	Ni	Mo	Si	Mn	C	Fe	Other
410	S41000	12	—	—	0.3	0.4	0.14	87	
410S	S41008	12	—	—	0.3	0.4	0.05	97	
416	S41610	13	—	—	0.4	0.2	0.1	84	0.2S 0.05P
420	S42000	13	—	—	0.4	0.4	0.2	86	
431	S43100	15.6	1.9	—	0.2	0.4	0.1	81	
440A	S44002	17	—	0.5	0.2	0.4	0.67	81	
440B	S44003	17	—	0.5	0.2	0.4	0.8	81	
440C	S44004	17	—	0.5	0.2	0.4	1.07	80	
154CM <sup>®</sup>	—	14	—	4	0.3	0.5	1.05	80	

## 7 AGE-HARDENING MARTENSITIC STAINLESS STEELS

Age-Hardening Alloys (%)

Alloy	UNS	Cr	Ni	Mo	Cu	Mn	Al	Ti	C	Fe	Other
455	S45500	11.5	8.5	—	2	0.2	—	1.1	0.2	76	0.3Cb
PH15-7Mo <sup>®</sup>	S15700	15	7	2.5	—	0.4	1	—	0.04	74	—
17-4PH <sup>®</sup>	S17400	15.5	4.7	—	3.3	0.5	—	—	0.05	75	0.3Cb
17-7PH <sup>®</sup>	S17780	17	7.3	—	—	0.7	1.2	—	0.06	74	—
PH13-8Mo <sup>®</sup>	S13800	23	8	2.5	—	—	1.2	—	0.03	76	—

## 8 DUPLEX STAINLESS STEELS

Duplex stainless steels are characterized by high strength and good resistance to chloride SCC. They represent a more economical solution to the problem of stainless SCC than does the use of a high-nickel alloy. Some of the newer lean duplex grades, such as LDX 2101, are replacing carbon steels as well as 304L and 316L stainless. AL 2003 is intended to offer a cost reduction compared with 2205. Carbon steel may be replaced in part because the higher strength permits such weight reduction as well as eliminating maintenance costs. The grades most commonly available from North American service centers are alloys LDX 2101, 2205, 2507, and ZERON 100. LDX 2101 was first used in Europe. Other grades are available from steel mills in heat lot quantities, appropriate for large projects.

Alloy	UNS	Cr	Ni	Mo	Cu	Mn	Si	N	C	Fe	Other
LDX 2101 <sup>®</sup>	S32101	21.5	1.5	0.3	0.3	5	0.7	0.22	0.03	70	
ATI 2102 <sup>™</sup>	S82011	21.5	1.5	0.5	0.3	2.8	0.5	0.22	0.02	72	
AL 2003 <sup>™</sup>	S32003	21	3.5	1.6	—	1	0.5	0.17	0.02	73	
SAF 2304	S32304	23	4	0.3	0.3	2	—	0.1	0.03	70	
3RE60	S31500	18.4	4.8	2.7	—	1.6	1.7	0.07	0.03	70	
Nitronic <sup>®</sup> 19D	S32001	21.2	1.3	—	—	5	0.4	0.15	0.02	71	
LDX 2404 <sup>™</sup>	S82441	24	3.6	1.6	—	3	—	0.27	0.02	67	
2205	S32205	22.1	5.6	3.1	—	1.5	0.5	0.16	0.02	67	
ZERON <sup>®</sup> 100	S32760	25	7	3.5	0.5	0.5	0.3	0.22	0.02	62	0.7W
2507	S32750	25	7	4	—	0.1	0.2	0.3	0.02	63	
255	S32550	25.5	5.7	3.1	1.8	0.8	0.5	0.17	0.02	62	

## 9 AUSTENITIC STAINLESS AND NICKEL ALLOYS

These nickel-bearing alloys are used for the majority of corrosive environments. Alloy 316L is by far the most common choice for chemical process equipment. Formerly, when 316L was inadequate, the designer switched to the high end of the spectrum, alloy C-276, which is still considered the most broadly useful of the high-nickel alloys. Today there are numerous other choices, ranging from those of intermediate cost to alloys superior to C-276 in specific environments.

Types S30600 and S32615 and alloy D-205<sup>™</sup> are specialized high-silicon materials intended for concentrated sulfuric acid heat exchanger service. Weldability is limited. A very high chromium grade, R20033, is also intended for hot concentrated sulfuric acid. It is weldable and has a broader range of potential uses than do the high-silicon alloys.

Materials in the 5–7% molybdenum range are used for seawater service and chemical process vessels in general. Alloys N08367, S31254, and N08926 constitute the “6 moly” alloys. These both have corrosion resistance and are cost intermediate between 316L and alloy C-276. All are readily fabricated and broadly available. Nitrogen in these alloys retards sigma formation, in spite of rather high Mo and moderate Ni levels. Prolonged exposure in the 1000–1800°F (540–980°C) temperature range may cause sigma-phase precipitation.

Alloys in the 13–16% Mo range include C-276, C-22, 59, C-2000, and 686. The latter four are regarded as improvements over C-276, with higher Cr for oxidizing environments. One of the more impressive new high-end nickel alloys, MAT 21, makes use of a tantalum addition, as well as 19% Mo. Availability in the United States is questionable.

Alloy selection for corrosive process environments is a complex process. It should include experience with similar equipment, extensive testing in the exact corrosive environment of interest, and detailed knowledge of the various alloys to be considered. Oftentimes, apparently minor contaminants can cause major changes in corrosion rates. One example is contamination of organic chlorides with small amounts of water. This can permit the organic compound to hydrolyze, forming hydrochloric acid. The HCl in turn may aggressively pit or stress corrode the standard 18-8 stainless steels. Other examples are the alloys B-2, 200, and 400, which contain no chromium. While they have excellent corrosion resistance in reducing environments, they have little or no resistance to oxidizing environments. Unexpected failures may therefore arise from contamination by small amounts of oxidizing salts (e.g., FeCl<sub>3</sub>, CuCl<sub>2</sub>, or NaClO<sub>3</sub>) or even dissolved oxygen. Titanium behaves in the opposite manner and requires the presence of oxidizing species to develop its protective oxide film.

Alloy	UNS	Cr	Ni	Mo	Si	Mn	Cu	C	Fe	Other
302	S30200	18.5	8.2	—	0.5	0.75	—	0.1	72	—
304L	S30403	18.3	9	—	9.5	1.7	—	0.02	70	—
321	S32100	17.3	9.3	—	0.7	1.8	—	0.01	70	0.2Ti
347	S34700	17	9.5	—	0.7	1.5	—	0.04	70	0.5Cb
316L	S31603	16.4	10.2	2.1	0.5	1.6	—	0.02	69	—
317L	S31703	18	11.6	3.1	0.4	1.5	—	0.02	65	—
Nitronic 50	S20910	22	12.5	2	0.4	0.5	—	0.03	57	0.3N 0.2Cb
317LMN	S31726	17	13	4.2	0.5	1.5	—	0.03	62	0.15N
A610	S30600	18	15	—	4	0.7	—	0.01	62	—
254 SMO®	S31254	20	18	6.1	0.4	0.7	0.7	0.015	54	0.2N
SX	S32615	18	20.5	0.9	5.5	1.5	2	0.04	51	—
(Chinese)	S32050	23	21.5	6.4	0.5	1	—	0.03	47	0.25N
654 SMO®	S32654	24	22	7.3	0.3	2	0.45	0.02	43	0.45N
B66	S31266	24.5	22	5.6	—	3	1.5	0.02	44	2W
904L	N08904	21	25	4.5	0.5	1.7	1.6	0.015	45	—
AL4565™	S34565	25	17.6	4.7	—	6	—	0.03	46	0.1Cb 0.5N
25-6MO, 1925 hMO,	N08926	20	25	6.2	0.4	0.7	0.9	0.01	46	0.2N
<b>AL-6XN®</b>	<b>N08367</b>	<b>20.5</b>	<b>24</b>	<b>6.3</b>	<b>0.4</b>	<b>0.3</b>	—	<b>0.02</b>	<b>48</b>	<b>0.22N</b>
27-7Mo	N08927	22	27	7.3	0.2	1	—	0.01	42	0.35N
28	N08028	27	31	3.5	0.2	1.8	1	0.01	35	—
<b>31</b>	<b>N08031</b>	<b>27</b>	<b>31</b>	<b>6.5</b>	<b>0.2</b>	<b>1</b>	<b>1.2</b>	<b>0.01</b>	<b>33</b>	<b>0.2N</b>
33	R20033	33	31	1.4	0.3	0.7	0.7	0.01	32	—
20Cb-3	N08020	20	33	2.2	0.4	0.4	3.3	0.02	40	0.5Cb
3620 Nb	N08020	20	37	2.1	0.5	1.6	3.4	0.02	35	0.6Cb
<b>825</b>	<b>N08825</b>	<b>21.5</b>	<b>40</b>	<b>2.8</b>	<b>0.3</b>	<b>0.6</b>	<b>2</b>	<b>0.01</b>	<b>29</b>	<b>0.8Ti</b>
<b>G-30</b>	<b>N06030</b>	<b>29.5</b>	<b>45</b>	<b>5.5</b>	—	—	<b>1.9</b>	<b>0.01</b>	<b>15</b>	<b>0.7Cb 2.5W</b>
G	N06007	22	45	6.5	0.3	1.5	2	0.01	20	2.1Cb 0.8W
G-3	N06985	22	48	7	0.4	0.8	2	0.01	18	0.3Cb 0.8W
625	N06625	21.5	61	9	0.1	0.1	—	0.05	4	3.6Cb
<b>C-276</b>	<b>N10276</b>	<b>15.5</b>	<b>57</b>	<b>15.5</b>	<b>0.05</b>	<b>0.5</b>	—	<b>0.005</b>	<b>5.5</b>	<b>0.2V 4W</b>
686	N06686	20.5	57	16.3	0.1	0.2	—	0.005	1	3.9W 0.2Al
C-2000®	N06200	23	58.5	16	0.02	0.2	1.6	0.003	0.3	0.25Al
C-22	N06022	21	57	13	0.05	0.3	—	0.003	4	0.2V 3W
59	N06059	23	59	16	0.05	0.4	—	0.005	0.3	0.2Al
MAT 21	—	19	60	19	—	—	—	—	—	1.8Ta

Alloy	UNS	Cr	Ni	Mo	Si	Mn	Cu	C	Fe	Other
B-2	N10665	—	71	28	0.01	0.15	—	0.002	0.8	—
B	N10001	—	66	30	—	0.5	—	0.06	3	0.3V
<b>B-3</b>	<b>N10675</b>	<b>1.3</b>	<b>67.7</b>	<b>28</b>	<b>0.03</b>	<b>0.5</b>	—	<b>0.002</b>	<b>1.5</b>	—
B-4	N10629	1.3	67	28	—	—	—	0.005	3	—
400	N04400	—	66	—	0.02	1	31	0.1	1.5	—
K500	N05500	—	66	—	—	1	28	0.1	1.5	2.7Al 0.6Ti
600	N06600	15.5	76	—	0.2	0.3	—	0.08	8	0.2Ti
201	N02201	—	99.5	—	0.2	—	—	0.01	0.2	—

Note: Alloys listed in boldface are those most commonly available from stocking distributors.



## 10 WELDING<sup>9</sup>

There are some important differences between welding carbon steel and welding stainless steel. Alloys containing more than about 20% nickel have somewhat different requirements than the lower nickel austenitic stainless steels. There are specific issues regarding duplex stainless steels and weld fillers for the high-molybdenum alloys.

### 10.1 Carbon versus Stainless Steel

Six important differences between welding the carbon or low-alloy structural steels and the austenitic stainless and nickel alloys are surface preparation, shielding gases, cold cracking versus hot cracking, distortion, penetration, and fabrication time.

**1. Surface Preparation.** When fabricating carbon steel it is common practice to weld right over the scale (a so-called mill finish is a layer of blue-black oxide, or scale, on the metal surface), red rust, and even paint. The steel weld fillers normally contain sufficient deoxidizing agents, such as manganese and silicon, to reduce these surface iron oxides back to metallic iron. The resultant Mn–Si slag floats to the weld surface. Iron oxide, or scale, melts at a lower temperature, 2500°F (1371°C), than does the steel itself. One can see this in a steel mill when a large ingot is removed from the soaking pit for forging—the molten scale literally drips off the white-hot steel.

Stainless steel, by contrast, must be clean and free of any black scale from hot-rolling, forging, or annealing operations. Such scale is predominately chromium oxide. Normally, stainless is produced with a descaled white or bright finish. Stainless steel melts at a lower temperature than does its chromium oxide scale, and the stainless weld filler chemistry is not capable of reducing this scale back to metallic chromium. As a result, with gas-shielded processes it is difficult to get the weld bead to even “wet,” or stick to, a scaled piece of stainless steel.

The need to clean or grind down to bright metal is more likely to cause trouble when stainless is being joined to carbon steel. In this dissimilar metal joint it is necessary to grind that carbon steel to bright metal, on both sides of the joint, free of all rust, mill scale, grease, and paint. The preferred weld fillers for this particular joint, to minimize the hard martensitic layer on the steel side, are ENiCrFe-3 covered electrodes or ERNiCr-3 bare filler wire. E309 electrodes are commonly used but are not the optimum choice.

Both stainless and high-nickel alloys designed for corrosion resistance are produced to very low carbon contents, less than 0.03% and sometimes less than 0.01% carbon. Any higher carbon will reduce the metal’s corrosion resistance. For this reason it is necessary to clean the alloy thoroughly of all grease and oil before welding. In addition, the very high nickel alloys, such as Monel<sup>®</sup> 400 or commercially pure nickel 200/201, are very sensitive to weld cracking from the sulfur in machining oil or marking crayons.

Metallic zinc paint is a common way to protect structural steel from corrosion. Even a small amount of that zinc paint overspray on stainless will cause the stainless to crack badly when welded. Consider finishing all stainless welding before painting the structural steel in the area.

**2. Shielding Gases.** For gas–metal arc welding (GMAW, also called MIG) of carbon steel the shielding gases are usually 95% Ar–5% O<sub>2</sub>, 75% Ar–25% CO<sub>2</sub> (carbon dioxide), or 100% CO<sub>2</sub>. While suitable for carbon or low-alloy steel welding wire, such gases are far too oxidizing for use with stainless or nickel alloys. It is not unknown to hear the complaint “Clouds of red smoke are coming off when I weld this stainless ... heavy spatter” and then learn that the shielding gas used was 75% Ar–25% CO<sub>2</sub>—a fine gas for carbon steel but not for any stainless steel.

One exception to this high-CO<sub>2</sub> prohibition is when using flux-cored wire, either stainless or nickel alloy. Some of these wires are specifically formulated to run best with 75Ar–25CO<sub>2</sub>.

Stainless and nickel alloys may be GMAW spray-arc welded using 100% argon shielding gas, though it is not necessarily the ideal choice. Stainless steels possess a passive chromium oxide film. The basis of stainless corrosion resistance, this film is not desirable when welding. Some 80% argon is necessary to get into a spray transfer mode. Beyond this, a helium addition, up to about 20%, gives a hotter arc and helps break up the oxide film. A very slight amount of carbon dioxide, perhaps 1%, will prevent arc wander. Too much CO<sub>2</sub> may begin to add carbon to the weld, undesirable for corrosion resistance. Nitrogen may be added in gases specifically designed for welding the duplex stainless steels.

Pulse-arc welding is usually done with a 75% Ar–25% He mix. Short-circuiting arc transfer may be done with this 75% Ar–25% He mix but a 90% He–7 1/2% argon–2 1/2% CO<sub>2</sub> “trimix” is more commonly used for stainless steel.

**3. Cold Cracking versus Hot Cracking.** Carbon steel weldments may harden and crack as they cool from welding. High hardness and the resulting cracking may occur when the steel contains more than 0.25% carbon. Alloying elements which increase hardenability, such as manganese, chromium, molybdenum, etc., can make steels of lower carbon content also harden. Hydrogen pickup from moisture in the air causes underbead cracking in steels that harden as they cool from welding. To prevent such cracking, the steel is usually preheated before welding. This retards the cooling rate of the weld and avoids martensite formation. Postweld heat treatment, or stress relief, is also applied to some steels or for certain applications. The martensitic stainless steels behave in this fashion and because of their high hardenability are quite difficult to weld.

Austenitic stainless and nickel alloys do not harden, no matter how fast they cool from welding. So, it is not necessary to preheat austenitic stainless or to postweld heat treat. Indeed, preheating austenitic alloys beyond what may be necessary to dry the metal can be positively harmful. Stress relief 1100–1200°F (600–650°C) as applied to carbon steel is ineffective with stainless or nickel alloys and may damage the corrosion resistance of some grades.

Stainless steel weldments are usually quite resistant to cracking, unless contaminated, possibly by zinc or copper, more rarely by aluminum. A small amount of ferrite in the austenitic weld bead provides this hot cracking resistance.

High-nickel alloys are less forgiving and may be susceptible to cracking in restrained joints, including heavy sections. This is a hot tearing, not a cold crack. That is, the weld bead tears rather than stretches, as the bead contracts upon solidifying.

This hot tearing/hot cracking has nothing to do with hardness. The faster a nickel alloy weld freezes solid, the less time it spends in the temperature range where it can tear. For this reason preheating, which slows down the cooling rate, is actually harmful, as it permits more opportunity for hot tearing to occur.

**4. Distortion.** Stainless steel has poor thermal conductivity, only about one-fourth that of ASTM A 36 structural steel. This means the welding heat tends to remain concentrated, rather than spread out. Stainless also expands with heat about half again as much as does carbon steel. The combination of these two factors means that stainless or nickel alloy fabrications distort significantly more than similar designs in carbon steel.

Tack welds should be closer than with carbon steel and sequenced in a pattern, left side, right side, middle, etc. If the tacks are simply done in order from one end, the plate edges close up. In order to balance stresses, weld runs should be done symmetrically about the joint's center of gravity. Back step welding is helpful. This subject is well covered in Refs. 10 and 11.

Reducing heat input reduces the stresses and distortions from the welding operation. Heat into the workpiece is controlled by welding current, arc voltage, travel speed, and the specific welding process used. For the same amperes, voltages, and speed, submerged arc welding (SAW) transfers the most heat; shielded-metal arc welding (SMAW) and GMAW with argon

shielding next and roughly equivalent. Gas–tungsten arc welding (GTAW) can put the least heat into the work.

**5. Penetration.** There is some tendency for welders to want to increase heat input with the stainless and high-nickel alloys. First, the weld fillers tend to be sluggish and not flow well, as compared with carbon steel. Second, the arc simply will not penetrate stainless steel as it does carbon steel. The higher the nickel content, the less the penetration. Increasing welding current will not solve the problem! Stainless, and especially nickel alloy, joint designs must be more open. The base metal should be single or double beveled, with a root gap, so that the weld metal may be placed in the joint.

**6. Fabrication Time.** Cleanliness, distortion control measures, maintaining low interpass temperatures, and even machining add up to more time spent fabricating stainless than carbon steel. A shop experienced with stainless may require 1.6 times as long to complete the same fabrication in stainless as in carbon steel. A good carbon steel shop encountering stainless or nickel alloys for the first time may easily spend twice as long, maybe even three times as long, to do the stainless fabrication as it would the same job in carbon steel.

## 10.2 Austenitic Alloys

The fundamental problem to be overcome in welding austenitic nickel-bearing alloys is the tendency of the weld to hot tear upon solidification from the melt. This matter is readily handled in stainless steels of up to about 15% or so nickel. In these stainless grades the weld metal composition is adjusted, usually by slightly higher chromium and reduced nickel, to form a small amount of ferrite upon solidification. The amount of ferrite in the weld may be measured magnetically and is reported as a ferrite number (FN). This ferrite acts to nullify the effects of the elements responsible for hot cracking in the Ni–Cr–Fe austenitics. These elements are chiefly phosphorus, sulfur, silicon, and boron. In higher nickel grades, about 20% nickel and over, it is metallurgically not possible to form any measurable amount of ferrite. Therefore other means of minimizing hot cracking must be used. Foremost among these is to use high-purity raw materials in the manufacture of weld fillers. Simply reducing the amounts of harmful P, S, Si, and B in the weld metal improves its ability to make a sound weld.

Phosphorus, in particular, must be kept below 0.015% in the weld wire itself. Certain alloy additions such as manganese, columbium (niobium), and molybdenum serve in one way or another to reduce the austenitic propensity for weld hot cracking. Manganese ranges from about 2% in AWS E310-15–covered electrodes to 8% in ENiCrFe-3 nickel alloy–covered electrodes. Columbium at the 0.5% level, as in 347 or 20Cb-3 stainless, is harmful whereas 2–4% Cb is quite beneficial in many nickel-based weld fillers. Molybdenum is not added with the intention of increasing weldability; nevertheless it does so. The 2% Mo contributes to 316L being the most weldable of the stainless steels, and 15% in C-276 accounts for the popularity of the various “C-type” electrodes in repair welding.

The distinction between the lower nickel stainless grades, which depend upon ferrite to ensure weldability, and the high-nickel alloys, which require high-purity weld fillers, is an important one to remember. Most ferrite-containing (stainless) weld fillers are useless with nickel alloy base metal, as dilution of the weld bead with nickel from the base metal eliminates this ferrite. Likewise, a high-purity nickel alloy weld filler, such as ER320LR, may not be so crack resistant when contaminated by phosphorus from use on 316L or carbon steel base metal.

### *Alloys under 20% Nickel*

Most austenitic grades containing less than 20% nickel are joined with weld fillers that utilize some ferrite, perhaps 4–12 FN, to ensure freedom from hot cracks. In practice, this means

stainless steels up through 317LMN or 309S, both about 13% nickel. The 310S type stands in an odd position between the stainless and the nickel alloys, having neither ferrite nor any particular alloy addition to the weld metal to ensure sound welds. Not surprisingly, 310S welds have a reputation for fissuring, unless the ER310 weld filler contains less than 0.015% P alloys over 20% nickel. Corrosion-resistant alloys in this category begin with the 18% nickel 254 SMO<sup>®</sup>, for this and other “6 moly” grades are welded with an overmatching nickel alloy filler such as ERNiCrMo-3.

Other nickel alloys are joined with matching composition weld fillers modified only by restrictions on P, S, Si, and B. A minor amount of titanium may be added for deoxidation. Other fillers contain significant manganese or columbium to improve resistance to fissuring and hot cracking.

Such chemistry modifications are rarely as effective in preventing hot cracking as is the use of ferrite in the lower nickel stainless weld fillers. Welding technique and attention to cleanliness, then, become increasingly important to ensure the soundness of fully austenitic welds. These techniques include bead contour and low interpass temperature. Reinforced, convex stringer beads are much more resistant to centerbead cracking than are shallow, concave beads. Interpass temperature for most nickel alloy weldments is kept below 300°F (150°C). Cleanliness includes not using oxygen additions to the GMAW shielding gases for nickel alloys.

It is worth repeating here that high-nickel alloys cannot be reliably welded using stainless steel weld fillers. Stainless steel fillers (308, 309, etc.) depend upon a chemistry which will solidify from the melt as a duplex structure, containing a small amount of ferrite in with the austenite.

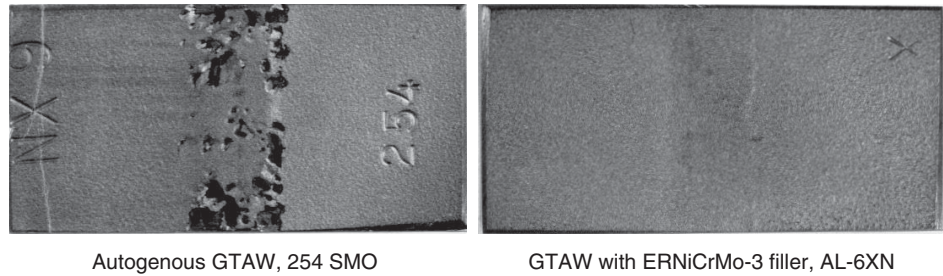
### 10.3 Duplex Stainless Steels<sup>12</sup>

When welding duplex stainless the issues are maintaining the austenite–ferrite balance in the weldment and avoiding precipitation of nitrides and sigma. Rather high heat input is used to weld duplex, similar to welding 316L stainless. This is in contrast to the lower heat preferred with the high-nickel alloys. Low heat input is *not* desirable with a duplex, as it may not permit sufficient transformation of ferrite to austenite upon cooling. Modern duplex weld fillers have a nitrogen addition as well as slightly higher nickel content than the base metal. This is to ensure that enough weld metal ferrite transforms to austenite to maintain a balance of the two phases as welded. Weldments made using weld fillers overalloyed in nickel should not be annealed. The superduplex grades 2705, Ferralium, and Zeron 100 may also be welded with the nickel alloy ERNiCrMo-14.<sup>13</sup>

Toughness and critical pitting temperature of duplex weldments vary with the choice of welding process, in opposite directions—in order of increasing notch impact toughness: SMAW AC/DC, FCAW (flux-cored arc welding), SMAW DC-basic, SAW, GMAW argon shielding, GMAW 95% Ar–3% He–2% N<sub>2</sub> shielding, and GTAW; in order of increasing pitting resistance, as measured by critical pitting temperature, GTAW, GMAW, SAW, FCAW, SMAW DC-basic, and SMAW AC/DC.

### 10.4 High-Molybdenum Alloys<sup>14,15</sup>

When high-molybdenum containing stainless and nickel alloys are welded there is considerable segregation of molybdenum and chromium in the weld bead. The reason is that both these metals have very high melting points, 6170°F and 3407°F (respectively). This leaves small local areas depleted in these elements. Pitting corrosion can start in the low-Mo areas, with the pits eventually growing even into metal with high molybdenum content. This situation



**Figure 1** Welds in 6% molybdenum alloy 1/4" plate. Tested per ASTM G 48 for 72 h in 10% FeCl<sub>3</sub>•6H<sub>2</sub>O, at 50°C (122°F). AL-6XN alloy FABRICATION, Bulletin 203, Rolled Alloys.

occurs in alloys ranging from 316L stainless up through C-276, generally being more severe at higher alloy contents. In order to counteract the problem, high-molybdenum stainless and nickel alloys are welded with an overmatching filler metal. For stainless steels 316L through super-austenitics such as AL-6XN, weld fillers ERNiCrMo-3 (N06625) and ERNiCrMo-10 (N06022) have worked well. See Fig. 1.

In the case of tubular products autogenously welded in production, a high-temperature anneal is used to homogenize the metal. In some cases the line speed and temperature chosen may not completely homogenize the structure. A small amount of nitrogen, 3–5%, may be added to the torch gas to improve weld bead pitting resistance. Autogenous welds in thin sheet, which cannot be annealed after welding, should have this nitrogen addition to minimize the loss of corrosion. Even so, because thin-sheet welds solidify more quickly, the segregation is less severe.

In the nickel alloys, weld filler 686 CPT (ERNiCrMo-14) appears to be markedly less susceptible to segregation problems than are other high-molybdenum alloys. This filler may be chosen for high-nickel alloys such as C-276, C-22, 59, C-2000 and, of course, alloy 686 itself. It is also suggested for some of the superaustenitics such as 27Mo and 654 SMO®.

The corrosion tests of weldments in Fig. 2 illustrate the behavior of this filler metal.

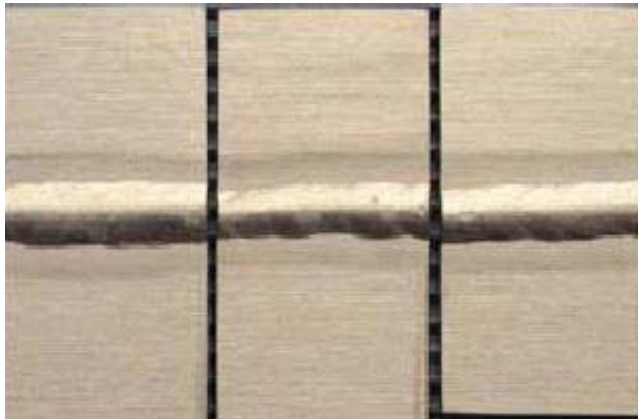
### *Duplex Stainless and Nickel Alloy Weld Fillers of Interest*

#### Duplex

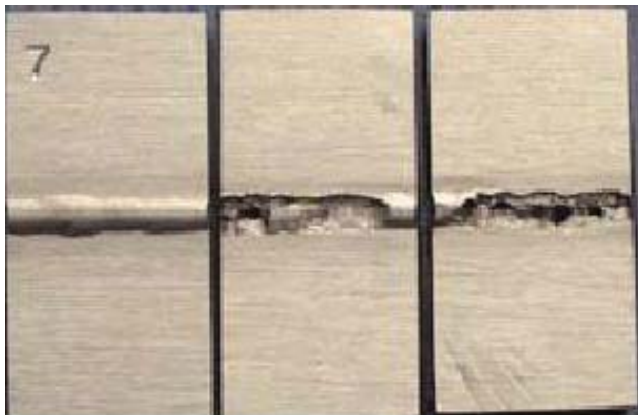
AWS Class	UNS	Cr	Ni	Mo	W	C	N	Other
ER2209	S39209	22.5	8	3	—	0.02	0.14	65Fe
ER2594	S32750	25	9.2	3.9	—	0.01	0.3	0.1Cu, 60Fe
ZERON 100X	—	25	9.2	3.6	0.6	0.01	0.2	0.5Cu, 60Fe

#### Nickel Alloy

AWS Class	UNS	Cr	Ni	Mo	W	C	Fe	Other
ER320LR	N08022	20.5	33.5	2.3	—	0.02	35	3.3Cu, 0.3Cb
ERNiCrMo-3	N06625	22	64	9	—	0.04	1	3.5Cb
ERNiCrMo-10	N06022	21	57	13	3	0.003	4e	1.7Co, 0.2V
ERNiCrMo-14	N06686	22	56	16	3.7	0.005	2	0.1Ti



Alloy N06022 welded with  
INCO-WELD filler metal 686CPT



Alloy N06022 welded with matching  
N06022 (ERNiCrMo-10) filler metal.

**Figure 2** Corrosion resistance of weldments in corrosion-resistant alloys in boiling Green Death test medium: 11.9%  $\text{H}_2\text{SO}_4$  + 1.3%  $\text{HCl}$  + 1.0%  $\text{FeCl}_3$  + 1.0%  $\text{CuCl}_2$ . Corrosion test data are from Special Metals Corporation. The Green Death test solution was originally developed, and named, by Haynes International.

## WEBSITES

Detailed technical information on heat- and corrosion-resistant stainless and nickel alloys is available at [www.rolledalloys.com](http://www.rolledalloys.com), nickel alloys at [www.specialmetals.com](http://www.specialmetals.com), with stainless steel data at [www.alleghenyludlum.com](http://www.alleghenyludlum.com) and [www.outokumpu.com](http://www.outokumpu.com).

## REFERENCES

1. H. H. Uhlig, *The Corrosion Handbook*, Wiley, New York, 1948.
2. J. Kelly, "Corrosion Resistant Alloy Specifications & Operating Data," Bulletin 151, Rolled Alloys, Temperance, MI, 2003.



3. M. Ueda, H. Abo, T. Sunami, T. Muta, and H. Yamamoto, "A New Austenitic Stainless Steel Having Resistance to Stress Corrosion Cracking," Nippon Steel Technical Report, Overseas No. 2, January 1973, p. 66.
4. C. H. Samans, "Stress Corrosion Cracking Susceptibility of Stainless Steels and Nickel Base Alloys in Polythionic Acids and Acid Copper Sulfate Solution," *Corrosion*, 20 (Aug), NACE, Houston, TX, 1964.
5. J. Kelly, "AL-6XN<sup>®</sup> Alloy Physical, Mechanical and Corrosion Properties," Bulletin No. 210, Rolled Alloys, Temperance, MI, 2002.
6. R. Kirchheiner, H. Portisch, R. Solomon, M. Jahudka, and J. Ettore, "Designing Components for Radioactive Waste Liquids in a Modern NiCrMo-Alloy," Paper No. 166, Corrosion 98, NACE International, Houston, TX, 1998.
7. Paper No. 338, Corrosion 95, NACE International, Houston, TX, 1995.
8. Special Metals Publication No. SMC-092, Huntington, WV.
9. J. Kelly, "Heat Resistant Alloy Welding," Bulletin 200, Rolled Alloys, Temperance, MI, 2002.
10. Avesta, *Handbook for the Welding of Stainless Steel*, Inf. 8901, Avesta Welding AB, S-774 80, Avesta, Sweden.
11. B. Lundqvist, *Sandvik Welding Handbook*, AB Sandvik Steel, Sandviken, Sweden, 1977.
12. J. Kelly, "RA2205 Duplex Stainless," Bulletin 1071, Rolled Alloys, Temperance, MI, 2003.
13. G. Furmanski, S. D. Kiser, and L. E. Shoemaker, "A NiCrMo Welding Product Provides Optimum Weldments in SuperDuplex Pipeline for Geothermal Power Service," Paper No. 08177, NACE International, Houston, TX, 2008.
14. J. Kelly, "AL-6XN Alloy Fabrication," Bulletin 203, Rolled Alloys, Temperance, MI, 2001.
15. M. B. Rockel and M. Renner, "Pitting, Crevice and Stress Corrosion Resistance of High Chromium and Molybdenum Alloy Stainless Steels," *Werkstoff und Korrosion*, 35, 537-542, 1984.
16. S. McCoy, L. E. Shoemaker, and J. Crum, *Corrosion Performance and Fabricability of the New Generation of Highly Corrosion-Resistant Nickel-Chromium—Molybdenum Alloys*, Special Metals Wiggin Ltd UK and Special Metals Corporation.

## TRADEMARKS

ZERON 100 is a registered trademark of Rolled Alloys.

AL-6XN, E-BRITE, and AL 29-4C are registered trademarks; 2003 and 2102 are trademarks, of ATI Properties, Inc.

20Cb-3 is a registered trademark of Carpenter Technology Corporation.

254 SMO, 654 SMO, and LDX 2101 are registered trademarks, and LDX 2404 a trademark, of Outokumpu AB.

U-3CR12L is a registered trademark of Columbus Stainless (Pty) Ltd.

Nicrofer is a registered trademark of ThyssenKrupp VDM.

Duraloy is a registered trademark of Duraloy Technologies, Inc.

HASTELLOYS, Haynes, G-30, and C-2000 are registered trademarks of Haynes International.

INCOLOY, INCONEL, INCO-WELD, MONEL, 800HT, 25-6MO, 27-7MO, and 686CPT are registered trademarks of Special Metals, Inc.

NITRONIC, 17-4PH, PH15-7MO, 17-7PH, and PH13-8MO are registered trademarks of AK Steel Corporation.

Sandvik SX and SAF are registered trademarks of Sandvik AB.



# CHAPTER 3

---

## ALUMINUM ALLOYS

**J. G. Kaufman**  
Kaufman Associates  
Lewes, Delaware

<b>1 NATURE OF ALUMINUM ALLOYS</b>	<b>61</b>	<b>6 MACHINING ALUMINUM ALLOYS</b>	<b>89</b>
<b>2 ADVANTAGES OF ALUMINUM ALLOYS</b>	<b>62</b>	6.1 Single-Point Tool Operations	90
2.1 Wrought Aluminum Alloys	62	6.2 Multipoint Tool Operations	90
2.2 Cast Aluminum Alloys	64	<b>7 FINISHING ALUMINUM</b>	<b>91</b>
2.3 Limitations of Wrought and Cast Aluminum Alloys	65	7.1 Mechanical Finishes	91
<b>3 DESIGNATION SYSTEMS</b>	<b>65</b>	7.2 Chemical Finishes	92
3.1 Wrought Aluminum Alloy Designation System	66	7.3 Electrochemical Finishes	92
3.2 Cast Aluminum Alloy Designation System	67	7.4 Clear Anodizing	92
3.3 Aluminum Alloy Temper Designation System	70	7.5 Color Anodizing	92
<b>4 MECHANICAL PROPERTIES OF ALUMINUM ALLOYS</b>	<b>73</b>	7.6 Integral Color Anodizing	92
<b>5 CORROSION BEHAVIOR OF ALUMINUM ALLOYS</b>	<b>87</b>	7.7 Electrolytically Deposited Coloring	92
5.1 General Corrosion	87	7.8 Hard Anodizing	92
5.2 Pitting Corrosion	88	7.9 Electroplating	93
5.3 Galvanic Corrosion	89	7.10 Applied Coatings	93
		<b>8 APPLICATIONS OF ALUMINUM ALLOYS</b>	<b>93</b>
		8.1 Applications by Alloy Class	93
		8.2 Applications by Market Area	112
		<b>9 SUMMARY</b>	<b>114</b>
		<b>REFERENCES</b>	<b>115</b>

### 1 NATURE OF ALUMINUM ALLOYS

Aluminum is the most abundant metal and the third most abundant chemical element in Earth's crust, comprising over 8% of its weight. Only oxygen and silicon are more prevalent. Yet, until about 150 years ago aluminum in its metallic form was unknown to humans. The reason for this is that aluminum, unlike iron or copper, does not exist as a metal in nature. Because of its chemical activity and its affinity for oxygen, aluminum is always found combined with other elements, mainly as aluminum oxide. As such it is found in nearly all clays and many minerals. Rubies and sapphires are aluminum oxide colored by trace impurities, and corundum, also aluminum oxide, is the second hardest naturally occurring substance on Earth—only diamond is harder. It was not until 1886 that scientists learned how to economically extract aluminum from aluminum oxide via electrolytic reduction. Yet in the more than 100 years since that time, aluminum has become the second most widely used of the approximately 60 naturally occurring metals, second only to iron.

Aluminum alloys are broadly used in products and applications that touch us regularly in our daily lives, from aluminum foil for food packaging and easy-open aluminum cans for your beverages to the structural members of the ground vehicles and the aircraft in which we travel. The broad use of aluminum alloys is dictated by a very desirable combination of properties, combined with the ease with which they may be produced in a great variety of forms and shapes plus the ease with which they may be recycled and reused endlessly. In this chapter, we will review the characteristics of aluminum alloys that make them so attractive and note the variety of applications in which they are used.

For readers who are interested in a broader look at the aluminum industry as a whole, the publications of the Aluminum Association are highly recommended, especially:

- *Aluminum: Technology, Applications and Environment*<sup>1</sup>
- *Aluminum Standards and Data (Standard and Metric Editions)*<sup>2</sup>
- *Standards for Aluminum Sand and Permanent Mold Castings*<sup>3</sup>
- *The Aluminum Design Manual*<sup>4</sup>

See the References at the end of the chapter for a more complete listing.

## 2 ADVANTAGES OF ALUMINUM ALLOYS

The first step in becoming familiar with the opportunities to utilize aluminum alloys advantageously is to briefly note some of the basic characteristics of wrought and cast aluminum alloys that make them desirable candidates for such a wide range of applications as well as their limitations. Wrought alloys (those mechanically formed by rolling, forging, and extrusion into useful products) are addressed first, then cast alloys (those cast directly to the near-final finished shape).

### 2.1 Wrought Aluminum Alloys

*Low Density/Specific Gravity.* One property of aluminum that everyone is familiar with is its light weight or, technically, its low density or specific gravity. The specific gravity of aluminum is only 2.7 times that of water and roughly one-third that of steel and copper. An easy number to remember is that 1 cubic inch (in.<sup>3</sup>) of aluminum weighs 0.1 lb; 1 cubic foot (ft<sup>3</sup>) weighs 170 lb compared to 62 lb for water and 490 lb for steel.

*High Strength–Weight Ratio.* The combination of relatively high strength with low density means a high-strength efficiency for aluminum alloys and many opportunities for replacement of heavier metals with no loss (and perhaps a gain) in load-carrying capacity. This characteristic, combined with the excellent corrosion resistance and recyclability, has led to aluminum's broad use in containers, aircraft, and automotive applications.

*Excellent Corrosion Resistance.* As a result of a naturally occurring tenacious surface oxide film, many aluminum alloys provide exceptional resistance to corrosion in many atmosphere and chemical environments. Alloys of the 1xxx, 3xxx, 5xxx, and 6xxx systems are especially favorable in this respect and are even used in applications where they are in direct contact with seawater and antiskid salts. With some electrocoating enhancements (e.g., anodizing), the oxide coating can be thickened for even greater protection. Aluminum and a number of its alloys possess excellent resistance to corrosive attack by many foods and chemicals as well as natural environments.

*High Thermal Conductivity.* Aluminum and its alloys are good conductors of heat, and, while they melt at lower temperatures than steels, about 1000°F (about 535°C), they are slower to reach very high temperatures than steel in fire exposure.

*High Electrical Conductivity.* Pure aluminum and some of its alloys have exceptionally high electrical conductivity (i.e., very low electrical resistivity), second only to copper among common metals as conductors.

*Excellent Reflectivity.* Aluminum with appropriate surface treatment becomes an excellent reflector and does not dull from normal atmospheric oxidation.

*High Fracture Toughness and Energy Absorption Capacity.* Many aluminum alloys are exceptionally tough and excellent choices for critical applications where resistance to unstable crack growth and brittle fracture are imperatives. Alloys of the 5xxx series, for example, are prime choices for liquefied natural gas (LNG) tankage. Special high-toughness versions of aerospace alloys, such as 2124, 7050, and 7475, replace the standard versions of these alloys for critical bulkhead applications.

*Superior Cryogenic Toughness.* Aluminum alloys, especially of the 3xxx, 5xxx, and 6xxx series, are ideal for very low temperature applications because the ductility and toughness as well as strength of many alloys at subzero temperatures are as high as or higher than at room temperature, even down to near absolute zero. As noted above, the 5xxx series alloys are regularly used for liquefied gas tankage operating at temperatures from -150 to -452°F (-65 to -269°C).

*Fatigue Strength.* On an efficiency basis (strength to density) the fatigue strengths of many aluminum alloys are comparable to those of steels.

*Low Modulus of Elasticity.* Aluminum alloys have elastic moduli about one-third those of steels (about  $10 \times 10^6$  psi vs. about  $30 \times 10^6$  psi), so they absorb about three times as much elastic energy upon deformation to the same stress. They also deflect three times more under load (see Section 2.3).

*Superior Workability.* Aluminum alloys are readily workable by virtually all metalworking technologies and especially amenable to extrusion (the process of forcing heated metal through shaped dies to produce specific shaped sections). This enables aluminum to be produced in a remarkable variety of shapes and forms in which the metal can be placed in locations where it can most efficiently carry the applied loads.

*Ease of Joining.* Aluminum alloys may be joined by a very broad variety of commercial methods, including welding, brazing, soldering, riveting, bolting, and even nailing in addition to an unlimited variety of mechanical procedures. Welding, while considered difficult by those familiar only with joining steel and who try to apply the same techniques to aluminum, is particularly easy when performed by proven techniques such as gas-metal arc welding (GMAW or MIG) or gas-tungsten arc welding (GTAW or TIG).

*Versatile Array of Finishes.* Aluminum can be finished in more ways than any other metal used today, including a variety of techniques that build upon its strong oxide coating and employ coloring, plus more conventional means such as painting and enameling.

*Ease of Recycling.* Aluminum and its alloys are among the easiest to recycle of any structural materials. In addition, they are recyclable in the truest sense, unlike materials which are reused but in lower quality products: Aluminum alloys may be recycled *directly* back into the same high-quality products like rigid container sheet (cans) and automotive components. Through such recycling, the life-cycle assessment advantages for aluminum are optimized.

## 2.2 Cast Aluminum Alloys

The desirable characteristics of wrought alloys, including recyclability, are also generally applicable to cast alloys, but in fact the choice of one casting alloy or another tends to be more often made on the basis of their relative abilities to meet one or more of the four following characteristics:

- Ease of casting
- Quality of finish
- High strength, especially at high temperatures
- High toughness

**1. *Ease of Casting.*** Many aluminum casting alloys have relatively high silicon contents that provide excellent flow characteristics during casting, enabling them to be utilized for large and complex castings (e.g., even complete engines). Relatively minute details in the shape of the casting can be accurately and reliably replicated.

**2. *Quality of Finish.*** By proper selection of aluminum casting alloy, extremely fine surface quality can be achieved. While such alloys typically require more attention to casting practice, they are widely used in applications where the finished casting surface mirrors the finish needed in surface.

**3. *High Strength.*** Many aluminum casting alloys respond to heat treatment following casting and achieve relatively high levels of strength and excellent strength–weight ratios. With careful design of molds, high chill rates can be assured and both high strength and high toughness can be achieved.

**4. *High Toughness.*** With careful selection of alloy and heat treatment combined with process technology often referred to as premium engineered casting, optimizing metal flow and chill rate, the toughness of castings may be comparable to that of wrought alloys at comparable strength levels. Techniques such as hot isostatic pressing (HIP) are available to further reduce porosity and improve performance.

Unfortunately few casting alloys possess all four characteristics, but some generalizations useful in alloy selection for specific applications may be made:

**1. *Ease of Casting.*** The high-silicon 3xx.x series are outstanding in this respect as the relatively high silicon contents lend a characteristic of good flow and mold-filling capability. As a result, the 3xxx.x series are the most widely used and are especially chosen for large and very complex casting.

**2. *Finish.*** The 5xx.x and 7xx.x series are noteworthy for the fine finish they provide, but they are more difficult to cast than the 3xx.x series and so are usually limited to those applications where that finish is paramount. A good example is the use of 7xx.x alloys for bearings.

**3. *Strength and Toughness.*** The 2xx.x alloys typically provide the very highest strengths, especially at high temperatures, but are among the more difficult to cast and lack good surface characteristics. Therefore their use is usually limited to situations where sophisticated



casting techniques can be applied and where strength and toughness are at a premium, as in the aerospace industry. Relatively high strengths and superior toughness can also be achieved with some of the higher purity 3xx.x alloys (e.g., A356.0, A357.0) in heat-treated conditions.

### 2.3 Limitations of Wrought and Cast Aluminum Alloys

There are several characteristics of aluminum alloys that require special attention in alloy selection or design:

*Moduli of Elasticity.* As noted earlier, the elastic moduli of aluminum alloys are about one-third those of steel. In applications such as bridges, where some designs may be deflection critical, this is a disadvantage and consideration should be given to the fact that aluminum alloys will deflect about three times more than comparably sized steel members. To compensate for this, aluminum members subject to bending loads are usually made deeper or thicker in their upper and lower extremities to reduce stresses and/or deflections.

*Melting Temperature.* Aluminum alloys melt at about 1000°F (535°C), well below where steels melt, and so they should not be selected for applications such as flue pipes and fire doors where the low melting point may result in unsatisfactory performance. The useful limit of high-temperature structural application of aluminum alloys is about 500°F (about 260°C) for conventional alloys or about 600°F (315°C) for alumina-enhanced alloys. It is useful to note, however, that even in the most intense fires, aluminum alloys do not burn; they are rated non-combustible in all types of fire tests and achieve the highest ratings in flame-spread tests. Further, as noted earlier, they are slower to reach high temperatures in fires than other metals such as steels because of their higher thermal conductivity and emissivity. Nevertheless, they should not be used where service requirements include structural strength above 500°F (260°C) or exposure above 700°F (370°C).

*Stress Corrosion Susceptibility of Some Alloys.* Some aluminum alloys, notably the 2xxx and 7xxx alloys, when stressed perpendicular to the major plane of grain flow (i.e., in the short-transverse direction), may be subject to intergranular stress corrosion cracking (SCC) unless they have been given a special thermal treatment to reduce or eliminate this type of behavior. If short-transverse stresses are anticipated in relatively thick components, 2xxx alloys should only be utilized in the T6- or T8-type tempers (not T3- or T4-type tempers), and 7xxx alloys should only be used in the T7-type tempers (not T6- or T8-type tempers). Similarly, 5xxx alloys with more than 3% Mg should not be used in applications where a combination of high stress and high temperature will be experienced over a long period of time (more than several hundred hours at or above 150°F, or 65°C) because some susceptibility to SCC may be encountered (i.e., the alloys may become “sensitized”); for applications where temperatures above about 150°F (65°C) are likely to be encountered for long periods, the use of 5xxx wrought alloys or 5xxx casting alloys with 3% or less Mg, e.g., 5454, is recommended.

*Mercury Embrittlement.* Aluminum alloys should never be used when they may be in direct contact with liquid or vaporized mercury; severe grain boundary embrittlement may result. This is an unlikely exposure for the vast majority of applications, but in any instance where there is the possibility of mercury being present, the use of aluminum alloys should be avoided.

## 3 DESIGNATION SYSTEMS

One advantage in using aluminum alloys and tempers is the universally accepted and easily understood alloy and temper systems by which they are known. It is extremely useful for

both secondary fabricators and users of aluminum products and components to have a working knowledge of those designation systems. The alloy system provides a standard form of alloy identification that enables the user to understand a great deal about the chemical composition and characteristics of the alloy, and similarly, the temper designation system permits one to understand a great deal about the way in which the product has been fabricated.

The alloy and temper designation systems in use today for wrought aluminum were adopted by the aluminum industry in about 1955, and the current cast system was developed somewhat later. The aluminum industry created and continues to maintain the designation of the systems through its industry organization, the Aluminum Association. The alloy registration process is carefully controlled and its integrity maintained by the Technical Committee on Product Standards of the Aluminum Association, made up of industry standards experts.<sup>5</sup> Further, as noted earlier, the Aluminum Association designation system is the basis of the American National Standards Institute (ANSI) standards, incorporated in ANSI H35.1<sup>6</sup> and, for the wrought alloy system at least, is the basis of the near-worldwide *International Accord on Aluminum Alloy Designations*.<sup>7</sup> It is useful to note that the international accord does not encompass casting alloy designations, so more variation will be encountered in international designations for casting alloys than for wrought aluminum alloys.

The Aluminum Association *American National Standard Alloy and Temper Designation Systems for Aluminum* covered in ANSI H35.1<sup>6</sup> and *Aluminum Standards and Data*<sup>2</sup> are outlined in this chapter.

### 3.1 Wrought Aluminum Alloy Designation System

The Aluminum Association wrought alloy designation system consists of four numerical digits, sometimes with alphabetic prefixes or suffices, but normally just the *four* numbers:

- The *first* digit defines the major alloying class of the series starting with that number.
- The *second* defines variations in the original basic alloy; that digit is always a 0 for the original composition, a 1 for the first variation, a 2 for the second variation, and so forth; variations are typically defined by differences in one or more alloying elements of 0.15–0.50% or more, depending upon the level of the added element.
- The *third* and *fourth* digits designate the specific alloy within the series; there is no special significance to the values of those digits, and they are not necessarily used in sequence.

Table 1 shows the meaning of the first of the four digits in the wrought alloy designation system. The alloy family is identified by that number and the associated main alloying ingredient(s), with three exceptions:

- Members of the 1000 series family are commercially pure aluminum or special-purity versions and as such do not typically have any alloying elements intentionally added; however, they do contain minor impurities that are not removed unless the intended application requires it.
- The 8000 series family is an “other elements” series, comprised of alloys with rather unusual major alloying elements such as iron and nickel.
- The 9000 series is unassigned.

The major benefit of understanding this designation system is that one can tell a great deal about the alloy just from knowledge of which it is a member. For example:

- As indicated earlier, the 1xxx series are pure aluminum and its variations; compositions of 99.0% or more aluminum are by definition in this series. Within the 1xxx series,

**Table 1** Main Alloying Elements in Wrought Alloy Designation System

Alloy	Main Alloying Element
1000	Mostly pure aluminum; no major alloying additions
2000	Copper
3000	Manganese
4000	Silicon
5000	Magnesium
6000	Magnesium and silicon
7000	Zinc
8000	Other elements (e.g., iron or tin)
9000	Unassigned

the last two of the four digits in the designation indicate the minimum aluminum percentage. These digits are the same as the two digits to the right of the decimal point in the minimum aluminum percentage specified for the designation when expressed to the nearest 0.01%. As with the rest of the alloy series, the second digit indicates modifications in impurity limits or intentionally added elements. Compositions of the 1xxx series do not respond to any solution heat treatment but may be strengthened modestly by strain hardening.

- The 2xxx series alloys have copper as their main alloying element and, because it will go in significant amounts into solid solution in aluminum, they will respond to solution heat treatment; they are referred to as heat treatable.
- The 3xxx series alloys are based on manganese and are strain hardenable; they do not respond to solution heat treatment.
- The 4xxx series alloys are based on silicon; some alloys are heat treatable, others are not, depending upon the amount of silicon and the other alloying constituents.
- The 5xxx series alloys are based on magnesium and are strain hardenable, not heat treatable.
- The 6xxx series alloys have both magnesium and silicon as their main alloying elements; these combine as magnesium silicide ( $Mg_2Si$ ) following solid solution, and so the alloys are heat treatable.
- The 7xxx series alloys have zinc as their main alloying element, often with significant amounts of copper and magnesium, and they are heat treatable.
- The 8xxx series contain one or more of several less frequently used major alloying elements like iron or tin; their characteristics depend on the major alloying element(s).

The compositions of a representative group of widely used commercial wrought aluminum alloys are given in Table 2, from *Aluminum Standards and Data*<sup>2</sup> and other Aluminum Association publications.

### 3.2 Cast Aluminum Alloy Designation System

The designation system for cast aluminum alloys is similar in some respects to that for wrought alloys but has a few very important differences as noted by the following description.

Like the wrought alloy system, the cast alloy designation system also has four digits but differs from the wrought alloy system in that a decimal point is used between the third and

**Table 2** Nominal Compositions of Wrought Aluminum Alloy<sup>a</sup>

Alloy	Percent of Alloying Elements <sup>b</sup>								Notes <sup>c</sup>
	Silicon	Copper	Manganese	Magnesium	Chromium	Nickel	Zinc	Titanium	
1060	—	—	—	—	—	—	—	—	1
1100	—	—	—	—	—	—	—	—	1
1145	—	—	—	—	—	—	—	—	1
1350	—	—	—	—	—	—	—	—	2
2008	0.65	0.9	—	0.38	—	—	—	—	3
2010	—	1.0	0.25	0.7	—	—	—	—	
2011	—	5.5	—	—	—	—	—	—	4
2014	0.8	4.4	0.8	0.50	—	—	—	—	
2017	0.50	4.0	0.7	0.6	—	—	—	—	
2024	—	4.4	0.6	1.5	—	—	—	—	
2025	0.8	4.4	0.8	—	—	—	—	—	
2036	—	2.6	0.25	0.45	—	—	—	—	
2117	—	2.6	—	0.35	—	—	—	—	
2124	—	4.4	0.6	1.5	—	—	—	—	5
2195	—	4.0	—	0.50	—	—	—	—	5
2219	—	6.3	0.30	—	—	—	—	0.06	7
2319	—	6.3	0.30	—	—	—	—	0.15	7
2618	0.18	2.3	—	1.6	—	1	—	0.07	8
3003	—	0.12	1.2	—	—	—	—	—	
3004	—	—	1.2	1	—	—	—	—	
3005	—	—	1.2	0.40	—	—	—	—	
3105	—	—	0.6	0.50	—	—	—	—	
4032	12.2	0.9	—	—	—	—	0.9	—	
4043	5.2	—	—	—	—	—	—	—	
4643	4.1	—	—	0.20	—	—	—	—	
5005	—	—	—	0.8	—	—	—	—	
5050	—	—	—	1.4	—	—	—	—	
5052	—	—	—	2.5	0.25	—	—	—	
5056	—	—	0.12	5.0	0.12	—	—	—	
5083	—	—	0.7	4.4	0.15	—	—	—	
5086	—	—	0.45	4.0	0.15	—	—	—	
5154	—	—	—	3.5	0.25	—	—	—	
5183	—	—	0.8	4.8	0.15	—	—	—	
5356	—	—	0.12	5.0	0.12	—	—	0.13	
5454	—	—	0.8	2.7	0.12	—	—	—	
5456	—	—	0.8	5.1	0.12	—	—	—	
5457	—	—	0.30	1.0	—	—	—	—	
5554	—	—	0.8	2.7	0.12	—	—	0.12	
5556	—	—	0.8	5.1	0.12	—	—	0.12	
5657	—	—	—	0.8	—	—	—	—	
5754	—	—	0.5	3.1	0.3	—	—	—	
6005	0.8	—	—	0.50	—	—	—	—	
6009	—	—	—	—	—	—	—	—	
6013	0.8	0.8	0.50	1.0	—	—	—	—	
6053	0.7	—	—	1.2	0.25	—	—	—	
6061	0.6	0.28	—	1.0	0.20	—	—	—	
6063	0.40	—	—	0.7	—	—	—	—	

**Table 2** (Continued)

Alloy	Percent of Alloying Elements <sup>b</sup>								Notes <sup>c</sup>
	Silicon	Copper	Manganese	Magnesium	Chromium	Nickel	Zinc	Titanium	
6066	1.4	1.0	0.8	1.1	—	—	—	—	
6070	1.4	0.28	0.7	0.8	—	—	—	—	
6101	0.50	—	—	0.6	—	—	—	—	
6111	0.85	0.7	0.28	0.75	—	—	—	—	
6151	0.9	—	—	0.6	0.25	—	—	—	
6201	0.7	—	—	0.8	—	—	—	—	
6262	0.6	0.28	—	1.0	0.09	—	—	—	9
6351	1.0	—	0.6	0.6	—	—	—	—	
6951	0.35	0.28	—	0.6	—	—	—	—	
7005	—	—	0.45	1.4	0.13	—	4.5	0.04	10
7049	—	1.6	—	2.4	0.16	—	7.7	—	
7050	—	2.3	—	2.2	—	—	6.2	—	11
7072	—	—	—	—	—	—	1.0	—	
7075	—	1.6	—	2.5	0.23	—	5.6	—	
7116	—	0.8	—	1.1	—	—	4.7	—	12
7129	—	0.7	—	1.6	—	—	4.7	—	12
7175	—	1.6	—	2.5	0.23	—	5.6	—	5
7178	—	2.0	—	2.8	0.23	—	6.8	—	
7475	—	1.6	—	2.2	0.22	—	5.7	—	5
8017	—	0.15	—	0.03	—	—	—	—	13
8090	—	1.3	—	0.95	—	—	—	—	14
8176	0.09	—	—	—	—	—	—	—	13

<sup>a</sup>Based on industry handbooks.<sup>2,3</sup> Consult those references for specified limits. Values are nominal, i.e., middle range of limits for elements for which a composition range is specified.

<sup>b</sup>Aluminum and normal impurities constitute remainder.

<sup>c</sup>1. Percent minimum aluminum— for 1060: 99.60%; for 1100: 99.00%; for 1145: 99.45%; for 1350: 99.50%. Also, for 1100, 0.12% iron.

2. Formerly designated EC.
3. Also contains 0.05% vanadium (max.).
4. Also contains 0.40% lead and 0.4% bismuth.
5. This alloy has tighter limits on impurities than does its companion alloy (2024 or 7075).
6. Also contains 1.0% lithium, 0.42% silver, and 0.12% zirconium.
7. Also contains 0.10% vanadium plus 0.18% zirconium.
8. Also contains 1.1% iron.
9. Also contains 0.55% lead and 0.55% bismuth.
10. Also contains 0.14% zirconium.
11. Also contains 0.12% zirconium.
12. Also contains 0.05% max. vanadium plus 0.03% max. gallium.
13. Also contains 0.7% iron.
14. Also contains 2.4% lithium plus 0.10% zirconium.

fourth digits to make clear that these are designations to identify alloys in the form of castings or foundry ingot.

As for the wrought alloy designation system, the various digits of the cast alloy system convey information about the alloy:

- The first digit indicates the alloy group, as can be seen in Table 3. For 2xx.x through 8xx.x alloys, the alloy group is determined by the alloying element present in the greatest

**Table 3** Cast Alloy Designation System

Alloy	Main Alloying Element
1xx.x	Pure aluminum, 99.00% maximum
2xx.x	Copper
3xx.x	Silicon, with added copper and/or magnesium
4xx.x	Silicon
5xx.x	Magnesium
7xx.x	Zinc
8xx.x	Tin
9xx.x	Other elements
6xx.x	Unused series

mean percentage, except in cases in which the composition being registered qualifies as a modification of a previously registered alloy. Note that in Table 3 the 6xx.x series is shown last and for cast alloys is designated as the unused series.

- The second and third digits identify the specific aluminum alloy or, for the aluminum 1xx.x series, indicate purity. If the greatest mean percentage is common to more than one alloying element, the alloy group is determined by the element that comes first in sequence. For the 1xx.x group, the second two of the four digits in the designation indicate the minimum aluminum percentage. These digits are the same as the two digits to the right of the decimal point in the minimum aluminum percentage when expressed to the nearest 0.01%.
- The fourth digit indicates the product form: xxx.0 indicates castings and xxx.1 for the most part indicates ingot having limits for alloying elements the same as those for the alloy in the form of castings. A fourth digit of xxx.2 may be used to indicate that the ingot has composition limits that differ from but fall within the xxx.1 limits; this typically represents the use of tighter limits on certain impurities to achieve specific properties in the cast product produced from that ingot.
- A letter before the numerical designation indicates a modification of the original alloy or an impurity limit. These serial letters are assigned in alphabetical sequence starting with A, but omitting I, O, Q, and X, with X being reserved for experimental alloys. Note that explicit rules have been established for determining whether a proposed composition is a modification of an existing alloy or if it is a new alloy.

Experimental alloys of either the wrought or cast series are indicated by the addition of the prefix X. The prefix is dropped when the alloy is no longer experimental. However, during development and before an alloy is designated as experimental, a new composition may be identified by a serial number assigned by the originator. Use of the serial number is discontinued when the composition is registered with the Aluminum Association and the ANSI H35.1 designation is assigned.

The compositions of a representative group of widely used commercial cast aluminum alloys are given in Table 4, from *Standards for Aluminum Sand and Permanent Mold Castings*<sup>3</sup> and other aluminum casting industry publications.<sup>5,8-10</sup>

### 3.3 Aluminum Alloy Temper Designation System

The temper designation is always presented immediately following the alloy designation (Section 3.2), with a dash between the two, e.g., 2014-T6 or A356.0-T6.



**Table 4** Nominal Compositions of Aluminum Alloy Castings <sup>a</sup>

Alloy	Percent of Alloying Elements <sup>b</sup>								Notes <sup>c</sup>
	Silicon	Copper	Manganese	Magnesium	Chromium	Nickel	Zinc	Titanium	
201.0	—	4.6	0.35	0.35	—	—	—	0.25	1
204.0	—	4.6	—	0.25	—	—	—	—	
A206.0	—	4.6	0.35	0.25	—	—	—	0.22	
208.0	3.0	4.0	—	—	—	—	—	—	
213.0	2.0	7.0	—	—	—	—	2.5	—	2
222.0	—	10.0	—	0.25	—	—	—	—	
224.0	—	5.0	0.35	—	—	—	—	—	3
240.0	—	8.0	0.5	6.0	—	0.5	—	—	
242.0	—	4.0	—	1.5	—	2.0	—	—	
A242.0	—	4.1	—	1.4	0.20	2.0	—	0.14	
295.0	1.1	4.5	—	—	—	—	—	—	
308.0	5.5	4.5	—	—	—	—	—	—	
319.0	6.0	3.5	—	—	—	—	—	—	
328.0	8.0	1.5	0.40	0.40	—	—	—	—	
332.0	9.5	3.0	—	1.0	—	—	—	—	
333.0	9.0	3.5	—	0.28	—	—	—	—	
336.0	12.0	1.0	—	1.0	—	2.5	—	—	
354.0	9.0	1.8	—	0.5	—	—	—	—	
355.0	5.0	1.25	—	0.5	—	—	—	—	
C355.0	5.0	1.25	—	0.5	—	—	—	—	4
356.0	7.0	—	—	0.32	—	—	—	—	
A356.0	7.0	—	—	0.35	—	—	—	—	4
357.0	7.0	—	—	0.52	—	—	—	—	
A357.0	7.0	—	—	0.55	—	—	—	0.12	4, 5
359.0	9.0	—	—	0.6	—	—	—	—	
360.0	9.5	—	—	0.5	—	—	—	—	
A360.0	9.5	—	—	0.5	—	—	—	—	4
380.0	8.5	3.5	—	—	—	—	—	—	
A380.0	8.5	3.5	—	—	—	—	—	—	4
383.0	10.5	2.5	—	—	—	—	—	—	
384.0	11.2	3.8	—	—	—	—	—	—	
B390.0	17.0	4.5	—	0.55	—	—	—	—	
413.0	12.0	—	—	—	—	—	—	—	
A413.0	12.0	—	—	—	—	—	—	—	
443.0	5.2	—	—	—	—	—	—	—	
B443.0	5.2	—	—	—	—	—	—	—	4
C443.0	5.2	—	—	—	—	—	—	—	6
A444.0	7.0	—	—	—	—	—	—	—	
512.0	1.8	—	—	4.0	—	—	—	—	
513.0	—	—	—	4.0	—	—	1.8	—	
514.0	—	—	—	4.0	—	—	—	—	
518.0	—	—	—	8.0	—	—	—	—	
520.0	—	—	—	10.0	—	—	—	—	
535.0	—	—	0.18	6.8	—	—	—	0.18	7
705.0	—	—	0.5	1.6	0.30	—	3.0	—	
707.0	—	—	0.50	2.1	0.30	—	4.2	—	

(continued)

**Table 4** (Continued)

Alloy	Percent of Alloying Elements <sup>b</sup>								Notes <sup>c</sup>
	Silicon	Copper	Manganese	Magnesium	Chromium	Nickel	Zinc	Titanium	
710.0	—	0.50	—	0.7	—	—	6.5	—	
711.0	—	0.50	—	0.35	—	—	6.5	—	8
712.0	—	—	—	0.58	0.50	—	6.0	0.20	
713.0	—	0.7	—	0.35	—	—	7.5	—	
771.0	—	—	—	0.9	0.40	—	7.0	0.15	
850.0	—	1.0	—	—	—	1.0	—	—	9
851.0	2.5	1.0	—	—	—	0.50	—	—	9
852.0	—	2.0	—	0.75	—	1.2	—	—	9

<sup>a</sup>Based on industry handbooks,<sup>3,5,8-10</sup> consult those references for specified limits. Values are nominal, i.e., average of range of limits for elements for which a range is shown; values are representative of separately cast test bars, not of specimens taken from commercial castings.

<sup>b</sup>Aluminum and normal impurities constitute remainder.

- <sup>c</sup>
1. Also contains 0.7% silver.
  2. Also contains 1.2% iron.
  3. Also contains 0.10% vanadium and 0.18% zirconium.
  4. Impurity limits are much lower for this alloy than for alloy listed above it.
  5. Also contains 0.055% beryllium.
  6. Also contains up to 2.0% total iron.
  7. Also contains 0.005% beryllium and 0.005% boron.
  8. Also contains 1.0 iron.
  9. Also contains 6.2% tin.

The first character in the temper designation is a capital letter indicating the general class of treatment as follows:

- F = as fabricated  
 O = annealed  
 H = strain hardened  
 W = solution heat treated  
 T = thermally treated

Further information on each of these designations is provided by the descriptions that follow:

*F = as fabricated.* Applies to wrought or cast products made by shaping processes in which there is no special control over thermal conditions or strain-hardening processes employed to achieve specific properties. For wrought alloys there are no mechanical property limits associated with this temper, though for cast alloys there may be.

*O = annealed.* Applies to wrought products that are annealed to obtain the lower strength temper, usually to increase subsequent workability, and to cast products that are annealed to improve ductility and dimensional stability. The O may be followed by a digit other than zero.

*H = strain hardened.* Applies to products that have their strength increased by strain hardening. They may or may not have supplementary thermal treatments to produce some reduction in strength. The H is always followed by two or more digits.

*W* = solution heat treated. Applies only to alloys that age spontaneously after solution heat treating. This designation is specific only when digits are used in combination with W to indicate the period of natural aging, i.e., W $\frac{1}{2}$ h.

*T* = thermally treated to produce stable tempers other than *F*. Applies to products that are thermally treated with or without supplementary strain hardening to produce stable tempers. The T is always followed by one or more digits.

The most widely used temper designations above are the H and T categories, and these are always followed by from one to four numeric digits that provide more detail about how the alloy has been fabricated. It is beyond the scope of this volume to describe the system in further detail and the reader is referred to Refs. 2 and 6 for additional needed information.

## 4 MECHANICAL PROPERTIES OF ALUMINUM ALLOYS

The typical properties of a representative group of wrought aluminum alloys are shown in Table 5,<sup>2</sup> presented in engineering units in Table 5A and in metric units in Table 5B. The typical properties of a representative group of cast aluminum alloys are shown in Table 6<sup>3,8-10</sup> presented in engineering units in Table 6A and in metric units in Table 6B. In aluminum industry usage, the typical values are indicative of average or mean values for all products of the respective alloys. In the case of castings, the values represent average or mean values from tests of separately cast test bars for quality control purposes. *These are not intended and should not be used for design purposes.*

For design mechanical properties, readers are referred to the materials specifications,<sup>2,3</sup> including ASTM standards, and to design handbooks such as *The Aluminum Design Manual*<sup>4</sup> and MMPDS/MIL-HDBK-5.<sup>11</sup> For design rules and guidelines, readers are referred to *The Aluminum Design Manual*<sup>4</sup> and Refs. 12–16.

For the physical properties of wrought aluminum alloys, readers are referred to *Aluminum Standards and Data (Standard and Metric Editions)*<sup>2</sup> and for the physical properties of cast aluminum alloys to casting industry standards.<sup>3,8-10</sup>

**Table 5A** Typical Mechanical Properties of Wrought Aluminum Alloys (Engineering Units)<sup>a</sup>

Alloy & Temper	Tension				Hardness Brinell Number (500 kg/10 mm)	Shear Ultimate Strength (ksi)	Fatigue Endurance Limit <sup>d</sup> (ksi)	Modulus of Elasticity (10 <sup>3</sup> ksi)
	Ultimate Strength (ksi)	Yield Strength (ksi)	Elongation (%)					
			In 2 in. <sup>b</sup>	In 4D <sup>c</sup>				
1060-O	10	4	43	—	19	7	3	10.0
1060-H12	12	11	16	—	23	8	4	10.0
1060-H14	14	13	12	—	26	9	5	10.0
1060-H16	16	15	8	—	30	10	6.5	10.0
1060-H18	19	18	6	—	35	11	6.5	10.0
1100-O	13	5	35	45	23	9	5	10.0
1100-H12	16	15	12	25	28	10	6	10.0
1100-H14	18	17	9	20	32	11	7	10.0
1100-H16	21	20	6	17	38	12	9	10.0
1100-H18	24	22	5	15	44	13	9	10.0
1350-O	12	4	23 <sup>f</sup>	—	—	8	—	10.0
1350-H12	14	12	—	—	—	9	—	10.0

(continued)

## 74 Aluminum Alloys

**Table 5A** (Continued)

Alloy & Temper	Tension				Hardness Brinell Number (500 kg/10 mm)	Shear Ultimate Strength (ksi)	Fatigue Endurance Limit <sup>d</sup> (ksi)	Modulus <sup>e</sup> of Elasticity (10 <sup>3</sup> ksi)
	Ultimate Strength (ksi)	Yield Strength (ksi)	Elongation (%)					
			In 2 in. <sup>b</sup>	In 4D <sup>c</sup>				
1350-H14	16	14	—	—	—	10	—	10.0
1350-H16	18	16	—	—	—	11	—	10.0
1350-H19	27	24	1.5 <sup>f</sup>	—	—	15	—	10.0
2008-T4	36	18	28	—	21	—	10.2	
2010-T4	35	19	25	21	8	10.2		
2011-T3	55	43	—	15	96	32	18	10.2
2011-T8	59	45	—	12	100	35	18	10.2
2014-O	27	14	—	18	45	18	13	10.6
2014-T4, T451	62	42	—	20	105	38	20	10.6
2014-T6, T651	70	60	—	13	135	42	18	10.6
2017-O	26	10	—	22	45	18	13	10.5
2017-T4, T451	62	40	—	22	105	38	18	10.5
2024-O	27	11	20	22	47	18	13	10.6
2024-T3	70	50	18	—	120	41	20	10.6
2024-T4, T351	68	47	20	19	120	41	20	10.6
2024-T361	72	57	13	—	130	42	18	10.6
2025-T6	58	37	—	19	110	35	18	10.4
2036-T4	49	28	24	—	—	—	18 <sup>g</sup>	10.3
2117-T4	43	24	—	27	70	28	14	10.3
2124-T851	70	64	—	8	—	—	—	10.6
2195-T351	52	36	17	—	—	—	—	10.6
2195-T851	66	51	10	—	—	—	—	10.6
2219-O	25	11	18	—	—	—	—	10.6
2219-T62	60	42	10	—	—	—	15	10.6
2219-T81, T851	66	51	10	—	—	—	15	10.6
2219-T87	69	57	10	—	—	—	15	10.6
2618-T61	64	54	—	10	115	38	18	10.8
3003-O	16	6	30	40	28	11	7	10.0
3003-H12	19	18	10	20	35	12	8	10.0
3003-H14	22	21	8	16	40	14	9	10.0
3003-H16	26	25	5	14	47	15	10	10.0
3003-H18	29	27	4	10	55	16	10	10.0
3004-O	26	10	20	25	45	16	14	10.0
3004-H32	31	25	10	17	52	17	15	10.0
3004-H34	35	29	9	12	63	18	15	10.0
3004-H36	38	33	5	9	70	20	16	10.0
3004-H38	41	36	5	6	77	21	16	10.0
3105-O	17	8	24	—	—	12	—	10.0
3105-H12	22	19	7	—	—	14	—	10.0
3105-H14	25	22	5	—	—	15	—	10.0
3105-H16	28	25	4	—	—	16	—	10.0
3105-H18	31	28	3	—	—	17	—	10.0
3105-H25	26	23	8	—	—	15	—	10.0
4032-T6	55	46	9	120	38	16	11.4	

Table 5A (Continued)

Alloy & Temper	Tension				Hardness Brinell Number (500 kg/10 mm)	Shear Ultimate Strength (ksi)	Fatigue Endurance Limit <sup>d</sup> (ksi)	Modulus <sup>e</sup> of Elasticity (10 <sup>3</sup> ksi)
	Ultimate Strength (ksi)	Yield Strength (ksi)	Elongation (%)					
			In 2 in. <sup>b</sup>	In 4D <sup>c</sup>				
5005-O	18	6	25	—	28	11	—	10.0
5005-H32	20	17	11	—	36	14	—	10.0
5005-H34	23	20	8	—	41	14	—	10.0
5005-H36	26	24	6	—	46	15	—	10.0
5005-H38	29	27	6	—	51	16	—	10.0
5050-O	21	8	24	—	36	15	12	10.0
5050-H32	25	21	9	—	46	17	13	10.0
5050-H34	28	24	8	—	53	18	13	10.0
5050-H36	30	26	7	—	58	19	14	10.0
5050-H38	32	29	6	—	63	20	14	10.0
5052-O	28	13	25	30	47	18	16	10.2
5052-H32	33	28	12	18	60	20	17	10.2
5052-H34	38	31	10	14	68	21	18	10.2
5052-H36	40	35	8	10	73	23	19	10.2
5052-H38	42	37	7	8	77	24	20	10.2
5056-O	42	22	—	35	65	26	20	10.3
5056-H18	63	59	—	10	105	34	22	10.3
5056-H38	60	50	—	15	100	32	22	10.3
5083-O	42	21	—	22	—	25	—	10.3
5083-H116	46	33	—	16	—	—	23	10.3
5083-H321	46	33	—	16	—	—	23	10.3
5086-O	38	17	22	—	—	23	—	10.3
5086-H32	42	30	12	—	—	—	—	10.3
5086-H34	47	37	10	—	—	27	—	10.3
5086-H116	42	30	12	—	—	—	—	10.3
5154-O	35	17	27	—	58	22	17	10.2
5154-H32	39	30	15	—	67	22	18	10.2
5154-H34	42	33	13	—	73	24	19	10.2
5154-H36	45	36	12	—	78	26	20	10.2
5154-H38	48	39	10	—	80	28	21	10.2
5454-O	36	17	22	—	62	23	—	10.2
454-H32	40	30	10	—	73	24	—	10.2
5454-H34	44	35	10	—	81	26	—	10.2
5454-H111	38	26	14	—	70	23	—	10.2
5456-O	45	23	—	24	—	—	—	10.3
5456-H116	51	37	—	16	90	30	—	10.3
5456-H321	51	37	—	16	90	30	—	10.3
5657-H25	23	20	12	—	40	12	—	10.0
5657-H28, H38	28	24	7	—	50	15	—	10.0
5754-O	32	14	26	—	—	19	—	10.3
6009-T4	32	18	25	—	—	19	—	10.0
6022-T4	37	22	26	—	—	22	—	10.0
6061-O	18	8	25	30	30	12	9	10.0
6061-T4, T451	35	21	22	25	65	24	14	10.0
6061-T6, T651	45	40	12	17	95	30	14	10.0

(continued)

## 76 Aluminum Alloys

**Table 5A** (Continued)

Alloy & Temper	Tension				Hardness Brinell Number (500 kg/10 mm)	Shear Ultimate Strength (ksi)	Fatigue Endurance Limit <sup>d</sup> (ksi)	Modulus <sup>e</sup> of Elasticity (10 <sup>3</sup> ksi)
	Ultimate Strength (ksi)	Yield Strength (ksi)	Elongation (%)					
			In 2 in. <sup>b</sup>	In 4D <sup>c</sup>				
6063-O	13	7	—	—	25	10	8	10.0
6063-T4	25	13	22	—	—	—	—	10.0
6063-T5	27	21	12	—	60	17	10	10.0
6063-T6	35	31	12	—	73	22	10	10.0
6063-T83	37	35	9	—	82	22	—	10.0
6066-O	22	12	—	18	43	14	—	10.0
6066-T4, T451	52	30	—	18	90	29	—	10.0
6066-T6, T651	57	52	—	12	120	34	16	10.0
6070-T6	55	51	10	—	—	34	14	10.0
6101-H111	14	11	—	—	—	—	—	10.0
6101-T6	32	28	15	—	71	20	—	10.0
6111-T4	42	22	26	—	—	25	—	10.0
6111-T41	39	22	26	—	—	23	—	10.0
6262-T9	58	55	—	10	120	35	13	10.0
6351-T4	36	22	20	—	—	44	—	10.0
6351-T6	45	41	14	—	95	29	13	10.0
7049-T73	75	65	—	12	135	44	—	10.4
7049-T7352	75	63	—	11	135	43	10.4	—
7050-T7351X	72	63	—	12	—	—	—	10.4
7050-T7451	76	68	—	11	—	44	—	10.4
7050-T7651	80	71	—	11	—	47	—	10.4
7075-O	33	15	17	16	60	22	—	10.4
7075-T6, T651	83	73	11	11	150	48	23	10.4
7175-T74	76	66	11	135	42	23	10.4	—
7178-O	33	15	16	—	—	—	—	10.4
7178-T6, T651	88	78	11	—	—	—	—	10.4
7178-T76, T7651	83	73	11	—	—	—	—	10.4
7475-T61	82	71	11	—	—	—	—	10.4
7475-T651	85	74	—	13	—	—	—	10.4
7475-T7351	72	61	—	13	—	—	—	10.4
7475-T761	75	65	12	—	—	—	—	10.4
7475-T7651	77	67	—	12	—	—	—	10.4
8176-H24	17	14	15	—	80	—	—	10.0

<sup>a</sup>Based on *Aluminum Standards and Data*.<sup>2</sup> Consult that reference for limits. For tensile yield strengths, offset = 0.2%.

<sup>b</sup>Elongation measured over 2 in. gauge length on  $\frac{1}{16}$ -in.-thick sheet-type specimens.

<sup>c</sup>Elongation measured over 2 in. gauge length (4D) in  $\frac{1}{2}$ -in.-diameter specimens.

<sup>d</sup>Based on 500,000,000 cycles of completely reversed stress using R. R. Moore type of machines and specimens.

<sup>e</sup>Average of tension and compression moduli; compressive modulus is nominally about 2% greater than the tension modulus.

<sup>f</sup>Measured over 10 in. gauge length in wire.

<sup>g</sup>At 10<sup>7</sup> cycles with flexural fatigue specimens.



**Table 5B** Typical Mechanical Properties of Wrought Aluminum Alloys (Metric Units)<sup>a</sup> Alloy and Temper

Alloy & Temper	Tension				Hardness Brinell Number (500 kg/10 mm)	Shear Ultimate Strength (MPa)	Fatigue Endurance Limit <sup>d</sup> (MPa)	Modulus of Elasticity (GPa)
	Ultimate Strength (MPa)	Yield Strength (MPa)	Elongation (%)					
			in 50 mm <sup>b</sup>	in 5D <sup>c</sup>				
1060-O	70	30	43	—	19	50	20	69
1060-H12	85	75	16	—	23	55	30	69
1060-H14	100	90	12	—	26	60	35	69
1060-H16	115	105	8	—	30	70	45	69
1060-H18	130	125	6	—	35	75	45	69
1100-O	90	35	35	42	23	60	35	69
1100-H12	110	105	12	22	28	70	40	69
1100-H14	125	115	9	18	32	75	50	69
1100-H16	145	140	6	15	38	85	60	69
1100-H18	165	150	5	13	44	90	60	69
1350-O	85	30	23 <sup>f</sup>	—	—	55	—	69
1350-H12	95	85	—	—	—	60	—	69
1350-H14	110	95	—	—	—	70	—	69
1350-H16	125	110	—	—	—	75	—	69
1350-H19	185	165	1.5 <sup>f</sup>	—	—	105	—	69
2008-T4	250	125	28	—	145	70	—	70
2010-T4, T41	240	130	25	—	145	70	—	70
2011-T3	380	295	—	13	95	220	125	70
2011-T8	405	310	—	10	100	240	125	70
2014-O	185	95	—	16	45	125	90	73
2014-T4, T451	425	290	—	18	105	260	140	73
2014-T6, T651	485	415	—	11	135	290	125	73
2017-O	180	70	—	20	45	125	90	73
2017-T4, T451	425	275	—	20	105	260	125	73
2024-O	185	75	20	20	47	125	90	73
2024-T3	485	345	18	—	120	285	140	73
2024-T4, T351	472	325	20	17	120	285	140	73
2024-T361	495	395	13	—	130	290	125	73
2025-T6	400	255	—	17	110	240	125	72
2036-T4	340	195	24	—	—	205	125 <sup>g</sup>	71
2117-T4	295	165	—	24	70	195	95	71
2124-T851	485	440	—	8	—	—	—	73
2195-T351	360	250	17	—	—	—	—	73
2195-T851	455	350	10	—	—	—	—	73
2219-O	170	75	18	—	—	—	—	73
2219-T62	415	290	10	—	—	—	105	73
2219-T81, T851	455	350	10	—	—	—	105	73
2219-T87	475	395	10	—	—	—	105	73
2618-T61	440	370	10	115	260	90	73	
3003-O	110	40	30	37	28	75	50	69
3003-H12	130	125	10	18	35	85	55	69
3003-H14	150	145	8	14	40	95	60	69
3003-H16	175	170	5	12	47	105	70	69
3003-H18	200	185	4	9	55	110	70	69
3004-O	180	70	20	22	45	110	95	69
3004-H32	215	170	10	15	52	115	105	69

(continued)

Table 5B (Continued)

Alloy & Temper	Tension				Hardness Brinell Number (500 kg/10 mm)	Shear Ultimate Strength (MPa)	Fatigue Endurance Limit <sup>d</sup> (MPa)	Modulus <sup>e</sup> of Elasticity (GPa)
	Ultimate Strength (MPa)	Yield Strength (MPa)	Elongation (%)					
			in 50 mm <sup>b</sup>	in 5D <sup>c</sup>				
3004-H34	240	200	9	10	63	125	105	69
3004-H36	260	230	5	8	70	140	110	69
3004-H38	285	250	5	5	77	145	110	69
3105-O	115	55	24	—	—	85	—	69
3105-H12	150	130	7	—	—	95	—	69
3105-H14	170	150	5	—	—	105	—	69
3105-H16	195	170	4	—	—	110	—	69
3105-H18	215	195	3	—	—	115	—	69
3105-H25	180	160	8	—	—	95	—	69
4032-T6	380	315	—	9	120	260	110	79
5005-O	125	40	25	—	28	75	—	69
5005-H32	140	115	11	—	36	95	—	69
5005-H34	160	140	8	—	41	95	—	69
5005-H36	180	165	6	—	46	105	—	69
5005-H38	200	185	5	—	51	110	—	69
5050-O	145	55	24	—	36	105	85	69
5050-H32	170	145	9	—	46	115	90	69
5050-H34	190	165	8	—	53	125	90	69
5050-H36	205	180	7	—	58	130	95	69
5050-H38	220	200	6	—	63	140	95	69
5052-O	195	90	25	27	47	125	110	70
5052-H32	230	195	12	16	60	140	115	70
5052-H34	260	215	10	12	68	145	125	70
5052-H36	275	240	8	9	73	160	130	70
5052-H38	290	255	7	7	77	165	140	70
5056-O	290	150	—	32	65	180	140	71
5056-H18	435	405	—	9	105	235	150	71
5056-H38	415	345	—	13	100	220	150	71
5083-O	290	145	—	20	—	170	—	71
5083-H116	315	230	—	14	—	—	160	71
5083-H321	315	230	—	14	—	—	160	71
5086-O	260	115	22	—	—	165	—	71
5086-H32	290	205	12	—	—	—	—	71
5086-H34	325	255	10	—	—	185	—	71
5086-H116	290	205	12	—	—	—	—	71
5154-O	240	115	27	—	58	150	115	70
5154-H32	270	205	15	—	67	150	125	70
5154-H34	290	230	13	—	73	165	130	70
5154-H36	310	250	12	—	78	180	140	70
5154-H38	330	270	10	—	80	195	145	70
5454-O	250	115	22	—	62	160	—	70
5454-H32	275	205	10	—	73	165	—	70
5454-H34	305	240	10	—	81	180	—	70
5454-H111	260	180	14	—	70	160	—	70
5456-O	310	160	—	22	—	—	—	71
5456-H116	350	255	—	14	90	205	—	71
5456-H321	350	255	—	14	90	205	—	71

Table 5B (Continued)

Alloy & Temper	Tension				Hardness Brinell Number (500 kg/10 mm)	Shear Ultimate Strength (MPa)	Fatigue Endurance Limit <sup>d</sup> (MPa)	Modulus of Elasticity (GPa)
	Ultimate Strength (MPa)	Yield Strength (MPa)	Elongation (%)					
			in 50 mm <sup>b</sup>	in 5D <sup>c</sup>				
5657-H25	160	140	12	—	40	95	—	69
5657-H28, H38	195	165	7	—	50	105	—	69
5754-O	220	100	26	—	—	130	—	71
6009-T4	220	125	25	—	—	130	—	69
6061-O	125	55	25	27	30	85	60	69
6061-T4, T451	240	145	22	22	65	165	95	69
6061-T6, T651	310	275	12	15	95	205	95	69
6063-O	90	50	—	—	25	70	55	69
6063-T4	170	90	22	—	—	—	—	69
6063-T5	185	145	12	—	60	115	70	69
6063-T6	240	215	12	—	73	150	70	69
6063-T83	255	240	9	—	82	150	—	69
6066-O	150	85	—	16	43	95	—	69
6066-T4, T451	360	205	—	16	90	200	—	69
6066-T6, T651	395	360	—	10	120	235	110	69
6070-T6	380	350	10	—	—	235	95	69
6101-H111	95	75	—	—	—	—	—	69
6101-T6	220	195	15 <sup>f</sup>	—	71	140	—	69
6111-T4	280	150	26	—	—	175	—	69
6111-T41	270	150	26	—	—	160	—	69
6262-T9	400	380	—	9	120	240	90	69
6351-T4	250	150	20	—	—	44	—	69
6351-T6	310	285	14	—	95	200	90	69
7049-T73	515	450	—	10	135	305	—	72
7049-T7352	515	435	—	9	135	295	—	72
7050-T7351X	495	435	—	11	—	—	—	72
7050-T7451	525	470	—	10	—	305	—	72
7050-T7651	550	490	—	10	—	325	—	72
7075-O	230	105	17	14	60	150	—	72
7075-T6, T651	570	505	11	9	150	330	160	72
7175-T74	525	455	—	10	135	290	160	72
7178-O	230	105	15	14	—	—	—	72
7178-T6, T651	605	540	10	9	—	—	—	72
7178-T76, T7651	570	505	11	9	—	—	—	71
7475-T61	565	490	11	—	—	—	—	70
7475-T651	585	510	—	13	—	—	—	72
7475-T7351	495	420	—	13	—	—	—	72
7475-T761	515	450	12	—	—	—	—	70
7475-T7651	530	460	—	12	—	—	—	72
8176-H24	160	95	15	—	—	70	—	10

<sup>a</sup>Based on *Aluminum Standards and Data*.<sup>2</sup> Consult that reference for limits. For tensile yield strengths, offset = 0.2%.

<sup>b</sup>Elongation measured over 500 mm gauge length on 1.60-mm-thick sheet-type specimens.

<sup>c</sup>Elongation measured over 500 mm gauge length (5D) in 12.5-mm-diameter specimens.

<sup>d</sup>Based on 500,000,000 cycles of completely reversed stress using R. R. Moore type of machines and specimens.

<sup>e</sup>Average of tension and compression moduli; compressive modulus is nominally about 2% greater.

<sup>f</sup>Measured over 250 mm gauge length in wire.

<sup>g</sup>At 10<sup>7</sup> cycles with flexural fatigue specimens.

**Table 6A** Typical Mechanical Properties of Wrought Aluminum Alloy Castings (Engineering Units)<sup>a</sup>

Alloy and Temper	Tension			Hardness Brinell Number (500 kg / 10 mm)	Shear Ultimate Strength (ksi)	Fatigue Endurance Limit <sup>b</sup> (ksi)	Modulus of Elasticity (10 <sup>3</sup> ksi)
	Ultimate Strength (ksi)	Yield Strength (ksi)	Elongation in 2 in. or 4D (%)				
<b>Sand Cast</b>							
201.0-T6	65	55	8	130	—	—	—
201.0-T7	68	60	6	—	—	14	—
201.0-T43	60	37	17	—	—	—	—
204.0-T4	45	28	6	—	—	—	—
A206.0-T4	51	36	7	—	40	—	—
208.0-F	21	14	3	—	17	11	—
213.0-F	24	15	2	70	20	9	—
222.0-O	27	20	1	80	21	9.5	—
222.0-T61	41	40	< 0.5	115	32	8.5	10.7
224.0-T72	55	40	10	123	35	9	10.5
240.0-F	34	28	1	90	—	—	—
242.0-F	31	20	1	—	—	—	10.3
242.0-O	27	18	1	70	21	8	10.3
242.0-T571	32	30	1	85	26	11	10.3
242.0-T61	32	20	—	90–120	—	—	10.3
242.0-T77	30	23	2	75	24	10.5	10.3
A242.0-T75	31	—	2	—	—	—	—
295.0-T4	32	16	9	80	26	7	10.0
295.0-T6	36	24	5	75	30	7.5	10.0
295.0-T62	41	32	2	90	33	8	10.0
295.0-T7	29	16	3	55–85	—	—	10.0
319-F	27	18	2	70	22	10	10.7
319.0-T5	30	26	2	80	24	11	10.7
319.0-T6	36	24	2	80	29	11	10.7
328.0-F	25	14	1	45–75	—	—	—
328.0-T6	34	21	1	65–95	—	—	—
355.0-F	23	12	3	—	—	—	10.2
355.0-T51	28	23	2	65	22	8	10.2
355.0-T6	35	25	3	80	28	9	10.2
355.0-T61	35	35	1	90	31	9.5	10.2
355.0-T7	38	26	1	85	28	10	10.2
355.0-T71	35	29	2	75	26	10	10.2
C355.0-T6	39	29	5	85	—	—	—
356.0-F	24	18	6	—	—	—	10.5
356.0-T51	25	20	2	60	20	8	10.5
356.0-T6	33	24	4	70	26	8.5	10.5
356.0-T7	34	30	2	75	24	9	10.5
356.0-T71	28	21	4	60	20	8.5	10.5
A356.0-F	23	12	6	—	—	—	10.5
A356.0-T51	26	18	3	—	—	—	10.5
A356.0-T6	40	30	6	75	—	—	10.5
A356.0-T71	30	20	3	—	—	—	10.5
357.0-F	25	13	5	—	—	—	—
357.0-T51	26	17	3	—	—	—	—
357.0-T6	50	43	2	—	—	—	—
357.0-T7	40	34	3	60	—	—	—
A357.0-T6	46	36	3	85	40	12	—

Table 6A (Continued)

Alloy and Temper	Tension			Hardness Brinell Number (500 kg / 10 mm)	Shear Ultimate Strength (ksi)	Fatigue Endurance Limit <sup>b</sup> (ksi)	Modulus <sup>c</sup> of Elasticity (10 <sup>3</sup> ksi)
	Ultimate Strength (ksi)	Yield Strength (ksi)	Elongation in 2 in. or 4D (%)				
359.0-T62	50	42	6	—	—	—	—
A390.0-F	26	26	< 1.0	100	—	—	—
A390.0-T5	26	26	< 1.0	100	—	—	—
A390.0-T6	40	40	< 1.0	140	—	13	—
A390.0-T7	36	36	< 1.0	115	—	—	—
443.0-F	19	8	8	40	14	8	10.3
B443.0-F	17	6	3	25–55	—	—	—
A444.0-F	21	9	9	44	—	—	—
A444.0-T4	23	9	12	45	—	—	—
511.0-F	21	12	3	50	17	8	—
512.0-F	20	13	2	50	17	9	—
514.0-F	25	12	9	50	20	7	—
520.0-T4	48	26	16	75	34	8	—
535.0-F	35	18	9	60–90	—	—	—
535.0-T5	35	18	9	60–90	—	—	—
A535.0-F	36	18	9	65	—	—	—
707.0-T5	33	22	2	70–100	—	—	—
707.0-T7	37	30	1	65–95	—	—	—
710.0-F	32	20	2	60–90	—	—	—
710.0-T5	32	20	2	60–90	—	—	—
712.0-F	34	25	4	60–90	—	—	—
712.0-T5	34	25	4	60–90	—	—	—
713.0-F	32	22	3	60–90	—	—	—
713.0-T5	32	22	3	60–90	—	—	—
771.0-T5	32	27	3	70–100	—	—	—
771.0-T52	36	30	2	70–100	—	—	—
771.0-T53	36	27	2	—	—	—	—
771.0-T6	42	35	5	75–105	—	—	—
771.0-T71	48	45	2	105–135	—	—	—
850.0-T5	20	11	8	45	14	—	10.3
851.0-T5	20	11	5	45	14	—	10.3
852.0-T5	27	22	2	65	18	10	10.3
<b>Permanent Mold</b>							
201.0-T6	65	55	8	130	—	—	—
201.0-T7	68	60	6	—	—	14	—
201.0-T43	60	37	17	—	—	—	—
204.0-T4	48	29	8	—	—	—	—
A206.0-T4	62	38	17	—	42	—	—
A206.0-T7	63	50	12	—	37	—	—
208.0-T6	35	22	2	75–105	—	—	—
208.0-T7	33	16	3	65–95	—	—	—
213.0-F	30	24	2	85	24	9.5	—
222.0-T551	37	35	< 0.5	115	30	8.5	10.7
222.0-T52	35	31	1	100	25	—	10.7
238.0-F	30	24	2	100	24	—	—
242.0-T571	40	34	1	105	30	10.5	10.3
242.0-T61	47	42	1	110	35	10	10.3

(continued)

## 82 Aluminum Alloys

**Table 6A** (Continued)

Alloy and Temper	Tension			Hardness Brinell Number (500 kg / 10 mm)	Shear Ultimate Strength (ksi)	Fatigue Endurance Limit <sup>b</sup> (ksi)	Modulus <sup>c</sup> of Elasticity (10 <sup>3</sup> ksi)
	Ultimate Strength (ksi)	Yield Strength (ksi)	Elongation in 2 in. or 4D (%)				
A249.0-T63	69	60	6	—	—	—	—
296.0-T7	39	20	5	80	30	9	10.1
308.0-F	28	16	2	70	22	13	—
319.0-F	34	19	3	85	24	—	10.7
319.0-T6	40	27	3	95	—	—	10.7
324.0-F	30	16	4	70	—	—	—
324.0-T5	36	26	3	90	—	—	—
324.0-T62	45	39	3	105	—	—	—
332.0-T5	36	28	1	105	—	—	—
328.0-T6	34	21	1	65–95	—	—	—
333.0-F	34	19	2	90	27	15	—
333.0-T5	34	25	1	100	27	12	—
333.0-T6	42	30	2	105	33	15	—
333.0-T7	37	28	2	90	28	12	—
336.0-T551	36	28	1	105	28	14	—
336.0-T65	47	43	1	125	36	—	—
354.0-T61	48	37	3	—	—	—	—
354.0-T62	52	42	2	—	—	—	—
355.0-F	27	15	4	—	—	—	10.2
355.0-T51	30	24	2	75	24	—	10.2
355.0-T6	42	27	4	90	34	10	10.2
355.0-T61	45	40	2	105	36	10	10.2
355.0-T7	40	30	2	85	30	10	10.2
355.0-T71	36	31	3	85	27	10	10.2
C355.0-T6	48	28	8	90	—	—	10.2
C355.0-T61	46	34	6	100	—	—	10.2
C355.0-T62	48	37	5	100	—	—	10.2
356.0-F	26	18	5	—	—	—	10.5
356.0-T51	27	20	2	—	—	—	10.5
356.0-T6	38	27	5	80	30	13	10.5
356.0-T7	32	24	6	70	25	11	10.5
356.0-T71	25	—	3	60–90	—	—	10.5
A356.0-F	27	13	8	—	—	—	10.5
A356.0-T51	29	20	5	—	—	—	10.5
A356.0-T6	41	30	12	80	—	—	10.5
357.0-F	28	15	6	—	—	—	—
357.0-T51	29	21	4	—	—	—	—
357.0-T6	52	43	5	100	35	13	—
357.0-T7	38	30	5	70	—	—	—
A357.0-T6	52	42	5	100	35	15	—
359.0-T61	48	37	6	—	—	—	—
359.0-T62	50	42	6	—	—	16	—
A390.0-F	29	29	< 1.0	110	—	—	—
A390.0-T5	29	29	< 1.0	110	—	—	—
A390.0-T6	45	45	< 1.0	145	—	17	—
A390.0-T7	38	38	< 1.0	120	—	15	—
443.0-F	23	9	10	45	16	8	10.3
B443.0-F	21	6	6	30–60	—	—	—
A444.0-F	24	11	13	44	—	—	—

**Table 6A** (Continued)

Alloy and Temper	Tension			Hardness Brinell Number (500 kg / 10 mm)	Shear Ultimate Strength (ksi)	Fatigue Endurance Limit <sup>b</sup> (ksi)	Modulus <sup>c</sup> of Elasticity (10 <sup>3</sup> ksi)
	Ultimate Strength (ksi)	Yield Strength (ksi)	Elongation in 2 in. or 4D (%)				
A444.0-T4	23	10	21	45	16	8	—
513.0-F	27	16	7	60	22	10	—
535.0-F	35	18	8	60–90	—	—	—
705.0-T5	37	17	10	55–75	—	—	—
707.0-T7	45	35	3	80–110	—	—	—
711.0-T1	28	18	7	55–85	—	—	—
713.0-T5	32	22	4	60–90	—	—	—
850.0-T5	23	11	12	45	15	9	10.3
851.0-T5	20	11	5	45	14	9	10.3
851.0-T6	18	—	8	—	—	—	10.3
852.0-T5	32	23	5	70	21	11	10.3
<b>Die Cast</b>							
360.0-F	44	25	3	75	28	20	10.3
A360.0-F	46	24	4	75	26	18	10.3
380.0-F	46	23	3	80	28	20	10.3
A380.0-F	47	23	4	80	27	20	10.3
383.0-F	45	22	4	75	—	21	10.3
384.0-F	48	24	3	85	29	20	—
390.0-F	40.5	35	< 1	—	—	—	—
B390.0-F	46	36	< 1	120	—	20	11.8
392.0-F	42	39	< 1	—	—	—	—
413.0-F	43	21	3	80	25	19	10.3
A413.0-F	42	19	4	80	25	19	—
C443.0-F	33	14	9	65	29	17	10.3
518.0-F	45	28	5	80	29	20	—

<sup>a</sup>Based upon industry handbooks.<sup>3,8–10</sup> Consult those references for limits. Values are representative of separately cast test bars, not of specimens taken from commercial castings. For tensile yield strengths, offset = 0.2%.

<sup>b</sup>Based on 500,000,000 cycles of completely reversed stress using R. R. Moore type of machines and specimens.

<sup>c</sup>Average of tension and compression moduli; compressive modulus is nominally about 2% greater than the tension modulus.

**Table 6B** Typical Mechanical Properties of Aluminum Alloy Castings (Metric Units)<sup>a</sup>

Alloy and Temper	Tension			Hardness Brinell Number (500 kg / 10 mm)	Shear Ultimate Strength (MPa)	Fatigue Endurance Limit <sup>b</sup> (MPa)	Modulus <sup>c</sup> of Elasticity (GPa)
	Ultimate Strength (MPa)	Yield Strength (MPa)	Elongation in 5D (%)				
<b>Sand Cast</b>							
201.0-T6	450	380	8	130	—	—	—
201.0-T7	470	415	6	—	—	95	—
201.0-T43	415	255	17	—	—	—	—
204.0-T4	310	195	6	—	—	—	—
A206.0-T4	350	250	7	—	275	—	—
2008.0-F	145	655	3	—	115	75	—

(continued)



## 84 Aluminum Alloys

**Table 6B** (Continued)

Alloy and Temper	Tension			Hardness Brinell Number (500 kg / 10 mm)	Shear Ultimate Strength (MPa)	Fatigue Endurance Limit <sup>b</sup> (MPa)	Modulus of Elasticity (GPa)
	Ultimate Strength (MPa)	Yield Strength (MPa)	Elongation in 5D (%)				
213.0-F	165	105	2	70	140	60	—
222.0-O	185	140	1	80	145	65	—
222.0-T61	285	275	< 0.5	115	220	60	74
224.0-T72	380	275	10	123	240	60	73
240.0-F	235	195	1	90	—	—	—
242.0-F	145	140	1	—	—	—	71
242.0-O	185	125	1	70	145	55	71
242.0-T571	220	205	1	85	180	75	71
242.0-T61	220	140	—	90–120	—	—	71
242.0-T77	205	160	2	75	165	70	71
A242.0-T75	215	—	2	—	—	—	—
295.0-T4	220	110	9	80	180	50	69
295.0-T6	250	165	5	75	205	50	69
295.0-T62	285	220	2	90	230	55	69
295.0-T7	200	110	3	55–85	—	—	69
319-F	185	125	2	70	150	70	74
319.0-T5	205	180	2	80	165	75	74
319.0-T6	250	165	2	80	200	75	74
328.0-F	170	95	1	45–75	—	—	—
328.0-T6	235	145	1	65–95	—	—	—
355.0-F	160	85	3	—	—	—	70
355.0-T51	195	160	2	65	150	55	70
355.0-T6	240	170	3	80	195	60	70
355.0-T61	240	240	1	90	215	65	70
355.0-T7	260	180	1	85	195	70	70
355.0-T71	240	200	2	75	180	70	70
C355.0-T6	270	200	5	85	—	—	—
356.0-F	165	125	6	—	—	—	73
356.0-T51	170	140	2	60	140	55	73
356.0-T6	230	165	4	70	180	60	73
356.0-T7	235	205	2	75	165	60	73
356.0-T71	195	145	4	60	140	60	73
A356.0-F	160	85	6	—	—	—	73
A356.0-T51	180	125	3	—	—	—	73
A356.0-T6	275	205	6	75	—	—	73
A356.0-T71	205	140	3	—	—	—	73
357.0-F	170	90	5	—	—	—	—
357.0-T51	180	115	3	—	—	—	—
357.0-T6	345	295	2	—	—	—	—
357.0-T7	275	235	3	60	—	—	—
A357.0-T6	315	250	3	85	275	95	—
359.0-T62	345	290	6	16	—	—	—
A390.0-F	180	180	< 1.0	100	—	—	—
A390.0-T5	180	180	< 1.0	100	—	—	—
A390.0-T6	275	275	< 1.0	140	—	90	—
A390.0-T7	250	250	< 1.0	115	—	—	—
443.0-F	130	55	8	40	95	55	71
B443.0-F	115	40	3	25–55	—	—	—

Table 6B (Continued)

Alloy and Temper	Tension			Hardness Brinell Number (500 kg / 10 mm)	Shear Ultimate Strength (MPa)	Fatigue Endurance Limit <sup>b</sup> (MPa)	Modulus <sup>c</sup> of Elasticity (GPa)
	Ultimate Strength (MPa)	Yield Strength (MPa)	Elongation in 5D (%)				
A444.0-F	145	60	9	43,400	—	—	—
A444.0-T4	23	60	12				
511.0-F	145	85	3	50	115	55	
512.0-F	140	90	2	50	115	60	
514.0-F	170	85	9	50	140	50	—
520.0-T4	330	180	16	75	235	55	—
535.0-F	240	125	9	60–90	—	—	—
535.0-T5	240	125	9	60–90	—	—	—
A535.0-F	250	125	9	65	—	—	—
707.0-T5	230	150	2	70–100	—	—	—
707.0-T7	255	205	1	65–95	—	—	—
710.0-F	220	140	2	60–90	—	—	—
710.0-T5	220	140	2	60–90	—	—	—
712.0-F	235	170	4	60–90	—	—	—
712.0-T5	235	170	4	60–90	—	—	—
713.0-F	220	150	3	60–90	—	—	—
713.0-T5	220	150	3	60–90	—	—	—
771.0-T5	220	185	3	70–100	—	—	—
771.0-T52	250	205	2	70–100	—	—	—
771.0-T53	250	185	2	—	—	—	—
771.0-T6	290	240	5	75–105	—	—	—
771.0-T71	330	310	2	105–135	—	—	—
850.0-T5	140	75	8	45	95	—	71
851.0-T5	140	75	5	45	95	—	71
852.0-T5	185	150	2	n65	125	60	71
<b>Permanent Mold</b>							
201.0-T6	450	380	8	130	—	—	—
201.0-T7	470	415	6	—	—	95	—
201.0-T43	415	255	17	—	—	—	—
204.0-T4	330	200	8	—	—	—	—
A206.0-T4	430	260	17	—	290	—	—
A206.0-T7	435	345	12	—	255	—	—
208.0-T6	240	150	2	75–105	—	—	—
208.0-T7	230	110	3	65–95	—	—	—
213.0-F	205	165	2	85	165	65	—
222.0-T551	255	240	< 0.5	115	205	60	74
222.0-T52	240	215	1	100	170	—	74
238.0-F	205	165	2	100	165	—	—
242.0-T571	275	235	1	105	205	70	74
242.0-T61	325	290	1	110	450	70	74
A249.0-T63	475	415	6	—	—	—	—
296.0-T7	270	140	5	80	205	60	70
308.0-F	195	110	2	70	150	90	—
319.0-F	235	130	3	85	165	—	74
319.0-T6	275	185	3	95	—	—	74
324.0-F	205	110	4	70	—	—	—

(continued)

Table 6B (Continued)

Alloy and Temper	Tension			Hardness Brinell Number (500 kg / 10 mm)	Shear Ultimate Strength (MPa)	Fatigue Endurance Limit <sup>b</sup> (MPa)	Modulus <sup>c</sup> of Elasticity (GPa)
	Ultimate Strength (MPa)	Yield Strength (MPa)	Elongation in 5D (%)				
324.0-T5	250	180	3	90	—	—	—
324.0-T62	310	270	3	105	—	—	—
332.0-T5	250	195	1	105	—	—	—
328.0-T6	235	145	1	65–95	—	—	—
333.0-F	235	130	2	90	185	105	—
333.0-T5	235	170	1	100	185	85	—
333.0-T6	290	205	2	105	230	105	—
333.0-T7	255	195	2	90	195	85	—
336.0-T551	250	193	1	105	193	95	—
336.0-T65	325	295	1	125	250	—	—
354.0-T61	330	255	3	—	—	—	—
354.0-T62	360	290	2	—	—	—	—
355.0-F	185	105	4	—	—	—	70
355.0-T51	205	165	2	75	165	—	70
355.0-T6	290	185	4	90	235	70	70
355.0-T61	310	275	2	105	250	70	70
355.0-T7	275	205	2	85	205	70	70
355.0-T71	250	215	3	85	185	70	70
C355.0-T6	330	195	8	90	—	—	70
C355.0-T61	315	235	6	100	—	—	70
C355.0-T62	330	255	5	100	—	—	70
356.0-F	180	125	5	—	—	—	73
356.0-T51	185	140	2	—	—	—	73
356.0-T6	260	185	5	80	205	90	73
356.0-T7	220	165	6	70	170	75	73
356.0-T71	170	—	3	60–90	—	—	73
A356.0-F	185	90	8	—	—	—	73
A356.0-T51	200	140	5	—	—	—	73
A356.0-T6	285	205	12	80	—	—	73
357.0-F	195	105	6	—	—	—	—
357.0-T51	200	145	4	—	—	—	—
357.0-T6	360	295	5	100	240	90	—
357.0-T7	260	205	5	70	—	—	—
A357.0-T6	360	290	5	100	240	105	—
359.0-T61	330	255	6	—	—	—	—
359.0-T62	345	290	6	—	—	110	—
A390.0-F	200	200	< 1.0	110	—	—	—
A390.0-75	200	200	< 1.0	110	—	—	—
A390.0-T6	310	310	< 1.0	145	—	115	—
A390.0-T7	260	260	< 1.0	120	—	105	—
443.0-F	160	60	10	45	110	55	71
B443.0-F	145	40	6	30–60	—	—	—
A444.0-F	165	75	13	44	—	—	—
A444.0-T4	160	70	21	45	110	55	—
513.0-F	185	110	7	60	150	70	—
535.0-F	240	125	8	60–90	—	—	—
705.0-T5	255	115	10	55–75	—	—	—
707.0-T7	310	240	3	80–110	—	—	—

Table 6B (Continued)

Alloy and Temper	Tension			Hardness Brinell Number (500 kg / 10 mm)	Shear Ultimate Strength (MPa)	Fatigue Endurance Limit <sup>b</sup> (MPa)	Modulus <sup>c</sup> of Elasticity (GPa)
	Ultimate Strength (MPa)	Yield Strength (MPa)	Elongation in 5D (%)				
711.0-T1	195	125	7	55–85	—	—	—
713.0-T5	220	150	4	60–90	—	—	—
850.0-T5	160	75	12	45	105	60	71
851.0-T5	140	75	5	45	95	60	71
851.0-T6	125	—	8	—	—	—	71
852.0-T5	220	160	5	70	145	75	71
<b>Die Cast</b>							
A360.0-F	315	165	4	75	180	124	71
380.0-F	315	160	3	80	195	140	71
A380.0-F	325	160	4	80	185	140	71
383.0-F	310	150	4	75	—	145	71
384.0-F	330	165	3	85	200	140	—
390.0-F	280	240	< 1	—	—	—	—
B390.0-F	315	250	< 1	120	—	140	81
392.0-F	290	270	< 1	—	—	—	—
413.0-F	295	145	3	80	170	130	71
A413.0-F	290	130	4	80	170	130	—
C443.0-F	230	95	9	65	200	115	71
518.0-F	310	193	5	80	200	140	—

<sup>a</sup>Based upon industry handbooks.<sup>3,8–10</sup> Consult those references for limits. Values are representative of separately cast test bars, not of specimens taken from commercial castings. For tensile yield strengths, offset = 0.2%.

<sup>b</sup>Based on 500,000,000 cycles of completely reversed stress using R. R. Moore type of machines and specimens.

<sup>c</sup>Average of tension and compression moduli; compressive modulus is nominally about 2% greater.

## 5 CORROSION BEHAVIOR OF ALUMINUM ALLOYS

Although aluminum is a chemically active metal, its resistance to corrosion is attributable to an invisible oxide film that forms naturally and is always present unless it is deliberately prevented from forming. Scratch the oxide from the surface and, in air, the oxide immediately re-forms. Once formed, the oxide effectively protects the metal from chemical attack and also from further oxidation. Some properties of this natural oxide are as follows:

- It is very thin—200–400 billionths of an inch thick.
- It is tenacious. Unlike iron oxide or rust that spalls from the surface leaving a fresh surface to oxidize, aluminum oxide adheres tightly to aluminum.
- It is hard. Aluminum oxide is one of the hardest substances known.
- It is relatively stable and chemically inert.
- It is transparent and does not detract from the metal's appearance.

### 5.1 General Corrosion

The general corrosion behavior of aluminum alloys depends basically on three factors: (1) the stability of the oxide film, (2) the environment, and (3) the alloying elements; these factors are

not independent of one another. The oxide film is considered stable between pH 4.5 and 9.0; however, aluminum can be attacked by certain anions and cations in neutral solutions, and it is resistant to some acids and alkalis.

In general, aluminum alloys have good corrosion resistance in the following environments: atmosphere, most fresh waters, seawater, most soils, most foods, and many chemicals. Since “good corrosion resistance” is intended to mean that the material will give long service life without surface protection, in support of this rating is the following list of established applications of aluminum in various environments:

*In Atmosphere.* Roofing and siding, truck and aircraft skin, architectural.

*With Most Fresh Waters.* Storage tanks, pipelines, heat exchangers, pleasure boats.

*In Seawater.* Ship hulls and superstructures, buoys, pipelines.

*In Soils.* Pipelines and drainage pipes.

*With Foods.* Cooking utensils, tanks and equipment, cans and packaging.

*With Chemicals.* Storage tanks, processing and transporting equipment.

It is generally true that the higher the aluminum purity, the greater is its corrosion resistance. However, certain elements can be alloyed with aluminum without reducing its corrosion resistance and in some cases an improvement actually results. Those elements having little or no effect include Mn, Mg, Zn, Si, Sb, Bi, Pb, and Ti; those having a detrimental effect include Cu, Fe, and Ni. Some guidelines for the different alloy groupings include the following:

*Al–Mn Alloys.* Al–Mn alloys (3xxx series) have good corrosion resistance and may possibly be better than 1100 alloy in marine environments and for cooking utensils because of a reduced effect by Fe in these alloys.

*Al–Mg Alloys.* Al–Mg alloys (5xxx series) are as corrosion resistant as 1xxx alloys and even more resistant to salt water and some alkaline solutions. In general, they offer the best combination of strength and corrosion resistance of all aluminum alloys. As a result, they are a popular choice for marine vessels such as fishing boats and ferries.

*Al–Mg–Si Alloys.* Al–Mg–Si alloys (6xxx series) have good resistance to atmosphere corrosion but generally slightly lower resistance than Al–Mg alloys. Like the Al–Mg (5xxx) alloys, they can be used unprotected in most atmospheres and waters.

*Alclad Alloys.* Alclad alloys are composite wrought products comprised of an aluminum alloy core with a thin layer of corrosion-protective pure aluminum or aluminum alloy metallurgically bonded to one or both surfaces of the core. As a class, alclad alloys have a very high resistance to corrosion. The cladding is anodic to the core and thus protects the core.

## 5.2 Pitting Corrosion

Pitting is the most common corrosive attack on aluminum alloy products. Pits may form at localized discontinuities in the oxide film on aluminum exposed to atmosphere, fresh water or saltwater, or other neutral electrolytes. Since in highly acidic or alkaline solutions the oxide film is usually unstable, pitting generally occurs in a pH range of about 4.5–9.0. The pits can be minute and concentrated and can vary in size and be widely scattered, depending on alloy composition, oxide film quality, and the nature of the corrodent. The resistance of aluminum to pitting depends significantly on its purity; the purest metal is the most resistant. The presence of other elements in aluminum, except Mn, Mg, and Zn, increases in susceptibility to pitting.

Copper and iron have the greatest effect on susceptibility. Alclad alloys have greatest resistance to penetration since any pitting is confined to the more anodic cladding until the cladding is consumed.

### 5.3 Galvanic Corrosion

Aluminum in contact with a dissimilar metal in the presence of an electrolyte tends to corrode more rapidly than if exposed by itself to the same environment; this is referred to as galvanic corrosion. The tendency of one metal to cause galvanic corrosion of another can be predicted from a “galvanic series,” which depends on environments. Such a series is listed below; the anodic metal is usually corroded by contact with a more cathodic one:

Anodic	Magnesium and zinc	Protect aluminum
	Aluminum, cadmium, and chromium	Neutral and safe in most environments
	Steel and iron	Cause slow action on aluminum except in marine environments
	Lead	Safe except for severe marine or industrial atmospheres
Cathodic	Copper and nickel	Tend to corrode aluminum
	Stainless steel	Safe in most atmospheres and fresh water; tends to corrode aluminum in severe marine atmospheres

Since galvanic corrosion is akin to a battery and depends on current flow, several factors determine the severity of attack:

*Electrolyte Conductivity.* The higher the electrical conductivity, the greater the corrosive effect.

*Polarization.* Some couples polarize strongly to reduce the current flow appreciably. For example, stainless steel is highly cathodic to aluminum, but because of polarization, the two can safely be used together in many environments.

*Anode–Cathode Area Ratios.* A high ratio minimizes galvanic attack; a low ratio tends to cause severe galvanic corrosion.

## 6 MACHINING ALUMINUM ALLOYS

Aluminum alloys are readily machined and offer such advantages as almost unlimited cutting speed, good dimensional control, low cutting force, and excellent life.

The cutting tool geometry used in machining aluminum alloys is described by seven elements: top or back rake angle, side rake angle, end-relief angle, side-relief angle, end cutting edge angle, and nose radius. The depth of cut may be in the range of  $\frac{1}{16}$ – $\frac{1}{4}$  in. (1.6–6.3 mm) for small work up to  $\frac{1}{2}$ – $1\frac{1}{2}$  in. (12.5–38 mm) for large work. The feed depends on finish. Rough cuts vary from 0.006 to 0.080 in. (0.15–2 mm) and finishing cuts from 0.002 to 0.006 in. (0.05–0.15 mm). Speed should be as high as possible, up to about 15,000 feet per minute (fpm) [about 5000 meters per minute (mpm)]. Cutting forces for an alloy such as 6061-T651 are 0.30–0.50 hp/in.<sup>3</sup>/min for a 0° rake angle and 0.25–0.35 hp/in.<sup>3</sup>/min for a 20° rake angle. Lubrication such as light mineral or soluble oil is desirable for high production. Alloys with a machinability rating of A or B may not need lubrication.

Cutting tool materials for machining aluminum alloys include water-hardening steels, high-speed steels, hard-cast alloys, sintered carbides, and diamonds:

1. Water-hardening steels (plain carbon or with additions of chromium, vanadium, or tungsten) are lowest in first cost. They soften if cutting edge temperatures exceed 300°F (150°C), have low resistance to edge wear, and are suitable for low cutting speeds and limited production runs.
2. High-speed steels are available in a number of forms, are heat treatable, permit machining at rapid rates, allow cutting edge temperatures of over 1000°F (540°C), and resist shock better than hard-cast or sintered carbides.
3. Hard-cast alloys are cast closely to finish size, are not heat treated, and lie between high-speed steels and carbides in terms of heat resistance, wear, and initial cost. They will not take severe shock loads.
4. Sintered carbide tools are available in solid form or as inserts. They permit speeds 10–30 times faster than for high-speed steels. They can be used for most machining operations. They should be used only when they can be supported rigidly and when there is sufficient power and speed. Many types are available.
5. Mounted diamonds are used for finishing cuts where an extremely high quality surface is required.

## 6.1 Single-Point Tool Operations

1. *Turning.* Aluminum alloys should be turned at high speeds with the work held rigidly and supported adequately to minimize distortion.
2. *Boring.* All types of tooling are suitable. Much higher speeds can be employed than for boring ferrous materials. Carbide tips are normally used in high-speed boring in vertical or horizontal boring machines.
3. *Planing and Shaping.* Aluminum permits maximum table speeds and high metal removal rates. Tools should not strike the work on the return stroke.

## 6.2 Multipoint Tool Operations

*Milling.* Removal rate is high with correct cutter design, speed and feed, machine rigidity, and power. When cutting speeds are high, the heat developed is retained mostly in the chips, with the balance absorbed by the coolant. Speeds are high with cutters of high-speed and cast alloys and very high with sintered carbide cutters. All common types of solid-tooth, high-carbon, or high-speed steel cutters can be employed. High-carbon cutters operating at a maximum edge temperature of 400°F are preferred for short-run production. For long runs, high-speed steel or inserted-tooth cutters are used. Speeds of 15,000 fpm (5000 mpm) are not uncommon for carbide cutters. Maximum speeds for high-speed and high-carbon steel cutters are around 5000 and 600 fpm (1650 and 200 mpm), respectively.

*Drilling.* General-purpose drills with bright finishes are satisfactory for use on aluminum. Better results may be obtained with drills having a high helix angle. Flute areas should be large; the point angle should be 118° (130°–140° for deeper holes). Cutting lips should be equal in size. Lip relief angles are between 12° and 20°, increasing toward the center to hold the chisel angle between 130° and 145°. No set rule can be given for achieving the correct web thickness. Generally, for aluminum, it may be thinner at the point without tool breakage. A 1Xs-Hi drill



at 6000 rpm has a peripheral speed of 2000 fpm (680 mpm). For drilling aluminum, machines are available with speeds up to 80,000 rpm. If excessive heat is generated, hold diameter may be reduced even below drill size. With proper drills, feeds, speeds, and lubrication, no heat problem should occur.

For a feed of 0.008 inches per rotation (ipr) and a depth-to-diameter ratio of 4:1, the thrust value is 170 lb and the torque value is 10 lb-in. for a 1A-Ui drill with alloy 6061-T651. Aluminum alloys can be counterbored, tapped, threaded by cutting or rolling, and broached. Machining fluid should be used copiously.

*Grinding.* Resin-bonded silicon carbide wheels of medium hardness are used for rough grinding of aluminum. Finish grinding requires softer, vitrified-bonded wheels. Wheel speeds can vary from 5500 to 6000 fpm (1800–2000 mpm). Abrasive belt grinding employs belt speeds from 4600 to 5000 square feet per minute (sfpm). Grain size of silicon carbide abrasive varies from 36 to 80 for rough cuts and from 120 to 180 for finishing cuts. For contact wheel abrasive belt grinding, speeds are 4500–6500 sfpm. Silicon carbide or aluminum oxide belts (24–80 grit) are used for rough cuts.

*Sawing, Shearing, Routing, and Arc Cutting Aluminum.* Correct tooth contour is most important in *circular sawing*. The preferred saw blade has an alternate hollow ground side—rake teeth at about 15°. Operating speeds are 4000–15,000 fpm (1300–5000 mpm). Lower speeds are recommended for semi-high-speed steel, intermediate speeds for high-speed inserted-tooth steel blades, and high speeds for carbide-tipped blades. Band-sawing speeds should be between 2000 and 5000 fpm (655–1640 mpm). Spring-tempered blades are recommended for sheet and soft blades with hardened teeth for plate. Tooth pitch should not exceed material thickness: four to five teeth to the inch for spring tempered, six to eight teeth to the inch for flexible backed. Contour sawing is readily carried out. Lubricant should be applied to the back of the blade. Shearing of sheet may be done on guillotine shears. The clearance between blades is generally 10–12% of sheet thickness down to 5–6% for light-gauge soft-alloy sheet. Hold-down pads, shear beds, and tables should be covered to prevent marring. Routing can also be used with 0.188–0.50-in. (4.8–12.7-mm) material routed at feeds of 10–30 ipm [25–75 centimeters per minute (cmppm)]. Heat-treated plates up to 3 in. (7.6 cm) in thickness material can be routed at feeds up to 10 ipm (25 cmppm). Chipless machining of aluminum can be carried out using shear spinning rotary swaging, internal swaging, thread rolling, and flame cutting.

## 7 FINISHING ALUMINUM

The aluminum surface can be finished in more different ways than any other metal. The normal finishing operations fall into four categories: mechanical, chemical, electrochemical, and applied. They are usually performed in the order listed, although one or more of the processes can be eliminated depending upon the final effect desired.

### 7.1 Mechanical Finishes

This is an important starting point since even with subsequent finishing operations a rough, smooth, or textured surface may be retained and observed. For many applications, the as-fabricated finish may be good enough. Or this surface can be changed by grinding, polishing, buffing, abrasive or shot blasting, tumbling or burnishing, or even hammering for special effects. Rolled surfaces of sheet or foil can be made highly specular by use of polishing rolls; one side or two sides bright and textures can be obtained by using textured rolls.

## 92 Aluminum Alloys

### 7.2 Chemical Finishes

A chemical finish is often applied after the mechanical finish. The most widely used chemical finishes include caustic etching for a matte finish, design etching, chemical brightening, conversion coatings, and immersion coatings. Conversion coatings chemically convert the natural oxide coating on aluminum to a chromate, a phosphate, or a combination chromate–phosphate coating, and they are principally used and are the recommended ways to prepare the aluminum surface for painting.

### 7.3 Electrochemical Finishes

These include electrobrightening for maximum specularity, electroplating of another metal such as nickel or chromium for hardness and wear resistance, and, most importantly, anodizing. Anodizing is an electrochemical process whereby the natural oxide layer is increased in thickness over a thousand times and made more dense for increased resistance to corrosion and abrasion resistance. The anodic oxide forms by the growth of cells, each cell containing a central pore. The pores are sealed by immersing the metal into very hot or boiling water. Sealing is an important step and will affect the appearance and properties of the anodized coating. There are several varieties of anodized coatings.

### 7.4 Clear Anodizing

On many aluminum alloys a thick, transparent oxide layer can be obtained by anodizing in a sulfuric acid solution—this is called clear anodizing. The thickness of the layer depends on the current density and the time in solution and is usually between 0.1 and 1 mil in thickness.

### 7.5 Color Anodizing

Color can be added to the film simply by immersing the metal immediately after anodizing and before sealing into a vat containing a dye or metallic coloring agents and then sealing the film. A wide range of colors have been imparted to aluminum in this fashion for many years. However, the colors imparted in this manner tend to fade from prolonged exposure to sunlight.

### 7.6 Integral Color Anodizing

More lightfast colors for outdoor use are achieved through integral color anodizing. These are proprietary processes utilizing electrolytes containing organic acids and, in some cases, small amounts of impurities are added to the metal itself to bring about the desired colors. This is usually an onstage process and the color forms as an integral part of the anodization. Colors are for the most part limited to golds, bronzes, grays, and blacks.

### 7.7 Electrolytically Deposited Coloring

Electrolytically deposited coloring is another means of imparting lightfast colors. Following sulfuric acid anodizing, the parts are transferred to a second solution containing metallic pigments that are driven into the coating by an electric current.

### 7.8 Hard Anodizing

Hard anodizing, or hardcoating as it is sometimes called, usually involves anodizing in a combination of acids and produces a very dense coating, often 1–5 mils thick. It is very resistant to wear and is normally intended for engineering applications rather than appearance.

## 7.9 Electroplating

In electroplating, a metal such as chromium or nickel is deposited on the aluminum surface from a solution containing that metal. This usually is done for appearance or to improve the hardness or abrasion resistance of the surface. Electroplating has a “smoothing-out” effect, whereas anodized coatings follow the contours of the base-metal surface, thus preserving a matte or a polished surface as well as any other patterns applied prior to the anodizing.

## 7.10 Applied Coatings

Applied coatings include porcelain enamel, paints and organic coatings, and laminates such as plastic, paper, or wood veneers. Probably as much aluminum produced today is painted as is anodized. Adhesion can be excellent when the surface has been prepared properly. For best results paint should be applied over a clean conversion-coated or anodized surface.

# 8 APPLICATIONS OF ALUMINUM ALLOYS

There are at least two approaches to overviewing important applications of aluminum alloys: *by alloy class*, as introduced in Section 3, and *by type of application*. We will consider both approaches in the information below, reviewing by alloy class in Section 8.1 and by application in Section 8.2.

All photographs are courtesy of the Aluminum Association unless otherwise indicated. For a more complete discussion of these and other applications of aluminum alloys, the reader is referred to Altenpohl’s very complete treatise on the aluminum industry, *Aluminum: Technology, Applications and Environment*,<sup>1</sup> and to *Aluminum Alloy Castings—Properties, Processes, and Applications*.<sup>17</sup>

## 8.1 Applications by Alloy Class

### *Wrought Alloys*

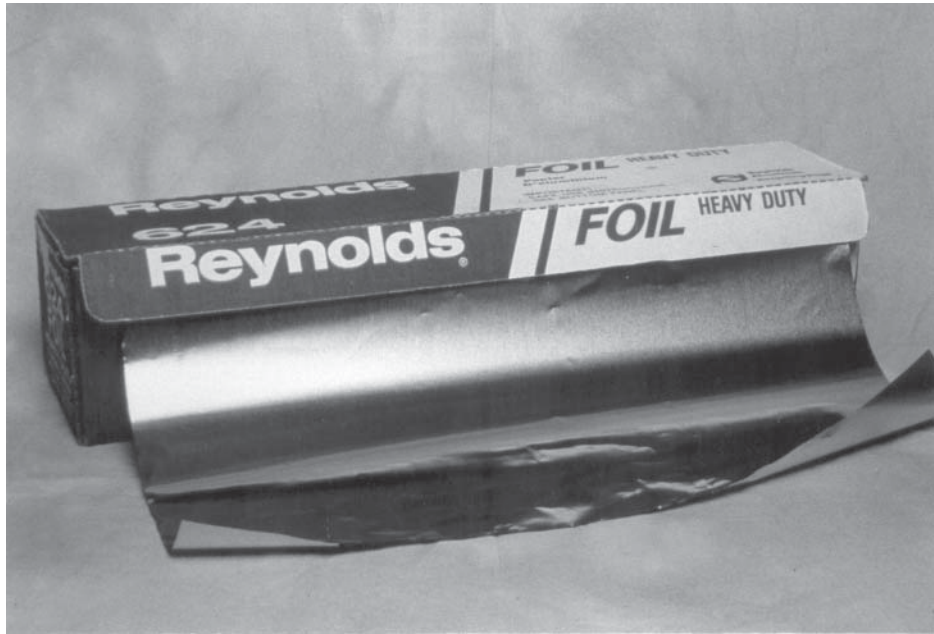
*1xxx—Pure Al.* The major characteristics of the 1xxx series are:

- Strain hardenable
- Exceptionally high formability, corrosion resistance, and electrical conductivity
- Typical ultimate tensile strength range: 10–27 ksi (70–185 MPa)
- Readily joined by welding, brazing, and soldering

The 1xxx series represents the commercially pure aluminum, ranging from the baseline 1100 (99.00% minimum Al) to relatively purer 1050/1350 (99.50% minimum Al) and 1175 (99.75% minimum Al). The 1xxx series are strain hardenable but would not be used where strength is a prime consideration.

The primary uses of the 1xxx series include applications where the combination of extremely high corrosion resistance, formability, and/or electrical conductivity are required, e.g., foil and strip for packaging (Fig. 1), chemical equipment, tank car or truck bodies, spun hollowware, and elaborate sheet metal work.

Electrical applications are one major use of the 1xxx series, primarily 1350, which has relatively tight controls on impurities that would lower electrical conductivity. As a result, an electrical conductivity of 62% of the International Annealed Copper Standard (IACS) is guaranteed for this material which, combined with the natural light weight of aluminum, means a significant weight and therefore cost advantage over copper in electrical applications (Fig. 2).



**Figure 1** Reynolds Heavy Duty Foil product, an example of aluminum food wrapping products made of various grades of 1xxx commercially pure aluminum. (Courtesy of the Aluminum Association.)

*2xxx—Al—Cu Alloys.* The major characteristics of the 2xxx series are:

- Heat treatable
- High strength at room and elevated temperatures
- Typical ultimate tensile strength range: 27–62 ksi (185–430 MPa)
- Usually joined mechanically but some alloys are weldable

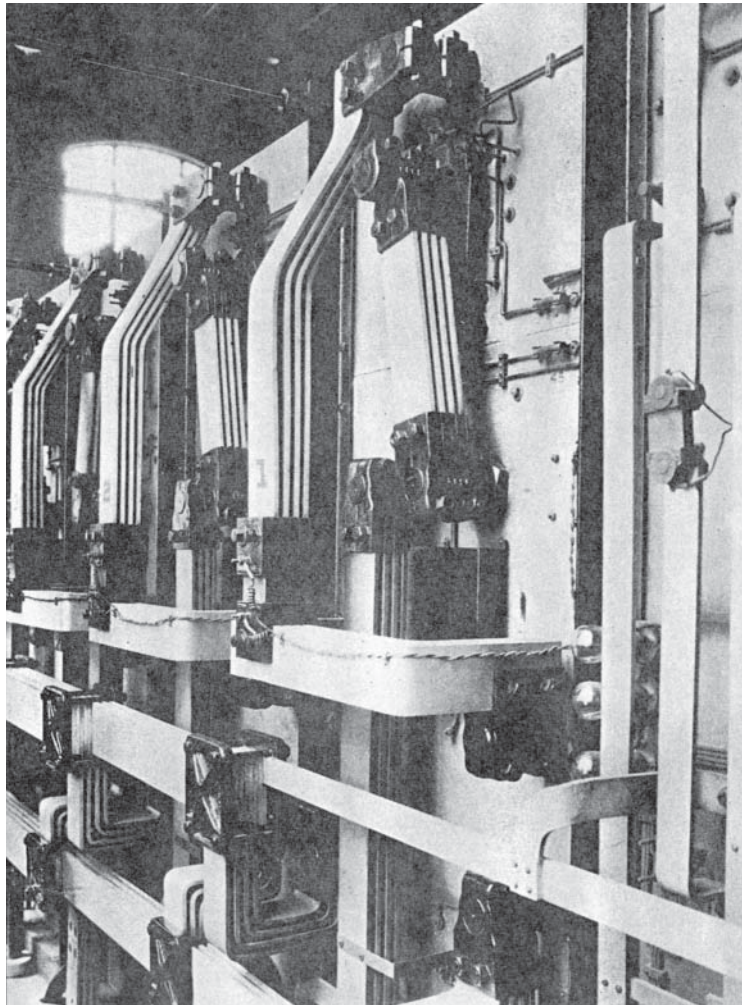
The 2xxx series are heat treatable and possess in certain individual alloys (e.g., 2219) good combinations of high strength (especially at elevated temperatures), toughness, and weldability. Aluminum–copper alloys are not as resistant to atmospheric corrosion as several other series and so are usually painted or clad for added protection.

The higher strength 2xxx alloys are widely used in aircraft wings and fuselage components (2X24; Fig. 3) and in truck body construction (2014; Fig. 4). Some specific alloys in the series (e.g., 2219 and 2048) are readily joined by gas–metal arc (GMA) and gas–tungsten arc (GTA) welding and so are used for aerospace applications where that is the preferred method of joining.

Alloy 2195 is a new Li-bearing aluminum alloy providing very high modulus of elasticity along with higher strength and comparable weldability to 2219; it is being utilized for space applications (Fig. 5).

For applications requiring high strength plus high fracture toughness, there are high-toughness versions of several of the alloys (e.g., 2124, 2324, 2419, 2524) that have tighter control on the impurities that increases their resistance to unstable fracture, all developed specifically for the aircraft industry.

Alloys 2011, 2017, and 2117 are widely used for fasteners and screw-machine stock.



**Figure 2** Aluminum electrical bus bar installation with 1350 bus bar. (Courtesy of the Aluminum Association.)

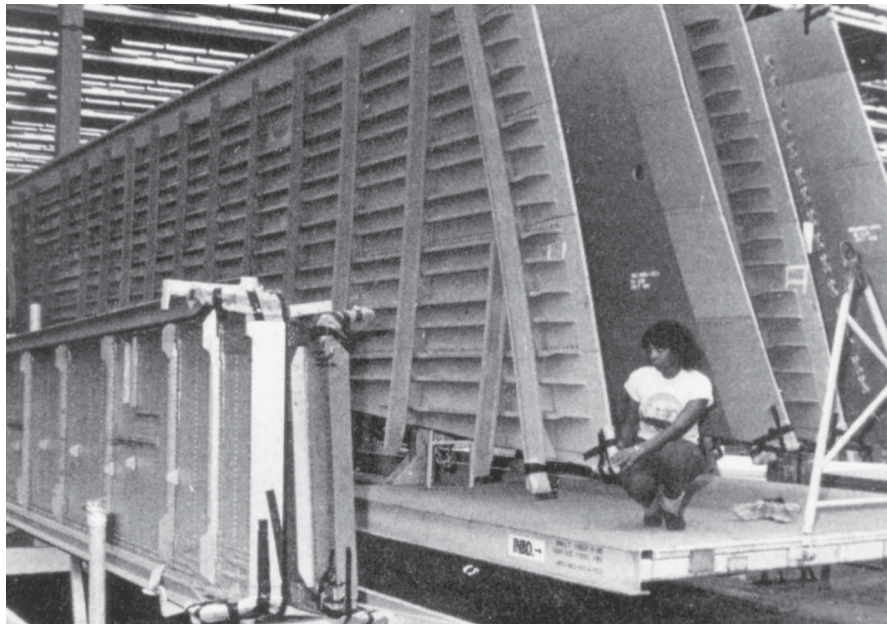
*3xxx—Al–Mn Alloys.* The major characteristics of the 3xxx series are:

- High formability and corrosion resistance with medium strength
- Typical ultimate tensile strength range: 16–41 ksi (110–285 MPa)
- Readily joined by all commercial procedures

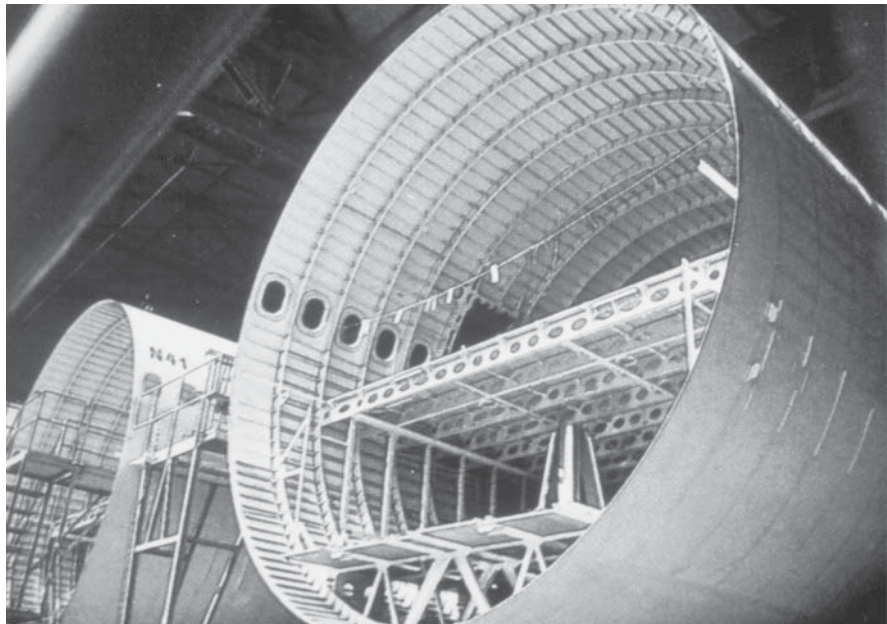
The 3xxx series are strain hardenable, have excellent corrosion resistance, and are readily welded, brazed, and soldered.

Alloy 3003 is widely used in cooking utensils and chemical equipment because of its superiority in handling many foods and chemicals and in builders' hardware because of its superior corrosion resistance. Alloy 3105 is a principal for roofing and siding.





(a)



(b)

**Figure 3** (a) Aircraft wing and fuselage structures includes extrusions and plate of 2xxx alloys like 2024, 2124, and 2618 and 7xxx alloys like 7050 and 7475. (b) External sheet skin may be Alclad 2024, 2524, 2618, or 7475; the higher purity cladding provides corrosion protection to the Al-Cu and Al-Zn-Mg alloys that may darken with age otherwise. (Courtesy of the Aluminum Association.)



**Figure 4** Heavy dump and tank trucks and trailer trucks employ high-strength 2xxx or 6xxx extrusions for their structural members and tough 5xxx alloy sheet and plate for their load-carrying components. (Courtesy of the Aluminum Association.)

Because of their ease and flexibility of joining, 3003 and other members of the 3xxx series are widely used in sheet and tubular form for heat exchangers in vehicles and power plants (Fig. 6).

Alloy 3004 and its modification 3104 are the principals for the bodies of drawn and ironed can bodies for beverage cans for beer and soft drinks (Fig. 7). As a result, they are among the most used individual alloys in the aluminum system, in excess of 3.5 billion pounds per year.

*4xxx—Al–Si Alloys.* The major characteristics of the 4xxx series are:

- Heat treatable
- Good flow characteristics, medium strength
- Typical ultimate tensile strength range: 25–55 ksi (170–380 MPa)
- Easily joined, especially by brazing and soldering





**Figure 5** Fuel tanks and booster rockets such as those of the Space Shuttle are 2xxx alloys, originally 2219 and 2419, now Al–Li “Weldalite” alloy 2195. (Courtesy of the Aluminum Association.)

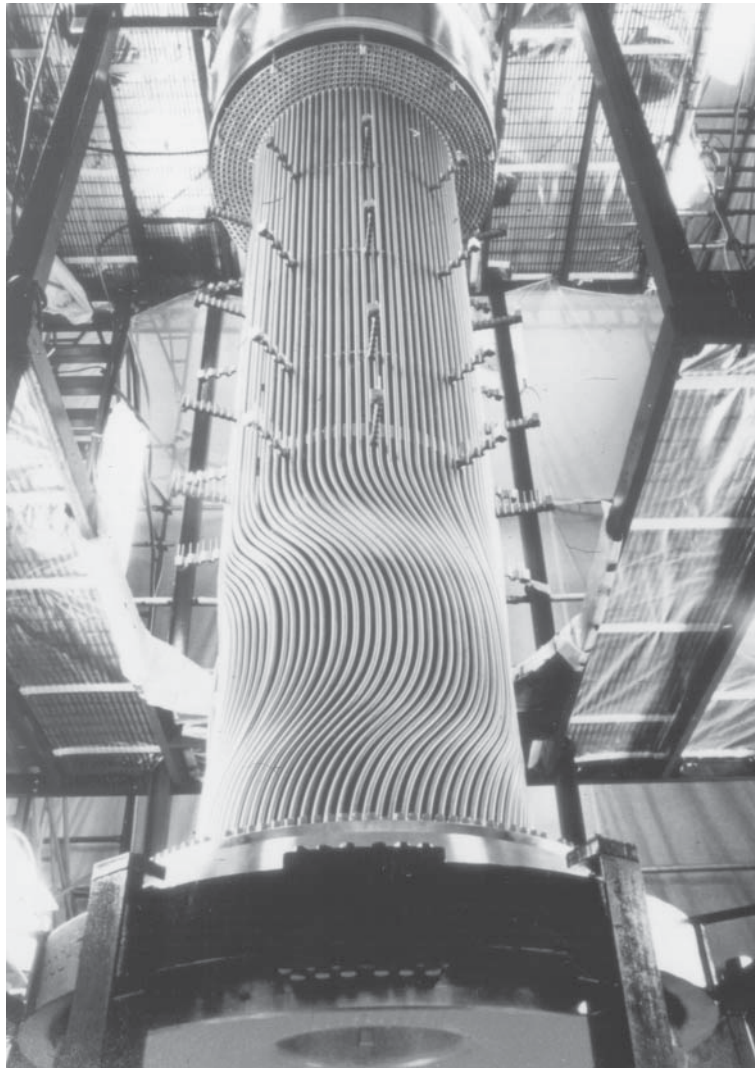
There are two major uses of the 4xxx series, both generated by their excellent flow characteristics provided by their relatively high silicon contents. The first is for forgings: The workhorse alloy is 4032, a medium- to high-strength, heat-treatable alloy used principally in applications such as forged aircraft pistons. The second major application is as filler alloy; here the workhorse is 4043, used for GMA welding of 4xxx and 6xxx alloys for structural and automotive applications.

As noted, the same characteristic leads to both types of application: good flow characteristic provided by the high silicon content. In the case of forgings, this ensures the complete and precise filling of complex dies; in the case of welding, it ensures complete filling of grooves in the members to be joined. For the same reason, other variations of the 4xxx alloys are used for the cladding on brazing sheet, the component that flows to complete the bond.

*5xxx—Al–Mg Alloys.* The major characteristics of the 5xxx series are:

- Strain hardenable
- Excellent corrosion resistance, toughness, weldability; moderate strength
- Building and construction, automotive, cryogenic, marine applications
- Representative alloys: 5052, 5083, 5754
- Typical ultimate tensile strength range: 18–51 ksi (125–350 MPa)

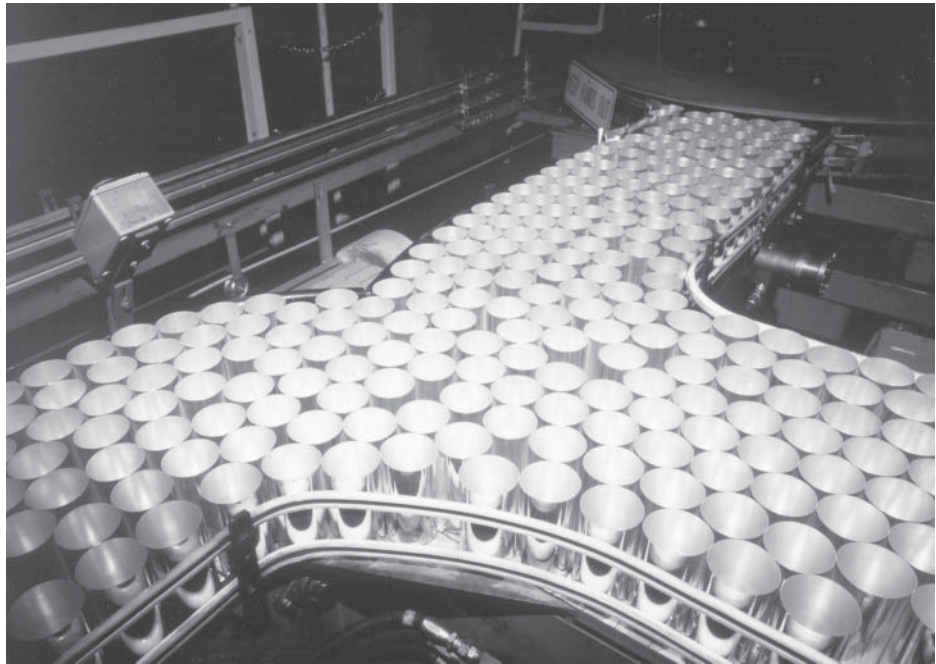
Aluminum–magnesium alloys of the 5xxx series are strain hardenable and have moderately high strength, excellent corrosion resistance even in salt water, and very high toughness even at cryogenic temperatures to near absolute zero. They are readily welded by a variety of techniques, even at thicknesses up to 8 in. (20 cm).



**Figure 6** Alloy 3003 tubing in large commercial power plant heat exchanger. (Courtesy of the Aluminum Association.)

As a result, 5xxx alloys find wide application in building and construction (Fig. 8), highway structures including bridges (Fig. 9), storage tanks and pressure vessels, cryogenic tankage and systems for temperatures as low as  $-459^{\circ}\text{F}$  ( $-270^{\circ}\text{C}$ ) near absolute zero, transportation (Fig. 10), and marine applications (Fig. 11), including offshore drilling rigs (Fig. 12).

Alloys 5052, 5086, and 5083 are the workhorses from the structural standpoint, with increasingly higher strength associated with the higher Mg content. Specialty alloys in the group include 5182, the beverage can end alloy (Fig. 7), and thus among the largest in tonnage used; 5754 for automotive body frames and panels (Fig. 13); and 5252, 5457, and 5657 for bright trim applications, including automotive trim.



**Figure 7** Bodies of most beverage cans are alloy 3004, the ends are 5182, making it the largest volume alloy combination in the industry. (Courtesy of the Aluminum Association.)

Care must be taken to avoid use of 5xxx alloys with more than 3% Mg content in applications where they receive continuous exposure to temperatures above 212°F (100°C). Such alloys may become sensitized and susceptible to SCC. For this reason, alloys such as 5454 and 5754 are recommended for applications where high-temperature exposure is likely.

*6xxx—Al—Mg—Si Alloys.* The major characteristics of the 6xxx series are:

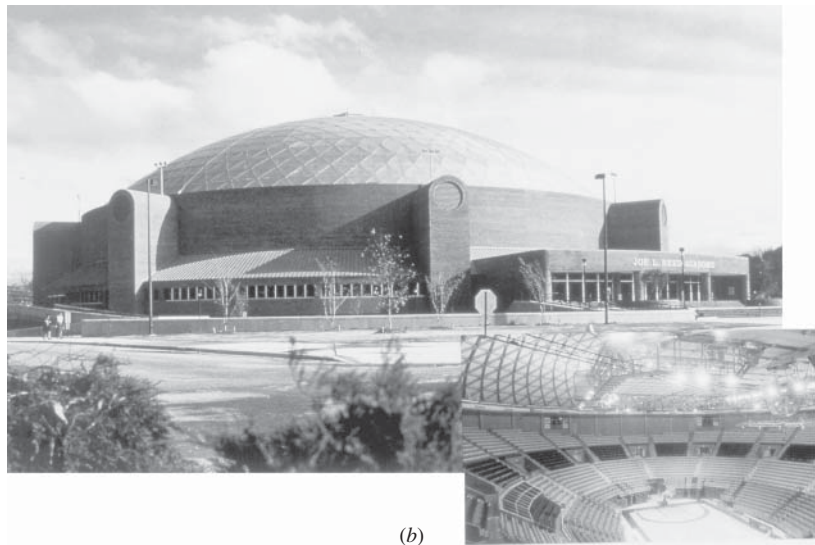
- Heat treatable
- High corrosion resistance, excellent extrudability, moderate strength
- Typical ultimate tensile strength range: 18–58 ksi (125–400 MPa)
- Readily welded by GMA and GTA welding methods

The 6xxx alloys are heat treatable and have moderately high strength coupled with excellent corrosion resistance. A unique feature is their great extrudability, making it possible to produce in single shapes relatively complex architectural forms and also to design shapes that put the majority of the metal where it will most efficiently carry the highest tensile and compressive stresses (Fig. 14). This is a particularly important advantage for architectural and structural members where stiffness criticality is important.

Alloy 6063 is perhaps the most widely used because of its extrudability; it is not only the first choice for many architectural and structural members but also has been the choice for the Audi automotive space frame members. A good example of its structural use was the all-aluminum bridge structure in Foresmo, Norway (Fig. 9); it was prefabricated in a shop and erected on the site in only a few days.



(a)



(b)

**Figure 8** Sheet of 5xxx alloys often forms the surface of geodesic dome structures, as in these examples of (a) a water treatment plant and (b) a wide-span arena roof. The structural supports are typically 6061 or 6063 extruded shapes or tubular members. (Courtesy of the Aluminum Association.)





(a)



(b)

**Figure 9** The Foresmo bridge in northern Norway is an excellent example of the use of Al–Mg alloys for built-up girders systems; these photos illustrate a major advantage of replacement aluminum bridges: the ability to prefabricate the spans, (a) transport them, and (b) erect them in place quickly, minimizing the disruption to traffic. (Courtesy of the Aluminum Association.)



**Figure 10** Alloy 5454 has been widely used for railcar body construction where heavy loads, such as coal, and potentially high temperatures may be involved. (Courtesy of the Aluminum Association.)

Higher strength alloy 6061 extrusions and plates find broad use in welded structural members such as automotive, truck (Fig. 4), and marine frames, railroad cars, and pipelines. Alloys like 6111 provide a fine combination of strength and formability, useful for external automotive panels (Fig. 13*b*).

Among specialty alloys in the series are 6066-T6, with high strength for forgings; 6071 for the highest strength available in 6xxx extrusions; and 6101 and 6201 for high-strength electrical bus and electrical conductor wire, respectively.

*7xxx—Al–Zn Alloys.* The major characteristics of the 7xxx series are:

- Heat treatable
- Very high strength; special high-toughness versions
- Typical ultimate tensile strength range: 32–88 ksi (220–605 MPa)
- Mechanically joined

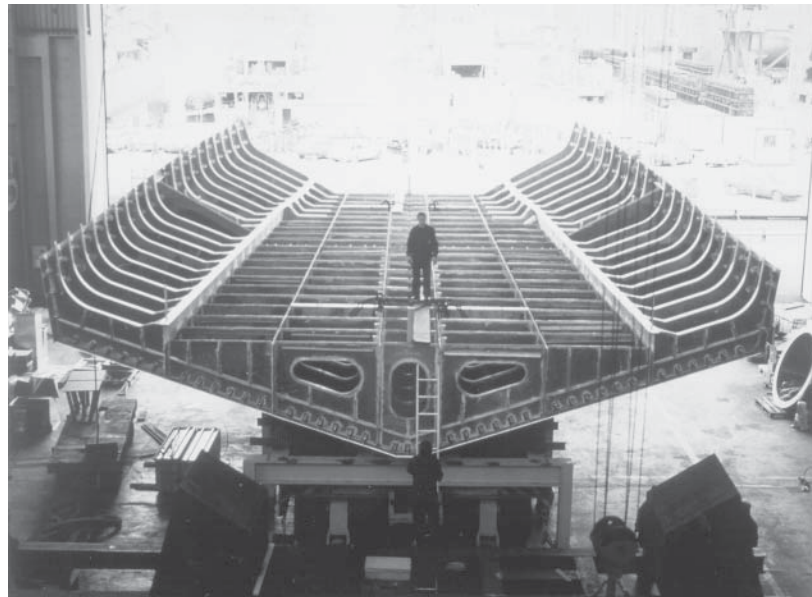
The 7xxx alloys are heat treatable and, among the Al–Zn–Mg–Cu versions in particular, provide the highest strengths of all aluminum alloys. These alloys are not considered weldable by commercial processes and are regularly used with riveted construction.

The widest application of the 7xxx alloys has historically been in the aircraft industry (Fig. 3), where fracture-critical design concepts have provided the impetus for the high-toughness alloy development. There are several alloys in the series that are produced especially for their high toughness, notably 7050, 7055, 7150, 7175, and 7475; for these alloys, controlled impurity levels, particularly of Fe and Si, maximize the combination of strength and fracture toughness. Forgings of these alloys (Fig. 15) are often used for large structural members in aircraft.

The high strength–density combination for 7075-T73 (as well as 2014-T6) has made them choices for drill pipe, where the long lengths needed for deep wells require lightweight alloys.



(a)



(b)

**Figure 11** High-speed single-hull ships (a) like the Proserio employ 5083 or 5383-H113 / H321 machined plate for hulls, (b) internal hull stiffeners, decking, and superstructure. (Courtesy of the Aluminum Association.)





**Figure 12** Demands of the superstructures of offshore oil rigs in high humidity and water exposure are met with 5454, 5086, and 5083 Al–Mg alloy welded construction. (Courtesy of the Aluminum Association.)

The atmospheric corrosion resistance of the 7xxx alloys is not as high as that of the 5xxx and 6xxx alloys, so in such service they are usually coated or, for sheet and plate, used in an alclad version. Also, special tempers have been developed to improve their resistance to exfoliation and SCC, the T76 and T73 types, respectively. These tempers are especially recommended in situations where there may be high short transverse (through-the-thickness) stresses present during exposure to atmospheric or more severe environments.

The Cu-free 7xxx alloys have lower strength but are tougher and are both readily extrudable and weldable, so alloys like 7005 and 7029 find their way into applications like guard rail and automotive and truck bumpers.

*8xxx—Alloys with Al+Other Elements (Not Covered by Other Series).* The major characteristics of the 8xxx series are:

- Heat treatable
- High conductivity, strength, and hardness
- Typical ultimate tensile strength range: 17–35 ksi (115–240 MPa)

The 8xxx series is used for those alloys with lesser used alloying elements such as Fe, Ni, and Li. Each is used for the particular characteristics it provides the alloys.

Iron and Ni provide strength with little loss in electrical conductivity and so are used in a series of alloys represented by 8017 for conductors.

Lithium in alloy 8090 provides exceptionally high strength and modulus, and so this alloy is used for aerospace applications where increases in stiffness combined with high strength reduces component weight.

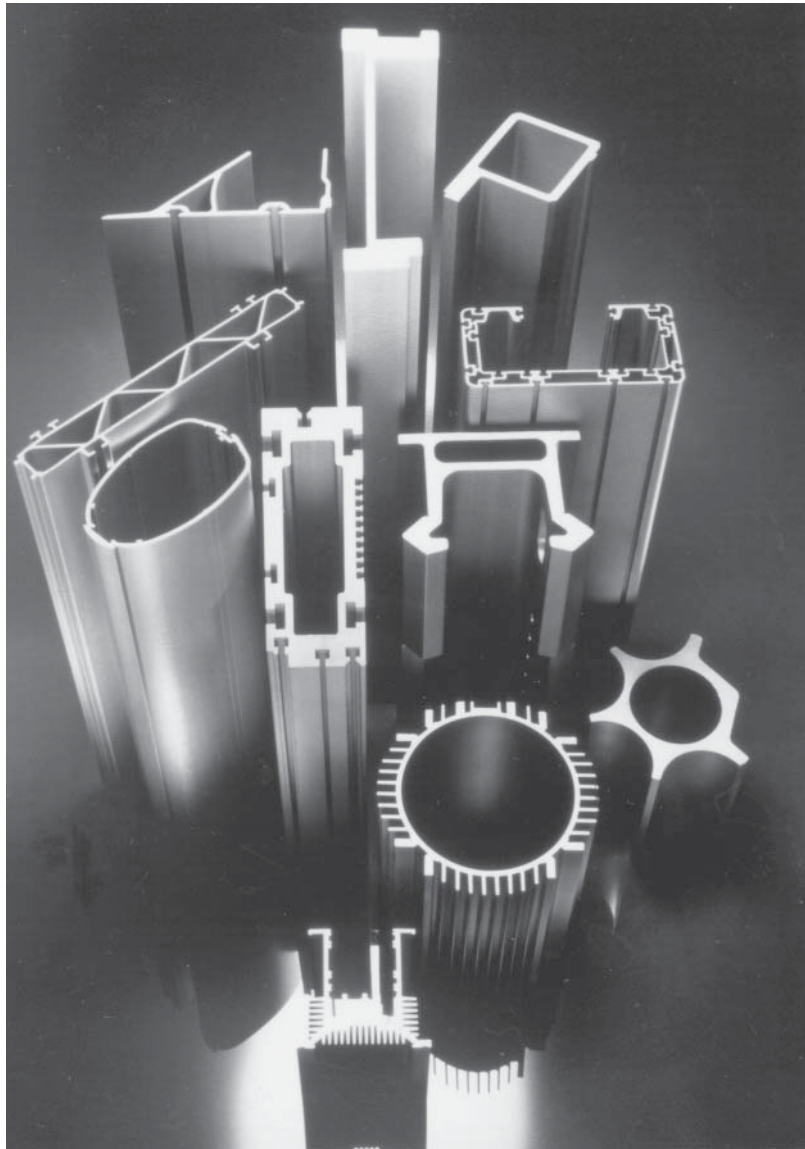


(a)



(b)

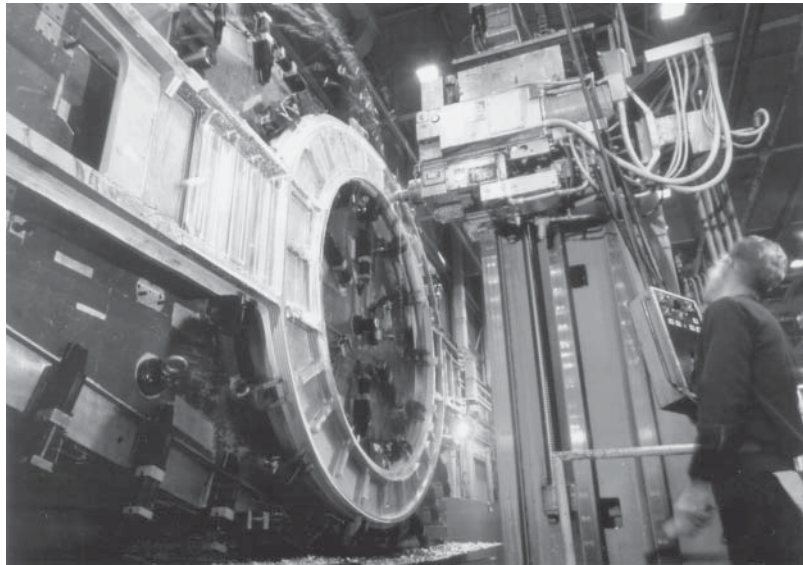
**Figure 13** Automotive structures are likely to employ increasing amounts of 5754-0 formed sheet for parts such as internal door stiffeners or (a) the entire body in white; (b) external body panels are more likely to be higher strength 6111-T4. (Courtesy of the Aluminum Association.)



**Figure 14** Power of extruded Al–Mg–Si alloys is the “put the metal where you need it” flexibility these alloys and the extrusion process provide. (Courtesy of the Aluminum Association.)

### *Cast Alloys*

In comparison with wrought alloys, casting alloys contain larger proportions of certain alloying elements such as silicon and impurity elements like iron. This results in a largely heterogeneous cast structure, i.e., one having a substantial volume of second phases. This second-phase material warrants careful study, since any coarse, sharp, and/or brittle constituent can create harmful internal notches and nucleate cracks when the component is later put under load. Fatigue performance is very sensitive to large heterogeneities, especially at or near the surface. As will be



**Figure 15** Example of a premium forged aircraft part, usually of alloys such as 7050 or 7175-T74. (Courtesy of the Aluminum Association.)

shown later, careful alloy selection combined with good metallurgical and foundry practices can largely prevent such defects and provide exceptional quality castings for critical applications.

The elongation and strength, especially in fatigue, of most cast products are relatively lower than those of wrought products. This is because current casting practice is as yet unable to reliably prevent casting defects. In recent years, however, innovations in casting processes such as squeeze casting have brought about some significant improvement in the consistency and level of properties of castings, and these should be taken into account in selecting casting processes for critical applications. Another significant enhancement addressing porosity problems is HIP; its use has been shown to substantially improve the fatigue performance of aluminum castings.<sup>17</sup>

For applications where high ductility and toughness along with high strength are required, relatively high purity versions of casting alloys like A356.0-T6 (rather than 356.0-T6) and A357.0-T6 (rather than 357.0-T6) are recommended.

*2xx.x—Al—Cu Alloys.* The major characteristics of the 2xx.x series are:

- Heat treatable; sand and permanent mold castings
- High strength at room and elevated temperatures; some high-toughness alloys
- Approximate ultimate tensile strength range: 19–65 ksi (130–450 MPa)

The strongest of the common casting alloys are heat-treated 201.0 and 204.0, which have found important application in the aerospace industry. Their castability is somewhat limited by a tendency to microporosity and hot tearing, so that they are best suited to investment casting. Their high toughness makes them particularly suitable for highly stressed components in machine tool construction, in electrical engineering (pressurized switchgear casings), and in aircraft construction.

Besides the standard aluminum casting alloys, there are special alloys for particular components, for instance, for engine piston heads, integral engine blocks, or bearings. For these



applications the chosen alloy needs good wear resistance and a low friction coefficient as well as adequate strength at elevated service temperatures. A good example is the alloy 203.0, which to date is the aluminum casting alloy with the highest strength at around 400°F (200°C).

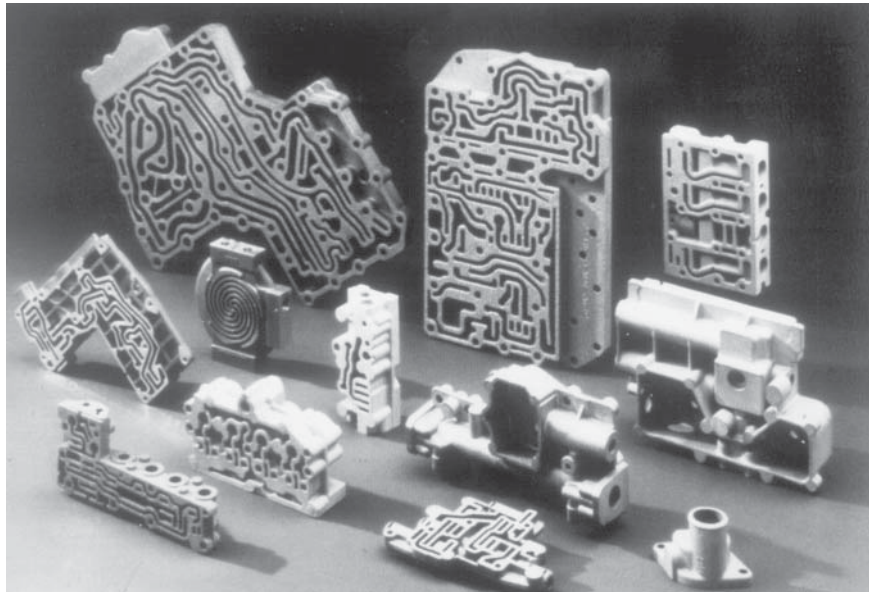
*3xx.x—Al–Si+Cu or Mg Alloys.* The major characteristics of the 3xx.x series are:

- Heat treatable; sand, permanent mold, and die castings
- Excellent fluidity, high strength, some high-toughness alloys
- Approximate ultimate tensile strength range: 19–40 ksi (130–275 MPa)
- Readily welded

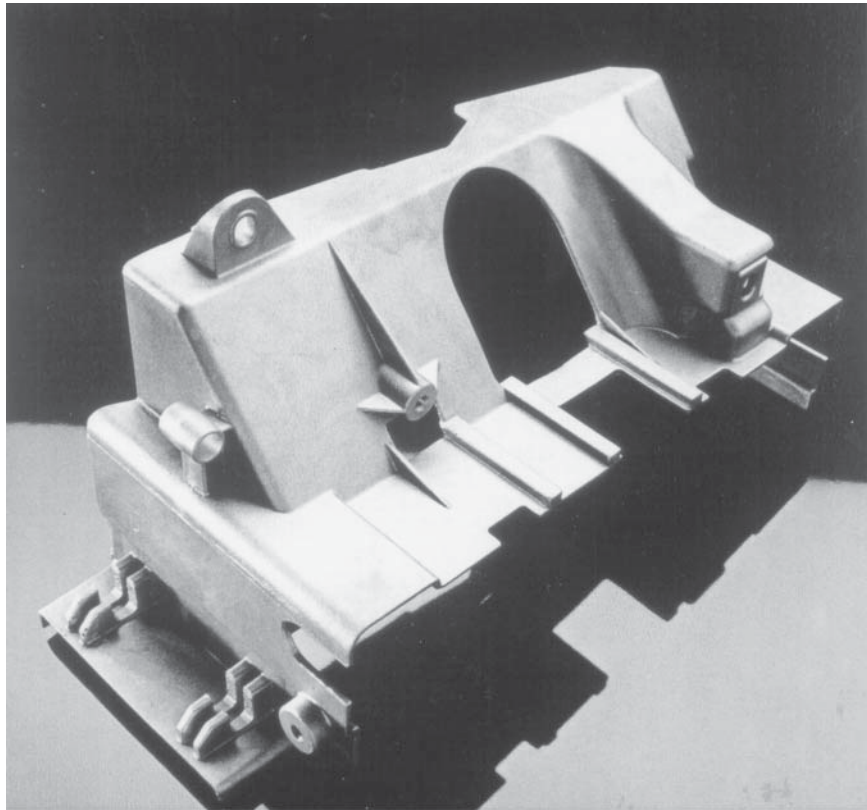
The 3xx.x series of castings are one of the most widely used because of the flexibility provided by the high silicon content and its contribution to fluidity plus their response to heat treatment, which provides a variety of high-strength options. As a result, they are the best choice for large and complex castings (Fig. 16). Further the 3xx.x series may be cast by a variety of techniques ranging from relatively simple sand or die casting to very intricate permanent mold, investment castings, and the newer thixocasting and squeeze-casting technologies (Fig. 17).

Among the workhorse alloys are 319.0 and 356.0/A356.0 for sand and permanent mold casting, with A356.0-T6 for such critical applications as automotive wheels (Fig. 18). For die castings, 360.0, 380.0/A380.0, and 390.0 are the most widely used. The newer squeeze-cast technologies have generally employed 357.0-T6 and A357.0-T6.

Alloy 332.0 is also one of the most frequently used aluminum casting alloys because it can be made almost exclusively from recycled scrap.



**Figure 16** Complex 3xx.x castings made by the investment casting processes provide the ability to obtain exceptionally intricate detail and fine quality. (Courtesy of the Aluminum Association.)



**Figure 17** Thixoformed A356.0-T6 and A357.0-T6 may be used for critical aircraft components. (Courtesy of the Aluminum Association.)

*4xx.x—Al–Si Alloys.* The major characteristics of the 4xx.x series are:

- Non-heat treatable; sand, permanent mold, and die castings
- Excellent fluidity, good for intricate castings
- Approximate ultimate tensile strength range: 17–25 ksi (115–170 MPa)

Alloy B413.0 is notable for its very good castability and excellent weldability, which are due to its eutectic composition and low melting point of 700°C. It combines moderate strength with high elongation before rupture and good corrosion resistance. The alloy is particularly suitable for intricate, thin-walled, leak-proof, fatigue-resistant castings.

These alloys have found applications in relatively complex cast parts for typewriter and computer housings and dental equipment and also for fairly critical components in marine and architectural applications.

*5xx.x—Al–Mg Alloys.* The major characteristics of the 5xx.x series are:

- Non-heat treatable; sand, permanent mold, and die
- Tougher to cast, provides good finishing characteristics
- Excellent corrosion resistance, machinability, surface appearance
- Approximate ultimate tensile strength range: 17–25 ksi (115–170 MPa)



**Figure 18** Automotive wheels are often cast A356.0-T6. (Courtesy of the Aluminum Association.)

The common feature of this group of alloys is good resistance to corrosion. Alloys 512.0 and 514.0 have medium strength and good elongation and are suitable for components exposed to seawater or to other similar corrosive environments. These alloys are often used for door and window fittings, which can be decoratively anodized to give a metallic finish or in a wide range of colors. Their castability is inferior to that of the Al–Si alloys because of their magnesium content and consequently long freezing range. For this reason they tend to be replaced by 355.0/AlSi5Mg, which has long been used for similar applications.

For die castings where decorative anodizing is particularly important, alloy 520.0 is quite suitable.

*7xx.x—Al–Zn Alloys.* The major characteristics of the 7xx.x series are:

- Heat treatable; sand and permanent mold cast (harder to cast)
- Excellent machinability, appearance
- Approximate ultimate tensile strength range: 30–55 ksi (205–380 MPa)

Because of the increased difficulty in casting 7xx.x alloys, they tend to be used only where the excellent finishing characteristics and machinability are important. Representative applications include furniture, garden tools, office machines, and farming and mining equipment.

*8xx.x—Al–Sn Alloys.* The major characteristics of the 8xx.x series are:

- Heat treatable; sand and permanent mold castings (harder to cast)
- Excellent machinability
- Bearings and bushings of all types
- Approximate ultimate tensile strength range: 15–30 ksi (105–210 MPa)



Like the 7xx.x alloys, 8xx.x alloys are relatively hard to cast and tend to be used only where their combination of superior surface finish and relative hardness are important. The prime examples are for parts requiring extensive machining and for bushings and bearings.

## 8.2 Applications by Market Area

In the paragraphs that follow, a review will be made of the alloys often selected for products in a number of the major markets in which aluminum is used.

### *Electrical Markets*

The major products for which aluminum is used in electrical applications are electric cables and bus conductors, where the high electrical conductivity (60% IACS) makes aluminum a cost-effective replacement for copper products:

- Electrical conductor wire—1350 where no special strength requirements exist and 6201 where a combination of high strength and high conductivity are needed
- Bus conductor—6101 (Fig. 2)
- Electrical cable towers—6063 or 6061 extruded shapes

### *Building and Construction Markets*

Building and construction encompass those markets where architectural and/or structural requirements come together. Such applications include residential housing, commercial store fronts and structures, conference centers and areas (i.e., long roof bay requirements), highway bridges and roadside structures, and a variety of holding tanks and chemical structures (also considered below under Petroleum and Chemical Industry Components). Among the choices are the following:

- Bridges and other highway structures—6063 and 6061 extrusions (Figs. 8 and 9); 5083, 5083, and 5454 plate (Fig. 9)
- Bridge rail mounts—357.0-T6
- Store fronts, curtain wall—6063 extrusions
- Building sheet, siding—3005, 3105, and 5005 sheet
- Arena and convention center roofs—6061 extrusions with 5xxx alloy sheet panels (Fig. 8)
- Residential housing structures—6063 extrusions
- Architectural trim—5257, 5657, 6463
- Composite wall panels—5xxx alloy sheet plus expanded polymers

### *Automobile, Van, SUV, Bus, and Truck Applications*

Automotive structures require a combination of aluminum castings, sheet, and extrusions to cover all good opportunities to increase gasoline mileage and reduce pollutants. Some examples are the following:

- Frame—5182 or 5754 sheet (Fig. 13a) or, for space frame designs, 6063 or 6061 extrusions
- External body sheet panels where dent resistance is important—2008, 6111 (Fig. 13b)
- Inner body panels—5083, 5754
- Bumpers—7029, 7129

- Air conditioner tubes, heat exchangers—3003 (Fig. 6)
- Auto trim—5257, 5657, 5757
- Door beams, seat tracks, racks, rails—6061 or 6063
- Hood, decklids—2036, 6016, 6111
- Truck beams—2014, 6070 (Fig. 4)
- Truck trailer bodies—5454, 5083, 5456 (Fig. 4)
- Wheels—A356.0 (Fig. 18), formed 5xxx sheet, or forged 2014-T6
- Housings, gear boxes—357.0, A357.0 (Fig. 16)

### ***Aircraft and Aerospace Applications***

Aircraft and aerospace applications require high strength combined with, depending upon the specific component, high fracture toughness, high corrosion resistance, and/or high modulus (sometimes all three). The result has been a great number of alloys and tempers developed specifically for this market, as illustrated by the examples below:

- Space mirror—high-purity aluminum
- Wing and fuselage skin—2024, alclad 2024, 7050 plate or extrusions (Fig. 3)
- Wing structures—2024, 2124, 2314, 7050 stiffened extrusions (Fig. 3)
- Bulkhead—2197, 7049, 7050, 7175
- Rocket tankage—2195, 2219, 2419 (Fig. 5)
- Engine components—2618
- Propellers—2025
- Rivets—2117, 6053
- If high modulus is critical—Li-bearing alloys 2090, 2091, 2195, or 8090
- If high fracture toughness is critical—2124, 2224, 2324, 7175, 7475
- For maximum fracture toughness—7475
- If stress corrosion resistance is important—7X50 or 7X75 in the T73-type temper
- If resistance to exfoliation attack is vital—7xxx alloys in the T76-type temper
- For welded construction, as for shuttle tanks—5456, 2219, 2195

### ***Marine Transportation***

Many aluminum alloys readily withstand the corrosive attack of marine salt water and so find applications in boats, ships, offshore stations, and other components that are immersed in salt-water:

- Hull material—5083, 5383, 6063, 6061 (Fig. 11)
- Superstructure—5083, 5456
- Structural beams—5083, 5383, 6063, 6061 (Fig. 11)
- Off-shore stations, tanks—5083, 5456 (Fig. 12)

### ***Rail Transportation***

Much as for auto and truck bodies, aluminum lends itself to railcar structural and exterior panel applications:

- Beams—2014, 6061, 6070
- Exterior panels—5456, 6111

- Tank cars—5454, 5083
- Coal cars—5454, 5083, 5456 (Fig. 10)
- Cars for hot cargo—5454

### ***Packaging Applications***

Packaging applications require either great ductility and corrosion resistance for foil and wrapping applications or great strength and workability for rigid container sheet applications, i.e., cans. Alloy choices include the following:

- Aluminum foil for foods—1175 (Fig. 1)
- Rigid container (can) bodies—3004 (Fig. 7)
- Rigid container (can) ends—5182

### ***Petroleum and Chemical Industry Components***

The excellent combination of high strength combined with superior corrosion resistance plus weldability makes a number of aluminum alloys ideal for chemical industry applications, even some involving very corrosive fluids:

- Chemical piping—1060, 5254, 6063
- Pressure vessels (ASME Code)—5083, 5086, 6061, 6063
- Pipelines—6061, 6063, 6070
- Cryogenic tankage—5052, 5083, 5454, 6063, 6061
- Containers for hydrogen peroxide—5254, 5652

### ***Other Markets***

While not major markets in themselves, a variety of specialty products find great advantage in aluminum alloys:

- Screw machine products—2011, 6262
- Appliances—5005, 5052
- Tread plate—6061
- Weld wire—4043 (for welding 6xxx alloys), 5356, 5183, 5556 (for welding 5xxx alloys)

## **9 SUMMARY**

Listed below are some of the characteristics of aluminum and its alloys that lead to their widespread application in nearly every segment of the economy. It is safe to say that no other material offers the same combination of properties.

- *Lightweight.* Very few metals have a lower density than aluminum, and they are not in common usage. Iron and copper are roughly three times as dense and titanium over 60% more dense than aluminum.
- *Good Formability.* Aluminum can be fabricated or shaped by just about every known method and is consequently available in a wide variety of forms.
- *Wide Range of Mechanical Properties.* Aluminum can be utilized as a weak, highly ductile material or, through alloying, as a material with a tensile strength approaching 100,000 psi.

- *High Strength-to-Weight Ratio.* Because of the combination of low density and high tensile strength, some aluminum alloys possess superior strength-to-weight ratios, equaled or surpassed only by highly alloyed and strengthened steels and titanium.
- *Good Cryogenic Properties.* Aluminum does not become brittle at very low temperatures; indeed, mechanical properties of most aluminum alloys actually improve with decreasing temperature.
- *Good Weatherability and General Corrosion Resistance.* Aluminum does not rust away in the atmosphere and usually requires no surface protection. It is highly resistant to attack from a number of chemicals.
- *High Electrical and Thermal Conductivity.* Pound for pound, aluminum conducts electricity and heat better than any other material except sodium, which can only be used under very special conditions. On a volume basis, only copper, silver, and gold are better conductors.
- *High Reflectivity.* Normally, aluminum reflects 80% of white light, and this value can be increased with special processing.
- *Finishability.* Aluminum is unique among the architectural metals with respect to the variety of finishes employed.

## REFERENCES

1. D. G. Altenpohl, *Aluminum: Technology, Applications and Environment*, Aluminum Association, Washington, DC, and TMS, Warrendale, PA, 1999.
2. *Aluminum Standards and Data (Standard and Metric Editions)*, Aluminum Association, Washington, DC, published periodically.
3. *Standards for Aluminum Sand and Permanent Mold Casting*, Aluminum Association, Washington, DC, December 1992.
4. *The Aluminum Design Manual*, Aluminum Association, Washington, DC, 2005.
5. *The Aluminum Association Alloy and Temper Registrations Records:*
  - (i) International Alloy Designations and Chemical Composition Limits for Wrought Aluminum and Aluminum Alloys, Aluminum Association, Washington, DC, January 2001.
  - (ii) Designations and Chemical Composition Limits for Aluminum Alloys in the Form of Castings and Ingot, Aluminum Association, Washington, DC, January 1996.
  - (iii) Tempers for Aluminum and Aluminum Alloy Products, Aluminum Association, Washington, DC, August 2001.
6. *American National Standard Alloy and Temper Designation Systems for Aluminum*, ANSI H35.1-1997, American National Standards Institute, Aluminum Association, Secretariat, Washington, DC, 1997.
7. *International Accord on Wrought Aluminum Alloy Designations*, Aluminum Association, Washington, DC, published periodically.
8. D. Zalenas (Ed.), *Aluminum Casting Technology*, 2nd ed., American Foundrymen's Society, Des Plaines, IL, 1993.
9. *Product Design for Die Casting in Recyclable Aluminum, Magnesium, Zinc, and ZA Alloys*, Die Casting Development Council, La Grange, IL, 1996.
10. *The NFFS Guide to Aluminum Casting Design: Sand and Permanent Mold*, Non-Ferrous Founders Society, Des Plaines, IL, 1994.
11. *Strength of Aircraft Elements*, MMPDS-01/MIL-HDBK-5J, Federal Aviation Administration, Washington, DC, 2004.
12. M. L. Sharp, *Behavior and Design of Aluminum Structures*, McGraw-Hill, New York, 1993.
13. M. L. Sharp, G. E. Nordmark, and C. C. Menzemer, *Fatigue Design of Aluminum Components and Structures*, McGraw-Hill, New York, 1996.

14. *Fatigue Design Handbook*, 2nd ed., SAE AE-10, Society of Automotive Engineers, Warrendale, PA, 1988.
15. J. R. Kissell and R. L. Ferry, *Aluminum Structures, a Guide to Their Specifications and Design*, Wiley, New York, 1995.
16. *Boiler & Pressure Vessel Code*, American Society of Mechanical Engineers, New York, updated periodically.
17. J. G. Kaufman and E. Rooy, *Aluminum Alloy Castings—Properties, Processes, and Applications*, ASM International, Materials Park, OH, 2004.

### Additional Selected Reading

18. *Aluminum Alloys—Selection and Application*, Aluminum Association, Washington, DC, December 1998.
19. J. R. Davis (Ed.), *Aluminum and Aluminum Alloys*, ASM Specialty Handbook, ASM International, Materials Park, OH, February 1994.
20. H. Chandler (Ed.), *Heat Treater's Guide—Practices and Procedures for Nonferrous Alloys*, ASM International, Materials Park, OH, February 1994.
21. J. G. Kaufman (Ed.), *Properties of Aluminum Alloys—Tensile, Creep, and Fatigue Data at High and Low Temperatures*, Aluminum Association and ASM International, Materials Park, OH, December 1999.
22. *Aluminum Alloys for Cryogenic Applications*, Aluminum Association, Washington, DC, 1999.
23. *Life-Cycle Assessments for Aluminum Alloy Products*, Aluminum Association, Washington, DC, February 1996.
24. *Aluminum for Automotive Body Sheet Panels*, Publication AT3, Aluminum Association, Washington, DC, 1998.
25. *Aluminum Automotive Extrusion Manual*, Publication AT6, Aluminum Association, Washington, DC, 1998.
26. J. G. Kaufman, *Introduction to Aluminum Alloys and Tempers*, Aluminum Association and ASM International, Materials Park, OH, 2000.
27. J. G. Kaufman, *Fracture Resistance of Aluminum Alloys—Notch Toughness, Tear Resistance, and Fracture Toughness*, Aluminum Association and ASM International, Materials Park, OH, 2001.
28. *Aluminum and Aluminum Alloys*, American Society for Metals, Materials Park, OH, 1993.
29. *Aluminum Brazing Handbook*, Aluminum Association, Washington, DC, 1998.
30. *Aluminum Electrical Conductor Handbook*, Aluminum Association, Washington DC, 1998.
31. *Aluminum: Properties and Physical Metallurgy*, ASM International, Materials Park, OH, 1984.
32. *Aluminum Soldering Handbook*, Aluminum Association, Washington, DC, 2004.
33. *Forming and Machining Aluminum*, Aluminum Association, Washington, DC, 1988.
34. H. P. Goddard et al., *The Corrosion of Light Metals*, Wiley, New York, 1967.
35. *Guidelines for the Use of Aluminum with Food and Chemicals*, Aluminum Association, Washington, DC, 1994.
36. *Handbook of Corrosion Data*, ASM International, Materials Park, OH, 1989.
37. J. D. Minford, *Handbook of Aluminum Bonding Technology and Data*, Marcel Dekker, New York, 1993.
38. *Metals Handbook Series*, ASM International, Materials Park, OH, updated periodically.
39. *The Surface Treatment and Finishing of Aluminum and Its Alloys*, Aluminum Association, Washington, DC, 2001.
40. *Welding Aluminum: Theory and Practice*, Aluminum Association, Washington, DC, 2002.

# CHAPTER 4

## COPPER AND COPPER ALLOYS

**Konrad J. A. Kundig**  
Metallurgical Consultant  
Tucson, Arizona

**Robert D. Weed**  
Copper Development Association  
New York, New York

<b>1 INTRODUCTION</b>	<b>117</b>	4.7 Welding Processes	212
<b>2 COPPER ALLOY FAMILIES</b>	<b>118</b>	4.8 Joint Preparation	213
2.1 Compositions	119	4.9 Filler Metals	213
2.2 Physical Properties of Copper and Copper Alloys	150	4.10 Distortion Control	213
<b>3 MECHANICAL PROPERTIES OF COPPER AND COPPER ALLOYS</b>	<b>150</b>	4.11 Avoiding Cracking	214
3.1 Strengthening Mechanisms	150	4.12 Weld Properties	214
3.2 Temper	159	4.13 Safety and Health	214
3.3 Mechanical Properties Data	162	<b>5 TUBE AND PIPE PRODUCTS</b>	<b>215</b>
<b>4 CORROSION BEHAVIOR</b>	<b>199</b>	5.1 Plumbing Tube	215
4.1 Forms of Corrosion	201	5.2 Nonflammable Medical Gas Piping Systems	217
4.2 Biostatic and Antimicrobial Properties	202	5.3 Fuel Gas Distribution Systems	217
4.3 Fabrication	204	<b>6 COPPER ALLOY SLEEVE BEARINGS</b>	<b>224</b>
4.4 Casting	209	<b>7 STANDARDS AND SPECIFICATIONS</b>	<b>226</b>
4.5 Forging	211	<b>ADDITIONAL INFORMATION</b>	<b>227</b>
4.6 Welding, Brazing, and Soldering	211	<b>REFERENCES</b>	<b>227</b>

### 1 INTRODUCTION

Copper was among the first metals to be put into utilitarian service. Fabricated copper objects dating to approximately 8500 B.C. place the probable origin of the metal's use in Asia Minor, although prehistoric artifacts can be associated with civilizations on almost all inhabited continents. Copper is one of a few metals found in its native (metallic) state, and the earliest copper "products," mainly ornamental or votive objects, were undoubtedly made from nuggets. A solid copper mace head, found near Cata Huyuk, Anatolia (now Turkey), has been dated to 8000 B.C. Smelting is believed to have begun in what is now Israel as early as 5000 B.C., and a vigorous



trade in the metal was well established within several hundred years. That prehistoric copper objects have survived through millennia attests to the metal's inherent chemical stability.<sup>1,2</sup>

Copper alloys first appeared, in Mesopotamia, around 3500 B.C. through the inclusion of tin (ushering in the Bronze Age) and later zinc (creating brass). The resulting alloys were stronger than pure copper, which brought them more-demanding applications, but the discovery of iron soon supplanted the alloys in such items as tools and weaponry. Nevertheless, copper "consumption"—if it can be called that—remained quite small for millennia. It was not until the introduction of electricity in the nineteenth century that copper came into widespread use. Consumption grew quickly, reflecting, as it does to this day, global rates of electrification and industrialization and, more recently, the growth of communications and data-processing systems.

In 2011, worldwide consumption of refined copper was approximately 21.6 million short tons. The United States consumed more than 1.9 million tons of refined copper in 2011, of which 1.2 million tons was mined domestically. About 33% of consumption was in the form of refined scrap. Chile is the world's leading copper miner, followed by the United States. Arizona, with approximately 65% of domestic output, is the principal copper-producing state, followed by Utah and New Mexico. The United States has ample resources and exports as well and imports both metal and ore concentrates. Several new ore bodies are currently (2012) under development in Arizona and elsewhere.

The properties that drive the use of copper and its alloys include high electrical and thermal conductivities, favorable combinations of strength and ductility, ease of fabrication (machinability, castability, weldability, and joining properties), resistance to corrosion, aesthetic appeal, and the metal's ability to form literally hundreds of useful alloys, usually with specifically tailored properties.

In the United States in 2010, 66% of all copper and copper alloys consumed found its way into electrical applications. Applications related to corrosion resistance, mainly plumbing goods (22.5%), heat transfer, radiators, air conditioners, etc. (9%), structural properties (7%), and aesthetics (2%) accounted for the remainder. In terms of product form, wire and cable products made up about one-half of total metallic copper consumption, followed by plumbing and commercial tube; rod, bar, and mechanical wire; and strip, sheet, and plate, each ranging between approximately 14 and 17%. Castings, metal powder, and chemicals together make up a bit more than 5%. A growing fraction of copper use derives from the metal's intrinsic antimicrobial properties. This topic is addressed elsewhere in the chapter.

## 2 COPPER ALLOY FAMILIES

The Unified Numbering System (UNS) is the accepted alloy designation system in North America for wrought and cast coppers and copper alloys. Identification is by five-digit numbers preceded by the letter C. The numbering system is based on an earlier and still occasionally cited three-digit system developed by the U.S. copper and brass industry. Older descriptive alloy names also remain in wide use, although they are not suitable for specification purposes. For example, *forging brass* became copper alloy no. 377 and, eventually, alloy C37700. The UNS is administered by the Copper Development Association, Inc. (CDA) and is managed jointly by the American Society for Testing and Materials (ASTM) and the Society of Automotive Engineers (SAE). Alloy designations are common to standards issued by those organizations. Producers may register new alloys with CDA, which assigns an appropriate number and publishes properties on its website ([www.copper.org](http://www.copper.org)). Numbers from C10000 through C79999 denote wrought alloys, i.e., rolled, drawn, forged, or extruded. Cast alloys are numbered from C80000 through C99999. Descriptions of the copper alloy families are presented in Table 1.

**Table 1** Copper Alloy Families

<b>Coppers</b> C10100–C15999 (wrought), C80000–C83199 (cast)	Wrought coppers have a designated minimum copper content of 99.3% or higher, including several grades containing a minimum of 99.99% Cu. Cast coppers have a designated minimum copper content of 98.5% or higher, including one grade at 99.9% Cu. Uses are principally electrical products or those requiring very high thermal conductivity.
<b>High-Copper Alloys</b> C160000–C19999 (wrought) C81400–83299 (cast)	For wrought products, these are alloys with designated copper contents less than 99.3% but more than 96% that do not fall into any other copper alloy group. The cast high-copper alloys have designated copper contents in excess of 94%, to which silver may be added for special properties. They are often specified where good electrical and thermal conductivity in conjunction with higher mechanical strengths than those available in coppers are needed.
<b>Brasses</b> C20000–C49990 (wrought) C83300–C89999 (wrought)	These alloys contain zinc as the principal alloying element with or without other designated alloying elements such as iron, aluminum, nickel, and silicon. The <b>wrought alloys</b> comprise three main families of brasses: copper–zinc alloys; copper–zinc–lead alloys (lead brasses); and copper–zinc–tin alloys (tin brasses). The <b>cast alloys</b> comprise four main families of brasses: copper–tin–zinc alloys (red, semi-red, and yellow brasses); “manganese bronze” alloys (high-strength yellow brasses); leaded “manganese bronze” alloys (leaded high-strength yellow brasses); copper–zinc–silicon alloys (silicon brasses and bronzes); and cast copper–bismuth and copper–bismuth–selenium alloys. Ingot for remelting for the manufacture of castings may vary slightly from the ranges shown in the tables. Brasses are widely used for a large variety of products.
<b>Bronzes</b> C50000–C69999 (wrought) C90000–C95999 (cast)	Broadly speaking, bronzes are copper alloys in which the major alloying element is not zinc or nickel. Originally “bronze” described alloys with tin as the only or principal alloying element. Today, the term is generally used not by itself but with a modifying adjective. For <b>wrought alloys</b> , there are four main families of bronzes: copper–tin–phosphorus alloys (phosphor bronzes); copper–tin–lead–phosphorus alloys (leaded phosphor bronzes); copper–aluminum alloys (aluminum bronzes); and copper–silicon alloys (silicon bronzes). The <b>cast alloys</b> have four main families of bronzes: copper–tin alloys (tin bronzes); copper–tin–lead alloys (leaded and high-leaded tin bronzes); copper–tin–nickel alloys (nickel–tin bronzes); and copper–aluminum alloys (aluminum bronzes). The family of alloys known as “manganese bronzes,” in which zinc is the major alloying element, is included in the brasses, above. Bronzes are generally specified where the intrinsic properties of copper-based metals are needed, along with improved mechanical and/or chemical properties than those offered by most brasses.
<b>Copper Nickels</b>	These are alloys with nickel as the principal alloying element, with or without other designated alloying elements. They are especially resistant to salt-water corrosion and are used in some marine equipment. Flat-rolled copper–nickels are also used in coinage.
<b>Nickel Silvers</b> C73500–C79999 (wrought) C97000–97999 (cast)	Technically, these alloys are nickel brasses. Named for their silvery color, contain zinc and nickel as the principal and secondary alloying elements, with or without other designated elements, including sulfur or lead for enhanced machinability. They have traditionally been used in the dairy industry and some grades also still occasionally called “dairy metal.”
<b>Leaded Coppers</b> C98000–C98999 (cast)	These compositions comprise a series of <b>cast alloys</b> of copper containing 20% or more lead, sometimes with a small amount of silver but without tin or zinc. They are important bearing materials.
<b>Special Alloys</b> C99000–C99999 (cast)	Alloys whose chemical compositions do not fall into any of the above categories are combined in the family of “special alloys.”

## 2.1 Compositions

Compositions of currently accepted wrought and cast coppers and copper alloys arranged by alloy families and similar alloys within families are given in Tables 2–21 and 22–38, respectively.<sup>3</sup> For example, leaded and nonleaded brasses and bronzes are tabulated separately. Compositions are given as weight percent maximum unless shown as a range or minimum. These data are kept current on the CDA website, [www.copper.org](http://www.copper.org).

120 Copper and Copper Alloys

Table 2 Compositions of Wrought Coppers, UNS C10100–C12000

Copper No.	Designation	Description	Cu (incl Ag)	Ag		As	Sb	P	Te	Other Named Elements
				% Min	Troy oz Min					
C10100 <sup>b</sup>	OFE	Oxygen-free electronic	99.99 min <sup>c</sup>	—	—	.0005	.0004	.0003	.0002	1 .0005 Oxygen
C10200 <sup>b</sup>	OF	Oxygen free	99.95 min <sup>d</sup>	—	—	—	—	—	—	.0010 Oxygen
C10300	OFXLP	Oxygen-free copper	99.95 min <sup>e</sup>	—	—	—	—	.001–.005	—	—
C10400 <sup>b</sup>	OFS	Oxygen free with Ag	99.95 min <sup>d</sup>	.027	8.	—	—	—	—	.0010 Oxygen
C10500 <sup>b</sup>	OFS	Oxygen free with Ag	99.95 min <sup>d</sup>	.034	10.	—	—	—	—	.0010 Oxygen
C10700 <sup>b</sup>	OFS	Oxygen free with Ag	99.95 min <sup>d</sup>	.085	25.	—	—	—	—	.0010 Oxygen
C10800	OFLP	—	99.95 min <sup>e</sup>	—	—	—	—	.005–.012	—	—
C10910 <sup>b</sup>	—	—	99.95 min <sup>d</sup>	—	—	—	—	—	—	.005 Oxygen
C10920	—	—	99.90 min	—	—	—	—	—	—	.02 Oxygen
C10930	—	—	99.90 min	.044	13.	—	—	—	—	.02 Oxygen
C10940	—	—	99.90 min	.085	25.	—	—	—	—	.02 Oxygen
C11000 <sup>b</sup>	ETP	Electrolytic tough pitch	99.90 min	—	—	—	—	—	—	<sup>f</sup>
C11010 <sup>b</sup>	RHC	Remelted high conductivity	99.90 min	—	—	—	—	—	—	<sup>f</sup>
C11020 <sup>b</sup>	FRHC	Fire-refined high conductivity	99.90 min	—	—	—	—	—	—	<sup>f</sup>
C11030 <sup>b</sup>	CRTP	Chemically refined tough pitch	99.90 min	—	—	—	—	—	—	<sup>f</sup>
C11040 <sup>b</sup>	—	—	99.90 min	—	—	.0005	.0004	—	.0002	<sup>g</sup>
C11045	—	—	—	—	—	—	—	—	—	—
C11100 <sup>b</sup>	ETP	Electronic tough pitch, anneal resistant	99.90 min	—	—	—	—	—	—	<sup>h</sup>
C11300 <sup>b</sup>	STP	Tough pitch with Ag	99.90 min	.027	8.	—	—	—	—	<sup>f</sup>
C11400 <sup>b</sup>	STP	Tough pitch with Ag	99.90 min	.034	10.	—	—	—	—	<sup>f</sup>
C11500 <sup>b</sup>	STP	Tough pitch with Ag	99.90 min	.054	16.	—	—	—	—	<sup>f</sup>
C11600 <sup>b</sup>	STP	Tough pitch with Ag	99.90 min	.085	25.	—	—	—	—	<sup>f</sup>
C11700	—	—	99.9 min <sup>i</sup>	—	—	—	—	.04	—	.004–.02 B
C12000	DLP	Phosphorus-deoxidized, low-residual P	99.90 min	—	—	—	—	.004–.012	—	—

<sup>a</sup>The following additional maximum limits shall apply: Bi, 1 ppm (.0001%); Cd, 1 ppm (.0001%); Fe, 10 ppm (.0010%); Pb, 5 ppm (.0005%); Mn, 0.5 ppm (.00005%); Ni, 10 ppm (.0010%); Se, 3 ppm (.0003%); Ag, 25 ppm (.0025%); S, 15 ppm (.0015%); Sn, 2 ppm (.0002%); Zn, 1 ppm (.0001%).

<sup>b</sup>This is a high-conductivity copper which has, in the annealed condition, a minimum conductivity of 100% IACS except for alloy C10100, which has a minimum conductivity of 101% IACS.

<sup>c</sup>Cu is determined by the difference between the impurity total and 100%. The Cu value is exclusive of Ag.

<sup>d</sup>Cu is determined by the difference between the impurity total and 100%.

<sup>e</sup>Includes P.

<sup>f</sup>Oxygen and trace elements may vary depending on the process.

<sup>g</sup>The following additional maximum limits shall apply: Se, 2 ppm (.0002%); Bi, 1.0 ppm (.00010%); Group Total, Te + Se + Bi, 3 ppm (.0003%). Sn, 5 ppm (.0005%); Pb, 5 ppm (.0005%); Fe, 10 ppm (.0010%); Ni, 10 ppm (.0010%), S, 15 ppm (.0015%); Ag, 25 ppm (.0025%); oxygen, 100–65 ppm (.010–.065%). The total maximum allowable of 65 ppm (.0065%) does not include oxygen.

<sup>h</sup>Small amounts of Cd or other elements may be added by agreement to improve the resistance to softening at elevated temperatures.

<sup>i</sup>Includes B + P.

**Table 3** Compositions of Wrought Coppers, UNS C12100–C14181

Copper No.	Designation	Description	Cu (incl Ag)	Ag		As	Sb	P	Te	Other Named Elements
				% Min	Troy oz Min					
C12100	DLPS	Phosphorus-deoxidized, low-residual P	99.90 min	.014	4.	—	—	.005–.012	—	—
C12200 <sup>a</sup>	DHP	Phosphorus-deoxidized, high-residual P	99.9 min	—	—	—	—	.015–.040	—	—
C12210 <sup>d</sup>	—	—	99.90 min	—	—	—	—	.015–.025	—	—
C12220 <sup>d</sup>	—	—	99.9 min	—	—	—	—	.040–.065	—	—
C12300 <sup>d</sup>	DHPS	Phosphorus-deoxidized, high-residual P	99.90 min	—	—	—	—	.015–.040	—	—
C12500 <sup>d</sup>	FRTP	Fire-refined tough pitch	99.88 min	—	—	.012	.003	—	.025 <sup>b</sup>	.003 Bi .004 Pb .050 Ni .005 Bi .05 Fe
C12510 <sup>d</sup>	—	—	99.9 min	—	—	—	.003	.03	.025 <sup>b</sup>	.020 Pb .050 Ni .05 Sn .080 Zn .003 Bi .004 Pb .050 Ni
C12900 <sup>d</sup>	FRSTP	Fire-refined tough pitch with Ag	99.88 min	.054	16.	.012	.003	—	.025 <sup>c</sup>	—
C13100 <sup>d</sup>	—	—	99.8 min	—	—	—	—	—	—	—
C13150 <sup>d</sup>	FRTP	Fire-refined tough pitch	99.88	—	—	0.012	—	—	0.025	.01 Al .02 Pb
C14180 <sup>d</sup>	—	—	99.90 min	—	—	—	—	.075	—	—
C14181 <sup>d</sup>	—	—	99.90 min	—	—	—	—	.002	—	.002 Cd .005 C .002 Pb .002 Zn

<sup>a</sup>This includes oxygen-free Cu which contains P in an amount agreed upon.

<sup>b</sup>0.025 Te + Se.

<sup>c</sup>Includes Te + Se.

<sup>d</sup>Antimicrobial.

Table 4 Compositions of Wrought Coppers, UNS C14200–C15500

Copper No.	Designation	Description	Cu (incl Ag)	Ag		As	Sb	P	Te	Other Named Elements
				% Min	Troy oz Min					
C14200	DPA	Phosphorus deoxidized, arsenical	99.4 min	—	.15–.50	—	.015–.040	—	—	—
C14300	—	Cadmium copper, deoxidized	99.90 min <sup>a</sup>	—	—	—	—	—	—	.05–.15 Cd
C14410	—	—	99.90 min <sup>b</sup>	—	—	—	.005–.020	—	—	.05 Fe .05 Pb .10–.20 Sn
C14415	—	—	99.96 min <sup>b</sup>	—	—	—	—	—	—	.10–.15 Sn
C14420	—	—	99.90 min <sup>c</sup>	—	—	—	—	—	.005–.05	.04–.15 Sn
C14425	—	—	99.97	—	—	—	—	—	—	0.020 Fe 0.10 Pb 0.020 Ni 0.010 P 0.25–0.35 Sn 0.10 Zn
C14500 <sup>(4)</sup>	PTE	Tellurium bearing	99.90 min <sup>e</sup>	—	—	—	—	.004–.012	.40–.7	—
C14510 <sup>*</sup>	—	Tellurium bearing	99.85 min <sup>e</sup>	—	—	—	—	.010–.030	.30–.7	.05 Pb
C14520 <sup>*</sup>	DPTE	Phosphorus deoxidized, tellurium bearing	99.90 min <sup>e</sup>	—	—	—	—	.004–.020	.40–.7	—
C14530 <sup>*</sup>	—	—	99.90 min <sup>b</sup>	—	—	—	—	.001–.010	.003–.023 <sup>f</sup>	<i>f</i>
C14700 <sup>(4)*</sup>	—	Sulfur bearing	99.90 min <sup>g</sup>	—	—	—	—	.002–.005 <sup>g</sup>	—	.003–.023 Sn <i>g</i>
C14750	—	—	99.6	0.05–0.50	—	—	—	—	—	.20–.50 S 0.012 P
C15000 <sup>(8)*</sup>	—	Zirconium copper	99.80 min	—	—	—	—	—	—	0.20–0.50 S
C15100 <sup>(8)*</sup>	—	—	99.80 min	—	—	—	—	—	—	.10–.20 Zr
C15150 <sup>*</sup>	—	—	99.90 min	—	—	—	—	—	—	.05–.15 Zr
C15500 <sup>*</sup>	—	—	99.75 min	.027–.10	8. –30.	—	—	.040–.080	—	.015–.030 Zr .08–.13 Mg
C15650 <sup>*</sup>	MA5J	—	99.9	—	—	—	—	—	—	0.04–0.06 Co 0.015–0.040 P

<sup>a</sup>Includes Cd. Deoxidized with Li or other suitable elements as agreed upon.<sup>b</sup>Includes Cu + Ag + Sn.<sup>c</sup>Includes Te + Sn.<sup>d</sup>Includes oxygen-free or deoxidized grades with deoxidizers (such as phosphorus, boron, lithium, or others) in an amount agreed upon.<sup>e</sup>Includes Te.<sup>f</sup>Includes Te + Se.<sup>g</sup>Includes Cu + S + P.<sup>h</sup>Cu + sum of named elements, 99.9% min.

**Table 5** Compositions of Wrought Coppers, UNS C15715–C15900

Copper No.	Designation	Description	Cu (incl Ag)	Al	Fe	Pb	Oxygen	Boron	Other Named Elements
C15715*	Glidcop Al-15	MMC	99.62 min	.13–.17 <sup>a</sup>	.01	.01	.12–.19 <sup>a</sup>	—	—
C15720	Glidcop Al-20	MMC	99.52 min	.18–.22 <sup>a</sup>	.01	.01	.16–.24 <sup>a</sup>	—	—
C15725*	Glidcop Al-20	MMC	99.43 min	.23–.27 <sup>a</sup>	.01	.01	.20–.28 <sup>a</sup>	—	—
C15730*	Glidcop Al-30	MMC	99.94 min	0.26–0.34 <sup>a</sup>	0.04	—	0.32–0.46	0.22	—
C15750*	Glidcop-A;-50	MMC	99.56 min	0.42–0.50	0.04 Fe 0.52 O	—	0.52–0.68	0.22	—
C15760*	Gliddop Al-60	MMC	98.77 min	.58–.62 <sup>a</sup>	.01	.01	0.52–0.59	0.22–	—
C15780*	Glidcop Al-80	MMC	98.10 min	0.66–0.74	0.04	—	0.76–0.90	0.22	—
C15790*	Glidcop Al-90	MMC	97.68 min	0.88–0.96	0.04	—	0.96–1.10	0.22	—
C15815*	—	MMC	97.82	.13–.17 <sup>a</sup>	.01	.01	.19 <sup>a</sup>	1.2–1.8	—
C15900*	—	MMC	97.51 min	0.76–0.84 Al	0.04	—	0.40–0.54	—	0.27–0 0.33 C 0.66–0.74 Ti

<sup>a</sup>All aluminum present as Al<sub>2</sub>O<sub>3</sub>; .04% oxygen present as Cu<sub>2</sub>O with a negligible amount in solid solution with copper.  
 Note: MMC = metal matrix composite = dispersion-strengthened copper.



Table 6 Compositions of Wrought High-Copper Alloys, UNS C16200–C18090

Copper Alloy No.	Previous Trade Name	MMC	Cu (incl Ag)	Fe	Sn	Ni	Co	Cr	Si	Be	Pb	Other Named Elements
C16200 <sup>a</sup>	Cadmium copper		Rem.	.02	—	—	—	—	—	—	—	.7–1.2 Cd
C16500 <sup>a</sup>	—		Rem.	.02	.50–.7	—	—	—	—	—	—	.6–1.0 Cd
C17000 <sup>a</sup>	Beryllium copper		Rem.	—	—	—	.20 min <sup>b</sup>	—	.20	1.60–1.79	—	.20 Al
C17200 <sup>a</sup>	Beryllium copper		Rem.	—	—	—	.20 min <sup>b</sup>	—	.20	1.80–2.00	—	.20 Al
C17300 <sup>a</sup>	Beryllium copper		Rem.	—	—	—	.20 min <sup>b</sup>	—	.20	1.80–2.00	.20–.6	.20 Al
C17410 <sup>a</sup>	Beryllium copper		Rem.	.20	—	—	.35–.6	—	.20	.15–.50	—	.20 Al
C17450 <sup>a</sup>	Beryllium copper		Rem.	.20	.25	.50–1.0	—	—	.20	.15–.50	—	.20 Al .50 Zr
C17455 <sup>a</sup>	Beryllium copper		Rem.	.20	.25	.50–1.0 <sup>c</sup>	—	—	.20	.15–.50	.20–.6	.20 Al .50 Zr
C17460 <sup>a</sup>	Beryllium copper		Rem.	.20	.25	1.0–1.4	—	—	.20	.15–.50	—	.20 Al
C17465 <sup>a</sup>	Beryllium copper		Rem.	.20	.25	1.0–1.4 <sup>c</sup>	—	—	.20	.15–.50	.20–.6	.20 Al .50 Zr
C17500 <sup>a</sup>	Beryllium copper		Rem.	.10	—	—	2.4–2.7	—	.20	.4–.7	—	.20 Al
C17510 <sup>a</sup>	Beryllium copper		Rem.	.10	—	1.4–2.2	.3	—	.20	.2–.6	—	.20 Al
C17530 <sup>a</sup>	Beryllium copper		Rem.	.20	—	1.8–2.5 <sup>c</sup>	—	—	.20	.20–.40	—	.6 Al
C18000 <sup>a</sup>	—		Rem.	.15	—	1.8–3.0 <sup>d</sup>	—	.10–.8	.40–.8	—	—	—
C18020 <sup>e</sup>	—		Rem.	—	.05–.25	—	—	.10–.30	.05	—	—	.10–.30 Zn
C18025 <sup>e</sup>	Chromium copper		Rem.	—	0.015–0.25	—	—	0.20–0.30	—	—	—	0.01–0.03 Mg 0.03–0.07 Si
C18030 <sup>f</sup>	—		Rem.	—	.08–.12	—	—	.10–.20	—	—	—	0.05–0.15 Zn
C18040 <sup>f</sup>	—		Rem.	—	.20–.30	—	—	.25–.35	—	—	—	.005–.015 P .005–.015 P
C18045 <sup>e</sup>	—		99.1 min	—	.20–.30	—	—	.20–.35	.05	—	—	.05–.15 Zn .15–.30 Zn
C18050 <sup>g</sup>	—		Rem.	—	—	—	—	.05–.15	—	—	—	.005–.015 Te
C18070 <sup>g</sup>	—		99.0 min	—	—	—	—	.15–.40	.02–.07	—	—	.01–.40 Ti
C18080 <sup>g</sup>	—		Rem.	.02–.20	—	—	—	.20–.7	.01–.10	—	—	.01–.30 Ag .01–.15 Ti
C18090 <sup>h</sup>	—		96.0 min	—	.50–1.2	.30–1.2	—	.20–1.0	—	—	—	.15–.8 Ti

<sup>a</sup>Cu + sum of named elements, 99.5% min.<sup>b</sup>Ni + Co, .20% min.; Ni + Fe + Co, .6% max. Ni +<sup>c</sup>Ni value includes Co.<sup>d</sup>Includes Co.<sup>e</sup>Cu + sum of named elements, 99.9% min.<sup>f</sup>Includes oxygen-free or deoxidized grades with deoxidizers (such as phosphorus, boron, lithium, or others) in an amount agreed upon.<sup>g</sup>Cu + sum of named elements, 99.8% min.<sup>h</sup>Cu + sum of named elements, 99.85% min.

**Table 7** Compositions of Wrought High-Copper Alloys, UNS C18100–C18835

Copper Alloy No.	Previous Trade Name	Description	Cu (incl Ag)	Fe	Sn	Ni	Co	Cr	Si	Be	Pb	Other Named Elements
C18100 <sup>a</sup>		Chromium copper	98.7 min	—	—	—	—	.40–1.2	—	—	—	.03–.06 Mg, .08–.20 Zr
C18135 <sup>a</sup>		—	Rem.	—	—	—	—	.20–.6	—	—	—	.20–.6 Cd
C18140 <sup>a</sup>		—	Rem.	—	—	—	—	.15–.45	.005–.05	—	—	.05–.25 Zr
C18141 <sup>a</sup>		—	Rem.	—	.20	—	—	0.20–0.40 Cr	0.01–0.03 Si	—	—	0.01 Al, 0.02–0.05 Mg, .07–.13 Zr
C18143 <sup>a</sup>		—	Rem.	—	.20	—	—	.20–.40	.01–.03 Si	—	—	.01 Al, .05 Mn, .07–.13 Zr
C18145 <sup>a</sup>		—	Rem.	—	—	—	—	.10–.30	—	—	—	.10–.30 Zn, .05–.15 Zr
C18150 <sup>b</sup>		—	Rem.	—	—	—	—	.50–1.5	—	—	—	.05–.25 Zr
C18200 <sup>a</sup>		Chromium copper	Rem.	.10	—	—	—	.6–1.2	.10	—	.05	—
C18400 <sup>a</sup>		Chromium copper	Rem.	.15	—	—	—	.40–1.2	.10	—	—	.005 As, .005 Ca, .05 Li, .05 P, .7 Zn
C18600 <sup>a</sup>		—	Rem.	.25–.8	—	.25	.10	.10–1.0	—	—	—	.05–.50 Ti, .05–.40 Zr
C18610 <sup>a</sup>		—	Rem.	.10	—	.25	.25–.8	.10–1.0	—	—	—	.05–.50 Ti, .05–.40 Zr
C18620		—	99.40 min	—	.03–.15	.02–.06	—	—	—	—	—	.14–.21 Co, .040–.075 P, .02–.1 Zr
C18660		—	Rem.	.10–.15	.08 min	—	—	.01–.02	.01–.02 Si	—	—	.03–.07 Mg, .03–.08 P,
C18661 <sup>a</sup>		—	Rem.	.10	.20	—	—	—	—	—	—	.10–.7 Mg, .001–.02 P,
C18665		—	99.0 min	—	—	—	—	—	—	—	—	.40–.9 Mg, .002–.04 P
C18700		Free-machining Cu	99.5 min <sup>c</sup>	—	—	—	—	—	—	—	—	.8–1.5
C18835		—	99.0 min <sup>a</sup>	.10	.15–.55	—	—	—	—	—	.05	.01 P, .30 Zn

<sup>a</sup>Cu + sum of named elements, 99.5% min.

<sup>b</sup>Cu + sum of named elements, 99.7% min.

<sup>c</sup>Includes Pb.

**Table 8** Compositions of Wrought High-Copper Alloys, UNS C18900–19160

Alloy No.	Previous Trade Name	Cu (incl Ag)	Fe	Sn	Ni	Co	Cr	Si	Be	Pb	Other Named Elements
C18900 <sup>a</sup>	—	Rem.	—	.6–.9	—	—	—	.15–.40	—	.02	.01 Al .10–.30 Mn .05 P .10 Zn
C18980 <sup>a</sup>	—	98.0 min	—	1.0	—	—	—	.50	—	.02	.50 Mn .15 P
C18990 <sup>b</sup>	—	Rem.	—	1.8–2.2	—	—	.10–.20	—	—	—	.005–.015 P
C19000 <sup>a</sup>	—	Rem.	.10	—	.9–1.3	—	—	—	—	.05	.15–.35 P .8 Zn
C19002 <sup>a</sup>	—	Rem.	.10	.02–.30	1.4–1.7 <sup>c</sup>	—	—	.20–.35	—	.05	.01 Mg .05 P .02–.50 Ag .04–.35 Zn .005–.05 Zr
C19010 <sup>a</sup>	—	Rem.	—	—	.8–1.8	—	—	.15–.35	—	—	.01–.05 P
C19015 <sup>d</sup>	—	Rem.	—	—	.50–2.4	—	—	.10–.40	—	—	.02–.15 Mg .02–.20 P
C19020 <sup>d</sup>	—	Rem.	—	.30–.9	.50–3.0	—	—	—	—	—	.01–.20 P
C19024	—	Rem.	.02	.20–.80	.10–.6	—	—	—	—	—	.008–.05 P, .05 Zn
C19025 <sup>e</sup>	—	Rem.	.10	.7–1.1	.8–1.2	—	—	—	—	—	.03–.07 P .20 Zn
C19027	NB 115	Rem.	.10	1.20–1.80	.0–1.2	—	—	—	—	—	.20 Mg, .03–.15 P, .2 Zn
C19030 <sup>e</sup>	—	Rem.	.10	1.0–1.5	1.5–2.0	—	—	.010	—	.02	.01–.03 P
C19040	NB 115	96.1 min.	.06	1.0–2.0	.7–.9	—	—	—	—	.02	.02 M, .55 P
C19100 <sup>a</sup>	—	Rem.	.20	—	.9–1.3	—	—	—	—	.10x	.15–.35 P .35–.6 Te .50 Zn
C19140 <sup>a</sup>	—	Rem.	.05	.05	.8–1.2	—	—	—	—	.40–.8	.15–.35 P .50 Zn
C19150 <sup>a</sup>	—	Rem.	.05	.05	.8–1.2	—	—	—	—	.50–1.0	.15–.35 P
C19160 <sup>a</sup>	—	Rem.	.05	.05	.8–1.2	—	—	—	—	.8–1.2	.15–.35 P .50 Zn

<sup>a</sup>Cu + sum of named elements, 99.5% min.<sup>b</sup>Cu + sum of named elements, 99.9% min.<sup>c</sup>Ni value includes Co<sup>d</sup>Cu + sum of named elements, 99.8% min.<sup>e</sup>Cu + sum of named elements, 99.7% min.

**Table 9** Compositions of Wrought High-Copper Alloys, UNS C19170–C19910

Copper Alloy No.	Previous Trade Name	Cu	Fe	Sn	Zn	Al	Pb	P	Other Named Elements
C19170	KLF 170	96.8 min	.05–.15					.08–.20	.02 Pb, 50–1.0 Ni, .010 Si, 1.0 Zn
C19200 <sup>a</sup>	—	98.5 min	.8–1.2	—	.20	—	—	.01–.04	—
C19210 <sup>a</sup>	—	Rem.	.05–.15	—	—	—	—	.025–.04	—
C19215 <sup>a</sup>	—	Rem.	.05–.20	—	1.1–3.5	—	—	.025–.050	—
C19220 <sup>a</sup>	—	Rem.	.10–.30	.05–.10	—	—	—	.03–.07	.005–.015 B, .10–.25 Ni
C19240	Super KFC	97.5 min	.15–.45	.20–.80	1.0	—	.02	.04–.20	.02 Mn, .010 Si
C19250	SPKFC	95.8 min	.15–.45	.8–2.5	1.0	—	.02	.04–.20	.02 Mn, .010 Si
C19260 <sup>b</sup>	—	98.5 min	.40–.8	—	—	—	—	—	.02–.15 Mg, .20–.40 Ti
C19280 <sup>a</sup>	—	Rem.	.50–1.5	.30–.7	.30–.7	—	—	.005–.015	—
C19400	—	97.0 min	2.1–2.6	—	.05–.20	—	.03	.015–.15	—
C19410 <sup>a</sup>	—	Rem.	1.8–2.3	.6–.9	.10–.20	—	—	.015–.050	—
C19419	CAC19	96.7 min	1.7–2.5	.05–.18	.10–.40	—	.02	.03	.04 Mn, .04 Ni, .03–.09 Si
C19450 <sup>a</sup>	—	Rem.	1.5–3.0	.8–2.5	—	—	—	.005–.05	—
C19500 <sup>a</sup>	—	96.0 min	1.0–2.0	.10–1.0	.20	.02	.02	.01–.35	.30–1.3 Co
C19520 <sup>a</sup>	—	96.6 min	.50–1.5	—	—	—	.01–3.5	—	—
C19700 <sup>a</sup>	—	Rem.	.30–1.2	.20	.20	—	.05	.10–.40	.05 Co, .01–.20 Mg, .05 Mn, .05 Ni
C19710 <sup>c</sup>	—	Rem.	.05–.40	.20	.20	—	.05	.07–.15	.03–.06 Mg, .05 Mn, .10 Ni <sup>d</sup>
C19720 <sup>c</sup>	—	Rem.	.05–.50	.20	.20	—	.05	.05–.15	.06–.20 Mg, .05 Mn, .10 Ni <sup>d</sup>
C19750 <sup>a</sup>	—	Rem.	.35–1.2	.05–.40	.20	—	.05	.10–.40	.05 Co, .01–.20 Mg, .05 Mn, .05 Ni
C19800 <sup>a</sup>	—	Rem.	.02–.50	.10–1.0	.30–1.5	—	—	.01–.10	.10–1.0 Mg
C19810 <sup>a</sup>	—	Rem.	1.5–3.0	—	1.0–5.0	—	—	.10	.10 Cr, .10 Mg, .10 Ti, .10 Zr
C19900 <sup>c</sup>	—	Rem.	—	—	—	—	—	—	2.9–3.4 Ti
C19910	NKT322	Rem.	.01–.23	—	—	—	—	—	2.9–3.4 Ti

<sup>a</sup>Cu + sum of named elements, 99.8% min.<sup>b</sup>Cu + sum of named elements, 99.9% min.<sup>c</sup>Cu + sum of named elements, 99.5% min.<sup>d</sup>Ni value includes Co.

**Table 10** Compositions of Wrought Copper–Zinc Alloys (Yellow Brasses), UNS C21000–C28000

No.	Previous Trade Name	Cu	Pb	Fe	Zn	Other Named Elements
C21000 <sup>a</sup>	Gilding, 95%	94.0–96.0	.05	.05	Rem.	—
C22000 <sup>a</sup>	Commercial bronze, 90%	89.0–91.0	.05	.05	Rem.	—
C22600 <sup>a</sup>	Jewelry bronze, 87-1/2%	86.0–89.0	.05	.05	Rem.	—
C23000 <sup>a</sup>	Red brass, 85%	84.0–86.0	.05	.05	Rem.	—
C23030 <sup>a</sup>	—	83.5–85.5	.05	.05	Rem.	.20–.40 Si
C23400 <sup>a</sup>	—	81.0–84.0	.05	.05	Rem.	—
C24000 <sup>a</sup>	Low brass, 80%	78.5–81.5	.05	.05	Rem.	—
C24080 <sup>a</sup>	—	78.0–82.0	.20	—	Rem.	.10 Al
C25600 <sup>b</sup>	—	71.0–73.0	.05	.05	Rem.	—
C26000 <sup>b</sup>	Cartridge brass, 70%	68.5–71.5	.07	.05	Rem.	—
C26130 <sup>b</sup>	—	68.5–71.5	.05	.05	Rem.	.02–.08 As
C26200 <sup>b</sup>	—	67.0–70.0	.07	.05	Rem.	—
C26800 <sup>b</sup>	Yellow brass, 66%	64.0–68.5	.15	.05	Rem.	—
C27000 <sup>b</sup>	Yellow brass, 65%	63.0–68.5	.10	.07	Rem.	—
C27200 <sup>b</sup>	—	62.0–65.0	.07	.07	Rem.	—
C27400 <sup>b</sup>	Yellow brass, 63%	61.0–64.0	.10	.05	Rem.	—
C27450	Yellow brass	60.0–65.0	.25	.35	Rem.	—
C27451	Yellow brass	61.0–65.0	.25	.35	Rem.	.05–.20 P
C28000 <sup>b</sup>	Muntz metal, 60%	59.0–63.0	.30	.07	Rem.	—

<sup>a</sup>Cu + sum of named elements, 99.8% min.<sup>b</sup>Cu + sum of named elements, 99.7% min.**Table 11** Compositions of Wrought Copper–Zinc–Lead Alloys (Leaded Brasses), UNS C28300–C38500

Copper Alloy No.	Previous Trade Name	Cu	Pb	Fe	Zn	Other Named Elements
C28300	Yellow brass	58.0–62.0	.09	.35	31.0–41.0	.01 Mn, .20 Zr
C28310	Yellow brass	58.0–62.0	.09	.35	31.0–41.0	.01–.20 Mn, .1–.65 S, .20 B, .20 Zr
C28320	Yellow brass	58.0–62.0	.09	.35	31.0–41.0	.20 B, .10 C, .20 Mn, .10–.65 S, .30 Ti
C28330	Yellow brass	58.0–62.0	.09	.35	31.0–41.0	.20 B, .10–1.5 Sb, .10 C, .30 Ti, .20 Zr
C28500	Copper–zinc alloy	57.0–59.0	.25	.35	Rem.	—
C31200 <sup>a</sup>	—	87.5–90.5	.7–1.2	.10	Rem.	.25 Ni
C31400 <sup>a</sup>	Leaded commercial bronze	87.5–90.5	1.3–2.5	.10	Rem.	.7 Ni
C31600 <sup>a</sup>	Leaded commercial bronze (nickel bearing)	87.5–90.5	1.3–2.5	.10	Rem.	.7–1.2 Ni .04–.10 P
C32000 <sup>a</sup>	Leaded red brass	83.5–86.5	1.5–2.2	.10	Rem.	.25 Ni
C33000 <sup>a</sup>	Low-leaded brass (tube)	65.0–68.0	.25–.7	.07	Rem.	—
C33200 <sup>a</sup>	High-leaded brass (tube)	65.0–68.0	1.5–2.5	.07	Rem.	—
C33500 <sup>a</sup>	Low-Leaded Brass	62.0–65.0	.25–.7	.15 <sup>b</sup>	Rem.	—
C34000 <sup>a</sup>	Medium-leaded brass, 64-1/2%	62.0–65.0	.8–1.5	.15 <sup>b</sup>	Rem.	—
C34200 <sup>a</sup>	High-leaded brass, 64-1/2%	62.0–65.0	1.5–2.5	.15 <sup>b</sup>	Rem.	—
C34500 <sup>a</sup>	—	62.0–65.0	1.5–2.5	.15	Rem.	—
C35000 <sup>a</sup>	Medium-leaded brass, 62%	60.0–63.0 <sup>c</sup>	.8–2.0	.15 <sup>b</sup>	Rem.	—
C35300 <sup>d</sup>	High-leaded brass, 62%	60.0–63.0 <sup>c</sup>	1.5–2.5	.15 <sup>b</sup>	Rem.	—
C35330 <sup>d</sup>	—	59.5–64.0	1.5–3.5 <sup>e</sup>	—	Rem.	.02–.25 As

**Table 11** (Continued)

Copper Alloy No.	Previous Trade Name	Cu	Pb	Fe	Zn	Other Named Elements
C35350	Leaded brass	61.0–63.0	2.0–4.5	.40	Rem.	.05–.30 Ni, .05–.2 P, .30 Sn
C35600 <sup>d</sup>	Extra high leaded brass	60.0–63.0	2.0–3.0	.15 <sup>b</sup>	Rem.	—
C36000 <sup>d</sup>	Free-cutting brass	60.0–63.0	2.5–3.7	.35	Rem.	—
C36010	Leaded brass	60.0–63.0	3.1–3.7	.35	Rem.	—
C36300	Copper–Zinc–Lead Alloy	61.0–63.0	.25–.7	.15	Rem.	.04–.15 P
C36500 <sup>a</sup>	Leaded Muntz metal, uninhibited	58.0–61.0	.25–.7	.15	Rem.	.25 Sn
C37000 <sup>a</sup>	Free-cutting Muntz metal	59.0–62.0	.8–1.5	.15	Rem.	—
C37100 <sup>a</sup>	—	58.0–62.0	.6–1.2	.15	Rem.	—
C37700 <sup>d</sup>	Forging brass	58.0–61.0	1.5–2.5	.30	Rem.	—
C37710 <sup>d</sup>	—	56.5–60.0	1.0–3.0	.30	Rem.	—
C38000 <sup>d</sup>	Architectural bronze, low leaded	55.0–60.0	1.5–2.5	.35	Rem.	.50 Al .30 Sn
C38500 <sup>d</sup>	Architectural bronze	55.0–59.0	2.5–3.5	.35	Rem.	—

<sup>a</sup>Cu + sum of named elements, 99.6% min.<sup>b</sup>For flat products, the iron shall be .10% max.<sup>c</sup>Cu, 61.0% min. for rod.<sup>d</sup>Cu + sum of named elements, 99.5% min.<sup>e</sup>Pb may be reduced to 1.0% by agreement.**Table 12** Compositions of Wrought Copper–Zinc–Tin Alloys (Tin Brasses), UNS C40000–C49999

Copper Alloy No.	Previous Trade Name	Cu	Pb	Fe	Sn	Zn	P	Other Named Elements
C40400 <sup>a</sup>	—	Rem.	—	—	.35–.7	2.0–3.0	—	—
C40410	Copper–zinc–tin alloy	95.0–99.0	.05	.05	0–.40	Rem.	—	—
C40500 <sup>a</sup>	Penny bronze	94.0–96.0	.05	.05	.7–1.3	Rem.	—	—
C40810 <sup>a</sup>	—	94.5–96.5	.05	.08–.12	1.8–2.2	Rem.	.028–.04	.11–.20 Ni
C40820 <sup>b</sup>	—	94.0 min	.02	—	1.0–2.5	.20–2.5	.05	.10–.50 Ni
C40850 <sup>a</sup>	—	94.5–96.5	.05	.05–.20	2.6–4.0	Rem.	.01–.20	.05–.20 Ni
C40860 <sup>a</sup>	—	94.0–96.0	.05	.01–.05	1.7–2.3	Rem.	.02–.04	.05–.20 Ni
C41000 <sup>a</sup>	—	91.0–93.0	.05	.05	2.0–2.8	Rem.	—	—
C41100 <sup>a</sup>	—	89.0–92.0	.10	.05	.30–.7	Rem.	—	—
C41110	Copper–zinc–tin alloy	90.0–94.0	.05	.05	.10–.50 Rem.	—	—	—
C41120 <sup>a</sup>	—	89.0–92.0	.05	.05–.20	.30–.7	Rem.	.01–.35	.05–.20 Ni
C41300 <sup>a</sup>	—	89.0–93.0	.10	.05	.7–1.3	Rem.	—	—
C41500 <sup>a</sup>	—	89.0–93.0	.10	.05	1.5–2.2	Rem.	—	—
C42000 <sup>a</sup>	—	88.0–91.0	—	—	1.5–2.0	Rem.	.25	—
C42200 <sup>a</sup>	—	86.0–89.0	.05	.05	.8–1.4	Rem.	.35	—
C42210	Tin brass	86.0–89.0	.01	.035	1.0–1.06	Rem.	P, .005	.5 Ni, .001–.01 Se, .005 Te,
C42220 <sup>a</sup>	—	88.0–91.0	.05	.05–.20	.7–1.4	Rem.	.02–.05	.05–.20 Ni
C42500 <sup>a</sup>	—	87.0–90.0	.05	.05	1.5–3.0	Rem.	.35	—
C42520 <sup>a</sup>	—	88.0–91.0	.05	.05–.20	1.5–3.0	Rem.	.01–.20	.05–.20 Ni

(continued)

130 Copper and Copper Alloys

Table 12 (Continued)

Copper Alloy No.	Previous Trade Name	Cu	Pb	Fe	Sn	Zn	P	Other Named Elements
C42600 <sup>a</sup>	—	87.0–90.0	.05	.05–.20	2.5–4.0	Rem.	.01–.20	.05–.20 Ni <sup>c</sup>
C43000 <sup>a</sup>	—	84.0–87.0	.10	.05	1.7–2.7	Rem.	—	—
C43400 <sup>a</sup>	—	84.0–87.0	.05	.05	.40–1.0	Rem.	—	—
C43500 <sup>a</sup>	—	79.0–83.0	.10	.05	.6–1.2	Rem.	—	—
C43600 <sup>a</sup>	—	80.0–83.0	.05	.05	.20–.50	Rem.	—	—
C44250 <sup>d</sup>	—	73.0–76.0	.07	.20	.50–1.5	Rem.	.10	.20 Ni
C44300 <sup>d</sup>	Admiralty, arsenical	70.0–73.0	.07	.06	.8–1.2 <sup>e</sup>	Rem.	—	.02–.06 As
C44400 <sup>d</sup>	Admiralty, antimonial	70.0–73.0	.07	.06	.8–1.2 <sup>e</sup>	Rem.	—	.02–.10 Sb
C44500 <sup>d</sup>	Admiralty, phosphorized	70.0–73.0	.07	.06	.8–1.2 <sup>e</sup>	Rem.	.02–.10	—
C44750	Tin brass	Rem.	.05	1.0–1.5	.30–3.0	27.0–31.5	—	—
C45470	Copper–zinc–aluminum–tin alloy	64.0–69.0	—	—	.6–.9	Rem.	—	.30–.80
C46200 <sup>d</sup>	Naval brass, 63-1/2%	62.0–65.0	.20	.10	.50–1.0	Rem.	—	—
C46400 <sup>d</sup>	Naval brass, uninhibited	59.0–62.0	.20	.10	.50–1.0	Rem.	—	—
C46500 <sup>d</sup>	Naval brass, arsenical	59.0–62.0	.20	.10	.50–1.0	Rem.	—	.02–.06 As
C47000 <sup>d</sup>	Naval brass welding and brazing rod	57.0–61.0	.05	—	.25–1.0	Rem.	—	.01 Al
C47940 <sup>d</sup>	—	63.0–66.0	1.0–2.0	.10–1.0	1.2–2.0	Rem.	—	.10–.50 Ni <sup>c</sup>
C48200 <sup>d</sup>	Naval brass, medium leaded	59.0–62.0	.40–1.0	.10	.50–1.0	Rem.	—	—
C48500 <sup>d</sup>	Naval brass, high leaded	59.0–62.0	1.3–2.2	.10	.50–1.0	Rem.	—	—
C48600 <sup>d</sup>	—	59.0–62.0	1.0–2.5	—	.30–1.5	Rem.	—	.02–.25 As
C49250	Copper–zinc–bismuth alloy	58.0–61.0	.09	.50	.30	Rem.	—	1.8–2.4 Bi, .001 Cd,
C49255	Copper–zinc–bismuth alloy	58.0–60.0	.10	.01	.50	Rem.	.10 P,	1.7–2.9 Bi, .01 Cd, .10–.30 Ni, .02–.07 Se, .10 Si,
C49260	GEM brass	58.0–63.0	.09	.05	.50	Rem.	.05–.15	1.10 Bi, .001 Cd, 10 Si
C49300	Lead-free copper–bismuth alloy	58.0–62.0	.01	.10	1.0–1.8	Rem.	.20	.5 Al, .50 Sb, .50–2.0 Bi, .03 Mn, 1.5 Ni, .20 Se, .10 Si,
C49340	GEM brass	60.0–63.0	.09	.12	.50–1.5	Rem.	.05–.15	.50–2.2 Bi, .001 Cd, .10 Si,
C49350	Bismuth brass alloy	61.0–63.0	.09	.12	1.5–3.0	Rem.	.04–.15	.02–.10 Sb, .50–2.5 Bi, .30 Si
C49355	Copper–zinc–bismuth alloy	63.0–69.0	.09	.10	.50–2.0	27.0–35.0	—	.5–1.5 Bi, .001 B, .10 Mn, 1.5 Si,
C49360	Tin-Eco(Bismuth)	Rem.	.09	—	1.0–2.0	19.0–22.0	—	.5–1.5 Bi, 2.0–3.5 Si,

<sup>a</sup>Cu + sum of named elements, 99.7% min.

<sup>b</sup>Cu + sum of named elements, 99.5% min.

<sup>c</sup>Ni value includes Co

<sup>d</sup>Cu + sum of named elements, 99.6% min.

<sup>e</sup>For tubular products, the minimum Sn content may be .9%.



**Table 13** Compositions of Wrought Copper–Tin–Phosphorus Alloys (Phosphor Bronzes), UNS C50000–C52999

Copper Alloy No.	Previous Trade Name	Cu	Pb	Fe	Sn	Zn	P	Other Named Elements
C50100 <sup>a</sup>	—	Rem.	.05	.05	.50–.8	—	.01–.05	—
C50150	Copper–tin–phosphorus–zirconium	99.0	—	—	.50–.80	—	.004	.04–.08 Zr
C50200 <sup>a</sup>	—	Rem.	.05	.10	1.0–1.5	—	.04	—
C50500 <sup>a</sup>	Phosphor bronze, 1.25% E	Rem.	.05	.10	1.0–1.7	.30	.03–.35	—
C50510 <sup>b</sup>	—	Rem.	—	—	1.0–1.5	.10–.25	.02–.07	.15–.40 Ni
C50580 <sup>a</sup>	—	Rem.	.05	.05–.20	1.0–1.7	.30	.01–.35	.05–.20 Ni
C50590 <sup>a</sup>	—	97.0 min	.02	.05–.40	.50–1.5	.50	.02–.15	—
C50700 <sup>a</sup>	—	Rem.	.05	.10	1.5–2.0	—	.30	—
C50705 <sup>a</sup>	—	96.5 min	.02	.10–.40	1.5–2.0	.50	.04–.15	—
C50710 <sup>a</sup>	—	Rem.	—	—	1.7–2.3	—	.15	.10–.40 Ni
C50715 <sup>c</sup>	—	Rem.	.02	.05–.15	1.7–2.3	—	.025–.04	—
C50725 <sup>a</sup>	—	94.0 min	.02	.05–.20	1.5–2.5	1.5–3.0	.02–.06	—
C50780 <sup>a</sup>	—	Rem.	.05	.05–.20	1.7–2.3	.30	.01–.35	.05–.20 Ni
C50900 <sup>a</sup>	—	Rem.	.05	.10	2.5–3.8	.30	.03–.30	—
C51000 <sup>a</sup>	Phosphor bronze, 5% A	Rem.	.05	.10	4.2–5.8	.30	.03–.35	—
C51080 <sup>a</sup>	—	Rem.	.05	.05–.20	4.8–5.8	.30	.01–.35	.05–.20 Ni
C51100 <sup>a</sup>	—	Rem.	.05	.10	3.5–4.9	.30	.03–.35	—
C51180 <sup>a</sup>	—	Rem.	.05	.05–.20	3.5–4.9	.30	.01–.35	.05–.20 Ni
C51190 <sup>a</sup>	—	Rem.	.02	.05–.15	3.0–6.5	—	.025–.045	.15 Co
C51800 <sup>a</sup>	Phosphor bronze	Rem.	.02	—	4.0–6.0	—	.10–.35	.01 Al
C51900 <sup>a</sup>	—	Rem.	.05	.10	5.0–7.0	.30	.03–.35	—
C51980 <sup>a</sup>	—	Rem.	.05	.05–.20	5.5–7.0	.30	.01–.35	.05–.20 Ni
C52100 <sup>a</sup>	Phosphor bronze, 8% C	Rem.	.05	.10	7.0–9.0	.20	.03–.35	—
C52180 <sup>a</sup>	—	Rem.	.05	.05–.20	7.0–9.0	.30	.01–.35	.05–.20 Ni
C52400 <sup>a</sup>	Phosphor bronze 10% D	Rem.	.05	.10	9.0–11.0	.20	.03–.35	—
C52480 <sup>a</sup>	—	Rem.	.05	.05–.20	9.0–11.0	.30	.01–.35	.05–.20 Ni

<sup>a</sup>Cu + sum of named elements, 99.5% min.

<sup>b</sup>Cu + sum of named elements, 99.7% min.

<sup>c</sup>Cu + Sn + Fe + P, 99.5% min

**Table 14** Compositions of Wrought Copper–Tin–Lead–Phosphorus Alloys (Leaded Phosphor Bronzes), UNS C53000–C54999

Copper Alloy No.	Previous Trade Name	Cu	Pb	Fe	Sn	Zn	P	Other Named Elements
C53400 <sup>a</sup>	Phosphor bronze B-1	Rem.	.8–1.2	.10	3.5–5.8	.30	.03–.35	—
C53800 <sup>b</sup>	—	Rem.	.40–.6	.030	13.1–13.9	.12	—	.06 Mn .03 Ni <sup>c</sup>
C54400 <sup>a</sup>	Phosphor bronze B-2	Rem.	3.5–4.5	.10	3.5–4.5	1.5–4.5	.01–.50	—

<sup>a</sup>Cu + sum of named elements, 99.5% min.<sup>b</sup>Cu + sum of named elements, 99.8% min.<sup>c</sup>Ni value includes Co.**Table 15** Compositions of Wrought Copper–Phosphorus and Copper–Silver–Phosphorus Alloys (Brazing Alloys), UNS C55000–C55299

Copper Alloy No.	Previous Trade Name	Cu	Ag	P	Other Named Elements
C55180 <sup>a</sup>	—	Rem.	—	4.8–5.2	—
C55181 <sup>a</sup>	—	Rem.	—	7.0–7.5	—
C55280 <sup>a</sup>	—	Rem.	1.8–2.2	6.8–7.2	—
C55281 <sup>a</sup>	—	Rem.	4.8–5.2	5.8–6.2	—
C55282 <sup>a</sup>	—	Rem.	4.8–5.2	6.5–7.0	—
C55283 <sup>a</sup>	—	Rem.	5.8–6.2	7.0–7.5	—
C55284 <sup>a</sup>	—	Rem.	14.5–15.5	4.8–5.2	—
C55285	Copper-silver-phosphorus alloy	Rem.	7.2–18.0	6.0–6.7	—
C55385	Copper brazing alloy	Rem.	6.0–7.0	6.0–6.7	.01–.40 Si
C55385	Copper brazing alloy	Rem.	—	6.0–8.7	.30–5.0 Ni, 505-605 Sn
C56000	—	Rem.	—	—	29.0–31.0 Ag, 30.0.35.0 Zn

<sup>a</sup>Cu + sum of named elements, 99.85% min.**Table 16** Copper–Silver–Zinc Alloys C55300–C60799

Copper Alloy No.	Previous Trade Name	Cu	Ag	Zn	Other Named Elements
C55385 <sup>a</sup>	—	Rem.	—	—	6.0–7.0 P .01–.40 Si 6.0–7.0 Sn
C55386 <sup>a</sup>	Other copper brazing alloy	Rem.	—	—	3.0–5.0 Ni 6.8–7.2 P 5.5–6.5 Sn
C56000 <sup>b</sup>	—	Rem.	29.0–31.0	30.0–34.0	—
C60600	—	Rem.	—	—	4.0–7.0 Al — .50 Fe

<sup>a</sup>Cu + sum of named elements, 99.85% min.<sup>b</sup>Cu + sum of named elements, 99.5% min.

**Table 17** Compositions of Copper–Aluminum Alloys (Aluminum Bronzes), UNS C60800–64699

Copper Alloy No.	Previous Trade Name	Cu (incl Ag)	Al	Fe	Pb	Zn	Si	Ni	Other Named Elements
C60800	Aluminum bronze	Rem.	5.0–6.5	.10	—	—	—	—	.02–.35 As
C61000	Aluminum bronze	Rem.	6.8–8.0	.5	.02	.20	.10	—	—
C61300	Aluminum bronze	Rem.	6.0–7.50	2.0–3.0	.01	..	.10	—	.20 Mn, .015 P, .20–.50 Sn
C61400	Aluminum bronze	Rem.	6.0-8-0	1.5–3.5	.01	.2	—	—	1.0 Mn
C61500	Nickel–aluminum bronze	Rem.	7.7–8.3	—	.015	—	—	1.8–2.2	—
C61550	Nickel–aluminum bronze	Rem.	5.5–6.5	.2	.05	—	—	1.5–2.5	1.0 Mn, .05 Sn
C61800	Aluminum bronze	Rem.	8.5–11.0	.5–1.05	.02	.02	.10	—	—
C61900	Aluminum bronze	Rem.	8.5–10.0	3.0–4.5	.02	.84	—	—	.6 Sn
C62200	Aluminum bronze	Rem.	11.0–12.0	.3–4.2	.02	.02	.10	—	—
C62300	Aluminum bronze	Rem.	8.5–10.0	2.0–4.0	—	—	.25	—	.50 Mn
C62400	Aluminum bronze	Rem.	10.0–11.50	2.0–4.5	—	.30	.25	—	.30 Mn, .20 Sn
C62500	Aluminum bronze	Rem.	12.5–13.5	3.5–5.5	—	—	—	—	2.0 Mn
C62580	Aluminum bronze	Rem.	12.0–13.0	3.0–5.0	.02	0.20	0.40	—	—
C62581	Aluminum bronze	Rem.	13.0–14.0	3.0–5.0	.02	.02	.04	—	—
C62582	Aluminum bronze	Rem.	14.0–15.0	3.0–5.0	.02	.20	.04	—	—
C63000	Nickel–aluminum bronze	Rem.	9.0–11.0	2.0–4.0	—	.30	.25	4.0–5.5	1.5 Mn
C63010	Nickel–aluminum bronze	Rem.	9.7–10.9	2.0–3.5	—	.30	—	4.5–5.5	1.5 Mn, .20 Sn
CC6320	Nickel–aluminum bronze	Rem.	10.0–11.0	4.0–5.5	.03	.30	—	4.2–6.0	.050 Cr, .02 Co, 1.5 Mn, .25 Sn
C63200	Nickel–aluminum bronze	Rem.	8.7–9.5	3.5–4.3	.02	—	.10	4.0–4.8	1.2–2.0 Mn,
C63280	Nickel–aluminum bronze	Rem.	8.5–9.5	3.0–5.0	.02	—	—	4.0–5.5	.6–3.5 Mn
C63380	Nickel–aluminum bronze	Rem.	7.0–8.5	2.0–4.0	.02	.15	.10	1.5–3.0	11.0–14.0 Mn,
C63400	Aluminum bronze	Rem.	2.6–3.2	.15	.05	.50	.25–.45	.15	.09 As, .20 Sn
C63500	Aluminum bronze	Rem.	4.5–7.0	.15–.50	—	4.5–7.0	—	—	.50–2.0 Sn
C63600	Aluminum bronze	Rem.	3.0–4.0	.15	.05	.50	.70–1.3	.15	—
C63800	Aluminum bronze	Rem.	2.5–3.1	.20	.05	.8	1.5–2.1	.20	.25–.55 Co.
C64200	Aluminum bronze	Rem.	6.3–7.6	.30	.05	.50	1.5–2.2	.25	.09 As, .10 Mn,
C64210	Aluminum–silicon bronze	Rem.	6.3–7.0	.30	.05	.50	1.5–2.0	.25	.09 As, .10 Mn, .20Sn

### 134 Copper and Copper Alloys

**Table 18** Compositions of Copper–Silicon Alloys (Silicon Bronzes and Silicon Brasses) C64700–C66199

Copper Alloy No.	Previous Trade Name	Cu (incl Ag)	Pb	Fe	Sn	Zn	Mn	Si	Ni	Other Named Elements
C64700 <sup>a</sup>	—	Rem.	.10	.10	—	.50	—	.40–.8	1.6–2.2 <sup>b</sup>	—
C64710 <sup>a</sup>	—	95.0 min	—	—	—	.20–.50	.10	.50–.9	2.9–3.5 <sup>b</sup>	—
C64725 <sup>a</sup>	—	95.0 min	.01	.25	.20–.8	.50–1.5	—	.20–.8	1.3–2.7 <sup>b</sup>	.01 Ca .20 Cr .20 Mg
C64727	Copper silicon alloy	Rem.	.01	.25	.20–.8	.20–1.0	—	.50–.8	2.5–3.0	.002–.20 Mg
C64728	Copper–nickel–zinc–silicon alloy	Rem.	.05	.20	.10–1.0	.10–2.0	—	.30–.90	2.0–3.6	—
C64730 <sup>a</sup>	—	93.5 min	—	—	1.0–1.5	.20–.50	.10	.50–.9	2.9–3.5 <sup>b</sup>	—
C64740 <sup>a</sup>	—	95.0 min	.01	.25	1.5–2.5	.20–1.0	—	.05–.50	1.0–2.0 <sup>b</sup>	.01 Ca .05 Mg
C64745	NKC164	Rem.	.05	.20	.20–.80	.20–.80	.10	.10–.70	.20	—
C64750 <sup>c</sup>	—	Rem.	—	1.0	.05–.8	1.0	—	.10–.7	1.0–3.0	.10 Mg .10 P .10 Zr
C64760 <sup>a</sup>	—	93.5 min	.02	—	.30	.20–2.5	—	.05–.6	.40–2.5	.05 Mg
C64770 <sup>a</sup>	—	Rem.	.05	.10	.05–.50	.30–.8	.10	.40–.8	1.5–3.0 <sup>b</sup>	.30 Mg
C64575	Copper–nickel–silicon alloy	Rem.	.10	.05	.05–1.0	.30–.80	.10	.40–.90	1.5–3.5	.50 Cr, .30 Mg,
C64780 <sup>a</sup>	—	90.0 min	.02	—	.10–2.0	.20–2.5	.01–1.0	.20–.9	1.0–3.5	.01 Cr .01 Mg .01 Ti .01 Zr
C64785 <sup>a</sup>	—	Rem.	.015	.02	.50–2.0	3.0–6.0	.20–1.0	.15	.40–1.6 <sup>d</sup>	3.0–6.0 Al .015 P
C64790 <sup>a</sup>	—	Rem.	.05	.10	.05–.50	.30–.8	.10	.6–1.2	2.5–4.5 <sup>b</sup>	.05–.50 Cr .05–.30 Mg
C64800	NKC4419	Rem.	1.0	.05	.50	.50	—	.20–1.0	.50	.09 Cr, .50P, 1.0–3.0 Co,
C64900 <sup>a</sup>	—	Rem.	.05	.10	1.2–1.6	.20	—	.8–1.2	.10 <sup>b</sup>	.10 Al
C65100 <sup>a</sup>	Low-silicon bronze B	Rem.	.05	.8	—	1.5	.7	.8–2.0	—	—
C65400 <sup>a</sup>	—	Rem.	.05	—	1.2–1.9	.50	—	2.7–3.4	—	.01–.12 Cr
C65500 <sup>a</sup>	High-silicon bronze A	Rem.	.05	.8	—	1.5	.50–1.3	2.8–3.8	.6 <sup>b</sup>	—
C65600 <sup>a</sup>	—	Rem.	.02	.50	1.5	1.5	1.5	2.8–4.0	—	.01 Al
C66100 <sup>a</sup>	—	Rem.	.20–.8	.25	—	1.5	1.5	2.8–3.5	—	—

<sup>a</sup>Cu + sum of named elements, 99.5% min.

<sup>b</sup>Ni value includes Co.

<sup>c</sup>Cu + sum of named elements, 99.92% min.

<sup>d</sup>Not including Co.

**Table 19** Compositions of Other Wrought Copper–Zinc Alloys, UNS C66200–C69999

Copper Alloy No.	Previous Trade Name	Cu (incl Ag)	Pb	Fe	Sn	Zn	Ni	Al	Mn	Si	Other Named Elements
C66200 <sup>a</sup>	—	86.6–91.0	.05	.05	.20–.7	Rem.	.30–1.0 <sup>b</sup>	—	—	—	.05–.20P
C66300 <sup>a</sup>	—	84.5–87.5	.05	1.4–2.4 <sup>c</sup>	1.5–3.0	Rem.	—	—	—	—	.20 Co <sup>c</sup> .35 P .30–.7 Co <sup>d</sup>
C66400 <sup>a</sup>	—	Rem.	.015	1.3–1.7 <sup>d</sup>	.05	11.0–12.0	—	—	—	—	—
C66410 <sup>a</sup>	—	Rem.	.015	1.8–2.3	.05	11.0–12.0	—	—	—	—	—
C66420 <sup>a</sup>	—	Rem.	—	.50–1.5	—	12.7–17.0	—	—	—	—	—
C66430 <sup>a</sup>	—	Rem.	.05	.6–.9	.6–.9	13.0–15.0	—	—	—	—	.10P
C66700 <sup>a</sup>	Manganese brass	68.5–71.5	.07	.10	—	Rem.	—	—	.8–1.5	—	—
C66800 <sup>a</sup>	—	60.0–63.0	.50	.35	.30	Rem.	.25 <sup>b</sup>	.25	2.0–3.5	.50–1.5	—
C66900 <sup>e</sup>	—	62.5–64.5	.05	.25	—	Rem.	—	—	11.5–12.5	—	—
C66908	Copper–zinc–manganese	Rem.	.05	.01–2.0	.50	6.0–9.0	.01–3.5	.25	4.0–7.0	—	—
C66910	Copper–zinc–manganese	Rem.	.05	.10–1.5	.05	6.0–8.0	—	.25	12.0–15.0	—	.01 Co .05 Nb. .15 Ti .15 Zr
C66913	Copper–zinc–manganese	Rem.	.05	.01–1.5	.50	8.0–12.5	.01–3.5	.25	12.0–15.0	—	.01 Co
C66915	Copper–zinc–manganese	Rem.	.05	.01–1.5	.50	8.0–12.5	.01–3.5	.25	12.0–15.0	—	.25 Al. .01–.50 Co
C66925	Copper–zinc–manganese	Rem.	.05	.50	.50	17.0–21.0	.01–3.5	.25	8.0–11.0	—	.01 Co
C66930	Copper–manganese alloy	Rem.	.02	.05	.05	.05	.02	—	19.0–20.50	—	.02P
C66950 <sup>a</sup>	—	Rem.	.01	.50	—	14.0–15.0	—	1.0–1.5	14.0–15.0	—	—
C67000 <sup>a</sup>	Manganese bronze B	63.0–68.0	.20	2.0–4.0	.50	Rem.	—	3.0–6.0	2.5–5.0	—	—
C67300 <sup>a</sup>	—	58.0–63.0	.40–3.0	.50	.30	Rem.	.25 <sup>b</sup>	.25	2.0–3.5	.50–1.5	—
C67400 <sup>a</sup>	—	57.0–60.0	.50	.35	.30	Rem.	.25 <sup>b</sup>	.50–2.0	2.0–3.5	.50–1.5	—
C67420 <sup>a</sup>	—	57.0–58.5	.25–.8	.15–.55	.35	Rem.	.25 <sup>b</sup>	1.0–2.0	1.5–2.5	.25–.7	—
C67500 <sup>a</sup>	Manganese bronze A	57.0–60.0	.20	.8–2.0	.50–1.5	Rem.	—	.25	.05–.50	—	—

(continued)

Table 19 (Continued)

Copper Alloy No.	Previous Trade Name	Cu (incl Ag)	Pb	Fe	Sn	Zn	Ni	Al	Mn	Si	Other Named Elements
C67600 <sup>a</sup>	—	57.0–60.0	.50–1.0	.40–1.3	.50–1.5	Rem.	—	—	.05–.50	—	—
C68000 <sup>a</sup>	Bronze, low fuming (nickel)	56.0–60.0	.05	.25–1.25	.75–1.10	Rem.	.20–.8 <sup>b</sup>	.01	.01–.50	.04–.15	—
C68100 <sup>a</sup>	Bronze, low fuming	56.0–60.0	.05	.25–1.2	.75–1.10	Rem.	—	.01	.01–.50	.04–.15	—
C68300	Copper–zinc alloy	59.0–63.0	.09	—	.05–.20	Rem.	—	—	—	.30–1.0	.30–1.0 Sb .01 Cd
C68350	Low-silicon brass	59.0–64.0	.09	.15	.60	Rem.	.20	.30	—	.60	.05–.40 P
C68600	Copper–zinc	56.0–60.0	.50–1.5	.50–1.2	.20–1.0	Rem.	—	.30–1.5	.30–2.0	—	—
C68700 <sup>a</sup>	Aluminum Brass, arsenical	76.0–79.0	.07	.06	—	Rem.	—	1.8–2.5	—	—	.02–.06 As
C68800 <sup>a</sup>	—	Rem.	.05	.20	—	21.3–24.1 <sup>f</sup>	—	3.0–3.8 <sup>f</sup>	—	—	.25–.55 Co
C69050 <sup>a</sup>	—	70.0–75.0	—	—	—	Rem.	.50–1.5 <sup>b</sup>	3.0–4.0	—	.10–.6	.01–.20 Zr
C69100 <sup>a</sup>	—	81.0–84.0	.05	.25	.10	Rem.	.8–1.4 <sup>b</sup>	.7–1.2	.10	.8–1.3	—
C69150	Copper–zinc alloy	82.5–87.5	.05	.25	.025	Rem.	.20	.70–1.3	.25–.60	.02	—
C69220	Copper–zinc alloy	69.0–71.0	.08	.10	.30	Rem.	.20	—	.8–1.8	1.8–2.6	.10 Sb .05–.20 P
C69250	Copper–zinc–manganese	Rem.	.05	.20	.20	7.5–8.5	2.0–3.0	1.0–2.0	5.0–6.0	.10	—
C69300 <sup>a</sup>	—	73.0–77.0	.10	.10	.20	Rem.	.10 <sup>b</sup>	—	.10	2.7–3.4	.04–.15 P
C69400 <sup>a</sup>	Silicon red brass	80.0–83.0	.30	.20	—	Rem.	—	—	—	3.5–4.5	—
C69430 <sup>a</sup>	—	80.0–83.0	.30	.20	—	Rem.	—	—	—	3.5–4.5	.03–.06 As
C69700 <sup>a</sup>	—	75.0–80.0	.50–1.5	.20	—	Rem.	—	—	.40	2.5–3.5	—
C69710 <sup>a</sup>	—	75.0–80.0	.50–1.5	.20	—	Rem.	—	—	.40	2.5–3.5	.03–.06 As
C69750 <sup>a</sup>	—	78.0–83.0	.8–1.3	.05	.05	Rem.	.01	—	.05	1.9–2.22	.02 P

<sup>a</sup>Cu + sum of named elements, 99.5% min.<sup>b</sup>Ni value includes Co.<sup>c</sup>Fe + Co, 1.4–2.4%<sup>d</sup>Fe + Co, 1.8–2.3%<sup>e</sup>Cu + sum of named elements, 99.8% min.<sup>f</sup>Al + Zn, 25.1–27.1%.

**Table 20** Compositions of Wrought Copper–Nickel Alloys (Copper Nickels), C70000–C73499

Copper Alloy No.	Previous Trade Name	Cu (incl Ag)	Pb	Fe	Zn	Ni	Sn	Mn	Other Named Elements
C70100 <sup>a</sup>	—	Rem.	—	.05	.25	3.0–4.0 <sup>b</sup>	—	.50	—
C70200 <sup>a</sup>	—	Rem.	.05	.10	—	2.0–3.0 <sup>b</sup>	—	.40	—
C70230 <sup>a</sup>	—	Rem.	—	—	.50–2.0	2.2–3.2	.10–.50	—	<sup>c</sup> .40–.8 Si .10 Ag
C70240 <sup>a</sup>	—	Rem.	.05	.10	.30–.8	1.0–4.0 <sup>b</sup>	—	.01–.20	.40–.8 Si .01–.10 Ag
C70250 <sup>a</sup>	—	Rem.	.05	.20	1.0	2.2–4.2 <sup>b</sup>	—	.10	.05–.30 Mg .25–1.2 Si
C70252	Copper–nickel	Rem.	.05	.20	—	3.0–4.2	—	.11–.20	.05–.30 Mg .40–1.2 Si
C70260 <sup>a</sup>	—	Rem.	—	—	—	1.0–3.0 <sup>b</sup>	—	—	.010 P .20–.7 Si
C70265 <sup>a</sup>	—	Rem.	.05	—	.30	1.0–3.0 <sup>b</sup>	.05–.8	—	.01 P .20–.7 Si
C70270 <sup>a</sup>	—	Rem.	.05	.28–1.0	1.0	1.0–3.0 <sup>b</sup>	.10–1.0	.15	.20–1.0 Si
C70275	Copper–nickel	Rem.	.01	.25	.30–1.0	.50–1.5	.30–1.0	—	.01 Ca .06 Cr .002–.20 Mg
C70280 <sup>a</sup>	—	Rem.	.02	.015	.30	1.3–1.7 <sup>b</sup>	1.0–1.5	—	.10–.50 Si .02–.04 P .22–.30 Si
C70290 <sup>a</sup>	—	Rem.	.02	.015	.30	1.3–1.7 <sup>b</sup>	2.1–2.7	—	.02–.04 P .22–.30 Si
C70310 <sup>a</sup>	—	Rem.	.05	.10	2.0	1.0–4.0 <sup>b</sup>	1.0	—	.01 Mg .05 P .08–1.0 Si .02–.50 Ag
C70350 <sup>a</sup>	—	Rem.	.05	.20	1.0	1.0–2.0	—	.20	.005–.05 Zr 1.0–2.0 Co .04 Mg .50–1.0 Si
C70370 <sup>a</sup>	—	Rem.	0.	0.	1.	1.–2.	—	0.	1.–2. Co 0.–1. Si 0.–1. Ag
C70400 <sup>a</sup>	Copper–nickel, 5%	Rem.	.05	1.3–1.7	1.0	4.8–6.2 <sup>b</sup>	—	.30–.8	—
C70500 <sup>a</sup>	Copper–nickel, 7%	Rem.	.05	.10	.20	5.8–7.8 <sup>b</sup>	—	.15	—
C70600 <sup>a</sup>	Copper–nickel, 10%	Rem.	.05	1.0–1.8	1.0	9.0–11.0 <sup>b</sup>	—	1.0	—
C70610 <sup>a</sup>	—	Rem.	.01	1.0–2.0	—	10.0–11.0 <sup>b</sup>	—	.50–1.0	.05 C .05 S
C70620 <sup>a</sup>	—	86.5 min	.02	1.0–1.8	.50	9.0–11.0 <sup>b</sup>	—	1.0	.05 C .02 P .02 S
C70690 <sup>a</sup>	—	Rem.	.001	.005	.001	9.0–11.0 <sup>b</sup>	—	.001	<sup>d</sup>
C70700 <sup>a</sup>	—	Rem.	—	.05	—	9.5–10.5 <sup>b</sup>	—	.50	—
C70800 <sup>a</sup>	Copper–nickel, 11%	Rem.	.05	.10	.20	10.5–12.5 <sup>b</sup>	—	.15	—

(continued)



138 Copper and Copper Alloys

Table 20 (Continued)

Copper Alloy No.	Previous Trade Name	Cu (incl Ag)	Pb	Fe	Zn	Ni	Sn	Mn	Other Named Elements
C71000 <sup>a</sup>	Copper–nickel, 20%	Rem.	.05	1.0	1.0	19.0–23.0 <sup>b</sup>	—	1.0	—
C71100 <sup>a</sup>	—	Rem.	.05	.10	.20	22.0–24.0 <sup>b</sup>	—	.15	—
C71300 <sup>a</sup>	—	Rem.	.05	.20	1.0	23.5–26.5 <sup>b</sup>	—	1.0	—
C71500 <sup>a</sup>	Copper–nickel, 30%	Rem.	.05	.40–1.0	1.0	29.0–33.0 <sup>b</sup>	—	1.0	—
C71520 <sup>a</sup>	—	65.0 min	.02	.40–1.0	.50	29.0–33.0 <sup>b</sup>	—	1.0	.05 C .02 P .02 S
C71580 <sup>a</sup>	—	Rem.	.05	.50	.05	29.0–33.0 <sup>b</sup>	—	.30	<sup>e</sup>
C71581 <sup>a</sup>	—	Rem.	.02	.40–.7	—	29.0–32.0 <sup>b</sup>	—	1.0	<sup>f</sup>
C71590	—	Rem.	.001	.15	.001	29.0–31.0 <sup>b</sup>	.001	.50	<sup>d</sup>
C71640 <sup>a</sup>	—	Rem.	.05 <sup>g</sup>	1.7–2.3	1.0 <sup>g</sup>	29.0–32.0 <sup>b</sup>	—	1.5–2.5	<sup>g</sup> .06 C .03 S
C71700 <sup>a</sup>	—	Rem.	—	.40–1.0	1.0	29.0–33.0 <sup>b</sup>	—	1.0	.30–.7 Be
C71900 <sup>a</sup>	—	Rem.	.015	.50	.05	28.0–33.0 <sup>b</sup>	—	.20–1.0	.04 C 2.2–3.0 Cr .02 P .25 Si .015 S .01–.20 Ti .02–.35 Zr
C72150 <sup>a</sup>	—	Rem.	.05	.10	.20	43.0–46.0 <sup>b</sup>	—	.05	.10 C .50 Si
C72200 <sup>h</sup>	—	Rem.	.05 <sup>g</sup>	.50–1.0	1.0 <sup>g</sup>	15.0–18.0 <sup>b</sup>	—	1.0	<sup>g</sup> .30–.7 Cr .03 Si .03 Ti
C72420 <sup>i</sup>	—	Rem.	.02	.7–1.2	.20	13.5–16.5 <sup>b</sup>	.10	3.5–5.5	1.0–2.0 Al .05 C .50 Cr .05 Mg .01 P .15 Si .15 S
C72500 <sup>h</sup>	—	Rem.	.05	.6	.50	8.5–10.5 <sup>b</sup>	1.8–2.8	.20	—
C72650 <sup>i</sup>	—	Rem.	.01	.10	.10	7.0–8.0 <sup>b</sup>	4.5–5.5	.10	—
C72700 <sup>i</sup>	—	Rem.	.02 <sup>j</sup>	.50	.50	8.5–9.5 <sup>b</sup>	5.5–6.5	.05–.30	.15 Mg .10 Nb
C72800 <sup>i</sup>	—	Rem.	.005	.50	1.0	9.5–10.5 <sup>b</sup>	7.5–8.5	.05–.30	.10 Al .02 Sb .001 Bi .001 B .005–.15 Mg .10–.30 Nb .005 P .05 Si .0025 S .01 Ti

**Table 20** (Continued)

Copper Alloy No.	Previous Trade Name	Cu (incl Ag)	Pb	Fe	Zn	Ni	Sn	Mn	Other Named Elements
C72900 <sup>i</sup>	—	Rem.	.02 <sup>j</sup>	.50	.50	14.5–15.5 <sup>b</sup>	7.5–8.5	.30	.15 Mg .10 Nb
C72950 <sup>i</sup>	—	Rem.	.05	.6	—	20.0–22.0 <sup>b</sup>	4.5–5.7	.6	—
C73100	Copper–zinc–nickel	Rem.	.05	.10	18.0–22.0	4.0–6.0	.10	.50	—

<sup>a</sup>Cu + Sum of Named Elements, 99.5% min.<sup>b</sup>Ni value includes Co.<sup>c</sup>Ag Includes B<sup>d</sup>Includes Co<sup>e</sup>The following additional maximum limits shall apply: .02% C, .015% Si, .003% S, .002% Al, .001% P, .0005% Hg, .001% Ti, .001% Sb, .001% As, .001% Bi, .05% Co, .10% Mg and .005% Oxygen. For C70690, Co shall be .02% max.<sup>f</sup>The following additional maximum limits shall apply: .07% C, .15% Si, .024% S, .05% Al and .03% P.<sup>g</sup>.02% P, max.; .25% Si, max.; .01% S, max.; .02–.50% Ti.<sup>h</sup>The following additional maximum limits shall apply: When the product is for subsequent welding applications and is so specified by the purchaser, .50% Zn, .02% P, .02% Pb, .02% S and .05% C.<sup>i</sup>Cu + Sum of Named Elements, 99.8% min.<sup>j</sup>Cu + Sum of Named Elements, 99.7% min.**Table 21** Compositions of Wrought Copper–Nickel–Zinc Alloys (Nickel Silvers)

Copper Alloy Number	Previous Trade Name	Cu (Including Ag)	Fe	Pb	Mn	Ni	Sn	Zn	Other Named Elements
C73100 <sup>a</sup>	Nickel silver	Rem. <sup>b</sup>	.10	.05	.50	4.0–6.0	.10	18.0–22.0	—
C73500 <sup>a</sup>	Nickel silver	70.5–73.5 <sup>b</sup>	.25	.09	.50	16.9–19.5 <sup>c</sup>	—	Rem.	—
C74000 <sup>a</sup>	Nickel silver	69.0–73.5	.25	.05	.50	9.0–11.0 <sup>b</sup>	—	Rem.	—
C74300 <sup>a</sup>	Nickel silver	63.0–66.0	.25	.09	.50	7.0–9.0 <sup>c</sup>	—	Rem.	—
C74400 <sup>a</sup>	Nickel silver	62.0 <sup>b</sup> –66.0	.05	.05	—	2.0–4.0 <sup>c</sup>	—	Rem.	—
C74500 <sup>a</sup>	Nickel silver	63.5 <sup>b</sup> –66.5	.25	.09	.50	9.0–11.0 <sup>c</sup>	—	Rem.	—
C75200 <sup>a</sup>	Nickel silver	63.0–66.5	.25	.05	.50	16.5–19.5 <sup>c</sup>	—	Rem.	—
C75400 <sup>a</sup>	Nickel silver	63.5–66.5	.25	–.10	.50	14.0–16.0 <sup>c</sup>	—	Rem.	—
C75700 <sup>a</sup>	Nickel silver	63.5–66.5	.25	.05	.50	11.0–13.0 <sup>c</sup>	—	Rem.	—
C76000 <sup>a</sup>	Nickel silver	60. <sup>b</sup> –63.0	.25	.10	.50	7.0 <sup>c</sup> –9.0 Rem.	—	—	—
C76200 <sup>a</sup>	Nickel silver	57.0–61.0	.25	.09	.50	11.0–13.5 <sup>c</sup>	—	Rem.	—
C76400 <sup>a</sup>	Nickel silver	58.5–61.5	.25	.05	.50	16.5–19.5 <sup>c</sup>	—	Rem.	—
C76700 <sup>a</sup>	Nickel silver, 56.6–15	55.0 <sup>b</sup> –58.0	—	—	.50	14.0 <sup>c</sup> –16.0	—	Rem.	—
C77000 <sup>a</sup>	Nickel silver, 55–18	53.5–56.5 <sup>b</sup>	.25	.05	.50	16.5 <sup>c</sup> –19.5	—	Rem.	—
C77300 <sup>a</sup>	Nickel silver	46.0–50.0 <sup>b</sup>	—	.05	—	9.0 <sup>c</sup> –11.0	—	Rem.	.01 Al, .25 P, .04–.25 Si
C77400 <sup>a</sup>	Nickel silver	43.0–47.0 <sup>b</sup>	—	.09	—	9.0 <sup>c</sup> –11.0	—	Rem.	—
C77600 <sup>a</sup>	Nickel silver	42.0–45.0	.20	.25	.25	12.0–14.0 <sup>c</sup>	.15	Rem.	—
C78200 <sup>a</sup>	Nickel silver	63.0–67.0	.35	1.5–2.5	.50	7.0–9.0 <sup>c</sup>	—	Rem.	—
C78270 <sup>a</sup>	Nickel silver	65.0 <sup>b</sup> –68.0	.35	1.0–1.8	.50	4.5–6.0 <sup>c</sup>	—	Rem.	—
C79000 <sup>a</sup>	Nickel silver	63.0 <sup>b</sup> –67.0	.35	1.5–2.2	.50	.11 <sup>c</sup> –.13	—	Rem.	—
C79200 <sup>a</sup>	Nickel silver	59.0–65.0	.25	.8–1.4	.50	11.0–13.0 <sup>c</sup>	—	Rem.	—
C79350 <sup>a</sup>	Nickel silver	59.0–63.0	.25	.8–1.1	.50	23.0 <sup>c</sup> –26.0	.40–.60	Rem.	—

(continued)

140 Copper and Copper Alloys

Table 21 (Continued)

Copper Alloy Number	Previous Trade Name	Cu (Including Ag)	Fe	Pb	Mn	Ni	Sn	Zn	Other Named Elements
C79600 <sup>a</sup>	Nickel silver	43.5–46.5	—	.80–1.2	1.5–2.5	9.0 <sup>c</sup> –11.0	—	Rem.	—
C79800	Nickel silver	45.5–48.5 <sup>b</sup>	.25	1.5–2.5	1.5–2.5	9.0–11.0	—	Rem.	—
C79830 <sup>a</sup>	Nickel silver	45.5–47.0	.45	1.0–2.5	.15–.55	9.0 <sup>c</sup> –10.0	—	Rem.	—
C79860 <sup>a</sup>	Nickel silver	42.3–43.7 <sup>b</sup>	.20	1.3–1.8	5.6–6.4	11.8 <sup>c</sup> –12.7	.10	Rem.	.005 P, .06 Si

<sup>a</sup>Cu + sum of named elements, 99.5% min.

<sup>b</sup>Ni value includes Co.

<sup>c</sup>Cu + sum of named elements, 99.7% min.

<sup>d</sup>.05% Pb, max., for rod, wire, and tube.

<sup>e</sup>Includes Ag.

<sup>f</sup>Includes Co.

Table 22 Compositions of Cast Coppers, UNS C80000–C81399

Copper No.	Cu(incl Ag)	P
C80100	99.95 min	—
C80300	99.95 min	—
C80410	99.9 min	—
C80500	99.75 min	—
C80700	99.75 min	—
C80900	99.70 min	—
C81100	99.70 min	—
C81200	99.9 min	.045–.065
C81300 <sup>a</sup>	98.5 min	—
C80100	99.95 min	—
C80300	99.95 min	—
C80410	99.9 min	—

<sup>a</sup>Cu + sum of named elements, 99.5% min.

Table 23 Compositions of Cast High-Copper Alloys, UNS C81400–C83299

Copper Alloy No.	Cu	Ag	Be	Co	Si	Ni	Fe	Al	Sn	Pb	Zn	Cr	Other Named Elements
C81400 <sup>a</sup>	Rem.	—	.02–.10	—	—	—	—	—	—	—	—	.6–1.0	—
C81500 <sup>a</sup>	Rem.	—	—	—	.15	—	.10	.10	.10	.02	.10	.40–1.5	—
C81540 <sup>a</sup>	95.1 min <sup>b</sup>	—	—	—	.40–.8	2.0–3.0 <sup>c</sup>	.15	.10	.10	.02	.10	.10–.6	—
C82000 <sup>a</sup>	Rem.	—	.45–.8	2.40–2.70 <sup>d</sup>	.15	.20 <sup>d</sup>	.10	.10	.10	.02	.10	.10	—
C82200 <sup>a</sup>	Rem.	—	.35–.8	.30	—	1.0–2.0	—	—	—	—	—	—	—
C82400 <sup>a</sup>	Rem.	—	1.60–1.85	.20–.65	—	.20	.20	.15	.10	.02	.10	.10	—
C82500 <sup>a</sup>	Rem.	—	1.90–2.25	.35–.70 <sup>d</sup>	.20–.35	.20 <sup>d</sup>	.25	.15	.10	.02	.10	.10	—
C82510 <sup>a</sup>	Rem.	—	1.90–2.15	1.0–1.2	.20–.35	.20	.25	.15	.10	.02	.10	.10	—
C82600 <sup>a</sup>	Rem.	—	2.25–2.55	.35–.65	.20–.35	.20	.25	.15	.10	.02	.10	.10	—
C82700 <sup>a</sup>	Rem.	—	2.35–2.55	—	.15	1.0–1.5	.25	.15	.10	.02	.10	.10	—
C82800 <sup>a</sup>	Rem.	—	2.50–2.85	.35–.70 <sup>d</sup>	.20–.35	.20 <sup>d</sup>	.25	.15	.10	.02	.10	.10	—

<sup>a</sup>Cu + sum of named elements, 99.5% min.

<sup>b</sup>Includes Ag.

<sup>c</sup>Ni value includes Co.

<sup>d</sup>Ni + Co.

**Table 24** Copper–Tin–Zinc and Copper–Tin–Zinc–Lead Alloys (Red and Leaded Red Brasses) C83300–C83999

Copper Alloy Number	Cu	Sn	Pb	Zn	Fe	Sb	As	Nb	S	P	Si	Other Named Elements
C83300 <sup>a</sup>	92.0–94.0 <sup>b</sup>	1.0–2.0	1.0–2.0	2.0–6.0	—	—	—	—	—	—	—	—
C83400 <sup>a</sup>	88.0–92.0 <sup>b</sup>	.20	.50	8.0–12.0	.25	.25	—	1.0 <sup>c</sup>	.08	.03 <sup>d</sup>	.005	.005
C83410 <sup>a</sup>	88.0–91.0	1.0–2.0	.10	Rem.	.05	—	—	.05	—	—	.005	.005
C83420 <sup>a</sup>	88.0–92.0	.25–.7	.50	Rem.	.10	—	—	—	—	—	—	—
C83450 <sup>a</sup>	87.0–89.0 <sup>b</sup>	2.0–3.5	1.5–3.0	5.5–7.5	.30	.25	—	.8–2.0 <sup>c</sup>	.08	.03 <sup>d</sup>	.005	.005
C83470 <sup>a</sup>	90.0–96.0	3.0–5.	.09	1.0–3.0	.50	.20	.10–1.0	.20–.6	.05	.01	—	—
C83500 <sup>a</sup>	86.0–88.0 <sup>b</sup>	5.5–6.5	3.5–5.5	1.0–2.5	.25	.25	—	.50–1.0 <sup>c</sup>	.08	.03 <sup>d</sup>	.005	.005
C83520 <sup>a</sup>	Rem.	3.5–4.5	3.5–4.5	—	.30	.25	—	1.0	—	—	—	—
C83600 <sup>a</sup>	84.0–86.0 <sup>b</sup>	4.0–6.0	4.0–6.0	4.0–6.0	.30	.25	—	1.0 <sup>c</sup>	.08	.05 <sup>d</sup>	.005	.005
C83700 <sup>a</sup>	83.0–88.0	1.00	.50	Rem.	.30	—	.05–.20	.30	—	.05	.005	.005
C83800 <sup>a</sup>	82.0–83.8 <sup>b</sup>	3.3–4.2	5.0–7.0	5.0–8.0	.30	.25	—	1.0 <sup>c</sup>	.08	.03 <sup>d</sup>	.005	.005
C83810 <sup>a</sup>	Rem. <sup>b</sup>	2.0–3.5	4.0–6.0	7.5–9.5	.50 <sup>g</sup>	—	—	2.0 <sup>c</sup>	—	—	.005	.10

<sup>a</sup>Cu + sum of named elements, 99.3% min.<sup>b</sup>In determining Cu min., Cu may be calculated as Cu + Ni.<sup>c</sup>Ni value includes Co.<sup>d</sup>For continuous castings, P shall be 1.5%, max.<sup>e</sup>Cu + sum of named elements, 99.5% min.<sup>f</sup>Cu + sum of named elements, 99.8% min.<sup>g</sup>Fe + Sb + As shall be .50% max.**Table 25** Compositions of Cast Copper–Tin–Zinc and Copper–Tin–Zinc–Lead Alloys (Semi-Red and Leaded Semi-Red Brasses), UNS C84000–C84999

Copper Alloy No.	Cu	Sn	Pb	Zn	Fe	Sb	Ni	S	P	Al	Si	Bi	Other Named Elements
C84000 <sup>a</sup>	82.0–89.0	2.0–4.0	.09	5.0–14.0	.40	.02	.50–2.0	.10–.65	.05	.005	.005	—	.20 B .01 Mn .20 Zr
C84010 <sup>a</sup>	82.0–89.0	2.0–4.0	.09	5.0–14.0	.40	.02	.50–2.0	.10–.65	.05	.005	.005	—	.20 B .01–.20 Mn .20 Zr
C84020 <sup>a</sup>	82.0–89.0	2.0–4.0	.09	5.0–14.0	.40	.02	.50–2.0	.10–.65	.05	.005	.005	—	.20 B .10 C .20 Mn .30 Ti .20 Zr
C84200 <sup>a</sup>	78.0–82.0 <sup>b</sup>	4.0–6.0	2.0–3.0	10.0–16.0	.40	.25	.8 <sup>c</sup>	.08	.05 <sup>d</sup>	.005	.005	—	—
C84400 <sup>a</sup>	78.0–82.0 <sup>b</sup>	2.3–3.5	6.0–8.0	7.0–10.0	.40	.25	1.0 <sup>c</sup>	.08	.02 <sup>d</sup>	.005	.005	—	—
C84410 <sup>a</sup>	Rem. <sup>b</sup>	3.0–4.5	7.0–9.0	7.0–11.0	—	—	1.0 <sup>c</sup>	—	—	.01	.2	.05	<sup>e</sup>
C84500 <sup>a</sup>	77.0–79.0 <sup>b</sup>	2.0–4.0	6.0–7.5	10.0–14.0	.40	.25	1.0 <sup>c</sup>	.08	.02 <sup>d</sup>	.005	.005	—	—
C84800 <sup>a</sup>	75.0–77.0 <sup>b</sup>	2.0–3.0	5.5–7.0	13.0–17.0	.40	.25	1.0 <sup>c</sup>	.08	.02 <sup>d</sup>	.005	.005	—	—

<sup>a</sup>Cu + sum of named elements, 99.3% min.<sup>b</sup>In determining Cu min., Cu may be calculated as Cu + Ni.<sup>c</sup>Ni value includes Co.<sup>d</sup>For continuous castings, P shall be 1.5%, max.<sup>e</sup>Fe + Sb + As shall be .8% max.

**Table 26** Compositions of Cast Copper-Zinc Alloys (Yellow Brasses), UNS C85000–C85999

Copper Alloy No.	Cu	Sn	Pb	Zn	Fe	Sb	Ni	Mn	As	S	P	Al	Si	Other Named Elements
C85200 <sup>a</sup>	70.0–74.0 <sup>b</sup>	.7–2.0	1.5–3.8	20.0–27.0	.6	.20	1.0 <sup>c</sup>	—	—	.05	.02	.005	.05	—
C85210 <sup>d</sup>	70.0–75.0 <sup>b</sup>	1.0–3.0	2.0–5.0	Rem.	.8	—	1.0	—	.02–.06	—	—	.005	.005	—
C85300 <sup>a</sup>	68.0–72.0	.50	.50	Rem.	—	—	—	—	—	—	.50	—	—	—
C85310 <sup>d</sup>	68.0–73.0 <sup>b</sup>	1.5	2.0–5.0	Rem.	.8	—	1.0	—	.02–.06	—	—	.0	—	—
C85400 <sup>d</sup>	65.0–70.0 <sup>b</sup>	.50–1.5	1.5–3.8	24.0–32.0	.7	—	1.0 <sup>c</sup>	—	—	—	—	.35	.05	—
C85450 <sup>e</sup>	60.0–64.0	.50–1.5	.09	Rem.	.30–1.0	—	1.0 <sup>c</sup>	.6	—	—	—	1.0	—	—
C85500 <sup>a</sup>	59.0–63.0 <sup>b</sup>	.20	.20	Rem.	.20	—	.20 <sup>c</sup>	.20	—	—	—	—	—	—
C85550 <sup>e</sup>	59.0–64.0	.30	.09	Rem.	.15	—	.20 <sup>f</sup>	—	—	—	—	.30	.30–1.0	—
C85600	59.0–63.0	.20	.20	Rem.	—	—	.20	.20	—	—	—	—	—	—
C85610	63.0–66.0	1.2–2.0	1.0–2.0	Rem.	.10–1.0	—	2.0	—	—	—	—	—	—	1.0 Be
C85700 <sup>g</sup>	58.0–64.0 <sup>b</sup>	.50–1.5	.8–1.5	32.0–40.0	.7	—	1.0 <sup>c</sup>	—	—	—	—	.8	.05	—
C85710	58.0–63.0	1.0	1.0–2.5	Rem.	.8	—	1.0	.50	—	—	—	.20–.8	.05	—
C85800 <sup>g</sup>	57.0 min <sup>b</sup>	1.5	1.5	31.0–41.0	.50	.05	.50 <sup>c</sup>	.25	.05	.05	.01	.55	.25	—
C85900 <sup>h</sup>	58.0–62.0	1.5	.09	31.0–41.0	.50	.20	1.5	.01	—	.10–.65	.01	.10–.6	.25	.20 B .20 Zr
C85910 <sup>h</sup>	58.0–62.0	1.5	.09	31.0–41.0	.50	.20	1.5	.01–.20	—	.10–.65	.01	.10–.6	.25	.20 B .20 Zr
C85920 <sup>h</sup>	58.0–62.0	1.5	.09	31.0–41.0	.50	.20	1.5	.20	—	.1	.01	.10–.6	.25	.20 B .20 Zr
C85930 <sup>h</sup>	58.0–62.0	1.5	.09	31.0–41.0	.50	.10–1.5	1.5	.20	—	.10–.65	.01	.10–.6	.25	.10 C .30 Ti .20 Zr .20 B .10 C .30 Ti .20 Zr

<sup>a</sup>Cu + Sum of Named Elements, 99.1% min.<sup>b</sup>In determining Cu min., Cu may be calculated as Cu + Ni.<sup>c</sup>Ni value includes Co.<sup>d</sup>Cu + Sum of Named Elements, 98.9% min.<sup>e</sup>Cu + Sum of Named Elements, 98.7% min.<sup>f</sup>For continuous castings, P shall be 1.0% max.<sup>g</sup>Cu + sum of named elements, 99.8% min.<sup>h</sup>Fe + Sb + As shall be .50% max.

**Table 27** Compositions of Cast Manganese Bronze and Leaded Manganese Bronze Alloys (High-Strength Yellow Brasses), C86000–C86999

Alloy No.	Cu	Sn	Pb	Zn	Fe	Ni	Al	Mn	Si	Other Named Elements
C86100 <sup>a</sup>	66.0–68.0 <sup>b</sup>	.20	.20	Rem.	2.0–4.0	—	4.5–5.5	2.5–5.0	—	—
C86200 <sup>a</sup>	60.0–66.0 <sup>b</sup>	.20	.20	22.0–28.0	2.0–4.0	1.0 <sup>c</sup>	3.0–4.9	2.5–5.0	—	—
C86300 <sup>a</sup>	60.0–66.0 <sup>b</sup>	.20	.20	22.0–28.0	2.0–4.0	1.0 <sup>c</sup>	5.0–7.5	2.5–5.0	—	—
C86350 <sup>(4)</sup>	60.0–64.0 <sup>b</sup>	.8	.09	Rem.	1.0	.50 <sup>c</sup>	.30–1.1	2.0–5.0	—	.10 Mg
C86400 <sup>a</sup>	56.0–62.0 <sup>b</sup>	.50–1.5	.50–1.5	34.0–42.0	.40–2.0	1.0 <sup>c</sup>	.50–1.5	.10–1.5	—	—
C86500 <sup>a</sup>	55.0–60.0 <sup>b</sup>	1.0	.40	36.0–42.0	.40–2.0	1.0 <sup>c</sup>	.50–1.5	.10–1.5	—	—
C86550 <sup>a</sup>	57.0 min <sup>b</sup>	1.0	.50	Rem.	.7–2.0	1.0 <sup>c</sup>	.50–2.5	.10–3.0	.10	—
C86700 <sup>a</sup>	55.0–60.0 <sup>b</sup>	1.5	.50–1.5	30.0–38.0	1.0–3.0	1.0 <sup>c</sup>	1.0–3.0	.10–3.5	—	—
C86800 <sup>a</sup>	53.5–57.0 <sup>b</sup>	1.0	.20	Rem.	1.0–2.5	2.5–4.0 <sup>c</sup>	2.0	2.5–4.0	—	—

<sup>a</sup>Cu + sum of named elements, 99.0% min.<sup>b</sup>In determining Cu min., Cu may be calculated as Cu + Ni.<sup>c</sup>Ni value includes Co.**Table 28** Compositions of Cast Copper–Silicon Alloys (Silicon Bronzes and Silicon Brasses), UNS C87000–C87999

Copper Alloy No.	Cu	Sn	Pb	Zn	Fe	Al	Si	Mn	Mg	Ni	S	Other Named Elements
C87200	89.0 min	1.0	.50	5.0	2.5	1.5	1.0–5.0	1.5	—	—	—	.50 P
C87300 <sup>a</sup>	94.0 min	—	.09	.25	.20	—	3.5–4.5	.8–1.5	—	—	—	—
C87400 <sup>b</sup>	79.0 min	—	1.0	12.0–16.0	—	.8	2.5–4.0	—	—	—	—	—
C87410 <sup>b</sup>	79.0 min	—	1.0	12.0–16.0	—	.8	2.5–4.0	—	—	—	—	.03–.06 As
C87420 <sup>b</sup>	79.0 min	—	1.0	12.0–16.0	—	.8	2.5–4.0	—	—	—	—	.03–.06 Sb
C87430 <sup>b</sup>	79.0 min	—	1.0	12.0–16.0	—	.8	2.5–4.0	—	—	—	—	.03–.06 P
C87500 <sup>a</sup>	79.0 min	—	.09	12.0–16.0	—	.50	3.0–5.0	—	—	—	—	—
C87510	79.0 min	—	.50	12.0–16.0	—	.50	3.0–5.0	—	—	—	—	.03–.06 As
C87520	79.0 min	—	.50	12.0–16.0	—	.50	3.0–5.0	—	—	—	—	.03–.06 Sb
C87530	79.0 min	—	.50	12.0–16.0	—	.50	3.0–5.0	—	—	—	—	.03–.06 P
C87600 <sup>a</sup>	88.0 min	—	.09	4.0–7.0	.20	—	3.5–5.5	.25	—	—	—	—
C87610 <sup>a</sup>	90.0 min	—	.09	3.0–5.0	.20	—	3.0–5.0	.25	—	—	—	—
C87700 <sup>b</sup>	87.5 min	2.0	.09	7.0–9.0	.50	—	2.5–3.5	.8	—	.25	—	.10 Sb .15 P
C87710 <sup>b</sup>	84.0 min	2.0	.09	9.0–11.0	.50	—	3.0–5.0	.8	—	.25	—	.10 Sb .15 P
C87800 <sup>a</sup>	80.0 min	.25	.09	12.0–16.0	.15	.15	3.8–4.2	.15	.01	.20 <sup>c</sup>	.05	.05 Sb .05 As .01 P
C87845 <sup>a</sup>	75.0–78.0	.10	.02	Rem.	.10	.09	2.5–2.9	.10	—	.20 <sup>c</sup>	—	.015 Sb .015 As .015 Cr .03–.06 P
C87850 <sup>a</sup>	74.0–78.0	.30	.09	Rem.	.10	—	2.7–3.4	.10	—	.20 <sup>c</sup>	—	.10 Sb .05–.20 P
C87900	63.0 min	.25	.25	30.0–36.0	.40	.15	.8–1.2	.15	—	.50	.05	.05 Sb .05 As .01 P

<sup>a</sup>Cu + sum of named elements, 99.5% min.<sup>b</sup>Cu + sum of named elements, 99.2% min.<sup>c</sup>Ni value includes Co.

**Table 29** Compositions of Cast Copper–Bismuth and Copper–Bismuth–Selenium Alloys, (EnviroBrasses) UNS C88000–C89999

Copper Alloy No.	Cu	Sn	Pb	Zn	Fe	Sb	Ni	S	P	Al	Si	Bi	Se	Other Named Elements
C89320 <sup>a</sup>	87.0–91.0	5.0–7.0	.09	1.0	.20	.35	1.0 <sup>b</sup>	.08	.30	.005	.005	4.0–6.0	—	—
C89325 <sup>c</sup>	84.0–88.0	9.0–11.0	.10	1.0	.15	.50	1.0 <sup>b</sup>	.08	.10	.005	.005	2.7–3.7	—	<i>d</i>
C89510 <sup>a</sup>	86.0–88.0	4.0–6.0	.09	4.0–6.0	.20	.25	1.0 <sup>b</sup>	.08	.05	.005	.005	.50–1.5 <sup>e</sup>	.35–.75 <sup>e</sup>	—
C89520 <sup>a</sup>	85.0–87.0	5.0–6.0	.09	4.0–6.0	.20	.25	1.0 <sup>b</sup>	.1	—	.005	—	1.6–2.2 <sup>f</sup>	.8–1.1 <sup>f</sup>	—
C89530 <sup>a</sup>	84.0–89.0	3.5–6.0	.20	7.0–9.0	.30	.20	1.0 <sup>b</sup>	—	.05	.01	.01	1.0–2.0	.10–.30	—
C89535 <sup>a</sup>	84.0–89.0	2.5–5.5	.25	5.0–9.0	.30	.20	.30–1.0 <sup>g</sup>	—	.40	.01	.01	.8–2.0	.50	—
C89540 <sup>a</sup>	58.0–64.0	1.2	.10	32.0–38.0	.50	—	1.0 <sup>b</sup>	—	—	.10–.60	—	.6–1.2	.10	—
C89550 <sup>a</sup>	58.0–64.0	1.2	.09	32.0–38.0	.50	.05	1.0 <sup>b</sup>	.05	.01	.10–.6	.25	.6–1.2	.01–.10	—
C89560 <sup>a,h</sup>	58.0–61.0	.25	.09	Rem.	.12	—	—	—	—	.30–.8	—	1.0–2.4	—	.0003–.0015 B .001 Cd
C89720 <sup>a</sup>	63.0min	.6–1.5	.09	26.0–32.0	.10	.02–.20	1.0 <sup>b</sup>	—	.02	.35–1.5	.40–1.0	.50–2.0	—	.0005–.01 B .10 Mn
C89831 <sup>c</sup>	87.0–91.0	2.7–3.7	.10	2.0–4.0	.30	.25	1.0 <sup>b</sup>	.08	.050	.005	.005	2.7–3.7	—	<i>d</i>
C89833 <sup>i</sup>	86.0–91.0	4.0–6.0	.09	2.0–6.0	.30	.25	1.0 <sup>b</sup>	.08	.050	.005	.005	1.7–2.7	—	—
C89835 <sup>c</sup>	85.0–89.0	6.0–7.5	.09	2.0–4.0	.20	.35	1.0 <sup>b</sup>	.08	.10	.005	.005	1.7–2.7	—	<i>d</i>
C89836 <sup>a</sup>	87.0–91.0	4.0–7.0	.25	2.0–4.0	.35	.25	.90 <sup>b</sup>	.08	.06	.005	.005	1.5–3.5	—	—
C89837 <sup>c</sup>	84.0–88.0	3.0–4.0	.10	6.0–10.0	.30	.25	1.0 <sup>b</sup>	.08	.050	.005	.005	.7–1.2	—	<i>d</i>
C89841 <sup>a</sup>	73.0–77.0	.30	—	18.0–23.0	.10	.10	.20 <sup>g</sup>	—	—	.01	2.8–3.4	.50–1.0	—	.10 Mn
C89842 <sup>a</sup>	78.0–82.0	2.0–3.0	.09	Rem.	.30	.05	.10–.50 <sup>b</sup>	—	.005–.02	.005	.005	1.5–2.5	—	—
C89844 <sup>i</sup>	83.0–86.0	3.0–5.0	.20	7.0–10.0	.30	.25	1.0 <sup>b</sup>	.08	.05	.005	.005	2.0–4.0	—	—
C89845 <sup>a</sup>	82.5–87.5	3.0–5.0	.09	6.0–9.0	.30	.25	1.5–2.5 <sup>b</sup>	—	.05	.01	.01	1.0–2.0	—	—
C89940 <sup>a</sup>	64.0–68.0	3.0–5.0	.01	3.0–5.0	.7–2.0	.10	20.0–23.0 <sup>b</sup>	.05	.10–.15	.005	.15	4.0–5.5	—	.20 Mn

<sup>a</sup>Cu + sum of named elements, 99.5% min.<sup>b</sup>Ni value includes Co.<sup>c</sup>Cu + sum of named elements, 99.0% min.<sup>d</sup>.01–2.0% as any single or combination of Ce, La, or other rare earth(x) elements, as agreed upon. (x)ASM International definition: one of the group of chemically similar metals with atomic numbers 57–71, commonly referred to as lanthanides.<sup>e</sup>Experience favors Bi:Se ≥ 2:1.<sup>f</sup>Bi:Se ≥ 2:1.<sup>g</sup>Includes Co.<sup>h</sup>Includes Boron 3–15 ppm.<sup>i</sup>Cu + sum of named elements, 99.3% min.



**Table 30** Compositions of Cast Copper–Tin Alloys (Tin Bronzes), UNS C90000–C91999

Copper Alloy No.	Cu	Sn	Pb	Zn	Fe	Sb	Ni	S	P	Al	Si	Mn	Other Named Elements
C90200 <sup>a</sup>	91.0–94.0 <sup>b</sup>	6.0–8.0	.30	.50	.20	.20	.50 <sup>c</sup>	.05	.05 <sup>d</sup>	.005	.005	—	—
C90250	89.0–91.0	9.0–11.0	.30	.50	.25	.02	2.0	.05	.05	.005	.005	.20	—
C90300 <sup>a</sup>	86.0–89.0 <sup>b</sup>	7.5–9.0	.30	3.0–5.0	.20	.20	1.0 <sup>c</sup>	.05	.05 <sup>d</sup>	.005	.005	—	—
C90400 <sup>e</sup>	86.0–89.0	7.5–8.5	.09	1.0–5.0	.40	.02	1.0	.10–.65	.05	.005	.005	.01	.20 B .20 Zr
C90410 <sup>e</sup>	86.0–89.0	7.5–8.5	.09	1.0–5.0	.40	.02	1.0	.10–.65	.05	.005	.005	.01–.20	.20 B .20 Zr
C90420 <sup>e</sup>	86.0–89.0	7.5–8.5	.09	1.0–5.0	.40	.02	1.0	.10–.65	.05	.005	.005	.20	.20 B .10 C .30 Ti .20 Zr
C90430 <sup>e</sup>	86.0–89.0	7.5–8.5	.09	1.0–5.0	.40	.10–1.5	1.0	.10–.65	.05	.005	.005	.20	.20 B .10 C .30 Ti .20 Zr
C90500 <sup>f</sup>	86.0–89.0 <sup>b</sup>	9.0–11.0	.30	1.0–3.0	.20	.20	1.0 <sup>c</sup>	.05	.05 <sup>d</sup>	.005	.005	—	—
C90700 <sup>a</sup>	88.0–90.0 <sup>b</sup>	10.0–12.0	.50	.50	.15	.20	.50 <sup>c</sup>	.05	.30 <sup>d</sup>	.005	.005	—	—
C90710 <sup>a</sup>	Rem. <sup>b</sup>	10.0–12.0	.25	.05	.10	.20	.10 <sup>c</sup>	.05	.05–1.2 <sup>d</sup>	.005	.005	—	—
C90800 <sup>a</sup>	85.0–89.0 <sup>b</sup>	11.0–13.0	.25	.25	.15	.20	.50 <sup>c</sup>	.05	.30 <sup>d</sup>	.005	.005	—	—
C90810 <sup>a</sup>	Rem. <sup>b</sup>	11.0–13.0	.25	.30	.15	.20	.50 <sup>c</sup>	.05	.15–.8 <sup>d</sup>	.005	.005	—	—
C90900 <sup>a</sup>	86.0–89.0 <sup>b</sup>	12.0–14.0	.25	.25	.15	.20	.50 <sup>c</sup>	.05	.05 <sup>d</sup>	.005	.005	—	—
C91000 <sup>a</sup>	84.0–86.0 <sup>b</sup>	14.0–16.0	.20	1.5	.10	.20	.8 <sup>c</sup>	.05	.05 <sup>d</sup>	.005	.005	—	—
C91100 <sup>a</sup>	82.0–85.0 <sup>b</sup>	15.0–17.0	.25	.25	.25	.20	.50 <sup>c</sup>	.05	1.0 <sup>d</sup>	.005	.005	—	—
C91300 <sup>a</sup>	79.0–82.0 <sup>b</sup>	18.0–20.0	.25	.25	.25	.20	.50 <sup>c</sup>	.05	1.0 <sup>d</sup>	.005	.005	—	—
C91500	Rem.	9.0–11.0	2.0–3.2	—	—	—	2.8–4.0	—	.50	—	—	—	—
C91600 <sup>a</sup>	86.0–89.0 <sup>b</sup>	9.7–10.8	.25	.25	.20	.20	1.2–2.0 <sup>c</sup>	.05	.30 <sup>d</sup>	.005	.005	—	—
C91700 <sup>a</sup>	84.0–87.0 <sup>b</sup>	11.3–12.5	.25	.25	.20	.20	1.2–2.0 <sup>c</sup>	.05	.30 <sup>d</sup>	.005	.005	—	—

<sup>a</sup>Cu + sum of named elements, 99.4% min.<sup>b</sup>In determining Cu min., Cu may be calculated as Cu + Ni.<sup>c</sup>Ni value includes Co.<sup>d</sup>For continuous castings, P shall be 1.5%, max.<sup>e</sup>Cu + sum of named elements, 99.3% min.<sup>f</sup>Cu + sum of named elements, 99.7% min.**Table 31** Compositions of Cast Copper–Tin–Lead Alloys (Leaded Tin Bronzes), UNS C92000–C92900

Copper Alloy No.	Cu	Sn	Pb	Zn	Fe	Sb	Ni	S	P	Al	Si	Mn	Other Named Elements
C92200 <sup>a</sup>	86.0–90.0 <sup>b</sup>	5.5–6.5	1.0–2.0	3.0–5.0	.25	.25	1.0 <sup>c</sup>	.05	.05 <sup>d</sup>	.005	.005	—	—
C92210 <sup>a</sup>	86.0–89.0 <sup>b</sup>	4.5–5.5	1.7–2.5	3.0–4.5	.25	.20	.7–1.0 <sup>c</sup>	.05	.03 <sup>d</sup>	.005	.005	—	—
C92220 <sup>a</sup>	86.0–88.0 <sup>b</sup>	5.0–6.0	1.5–2.5	3.0–5.5	.25	—	.50–1.0 <sup>c</sup>	—	.05 <sup>d</sup>	—	—	—	—
C92300 <sup>a</sup>	85.0–89.0 <sup>b</sup>	7.5–9.0	.30–1.0	2.5–5.0	.25	.25	1.0 <sup>c</sup>	.05	.05 <sup>d</sup>	.005	.005	—	—
C92310 <sup>a</sup>	Rem. <sup>b</sup>	7.5–8.5	.30–1.5	3.5–4.5	—	—	1.0 <sup>c</sup>	—	—	.005	.005	.03	—
C92400 <sup>a</sup>	86.0–89.0 <sup>b</sup>	9.0–11.0	1.0–2.5	1.0–3.0	.25	.25	1.0 <sup>c</sup>	.05	.05 <sup>d</sup>	.005	.005	—	—

(continued)

**Table 31** (Continued)

Copper Alloy No.	Cu	Sn	Pb	Zn	Fe	Sb	Ni	S	P	Al	Si	Mn	Other Named Elements
C92410 <sup>a</sup>	Rem. <sup>b</sup>	6.0–8.0	2.5–3.5	1.5–3.0	.20	.25	.20 <sup>c</sup>	—	—	.005	.005	.05	—
C92500 <sup>a</sup>	85.0–88.0 <sup>b</sup>	10.0–12.0	1.0–1.5	.50	.30	.25	.8–1.5 <sup>c</sup>	.05	.30 <sup>d</sup>	.005	.005	—	—
C92600 <sup>a</sup>	86.0–88.5 <sup>b</sup>	9.3–10.5	.8–1.5	1.3–2.5	.20	.25	.7 <sup>c</sup>	.05	.03 <sup>d</sup>	.005	.005	—	—
C92610 <sup>a</sup>	Rem. <sup>b</sup>	9.5–10.5	.30–1.5	1.7–2.8	.15	—	1.0 <sup>c</sup>	—	—	.005	.005	.03	—
C92700 <sup>a</sup>	86.0–89.0 <sup>b</sup>	9.0–11.0	1.0–2.5	.7	.20	.25	1.0 <sup>c</sup>	.05	.25 <sup>d</sup>	.005	.005	—	—
C92710 <sup>a</sup>	Rem. <sup>b</sup>	9.0–11.0	4.0–6.0	1.0	.20	.25	2.0 <sup>c</sup>	.05	.10 <sup>d</sup>	.005	.005	—	—
C92800 <sup>a</sup>	78.0–82.0 <sup>b</sup>	15.0–17.0	4.0–6.0	.8	.20	.25	.8 <sup>c</sup>	.05	.05 <sup>d</sup>	.005	.005	—	—
C92810 <sup>a</sup>	78.0–82.0 <sup>b</sup>	12.0–14.0	4.0–6.0	.50	.50	.25	.8–1.2 <sup>c</sup>	.05	.05 <sup>d</sup>	.005	.005	—	—
C92900 <sup>a</sup>	82.0–86.0 <sup>b</sup>	9.0–11.0	2.0–3.2	.25	.20	.25	2.8–4.0 <sup>c</sup>	.05	.50 <sup>d</sup>	.005	.005	—	—

<sup>a</sup>Cu + sum of named elements, 99.3% min.

<sup>b</sup>In determining Cu min., Cu may be calculated as Cu + Ni.

<sup>c</sup>Ni value includes Co.

<sup>d</sup>For continuous castings, P shall be 1.5%, max.

**Table 32** Compositions of Cast Copper–Tin–Lead Alloys (High-Leaded Tin Bronzes), UNS C93000–C94500

Copper Alloy No.	Cu	Sn	Pb	Zn	Fe	Sb	Ni	S	P	Al	Si	Other Named Elements
C93100 <sup>a</sup>	Rem. <sup>b</sup>	6.5–8.5	2.0–5.0	2.0	.25	.25	1.0 <sup>c</sup>	.05	.30 <sup>d</sup>	.005	.005	—
C93200 <sup>a</sup>	81.0–85.0 <sup>b</sup>	6.3–7.5	6.0–8.0	1.0–4.0	.20	.35	1.0 <sup>c</sup>	.08	.15 <sup>d</sup>	.005	.005	—
C93400 <sup>a</sup>	82.0–85.0 <sup>b</sup>	7.0–9.0	7.0–9.0	.8	.20	.50	1.0 <sup>c</sup>	.08	.50 <sup>d</sup>	.005	.005	—
C93500 <sup>a</sup>	83.0–86.0 <sup>b</sup>	4.3–6.0	8.0–10.0	2.0	.20	.30	1.0 <sup>c</sup>	.08	.05 <sup>d</sup>	.005	.005	—
C93600 <sup>e</sup>	79.0–83.0	6.0–8.0	11.0–13.0	1.0	.20	.55	1.0 <sup>c</sup>	.08	.15 <sup>d</sup>	.005	.005	—
C93700 <sup>a</sup>	78.0–82.0	9.0–11.0	8.0–11.0	.8	.7 <sup>f</sup>	.50	.50 <sup>c</sup>	.08	.10 <sup>d</sup>	.005	.005	—
C93720 <sup>a</sup>	83.0 min	3.5–4.5	7.0–9.0	4.0	.7	.50	.50 <sup>c</sup>	—	.10 <sup>d</sup>	—	—	—
C93800 <sup>a</sup>	75.0–79.0	6.3–7.5	13.0–16.0	.8	.15	.8	1.0 <sup>c</sup>	.08	.05 <sup>d</sup>	.005	.005	—
C93900 <sup>g</sup>	76.5–79.5	5.0–7.0	14.0–18.0	1.5	.40	.50	.8 <sup>c</sup>	.08	1.5 <sup>d</sup>	.005	.005	—
C94000 <sup>h</sup>	69.0–72.0	12.0–14.0	14.0–16.0	.50	.25	.50	.50–1.0 <sup>c</sup>	.08 <sup>i</sup>	.05 <sup>d</sup>	.005	.005	—
C94100 <sup>h</sup>	72.0–79.0	4.5–6.5	18.0–22.0	1.0	.25	.8	1.0 <sup>c</sup>	.08 <sup>i</sup>	.50 <sup>d</sup>	.005	.005	—
C94200	68.5–75.5	3.0–4.0	3.0–4.0	3.0	.35	.50	.50	—	—	—	—	—
C94300 <sup>a</sup>	67.0–72.0	4.5–6.0	23.0–27.0	.8	.15	.8	1.0 <sup>c</sup>	.08 <sup>i</sup>	.08 <sup>d</sup>	.005	.005	—
C94310 <sup>a</sup>	Rem.	1.5–3.0	27.0–34.0	.50	.50	.50	.25–1.0 <sup>c</sup>	—	.05 <sup>d</sup>	—	—	—
C94320 <sup>a</sup>	Rem.	4.0–7.0	24.0–32.0	—	.35	—	—	—	—	—	—	—
C94330 <sup>a</sup>	68.5–75.5	3.0–4.0	21.0–25.0	3.0	.7	.50	.50 <sup>c</sup>	—	.10 <sup>d</sup>	—	—	—
C94400 <sup>a</sup>	Rem.	7.0–9.0	9.0–12.0	.8	.15	.8	1.0 <sup>c</sup>	.08	.50 <sup>d</sup>	.005	.005	—
C94500 <sup>a</sup>	Rem.	6.0–8.0	16.0–22.0	1.2	.15	.8	1.0 <sup>c</sup>	.08	.05 <sup>d</sup>	.005	.005	—

<sup>a</sup>Cu + sum of named elements, 99.0% min.

<sup>b</sup>In determining Cu min., Cu may be calculated as Cu + Ni.

<sup>c</sup>Ni value includes Co.

<sup>d</sup>For continuous castings, P shall be 1.5%, max.

<sup>e</sup>Cu + sum of named elements, 99.3% min.

<sup>f</sup>Fe shall be .35% max., when used for steel-backed

<sup>g</sup>Cu + sum of named elements, 98.9% min.

<sup>h</sup>Cu + sum of named elements, 98.7% min.

<sup>i</sup>For continuous castings, S shall be .25% max.

**Table 33** Compositions of Cast Copper–Tin–Nickel Alloys (Nickel–Tin Bronzes), UNS C94600–C94999

Copper Alloy No.	Cu	Sn	Pb	Zn	Fe	Sb	Ni	Mn	S	P	Al	Si	Other Named Elements
C94700 <sup>a</sup>	85.0–90.0	4.5–6.0	.09 <sup>b</sup>	1.0–2.5	.25	.15	4.5–6.0 <sup>c</sup>	.20	.05	.05	.005	.005	—
C94800 <sup>a</sup>	84.0–89.0	4.5–6.0	.30–1.0	1.0–2.5	.25	.15	4.5–6.0 <sup>c</sup>	.20	.05	.05	.005	.005	—
C94900 <sup>d</sup>	79.0–81.0	4.0–6.0	4.0–6.0	4.0–6.0	.30	.25	4.0–6.0 <sup>c</sup>	.10	.08	.05	.005	.005	—

<sup>a</sup>Cu + sum of named elements, 98.7% min.<sup>b</sup>The mechanical properties of C94700 (heat treated) may not be attainable if the Pb content exceeds .01%.<sup>c</sup>Ni value includes Co.<sup>d</sup>Cu + sum of named elements, 99.4% min.**Table 34** Compositions of Cast Copper–Aluminum–Iron and Copper–Aluminum–Iron–Nickel Alloys (Aluminum Bronzes), UNS C95000–C95999

Copper Alloy No.	Cu	Pb	Fe	Ni	Al	Mn	Mg	Si	Zn	Sn	Other Named Elements
C95200 <sup>a</sup>	86.0 min	—	2.5–4.0	—	8.5–9.5	—	—	—	—	—	—
C95210 <sup>a</sup>	86.0 min	.05	2.5–4.0	1.0 <sup>b</sup>	8.5–9.5	1.0	.05	.25	.50	.10	—
C95220 <sup>c</sup>	Rem.	—	2.5–4.0	2.5 <sup>b</sup>	9.5–10.5	.50	—	—	—	—	—
C95300 <sup>a</sup>	86.0 min	—	.8–1.5	—	9.0–11.0	—	—	—	—	—	—
C95400 <sup>c</sup>	83.0 min	—	3.0–5.0	1.5 <sup>b</sup>	10.0–11.5	.50	—	—	—	—	—
C95410 <sup>c</sup>	83.0 min	—	3.0–5.0	1.5–2.5 <sup>b</sup>	10.0–11.5	.50	—	—	—	—	—
C95420 <sup>c</sup>	83.5 min	—	3.0–4.3	.50 <sup>b</sup>	10.5–12.0	.50	—	—	—	—	—
C95430	Rem.	—	—	.50	10.5–12.0	.50	—	—	—	—	—
C95500 <sup>c</sup>	78.0 min	—	3.0–5.0	3.0–5.5 <sup>b</sup>	10.0–11.5	3.5	—	—	—	—	—
C95510 <sup>d</sup>	78.0 min	—	2.0–3.5	4.5–5.5 <sup>b</sup>	9.7–10.9	1.5	—	—	.30	.20	—
C95520 <sup>c</sup>	74.5 min	.03	4.0–5.5	4.2–6.0 <sup>b</sup>	10.5–11.5	1.5	—	.15	.30	.25	.05 Cr .20 Co
C95600 <sup>a</sup>	88.0 min	—	—	.25 <sup>b</sup>	6.0–8.0	—	—	1.8–3.2	—	—	—
C95700 <sup>c</sup>	71.0 min	—	2.0–4.0	1.5–3.0 <sup>b</sup>	7.0–8.5	11.0–14.0	—	.10	—	—	—
C95710 <sup>c</sup>	71.0 min	.05	2.0–4.0	1.5–3.0 <sup>b</sup>	7.0–8.5	11.0–14.0	—	.15	.50	1.0	.05 P
C95720 <sup>c</sup>	73.0 min	.03	1.5–3.5	3.0–6.0 <sup>b</sup>	6.0–8.0	12.0–15.0	—	.10	.10	.10	.09 Cr
C95800 <sup>c</sup>	79.0 min	.03	3.5–4.5 <sup>e</sup>	4.0–5.0 <sup>e</sup>	8.5–9.5	.8–1.5	—	.10	—	—	—
C95810 <sup>c</sup>	79.0 min	.09	3.5–4.5 <sup>e</sup>	4.0–5.0 <sup>e</sup>	8.5–9.5	.8–1.5	.05	.10	.50	—	—
C95820 <sup>f</sup>	77.5 min	.02	4.0–5.0	4.5–5.8 <sup>b</sup>	9.0–10.0	1.5	—	.10	.20	.20	—
C95900 <sup>c</sup>	Rem.	—	3.0–5.0	.50 <sup>b</sup>	12.0–13.5	1.5	—	—	—	—	—

<sup>a</sup>Cu + sum of named elements, 99.0% min.<sup>b</sup>Ni value includes Co.<sup>c</sup>Cu + sum of named elements, 99.5% min.<sup>d</sup>Cu + sum of named elements, 99.8% min.<sup>e</sup>Fe content shall not exceed Ni content.<sup>f</sup>Cu + sum of named elements, 99.2% min.

**Table 35** Composition of Cast Copper–Nickel Alloys (Copper Nickels), UNS C96000–C96999

Copper Alloy No.	Cu	Pb	Fe	Ni	Mn	Si	Nb	C	Be	Other Named Elements
C96200 <sup>a</sup>	Rem.	.01	1.0–1.8	9.0–11.0 <sup>b</sup>	1.5	.50	1.0 <sup>c</sup>	.10	—	.02 P .02 S
C96300 <sup>a</sup>	Rem.	.01	.50–1.5	18.0–22.0 <sup>b</sup>	.25–1.5	.50	.50–1.5	.15	—	.02 P .02 S
C96400 <sup>a</sup>	Rem.	.01	.25–1.5	28.0–32.0 <sup>b</sup>	1.5	.50	.50–1.5	.15	—	.02 P .02 S
C96600 <sup>a</sup>	Rem.	.01	.8–1.1	29.0–33.0 <sup>b</sup>	1.0	.15	—	—	.40–.7	—
C96700 <sup>a</sup>	Rem.	.01	.40–1.0	29.0–33.0 <sup>b</sup>	.40–1.0	.15	—	—	1.1–1.2	.15–.35 Ti .15–.35 Zr
C96800 <sup>a(4)</sup>	Rem.	.005	.50	9.5–10.5 <sup>b</sup>	.05–.30	.05	.10–.30	—	—	.005–.15 Mg 7.5–8.5 Sn 1.0 Zn
C96900 <sup>a</sup>	Rem.	.02	.50	14.5–15.5 <sup>b</sup>	.05–.30	—	.10	—	—	.15 Mg 7.5–8.5 Sn .50 Zn
C96950 <sup>a</sup>	Rem.	.02	.05	11.0–15.5 <sup>b</sup>	.05–.40	.30	.10	—	—	.15 Mg 5.8–8.5 Sn
C96970 <sup>a</sup>	Rem.	.02	.50	8.5–9.5 <sup>b</sup>	.30	—	.10	—	—	.15 Mg 5.5–6.5 Sn .50 Zn

<sup>a</sup>Cu + sum of named elements, 99.5% min.

<sup>b</sup>Ni value includes Co.

<sup>c</sup>The following additional maximum impurity limits shall apply: .10% Al, .001% B, .001% Bi, .005% P, .0025% S, .02% Sb, .01% Ti

**Table 36** Compositions of Cast Copper–Nickel–Zinc Alloys (Nickel Silvers) C97000–C97999

Copper Alloy No.	Cu	Sn	Pb	Zn	Fe	Sb	Ni	S	P	Al	Mn	Si	Other Named Elements
C97300 <sup>a</sup>	53.0–58.0	1.5–3.0	8.0–11.0	17.0–25.0	1.5	.35	11.0–14.0 <sup>b</sup>	.08	.05	.005	.50	.15	—
C97400 <sup>a</sup>	58.0–61.0	2.5–3.5	4.5–5.5	Rem.	1.5	—	15.5–17.0 <sup>b</sup>	—	—	—	.50	—	—
C97600 <sup>c</sup>	63.0–67.0	3.5–4.5	3.0–5.0	3.0–9.0	1.5	.25	19.0–21.5 <sup>b</sup>	.08	.05	.005	1.0	.15	—
C97800 <sup>d</sup>	64.0–67.0	4.0–5.5	1.0–2.5	1.0–4.0	1.5	.20	24.0–27.0 <sup>b</sup>	.08	.05	.005	1.0	.15	—

<sup>a</sup>Cu + sum of named elements, 99.0% min.

<sup>b</sup>Ni value includes Co.

<sup>c</sup>Cu + sum of named elements, 99.7% min.

<sup>d</sup>Cu + sum of named elements, 99.6% min.

**Table 37** Compositions of Cast Copper–Lead Alloys (Leaded Coppers), UNS C98000–C98999

Copper Alloy No.	Cu	Sn	Pb	Ag	Zn	P	Fe	Ni	Sb	Other Named Elements
C98200 <sup>a</sup>	Rem.	.6–2.0	21.0–27.0	—	.50	.10	.7	.50	.50	—
C98400 <sup>a</sup>	Rem.	.50	26.0–33.0	1.5	.50	.10	.7	.50	.50	—
C98600	60.0–70.0	.50	30.0–40.0	1.5	—	—	.35	—	—	—
C98800	56.5–62.5 <sup>b</sup>	.25	37.5–42.5 <sup>c</sup>	5.5 <sup>c</sup>	.10	.02	.35	—	—	—
C98820	Rem.	1.0–5.0	40.0–44.0	—	—	—	.35	—	—	—
C98840	Rem.	1.0–5.0	44.0–58.0	—	—	—	.35	—	—	—

<sup>a</sup>Cu + sum of named elements, 99.5% min.

<sup>b</sup>Includes Ag.

<sup>c</sup>Pb and Ag may be adjusted to modify alloy hardness.

**Table 38** Compositions of Cast Special Alloys, UNS C99000–C99999

Copper Alloy No.	Other Designation	Cu	Sn	Pb	Ni	Fe	Al	Co	Si	Mn	Other Named Elements
C99300 <sup>a</sup>	Increment 800	Rem.	.05	.02	13.5–16.5	.40–1.0	10.7–11.5	1.0–2.0	.02	—	—
C99350 <sup>a</sup>	—	Rem.	—	.15	14.5–16.0 <sup>b</sup>	1.0	9.5–10.5	—	—	.25	7.5–9.5 Zn
C99400 <sup>a</sup>	—	Rem.	—	.09	1.0–3.5	1.0–3.0	.50–2.0	—	.50–2.0	.50	.50–5.0 Zn
C99500 <sup>a</sup>	—	Rem.	—	.09	3.5–5.50	3.0–5.0	.50–2.0	—	.50–2.0	.50	.50–2.0 Zn
C99600 <sup>a</sup>	Increment 1	Rem.	.10	.02	.20	.20	1.0–2.8	.20	.10	39.0–45.0	.05 C .20 Zn
C99700 <sup>a</sup>	—	54.0min	1.0	2.0	4.0–6.0	1.0	.50–3.0	—	—	11.0–15.0	19.0–25.0 Zn
C99710 <sup>a</sup>	—	60.0min	1.0	.09	4.0–6.0	1.0	1.0	—	—	11.0–15.0	19.0–25.0 Zn
C99720 <sup>c</sup>	—	54.0–59.0	1.5–2.0	.05	5.0–6.0	.6–1.0	1.0–1.4	—	.05	11.0–14.0	2.0–3.0 Bi .05 P
C99740 <sup>c</sup>	—	55.0–60.0	1.5–2.0	.05	5.0–6.0	.6–1.0	1.0–1.4	—	.05	11.0–14.0	18.0–24.0 Zn 4.0 Bi .0 P
C99750 <sup>a</sup>	—	55.0–61.0	—	.50–2.5	5.0	1.0	.25–3.0	—	—	17.0–23.0	17.0–23.0 Zn
C99780 <sup>c</sup>	—	62.0–66.0	.50–2.0	.05	4.0–6.0	.50	.30–1.0	—	.05	12.0–15.0	.50–2.0 Bi .05 P 16.0–22.0 Zn

<sup>a</sup>Cu + sum of named elements, 99.7% min.

<sup>b</sup>Ni value includes Co.

<sup>c</sup>Cu + sum of named elements, 99.8% min.

## 2.2 Physical Properties of Copper and Copper Alloys

### *Pure Copper*

Copper, atomic number 29, is a member of subgroup IB in the periodic chart of the elements. Other so-called noble metals in the subgroup include silver and gold, with which copper shares properties such as high ductility and chemical stability. Copper's atomic structure is  $1s^2 2s^2 2p^6 3s^2 3p^6 3d^{10} 4s^1$ . Its filled  $3d$  state and loosely bound  $4s$  electrons and the optical transitions between filled  $3d$  and empty  $4s$  states are responsible for copper's high electrical and thermal conductivities and its distinctive red color.

Copper's atomic weight is 63.546. Almost all copper found in nature exists as one of two stable isotopes,  $\text{Cu}^{63}$  (occurring 69.09%) and  $\text{Cu}^{65}$  (30.91%). Unstable isotopes, ranging from  $\text{Cu}^{58}$  to  $\text{Cu}^{68}$ , are  $\beta$  emitters. Naturally occurring copper is not considered harmfully radioactive.

Table 39<sup>4,5</sup> contains a compilation of physical properties for the pure metal; those for wrought and cast copper alloys are listed in Tables 40 and 41, respectively. Most important among these from an engineering standpoint are its high electrical and thermal conductivities. Copper is the standard for electrical conductivity against which other metals are compared. The International Annealed Copper Standard (IACS) for conductivity is defined as  $\sigma = 5.8 \times 10^7$  S/m. The value is based on the resistance,  $1/58 \Omega$  (0.017241  $\Omega$ ), of an annealed, *commercially* pure copper wire, one meter long, having a uniform cross section of one millimeter square, weighing one gram and having a density of 8.89 g/cm<sup>3</sup> at 293 K (20°C). The corresponding volume resistivity is  $\rho = 7241 \times 10^{-8} \Omega\text{-m}$ .

The conductivity of copper produced using modern technology often exceeds that of "commercially available" metal when the IACS was adopted, and it is not unusual for today's electrical and electronic grades of copper (C10100, C10300, C11000, etc.) to exceed the IACS value by one or more percentage points.<sup>6</sup> IACS remains defined at  $5.8 \times 10^7$  S/m, "modern" copper may exhibit conductivity as high or higher than  $5.96 \times 10^7$  S/m

All conductivities given above are volumetric, which may be a design consideration when making materials selections. For example, aluminum's volumetric electrical conductivity and resistivity at 20°C are  $3.7 \cdot 10 \times 10^7$  S/m and  $2.82 \times 10^{-8} \Omega\text{-m}$ , respectively; carbon steel's are  $6.99 \times 10^6$  S/m and  $1.43 \times 10^{-7} \Omega\text{-m}$ , and austenitic (type 304) stainless steel's are  $1.45 \times 10^6$  S/m and  $9 \times 10^{-7} \Omega\text{-m}$ . Thus, the *volumetric* electrical conductivity of copper is approximately 62% higher than that of aluminum, but aluminum's conductivity is roughly twice that of copper on a weight basis. Copper is therefore normally preferred where space is at a premium, as in conduit, whereas aluminum is favored for products such as overhead transmission cables, where low weight is important. Despite its higher density, however, copper remains the dominant electrical conductor of choice for aircraft and aerospace applications for reasons of long-term reliability.

Alloying reduces electrical conductivity and, to a lesser degree, thermal conductivity. The effects are proportional to alloy content *in solution* at low alloying concentrations but increase significantly at the concentrations found in alloys such as brasses, bronzes, and copper nickels. The effect of individual alloying elements is additive.

Copper's high thermal conductivity is exploited in applications such as heat exchangers, low-pressure heaters and condensers, welding and plasma-cutting equipment, and as thermal buffers in superconducting cables (copper itself is not a superconductor). Copper's thermal conductivity decreases by about 7% between room temperature and the melting point. Copper's temperature coefficient of electrical conductivity is  $0.0039 \text{ K}^{-1}$ .

## 3 MECHANICAL PROPERTIES OF COPPER AND COPPER ALLOYS

### 3.1 Strengthening Mechanisms

Pure copper exists in a single crystal form at all temperatures below its melting point (Fig. 1). In the unalloyed metal, hardening (strengthening) is achieved mainly through cold working

**Table 39** Physical Properties of Pure Copper

Property	Value
Atomic weight	63.546
Atomic volume, cm <sup>3</sup> /mol	7.11
Mass numbers, stable isotopes	63 (69.1%), 65 (30.9%)
Oxidation states	1, 2, 3
Standard electrode potential, V	Cu/Cu <sup>+</sup> = 0.520 Cu <sup>+</sup> /Cu <sup>2+</sup> = 0.337
Electrochemical equivalent, mg/°C <sup>(5)</sup>	0.3294 for Cu <sup>2+</sup> 0.6588 for Cu <sup>+</sup>
Electrolytic solution potential, V (SCE) <sup>(5)</sup>	0.158 (Cu <sup>2+</sup> + e <sup>-</sup> = Cu <sup>+</sup> ) 0.3402 (Cu <sup>2+</sup> + 2e <sup>-</sup> = Cu) 0.522 (Cu <sup>+</sup> + e <sup>-</sup> = Cu)
Density, g/m <sup>3</sup>	8.95285 (pure, single crystal) 8.94 (nominal)
Metallic (Goldschmidt) radius, nm	0.1276 (12-fold coordination)
Ionic radius, M <sup>+</sup> , nm <sup>(3)</sup>	0.096
Covalent radius, nm <sup>(3)</sup>	0.138
Crystal structure	fcc, A1, Fm3m: cF4
Lattice parameter	0.361509 ± 0.000004 nm (25°C, 77 °F)
Electronegativity <sup>(3)</sup>	2.43
Ionization energy, kJ/mol <sup>(3)</sup>	
1 <sup>st</sup>	745
2 <sup>nd</sup>	1950
Ionization potential, eV <sup>(5)</sup>	7.724 Cu(I) 20.29 Cu(II) 36.83 Cu(III)
Hall effect <sup>(5)</sup>	
Hall voltage, V at 0.30 to 0.8116T	-5.24 × 10 <sup>-4</sup>
Hall coefficient, mV·mA·T	-5.5
Heat of atomization, kJ/mol <sup>(3)</sup>	339
Thermal conductivity, W/m·K	394 <sup>(3)</sup> , 398 <sup>(5)</sup>
Electrical conductivity, MS/cm at 20°C	0.591
Electrical resistivity at 20°C, nΩ·m	16.70
Temperature coefficient of electrical resistivity, 0–100°C <sup>(5)</sup>	0.0068
Melting point	1358.03 K (1084.88°C, 1984.79°F) <sup>(5)</sup> 1356 K (1083°C, 1981.4°F) <sup>(3)</sup>
Heat of fusion, kJ/kg	205, 204.9, 206.8 <sup>(15)</sup> 212 <sup>(3)</sup>
Boiling point	2868 K (2595°C, 4703°F), 2840 K (2567°C, 4652°F) <sup>(5)</sup> 2595 K (2868°C, 5194°F) <sup>(5)</sup>
Heat of vaporization, kJ/kg	7369 <sup>(3)</sup> 4729, 4726, 4793 <sup>(5)</sup>
Specific heat, kJ/kg·K	0.255 (100 K) <sup>(5)</sup> 0.384 (293 K) <sup>(3)</sup> 0.386 (293 K) <sup>(5)</sup> 0.494 (2000 K) <sup>(15)</sup>
Coefficient of expansion, linear, μm/m	16.5
Coefficient of expansion, volumetric, 10 <sup>-6</sup> /K	49.5
Tensile strength, MPa	230 (annealed) <sup>(3)</sup> 209 (annealed) <sup>(5)</sup> 344 (cold drawn) <sup>(5)</sup>

(continued)



Table 39 (Continued)

Property	Value
Elastic modulus, GPa	125 (tension, annealed) <sup>(5)</sup> 102–120 (tension, hard drawn) <sup>(3)</sup> 128 (tension, cold drawn) <sup>(5)</sup> 46.4 (shear, annealed) <sup>(5)</sup> 140 (bulk) <sup>(5)</sup>
Magnetic susceptibility, 291 K, mks	−0.086 × 10 <sup>−6</sup> (3) −1.08 × 10 <sup>−6</sup> (5)
Emissivity	0.03 (unoxidized metal, 100°C) (3) 0.8 (heavily oxidized surface) <sup>(5)</sup>
Spectral reflection coefficient, incandescent light	0.63 <sup>(5)</sup>
Nominal spectral emittance, λ=655 nm, 800°C	0.15 <sup>(5)</sup>
Absorptivity, solar radiation	0.25 <sup>(5)</sup>
Viscosity, mPa·s (cP)	3.36 (1085°C, 1985 °F) <sup>(5)</sup> 3.33 (1100°C, 2012 °F) (5) 3.41 (1145°C, 2093 °F) <sup>(3)</sup> 3.22 (1150°C, 2102 °F) (5) 3.12 (1200°C, 2192 °F) (5)
Surface tension mN/m (dyn/cm)	1300 (99.99999% Cu, 1084°C, 1983 °F, vacuum) <sup>(5)</sup> 1341 (99.999% Cu, N <sub>2</sub> , 1150°C, 2102 °F) <sup>(5)</sup> 1104 (1145°C, 2093 °F) <sup>(3)</sup> (see Ref. 5 for additional data)
Coefficient of friction	4.0 (Cu on Cu) in H <sub>2</sub> or N <sub>2</sub> (5) 1.6 (Cu on Cu) in air or O <sub>2</sub> (5) 1.4 (clean) (15) 0.8 (in paraffin oil) (5)
Velocity of sound, m/s	4759 (longitudinal bulk waves) <sup>(5)</sup> 3813 (irrotational rod waves) <sup>(5)</sup> 2325 (shear waves) <sup>(5)</sup> 2171 (Rayleigh waves) <sup>(5)</sup>

(drawing, cold rolling) and, to a lesser extent, by grain refinement and the addition of non-metallic dispersoids.

The specific type(s) of strengthening produced by alloying varies with the type and concentration of the constituent(s) added: Nickel, tin, cadmium, zinc, silicon, aluminum, and many of the other elements commonly present in copper alloys produce at least some of their effect through solid-solution hardening. Copper nickels and low-zinc brasses are the most common examples. Some elements additionally induce the formation of strength-raising secondary phases over specific concentrations ranges. Chromium, zirconium, and beryllium form microscopic particles in the metal matrix after suitable heat treatment. Known as *precipitation strengthening* or *hardening*, the mechanism can produce tensile strengths greater than 200,000 psi (1379 MPa) and hardness exceeding Rockwell C 40. High strength levels can also be generated by a combination of mechanisms. Aluminum bronzes and manganese bronzes rely on solution strengthening and secondary-phase strengthening. Some nickel–aluminum bronzes can also undergo a martensitic transformation similar to, but much less potent than, that seen in steels. Manganese bronzes (which are actually brasses as defined above) are capable of attaining 100,000 psi tensile strengths. Nickel and tin, when added together in proper proportions produce, an order–disorder transformation known as spinodal decomposition, which is capable of raising strength nearly to the levels achieved in copper–beryllium

**Table 40** Physical Properties of Selected Wrought Coppers and Copper Alloys

UNS Number	Melting Point, °F, °C	Melting Point, °F, °C	Density lb/in. <sup>3</sup> , 68°F, gm/cm <sup>3</sup> , 20°C	Electrical Resistivity Ω-cmil/ft, 68°F, μΩ-cm, 20°C	Electrical Conductivity* %IACS, 68°F, MS/cm at 20°C	Thermal Conductivity Btu · ft/(h · ft <sup>2</sup> · °F), 68°F, W/m · K at 20°C	Coefficient of Thermal Expansion		Specific Heat Btu/lb/°F, 68°F, J/kg · K, 293 K	Modulus of Elasticity in Tension ksi, MPa	Modulus of Rigidity ksi, MPa	
							(68–212°F) (68–392°F)	(10–6°F) (68–572°F)				
C10100–C10300	1981	1083	0.323	10.3	101	226	9.4	9.6	9.8	0.092	17000	6400
C11000	1981	1083	8.94	1.71	0.591	391.1	16.9	17.3	17.6	393.5	117000	44130
C12200	1981	1083	0.322	12.2	85	196	9.4	9.5	9.8	0.092	17000	6400
C15000	1976	1083	8.91	2.03	0.497	339.2	16.9	17.1	17.6	393.5	117000	44130
C17200	1980	1083	0.321	11.2	93	212.3	9.4	9.8	—	0.092	187000	—
C17500	1982	1083	8.89	1.86	0.544	366.9	16.9	17.6	—	393.5	129000	—
C18100	1975	1083	0.298	46.2	22	62	—	—	9.9	0.1	18500	7300
C19100	1983	1083	8.26	7.68	0.129	107.3	—	—	17.8	419.0	128000	50330
C19200	1980	1083	0.311	22.8	45	120.0	—	9.8	—	0.1	19000	7500
C23000	1980	1083	8.61	3.79	0.263	207.7	9.3	17.6	10.7	419.0	131000	51710
C26000	1980	1083	0.319	13	80	187.0	16.7	18.4	19.3	0.094	182000	125000
C27000	1980	1083	8.83	2.16	0.468	323.6	16.7	—	17.6	393.9	6800	46880
	1980	1083	0.32	15	65	150.0	9	—	—	0.09	17000	6400
	1980	1083	8.86	2.49	0.38	259.6	16.2	—	—	377.1	117000	44130
	1980	1083	0.323	18.9	55	145	—	—	9.8	0.092	16000	6000
	1980	1083	8.94	3.14	0.322	251.0	—	—	17.6	385.5	110000	41370
	1980	1083	0.316	28	37	92.0	—	—	10.4	0.09	17000	6400
	1980	1083	8.75	4.65	0.216	159.2	—	—	18.7	377.1	117000	44130
	1980	1083	0.308	37	28	70.0	—	—	11.1	0.09	16000	6000
	1980	1083	8.53	6.15	0.164	121.2	—	—	20	377.1	110000	41370
	1980	1083	0.306	38.4	27	67.0	—	—	11.3	0.09	15000	5600
	1980	1083	8.47	6.38	0.158	116.0	—	—	20.3	377.1	103400	38610

(continued)

Table 40 (Continued)

UNS Number	Melting Point, °F, °C	Melting Point, °F, °C	Density lb/in. <sup>3</sup> , 68°F, gm/cm <sup>3</sup> , 20°C	Electrical Resistivity Ω-cmil/ft., 68°F, μΩ-cm, 20°C	Electrical Conductivity* %IACS, 68°F MS/cm at 20°C	Thermal Conductivity Btu · ft/(h · ft <sup>2</sup> · °F), 68°F W/m · K at 20°C	Coefficient of Thermal Expansion			Specific Heat Btu/lb/°F, 68°F J/kg · K, 293 K	Modulus of Elasticity in Tension		Modulus of Rigidity of ksi MPa
							Expansion, 10 <sup>-6</sup> /°F (68–212°F) 10 <sup>-6</sup> /°C (20–100°C)	Expansion, 10 <sup>-6</sup> /°F (68–392°F) 10 <sup>-6</sup> /°C (20–200°C)	Expansion, 10 <sup>-6</sup> /°F (68–572°F) 10 <sup>-6</sup> /°C (20–300°C)		ksi MPa	ksi MPa	
C28000	1660	1650	0.303	37.0	28	71.0	—	—	11.6	0.09	15000	5600	
	904	899	8.39	6.15	0.164	122.9	—	—	20.9	377.1	103400	38610	
C36000	1650	1630	0.307	39.9	26	67.0	—	—	11.4	0.09	14000	5300	
	899	888	8.5	6.63	0.152	116.0	—	—	20.5	377.1	96500	36500	
C37700	1640	1620	0.305	39.4	27	69.0	—	—	11.5	0.09	15000	5600	
	893	882	8.44	6.38	0.158	119.4	—	—	20.7	377.1	103400	38610	
C44400	1720	1650	0.308	41.5	25	64.0	—	—	11.2	0.09	16000	6000	
	938	899	8.53	6.9	0.146	110.8	—	—	20.2	377.1	110000	41370	
C46500	1650	1630	0.304	39.9	26	67.0	—	—	11.8	0.09	15000	5600	
	899	888	8.41	6.63	0.152	116.0	—	—	21.2	377.1	103400	38610	
C46500	1650	1630	0.304	39.9	26	67.0	—	—	11.8	0.09	15000	5600	
	899	888	8.41	6.63	0.152	116.0	—	—	21.2	377.1	103400	38610	
C50500	1970	1900	0.321	21.6	48	120.0	—	—	9.9	0.09	17000	17000	
	1077	1038	8.89	3.59	10.281	207.7	—	—	17.8	377.1	117000	16000	
C51100	1945	1785	0.32	52.0	20	48.4	—	—	9.9	0.09	16000	16000	
	1063	974	8.86	8.64	0.117	83.8	—	—	17.87	377.1	110000	110000	
C52100	1880	1620	0.318	79.8	13	36.0	—	—	10.1	0.09	16000	16000	
	1027	882	8.8	13.27	0.076	62.3	—	—	18.2	377.1	110000	110000	
C61300	1915	1905	0.287	86.8	12	32.0	—	—	9	0.09	17000	17000	
	1046	1041	7.95	14.43	0.070	55.4	—	—	16.2	377.1	117000	117000	
C61800	1913	1904	0.272	79.8	13	37.0	—	—	9.0	0.09	17000	17000	
	1045	1040	7.53	13.27	0.076	64.0	—	—	16.2	377.1	117000	117000	
C62400	1900	1880	0.269	86.4	12	34.0	—	—	9.0	0.09	17000	17000	
	1038	1027	7.45	14.36	0.070	58.8	—	—	16.2	377.1	117000	117000	
C63200	1940	1905	0.276	148.0	7	20.0	—	—	9.0	0.09	17000	17000	
	1060	1041	7.64	24.6	0.041	34.6	—	—	16.2	377.1	117000	117000	

C65500	1880	1780	0.308	148.0	7	21.0	—	—	10.0	0.09	15000
	1027	971	8.53	24.6	0.041	36.3	—	—	18.0	377.1	103400
C66700	2000	1920	0.308	61.0	17	56.0	—	—	11.1	0.09	16000
	1093	1049	8.53	10.14	0.099	96.9	—	—	20.0	377.1	110000
C67500	1630	1590	0.302	43.2	24	61.0	—	—	11.8	0.09	15000
	888	866	8.36	7.18	0.14	105.6	—	—	21.2	377.1	103400
C69400	1685	1510	0.296	167.0	6	15.0	—	—	11.2	0.09	16000
	918	821	8.19	27.76	0.036	26.0	—	—	20.2	377.1	110000
C70600	2100	2010	0.323	115.0	9	26.0	—	—	9.5	0.09	18000
	1149	1099	8.94	19.12	0.053	45.0	—	—	17.1	377.1	124000
C71500	2260	2140	0.323	225.0	4	17.0	—	—	9.0	0.09	22000
	1238	1171	8.94	37.4	0.027	29.4	—	—	16.2	377.1	152000
C72200	2148	2052	0.323	159.0	6	19.9	—	—	8.8	0.094	20000
	1176	1122	8.94	26.43	0.038	34.4	—	—	15.8	393.9	138000
C74500	1870	—	0.314	115.0	9	26.0	—	—	9.1	0.09	17500
	1021	—	8.69	19.12	0.053	45.0	—	—	16.4	377.1	121000
C77000	1930	—	0.314	189.0	5	17.0	—	—	9.3	0.09	18000
	1054	—	8.69	31.42	0.032	29.4	—	—	16.7	377.1	124000
C66700	2000	1920	0.308	61.0	17	56.0	—	—	11.1	0.09	16000
	1093	1049	8.53	10.14	0.099	96.9	—	—	20.0	377.1	110000
C67500	1630	1590	0.302	43.2	24	61.0	—	—	11.8	0.09	15000
	888	866	8.36	7.18	0.14	105.6	—	—	21.2	377.1	103400

Table 41 Physical Properties of Selected Cast Copper Alloys

UNS Number	Melting Point, °F, °C	Melting Point, °F, °C	Density lb/in <sup>3</sup> , 68°F; gm/cm <sup>3</sup> , 20°C	Electrical Resistivity Ω-cmil/ft, 68 μΩ-cm, 20°C	Electrical Conductivity* % IACS, 68°F MS/cm, 20°C	Thermal Conductivity Btu · ft/(h · ft <sup>2</sup> · °F), 68°F; W/m · K at 20°C	Coefficient of Thermal Expansion		Specific Heat Btu/lb/°F, 68°F; J/kg · K, 293 K	Modulus of Elasticity in Tension ksi, MPa	Relative Magnetic Permeability	Poisson's Ratio
							(68–392°F) 10 <sup>-6</sup> /°F	(20–200°C) 10 <sup>-6</sup> /°C				
C81100	1981	1948	0.323	11.3	92	200.0	9.4	0.09	17,000	1.0		
	1083	1064	8.94	1.87	0.538	346.1	16.9	377.1	1,17,000			
C81400	2000	1950	0.318	17.3	60	150.0	10.0	0.093	16,000			
	1093	1066	8.81	2.87	0.348	259.0	18.0	389.7	1,10,000			
82000	1990	1780	0.311 <sup>a</sup>	23.1	45	150.0	9.9	0.1	17,000	1.001	0.33	
	1088	971	8.61	3.85	0.263	259.6	17.8	419.0	1,17,000			
C82500	1800	1575	0.297 <sup>b</sup>	51.6	20	74.9	9.4	0.1	18,500	1.002	0.3	
	982	857	8.09	8.62	0.116	129.8	16.9	419.0	1,28,000			
C83300	1940	1886	0.318	32.3	32			0.09	15,000			
	1060	1030	8.8	5.38	0.187			377.1	10,340			
C83450	1860	1580	0.319		20							
	1015	860	8.83		0.115							
C83600	1850	1570	0.318	69.1	15	41.6	10.0	0.09	13,500	1.0		
	1010	854	8.83	11.49	0.087	72.0	18.0	377.1	93,100			
C83800	1840	1550	0.312	69.1	15	41.8	10.0	0.09	13,300	1.0		
	1004	843	8.64	11.49	0.087	72.4	18.0	377.1	91,700			
C84400	1840	1549	0.314	63.3	16	41.8	10.0 <sup>c</sup>	0.09	13,000	1.0		
	1004	843	8.69	10.53	0.095	72.4		377.1	89,600			
C85200	1725	1700	0.307	57.8	18	48.5	11.5	0.09	11,000			
	941	927	8.5	9.62	0.104	83.9	20.7 <sup>d</sup>	377.1	75,800			
C85400	1725	1700	0.305	53.2	20	50.8	11.1	0.09	12,000	1.0		
	941	927	8.44	8.85	0.113	87.9	20.2 <sup>d</sup>	377.1	82,700			
C85700	1725	1675	0.304	47	22	48.5		0.09	14,000	1.0		
	941	913	8.41	7.81	0.128	83.9		377.1	87,000			
C86200	1725	1650	0.288	136.7	8	20.5	12.0	0.09	15,000	1.24 <sup>e</sup>		
	941	899	7.97	22.73	0.044	35.5		377.1	1,03,400			
C86300	1693	1625	0.283	130.8	8	20.5	12	0.09	14,200	1.09 <sup>e</sup>		
	923	885	7.83	21.74	0.044	35.5	21.6	377.1	97,900			
C86400	1616	1583	0.301	54.2	19	51	11.0 <sup>c</sup>	0.09	14,000			
	880	862	8.33	9.01	0.111	88.3	19.8	377.1	87,000			
C86500	1616	1583	0.301	47.0	22	49.6	11.3 <sup>d</sup>	0.09	15,000	1.09 <sup>e</sup>		
	880	862	8.33	7.81	0.128	85.8	20.3	377.1	1,03,400			

C87300	1780	1510	0.302				6	16.4			11.0	16,000
	971	821	8.36				0.035	28.4			19.8	1,10,000
C89510	1871	1500	0.313									
	1021	815	8.66									
C89520	1842	353										
	1005	196										
C89550	1638	1588										
	892	864										
C87500	1680	1510	0.299	154.2	6	16.0	6	16.0		10.9	0.09	15,400
	916	821	8.28	25.64	0.039	27.7	0.039	27.7		19.6	377.1	1,06,000
C90300	1832	1570	0.318	87.2	12	43.2	12	43.2	10.0		0.09	14,000
	1000	854	8.8	14.49	0.069	74.8	0.069	74.8	18.0		377.1	87,000
C90500	1830	1570	0.315	94.0	11	43.2	11	43.2	11.0		0.09	15,000
	999	854	8.72	15.63	0.064	74.8	0.064	74.8	19.8		377.1	1,03,400
C90700	1830	1528	0.317	107.4	10	40.8	10	40.8	10.2		0.09	15,000
	999	831	8.77	17.86	0.056	70.6	0.056	70.6	18.4		377.1	1,03,400
C91100	1742	1505		122.8	8		8				0.09	15,000
	950	818		20.41	0.049		0.049				377.1	1,03,400
C91300	1632	1505		150.4	7		7				0.09	16,000
	889	818		25.0	0.04		0.04				377.1	1,10,000
C91600	1887	1575	0.32	103.7	10	40.8	10	40.8	9.0		0.09	16,000
	1031	857	8.86	17.24	0.058	70.6	0.058	70.6	16.2		377.1	1,10,000
C92200	1810	1518	0.312	72.5	14	40.2	14	40.2	10.0		0.09	14,000
	988	826	8.64	12.0	0.083	69.6	0.083	69.6	18.0		377.1	87,000
C92300	1830	1570	0.317	85.9	12	43.2	12	43.2	10.0		0.09	14,000
	999	854	8.77	14.29	0.069	74.8	0.069	74.8	18.0		377.1	87,000
C92600	1800	1550	0.315	115.7	9		9				0.09	15,000
	982	843	8.72	19.23	0.052		0.052				377.1	1,03,400
C92900	1887	1575	0.32	113.5	9	33.6	9	33.6	9.5		0.09	14,000
	1031	857	8.86	18.87	0.052	58.2	0.052	58.2	17.1		377.1	87,000
C93200	1790	1570	0.332	85.9	12	33.6	12	33.6	10.0 <sup>d</sup>		0.09	14,500
	977	854	8.91	14.29	0.07	58.2	0.07	58.2	18.0		377.1	1,00,000
C93700	1705	1403	0.32	102	10	27.1	10	27.1	10.3		0.09	11,000
	929	762	8.86	16.95	0.059	46.9	0.059	46.9	18.5		377.1	75,800
C93800	1730	1570	0.334	91.1	11	30.2	11	30.2	10.3		0.09	10,500
	943	854	9.25	15.15	0.066	52.3	0.066	52.3	18.5		377.1	72,400
C95200	1913	1907	0.276	94	11	29.1	11	29.1		9.0	0.09	15,000
	1045	1042	7.64	15.63	0.066	50.4	0.066	50.4		16.2	377.1	1,03,400
C95300	1913	1904	0.272	80.2	13	36.3	13	36.3		9.0	0.09	16,000
	1045	1040	7.53	13.33	0.075	62.8	0.075	62.8		16.2	377.1	1,10,000

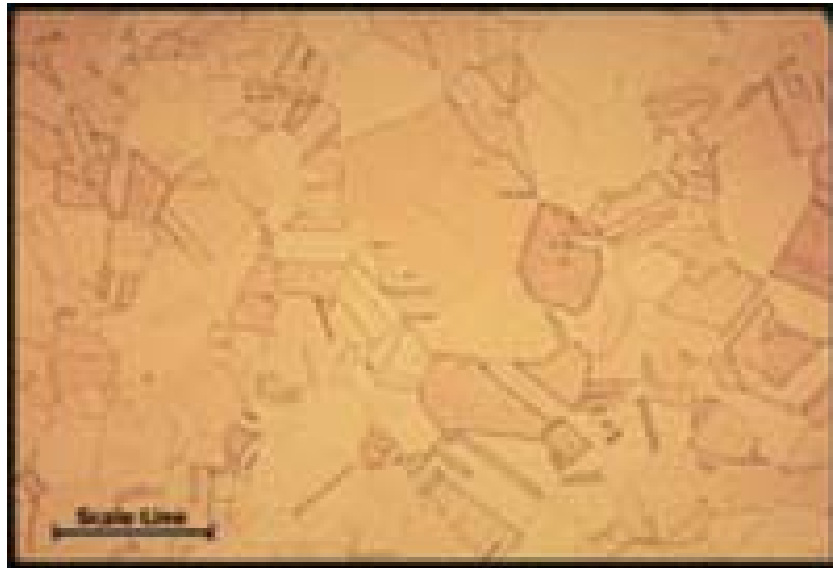
(continued)

Table 41  
(Continued)

UNS Number	Melting Point, °F, °C	Melting Point, °F, °C	Density lb/in <sup>3</sup> , 68°F, gm/cm <sup>3</sup> , 20°C	Electrical Resistivity Ω-cmil/ft, 68°F, 68 μΩ-cm, 20°C	Electrical Conductivity* % IACS, 68°F MS/cm, 20°C	Thermal Conductivity Btu · ft/(h · ft <sup>2</sup> · °F), 68°F, W/m · K at 20°C	Coefficient of Thermal Expansion, 10 <sup>-6</sup> /°F (68-392°F), 10 <sup>-6</sup> /°C (20-200°C)	Coefficient of Thermal Expansion, 10 <sup>-6</sup> /°F (68-572°F), 10 <sup>-6</sup> /°C (20-300°C)	Specific Heat Btu/lb/°F, 68°F, J/kg · K, 293 K	Modulus of Elasticity in Tension ksi, MPa	Relative Magnetic Permeability	Poisson's Ratio
	C95400	1900	1880	0.269	80.2	13	33.9	9.0	9.0	0.09	15,500	1.27 <sup>f</sup>
	1038	1027	7.45	13.33	0.075	58.7	16.2	16.2	377.1	1,07,000		
C95410	1900	1880	0.269	80.2	13	33.9	9.0	9.0	0.10	15,500		
	1038	1027	7.45	13.33	0.075	58.7	16.2	16.2	419.0	1,07,000		
C95500	1930	1900	0.373	122.8	8	24.2	9.0	9.0	0.10	16,000	1.32 <sup>f</sup>	0.32
	1054	1038	7.53	20.41	0.049	41.9	16.2	16.2	419.0	1,10,000	1.2 <sup>g</sup>	
C95800	1940	1910	0.276	146.7	7	20.8	9.0	9.0	0.105	16,500	1.05 <sup>f</sup>	0.32
	1060	1043	7.64	24.39	0.041	36.0	16.2	16.2	440.0	1,14,000		
C96400	2260	2140	0.323	214.8	5	16.4	9.0	9.0	0.09	21,000		
	1238	1171	8.94	35.71	0.028	28.5	16.2	16.2	377.1	1,45,000		
C97300	1904	1850	0.321	182.3	6	16.5	9.0	9.0	0.09	16,000		
	1040	1010	8.89	30.3	0.033	28.6	16.2	16.2	377.1	1,10,000		
C97400	2012	1958	0.32	188	6	15.8	9.2	9.2	0.09	16,000		
	1100	1070	8.86	31.25	0.032	27.3	16.6	16.6	377.1	1,10,000		
C97600	2089	2027	0.321	207.4	5	13.0	9.3	9.3	0.09	19,000		
	1143	1108	8.89	34.48	0.029	22.6	16.7	16.7	377.1	1,31,000		
C97800	2089	2027	0.321	207.4	5	13.0	9.3	9.3	0.09	19,000		
	1143	1108	8.89	34.48	0.029	22.6	16.7	16.7	377.1	1,31,000		
C99400			0.3	85.9	16					19,300		
			8.3	14.29	0.098					1,33,000		
C99500			0.3	71.0	10					19,000		
			8.3	11.64	0.057					1,31,000		
C99700	1655	1615	0.296	353.8	3					16,500		
	902	879	8.19	58.82	58.82					1,14,000		
C99750	1550	1505	0.29	501.3	2					17,000		
	843	818	8.03	83.3	0.012					1,17,000		

<sup>a</sup>TFOO condition.<sup>b</sup>Change in density upon aging=0.6%.<sup>c</sup>At 20°C, 68°F.<sup>d</sup>20-100°C, 68-212°F<sup>e</sup>Field strength 16 kA/m (200 Oe).<sup>f</sup>As cast, field strength 16 kA/m (200 Oe).<sup>g</sup>TQ50 temper, field strength 16 kA/m (200 Oe).





**Figure 1** Microstructure of pure copper. Courtesy of The Copper Development Association, Inc.

alloys while retaining relatively good electrical conductivity. The high-performance copper alloys are generally used in demanding applications such as high-strength bolts, special-purpose electrical connectors, and terminals, particularly those destined for elevated temperature service or which require high “burn-in” resistance. These requirements are often combined with the need for good formability, corrosion resistance, and an appropriate level of electrical conductivity.

Finally, there are the copper–metal matrix materials (CMMs) such as C15715–C15760, which are actually composites rather than alloys. They attain quite high strength levels along with very strong softening resistance at elevated temperatures due to the presence of a dispersion of ultrafine aluminum oxide particles. Because it does not alloy with copper, the alumina has a weak effect on electrical conductivity. MMCs are most commonly specified for high-performance electrical connectors and resistance welding electrodes and wheels. Electrodes made from the composites meet the Resistance Welding Manufacturers’ Association (RWMA) Class III standards.

### 3.2 Temper

“Temper” is the term that describes a metal’s processing history. It is commonly applied to coppers and copper alloys and is more semiquantitative than technically precise in terms of mechanical properties. Metals are said to have a hard temper if they have been cold worked, heat treated, or both, and in one of the softer tempers when they are in an as-cast, as-hot-wrought, as-cast or annealed state. When specifying copper alloys for a particular application, it is only necessary to call out the UNS designation, the product form and size (wire, rod, sheet, etc.), and a temper. Tempers are defined in ASTM Standard Practice B 601, *Temper Designations for Copper and Copper Alloys—Wrought and Cast*, an extract from which is shown in Table 42.<sup>7</sup>

**Table 42** Standard Temper Designations for Copper-Based Alloys (Based on ASTM B 601)

<b>Annealed Tempers—O</b>	<b>Temper Names</b>	<b>Cold-Worked Tempers Based on Particular Products (Wire)—H</b>	<b>Temper Names</b>
O10	Cast & Annealed	H50	
O11	As Cast & Precipitation Heat Treated	H52	
O25	Hot Rolled & Annealed	H58	
O30	Hot Extruded & Annealed	H60	Cold Heading, Forming
O31	Hot Extruded & Annealed	H63	Rivet
O32	Extruded & Precipitation Heat Treated	H64	Screw
O30	Light Anneal	H66	Bolt
O50	Soft Anneal	H70	Bending
O60	Annealed (Also Mill Annealed)	H80	Hard Drawn
O61	Soft Anneal	H85	Medium-Hard Drawn Electrical Wire
O65	Annealed		
O68	Drawing Anneal	H86	Hard-Hard Drawn Electrical Wire
O70	Dead Soft Annealed		
O80	Annealed to Temper, 1/8 Hard	H90	As Finned
O81	Annealed to Temper, 1/4 Hard		
O82	Annealed to Temper, 1/2 Hard		
<b>Annealed Tempers With Grain Size Prescribed—OS</b>	<b>Nominal Average Grain Size, mm</b>	<b>Cold Worked and Stress Relieved—HR</b>	<b>Temper Names</b>
OS005	0.005	HR01	1/4 Hard and Stress Relieved
OS010	0.010	HR02	1/2 Hard and Stress Relieved
OS015	0.015	HR04	Hard & Stress Relieved
OS020	0.020	HR08	Spring & Stress Relieved
OS025	0.025	HR10	Extra Spring & Stress Relieved
OS035	0.035	HR12	Special Spring & Stress Relieved
OS050	0.050	HR20	As Finned
OS060	0.060		
OS070	0.070	<b>Cold Rolled &amp; Order Strengthened</b>	<b>Temper Names</b>
OS100	0.100	HT04	Hard Temper & Treated
OS120	0.120	HT08	Spring Temper & Treated
OS150	0.150		
OS200	0.200	<b>Hard Drawn End Annealed</b>	<b>Temper Names</b>
		HE80	Hard Drawn & End Annealed
<b>Cold-Worked Tempers Based on Cold Rolling or Drawing—H</b>	<b>Temper Names</b>	<b>Cold-Worked Tempers With Added Treatments—HR</b>	<b>Temper Names</b>
H00	1/8 Hard	HR50	Drawn & Stress Relieved
H01	1/4 Hard		
H02	1/2 Hard	<b>As-Manufactured Tempers—M</b>	<b>Temper Names</b>
H03	3/4 Hard	M01	As Sand Cast
H04	Hard	M02	As Centrifugal Cast
H06	Extra Hard	M03	As Plaster Cast
H08	Spring	M05	As Pressure Die Cast
H10	Extra Spring	M06	As Permanent Mold Cast
H12	Special Spring	M07	As Investment Cast
H13	Ultra Spring	M10	As Hot Forged, Air Cooled
H14	Super Spring	M11	As Hot Forged, Quenched
		M20	As Hot Rolled
		M25	As Hot Rolled & Re-Rolled
		M30	As Extruded
		M40	As Hot Pierced
		M45	As Hot Pierced & Re-Rolled

Table 42 (Continued)

<b>Heat-Treated Tempers, T; Quench Hardened, TQ</b>	<b>Temper Names</b>	<b>Cold-Worked Tempers &amp; Spinodal Heat Treated to Meet Standard Requirements Based on Cold Rolling or Cold Drawing—TS</b>	<b>Temper Names</b>
TQ00	Quench Hardened	TS00	1/8 Hard & Spinodal Hardened (1/8TS)
TQ30	Quench Hardened Tempered	TS01	1/4 Hard & Spinodal Hardened (1/4TS)
TQ50	Quench Hardened Temper Annealed	TS02	1/4 Hard & Spinodal Hardened (1/4TS)
TQ55	Quench Hardened Temper Annealed, Cold Drawn and Stress Relieved	TS03	3/4 Hard & Spinodal Hardened (3/4TS)
TQ75	Interrupted Quench	TS04	Hard & Spinodal Hardened
<b>Solution Heat Treated—TB</b>	<b>Temper Names</b>	TS06	Extra Hard & Spinodal Hardened
TB00	Solution Heat Treated (A)	TS08	Spring & Spinodal Hardened
<b>Solution Treated &amp; Cold Worked—TD</b>	<b>Temper Names</b>	TS10	Extra Spring & Spinodal Hardened
TD00	Solution Treated & Cold Worked: 1/8 Hard	TS12	Special Spring & Spinodal Hardened
TD01	Solution Treated & Cold Worked: 1/4 Hard	TS13	Special Spring & Spinodal Hardened
TD02	Solution Treated & Cold Worked: 1/2 Hard	TS14	Ultra Spring & Spinodal Hardened
TD03	Solution Treated & Cold Worked: 3/4 Hard		
TD04	Solution Treated & Cold Worked: Hard (H)	<b>Mill Hardened Tempers—TM</b>	<b>Manufacturing Designation</b>
<b>Solution Heat Treated &amp; Precipitation Heat Treated—TF</b>	<b>Temper Names</b>	TM00	AM
TF00	Precipitation Hardened (AT)	TM01	1/4 HM
TF01	Precipitation Heat-Treated Plate—Low Hardness (ATLH)	TM02	1/2 HM
TF02	Precipitation Heat-Treated Plate—High Hardness (ATHH)	TM04	HM
		TM06	XHM
		TM08	XHMS
<b>Solution Heat Treated &amp; Spinodal Heat Treated—TX</b>	<b>Temper Names</b>	<b>Precipitation Heat Treated or Spinodal Heat Treated and Cold Worked—TL</b>	<b>Temper Names</b>
TX00	Spinodal Hardened	TL00	Precipitation Heat Treated or Spinodal Heat Treated & 1/8 Hard
<b>Solution Heat Treated, Cold Worked, &amp; Precipitation Heat Treated—TH</b>	<b>Temper Names</b>	TL01	Precipitation Heat Treated or Spinodal Heat Treated & 1/4 Hard
TH01	1/4 Hard and Precipitation Heat Treated (1/4 HT)	TL02	Precipitation Heat Treated or Spinodal Heat Treated & 1/2 Hard
TH02	1/2 Hard and Precipitation Heat Treated (1/2 HT)	TL04	Precipitation Heat Treated or Spinodal Heat Treated & Hard
TH03	3/4 Hard and Precipitation Heat Treated (3/4 HT)	T008	Precipitation Heat Treated or Spinodal Heat Treated & Spring
TH04	Hard and Precipitation Heat Treated (HT)	TL10	Precipitation Heat Treated or Spinodal Heat Treated & Extra Spring

Table 42 (Continued)

<b>Precipitation Heat Treated or Spinodal Heat Treated, Cold Worked, &amp; Stress Relief Annealed—TR</b>	<b>Temper Names</b>	<b>Welded Tube and Annealed—WO</b>	<b>Temper Names</b>
TR01	Precipitation Heat Treated or Spinodal Heat Treated, $\frac{1}{4}$ Hard & Stress Relieved	WO50 WO60 WO61	Welded and Light Annealed Welded and Soft Annealed Welded and Annealed
TR02	Precipitation Heat Treated or Spinodal Heat Treated, $\frac{1}{2}$ Hard & Stress Relieved	<b>Welded Tube and Light Cold Worked—WH</b> WH55	<b>Temper Names</b> Welded and Light Cold Worked
TR04	Precipitation Heat Treated or Spinodal Heat Treated, Hard & Stress Relieved	<b>Welded Tube and Cold Drawn—WH</b> WH00 WH01 WH02 WH03 WH04 WH06 WH55	<b>Temper Names</b> Welded & Drawn: $\frac{1}{8}$ Hard Welded & Drawn: $\frac{1}{4}$ Hard Welded & Drawn: $\frac{1}{2}$ Hard Welded & Drawn: $\frac{3}{4}$ Hard Welded & Drawn: Hard Welded & Drawn: Extra Hard Welded & Cold Reduced or Light Drawn
<b>Tempers of Welded Tube—W; As Welded—WM</b>	<b>Temper Names</b>	WH58 WH80	Welded & Drawn, General Purpose Welded & Reduced or Hard Drawn
WM50	As Welded from Annealed Strip	<b>Welded Tube, Cold Drawn, &amp; Stress Relieved—WR</b> WR00	<b>Temper Names</b> Welded, Drawn, & Stress Relieved from: $\frac{1}{8}$ Hard
WM00	As Welded from Annealed $\frac{1}{8}$ Hard Strip	WR01	Welded, Drawn, & Stress Relieved from: $\frac{1}{4}$ Hard
WM01	As Welded from Annealed $\frac{1}{4}$ Hard Strip	WR02	Welded, Drawn, & Stress Relieved from: $\frac{1}{2}$ Hard
WM02	As Welded from Annealed $\frac{1}{2}$ Hard Strip	WR03	Welded, Drawn, & Stress Relieved from: $\frac{3}{4}$ Hard
WM03	As Welded from Annealed $\frac{3}{4}$ Hard Strip	WR04	Welded, Drawn, & Stress Relieved from: $\frac{1}{8}$ Hard
WM04	As Welded from Annealed Hard Strip	WR06	Welded, Drawn, & Stress Relieved from: Extra Hard
WM06	As Welded from Annealed Extra Hard Strip		
WM08	As Welded from Annealed Spring Strip		
WM10	As Welded from Annealed Extra Spring Strip		
WM15	As Welded from Annealed Strip, Thermal Stress Relieved		
WM20	As Welded from $\frac{1}{8}$ Hard Strip, Thermal Stress Relieved		
WM21	As Welded from $\frac{1}{4}$ Hard Strip, Thermal Stress Relieved		
WM22	As Welded from $\frac{1}{2}$ Hard Strip, Thermal Stress Relieved		

Note that higher strength and hardness are usually gained at the cost of reduced ductility and, especially in the case of alloys, somewhat reduced electrical and thermal conductivity. A broad range of tempers are available to permit selection of the most appropriate combination of properties.

### 3.3 Mechanical Properties Data

Mechanical properties of selected wrought and cast coppers and copper alloys are listed in Tables 43 and 44, respectively. Note that the tables identify typical and/or minimum properties.

**Table 43** Mechanical Properties of Selected Wrought Copper Alloys

Temper	Section Size in. mm.	Cold Work %	Temp Typ/ Min C	Tensile Strength ksi MPa	Yield Strength (0.5% ext. under load) ksi MPa	Yield Strength (0.2% offset) ksi MPa	Yield Strength (0.05% offset) ksi MPa	Rockwell Hardness			Vickers Hard.		Brinell Hard.		Shear Strength ksi MPa	Fatigue Strength <sup>a</sup> ksi MPa	Izod Impact Strength ft-lb J	
								EI	B	C	F	30T	500	500				3000
<b>C10100—C10300</b> —Automotive Rectifiers, Conductors, Glass-to-Metal Seals, High-Resistance-Ratio Cryogenic Shunts, Bus Bars, Lead-in Wire, Vacuum Seals, Transistor Component Bases, Bus Conductors, Wave Guides, Hollow Conductors, Anodes for Vacuum Tubes, Coaxial Cable, Coaxial Tube, Klystrons, Microwave Tubes																		
<b>Rod</b>																		
H04	2	16	TYP	68	45	40	—	—	20	45	—	85	—	—	—	—	26	—
	51			20	310	276	—	—	20	45	—	85	—	—	—	—	179	—
M20	1	0	TYP	68	32	10	—	—	55	—	—	40	—	—	—	—	22	—
	25.4			20	221	69	—	—	55	—	—	40	—	—	—	—	152	—
<b>Tube</b>																		
H55	0.065	0	TYP	68	40	32	—	—	25	35	—	77	45	—	—	—	26	—
	1.65			20	276	221	—	—	25	35	—	77	45	—	—	—	179	—
H80	0.065	0	TYP	68	55	50	—	—	8	60	—	95	63	—	—	—	29	—
	1.65			20	379	345	—	—	8	60	—	95	63	—	—	—	200	—
<b>Wire</b>																		
H04	—8	0	TYP	68	55	—	—	—	1	—	—	—	—	—	—	—	29	—
	2			20	379	—	—	—	1	—	—	—	—	—	—	—	200	—
H08	—8	0	TYP	68	66	—	—	—	1	—	—	—	—	—	—	—	33	—
	2			20	455	—	—	—	1	—	—	—	—	—	—	—	228	—
<b>Shapes</b>																		
H04	0.5	15	TYP	68	40	32	—	—	30	35	—	—	—	—	—	—	26	—
	12.7			20	276	221	—	—	30	35	—	—	—	—	—	—	179	—
<b>Flat Products</b>																		
H00	0.25	0	TYP	68	36	28	—	—	40	10	—	60	—	—	—	—	25	—
	6.35			20	248	193	—	—	40	10	—	60	—	—	—	—	172	—
H04	1	0	TYP	68	45	40	—	—	20	45	—	85	—	—	—	—	26	—
	25.4			20	310	276	—	—	20	45	—	85	—	—	—	—	179	—

(continued)

Table 43 (Continued)

Temper	Section Size in.	Cold Work %	Temp Typ/Min	Temp F/C	Tensile Strength ksi/MPa	Yield Strength (0.5% ext. under load)		Elongation %	Rockwell Hardness			Vickers Hard.	Brinell Hard.	Shear Strength ksi/MPa	Fatigue Strength <sup>a</sup> ksi/MPa	Izod Impact Strength ft-lb/J
						ksi	MPa		B	C	F					
<b>C11000</b> —Conductors, Electrical, Terminal Connectors, Bus Bars, Magnet Wire, Stranded Conductors, Wire, Electrical, Terminals, Switches, Radio Parts, Contacts, Trolley Wire, Gaskets, Radiators, Downspouts, Flashing, Roofing, Gutters, Building Fronts, Skylight Frames, Spouting, Ball Floats, Butts, Rivets, Nails, Cotter Pins, Soldering Copper, Tacks, Wire Screening, Fasteners, Heat Exchangers, Pans, Vats, Road Bed Expansion Plates, Rotating Bands, Kettles, Chimney Cap Screens, Chlorine Cells, Pressure Vessels, Anodes, Chemical Process Equipment, Printing Rolls																
<b>Rod</b>																
H04	0.25	40	TYP	68	55	50	—	—	10	60	—	—	—	—	—	—
	6.35			20	379	345	—	—	10	60	—	—	—	—	—	—
M20	1	0	TYP	68	32	10	—	—	55	—	—	—	—	—	—	—
	25.4			20	221	69	—	—	55	—	—	—	—	—	—	—
<b>Tube</b>																
H80	0.065	40	TYP	68	55	50	—	—	8	60	—	—	—	—	—	—
	1.65			20	379	345	—	—	8	60	—	—	—	—	—	—
<b>Wire</b>																
H04	0.08	0	TYP	68	55	—	—	—	1	—	—	—	—	—	—	—
	2			20	379	—	—	—	1	—	—	—	—	—	—	—
OS050	0.08	0	TYP	68	35	—	—	—	35	—	—	—	—	—	—	—
	2			20	241	—	—	—	35	—	—	—	—	—	—	—
<b>Shapes</b>																
H04	0.5	15	TYP	68	40	32	—	—	30	35	—	—	—	—	—	—
	12.7			20	276	221	—	—	30	35	—	—	—	—	—	—
<b>C12200</b> —Gutters, Downspouts, Flashing, Roofing, Air Lines, Hydraulic Lines, Oil Lines, Air Conditioner Tubes and Condenser Sheets, Gas Lines, Heater Units, Heater Lines, Oil Burner Tubes, Air Conditioners, Refrigerators, Heater Elements, Wire Connectors, Tubing, LP Gas Service, Tubing, Medical Gas—Oxygen, Steam Lines, Paper Lines, Pulp Lines, Distiller Tubes, Dairy Tubes, Heat Exchanger Tubes, Evaporator Tubes, Condenser Tubes, Brewery Tubes, Oil Lines in Airplanes, Hydraulic Lines in Airplanes, Gasoline Lines in Airplanes, Air Lines in Airplanes, Oil Coolers in Airplanes, Tanks, Water Lines, Plating Hangers, Plating Anodes, Sugar House Refinery Lines, Print Rolls, Paper Rolls, Expansion Joint Tubes, Heat Exchanger Shells, Anodes for Electroplating, Kettles, Rotating Bands, Gage Lines, Casting Molds, Plating Anodes, Plating Racks, Plumbing Tube, Oil Coolers, Gasoline Lines, Plumbing Fittings, Plumbing Pipe																
<b>Pipe</b>																
H04	—	30	TYP	68	50	45	—	—	10	50	—	—	—	—	—	—
	—			20	345	310	—	—	10	50	—	—	—	—	—	—





Table 43 (Continued)

Temper	Section Size in. mm.	Cold Work %	Temp Typ/Min C	Tensile Strength ksi MPa	Yield Strength (0.5% ext. under load) ksi MPa	Yield Strength (0.2% offset) ksi MPa	Yield Strength (0.05% offset) ksi MPa	Rockwell Hardness			Vickers Hard.			Shear Strength ksi MPa	Fatigue Strength <sup>a</sup> ksi MPa	Izod Impact Strength ft-lb J
								El %	B	C	F	30T	500			
<b>C17500</b> —Fuse Clips, Switch Parts, Relay Parts, Conductors, Connectors, Fasteners, Resistance Welding Equipment, Seam Welding Dies, Resistance and Spot Welding Tips, Springs, Die Casting Plunger Tips, Tooling for Plastic Molds, Stressed Parts																
<b>Rod</b>																
TB00	0.0	0	TYP	68	45	25	—	—	28	35	—	—	—	—	—	—
	0.0			20	310	172	—	—	28	35	—	—	—	—	—	—
TF00	0.0	0	TYP	68	110	90	—	—	18	96	—	—	—	—	40	—
	0.0			20	758	621	—	—	18	96	—	—	—	—	276	—
TH04	0.0	0	TYP	68	115	110	—	—	14	98	—	—	—	—	40	—
	0.0			20	793	758	—	—	14	98	—	—	—	—	276	—
<b>Forgings</b>																
TB00	0.0	0	TYP	68	42	—	20	—	—	50	—	—	—	—	—	—
	0.0			20	293	—	138	—	—	50	—	—	—	—	—	—
TF00	4	0	TYP	68	115	—	90	—	—	92	—	—	—	—	—	—
	102			20	794	—	620	—	—	92	—	—	—	—	—	—
TB00	0.0	0	TYP	68	42	—	20	—	—	50	—	—	—	—	—	—
	0.0			20	293	—	138	—	—	50	—	—	—	—	—	—
TF00	4	0	TYP	68	115	—	90	—	—	92	—	—	—	—	—	—
	102			20	794	—	620	—	—	92	—	—	—	—	—	—
<b>Flat Products</b>																
TB00	0.0	0	TYP	68	45	25	—	—	28	32	—	—	—	—	—	—
	0.0			20	310	172	—	—	28	32	—	—	—	—	—	—
TD02	0.0	0	TYP	68	68	60	—	—	8	70	—	—	—	—	—	—
	0.0			20	469	414	—	—	8	70	—	—	—	—	—	—
TD04	0.0	0	TYP	68	78	70	—	—	5	83	—	—	—	—	—	—
	0.0			20	538	483	—	—	5	83	—	—	—	—	—	—
TF00	0.0	0	TYP	68	110	90	—	—	12	96	—	—	—	—	—	—
	0.0			20	758	621	—	—	12	96	—	—	—	—	—	—
TH02	0.0	0	TYP	68	115	108	—	—	8	98	—	—	—	—	35	—
	0.0			20	793	745	—	—	8	98	—	—	—	—	241	—
TH04	0.0	0	TYP	68	115	110	—	—	8	98	—	—	—	—	—	—
	0.0			20	793	758	—	—	8	98	—	—	—	—	—	—

**C17500**—Fuse Clips, Switch Parts, Relay Parts, Conductors, Connectors, Fasteners, Resistance Welding Equipment, Seam Welding Dies, Resistance and Spot Welding Tips, Springs, Die Casting Plunger Tips, Tooling for Plastic Molds, Stressed Parts

**C18100**—Switches, Circuit Breakers, High-Temperature Wire, Contacts, Heat Sinks, Resistance Welding Wheels, Resistance Welding Tips, Semiconductor Bases, Resistance Welding Equipment, Fasteners, Fusion Energy Targets, Solar Collectors, Continuous Casting Molds, Stressed Parts

Wire													
H04	0.8	90	TYP	68	158	—	141	—	17	—	—	—	—
	20.3			20	1089	—	972	—	17	—	—	—	—
H04	9.16	60	TYP	68	75	—	68	—	11	80	—	—	—
	233			20	517	—	469	—	11	80	—	—	—

**Flat Products**

H04	0.04	40	TYP	68	139	—	128	—	16	—	—	—	—
	1			20	958	—	882	—	16	—	—	—	—

**C19100**—Connectors, Components, Bolts, Turn Buckle Barrels, Nuts, Forgings, Screw Machine Parts, Bushings, Tie Rods, Gears, Pinions, Welding Torch Tips, Hardware

Rod													
HR01	1	0	TYP	68	78	68	70	—	27	84	—	—	41
	25.4			20	538	469	483	—	27	84	—	—	283
HR01	0.125	75	TYP	68	104	77	92	—	6	95	—	—	56
	3.18			20	717	531	634	—	6	95	—	—	386
TH04	0.500	—			80	70	73	—	15	85	—	—	33
	12.7				552	483	503	—			—	—	228

**C19200**—Hydraulic Brake Lines, Gift Hollow Ware, Terminals, Circuit Breaker Parts, Fuse Clips, Cable Wrap, Contact Springs, Lead Frames, Connectors, Eyelets, Flexible Hose, Heat Exchanger Tubing, Gaskets, Air Conditioning Tubing

Tube													
H80	—	40	TYP	68	56	52	52	—	7	—	—	—	—
				20	386	359	359	—	7	—	—	—	—
<b>Flat Products</b>													
O60	0.0	0	TYP	68	45	—	20	—	25	38	—	—	—
	0.0			20	310	—	138	—	25	38	—	—	—
H08	0.04	0	TYP	68	74	—	71	—	2	76	—	—	—
	1			20	510	—	490	—	2	76	—	—	—

(continued)

Table 43 (Continued)

Temper	Section Size in.	Cold Work %	Temp Typ/Min	Temp F	Tensile Strength ksi	Yield Strength (0.5% ext. under load) ksi	Yield Strength (0.2% offset) ksi	Yield Strength (0.05% offset) ksi	Rockwell Hardness			Vickens Hard.		Shear Strength ksi	Fatigue Strength <sup>a</sup> ksi	Izod Impact Strength ft-lb	
									B	C	F	30T	500				3000
<b>C23000</b> —Weather Strip, Etching Parts, Trim, Kick Plates, Fire Extinguisher Cases, Costume Jewelry, Zippers, Medallions, Plaques, Tokens, Coinage, Rouge Boxes, Lipstick Containers, Dials, Compacts, Badges, Nameplates, Rotor Bars, AC Motors, Sockets, Conduit, Screw Shells, AC Motors, Sockets, Conduit, Screw Shells, Rotor Bars, AC Motors, Sockets, Conduit, Screw Shells, Pump Cylinder Liners, Heat Exchanger Shells, Flexible Metal Hose, Fire Extinguishers, Pickling Crates, Tags, Radiator Cores, Condenser Tubes, Tubing for Heat Exchangers, Tubing for Instrumentation, Heat Exchangers, Fire Hose Couplings, Pipe Nipples, Pipe, Pump Lines, J-Bends, Pipe Service Lines, Traps, Fittings, Service Lines																	
<b>Pipe</b>																	
OS015	0.0	0	TYP	68	44	18	—	—	45	—	71	—	—	—	—	—	—
	0.0			20	303	124	—	—	45	—	71	—	—	—	—	—	—
<b>Tube</b>																	
OS050	0.065	0	TYP	68	40	12	—	—	55	—	60	15	—	—	—	—	—
	1.65			20	276	83	—	—	55	—	60	15	—	—	—	—	—
H80	0.065	35	TYP	68	70	58	—	—	8	77	—	68	—	—	—	—	—
	1.65			20	483	400	—	—	8	77	—	68	—	—	—	—	—
<b>Wire</b>																	
H00	0.08	0	TYP	68	50	—	—	—	25	—	—	—	—	—	35	20	—
	2			20	345	—	—	—	25	—	—	—	—	—	241	138	—
H08	0.08	0	TYP	68	105	—	—	—	—	—	—	—	—	—	54	—	—
	2			20	724	—	—	—	—	—	—	—	—	—	372	—	—
<b>Flat Products</b>																	
OS015	0.04	0	TYP	68	45	18	—	—	42	—	71	38	—	—	33	—	—
	1			20	310	124	—	—	42	—	71	38	—	—	228	—	—
H08	0.04	0	TYP	68	84	63	—	—	3	86	—	74	—	—	46	—	—
	1			20	579	434	—	—	3	86	—	74	—	—	317	—	—

**C26000**—Grillwork, Radiator Tube, Radiator Tanks, Odometer Contacts, Electrical Connectors, Tanks, Radiator Cores, Thermostats, Heater Cores, Door Knobs, Locks, Push Plates, Kick Plates, Decorative Hardware, Hinges, Finish Hardware, Shells—Electrical Sockets, Syringe Parts, Chain Links, Planers, Etched Articles, Bird Cages, Buttons, Snaps, Fireplace Screens, Coinage, Pen/Pencil Inserts and Clips, Costume Jewelry, Watch Parts, Lamps, Terminal Connectors, Reflectors, Screw Shells, Flashlight Shells, Lamp Fixtures, Fasteners, Grommets, Eyelets, Screws, Pins, Rivets, Sound Proofing Equipment, Springs, Tubing for Instruments and Machines, Wire Screens, Pump Cylinders, Air Pressure Conveyor Systems, Liners, Chain, Bead Chain, Power Cylinders, Pumps, Heat Exchangers, Mechanical Housings for Lighters, Ammunition, Shells—Mechanical Housings for Ammunition, Ammunition Cartridge Cases, Washers, Stencils, Plumbing Accessories, Plumbing Brass Goods, Fittings, Traps, Bathroom Fixtures, Faucet Escutcheons

<b>Rod</b>																								
H00	1	6	TYP	68	55	40	—	48	60	—	—	—	—	—	—	—	—	—	—	36	—	—		
	25.4			20	379	276	—	48	60	—	—	—	—	—	—	—	—	—	—	248	—	—		
H02	1	20	TYP	68	70	52	—	30	80	—	—	—	—	—	—	—	—	—	—	42	22	—		
	25.4			20	483	359	—	30	80	—	—	—	—	—	—	—	—	—	—	290	152	—		
<b>Tube</b>																								
H80	0.0	35	TYP	68	78	64	—	8	82	—	73	—	—	—	—	—	—	—	—	—	—	—	—	
	0.0			20	538	441	—	8	82	—	73	—	—	—	—	—	—	—	—	—	—	—	—	
<b>Wire</b>																								
H00	0.08	0	TYP	68	58	—	—	35	—	—	—	—	—	—	—	—	—	—	—	38	—	—	—	
	2			20	400	—	—	35	—	—	—	—	—	—	—	—	—	—	—	262	—	—	—	
H08	0.08	0	TYP	68	130	—	—	3	—	—	—	—	—	—	—	—	—	—	—	60	22	—	—	
	2			20	896	—	—	3	—	—	—	—	—	—	—	—	—	—	—	414	152	—	—	

**Flat Products**

OS015	0.04	0	TYP	68	53	22	—	54	—	78	43	—	—	—	—	—	—	—	—	35	14	—	—
	1			20	365	152	—	54	—	78	43	—	—	—	—	—	—	—	—	241	97	—	—
H10	0.04	0	TYP	68	99	65	—	3	93	—	78	—	—	—	—	—	—	—	—	—	—	—	—
	1			20	683	448	—	3	93	—	78	—	—	—	—	—	—	—	—	—	—	—	—

**C27000**—Handrails, Grillwork, Radiator Cores, Tanks, Finish Hardware, Hinges, Locks, Stencils, Push Plates, Kick Plates, Flashlight Shells, Screw Shells, Socket Shells, Reflectors, Lamp Fixtures, Fasteners, Rivets, Pins, Screws, Grommets, Eyelets, Springs, Bead Chain, Chain, Fasteners, Plumbing Accessories, Sink Strainers

**Rod**

H00	1	6	TYP	68	55	40	—	48	55	—	—	—	—	—	—	—	—	—	—	36	—	—	—
	25.4			20	379	276	—	48	55	—	—	—	—	—	—	—	—	—	—	248	—	—	—
OS050	1	0	TYP	68	48	16	—	65	—	65	—	—	—	—	—	—	—	—	—	34	—	—	—
	25.4			20	331	110	—	65	—	65	—	—	—	—	—	—	—	—	—	234	—	—	—

**Wire**

H00	0.08	0	TYP	68	58	—	—	35	—	—	—	—	—	—	—	—	—	—	—	38	—	—	—
	2.0			20	400	—	—	35	—	—	—	—	—	—	—	—	—	—	—	262	—	—	—
H08	0.08	0	TYP	68	128	—	—	3	—	—	—	—	—	—	—	—	—	—	—	60	—	—	—
	2.0			20	883	—	—	3	—	—	—	—	—	—	—	—	—	—	—	414	—	—	—

(continued)

Table 43 (Continued)

Temper	Section Size in. mm.	Cold Work %	Temp Typ/Min	Temp F C	Tensile Strength ksi MPa	Yield Strength (0.5% ext. under load) ksi MPa	Yield Strength (0.2% offset) ksi MPa	Yield Strength (0.05% offset) ksi MPa	Rockwell Hardness			Vickers Hard.		Shear Strength ksi MPa	Fatigue Strength <sup>a</sup> ksi MPa	Izod Impact Strength ft-lb J
									El %	B	C	F	30T			
<b>Flat Products</b>																
OS015	0.04	0	TYP	68	53	22	—	—	—	54	—	78	43	—	—	0.0
	1			20	365	152	—	—	—	54	—	78	43	—	—	0.
H08	0.04	0	TYP	68	91	62	—	—	—	3	90	—	76	—	20	0.0
	1			20	627	427	—	—	—	3	90	—	76	—	138	0.0
<b>C28000</b> —Door Frames, Large Architectural Trim, Architectural Panels, Sheet, Hardware, Decoration, Structural, Heavy Plate, Large Sheets, Decorative Hardware, Bolts, Brazing Rod, Valve Stems, Condenser Plates, Hot Forgings, Evaporator Tubes, Large Nuts and Bolts, Condenser Tube, Heat Exchanger Tube																
<b>Rod</b>																
M30	1	0	TYP	68	52	20	—	—	—	52	—	78	—	—	—	0.0
	25.4			20	359	138	—	—	—	52	—	78	—	—	—	0.0
H01	1	0	TYP	68	72	50	—	—	—	25	78	—	—	—	—	0.0
	25.4			20	496	345	—	—	—	25	78	—	—	—	—	0.0
<b>Tube</b>																
O50	0.0	0	TYP	68	56	23	—	—	—	50	—	82	47	—	—	0.0
	0.0			20	386	159	—	—	—	50	—	82	47	—	—	0.
H04	0.0	30	TYP	68	74	55	—	—	—	10	80	—	—	—	—	0.0
	0.0			20	510	379	—	—	—	10	80	—	—	—	—	0.0
<b>Flat Products</b>																
O60	0.04	0	TYP	68	54	21	—	—	—	45	—	80	46	—	—	0.0
	1			20	372	145	—	—	—	45	—	80	46	—	—	0.0
H02	0.04	0	TYP	68	70	50	—	—	—	10	75	—	67	—	—	0.0
	1			20	483	345	—	—	—	10	75	—	67	—	—	0.0

**C36000**—Terrazzo Strip, Fluid Connectors, Threaded Inserts for Plastic, Sensor Bodies, Thermostat Parts, Lock Bodies, Hardware, Fittings, t Combs (to Straighten Hair), Bolts, Nuts, Screws, Nuts, Screws, Valve Stems, Valve Seats, Valve Trim, Fluid Connectors, Nozzles, Unions, Adapters, Screw Machine Products, Automatic Screw Machine Parts, Pinions, Gears, Faucet Components, Pneumatic Fittings, Gauges, Plumbers' Brass Goods, Faucet Stems, Faucet Seats, Plumbing Fittings

**Bar**  
H02 < 0.50 0 TYP 68 — — — — 65 — — — — 0.0  
< 12.7 20 — — — — 65 — — — — 0.0

**ROD**  
H04 0.375 0 TYP 68 — — — — 78 — — — — 34 0.0  
12.7 20 — — — — 78 — — — — 234 0.0

**Shapes**  
M30 0.5 0 TYP 68 49 18 — — 50 — — 68 — — 30 0.0  
12.7 20 338 124 — — 50 — — 68 — — 207 0.0

**Flat Products**  
H02 0.25 11 TYP 68 56 45 — — 20 62 — — — — 33 0.0  
4.76 20 386 310 — — 20 62 — — — — 228 0.0

**C37700**—Furniture Hardware, Decorative Knobs, Door Handles, Valve Bodies for Refrigeration, Chemicals, Golf Putters, Valve Bodies for Scuba & Propane Spray Tanks, Valve Bodies for Agricultural Spray Tanks, Fuse Bodies, Covers, Valve Components, Forgings and Pressings of All Kinds

**Rod**  
M30 1 0 TYP 68 52 20 — — 45 — — 78 — — — — 0.0  
25.4 20 359 138 — — 45 — — 78 — — — — 0.0

**Shapes**  
M30 1 0 TYP 68 52 20 — — 45 — — 78 — — — — 0.0  
25.4 20 359 138 — — 45 — — 78 — — — — 0.0

**C44000**—Condenser Tube, Evaporator Tubing, Heat Exchanger Tubing, Condenser Tube Plates, Distiller Tubes, Ferrules, Strainers

**Tube**  
OS025 0.0 0 TYP 68 53 22 — — 65 — — 75 37 — — 0.0  
0.0 20 365 152 — — 65 — — 75 37 — — 0.0

**Wire**  
OS015 0.08 0 TYP 68 55 — — 60 — — — — — — 0.0  
2 20 379 — — 60 — — — — — — 0.0

**Plate**  
M20 1 0 TYP 68 48 18 — — 65 — — 70 — — — — 0.0  
25.4 20 331 124 — — 65 — — 70 — — — — 0.0

(continued)

Table 43 (Continued)

Temper	Section Size in. mm.	Cold Work %	Temp Typ/Min C	Tensile Strength ksi MPa	Yield Strength (0.5% ext. under load) ksi MPa	Yield Strength (0.2% offset) ksi MPa	Yield Strength (0.05% offset) ksi MPa	Rockwell Hardness			Vickers Hard.		Shear Strength ksi MPa	Fatigue Strength <sup>a</sup> ksi MPa	Izod Impact Strength ft-lb J	
								El %	B	C	F	30T				500
<b>C46500</b> —Elevators, Architectural Metal, Bolts, Nuts, Rivets, Plater Bar for Jewelry, Plates, Baffles, Heat Sinks, Balls, Structural Uses, Welding Rod, Condenser Plates, Valve Stems, Aircraft Turn buckle Barrels, Petrochemical Tanks, Heat Exchanger Tube, Marine Hardware, Propeller Shafts, Fittings																
<b>Rod</b>																
O60	1	0	TYP	68	57	25	—	—	47	55	—	—	—	—	40	0.0
	25.4			20	393	172	—	—	47	55	—	—	—	—	276	0.0
H02	1	20	TYP	68	75	53	—	—	20	82	—	—	—	44	0.0	
	25.4			20	517	365	—	—	20	82	—	—	—	303	0.0	
<b>Tube</b>																
H04	0.0	35	TYP	68	88	66	—	—	18	95	—	—	—	—	—	0.0
	0.0			20	607	455	—	—	18	95	—	—	—	—	—	0.0
<b>Flat Products</b>																
O60	0.25	0	TYP	68	58	25	—	—	49	56	—	—	—	40	0.0	
	6.35			20	400	172	—	—	49	56	—	—	—	276	0.0	
H01	0.04	0	TYP	68	70	58	—	—	17	75	—	—	—	43	0.0	
	1			20	483	400	—	—	17	75	—	—	—	296	0.0	
<b>Wire</b>																
H04	0.08	80	TYP	68	79	—	—	—	1	—	—	—	—	32	0.0	
<b>Flat Products</b>																
OS025	0.04	0	TYP	68	40	14	—	—	48	—	68	—	—	—	0.0	
	1			20	276	97	—	—	48	—	68	—	—	—	0.0	
H08	0.04	0	TYP	68	75	—	—	—	4	79	—	70	—	—	0.0	
	1			20	517	—	—	—	4	79	—	70	—	—	0.0	
<b>C51100</b> —Bridge Bearing Plates, Resistance Wire, Electronic Connectors, Electrical Connectors, Electrical Flexing Contact Blades, Switch Parts, Wire Brushes, Fuse Clips, Electronic and Precision Instrument Parts, Electromechanical Spring Components, Fasteners, Cotter Pins, Lock Washers, Bellows, Springs, Chemical Hardware, Textile Machinery, Pressure Responsive Elements, Welding Rods, Perforated Sheets, Truss Wire, Sleeve Bushings, Beater Bar, Clutch Disks, Diaphragms, Bourdon Tubes																
<b>Flat Products</b>																
OS015	0.04	0	TYP	68	49	—	23	—	50	—	76	—	—	—	0.0	
	1			20	338	—	159	—	50	—	76	—	—	—	0.0	
HR08	0.0	0	TYP	68	98	—	88	—	8	—	—	—	—	—	0.0	
	0.0			20	676	—	607	—	8	—	—	—	—	—	0.0	



**C52100**—Bridge Bearing Plates, Thermostat Bellows, Power Conductor for Electrological Pencil, Cymbals, Coinage, Electronic Connectors, Electrical Flexing Contact Blades, Electrical Flexing Contact Blades, Electrical Connectors, Cold Headed Parts, Wire Brushes, Switch Parts, Fuse Clips, Fasteners, Heavy Duty, Lock Washers, Cotter Pins, Doctor Blades, Paper Industry, Welding Wire, Beater Bar, Clutch Disks, Bourdon Tubing, Diaphragms, Sleeve Bushings, Springs, Heavy Duty, Pneumatic Hammers, Well Drill Equipment, Thrust Bearings, Cold Headed Parts, Pinions, Gears, Clips, Heavy Duty, Springs, Helical Torsion, Springs, Helical Extension, Bellows, Truss Wire, Chemical Hardware, Perforated Sheets, Textile Machinery, Marine Parts

**Rod**  
H02 0.5 20 TYP 68 80 65 — — 33 85 — 0.0  
12.7 20 552 448 — — — 33 85 — 0.0

**Wire**  
OS035 0.08 0 TYP 68 60 24 — — 65 — 0.0  
2 20 414 165 — — 65 — 0.0  
H06 0.08 0 TYP 68 140 — 0.0  
2 20 965 — 0.0

**Flat Products**  
OS015 0.04 0 TYP 68 65 — — — — 60 — — — 85 — — — — — — — — — — — — — — — — — — 0.0  
1 20 448 — — — — 60 — — — 85 — — — — — — — — — — — — — — — — — — 0.0  
HR08 0.0 0 TYP 68 112 — — 102 — 11 — 0.0  
0.0 20 772 — — 703 — 11 — 0.0

**C61300**—Wire Screening, Fasteners, Bolts, Nuts, Gaskets, Tanks, Desalination Equipment, Sea Water Piping, Machine Parts, Tube Sheets, Seamless Tubing and Pipe, Columns, Heat Exchanger Tube, Piping Systems, Acid Resistant, Corrosion-Resistant Vessels, Condenser Tube, Water Boxes, Tie Rods, Mining Shovels, Marine Hardware, Protective Sheathing, Explosives Blending Chambers & Mixing Troughs, Ball Valve Seats

**Rod**  
H04 1 25 TYP 68 82 55 — — — 35 90 — — — — — — — — — 45 — — — 0.0  
25.4 20 565 379 — — — 35 90 — — — — — — — — — 310 — — — 0.0

**Flat Products**  
O60 1 0 TYP 68 76 33 — — — 42 79 — — — — — — — — — 45 25 0.0  
25.4 20 524 228 — — — 42 79 — — — — — — — — — 310 172 0.0

**C61800**—Welding Rod, Bushings, Bearing Liners, Pickling Hooks, Shafts, Welding Wire, Tie Rods, Bearings, Pump Impellers, Marine Hardware

**Rod**  
H02 1 15 TYP 68 85 43 — — — 23 89 — — — — — — — — — 47 82 0.0  
25.4 20 586 293 — — — 23 89 — — — — — — — — — 324 565 0.0

**Wire**  
H02 0.063 0 TYP 68 140 — 0.0  
1.60 20 965 — 0.0

(continued)

Table 43 (Continued)

Temper	Section Size in. mm.	Cold Work %	Typ/Min	Temp F C	Tensile Strength ksi MPa	Yield Strength ext. under load ksi MPa	Yield Strength (0.2% offset) ksi MPa	Yield Strength (0.05% offset) ksi MPa	Rockwell Hardness			Vickers Hard.		Shear Strength ksi MPa	Fatigue Strength <sup>a</sup> ksi MPa	Izod Impact Strength ft-lb J
									B	C	F	30T	500			
<b>C62400</b> —Nuts, Hydraulic Bushings, Support Bushings, Valve Balls, Welding Wire, Tie Rods, Wear Plates, Drift Pins, Bushings, Gears, Cams																
<b>Bar</b>																
O50	1	0	TYP	68	100	50	—	—	—	14	92	—	—	—	—	0.0
	25.4			20	689	345	—	—	—	14	92	—	—	—	—	0.0
M30	3	0	TYP	68	90	40	—	—	—	18	87	—	—	—	—	0.0
	76			20	621	276	—	—	—	18	87	—	—	—	—	0.0
<b>C63200</b> —Marine Fasteners, Bolts, Nuts, Sleeve Bearings, Valve Stems, Sea Water Pump Bodies, Bearing Cages, Shafts, Bushings, Cams, Sea Water Valves, Marine Drive Shafts																
<b>Rod</b>																
O50	1	0	TYP	68	105	53	—	—	—	22	96	—	—	—	—	0.0
	25.4			20	724	365	—	—	—	22	96	—	—	—	—	0.0
<b>Plate</b>																
O50	1	0	TYP	68	90	45	—	—	—	25	85	—	—	—	—	0.0
	25.4			20	621	310	—	—	—	25	85	—	—	—	—	0.0
<b>Forgings</b>																
O50	5	0	TYP	68	100	45	—	—	—	22	92	—	—	—	—	0.0
	127			20	689	310	—	—	—	22	92	—	—	—	—	0.0
<b>C65500</b> —Sculpture, Motors, Rotor Bar, Pole Line Hardware, Bolts, Cotter Pins, Screws, Hinges, Burrs, Rivets, Nuts, Nails, Clamps, Oil Refinery Plumbing Tube, Wire, Screen Cloth, Piston Rings, Kettles, Heat Exchanger Tubes, Chemical Equipment, Channels, Cable, Bushings, Tanks, Butts, Shuffling, Screen Plates, Welded Tanks, Doctor Blades, Paper Industry, Hydraulic Pressure Lines, Bearing Plates, Pressure Vessels, Welded Pressure Vessels, Wear Plates, Propeller Shafts, Hardware																
<b>Rod</b>																
OS050	1	0	TYP	68	58	22	—	—	—	60	60	—	—	—	43	0.0
	25.4			20	400	152	—	—	—	60	60	—	—	—	296	0.0
H06	1	50	TYP	68	108	60	—	—	—	13	95	—	—	—	62	0.0
	25.4			20	745	414	—	—	—	13	95	—	—	—	427	0.0
<b>Tube</b>																
OS050	0.065	0	TYP	68	57	—	—	—	—	70	45	—	—	—	—	0.0
	1.7			20	393	—	—	—	—	70	45	—	—	—	—	0.0
OS050	0.065	0	TYP	68	57	—	—	—	—	70	45	—	—	—	—	0.0
	1.7			20	393	—	—	—	—	70	45	—	—	—	—	0.0

<b>Wire</b>																							
OS035	0.08	0	TYP	68	60	25	—	—	—	—	—	—	—	—	—	—	—	—	—	—	43	—	0.0
	2			20	414	172	—	—	—	—	—	—	—	—	—	—	—	—	—	—	296	—	0.0
H08	0.08	0	TYP	68	145	70	—	—	—	—	—	—	—	—	—	—	—	—	—	—	70	30	0.0
	2			20	1000	483	—	—	—	—	—	—	—	—	—	—	—	—	—	—	483	207	0.0
<b>Flat Products</b>																							
OS015	0.04	0	TYP	68	63	30	—	—	—	—	—	—	—	—	—	—	—	—	—	—	—	—	—
	1			20	434	207	—	—	—	—	—	—	—	—	—	—	—	—	—	—	—	45	—
H08	0.04	0	TYP	68	110	62	—	—	—	—	—	—	—	—	—	—	—	—	—	—	—	63	—
	1			20	758	427	—	—	—	—	—	—	—	—	—	—	—	—	—	—	—	434	—
<b>C66700—Resistance Weldable Brass Products</b>																							
<b>Wire</b>																							
H02	0.08	0	TYP	68	90	—	—	—	—	—	—	—	—	—	—	—	—	—	—	—	—	—	—
	2			20	621	—	—	—	—	—	—	—	—	—	—	—	—	—	—	—	—	—	—
<b>Flat Products</b>																							
OS015	0.04	0	TYP	68	55	24	—	—	—	—	—	—	—	—	—	—	—	—	—	—	—	—	—
	1			20	379	165	—	—	—	—	—	—	—	—	—	—	—	—	—	—	—	—	—
H10	0.04	0	TYP	68	100	—	—	—	—	—	—	—	—	—	—	—	—	—	—	—	—	—	—
	1			20	689	—	—	—	—	—	—	—	—	—	—	—	—	—	—	—	—	—	—
<b>C67500—Clutch Disks, Pump Rods, Shafting, Bolts, Balls, Valve Stems, Valve Bodies, Aircraft Parts, Bushings, Hardware</b>																							
<b>Rod</b>																							
H01	1	10	TYP	68	77	45	—	—	—	—	—	—	—	—	—	—	—	—	—	—	—	—	—
	25.4			20	531	310	—	—	—	—	—	—	—	—	—	—	—	—	—	—	—	—	—
H02	1	20	TYP	68	84	60	—	—	—	—	—	—	—	—	—	—	—	—	—	—	—	—	—
	25.4			20	579	414	—	—	—	—	—	—	—	—	—	—	—	—	—	—	—	—	—
<b>C69400—Valve Stems</b>																							
<b>Rod</b>																							
O60	1	0	TYP	68	85	43	—	—	—	—	—	—	—	—	—	—	—	—	—	—	—	—	—
	25.4			20	586	296	—	—	—	—	—	—	—	—	—	—	—	—	—	—	—	—	—
H04	0.75	0	TYP	68	100	57	—	—	—	—	—	—	—	—	—	—	—	—	—	—	—	—	—
	19			20	689	393	—	—	—	—	—	—	—	—	—	—	—	—	—	—	—	—	—
<b>C70600—Power Steering Tube, Brake Lines, Screw Lamp Bases, Valve Bodies, Condensers, Evaporators, Pump Impellers for Oil Refining, Pressure Vessels, Condenser Plates, Weld Torch Tips, Distiller Tubes, Ferrules, Heat Exchanger Tubes, Evaporator Tubes, Salt Water Baffles, Salt Water Pipe Fittings, Water Hoses, Boat Hulls, Hot Water Tanks, Ship Hulls, Tube Sheet for Salt Water Service, Salt Water Piping Systems, Salt Water Piling Wrap, Propeller Sleeves, Flanges</b>																							
<b>Tube</b>																							
OS025	0.0	0	TYP	68	44	16	—	—	—	—	—	—	—	—	—	—	—	—	—	—	—	—	—
	0.0			20	303	110	—	—	—	—	—	—	—	—	—	—	—	—	—	—	—	—	—
H55	0.0	0	TYP	68	60	57	—	—	—	—	—	—	—	—	—	—	—	—	—	—	—	—	—
	0.0			20	414	393	—	—	—	—	—	—	—	—	—	—	—	—	—	—	—	—	—

(continued)

Table 43 (Continued)

Temper	Section Size in.	Cold Work %	Temp Typ/Min	Temp F/C	Tensile Strength ksi/MPa	Yield Strength (0.5% ext. under load) ksi/MPa	Yield Strength (0.2% offset) ksi/MPa	Yield Strength (0.05% offset) ksi/MPa	Rockwell Hardness			Vickers Hard.		Shear Strength ksi/MPa	Fatigue Strength <sup>a</sup> ksi/MPa	Izod Impact Strength ft-lb/J
									El %	B	C	F	30T			
<b>C71500</b> —Pump Impellers, Welding Backing Rings, Flexible Metal Hose, Boiler Parts, Evaporator Tubes, Distiller Tubes, Condenser Plates, Weld Wire, Heat Exchanger Tubes, Refrigerators, Process Equipment, Condenser Components, Heat Exchanger Components, Propeller Sleeves, Condensers, Ferrules, Sea Water Pump Bodies and Internal Parts, Sea Water Condensers, Valve Bodies, Salt Water Piping, Fittings, Salt Water Flanges, Water Boxes																
<b>Rod</b>																
H04	1	20	TYP	68	75	70	—	—	—	15	80	—	—	—	—	0.0
	25.4			20	517	483	—	—	—	15	80	—	—	—	—	0.0
<b>Tube</b>																
OS025	0.0	0	TYP	68	60	25	—	—	—	45	45	—	80	—	—	0.0
	0.0			20	414	172	—	—	—	45	45	—	80	—	—	0.0
<b>Flat Products</b>																
M20	1	0	TYP	68	55	20	—	—	—	45	35	—	—	—	—	0.0
	25.4			20	379	138	—	—	—	45	35	—	—	—	—	0.0
<b>C72200</b> —Condenser Tubing, Heat Exchanger Tubing, Salt Water Piping																
<b>Tube</b>																
H55	0.0	0	TYP	68	70	—	68	—	—	—	—	—	—	—	—	0.0
	0.0			20	483	—	469	—	—	—	—	—	—	—	—	0.0
O50	0.0	0	TYP	68	46	—	18	—	—	46	—	—	—	—	—	0.0
	0.0			20	317	—	124	—	—	46	—	—	—	—	—	0.0
<b>Strip</b>																
H04	0.0	0	TYP	68	70	—	66	—	—	6	—	—	—	—	—	0.0
	0.0			20	483	—	455	—	—	6	—	—	—	—	—	0.0
O61	0.0	0	TYP	68	46	—	18	—	—	46	—	—	—	—	—	0.0
	0.0			20	317	—	124	—	—	46	—	—	—	—	—	0.0

**C72500**—Electronic Contacts, Telecommunications Connectors, Relays, Switch Springs, Connectors, Lead Frames, Control and Sensing Bellows, Brazing Alloy

<b>Wire</b>															
OS015	0.08	0	TYP	68	60	25	—	—	—	—	—	—	—	0.0	
	2			20	414	172	—	—	—	—	—	—	—	0.0	
H14	0.08	99	TYP	68	120	—	—	—	—	—	—	—	—	0.0	
	2			20	827	—	—	—	—	—	—	—	—	0.0	
<b>Flat Products</b>															
OS015	0.04	0	TYP	68	55	22	22	—	35	42	—	—	44	—	0.0
	1			20	379	152	152	—	35	42	—	—	44	—	0.0
<b>Flat Products</b>															
OS015	0.04	0	TYP	68	55	22	22	—	35	42	—	—	44	—	0.0
	1			20	379	152	152	—	35	42	—	—	44	—	0.0
H08	0.04	0	TYP	68	91	83	90	—	1	90	—	—	—	—	0.0
	1			20	627	572	621	—	1	90	—	—	—	—	0.0

**C72650**—Connectors for High Temperatures, Switches, Relays, Springs, Cladding and Inlay

<b>Flat Products</b>															
TM00	0.0	0	TYP	68	110	—	80	75	18	—	—	—	—	—	0.0
	0.0			20	758	—	552	517	18	—	—	—	—	—	0.0
TM06	0.0	0	TYP	68	130	—	115	110	6	—	—	—	—	—	0.0
	0.0			20	896	—	793	758	6	—	—	—	—	—	0.0
TS04	0.0	0	TYP	68	147	—	—	122	4	—	—	—	—	—	0.0
	0.0			20	1013	—	—	841	4	—	—	—	—	—	0.0
TX00	0.0	0	TYP	68	130	—	—	78	6	—	—	—	—	—	0.0
	0.0			20	896	—	—	538	6	—	—	—	—	—	0.0

**C72700**—Connectors, Springs, Coil Springs

<b>Flat Products</b>															
TB00	0.012	0	TYP	68	66	29	—	—	36	—	—	—	—	—	0.0
	0.3			20	455	200	—	—	36	—	—	—	—	—	0.0
TD04	0.027	75	TYP	68	126	—	100	—	—	—	—	—	—	—	0.0
	0.69			20	869	—	689	—	—	—	—	—	—	—	0.0
TS12	0.0	0	TYP	68	165	—	—	145	2	—	—	—	—	—	0.0
	0.0			20	1138	—	—	1000	2	—	—	—	—	—	0.0
TX00	0.0	33	TYP	68	115	—	—	77	15	—	—	—	—	—	0.0
	0.0			20	793	—	—	531	15	—	—	—	—	—	0.0

(continued)

Table 43 (Continued)

Temper	Section Size in. mm.	Cold Work %	Typ/Min	Temp F C	Tensile Strength ksi MPa	Yield Strength ext. under load ksi MPa	Yield Strength (0.2% offset) ksi MPa	Yield Strength (0.05% offset) ksi MPa	Rockwell Hardness			Vickens Hard.			Shear Strength ksi MPa	Fatigue Strength <sup>a</sup> ksi MPa	Izod Impact Strength ft-lb J
									B	C	F	30T	500	500			
<b>C72800</b> —Springs, Extruded Shapes, Tubes, Bars, Rod, Wire, Forgings																	
<b>Rod</b>																	
TB00	0.25	0	TYP	68	76	—	36	—	23	—	—	—	—	—	—	—	0.0
	6.35			20	525	—	250	—	23	—	—	—	—	—	—	—	0.0
TF00	0.76	0	TYP	68	147	—	126	—	10	—	33	—	—	—	—	—	0.0
	19.3			20	1014	—	867	—	10	—	33	—	—	—	—	—	0.0
TH01	0.113	0	TYP	68	199	—	196	—	4	—	—	—	—	—	—	—	0.0
	2.87			20	1372	—	1351	—	4	—	—	—	—	—	—	—	0.0
<b>Tube</b>																	
TF00	0.0	0	TYP	68	294	—	250	—	5	—	67	—	—	—	—	—	0.0
	0.0			20	2024	—	1723	—	5	—	67	—	—	—	—	—	0.0
<b>Strip</b>																	
H01	0.089	0	TYP	68	89	—	76	—	13	89	—	—	—	—	—	—	0.0
	2.26			20	612	—	525	—	13	89	—	—	—	—	—	—	0.0
H08	0.063	0	TYP	68	139	—	132	—	3	—	30	—	—	—	—	—	0.0
	1.6			20	956	—	911	—	3	—	30	—	—	—	—	—	0.0
TH08	0.063	0	TYP	68	191	—	180	—	3	—	39	—	—	—	—	—	0.0
	1.6			20	1318	—	1242	—	3	—	39	—	—	—	—	—	0.0
<b>Forgings</b>																	
TF00	0.0	0	TYP	68	145	—	120	—	—	—	34	—	—	—	—	—	0.0
	0.0			20	1000	—	827	—	—	—	34	—	—	—	—	—	0.0
<b>C72900</b> —Connectors, Miniaturized Sockets, Relay Elements, Contacts, Controls, Wire, Marine Components, Springs, Wire, Marine Components																	
<b>Tube</b>																	
TF00	0.0	0	TYP	68	154	—	—	—	7	—	32	—	—	—	—	—	0.0
	0.0			20	1062	—	—	—	7	—	32	—	—	—	—	—	0.0

<b>Wire</b>																	
TF00	.030	0	TYP	68	160	—	174	—	—	—	—	—	—	—	—	—	0.0
	0.8			20	1103	—	1201	—	—	—	—	—	—	—	—	—	0.0
<b>Flat Products</b>																	
TD04	0.027	78	TYP	68	145	—	—	—	—	—	31	—	—	—	—	—	0.0
	0.69			20	1000	—	—	—	—	—	31	—	—	—	—	—	0.0
TM08	0.0	0	TYP	68	137	—	125	110	6	—	—	—	—	—	—	—	0.0
	0.0			20	944	—	862	758	6	—	—	—	—	—	—	—	0.0
TS12	0.0	0	TYP	68	181	—	—	163	—	—	—	—	—	—	—	—	0.0
	0.0			20	1248	—	—	1127	—	—	—	—	—	—	—	—	0.0
TX00	0.0	78	TYP	68	120	—	—	81	10	—	—	—	—	—	—	—	0.0
	0.0			20	827	—	—	558	10	—	—	—	—	—	—	—	0.0
<b>C74500—Hollow Ware, Name Plates, Connectors, Rivets, Screws, Slide Fasteners, Optical Parts, Plater Bar, Etching Stock</b>																	
<b>Wire</b>																	
OS015	0.08	0	TYP	68	63	—	—	—	—	—	35	—	—	—	—	—	0.0
	2			20	434	—	—	—	—	—	35	—	—	—	—	—	0.0
H04	0.08	84	TYP	68	130	—	—	—	—	—	1	—	—	—	—	—	0.0
	2			20	896	—	—	—	—	—	1	—	—	—	—	—	0.0
<b>Flat Products</b>																	
OS015	0.04	0	TYP	68	60	28	—	—	36	52	—	85	51	—	—	—	0.0
	1			20	414	193	—	—	36	52	—	85	51	—	—	—	0.0
H06	0.04	0	TYP	68	95	76	—	—	3	92	—	—	78	—	59	—	0.0
	1			20	655	524	—	—	3	92	—	—	78	—	407	—	0.0
<b>C77000—Resistance Wire, Springs, Optical Goods, Eyeglass Frames</b>																	
<b>Wire</b>																	
OS035	0.08	0	TYP	68	60	—	—	—	40	—	—	—	—	—	—	—	0.0
	2			20	414	—	—	—	40	—	—	—	—	—	—	—	0.0
H04	0.08	68	TYP	68	145	—	—	—	2	—	—	—	—	—	—	—	0.0
	2			20	1000	—	—	—	2	—	—	—	—	—	—	—	0.0
<b>Flat Products</b>																	
OS035	0.04	0	TYP	68	60	27	—	—	40	55	—	90	—	—	—	—	0.0
	1			20	414	186	—	—	40	55	—	90	—	—	—	—	0.0
H08	0.04	0	TYP	68	115	—	—	—	2	99	—	—	81	—	—	—	0.0
	1			20	793	—	—	—	2	99	—	—	81	—	—	—	0.0

<sup>a</sup>Fatigue Strength: 100 × 10<sup>6</sup> cycles.

Source: Copper Development Association





**C82500**—Sculpture, Safety Tools, Jewelry, Molds for Plastic Parts, Glass Molds, Aluminum Die Cast Plunger Tips, Valves, Business Machine Parts, Pressure Housings in Salt Water Environments, Sleeves, Permanent Molds for Brass and Aluminum Casting, Golf Clubs, Corrosion-Resistant Valves, Undersea Cable Housings, Ordnance Components

<i>As Sand Cast</i>																		
M01	0.0	0	TYP	68	80	—	45	—	20	82	—	—	—	—	—	—	—	0.0
	0.0			20	552	—	310	—	20	82	—	—	—	—	—	—	—	0.0
M01	0.0	0	SMIN	68	75	—	40	—	15	—	—	—	—	—	—	—	—	0.0
	0.0			20	518	—	276	—	15	—	—	—	—	—	—	—	—	0.0
TB00	0.0	0	TYP	68	60	—	25	—	35	63	—	—	—	—	—	—	—	0.0
	0.0			20	414	—	172	—	35	63	—	—	—	—	—	—	—	0.0
TF00	0.0	0	TYP	68	160	—	150	—	1	—	43	—	—	—	—	24	—	0.0
	0.0			20	1103	—	1035	—	1	—	43	—	—	—	—	165	—	0.0
TF00	0.0	0	SMIN	68	150	—	120	—	1	—	—	—	—	—	—	—	—	0.0
	0.0			20	1035	—	828	—	1	—	—	—	—	—	—	—	—	0.0

**C83300**—Adaptors, Electrical Hardware Parts, Connectors, Electrical Components, Terminal Ends for Electric Cables

<i>As Sand Cast</i>																		
M01	0.0	0	TYP	68	32	10	—	—	35	35	—	—	—	—	—	—	—	0.0
	0.0			20	221	69	—	—	35	35	—	—	—	—	—	—	—	0.0

**C83450**—Electrical Hardware, Low-Pressure Valve Bodies, Water Pump Parts, Iron Waterworks Valve Trim, Plumbing and Pipe Fittings

<i>As Sand Cast</i>																		
M01	0.0	0	TYP	68	37	15	—	—	31	—	—	—	—	—	62	—	—	0.0
	0.0			20	255	103	—	—	31	—	—	—	—	—	62	—	—	0.0
M01	0.0	0	SMIN	68	30	14	—	—	25	—	—	—	—	—	—	—	—	0.0
	0.0			20	207	97	—	—	25	—	—	—	—	—	—	—	—	0.0

**C83600**—Ornamental Fixtures, Hardware, Lightning Protection, Cooling Equipment, Heating Equipment, Trowels for Cement Working, Electrical Equipment, Switches, Electrical Hardware, Large Hold-Down Screws, Bearings, Small Gears, Low-Pressure Valves, Pumps, Valves for the Water Meter Industry, Valve Bodies for the Water Meter Industry, Transducer Housings, Valves, Rings, Printing Presses, Furnaces, Pump Fixtures, Impellers, Valve Bodies, Pumps, Couplings, Handles for Dental Equipment, Bearing Segments for Steel Industry, Pressure Blocks for Steel Industry, Air Actuators, Valve Bodies, Valves, Bushings, Pump Parts, Marine Products, Parts for Boats, Faucets, Pipe Fittings, Fixtures

<i>As Sand Cast</i>																		
M01	0.0	0	TYP	68	37	17	—	—	30	—	—	—	—	—	60	—	—	11
	0.0			20	255	117	—	—	30	—	—	—	—	—	60	—	—	76
M01	0.0	0	SMIN	68	30	14	—	—	20	—	—	—	—	—	—	—	—	0.0
	0.0			20	205	97	—	—	20	—	—	—	—	—	—	—	—	0.0
<i>As Continuous Cast</i>																		
M07	0.0	0	SMIN	68	36	19	—	—	15	—	—	—	—	—	—	—	—	0.0
	0.0			20	248	131	—	—	15	—	—	—	—	—	—	—	—	0.0

*As Centrifugal Cast*

M02	0.0	0	SMIN	68	30	14	—	—	20	—	—	—	—	—	—	—	—	0.0
	0.0			20	207	97	—	—	20	—	—	—	—	—	—	—	—	0.0

(continued)



<b>C85200</b> —Ornamental Castings, Builders Hardware, Andirons, Chandeliers, Valves, Plumbing Fixtures, Plumbing Fittings															
<i>As Sand Cast</i>															
M01	0.0	0	TYP	68	38	13	—	—	35	—	—	45	—	—	0.0
	0.0	0		20	262	90	—	—	35	—	—	45	—	—	0.0
M01	0.0	0	SMIN	68	35	12	—	—	25	—	—	—	—	—	0.0
	0.0	0		20	241	83	—	—	25	—	—	—	—	—	0.0
<i>As Centrifugal Cast</i>															
M02	0.0	0	SMIN	68	35	12	—	—	25	—	—	—	—	—	0.0
	0.0	0		20	241	83	—	—	25	—	—	—	—	—	0.
<b>C85400</b> —Emblem, Ornaments, Builder Hardware, Window Hardware, Ornamental Fittings, Door Hardware for Prisons, Furniture, Decorative Furniture Legs, Musical Instruments, Chandeliers, Andirons, Mechanical Components Where Looks Are Important, Gas Cocks, Radiator Fittings, Battery Clamps, Ferrules, Valves, Marine Hardware, Ship Trimmings, Plumbing Parts															
M01	0.0	0	TYP	68	38	13	—	—	35	—	—	50	—	—	0.0
	0.0	0		20	262	90	—	—	35	—	—	50	—	—	0.0
M01	0.0	0	SMIN	68	30	11	—	—	20	—	—	—	—	—	0.0
	0.0	0		20	207	76	—	—	20	—	—	—	—	—	0.0
<i>As Centrifugal Cast</i>															
M02	0.0	0	SMIN	68	30	11	—	—	20	—	—	—	—	—	0.0
	0.0	0		20	207	76	—	—	20	—	—	—	—	—	0.0
<b>C85700</b> —Ornamental Hardware, Window Hardware, Door Hardware for Prisons, Musical Instruments, Mechanical Components Where Appearance Is Important, Ship Trim, Marine Hardware, Flanges, Fittings															
<i>As Sand Cast</i>															
M01	0.0	0	TYP	68	50	18	—	—	40	—	—	75	—	—	0.0
	0.0	0		20	345	124	—	—	40	—	—	75	—	—	0.0
M01	0.0	0	SMIN	68	—	14	—	—	—	—	—	—	—	—	0.0
	0.0	0		20	—	97	—	—	—	—	—	—	—	—	0.0
<i>As Centrifugal Cast</i>															
M02	0.0	0	SMIN	68	40	14	—	—	15	—	—	—	—	—	0.0
	0.0	0		20	276	97	—	—	15	—	—	—	—	—	0.0

(continued)



**C86400**—Window Hardware, Door Hardware for Prison, Piano Keys, Musical Instruments, Electrical Equipment, Switches, Electrical Components, Screw Down Nuts, Roller Bearings, Valve Stems, Machinery Parts, Propellers, Cams, Bearings, Light-Duty Gears, Brackets, Lever Arms, Fittings, Pump Fixtures, Bushings, Bearing Cage Blanks, Covers for Marine Hardware, Marine Hardware, Marine Fittings, Boat Parts, Plumbing Fixtures

*As Sand Cast*

M01	0.0	0	TYP	68	65	25	—	20	—	—	—	90	105	—	25	30.0
	0.0	0		20	448	172	—	20	—	—	—	90	105	—	172	41.0
M01	0.0	0	SMIN	68	60	20	—	15	—	—	—	—	—	—	—	0.0
	0.0	0		20	414	138	—	15	—	—	—	—	—	—	—	0.0

*As Centrifugal Cast*

M02	0.0	0	SMIN	68	60	20	—	15	—	—	—	—	—	—	—	0.0
	0.0	0		20	414	138	—	15	—	—	—	—	—	—	—	0.0

**C86500**—Welding Guns, Brackets, Electrical Hardware, Gears, Machinery Parts (Substituted for Steel and Malleable Iron), Wear Rings for Pressing Dies for Wood Pulp Industry, Forming Dies for Wood Pulp Industry, Machinery, Struts, Hooks, Lever Arms, Machinery Parts Requiring High-Strength, Frames, Compressors, Pressing Dies for Wood Pulp, Propellers for Salt and Fresh Water, Covers for Marine Hardware, Rudders, Boat Parts, Clamps

*As Sand Cast*

M01	0.0	0	TYP	68	71	29	—	30	—	—	—	100	130	—	20	0.0
	0.0	0		20	490	200	—	30	—	—	—	100	130	—	138	0.0
M01	0.0	0	SMIN	68	65	25	—	20	—	—	—	—	—	—	—	0.0
	0.0	0		20	448	172	—	20	—	—	—	—	—	—	—	0.0

*As Continuous Cast*

M07	0.0	0	SMIN	68	70	25	—	25	—	—	—	—	—	—	—	0.0
	0.0	0		20	483	172	—	25	—	—	—	—	—	—	—	0.0

*As Centrifugal Cast*

M02	0.0	0	SMIN	68	65	25	—	20	—	—	—	—	—	—	—	0.0
	0.0	0		20	448	172	—	20	—	—	—	—	—	—	—	0.0

**C87300**

*As Sand Cast*

M02	0.0	0	SMIN	68	65	25	—	20	—	—	—	—	—	—	—	0.0
	0.0	0		20	448	172	—	20	—	—	—	—	—	—	—	0.0

*As Centrifugal Cast*

M02	0.0	0	SMIN	68	45	18	—	20	—	—	—	—	—	—	—	0.0
	0.0	0		20	310	124	—	20	—	—	—	—	—	—	—	0.0

(continued)

Table 44 (Continued)

Alloy	Temper	Section Size in.	Cold Work %	Typ/Min	Temp F	Tensile Strength ksi	Yield Strength (0.5% ext. under load) ksi	Yield Strength (0.2% offset) ksi	Yield Strength (0.05% offset) ksi	Rockwell Hardness			Vickens Hard.		Brinell Hard.	Shear Strength ksi	Fatigue Strength* ksi	Izod Impact Strength ft-lb
										B	C	F	30T	500				
<b>C87500</b> —Window Hardware, Levers, Pump Fixtures, Fittings, Bearings, Impellers, Gears, Valve Bodies, at Parts, Small Boat Propellers, Plumbing Fixtures																		
<i>As Sand Cast</i>																		
M01	0.0	0	TYP	68	67	30	—	—	—	21	—	—	115	134	—	22	0.0	
M01	0.0	0	SMIN	20	462	207	—	—	—	21	—	—	115	134	—	152	0.0	
M01	0.0	0	TYP	68	60	24	—	—	—	16	—	—	—	—	—	—	0.0	
M01	0.0	0	SMIN	20	414	165	—	—	—	16	—	—	—	—	—	—	0.0	
<i>As Centrifugal Cast</i>																		
M02	0.0	0	SMIN	68	60	24	—	—	—	16	—	—	—	—	—	—	0.0	
M02	0.0	0	TYP	20	414	165	—	—	—	16	—	—	—	—	—	—	0.0	
<i>As Permanent Mold Cast</i>																		
M05	0.0	0	SMIN	68	80	30	—	—	—	15	—	—	—	—	—	—	0.0	
M05	0.0	0	TYP	20	552	207	—	—	—	15	—	—	—	—	—	—	0.0	
<b>C89510</b> —Lead-Free Plumbing Castings																		
<i>As Sand Cast</i>																		
M01	0.0	0	TYP	68	30	20	—	—	—	12	—	—	37	—	—	—	0.0	
M01	0.0	0	SMIN	20	210	135	—	—	—	12	—	—	37	—	—	—	0.0	
<b>C89520</b> —Lead-Free Plumbing Castings																		
<i>As Sand Cast</i>																		
M01	0.0	0	TYP	68	31	21	—	—	—	10	—	—	54	—	—	—	0.0	
M01	0.0	0	SMIN	20	210	140	—	—	—	10	—	—	54	—	—	—	0.0	
<b>C89550</b> —Lead-Free Plumbing Castings																		
<i>As Sand Cast</i>																		
M01	0.0	0	MIN	68	35	21	20	—	—	5	—	—	—	—	—	—	0.0	
M01	0.0	0	TYP	20	240	140	135	—	—	5	—	—	—	—	—	—	0.0	
M01	0.0	0	TYP	68	48	29	28	—	—	8	—	—	—	—	—	—	0.0	
M01	0.0	0	SMIN	20	330	200	190	—	—	8	—	—	—	—	—	—	0.0	

**C90300**—Heavy-Construction Equipment Bearings, Swivels, Bearings, Bushings, Pump Impellers, Piston Rings, Valve Bodies, Gear Blanks, Gears, Pump Bodies, Valves, and Fittings

<i>As Sand Cast</i>															
M01	0.0	0	TYP	68	45	21	—	—	30	—	—	70	—	—	0.0
	0.0			20	310	145	—	—	30	—	—	70	—	—	0.0
M01	0.0	0	SMIN	68	40	18	—	—	20	—	—	—	—	—	0.0
	0.0			20	276	124	—	—	20	—	—	—	—	—	0.0
<i>As Continuous Cast</i>															
M07	0.0	0	SMIN	68	44	22	—	—	18	—	—	—	—	—	0.0
	0.0			20	303	152	—	—	18	—	—	—	—	—	0.0

**C90500**—Clamps, Heavy-Construction Equipment, Electrical Connectors, Nuts, Bearings, Pump Impellers, Pump Bodies, Valves, Finishing Dies for Wood Pulp Industry, Expansion Bearings, Worm Gears, Seal Rings, Valve Bodies, Gear Blanks, Gears, Piston Rings, Bushings, Water Conditioners, Steam Fittings

<i>As Sand Cast</i>															
M01	0.0	0	TYP	68	45	22	—	—	25	—	—	75	—	13	10.0
	0.0			20	310	152	—	—	25	—	—	75	—	90	13.0
M01	0.0	0	SMIN	68	40	18	—	—	20	—	—	—	—	—	0.0
	0.0			20	275	124	—	—	20	—	—	—	—	—	0.0
<i>As Continuous Cast</i>															
M07	0.0	0	SMIN	68	44	25	—	—	10	—	—	—	—	—	0.0
	0.0			20	303	172	—	—	10	—	—	—	—	—	0.0
<i>As Centrifugal Cast</i>															
M02	0.0	0	TYP	68	45	22	—	—	25	—	—	75	—	13	10.0
	0.0			20	310	152	—	—	25	—	—	75	—	90	13.0
M02	0.0	0	SMIN	68	40	18	—	—	20	—	—	—	—	—	0.0
	0.0			20	276	124	—	—	20	—	—	—	—	—	0.0

(continued)





<i>As Continuous Cast</i>												
M07	0.0	0	SMIN	68	—	—	—	—	—	—	—	0.0
	0.0			20	—	—	—	—	—	—	—	0.0
<b>C91600</b> —Nuts, Gears, Fittings, Bearings, Pump Impellers, Steam Castings, Bushings, Piston Rings												
<i>As Sand Cast</i>												
M01	0.0	0	TYP	68	44	22	—	—	—	—	—	0.0
	0.0			20	303	152	—	—	—	—	—	0.0
M01	0.0	0	SMIN	68	35	17	—	—	—	—	—	0.0
	0.0			20	241	117	—	—	—	—	—	0.0
<i>As Centrifugal Cast</i>												
M02	0.0	0	TYP	68	60	32	—	—	—	—	—	0.0
	0.0			20	414	221	—	—	—	—	—	0.0
M02	0.0	0	SMIN	68	45	25	—	—	—	—	—	0.0
	0.0			20	310	172	—	—	—	—	—	0.0
<i>As Permanent Mold Cast</i>												
M05	0.0	0	TYP	68	60	32	—	—	—	—	—	0.0
	0.0			20	414	221	—	—	—	—	—	0.0
<b>C92200</b> —Ornamental Castings, Heating Equipment, Cooling Equipment, Nuts, Medium-Pressure Hydraulic Equipment, Valves for Water Meters, Pumps Used to 550°F, Gears, Bushings, Pump Impellers, Bearings, Piston Rings, Fittings Used to 550°F, Cryogenic Valves, Valve Components, Marine Castings, Medium-Pressure Steam Equipment to 550°F												
<i>As Sand Cast</i>												
M01	0.0	0	TYP	68	40	20	—	—	—	—	—	0.0
	0.0			20	276	138	—	—	—	—	—	0.0
M01	0.0	0	SMIN	68	34	16	—	—	—	—	—	0.0
	0.0			20	234	110	—	—	—	—	—	0.0
<i>As Continuous Cast</i>												
M07	0.0	0	SMIN	68	38	19	—	—	—	—	—	0.0
	0.0			20	262	131	—	—	—	—	—	0.0
<i>As Centrifugal Cast</i>												
M02	0.0	0	SMIN	68	34	16	—	—	—	—	—	0.0
	0.0			20	234	110	—	—	—	—	—	0.0
<i>As Permanent Mold Cast</i>												
M05	0.0	0	SMIN	68	34	16	—	—	—	—	—	0.0
	0.0			20	234	110	—	—	—	—	—	0.0

(continued)



<i>As Permanent Mold Cast</i>															
M05	0.0	0	TYP	68	47	26	—	—	20	—	—	80	—	—	12.0
	0.0			20	324	179	—	—	20	—	—	80	—	—	16.0
<b>C93200</b> —Automotive Fittings, Washers, Insert Bearings, Bearings, Pumps, Machine Parts, Pump Fixtures, Machine Tool Bearings, Trunnion Bearings, Rolling Mill Bearings, Pump Impellers, Hydraulic Press Main Lining, Hydraulic Press Stuffing Box, Forging Press Toggle Lever Bearings, Diesel Engine Wrist Pin Bushings, Water Pump Bushings, Fuel Pump Bushings, Linkage Bushings for Presses, Roll Neck Bearings, Bearings for Cranes, Main Spindle Bearings, Fittings, Bushings, Thrust Washers, General-Purpose Bushings															
<i>As Sand Cast</i>															
M01	0.0	0	TYP	68	35	18	—	—	20	—	—	65	—	—	6.0
	0.0			20	241	124	—	—	20	—	—	65	—	—	8.0
M01	0.0	0	SMIN	68	30	14	—	—	15	—	—	—	—	—	0.0
	0.0			20	207	97	—	—	15	—	—	—	—	—	0.0
<i>As Continuous Cast</i>															
M07	0.0	0	SMIN	68	35	20	—	—	10	—	—	—	—	—	0.0
	0.0			20	241	138	—	—	10	—	—	—	—	—	0.0
<i>As Centrifugal Cast</i>															
M02	0.0	0	SMIN	68	30	14	—	—	15	—	—	—	—	—	0.0
	0.0			20	207	97	—	—	15	—	—	—	—	—	0.0
<b>C93700</b> —Brackets, Nuts, Washers for Engines, Bushings for High Speed and Heavy Pressure., Bushings, Machine Parts, Slide Guides for Steel Mills, Pumps, Impellers, Bearing Plates, Corrosion-Resistant Castings, Pressure-Tight Castings, High-Speed, Heavy-Load Bearings, Parts for Steel Mill Maintenance, Applications Requiring Acid Resistance to Sulfite Fluids, Bearings, Crank Shafts, Large Marine Bearings															
<i>As Sand Cast</i>															
M01	0.0	0	TYP	68	35	18	16	—	20	—	—	60	—	18	5.0
	0.0			20	241	124	110	—	20	—	—	60	—	124	7.0
M01	0.0	0	SMIN	68	30	12	—	—	15	—	—	—	—	—	0.0
	0.0			20	207	83	—	—	15	—	—	—	—	—	0.0
<i>As Continuous Cast</i>															
M07	0.0	0	SMIN	68	35	20	—	—	6	—	—	—	—	—	0.0
	0.0			20	241	138	—	—	6	—	—	—	—	—	0.0
<i>As Centrifugal Cast</i>															
M02	0.0	0	SMIN	68	30	12	—	—	15	—	—	—	—	—	0.0
	0.0			20	207	83	—	—	15	—	—	—	—	—	0.0

(continued)



**C95200**—Electrical Hardware, Nuts, Large Gear Parts, Pickling Tanks, Hydrant Parts, High-Strength Clamps, Valve Bodies, Mild Alkali Applications, Wear Plates, Bearing Liners, Valves, Worm Wheels, Worms, Pump Rods, Plungers, Gears, Bushings, Bearings, Acid-Resistant Pumps, Valve Seats, Hot Mill Guides, Welding Jaws, Pickling Equipment, Pump Parts, Thrust Pads, Marine Engines, Marine Hardware, Propellers, Covers for Marine Hardware, Gun Mountings, Gun Slides

<i>As Sand Cast</i>																		
M01	0.0	0	TYP	68	80	27	—	35	—	—	—	125	40	22	30.0			
	0.0			20	552	186	—	35	—	—	—	125	276	152	41.0			
M01	0.0	0	S MIN	68	65	25	—	20	—	—	—	110	—	—	0.0			
	0.0			20	448	172	—	20	—	—	—	110	—	—	0.0			
<i>As Continuous Cast</i>																		
M07	0.0	0	S MIN	68	68	26	—	20	—	—	—	—	—	—	0.0			
	0.0			20	469	179	—	20	—	—	—	—	—	—	0.0			
<i>As Centrifugal Cast</i>																		
M02	0.0	0	S MIN	68	65	25	—	20	—	—	—	110	—	—	0.0			
	0.0			20	450	170	—	20	—	—	—	110	—	—	0.0			
<i>As Permanent Mold Cast</i>																		
M05	0.0	0	TYP	68	93	35	—	38	78	—	—	—	—	—	0.0			
	0.0			20	640	240	—	38	78	—	—	—	—	—	0.0			
<i>As Permanent Mold Cast</i>																		
M05	0.0	0	TYP	68	93	35	—	38	78	—	—	—	—	—	0.0			
	0.0			20	640	240	—	38	78	—	—	—	—	—	0.0			

(continued)



**C95410**—Bearings, Spur Gears, Gears, Pickling Hooks, Worms, Valve Components, Bushings, Pickling Baskets

*As Sand Cast*

M01	0.0	0	TYP	68	85	35	—	18	—	—	—	170	47	28	14.0
	0.0	0		20	586	241	—	18	—	—	—	170	324	193	19.0
M01	0.0	0	SMIN	68	75	30	—	12	—	—	—	150	—	—	0.0
	0.0	0		20	515	205	—	12	—	—	—	150	—	—	0.0
TQ50	0.0	0	TYP	68	105	54	—	8	—	—	—	195	50	35	14.0
	0.0	0		20	724	372	—	8	—	—	—	195	345	241	19.0
TQ50	0.0	0	SMIN	68	90	45	—	6	—	—	—	190	—	—	0.0
	0.0	0		20	620	310	—	6	—	—	—	190	—	—	0.0

*As Continuous Cast*

M07	0.0	0	SMIN	68	85	32	—	12	—	—	—	—	—	—	—
	0.0	0		20	586	221	—	12	—	—	—	—	—	—	—
TQ50	0.0	0	SMIN	68	95	45	—	10	—	—	—	—	—	—	—
	0.0	0		20	655	310	—	10	—	—	—	—	—	—	—

*As Centrifugal Cast*

M02	0.0	0	SMIN	68	75	30	—	12	—	—	—	150	—	—	0.0
	0.0	0		20	515	205	—	12	—	—	—	150	—	—	0.0
TQ50	0.0	0	SMIN	68	90	45	—	6	—	—	—	190	—	—	0.0
	0.0	0		20	620	310	—	6	—	—	—	190	—	—	0.0

*As Permanent Mold Cast*

M05	0.0	0	SMIN	68	100	40	—	10	—	—	—	—	—	—	0.0
	0.0	0		20	690	275	—	10	—	—	—	—	—	—	0.0

(continued)





**C95800**—Nuts, Shafts, Propeller Hub, Propeller Blades, Pickling Equipment, Valve Bodies, Machinery, Worms, Bushings, Worm Wheels, Gears, Wear Plates, Valves in Contact with Sea Water; Covers for Marine Hardware, Ship Building, Marine Hardware, Elbows

*As Sand Cast*

M01	0.0	0	TYP	68	95	38	—	—	—	—	—	—	—	—	—	—	159	58	31	20.0
	0.0			20	655	262	—	—	—	—	—	—	—	—	—	—	159	400	214	27.0
M01	0.0	0	SMIN	68	85	35	—	—	—	—	—	—	—	—	—	—	—	—	—	0.0
	0.0			20	585	240	—	—	—	—	—	—	—	—	—	—	—	—	—	0.0

*As Continuous Cast*

M07	0.0	0	SMIN	68	85	35	—	—	—	—	—	—	—	—	—	—	—	—	—	0.0
	0.0			20	586	241	—	—	—	—	—	—	—	—	—	—	—	—	—	0.0

*As Centrifugal Cast*

M02	0.0	0	SMIN	68	85	35	—	—	—	—	—	—	—	—	—	—	—	—	—	0.0
	0.0			20	585	240	—	—	—	—	—	—	—	—	—	—	—	—	—	0.0

*As Permanent Mold Cast*

M05	0.0	0	TYP	68	96	52	—	—	—	—	—	—	—	—	—	—	—	—	—	—
	0.0			20	660	360	—	—	—	—	—	—	—	—	—	—	—	—	—	—
M05	0.0	0	SMIN	68	90	40	—	—	—	—	—	—	—	—	—	—	—	—	—	—
	0.0			20	620	275	—	—	—	—	—	—	—	—	—	—	—	—	—	—

**C96400**—Pump Fixtures, Fittings, Pump Bodies, Steam Fittings, Valves, Pump Bodies, Flanges and Elbows Used for Sea Water Corrosion Resistance, Boat Parts

*As Sand Cast*

M01	0.0	0	TYP	68	68	37	—	—	—	—	—	—	—	—	—	—	—	—	—	—
	0.0			20	469	255	—	—	—	—	—	—	—	—	—	—	—	—	—	—
M01	0.0	0	SMIN	68	60	32	—	—	—	—	—	—	—	—	—	—	—	—	—	—
	0.0			20	415	220	—	—	—	—	—	—	—	—	—	—	—	—	—	—

*As Continuous Cast*

M07	0.0	0	SMIN	68	65	35	—	—	—	—	—	—	—	—	—	—	—	—	—	—
	0.0			20	448	241	—	—	—	—	—	—	—	—	—	—	—	—	—	—

Source: Copper Development Association

Typical (nominal) properties may vary by as much as 5–10% in practice because of variations in processing and composition. They cannot be guaranteed except by special arrangement between customer and supplier and should not be used for design purposes, for which ASTM, SAE, ASME MIL, or other recognized standard specifications should be used instead. The tables include annealed tempers and representative hard or as-heat-treated tempers, as appropriate. There are numerous additional but less-common tempers, and readers are encouraged to contact ASTM or the Copper Development Association, Inc. or its website, [www.copper.org](http://www.copper.org), for current information. Note also that yield strength is presented as either 0.2% offset or 0.5% extension under load, depending on yielding behavior for the alloy in question. These two forms of expressing extension data accommodate alloys whose stress–strain curves do or do not exhibit a well-defined yield point,

Fatigue strength in copper metals decreases to approximately one-half the static tensile strength in  $10^8$  cycles. The rate of decrease, itself, decreases with the number of cycles,  $N$ , and may become independent of  $N$  in some alloys, for which an absolute endurance ratio (fatigue strength at  $N$  cycles divided by static tensile strength) can be identified.

### ***Effect of Temperature***

Copper alloys used at elevated temperatures are chosen on the basis of time-dependent deformation behavior. Slow deformation under constant load, or creep, eventually leads to stress rupture, in which case failure occurs at a stress as low as one-half the short-term tensile strength. Conversely, stress decreases when metals are held at constant strain at elevated temperatures. This phenomenon is known as stress relaxation; it is an important design element in products such as electrical connectors and springs used at elevated temperatures.

With some exceptions (welding equipment, furnace tuyeres, and burner components), high-purity coppers are generally not specified for elevated-temperature applications. Leaded coppers and copper alloys are likewise not suitable. On the other hand, many of the high-copper alloys and copper-based MMCs were designed specifically to retain strength and conductivity when heated. On the other hand, nonleaded brasses and bronzes, chromium copper, chromium–zirconium copper, beryllium coppers and other high-performance alloys, as well as copper-based MMCs have intermediate to very high strengths and stress relaxation resistance at elevated temperatures and are routinely used under such conditions. Aluminum bronzes, nickel–aluminum bronzes, and copper nickels have superior resistance to creep and stress rupture. Copper nickels and nickel–aluminum bronzes are considered to be the most suitable copper alloys for use at temperatures above 662F (350°C) based on their performance in a 100,000-h stress-rupture test. MMCs are also viable candidates in such applications. They also exhibit high corrosion resistance in chemical and marine environments.

### ***Impact Loading***

Copper alloys generally exhibit good ductility. Wrought products such as rod, plate, mechanical wire, and forgings are inherently better able to withstand impact loads and severe deformations before rupture than their cast counterparts. The ductility and impact resistance of copper and predominantly single-phase (alpha) alloys do not decrease significantly with decreasing temperature. Alloys containing high volume fractions of the body-centered-cubic (bcc)  $\beta$  phase may show some low-temperature sensitivity to impact loads. Charpy V-notch impact strengths of six copper alloys are listed as functions of temperature in Table 45. On the other hand, the temperature-dependent ductility of  $\beta$ -containing alloys at elevated temperatures is useful, as it facilitates hot forging, extrusion, and rolling operations.

**Table 45** Impact Properties of Cast Copper Alloys

Alloy (UNS)	Temperature °F (°C)	Charpy V-Notch Impact Strength, ft-lb (J)	Alloy (UNS)	Temperature °F (°C)	Charpy V-Notch Impact Strength, ft-lb (J)	Alloy (UNS)	Temperature °F (°C)	Charpy V-Notch Impact Strength, ft-lb (J)
C83600	-305 (-188)	11 (15)	C92200	-320 (-196)	13 (18)	C95500	-305 (-188)	12 (16)
	-100 (-74)	13 (18)		-108 (-78)	14 (19)		-200 (-130)	16 (22)
	68 (20)	19 (26)		68 (20)	19 (26)		-78 (-60)	18 (24)
	392 (200)	15 (20)		212 (100)	14 (19)		68 (20)	18 (24)
	572 (300)	13 (18)		392 (200)	13 (18)		392 (200)	28 (38)
C86500	-305 (-188)	12 (16)	C95200	572 (300)	12 (16)	C95700	572 (300)	26 (35)
	-100 (-74)	19 (26)		-320 (-196)	25 (34)		-290 (10)	10 (14)
	68 (20)	19 (26)		68 (20)	30 (41)		-148 (-100)	16 (22)
	212 (100)	18 (24)		212 (100)	33 (45)		-58 (-50)	23 (31)
							68 (20)	32 (41)

Source: Copper Development Association.

## 4 CORROSION BEHAVIOR

Copper and its alloys derive their inherent corrosion resistance from their tendency to form stable, adherent, and protective corrosion product films (tarnishes and patinas) when exposed to corrosive environments. Once established and left undisturbed, such films sharply limit the progress of corrosion reactions by inhibiting the ingress of oxygen, sulfur, and other corrodants.

Copper and brass tubes, valves, and fittings are widely used for handling of potable water. Stable corrosion films typically form and coat the insides of such tubes. Catastrophic corrosion is not encountered in properly treated waters, although copper and low-zinc brasses are affected by waters containing high concentrations of carbon dioxide. High iron concentrations can cause pitting, whereas low pH can lead to excessive copper dissolution and can also cause dezincification of so-called uninhibited (against dezincification) yellow brass. Hard, alkaline waters are generally benign toward copper. Untreated waters or waters containing inadequate concentrations of chlorine and copper can provoke pitting corrosion under biofilms that can form on the inside of copper tubes under certain conditions.

NSF standard 61<sup>8</sup> limits the amount of lead and copper permitted in potable waters contained in or transmitted through certain plumbing products. Metal can leach into the water from exposed surfaces under stagnant conditions at low pH. Lead and copper levels in such water can often be limited by redesigning the fixture, but where this option is not available, lead-free *EnviroBrasses* C89510, C89520, and C89550 can be specified in place of ordinary plumbing brasses. The alloys' bismuth and selenium contents provide the high machinability needed for cost-effective production rates.

Many copper alloys are well-suited for use in seawater environments, and indeed, some of these alloys—and copper itself—have been used in marine applications for centuries. Preferred marine alloys include copper nickels, which exhibit the highest corrosion and erosion resistance among copper metals, and also offer relatively high strengths, and aluminum bronzes, which are stronger still, as well as ultrahigh-strength beryllium copper, inhibited aluminum brass, phosphor bronzes, arsenical admiralty brass, and nickel silvers. Copper alloys that perform well in seawater are also often acceptable for use with industrial and process chemicals. Copper nickels, aluminum bronzes, silicon bronzes, manganese bronzes, and tin and phosphor bronzes should be considered for such environments. Table 46 provides general guidelines.

**Table 46** Guidelines for Copper Alloy Selection in Corrosive Environments

Environment	Comments
Concentrated or dilute acids or alkalis not containing air or other oxidants (nitric acid, dichromates, chlorine, and ferric salts), complexing agents [cyanides, ammonia, chlorides (when hot), amines], and compounds that react directly with copper (sulfur, hydrogen sulfide, silver salts, mercury and its compounds, acetylene).	Tin bronzes, silicon bronzes, nickel silver, copper aluminum bronzes, and low-zinc brasses are generally acceptable.
Dilute or concentrated acids or acid salts, both organic and inorganic.	Yellow brasses and other high-zinc alloys should not be specified.
Dilute or concentrated alkalis, neutral chloride or sulfate solutions, or mild oxidizing agents such as calcium hypochlorite, hydrogen peroxide, and sodium nitrate.	High-zinc alloys should not be specified.
Nonoxidizing acetic, hydrochloric, and phosphoric acids.	Tin bronzes, aluminum bronzes, nickel silver, copper, and silicon bronzes recommended. High-zinc alloys should not be specified.
Hot and concentrated hydrochloric acid.	May be aggressive toward alloys that resist attack when the acid is cold and dilute.
Nitric, chromic, and other oxidizing acids.	Copper alloys not recommended.
Alkalis.	70-30 copper-nickel alloys recommended for concentrated bases; high-tin bronzes, nickel silver, silicon bronzes, and most other alloys except high-zinc brasses can be used with dilute bases. Aluminum bronzes not containing tin are susceptible to dealumination in hot dilute alkalis.
Ammonium hydroxide, substituted ammonium compounds, amines, and cyanides. Mercury, mercury salts.	Copper alloys should be avoided.
Neutral salt solutions.	Generally safe with most copper alloys, although corrosion rates may vary. Chlorides are more aggressive than sulfates and carbonates, especially in aerated solutions. Copper nickels and aluminum bronzes are preferred for use with concentrated brines.
Basic salts.	Behavior similar to that of hydroxides but less aggressive.
Gases.	Do not attack copper alloys when dry but can become aggressive when moist. All copper alloys are attacked by moist chlorine, but chlorinated water can be handled by high-tin bronze, nickel silver, and copper. High-zinc brasses are attacked by moist carbon dioxide.
Organic compounds.	Generally benign toward copper alloys. Exceptions include hot, moist, chlorinated hydrocarbons and aerated organic acids. Moist acetylene forms explosive compounds in contact with copper and alloys containing more than 65% copper.
Foodstuffs and beverages.	Contact with acidic foodstuffs and beverages can impart a metallic taste and should be avoided. Copper and copper alloys are suitable for brewing and distilling, and nickel silvers are commonly used with dairy products. Leaded alloys should be used with caution.

## 4.1 Forms of Corrosion

Copper alloys are widely used in aggressive environments, but they should be used with caution in certain media, where corrosion can take one or more of the following forms:

1. *Dealloying* or “*parting*” corrosion is observed in brasses exposed to seawater and stagnant, neutral, or slightly acidic freshwaters, especially under sediments or biomass deposits. Additions of arsenic or antimony strongly reduce the phenomenon, forming *inhibited* dezincification-resistant brasses, such as C31400, C31600, C35330, C69430, C69710, C87800, or C87900. These alloys should be used where dealloying conditions are present. Certain aluminum-rich aluminum and nickel–aluminum bronzes are also vulnerable to dealloying, although susceptibility can be reduced through heat treatment and eliminated entirely by cathodic protection.

2. *Erosion–corrosion* and *cavitation* occur when protective corrosion films are removed by high-velocity fluids faster than the films can regenerate. The phenomenon is often encountered on bronze ship propellers and industrial impeller blades. Entrained particulates in the fluid accelerate the process. Critical flow velocities for selected copper alloys, below which erosion–corrosion does not occur, are listed in Table 47.

3. *Galvanic*, or *dissimilar-metal, corrosion* can occur when two metals with significantly different electrochemical potentials are joined in a corrosive environment. The more noble (cathodic) metal in the couple is protected at the expense of the more reactive (anodic) one. For example, copper alloys can accelerate corrosion in aluminum and mild steel, especially if the area ratio of copper to the anodic metal is large. Conversely, copper alloys can corrode when coupled to gold, silver, platinum group metals, or carbon (or graphite). In either case, electrically insulating the coupled metals from one another or physically isolating it from the aggressive environment with protective coatings prevents attack.

4. *Stress corrosion*, or *environmentally assisted cracking (EAC)*, occurs in many copper alloys exposed to aqueous ammonium ions, nitrites, mercury compounds, and moist atmospheres containing sulfur dioxide if the metals are under imposed or residual tensile stress. Yellow brasses are especially vulnerable. Tin bronzes, red brasses, and aluminum bronzes are less sensitive, while pure copper and copper nickels are essentially immune.

**Table 47** Velocity Guidelines for Copper Alloys in Pumps and Propellers Operating in Seawater

Alloy (UNS)	Peripheral Velocity, ft/s (m/s)
C83600	<30 (9.1)
C87600	< (9.1)
C90300, C92200	< (13.7)
C95200, C86500	< (22.8)
C95500, C95700, C95800	> (22.8)

Source: Copper Development Association.

### ***Corrosion, Copper, Health, and the Environment***

Corrosion implies the dissolution of metal and its release to the environment or to a medium from which it can be taken up by organisms, possibly with harmful consequences. Such releases can ensue from day-to-day use of copper products, such as plumbing goods and roofing sheet, or from disposal of copper-containing electronic equipment in a landfill. In an effort to avoid harmful impacts to the environment, regulations and, in some cases, design standards have been introduced to limit such releases.

However, It must be understood that toxicity occurs only at concentrations above certain minimum levels and that those levels can vary widely among the array of offended biospecies involved. Low concentrations of soluble copper in the food chain can be harmless or, more importantly, beneficial to health since copper is an essential nutrient for most living species, including humans. Inadequate copper intake can result in deficiency and detrimental physiological consequences from infancy to adulthood.

Copper, once thought to be “toxic, persistent, and bioaccumulative” by the U.S. Environmental Protection Agency (EPA), has been the subject of a large body of research over the past several decades that seeks to understand the metal’s behavior with respect to health and the environment. Results of those studies show that, while *ionic* copper exhibits some degree of toxicity in organisms above concentrations as described above, the offending ionic copper species are readily transformed in nature via rapid and nearly complete binding of the copper by organic complexing agents. In other cases, they are transformed to far less soluble, and hence less bioavailable, inorganic species. Toxicity is thereby sharply reduced. Changes have been made in environmental regulations as a result of our increased understanding of the behavior of copper in the environment. Significantly, copper was removed from the EPA list of persistent, bioaccumulative and toxic (PBT) substances in 2004.

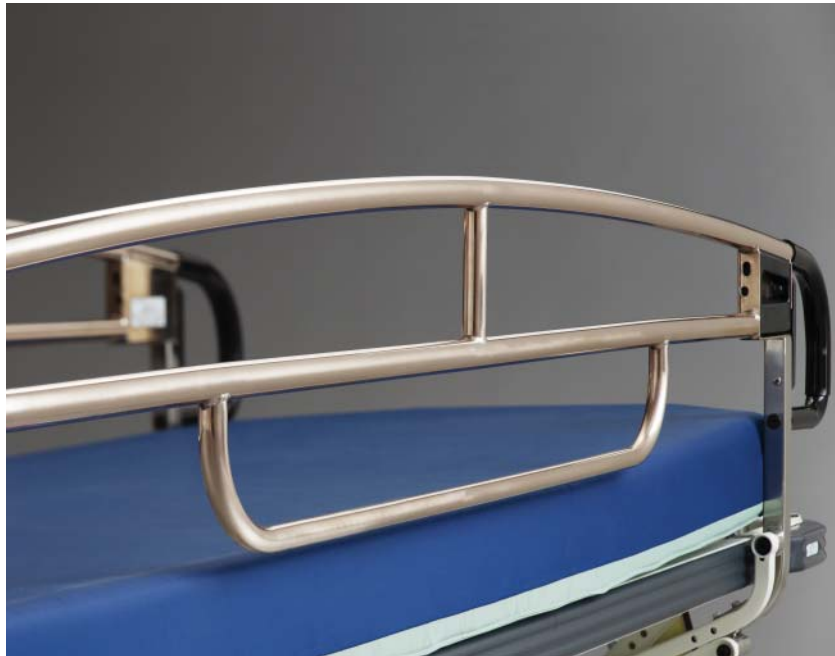
Copper and its alloys are among the most thoroughly recycled industrial metals. Scrap copper can be (and is) re-refined to primary purity standards, but it is more often used as feedstock for nonelectrical products and as a base for alloys. In 2003, the U.S. economy consumed approximately 26.4% as much scrap copper as it did primary refined copper. Recycling also conserves energy: Studies conducted in 1997 suggest that copper produced from ore consumes 62 MJ/kg, whereas clean scrap that requires only remelting requires approximately 8 MJ/kg for reuse; scrap that requires electrolytic refining consumes approximately 10 MJ/kg, and resmelted scrap requires approximately 28 MJ/kg.

## **4.2 Biostatic and Antimicrobial Properties**

### ***Biostatic Properties***

Copper and alloys containing at least 60% copper inhibit the growth of organisms on metallic surfaces, a property that has been exploited since copper plates were first used to protect wooden ship hulls centuries ago. The metal toxicity toward these organisms makes surfaces inhospitable to marine life forms such as algae and barnacles, while at the same time causing no harm to the environment. Most vessels are now protected by sacrificial anodes or copper-containing antifouling paints and coatings, although metallic copper sheathing is still applied to some smaller personal and commercial vessels. The biostatic properties of copper alloys themselves are widely exploited to maintain unobstructed flow in marine valves, condenser tubing, sea-water piping, and inlet screens. Copper water tubes, as well as copper and brass fittings and plumbing goods, are known to inhibit the growth of pathogens such as *Pneumophila legionella*, which causes Legionnaires’ disease, and it was observed as early as the 1980s that brass door-knobs and push plates used in hospitals remain essentially pathogen free.

Aqueous solutions of copper salts have a long history in agriculture, principally as fungicides. Of these, the centuries-old Bordeaux mixture (copper sulfate and hydrated lime) is the



**Figure 2** The handrails on this modern stretcher are constructed from an antimicrobial copper alloy. Antimicrobial copper alloys retard the growth of many pathogens. (Photo courtesy of Pedigo Products, Inc.)

best known; other copper fungicides in current use include copper ammonium carbonate and copper soap (copper octanoate).

### ***Antimicrobial Copper***

Extensive research has conclusively shown that copper and copper alloy surfaces continuously kill pathogens that commonly inhabit touch surfaces such as bannisters, bedrails, push plates, handrails, and doorknobs (Fig. 2).

Under laboratory conditions, bacteria counts of potentially lethal methicillin-resistant *Staphylococcus aureus* (MRSA), *Escherichia coli* O157:H7, and vancomycin-resistant *Enterococcus faecalis* (VRE), among others, are continuously reduced by greater than 99.9% within 2 h, whereas the same pathogens placed on stainless steel and polyethylene surfaces can survive for days. In a clinical setting, researchers found that antimicrobial copper surfaces continually reduced bacteria levels found on surfaces in hospital intensive care units (ICUs) by 83%.

Based on data such as these (and others), the EPA has granted official antimicrobial public health registration to hundreds of coppers and copper alloys and designers can lawfully claim antimicrobial action for registered product applications.

Antimicrobial copper's ability to kill pathogens, along with its commercial availability in all product forms and a full spectrum of copper alloy colors, has made it a viable option in architectural applications in which potential health issues exist. Examples include touch surfaces in hospitals, food-handling facilities, public transportation, and schools.



### 4.3 Fabrication

#### *Machining*

All copper alloys can be machined using standard tooling and machining operations. High-speed steel suffices for all but the hardest alloys, although both high-speed and carbide tooling can be used without lubrication when cutting leaded alloys such as free-cutting brass, alloy C36000, and leaded or bismuth-containing cast plumbing brasses.

*Chip Appearance and Machinability.* The copper alloys' wide range of physical and mechanical properties are expressed in three types of machining chips (Fig. 3). Free-cutting alloys containing lead, sulfur, tellurium, or combinations of selenium and bismuth produce type I chips. The chips are short and fragmented and are easily cleared from the cutting zone. These alloys are intended for high-productivity machining operations. Alloys with multiphase microstructures tend to produce short, curly, type II chips. The alloys are readily machinable but at slower rates than those of type I alloys. Copper and ductile single-phase alloys produce long and stringy- type III chips. The alloys' low hardness facilitates cutting, but attention to tool design is important for optimum workpiece quality.

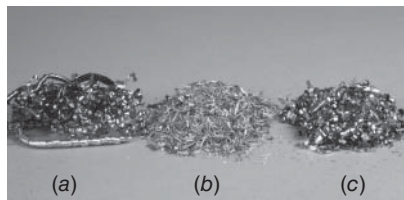
Machinability is commonly reported on a scale of 1 to 100, on which free-cutting brass, C36000, ranks 100. Other type I copper alloys are rated between 50 and 100; type II alloys, between 30 and 50; and type III alloys, between 20 and 40. By comparison, when tested according to ASTM E 618, *Tentative Method for Evaluating Machining Performance on an Automatic Screw/Bar Machine*, leaded free-machining steel 12L14 has a machinability rating of approximately 21.

Type I alloys include leaded coppers, brasses, bronzes and nickel silvers, architectural and forging brasses, tellurium, and sulfur-bearing coppers and alloys. Type II alloys include aluminum and nickel–aluminum bronzes, beryllium coppers, manganese bronze, Naval brass, silicon red brass, and aluminum oxide dispersion-strengthened coppers. Type III alloys include nonleaded brasses, bronzes, and nickel silvers, as well as silicon bronzes, coppers, high-copper alloys, low-aluminum bronzes, and copper nickels.

#### *Recommended Machining Practices*

Recommended tool geometries are illustrated in publications available from the Copper Development Association, Inc. The following guidelines can be used as starting points from which optimum conditions can be planned for various machining operations.

*Single-Point Turning Tools.* Type I alloys require little or no rake, and modest clearance angles can be used but are not necessary unless the tool tends to drag (Figs. 4a and 4b). Free-cutting brass can be cut at maximum attainable speed; speeds for other leaded alloys range from 300 to



**Figure 3** Three types of copper alloy machining chips: (a) type I (C36000 free-cutting brass), (b) type II (High-strength brass), (c) type III (C11000 copper). Courtesy of The Copper Development Association, Inc.

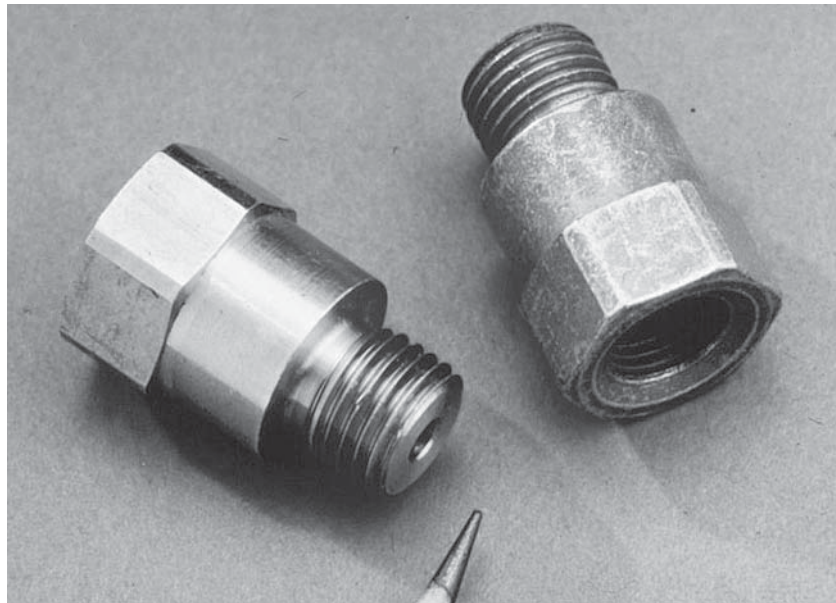
1000 sfm (91–305 m/min). Straight light mineral oils are generally preferred, but soluble oils also give good results.

Type II alloys exhibit a wide range of properties, and cutting parameters vary accordingly. Ductile alloys should be cut with rake angles of  $10^\circ$  with reasonable clearance. Less ductile alloys require little or no rake to avoid chatter. Cutting speeds between 150 and 300 sfm (46 and 92 m/min) are recommended for high-speed steel single-point and form tools. Speeds can be increased to between 400 and 600 sfm (122 and 183 m/min) with carbide tooling. Begin with light cuts, 0.002 in./rev (0.05 mm/rev) and increase feed until surface finish and/or wear rates deteriorate. Alloys that tend to type III behavior require cutting fluids that provide effective lubrication and cooling. Mineral oil fortified with between 5 and 15% lard oil or a sulfurized fatty oil base thinned with a light mineral oil gives good lubrication. Alloys with higher machinability ratings can be cut with soluble oils.

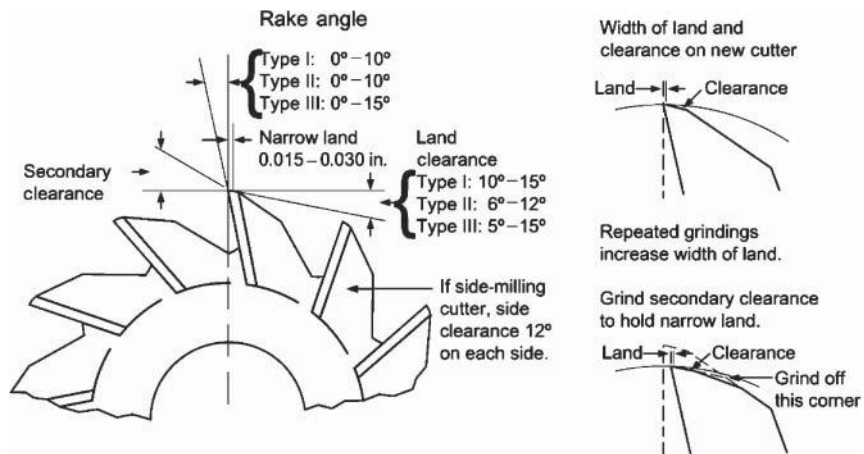
Type III alloys require generous rake angles. Single-point tools should be ground with a back rake of  $10^\circ$ – $20^\circ$  and a side rake of as much as  $20^\circ$ – $30^\circ$ . Rake angles can be reduced somewhat with single-point carbide tools and dovetail or circular form tools. Coppers and copper nickels tend to build up on the tool face, but burnishing the tool to a smooth finish reduces this tendency, as does the application of low-friction coatings such as titanium nitride. High-speed form tools should be ground with a front clearance angle between  $7^\circ$  and  $12^\circ$ ; the clearance angle can be reduced slightly with carbide tooling.

Recommended straight-blade and circular cut-off tool geometries are illustrated in Fig. 4c; geometries for carbide and high-speed circular and dovetail form tools are illustrated in Fig. 4d.

*Milling.* Free-cutting type I alloys can be milled at speeds up to 500 sfm (152 m/min) (Fig. 5). Carbide tooling permits the highest speeds. Rake angles of  $0^\circ$ – $10^\circ$  are recommended, and land clearance should be between  $5^\circ$  and  $15^\circ$ . Side milling cutters require a  $12^\circ$  clearance on



**Figure 4** Brass (left) and chromate-dipped leaded steel (right) pneumatic fittings. Courtesy of The Copper Development Association, Inc.



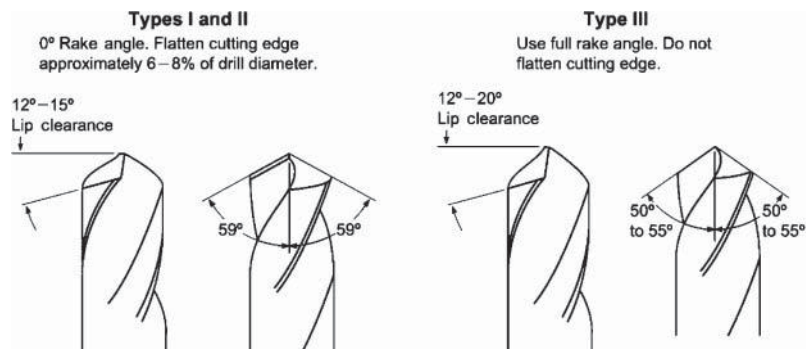
**Figure 5** Milling cutter rakes and clearances. Courtesy of The Copper Development Association, Inc.

each side. Cutting fluids are needed for heat removal at high speeds but are sometimes not used under moderate milling conditions.

Short-chip type II alloys can tolerate rake angles between  $0^\circ$  and  $10^\circ$ , but optimum conditions should be selected for individual alloys. Small-diameter cutters should be ground with  $0^\circ$  rake for hard aluminum bronzes. Milling speeds can be as high as 200 sfm (61 m/min) with feed rates between 0.016 and 0.022 in./rev (0.4 and 0.56 mm/rev) for spiral cutters and from 0.010 to 0.022 in./rev (0.25 to 0.056 mm/rev) per tooth for end mills. Soluble oils are satisfactory, as are mineral oils containing about 5% lard oil.

Long-chip type III alloys require milling cutters with tooth spacing no finer than four to eight teeth per inch to facilitate chip removal. Spiral cutters are useful for wide cuts, for which helix angles as large as  $53^\circ$  have been found to be satisfactory. Generous rake angles (up to  $15^\circ$ ) and adequate clearance (up to  $15^\circ$ ) should be provided. Radial undercuts prevent tooth edges from dragging, and cutting faces should be finely polished to reduce build-up. Recommended milling speeds range from 50 to 100 sfm (15–45 m/min); feed rates range from 0.007 to 0.030 in./rev (0.18–0.76 mm/rev).

*Drilling.* Standard twist drills are satisfactory for most copper alloys; however, high production rates might require special drill configurations (Fig. 6). Small-diameter holes in copper



**Figure 6** Drillpoint and clearance angles. Courtesy of The Copper Development Association, Inc.

are best cut with fast-twist drills, while free-cutting grades can be cut very rapidly with straight-fluted “brass” drills. Full rake angles are normally retained in drills used on long-chip type III alloys. Drill-tip angles should be between  $100^\circ$  and  $110^\circ$  and lip clearance angles may have to be as steep as  $20^\circ$ . Notching the cutting edge helps break up stringy chips. Drills for short-chip type II alloys and free-cutting type I alloys should be flat-ground to a  $0^\circ$  rake, with standard  $118^\circ$  tip angles and lip clearances between  $12^\circ$  and  $15^\circ$ . Speeds are similar to those for turning, and small-diameter holes can be drilled at maximum spindle speed. Recommended feed rates range from 0.002 to 0.030 in./rev (0.05–0.76 mm/rev) depending on alloy, i.e., higher rates for free-cutting alloys and lower rates for types II and III alloys. Cutting fluids are beneficial but not necessary with free-cutting alloys but may be required for others.

**Boring.** For best surface condition, free-cutting alloys should be bored with a  $0^\circ$  back rake angle, a  $5^\circ$  side rake angle, and speeds of 500–1000 sfm (152–305 m/min) (Fig. 7). Rake angle can be increased to between  $0^\circ$  and  $5^\circ$  in type II alloys and between  $5^\circ$  and  $10^\circ$  in type III alloys. Side rake angles will range between  $5^\circ$  and  $10^\circ$  and between  $15^\circ$  and  $20^\circ$  for types II and III alloys, respectively. Recommended cutting speeds will range between 400 and 600 sfm (122 and 183 m/min) for type II alloys and between 200 and 500 sfm (61 and 152 m/min) for type III alloys.

**Reaming.** Fluted reamers used with copper alloys are similar to those used with steel, except that clearances should be increased to  $8^\circ$ – $10^\circ$  (Fig. 8). A rake angle (hook) of  $5^\circ$  is used on all copper alloys except free-cutting alloys, which are generally reamed with zero or negative rake. Cutting tools must be lapped to a fine finish. Speeds for copper and other long-chip alloys will range from 40 to 90 sfm (12–27 m/min), 75 to 150 sfm (23–76 m/min) for short-chip alloys, and 100 to 200 sfm (30–61 m/min) for free-cutting type I alloys.

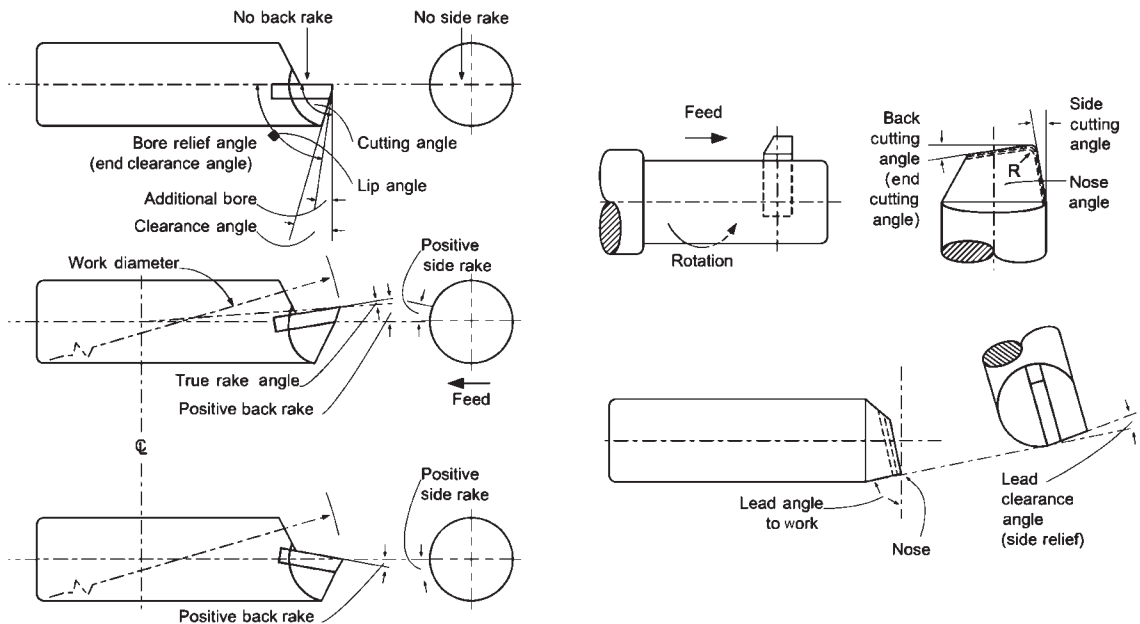
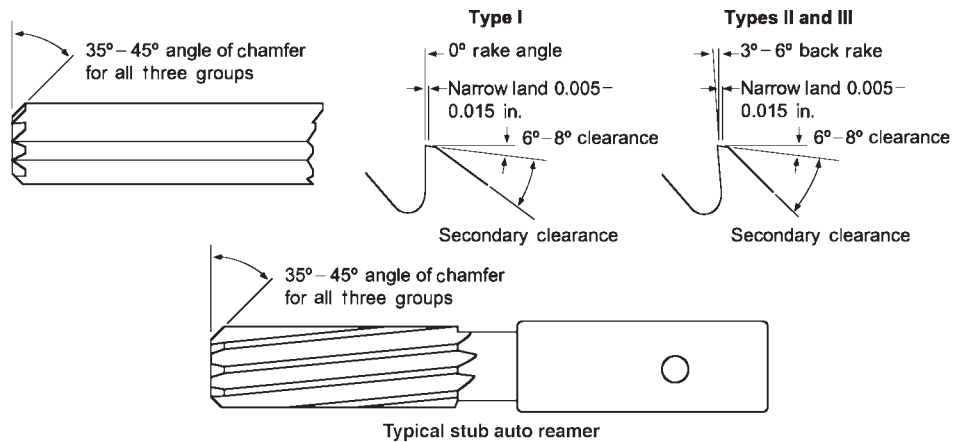


Figure 7 Boring tools. Courtesy of The Copper Development Association, Inc.



**Figure 8** Reamer angles and clearances. Courtesy of The Copper Development Association, Inc.

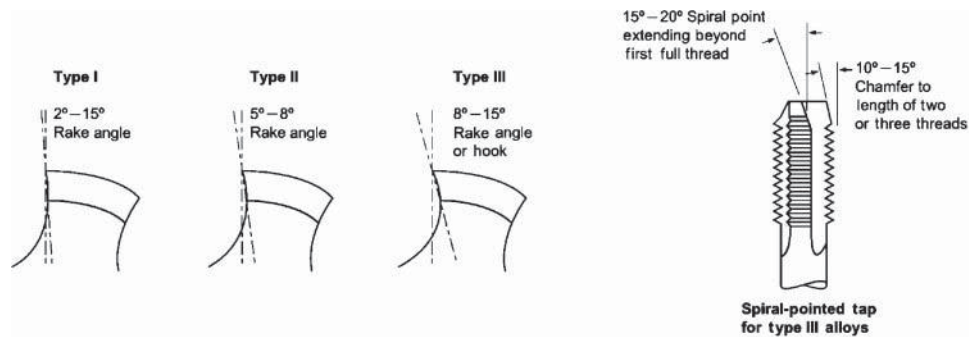
**Threading and Tapping.** Free-cutting brass accepts fine- to medium-pitch rolled threads quite well, but coarse or deep threads may call for alloys such as C34000, C34500, or C35300, which have lower lead contents and are more ductile than C36000. Ductile nonleaded alloys can be roll threaded; operations proceed best when alloys are in the annealed condition. Thread die cutting generally follows the recommendations for turning operations: soft, ductile long-chip alloys require large rake angles ( $17^{\circ}$ - $25^{\circ}$  and up to  $30^{\circ}$  for pure copper); hard multiphase type II alloys require intermediate rake angles, generally  $12^{\circ}$ - $17^{\circ}$  but up to  $25^{\circ}$  for high-strength aluminum bronze. Free-cutting brass and other highly leaded alloys require zero rake angles. See Figs. 9a and 9b for recommended tool geometries.

**Sawing.** Coarse teeth are better for cutting soft or thick materials; finer teeth should be used with hard materials and thin sections (Fig. 10). Sawing conditions range from between 130 and 150 strokes/min for type I alloys to between 90 and 120 strokes/min for type II alloys and between 60 and 90 strokes/min for type III alloys. Thin rods of type I alloys less than  $1\frac{1}{2}$  in. (38 mm) in diameter can be circular sawed at rim speeds between 4000 and 8000 sfm (1220 and 2440 m/min) at feeds of 60 in./min (1524 mm/min). Speeds and feeds are reduced by between one-third and one-half for types II and III alloys, respectively. Thicker sections require proportionately slower speeds and lower feed rates.

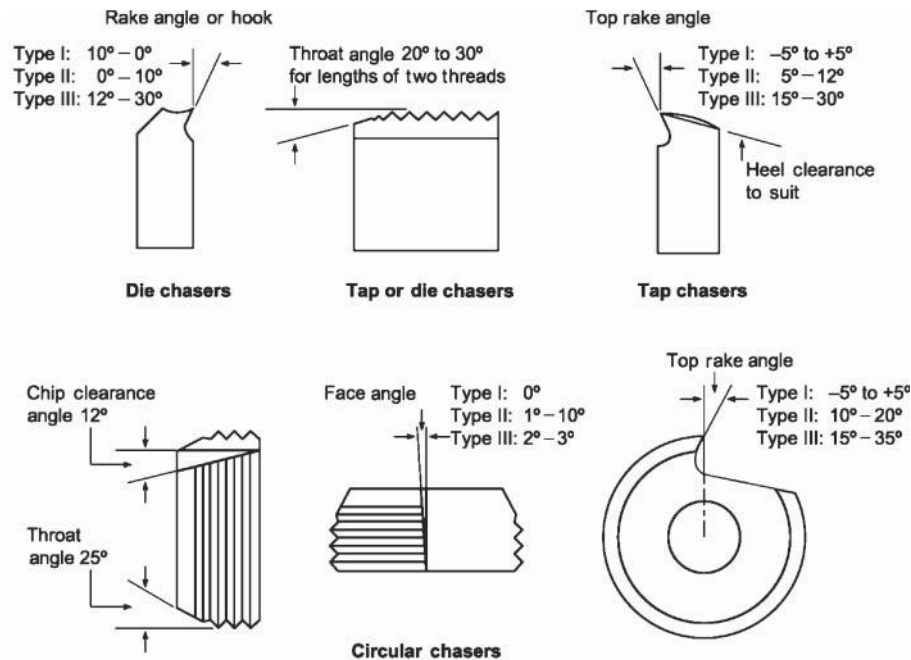
#### **Free-Cutting Brass Machining Economics**

Free-cutting brass (C36000) and leaded free-machining steel (12L14) have competed closely in the past on the basis of mechanical properties for large-volume screw-machined parts such as automotive fittings. Brass's faster machining rates along with the value of recycled brass scrap more than made up for differences in raw materials cost. When raw material cost differences are large, brass retains an advantage in environmental and quality issues such as its nearly 100% recycling rates and inherent corrosion resistance, which can reduce or eliminate the need for electroplating, conversion coating, or painting.

The high value of brass machining scrap reduces the effective difference between as-machined parts costs for brass and steel parts, especially in products that require extensive metal removal. The pneumatic fitting shown in Fig. 4, a typical screw-machine product machined from rod, generates 71% scrap in the form of readily recyclable turnings.



(a)



(b)

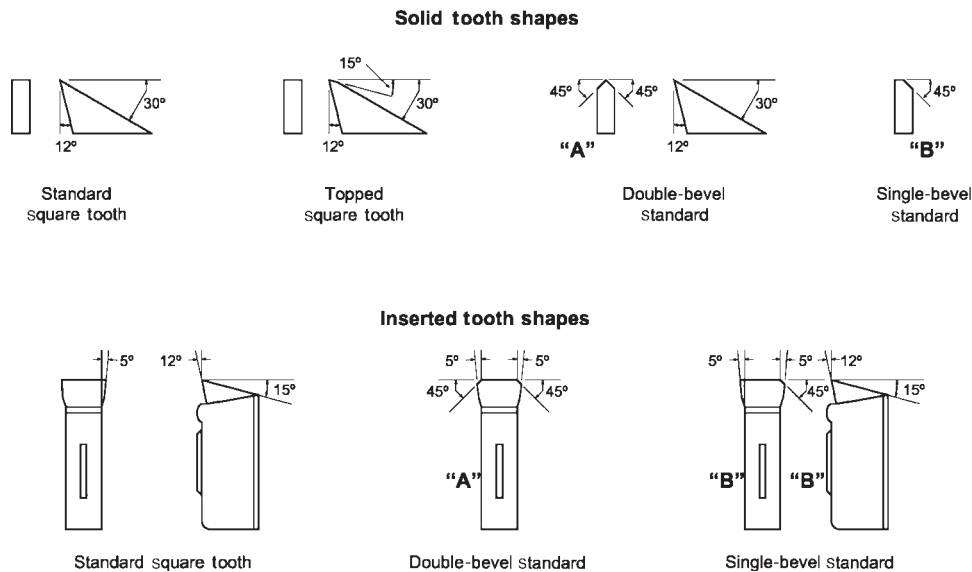
**Figure 9** (a) tap rake angle; (b) chasers for die heads and collapsible tools. Courtesy of The Copper Development Association, Inc.

## 4.4 Casting

Copper casting alloys are widely used in the manufacture of plumbing, electrical, and mechanical products and for bearings and industrial valves and fittings. The large selection of available alloys enables the designer to choose a combination of physical, mechanical chemical (corrosion-resistant), and antimicrobial properties that best suit product requirements.

Sand casting accounts for approximately 75% of U.S. copper alloy foundry production. It is relatively inexpensive, acceptably precise, and highly versatile, being applicable to castings ranging in size from a few ounces to many tons. It can be used with all copper alloys.





**Figure 10** Solid and insert tooth shapes for circular saws. Courtesy of The Copper Development Association, Inc.

Copper alloys can be cast by shell, plaster, and investment methods and the continuous and centrifugal processes. Centrifugal casting, in particular, is also used for a large variety of industrial goods such as valves, bearings (which are also continuously cast), marine propeller housings, hydraulic cylinders, flanges, fittings, and other cylindrical items. The choice among processes depends on product requirements, the number of castings to be produced, and, for small runs, cost.

Metal-mold processes such as static, low-pressure and vacuum permanent mold casting, pressure die casting, and semisolid casting are also used extensively with copper alloys. These processes are best applied to alloys with wide freezing ranges and are less well suited for (although not excluded from) pure copper, high-copper alloys, and other alloys that solidify over a narrow temperature span. Examples of acceptable alloys include red-, semi-red and yellow brasses, silicon brasses, manganese bronzes, nickel silvers, and aluminum and nickel–aluminum bronzes.

Permanent-mold castings are characterized by good part-to-part dimensional consistency and very good surface finishes (about  $70\ \mu\text{in.}$ ,  $1.8\ \mu\text{m}$ ). Rapid solidification tends to create finer grain sizes, which lead to somewhat higher mechanical properties than those for sand castings, as shown in Table 4. Die costs can be relatively high, but the overall costs of the processes are quite favorable for medium-to-large production runs.

Squirrel cages for high-efficiency AC induction motors, products formerly limited exclusively to aluminum, are now routinely cast as well in high-conductivity copper by using the high-pressure die-casting process. Such motors suffer fewer  $I^2R$  losses than aluminum motors. Additional information is available from the Copper Development Association, Inc.

The semisolid casting process is similar to pressure die casting except that it is performed between the liquidus and solidus temperatures while the alloy is in a semisolid or “slushy” state. Castings exhibit freedom from porosity (pressure tightness), improved mechanical properties compared with sand cast alloys, and excellent surface finish. Die costs are relatively high but can be offset by large production quantities and the process’s ability to cast to near-net shapes.

## 4.5 Forging

Hot forging is used effectively for the manufacture of high-quality, near-net shape products requiring combinations of soundness, uniform mechanical properties and dimensional tolerances, and good surface finish. Medical gas mixing valves, pressure regulator housings, and architectural and electrical hardware are typical examples. Forging brass, C37700, is the workhorse hot-forging alloy (in addition to its good forging characteristics, the alloy contains lead for high machinability), but the process is also applicable to other high-zinc brasses and alloys containing sufficient  $\beta$  phase to ensure hot ductility.

## 4.6 Welding, Brazing, and Soldering

### *Coppers and High-Copper Alloys*

Most coppers and many copper alloys are readily weldable, the exceptions being un-deoxidized coppers and alloys containing lead, bismuth, or selenium. All copper alloys can be brazed and soldered.

Welding processes used include gas–tungsten arc (GTAW), gas–metal arc (GMAW), and, to a much lesser degree, oxyfuel welding (OFW). Shielded metal arc welding (SMAW) and resistance welding are generally not recommended for copper. Less conventional processes such as friction welding, electron beam (EB) welding and laser welding produce very high quality joints in copper and high-copper alloys. The suitability of joining processes for coppers and high-copper alloys is given in Table 48.

Oxygen-free grades such as C10100 are highly weldable. Their low dissolved oxygen content (<10 ppm) avoids the generation of porosity that can arise in, for example, electrolytic tough pitch copper, C11000, when welding is performed in the presence of hydrogen, as in atmospheric moisture or surface contamination. This hydrogen reacts with dissolved oxygen to generate water vapor in the liquid metal pool. Susceptible coppers, such as C11000, should be joined by brazing or soldering. Deoxidized coppers, such as C12200, are not vulnerable to hydrogen-related welding defects.

Pure copper's high thermal conductivity requires higher heat input during welding than do other materials, including copper alloys. Preheat and maintenance of high interpass temperatures is important for adequate penetration. Note that the high heating requirements will anneal out the effects of cold work, if any, in the base metal.

High-copper alloys (C16000–C19900) are weldable, but the effect of prior heat treatment, if any, may be lost in the heat-affected zone (HAZ). For best results, these alloys should be welded in the solution-annealed condition and heat treated (aged) after welding. High-copper alloys have somewhat lower thermal conductivity than pure copper and require less preheat and lower interpass temperatures.

**Table 48** Welding Processes for Coppers and High-Copper Alloys<sup>a</sup>

Alloy	UNS No.	OFW	SMAW	GMAW	GTAW	RW	SSW	Brazing	Soldering	EBW
OF Cu	C10100-C10800	F	NR	G	G	NR	G	E	E	G
ETP Cu	C11000-C11900	NR	NR	F	F	NR	G	E	G	NR
Deox Cu	C12000-C12300-C17500	G	NR	E	E	NR	E	E	E	G
Be Cu	C17000-	NR	F	G	G	F	F	G	G	F
Cd/Cr Cu	C16200/ C18200	NR	NR	G	G	NR	F	G	G	F

<sup>a</sup>E=Excellent, G=Good, F=Fair, NR=Not Recommended.

Source: Copper Development Association.



***Dissimilar-Metal Combinations***

Successful and safe dissimilar-metal weld joints can be made in coppers and copper alloys and between copper metals and other metals if a reasonable amount of precaution is taken before and during welding, especially with regard to differing coefficients of thermal expansion.

Aluminum bronze (AWS A5.6/ER CuAl-A2) and silicon bronze (AWS A5.6/ER CuSi) are used to join dissimilar metals. Deoxidized coppers, including AWS A5.6/ERCu, can also be used for many dissimilar-metal combinations, but they are not as versatile as either the silicon or aluminum bronze alloys. (Note that these metals are *welding* alloys, which are different from copper-based brazing alloys.) Aluminum bronze is the strongest of the four alloys. It has a slightly higher thermal conductivity and slightly lower coefficient of thermal expansion than silicon bronze. All copper alloys have good corrosion resistance.

Both silicon bronze and aluminum bronze can be used to weld ferrous and nonferrous metals and alloys to each other and in various combinations (Table 49). Other combinations are also weldable.

***Shielding Gas Requirements***

Argon, helium, or mixtures of the two are commonly used as shielding gases for GTAW and GMAW welding of copper and high-copper alloys. The choice of gas depends on the degree of heat input needed. Helium produces a higher heat input than argon and is normally used with thick sections. Helium–argon mixtures give intermediate heat input. As rule of thumb, use argon when manually welding sections less than 1/8 in. (3.2 mm) thick, although a mixture of 75% helium–25% argon can be used for the automatic welding of thin sections.

With GMAW, straight argon requires approximately 100°F (55°C) higher preheat temperatures than when welding with 100% helium. With GTAW, preheat temperatures should be raised by 200°F (110°C) for pure argon.

**4.7 Welding Processes**

High-quality joints are best made using GTAW or GMAW processes. Plasma arc welding (PAW) is also used, and conditions used with GTAW also generally apply to this process. SMAW can be used for less-critical joints, and it is not discussed here.

***GTAW***

Manual GTAW is generally preferred for thin sections. Some fabricators use automatic GTAW for relatively thick sections, claiming that the process affords better control than GMAW and

**Table 49** Dissimilar Metal Combinations Welded with Silicon Bronze and Aluminum Bronze

	Mild Steel	Galvanized Steel	Stainless Steel	Cast Iron	Copper	Copper-Nickel	Silicon Bronze	Aluminum Bronze	Brass
Mild Steel		X	X	X	X	X	X	X	X
Galvanized Steel	X		X	X	X		X	X	X
Stainless Steel	X	X			X	X	X	X	X
Cast Iron	X	X	X		X	X	X	X	X
Copper	X	X	X	X		X	X	X	X
Copper-Nickel	X		X	X	X		X	X	X
Silicon Bronze	X	X	X	X	X	X		X	X
Aluminum Bronze	X	X	X	X	X	X	X		X

Source: Copper Development Association.

is capable of producing x-ray quality welds for especially critical applications. That preference is not meant to imply that GMAW is an inferior process. GMAW is widely and routinely used to weld copper at economically favorable speeds.

Preheat should be considered for all thicknesses, but it is absolutely necessary for work thicker than about 0.1 in. (0.25 mm). Preheat temperatures are about 100°F (55°C) higher than those used for GMAW.

GTAW can be used in all positions and is best for out-of-position welding. Pulsed current is recommended for vertical and overhead work. Use direct current, with electrode negative.

### ***GMAW***

GMAW is normally used when welding heavy sections in copper. Preheat is important, and straight helium or a 75% helium–25% argon mixture is normally used as a shielding gas. When welding with 100% argon, recommended preheat temperatures are raised by about 100°F (55°C) over what they would be with helium. GMAW can be used for vertical and overhead work but pulsed current and small-diameter wire is recommended in such cases.

## **4.8 Joint Preparation**

Joint designs for welding copper and copper alloys are based on the metals' high thermal conductivity and the need to gain good penetration. Joint angles are generally 10°–20° wider than those used with steels and low-conductivity alloys. A separation of 3/32 in. (2.4 mm) should be used for square-groove butt joints. For double V-groove joints, use a total included angle between 80° and 90° and 3/32–1/8 in. (2.4–3.2 mm) joint separation. An 80°–90° included angle is also recommended for single V-groove joints, although no joint separation is necessary in this case.

All welded surfaces should be thoroughly cleaned, dry and degreased. Wire brushing normally suffices for pure coppers, but beryllium coppers and other copper alloys that form tightly adhering oxide films may require grinding or chemical cleaning to provide completely bare surfaces.

## **4.9 Filler Metals**

The filler metal normally used to weld copper is deoxidized copper, supplied as wire or bare electrodes meeting AWS 5.6/ERCu. It contains 0.05% phosphorus maximum. In addition to phosphorus, deox copper contains manganese, tin, and silicon as deoxidizers and to increase fluidity and may also contain zinc and aluminum. Its conductivity ranges from about 15 to 40% IACS, which is considerably higher than other copper welding alloys.

Silicon bronze (AWS 5.6/ERCuSi) and aluminum bronzes (AWS 5.6/ERCuAl-1, AWS 5.6/ERCuAl-2, AWS 5.6/ERCuAl-3 ) also weld well with copper, and they are often used when joining copper to other metals (unless high conductivity is important). The alloys produce higher strength joints than are possible with deox copper (strength of CuAl-A1 < CuAl-A2 < CuAl-A3), although strength is often less important than conductivity in welded copper assemblies.

On the other hand, strength may be an important consideration when welding high-copper alloys. In such cases, aluminum bronzes or silicon bronzes can be used as filler metals.

## **4.10 Distortion Control**

The thermal expansion of copper metals is about 50% higher than that of carbon steels. Thermal conductivity can be as much as eight times higher. The potential for distortion during welding

is, therefore, considerably greater when welding copper than with steel. Small or light-gage components should be firmly clamped or fixtured to minimize warping. Multiple tack welds are also helpful, especially with large items or thick sections. Preheating, which is necessary in any case, is likewise beneficial since it tends to reduce temperature differences across large areas.

The thermal stresses that cause distortion can also lead to cracking, another reason for correct preheat, which minimizes these stresses. Root passes should be large. High heat input during the initial pass, along with copper's high conductivity, creates more uniform temperatures around the weld zone and, therefore, avoids the sharp thermal gradients that can lead to cracking. Copper or ceramic backing rings, when used in conjunction with GTAW, help control root-pass penetration.

### 4.11 Avoiding Cracking

Weld cracking most often occurs when the base and filler metals (or both of the base metals) have widely different melting points, thermal conductivities, or thermal expansion coefficients. The chance for cracking grows worse when more than one of these conditions is present at the same time. To prevent cracking caused by widely different melting points, filler metal with a melting point that lies between those of the base metals should be used. In some cases, it may be helpful to butter the filler metal onto the lower melting base metal before laying down the rest of the passes. Buttering also reduces dilution.

Differences in thermal conductivity between two base metals produce different heating and cooling rates on the two sides of the weld joint. The metal with the higher conductivity will tend to draw heat away from the weld zone, and in severe cases uneven heat flow may prevent complete fusion of the low-conductivity metal. Uneven heat flow can also lead to distortion in the finished assembly. Risk can be reduced by preheating the base metal with the higher conductivity, leading to a more even heating of the weld assembly. Heating the higher conductivity base metal also reduces the cooling rate after welding, reducing postweld thermal stresses.

Large differences in thermal expansion between two base metals (and between base metals and the filler metal) can arise during and after welding and during service. The stresses can be high enough to cause cracking in both cases. Cracking during welding is called hot cracking or hot tearing, and it results from the normal weakness of metals at high temperatures. Postweld cracking occurs when stresses are not adequately relieved. Cracking of this type is accelerated when the metals are cycled between low and high temperatures during service. Cracking can be avoided by selecting a filler metal with a thermal expansion coefficient that is intermediate between those of the two base metals and by applying preheat and, if necessary, postheat in order to reduce the level of thermal stresses during and after welding.

### 4.12 Weld Properties

As-cast copper is fairly soft, and ductility is high. Properties of welded joints are similar. That is, weld metal should have about the same strength and ductility as a fine-grained casting, and the properties of metal in the HAZ should resemble those of wrought and annealed metal. Any additional strength in the base metal due to prior cold work will be reduced, especially in regions in and near the HAZ. Welding reduces properties in heat-treated high-copper alloys.

### 4.13 Safety and Health

Copper and certain elements contained in high-copper alloys (chromium, beryllium, cadmium, arsenic, lead, manganese, and nickel) can cause serious health effects. Government regulations,

therefore, impose strict limits on exposure to welding fumes, dust, and grinding particles when elements that are known to be especially harmful are likely to be present. Respirators and fume exhaust systems must be used if called for, and eating or the storage of food and beverages near welding operations should be avoided.

## 5 TUBE AND PIPE PRODUCTS

### 5.1 Plumbing Tube

In the United States, copper plumbing tube is manufactured to meet the requirements of specifications established by ASTM. Table 50, reproduced from the Copper Development Association's *The Copper Tube Handbook*, lists the six standard types, applicable standards, uses, tempers, and commercially available lengths of plumbing tube.

Types K, L, M, DWV, and medical gas tube are designated by ASTM standard sizes, with the actual outside diameter always 1/8-in. larger than the standard size designation. Each type represents a series of sizes with different wall thicknesses. Type K tube has thicker walls than type L tube, and type L walls are thicker than type M, for any given diameter. All inside diameters depend on tube size and wall thickness. Copper tube for air-conditioning and refrigeration field service (ACR) is designated by actual outside diameter.

“Temper” describes the strength and hardness of the tube. In the piping trades, drawn temper tube is often referred to as “hard” tube and annealed as “soft” tube. Tube in the hard-temper condition is usually joined by soldering or brazing, using capillary fittings or by welding. Tube in the soft temper is commonly joined by the same techniques and also by the use of flare-type and compression fittings. It is also possible to expand the end of one tube so that it can be joined to another by soldering or brazing without a capillary fitting—a procedure that can be efficient and economical in many installations. Tube in both the hard and soft tempers can also be joined by a variety of mechanical joints that can be assembled without the use of the heat source required for soldering and brazing.

As for all materials, the allowable internal pressure for any copper tube in service is based on the formula used in the American Society of Mechanical Engineers Code for Pressure Piping (ASME B31):

$$P = \frac{2S(t_{\min} - C)}{D_{\max} - 0.8(t_{\min} - C)}$$

where  $P$  = allowable pressure, psi  
 $S$  = maximum allowable stress in tension, psi  
 $T_{\min}$  = wall thickness (min.), in.  
 $D_{\max}$  = outside diameter (max.), in.  
 $C$  = a constant

For copper tube, because of copper's superior corrosion resistance, the Code permits the factor  $C$  to be zero. Thus the formula becomes

$$P = \frac{2St_{\min}}{D_{\max} - 0.8t_{\min}}$$

The value of  $S$  in the formula is the maximum allowable stress (ASME B31) for continuous long-term service of the tube material. It is only a small fraction of copper's ultimate tensile strength or of the burst strength of copper tube and has been confirmed to be safe by years of service experience and testing. The allowable stress value depends on the service temperature and on the temper of the tube, drawn or annealed.

**Table 50** Types and Applications of Copper Tube Products\*

Tube type	Color code	Standard	Application <sup>d</sup>	Commercially available lengths <sup>b</sup>						
				Nominal or standard sizes	Drawn	Annealed				
Type K	Green	ASTM B 88 <sup>c</sup>	Domestic water service and distribution Fire protection Solar Fuel/fuel oil HVAC Snow melting Compressed air Natural gas Liquefied petroleum (LP) gas Vacuum	Straight lengths						
				1/4–8 in.	20 ft	20 ft				
				10 in.	18 ft	18 ft				
				12 in.	12 ft	12 ft				
				Coils						
				1/4–1 in.	—	60 ft				
				—	—	100 ft				
				1 1/4 and 1 1/2 in.	—	60 ft				
				2 in.	—	40 ft				
				—	—	45 ft				
				Type L	Blue	ASTM B 88	Domestic water service and distribution Fire protection Solar Fuel/fuel oil Natural gas Liquefied petroleum (LP) gas HVAC Snow melting Compressed air Vacuum	Straight lengths		
1/4–10 in.	20 ft	20 ft								
12 in.	18 ft	18 ft								
Coils										
1/4–1 in.	—	60 ft								
—	—	100 ft								
1 1/4–1 1/2 in.	—	60 ft								
2 in.	—	40 ft								
—	—	45 ft								
Type M	Red	ASTM B 88	Domestic water service and distribution Fire protection Solar Fuel/fuel oil HVAC Snow melting Vacuum					Straight lengths		
								1/4–12 in.	20 ft	N/A
				Coils						
				—						
				—						
				—						
DWV	Yellow	ASTM B 306	Drain, waste, vent HVAC Solar	Straight lengths						
				1 1/4–8 in.	20 ft	N/A				
				Coils						
—										
ACR	Blue	ASTM B 280	Air conditioning Refrigeration Natural gas Liquefied petroleum (LP) gas Compressed air	Straight lengths						
				3/8–4 1/8 in.	20 ft	<sup>d</sup>				
				Coils						
				1/8–1 5/8 in.	—	50				
				—						

**Table 50** (Continued)

Tube type	Color code	Standard	Application <sup>a</sup>	Commercially available lengths <sup>b</sup>		
				Nominal or standard sizes	Drawn	Annealed
OXY, MED, OXY/MED, OXY/ACR, ACR/MED	(K) Green, (L) Blue	ASTM B 819	Medical gas Compressed medical air Vacuum	Straight lengths		
				1/4–8 in.	20 ft	N/A

<sup>a</sup>There are many other copper and copper alloy tubes and pipes available for specialized applications.

<sup>b</sup>For information on these products, contact the Copper Development Association, Inc. Individual manufacturers may have commercially available lengths in addition to those shown in this table.

<sup>c</sup>Tube made to other ASTM standards is also intended for plumbing applications, although ASTM B 88 is by far the most widely used. ASTM Standard Classifications B 698 lists six plumbing tube standards including B 88.

<sup>d</sup>Available as special order only.

Source: Copper Development Association.

In Tables 50–54 the rated internal working pressures are shown for both annealed (soft) and drawn (hard) types K, L, M, and DWV copper tube for service temperatures from 100°F to 400°F. The ratings for drawn tube can be used for soldered systems and systems using properly designed mechanical joints. Fittings manufacturers can provide information about the strength of their various types and sizes of fittings.

When welding or brazing is used to join tubes, the annealed ratings must be used, since the heating involved in these joining processes will anneal (soften) the hard tube. This is the reason that annealed ratings are shown in Table 53 for type M and Table 54 for DWV tube, although they are not furnished in the annealed temper. Table 55 lists allowable internal working pressures for ACR tube. Table 56 gives pressure–temperature ratings for brazed and soldered joints.

## 5.2 Nonflammable Medical Gas Piping Systems

Safety standards for oxygen and other positive-pressure medical gases require the use of type K or L copper tube (see ASTM B 819). Special cleanliness requirements are called for because oxygen under pressure may cause the spontaneous combustion of some organic oils (the residual of lubricating oil used during manufacture) and for the safety of patients receiving medical gases.

## 5.3 Fuel Gas Distribution Systems

Until recently, nearly all interior fuel gas distribution systems in residential applications have used threaded steel pipe. Some areas of the United States, however, have extensive experience using copper tube for distribution of natural and liquefied petroleum (LP) gas, ranging from single-family attached and detached to multistory, multifamily dwellings. In addition, copper gas distribution lines have been installed for many years in commercial buildings such as strip malls, hotels, and motels. Major code bodies in the United States and Canada have approved copper tube for fuel gas systems. In 1989 in the United States, provisions for the use of copper

**Table 51** Rated Internal Working Pressures for Copper Tube: TYPE K<sup>a</sup>

Part 1: 1/4–2 in.

Nominal or Standard Size, in.	Annealed						
	S = 6000 psi 100°F	S = 5100 psi 150°F	S = 4900 psi 200°F	S = 4800 psi 250°F	S = 4700 psi 300°F	S = 4000 psi 350°F	S = 3000 psi 400°F
1/4	1074	913	877	860	842	716	537
3/8	1130	960	923	904	885	753	565
1/2	891	758	728	713	698	594	446
5/8	736	626	601	589	577	491	368
3/4	852	724	696	682	668	568	426
1	655	557	535	524	513	437	327
1 1/4	532	452	434	425	416	354	266
1 1/2	494	420	404	396	387	330	247
2	435	370	355	348	341	290	217

Nominal or Standard Size, in.	Drawn <sup>b</sup>						
	S = 10,300 psi 100°F	S = 10,300 psi 150°F	S = 10,300 psi 200°F	S = 10,300 psi 250°F	S = 10,000 psi 300°F	S = 9700 psi 350°F	S = 9400 psi 400°F
1/4	1850	1850	1850	1850	1796	1742	1688
3/8	1946	1946	1946	1946	1889	1833	1776
1/2	1534	1534	1534	1534	1490	1445	1400
5/8	1266	1266	1266	1266	1229	1193	1156
3/4	1466	1466	1466	1466	1424	1381	1338
1	1126	1126	1126	1126	1093	1061	1028
1 1/4	914	914	914	914	888	861	834
1 1/2	850	850	850	850	825	801	776
2	747	747	747	747	726	704	682

Part 2: 2 1/2–12 inches

Nominal or standard size, in.	Annealed						
	S = 6000 psi 100°F	S = 5100 psi 150°F	S = 4900 psi 200°F	S = 4800 psi 250°F	S = 4700 psi 300°F	S = 4000 psi 350°F	S = 3000 psi 400°F
2 1/2	398	338	325	319	312	265	199
3	385	328	315	308	302	257	193
3 1/2	366	311	299	293	286	244	183
4	360	306	294	288	282	240	180
5	345	293	281	276	270	230	172
6	346	295	283	277	271	231	173
8	369	314	301	295	289	246	184
10	369	314	301	295	289	246	184
12	370	314	302	296	290	247	185

**Table 51** (Continued)

Nominal or standard size, in.	Drawn <sup>b</sup>						
	S = 10,300 psi 100°F	S = 10,300 psi 150°F	S = 10,300 psi 200°F	S = 10,300 psi 250°F	S = 10,000 psi 300°F	S = 9700 psi 350°F	S = 9400 psi 400°F
2 1/2	684	684	684	684	664	644	624
3	662	662	662	662	643	624	604
3 1/2	628	628	628	628	610	592	573
4	618	618	618	618	600	582	564
5	592	592	592	592	575	557	540
6	595	595	595	595	578	560	543
8	634	634	634	634	615	597	578
10	634	634	634	634	615	597	578
12	635	635	635	635	617	598	580

<sup>a</sup>Based on maximum allowable stress in tension (psi) for the indicated temperatures (°F).

<sup>b</sup>When brazing or welding is used to join drawn tube, the corresponding annealed rating must be used.

Source: Copper Development Association.

**Table 52** Rated Internal Working Pressure for Copper Tube: TYPE L<sup>a</sup>

Part 1: 1/4–2 in.							
Nominal or Standard Size, in.	Annealed						
	S = 6000 psi 100°F	S = 5100 psi 150°F	S = 4900 psi 200°F	S = 4800 psi 250°F	S = 4700 psi 300°F	S = 4000 psi 350°F	S = 3000 psi 400°F
1/4	912	775	745	729	714	608	456
3/8	779	662	636	623	610	519	389
1/2	722	613	589	577	565	481	361
5/8	631	537	516	505	495	421	316
3/4	582	495	475	466	456	388	291
1	494	420	404	395	387	330	247
1 1/4	439	373	358	351	344	293	219
1 1/2	408	347	334	327	320	272	204
2	364	309	297	291	285	242	182

Nominal or Standard Size, in.	Drawn <sup>b</sup>						
	S = 10,300 psi 100°F	S = 10,300 psi 150°F	S = 10,300 psi 200°F	S = 10,300 psi 250°F	S = 10,000 psi 300°F	S = 9700 psi 350°F	S = 9400 psi 400°F
1/4	1569	1569	1569	1569	1524	1478	1432
3/8	1341	1341	1341	1341	1302	1263	1224
1/2	1242	1242	1242	1242	1206	1169	1133
5/8	1086	1086	1086	1086	1055	1023	991
3/4	1002	1002	1002	1002	972	943	914
1	850	850	850	850	825	801	776
1 1/4	755	755	755	755	733	711	689
1 1/2	702	702	702	702	682	661	641
2	625	625	625	625	607	589	570

(continued)



**Table 52** (Continued)

Part 2: 2½–12 in.

Nominal or Standard Size, in.	Annealed						
	S = 6000 psi 100°F	S = 5100 psi 150°F	S = 4900 psi 200°F	S = 4800 psi 250°F	S = 4700 psi 300°F	S = 4000 psi 350°F	S = 3000 psi 400°F
2½	336	285	274	269	263	224	168
3	317	270	259	254	248	211	159
3½	304	258	248	243	238	202	152
4	293	249	240	235	230	196	147
5	269	229	220	215	211	179	135
6	251	213	205	201	196	167	125
8	270	230	221	216	212	180	135
10	271	231	222	217	212	181	136
12	253	215	207	203	199	169	127

Nominal or Standard Size, in.	Drawn <sup>b</sup>						
	S = 10,300 psi 100°F	S = 10,300 psi 150°F	S = 10,300 psi 200°F	S = 10,300 psi 250°F	S = 10,000 psi 300°F	S = 9700 psi 350°F	S = 9400 psi 400°F
2½	577	577	577	577	560	544	527
3	545	545	545	545	529	513	497
3½	522	522	522	522	506	491	476
4	504	504	504	504	489	474	460
5	462	462	462	462	449	435	422
6	431	431	431	431	418	406	393
8	464	464	464	464	451	437	424
10	466	466	466	466	452	439	425
12	435	435	435	435	423	410	397

<sup>a</sup>Based on maximum allowable stress in tension (psi) for the indicated temperatures (°F).<sup>b</sup>When brazing or welding is used to join drawn tube, the corresponding annealed rating must be used.

Source: Copper Development Association.

**Table 53** Rated Internal Working Pressure for Copper Tube: TYPE M<sup>a</sup>

Part 1: ¼–2 in.

Nominal or Standard Size, in.	Annealed <sup>c</sup>						
	S=6000 psi 100°F	S=5100 psi 150°F	S=4900 psi 200°F	S=4800 psi 250°F	S=4700 psi 300°F	S=4000 psi 350°F	S=3000 psi 400°F
¼	—	—	—	—	—	—	—
⅜	570	485	466	456	447	380	285
½	494	420	403	395	387	329	247
⅝	—	—	—	—	—	—	—
¾	407	346	332	326	319	271	204
1	337	286	275	270	264	225	169
1¼	338	287	276	271	265	225	169
1½	331	282	270	265	259	221	166
2	299	254	244	239	234	199	149

**Table 53** (Continued)

Nominal or Standard Size, in.	Drawn <sup>b</sup>						
	S=10,300 psi 100°F	S=10,300 psi 150°F	S=10,300 psi 200°F	S=10,300 psi 250°F	S=10,000 psi 300°F	S=9700 psi 350°F	S=9400 psi 400°F
1/4	—	—	—	—	—	—	—
3/8	982	982	982	982	953	925	896
1/2	850	850	850	850	825	800	776
5/8	—	—	—	—	—	—	—
3/4	701	701	701	701	680	660	639
1	580	580	580	580	563	546	529
1 1/4	582	582	582	582	565	548	531
1 1/2	569	569	569	569	553	536	520
2	514	514	514	514	499	484	469

Part 2: 2 1/2–12 in.

Nominal or Standard Size, in.	Annealed <sup>c</sup>						
	S=6000 psi 100°F	S=5100 psi 150°F	S=4900 psi 200°F	S=4800 psi 250°F	S=4700 psi 300°F	S=4000 psi 350°F	S=3000 psi 400°F
2 1/2	<b>274</b>	<b>233</b>	<b>224</b>	<b>219</b>	<b>215</b>	<b>183</b>	<b>137</b>
<b>3</b>	<b>253</b>	<b>215</b>	<b>207</b>	<b>203</b>	<b>199</b>	<b>169</b>	<b>127</b>
3 1/2	<b>252</b>	<b>214</b>	<b>206</b>	<b>202</b>	<b>197</b>	<b>168</b>	<b>126</b>
<b>4</b>	<b>251</b>	<b>213</b>	<b>205</b>	<b>201</b>	<b>197</b>	<b>167</b>	<b>126</b>
<b>5</b>	<b>233</b>	<b>198</b>	<b>190</b>	<b>186</b>	<b>182</b>	<b>155</b>	<b>116</b>
<b>6</b>	<b>218</b>	<b>186</b>	<b>178</b>	<b>175</b>	<b>171</b>	<b>146</b>	<b>109</b>
<b>8</b>	<b>229</b>	<b>195</b>	<b>187</b>	<b>183</b>	<b>180</b>	<b>153</b>	<b>115</b>
<b>10</b>	<b>230</b>	<b>195</b>	<b>188</b>	<b>184</b>	<b>180</b>	<b>153</b>	<b>115</b>
<b>12</b>	<b>230</b>	<b>195</b>	<b>188</b>	<b>184</b>	<b>180</b>	<b>153</b>	<b>115</b>

Nominal or Standard Size, in.	Drawn <sup>b</sup>						
	S=10,300 psi 100°F	S=10,300 psi 150°F	S=10,300 psi 200°F	S=10,300 psi 250°F	S=10,000 psi 300°F	S=9700 psi 350°F	S=9400 psi 400°F
2 1/2	471	471	471	471	457	444	430
3	435	435	435	435	423	410	397
3 1/2	433	433	433	433	421	408	395
4	431	431	431	431	419	406	394
5	400	400	400	400	388	377	365
6	375	375	375	375	364	353	342
8	394	394	394	394	382	371	359
10	394	394	394	394	383	371	360
12	395	395	395	395	383	372	360

<sup>a</sup>Based on maximum allowable stress in tension (psi) for the indicated temperatures (°F).<sup>b</sup>When brazing or welding is used to join drawn tube, the corresponding annealed rating must be used.<sup>c</sup>Types M and DWV are not normally available in the annealed temper. Boldfaced values are provided for guidance when drawn temper tube is brazed or welded.

Source: Copper Development Association

**Table 54** Rated Internal Working Pressure for Copper Tube: TYPE DWV<sup>a</sup>

Part 1: 1 1/4–2 in.							
Nominal or Standard Size, in.	Annealed <sup>c</sup>						
	S=6000 psi 100°F	S=5100 psi 150°F	S=4900 psi 200°F	S=4800 psi 250°F	S=4700 psi 300°F	S=4000 psi 350°F	S=3000 psi 400°F
1 1/4	<b>330</b>	<b>280</b>	<b>269</b>	<b>264</b>	<b>258</b>	<b>220</b>	<b>165</b>
1 1/2	<b>293</b>	<b>249</b>	<b>240</b>	<b>235</b>	<b>230</b>	<b>196</b>	<b>147</b>
2	<b>217</b>	<b>185</b>	<b>178</b>	<b>174</b>	<b>170</b>	<b>145</b>	<b>109</b>

Part 2: 3–8 in.							
Nominal or Standard Size, in.	Annealed <sup>c</sup>						
	S=6000 psi 100°F	S=5100 psi 150°F	S=4900 psi 200°F	S=4800 psi 250°F	S=4700 psi 300°F	S=4000 psi 350°F	S=3000 psi 400°F
3	<b>159</b>	<b>135</b>	<b>130</b>	<b>127</b>	<b>125</b>	<b>106</b>	<b>80</b>
4	<b>150</b>	<b>127</b>	<b>122</b>	<b>120</b>	<b>117</b>	<b>100</b>	<b>75</b>
5	<b>151</b>	<b>129</b>	<b>124</b>	<b>121</b>	<b>119</b>	<b>101</b>	<b>76</b>
6	<b>148</b>	<b>126</b>	<b>121</b>	<b>119</b>	<b>116</b>	<b>99</b>	<b>74</b>
8	<b>146</b>	<b>124</b>	<b>119</b>	<b>117</b>	<b>114</b>	<b>97</b>	<b>73</b>

Nominal or Standard Size, in.	Drawn <sup>b</sup>						
	S=10,300 psi 100°F	S=10,300 psi 150°F	S=10,300 psi 200°F	S=10,300 psi 250°F	S=10,000 psi 300°F	S=9700 psi 350°F	S=9400 psi 400°F
1 1/4	566	566	566	566	549	533	516
1 1/2	503	503	503	503	489	474	459
2	373	373	373	373	362	352	341

Nominal or Standard Size, in.	Drawn <sup>b</sup>						
	S=10,300 psi 100°F	S=10,300 psi 150°F	S=10,300 psi 200°F	S=10,300 psi 250°F	S=10,000 psi 300°F	S=9700 psi 350°F	S=9400 psi 400°F
3	273	273	273	273	265	257	249
4	257	257	257	257	250	242	235
5	260	260	260	260	252	245	237
6	255	255	255	255	247	240	232
8	251	251	251	251	244	236	229

<sup>a</sup>Based on maximum allowable stress in tension (psi) for the indicated temperatures (°F).

<sup>b</sup>When brazing or welding is used to join drawn tube, the corresponding annealed rating must be used.

<sup>c</sup>Types M and DWV are not normally available in the annealed temper. Shaded values are provided for guidance when drawn temper tube is brazed or welded.

Source: Copper Development Association

**Table 55** Rated Internal Working Pressure for Copper Tube: ACR<sup>a</sup> (Air Conditioning and Refrigeration Field Service)

Part 1: 1/8–1 5/8 in.

Nominal or Standard Size, in.	Coils, Annealed (Coils, Drawn, not manufactured)						
	S = 6000 psi 100°F	S = 5100 psi 150F	S = 4900 psi 200F	S = 4800 psi 250F	S = 4700 psi 300F	S = 4000 psi 350F	S = 3000 psi 400F
1/8	3074	2613	2510	2459	2408	2049	1537
3/16	935	1645	1581	1548	1516	1290	968
1/4	1406	1195	1148	1125	1102	938	703
5/16	1197	1017	977	957	937	798	598
3/8	984	836	803	787	770	656	492
1/2	727	618	594	581	569	485	363
5/8	618	525	504	494	484	412	309
3/4	511	435	417	409	400	341	256
3/4	631	537	516	505	495	421	316
7/8	582	495	475	466	456	388	291
1 1/8	494	420	404	395	387	330	247
1 3/8	439	373	358	351	344	293	219
1 5/8	408	347	334	327	320	272	204

Part 2: 3/8–4 1/8 in.

Straight Lengths

Nominal or Standard Size, in.	Annealed						
	S = 6000 psi 100°F	S = 5100 psi 150°F	S = 4900 psi 200°F	S = 4800 psi 250°F	S = 4700 psi 300°F	S = 4000 psi 350°F	S = 3000 psi 400°F
3/8	914	777	747	731	716	609	457
1/2	781	664	638	625	612	521	391
5/8	723	615	591	579	567	482	362
3/4	633	538	517	506	496	422	316
7/8	583	496	477	467	457	389	292
1 1/8	495	421	404	39	388	330	248
1 3/8	440	374	359	352	344	293	220
1 5/8	409	348	334	327	320	273	205
2 1/8	364	309	297	291	285	243	182
2 5/8	336	286	275	269	263	224	168
3 1/8	317	270	259	254	249	212	159
3 5/8	304	258	248	243	238	203	152
4 1/8	293	249	240	235	230	196	147

(continued)

Table 55 (Continued)

Nominal or Standard Size, in.	Drawn						
	S = 10,300 psi 100°F	S = 10,300 psi 150°F	S = 10,300 psi 200°F	S = 10,300 psi 250°F	S = 10,000 psi 300°F	S = 9700 psi 350°F	S = 9400 psi 400°F
3/8	1569	1569	1569	1569	1524	1478	1432
1/2	1341	1341	1341	1341	1302	1263	1224
5/8	1242	1242	1242	1242	206	1169	1133
3/4	1086	1086	1086	1086	1055	1023	991
7/8	1002	1002	1002	1002	972	943	914
1 1/8	850	850	850	850	825	801	776
1 3/8	755	755	755	755	733	711	689
1 5/8	702	702	702	702	682	661	641
2 1/8	625	625	625	625	607	589	570
2 3/8	577	577	577	577	560	544	527
3 1/8	545	545	545	545	529	513	497
3 5/8	522	522	522	522	506	491	476
4 1/8	504	504	504	504	489	474	460

<sup>a</sup>Based on maximum allowable stress in tension (psi) for the indicated temperatures (°F).

<sup>b</sup>When brazing or welding is used to join drawn tube, the corresponding annealed rating must be used.

Source: Copper Development Association.

tube and copper alloy fittings for interior distribution systems were incorporated in the National Fuel Gas Code (ANSI Z223.1/NFPA 54). Similar provision is made in the Canadian document CAN/CGA-B149.1, Natural Gas Installation Code. Copper and copper alloy tube (except tin-lined copper tube) should not be used if the gas contains more than an average of 0.3 grain of hydrogen sulfide per 100 standard cubic feet (scf) of gas (0.7 mg/100 L).

## 6 COPPER ALLOY SLEEVE BEARINGS

Copper alloy sleeve bearings are available in wrought, sintered, and cast forms, the latter being the most commonly used type since they offer the broadest range of applicability. Table 57 summarizes the performance of the cast bearing bronze families with respect to five key bearing properties.

**Tin Bronzes** exhibit relatively high thermal conductivity and low friction coefficients against steel, both of which result in low bearing operating temperatures. The alloys are hard and strong and have good corrosion resistance, especially against seawater. They are wear resistant and withstand pounding well. The alloys are also somewhat abrasive and should be used against hardened steel shafts (300–400 HB minimum). The alloys work well with grease lubricants and can function as boundary-type bearings.

**Leaded Tin Bronzes** are essentially free-cutting versions of the tin bronzes. Properties and applications are similar.

**High-Leaded Tin Bronzes** comprise the most commonly used family of bronze bearing alloys. Although not quite so strong as tin bronzes and leaded tin bronzes, they operate well under moderate loads and medium-to-high speeds—applications that make up the bulk of sleeve bearing use. They are especially recommended for boundary-lubricated and mixed-film operation and provide a level of protection in the event of lubricant failure. They tolerate dirt in lubricants,

**Table 56** Pressure–Temperature Ratings of Soldered and Brazed Joints

Joining material <sup>d</sup>	Service temperature °F		Maximum working gage pressure (psi) for standard water tube sizes <sup>a</sup>				
			Nominal of Standard Size, in.				
			1/8–1	1 1/4–2	2 1/4–4	5–8	10–12
<b>Alloy Sn50 50-50 Tin–Lead Solder<sup>d</sup></b>	100	Pressure <sup>b</sup>	200	175	150	135	100
		DWV <sup>c</sup>	—	95	80	70	—
	150	Pressure <sup>b</sup>	150	125	100	90	70
		DWV <sup>c</sup>	—	70	55	45	—
	200	Pressure <sup>b</sup>	100	90	75	70	50
		DWV <sup>c</sup> ;	—	50	40	35	—
	250	Pressure <sup>b</sup>	85	75	50	45	40
		DWV <sup>c</sup> ;	—	—	—	—	—
	Saturated steam	Pressure	15	15	15	15	15
	<b>Alloy Sb5 95-5 Tin–Antimony Solder</b>	100	Pressure <sup>b</sup>	1090	850	705	660
DWV <sup>c</sup>			—	390	325	330	—
150		Pressure <sup>b</sup>	625	485	405	375	285
		DWV <sup>c</sup>	—	225	185	190	—
200		Pressure <sup>b</sup>	505	395	325	305	230
		DWV <sup>c</sup> ;	—	180	150	155	—
250		Pressure <sup>b</sup>	270	210	175	160	120
		DWV <sup>c</sup> ;	—	95	80	80	—
Saturated steam		Pressure	15	15	15	15	15
<b>Alloy E</b>		100	Pressure <sup>b</sup>	710	555	460	430
	DWV <sup>c</sup>		—	255	210	215	—
	150	Pressure <sup>b</sup>	475	370	305	285	215
		DWV <sup>c</sup>	—	170	140	140	—
	200	Pressure <sup>b</sup>	375	290	240	225	170
		DWV <sup>c</sup> ;	—	135	110	115	—
	250	Pressure <sup>b</sup>	320	250	205	195	145
		DWV <sup>c</sup> ;	—	115	95	95	—
	Saturated steam	Pressure	15	15	15	15	15
	<b>Alloy HB</b>	100	Pressure <sup>b</sup>	1035	805	670	625
DWV <sup>c</sup>			—	370	310	315	—
150		Pressure <sup>b</sup>	710	555	460	430	325
		DWV <sup>c</sup>	—	255	210	215	—
200		Pressure <sup>b</sup>	440	340	285	265	200
		DWV <sup>c</sup> ;	—	155	130	135	—
250		Pressure <sup>b</sup>	430	335	275	260	195
		DWV <sup>c</sup> ;	—	155	125	130	—
Saturated steam		Pressure	15	15	15	15	15
<b>Joining materials melting at or above 1100°C</b>		Pressure-temperature ratings consistent with the materials and procedures employed (see tables 47–51, annealed.)					

For extremely low working temperatures in the 0 to –200°F range, it is recommended that a joint material melting at or above 1100°F be employed (see Note 6).

<sup>a</sup>Standard water tube sizes per ASTM B 88.

<sup>b</sup>Ratings up to 8 in. in size are those given in ASME B16.22, Wrought Copper and Copper Alloy Solder Joint Pressure Fittings, and ASME B16.18, Cast Copper and Copper Alloy Solder Joint Fittings. Rating for 10–12-in. sizes are those given in ASME B16.18, Cast Copper and Copper Alloy Solder Joint Pressure Fittings.

<sup>c</sup>Using ASME B16.29, Wrought Copper and Wrought Copper Alloy Solder Joint Drainage Fittings—DWV, and ASME B16.23, Cast Copper Alloy Solder Joint Drainage Fittings—DWV.

<sup>d</sup>Alloy designations are per ASTM B 32.

<sup>e</sup>The Safe Drinking Water Act Amendment of 1986 prohibits the use in potable water systems of any solder having a lead content in excess of 0.2%.

<sup>f</sup>These joining materials are defined as brazing alloys by the American Welding Society.

Source: Copper Development Association

**Table 57** Comparison of Bearing Selection Criteria for Cast Copper Bearing Alloys

Bearing Alloy Families	Load Capacity and Fatigue Resistance	Maximum Operating Temperature	Conformability and Embeddability	Resistance to Seizure	Hardness and Wear Resistance
Lead red brasses	Moderate	Moderate	Low	Low	Good
High-lead tin bronzes	Moderate/high	High	Good	Good	High
Aluminum bronzes	Very high	Very high	Poor	Moderate	Very high
High-strength brasses	Moderate	Moderate	Poor	Moderate	High
Copper-beryllium alloys	High	High	Poor	Poor	Very high
Leaded coppers	Moderate	High	Very good	Very good	Moderate

Source: Copper Development Association

can accommodate misaligned shafts, and can be run against unhardened shafts. Alloy C93200 is the workhorse of the series.

**High-Strength Brasses** (sometimes called manganese bronzes) are modifications of yellow brasses made by addition of aluminum, manganese, and iron to achieve higher strength, which can reach more than 115 ksi (800 MPa). Fatigue resistance is moderate, but the alloys can operate under very high loads and at moderately high speeds. They require hardened, well-aligned shafts and reliable, clean lubrication.

**Aluminum Bronzes** are among the highest strength copper-based bearing alloys. Alloy C95500 can be heat treated (suffix “HT”) to tensile strengths of more than 115 ksi (800 MPa). The compressive strength of alloy C95400 at 500°F (260°C) is the same as that of tin bronzes at room temperature. The aluminum bronzes also have the highest fatigue strength among bearing alloys and resist heavy and repeated impact well. They must be used against shafts hardened to 500 HB or higher and require clean, reliable full-film lubrication. Both bearing and shaft surfaces should be machined to finishes finer than 15–20  $\mu\text{in.}$  (0.4–0.5  $\mu\text{m}$ ). Correct shaft alignment is important.

**Silicon Brasses** have good bearing characteristics at moderately high speeds. They are readily machinable, contain no lead, and are stronger than standard tin bearing alloys. Lubrication must be clean and reliable, and operation should be against hardened shafts.

**Copper–Beryllium Alloys** can be heat treated to attain very high hardness. Alloy C82800, for example, exhibits a tensile strength in excess of 165 ksi (1100 MPa). The beryllium coppers have good bearing properties and can withstand extremely high stresses. They require hardened and precisely aligned shafts and clean, reliable lubrication. Their moderate impact and fatigue strengths require that bearings be properly supported.

**Lead-Free Bearing Bronze** contains bismuth in place of lead. Properties are comparable. For example, lead-free alloy C89320 is very similar to the high-lead tin bronze C93200.

## 7 STANDARDS AND SPECIFICATIONS

Copper and copper alloys designated according to the UNS numbering system are cited in AMS, ASME, ASTM, RWMA, FED, and MIL specifications. In addition, ingot standards are listed for cast metal feedstock by North American ingot manufacturers. Cross references to all

relevant standards, by UNS number and product form, are available from the Copper Development Association and can be viewed on the *Standards and Properties* section of its website, [www.copper.org](http://www.copper.org).

## ADDITIONAL INFORMATION

Complete technical information regarding copper and its alloys is maintained by the Copper Development Association, Inc. ([www.copper.org](http://www.copper.org)) and the Canadian Copper and Brass Development Association ([www.coppercanada.ca](http://www.coppercanada.ca)). Copper development centers are located in 24 other countries. Information about these centers can be found through the International Copper Association, Ltd. ([www.copperinfo.com](http://www.copperinfo.com)).

## REFERENCES

1. G. Joseph and K. J. A. Kundig (Eds.), *Copper: Its Trade, Manufacture, Use, and Environmental Status*, ASM International and International Copper Association, Materials Park, OH, 1999.
2. R. Raymond, *Out of the Fiery Furnace—The Impact of Metals on Mankind*, The Macmillan Company of Australia, South Melbourne, Australia, 1984.
3. “ASTM Standard Designations for Wrought and Cast Copper and Copper Alloys,” Copper Development Association and ASTM International, New York, 2004. See also <http://www.copper.org/resources/properties/db/SDAPropertiesSelectionServlet.jsp?service=COPPERINTRA&Action=search>.
4. A. Sutulov, *Copper at the Crossroads*, Internmet Publications, Santiago, Chile, 1985, pp. 55–57.
5. R. E. Bolz and G. I. Tuve (Eds.), *Handbook of Tables of Applied Engineering Science*, 2nd ed., CRC Press, Boca Raton, Florida, 1974.
6. Wiley On-Line Library, *An Introduction to Materials Engineering and Science: For Chemical and Materials Engineers*, Appendix 8.
7. ASTM International, West Conshohocken, PA, [www.astm.org](http://www.astm.org).
8. NSF International, Ann Arbor, MI, [www.nsf.org](http://www.nsf.org).





# CHAPTER 5

## A GUIDE TO ENGINEERING SELECTION OF TITANIUM ALLOYS FOR DESIGN

**Matthew J. Donachie**

**Rensselaer at Hartford**

**Hartford Connecticut**

<b>1 INTRODUCTION</b>	<b>229</b>	3.9 Oxygen and Nitrogen (in CP Titanium)	244
1.1 Purpose	229	3.10 Mechanical Properties of Titanium Alloys	244
1.2 What Are Titanium Alloys?	230	<b>4 MANUFACTURING PROCESSES</b>	<b>254</b>
1.3 Temperature Capability of Titanium Alloys	230	4.1 General Aspects of the Manufacture of Titanium Articles	254
1.4 How Are Alloys Strengthened?	232	4.2 Production of Titanium via Vacuum Arc Melting	255
1.5 Manufacture of Titanium Articles	232	4.3 Cutting the Cost of Titanium Alloy Melting	255
1.6 Titanium Alloy Information	233	4.4 Defects and Their Control in Titanium Melting	256
<b>2 METALLURGY OF TITANIUM ALLOYS</b>	<b>233</b>	4.5 Forging Titanium Alloys	256
2.1 Structures	233	4.6 Casting	258
2.2 Crystal Structure Behavior in Alloys	234	4.7 Machining and Residual Stresses	259
2.3 Metals at High Temperatures	234	4.8 Joining	259
<b>3 MICROSTRUCTURE AND PROPERTIES OF TITANIUM AND ITS ALLOYS</b>	<b>236</b>	4.9 Other Aspects of Titanium Alloy Selection	260
3.1 Introduction	236	4.10 Corrosion	260
3.2 Alloy Composition and General Behavior	237	4.11 Biomedical Applications	261
3.3 Strengthening of Titanium Alloys	238	4.12 Cryogenic Applications	261
3.4 Effects of Alloy Elements	241	<b>5 FINAL COMMENTS</b>	<b>261</b>
3.5 Intermetallic Compounds and Other Secondary Phases	241	5.1 General	261
3.6 Elastic Constants and Physical Properties	242	5.2 Newer Titanium Products	263
3.7 Effects of Processing	243	5.3 Thoughts on Alloy Selection	263
3.8 Hydrogen (in CP Titanium)	243	<b>BIBLIOGRAPHY</b>	<b>265</b>

### 1 INTRODUCTION

#### 1.1 Purpose

This chapter is intended to create a sufficient understanding of titanium and its alloys so that selection of them for specific designs will be appropriate. Knowledge of titanium alloy types

and their processing will give a potential user the ability to understand the ways in which titanium alloys (and titanium) can contribute to a design. This chapter will provide the user with sufficient knowledge to ask the important technical questions of titanium alloy and product providers. You will be equipped to evaluate the capability of primary metal (largely melt shops) and component producers while addressing the necessary mechanical property and corrosion/environmental behavior that ultimately influence alloy selection.

There is no cookbook for titanium selection although there is a fair degree of standardization relative to generic alloy compositions. Since titanium metal matrix composites use existing alloys, there probably will be a degree of standardization of such composite materials as they continue to develop. Proprietary/restricted processing leads to titanium alloy conditions and properties not listed in a handbook or catalog of materials. Some proprietary alloy chemistries exist and metal matrix composites may also develop on a proprietary basis.

Larger volume customers, particularly those in the aerospace industry, frequently dictate the resultant material conditions that generally will be available from a supplier. Proprietary alloy chemistries and/or proprietary/restricted processing required by such customers can lead to alloys or alloy variants that may not be widely available as noted above. In general, proprietary processing is more likely to be encountered than proprietary chemistry nowadays. With few exceptions, critical applications for titanium and its alloys will require the customer to work with one or more titanium producers to develop an understanding of what is available and what a selector/designer can expect from a chosen titanium alloy.

Properties of the titanium alloy families sometimes are listed in handbooks or vendor/supplier brochures. However, not all data will be available.

## 1.2 What Are Titanium Alloys?

Titanium alloys for purposes of this chapter are those alloys of about 50% or higher titanium that offer exceptional strength to density benefits plus corrosion properties comparable to the excellent corrosion resistance of pure titanium. The range of operation is from cryogenic temperatures to around 538–595°C (1000–1100°F). Titanium alloys based on intermetallics such as gamma titanium aluminide (TiAl intermetallic compound which has been designated gamma) are included in this discussion. These alloys are meant to compete with superalloys at the lower end of superalloy temperature capability, perhaps up to 700°C (~1300°F). They may offer some mechanical advantages for now but often represent an economic debit. Limited experience is available with the titanium aluminides.

## 1.3 Temperature Capability of Titanium Alloys

Although the melting point of titanium is in excess of 1660°C (3000°F), commercial alloys operate at substantially lower temperatures. It is not possible to create titanium alloys that operate close to their melting temperatures. Attainable strengths, crystallographic phase transformations, and environmental interaction considerations cause restrictions. Thus, while titanium and its alloys have melting points higher than those of steels, their maximum upper useful temperatures for structural applications generally range from as low as 427°C (800°F) to the region of about 538–595°C (1000–1100°F) dependent on composition. As noted, titanium aluminide alloys show promise for applications at higher temperatures, perhaps up to 700°C (~1300°F) although at one time they were expected to offer benefits to higher temperatures. Actual application temperatures will vary with individual alloy composition. Since application temperatures are much below the melting points, incipient melting is not a factor in titanium alloy application.

**Table 1** Comparison of Typical Strength-to-Density Values at 20°C

Metal	Specific Gravity	Tensile Strength (lb/in. <sup>2</sup> )	Tensile Strength/Specific Gravity
CP	4.5	58,000	13,000
Ti-6Al-4V	4.4	130,000	29,000
Ti-4Al-3Mo-1V	4.5	200,000	45,000
Ultrahigh-strength steel (4340)	7.9	287,000	36,000

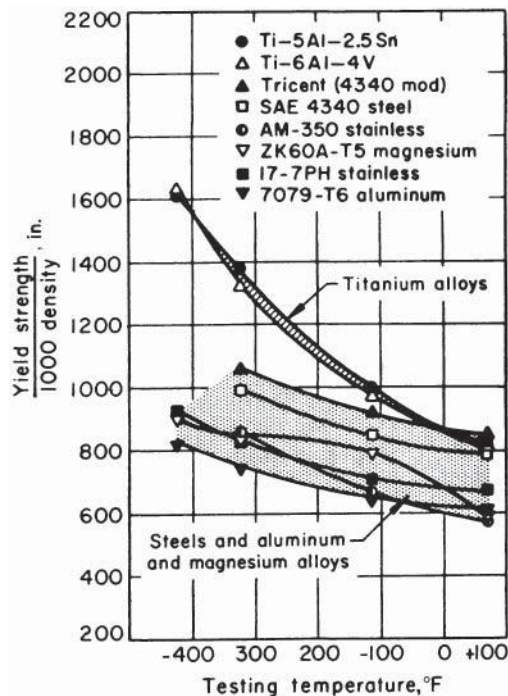
Source: Matthew Donachie, *Titanium: A Technical Guide*, 1st ed., ASM International, Materials Park, OH, 1988, p. 158.

### Strength and Corrosion Capability of Titanium and Its Alloys

Titanium owes its industrial use to two significant factors:

- Titanium has exceptional room temperature resistance to a variety of corrosive media.
- Titanium has a relatively low density and can be strengthened to achieve outstanding properties when compared with competitive materials on a strength-to-density basis.

Table 1 compares typical strength-to-density values for commercial purity (CP) titanium, several titanium alloys, and high-strength steel. Figure 1 visually depicts the strength



**Figure 1** Yield strength–density ratio as a function of temperature for several titanium alloys compared to some steel, aluminum, and magnesium alloys. (Source: Matthew Donachie, *Titanium: A Technical Guide*, 2nd ed., ASM International, Materials Park, OH, 2001, p. 158.) Reprinted with permission of ASM International.

improvements possible in titanium alloys compared to magnesium, aluminum, or steel. In addition to excellent strength characteristics, titanium's corrosion resistance makes it a desirable material for body replacement parts and other tough corrosion-prone applications. The modulus of elasticity (Young's modulus) is an important factor in addition to strength (specific strength) in some applications. Recently, after many years of standard titanium alpha-beta (such as Ti-6Al-4V) alloy composition use as biomaterials, titanium beta alloys (with lower moduli than the customary alpha-beta alloys) have been incorporated into biomedical orthopedic applications.

#### 1.4 How Are Alloys Strengthened?

Metals are crystalline. In the solid state, the atoms of a metal or alloy have various crystallographic arrangements, often occurring as cubic or hexagonal structures. Some crystal structures tend to be associated with better property characteristics than others. In addition, crystalline aggregates of atoms have orientation relationships making properties possibly directionally dependent. Unique crystalline aggregates are called grains and, in an alloy, there are usually many grains with random orientation directions from grain to grain. Metal alloys with multiple random grain directions are known as polycrystals, often referred to as equiaxed. However, columnar shaped grains (one long axis) are common as a result of casting operations and other elongated grains can result from plastic deformation during shape forming deformation of an alloy to a component. Grain size and shape are refined by deformation, application of heat, and transformation of existing grains into new ones of the same or different crystallographic structure. The occurrence of a particular crystal structure and chemistry (or range of chemistries) defines a phase, i.e., a chemically homogenous, physically distinct, mechanically separable part of a system. The basic phases in titanium are alpha and beta (see later sections for more information).

The peripheral surface of a grain is called a grain boundary. Aggregates of atoms without grain boundaries are rarely created in nature. Such aggregates, whether produced naturally or by human manipulation, are called single crystals. The introduction of different atom types, additional crystal phases, and/or manipulation of grain boundaries enable inhibition of the movement, through the crystal lattice or grains, of imperfections that cause deformation to occur. Titanium alloys are basis titanium modified by changes in chemistry, in a polycrystalline form, with various phases present in the grains or at grain boundaries.

#### 1.5 Manufacture of Titanium Articles

Appropriate compositions of all titanium alloy types can be wrought processed (forged, rolled to sheet, or otherwise mechanically formed) into a variety of shapes. Powder metallurgy also can be used to accomplish shape formation. Casting, particularly investment casting, is used to cast appropriate compositions in complex shapes usually with properties approaching those of the wrought forms. Fabricated titanium alloy structures can be built up by welding or brazing. Machining of titanium alloys requires forces about equal to those for machining austenitic stainless steel. Titanium alloys do have metallurgical characteristics that make them more difficult to machine than steels of comparable hardness.

In welding or machining of titanium, the effects of the energy input (heat energy, deformation energy) on the microstructure and properties of the final titanium alloy product must be considered. Many titanium alloys can combust if appropriate conditions of temperature are exceeded. Care is needed in machining and in storing scrap.

Many titanium alloys are available as wrought components in extruded, forged, or rolled form. Hot deformation is the preferred shape forming process. Cold rolling may be used to increase short-time strength properties for some lower temperature applications. Properties of

titanium alloys generally are controlled by adjustments in chemistry (composition) and by modification of the processing (including heat treatment). Many alloys are available in cast form as well. Limited alloys are available from powder processing.

## 1.6 Titanium Alloy Information

Some chemistries and properties are listed in this chapter, but there is no substitute for consultation with titanium manufacturers about the forms (some cast, some powder, mostly wrought) which can be provided and the exact chemistries available. It should be understood that not all titanium alloys, particularly those with specific processing, are readily available as off-the-shelf items. Design data for titanium alloys are not intended to be conveyed in this chapter, but typical properties are indicated for some materials. It is very important to note that design properties should be obtained from internal testing if possible. Barring in-house test results or other certified/analyzed properties data, data from titanium metal or component producers or from other validated sources may be useful. Typical properties are merely a guide for comparison. Exact chemistry, section size, heat treatment, and other processing steps must be known to generate adequate property values for design.

The properties of titanium alloy compositions, although developed over many years, are not normally well documented in the literature. However, since many consumers actually only use a few alloys within the customary user groups, data may be more plentiful for certain compositions. In the case of titanium, the most used and studied alloy, whether wrought or cast, is Ti-6Al-4V.

The extent to which data generated for specific applications are available to the general public is unknown. However, even if such data were disseminated widely, the alloy selector needs to be aware that apparently minor chemistry changes or variations in processing operations such as forging (a form of mechanical deformation) conditions, heat treatment, etc., dramatically affect properties of titanium alloys. All property data should be reconciled with the actual manufacturing specifications and processing conditions expected. It is most important that alloy selectors work with competent metallurgical engineers to establish the validity of data intended for design as well as to specify the processing conditions that will be used for component production.

Application of design data must take into consideration the probability that components may contain locally inhomogeneous regions. For titanium alloys, such inhomogeneities (segregation) can be disastrous in gas turbine applications. The probability of occurrence of these regions is dependent upon the melting procedures, being essentially eliminated by so-called triple melt. All facets of chemistry and processing need to be considered when selecting a titanium alloy for an application.

For sources of property data other than that of the producers (melters, forgers, etc.) or an alloy selector's own institution, one may refer to handbooks or to organizations such as ASM International which publish compilations of data that may form a basis for the development of design allowables for titanium alloys. Standards organizations such as ASTM publish information about titanium alloys, but that information does not ordinarily contain any design data. Additional information may be available from industry organizations (see Associations Providing Titanium Information at the end of the chapter).

## 2 METALLURGY OF TITANIUM ALLOYS

### 2.1 Structures

As noted above, metals are crystalline and the atoms take various crystallographic forms. Some of these forms tend to be associated with better property characteristics than other crystal

structures. Titanium, as does iron, exists in more than one crystallographic form. Titanium has two elemental crystal structures: in one, the atoms are arranged in a body-centered-cubic (bcc) array; in the other they are arranged in a hexagonal close-packed (hcp) array. The cubic structure is found only at high temperatures, unless the titanium is alloyed with other elements to maintain the cubic structure at lower temperatures. The bcc crystal structure is designated as beta and the hcp structure as alpha. Thus, titanium's two normal crystal structures are commonly known as alpha and beta phases.

Not only crystal structure but also overall “structure,” i.e. appearance, at levels above that of the atomic crystal structure is important. Structure for our purposes will be defined as the macrostructure and microstructure (i.e., macro- and micro-appearance) of (usually) a polished and etched cross section of metal visible at magnifications up to and including 10,000 $\times$ . Two other microstructural features which are not determined visually but are determined by other means such as x-ray diffraction or chemistry are phase type (alpha, beta, etc.) and texture (orientation) of grains.

Alpha actually means any hexagonal titanium, pure or alloyed, while beta means any cubic titanium, pure or alloyed. The alpha and beta “structures”—sometimes called systems or types—are the basis for the generally accepted classes of titanium alloys. These are alpha, near alpha, alpha–beta, and beta. Sometimes a category of near beta is also considered. The preceding categories denote the general type of microstructure after processing.

Crystal structure and grain structure (a component of microstructure) are not synonymous terms. Both (as well as the chemical composition and arrangement of phases in the microstructure) must be specified to completely identify the alloy and its expected mechanical, physical, and corrosion behavior. The important fact to keep in mind is that, while grain shape and size do affect behavior, the crystal structure changes (from alpha to beta and back again) which occur during processing play a major role in defining titanium properties.

## 2.2 Crystal Structure Behavior in Alloys

An alpha alloy (so described because its chemistry favors the alpha phase) does not normally form a beta phase on heating. A near-alpha (sometimes called “superalpha”) alloy forms only a limited beta phase on heating, and so it may appear microstructurally similar to an alpha alloy when viewed at lower temperatures. An alpha–beta alloy is one for which the composition permits complete transformation to beta on heating but transformation back to alpha plus retained and/or transformed beta at lower temperatures. A near-beta or beta alloy composition is one which tends to retain, indefinitely at lower temperatures, the beta phase formed at high temperatures. However, the beta that is retained on initial cooling to room temperature is metastable for many beta alloys. Dependent on chemistry, it may precipitate secondary phases during heat treatment.

## 2.3 Metals at High Temperatures

### *General*

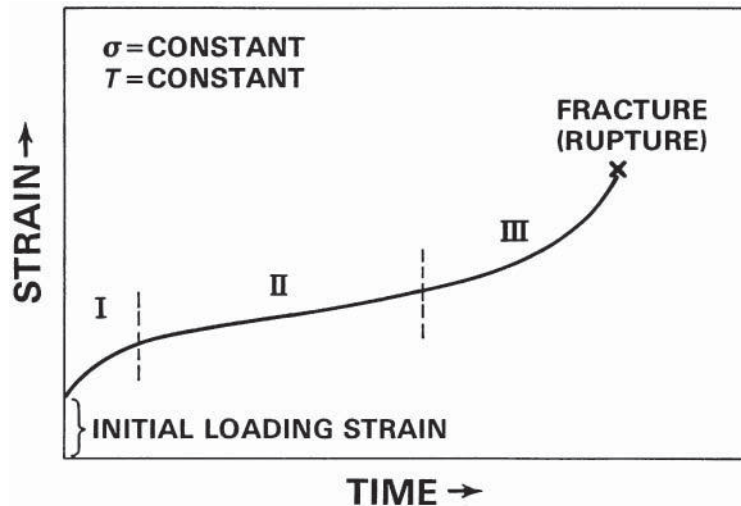
While material strengths at low temperatures usually are not a function of time, at high temperatures the time of load application becomes very significant for mechanical properties. Concurrently, the availability of oxygen at high temperatures accelerates the conversion of some of the metal atoms to oxides. Oxidation proceeds much more rapidly at high temperatures than at room or lower temperatures. For alloys of titanium there is the additional complication of titanium's high affinity for oxygen and its ability to “getter” oxygen (or nitrogen) from the air. Dissolved oxygen greatly changes the strength and ductility of titanium alloys. Hydrogen is another gaseous element which can significantly affect properties of titanium alloys. Hydrogen tends to cause hydrogen embrittlement while oxygen will strengthen but reduce the ductility yet not necessarily embrittle titanium as hydrogen does.

### Mechanical Behavior

In the case of short-time tensile properties of tensile yield strength (TYS) and ultimate tensile strength (UTS), the mechanical behavior of metals at higher temperatures is similar to that at room temperature but with metals becoming weaker as the temperature increases. However, when steady loads below the normal yield or ultimate strength determined in short-time tests are applied for prolonged times at higher temperatures, the situation is different. Figure 2 illustrates the way in which most materials respond to steady extended-time loads at high temperatures. A time-dependent extension (creep) is noticed under load. If the alloy is exposed for a long time, the alloy eventually fractures (ruptures). The degradation process is called creep or, in the event of failure, creep rupture (sometimes stress rupture) and alloys may be selected on their ability to resist creep and creep rupture failure. Cyclically applied loads that cause failure (fatigue) at lower temperatures also cause failures in shorter times (lesser cycles) at high temperatures. When titanium alloys operate for prolonged times at high temperature, they can fail by creep rupture. However, tensile strengths, fatigue strengths, and crack propagation criteria are more likely to dominate actual titanium alloy performance requirements.

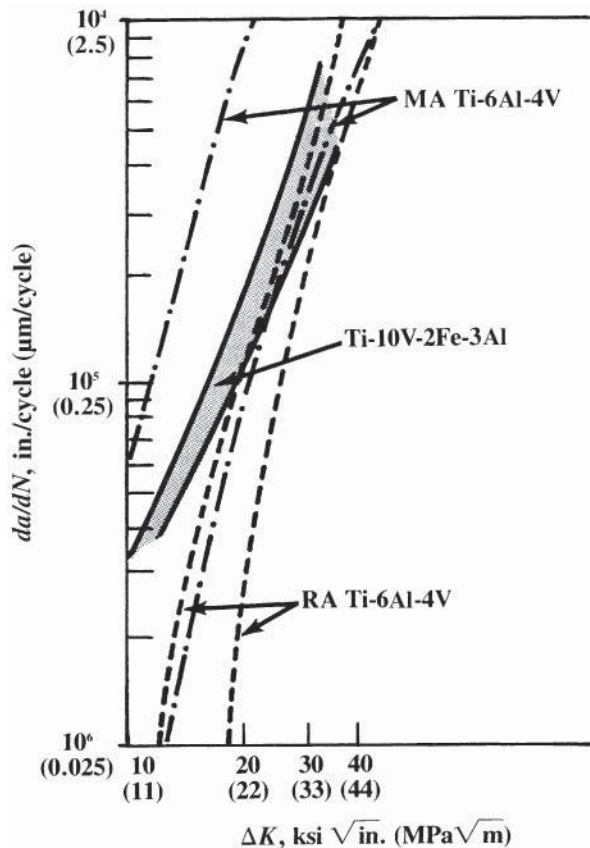
In highly mechanically loaded parts such as gas turbine fan and compressor disks, common titanium alloy applications, fatigue at high loads in short times, low-cycle fatigue (LCF), is the major concern. High-cycle fatigue (HCF) normally is not a problem with titanium alloys unless a design error occurs and subjects a component to a high-frequency vibration that forces rapid accumulation of fatigue cycles. While life under cyclic load (stress cycles, S-N, behavior) is a common criterion for design, resistance to crack propagation is an increasingly desired property. Thus, the crack growth rate vs. a fracture toughness parameter is required. The parameter in this instance may be the stress intensity factor ( $K$ ) range over an incremental distance which a crack has grown—the difference between the maximum and minimum  $K$  in the region of crack length measured. A plot of the resultant type ( $da/dn$  vs.  $\Delta K$ ) is shown in Fig. 3 for several wrought titanium alloys.

Creep–fatigue interactions can play a role in titanium alloy response to loading. This type of fatigue in titanium alloys is sometimes called “dwell time fatigue” or may be called



**Figure 2** Creep rupture schematic showing time-dependent deformation under constant load at constant high temperatures followed by final rupture. (All loads below the short-time yield strength. Roman numerals denote ranges of the creep rupture curve.)





For Ti-10V-2Fe-3Al:  $R = 0.05$ ;  $F = 1-30 \text{ Hz}$

For MA Ti-6Al-4V:  $R = 0.08$ ;  $F = 1-25 \text{ Hz}$

For RA Ti-6Al-4V:  $R = 0.08$ ;  $F = 6 \text{ Hz}$

**Figure 3** Comparison of fatigue crack growth rate ( $da/dn$ ) versus toughness change ( $\Delta K$ ); curves for several titanium alloys. Note that MA = mill annealed while RA = recrystallization annealed. (Source: Matthew Donachie, *Titanium: A Technical Guide*, 2nd ed., ASM International, Materials Park, OH, 2001, p. 109.) Reprinted with permission of ASM International.

interrupted low-cycle fatigue (ILCF). In dwell or interrupted fatigue, the cyclic loading is interrupted so a steady load is imposed for a short time before cyclic loading is resumed. This process causes an interaction between creep (steady load) and fatigue (cyclic load) to take place, occurring at surprisingly low temperature levels—less than  $200^\circ\text{C}$  ( $390^\circ\text{F}$ ). The fatigue life of alpha/beta titanium alloys in dwell loads is substantially reduced compared to continuously fatigue loaded alloys.

### 3 MICROSTRUCTURE AND PROPERTIES OF TITANIUM AND ITS ALLOYS

#### 3.1 Introduction

The grain size, grain shape, and grain boundary arrangements in titanium have a very significant influence on mechanical properties, and it is the ability to manipulate the phases/grains present

as a result of alloy composition that is responsible for the variety of properties that can be produced in titanium and its alloys. Transformed beta-phase products in alloys can affect tensile strengths, ductility, toughness, and cyclic properties. To these effects must be added the basic strengthening effects of alloy elements.

### 3.2 Alloy Composition and General Behavior

Alpha titanium alloys usually have high amounts of aluminum which contribute to oxidation resistance at high temperatures. Alpha–beta alloys also contain, as the principal element, high amounts of aluminum, but the primary reason is to control the alpha phase. Alpha alloys cannot be heat treated to develop higher mechanical properties because they are single-phase alloys.

The addition of certain alloy elements to pure titanium provides for a wide two-phase region where alpha and beta coexist. This behavior enables the resultant alloys to be heat treated or processed, if desired, in the temperature range where the alloy is two phase. The two-phase condition permits the structure to be refined by the alpha–beta–alpha transformation process on heating and cooling. The process of heating to a high temperature to promote subsequent transformation is known as solution heat treatment. By permitting some beta to be retained temporarily at lower temperature, beta-favoring alloy elements enable optimum control of the microstructure. After cooling alloys from the forging or solution heat treatment temperature, the microstructure is controlled by subsequent transformation as the alloys are “aged” (reheated, after the rapid cooling, to temperatures well below the beta transus). The alpha–beta alloys, when properly treated, have an excellent combination of strength and ductility. They generally are stronger than the alpha or the beta alloys.

The beta alloys are metastable; that is, they tend to transform to an equilibrium, or balance of structures. The beta alloys generate their strength from the intrinsic strength of the beta structure and the precipitation of alpha and other phases from the alloy through heat treatment after processing. The most significant commercial benefit provided by a beta structure is the increased formability of such alloys relative to the hexagonal crystal structure types (alpha and alpha–beta).

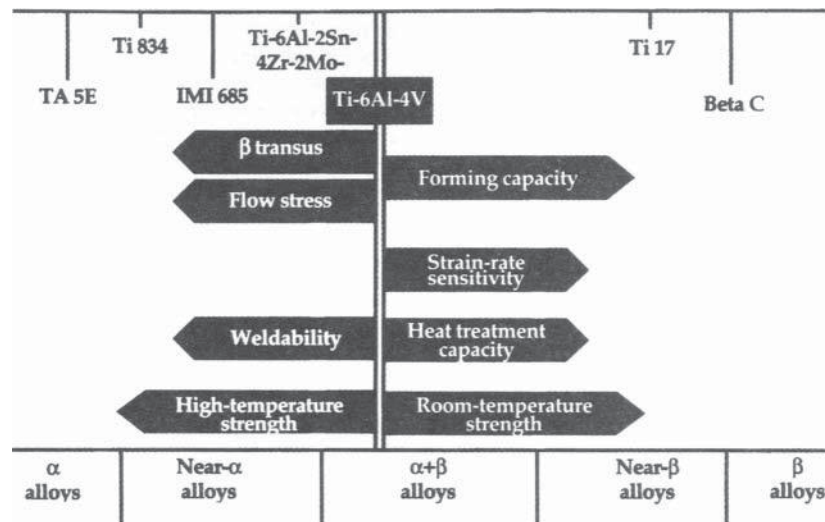
The three principal categories or classes (alpha, alpha–beta, beta) of titanium have been mentioned, as noted earlier, with the alpha category sometimes subdivided into alpha and near alpha and the beta category sometimes considered as near beta and beta. When CP titanium is added to the list, we may find titanium materials to be listed under one of the following:

- Unalloyed (CP)
- Alpha and near alpha
- Alpha–beta
- Beta and near beta

Figure 4 shows the main characteristics of the different titanium alloy family groupings. CP titanium is excluded from this figure. For purposes of alloy selection, separation as alpha, alpha–beta, and beta alloys plus CP titanium is usually sufficient.

Titanium aluminides differ from conventional titanium alloys in that they are principally chemical compounds alloyed to enhance strength, formability, etc. The aluminides have higher operational temperatures than conventional titanium but at higher cost and, generally, have lower ductility and formability.

In addition to alloys, titanium is sold and used in CP forms usually identified as grades. Pure titanium usually has some amount of oxygen alloyed with it. The strength of CP titanium is affected by the interstitial (oxygen and nitrogen) element content. A principal difference among grades is the oxygen (and nitrogen) content, which influences mechanical properties. Small additions of some alloy elements such as palladium are added for increased corrosion resistance



**Figure 4** Main characteristics of different titanium alloy family groupings. (Source: Matthew Donachie, *Titanium: A Technical Guide*, 2nd ed., ASM International, Materials Park, OH, 2001, p. 22.) Reprinted with permission of ASM International.

in certain grades. A summary of the compositions of many commercial and semicommercial titanium grades and alloys is given in Table 2.

### 3.3 Strengthening of Titanium Alloys

Desired mechanical properties such as yield or ultimate strength density (strength efficiency), perhaps creep and creep rupture strength as well as fatigue crack growth rate, and fracture toughness are extremely important. Manufacturing considerations such as welding and forming requirements play a major role in affecting titanium alloys' properties. Such considerations normally provide the criteria that determine the alloy composition, structure (alpha, alpha–beta, or beta), heat treatment (some variant of either annealing or solution treating and aging), and level of process control selected or prescribed for structural titanium alloy applications.

By introducing atoms, phases, grain boundaries, or other interfaces into titanium, the movement of imperfections that cause deformation to occur is inhibited. The process of modifying composition and microstructure enables titanium alloys to be strengthened significantly. Final strength is a function of composition and the various deformation processes used to form and strengthen alloys. It is quite important for the alloy selector to have a realistic understanding of the strengthening process in titanium alloys as the properties of titanium and its alloys can be modified considerably not only by chemistry modification but also by processing.

Titanium alloys derive their strength from a fineness of microstructure produced by transformation of crystal structures from beta to alpha in grains, plus dispersion of one phase in another, as in the case of precipitation of alpha phases from retained beta in metastable beta alloys. The fine structure of titanium alloys often can be martensitic in nature, created by transformations as temperatures on the component being produced are reduced during cooling from deformation processing or solution treatment. The reader may recall that martensitic structures are produced in steels (and in other systems) and can create very strong and hard alloys. Martensitic reactions are found in titanium alloys; they are not as effective as those in steels about causing hardening but do bring about microstructure refinements and thus strength improvements in titanium alloys. Fine dispersions in the alloys usually are produced by “aging” through

**Table 2** Some Commercial and Semicommercial Grades and Alloys of Titanium

Designation	Tensile Strength (min.)		0.2% Yield Strength (min.)		Impurity Limits wt. % (max.)					Nominal Composition, wt. %				
	MPa	ksi	MPa	ksi	N	C	H	Fe	O	Al	Sn	Zr	Mo	Others
<b>Unalloyed grades</b>														
ASTM grade 1	240	35	170	25	0.03	0.08	0.015	0.20	0.18	—	—	—	—	—
ASTM grade 2	340	50	280	40	0.03	0.08	0.015	0.30	0.25	—	—	—	—	—
ASTM grade 3	450	65	380	55	0.05	0.08	0.015	0.30	0.35	—	—	—	—	—
ASTM grade 4	550	80	480	70	0.05	0.08	0.015	0.50	0.40	—	—	—	—	—
ASTM grade 7	340	50	280	40	0.03	0.08	0.015	0.30	0.25	—	—	—	—	0.2Pd
ASTM grade 11	240	35	170	25	0.03	0.08	0.015	0.20	0.18	—	—	—	—	0.2Pd
<b><math>\alpha</math> and near-<math>\alpha</math> alloys</b>														
Ti-0.3Mo-0.8Ni	480	70	380	55	0.03	0.10	0.015	0.30	0.25	—	—	—	0.3	0.8Ni
Ti-5Al-2.5Sn	790	115	760	110	0.05	0.08	0.02	0.50	0.20	5	2.5	—	—	—
Ti-5Al-2.5Sn-ELI	690	100	620	90	0.07	0.08	0.0125	0.25	0.12	5	2.5	—	—	—
Ti-8Al-1Mo-1V	900	130	830	120	0.05	0.08	0.015	0.30	0.12	8	—	—	1	1V
Ti-6Al-2Sn-4Zr-2Mo	900	130	830	120	0.05	0.05	0.0125	0.25	0.15	6	2	4	2	0.08Si
Ti-6Al-2Nb-1Ta-0.8Mo	790	115	690	100	0.02	0.03	0.0125	0.12	0.10	6	—	—	1	2Nb, 1Ta
Ti-2.25Al-11Sn-5Zr-1Mo	1000	145	900	130	0.04	0.04	0.008	0.12	0.17	2.25	11	5	1	0.2Si
Ti-5.8Al-4Sn-3.5Zr-0.7Nb														
-0.5Mo-0.35Si	1030	149	910	132	0.03	0.08	0.006	0.05	0.15	5.8	4	3.5	0.5	0.7Nb, 0.35Si
Ti-1100	1030	150	920	134	.03	.04	?	.03	.09	6	2.8	4	.42	V .2, Si .4
<b><math>\alpha</math>-<math>\beta</math> alloys</b>														
Ti-6Al-4V <sup>a</sup>	900	130	830	120	0.05	0.10	0.0125	0.30	0.20	6	—	—	—	4V
Ti-6Al-4V-ELI <sup>a</sup>	830	120	760	110	0.05	0.08	0.0125	0.25	0.13	6	—	—	—	4V
Ti-6Al-6V-2Sn <sup>a</sup>	1030	150	970	140	0.04	0.05	0.015	1.0	0.20	6	2	—	—	0.7Cu, 6V
Ti-8Mn <sup>a</sup>	860	125	760	110	0.05	0.08	0.015	0.50	0.20	—	—	—	—	8.0Mn
Ti-7Al-4Mo <sup>a</sup>	1030	150	970	140	0.05	0.10	0.013	0.30	0.20	7.0	—	—	4.0	—
Ti-6Al-2Sn-4Zr-6Mo <sup>b</sup>	1170	170	1100	160	0.04	0.04	0.0125	0.15	0.15	6	2	4	6	—
Ti-5Al-2Sn-2Zr-4Mo-4Cr <sup>b,c</sup>	1125	163	1055	153	0.04	0.05	0.0125	0.30	0.13	5	2	2	4	4Cr
Ti-6Al-2Sn-2Zr-2Mo-2Cr <sup>c</sup>	1030	150	970	140	0.03	0.05	0.0125	0.25	0.14	5.7	2	2	2	2Cr, 0.25Si
Ti-3Al-2.5V <sup>d</sup>	620	90	520	75	0.015	0.05	0.015	0.30	0.12	3	—	—	—	2.5V
Ti-4Al-4Mo-2Sn-0.5Si	1100	160	960	139	<sup>e</sup>	0.02	0.0125	0.20	0.20	4	2	—	4	0.5Si
ATI 425	1007	146	931	135	.03	.08	.015	added	.30	4	—	—	—	V 2.5, Fe 1.5

(continued)

Table 2 (Continued)

Designation	Tensile Strength (min.)		0.2% Yield Strength (min.)		Impurity Limits wt. % (max.)					Nominal Composition, wt. %				
	MPa	ksi	MPa	ksi	N	C	H	Fe	O	Al	Sn	Zr	Mo	Others
<b><math>\beta</math> alloys</b>														
Ti-10V-2Fe-3Al <sup>6c</sup>	1170	170	1100	160	0.05	0.05	0.015	2.5	0.16	3	—	—	—	10V
Ti-13V-11Cr-3Al <sup>b</sup>	1170	170	1100	160	0.05	0.05	0.025	0.35	0.17	3	—	—	—	11.0Cr, 13.0V
Ti-8Mo-8V-2Fe-3Al <sup>6c</sup>	1170	170	1100	160	0.03	0.05	0.015	2.5	0.17	3	—	—	8.0	8.0V
Ti-3Al-8V-6Cr-4Mo-4Zr <sup>6c</sup>	900	130	830	120	0.03	0.05	0.20	0.25	0.12	3	—	4	4	6Cr, 8V
Ti-11.5Mo-6Zr-4.5Sn <sup>d</sup>	690	100	620	90	0.05	0.10	0.020	0.35	0.18	—	4.5	6.0	11.5	—
Ti-15V-3Cr-3Al-3Sn	1000 <sup>b</sup> 1241 <sup>f</sup>	145 <sup>b</sup> 180 <sup>f</sup>	965 <sup>b</sup> 1172 <sup>f</sup>	140 <sup>b</sup> 170 <sup>f</sup>	0.05	0.05	0.015	0.25	0.13	3	3	—	—	15V, 3Cr
Ti-15Mo-3Al-2.7Nb-0.2Si	862	125	793	115	0.05	0.05	0.015	0.25	0.13	3	—	—	15	2.7Nb, 0.2Si

<sup>a</sup>Mechanical properties given for the annealed condition; may be solution treated and aged to increase strength.

<sup>b</sup>Mechanical properties given for the solution-treated-and-aged condition; alloy not normally applied in annealed conditions.

<sup>c</sup>Semicommercial alloy; mechanical properties and composition limits subject to negotiation with suppliers.

<sup>d</sup>Primarily a tubing alloy; may be cold drawn to increase strength.

<sup>e</sup>Combined O<sub>2</sub> + 2N<sub>2</sub> = 0.27%.

<sup>f</sup>Also solution treated and aged using an alternative aging temperature (480°C, or 900°F)

Source: Matthew Donachie, *Titanium: A Technical Guide*, 2nd ed., ASM International, Materials Park, OH, 2001, p. 8, except:

Ti-1100 data from Timet data sheet TMC-0156 (2008)

ATI 425 data from ATI 425 technical data sheet (2011)

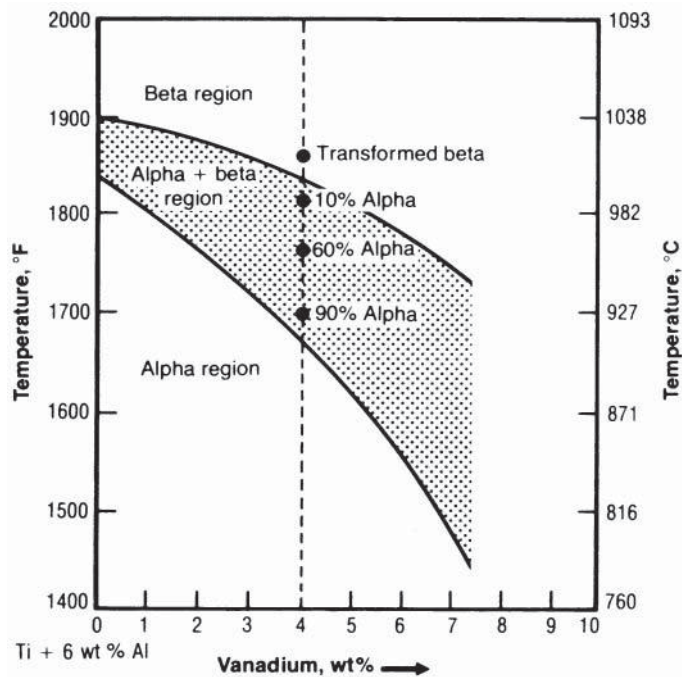
reheating and holding at an intermediate temperature after prior forging and heat treatment processing.

### 3.4 Effects of Alloy Elements

Alloy elements generally can be classified as alpha stabilizers or beta stabilizers. Alpha stabilizers, such as aluminum, oxygen, and nitrogen, increase the temperature at which the alpha phase is stable. On the other hand, beta stabilizers, such as vanadium and molybdenum, result in stability of the beta phase at lower temperatures. The transformation temperature from alpha plus beta, or from alpha, to all beta is known as the beta transus temperature. The beta transus is defined as the lowest equilibrium temperature above which the material is 100% beta. The beta transus is critical in deformation processing and in heat treatment, as described below. By reference to the beta transus, heat treatment temperatures can be selected to produce specific microstructures during heat treatment. See, for example, the amount of alpha phase that can be produced by temperature relative to the beta transus for Ti-6Al-4V as shown in Fig. 5.

### 3.5 Intermetallic Compounds and Other Secondary Phases

Intermetallic compounds and transient secondary phases are formed in titanium alloy systems along with microstructural variants of the traditional beta and alpha phases. The more important secondary phases, historically, have been omega and alpha-2 (chemically written as  $Ti_3Al$ ). The omega phase has not proven to be a factor in commercial systems using present-day processing practice. Alpha-2 has been a concern in some cases of stress corrosion cracking. Alloys



**Figure 5** Phase diagram that predicts the results of heat treatment or forging practice. (Source: Matthew Donachie, *Titanium: A Technical Guide*, 2nd ed., ASM International, Materials Park, OH, 2001, p. 34.) Reprinted with permission of ASM International.

with extrahigh aluminum were found to be prone to stress corrosion cracking. Some interest in alpha-2 centered on its use as a matrix for a high-temperature titanium alloy. However, the high-temperature alloy matrix of choice is gamma TiAl, mentioned previously. The gamma phase is not a factor in the property behavior of conventional titanium alloys.

### 3.6 Elastic Constants and Physical Properties

Titanium is a low-density element (approximately 60% of the density of steel and superalloys) which can be strengthened greatly by alloying and deformation processing. The physical and mechanical properties of elemental titanium are given in Table 3. Titanium is nonmagnetic and has good heat transfer properties. Its coefficient of thermal expansion is somewhat lower than that of steel and less than half that of aluminum.

**Table 3** Physical and Mechanical Properties of Elemental Titanium

Atomic number	22
Atomic weight	47.90
Atomic volume	10.6 W/D
Covalent radius	1.32 Å
First ionization energy	158 kcal/g · mol
Thermal neutron absorption cross section	5.6 barns/atom
Crystal structure	<ul style="list-style-type: none"> <li>• Alpha: hcp <math>\leq 882.5^{\circ}\text{C}</math> (1620°F)</li> <li>• Beta: bcc <math>\geq 882.5^{\circ}\text{C}</math> (1620°F)</li> </ul>
Color	Dark gray
Density	4.51 g/cm <sup>3</sup> (0.163 lb/in. <sup>3</sup> )
Melting point	1668 $\pm$ 10°C (3035°F)
Solidus/liquidus	1725°C
Boiling point	3260°C (5900°F)
Specific heat (at 25°C)	0.518 J/kg · K (0.124 Btu/lb · °F)
Thermal conductivity	9.0 Btu/h · ft <sup>2</sup> · °F
Heat of fusion	440 kJ/kg (estimated)
Heat of vaporization	9.83 MJ/kg
Specific gravity	4.5
Hardness	70–74 R <sub>B</sub>
Tensile strength	35 ksi · min
Modulus of elasticity	14.9 $\times$ 10 <sup>6</sup> psi
Young's modulus of elasticity	116 $\times$ 10 <sup>9</sup> N/m <sup>2</sup> 16.8 $\times$ 10 <sup>6</sup> lbf/in. <sup>2</sup> 102.7 GPa
Poisson's ratio	0.41
Coefficient of friction	0.8 at 40 m/min (125 ft/min) 0.68 at 300 m/min (1000 ft/min)
Specific resistance	554 $\mu\Omega$ · mm
Coefficient of thermal expansion	8.64 $\times$ 10 <sup>-6</sup> /°C
Electrical conductivity	3% IACS (copper 100%)
Electrical resistivity	47.8 $\mu\Omega$ · cm
Electronegativity	1.5 Pauling's
Temperature coefficient of electrical resistance	0.0026/°C
Magnetic susceptibility	1.25 $\times$ 10 <sup>-6</sup> 3.17 emu/g
Machinability rating	40

Source: Matthew Donachie, *Titanium: A Technical Guide, 1st ed.*, ASM International, Materials Park, OH, 1988, p. 11.

Titanium's modulus can vary with alloy type (beta vs. alpha) and processing, from as low as 93 GPa ( $13.5 \times 10^6$  psi) up to about 120.5 GPa ( $17.5 \times 10^6$  psi). For reference, titanium alloy moduli on average are about 50% greater than the moduli for aluminum alloys but only about 60% of the moduli for steels and nickel-based superalloys. Wrought titanium alloys can have their crystals oriented by processing such that a texture develops. When that happens, instead of the usual random orientation of grains leading to uniformity of mechanical properties, a nonuniform orientation occurs and leads to a greater than normal range of property values. By appropriate processing, it is possible to orient wrought titanium for optimum elastic modulus at the high end of the modulus values quoted above. Although textures can be produced, processing that leads to directional grain or crystal orientation similar to directional solidification in castings or directional recrystallization in oxide dispersion-strengthened alloys is not practical in titanium alloy systems. Directional processing, while providing control over the modulus, may not result in the best values for strength properties.

### 3.7 Effects of Processing

Properties of titanium alloys of a given composition generally are controlled by variations of the processing (including heat treatment) and are modified for optimum fatigue resistance by surface treatments such as shot peening. Process treatments can produce either acicular or equiaxed microstructures in most titanium alloys if phase transformations from alpha-to-beta-to-alpha (or to related phases) are permitted to occur. Microstructures have been identified which show alpha as acicular or equiaxed and with varying amounts of alpha phase. The platelike or acicular alpha produced by transformation from beta phase has special aspects as far as properties are concerned. Table 4 shows the relative behavior of equiaxed vs. platelike alpha. No one microstructure is best for all applications.

### 3.8 Hydrogen (in CP Titanium)

The solubility of hydrogen in alpha titanium at 300°C (572°F) is about 8 at.% (about 0.15 wt.%, or about 1000 ppm by weight). Hydrogen in solution has little effect on the mechanical properties. Damage is caused by hydrides which form. Upon precipitation of the hydride, titanium alloy ductility suffers. Hydrogen damage of titanium and titanium alloys, therefore, is manifested as a loss of ductility (embrittlement) and/or a reduction in the stress intensity threshold for crack propagation. Figure 6 shows the effect of hydrogen on reduction of area.

No embrittlement is found at 20 ppm hydrogen, which corresponds to about 0.1 at.% of hydrogen. Other data show that, independent of the heat treatment, this low a concentration has little effect on the impact strength, a different measure of embrittlement. However, as little as

**Table 4** Relative Advantages of Equiaxed and Acicular Microstructures

---

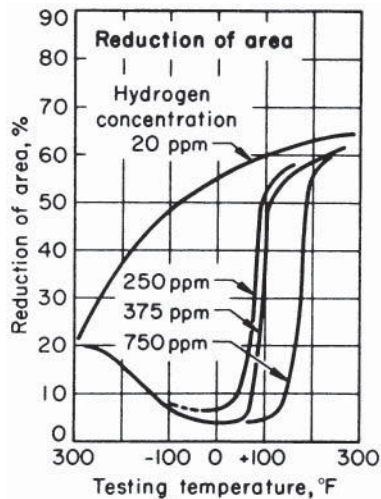
*Equiaxed*

- Higher ductility and formability
- Higher threshold stress for hot-salt stress corrosion
- Higher strength (for equivalent heat treatment)
- Better hydrogen tolerance
- Better low-cycle fatigue (initiation) properties

*Acicular*

- Superior creep properties
  - Higher fracture toughness values
-





**Figure 6** Ductility of alpha titanium versus test temperature, showing embrittling effects of hydrogen. (Source: M. Donachie, *Titanium: A Technical Guide*, 2nd ed., ASM International, Materials Park, OH, 2001, p. 96.) Reprinted with permission of ASM International.

0.5 at.% hydrogen (about 100 atom ppm) can cause measurable embrittlement. Slow cooling from the alpha region—e.g., 400°C (752°F)—allows sufficient hydride to precipitate to reduce the impact energy. The only practical approach to control the hydrogen problem is to maintain a low concentration of the element. Hydrogen also can have a potent effect on other titanium alloy properties. Contrary to the situation with oxygen and nitrogen (see below), hydrogen can be removed from alloys by vacuum heat treatment.

### 3.9 Oxygen and Nitrogen (in CP Titanium)

Oxygen and nitrogen have a significant effect on strength properties. As the amount of oxygen and nitrogen increases, the toughness decreases until the material eventually becomes quite brittle. Embrittlement occurs at a concentration considerably below the solubility limit. The allowed oxygen content is higher than the allowed nitrogen content. Yield and ultimate strengths increase as oxygen (and nitrogen) levels go up. The higher strengths in CP titanium grades come from higher oxygen levels. Oxygen (and nitrogen) can have a potent effect on other titanium alloy properties as well. Oxygen and nitrogen are not removed by vacuum heat treatment and so control must always be exerted during alloy processing to maintain component oxygen/nitrogen levels at desired or below permissible levels. Further discussion of the effects of interstitial elements such as oxygen follows below.

### 3.10 Mechanical Properties of Titanium Alloys

#### *General Aspects*

The grain size, grain shape, and grain boundary arrangements in titanium have a very significant influence on mechanical properties, and it is the ability to manipulate the phases/grains present as a result of alloy composition that is responsible for the variety of properties that can be produced in titanium and its alloys. Transformed beta-phase products in alloys can affect tensile strengths, ductility, toughness, and cyclic properties. To these effects must be added the basic strengthening effects of alloy elements.

Interstitial elements are those elements such as oxygen that are significantly smaller than the titanium atom and so may dissolve in the titanium-phase crystal lattice as solid solutions without substituting for titanium atoms. Of course, some interstitial elements also may form second phases with titanium. For example, as indicated earlier, hydrogen can combine with titanium atoms to form a titanium hydride. As is the case for comparable-size (substitutional) elements to titanium, interstitial elements may have a preference for one phase over another in the metal. As indicated above, a significant influence on mechanical behavior of CP titanium is brought about by the elements hydrogen, nitrogen, carbon, and oxygen, which dissolve interstitially in titanium and have a potent effect on mechanical properties. These effects carry over to titanium alloys in varying degrees.

The ELI (extralow interstitial) levels specified for some titanium alloys implicitly recognize the effect of reduced interstitials on ductility. ELI-type material is used for critical applications where enhanced ductility and toughness are produced by keeping interstitials at a very low level. Hydrogen is always kept at a low level to avoid embrittlement, yet there still remains concern about the most reasonable level to specify in both CP and alloyed titanium to protect against embrittlement but keep manufacturing cost low.

Although data are not provided here for grain size effects on titanium grades, it is generally accepted that fineness of structure (smaller particle size, grain size, etc.) is more desirable from the point of view of TYS in metallic materials. The UTS is not particularly affected by grain size, but ductility as represented by elongation or reduction in area generally is improved with smaller grain sizes. Ductility is a measure of toughness, but toughness is not normally at issue in CP titanium grades. Another measure of toughness is Charpy impact strength. Chemistry and minimum tensile properties for various specifications for CP and modified titanium grades at room temperature are given in Table 5.

Elevated-temperature behavior of titanium grades has been studied but titanium grades are not customarily used at high temperatures. The near-alpha or alpha-beta alloys are the preferred materials where high-temperature mechanical properties are desired. With allowance for grain size effects and possible minor chemistry variations, cast CP titanium materials should behave in much the same way as wrought.

### ***Alpha Alloys***

Alpha alloys such as Ti-5Al-2.5Sn, Ti-6Al-2Sn-4Zr-2Mo+Si, and Ti-8Al-1Mo-1V (see Table 2) are used primarily in gas turbine applications. Ti-8Al-1Mo-1V alloy and Ti-6Al-2Sn-4Zr-2Mo + Si are useful at temperatures above the normal range for the work horse alpha-beta alloy, Ti-6Al-4V. Ti-8Al-1Mo-1V and Ti-6Al-2Sn-4Zr-2Mo + Si alloys have better creep resistance than Ti-6Al-4V and creep resistance is enhanced with a fine acicular (Widmanstätten) structure. In its normal heat-treated condition, Ti-6Al-2Sn-4Zr-2Mo+Si alloy actually has a structure better described as alpha-beta. Ti-1100 alloy (Ti-6Al-2.7Sn-4Zr-0.4Mo-0.45Si) is a near-alpha alloy designed for the highest operating temperatures.

Alpha and near-alpha alloys are usually employed in the solution-annealed and stabilized condition. Solution annealing may be done at a temperature some 35°C (63°F) below the beta transus temperature while stabilization is commonly produced by heating for 8 h at about 590°C (1100°F). These alloys are more susceptible to the formation of ordered Ti<sub>3</sub>Al, which promotes stress corrosion cracking (SCC).

### ***Alpha-Beta Alloys***

The most important titanium alloy is the alpha-beta alloy, Ti-6Al-4V. This alloy has found application for a wide variety of aerospace components and fracture-critical parts. With a strength-to-density ratio of 25 × 10<sup>6</sup> mm (1 × 10<sup>6</sup> in.), Ti-6Al-4V is an effective

**Table 5** CP and Modified Ti: Minimum Room Temperature Tensile Properties for Various Specifications

Designation	Chemical Composition (% max.)				Tensile Properties <sup>a</sup>				Minimum Elongation (%)
	C	O	N	Fe	Tensile Strength		Yield Strength		
					MPa	ksi	MPa	ksi	
JIS class 1	—	0.15	0.05	0.20	275–410	40–60	165 <sup>b</sup>	24 <sup>b</sup>	27
ASTM grade 1 (UNS R50250)	0.10	0.18	0.03	0.20	240	35	170–310	25–45	24
DIN 3.7025	0.08	0.10	0.05	0.20	295–410	43–60	175	25.5	30
GOST BT1-00	0.05	0.10	0.04	0.20	295	43	—	—	20
BS 19-27t/in. <sup>2</sup>	—	—	—	0.20	285–410	41–60	195	28	25
JIS class 2	—	0.20	0.05	0.25	343–510	50–74	215 <sup>b</sup>	31 <sup>b</sup>	23
ASTM grade 2 (UNS R50400)	0.10	0.25	0.03	0.30	343	50	275–410	40–60	20
DIN 3.7035	0.08	0.20	0.06	0.25	372	54	245	35.5	22
GOST BTI-0	0.07	0.20	0.04	0.30	390–540	57–78	—	—	20
BS 25-35t/in. <sup>2</sup>	—	—	—	0.20	382–530	55–77	285	41	22
JIS class 3	—	0.30	0.07	0.30	480–617	70–90	343 <sup>b</sup>	50 <sup>b</sup>	18
ASTM grade 3 (UNS R50500)	0.10	0.35	0.05	0.30	440	64	377–520	55–75	18
ASTM grade 4 (UNS R50700)	0.10	0.40	0.05	0.50	550	80	480	70	15
DIN 3.7055	0.10	0.25	0.06	0.30	460–590	67–85	323	47	18
ASTM grade 7 (UNS R52400)	0.10	0.25	0.03	0.30	343	50	275–410	40–60	20
ASTM grade 11 (UNS R52250)	0.10	0.18	0.03	0.20	240	35	170–310	25–45	24
ASTM grade 12 (UNS R53400)	0.10	0.25	0.03	0.30	480	70	380	55	12

<sup>a</sup>Unless a range is specified, all listed values are minimums.

<sup>b</sup>Only for sheet, plate, and coil.

Source: G Welsch, R. Boyer, and E. Collins, Principal Eds., *Materials Property Handbook—Titanium Alloys*, ASM International, Materials Park, OH, 1994, p. 224.

lightweight structural material and has strength–toughness combinations between those of steel and aluminum alloys. High-strength alpha–beta alloys include Ti–6Al–6V–2Sn and Ti–6Al–2Sn–4Zr–6Mo. Alpha is the dominant phase in all of these alloys. These high-strength alloys are stronger and more readily heat treated than Ti–6Al–4V.

When alpha–beta titanium alloys are heat treated high in the alpha–beta range and then cooled, the resulting structure, because of the presence of globular (equiaxed) primary alpha in the transformed beta (platelike) matrix, is called equiaxed. When a 100% transformed beta structure is achieved by cooling from above the beta transus, the structure may be called acicular, or needlelike. Generally speaking, alpha–beta alloys would be annealed just below the beta transus to produce a maximum of transformed acicular beta with approximately 10% of equiaxed alpha present. Some titanium alloys—for example Ti–6Al–2Sn–4Zr–2Mo—are given beta heat treatments to enhance high-temperature creep resistance. (Castings and powder products may be given a beta anneal, too, in order to break up the structure, although not necessarily for optimizing creep strength.)

In actual components, the structure of titanium alpha–beta alloys is controlled not only by how much working (mechanical deformation in processing) is done and by how close to, or above, the beta transus the alloy is processed but also by the section size of the component. Ideally, alloys should have good hardenability, i.e., ability to reach desired cooling rates and attendant microstructures in fairly thick sections. Many alpha–beta alloys do not have great hardenability. Ti–6Al–4V alloy only has sufficient hardenability to be effectively heat treated to full property levels in sections less than 25 mm (1 in.) thick.

One of the least understood concepts in the behavior of alpha–beta titanium alloys is that of aging. With few exceptions titanium alloys do not age in the classical sense: that is, where

a secondary metastable precipitate or a strong intermetallic compound appears and strengthens the matrix by its dispersion. A dispersion is produced on aging titanium alpha–beta alloys, but it is thought to be beta dispersed in the alpha or in martensitic alpha prime. Beta is not materially different from the alpha phase with respect to strength; however, the effectiveness of strengthening in titanium alloys appears to center in the number and fineness of alpha–beta phase boundaries. Annealing and rapid cooling, which maximize alpha–beta boundaries for a fixed primary alpha content, along with aging, which may promote additional boundary structure, can significantly increase alloy strength.

### ***Beta Alloys***

An alloy is considered to be a beta alloy if it contains sufficient beta stabilizer alloying element to retain the beta phase without transformation to martensite on quenching to room temperature. A number of titanium alloys (see Table 2) contain more than this minimum amount of beta stabilizer alloy addition. The more highly beta-stabilized alloys are alloys such as Ti–3Al–8V–6Cr–4Mo–4Zr (beta C) and Ti–15V–3Cr–3Al–3Sn. Solute-lean beta alloys are sometimes classified as beta-rich alpha–beta alloys, and this class includes Ti–10V–2Fe–3Al and proprietary alloys such as Ti-17 (Ti–5Al–2Sn–2Zr–4Mo–4Cr) and beta CEZ (Ti–5Al–2Sn–4Zr–4Mo–2Cr).

In a strict sense there is no truly stable beta alloy because even the most highly alloyed beta will, on holding at elevated temperatures, begin to precipitate omega, alpha, Ti<sub>3</sub>Al, or silicides, depending on temperature, time, and alloy composition. All beta alloys contain a small amount of aluminum, an alpha stabilizer, in order to strengthen alpha that may be present after heat treatment. The composition of the precipitating alpha is not constant and will depend on the temperature of heat treatment. The higher the temperature in the alpha–beta phase field, the higher will be the aluminum content of alpha.

The processing window for beta alloys is tighter than that normally used for the other alloy types (alpha and alpha–beta alloys). For the less highly beta-stabilized alloys, Ti–10V–2Fe–3Al for example, the thermomechanical process is critical to the property combinations achieved as this processing has a strong influence on the final microstructure and the resultant tensile strength and fracture toughness that may be achieved. Exact control of thermomechanical processing is somewhat less important in the more highly beta-stabilized alloys, such as Ti–3Al–8V–6Cr–4Mo–4Zr and Ti–15V–3Cr–3Al–3Sn. In these alloys, the final microstructure, precipitated alpha in the beta phase, is so fine that microstructural manipulation through thermomechanical processing is not as effective.

### ***Properties—Wrought Alloys***

Typical minimum property values for titanium alloy mill products are listed in Table 6. Fractions of room temperature strength retained at elevated temperatures by the same titanium alloys are shown in Table 7. Data for unalloyed titanium is included in Table 7 to illustrate that alloys not only have higher room temperature strengths than unalloyed titanium but also retain much larger fractions of that strength at elevated temperatures. Typical tensile strengths and 0.1% creep strengths as functions of temperature of some selected alloys are shown in Figs. 7 and 8, respectively.

Fatigue life in unalloyed titanium (and in alloys) depends on grain size, interstitial (oxygen, etc.) level, and degree of cold work, as illustrated in Fig. 9. A decrease in grain size in unalloyed titanium from 110 μm down to 6 μm improves the 10<sup>7</sup> cycle fatigue endurance limit by 30%. HCF endurance limits of unalloyed titanium depend on interstitial contents just as do the TYS and UTS. The ratio of HCF endurance limit and TYS at ambient temperature appears to remain relatively constant as TYS changes with changing interstitial content but does show temperature dependence.

**Table 6** Tensile Strengths of Several Commercial Titanium-Based Alloys: Typical Room Temperature Values

Alloy Name	Nominal Composition	Condition	Tensile Strength		Yield Strength		Elongation (%)
			ksi	10 <sup>8</sup> N/m <sup>2</sup>	ksi	10 <sup>8</sup> N/m <sup>2</sup>	
5-2-5	Ti-5Al-2.5Sn	Annealed (0.25-4 h/1300-1600°F)	120-130	8.3-9.0	115-120	7.9-8.3	13-18
3-2-5	Ti-3Al-2.5V	Annealed (1-3 h/1200-1400°F)	95	6.5	90	6.2	22
6-2-1-1	Ti-6Al-2Nb-1Ta-1Mo	Annealed (0.25-2 h/1300-1700°F)	125	8.6	110	7.6	14
8-1-1	Ti-8Al-1Mo-1V	Annealed (8 h/1450°F)	145	10.0	135	9.3	12
Ti-1100	6Al-2.7Sn-4Zr-0.4Mo-0.45Si	Beta anneal +1400 F/1 h	150	10.3	134	9.2	
Corona 5	Ti-4.5Al-5Mo-1.5Cr	$\alpha$ - $\beta$ annealed after $\beta$ processing	140-160	9.7-11.0	135-150	9.3-10.3	12-15
Ti-17	Ti-5Al-2Sn-2Zr-4Mo-4Cr	$\alpha$ - $\beta$ or $\beta$ processed plus aged	165	11.4	155	10.7	8
6-4	Ti-6Al-4V	Annealed (2 h/1300-1600°F)	140	9.6	130	9.0	17
ATI 425	4Al-2.5V-1.5Fe	Hot work bar/billet-mill annealed	146	10.1	135	9.3	
6-6-2	Ti-6Al-6V-2Sn	Aged	170	11.7	160	11.0	12
		Annealed (3 h/1300-1500°F)	155	10.7	145	10.0	14
6-2-4-2	Ti-6Al-2Sn-4Zr-2Mo	Aged	185	12.8	175	12.1	10
6-2-4-6	Ti-6Al-2Sn-4Zr-6Mo	Annealed (4 h/1300-1550°F)	145	10.0	135	9.3	15
		Annealed (2 h/1500-1600°F)	150	10.3	140	9.7	11
6-22-22	Ti-6Al-2Sn-2Zr-2Mo-2Cr-0.25Si	Aged	175	12.1	165	11.4	8
10-2-3	Ti-10V-2Fe-3Al	$\alpha$ - $\beta$ processed plus aged	162	11.2	147	10.1	14
		Annealed (1 h/1400°F)	140	9.7	130	9.0	9
15-3-3-3	Ti-15V-3Cr-3Sn-3Al	Aged	180-195	12.4-13.4	165-180	11.4-12.4	7
		Annealed (0.25 h/1450°F)	115	7.9	112	7.7	20-25
13-11-3	Ti-13V-11Cr-3Al	Aged	165	11.4	155	10.7	8
		Annealed (0.5 h/1400-1500°F)	135-140	9.3-9.7	125	8.6	18
38-6-44	Ti-3Al-8V-6Cr-4Mo-4Zr	Aged	175	12.1	165	11.4	7
		Annealed (0.5 h/1500-1700°F)	120-130	8.3-9.0	113-120	7.8-8.3	10-15
$\beta$ -III	Ti-4.5Sn-6Zr-11.5Mo	Aged	180	12.4	170	11.7	7
		Annealed (0.5 h/1300-1600°F)	100-110	6.9-7.6	95	6.5	23
		Aged	180	12.4	170	11.7	7

International, Materials Park, OH, 1994, p. 106, except:

Ti-1100 (Timetal 1100) data from oral communication (2012) and Timet data sheet TMC-0156 Titanium Metal Corp., Exton, PA, 2008

ATI425 data from ATI 425 Technical Data Sheet, Allegheny Technologies Inc., Pittsburgh, PA, 2010.

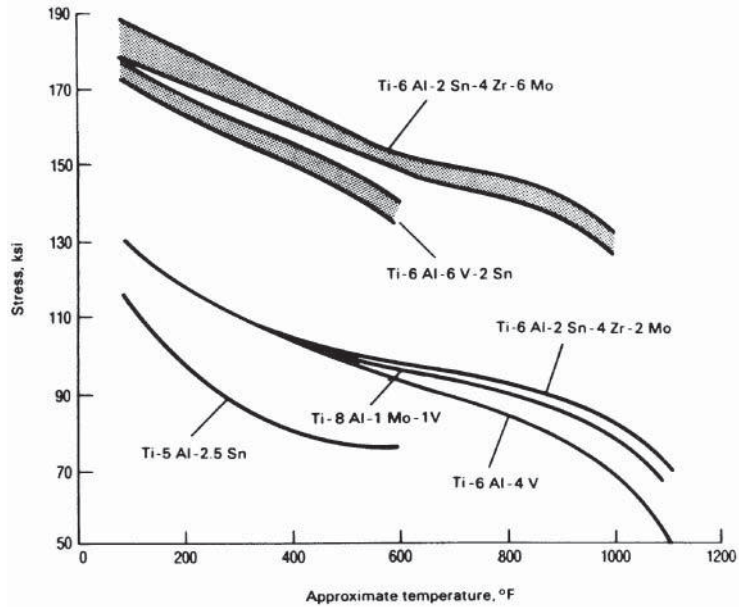
Source: G. Welsch, R. Boyer, and E. Collins, Principal Eds., *Materials Property Handbook—Titanium Alloys*, ASM International, Materials Park, OH, 1994, p. 106.

**Table 7** Fraction of Room Temperature Strength Retained at Elevated Temperature for Several Titanium Alloys<sup>a</sup>

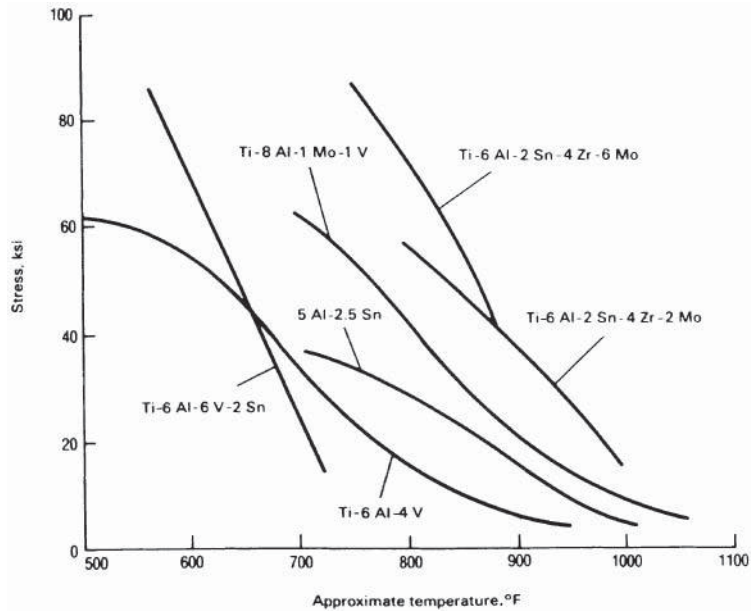
Temperature °C	°F	Unalloyed Ti		Ti-6Al-4V		Ti-6Al-6V-2Sn		Ti-6Al-2Sn-4Zr-6Mo		Ti-6Al-2Sn-4Zr-2Mo		Ti-1100 <sup>d</sup>		IMI-834	
		TS	YS	TS	YS	TS	YS	TS	YS	TS	YS	TS	YS	TS	YS
93	200	0.80	0.75	0.90	0.87	0.91	0.89	0.90	0.89	0.93	0.90	0.93	0.92	—	—
204	400	0.57	0.45	0.78	0.70	0.81	0.74	0.80	0.80	0.83	0.76	0.81	0.85	0.85	0.78
316	600	0.45	0.31	0.71	0.62	0.76	0.69	0.74	0.75	0.77	0.70	0.76	0.79	—	—
427	800	0.36	0.25	0.66	0.58	0.70	0.63	0.69	0.71	0.72	0.65	0.75	0.76	—	—
482	900	0.33	0.22	0.60	0.53	—	—	0.66	0.69	0.69	0.62	0.72	0.74	—	—
538	1000	0.30	0.20	0.51	0.44	—	—	0.61	0.66	0.66	0.60	0.69	0.69	—	—
593	1100	—	—	—	—	—	—	—	—	—	—	0.66	0.63	0.63	0.61

<sup>a</sup>Short-time tensile test with less than 1 h at temperature prior to test. TS = tensile strength; YS = yield strength.

Source: Author/Editor unlisted, *Fatigue Data Handbook: Light Structural Alloys*, ASM International, Materials Park, OH, 1995, p. 189.

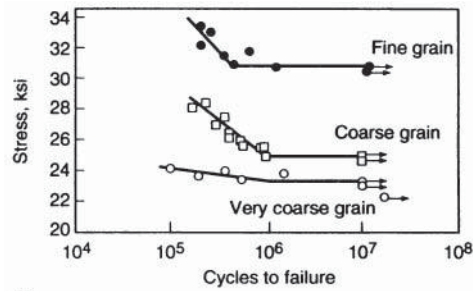


**Figure 7** Comparison of typical ultimate tensile strengths of selected titanium alloys as a function of temperature. (Source: M. Donachie, *Titanium: A Technical Guide*, 2nd ed., ASM International, Materials Park, OH, 2001, p. 104.) Reprinted with permission of ASM International.

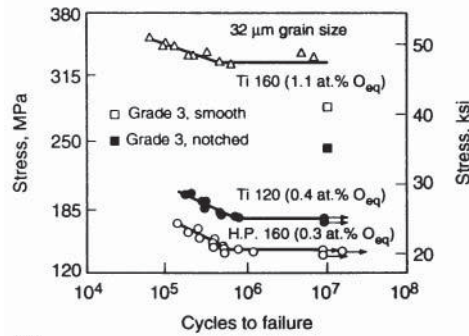


**Figure 8** Comparison of typical 150-h, 0.1% creep strengths for selected titanium alloys. (Source: M. Donachie, *Titanium: A Technical Guide*, 2nd ed., ASM International, Materials Park, OH, 2001, p. 104.) Reprinted with permission of ASM International.

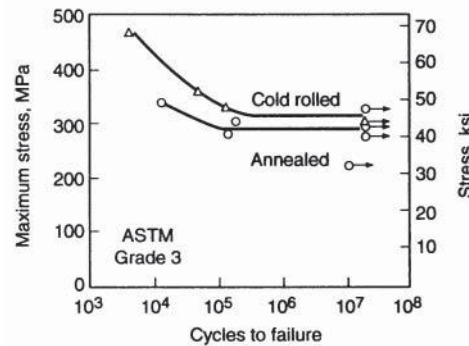




(a)



(b)



(c)

**Figure 9** Stress–cycles to failure curves for pure titanium as affected by (a) grain size, (b) oxygen content, and (c) cold work. (Source: Steven Lampman, Ed., *Metal Handbook*, Vol. 19, ASM International, Metals Park, OH, 1996, p. 837.) Reprinted with permission of ASM International.

There are significant differences among titanium alloys in fracture toughness, but there also is appreciable overlap in their properties. Table 8 gives examples of typical plane-strain fracture toughness ranges for alpha–beta titanium alloys. From these data it is apparent that the basic alloy chemistry affects the relationship between strength and toughness. From Table 8 it also is evident, as noted earlier, that transformed microstructures may greatly enhance toughness while only slightly reducing strength. It is well known that toughness depends on thermomechanical processing (TMP) to provide the desired structure. However, the enhancement of fracture



**Table 8** Typical Fracture Toughness Values of Several Titanium Alloys

Alloy	Alpha Morphology	Yield Strength		Fracture Toughness $K_{Ic}$	
		MPa	ksi	MPa · m <sup>1/2</sup>	ksi · in. <sup>1/2</sup>
Ti-6Al-4V	Equiaxed	910	130	44-66	40-60
	Transformed	875	125	88-110	80-100
Ti-6Al-6V-2Sn	Equiaxed	1085	155	33-55	30-50
	Transformed	980	140	55-77	50-70
Ti-6Al-2Sn-4Zr-6Mo	Equiaxed	1155	165	22-23	20-30
	Transformed	1120	160	33-55	30-50

Source: M. Donachie, *Titanium: A Technical Guide*, 1st ed., ASM International, Materials Park, OH, 1988, p. 168.

toughness at one stage of an operation— for example, a forging billet—does not necessarily carry over to a forged part.

Because welds in alloy Ti-6Al-4V contain transformed products, one would expect such welds to be relatively high in toughness. This is, in fact, the case. In addition to welding, many other factors such as environment, cooling rates occurring in large sections (i.e., hardenability), and hydrogen content, may affect  $K_{Ic}$ .

Titanium alloys may show less resistance to notches than other alloys. Notch strength in fatigue is significantly lower than smooth strength. Scratches on the surfaces of titanium alloy components can lead to reduced fatigue capability. Weld spatter is known to reduce fatigue capability. High levels of favorable compressive residual stresses usually exist in titanium alloys as a result of machining. These levels are sometimes enhanced by surface processing such as glass bead or shot peening. Electropolishing of titanium surfaces will reduce fatigue capability.

#### **Properties—Cast Alloys**

Cast titanium alloys generally are alpha-beta alloys. They are equal, or nearly equal, in strength to wrought alloys of the same compositions. Typical room temperature tensile properties of several cast titanium alloys are shown in Table 9 while creep strength of cast Ti-6Al-4V is shown in Table 10. Virtually all existing data have been generated from alloy Ti-6Al-4V; consequently, the basis for most cast alloy property data is Ti-6Al-4V. Because the microstructure of cast titanium alloy parts is comparable to that of wrought material, many properties of cast plus HIP parts are at similar levels to those for wrought alloys. These properties include tensile strength, creep strength, fracture toughness, and fatigue crack propagation.

Generally, castings of titanium alloys are hot isostatically pressed (HIPed) to close casting porosity. HIP conditions may affect the resultant properties since HIP is just another heat treatment as far as microstructure is concerned. It also should be noted that test results are often on small separately cast test coupons and will not necessarily reflect the property level achievable with similar processing on a full-scale cast part. Property levels of actual cast parts, especially larger components, probably will be somewhat lower, the result of coarser grain structure or slower quench rates achieved.

#### **Properties—Powder Formed Alloys**

It has been a goal of titanium alloy development to reduce costs by introducing powder metal processing. Very high purity powder is needed. Some applications for less demanding industries than the aerospace or biomedical markets may be able to use lower cost powder with lesser properties than conventional wrought alloys are capable of producing. High-purity powder is produced by special rotating electrode or similar processes under inert conditions. Subsequent

**Table 9** Typical Room Temperature Tensile Properties of Several Cast Titanium Alloys (bars machined from castings)<sup>a</sup>

Alloy <sup>b,c</sup>	Yield Strength		Tensile Strength		Elongation (%)	Reduction of area (%)
	MPa	ksi	MPa	ksi		
Commercially pure (grade 2)	448	65	552	80	18	32
Ti-6Al-4V, annealed	855	124	930	135	12	20
Ti-6Al-4V-ELI	758	110	827	120	13	22
Ti-1100, beta-STA <sup>c</sup>	848	123	938	136	11	20
Ti-6Al-2Sn-4Zr-2Mo, annealed	910	132	1006	146	10	21
IMI-834, beta-STA <sup>c</sup>	952	138	1069	155	5	8
Ti-6Al-2Sn-4Zr-6Mo, beta-STA <sup>c</sup>	1269	184	1345	195	1	1
Ti-3Al-8V-6Cr-4Zr-4Mo, beta-STA <sup>c</sup>	1241	180	1330	193	7	12
Ti-15V-3Al-3Cr-3Sn, beta-STA <sup>c</sup>	1200	174	1275	185	6	12

<sup>a</sup>Specification minimums are less than these typical properties.

<sup>b</sup>Solution-treated and aged (STA) heat treatments can be varied to produce alternate properties. <sup>c</sup>ELI, extralow interstitial.

<sup>c</sup>Beta-STA, solution treatment within  $\beta$ -phase field followed by aging.

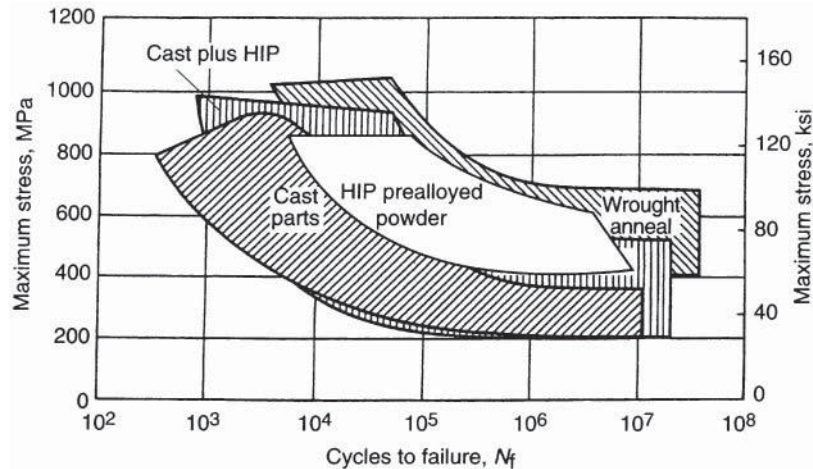
Source: Author/Editor unlisted, *Metals Handbook*, Vol. 2, ASM International, Materials Park, OH, 1990, p. 637.

**Table 10** Ti-6Al-4V: Creep Strength of Cast Material

Test Temperature		Stress		Plastic Strain on Loading (%)	Test Duration (h)	Time, h, to Reach Creep of		
°C	°F	MPa	ksi			0.1%	0.2%	1.0%
455	850	276	40.0	0	611.2	2.0	9.6	610.0
425	800	276	40.0	0	500.0	15.0	60.0	—
425	800	345	60.0	0	297.5	3.5	11.0	291.5
400	750	448	65.0	0.7	251.4	7.5	22.0	—
370	700	414	60.0	0.3	500	240.0	—	—
315	600	517	75.0	2.04	330.9	0.02	0.04	0.1
260	500	534	77.5	2.1	307.9	0.01	0.02	0.1
205	400	552	80.0	0.56	138.0	0.1	0.13	1.5
205	400	531	77.0	0.8	18.2	0.02	0.04	0.16
175	350	517	75.0	0.01	1006.0	0.4	2.2	—
150	300	517	75.0	—	500	0.25	1.2	—
150	300	517	75.0	—	500	1.7	12.2	—
120	250	517	75.0	0.0	1006.1	9.8	160.0	—

Note: Specimens from hubs of centrifugal compressor impellers that were cast, HIPed (2 h at 900°C, or 1650°F), and 103.5 MPa, 15.0 ksi, and aged 1.5 h at 675°C (1250°F). Specimen blanks approximately 5.72 × 0.95 × 0.96 cm (2.25 × 0.37 × 0.37 in.) in section size, with the long axis oriented tangential to the hub section, were machined to standard-type creep specimens 3.81 mm (0.150 in.) in diameter. The specimens were lathe turned and then polished with 320-grit emery paper. The creep rupture tests were performed at 120–455°C (250–850°F) using dead-load-type creep frames in air over a stress range of 276–552 MPa (40–80 ksi). The microstructure consisted of transformed  $\beta$ -grains with discontinuous grain boundary  $\alpha$  and colonies of transformed  $\beta$  that contained packets of parallel-oriented  $\alpha$ -platelets separated by a thin layer of aged  $\beta$ .

Source: A. Chakrabarti and E. Nichols, "Creep Behavior of Cast Ti-6Al-4V Alloy," *Titanium '80: Science and Technology*, Proceedings of the 4th International Conference on Titanium, Kyoto, Japan, May 19–22, 1980, Vol. 2, H. Kimura and O. Izumi, Ed., TMS/AIME, New York, 1980, pp. 1081–1096.



**Figure 10** Fatigue scatterbands for ingot metallurgy, castings, and powder metallurgy products of Ti-6Al-4V Alloy. (Source: Matthew Donachie, *Titanium: A Technical Guide*, 2nd ed., ASM International, Metals Park, OH, 2001, p. 116.) Reprinted with permission of ASM International.

handling and consolidation of the powder to form a net or near-net-shape (NNS) component also requires a highly inert environment. While powder-based components have shown comparable mechanical properties to wrought products, the costs of powder and the powder consolidation processes have not produced cost savings.

#### **Property Summary—Wrought, Cast, Powder Metallurgy Products**

Powder metallurgy technology has been applied to titanium alloy processing with limited success, partially owing to economic issues. Wrought processing remains the preferred method of achieving shape and property control. Cast alloy processing is used but for a limited alloy base. Figure 10 shows fatigue scatterbands for wrought, cast, and powder metallurgy products of Ti-6Al-4V alloy for comparison of attainable properties.

## **4 MANUFACTURING PROCESSES**

### **4.1 General Aspects of the Manufacture of Titanium Articles**

Appropriate compositions of all titanium alloys can be forged, rolled to sheet, or otherwise formed into a variety of shapes. Some compositions can be processed as large investment castings. Commercial large castings are made mostly in the titanium alloy, Ti-6Al-4V, which has been in production for about 60 years. Fabricated titanium structures can be built up by welding or brazing. Fabricated structures are primarily made with Ti-6Al-4V although stronger or more workable alloys are sometimes used. Fabricated structures may contain cast as well as wrought parts although wrought parts are assembled in most applications.

Single-piece forged gas turbine fan and compressor disks are prime applications for titanium alloys. Titanium wrought, cast, and powder metallurgy products find use in the biomedical arena. Fan blades and compressor blades of titanium represent areas that continue to receive support despite the recent use of titanium metal matrix composites. By and large, most titanium alloys are wrought, in particular, forged.

The manufacture of titanium alloys consists of a number of separate steps of which the following represent the transfer of titanium from an ore to an ingot ready for either wrought or cast processing or to mill products:

- Production of titanium sponge (reduction of titanium ore to an impure porous form of titanium metal)
- Purification of the sponge
- Melting of sponge or sponge plus alloy elements (or a master alloy) to form an electrode
- Remelting and, possibly, remelting again to homogenize the first electrode and create an ingot for further processing
- Primary fabrication, in which ingots are converted into billets or general mill products such as bar, plate, sheet, strip, or wire
- Secondary fabrication where a billet or bar may be forged into an approximate final shape

#### 4.2 Production of Titanium via Vacuum Arc Melting

Whether the final product is to be a forged or investment cast one, the essence of a titanium alloy's ability to create the properties desired hinges on the correct application of melting principles. Melting practices may be classified as either primary (the initial melt of elemental materials and /or scrap which sets the composition) or secondary (remelt, often more than once, of a primary melt for the purpose of controlling the solidification structure for subsequent wrought processing). The melt type or combination of melt types selected depends upon the alloy composition, mill form and size desired, properties desired, and sensitivity of the final component to localized inhomogeneity in the alloy.

The principal method for the production of titanium electrodes and ingots since commercial introduction of titanium alloys occurred in the 1950s has been the use of vacuum arc remelting (VAR). The purity of the titanium alloys produced is a function of the purity of the starting materials. Control of raw materials is extremely important in producing titanium and its alloys because there are many elements of which even small amounts can produce major, and at times undesirable, effects on the properties of the titanium alloys in finished form. In order to produce ingots of titanium or its alloys for commercial application, titanium from sponge is commonly alloyed with pure other elements, master melt of titanium plus alloy elements, and/or reclaimed titanium scrap (usually called "revert").

Because sponge is an uneven product consisting of a loose, granular mass, it does not compact as well as might be desired in some instances. Compacting of sponge titanium is needed to make an electrode from which to melt the alloy. During melting, a piece of the sponge might fall unmelted into the solidifying electrode. Perhaps a chunk of revert (or master melt) might fall in. Whatever the situation, a gross inhomogeneity would result. Depending on the type and size of the inhomogeneity, a major structural defect could exist. Consequently, after some significant incidents in aircraft gas turbine engines 50 years or more ago, second and then third melts were instituted to provide almost certain homogenization of the alloy.

#### 4.3 Cutting the Cost of Titanium Alloy Melting

Electron beam and plasma arc melting technologies are now available for the melting of titanium alloys or the remelting of scrap. The use of these technologies permits the controlled hearth melting (CHM) of titanium alloys. Processes such as electron beam controlled hearth melting (EBCHM) and plasma arc melting (PAM) have already demonstrated chemistry and quality improvements but not necessarily cost improvements for melting titanium alloys.

Other schemes have been suggested, including recovery of titanium as powder which would be sufficiently pure as to be electron beam melted just once to achieve ingot product. There is no widespread use of such technology at this time.

#### 4.4 Defects and Their Control in Titanium Melting

Defects have been a concern for titanium ingot metallurgy production since the early days of the industry. Different types of defects were recognized, most stemming from sponge handling, electrode preparation, and melt practice. The principal characterization of these defects is as random hard and brittle particles such as titanium nitride (type I defect) or tungsten carbide particles [high-density inclusions (HDIs)]. Solidification segregation can result in type II defects. Low-density inclusions (LDIs) are a variant of type II defects.

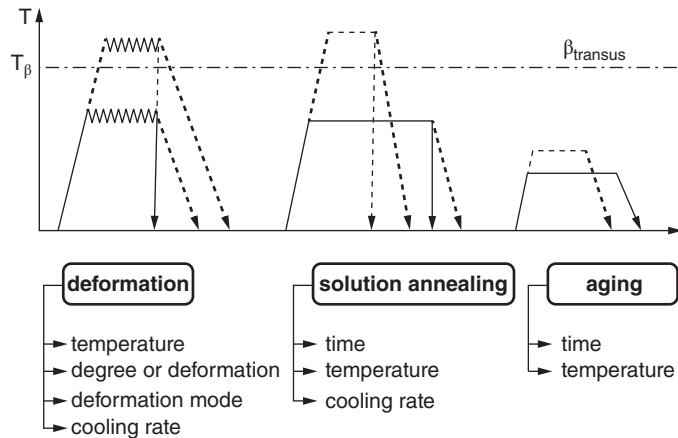
Over two dozen different defects have been cataloged. Defects prompted strict process controls which were agreed upon jointly by metal suppliers and customers alike. These controls have done much to attain either reduced-defect or defect-free materials. Despite the controls, occasional defects were involved in significant titanium alloy-related failures. The introduction of cold hearth technologies may further reduce the incidence of defects in titanium ingots. Studies on EBCHM and PAM demonstrated the ability of hearth melting to remove HDIs with great confidence (the HDIs fall to the bottom of the molten hearth). Type II defects can be avoided by better process control and use of improved melting methods; segregation defects are minimized by CHM.

#### 4.5 Forging Titanium Alloys

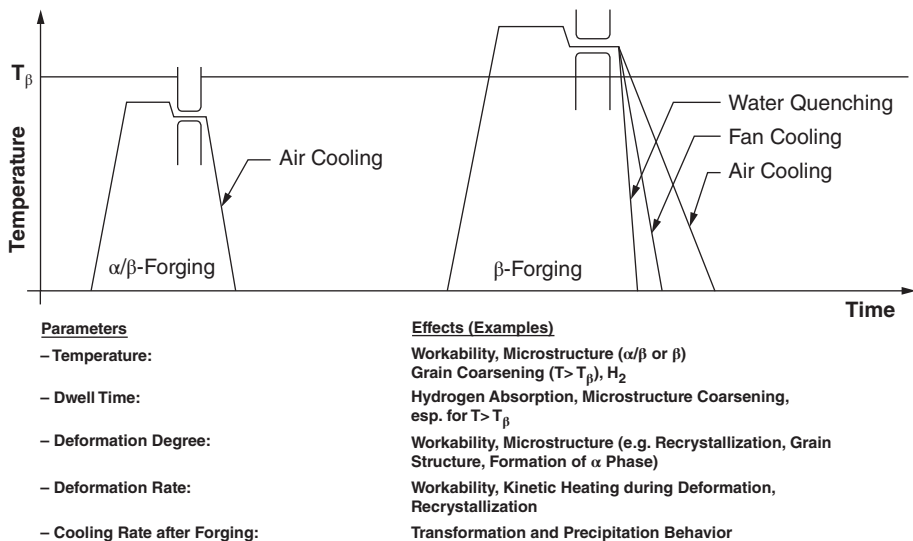
Manufacturing processes such as die forging, hot and cold forming, machining, chemical milling, joining, and sometimes extrusion are all secondary fabrication processes used for producing finished parts from billet or mill products. Each of these processes may strongly influence properties of titanium and its alloys, either alone or by interacting with effects of processes to which the metal has previously been subjected. Titanium alloy forgings are produced by all the forging methods currently available. These include open-die, closed-die, rotary forging, and others. One of the main purposes of forging, in addition to shape control, is to obtain a combination of mechanical properties that generally does not exist in bar or billet. Tensile strength, creep resistance, fatigue strength, and toughness all may be better in forgings than in bar or other forms. Selection of the optimal forging method is based on the shape desired for the forged component as well as its desired mechanical properties and microstructure (which largely determines properties after alloy composition is set).

Open-die forging is used to produce some shapes in titanium when volume and/or size do not warrant the development of closed dies for a particular application. However, closed-die forging is used to produce the greatest amount of forged titanium alloys. Closed-die forging can be classified as blocker-type (single die set), conventional (two or more die sets), or high definition (two or more die sets). Precision die forging is also conducted, usually employing hot-die/isothermal forging techniques. Conventional closed-die titanium forgings cost more than the blocker type but the increase in cost is justified because of reduced machining costs and better property control. The dies used in titanium forging are heated to facilitate the forging process and to reduce surface chilling and metal temperature losses which can lead to inadequate die filling and/or excessive surface cracking of the forged component. Hot-die/isothermal forging takes the die temperature to higher levels.

Forging is more than just a shape-making process. The key to successful forging and heat treatment is the beta transus temperature. Fundamentally there are two principal approaches to



**Figure 11** Thermomechanical treatment of titanium alloys. (Source: C. Leyens and M. Peters (Eds.), *Titanium and Titanium Alloys: Fundamentals and Applications*, Wiley, Hoboken, NJ, 2003.) This material is reproduced with permission of John Wiley & Sons, Inc., Germany.



**Figure 12** Parameters influencing forging of titanium alloys. (Source: C. Leyens and M. Peters (Eds.), *Titanium and Titanium Alloys: Fundamentals and Applications*, Wiley, Hoboken, NJ, 2003.) This material is reproduced with permission of John Wiley & Sons, Inc., Germany.

the forging of titanium alloys as illustrated schematically in Fig. 11 for forging deformation and heat treatment cycles:

- Forging the alloy predominantly below the beta transus
- Forging the alloy predominantly above the beta transus

Titanium forging is really about thermomechanically inducing favorable mechanical properties in the workpiece. Figure 12 illustrates schematically pertinent aspects of alpha–beta and beta forging processes for titanium.

Conventional alpha–beta forging is best described as a forging process in which all or most of the deformation is conducted below the beta transus. Alpha, beta, and transformed beta phases will be present in the microstructure at some time. Structures resulting from alpha–beta forging are characterized by deformed or equiaxed primary alpha phase (alpha present during the forging process) and transformed beta phase (acicular in appearance). Beta forging is a forging technique in which the deformation of the alloy is done above the beta transus. In commercial practice, beta forging actually involves initial deformation above the beta transus but final finishing with controlled amounts of deformation below the beta transus of the alloy. In beta forging, the influences of mechanical working (deformation) are not necessarily cumulative because of the high temperature and because of the formation of new grains by recrystallization each time the beta transus is surpassed on reheating for forging. Beta forging, particularly of alpha and alpha–beta alloys, results in significant reductions in forging pressures and reduced cracking tendency of the billet during forging.

An alternative titanium die-forging procedure involves the use of precision isothermal (sometimes superplastic) forging techniques. Precision isothermal forging produces a product form that requires much less machining than conventionally forged alloy to achieve final dimensions of the component. Precision forged titanium is a significant factor in titanium usage in the aircraft and gas turbine engine field. Most precision forged titanium is produced as near-net-shape (NNS) product, meaning that the forging is close to final dimensions but some machining is required.

Superplastic forming, a variant of superplastic isothermal forging, currently is widely used in the aircraft industry and to a lesser extent is used in the gas turbine industry. Advantages of superplastic forming are, among others:

- Very complex parts can be formed.
- Lighter, more efficient structures can be designed and formed.
- It is performed in a single operation.
- More than one piece may be produced in a machine cycle.
- Pressure (force) is uniformly applied to all areas of the workpiece.

Superplastic forming coupled with diffusion bonding (SPFDB) has been used on titanium alloys to produce complex fabricated structures.

## 4.6 Casting

Cost factors associated with wrought alloy processing led to continual efforts to develop and improve casting methods for titanium and its alloys. The two principal casting methods have been investment casting or the use of a rammed graphite mold. Investment casting is preferred when close tolerances, thin sections, and better surface finishes are required.

The result of casting development has been a somewhat checkered application of titanium castings with a more widespread acceptance of the practice in the last 25 years. Titanium castings now are used extensively in the aerospace industry and to lesser measure in the chemical process, marine, biomedical, automotive, and other industries. While many investment cast parts are relatively small, the maximum pour weights of titanium alloy castings can reach 727 kg (1600 lb). The shipped weight of a titanium case for a gas turbine engine can be nearly 273 kg (600 lb). For example, the Pratt & Whitney PW4084 engine intermediate case is about 263 kg (578 lb). Cast components by the rammed graphite mold process have reached 2700 kg (5950 lb) in CP and alloyed grades. Investment casting is the rule for castings used in aerospace and similar critical application areas.

The investment casting process uses a disposable mold to create a negative image of the desired component. Metal fills the mold and solidifies with the desired shape and dimensions



very close to final desired values. Some machining is necessary. An alpha case (surface area containing high oxygen or nitrogen which favor alpha phase of low ductility) can be created during the casting process and must be prevented or removed.

Several alloy compositions were evaluated in early studies of investment cast titanium but investigators soon concentrated on Ti–6Al–4V. Results supported the concept that cast titanium parts could be made with strength levels and characteristics approaching those of conventional wrought alloys. Subsequently, titanium components have been cast successfully from pure titanium, alpha–beta, and beta alloys. Ti–6Al–2Sn–4Zr–2Mo alloy thin-wall castings have been successfully produced with strength improvements over Ti–6Al–4V and comparable ductility. Nonetheless, the primary alloy used for casting of titanium components has been Ti–6Al–4V.

Some important casting concepts to remember are:

- Hot isostatic pressing may be required to close casting porosity.
- Heat treatment to develop properties may require close monitoring.
- Cast component properties will tend to fall in the lower end of the scatterband for wrought versions of the alloy chosen (usually Ti–6Al–4V – although other conventional alloys may be cast).
- Section thickness may affect properties generated in castings.

#### 4.7 Machining and Residual Stresses

As noted earlier, machining of titanium alloys is similar to but more difficult than that of machining stainless steels. In welding or machining of titanium alloys, the effects of the energy input (heat energy, deformation energy) on the microstructure and properties of the final product must be considered, just as it must be done in forging. Favorable residual stresses have been generated on titanium surfaces for years. Properties measured will degrade dramatically if the favorable surface residual stresses are reduced, for example, by chemical polishing as mentioned previously. Shot peening is a common method of increasing a titanium alloy's fatigue strength, at least in airfoil roots and other non–gas path regions.

#### 4.8 Joining

Components of titanium alloys are routinely welded. Titanium and most titanium alloys can be joined by the following fusion welding techniques:

- Gas–tungsten arc welding (GTAW)
- Gas–metal arc welding (GMAW)
- Plasma arc welding (PAW)
- Electron beam welding (EBW)
- Laser beam welding (LBW)

and by brazing or such solid-state joining techniques as diffusion bonding, inertia bonding, and friction welding.

Just as occurs in the heat treatment of titanium and its alloys, fusion welding processes can lead to pickup of detrimental gases. Alloys must be welded in such a way as to preclude interstitial gases such as oxygen from being incorporated in the weld or weld heat affected area. For successful arc welding of titanium and titanium alloys, complete shielding of the weld is necessary, because of the high reactivity of titanium to oxygen and nitrogen at welding temperatures. Excellent welds can be obtained in titanium and its alloys in a welding chamber, where welding is done in a protective gas atmosphere, thus giving adequate shielding. When welding titanium and titanium alloys, only argon or helium and occasionally a mixture of these two gases are



used for shielding. Since it is more readily available and less costly, argon is more widely used. Welding in a chamber, however, is not always practical. Open-air techniques can be used with fusion welding when the area to be joined is well shielded by an inert gas using a Mylar bag for gas containment. Such atmospheric control by means of a temporary bag, or chamber, is preferred. Because titanium alloy welds are commonly used in fatigue-critical applications, a stress relief operation is generally required following welding to minimize potentially detrimental residual stresses. The essence of joining titanium and its alloys is adhering to the following principal conditions which need to be met:

- Detrimental interstitial elements must be excluded from the joint region.
- Contaminants ( scale, oil, etc.) must be excluded from the joint region.
- Detrimental phase changes must be avoided to maintain joint ductility.

When proper techniques are developed and followed, the welding of thin-to-moderate section thickness in titanium alloys can be accomplished successfully using all of the processes mentioned. For welding titanium thicker than about 2.54 mm (0.10 in.) by the GTAW process, a filler metal must be used. For PAW, a filler metal may or may not be used for welding metal less than 12.7 mm (0.5 in.) thick. Friction stir welding of long sections of titanium alloy has been reported with excellent results.

Titanium and its alloys can be brazed. Argon, helium, and vacuum atmospheres are satisfactory for brazing titanium. For torch brazing, special fluxes must be used on the titanium. Fluxes for titanium are primarily mixtures of fluorides and chlorides of the alkali metals, sodium, potassium, and lithium. Vacuum and inert-gas atmospheres protect titanium during furnace and induction brazing operations. Titanium assemblies frequently are brazed in high-vacuum, cold-wall furnaces. A vacuum of  $10^{-3}$  torr or more is required to braze titanium. Ideally, brazing should be done in a vacuum at a pressure of about  $10^{-5}$ – $10^{-4}$  torr or done in a dry inert-gas atmosphere if vacuum brazing is not possible.

## 4.9 Other Aspects of Titanium Alloy Selection

### 4.10 Corrosion

Although titanium and its alloys are used chiefly for their desirable mechanical properties, among which the most notable is their high strength-to-weight ratio, another important characteristic of the metal and its alloys is titanium's outstanding resistance to corrosion. CP titanium offers excellent corrosion resistance in most environments, except those media that contain fluoride ions. Unalloyed titanium is highly resistant to the corrosion normally associated with many natural environments, including seawater, body fluids, and fruit and vegetable juices. Titanium exposed continuously to seawater for about 18 years has undergone only superficial discoloration. Titanium is more corrosion resistant than stainless steel in many industrial environments and its use in the chemical process industry has been continually increasing. Titanium exhibits excellent resistance to atmospheric corrosion in both marine and industrial environments. Titanium and some alloys have found use in sour (oil) well operations.

Titanium and its alloys have found use in flue gas desulfurization as well as in the food, pharmaceutical, and brewing industries. Titanium and its alloys exhibit outstanding resistance to corrosion in human tissue and fluid environments (see following). Other applications which rely on the corrosion resistance of titanium and its alloys are chemical refineries, seawater piping, power industry condensers, desalination plants, pulp and paper mills, and marine piping systems.

The major corrosion problems for titanium alloys appear to be with crevice corrosion, which occurs in locations where the corroding media are virtually stagnant. Pits, if formed, may progress in a similar manner. Other problem areas are with a potential for stress corrosion, particularly at high temperatures, resulting in hot salt stress corrosion cracking (HSSCC).

HSSCC has been observed in experimental testing and an occasional service failure. Stress corrosion cracking is a fracture, or cracking, phenomenon caused by the combined action of tensile stress, a susceptible alloy, and a specific corrosive environment. The requirement that tensile stress be present is an especially important characteristic of SCC. Aluminum additions increase susceptibility to SCC; alloys containing more than 6% Al generally are susceptible to stress corrosion. In addition to SCC at high temperatures, SCC has been observed in salt water or other lower temperature fluid environments but is not a problem in most applications.

HSSCC of titanium alloys is a function of temperature, stress, and time of exposure. In general, HSSCC has not been encountered at temperatures below about 260°C (500°F). The greatest susceptibility occurs at about 290–425°C (about 550–800°F) based on laboratory tests. Time to failure decreases as either temperature or stress level is increased. All commercial alloys, but not unalloyed titanium, have some degree of susceptibility to HSSCC. Alpha alloys are more susceptible than other alloys.

#### 4.11 Biomedical Applications

Titanium alloys have become standards in dental applications and the orthopedic prosthesis industry where hip implants, for example, benefit from several characteristics of titanium:

- Excellent resistance to corrosion by body fluids
- High specific strength owing to good mechanical strengths and low density
- Modulus about 50–60% of that of competing cobalt-based superalloys

Corrosion resistance benefits are evident. High specific strength, however, enables a lighter implant to be made with attendant improvement in patient response to the device. Furthermore, the modulus of bone is very low, about 10% of that of stainless steel or cobalt-based alloys, and the degree of load transfer from an implant to the bony structure in which it is implanted (and which it replaces) is a direct function of the modulus. By reducing the elastic modulus, the bone can be made to receive a greater share of the load which is important since bone grows in response to stress.

The result of using implants of titanium alloys of lower modulus than stainless steel and cobalt alloys is that the implant operates for a longer time before breakdown of the implant–bone assembly. Ti–6Al–4V continues to be the standard titanium alloy for biomedical applications. However, the recent introduction of beta titanium alloys for orthopedic implant applications promises further modulus reductions. (The Ti–15 Mo beta titanium alloy now is covered by ASTM F-2066 for surgical implant applications and alloys such as Ti–12 Mo–6 Zr–2 Fe and Ti–13 Nb–13Zr have been developed specifically for orthopedic implants.)

#### 4.12 Cryogenic Applications

Many of the available alpha and alpha–beta titanium alloys have been evaluated at subzero temperatures, but service experience at such temperatures has been gained only for a few alloys. Ti–5Al–2.5Sn and Ti–6Al–4V have very high strength-to-weight ratios at cryogenic temperatures and have been the preferred alloys for special applications at temperatures from –196 to –269°C (–320 to –452°F). Impurities such as iron and the interstitials oxygen, carbon, nitrogen, and hydrogen tend to reduce the toughness of these alloys at both room and subzero temperatures. For maximum toughness, ELI grades are specified for critical applications.

## 5 FINAL COMMENTS

### 5.1 General

Many titanium alloys have been developed although the total number is small compared to other metals such as steels and superalloys. A principal reason for this situation is the high cost of

raw titanium and of titanium alloy development, which includes proving the worth and safety of a new material. In the sport world, use of titanium made a brief run as a high-volume application against commercial non-gas turbine applications when the golf club market virtually tied up titanium metal for a short time in the 1990s. Titanium bicycle frames are marketed but are quite expensive. Titanium glass frames and orthopedic devices all add to the user base. Titanium alloys find use in automotive applications, e.g., Ti-1100 finds use as valves in engines. However, none of the above uses rise to the level of aerospace where gas turbines and airframe applications use significant amounts. Owing to the needs of the aerospace industry, alloys invented primarily for and used by the aerospace industry will continue to dominate the use and inventive talents of producers and designers in the foreseeable future.

Users and inventors obviously have limits on expenditures to bring a new composition to market. There has not been a major inventor's market for new alloys for the past 20 years. What has been accomplished is refinement in the way titanium alloys are produced and wider use of castings plus some powder in design.

There continue to be relatively novel areas of application that are attractive for titanium alloys. A low-cost beta alloy has been evaluated for automotive springs. For example, for a drag racer, a titanium valve spring offered a 34% weight reduction, improved performance in the high-rpm range, and reduced fuel consumption. Again, the question remains as to the cost effectiveness of titanium technology in normal automotive consumer markets. Beta titanium alloys have become available for biomedical needs.

New applications of old technology continue to be evaluated to produce elemental titanium at lower cost with the expectation of lowering titanium alloy costs as well. It took about 15 years from conception to bring one new powder process aimed at reduced costs of bulk titanium and its alloys to the commercialization stages. The ability of such a process to produce lower pure titanium powder at costs comparable to titanium sponge and so enter the titanium ingot metallurgy chain is still unclear.

Titanium alloy castings have made inroads. Cast alloy properties now seem to rival those of wrought alloys. A 53-in. titanium investment cast fan frame hub casting supports the front fan section of a General Electric engine on several aircraft. The casting replaced 88 stainless steel parts that required welding and machining. In another application, a 330-lb titanium thrust beam was cast for a satellite launch vehicle. The casting replaced an aluminum part. Another application for Ti-6Al-4V was a casting for a lightweight and mobile 155-mm towed howitzer using thin-walled casting technology. While these are impressive applications, it is important to recognize that there are limits on the range of capability and availability of cast titanium alloys. In addition, the amount of titanium used in nonaerospace applications is a fraction of what airframes and aircraft gas turbine usage is projected to be. Gas turbine applications and aerospace structures remain the most significant part of the application market with current estimates that 55% or more of titanium production goes into these markets.

Within most aerospace and aircraft gas turbine engine companies, only a few alloys have ever made it to production. Admittedly this list differs from company to company and product to product in the United States and somewhat more when considering alloys used outside the United States. Nevertheless, it is apparent that, although the ability to push titanium's operating environment higher in temperature has resulted in significant gains, advances have tapered off. Since the mid-1950s, when Pratt & Whitney put the first titanium in U.S. gas turbines, much industrial and government funding has been used to increase alloy capabilities. It is obvious that the titanium alloy market for design is closely related to military or commercial high-end systems and will continue to be so for many years. The Boeing 787 Dreamliner has almost trebled the titanium weight in such an aircraft and no doubt future commercial aircraft may push the level higher.

Other applications are possible for titanium alloys. When cost is not a major stumbling block, particularly for high-end uses such as auto racing vehicles or snowmobiles

or for military applications such as body armor or for other people safety-related applications, titanium alloys are available to do the job. A relatively new alloy, ATI 425 titanium (Ti-4Al-2.5V-1.5Fe-0.25O), is available with good workability to produce body armor for the military. Alloy properties are reported to be comparable to those with Ti-6Al-4V alloy and the alloy appears to have gained acceptance.

Marine applications of titanium alloys have been discussed for years. Titanium and alloys have been used for shafts and propellers plus shipboard piping systems. More mundane uses have been kayak paddles. The Soviets manufactured several titanium hulled submarines in the early 1970s. The Alvin research submersible had a titanium hull. Alloys like Ti-64 and Ti-6Al-2Nb-1Ta-0.8Mo were used and such submersibles could dive over 3 miles. The high strength-to-weight ratio plus outstanding corrosion resistance of titanium alloys makes them ideal candidates for marine structural applications. Titanium alloy costs plus difficulties in welding very large titanium plates and structures have held back use. Recent development of friction stir welding techniques for titanium suggest that its alloys could eventually find use in military ship hull construction. It is unlikely that marine applications for titanium alloys will materially change the gas turbine and aerospace vehicle status as the primary titanium consumers in the foreseeable future.

Relative to introduction of any new alloys in advanced concepts, the message is still as follows. If an existing alloy works and a new alloy does not offer some benefit that overrides the alloy and processing cost plus the development cost of proving up the alloy for its new use, do not change alloys. For the ever shrinking cadre of developers in industry, the current status suggests that efforts to tailor existing alloys and “sell” them for new or existing applications may have better return on investment.

## 5.2 Newer Titanium Products

The areas of gamma titanium aluminide application and the use of titanium metal matrix composites continue to pique interest in the improvement of the high-temperature capability of titanium alloys (gamma titanium) as well as the possibility of significant density-adjusted short-time properties (such as yield and ultimate strength) of titanium structures (composites). Titanium aluminides have been the subject of multidecades of consideration with interesting but limited economically viable results. A great deal of promise for gamma aluminides was thought to exist in the mid-1990s but appears to have waned. There is still a degree of continued interest in military use of gamma titanium aluminides as well as a limited market for high-temperature use in high-performance automotive engines.

As for shorter time, higher strength property adjustment, composites of fibers with titanium metal matrices are being produced commercially, but the extent of the use and the likelihood that such composites will be used more widely remain to be seen. At present titanium matrix composite parts have been made for a variety of aerospace and space applications, including arresting gear shanks, shuttle carrier pallet trunions, exhaust nozzle links, actuator pistons, and drive shafts. Titanium composite materials can be expected to be increasingly available for limited applications, but they will have to be developed and evaluated on a case-by-case basis. Gamma titanium aluminides and titanium composites will probably be available as niche alloy materials but widespread use is unlikely.

## 5.3 Thoughts on Alloy Selection

If an alloy selector is starting from scratch to pick an alloy for an application, then any commercially available alloy may be fair game. On the other hand, the best alloy sometimes may not be available owing to corporate patent protection or insufficient market to warrant its continued production by the limited number of manufacturers. Then, selection of another alloy from a

producer may be necessary but may possibly require development costs to get the product in workable form and to determine design properties. Titanium matrix composites may warrant more widespread use in aerospace structures in the future, but a series of standard specifications and production methods needs to be developed. The material selector and the designer need to be certain that advanced technologies can reliably and cost effectively deliver the properties and benefits promised.

If possible, select a known alloy that has more than one supplier and more than one melter, casting, forging, or powder source. In all likelihood, unless a special need (such as formability of sheet or maximum high-temperature strength) is required, Ti-6Al-4V might be the first choice for intermediate temperatures. For formability, beta alloys may be the choice while near alpha alloys may be required for higher temperature applications.

For special needs such as in marine applications or biomedical orthopedic situations, choice of other, newer alloys may be warranted. In any event, the designer should work with relevant materials engineers plus the suppliers and others in the manufacturing chain to acquire typical or design properties for the alloy in the form it will be used. Generic alloys may be best for the alloy selector not associated with one of the big corporate users of titanium alloys. User companies with proprietary interests usually have nothing to benefit from giving up a technological advantage by sharing design data or even granting a production release to use a proprietary alloy. However, the major titanium producers, at least in the United States, can provide extensive information (usually as data sheets and customer interaction with technical personnel) for specific alloys which they manufacture.

The Bibliography at the end of the chapter lists selected publications in the field. The publications include sources of much additional technical information on titanium and its alloys. Several information organizations in the titanium field are given below. Contact information on alloy melters, fabricators, etc., might be available from their websites. The judicious use of an Internet search engine can provide data sheets and interactive information with titanium producers or fabricators.

### *Associations Providing Titanium Information*

---

#### **Titanium Information Group**

National Metals Technology Centre (NAMTEC)  
 Dr. Alan McLelland  
 TIG Chairman  
 University of Sheffield  
 Wallis Way, Catliffe, Rotherham  
 South Yorkshire, United Kingdom S60 5TZ  
 Phone: 0114-222-4781  
[www.titaniuminfogroup.co.uk](http://www.titaniuminfogroup.co.uk)  
 E-mail: [enquiries@titaniuminfogroup.co.uk](mailto:enquiries@titaniuminfogroup.co.uk)

#### **Japan Titanium Society**

22-9 Kanda Nishiki-Cho  
 Chiyoda-Ku, Tokyo ZIP 101  
 Japan  
 Phone: 081 (3) 3293 5958  
 Fax: 081 (3) 3293 6187  
[www.titan-japan.com](http://www.titan-japan.com)

#### **International Titanium Association**

Jennifer Simpson  
 Executive Director  
 350 Interlocken Blvd., Suite 390  
 Broomfield, CO 80021-3485  
 Phone: 303-404-2221  
[www.titanium.org](http://www.titanium.org)  
 E-mail: [jsimpson@titanium.org](mailto:jsimpson@titanium.org)

---

**BIBLIOGRAPHY**

- Annual Meeting Proceedings of the International Titanium Association (some prior issues available on DVD), International Titanium Association, Northglenn, CO.
- ASM Handbook*, current edition, appropriate volumes on topics of interest, ASM International, Materials Park, OH.
- ASM Handbooks Online*, ASM International, available: <http://products.asminternational.org/hbk>.
- E. W. Collings, "Physical Metallurgy of Titanium Alloys," in G. Welsch, R. Boyer, and E. Collings (Principal Eds.), *Materials Property Handbook: Titanium Alloys*, ASM International, Materials Park, OH, 1994, pp. 1–122.
- M. Donachie, *Titanium: A Technical Guide*, 2nd ed., ASM International, Metals Park, OH, 2001.
- The Effective Use of Titanium: A Designer and User's Guide*, brochure, The Titanium Information Group, Kidderminster, England, 1992.
- B. Hanson, *The Selection and Use of Titanium*, The Institute of Materials, London, England, 1995.
- International (World) Conferences on Titanium, A series of conferences held roughly every 4 years starting in 1968, more frequently at present. Multiple society sponsors from major countries. Proceedings published by International Titanium Association, Northglenn, CO.
- C. Leyens and M. Peters (Eds.), *Titanium and Titanium Alloys: Fundamentals and Applications*, Wiley, Hoboken, NJ, 2003.
- Metallic Materials Properties Development and Standardization Handbook*, formerly MIL-HDBK-5, Battelle, Columbus, OH ongoing, available: <http://projects.battelle.org/mmpds>.
- V. N. Moiseyev, *Titanium Alloys: Russian Aircraft and Aerospace Applications*, Taylor & Francis Group, Boca Raton, FL, 2006.
- Titanium Reference Library* (DVD), ASM International, Materials Park, OH, 2010.
- G. Welsch, R. Boyer, and E. Collings (Principal Eds.), *Materials Property Handbook: Titanium Alloys*, ASM International, Materials Park, OH, 1994.



# CHAPTER 6

## NICKEL AND ITS ALLOYS

Gaylord D. Smith and Brian A. Baker

Special Metals Corporation  
Huntington, West Virginia

<b>1 INTRODUCTION</b>	<b>267</b>	<b>5 HEAT TREATMENT</b>	<b>285</b>
<b>2 NICKEL ALLOYS</b>	<b>268</b>	5.1 Reducing Atmosphere	285
2.1 Classification of Alloys	268	5.2 Prepared Atmosphere	286
2.2 Discussion and Applications	269	<b>6 WELDING</b>	<b>287</b>
<b>3 CORROSION</b>	<b>278</b>	<b>7 MACHINING</b>	<b>287</b>
<b>4 FABRICATION</b>	<b>282</b>	<b>8 CLOSURE</b>	<b>287</b>
4.1 Resistance to Deformation	283	<b>REFERENCES</b>	<b>288</b>
4.2 Strain Hardening	283		

### 1 INTRODUCTION

Nickel, the 24th element in abundance, has an average content of 0.016% in the outer 10 miles of the earth's crust. This is greater than the total for copper, zinc, and lead. However, few of these deposits scattered throughout the world are of commercial importance. Oxide ores commonly called laterites are largely distributed in the tropics. The igneous rocks contain high magnesium contents and have been concentrated by weathering. Of the total known ore deposits, more than 80% is contained in laterite ores. The sulfide ores found in the Northern Hemisphere do not easily concentrate by weathering. The sulfide ores in the Sudbury district of Ontario, which contain important by-products such as copper, cobalt, iron, and precious metals, are the world's greatest single source of nickel.<sup>1</sup>

Nickel has an atomic number of 28 and is one of the transition elements in the fourth series in the periodic table. The atomic weight is 58.71 and density is 8.902 g/cm<sup>3</sup>. Nickel has a high melting temperature (1453°C) and a ductile crystal structure (fcc). Nickel exhibits mild ferromagnetism at room temperature (saturation magnetization of 0.617 T and residual magnetism of 0.300 T) and has an electrical conductivity at 100°C of 82.8 W/m·K. The thermal expansion coefficient between 20 and 100°C is  $13.3 \times 10^{-6} / \text{C}^{-1}$ . The electrical resistivity of nickel at 20°C is 6.97  $\mu\Omega\cdot\text{cm}$  and the specific heat at 20°C is 0.44 kJ/kg·K. The modulus of elasticity in tension is 206 GPa and 73.6 GPa in shear. The Poisson ratio is 0.30.<sup>2</sup>

Nickel can be readily alloyed with other metallic elements to form a wide range of commercial alloys. As an alloying element, nickel is used in hardenable steels, stainless steels, special corrosion-resistant and high-temperature alloys, copper–nickel, “nickel– silvers,” and aluminum–nickel. Nickel imparts ductility and toughness to cast iron. Nickel alloys are used in a multiplicity of consumer applications, such as household appliances, electronics, and automotive components. Selected nickel alloys are used in critical industrial technologies, including chemical processing, pollution control, and aircraft, missile, and ship production as well as electric power generation.



Unalloyed nickel is used for porous electrodes in batteries and fuel cells and as fine catalyst powders. It has long been employed for electroplating on more corrosive substrates. Unalloyed wrought nickel is very resistant to corrosion in marine and industrial atmospheres as well as natural and flowing seawater. It is resistant to corrosion by alkalis and nonoxidizing acids, by neutral and alkaline salt solutions, and by chlorine, hydrogen chloride, fluorine, and certain molten salts.

## 2 NICKEL ALLOYS

Most of the alloys listed and discussed are in commercial production. However, producers from time to time introduce improved modifications that make previous alloys obsolete. For this reason or for economic reasons, they may remove certain alloys from their commercial product line. Some of these alloys have been included to show how a particular composition compares with the strength or corrosion resistance of currently produced commercial alloys.

### 2.1 Classification of Alloys

Nickel and its alloys can be classified into the following groups on the basis of chemical composition.<sup>3</sup>

#### *Nickel*

(1) Pure nickel, electrolytic (99.56% Ni), carbonyl nickel powder and pellet (99.95% Ni); (2) commercially pure wrought nickel (99.6–99.97% nickel); and (3) anodes (99.3% Ni).

#### *Nickel and Copper*

(1) Low-nickel alloys (2–13% Ni); (2) cupronickels (10–30% Ni); (3) coinage alloy (25% Ni); (4) electrical resistance alloy (45% Ni); (5) nonmagnetic alloys (up to 60% Ni); and (6) high-nickel alloys, Monel (over 50% Ni).

#### *Nickel and Iron*

(1) Wrought alloy steels (0.5–9% Ni); (2) cast alloy steels (0.5–9% Ni); (3) alloy cast irons (1–6 and 14–36% Ni); (4) magnetic alloys (20–90% Ni): (a) controlled coefficient of expansion (COE) alloys (29.5–32.5% Ni) and (b) high-permeability alloys (49–80% Ni); (5) nonmagnetic alloys (10–20% Ni); (6) clad steels (5–40% Ni); and (7) thermal expansion alloys: (a) low expansion (36–50% Ni) and (b) selected expansion (22–50% Ni).

#### *Iron, Nickel, and Chromium*

(1) Heat-resisting alloys (40–85% Ni); (2) electrical resistance alloys (35–60% Ni); (3) iron-based superalloys (9–26% Ni); (4) stainless steels (2–25% Ni); (5) valve steels (2–13% Ni); (6) iron-based superalloys (0.2–9% Ni); and (7) maraging steels (18% Ni).

#### *Nickel, Chromium, Molybdenum, and Iron*

(1) Nickel-based solution-strengthened alloys (40–70% Ni) and (2) nickel-based precipitation-strengthened alloys (40–80% Ni).

The nominal chemical composition of nickel-based alloys is given in Table 1. This table does not include alloys with less than 30% Ni, cast alloys, or welding products. For these and

those alloys not listed, the chemical composition and applicable specifications can be found in the *Unified Numbering System for Metals and Alloys*, published by the Society of Automotive Engineers.<sup>4</sup>

## 2.2 Discussion and Applications

The same grouping of alloys used in Tables 1, 2, and 3, which give chemical composition and mechanical properties, will be used for discussion of the various attributes and uses of the alloys as a group. Many of the alloy designations are registered trademarks of producer companies.

### *Nickel Alloys*

The corrosion resistance of nickel makes it particularly useful for maintaining product purity in the handling of foods, synthetic fibers, and caustic alkalis and also in structural applications where resistance to corrosion is a prime consideration. It is a general-purpose material used when the special properties of the other nickel alloys are not required. Other useful features of the alloy are its magnetic and magnetostrictive properties, high thermal and electrical conductivity, low gas content, and low vapor pressure.<sup>5</sup>

Typical nickel 200 applications are food-processing equipment, chemical shipping drums, electrical and electronic parts, aerospace and missile components, caustic handling equipment and piping, and transducers.

*Nickel 201* is preferred to nickel 200 for applications involving exposure to temperatures above 316°C (600°F). Nickel 201 is used as coinage, plater bars, and combustion boats in addition to some of the applications for nickel 200.

*Permanickelalloy 300*, by virtue of the magnesium content, is age hardenable. But, because of its low alloy content, alloy 300 retains many of the characteristics of nickel. Typical applications are grid lateral winding wires, magnetostriction devices, thermostat contact arms, solid-state capacitors, grid side rods, diaphragms, springs, clips, and fuel cells.

*Duranickel alloy 301* is another age-hardenable high-nickel alloy but is made heat treatable by aluminum and titanium additions. The important features of alloy 301 are high strength and hardness, good corrosion resistance, and good spring properties up to 316°C (600°F); it is on these mechanical considerations that selection of the alloy is usually based. Typical applications are extrusion press parts, molds used in the glass industry, clips, diaphragms, and springs.

### *Nickel–Copper Alloys*

Nickel–copper alloys are characterized by high strength, weldability, excellent corrosion resistance, and toughness over a wide temperature range. They have excellent service in seawater or brackish water under high-velocity conditions, as in propellers, propeller shafts, pump shafts, and impellers and condenser tubes, where resistance to the effects of cavitation and erosion are important. Corrosion rates in strongly agitated and aerated seawater usually do not exceed 1 mil/year.

*Monel alloy 400* has low corrosion rates in chlorinated solvents, glass-etching agents, sulfuric and many other acids, and practically all alkalis, and it is resistant to stress corrosion cracking. Alloy 400 is useful up to 538°C (1000°F) in oxidizing atmospheres, and even higher temperatures may be used if the environment is reducing. Springs of this material are used in corrosive environments up to 232°C (450°F). Typical applications are valves and pumps; pump and propeller shafts; marine fixtures and fasteners; electrical and electronic components; chemical processing equipment; gasoline and freshwater tanks; crude petroleum stills,

**Table 1** Nominal Chemical Composition (wt. %)

Material	Ni	Cu	Fe	Cr	Mo	Al	Ti	Nb	Mn	Si	C	Other Elements
<i>Nickel</i>												
Nickel 200	99.6	—	—	—	—	—	—	—	0.23	0.03	0.07	—
Nickel 201	99.7	—	—	—	—	—	—	—	0.23	0.03	0.01	—
Permanickel alloy 300	98.7	—	0.02	—	—	—	0.49	—	0.11	0.04	0.29	0.38 Mg
Duranickel alloy 301	94.3	—	0.08	—	—	4.44	0.44	—	0.25	0.50	0.16	—
<i>Nickel–Copper</i>												
Monel alloy 400	65.4	32	1.00	—	—	—	—	—	1.0	0.10	0.12	—
Monel alloy 404	54.6	45.3	0.03	—	—	—	—	—	0.01	0.04	0.07	—
Monel alloy R-405	65.3	31.6	1.25	—	—	0.1	—	—	1.0	0.17	0.15	0.04 S
Monel alloy K-500	65.0	30	0.64	—	—	2.94	0.48	—	0.70	0.12	0.17	—
<i>Nickel–Chromium–Iron</i>												
Inconel alloy 600	76	0.25	8.0	15.5	—	—	—	—	0.5	0.25	0.08	—
Inconel alloy 601	60.5	0.50	14.1	23.0	—	1.35	—	—	0.5	0.25	0.05	—
Inconel alloy 690	60	—	9.0	30	—	—	—	—	—	—	0.01	—
Inconel alloy 706	41.5	0.15	40	16	—	0.20	1.8	3	0.18	0.18	0.03	—
Inconel alloy 718	53.5	0.15	18.5	19	3.0	0.5	0.9	5.1	0.18	—	0.04	—
Inconel alloy X-750	73	0.25	7	15.5	—	0.70	2.5	1	0.50	0.25	0.04	—
<i>Nickel–Iron–Chromium</i>												
Incoloy alloy 800	31	0.38	46	20	—	0.38	0.38	—	0.75	0.50	0.05	—
Incoloy alloy 800H	31	0.38	46	20	—	0.38	0.38	—	0.75	0.50	0.07	—
Incoloy alloy 825	42	1.75	30	22.5	3	0.10	0.90	—	0.50	0.25	0.01	—
Incoloy alloy 925	43.2	1.8	28	21	3	0.35	2.10	—	0.60	0.22	0.03	—
Pyromet 860	44	—	Bal	13	6	1.0	3.0	—	0.25	0.10	0.05	4.0 Co
Refractaloy 26	38	—	Bal	18	3.2	0.2	2.6	—	0.8	1.0	0.03	20 Co

<i>Nickel-Iron</i>															
Ni10 alloy 36	36	—	61.5	—	—	—	—	—	—	—	—	0.5	0.09	0.03	—
Ni10 alloy 42	41.6	—	57.4	—	—	—	—	—	—	—	—	0.5	0.06	0.03	—
Ni-Span-C alloy 902	42.3	0.05	48.5	5.33	—	—	2.6	—	—	—	—	0.40	0.50	0.03	—
Incoloy alloy 903	38	—	41.5	—	—	—	1.40	—	—	—	—	0.09	0.17	0.02	14 Co
Incoloy alloy 907	37.6	0.10	41.9	—	—	—	—	—	—	—	—	0.05	0.08	0.02	14 Co
<i>Nickel-Chromium-Molybdenum</i>															
Hastelloy alloy X	Bal <sup>a</sup>	—	19	22	9	—	—	—	—	—	—	—	—	0.10	—
Hastelloy alloy G	Bal	2	19.5	22	6.5	—	—	—	—	—	—	< 1	1.5	< 0.05	<1W, <2.5 Co
Hastelloy alloy C-276	Bal	—	5.5	15.5	16	—	—	—	—	—	—	< 0.08	< 1	< 0.01	2.5 Co, 4 W, 0.35 V
Hastelloy alloy C	Bal	—	< 3	16	15.5	—	< 0.7	—	—	—	—	< 0.08	< 1	< 0.01	<2Co
Inconel alloy 617	54	—	—	22	9	—	—	—	—	—	—	—	—	0.07	12.5 Co
Inconel alloy 625	Bal	—	2.5	21.5	9	< 0.4	< 0.4	—	—	—	—	—	—	0.03	—
MAR-M-252	Bal	—	—	19	10	1	2.6	—	—	—	—	< 0.5	< 0.5	0.15	10 Co, 0.005 B
René 41	Bal	—	—	19	10	1.5	3.1	—	—	—	—	—	—	0.09	11 Co, <0.010 B
René 95	Bal	—	—	14	3.5	3.5	2.5	—	—	—	—	—	—	0.15	8 Co, 3.5 W, 0.01 B, 0.05 Zr
Astroloy	Bal	—	—	15	5.3	4.4	3.5	—	—	—	—	—	—	0.06	15 Co
Udimet 500	Bal	—	< 0.5	19	4	3.0	3.0	—	—	—	—	—	—	0.08	18 Co, 0.007 B
Udimet 520	Bal	—	—	19	6	2.0	3.0	—	—	—	—	—	—	0.05	12 Co, 1 W, 0.005 B
Udimet 600	Bal	—	< 4	17	4	4.2	2.9	—	—	—	—	—	—	0.04	16 Co, 0.02 B
Udimet 700	Bal	—	—	15	5.0	4.4	3.5	—	—	—	—	—	—	0.07	18.5 Co, 0.025 B
Udimet 1753	Bal	—	9.5	16.3	1.6	1.9	3.2	—	—	—	—	0.1	0.05	0.24	7.2 Co, 8.4 W, 0.008 B, 0.06 Zr
Waspaloy	Bal	< 0.1	< 2	19	4.3	1.5	3	—	—	—	—	—	—	0.08	14 Co, 0.006 B, 0.05 Zr

<sup>a</sup>Balance.

**Table 2** Mechanical Properties of Nickel Alloys

Material	0.2% Yield Strength (ksi) <sup>a</sup>	Tensile Strength (ksi) <sup>a</sup>	Elongation (%)	Rockwell Hardness
<i>Nickel</i>				
Nickel 200	21.5	67	47	55 R <sub>b</sub>
Nickel 201	15	58.5	50	45 R <sub>b</sub>
Permanickel alloy 300	38	95	30	79 R <sub>b</sub>
Duranickel alloy 301	132	185	28	36 R <sub>c</sub>
<i>Nickel–Copper</i>				
Monel alloy 400	31	79	52	73 R <sub>b</sub>
Monel alloy 404	31	69	40	68 R <sub>b</sub>
Monel alloy R-405	56	91	35	86 R <sub>b</sub>
Monel alloy K-500	111	160	24	25 R <sub>c</sub>
<i>Nickel–Chromium–Iron</i>				
Inconel alloy 600	50	112	41	90 R <sub>b</sub>
Inconel alloy 601	35	102	49	81 R <sub>b</sub>
Inconel alloy 690	53	106	41	97 R <sub>b</sub>
Inconel alloy 706	158	193	21	40 R <sub>c</sub>
Inconel alloy 718	168	205	20	46 R <sub>c</sub>
Inconel alloy X-750	102	174	25	33 R <sub>c</sub>
<i>Nickel–Iron–Chromium</i>				
Incoloy alloy 800	48	88	43	84 R <sub>b</sub>
Incoloy alloy 800H	29	81	52	72 R <sub>b</sub>
Incoloy alloy 825	44	97	53	84 R <sub>b</sub>
Incoloy alloy 925	119	176	24	34 R <sub>c</sub>
Pyromet 860	115	180	21	37 R <sub>c</sub>
Refractaloy 26	100	170	18	—
<i>Nickel–Iron</i>				
Nilo alloy 42	37	72	43	80 R <sub>b</sub>
Ni–Span–C alloy 902	137	150	12	33 R <sub>c</sub>
Incoloy alloy 903	174	198	14	39 R <sub>c</sub>
Incoloy alloy 907	163	195	15	42 R <sub>c</sub>
<i>Nickel–Chromium–Molybdenum</i>				
Hastelloy alloy X	52	114	43	—
Hastelloy alloy G	56	103	48.3	86 R <sub>b</sub>
Hastelloy alloy C-276	51	109	65	—
Inconel alloy 617	43	107	70	81 R <sub>b</sub>
Inconel alloy 625	63	140	51	96 R <sub>b</sub>
MAR-M-252	122	180	16	—
René 41	120	160	18	—
René 95	190	235	15	—
Astroloy	152	205	16	—
Udimet 500	122	190	32	—
Udimet 520	125	190	21	—
Udimet 600	132	190	13	—
Udimet 700	140	204	17	—
Udimet 1753	130	194	20	39 R <sub>c</sub>
Waspaloy	115	185	25	—

<sup>a</sup>MPa = ksi × 6.895.

**Table 3** 1000-h Rupture Stress (ksi)<sup>a</sup>

Material	1200°F	1500°F	1800°F	2000°F
<i>Nickel–Chromium–Iron</i>				
Inconel alloy 600	14.5	3.7	1.5	—
Inconel alloy 601	28	6.2	2.2	1.0
Inconel alloy 690	16	—	—	—
Inconel alloy 706	85	—	—	—
Inconel alloy 718	85	—	—	—
Inconel alloy X-750	68	17	—	—
<i>Nickel–Iron–Chromium</i>				
Incoloy alloy 800	20	—	—	—
Incoloy alloy 800H	23	6.8	1.9	0.9
Incoloy alloy 825	26	6.0	1.3	—
Pyromet 860	81	17	—	—
Refractaloy 26	65	15.5	—	—
<i>Nickel–Chromium–Molybdenum</i>				
Hastelloy alloy X	31	9.5	—	—
Inconel alloy 617	52	14	3.8	1.5
Inconel alloy 625	60	7.5	—	—
MAR-M-252	79	22.5	—	—
René 41	102	29	—	—
René 95	125	—	—	—
Astroloy	112	42	8	—
Udimet 500	110	30	—	—
Udimet 520	85	33	—	—
Udimet 600	—	37	—	—
Udimet 700	102	43	7.5	—
Udimet 1753	98	34	6.5	—
Waspaloy	89	26	—	—

<sup>a</sup>MPa = ksi × 6.895.

process vessels, and piping; boiler feedwater heaters and other heat exchangers; and deaerating heaters.

*Monel alloy 404* is characterized by low magnetic permeability and excellent brazing characteristics. Residual elements are controlled at low levels to provide a clean, wettable surface even after prolonged firing in wet hydrogen. Alloy 404 has a low Curie temperature and its magnetic properties are not appreciably affected by processing or fabrication. This magnetic stability makes alloy 404 particularly suitable for electronic applications. Much of the strength of alloy 404 is retained at outgassing temperatures. Thermal expansion of alloy 404 is sufficiently close to that of many other alloys as to permit the firing of composite metal tubes with negligible distortion. Typical applications are waveguides, metal-to-ceramic seals, transistor capsules, and power tubes.

*Monel alloy R-405* is a free-machining material intended almost exclusively for use as stock for automatic screw machines. It is similar to alloy 400 except that a controlled amount of sulfur is added for improved machining characteristics. The corrosion resistance of alloy R-405 is essentially the same as that of alloy 400, but the range of mechanical properties differs slightly. Typical applications are water meter parts, screw machine products, fasteners for nuclear applications, and valve seat inserts.

*Monel alloy K-500* is an age-hardenable alloy that combines the excellent corrosion resistance characteristics of the Monel nickel–copper alloys with the added advantage of increased

strength and hardness. Age hardening increases its strength and hardness. Still better properties are achieved when the alloy is cold worked prior to the aging treatment. Alloy K-500 has good mechanical properties over a wide temperature range. Strength is maintained up to about 649°C (1200°F), and the alloy is strong, tough, and ductile at temperatures as low as -253°C (-423°F). It also has low permeability and is nonmagnetic to -134°C (-210°F). Alloy K-500 has low corrosion rates in a wide variety of environments. Typical applications are pump shafts and impellers, doctor blades and scrapers, oil-well drill collars and instruments, electronic components, and springs.

### *Nickel–Chromium–Iron Alloys*

This family of alloys was developed for high-temperature oxidizing environments. These alloys typically contain 50–80% nickel, which permits the addition of other alloying elements to improve strength and corrosion resistance while maintaining toughness.

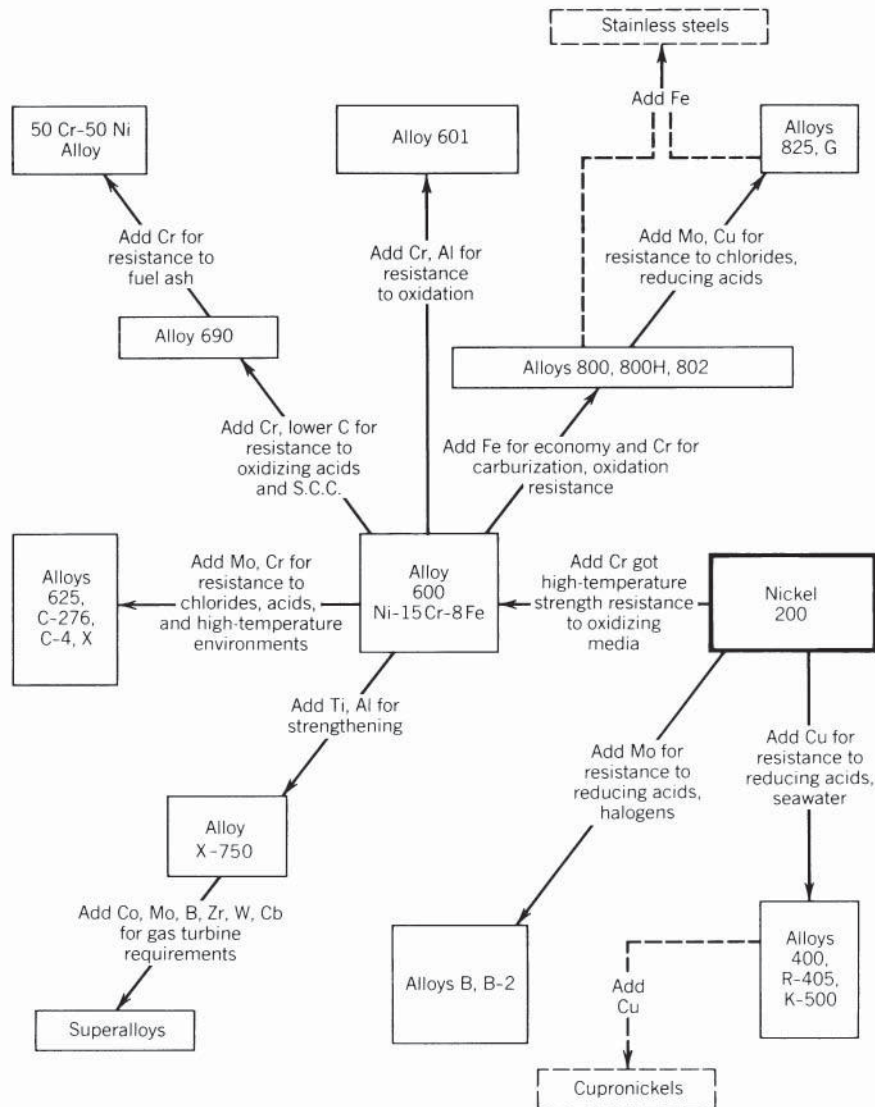
*Inconel alloy 600* is a standard engineering material for use in severely corrosive environments at elevated temperatures. It is resistant to oxidation at temperatures up to 1177°C (2150°F). In addition to corrosion and oxidation resistance, alloy 600 presents a desirable combination of high strength and workability and is hardened and strengthened by cold working. This alloy maintains strength, ductility, and toughness at cryogenic as well as elevated temperatures. Because of its resistance to chloride ion stress corrosion cracking and corrosion by high-purity water, it is used in nuclear reactors. For this service, the alloy is produced to exacting specifications and is designated Inconel alloy 600T. Typical applications are furnace muffles, electronic components, heat exchanger tubing, chemical- and food-processing equipment, carburizing baskets, fixtures and rotors, reactor control rods, nuclear reactor components, primary heat exchanger tubing, springs, and primary water piping. Alloy 600, being one of the early high-temperature, corrosion-resistant alloys, can be thought of as being the basis of many of our present-day special-purpose high-nickel alloys, as illustrated in Fig. 1 later in the chapter.

*Inconel alloy 601* has shown very low rates of oxidation and scaling at temperatures as high as 1093°C (2000°F). The high chromium content (nominally 23%) gives alloy 601 resistance to oxidizing, carburizing, and sulfur-containing environments. Oxidation resistance is further enhanced by the aluminum content. Typical applications are heat-treating baskets and fixtures, radiant furnace tubes, strand-annealing tubes, thermocouple protection tubes, and furnace muffles and retorts.

*Inconel alloy 690* is a high-chromium nickel alloy having very low corrosion rates in many corrosive aqueous media and high-temperature atmospheres. In various types of high-temperature water, alloy 690 also displays low corrosion rates and excellent resistance to stress corrosion cracking—desirable attributes for nuclear steam generator tubing. In addition, the alloy's resistance to sulfur-containing gases makes it a useful material for such applications as coal gasification units, burners and ducts for processing sulfuric acid, furnaces for petrochemical processing, and recuperators and incinerators.

*Inconel alloy 706* is a precipitation-hardenable alloy with characteristics similar to alloy 718, except that alloy 706 has considerably improved machinability. It also has good resistance to oxidation and corrosion over a broad range of temperatures and environments. Like alloy 718, alloy 706 has excellent resistance to postweld strain age cracking. Typical applications are gas turbine components and other parts that must have high strength combined with good machinability and weldability.

*Inconel alloy 718* is an age-hardenable high-strength alloy suitable for service at temperatures from -253°C (-423°F) to 704°C (1300°F). The fatigue strength of alloy 718 is high, and the alloy exhibits high stress rupture strength up to 704°C (1300°F) as well as oxidation resistance up to 982°C (1800°F). It also offers good corrosion resistance to a wide variety of environments. The outstanding characteristic of alloy 718 is its slow response to age hardening. The slow response enables the material to be welded and annealed with no spontaneous hardening unless it is cooled slowly. Alloy 718 can also be repair welded in the fully aged condition.



**Figure 1** Some compositional modifications of nickel and its alloys to produce special properties.

Typical applications are jet engine components, pump bodies and parts, rocket motors and thrust reversers, and spacecraft.

*Inconel alloy X-750* is an age-hardenable nickel–chromium–iron alloy used for its corrosion and oxidation resistance and high creep rupture strength up to 816°C (1500°F). The alloy is made age hardenable by the addition of aluminum, columbium, and titanium, which combine with nickel, during proper heat treatment, to form the intermetallic compound  $\text{Ni}_3(\text{Al}, \text{Ti})$ . Alloy X-750, originally developed for gas turbines and jet engines, has been adopted for a wide variety of other uses because of its favorable combination of properties. Excellent relaxation resistance makes alloy X-750 suitable for springs operating at temperatures up to about



649°C (1200°F). The material also exhibits good strength and ductility at temperatures as low as -253°C (-423°F). Alloy X-750 also exhibits high resistance to chloride ion stress corrosion cracking even in the fully age-hardened condition. Typical applications are gas turbine parts (aviation and industrial), springs (steam service), nuclear reactors, bolts, vacuum envelopes, heat-treating fixtures, extrusion dies, aircraft sheet, bellows, and forming tools.

#### *Nickel–Iron–Chromium Alloys*

This series of alloys typically contains 30–45% Ni and is used in elevated- or high-temperature environments where resistance to oxidation or corrosion is required.

*Incoloy alloy 800* is a widely used material of construction for equipment that must resist corrosion, have high strength, or resist oxidation and carburization. The chromium in the alloy imparts resistance to high-temperature oxidation and general corrosion. Nickel maintains an austenitic structure so that the alloy remains ductile after elevated-temperature exposure. The nickel content also contributes resistance to scaling, general corrosion, and stress corrosion cracking. Typical applications are heat-treating equipment and heat exchangers in the chemical, petrochemical, and nuclear industries, especially where resistance to stress corrosion cracking is required. Considerable quantities are used for sheathing on electric heating elements.

*Incoloy alloy 800H* is a version of Incoloy alloy 800 having significantly higher creep and rupture strength. The two alloys have the same chemical composition with the exception that the carbon content of alloy 800H is restricted to the upper portion of the standard range for alloy 800. In addition to a controlled carbon content, alloy 800H receives an annealing treatment that produces a coarse grain size—an ASTM number of 5 or coarser. The annealing treatment and carbon content are responsible for the alloy's greater creep and rupture strength.

Alloy 800H is useful for many applications involving long-term exposure to elevated temperatures or corrosive atmospheres. In chemical and petrochemical processing, the alloy is used in steam/hydrocarbon re-forming for catalyst tubing, convection tubing, pigtails, outlet manifolds, quenching-system piping, and transfer piping; in ethylene production for both convection and cracking tubes; in oxo-alcohol production for tubing in hydrogenation heaters; in hydrodealkylation units for heater tubing; and in production of vinyl chloride monomer for cracking tubes, return bends, and inlet and outlet flanges.

Industrial heating is another area of wide usage for alloy 800H. In various types of heat-treating furnaces, the alloy is used for radiant tubes, muffles, retorts, and assorted furnace fixtures. Alloy 800H is also used in power generation for steam superheater tubing and high-temperature heat exchangers in gas-cooled nuclear reactors.

*Incoloy alloy 825* was developed for use in aggressively corrosive environments. The nickel content of the alloy is sufficient to make it resistant to chloride ion stress corrosion cracking, and, with molybdenum and copper, alloy 825 has resistance to reducing acids. Chromium confers resistance to oxidizing chemicals. The alloy also resists pitting and intergranular attack when heated in the critical sensitization temperature range. Alloy 825 offers exceptional resistance to corrosion by sulfuric acid solutions, phosphoric acid solutions, and seawater. Typical applications are phosphoric acid evaporators, pickling-tank heaters, pickling hooks and equipment, chemical process equipment, spent nuclear fuel element recovery, propeller shafts, tank trucks, and oil-country cold-worked tubulars.

*Incoloy alloy 925* was developed for severe conditions found in corrosive wells containing H<sub>2</sub>S, CO<sub>2</sub>, and brine at high pressures. Alloy 925 is a weldable, age-hardenable alloy having corrosion and stress corrosion resistance similar to Incoloy alloy 825. It is recommended for applications where alloy 825 does not have adequate yield or tensile strength for service in the production of oil and gas, such as valve bodies, hanger bars, flow lines, casing, and other tools and equipment.

*Pyromet 860* and *Refractaloy 26* are high-temperature precipitation-hardenable alloys with lower nickel content than Inconel alloy X-750 but with additions of cobalt and molybdenum.

The precipitation-hardening elements are the same except the Al/Ti ratio is reversed with titanium content being greater than aluminum. Typical applications of both alloys are critical components of gas turbines, bolts, and structural members.<sup>6</sup>

### ***Nickel–Iron***

The nickel–iron alloys listed in Table 1 as a group have a low coefficient of expansion that remains virtually constant to a temperature below the Curie temperature for each alloy. A major application for *Nilo alloy 36* is tooling for curing composite airframe components. The thermal expansion characteristics of *Nilo alloy 42* are particularly useful for semiconductor lead frames and glass-sealing applications.

*Ni-Span-C alloy 902* and *Incoloy alloys 903 and 907* are precipitation-hardenable alloys with similar thermal expansion characteristics to *Nilo alloy 42* but having different constant coefficient of expansion temperature range. Alloy 902 is frequently used in precision apparatus where elastic members must maintain a constant frequency when subjected to temperature fluctuations. Alloys 903 and 907 are being used in aircraft jet engines for members requiring high-temperature strengths to 649°C (1200°F) with thermal expansion controlled to maintain low clearance.

### ***Nickel–Chromium–Molybdenum Alloys***

This group of alloys contains 45–60% Ni and was developed for severe corrosion environments. Many of these alloys also have good oxidation resistance and some have useful strength to 1093°C (2000°F).

*Hastelloy alloy X* is a non-age-hardenable nickel–chromium–iron–molybdenum alloy developed for high-temperature service up to 1204°C (2200°F). Typical applications are furnace hardware subjected to oxidizing, reducing, and neutral atmospheres; aircraft jet engine tail pipes; and combustion cans and afterburner components.<sup>7,8</sup>

*Hastelloy alloy C* is a mildly age-hardenable alloy similar in composition to alloy X except nearly all the iron is replaced with molybdenum and nickel. It is highly resistant to strongly oxidizing acids, salts, and chlorine. It has good high-temperature strength. Typical applications are chemical, petrochemical, and oil refinery equipment; aircraft jet engines; and heat-treating equipment.<sup>9,10</sup>

*Hastelloy alloy C-276* is a modification of *Hastelloy alloy C* where the carbon and silicon contents are reduced to very low levels to diminish carbide precipitation in the heat-affected zone of weldments. Alloy C-276 is non-age hardenable and is used in the solution-treated condition. No postwelding heat treatment is necessary for chemical process equipment. Typical applications are chemical and petrochemical process equipment, aircraft jet engines, and deep sour gas wells.<sup>9,10</sup>

*Hastelloy alloy G* is a non-age-hardenable alloy similar to the composition of alloy X but with 2% copper and 2% columbium and lower carbon content. Alloy G is resistant to pitting and stress corrosion cracking. Typical applications are paper and pulp equipment, phosphate fertilizer, and synthetic fiber processing.<sup>9,10</sup>

*Inconel alloy 617* is a solid-solution-strengthened alloy containing cobalt that has an exceptional combination of high-temperature strength and oxidation resistance, which makes alloy 617 a useful material for gas turbine aircraft engines and other applications involving exposure to extreme temperatures, such as steam generator tubing and pressure vessels for advanced high-temperature gas-cooled nuclear reactors.

*Inconel alloy 625*, like alloy 617, is a solid-solution-strengthened alloy but containing columbium instead of cobalt. This combination of elements is responsible for superior resistance to a wide range of corrosive environments of unusual severity as well as to high-temperature effects such as oxidation and carburization. The properties of alloy 625 that make

it attractive for seawater applications are freedom from pitting and crevice corrosion, high corrosion fatigue strength, high tensile strength, and resistance to chloride ion stress corrosion cracking. Typical applications are wire rope for mooring cables; propeller blades; submarine propeller sleeves and seals; submarine snorkel tubes; aircraft ducting, exhausts, thrust-reverser, and spray bars; and power plant scrubbers, stack liners, and bellows.

*MAR-M-252, René 41, René 95, and Astroloy* are a group of age-hardenable nickel-based alloys containing 10–15% cobalt designed for highly stressed parts operating at temperatures from 871 to 982°C (1600–1800°F) in jet engines. MAR-M-252 and René 41 have nearly the same composition but René 41 contains more of the age-hardening elements allowing higher strengths to be obtained. René 95, of similar base composition but in addition containing 3.5% columbium and 3.5% tungsten, is used at temperatures between 371 and 649°C (700 and 1200°F). Its primary use is as disks, shaft retaining rings, and other rotating parts in aircraft engines of various types.<sup>6,8,9</sup>

*Udimet 500, 520, 600, and 700* and *Unitemp 1753* are age-hardenable, nickel-based alloys having high strength at temperatures up to 982°C (1800°F). All contain a significant amount of cobalt. Applications include jet engine gas turbine blades, combustion chambers, rotor disks, and other high-temperature components.<sup>6,8,9</sup>

*Waspaloy* is an age-hardenable nickel-based alloy developed to have high strength up to 760°C (14,000°F) combined with oxidation resistance to 871°C (1600°F). Applications are jet engine turbine buckets and disks, air frame assemblies, missile systems, and high-temperature bolts and fasteners.<sup>6,8,9</sup>

### 3 CORROSION

It is well recognized that the potential saving is very great by utilizing available and economic practices to improve corrosion prevention and control. Not only should the designer consider initial cost of materials, but he or she should also include the cost of maintenance, length of service, downtime cost, and replacement costs. This type of cost analysis can frequently show that more highly alloyed, corrosion-resistant materials are more cost effective. The National Commission on Materials Policy concluded that one of the “most obvious opportunities for material economy is control of corrosion.”

Studies have shown that the total cost of corrosion is astonishing. The overall cost of corrosion in the United States was estimated by a study funded by the U.S. Federal Highway Administration. The report was published by NACE in July 2002. According to the report, metallic corrosion costs the United States about \$276 billion a year. The report claims that about 25–30% of the costs of corrosion (\$80 billion) is avoidable and could be saved by broader use of corrosion-resistant materials and the application of best anticorrosion technology from design through maintenance.

Since becoming commercially available shortly after the turn of the century, nickel has become very important in combating corrosion. It is a major constituent in the plated coatings and claddings applied to steel, corrosion-resistant stainless steels, copper–nickel and nickel–copper alloys, high-nickel alloys, and commercially pure nickel alloys. Not only is nickel a corrosion-resistant element in its own right, but, owing to its high tolerance for alloying, it has been possible to develop many metallurgically stable, special-purpose alloys.<sup>11</sup>

Figure 1 shows the relationship of these alloys and the major effect of alloying elements. Alloy 500 with 15% chromium, one of the earliest of the nickel–chromium alloys, can be thought of as the base for other alloys. Chromium imparts resistance to oxidizing environments and high-temperature strength. Increasing chromium to 30%, as in alloy 690, increases resistance to stress corrosion cracking, nitric acid, steam, and oxidizing gases.

Increasing chromium to 50% increases resistance to melting sulfates and vanadates found in fuel ash. High-temperature oxidation resistance is also improved by alloying with aluminum in conjunction with high chromium (e.g., alloy 601). Without chromium, nickel by itself is used as a corrosion-resistant material in food processing and in high-temperature caustic and gaseous chlorine or chloride environments.

Of importance for aqueous reducing acids, oxidizing chloride environments, and seawater are alloy 625 and alloy C-276, which contain 9 and 16% molybdenum, respectively, and are among the most resistant alloys currently available. Low-level titanium and aluminum additions provide V strengthening while retaining good corrosion resistance, as in alloy X-750. Cobalt and other alloying element additions provide jet engine materials (superalloys) that combine high-temperature strength with resistance to gaseous oxidation and sulfidation.

Another technologically important group of materials are the higher iron alloys, which were originally developed to conserve nickel and are often regarded as intermediate in performance and cost between nickel alloys and stainless steels. The prototype, alloy 800 (Fe–33% Ni–21% Cr), is a general-purpose alloy with good high-temperature strength and resistance to steam and oxidizing or carburizing gases. Alloying with molybdenum and chromium, as in alloy 825 and alloy G, improves resistance to reducing acids and localized corrosion in chlorides.

Another important category is the nickel–copper alloys. At the higher nickel end are the Monel alloys (30–45% Cu, balance Ni) used for corrosive chemicals such as hydrofluoric acid and severe marine environments. At the higher copper end are the cupronickels (10–30% Ni, balance Cu), which are widely used for marine applications because of their fouling resistance.

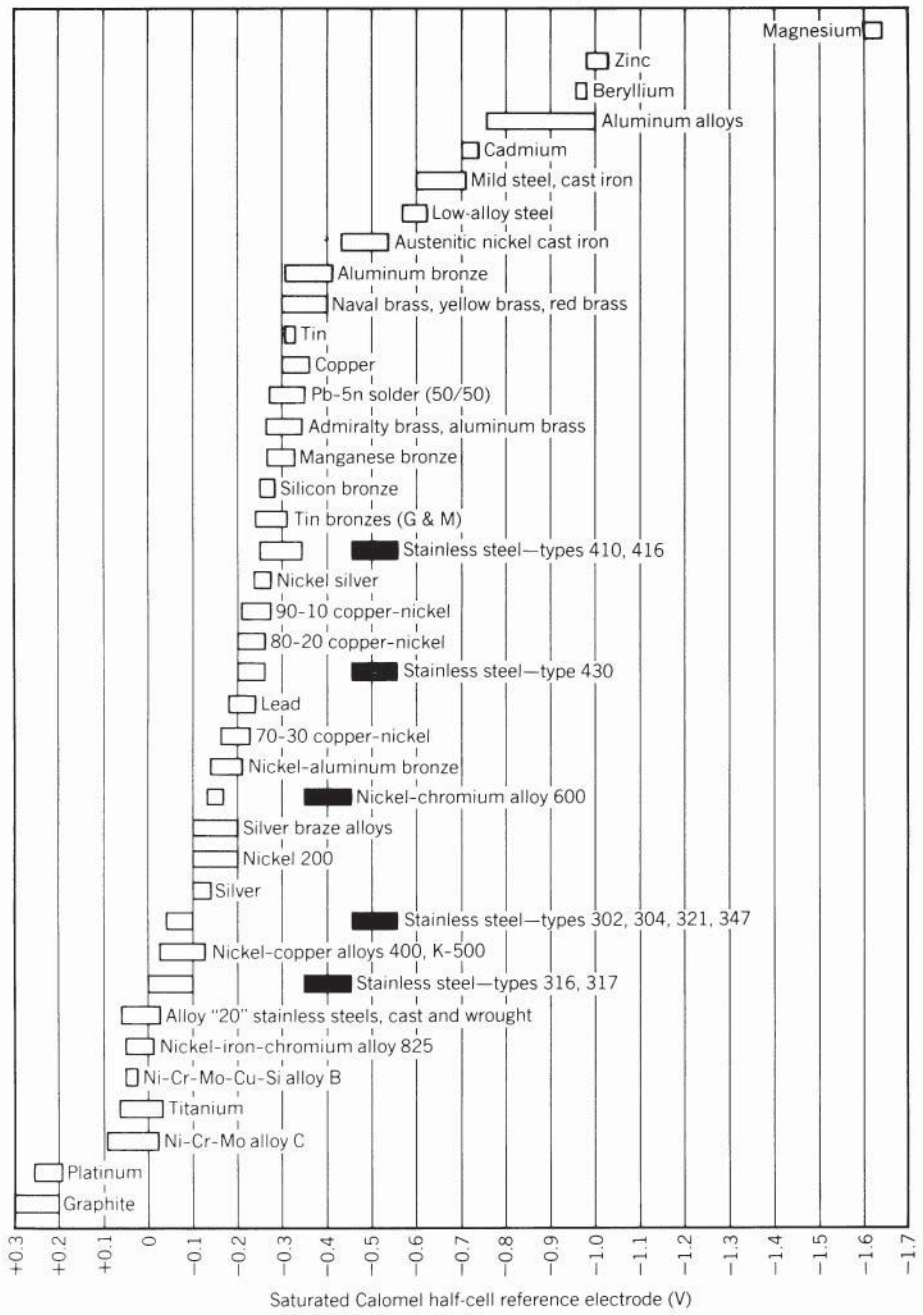
Nickel alloys exhibit high resistance to attack under nitriding conditions (e.g., in dissociated ammonia) and in chlorine or chloride gases. Corrosion in the latter at elevated temperatures proceeds by the formation and volatilization of chloride scales, and high-nickel contents are beneficial since nickel forms one of the least volatile chlorides. Conversely, in sulfidizing environments, high-nickel alloys without chromium can exhibit attack due to the formation of a low-melting-point Ni–Ni<sub>3</sub>Si<sub>2</sub> eutectic. However, high chromium contents appear to limit this form of attack.

Friend explains corrosion reactions as wet or dry (Ref. 10, pp. 3–5):

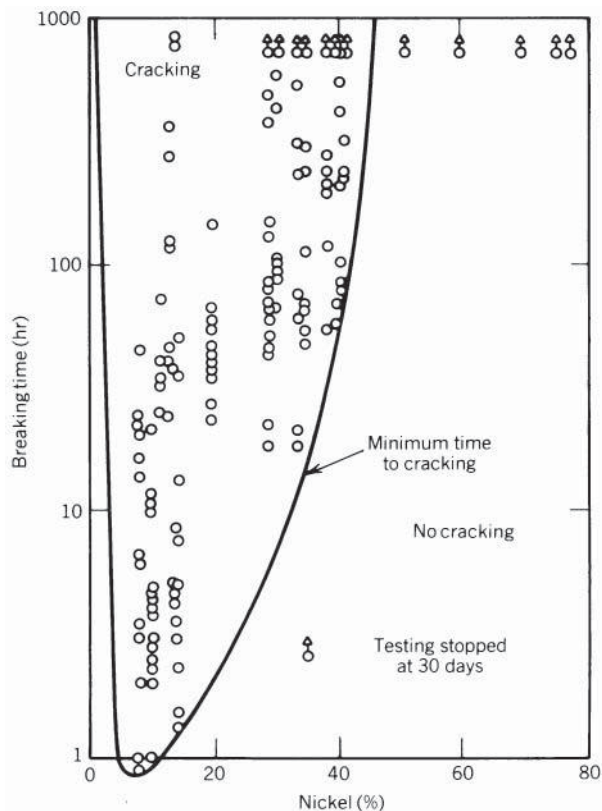
The term wet corrosion usually refers to all forms of corrosive attack by aqueous solutions of electrolytes, which can range from pure water (a weak electrolyte) to aqueous solutions of acids or bases or of their salts, including neutral salts. It also includes natural environments such as the atmosphere, natural waters, soils, and others, irrespective of whether the metal is in contact with a condensed film or droplets of moisture or is completely immersed. Corrosion by aqueous environments is electrochemical in nature, assuming the presence of anodic and cathodic areas on the surface of the metal even though these areas may be so small as to be indistinguishable by experimental methods and the distance between them may be only of atomic dimensions.

The term dry corrosion implies the absence of water or an aqueous solution. It generally is applied to metal/gas or metal/vapor reactions involving gases such as oxygen, halogens, hydrogen sulfide, and sulfur vapor and even to “dry” steam at elevated temperatures. ... High-temperature oxidation of metals has been considered to be an electrochemical phenomenon since it involves the diffusion of metal ions outward, or of reactant ions inward, through the corrosion product film, accompanied by a flow of electrons.

The decision to use a particular alloy in a commercial application is usually based on past corrosion experience and laboratory or field testing using test spools of candidate alloys. Most often weight loss is measured to rank various alloys; however, many service failures are due to localized attack such as pitting, crevice corrosion, intergranular corrosion, and stress corrosion cracking, which should be measured by other means.



**Figure 2** Corrosion potentials in flowing seawater (8–13 ft/s), temperature range 50–80°F. Alloys are listed in the order of the potential they exhibit in flowing seawater. Certain alloys, indicated by solid boxes, in low-velocity or poorly aerated water and at shielded areas may become active and exhibit a potential near -0.5 V.



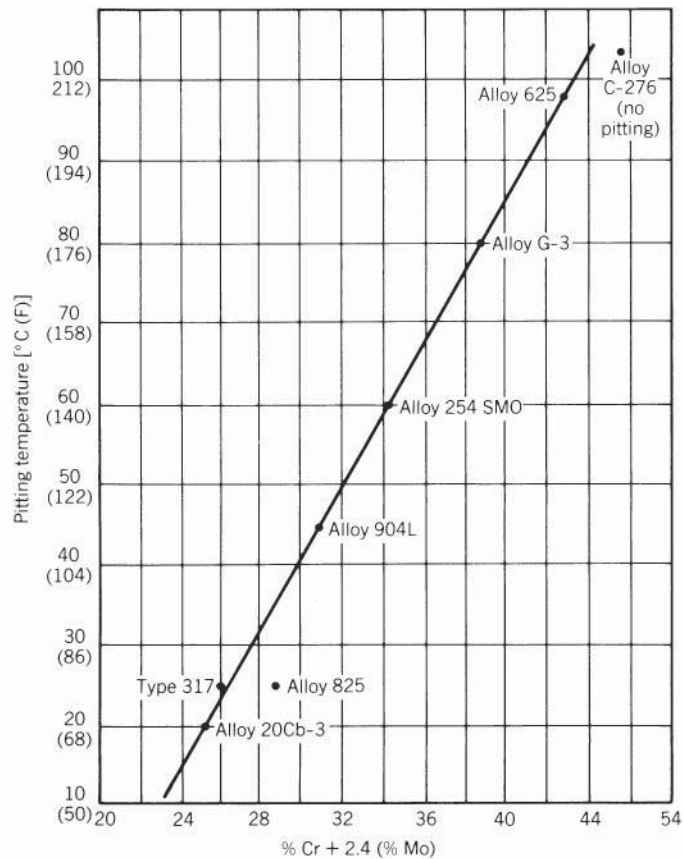
**Figure 3** Breaking time of iron–nickel–chromium wires under tensile stress in boiling 42% magnesium chloride.

A number of investigations have shown the effect of nickel on the different forms of corrosion. Figure 2 shows the galvanic series of many alloys in flowing seawater. This series gives an indication of the rate of corrosion between different metals or alloys when they are electrically coupled in an electrolyte. The metal close to the active end of the chart will behave as an anode and corrode, and the metal closer to the noble end will act as a cathode and be protected. Increasing the nickel content will move an alloy more to the noble end of the series. There are galvanic series for other corrosive environments, and the film-forming characteristics of each material may change this series somewhat. Seawater is normally used as a rough guide to the relative positions of alloys in solution of good electrical conductivity such as mineral acids or salts.

Residual stresses from cold rolling or forming do not have any significant effect on the general corrosion rate. However, many low-nickel-containing steels are subject to stress corrosion cracking in chloride-containing environments. Figure 3 from work by LaQue and Copson<sup>11</sup> shows that nickel–chromium and nickel–chromium–iron alloys containing about 45% Ni or more are immune from stress corrosion cracking in boiling 42% magnesium chloride.<sup>10</sup>

When localized corrosion occurs in well-defined areas, such corrosion is commonly called *pitting attack*. This type of corrosion typically occurs when the protective film is broken or is penetrated by a chloride ion and the film is unable to repair itself quickly. The addition of





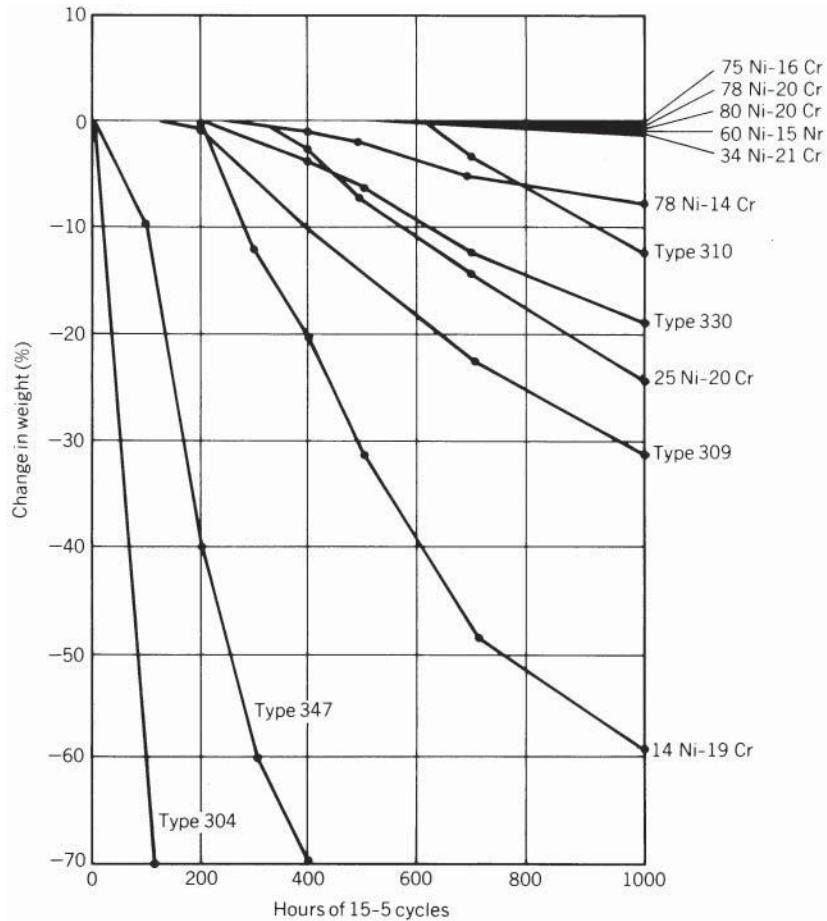
**Figure 4** Critical temperature for pitting in 4% NaCl + 1%  $\text{Fe}_2(\text{SO}_4)_3$  + 0.01 M HCl versus composition for Fe–Ni–Cr–Mo alloys.

chromium and particularly molybdenum makes nickel-based alloys less susceptible to pitting attack, as shown in Fig. 4, which shows a very good relationship between critical<sup>11</sup> pitting temperature in a salt solution. Along with significant increases in chromium and/or molybdenum, the iron content must be replaced with more nickel in wrought alloys to resist the formation of embrittling phases.<sup>11,12</sup>

Air oxidation at moderately high temperatures will form an intermediate subsurface layer between the alloy and gas quickly. Alloying of the base alloy can affect this subscale oxide and, therefore, control the rate of oxidation. At constant temperature, the resistance to oxidation is largely a function of chromium content. Early work by Eiselstein and Skinner has shown that nickel content is very beneficial under cyclic temperature conditions, as shown in Fig. 5.<sup>13</sup>

## 4 FABRICATION

The excellent ductility and malleability of nickel and nickel-based alloys in the annealed condition make them adaptable to virtually all methods of cold fabrication. As other engineering properties vary within this group of alloys, formability ranges from moderately easy to difficult in relation to other materials.



**Figure 5** Effect of nickel content on air oxidation of alloys. Each cycle consisted of 15 min at 1800°F followed by 5 min air cooling.

#### 4.1 Resistance to Deformation

Resistance to deformation, usually expressed in terms of hardness or yield strength, is a primary consideration in cold forming. Deformation resistance is moderately low for the nickel and nickel-copper systems and moderately high for the nickel-chromium and nickel-iron-chromium systems. However, when properly annealed, even the high-strength alloys have a substantial range between yield and ultimate tensile strength. This range is the plastic region of the material and all cold forming is accomplished within the limits of this region. Hence, the high-strength alloys require only stronger tooling and more powerful equipment for successful cold forming. Nominal tensile properties and hardnesses are given in Table 2.

#### 4.2 Strain Hardening

A universal characteristic of the high-nickel alloys is that they have face-centered-cubic crystallographic structures and, consequently, are subject to rapid strain hardening. This characteristic is used to advantage in increasing the room temperature tensile properties and hardness of alloys



that otherwise would have low mechanical strength or in adding strength to those alloys that are hardened by a precipitation heat treatment. Because of this increased strength, large reductions can be made without rupture of the material. However, the number of reductions in a forming sequence will be limited before annealing is required, and the percentage reduction in each successive operation must be reduced.

Since strain hardening is related to the solid-solution strengthening of alloying elements, the strain-hardening rate generally increases with the complexity of the alloy. Accordingly, strain-hardening rates range from moderately low for nickel and nickel-copper alloys to moderately high for nickel-chromium and nickel-iron-chromium alloys. Similarly, the age-hardenable alloys have higher strain-hardening rates than their solid-solution equivalents. Figure 6 compares the strain-hardening rates of some nickel alloys with those of other materials as shown by the increase in hardness with increasing cold reduction.

Laboratory tests have indicated that the shear strength of the high-nickel alloys in double shear averages about 65% of the ultimate tensile strength (see Table 4). These values, however,

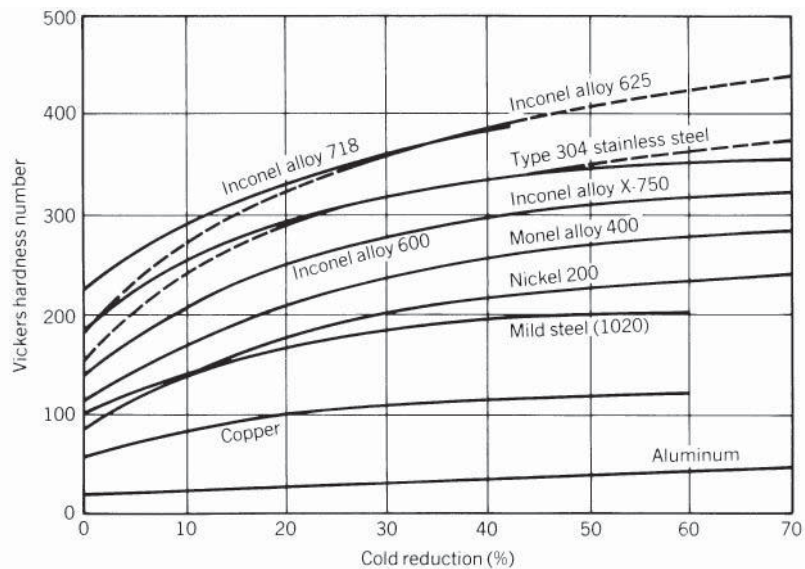


Figure 6 Effect of cold work on hardness.

Table 4 Strength in Double Shear of Nickel and Nickel Alloys

Alloy	Condition	Shear Strength (ksi) <sup>a</sup>	Tensile Strength (ksi)	Hardness
Nickel 200	Annealed	52	68	46 $R_b$
	Half hard	58	79	84 $R_b$
	Full hard	75	121	100 $R_b$
Monel alloy 400	Hot rolled, annealed	48	73	65 $R_b$
	Cold rolled, annealed	49	76	60 $R_b$
Inconel alloy 600	Annealed	60	85	71 $R_b$
	Half hard	66	98	98 $R_b$
	Full hard	82	152	31 $R_c$
Inconel alloy X-750	Age hardened <sup>b</sup>	112	171	36 $R_c$

<sup>a</sup>MPa = ksi  $\times$  6.895.

<sup>b</sup>Mill annealed and aged 1300°F (750°C)/20 h.

**Table 5** Shear Load for Power Shearing of 6.35-mm (0.250-in.) Gauge Annealed Nickel Alloys at 31 mm/m ( $\frac{3}{8}$  in./ft.) Rake as Compared with Mild Steel

Alloy	Tensile Strength (ksi) <sup>a</sup>	Hardness ( $R_b$ )	Shear Load ( $l_b$ ) <sup>b</sup>	Shear Load in Percent of Same Gauge of Mild Steel
Nickel 200	60	60	61,000	200
Monel alloy 400	77	75	66,000	210
Inconel alloy 600	92	79	51,000	160
Inconel alloy 625	124	95	55,000	180
Inconel alloy 718	121	98	50,000	160
Inconel alloy X-750	111	88	57,000	180
Mild steel	50	60	31,000	100

<sup>a</sup>MPa = ksi  $\times$  6.895.<sup>b</sup>kg = lb  $\times$  0.4536.

were obtained under essentially static conditions using laboratory testing equipment having sharp edges and controlled clearances. Shear loads for well-maintained production equipment can be found in Table 5. These data were developed on a power shear having a 31-mm/m ( $\frac{3}{8}$ -in./ft) rake.

## 5 HEAT TREATMENT

High-nickel alloys are subject to surface oxidation unless heating is performed in a protective atmosphere or under vacuum. A protective atmosphere can be provided either by controlling the ratio of fuel and air to minimize oxidation or by surrounding the metal being heated with a prepared atmosphere.

Monel alloy 400, Nickel 200, and similar alloys will remain bright and free from discoloration when heated and cooled in a reducing atmosphere formed by the products of combustion. The alloys that contain chromium, aluminum, or titanium form thin oxide films in the same atmosphere and, therefore, require prepared atmospheres to maintain bright surfaces.

Regardless of the type of atmosphere used, it must be free of sulfur. Exposure of nickel alloys to sulfur-containing atmospheres at high temperatures can cause severe sulfidation damage.

The atmosphere of concern is that in the immediate vicinity of the work, that is, the combustion gases that actually contact the surface of the metal. The true condition of the atmosphere is determined by analyzing gas samples taken at various points about the metal surface.

Furnace atmospheres can be checked for excessive sulfur by heating a small test piece of the material, for example, 13-mm- ( $\frac{1}{2}$ -in.-) diameter rod or 13 mm  $\times$  25 mm ( $\frac{1}{2}$  in.  $\times$  1 in.) flat bar, to the required temperature and holding it at temperature for 10–15 min. The piece is then air cooled or water quenched and bent through 180° flat on itself. If heating conditions are correct, there will be no evidence of cracking.

### 5.1 Reducing Atmosphere

The most common protective atmosphere used in heating the nickel alloys is that provided by controlling the ratio between the fuel and air supplied to the burners. A suitable reducing condition can be obtained by using a slight excess of fuel so that the products of combustion contain at least 4%, preferably 6%, of carbon monoxide plus hydrogen. The atmosphere should not be permitted to alternate from reducing to oxidizing; only a slight excess of fuel over air is needed.

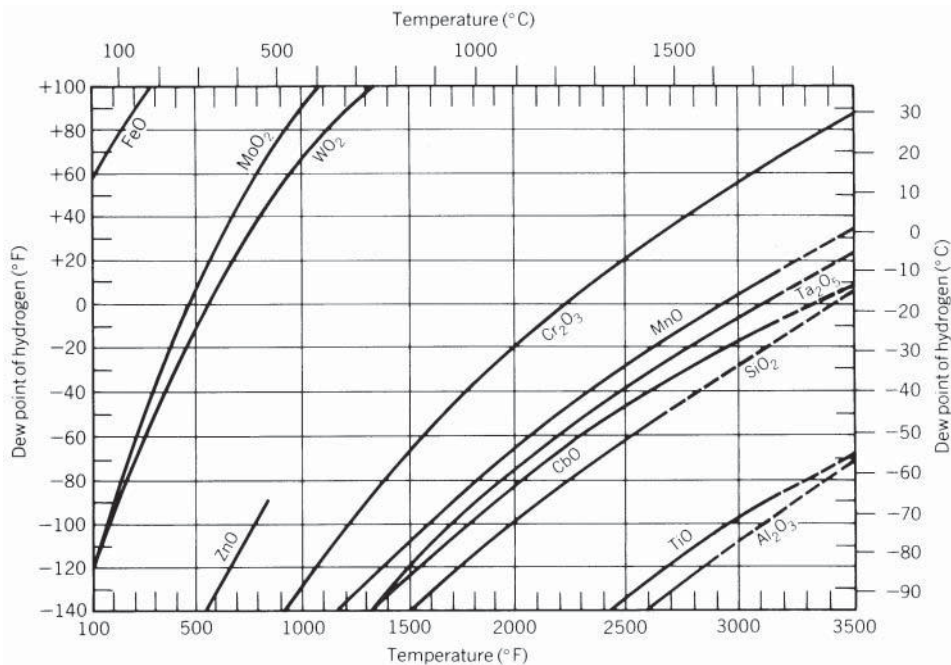
It is important that combustion take place before the mixture of fuel and air comes into contact with the work, otherwise the metal may be embrittled. To ensure proper combustion, ample space should be provided to burn the fuel completely before the hot gases contact the work. Direct impingement of the flame can cause cracking.

## 5.2 Prepared Atmosphere

Various prepared atmospheres can be introduced into the heating and cooling chambers of furnaces to prevent oxidation of nickel alloys. Although these atmospheres can be added to the products of combustion in a directly fired furnace, they are more commonly used with indirectly heated equipment. Prepared protective atmospheres suitable for use with the nickel alloys include dried hydrogen, dried nitrogen, dried argon or any other inert gas, dissociated ammonia, and cracked or partially reacted natural gas. For the protection of pure nickel and nickel-copper alloys, cracked natural gas should be limited to a dew point of  $-1$ – $4^{\circ}\text{C}$  ( $30$ – $40^{\circ}\text{F}$ ).

Figure 7 indicates that at a temperature of  $1093^{\circ}\text{C}$  ( $2000^{\circ}\text{F}$ ), a hydrogen dew point of less than  $-30^{\circ}\text{C}$  ( $-20^{\circ}\text{F}$ ) is required to reduce chromium oxide to chromium; at  $815^{\circ}\text{C}$  ( $1500^{\circ}\text{F}$ ) the dew point must be below  $-50^{\circ}\text{C}$  ( $-60^{\circ}\text{F}$ ). The values were derived from the thermodynamic relationships of pure metals with their oxides at equilibrium and should be used only as a guide to the behavior of complex alloys under nonequilibrium conditions. However, these curves have shown a close correlation with practical experience. For example, Inconel alloy 600 and Incoloy alloy 800 are successfully bright annealed in hydrogen having a dew point of  $-35$  to  $-40^{\circ}\text{C}$  ( $-30$  to  $-40^{\circ}\text{F}$ ).

As indicated in Fig. 7, lower dew points are required as the temperature is lowered. To minimize oxidation during cooling, the chromium-containing alloys must be cooled rapidly in a protective atmosphere.



**Figure 7** Metal/metal oxide equilibria in hydrogen atmospheres.

## 6 WELDING

Nickel alloys are characterized by good weldability by a variety of common joining processes. Thin sheet is generally joined without filler metal (autogenous) using gas–tungsten arc welding (GTAW) or plasma arc welding (PAW) processes. High-speed welding, using the GTAW process, requires magnetic arc deflection to maintain the arc in proper relation to the torch. While thin gauges can be welded at high speeds, the weld grain structure will be coarse and not exhibit the highest ductility. For optimum ductility, travel speed must be slow enough to produce an elliptical weld puddle rather the tear-drop shape which results from high-speed welding.

When filler metals are used, they usually are overmatching in composition to minimize galvanic corrosion effects in the weld metal. To minimize the amount of segregation which occurs in the fusion zone of the weld deposit, low heat input should be incorporated into the welding process when possible to optimize the corrosion resistance of the weld. Interpass weld temperature should not exceed 300°F (150°C) when joining thicker sections. Quality weld joints require careful consideration of the compatibility of weld metal with material being joined, the process used, dilution effects, joint design, service conditions, and the joint properties required. It is a good idea to involve a welding engineer where critical component requirements exist.

## 7 MACHINING

Nickel and nickel-based alloys can be machined by the same techniques used for iron-based alloys. However, higher loads will be imparted to the tooling requiring heavy-duty equipment to withstand the load and coolants to dissipate the heat generated. The cutting tool edge must be maintained sharp and have the proper geometry.

## 8 CLOSURE

It has not been possible to give the composition of and discuss each commercial alloy and, therefore, one should refer to publications like Refs. 5, 7, and 8 for alloy listings, which are revised periodically to include the latest alloys available. (See Table 6 for the producer companies of some of the alloys mentioned in this chapter.)

**Table 6** Registered Trademarks of Producer Company

Trademark	Owner
Duranickel	Special Metals Corporation
Hastelloy	Haynes International
Incoloy	Special Metals Corporation
Inconel	Special Metals Corporation
MAR-M	Martin Marietta Corporation
Monel	Special Metals Corporation
Nilo	Special Metals Corporation
Ni-Span-C	Special Metals Corporation
Permanickel	Special Metals Corporation
Pyromet	Carpenter Technology Corporation
René	General Electric Company
René 41	Allvac Metals Corporation
Udimet	Special Metals Corporation
Waspaloy	United Aircraft Corporation

## REFERENCES

1. J. R. Boldt, Jr., *The Winning of Nickel*, Van Nostrand, New York, 1967.
2. *Nickel and Its Alloys*, NBS Monograph 106, May 1968.
3. T. H. Bassford and J. Hosier, "Nickel and Its Alloys," in M. Kutz (Ed.), *Mechanical Engineers' Handbook*, 2nd ed., Wiley, New York, 1989, pp. 71–89.
4. *Unified Numbering System for Metals and Alloys*, 9th ed., Society of Automotive Engineers, Warrendale, PA, and Conshohocken, PA, 2001.
5. *Alloy Handbooks and Bulletins*, Special Metals Corporation, Huntington, WV, 2005.
6. *ASM Handbook*, 10th ed., Vol. 2, *Properties and Selection: Nonferrous Alloys and Special-Purpose Materials*, ASM International, Materials Park, OH, 1990.
7. *Hastelloy Alloy X Technical Bulletin*, Haynes International, Kokomo, IN.
8. *Alloy Digest*, ASM International, Materials Park, OH, 2003.
9. *Aerospace Structural Metals Handbook*, CINDA / USAF CRDA Handbook Operation, Purdue University, West Lafayette, IN, 2000.
10. W. Z. Friend, *Corrosion of Nickel and Nickel-Base Alloy*, Wiley, New York, 1980, pp. 3–5.
11. F. L. LaQue and H. R. Copson, *Corrosion Resistance of Metals and Alloys*, 2nd ed., Reinhold, New York, 1963.
12. J. Kolts et al., "Highly Alloyed Austenitic Materials for Corrosion Service," *Metal Progress*, September 1983, pp. 25–36.
13. Eiselstein and Skinner, *High Temperature Corrosion in Refinery and Petrochemical Service*, Inco Publication, 1960.

# CHAPTER 7

## MAGNESIUM AND ITS ALLOYS

**Robert E. Brown**

Magnesium Monthly Review  
Prattville Alabama

<b>1 INTRODUCTION</b>	<b>289</b>	<b>5 CORROSION AND FINISHING</b>	<b>296</b>
<b>2 USES</b>	<b>290</b>	5.1 Chemical Conversion	
2.1 Nonstructural Applications	290	Coatings	296
2.2 Structural Applications	290	5.2 Anodic Coatings	296
<b>3 ALLOYS AND PROPERTIES</b>	<b>291</b>	5.3 Painting	296
3.1 Mechanical Properties of Castings	292	5.4 Electroplating	296
3.2 Mechanical Properties of Wrought Materials	292	<b>6 RECYCLING</b>	<b>296</b>
3.3 Physical Properties of Magnesium	293	<b>7 LIFE-CYCLE ASSESSMENT</b>	<b>297</b>
<b>4 FABRICATION</b>	<b>293</b>	<b>REFERENCES</b>	<b>297</b>
4.1 Machining	293	<b>BIBLIOGRAPHY</b>	<b>297</b>
4.2 Joining	293		
4.3 Forming	295		

### 1 INTRODUCTION

Magnesium, with a density of 1.74 g/cm<sup>3</sup>, is the lightest of all structural metals. It is used mainly as an alloyed material in many forms, including castings, forgings, extrusions, rolled sheet, and plate. It is a plentiful element, representing 2.7% of the earth's crust. Magnesium is not found in its metallic form but occurs mainly in nature as carbonates, dolomite, and magnesite. It is also found as carnallite in brines or in salt lakes in many areas of the world. A major source of magnesium is in seawater. There is 6 million tons of magnesium in one cubic mile of seawater.

Incorrect ideas prevail as to the fire risk and inflammability of magnesium. Many people first encounter magnesium metal as a powder or ribbon and assume that it is readily inflammable and hazardous to handle. This is not true. Solid magnesium such as finished parts and coarse scrap is completely harmless. A match cannot ignite it, and only if heated above the melting point will the metal burn, the solid remaining unburnt (Ref. 1, p. 1).

There are two major methods of producing magnesium, electrolytic and thermal reduction. The main electrolytic method of reduction is by electrolysis of magnesium chloride. Thermal reduction is principally achieved by reducing magnesium oxide by ferrosilicon. The world's largest producing country is China and it produces magnesium by the Pidgeon process, which uses ferrosilicon to reduce calcined dolomite.

The total production of magnesium in all areas of the world is relatively small. In 2011, estimated world magnesium production was about 750,000 metric tons. China produced 610,000 metric tons, or 82% of the total world production.<sup>2</sup>

## 2 USES

Magnesium is used in many forms and in many applications. However, the largest percent of primary magnesium produced each year is used as an alloying element in aluminum, where it is added to improve strength and corrosion resistance. Aluminum beverage cans use magnesium alloys for the can body stock and lids. The next largest use is in die castings, most of which go to automotive use. The electronics industry uses many die castings for computers and hand-held communications devices. The notebook (laptop) computers are very large users of magnesium cases. Desulfurization of iron and steel is a large user of magnesium (powder or granules) also. A much smaller percent of the total annual use goes to many uses, including, forging, sheet and plate, and sand casting.

### 2.1 Nonstructural Applications

Magnesium occupies a very high position in the electromotive series. This property allows magnesium to be used as a sacrificial anode to protect steel from corrosion. As an example, magnesium is used to protect buried pipelines and to protect the inside of household hot-water heaters. It is also used for protection of ship hulls, ballast tanks, seawater condensers, and steel pilings in marine environments. Alloys used for this service are either cast or extruded.

Magnesium is added to grey cast iron to produce nodular or ductile iron. Magnesium causes the carbon flakes in the cast iron to draw up into balls, thus giving the castings, fewer breakage planes, and strength that is equivalent of steel.

Magnesium in powder or granule form is added to molten iron to reduce the sulfur content prior to its conversion to steel. This improves the strength and toughness of the final steel products. Magnesium also is used as a deoxidizer or scavenger in the manufacture of copper-based alloys, such as brass and bronze, and the manufacture of nickel alloys. Magnesium is used with calcium to remove bismuth from lead.

Magnesium is also used as a reducing agent in the production of titanium, zirconium, and beryllium. Very pure magnesium is used to reduce  $UF_4$  into uranium metal.

Magnesium powder is also used to produce the Grignard reagent, an organic or organometallic intermediate used in turn to produce fine chemicals and pharmaceuticals.

Magnesium sheet and plate are used for photoengraving and for large printing plates for fine quality printing. Magnesium is also used for the construction of batteries, both dry cell and reserve-cell types such as seawater-activated cells.

### 2.2 Structural Applications

Magnesium has many attractive properties that have enabled the metal to be used in many structural applications. Its extreme lightness alone makes it attractive to all parts that are moved or lifted during their manufacture or use. Low inertia, which results from the low density of magnesium, is especially advantageous in rapidly moving parts. In addition, the low density of magnesium allows thicker sections to be used in parts, eliminating the need for a large amount of stiffening, simplifying the part and its manufacture (Ref. 3, p. 4). Magnesium alloys have other attractive properties such as elevated-temperature properties for aircraft and missile applications. There is fatigue strength in wheels, damping in electronic housings and in jigs and fixtures, machinability in tooling plate, dent resistance in magnesium sheet used for luggage, alkaline resistance to concrete and low resistance to the passage of x-rays, and thermal neutrons in x-ray cassettes and nuclear fuel cans (Ref. 3, p. 4).

Magnesium is easily fabricated by most of the traditional metal-forming processes, including casting of all types, forging, extrusion, rolling, and injection molding (thixocasting). The base forms are transformed into finished products by machining, forming, and joining. Finishing for protective or decorative purposes is by chemical conversion coatings, painting, or electroplating.



Those properties mainly significant for structural applications are density (automotive and aerospace vehicle parts; portable tools such as chain saws, containers such for computers, cameras, briefcases; sports equipment such as catcher's masks, archery bows); high damping capacity (antivibration platforms for electronic equipment; walls for sound attenuation); excellent machinability (jigs and fixtures for manufacturing processes); and high corrosion resistance in an alkaline environment (cement tools).

Weight reduction of vehicles is an issue for many carmakers. Magnesium helps give a lighter weight car that improves fuel economy and reduces emission regardless of the propulsion system used. The major parts made in the standard traditional magnesium alloys include instrument panel support beams (dash boards), steering wheels, steering columns, four-wheel drive gear boxes, and various support brackets and pieces. The most successful car ever built was the Volkswagen Beetle with 24,000,000 cars sold into the market. This car used magnesium for the crankcase and transmission housing and other parts averaging 22 kg per car or more than 520,000 tons of magnesium during its life.

### 3 ALLOYS AND PROPERTIES

Many alloys have been developed to provide a range of properties and characteristics to meet the needs of a wide variety of applications. The most frequently used are listed in Table 1. There are two major classes—those containing aluminum as the principal alloying ingredient, the other containing more exotic metals for alloying. Those containing aluminum are strong

**Table 1** Magnesium Alloys in Common Use

ASTM Designation	Ag	Al	Fe max	Mn	Ni max	Rare Earth	Si	Zn	Zr	Forms
AM50A	—	4.9	0.004	0.32	0.002	—	—	0.22	—	DC
AM60B	—	6.0	0.005	0.42	0.002	—	—	0.22 max.	—	DC
AS41B	—	4.2	0.0035	0.52	0.002	—	1.0	0.12	—	DC
AZ91D	—	9	0.005	0.33	0.002	—	—	0.7	—	DC
ACM522	—	5.3	—	0.17	—	2.6	E	—	—	DC
AJ52A	—	5	—	0.38	—	C	—	0.20	—	DC
AJ62A	—	6	—	0.38	—	D	—	0.20	—	DC
AZ31B	—	3	0.005	0.6	0.005	—	—	1	—	S, P, F, E
AZ61A	—	6.5	0.005	0.33	0.005	—	—	0.9	—	F, E
AZ80A	—	8.5	0.005	0.31	0.005	—	—	0.5	—	F, E
AZ81A	—	7.6	—	0.24	—	—	—	0.7	—	SC, PM, IC
AZ91E	—	9	0.005	0.26	0.0010	—	—	0.7	—	SC, PM
EZ33A	—	—	—	—	—	3.2	—	2.5	0.7	SC, PM
K1A	—	—	—	—	—	—	—	—	0.7	SC, PM
M1A	—	—	—	1.6	—	—	—	—	—	E
QE22A	2.5	—	—	—	—	2.2	—	—	0.7	SC, PM, IC
WE43A	—	—	0.01	0.15	0.005	A	—	0.20	0.7	SC, PM, IC
WE54A	—	—	—	0.15	0.005	B	—	—	0.7	SC, PM, IC
ZE41A	—	—	—	0.15	—	1.2	—	4.2	0.7	SC, PM, IC
ZE63A	—	—	—	—	—	2.6	—	5.8	0.7	SC, PM, IC
ZK40A	—	—	—	—	—	—	—	4	0.7	E
ZK60A	—	—	—	—	—	—	—	5.5	0.7	F, E

A = 4 Yttrium; 3 RE. C = 2.0 Strontium. E = 2.0 Calcium.

B = 5.1 Yttrium; 4 RE. D = 2.5 Strontium.

DC = die casting; E = extrusion; F = forging; IC = investment casting; P = plate; PM = permanent mold; S = sheet; SC = sand casting.



and ductile and have excellent resistance to atmospheric corrosion. Zirconium is an excellent grain refiner for magnesium but cannot be used with aluminum. Within this class, those alloys containing rare earth or yttrium are especially suited for applications at higher temperatures up to 300°C. Those not containing rare earth or yttrium have zinc as a principal alloying ingredient and are strong, ductile, and tough (Ref. 4, p. 43).

### 3.1 Mechanical Properties of Castings

The largest and most rapidly growing structural use of magnesium alloys is in die casting. The majority of the die castings are for the automotive or electronic industry in all areas of the world. Both hot- and cold-chamber die casting processes are being used to produce automotive parts of all sizes and shapes. Weight limits are usually restricted to parts with net weights less than 25 lb. This method is frequently the most economical to produce a magnesium part and is especially effective in producing parts with very thin sections. The acceptance of magnesium die casting has been greatly assisted by the development of high-purity Mg–Al alloys with very low impurity levels, i.e., Fe, Ni, and Cu, at less than 0.002, 0.010, and 0.030%, respectively. These low levels of impurities enable magnesium alloy components to withstand standard salt spray corrosion testing with results equal to or better than those of competitive aluminum alloys.

AM60B and AM50A are being used for their higher elongation. This alloy is used for the instrument panel support beam (dashboard). The finished part, cast in one piece, extends from the right door pillar to the left door pillar; hence it is a vital structural part of the automobile frame.

New creep-resistant magnesium alloys have been developed to expand the use of magnesium in vehicles. The major area of a car that is most important in weight savings is the front end. If magnesium parts such as a crankcase or transmission can be converted to magnesium, large amounts of weight can be saved. Crankcases, oil pans, and transmissions all operate at temperatures over 150°C.

Development of sand cast magnesium alloys that can operate effectively at higher temperatures has been going on for many years. These high-temperature sand cast alloys are used for helicopter transmission housings and jet engine gearboxes. Most of these alloys are based on adding rare earths, zirconium, and yttrium. These alloys are not compatible with the high-pressure die casting process.

Newer heat-resistant and high-temperature creep-resistant alloys for die casting are being developed using several new types of compositions. Several new alloys used calcium to help develop creep resistance. An alloy developed by Noranda and now supplied by Magnesium Elektron Limited (MEL) of Manchester is based on Mg–Al–Sr–Ca. The alloy composition contains 5% Al and 2% Sr (AJ52X—“J” denotes strontium). General Motors is developing a similar alloy with large amounts of calcium. Dead Sea Magnesium and Volkswagen developed a high-temperature-resistant alloy based on Mg–Al–Ca–RE with optional additions of Sr and Zn. These alloys are able to give improved elevated-temperature properties, die castability, and excellent salt spray corrosion resistance. These alloys are being used as part of a program to expand the use of magnesium into automatic transmission casings, crankcases, oil pump body, oil pan, belt pulley, cylinder cover, and engine fan applications.

Other creep-resistant alloys being investigated include both high-pressure die cast alloys and sand cast alloys. The large size and complexity of engine blocks and transmission housings may create a need for additional higher temperature alloys that could be sand cast.

Mechanical properties of cast alloys are in Table 2.

### 3.2 Mechanical Properties of Wrought Materials

Wrought products are produced as forgings, extrusions, sheet, and plate. Mechanical properties are given in Table 3.

**Table 2** Typical Mechanical Properties for Castings

Alloy	Temper	Tensile Strength (MPa)	Yield Strength (MPa)	Elongation in 2 in. (%)
<i>Sand and Permanent Mold Castings</i>				
AZ81A	T4	276	85	15
AZ91E	F	165	95	3
	T4	275	85	14
	T6	275	195	6
EZ33A	T5	160	105	3
K1A	F	185	51	20
QE22A	T6	275	205	4
WE43A	T6	235	190	4
WE54A	T6	270	195	4
ZE63A	T6	295	190	7
<i>Investment Castings</i>				
AZ81A	T4	275	100	12
AZ91E	F	165	100	2
	T4	275	100	12
	T5	180	100	3
	T7	275	140	5
EZ33A	T5	255	110	4
K1A	F	175	60	20
QE22A	T6	260	185	4
<i>Die Castings</i>				
AM50A	F	200	110	10
AM60B	F	220	130	8
AS41B	F	210	140	6
AZ91D	F	230	160	3
<i>Die Castings for Elevated Temperatures</i>				
ACM522	F (20°C)	200	158	4
	F (175°C)	152	132	9
AJ52X	F (20°C)	228	161	13
	F (175°C)	141	100	18
AJ62X	F (20°C)	240	143	7
	F (175°C)	143	103	19

### 3.3 Physical Properties of Magnesium

A selection of physical properties of pure magnesium is given in Table 4. Most of these are insensitive to alloy addition, but melting point, density, and electrical resistivity may vary slightly.

## 4 FABRICATION

### 4.1 Machining

Magnesium is the easiest metal to machine. It requires less power for removing a given volume of metal by machining than any other commonly machined metal (Ref. 3, p. 3).

### 4.2 Joining

Magnesium can be joined by using the many traditional joining methods, both mechanical and thermal. Joining methods that have been used successfully include mechanical fasteners such

**Table 3** Typical Mechanical Properties of Wrought Products

Alloy	Temper	Tensile Strength (MPa)	Yield Strength (MPa)		Elongation in 2 in. (%)
			Tensile	Compressive	
<i>Sheet and Plate</i>					
AZ31B	O	255	150	110	21
	H24	290	220	180	15
<i>Extrusions</i>					
AZ31B	F	260	200	95	15
AZ61A	F	310	230	130	16
AZ80A	F	340	250	140	11
	T5	380	275	240	7
M1A	F	255	180	125	12
ZK40A	T5	275	255	140	4
ZK60A	F	340	250	185	14
	T5	365	305	250	11
<i>Forgings</i>					
AZ31B	F	260	195	85	9
AZ61A	F	195	180	115	12
AZ80A	F	315	215	170	8
	T5	345	235	195	6
	T6	345	250	185	5
ZK60A	T5	305	205	195	16
	T6	325	270	170	11

**Table 4** Physical Properties of Pure Magnesium

Latent heat of vaporization	5150–5400 kJ/kg
Latent heat of sublimation	6113–6238 kJ/kg
Density	1.738 g/cm <sup>3</sup>
Melting point	650°C
Thermal expansion	25.2 × 10 <sup>-6</sup> /K
Specific heat	1.025 kJ/kg · Kat 20°C
Latent heat of fusion	360–377 kJ/kg
Heat of combustion	25,020 kJ/kg
Boiling point	1090°C
Electrical resistivity	4.45 Ω · m × 10 <sup>-8</sup>
Crystal structure	Close-packed hexagonal
	<i>a</i> = 0.32092
	<i>c</i> = 0.52105
	<i>c/a</i> = 1.633

Source: From Ref. 2, p. 9.

as rivets and threaded fasteners (bolts and screws). Welding is done by protected arc processes such as metal inert gas (MIG) and tungsten inert gas (TIG) welding. Other welding methods such as plasma, electron beam, and friction stir welding, explosion joining, and ultrasonic joining are also used.

Magnesium has been joined by adhesive bonding for many years. Large structural components have been joined by the use of adhesives. The large six-engine U.S. Bomber, the B-36, used over 12,000 lb of magnesium sheet attached to frames by adhesives.

Magnesium welding can also be used to repair casting defects in magnesium cast parts.

### 4.3 Forming

Magnesium can be formed by most common wrought processes such as forging, extrusion, deep drawing, bending, spinning, stretch forming, and dimpling. Magnesium has a hexagonal close-packed crystalline structure with little cold workability. Magnesium is best formed when hot (80–225°C) (Ref. 1, p. 584).

Forging is accomplished with hydraulic presses or slow-acting mechanical presses. Magnesium deforms laterally rather than longitudinally. Forging temperatures are relatively low (27–400°C), so conventional low-alloy, hot-work steels are satisfactory materials for forging dies (Ref. 1, p. 559). The ease with which magnesium can be worked greatly reduces the number of forging operations needed to produce finished parts (Ref. 3, p. 47).

Magnesium alloys have been extruded for many years. Both indirect and direct extrusion has been used. Hydrostatic extrusion presses are being developed in Europe for magnesium alloys. Extrusion billet temperatures usually range from 320 to 400°C (Ref. 1, p. 555).

Magnesium is rolled to sheet and plate by conventional methods of reducing large, preheated slabs in successive passes through a conventional rolling mill. Because the metal structure is hexagonal, it requires careful handling and reheating after a series of passes when the temperature of the product gets too cold. Starting slab temperatures for breakdown should be 425–450°C. Sheet rolling range should be 350–440°C with about 25–50% reduction before reheating (Ref. 1, p. 555).

Twin roll casting is also being used to produce thin magnesium sheet directly from molten magnesium alloy (Fig. 1). Work is being done to produce sheet to a final thickness as it is cast between the rolls. POSCO, the Korean steel maker, is the leader in producing commercial magnesium sheet which has many potential uses in both autos and electronics. The latest twin roll caster can produce ~16-ton coils of magnesium alloy that are 2000 mm wide, 2500 mm in diameter, and 4–8 mm thick. Surface defects like inverse segregation can be minimized by adequate process control.<sup>5</sup>



**Figure 1** Twin roll cast magnesium alloy strip cast coil, 2000 mm wide.<sup>5</sup>

## 5 CORROSION AND FINISHING

Magnesium, as castings or as wrought products, has always faced corrosion problems. It is anodic to any other structural metal and will be preferentially attacked in the presence of an electrolyte. Galvanic contact must be avoided in structural assemblies by separating magnesium from other metals by the use of films, spacers, or tapes.

### 5.1 Chemical Conversion Coatings

The development of high-purity alloy helped reduce the surface corrosion of finished magnesium products, but more protection is needed, especially for automotive parts. Many types of finishing and protective coatings have been tried over the years. Chromate treatments to fully cleaned magnesium surfaces have worked quite well in the past. The environmental hazards of elemental hexavalent chromium have dictated the elimination of many coatings that contain hazardous materials. Many new methods have been developed that do not contain chromium and are even more effective in providing protection to the magnesium.

### 5.2 Anodic Coatings

Conversion coatings without chromium are being used followed by many surface-modifying treatments. The most widely used is anodic coating applied by placing the part in a bath as an anode while the tank is the cathode. Anodic coatings (Mag-Oxide, Tagnite, Keronite) have been very successful. Also microplasmic coatings and others are being used.

### 5.3 Painting

If a good chemical conversion or anodic coating is present, any paint or powder coating will provide protection. Best protection results from the application of baked, alkaline-resistant paints.

### 5.4 Electroplating

Magnesium can be electroplated fairly easily. This can be the traditional electroplating or the new “electroless” type of coating. Once a base coating is applied chemically, standard electroplating procedures can be applied to magnesium to give decorative and protective finishes.

## 6 RECYCLING

Magnesium is a highly recyclable material consuming only 5% of the energy required to manufacture the primary metal.<sup>6</sup> The continual growth of the demand for magnesium applications has created large quantities of scrap. The treatment of the secondary material that becomes available not only is an ecological necessity but also offers economic potential.

Present die casting methods have a yield of 50–75% based on total cast weight. That means that 25–50% must be recycled. There are two basic types of recycling processes: with the use of flux (usually a chloride salt mixture) and fluxless refining. Both are being used effectively.

The clean die casting scrap, consisting of gates and runners, is called type 1. This is the most highly sought after scrap. For many years it was sold to secondary magnesium plants for remelting and refining. Now, some larger die cast producers are working to recycle the type 1 scrap in their own plants. Type 1 can be easily remelted without flux. Most of the other types of die casting and industry scrap require flux to melt it and refine out impurities.<sup>7</sup>

## 7 LIFE-CYCLE ASSESSMENT

In many cases, the use of magnesium creates environmental benefits due to an efficient use of resources and energy, especially in vehicle lightweight construction. Several studies have been published in which the ecological benefits and risks for automotive magnesium components have been assessed. The studies show that whether an overall benefit from the use of magnesium can be achieved or not depends on the production and recycling conditions for magnesium. Magnesium production technology has been subject to significant improvements in the last several years.

In order to provide an up-to-date picture of a current magnesium life cycle in a transport application, the International Magnesium Association (IMA) has initiated a study on the life-cycle assessment (LCA) of magnesium in 2012. The study is being conducted by the Institute of Vehicle Concepts (German Aerospace Centre—DLR) and the Magnesium Innovation Centre (Helmholtz Centre Geesthacht—HZG). Valuable support is being given by several institutions and companies which provide data and background information for the LCA models. Results will be published as they become available.<sup>8</sup>

## REFERENCES

1. E. F. Emley, *Principles of Magnesium Technology*, Pergamon, New York, 1966.
2. A. Clark., "Update on Chinese Production, Costs and Shipments," IMA Proceedings for 2012, unpublished paper.
3. M. Avedesian and H. Baker, ASM Specialty Handbook, *Magnesium and Magnesium Alloys*, ASM International, Materials Park, OH, 1999.
4. R. Busk, *Magnesium Products Design*, Marcel Dekker, New York, 1987.
5. W. Park, I. Kim, J. Kim, and D. Choo, "Wide Strip Casting Technology of Magnesium Alloys," *Magnesium Technology 2011*, TMS, Warrendale, PA., 2011 p. 143.
6. L. Riopelle, "The Recycling of Magnesium Makes Cents," *Journal of Metals*, Vol. 48(10), 44–46, October, 1996.
7. G. Hanko et al., "Magnesium," in K. Kainer (Ed.), *Proceedings of the 6th International Conference on Magnesium Alloys and Their Applications*, Wiley VCH, Weinbein, 2004, p. 991.
8. H. Freidrich and S. Ehrenberger, "Goals and Methodological Approach of the IMA Life Cycle Assessment (LCA) Study," in *Proceedings of the 69th World Magnesium Conference, International Magnesium Association*, Wauconda, IL, 2012.

## BIBLIOGRAPHY

- A. Beck, *The Technology of Magnesium and its Alloys*, F. A. Hughes, Abbey House, London, 1940.
- E. Aghion and D. Eliezer, *Magnesium 2000*, Magnesium Research Institute, Potash House, Beer-Sheva, Israel, 2000.
- E. Aghion and D. Eliezer, *Magnesium Alloys-Science, Technology, and Applications*, Israeli Consortium for Magnesium Technology Development, S. Neaman Institute, Technion City, Haifa, 2004.
- H. Friedrich and B. Mordike, *Magnesium Technology, Metallurgy, Design Data, Applications*, Springer-Verlag, Berlin, 2006.
- T. Ruden, *Lightweight Magnesium Technology 2001–2005*, SAE International, Warrendale, PA, 2006.
- D. Jenkins, *Magnesium Overcast—Story of the Convair B-36*, Specialty Press, North Branch, MN, 2005.
- H. Kaplan, J. Hryn, and B. Clow, *Magnesium Technology 2000*, TMS, Warrendale, PA, 2000.
- W. Sillikens, S. Agnew, N. Neelameggham, and S. Mathaudhu, *Magnesium Technology 2011*, TMS, Warrendale, PA, 2011.
- Proceedings of the 69th Annual World Magnesium Conference (2012)*, International Magnesium Association (IMA), Wauconda, IL, May 2012.



# CHAPTER 8

## A GUIDE TO ENGINEERING SELECTION OF SUPERALLOYS FOR DESIGN

**Matthew J. Donachie and John Marcin**  
Rensselaer at Hartford  
Hartford, Connecticut

**Stephen J. Donachie (deceased)**  
Special Metals Corporation  
Huntington, West Virginia

<b>1 INTRODUCTION</b>	<b>300</b>	<b>6 COMPONENT PRODUCTION</b>	<b>337</b>
1.1 Purpose	300	6.1 Casting Practices to Produce Parts	337
1.2 What Are Superalloys?	300	6.2 Casting Considerations in Alloy Selection	339
1.3 How Are Superalloys Strengthened?	300	6.3 Wrought Processing—Forging and Powder Metal Superalloys	340
1.4 Manufacture of Superalloy Articles	302	6.4 Wrought Processing—Forging/Working Considerations in Alloy Selection	341
1.5 Superalloy Information	303	6.5 Joining	341
<b>2 METALS AT HIGH TEMPERATURES</b>	<b>304</b>	6.6 Summary of Component Production	343
2.1 General	304	6.7 Some Superalloy Information Sources	343
2.2 Mechanical Behavior	310	<b>7 OTHER ASPECTS OF SUPERALLOY SELECTION</b>	<b>345</b>
<b>3 PROPERTIES OF SUPERALLOYS</b>	<b>325</b>	7.1 Corrosion and Coatings for Protection	345
3.1 Physical/Environmental	325	7.2 Special Alloys for Hot-Corrosion Resistance	346
3.2 Mechanical	328	7.3 Thermal Barrier Coatings	346
<b>4 THE EVOLUTION OF SUPERALLOYS</b>	<b>330</b>	7.4 Postservice Refurbishment and Repair	346
4.1 Introduction	330	<b>8 ALLOY SELECTION SUMMARY</b>	<b>348</b>
4.2 Superalloy Modifications	331	8.1 What Alloys Are Available Off the Shelf for Intermediate Temperature Applications?	348
4.3 Improvement of Superalloys by Chemistry and Process Control or Minor Additions of New Elements	331	8.2 Comments on Wrought Alloys for Intermediate-Temperature Applications	348
<b>5 MELTING AND CASTING PRACTICES</b>	<b>332</b>		
5.1 General Aspects	332		
5.2 Melting and Refining Superalloys	332		
5.3 Pros and Cons of Remelted Ingot Processing	335		
5.4 Melting Considerations in Alloy Selection	336		



8.3	Comments on Wrought Alloys for Intermediate-Strength Higher Temperature Applications	349	8.5	Comments on Cast Alloys for High-Temperature Applications	350
8.4	What Alloys Are Available for High-Strength, High-Temperature Applications?	349	<b>9</b>	<b>FINAL COMMENTS</b>	<b>350</b>
				<b>BIBLIOGRAPHY</b>	<b>351</b>

## 1 INTRODUCTION

### 1.1 Purpose

This chapter is intended to create a sufficient understanding of superalloys so that selection of them for specific designs will be appropriate. Knowledge of types of superalloys and their processing will give a potential user the ability to understand the ways in which superalloys can contribute to a design. The information provided in this chapter should enable the user to ask the important questions of superalloy providers. Understanding the basics will enable an engineer to evaluate the capability of primary melt shops and component producers while addressing the necessary mechanical property and corrosion/environmental behavior that will influence alloy selection. However, there is no cook book for superalloy selection. Proprietary alloys and/or restricted or proprietary processing often lead to superalloy conditions and properties not listed in a handbook or catalog of materials. With few exceptions, critical design applications will require work with one or more superalloy manufacturers to develop an understanding of what is available and what a selector and/or designer can expect from a chosen superalloy.

### 1.2 What Are Superalloys?

For purposes of this chapter superalloys are those nickel-, iron–nickel-, and cobalt-based corrosion-resistant alloys generally used above a nominal temperature of 540°C (1000°F). The iron–nickel-based superalloys are an extension of stainless steel technology and generally are melted and cast to electrode/ingot shapes for subsequent fabrication to components. These iron–nickel-based superalloys usually are formed to shape or near net shape by wrought processing techniques such as hot rolling, forging, etc. On the other hand, after primary production by melting and ingot casting, the cobalt- and nickel-based superalloys may be used either in wrought or cast form depending on the application or the alloy composition involved. The stainless steels, nickel–chromium alloys, and cobalt dental alloys, which evolved into the superalloys, used chromium to provide elevated-temperature corrosion resistance. A Cr<sub>2</sub>O<sub>3</sub> layer on the surface proved very effective in protection against oxidation. Eventually, cast superalloys for the highest temperatures were protected against oxidation by chromium and aluminum. In our opinion, superalloys must contain chromium, probably at the level of 5 wt % (some would argue 8 wt %) or higher for reasonable corrosion resistance. The exact minimum amount will depend on the expected operating conditions. Extremely low chromium levels (2 wt %) have resulted from composition modifications of nickel-based superalloys to maximize high-temperature strength. (*Note:* wt % = percent by weight.)

### 1.3 How Are Superalloys Strengthened?

In the solid state, metals are crystalline and composed of grains. An individual grain is comprised of a repeating crystal arrangement of its atoms. This means that atom positions in

the basic building blocks (unit cell) for a metal or alloy piece have specific crystallographic arrangements, with atoms often arranged in cubic structures. There are various basic crystal structures; in particular, face-centered cubic (fcc), body-centered cubic (bcc), and hexagonal close packed (hcp) define most metallic materials. Some crystal structures tend to be associated with better property characteristics than others. For example, components with fcc crystals tend to have better ductility than components with other common crystal structures.

Crystalline aggregates of atoms have orientation relationships related to directions in the basic crystal structure. Each uniformly oriented crystalline aggregate is called a grain. In an alloy, there are usually many grains with each grain randomly oriented relative to surrounding grains. Metal alloys with random directions among its many grains are known as polycrystals (PCs) or equiaxed (EQX), having roughly equal dimensions of the grains in all directions. However, columnar shaped grains formed by dendritic growth (one long axis) are common in cast products.

The peripheral surface of a grain is called a grain boundary. Aggregates of atoms without grain boundaries are rarely created in nature. However, metals without grain boundaries (single crystals) or metals with aligned boundaries (columnar grained structures) can be produced in superalloys by appropriate manufacturing techniques. The introduction of different atom types, new crystal phases, and/or the manipulation of grain boundaries enables inhibition of the movement through the crystal lattice or grains of the imperfections (dislocations) that cause deformation to occur. [Note: A phase is any chemically homogenous, mechanically separable, physically distinct entity. Different phases may have the same crystal structure as, for example, the basic matrix phase ( $\gamma$ ) and the hardening phase ( $\gamma'$ ) in nickel-base superalloys.]

Superalloys are the basis metals (iron, nickel, cobalt) modified by changes in chemistry, generally in a PC form, with various phases present in the grains or at grain boundaries. Superalloys consist of an austenitic fcc crystal structure matrix phase,  $\gamma$ , plus a variety of secondary phases. Important secondary phases are:  $\gamma'$  fcc ordered  $\text{Ni}_3(\text{Al}, \text{Ti})$  and various MC,  $\text{M}_{23}\text{C}_6$ ,  $\text{M}_6\text{C}$ , and  $\text{M}_7\text{C}_3$  (rare) carbides in nickel- and iron–nickel-based superalloys. M represents various metal elements such as titanium, zirconium, hafnium, niobium, tungsten, molybdenum and chromium. Carbides are the principal secondary phases in cobalt-based alloys. Also,  $\gamma''$  double prime, a body-centered-tetragonal (bct) phase of ordered  $\text{Ni}_3\text{Nb}$ , a hexagonal ordered  $\text{Ni}_3\text{Ti}$  ( $\eta$ ) phase, and the delta orthorhombic  $\text{Ni}_3\text{Nb}$  intermetallic phase can be found in nickel- and iron–nickel-based superalloys. Ordered structures are those in which specific metal atoms occur on defined locations in the crystal lattice in contrast to disordered structures wherein the atoms of a phase occur randomly in location within the crystal structure. An example of an ordered strengthening phase is  $\gamma'$ , as noted above. Its nickel atoms are found on the faces of the cube and the aluminum or titanium atoms occupy the corners of the cube.

It is quite important for the engineer selecting alloys to have a realistic understanding of the strengthening process in superalloys, as the properties of superalloys can be modified not only by chemistry changes but also considerably by processing to manipulate the strengthening level achieved. Superalloys derive their strength from solid-solution hardeners and from secondary precipitate phases that form in the  $\gamma$  matrix and produce precipitation (age) hardening. Principal strengthening precipitate phases in nickel- and iron–nickel-based superalloys are  $\gamma'$  and  $\gamma''$ . Carbides may provide limited strengthening directly (e.g., through dispersion hardening) or, more commonly, indirectly (e.g., by stabilizing grain boundaries against movement). The delta and eta phases are useful (along with  $\gamma'$ ) in control of grain structure of wrought (i.e., mechanically deformed) superalloys during wrought processing after melting. By controlling grain structure, strength can be significantly influenced. The extent to which the secondary phases contribute directly to

**Table 1** Common Ranges of Major Alloying Additions in Superalloys

Element	Range (%)	
	Fe–Ni and Ni Base	Co Base
Cr	3–25	19–30
Mo, W	0–12	0–11
Al	0–6	0–4.5
Ti	0–6	0–4
Co	0–20	—
Ni	—	0–22
Nb	0–5	0–4
Ta	0–12	0–9
Re	0–6	0–2
Ru	0–6	—

Source: *Metals Handbook Desk Edition*, ASM International, Materials Park, OH, 1999, p. 395.

strengthening depends on the alloy and its processing. It should be noted that improper distributions of carbides and precipitate phases can be detrimental to properties.

In addition to those elements that produce solid-solution hardening and/or promote carbide and gamma prime formation, other elements (e.g., boron, zirconium, and hafnium) are added to enhance mechanical or chemical properties. Superalloy microstructure and property control can be complex. As many as 14 elements may be controlled in some superalloys. Some carbide- and  $\gamma'$ -forming elements may contribute significantly to corrosion properties as well. Starting in the decade of the 1980s, unusual, rare and thus expensive elements were found to contribute significantly to the high-temperature strength of nickel-based superalloys. Table 1 gives a generalized list of the ranges of alloying elements in superalloys. Table 2 provides a tabulation of the specific effects of the various alloying elements.

#### 1.4 Manufacture of Superalloy Articles

Appropriate compositions of all superalloy types can be forged, rolled to sheet, or otherwise formed into a variety of shapes. The more highly alloyed superalloy compositions for very high temperature use are normally processed as small castings. Large superalloy castings are made principally in the weldable nickel-based superalloy IN 718 although single-crystal turbine blades of complex higher temperature capability nickel-based superalloys have been cast in lengths up to several feet for applications in land-based gas turbine frames. Fabricated superalloy structures can be built up by welding or brazing, but the more highly alloyed the superalloy composition (i.e., higher amount of hardening phase), the more difficult it is to weld a superalloy. Machining of superalloys is similar to but more difficult than that of machining stainless steels. In welding or machining of superalloys, the effects of the energy input (heat energy, deformation energy) on the microstructure and properties of the final superalloy product must be considered.

Iron–nickel- and nickel-based superalloys are readily available as wrought components produced in extruded, forged, or rolled form; the higher strength nickel-based superalloys generally are found only in the cast condition. Powder metallurgy processing is an accepted method to produce wrought components of certain higher temperature strength alloys. Hot deformation is the preferred forming process, cold forming usually being restricted to thin sections (sheet). Cold rolling may be used to increase short-time strength properties

**Table 2** Role of Alloying Elements in Superalloys

Effect <sup>a</sup>	Iron Base	Cobalt Base	Nickel Base
Solid-solution strengtheners	Cr, Mo	Nb, Cr, Mo, Ni, W, Ta	Co, Cr, Fe, Mo, W, Ta, Re, Ru
fcc matrix stabilizer	C, W, Ni	Ni	—
Carbide form			
MC	Ti	Ti	W, Ta, Ti, Mo, Nb, Hf
M <sub>7</sub> C <sub>3</sub>	—	Cr	Cr
M <sub>23</sub> C <sub>6</sub>	Cr	Cr	Cr, Mo, W
M <sub>6</sub> C	Mo	Mo, W	Mo, W, Nb
Carbonitrides: M(CN)	C, N	C, N	C, N
Promotes general precipitation of carbides	P	—	—
Forms $\gamma'$ Ni <sub>3</sub> (Al,Ti)	Al, Ni, Ti	—	Al, Ti
Retards formation of hexagonal $\eta$ (Ni <sub>3</sub> Ti)	Al, Zr	—	—
Raises solvus temperature of $\gamma'$	—	—	Co
Hardening precipitates and/or intermetallics	Al, Ti, Nb	Al, Mo, Ti, <sup>b</sup> W, Ta	Al, Ti, Nb
Oxidation resistance	Cr	Al, Cr	Al, Cr, Y, La, Ce
Improves hot-corrosion resistance	La, Y	La, Y, Ti	La, Ti
Sulfidation resistance	Cr	Cr	Cr, Co, Si
Improves creep properties	B	—	B
Increases rupture strength	B	B, Zr	B <sup>c</sup>
Grain boundary refiners	—	—	B, C, Zr, Hf
Facilitates working	—	Ni <sub>3</sub> Ti	—
Retards $\gamma'$ coarsening	—	—	Re
Suppresses TCP Information	—	—	Ru <sup>d</sup>

<sup>a</sup>Not all these effects necessarily occur in a given alloy.

<sup>b</sup>Hardening by precipitation of Ni<sub>3</sub>Ti also occurs if sufficient Ni is present.

<sup>c</sup>If present in large amounts, borides are formed.

<sup>d</sup>Ru has significant effect on alloy element partitioning to phases.

Source: *Metals Handbook Desk Edition*, ASM International, Materials Park, OH, 1999, p. 395.

for applications at temperatures below the nominal lower temperature of 540°C (1000°F) established in Section 1.2 for superalloy use. Properties of superalloys generally are controlled by adjustments in chemistry (composition), control of grain size, and modification of the processing (including heat treatment).

## 1.5 Superalloy Information

While some chemistries and properties are listed in this chapter, there is no substitute for consultation with superalloy manufacturers about the forms (cast, wrought) which can be provided and the exact chemistries available. It should be understood that not all superalloys are readily available as off-the-shelf items. *While literally hundreds, perhaps thousands, of superalloy compositions have been evaluated since the mid-1930s, only a handful are routinely produced. Moreover, some superalloys are not available for use in all forms and sizes. Many of the highest strength alloys will be useful only as powder metal products or as castings. Many alloys have proprietary chemistry and production specifications.*

Design data for superalloys are not intended to be conveyed here but typical properties are indicated for some materials. Design properties should be obtained from internal testing,

if possible, or from producers or other validated sources if sufficient test data are not available in-house. Typical properties are merely a guide for comparison. Exact chemistry, section size, heat treatment, and other processing steps must be known to generate adequate property values for design.

The properties of the extraordinary range of superalloy compositions which have been developed over the years are not normally well documented in the literature. However, since many consumers of superalloys actually only use a few alloys within the customary user groups, data may be more plentiful for certain compositions. The extent to which such data are available to the general public is unknown. However, even if such data were disseminated widely, the alloy selector needs to be aware that processing treatments such as forging conditions, heat treatment, coatings for corrosion protection, etc., dramatically affect properties of superalloys. All data should be reconciled with the actual manufacturing specifications and processing conditions expected. Alloy selectors should work with competent metallurgical engineers to establish the validity of data intended for design as well as to specify the processing conditions that will be used for component production.

Application of design data must take into consideration the probability of components containing locally inhomogeneous regions. For wrought superalloys, the probability of occurrence of these regions (which are highly detrimental to fatigue life) is dependent upon the melting method selected for alloy production (see Section 5.2 on melting for details) or on the powder production and consolidation process. For superalloys used as castings, the degree of inhomogeneity and the likelihood of defects such as porosity are related to the alloy composition, the investment casting technique used, and the complexity of the final component.

For sources of property data other than that of the producers (melters, forgers, etc.) or an alloy selector's own institution, one may refer to organizations such as ASM International which publish compilations of data that may form a basis for the development of design allowances for superalloys.

Standards organizations such as ASTM publish information about superalloys but that information does not ordinarily contain design data. The great versatility of superalloys in property modification is also a detriment to the universal compilation of property values. The same nominal alloy may have some composition modifications made from one manufacturer or customer to another. Sometimes this extends from one country to another. Tweaking of the casting or forging process or the heat treatment, in addition to what seem like minor composition changes, can cause significant variations in properties. All facets of chemistry and processing need to be considered when selecting a superalloy for an application.

Some information is given on chemistry and properties of a few superalloys as follows: nominal compositions of selected superalloys in Tables 3 and 4; allowable trace element concentrations in Table 5; short-time (tensile) properties in Tables 6 and 7; time-dependent (creep rupture) properties in Tables 8 and 9; physical properties in Tables 10 and 11; and dynamic modulus values in Tables 12 and 13. It should be noted that time-dependent mechanical properties are particularly affected by grain size. Selected publications providing superalloy technical information or properties are indicated at the end of the chapter.

## 2 METALS AT HIGH TEMPERATURES

### 2.1 General

While material strengths at low temperatures are usually not a function of time, at high temperatures the time of load application becomes very significant for mechanical properties. Concurrently, the availability of oxygen at high temperatures accelerates the conversion of some of the metal atoms to oxides. Oxidation proceeds much more rapidly at high temperatures than at room or lower temperatures.

**Table 3** Nominal Compositions of Wrought Superalloys

Alloy	Composition, wt.%										
	Cr	Ni	Co	Mo	W	Nb	Ti	Al	Fe	C	Other
<b>Solid-Solution Alloys</b>											
<i>Iron-Nickel Base</i>											
Alloy N-155 (Multimet)	21.0	20.0	20.0	3.00	2.5	1.0	—	—	32.2	0.15	0.15 N, 0.2 La, 0.02 Zr
Haynes 556	22.0	21.0	20.0	3.0	2.5	0.1	—	0.3	29.0	0.10	0.50 Ta, 0.02 La, 0.02 Zr
I9-9 DL	19.0	9.0	—	1.25	1.25	0.4	0.3	—	66.8	0.30	1.10 Mn, 0.60 Si
Incoloy 800	21.0	32.5	—	—	—	—	0.38	0.38	45.7	0.05	—
Incoloy 800H	21.0	33.0	—	—	—	—	—	—	45.8	0.08	—
Incoloy 800HT	21.0	32.5	—	—	—	—	0.4	0.4	46.0	0.08	0.8 Mn, 0.5 Si, 0.4 Cu
Incoloy 801	20.5	32.0	—	—	—	—	1.13	—	46.3	0.05	—
Incoloy 802	21.0	32.5	—	—	—	—	0.75	0.58	44.8	0.35	—
<i>Nickel Base</i>											
Haynes 214	16.0	76.5	—	—	—	—	—	4.5	3.0	0.03	—
Haynes 230	22.0	55.0	5.0 max.	2.0	14.0	—	—	0.35	3.0 max.	0.10	0.15 max. B, 0.02 La
Inconel 600	15.5	76.0	—	—	—	—	—	—	8.0	0.08	0.25 Cu
Inconel 601	23.0	60.5	—	—	—	—	—	1.35	14.1	0.05	0.5 Cu
Inconel 617	22.0	55.0	12.5	9.0	—	—	—	1.0	—	0.07	—
Inconel 625	21.5	61.0	—	9.0	—	3.6	0.2	0.2	2.5	0.05	—
RA333	25.0	45.0	3.0	3.0	3.0	—	—	—	18.0	0.05	—
Hastelloy B	1.0 max.	63.0	2.5 max.	28.0	—	—	—	—	5.0	0.05 max.	0.03 V
Hastelloy N	7.0	72.0	—	16.0	—	—	0.5 max.	—	5.0 max.	0.06	—
Hastelloy S	15.5	67.0	—	15.5	—	—	—	0.2	1.0	0.02 max.	0.02 La
Hastelloy W	5.0	61.0	2.5 max.	24.5	—	—	—	—	5.5	0.12 max.	0.6 V
Hastelloy X	22.0	49.0	1.5 max.	9.0	0.6	—	—	2.0	15.8	0.15	—
Hastelloy C-276	15.5	59.0	—	16.0	3.7	—	—	—	5.0	0.02 max.	—
Haynes HR-120	25.0	37.0	3.0	2.5	2.5	0.7	—	0.1	33.0	0.05	0.7 Mn, 0.6 Si, 0.2 N, 0.004 B
Haynes HR-160	28.0	37.0	29.0	—	—	—	—	—	2.0	0.05	2.75 Si, 0.5 Mn
Nimonic 75	19.5	75.0	—	—	—	—	0.4	0.15	2.5	0.12	0.25 max. Cu
Nimonic 86	25.0	65.0	—	10.0	—	—	—	—	—	0.05	0.03 Ce, 0.015 Mg
<i>Cobalt Base</i>											
Haynes 25 (L605)	20.0	10.0	50.0	—	15.0	—	—	—	3.0	0.10	1.5 Mn
Haynes 188	22.0	22.0	37.0	—	14.5	—	—	—	3.0 max.	0.10	0.90 La
Alloy S-816	20.0	20.0	42.0	4.0	4.0	4.0	—	—	4.0	0.38	—
MP35-N	20.0	35.0	35.0	10.0	—	—	—	—	—	—	—
MP159	19.0	25.0	36.0	7.0	—	0.6	3.0	0.2	9.0	—	—
Stellite B	30.0	1.0	61.5	—	4.5	—	—	—	1.0	1.0	—
UMCo-50	28.0	—	49.0	—	—	—	—	—	21.0	0.12	—
<b>Precipitation-Hardening Alloys</b>											
<i>Iron-Nickel Base</i>											
A-286	15.0	26.0	—	1.25	—	—	2.0	0.2	55.2	0.04	0.005 B, 0.3 V
Discaloy	14.0	26.0	—	3.0	—	—	1.7	0.25	55.0	0.06	—
Incoloy 903	0.1 max.	38.0	15.0	0.1	—	3.0	1.4	0.7	41.0	0.04	—
Pyromet CTX-1	0.1 max.	37.7	16.0	0.1	—	3.0	1.7	1.0	39.0	0.03	—
Incoloy 907	—	38.4	13.0	—	—	4.7	1.5	0.03	42.0	0.01	0.15 Si
Incoloy 909	—	38.0	13.0	—	—	4.7	1.5	0.03	42.0	0.01	0.4 Si
Incoloy 925	20.5	44.0	—	2.8	—	—	2.1	0.2	29	0.01	1.8 Cu
V-57	14.8	27.0	—	1.25	—	—	3.0	0.25	48.6	0.08 max.	0.01 B, 0.5 max. V
W-545	13.5	26.0	—	1.5	—	—	2.85	0.2	55.8	0.08 max.	0.05 B
<i>Nickel Base</i>											
Astroloy	15.0	56.5	15.0	5.25	—	—	3.5	4.4	<0.3	0.06	0.03 B, 0.06 Zr
Custom Age 625 PLUS	21.0	61.0	—	8.0	—	3.4	1.3	0.2	5.0	0.01	—

(continued)

Table 3 (Continued)

Alloy	Composition, wt.%										
	Cr	Ni	Co	Mo	W	Nb	Ti	Al	Fe	C	Other
Haynes 242	8.0	62.5	2.5 max.	25.0	—	—	—	0.5 max.	2.0 max.	0.10 max.	0.006 max. B
Haynes 263	20.0	52.0	—	6.0	—	—	2.4	0.6	0.7	0.06	0.6 Mn, 0.4 Si, 0.2 Cu
Haynes R-41	19.0	52.0	11.0	10.0	—	—	3.1	1.5	5.0	0.09	0.5 Si, 0.1 Mn, 0.006 B
Inconel 100	10.0	60.0	15.0	3.0	—	—	4.7	5.5	<0.6	0.15	1.0 V, 0.06 Zr, 0.015 B
IN-100	10	60	15	3	—	—	4.7	5.5	<0.6	0.15	0.06 Zr, 1.0 V
Inconel 102	15.0	67.0	—	2.9	3.0	2.9	0.5	0.5	7.0	0.06	0.005 B, 0.02 Mg, 0.03 Zr
Incoloy 901	12.5	42.5	—	6.0	—	—	2.7	—	36.2	0.10 max.	—
Inconel 702	15.5	79.5	—	—	—	—	0.6	3.2	1.0	0.05	0.5 Mn, 0.2 Cu, 0.4 Si
Inconel 706	16.0	41.5	—	—	—	—	1.75	0.2	37.5	0.03	2.9 (Nb + Ta), 0.15 max. Cu
Inconel 718	19.0	52.5	—	3.0	—	5.1	0.9	0.5	18.5	0.08 max.	0.15 max. Cu
Inconel 721	16.0	71.0	—	—	—	—	3.0	—	6.5	0.4	2.2 Mn, 0.1 Cu
Inconel 722	15.5	75.0	—	—	—	—	2.4	0.7	7.0	0.04	0.5 Mn, 0.2 Cu, 0.4 Si
Inconel 725	21.0	57.0	—	8.0	—	3.5	1.5	0.35 max.	9.0	0.03 max.	—
Inconel 751	15.5	72.5	—	—	—	1.0	2.3	1.2	7.0	0.05	0.25 max. Cu
Inconel X-750	15.5	73.0	—	—	—	1.0	2.5	0.7	7.0	0.04	0.25 max. Cu
M-252	19.0	56.5	10.0	10.0	—	—	2.6	1.0	<0.75	0.15	0.005 B
MERL-76	12.4	54.4	18.6	3.3	—	1.4	4.3	5.1	—	0.02	0.35 Hf, 0.06 Zr
Nimonic 80A	19.5	73.0	1.0	—	—	—	2.25	1.4	1.5	0.05	0.10 max. Cu
Nimonic 90	19.5	55.5	18.0	—	—	—	2.4	1.4	1.5	0.06	—
Nimonic 95	19.5	53.5	18.0	—	—	—	2.9	2.0	5.0 max.	0.15 max.	+B, +Zr
Nimonic 100	11.0	56.0	20.0	5.0	—	—	1.5	5.0	2.0 max.	0.30 max.	+B, +Zr
Nimonic 105	15.0	54.0	20.0	5.0	—	—	1.2	4.7	—	0.08	0.005 B
Nimonic 115	15.0	55.0	15.0	4.0	—	—	4.0	5.0	1.0	0.20	0.04 Zr
C-263	20.0	51.0	20.0	5.9	—	—	2.1	0.45	0.7 max.	0.06	—
C-1023	15.5	bal	10	8.5	—	—	3.6	4.2	—	0.16	0.006 B
GTD 222	22.5	bal	19	—	2	0.8	2.3	1.2	—	0.1	1 Ta, 0.012 Zr, 0.005 B
Pyromet 860	13.0	44.0	4.0	6.0	—	—	3.0	1.0	28.9	0.05	0.01 B
Pyromet 31	22.7	55.5	—	2.0	—	1.1	2.5	1.5	14.5	0.04	0.005 B
Refractaloy 26	18.0	38.0	20.0	3.2	—	—	2.6	0.2	16.0	0.03	0.015 B
René 41	19.0	55.0	11.0	10.0	—	—	3.1	1.5	<0.3	0.09	0.01 B
René 88	16	56.4	13.0	4	4	0.7	3.7	2.1	—	0.03	0.03 Zr
René 95	14.0	61.0	8.0	3.5	3.5	3.5	2.5	3.5	<0.3	0.16	0.01 B, 0.05 Zr
René 100	9.5	61.0	15.0	3.0	—	—	4.2	5.5	1.0 max.	0.16	0.015 B, 0.06 Zr, 1.0 V
René 220	18	bal	12	3	—	5	1	0.5	—	0.02	0.01 B
Udimet 500	19.0	48.0	19.0	4.0	—	—	3.0	3.0	4.0 max.	0.08	0.005 B
Udimet 520	19.0	57.0	12.0	6.0	1.0	—	3.0	2.0	—	0.08	0.005 B
Udimet 630	17.0	50.0	—	3.0	3.0	6.5	1.0	0.7	18.0	0.04	0.004 B
Udimet 700	15.0	53.0	18.5	5.0	—	—	3.4	4.3	<1.0	0.07	0.03 B
Udimet 710	18.0	55.0	14.8	3.0	1.5	—	5.0	2.5	—	0.07	0.01 B
Udimet 720	18	55	14.8	3	1.25	—	5	2.5	—	0.035	0.03 Zr
Udimet 720LI	16	57	15.0	3	1.25	—	5	2.5	—	0.025	0.03 Zr
Unitemp AF2-1DA	12.0	59.0	10.0	3.0	6.0	—	3.0	4.6	<0.5	0.35	1.5 Ta, 0.015 B, 0.1 Zr
Waspaloy	19.5	57.0	13.5	4.3	—	—	3.0	1.4	2.0 max.	0.07	0.006 B, 0.09 Zr
Waspaloy	19.5	57.0	13.5	4.3	—	—	3.0	1.4	2.0 max.	0.07	0.006 B, 0.09 Zr

Source: Compositions of Superalloys, Online update of ASM Handbook Supplement, *Superalloys*. Approved by the ASM Handbook Committee for addition to the ASM Handbook Supplements, 2011.

**Table 4** Nominal Compositions of Cast Nickel-Based Superalloys

Alloy <sup>a</sup>	Co	Cr	Mo	W	Ta	Re	Ru	Nb	Al	Ti	Hf	C	Zr	B	Other
AM1	8.0	7.0	2.0	5.0	8.0	...	...	1.0	5.0	1.8	...	...	...	...	
AM3	5.5	8.0	2.25	5.0	3.5	...	...	...	6.0	2.0	...	...	...	...	
B-1900	10.0	8.0	6.0	...	4.3	...	...	...	6.0	1.0	...	0.10	0.08	0.015	...
B-1900+Hf	10.0	8.0	6.0	...	4.3	...	...	...	6.00	1	1.00	0.1	...	...	...
B-1910	10.0	10.0	3.0	...	7.0	...	...	...	6.0	1.0	...	0.10	0.10	0.015	...
C 1023	10.0	15.5	8.0	...	...	...	...	...	4.2	3.6	...	0.15	...	0.006	...
C 130	...	21.5	10.0	...	...	...	...	...	0.8	2.6	...	0.04	...	...	...
C 242	10.0	20.0	10.3	...	...	...	...	...	0.1	0.2	...	0.30	...	...	...
C 263	20.0	20.0	5.9	...	...	...	...	...	0.45	2.15	...	0.06	0.02	0.001	...
CM 186LC	9.3	6.0	0.5	8.4	3.4	3.0	...	...	5.70	...	1.40	0.070	0.005	0.015	...
CM 247LC	9.3	8.0	0.5	9.5	3.2	...	...	...	5.60	0.7	1.40	0.070	0.010	0.015	...
CMSX 486	9.3	4.8	0.7	8.6	4.5	3.0	...	...	5.70	0.7	1.20	...	0.005	0.015	...
CMSX-10	3	2	0.4	5	8	6	...	...	5.70	0.2	0.03	...	...	...	...
CMSX-2	4.6	8.0	0.6	8.0	6.0	...	...	...	5.6	1.0	...	...	...	...	...
CMSX-3	4.6	8.0	0.6	8.0	6.0	...	...	...	5.6	1.0	0.10	...	...	...	...
CMSX-4	9.6	6.4	0.6	6.4	6.5	...	...	...	5.6	1.0	0.10	...	...	...	3.0 Re
CMSX-4	9.6	6.6	0.6	6.4	6.5	3.0	...	...	5.6	1.0	0.10	60 ppm max	75 ppm max	25 ppm max	...
CMSX-4 (high carbon)	9.3–10.0	6.4–6.8	0.5–0.7	6.2–6.6	6.3–6.7	2.8–3.2	...	...	5.45–5.75	0.8–1.2	0.07–0.12	0.04–0.06	...	...	...
CMSX-6	5.0	9.9	3.0	...	2.0	...	...	...	4.8	4.7	0.05	...	...	...	...
CMSX-10	3.0	2.0	0.4	5.0	8.0	6.0	...	...	5.7	0.2	0.03	...	...	...	...
EPM-102	16.5	2.0	2.0	6.0	8.3	6.0	3.0	...	5.55	...	0.15	0.030	...	...	...
GMR-235	...	15.0	4.8	...	...	...	...	...	3.5	2.5	...	0.15	...	0.05	4.5 Fe
GTD 111	9.5	14.0	1.5	3.8	2.8	...	...	...	3.00	4.9	...	0.100	0.030	0.012	...
GTD 222	19.0	22.5	...	2.0	1.0	...	...	...	1.20	2.3	...	0.100	...	0.008	...
GTD 444(N4 mod)	7.5	9.8	1.5	6.0	4.8	...	...	0.5	4.20	3.5	0.15	0.080	...	0.009	...
Hastelloy S	...	16.0	15.0	...	...	...	...	...	0.40	...	...	0.01	...	0.009	3.0 Fe, 0.02 La, 0.65 Si, 0.55 Mn
Hastelloy X	1.5	...	9.0	0.6	...	...	...	...	...	...	...	0.08	...	...	18.5 Fe, 0.5 Mn, 0.3 Si
IN 100	15.0	10.0	3.0	...	...	...	...	...	5.50	4.7	...	0.180	0.060	0.014	...
IN-625	...	21.5	8.5	...	...	...	...	4.0	0.0	0.0	...	0.06	...	...	2.5 Fe
IN-713C	...	12.5	4.2	...	...	...	...	2.0	6.1	0.8	...	0.12	0.10	0.012	...
IN-713LC	...	12.0	4.5	...	...	...	...	2.0	5.9	0.6	...	0.05	0.10	0.01	...
IN-713 Hf (MM 004)	...	12.0	4.5	...	...	...	...	2.0	5.9	0.6	1.3	0.05	0.10	0.01	...
IN-718	...	18.5	3.0	...	...	...	...	5.1	0.5	0.9	...	0.04	...	...	18.5 Fe
IN-731	10.0	9.5	2.5	...	...	...	...	...	5.5	4.6	...	0.18	0.06	0.015	1.0 V
IN 738	8.5	16.0	1.7	2.6	1.7	...	...	0.9	3.40	3.4	...	0.100	0.100	0.010	...
IN 792	9.0	12.5	1.9	4.1	4.1	...	...	...	3.40	3.8	1.00	0.080	0.020	0.015	...
IN 792 DS +Hf	9.0	12.5	1.9	4.1	4.1	...	...	...	3.40	3.8	1.00	0.80	0.020	0.015	...
IN 939	19.0	22.4	...	2.0	1.4	...	...	1.0	1.90	3.7	...	0.150	1.100	0.009	...
IN-939	19.0	22.4	...	2.0	1.4	...	...	1.0	1.9	3.7	...	0.15	0.100	0.009	...
M-22	...	5.7	2.0	11.0	3.0	...	...	...	6.3	...	...	0.13	0.60	...	...
M-252	10	20	10	...	...	...	...	...	1	2.6	...	0.15	...	0.005	...
Mar-M002	10.0	8.0	...	10.0	2.6	...	...	...	...	1.5	1.50	0.150	0.030	0.015	...
MAR-M 200	10.0	9.0	...	12.5	...	...	...	1.8	5.0	2.0	...	0.15	0.05	0.015	...
Mar-M200Hf	9.0	8.0	...	12.0	...	...	...	1.0	5.00	1.9	2.00	0.130	0.030	0.015	...
MAR-M 246	10.0	9.0	2.5	10.0	1.5	...	...	...	5.5	1.5	...	0.15	0.05	0.015	...
MAR-M 246 Hf (MM 006)	10.0	9.0	2.5	10.0	1.5	...	...	...	5.5	1.5	1.4	0.15	0.05	0.015	...
Mar-M247	10.0	8.0	0.6	10.0	3.0	...	...	...	5.50	1.0	1.50	0.150	0.030	0.015	...
MAR-M241	9.5	15.8	2.0	3.8	...	...	...	...	4.3	1.8	...	0.14	0.05	0.015	...
MAR-M 432	20.0	15.5	...	3.0	2.0	...	...	2.0	2.8	4.3	...	0.15	0.05	0.015	...

(continued)



Table 4 (Continued)

Alloy <sup>a</sup>	Co	Cr	Mo	W	Ta	Re	Ru	Nb	Al	Ti	Hf	C	Zr	B	Other
MC2	5.0	8.0	2.0	8.0	6.0	...	...	...	5.0	1.5	0.1	...	...	...	...
MC-NG	...	4.0	1.0	5.0	5.0	4.0	...	...	6.0	0.5	0.1	...	...	...	...
MC-102	...	20.0	6.0	2.5	0.6	...	...	6.0	...	...	...	0.04	...	...	0.25 Si, 0.30 Mn
MK-4	9.4-9.6	6.4-6.6	0.6	6.4-6.6	7.2-7.5	3.0-3.2	...	...	5.60	0.6-0.9	0.15-0.2	0.02-0.03	...	50-60 ppm	...
MX-4	16.5	2	2	6	8.25	5.95	3	...	5.55	...	0.15	0.03	...	...	...
N 5	7.5	7	1.5	5	6.5	3	...	...	6.20	...	0.15	0.05	...	40 ppm	0.01 Y
Nasair 100	...	9.0	1.0	10.5	3.3	...	...	...	5.75	1.2	...	...	...	...	...
Nimocast 100	20.0	11.0	5.0	...	...	...	...	...	5.0	1.5	...	0.20	0.03	0.015	...
Nimocast 242	10.0	20.5	10.5	...	...	...	...	...	0.2	0.3	...	0.34	...	...	1.0 Fe, 0.3 Mn, 0.3 Si
Nimocast 263	20.0	20.0	5.8	...	...	...	...	...	0.5	2.0	...	0.06	0.04	0.008	0.5 Fe, 0.5 Mn
Nimocast 75	...	20.0	...	...	...	...	...	...	...	0.5	...	0.12	...	...	...
Nimocast 80	...	19.5	...	...	...	...	...	...	1.4	2.3	...	0.05	...	...	1.5 Fe
Nimocast 90	18.0	19.5	...	...	...	...	...	...	1.4	2.4	...	0.06	...	...	1.5 Fe
Nimocast 95	18.0	19.5	...	...	...	...	...	...	2.0	2.9	...	0.07	0.02	0.015	...
NX 188	...	...	18.0	...	...	...	...	...	8.0	...	...	0.04	...	...	...
PWA 1422	10.0	9.0	...	12.0	...	...	...	1.0	5.00	2.0	1.50	0.140	0.100	0.015	...
PWA 1426	10.0	6.5	1.7	6.5	4.0	3.0	...	...	6.00	...	1.50	0.100	0.100	0.015	...
PWA 1432	9.0	12.2	1.9	3.8	5.0	...	...	...	3.60	4.2	...	0.11	0.002	0.013	...
PWA 1437	9.0	12.2	1.9	3.8	5.0	...	...	...	3.60	4.2	...	0.11	0.02 max	0.013	...
PWA 1480	5.0	10.0	...	4.0	12.0	...	...	...	5.00	1.5	...	<.006	<0.0075	<0.0075	...
PWA 1483	9.0	12.2	1.9	3.8	5.0	...	...	...	3.60	4.2	...	0.07	-	-	...
PWA 1487	10.0	5.0	1.9	5.9	8.7	3.0	...	...	5.65	...	0.10	...	...	...	...
PWA 1497	2.0	2.0	6.0	8.3	6.0	3.0	...	5.55	...	0.15	0.030	...	...	...	...
Rene 100	15.0	9.5	3.0	...	...	...	...	...	5.5	4.2	...	0.15	0.06	0.015	1.0 V
Rene 125	10.0	9.0	2.0	7.0	3.8	...	...	...	1.40	2.5	0.05	0.110	0.050	0.017	...
Rene 125 Hf (MM 005)	10.0	9.0	2.0	7.0	3.8	...	...	...	4.8	2.6	1.6	0.10	0.05	0.015	...
Rene 142	12.0	6.8	1.5	4.9	6.35	2.8	...	...	6.15	...	1.56	0.12	...	0.015	...
Rene 200	12.0	19.0	3.2	...	3.1	...	...	...	5.1	0.5	1.0	...	0.03	...	...
Rene 220	10.5	19.0	9.5	...	3.0	...	...	...	5.0	0.5	1.0	...	0.02	...	0.010
Rene 41	10.5	19.0	9.5	...	...	...	...	...	1.7	3.2	...	0.08	0.01	0.005	...
Rene 77 (U700)	17.0	15.0	5.3	...	...	...	...	...	4.25	3.4	...	0.070	...	0.020	...
Rene 80	9.5	14.0	4.0	4.0	...	...	...	...	3.00	5.0	...	0.170	0.030	0.015	...
Rene 80 Hf	9.0	14.0	4.0	4.0	...	...	...	...	3.00	4.7	0.80	0.160	0.010	0.015	...
Rene N4	8.0	9.0	2.0	6.0	4.0	...	...	0.5	3.7	4.2	...	...	...	...	...
Rene N4+	7.0	10.0	2.0	6.0	5.0	...	...	...	4.20	3.5	...	0.060	...	0.004	...
Rene N5	8	7	2	5	7	...	...	...	6.2	...	...	...	...	...	...
Rene N6	12.5	4.2	1.4	6.0	7.2	5.4	...	...	5.75	...	0.15	...	...	...	...
Rene 2000	15	10	3	...	...	...	...	...	5.5	4.0	...	...	...	...	...
SEL	26.0	15.0	4.5	...	...	...	...	...	4.4	2.4	...	0.08	...	0.015	...
SEL-15	14.5	11.0	6.5	1.5	...	...	...	0.5	5.4	2.5	...	0.07	...	0.015	...
SRR 99	5	8	...	10	3	...	...	...	5.5	2.2	...	...	...	...	...
TMS-138	5.9	2.9	2.9	5.9	5.6	4.9	2.0	...	5.90	...	0.10	...	...	...	...
TMS-162	5.8	2.9	3.9	5.8	5.6	4.9	6.0	...	5.80	...	0.09	...	...	...	...
TMS-173	5.6	3.0	2.8	5.6	5.6	6.9	5.0	...	5.60	...	0.10	...	...	...	...
TMS-196	5.6	4.6	2.4	5.0	5.6	6.4	5.0	...	5.60	...	0.10	...	...	...	...
TMS-75	12.0	3.0	2.0	6.0	6.0	5.0	...	...	6.00	...	0.10	...	...	...	...
Udimet 500	16.5	18.5	3.5	...	...	...	...	...	3.0	3.0	...	0.08	...	0.006	...
Udimet 700	14.5	14.3	4.3	...	...	...	...	...	4.25	3.5	...	0.13	0.02	0.015	...
Udimet 710	15.0	18.0	3.0	1.5	...	...	...	...	2.5	5.0	...	0.02	0.03	0.070	0.5 V
UDM 56	5.0	16.0	1.5	6.0	...	...	...	...	2.5	5.0	...	0.06	0.03	0.070	0.5 V
Waspaloy	12.3	19.0	3.8	...	...	...	...	...	1.2	3.0	...	0.06	0.01	0.005	0.45 Mn
Wax-20	...	...	...	20	...	...	...	...	6.5	...	...	0.20	1.5	...	...
X-750	...	15	...	...	...	...	...	0.9	0.7	2.5	...	0.04	...	...	7Fe, 0.25 Cu

**Table 4** (Continued)

**Nominal compositions of cast cobalt-base superalloys**

Alloy designation	Nominal composition %												
	C	Ni	Cr	Co	Mo	Fe	Al	B	Ti	Ta	W	Zr	Other
AiResist 13	0.45	...	21	62	...	...	3.4	...	...	2	11	...	0.1 Y
AiResist 213	0.20	0.5	20	64	...	0.5	3.5	...	...	6.5	4.5	0.1	0.1 Y
AiResist 215	0.35	0.5	19	63	...	0.5	4.3	...	...	7.5	4.5	0.1	0.1 Y
FSX-414	0.25	10	29	52.5	...	1	...	0.010	...	...	7.5	...	...
Haynes 21	0.25	3	27	64	...	1	...	...	...	...	...	...	5 Mo
Haynes 25: L-605	0.1	10	20	54	...	1	...	...	...	...	15	...	...
J-1650	0.20	27	19	36	...	...	...	0.02	3.8	2	12	...	...
MAR-M 302	0.85	...	21.5	58	...	0.5	...	0.005	...	9	10	0.2	...
MAR-M 322	1.0	...	21.5	60.5	...	0.5	...	...	0.75	4.5	9	2	...
MAR-M 509	0.6	10	23.5	54.5	...	...	...	...	0.2	3.5	7	0.5	...
MAR-M 918	0.05	20	20	52	...	...	...	...	...	7.5	...	0.5	...
NASA Co-W-Re	0.40	...	3	67.5	...	...	...	...	1	...	25	1	2 Re
S-816	0.4	20	20	42	...	4	...	...	...	...	4	...	4 Mo, 4 Nb, 1.2 Mn, 0.4 Si
V-36	0.27	20	25	42	...	3	...	...	...	...	2	...	4 Mo, 2 Nb, 1 Mn, 0.4 Si
W1-52	0.45	...	21	63.5	...	2	...	...	...	...	11	...	2 Nb + Ta
X-40 (Stellite alloy 31)	0.50	10	22	57.5	...	1.5	...	...	...	...	7.5	...	0.5 Mn, 0.5 Si

**Single crystal nickel-base superalloys**

Alloy generation	Alloy <sup>a</sup>	Nominal composition %													
		Co	Cr	Mo	W	Ta	Re	Ru	Al	Ti	Hf	C	Zr	B	Y
1	PWA 1483	9.0	12.2	1.9	3.8	5.0	...	...	3.60	4.2	...	0.07	...	...	...
1	PWA 1480	5.0	10.0	...	4.0	12.0	...	...	5.00	1.5	...	<0.06	<0.0075	<0.0075	...
1	Rene N4+	7.0	10.0	2.0	6.0	5.0	...	...	4.20	3.5	...	0.060	...	0.004	...
2	CMSX-4	9.6	6.6	0.6	6.4	6.5	3.0	...	5.6	1.0	0.10	60 ppm max	75 ppm max	25 ppm max	...
2	CMSX 486	9.3	4.8	0.7	8.6	4.5	3.0	...	5.70	0.7	1.20	0.070	0.005	0.015	...
2	PWA 1484	10.0	5.0	1.9	5.9	8.7	3.0	...	5.65	...	0.10	...	...	...	...
2	PWA 1487	10.0	5.0	1.9	5.9	8.4	3.0	...	5.60	...	0.25	...	...	...	...
2	N5	7.5	7	1.5	5	6.5	3	...	6.20	...	0.15	0.05	...	40 ppm	0.01
2	MK-4	9.4–9.6	6.4–6.6	0.6	6.4–6.6	7.2–7.5	3.0–3.2	...	5.60	0.6–0.9	0.15–0.2	0.02–0.03	...	50–60 ppm	...
2	High Carbon CMSX-4	9.3–10.0	6.4–6.8	0.5–0.7	6.2–6.6	6.3–6.7	2.8–3.2	...	5.45–5.75	0.8–1.2	0.07–0.12	0.04–0.06	...	...	...
2	CMSX-10	3	2	0.4	5	8	6	...	5.70	0.2	0.03	...	...	...	...
3	TMS-75	12.0	3.0	2.0	6.0	6.0	5.0	...	6.00	...	0.10	...	...	...	...
3	Rene N6	12.5	4.2	1.4	6.0	7.2	5.4	...	5.75	...	0.15	...	...	...	...
3	MX-4	16.5	2	2	6	8.25	5.95	3	5.55	...	0.15	0.03	...	...	...
4	PWA 1497	16.5	2.0	2.0	6.0	8.3	6.0	3.0	5.55	...	0.15	0.030	...	...	...
4	TMS-138	5.9	2.9	2.9	5.9	5.6	4.9	2.0	5.90	...	0.10	...	...	...	...
4	EPM-102	16.5	2.0	2.0	6.0	8.3	6.0	3.0	5.55	...	0.15	0.030	...	...	...
5	TMS-162	5.8	2.9	2.9	5.8	5.6	4.9	6.0	5.80	...	0.09	...	...	...	...
5	TMS-173	5.6	3.0	3.0	5.6	5.6	6.9	5.0	5.60	...	0.10	...	...	...	...
5	TMS-196	5.6	4.6	4.6	5.0	5.6	6.4	5.0	5.60	...	0.10	...	...	...	...

**Column or Grain nickel-base superalloys**

Alloy <sup>a</sup>	Ni	Co	Cr	Mo	W	Ta	Re	Ru	Nb	Al	Ti	Hf	C	Zr	B
MarM200 Hf	bal	9.0	8.0	0.0	12.0	0.0	0.0	0.0	1.0	5.0	1.9	2.00	0.130	0.030	0.015
PWA 1422	bal	10.0	9.0	0.0	12.0	0.0	0.0	0.0	1.0	5.0	2.0	1.50	0.14	0.1	0.015
PWA 1426	bal	10.0	6.5	1.7	6.5	4.0	3.0	0.0	0.0	6.0	0.0	1.50	0.100	0.100	0.015
IN 792 DS + Hf	bal	9.0	12.5	1.9	4.1	4.1	0.0	0.0	0.0	3.4	3.8	1.00	0.080	0.020	0.015
Rene 80 H	bal	9.0	14.0	4.0	4.0	...	0.0	0.0	0.0	3.0	4.7	0.80	0.160	0.010	0.015
Rene 125	bal	10.0	9.0	2.0	7.0	3.8	0.0	0.0	0.0	1.4	2.5	0.05	0.110	0.050	0.017
GTD 111	bal	9.5	14.0	4.0	4.0	...	0.0	0.0	0.0	3.0	5.0	0.00	0.170	0.030	0.015
CM186L C	bal	9.3	6.0	0.5	8.4	3.4	3.0	0.0	0.0	5.7	0.0	1.40	0.070	0.005	0.015
CM247L C	bal	9.3	8.0	0.5	9.5	3.2	0.0	0.0	0.0	5.6	0.7	1.40	0.070	0.010	0.015
Rene 142	bal	12.0	6.8	1.5	4.9	6.4	2.8	0.0	0.0	6.2	0.0	1.50	0.120	0.020	0.015
PWA 1437 (1483 mod)	bal	9.0	12.2	1.9	3.8	5.0	0.0	0.0	0.0	3.6	4.2	0.00	0.11	0.02 max	0.013
GTD 444 (N4 mod)	bal	7.5	9.8	1.5	6.0	4.8	0.0	0.0	0.0	4.2	3.5	0.080	0.080	...	0.009

<sup>a</sup>For each alloy composition, Ni is the balance.

Source: Compositions of Superalloys, Online update of ASM Handbook Supplement, *Superalloys*. Approved by the ASM Handbook Committee for addition to the ASM Handbook Supplements, 2011.

**Table 5** Allowable Trace Element Concentrations for Selected Nickel-Based Superalloys

IN 718/MAR-M-247, typical alloy concentration						
Element	Commercial Grade		Aerospace Quality	Premium Quality		
	Tooling Applications	Other				
N, ppm	20+	60–100	60	5–15	10–25	1
O, ppm	5+	5–10	<5	<5	2	1
Si, wt.%	0.05+	0.10–0.30	0.05–0.10	0.02–0.04	<0.02	0.009
Mn, wt.%	0.01+	0.05+	<0.002	<0.002	<0.002	<0.002
S, ppm	15+	10–40	10–30	5–15	10	<5
Zr, wt.%	—	<0.01	0.001	—	<10 ppm	—
Fe, wt.%	0.10+	—	—	0.05–0.10	—	<0.03
Cu, wt.%	0.002+	0.08	0.01–0.05	0.002–0.005	<0.001	<0.001
P, wt.%	0.002	0.005	0.005	0.005	0.001–0.002	<0.001
Pb, ppm	<1	1–5	<1	<1	<1	<0.5
Ag, ppm	<0.5	<1	<1	<0.5	<0.5	<0.5
Bi, ppm	<0.3	<0.5	<0.5	<0.3	<0.2	<0.2
Se, ppm	<0.5	<1	<1	<0.5	<0.5	<0.5
Te, ppm	<0.3	<0.5	<0.5	<0.2	<0.2	<0.2
Tl, ppm	<0.3	<0.5	<0.5	<0.2	<0.2	<0.2
Sn, ppm	<5	15–40	<10	<5	<10	<5
Sb, ppm	<2	2+	<2	<1	<2	<1
As, ppm	<2	5	<2	<1	<2	<1
Zn, ppm	<2	2+	<2	<1	<2	<1

Source: *Superalloys, Alloying, and Performance*, ASM International, Materials Park, OH, 2010.

## 2.2 Mechanical Behavior

In the case of short-time tensile properties (yield strength, ultimate strength), the mechanical behavior of metals at higher temperatures is similar to that at room temperature, but with metals becoming weaker as the temperature increases. However, when steady loads below the normal yield or ultimate strength determined in short-time tests are applied for prolonged times at higher temperatures, the situation is different. Figure 1 illustrates the way in which most materials respond to steady extended-time loads at high temperatures.

Owing to the higher temperature, a time-dependent extension (creep) is noticed under load. If the alloy is exposed for a long time, the alloy eventually fractures (ruptures). The degradation process is called creep or, in the event of failure, creep rupture (sometimes stress rupture) and alloys are selected on their ability to resist creep and creep rupture failure. Data for superalloys frequently are provided as the stress which can be sustained for a fixed time (e.g., 100 h rupture) vs. the temperature. Figure 2 shows such a plot with ranges of expected performance for various superalloy families. One of the contributory aspects of elevated-temperature failure is that metals tend to come apart at the grain boundaries when tested for long times above about 0.5 of their absolute melting temperature. Thus, fine-grained alloys which are usually favored for lower temperature applications may not be the best materials for creep rupture limited applications at high temperatures as they have more grain boundaries than coarse-grained materials. Elimination or reorientation/alignment of grain boundaries is sometimes a key factor in maximizing the higher temperature life of an alloy.

**Table 6** Effect of Temperature on Short-Time Mechanical Properties of Selected Wrought Superalloys

Alloy	Form	Ultimate Tensile Strength at						Yield Strength at 0.2% offset at						Tensile Elongation (%) at		
		21°C (70°F)		540°C (1000°F)		760°C (1400°F)		21°C (70°F)		540°C (1000°F)		760°C (1400°F)		21°C (70°F)	540°C (1000°F)	760°C (1400°F)
		MPa	ksi	MPa	ksi	MPa	ksi	MPa	ksi	MPa	ksi	MPa	ksi	ksi	MPa	ksi
<i>Nickel Base</i>																
Astroloy	Bar	1415	205	1240	180	1160	168	1050	152	965	140	910	132	16	16	21
Cabot 214	—	915	133	715	104	560	84	560	81	510	74	495	72	38	19	9
D-979	Bar	1410	204	1295	188	720	104	1005	146	925	134	655	95	15	15	17
Hastelloy C-22	Sheet	800	116	625	91	525	76	405	59	275	40	240	35	57	61	63
Hastelloy G-30	Sheet	690	100	490	71	—	—	315	46	170	25	—	—	64	75	—
Hastelloy S	Bar	845	130	775	112	575	84	455	65	340	49	310	45	49	50	70
Hastelloy X	Sheet	785	114	650	94	435	63	360	52	290	42	260	38	43	45	37
Haynes 230	<sup>a</sup>	870	126	720	105	575	84	390	57	275	40	285	41	48	56	46
Inconel 587	Bar	1180	171	1035	150	830	120	705	102	620	90	605	88	28	22	20
Inconel 597	Bar	1220	177	1140	165	930	135	760	110	720	104	665	96	15	15	16
Inconel 600	Bar	660	96	560	81	260	38	285	41	220	32	180	26	45	41	70
Inconel 601	Sheet	740	107	725	105	290	42	455	66	350	51	220	32	40	34	78
Inconel 617	Bar	740	107	580	84	440	64	295	43	200	29	180	26	70	68	84
Inconel 617	Sheet	770	112	590	86	470	68	345	50	230	33	230	33	55	62	59
Inconel 625	Bar	965	140	910	132	550	80	490	71	415	60	415	60	50	50	45
Inconel 706	Bar	1310	190	1145	166	725	105	1005	146	910	132	660	96	20	19	32
Inconel 718	Bar	1435	208	1275	185	950	138	1185	172	1065	154	740	107	21	18	25
Inconel 718 Direct Age	Bar	1530	222	1350	196	—	—	1365	198	1180	171	—	—	16	15	—
Inconel 718 Super	Bar	1350	196	1200	174	—	—	1105	160	1020	148	—	—	16	18	—
Inconel X750	Bar	1200	174	1050	152	—	—	815	118	725	105	—	—	27	26	—
M-252	Bar	1240	180	1230	178	945	137	840	122	765	111	720	104	16	15	10
Nimonic 75	Bar	745	108	675	98	310	45	285	41	200	29	160	23	40	40	67
Nimonic 80A	Bar	1000	145	875	127	600	87	620	90	530	77	505	73	39	37	17
Nimonic 90	Bar	1235	179	1075	156	655	95	810	117	725	105	540	78	33	28	12

(continued)

Table 6 (Continued)

Alloy	Form	Ultimate Tensile Strength at						Yield Strength at 0.2% offset at						Tensile Elongation (%) at		
		21°C (70°F)		540°C (1000°F)		760°C (1400°F)		21°C (70°F)		540°C (1000°F)		760°C (1400°F)		21°C (70°F)	540°C (1000°F)	760°C (1400°F)
		MPa	ksi	MPa	ksi	MPa	ksi	MPa	ksi	MPa	ksi	MPa	ksi	ksi	MPa	ksi
Nimonic 105	Bar	1180	171	1130	164	930	135	830	120	775	112	740	107	16	22	25
Nimonic 115	Bar	1240	180	1090	158	1085	157	865	125	795	115	800	116	27	18	24
Nimonic 263	Sheet	970	141	800	116	650	94	580	84	485	70	460	67	39	42	21
Nimonic 942	Bar	1405	204	1300	189	900	131	1060	154	970	141	860	125	37	26	42
Nimonic PE 11	Bar	1080	157	1000	145	760	110	720	105	690	100	560	81	30	30	18
Nimonic PE 16	Bar	885	128	740	107	510	74	530	77	485	70	370	54	37	26	42
Nimonic PK 33	Sheet	1180	171	1000	145	885	128	780	113	725	105	670	97	30	30	18
Pyromet 860	Bar	1295	188	1255	182	910	132	835	121	840	122	835	121	22	15	18
René 41	Bar	1420	206	1400	203	1105	160	1060	154	1020	147	940	136	14	14	11
René 95	Bar	1620	235	1550	224	1170	170	1310	190	1255	182	1100	160	15	12	15
Udimet 400	Bar	1310	190	1185	172	—	—	930	135	830	120	—	—	30	26	—
Udimet 500	Bar	1310	190	1240	180	1040	151	840	122	795	115	730	106	32	28	39
Udimet 520	Bar	1310	190	1240	180	725	105	860	125	825	130	725	105	21	20	15
Udimet 630	Bar	1520	220	1380	200	965	140	1310	190	1170	170	860	125	15	15	5
Udimet 700	Bar	1410	204	1275	185	1035	150	965	140	895	130	825	120	17	16	20
Udimet 710	Bar	1185	172	1150	167	1020	148	910	132	850	123	815	118	7	10	25
Udimet 720	Bar	1570	228	—	—	1455	211	1195	173	—	—	1050	152	13	—	9
Unitemp AF2-IDA6	Bar	1560	226	1480	215	1290	187	1015	147	1040	151	995	144	20	19	16
Waspaloy	Bar	1275	185	1170	170	650	94	795	115	725	105	675	98	25	23	28
<i>Iron Base</i>																
A-286	Bar	1005	146	905	131	440	64	725	105	605	88	430	62	25	19	19
Alloy 901	Bar	1205	175	1030	149	725	105	895	130	780	113	635	92	14	14	19
Discaloy	Bar	1000	145	865	125	485	70	730	106	650	94	430	62	19	16	—
Haynes 556	Sheet	815	118	645	93	470	69	410	60	240	35	220	32	48	54	49
Incoloy 800	Bar	595	86	510	74	235	34	250	36	180	26	150	22	44	38	83
Incoloy 801	Bar	785	114	660	96	325	47	385	56	310	45	290	42	30	28	55
Incoloy 802	Bar	690	100	600	87	400	58	290	42	195	28	200	29	44	39	15
Incoloy 807	Bar	655	95	470	68	350	51	380	55	255	37	225	32.5	48	40	34
Incoloy 825 <sup>b</sup>	—	690	100	~ 590	~ 86	~ 275	~ 40	310	45	~ 234	~ 34	180	~ 26	45	~ 44	~ 86



**Table 7** Effect of Temperature on Short-Time Mechanical Properties of Selected Cast Superalloys (Numbers in Parentheses Are Estimated)

Alloy	Ultimate Tensile Strength at						0.2% Yield Strength at						Tensile Elongation, % at		
	21°C (70°F)		538°C (1000°F)		1093°C (2000°F)		21°C (70°F)		538°C (1000°F)		1093°C (2000°F)				
<i>Nickel Base</i>															
IN-713 C	850	123	860	125	—	—	740	107	705	102	—	—	8	10	—
IN-713 LC	895	130	895	130	—	—	750	109	760	110	—	—	15	11	—
B-1900	970	141	1005	146	270	38	825	120	870	126	195	28	8	7	11
IN-625	710	103	510	74	—	—	350	51	235	34	—	—	48	50	—
IN-718	1090	158	—	—	—	—	915	133	—	—	—	—	11	—	—
IN-100	1018	147	1090	150	(380)	(55)	850	123	885	128	(240)	(35)	9	9	—
IN-162	1005	146	1020	148	—	—	815	118	795	115	—	—	7	6.5	—
IN-731	835	121	—	—	275	40	725	105	—	—	170	25	6.5	—	—
IN-738	1095	159	—	—	—	—	950	138	—	—	—	—	—	—	—
IN-792	1170	170	—	—	—	—	1060	154	—	—	—	—	4	—	—
M-22	730	106	780	113	—	—	685	99	730	106	—	—	5.5	4.5	—
MAR-M200	930	135	945	137	325	47	840	122	880	123	—	—	7	5	—
MAR-M246	965	140	1000	145	345	50	860	125	860	125	—	—	5	5	—
MAR-M247	965	140	1035	150	—	—	815	118	825	120	—	—	7	—	—
MAR-M421	1085	157	995	147	—	—	930	135	815	118	—	—	4.5	3	—
MAR-M432	1240	180	1105	160	—	—	1070	155	910	132	—	—	6	—	—
MC-102	675	98	655	95	—	—	605	88	540	78	—	—	5	9	—
Nimocast 75	500	72	—	—	—	—	179	26	—	—	—	—	39	—	—
Nimocast 80	730	106	—	—	—	—	520	75	—	—	—	—	15	—	—
Nimocast 90	700	102	595	86	—	—	520	75	420	61	—	—	14	15	—
Nimocast 242	460	67	—	—	—	—	300	44	—	—	—	—	8	—	—
Nimocast 263	730	106	—	—	—	—	510	74	—	—	—	—	18	—	—
René 77	—	—	—	—	—	—	—	—	—	—	—	—	—	—	—
René 80	—	—	—	—	—	—	—	—	—	—	—	—	—	—	—
Udimet 500	930	135	895	130	—	—	815	118	725	105	—	—	13	13	—
Udimet 710	1075	156	—	—	240	35	895	130	—	—	170	25	8	—	—
CMSX-2 <sup>a</sup>	1185	172	1295 <sup>b</sup>	188 <sup>b</sup>	—	—	1135	165	1245 <sup>b</sup>	181 <sup>b</sup>	—	—	10	17 <sup>b</sup>	—
GMR-235	710	103	—	—	—	—	640	93	—	—	—	—	3	—	18 <sup>b</sup>
IN-939	1050	152	915 <sup>b</sup>	133 <sup>b</sup>	325 <sup>c</sup>	47 <sup>c</sup>	800	116	635 <sup>b</sup>	92 <sup>b</sup>	205 <sup>c</sup>	30 <sup>c</sup>	5	7 <sup>b</sup>	25 <sup>b</sup>
MM 002 <sup>d</sup>	1035	150	1035 <sup>b</sup>	150 <sup>b</sup>	550 <sup>c</sup>	80 <sup>c</sup>	825	120	860 <sup>b</sup>	125 <sup>b</sup>	345 <sup>c</sup>	50 <sup>c</sup>	7	5 <sup>b</sup>	12 <sup>b</sup>
IN-713 Hf <sup>e</sup>	1000	145	895 <sup>b</sup>	130 <sup>b</sup>	380 <sup>c</sup>	55 <sup>c</sup>	760	110	620 <sup>b</sup>	90 <sup>b</sup>	240 <sup>c</sup>	35 <sup>c</sup>	11	6 <sup>b</sup>	20 <sup>b</sup>
Rene 125 Hf	1070	155	1070 <sup>b</sup>	155 <sup>b</sup>	550 <sup>c</sup>	80 <sup>c</sup>	825	120	860 <sup>b</sup>	125 <sup>b</sup>	345 <sup>c</sup>	50 <sup>c</sup>	5	5 <sup>b</sup>	12 <sup>b</sup>
MAR-M 246 Hf <sup>e</sup>	1105	160	1070 <sup>b</sup>	155 <sup>b</sup>	565 <sup>c</sup>	82 <sup>c</sup>	860	125	860 <sup>b</sup>	125 <sup>b</sup>	345 <sup>c</sup>	50 <sup>c</sup>	6	7 <sup>b</sup>	14 <sup>b</sup>
MAR-M 200 Hf <sup>h</sup>	1035	150	1035 <sup>b</sup>	150 <sup>b</sup>	540 <sup>c</sup>	78 <sup>c</sup>	825	120	860 <sup>b</sup>	125 <sup>b</sup>	345 <sup>c</sup>	50 <sup>c</sup>	5	5 <sup>b</sup>	10 <sup>b</sup>
PWA-1480 <sup>a</sup>	—	—	1130 <sup>b</sup>	164 <sup>b</sup>	685 <sup>c</sup>	99 <sup>c</sup>	895	130	905 <sup>b</sup>	131 <sup>b</sup>	495 <sup>c</sup>	72 <sup>c</sup>	4	8 <sup>b</sup>	—
SEL	1020	148	875 <sup>b</sup>	127 <sup>b</sup>	—	—	905	131	795 <sup>b</sup>	115 <sup>b</sup>	—	—	6	7 <sup>b</sup>	—
UDM 56	945	137	945 <sup>b</sup>	137 <sup>b</sup>	—	—	850	123	725 <sup>b</sup>	105 <sup>b</sup>	—	—	3	5 <sup>b</sup>	—
SEL-15	1060	154	1090 <sup>b</sup>	158 <sup>b</sup>	—	—	895	130	815 <sup>b</sup>	118 <sup>b</sup>	—	—	9	5 <sup>b</sup>	—
<i>Cobalt Base</i>															
AiResist 13 <sup>i</sup>	600	87	420 <sup>b</sup>	61 <sup>b</sup>	—	—	530	77	330 <sup>b</sup>	48 <sup>b</sup>	—	—	1.5	4.5 <sup>b</sup>	—
AiResist 215 <sup>i</sup>	690	100	570 <sup>j</sup>	83 <sup>j</sup>	—	—	485	70	315 <sup>i</sup>	46 <sup>i</sup>	—	—	4	12 <sup>i</sup>	—
FSX-414	—	—	—	—	—	—	—	—	—	—	—	—	—	—	—
Haynes 1002	770	112	560	81	115	17	470	68	345	50	95	14	6	8	28
MAR-M 302	930	135	795	115	150	22	690	100	505	73	150	22	2	—	21
MAR-M 322 <sup>i</sup>	830	120	595 <sup>b</sup>	86 <sup>b</sup>	—	—	630	91	345 <sup>b</sup>	50 <sup>b</sup>	—	—	4	6.5 <sup>b</sup>	—
MAR-M 509	785	114	570	83	—	—	570	83	400	58	—	—	4	6	—
WL-52	750	109	745	108	160	23	585	85	440	64	105	15	5	7	35
X-40	745	108	550	80	—	—	525	76	275	40	—	—	9	17	—

<sup>a</sup>Single crystal [001].

<sup>b</sup>At 760°C (1400°F).

<sup>c</sup>At 980°C (1800°F).

<sup>d</sup>RR-7080.

<sup>e</sup>MM 004.

<sup>f</sup>M 005.

<sup>g</sup>MM 006.

<sup>h</sup>MM 009.

<sup>i</sup>Data from *Metals Handbook*, Vol. 3, 9th ed., ASM International, Metals Park, OH, 1980.

<sup>j</sup>At 650°C (1200°F).

Source: Nickel Development Institute, Toronto, Canada except as noted

**Table 8** Effect of Temperature on 1000 h Stress Rupture Strengths of Selected Wrought Superalloys

Alloy	Form	Rupture Strength at							
		650°C (1200°F)		760°C (1400°F)		870°C (1600°F)		980°C (1800°F)	
		MPa	ksi	MPa	ksi	MPa	ksi	MPa	ksi
<i>Nickel Base</i>									
Astroloy	Bar	770	112	425	62	170	25	55	8
Cabot 214	—	—	—	—	—	30	4	15	2
D-979	Bar	515	75	250	36	70	10	—	—
Hastelloy S	Bar	—	—	90	13	25	4	—	—
Hastelloy X	Sheet	215	31	105	15	40	6	15	2
Haynes 230	—	—	—	125	18	55	8	15	2
Inconel 587	Bar	—	—	285	41	—	—	—	—
Inconel 597	Bar	—	—	340	49	—	—	—	—
Inconel 600	Bar	—	—	—	—	30	4	15	2
Inconel 601	Sheet	195	28	60	9	30	4	15	2
Inconel 617	Bar	360	52	165	24	60	9	30	4
Inconel 617	Sheet	—	—	160	23	60	9	30	4
Inconel 625	Bar	370	54	160	23	50	7	20	3
Inconel 706	Bar	580	84	—	—	—	—	—	—
Inconel 718	Bar	595	86	195	28	—	—	—	—
Inconel 718 Direct Age	Bar	405	59	—	—	—	—	—	—
Inconel 718 Super	Bar	600	87	—	—	—	—	—	—
Inconel X750	Bar	470	68	—	—	50	7	—	—
M-252	Bar	565	82	270	39	95	14	—	—
Nimonic 75	Bar	170	25	50	7	5	1	—	—
Nimonic 80A	Bar	420	61	160	23	—	—	—	—
Nimonic 90	Bar	455	66	205	30	60	9	—	—
Nimonic 105	Bar	—	—	330	48	130	19	30	4
Nimonic 115	Bar	—	—	420	61	185	27	70	10
Nimonic 942	Bar	520	75	270	39	—	—	—	—
Nimonic PE.11	Bar	335	49	145	21	—	—	—	—
Nimonic PE.16	Bar	345	50	150	22	—	—	—	—
Nimonic PK.33	Sheet	655	95	310	45	90	13	—	—
Pyromet 860	Bar	545	79	250	36	—	—	—	—
René 41	Bar	705	102	345	50	115	17	—	—
René 95	Bar	860	125	—	—	—	—	—	—
Udimet 400	Bar	600	87	305	44	110	16	—	—
Udimet 500	Bar	760	110	325	47	125	18	—	—
Udimet 520	Bar	585	85	345	50	150	22	—	—
Udimet 700	Bar	705	102	425	62	200	29	55	8
Udimet 710	Bar	870	126	460	67	200	29	70	10
Udimet 720	Bar	670	97	—	—	—	—	—	—
Unitemp AF2-IDA6	Bar	885	128	360	52	—	—	—	—
Waspaloy	Bar	615	89	290	42	110	16	—	—
<i>Iron Base</i>									
A286	Bar	315	46	105	15	—	—	—	—
Alloy 901	Sheet	525	76	205	30	—	—	—	—
Discaloy	Bar	275	40	60	9	—	—	—	—
Haynes 556	Sheet	275	40	125	18	55	8	20	3
Incoloy 800	Bar	165	24	66	9.5	30	4.4	13	1.9

(continued)



Table 8 (Continued)

Alloy	Form	Rupture Strength at							
		650°C (1200°F)		760°C (1400°F)		870°C (1600°F)		980°C (1800°F)	
		MPa	ksi	MPa	ksi	MPa	ksi	MPa	ksi
Incoloy 801	Bar	—	—	—	—	—	—	—	—
Incoloy 802	Bar	170	25	110	15	69	10	24	3.5
Incoloy 807	Bar	—	—	105	15	43	6.2	19	2.7
Incoloy 903	Bar	510	74	—	—	—	—	—	—
Incoloy 909	Bar	345	50	—	—	—	—	—	—
N-155	Bar	295	43	140	20	70	10	20	3
V-57	Bar	485	70	—	—	—	—	—	—
<i>Cobalt Base</i>									
Haynes 188	Sheet	—	—	165	24	70	10	30	4
L-605	Sheet	270	39	165	24	75	11	30	4
MAR-M918	Sheet	—	—	60	9	20	3	5	1
Haynes 150	—	—	—	40 <sup>a</sup>	5.8	—	—	—	—

<sup>a</sup>At 815°C (1500°F).

A factor in mechanical behavior not often recognized is that the static modulus (e.g., Young's modulus  $E$ ) is affected by increases in temperature. This should be obvious from the above discussion about creep. Dependent on rate of load application, moduli determined by measurements from a tensile test tend to gradually fall below moduli determined by dynamic means. Since moduli are used in design and may affect predictions of life and durability, every effort should be made to determine the dynamic, not just static, moduli of superalloys for high-temperature applications. Moduli of cast alloys also may be affected dramatically by the orientation of grains or by use of single crystals. A more accurate method of depicting moduli would be to use the appropriate single-crystal elastic constants (three needed), but these are rarely available.

Cyclically applied loads that cause failure (fatigue) at lower temperatures also cause failures in shorter times (lesser cycles) at high temperatures. For example, Fig. 3 shows schematically how the cyclic resistance is degraded at high temperatures when the locus of failure is plotted as stress vs. applied cycles ( $S-N$ ) of load. From the  $S-N$  curves shown, it should be clear that there is not necessarily an endurance limit for metals and alloys at high temperatures. Cyclic loads can be induced not only by mechanical loads in a structure but also by thermal changes. The combination of thermally induced and mechanically induced loads leads to failure in thermal-mechanical fatigue (TMF). TMF failures occur in a relatively low number of cycles. Thus TMF is a low-cycle-fatigue (LCF) process. LCF can be induced by high repeated mechanical or thermal loads while lower stress, repeated, mechanical loads lead to fatigue failure in a high number of cycles (HCF).

Dependent on application, LCF failures in structures can be either mechanically induced or TMF type. In airfoils in the hot section of gas turbines, TMF is a major concern. In highly mechanically loaded parts such as gas turbine disks, mechanically induced LCF is the major concern. HCF normally is not a problem with superalloys unless a design error occurs and a component is subjected to a high-frequency vibration that forces rapid accumulation of fatigue cycles. Although  $S-N$  plots are common, the designer should be aware that data for LCF and TMF behavior are frequently gathered as plastic strain (epsilon plastic,  $\epsilon_p$  or delta epsilon plastic,  $\Delta\epsilon_p$ ) vs. applied cycles. The final component application will determine the preferred method of depicting fatigue behavior.

**Table 9** Effect of Temperature on Stress Rupture Strengths of Selected Cast Superalloys

Alloy	Rupture Strength at											
	815°C (1500°F)				870°C (1600°F)				980°C (1800°F)			
	100 h		1000 h		100 h		1000 h		100 h		1000 h	
	MPa	ksi	MPa	ksi	MPa	ksi	MPa	ksi	MPa	ksi	MPa	ksi
<i>Nickel Base</i>												
IN-713 LC	425	62	325	47	295	43	240	35	140	20	105	15
IN-713 C	370	54	305	44	305	44	215	31	130	19	70	10
IN-738 C	470	68	345	50	330	38	235	34	130	19	90	13
IN-738 LC	430	62	315	46	295	43	215	31	140	20	90	13
IN-100	455	66	365	53	360	52	260	38	160	23	90	13
MAR-M 247 (MM 0011)	585	85	415	60	455	66	290	42	185	27	125	18
MAR-M 246	525	76	435	62	440	63	290	42	195	28	125	18
MAR-M 246 Hf (MM 006)	530	77	425	62	425	62	285	41	205	30	130	19
MAR-M 200	495	72	415	60	385	56	295	43	170	25	125	18
MAR-M 200 Hf (MM 009)	—	—	—	—	—	—	305	44	—	—	125	18
B-1900	510	74	380	55	385	56	250	36	180	26	110	16
René 77	—	—	—	—	310	45	215	31.5	130	19	62	9.0
René 80	—	—	—	—	350	51	240	35	160	23	105	15
IN-625	130	19	110	16	97	14	76	11	34	5	28	4
IN-162	505	73	370	54	340	49	255	37	165	24	110	16
IN-731	505	73	365	53	—	—	—	—	165	24	105	15
IN-792	515	75	380	55	365	53	260	38	165	24	105	15
M-22	515	75	385	56	395	57	285	41	200	29	130	19
MAR-M 421	450	65	305	44	310	46	215	31	125	18	83	12
MAR-M 432	435	63	330	48	295	40	215	31	140	20	97	14
MC-102	195	28	145	21	145	21	105	15	—	—	—	—
Nimocast 90	160	23	110	17	125	18	83	12	—	—	—	—
Nimocast 242	110	16	83	12	90	13	59	8.6	45	6.5	—	—
Udimet 500	330	48	240	35	230	33	165	24	90	13	—	—
Udimet 710	420	61	325	47	305	44	215	31	150	22	76	11
CMSX-2	—	—	—	—	—	—	345	50	—	—	170	25
GMR-235	—	—	—	—	—	—	180	26	—	—	75	11
IN-939	—	—	—	—	—	—	195	28	—	—	60	9
MM002	—	—	—	—	—	—	305	44	—	—	125	18
IN-713 Hf (MM 004)	—	—	—	—	—	—	205	30	—	—	90	13
Ren 125 Hf (MM 005)	—	—	—	—	—	—	305	44	—	—	115	17
SEL-15	—	—	—	—	—	—	295	43	—	—	75	11
UDM56	—	—	—	—	—	—	270	39	—	—	125	18
<i>Cobalt Base</i>												
HS-21	150	22	95	14	115	17	90	13	60	9	50	7
X-40 (HS-31)	180	26	140	20	130	19	105	15	75	11	55	8
MAR-M 509	270	39	225	33	200	29	140	20	115	17	90	13
PSX-414	150	22	115	17	110	16	85	12	55	8	35	5
WI-52	—	—	195	28	175	25	150	22	90	13	70	10

**Table 10** Physical Properties of Selected Wrought Superalloys

Designation	Form	Density, g/cm <sup>d</sup>	Melting Range		Specific Heat Capacity					
					At 21°C (70°F)		At 538°C (1000°F)		At 871°C (1600°F)	
			°C	°F	J/kg • K	Btu/ lb • °F	J/kg • K	Btu/ lb • °F	J/kg • K	Btu/ lb • °F
<i>Nickel Base</i>										
Astroloy	Bar	7.91	—	—	—	—	—	—	—	—
D-979	Bar	8.19	1200–1390	2225–2530	—	—	—	—	—	—
Hastelloy X	Sheet	8.21	1260–1355	2300–2470	485	0.116	—	—	700	0.167
Hastelloy S	Bar	8.76	1335–1380	2435–2515	405	0.097	495	0.118	595	0.142
Inconel 597	Bar	8.04	—	—	—	—	—	—	—	—
Inconel 600	Bar	8.41	1355–1415	2470–2575	445	0.106	555	0.132	625	0.149
Inconel 601	Bar	8.05	1300–1370	2375–2495	450	0.107	590	0.140	680	0.162
Inconel 617	Bar	8.36	1330–1375	2430–2510	420	0.100	550	0.131	630	0.150
Inconel 625	Bar	8.44	1290–1350	2350–2460	410	0.098	535	0.128	620	0.148
Inconel 690	Bar	8.14	1345–1375	2450–2510	—	—	—	—	—	—
Inconel 706	Bar	8.08	1335–1370	2435–2500	445	0.106	580	0.138	670	0.159
Inconel 718	Bar	8.22	1260–1335	2300–2435	430	0.102	560	0.133	645	0.153
Inconel X750	Bar	8.25	1395–1425	2540–2600	430	0.103	545	0.130	715	0.171
Haynes 230	—	8.8	1300–1370	2375–2500	397	0.095	473	0.112	595	0.145
M-252	Bar	8.25	1315–1370	2400–2500	—	—	—	—	—	—
Nimonic 75	Bar	8.37	—	—	460	0.11	—	—	—	—
Nimonic 80A	Bar	8.16	1360–1390	2480–2535	460	0.11	—	—	—	—
Nimonic 81	Bar	8.06	—	—	460	0.11	585	0.14	670	0.16
Nimonic 90	Bar	8.19	1335–1360	2435–2480	460	0.11	585	0.14	670	0.16
Nimonic 105	Bar	8.00	—	—	420	0.10	545	0.13	670	0.16
Nimonic 115	Bar	7.85	—	—	460	0.11	—	—	—	—
Nimonic 263	Sheet	8.36	—	—	460	0.11	—	—	—	—
Nimonic 942	Bar	8.19	1240–1300	2265–2370	420	0.10	—	—	—	—
Nimonic PE 11	Bar	8.02	1280–1350	2335–2460	420	0.10	585	0.14	—	—
Nimonic PE 16	Bar	8.02	—	—	545	0.13	—	—	—	—
Nimonic PK 33	Sheet	8.21	—	—	420	0.10	545	0.13	670	0.16
Pyromet 860	Bar	8.21	—	—	—	—	—	—	—	—
René 41	Bar	8.25	1315–1370	2400–2500	—	—	545	0.13	725	0.173
René 95	Bar	—	—	—	—	—	—	—	—	—
Udimet 500	Bar	8.02	1300–1395	2375–2540	—	—	—	—	—	—
Udimet 520	Bar	8.21	1260–1405	2300–2560	—	—	—	—	—	—
Udimet 700	Bar	7.91	1205–1400	2200–2550	—	—	575	0.137	590	0.141
Unitemp AFL-IDA	Bar	8.26	—	—	420	0.100	—	—	—	—
Waspaloy	Bar	8.19	1330–1355	2425–2475	—	—	—	—	—	—
<i>Iron Base</i>										
Alloy 901	Bar	8.21	1230–1400	2250–2550	—	—	—	—	—	—
A-286	Bar	7.91	1370–1400	2500–2550	460	0.11	—	—	—	—
Discaloy	Bar	7.97	1380–1465	2515–2665	475	0.113	—	—	—	—
Haynes 556	Sheet	8.23	—	—	450	0.107	—	—	—	—
Incoloy 800	Bar	7.95	1355–1385	2475–2525	455	0.108	—	—	—	—
Incoloy 801	Bar	7.95	1355–1385	2475–2525	455	0.108	—	—	—	—
Incoloy 802	Bar	7.83	1345–1370	2450–2500	445	0.106	—	—	—	—
Incoloy 807	Bar	8.32	1275–1355	2325–2475	—	—	—	—	—	—
Incoloy 825 <sup>d</sup>	—	8.14	1370–1400	2500–2550	440	0.105	—	—	—	—
Incoloy 903	Bar	8.14	1320–1395	2405–2540	435	0.104	—	—	—	—

Table 10 (Continued)

Designation	Form	Density, g/cm <sup>a</sup>	Melting Range		Specific Heat Capacity					
					At 21°C (70°F)		At 538°C (1000°F)		At 871°C (1600°F)	
			°C	°F	J/kg • K	Btu/ lb • °F	J/kg • K	Btu/ lb • °F	J/kg • K	Btu/ lb • °F
Incoloy 904	Bar	8.12	—	—	460	0.11	—	—	—	—
Incoloy 907	—	8.33	1335–1400	2440–2550	431	0.103	—	—	—	—
Incoloy 909	—	8.30	1395–1430	2540–2610	427	0.102	—	—	—	—
N-155	Bar	8.19	1275–1355	2325–2475	430	0.103	—	—	—	—
19-9 DL	—	7.9	1425–1430	2600–2610	—	—	—	—	—	—
16-25-6	—	8.0	—	—	—	—	—	—	—	—
<i>Cobalt Base</i>										
Haynes	Sheet	8.98	1300–1330	2375–2425	405	0.097	510	0.122	565	0.135
L-605	Sheet	9.13	1330–1410	2425–2570	385	0.092	—	—	—	—
Haynes 150	—	8.05	1395	2540	—	—	—	—	—	—
MP35N	—	8.41	1315–1425	2400–2600	—	—	—	—	—	—
Elgiloy	—	8.3	1495	2720	—	—	—	—	—	—
Designation	Form	Thermal Conductivity						Mean Coefficient of Thermal Expansion, 10 <sup>-6</sup> K		Electrical Resistivity, Ω - m
		At 21°C (70°F)		At 538°C (1000°F)		At 871°C (1600°F)		At 538°C (1000°F)	At 871°C (1600°F)	
		W/m • K	Btu/ft <sup>2</sup> • in. h • °F	W/m • K	Btu/ft <sup>2</sup> • in. h • °F	W/m • K	Btu/ft <sup>2</sup> • in. h • °F			
<i>Nickel Base</i>										
Astroloy	Bar	—	—	—	—	—	—	13.9	16.2	—
D-979	Bar	12.6	87	18.5	128	—	—	14.9	17.7	—
Hastelloy X	Sheet	9.1	63	19.6	136	26.0	180	15.1	16.2	1180
Hastelloy S	Bar	—	—	20.0	139	26.1	181	13.3	14.9	—
Inconel 597	Bar	—	—	18.2	126	—	—	—	—	—
Inconel 600	Bar	14.8	103	22.8	158	28.9	200	15.1	16.4	1030
Inconel 601	Bar	11.3	78	20.0	139	25.7	178	15.3	17.1	1190 <sup>a</sup>
Inconel 617	Bar	13.6	94	21.5	149	26.7	185	13.9	15.7	1220 <sup>a</sup>
Inconel 625	Bar	9.8	68	17.5	121	22.8	158	14.0	15.8	1290
Inconel 690	Bar	13.3	95	22.8	158	27.8	193	—	—	148
Inconel 706	Bar	12.6	87	21.2	147	—	—	15.7	—	—
Inconel 718	Bar	11.4	79	19.6	136	24.9	173	14.4	—	1250 <sup>a</sup>
Inconel X750	Bar	12.0	83	18.9	131	23.6	164	14.6	16.8	1220 <sup>a</sup>
Haynes 230	—	8.9	62	18.4	133	24.4	179	14.0	15.2	1250
M-252	Bar	11.8	82	—	—	—	—	13.0	15.3	—
Nimonic 75	Bar	—	—	—	—	—	—	14.7	17.0	1090 <sup>a</sup>
Nimonic 80A	Bar	8.7	60	15.9	110	22.5	156	13.9	15.5	1240 <sup>a</sup>
Nimonic 81	Bar	10.8	75	19.2	133	25.1	174	14.2	17.5	1270 <sup>a</sup>
Nimonic 90	Bar	9.8	68	17.0	118	—	—	13.9	16.2	1180 <sup>a</sup>
Nimonic 105	Bar	10.8	75	18.6	129	24.0	166	13.9	16.0	1310 <sup>a</sup>
Nimonic 115	Bar	10.7	74	17.6	124	22.6	154	13.3	16.4	1390 <sup>a</sup>
Nimonic 263	Sheet	11.7	81	20.4	141	26.2	182	13.7	16.2	1150 <sup>a</sup>
Nimonic 942	Bar	—	—	—	—	—	—	14.7	16.5	—
Nimonic PE 11	Bar	—	—	—	—	—	—	15.2	—	—

(continued)

Table 10 (Continued)

Designation	Form	Thermal Conductivity						Mean Coefficient of Thermal Expansion, $10^{-6}$ K		Electrical Resistivity, $\Omega \cdot m$
		At 21°C (70°F)		At 538°C (1000°F)		At 871°C (1600°F)		At 538°C (1000°F)	At 871°C (1600°F)	
		W/m • K	Btu/ft <sup>2</sup> •in. h • °F	W/m • K	Btu/ft <sup>2</sup> •in. h • °F	W/m • K	Btu/ft <sup>2</sup> •in. h • °F	(1000°F)	(1600°F)	
Nimonic PE 16	Bar	11.7	81	20.2	140	26.4	183	15.3	18.5	1100 <sup>a</sup>
Nimonic PK 33	Sheet	10.7	74	19.2	133	24.7	171	13.1	16.2	1260 <sup>a</sup>
Pyromet 860	Bar	—	—	—	—	—	—	15.4	16.4	—
René 41	Bar	9.0	62	18.0	125	23.1	160	13.5	15.6	1308
René 95	Bar	8.7	60	17.4	120	—	—	—	—	—
Udimet 500	Bar	11.1	77	18.3	127	24.5	170	14.0	16.1	1203
Udimet 700	Bar	19.6	136	20.6	143	27.7	192	13.9	16.1	—
Unitemp AFI-IDA	Bar	10.8	75	16.5	114	19.5	135	12.4	14.1	—
Waspaloy	Bar	10.7	74	18.1	125	24.1	167	14.0	16.0	1240
<i>Iron Base</i>										
Alloy 901	Bar	13.3	92	—	—	—	—	15.3	—	—
A-286	Bar	12.7	88	22.5	156	—	—	17.6	—	—
Discaloy	Bar	13.3	92	21.1	146	—	—	17.1	—	—
Haynes 556	Sheet	11.6	80	17.5	121	—	—	16.2	17.5	—
Incoloy 800	Bar	11.6	80	20.1	139	—	—	16.4	18.4	989
Icolony 801	Bar	12.4	86	20.7	143	25.6	177	17.3	18.7	—
Incoloy 802	Bar	11.9	82	19.8	137	24.2	168	16.7	18.2	—
Incoloy 807	Bar	—	—	—	—	—	—	15.2	17.6	—
Incoloy 825	—	11.1	76.8	—	—	—	—	14.0 <sup>a</sup>	—	1130
Incoloy 903	Bar	16.8	116	20.9	145	—	—	8.6	—	610
Incoloy 904	Bar	16.8	116	22.4	155	—	—	—	—	—
Incoloy 907	—	14.8	103	—	—	—	—	7.7 <sup>b</sup>	—	697
Incoloy 909	—	14.8	103	—	—	—	—	7.7 <sup>b</sup>	—	728
N-155	Bar	12.3	85	19.2	133	—	—	16.4	17.8	—
19-9 DL	—	—	—	—	—	—	—	17.8	—	—
16-25-6	—	—	—	15	104	—	—	16.9	—	—
<i>Cobalt Base</i>										
Haynes 188	Sheet	—	—	19.9	138	25.1	174	14.8	17.0	922
L-605	Sheet	9.4	65	19.5	135	26.1	181	14.4	16.3	890
Stellite 6B	—	14.7	101	—	—	—	—	15.0	16.9	910
Haynes 150	—	—	—	0.75 <sup>c</sup>	5.2	—	—	—	16.8 <sup>d</sup>	810
MP35N	—	—	—	—	—	—	—	—	15.7 <sup>d</sup>	1010
Eligiloy	—	1.0	7.2	1.4	10	—	—	—	15.8 <sup>d</sup>	995

<sup>a</sup>At 21–93°C (70–200°F).<sup>b</sup>At 25–427°C (77–800°F).<sup>c</sup>At 705°C (1300°F).<sup>d</sup>At 980°C (1800°F).

While life under cyclic load ( $S$ - $N$  behavior) is a common criterion for design, resistance to crack propagation is an increasingly desired property. Thus, the crack growth rate ( $da/dn$ ) vs. a fracture toughness parameter is required. The parameter in this instance is the stress intensity factor ( $K$ ) range over an incremental distance through which a crack has grown—the difference between the maximum and minimum  $K$  in the region of crack length measured. Plots of the resultant type ( $da/dn$  vs.  $\Delta K$ ) are shown in Fig. 4 for several wrought superalloys.

**Table 11** Physical Properties of Selected Cast Superalloys

Alloy	Density, g/cm <sup>3</sup>	Melting Range		Specific Heat						Thermal Conductivity						Mean Coefficient of Thermal Expansion(s) <sup>a</sup> 10 <sup>-6</sup> K		
		°C	°F	At 21°C (70°F)		At 538°C (1000°F)		At 1093°C (2000°F)		At 193°C (200°F)		At 538°C (1000°F)		At 1093°C (2000°F)		At 93°C (200°F)	At 538°F (1000°C)	At 1093°C (2000°F)
				J/kg • K	Btu/lb • °F	J/kg • K	Btu/lb • °F	J/kg • K	Btu/lb • °F	W/m • K	• °F	W/m • K	• °F	W/m • K	• °F			
<i>Nickel Base</i>																		
IN-713 C	7.91	1260–1290	2300–2350	420	0.10	565	0.135	710	0.17	10.9	76	17.0	118	26.4	183	10.6	13.5	17.1
IN-713 LC	8.00	1290–1320	2350–2410	440	0.105	565	0.135	710	0.17	10.7	74	16.7	116	25.3	176	10.1	15.8	18.9
B-1900	8.22	1275–1300	2325–2375	—	—	—	—	—	—	(10.2) <sup>b</sup>	(71) <sup>b</sup>	16.3	113	—	—	11.7	13.3	16.2
Cast alloy 625	8.44	—	—	—	—	—	—	—	—	—	—	—	—	—	—	—	—	—
Cast alloy 718	8.22	1205–1345	2200–2450	—	—	—	—	—	—	—	—	—	—	—	—	—	—	—
IN-100	7.75	1265–1335	2305–2435	—	—	480	0.115	605	0.145	—	—	17.3	120	—	—	13.0	13.9	18.1
IN-162	8.08	1275–1305	2330–2380	—	—	—	—	—	—	—	—	—	—	—	—	12.2	14.1	—
IN-731	7.75	—	—	—	—	—	—	—	—	—	—	—	—	—	—	—	—	—
IN-738	8.11	1230–1315	2250–2400	420	0.10	565	0.135	710	0.17	—	—	17.7	123	27.2	189	11.6	14.0	—
IN-792	8.25	—	—	—	—	—	—	—	—	—	—	—	—	—	—	—	—	—
M-22	8.63	—	—	—	—	—	—	—	—	—	—	—	—	—	—	12.4	13.3	—
MAR-M-200	8.53	1315–1370	2400–2500	400	0.095	420	0.10	565	0.135	13.0	90	15.2	110	29.7	206	—	13.1	17.0
MAR-M-246	8.44	1315–1345	2400–2450	—	—	—	—	—	—	—	—	18.9	131	30.0	208	11.3	14.8	18.6
MAR-M-247	8.53	—	—	—	—	—	—	—	—	—	—	—	—	—	—	—	—	—
MAR-M-421	8.08	—	—	—	—	—	—	—	—	—	—	19.1	137	32.0	229	—	14.9	19.8
MAR-M-432	8.16	—	—	—	—	—	—	—	—	—	—	—	—	—	—	—	14.9	19.3
MC-102	8.84	—	—	—	—	—	—	—	—	—	—	—	—	—	—	12.8	14.9	—

(continued)



**Table 12** Dynamic Moduli of Selected Wrought Superalloys

Alloy	Form	Dynamic Modulus of Elasticity									
		At 21°C (70°F)		At 540°C (1000°F)		At 650°C (1200°F)		At 760°C (1400°F)		At 870°C (1600°F)	
		GPa	10 <sup>6</sup> psi	GPa	10 <sup>6</sup> psi	GPa	10 <sup>6</sup> psi	GPa	10 <sup>6</sup> psi	GPa	10 <sup>6</sup> psi
<i>Nickel Base</i>											
D-979	Bar	207	30.0	178	25.8	167	24.2	156	22.6	146	21.2
Hastelloy S	Bar	212	30.8	182	26.4	174	25.2	166	24.1	—	—
Hastelloy X	Sheet	197	28.6	161	23.4	154	22.3	146	21.1	137	19.9
Haynes 230	<sup>a</sup>	211	30.6	184	26.4	177	25.3	171	24.1	164	23.1
Inconel 587	Bar	222	32.1	—	—	—	—	—	—	—	—
Inconel 596	Bar	186	27.0	—	—	—	—	—	—	—	—
Inconel 600	Bar	214	31.1	184	26.7	176	25.5	168	24.3	157	22.8
Inconel 601 <sup>b</sup>	Sheet	207	30.0	175	25.4	166	24.1	155	22.5	141	20.5
Inconel 617	Bar	210	30.4	176	25.6	168	24.4	160	23.2	150	21.8
Inconel 625	Bar	208	30.1	179	25.9	170	24.7	161	23.3	148	21.4
Inconel 706	Bar	210	30.4	179	25.9	170	24.7	—	—	—	—
Inconel 718	Bar	200	29.0	171	24.8	163	23.7	154	22.3	139	20.2
Inconel X750	Bar	214	31.0	184	26.7	176	25.5	166	24.0	153	22.1
M-252	Bar	206	29.8	177	25.7	168	24.4	156	22.6	145	21.0
Nimonic 75	Bar	221	32.0	186	27.0	176	25.5	170	24.6	156	22.6
Nimonic 80A	Bar	219	31.8	188	27.2	179	26.0	170	24.6	157	22.7
Nimonic 90	Bar	226	32.7	190	27.6	181	26.3	170	24.7	158	22.9
Nimonic 105	Bar	223	32.3	186	27.0	178	25.8	168	24.4	155	22.5
Nimonic 115	Bar	224	32.4	188	27.2	181	26.3	173	25.1	164	23.8
Nimonic 263	Sheet	222	32.1	190	27.5	181	26.2	171	24.8	158	22.9
Nimonic 942	Bar	196	28.4	166	24.1	158	22.9	150	21.8	138	20.0
Nimonic PE 11	Bar	198	28.7	166	24.0	157	22.8	—	—	—	—
Nimonic PE 16	Bar	199	28.8	165	23.9	157	22.7	147	21.3	137	19.9
Nimonic PK 33	Sheet	222	32.1	191	27.6	183	26.5	173	25.1	162	23.5
Pyromet 860	Bar	200	29.0	—	—	—	—	—	—	—	—
René 95	Bar	209	30.3	183	26.5	176	25.5	168	24.3	—	—
Udimet 500	Bar	222	32.1	191	27.7	183	26.5	173	25.1	161	23.4
Udimet 700	Bar	224	32.4	194	28.1	186	27.0	177	25.7	167	24.2
Udimet 710	Bar	222	32.1	—	—	—	—	—	—	—	—
Waspaloy	Bar	213	30.9	184	26.7	177	25.6	168	24.3	158	22.9
<i>Iron Base</i>											
A-286	Bar	201	29.1	162	23.5	153	22.2	142	20.6	130	18.9
Alloy 901	Bar	206	29.9	167	24.2	153	22.1	—	—	—	—
Discaloy	Bar	196	28.4	154	22.3	145	21.0	—	—	—	—
Haynes 556	Sheet	203	29.5	165	23.9	156	22.6	146	21.1	137	19.9
Incoloy 800	Bar	196	28.4	161	23.4	154	22.3	146	21.1	138	20.0
Incoloy 801	Bar	208	30.1	170	24.7	162	23.5	154	22.3	144	20.9
Incoloy 802	Bar	205	29.7	169	24.5	161	23.4	156	22.6	152	22.0
Incoloy 807	Bar	184	26.6	155	22.4	146	21.2	137	19.9	128	18.5
Incoloy 903	Bar	147 <sup>c</sup>	21.3	152 <sup>d</sup>	22.1	—	—	—	—	—	—
Incoloy 907 <sup>d</sup>	—	165 <sup>c</sup>	23.9	165 <sup>d</sup>	23.9	159 <sup>c</sup>	23	—	—	—	—
N-155	Bar	202	29.3	167	24.2	159	23.0	149	21.6	138	20.0
V-57	Bar	199	28.8	163	23.6	153	22.2	144	20.8	130	18.9
19-9 DL	—	203	29.5	—	—	152	22.1	—	—	—	—
16-25-6	—	195	28.2	—	—	123	17.9	—	—	—	—

(continued)



**Table 12** (Continued)

Alloy	Form	Dynamic Modulus of Elasticity									
		At 21°C (70°F)		At 540°C (1000°F)		At 650°C (1200°F)		At 760°C (1400°F)		At 870°C (1600°F)	
		GPa	10 <sup>6</sup> psi	GPa	10 <sup>6</sup> psi	GPa	10 <sup>6</sup> psi	GPa	10 <sup>6</sup> psi	GPa	10 <sup>6</sup> psi
<i>Cobalt Base</i>											
Haynes 188	Sheet	207	30	—	—	—	—	—	—	—	—
L-605	Sheet	216	31.4	—	—	185	26.8	—	—	166	24.0
MAR-M-918	Sheet	225	32.6	186	27.0	176	25.5	168	24.3	159	23.0
MP35N	Bar	231 <sup>c</sup>	33.6	—	—	—	—	—	—	—	—
Haynes 150	—	217 <sup>c</sup>	31.5	—	—	—	—	—	—	—	—

<sup>a</sup>Cold-rolled and solution-annealed sheet, 1.2–1.6 mm (0.048–0.063 in.) thick.

<sup>b</sup>Data for bar, rather than sheet.

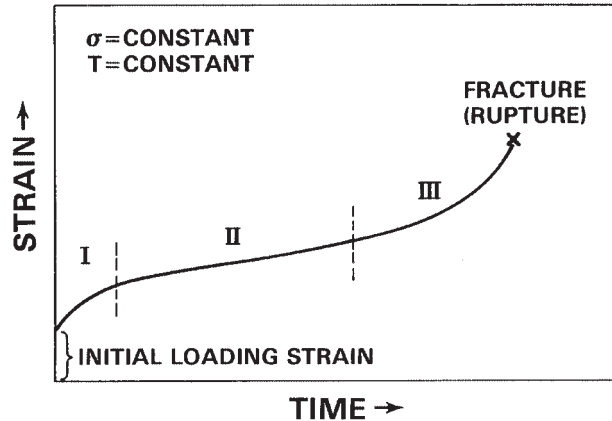
<sup>c</sup>Annealed.

<sup>d</sup>Precipitation hardened.

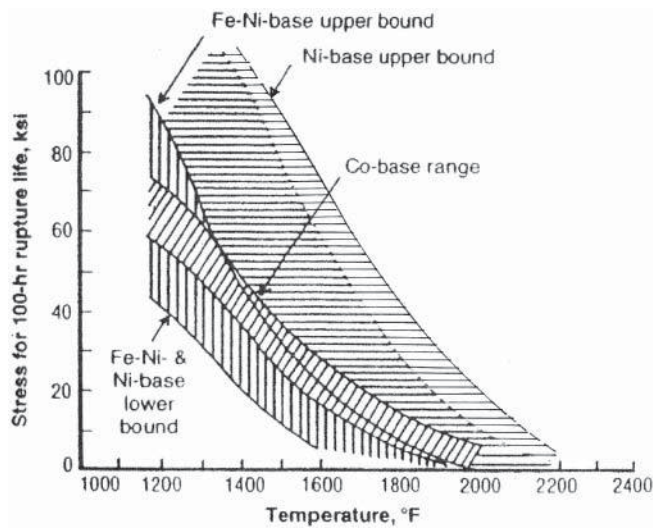
**Table 13** Dynamic Modulus of Elasticity for Selected Cast Superalloys

Alloy	Dynamic Modulus of Elasticity					
	At 21°C (70°F)		At 538°C (1000°F)		At 1093°C (2000°F)	
	GPa	10 <sup>6</sup> psi	GPa	10 <sup>6</sup> psi	GPa	10 <sup>6</sup> psi
<i>Nickel Base</i>						
IN-713 C	206	29.9	179	26.2	—	—
IN-713 LC	197	28.6	172	25.0	—	—
B-1900	214	31.0	183	27.0	—	—
IN-100	215	31.2	187	27.1	—	—
IN-162	197	28.5	172	24.9	—	—
IN-738	201	29.2	175	25.4	—	—
MAR-M-200	218	31.6	184	26.7	—	—
MAR-M-246	205	29.8	178	25.8	145	21.1
MAR-M-247	—	—	—	—	—	—
MAR-M-421	203	29.4	—	—	141	20.4
René 80	208	30.2	—	—	—	—
<i>Cobalt Base</i>						
Haynes 1002	210	30.4	173	25.1	—	—
MAR-M-509	225	32.7	—	—	—	—

The nature of superalloys is that they resist the creep rupture process better than other materials, have very good higher temperature short-time strength (yield, ultimate) and fatigue properties (including fatigue crack propagation resistance), and combine these mechanical properties with good to exceptional oxidation resistance. Consequently, superalloys are the obvious choice when structures are to operate at higher temperatures. Generally, the nominal temperature range of superalloy operation is broken up into the intermediate range of 540–760°C (1000–1400°F) and the high-temperature range which occurs above about 816°C (1500°F).



**Figure 1** Creep rupture schematic showing time-dependent deformation under constant load at constant high temperatures followed by final rupture. (All loads below the short-time yield strength. Roman numerals denote ranges of the creep rupture curve.)

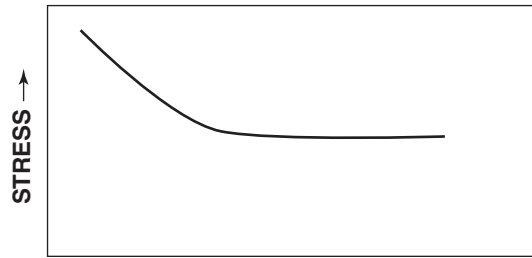


**Figure 2** Creep rupture curves showing ranges for superalloy families. *Source: Superalloys Source Book, ASM International, Materials Park, OH, 1984, p. 3.*

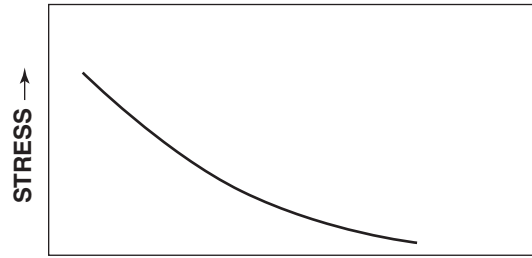
### 3 PROPERTIES OF SUPERALLOYS

#### 3.1 Physical/Environmental

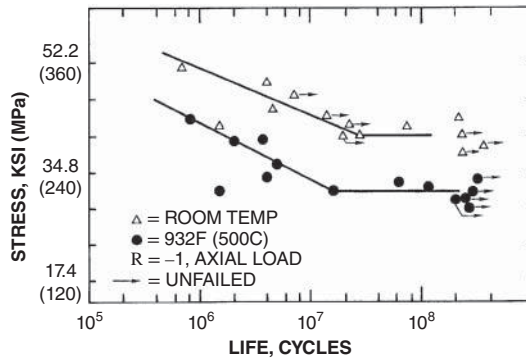
Iron, cobalt, and nickel, the bases of superalloys, are transition metals located in a similar area of the periodic table of the elements. The density, melting point, and physical properties of the superalloy base elements are given in Table 14. As can be seen, pure iron has a density of  $7.87 \text{ g/cm}^3$  ( $0.284 \text{ lb/in.}^3$ ), while pure nickel and cobalt have densities of about  $8.9 \text{ g/cm}^3$



LOG CYCLES →  
Typical Fatigue Curve at Low Temperature



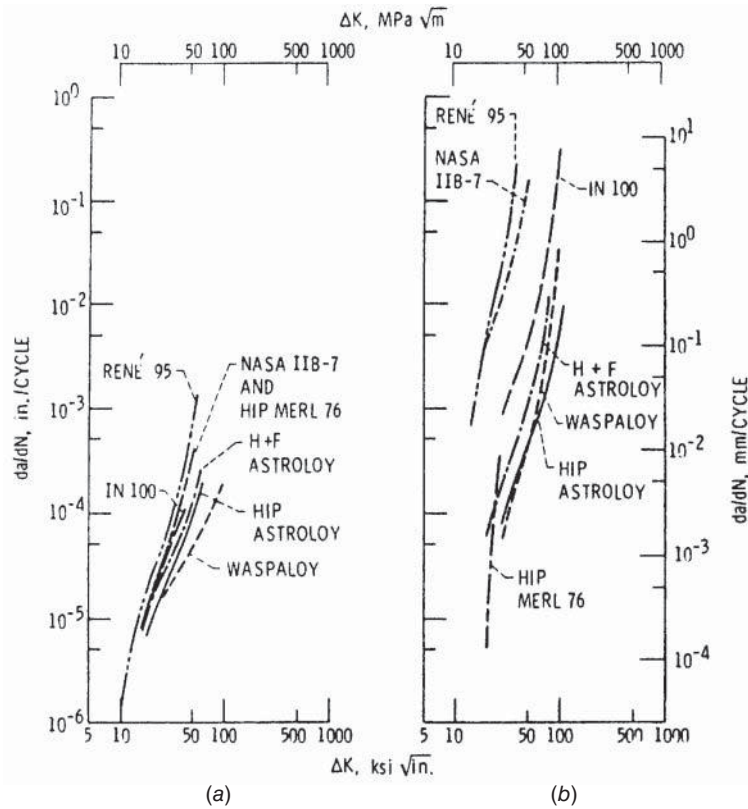
LOG CYCLES →  
Typical Fatigue Curve at High Temperature  
(a)



(b)

**Figure 3** Curves of stress versus cycles ( $S-N$ ) showing (a) schematic typical fatigue response at high temperature and (b) actual fatigue curves at room and elevated temperature for a specific nickel-based superalloy.

(0.322 lb/in.<sup>3</sup>). The superalloys are created usually by adding significant levels of the alloy elements chromium, aluminum, and titanium plus appropriate refractory metal elements such as tantalum, tungsten, and molybdenum to the base metal. Densities of superalloys are a function of the amounts of these elements in the final compositions. For example, iron–nickel-based superalloys have densities of around 7.9–8.3 g/cm<sup>3</sup> (0.285– 0.300 lb/in.<sup>3</sup>), not too dissimilar to densities of nickel-based superalloys, which may range from about 7.8 to 8.9 g/cm<sup>3</sup>



**Figure 4** Crack growth rate ( $da/dN$ ) versus toughness change ( $\Delta K$ ) curves for several superalloys at 649°C (1200°F); HIP = hot isostatically pressed; H + F = HIP + forge. Unless otherwise noted, all alloys are forged. Source: *Superalloys: Alloying and Performance*, ASM International, Materials Park, OH, 2010.

**Table 14** Some Physical Properties of Superalloy Base Elements

Crystal Structure	Melting Point		Density		Expansion Coefficient <sup>a</sup>		Thermal Conductivity <sup>a</sup>		
	°F	°C	lb/in. <sup>3</sup>	g/cm <sup>3</sup>	°F × 10 <sup>-6</sup>	°C × 10 <sup>-6</sup>	Btu/ft <sup>2</sup> /h/°F/in.	cal/cm <sup>2</sup> /s/°C/cm	
Co	hcp	2723	1493	0.32	8.9	7.0	12.4	464	0.215
Ni	fcc	2647	1452	0.32	8.9	7.4	13.3	610	0.165
Fe	bcc	2798	1535	0.28	7.87	6.7	11.7	493	0.175

<sup>a</sup>At room temperature.

Source: From *Superalloys II*, Wiley, New York, 1987, p. 14.

(0.282–0.326 lb/in.<sup>3</sup>). Cobalt-based superalloy densities, on the other hand, range from about 8.3 to 9.4 g/cm<sup>3</sup> (0.300–0.340 lb/in.<sup>3</sup>). Aluminum, titanium, and chromium reduce superalloy density whereas the refractory elements such as tungsten, rhenium, ruthenium, and tantalum increase it.

The melting temperatures of the basis superalloy elements are nickel, 1452°C (2647°F); cobalt, 1493°C (2723°F); and iron, 1535°C (2798°F). When metals are alloyed, there is no

longer a single melting point for a composition. Instead, alloys melt over a range. The lowest melting temperature (incipient melting temperature—lowest temperature at which melting will commence in a given alloy component) and melting ranges of superalloys are functions of composition and prior processing. Just as the basis metal is higher melting, so generally are incipient melting temperatures greater for cobalt-based superalloys than for nickel- or iron–nickel-based superalloys. Nickel-based superalloys may show incipient melting at temperatures as low as 1204°C (2200°F). However, advanced nickel-based single-crystal superalloys having limited amounts of melting point depressants tend to have incipient melting temperatures equal to or in excess of those of cobalt-based superalloys.

The physical properties, electrical conductivity, thermal conductivity, and thermal expansion of superalloys tend to be low (relative to other metal systems). These properties are influenced by the nature of the base metals (transition elements) and the presence of refractory-metal additions.

The corrosion resistance of superalloys depends primarily on the alloying elements added and the environment experienced. Chromium additions promote oxidation resistance and were on the order of 20 wt % or higher in early superalloys. In order to accommodate the addition of more strengthening elements, particularly in nickel-based superalloys, chromium levels were reduced, at first to the order of about 15 wt %, then to about 10 wt %, as aluminum additions were made that increased the oxidation resistance in addition to increasing alloy strength. When certain types of hot corrosion became a factor in operation, chromium levels were increased again to the order of 12–14 wt %. In more recent superalloys operating at the highest temperatures, the need to enhance strength and maintain microstructure stability has brought the chromium levels of recent single-crystal superalloys down to around or below 5 wt %.

Contaminants in the operating environment can cause unexpectedly high corrosion rates. Superalloys employed in furnace emission control and in certain oil and gas well applications face severe corrosion conditions. The superalloys employed at the highest temperatures in gas turbines are coated to increase oxidation/corrosion resistance. More information follows later in this chapter.

## 3.2 Mechanical

The superalloys are relatively ductile; the tensile ductilities of cobalt-based superalloys generally are less than those of iron–nickel- and nickel-based superalloys. Short-time tensile ductilities of all alloys generally range from as low as 10% to as high as 70% but gamma prime hardened alloys are in the lower end, usually between 10 and 40%. Creep rupture ductilities can range much lower. At the 760°C (1400°F) tensile ductility minimum area (see mention below for tensile testing), creep rupture ductilities of castings have gone below 1.5%, although most current high-strength PC equiaxed cast alloys have rupture ductilities in excess of 2.0%. Ductilities of columnar grain directionally solidified (CGDS) superalloys vary from the longitudinal to the transverse direction of testing. The transverse direction ductilities generally approximate ductilities of the same composition in polycrystalline form. Single-crystal directionally solidified (SCDS) superalloy ductilities will vary with orientation of the single crystal relative to the testing direction.

Superalloys typically have dynamic moduli of elasticity in the vicinity of 207 GPa ( $30 \times 10^6$  psi), although moduli of specific PC alloys can vary from 172 to 241 GPa ( $25 \times 10^6$ – $35 \times 10^6$  psi) at room temperature depending on the alloy system. Processing that leads to directional grain or crystal orientation can result in moduli of about 124–310 GPa (about  $18 \times 10^6$ – $45 \times 10^6$  psi) depending on the relation of grain or crystal orientation to testing direction. As noted above, dynamic measurement of modulus of elasticity at high temperatures is necessary because static modulus is greatly influenced by high temperatures and shows significant reductions over

the dynamic value at a common high temperature. Static modulus may drop by around 25–30% as temperatures increase from room temperature to 871°C (1600°F).

Short-time tensile yield properties of gamma prime hardened alloys range from around 550 to 1380 MPa (80–200 ksi) at room temperature. Actual values depend on composition and processing (cast vs. wrought). Wrought alloys tend to have the highest values, with the higher hardener content alloys (e.g., René 95, IN 100) having the highest strengths. However, strength also is a function of grain size and stored energy. Alloys such as U630 or IN 718 can be produced with very high yield strengths. Solid-solution-hardened alloys such as the sheet alloy, Hastelloy X, have lower strengths. The ultimate strengths of superalloys range from about 690 to 1520 MPa (100–230 ksi) at room temperature, with gamma prime hardened alloys in the high end of the range.

Superalloys tend to show an increase of yield strength from room temperature up to a nominal temperature of about 650°C (1200°F) or a bit higher and drop off thereafter. This is in contrast to non-superalloys, which tend to continuously decrease in short yield time strength as temperatures increase. Ultimate strengths generally do not show this trend. Concurrently, tensile ductility tends to decrease, with minimums in the range of 649–760°C (1200–1400°F). However, many published data for alloys do not show significant increases in tensile yield strength over the range from ambient temperature to 650°C (1200°F).

The highest tensile properties are found in the finer grain size wrought or powder metallurgy nickel-based superalloys which are used in applications at the upper end of the intermediate temperature regime, nominally 760°C (1400°F). The highest creep rupture properties invariably are found in the coarser grain PC cast superalloys or in directionally solidified superalloys in the CGDS and SCDS cast superalloys. Creep rupture strength tends to increase as structure goes from PC to CGDS to SCDS cast alloys.

Rupture strengths are a function of the time at which they are to be recorded. The 1000-h rupture stress capability is obviously lower than the 100-h capability. Creep capability also is a function of the amount of creep permitted in a test. For example, the time to 0.5%, 1.0%, 2.0%, and 5.0% might each be valuable for design, dependent on a component's intended use. It is much more difficult to find this information in the literature than it is to find creep rupture capability information. Handbooks generally do not carry much creep information. Creep rupture strengths for 100 h failure at 982°C (1800°F) may range from about 45 MPa (6.5 ksi) for an older gamma prime hardened PC wrought alloy such as U500 to 205 MPa (30 ksi) for the PC cast superalloy Mar-M 246. CGDS and SCDS alloys can be much stronger.

Cyclic properties, although of great importance, are not commonly tabulated for superalloys. Properties of interest would be the  $10^3$ – $10^5$  and  $10^6$ – $10^8$  cycle fatigue strength capabilities. This could mean stress for a fixed-cyclic-life-to-a-particular-sized-crack or stress for a fixed-cyclic-life-to-fracture for LCF regimes or only involve stress for a fixed-cyclic-life-to-fracture for HCF regimes. Also, crack propagation rates vs. the toughness parameter ( $da/dN$  vs.  $\Delta K$ ) are desired. The life values, when available, lend themselves to tabulation but the  $da/dN$  values are often represented by graphs for wrought alloys used at intermediate temperatures. LCF strengths are usually related to an alloy's yield strength while HCF strengths are usually related to an alloy's ultimate strength. For cast alloys used in the hottest sections of a gas turbine, there appears to be a relationship of TMF strength to the creep strength of an alloy when compared for a given alloy form, e.g., as for CGCS nickel-based superalloys.

Superalloys usually are processed to optimize one property in preference to others. The same composition, if used in the cast and wrought states, may have different heat treatments applied to the different product forms. Even when a superalloy is used in the same product form, process treatments may be used to optimize one property over others. For example, by adjusting the processing conditions (principally heat treatment) of different wrought Waspaloy components, substantial yield strength improvement can be made at the expense of creep rupture strengths.

## 4 THE EVOLUTION OF SUPERALLOYS

### 4.1 Introduction

During the first quarter of the twentieth century, chromium was added at various times to bases of cobalt, nickel, and iron. The resulting products were remarkably resistant to atmospheric (moisture-based) environments and to oxidation at high temperatures. By the time of World War II, some of these alloys, now containing additional alloy elements, had come into use for such applications as resistance wires, dental prostheses, cutlery, furnace and steam turbine components, etc. With emphasis on higher performance piston engines and the development of the gas turbine engine during the war, the need became apparent for corrosion-resistant materials to operate in demanding mechanical load conditions at high temperatures. At this point, the fledgling superalloy industry began to expand.

By modifying the stainless steels, higher strengths were achieved without the need for special high-temperature strengthening phases. Phases such as eta (a nickel–titanium compound) or gamma prime (a nickel–aluminum compound) had been introduced into the nickel–chromium families of alloys just prior to the war to produce high strength at high temperatures. The increasing application temperatures forced alloy developers to include these phases (eta, gamma prime) in the iron-based alloys to take the high-temperature strength characteristics beyond those of the modified stainless steels such as 19-9DL. Precipitation-hardened iron–nickel-based alloys were invented in Germany and, after modification, made their way to the United States and, as A-286 or V-57, are still in use today.

Nevertheless, the need for greater creep rupture strength continually increased. Some of this need was met in the early years by adapting a cobalt-based corrosion-resistant alloy (Vitallium) for use in aircraft engine superchargers and, later, to airfoils in the hot sections of gas turbines. Similar cobalt-based superalloys are still in use today. However, creep rupture requirements for aircraft gas turbine applications soon outstripped capabilities of the iron–nickel-based superalloys and the cobalt-based superalloys. Thus the use of nickel-based superalloys, modified to provide more of the hardening phase gamma prime, increased.

The development of nickel-based superalloys led to a reduction of titanium and an increase of aluminum to as much as 6 wt % in nickel-based superalloys. Concurrently, elements such as molybdenum, cobalt, and tungsten were added to or increased in nickel-based superalloys with alloy contents adjusted over time. Later, tantalum and niobium were added with amounts of all alloy elements varying with alloy and application.

Cobalt at one point was added in amounts to about 20 wt % but eventually cobalt amounts in nickel-based superalloys settled out at about 15%. In the 1950s, the best wrought nickel-based superalloys (e.g., Waspaloy) for high-temperature service had about 13 wt %. Economics then became important owing to a 10-fold increase in cobalt prices in the late 1970s. Most users of high cobalt-containing wrought nickel-based superalloys began to use much more of a wrought nickel-based superalloy, IN 718, which contains no cobalt. Subsequently IN 718 became the most widely used superalloy, at great cost savings for manufacturers. Cast nickel-based alloys with limitations on the maximum amount of cobalt in them were also used. However, in the development of rhenium- and ruthenium-containing high-strength SCDS superalloys, the chemistry changes that resulted in reduced chromium contents also enabled higher cobalt contents to once again emerge. Cobalt contents in such alloys may approach or exceed around 15 wt %.

It is obvious that the alloy selector must consider the extent to which geopolitical, geographical, and related alloy element costs can influence alloy cost per pound and the ability to create and effectively use new superalloys which contain critical or strategically important alloy elements.



As noted in the text, the introduction of up to 6 wt % of expensive specialty elements such as rhenium and ruthenium to single crystal directionally solidified nickel-base superalloys occurred in the late 1990s. There now is a trend to reduce the amounts of such added elements owing not only to the current cost but also to the realization that the miniscule amounts of such elements available in the earth's crust and thus available commercially would most likely cause even higher future costs and be insufficient to support the continued use of such elements in production.

## 4.2 Superalloy Modifications

Superalloys frequently are slightly modified for specific applications and a new name or specification is assigned. As an example, alloy PWA 1487 is PWA 1484 with a small addition of yttrium and slight changes in hafnium and tantalum (see Table 4). Sometimes, however, minor chemistry modifications are made without changing the specification or name assigned to an alloy. Actual chemistry levels can vary since individual superalloy suppliers and/or patent holders make modifications to the original alloy compositions. The same nominal alloy name may result in modest to significantly differing chemistries from one superalloy user to another.

A case in point relative to alloy design and designation is the improved superalloy, 718+, which allows about a 40°C (100°F) improvement in capability of IN 718 while retaining many of the superior properties of IN 718. This capability increase is achieved with the addition of about 9 wt % cobalt and so the alloy clearly is not IN 718.

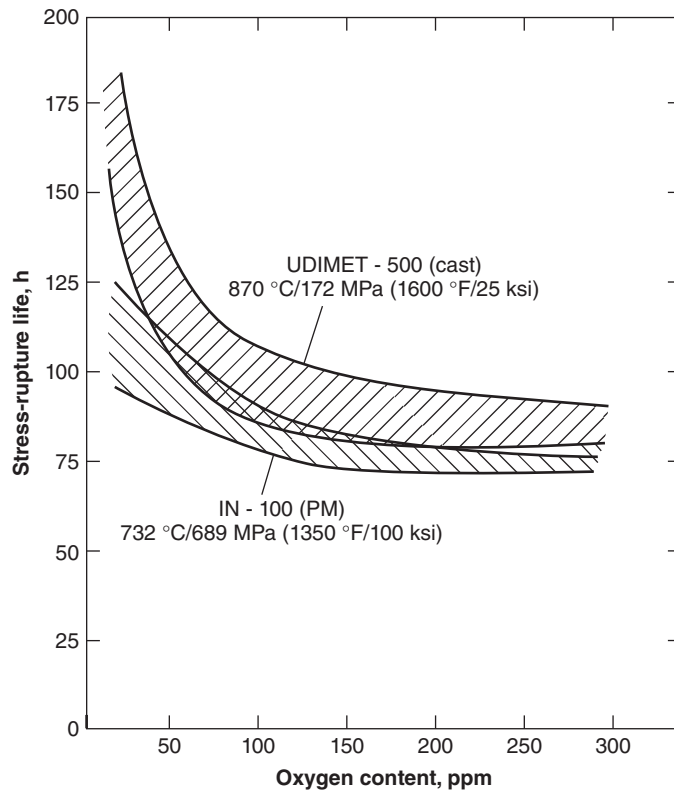
Although not uncommon now, proprietary additives once were added by some producers to assist in creating optimum properties of the resultant alloy product. For current chemistries, check with the appropriate superalloy producer or patent holder. Very small additions of zirconium and/or boron were known to superalloy developers and were proprietarily used long before the beneficial effects of minor elements were discovered in university research.

## 4.3 Improvement of Superalloys by Chemistry and Process Control or Minor Additions of New Elements

The production of superalloy components initially requires some sort of melting process. The melting produces ingots or electrodes. Electrodes are electrically remelted to produce ingot for forging, induction remelted to be converted to powder (for subsequent consolidation to a component), or induction remelted to be investment cast. Remelting is used to produce an ingot which can be processed to wrought mill forms (e.g., bar stock) or forged to a component shape. Until the start of the second half of the twentieth century, melting of superalloys was conducted in air or under slag environments. The properties of modern superalloys derive principally from the presence of many elements which are reactive with oxygen and so were being lost to some or a great degree in the melting and casting process. When vacuum melting techniques were introduced to commercial production of metals, they were pioneered by superalloys. The vacuum enabled the melting of superalloys containing higher amounts of the hardeners aluminum and titanium. Furthermore, the concurrent reduction in gases, oxides, and other impurities created a significant improvement in the ductility of superalloys. Moreover, with more hardener content, strengths of superalloys began to increase dramatically. Figure 5 shows the improvement in creep rupture life achieved with the reduction in oxygen content.

Figure 6 shows a somewhat stylized trend of improvements in superalloy creep rupture capability since the 1940s. Creep rupture strengths took a major jump around the early 1950s with the advent of vacuum melting and again a steady improvement in properties for cast alloys began with the introduction of CGDS processing in the 1970s and of SCDS processing in the 1980s.





**Figure 5** Influence of oxygen content on the stress rupture life of cast Udimet 500 and power metallurgy IN-100. *Source:* R. T. Holt and W. Wallace, "Impurities and Trace Elements in Nickel-Base Superalloys," *International Metals Reviews*, 21, 1–14, 1976. Republished with permission of American Society for Metals, from *International Metals Review*; permission conveyed through Copyright Clearance Center, Inc.

## 5 MELTING AND CASTING PRACTICES

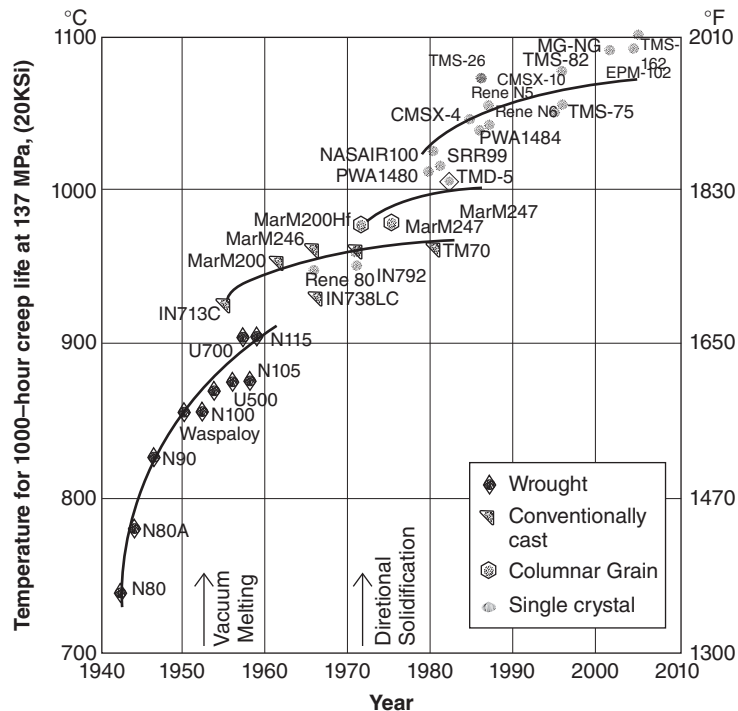
### 5.1 General Aspects

The development of superalloys as they are employed today is largely a story of the development of modern melting technology. Whether the final product is to be forged or investment cast, the essence of a superalloy's ability to create the properties desired hinges on the correct choice and adaptation of melting principles.

Superalloy melting practices may be classified as either primary (the initial melt of elemental materials and /or scrap which sets the composition) or secondary (remelt of a primary melt for the purpose of controlling the solidification structure). The melt type or combination of melt types selected depends upon the alloy composition, mill form and size/shape desired, properties desired, and sensitivity of the final component to localized inhomogeneity in the alloy.

### 5.2 Melting and Refining Superalloys

The two most common primary melt practices are argon–oxygen decarburizing treatment of electric arc processed metal (Arc-AOD) and vacuum induction melting (VIM). The two common secondary melt practices are vacuum arc remelting (VAR) and electroslag



**Figure 6** Temperature Capability (on Basis of Strength) versus Year of Alloy Introduction *Source:* Modified from R. G. Reed, *The Superalloys*, Cambridge University Press, New York, 2006.

remelting (ESR). A few alloy mill products may be manufactured from cast ingots after only primary melting. However, for the majority of superalloys to be worked, the common practice combinations are Arc-AOD + ESR, VIM + ESR, VIM + VAR, and VIM + ESR + VAR. Common material specifications, such as aerospace materials specifications (AMS), will specify acceptable melting practices.

The Arc-AOD practice used for superalloys is little different from that used for stainless steels. An electric arc furnace is the recipient of the initial charge and uses power from an arc struck between graphite electrodes and the charge to heat and melt the charge. Once the charge melts, no further electric power is needed. Heat is input into the charge by injecting (“blowing”) oxygen under the surface of the melt to react with elements such as aluminum, titanium, silicon, and carbon. A desulfurizing addition (usually CaO) is made. The slag formed by the oxidation products and the desulfurizing addition is physically removed from the furnace.

The deslagged charge is transferred to the AOD vessel, which is a refractory-lined steel shell with “tuyeres” in the bottom. The tuyeres are used to inject a mixture of argon and oxygen into the molten bath. By controlling the ratio of argon to oxygen, the selective oxidation or reduction of elements may be accomplished. The principal element reduced is carbon. Elements which need to be retained in the melt (particularly chromium) may also be oxidized into the slag. However, additions of aluminum made to the heat will react with the slag and reduce the chromium back into the molten charge. There is no external source of heat to an AOD vessel. The molten charge is heated by making additions of aluminum and oxidizing them ( $\text{Al}_2\text{O}_3$  has a very high heat of formation). Cooling is accomplished by adding solid scrap to the bath. When the desired composition and pouring temperature are reached, the heat is poured off into

a teeming ladle and transferred to the electrode/ingot pouring system. Precautions are taken (shrouding of the pour stream with argon) to minimize the reaction of the pour stream with atmospheric gases.

The other prevalent primary melt practice is VIM. The VIM furnace consists of a ceramic-lined crucible built up around water-cooled induction coils. The crucible is mounted in a vacuum chamber. The vacuum chamber may have several vacuum ports (of various sizes) built into it so that, without breaking vacuum, the charge material may be introduced into the crucible, molds may be introduced into the chamber, systems for removing slag from the pour stream (tundish) may be introduced, and sampling of the molten metal may be made for chemistry control.

The charge is separated into three types of components, virgin, reactive, and revert. Note that virgin material is usually elemental material but may also consist of any other type of material which has not been previously vacuum melted. Reactive elements refer to those elements which are strong oxide formers. For superalloys these are primarily aluminum, titanium, and zirconium. Operation of the VIM consists of charging the virgin portion of the charge (minus the reactive portion) into the crucible. The furnace is pumped down (if not already under vacuum) and a measurement made of the increase in pressure (as a function of time) when the vacuum ports are blanked off. This "leak-up rate" is a measurement of the baseline furnace vacuum integrity. Power is applied to the induction coils. The magnetic fields produced induce a current in the charge material, heating the charge. When the charge is molten, it will evolve gas (refining). The rate of gas evolution is measured by taking leak-up rates. When consecutive stable leak-up rates are obtained, then refining (degassing) is complete. This produces the lowest possible oxygen in the alloy. Reactive additions are then made and revert is added. (Revert is previously vacuum melted alloy which is of the same or nearly the same composition as the intended melt.)

Additions of some form of calcium are usually made to reduce sulfur in the charge by forming a CaS slag. A chemistry sample is taken and analyzed. "Trim" additions are made to bring the heat to a precise composition. The metal is (top) poured into the molds through a system for metal transfer plus slag control and regulation of the pour rate. Cast product for direct processing (e.g., for investment casting) is referred to as ingot. Most often, the VIM product is intended for secondary melting and is referred to as an electrode, as both secondary processes consume this product in an electrically heated manner.

Compared to VIM, Arc-AOD uses the lowest cost charge material and has higher production rates. That is, Arc-AOD is the lowest cost process. However, Arc-AOD is limited in its ability to precisely control composition in a narrow range (particularly for superalloys with high titanium levels) and also produces much higher oxygen content material. However, the choice of ESR as the secondary melting process may compensate to some degree for the higher oxide inclusion content of the Arc-AOD process).

ESR is the most frequently used secondary melt process for Arc-AOD electrodes. In ESR, alternating current is applied to an electrode situated inside a water-cooled crucible containing a molten slag charge. The intended circuit of current is from the electrode, through a molten slag, through the solidifying ingot, through the water-cooled stool, and by symmetrically located bus bars back to the electrode. The slag is generally a  $\text{CaF}_2$  base, modified by major additions of  $\text{CaO}$ ,  $\text{MgO}$ , and  $\text{Al}_2\text{O}_3$ . Minor additions of  $\text{TiO}_2$  and  $\text{ZrO}_2$  may be made to counteract loss of titanium and zirconium during the melting process. (Note that minor compositional changes may occur during ESR.) The current passing through the slag keeps the slag molten. The molten slag melts the immersed face of the electrode. As the molten metal gathers into drops on the melt surface of the electrode, it is reduced in sulfur (through reaction with the  $\text{CaF}_2$ ) and entrained oxides are incorporated into the slag. The fully formed drop falls through the slag and is collected in the water-cooled crucible. The slag, which has formed a solid layer against the cooled crucible wall, is partially remelted by the molten metal but remains as a layer between the ingot and the crucible. As the electrode is consumed, an ingot is built up in the crucible. At any given

time the ingot contains a pool of molten metal at the ingot top and a zone of liquid + solid between the solid portion of the ingot and the molten pool.

However, solidifying consumable melted ingots are susceptible to the formation of unacceptable segregation. For a given alloy there is a critical thickness and angle (to the growth direction) of the liquid + solid zone at which the liquid in that zone may form self-perpetuating channels in the solidification structure. Such channels are known as “freckles” and often are of such high-solute content that subsequent thermal treatment cannot eliminate the elemental concentration. Thus, the final product may contain channels of hard particles and be very detrimental to fatigue properties. *The more highly alloyed the material being melted, the smaller and shallower must be the liquid + solid zone in order to avoid freckle formation. The shape and thickness of the liquid + solid zone may be modified to be more resistant to freckle formation by reducing the melt rate (the rate of deposition of molten metal into the pool), reducing the ingot diameter or by improving the heat extraction from the sides of the crucible.*

VAR is used in preference to ESR where larger ingot sizes of highly alloyed materials are needed. VAR is a DC process which is conducted in a vacuum. As occurs in ESR, the electrode is melted into a water-cooled crucible. The melting is accomplished by initially striking an arc between the electrode face and the crucible stool. The arc melts the electrode face and the molten metal collects into drops which fall into the crucible to form an ingot against which the arc is maintained. Because there is no additional source of heat (as, for example, the cap of molten slag in ESR) and no insulating slag skin on the ingot, heat extraction in VAR is greater than in ESR. Thus the profile of the molten zone in VAR is generally shallower (than in ESR) for any given alloy, melt rate, and ingot diameter combination.

There is no compositional change in VAR with the exception of minor elements with high vapor pressures. Thus, residual amounts of detrimental elements such as bismuth and lead may be removed by VAR. Unfortunately, volatile elements such as magnesium (used for control of sulfide shape) are also removed. The removal of magnesium is generally compensated for by providing an elevated level in the primary melt process.

### 5.3 Pros and Cons of Remelted Ingot Processing

In VAR the interface between the ingot and the crucible does not contain the slag skin found in ESR. Instead, the surface of the ingot, being the first material to solidify, is low in solute elements. More importantly, any oxides or nitrides from the electrode are swept into this surface layer as they melt out of the electrode and onto the surface of the molten pool. This layer is called a “shelf.” A disruption in the arc stability may cause the arc to undercut a small section of this shelf. If this section drops into the pool, it is unlikely to remelt and thus forms an alloy lean “spot” which contains layers of entrapped oxide and nitride (“dirt”). These inhomogeneous regions are light or “white” etching and are known as “dirty white spots.” Their generation is triggered by conditions which do not generally leave any electronic signature (at current levels of detection capability) in the VAR records. While robust VAR process parameters and good electrode quality may minimize the frequency of dirty white spot occurrence, their formation cannot be completely avoided. Thus, the possible presence of dirty white spots in a component (and the degree of their degradation of properties) must be considered in material/melt process selection for a component.

In selecting ESR as the secondary melt practice, positive considerations are that ESR does not generally form dirty white spots, that ESR products may also have better hot workability than VAR products, and that the process yield may be modestly higher (lower cost). A negative consideration is that ESR products cannot be made in large ingot sizes (compared to VAR) without the formation of freckles. The state of the art in ESR controls is such that, at sizes where ESR will normally not form freckles, some undetected abnormality in the melt may cause sufficient disruption that freckles will be produced anyway. ESR is not a robust process

(with regard to avoiding defect formation) when operated towards the extreme end of its size capability. However, advances in ESR controls have allowed commercially useful ingots of ESR Waspaloy to be produced while maintaining an adequate distance from the melt regimes where freckle formation would become a concern. More highly alloyed materials (such as IN 718) cannot yet be robustly produced by ESR in similar sizes.

In selecting VAR as the secondary melt practice, positive considerations are that (for a given alloy) VAR will produce a larger ingot (than ESR) without the presence of freckles and that at the selected size the process should be much more robust (in freckle resistance) than is ESR. The principal negative considerations are that dirty white spots will exist in the ingot and that they cannot be detected or their removal assured.

Several producers of critical rotating components in the gas turbine industry have adopted the use of a hybrid secondary melt process. VIM is used to ensure a low-oxygen and nitrogen content precise chemistry initial electrode followed by ESR. The ESR electrode will be clean and sound but may contain freckles. The clean, sound electrode is then remelted by VAR. The improved cleanliness and soundness of the electrode facilitate VAR control. This product (referred to as “triple melt”) has a much reduced frequency of dirty white spot occurrence compared to standard double-melt (VIM + VAR) product. However, even in triple melt, dirty white spots will occur and must be considered in the component design. The trade-off is the additional cost of an extra processing step vs. the enhanced resistance to premature component failure from dirty white spots.

#### 5.4 Melting Considerations in Alloy Selection

As noted earlier, superalloys not only are available in standard mill forms (plate, sheet, and bar—from which components may be machined) but also may be produced as specific component shapes by the use of forging or casting. It is critically necessary that the property requirements of a component be fully understood. For instance, a component selected to resist corrosive attack may not need to be melted by a process that assures fatigue resistance.

The most critical feature of melt process selection is the size of the component to be manufactured from an ingot. The larger components require larger ingot sizes. As previously discussed, the more highly alloyed a material, the greater the restriction of maximum ingot size. For forged components consideration must be made not only of the final component size but also of the capability of the ingot to be sufficiently deformed to develop the properties characteristic of a forged structure. Internal cleanliness is also a consideration in selecting the melting route.

Generally, for fatigue-sensitive components, a melt practice is selected which will guarantee the absence of freckles from the structure. For larger size components this favors a final melt by VAR rather than ESR. However, while the absence of freckles may be guaranteed, there are no active VAR practices that can guarantee the elimination of dirty white spots. Thus, any component designed with a final melt practice of VAR must be designed with stress assumptions made assuming a specific flaw size is present in the new product. The flaw size is, of course, determined by knowledge of white spot frequency, size, and location within the component (for a specific alloy composition and melt route). White spot frequency and radial location in an ingot vary not only with ingot size but also with the precise melt conditions chosen to produce that size.

In forged applications the use of the triple melt process (VIM/ESR/VAR) is increasing as it has been demonstrated that this process reduces the frequency of dirty white spot formation while also it may be inferred that the average size of the dirty white spot is decreased. Further improvement in reduction of white spots may be made by a fourth melt (VIM/ESR/VAR/VAR). This process is not currently used commercially but may eventually be found useful for very high strength, highly stressed, freckle-prone alloys not produced by a powder metallurgy route.

For alloys such as Waspaloy, which may be produced in useful (for disk forgings) freckle-free ingot sizes, the process VIM/ESR is often chosen because of its complete freedom from formation of dirty white spots. VIM/ESR also may be selected for production of mill products whose manufacture does not require large initial ingot sizes.

For alloys to be used in the chemical industry, principally as sheet and plate, the need to assure absence of freckles may not be critical, although possible pinhole corrosion at freckles must be considered. These alloys are commonly produced by VIM/ESR or Arc-AOD/ESR. A driving force for the use of ESR is that ESR of rectangular shapes (slabs) is common. This allows the direct rolling of such alloys for flat mill products rather than the introduction of an intermediate forging process to reduce round ingot to slab.

In summary, it should be noted that no superalloy melting process produces a truly homogenous and uniform product. Specifying that the melted ingot *will* be uniform does not change the result. It is incumbent upon the component designer to understand the real and differing nature of each melt practice and select that practice which produces the properties needed while having the size capability to allow the component to be manufactured.

## 6 COMPONENT PRODUCTION

### 6.1 Casting Practices to Produce Parts

Casting is a manufacturing technology that takes a piece of non-useful metal, melts the metal, and creates a useful component via a casting mold. The principal casting practice for superalloy components is investment casting (also known as the lost wax process). This process is chosen since it can mass produce complex, near-net-shape component geometries to precise tolerances so that extensive machining of the component is not necessary after fabrication. Since the superalloys cast for aerospace components are quite expensive, conservation of metal is highly desirable. In addition, investment casting can create complex features internal to the components which can allow for weight reduction or for active cooling of the component during high-temperature operation. Much advancement has occurred in development of internal features that can enable more efficient and effective heat exchange to enable aerospace components to operate at high temperatures. For jet engine applications, this allows for improved fuel consumption, increased thrust, and lower nitrous oxide emissions.

The process begins with the creation of a tool or die that can create a wax replica of the component to be cast. This tool can be made of aluminum or steel depending on the quantity of parts to be produced. The tool is created through a series of milling and electrode machining operations to create a negative cavity inside the tool having the external geometry of the part to be manufactured. A wax replica of the component to be manufactured is created by injecting a molten wax material into the machined die and held until solid at which time it is removed from the die. The resultant replica is known as a wax pattern. The creation of a wax pattern via a permanent tool provides an economic advantage since many patterns can be made in a reproducible manner. If a hollow component is desired where the internal features are too fine to be created by the normal process, a positive replica of the negative hollow passage is created by fabrication of another injection tool. This tool also contains a machined cavity into which a ceramic formulation is injected to form the positive replica known as a ceramic core. This ceramic core requires removal from the tool after injection followed by a high-temperature firing cycle in a kiln to sinter the ceramic particles together. Once fired, the hardened ceramic core is placed into the wax injection die so wax can be injected around it. The wax pattern that is created has the external geometry formed by wax while the internal geometry is formed by the prefabricated ceramic core.

After wax pattern creation, a series of wax patterns are joined to gating that will provide metal flow from a central pour cup to the individual parts on the assembly. The pour cup,



gating, and component patterns are all created from wax and assembled together via hot irons or tools to create a wax assembly. For smaller parts, many wax patterns can be combined on the assembly, while for larger parts, a single component may be placed on the assembly. The gating is designed to allow for each part on the assembly to fill while providing extra metal to “feed” the parts until completely solid. The wax assembly is then coated (invested) with appropriate ceramic typically in a sequential fashion where a ceramic slurry suspension is applied followed by an application of dry ceramic particles known as stucco which adheres to the wet slurry via surface tension. The slurry fills in the details of the component while the stucco provides strength (like brick and mortar). Once a slurry/stucco layer is applied, the assembly is dried in a temperature- and humidity-controlled manner to dry the ceramic. This process is repeated many times until a ceramic “shell” is created on the outside of the wax assembly. The number of layers is dictated by the size of the mold to be cast and the amount of metal that will be eventually poured into the shell during the casting process.

After shell creation, the wax must be removed from inside the shell to create a hollow casting “mold” that can receive molten metal. To create this ceramic mold, the shell is dewaxed by placing the shell in a pressure vessel where superheated steam will be quickly introduced to remove wax without expansion to avoid cracking the ceramic shell or mold. After dewaxing, the ceramic shell is placed in a kiln and subjected to high temperature to sinter the ceramic particles together creating a stable, ceramic mold that has the strength to receive molten metal during casting. This ceramic mold is then cleaned, inspected, and prepared for casting.

To perform casting, a small amount of a vacuum induction melted master alloy is remelted and cast into the mold. The size of metal charge is dictated by the number of parts to be cast in the mold and the amount of gating that is feeding the parts. In some applications, a ceramic filter may be used to clean the VIM alloy before it enters the mold. After molten metal is poured into the ceramic casting mold, solidification of the metal will occur. Upon solidification, a series of components in the desired form are created. These objects, frequently gas turbine hot section airfoil components, are removed and then machined and processed to desired dimensions. For hollow components, the ceramic core inside the metal casting is removed by placing the parts in a heated pressure vessel filled with a caustic chemical which will dissolve the core, leaving behind a hollow passage. The investment castings are then inspected using x-rays to check internal quality, fluorescent penetrant inspection for external quality, ultrasonic for wall thickness, and dimensional inspection using coordinate measurement machines or bench gages.

Superalloy investment castings now are available in sizes from a few inches in length up to about 50 in. diameter/length. Turbine airfoils can now be made not only for aircraft gas turbines but also with airfoil lengths of several feet for land-based power turbines.

If hot molten metal is poured into a colder casting mold, a conventional polycrystalline (PC) investment casting is produced with more or less randomly oriented grains. The grains result from the randomness of solid production in the molten liquid metal. Many collections of solidified atoms grow from the mold surface inward in a direction normal to the mold surface and opposite to the direction of heat extraction. The inwardly growing crystals will eventually collide with one another, forming grain boundaries that must be strengthened by specific elements that create strengthening phases.

Mechanical properties of PC castings are nominally random but may show some directionality. Increased property strength levels have been achieved by columnar grain directional solidification (CGDS) which removes grain boundaries that are perpendicular to the applied principal load in turbine airfoils. Removal of these grain boundaries dramatically improves longitudinal (parallel to airfoil axis) creep rupture properties of nickel-based cast superalloys. Transverse boundaries continue to be a problem but are minimized by the addition of hafnium, which enhances grain boundary ductility. This CGDS structure is attained by pouring hot metal into a hotter mold and attaching the mold to a chillplate which will extract heat directionally downward. This directional heat extraction will cause the crystals to form directional columns. These directional columns will continue to grow parallel to each other by assistance

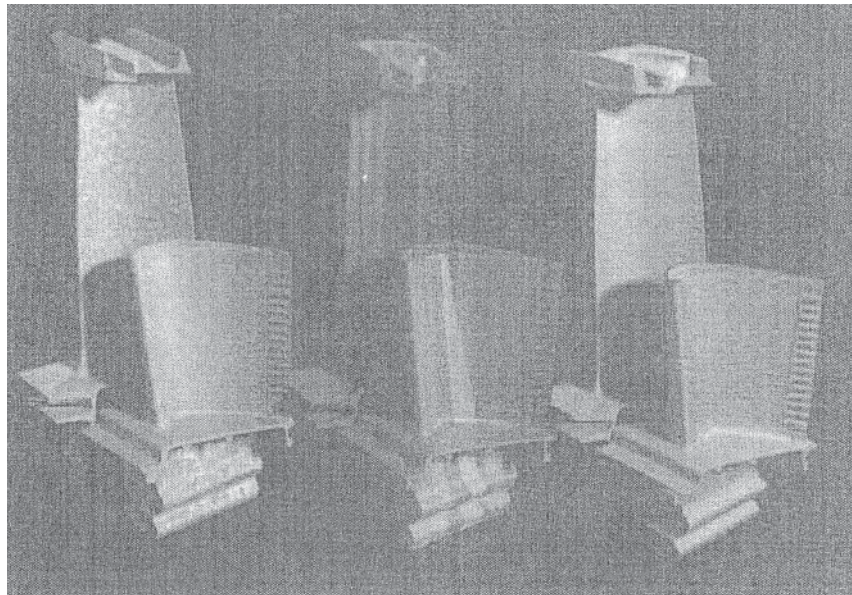
of a mechanical withdrawal of the mold from the hot portion of the furnace to a colder portion of the furnace.

The ultimate solution is to directionally solidify (DS) a superalloy as a single crystal, i.e., a superalloy with no grain boundaries. This is achieved in a similar manner as a columnar grain casting but a grain selector is used during the withdrawal process to preferentially “select” a predominant crystal orientation which will grow throughout the part to be manufactured. Through this method, a casting is created which has all the atoms stacked in a repeating orientation creating a single crystal with no grain boundaries. Maximum creep rupture strength in nickel-based superalloys now is achieved with single crystal directionally solidified (SCDS) alloys. SCDS has been applied not only to aircraft gas turbine engines but also to large-frame land-based gas turbines. Much progress has been made both in casting process development as well as alloy development to enable parts to operate at higher temperatures and/or longer times in their service application. Large, fully automated furnaces with advanced process control can make improved quality castings with high reproducibility. Alloy development has enabled the development of second-generation columnar grain directionally solidified alloys and fifth-generation single-crystal alloys.

An interesting benefit of directional solidification in nickel-based superalloys is the reduction of the elastic modulus in the primary solidification direction (parallel to the longitudinal axis). *Reduced moduli* means less thermal stress on hot-section airfoils and thus longer life in TMF.

## 6.2 Casting Considerations in Alloy Selection

Selection of cast superalloys is best conducted in conjunction with an investment casting foundry which can indicate the likelihood of success in casting a given design in the alloy selected. Figure 7 shows shapes and surface appearance of turbine blades produced to the three standard casting conditions (equiaxed, columnar grain, and single crystal). These parts



**Figure 7** Turbine blades produced by equiaxed grain (left), directionally solidified polycrystal (center), and directionally solidified single-crystal (right) casting processes



also contain complex internal cooling passages that effect the necessary cooling required for airfoil operation in ultra-hot-gas streams.

Not all alloys are equally good for casting. Casting defects occur and vary with the alloy composition and casting practice. Oxide (dross) carried over from the master melt may cause surface and internal inclusion problems. Porosity is another major concern, especially with large castings for the cases of gas turbines. Porosity may be controlled by mold design and pouring modifications. Non-surface-connected porosity may be closed by hot isostatic pressing (HIP) of cast articles. Surface porosity in large castings may be repaired by welding. Ceramic inclusions that evidence themselves as surface pits or subsurface x-ray indications could result from the breakdown of the ceramic crucible used for melting, ceramic filter media, or the ceramic shell. Metallic inclusions can also result from the improper melting of alloy elements or segregation of the elements during casting. Other casting concerns have included intergranular attack (IGA) caused during chemical removal of molding materials, selectively located coarse grains in PC materials, misoriented grains, and spurious grains in directionally solidified (DS), materials, etc. Alloys may be modified in chemistry to optimize product yield but with a possible compromise in properties. Product yield is an important determinant of final component cost.

### 6.3 Wrought Processing—Forging and Powder Metal Superalloys

Forging is the most common method of producing wrought components for superalloy applications. In the instance of gas turbine disks, the forging process requires the application of heat and pressure to move the alloy from its billet or powder metallurgy preform stage to a stage ready for machining to a finished disk. Forging normally consists of applying compressive loads by hydraulic or mechanically operated presses which can be very large. Forging is done hot, normally under continuously dropping temperatures. Some forging is done isothermally with appropriate techniques to maintain constant temperature. Forging or other forming techniques may produce mill products such as bar stock, wire, etc. However, the most demanding component applications such as gas turbine disks require the use of forged wrought ingot or powder metallurgy components. Disks are forged to near net size or to approximate shape using large presses with input stock from billets previously produced from consumably remelted ingots or consolidated powder. Forging processes may occur with flat platens but normally dies are used. Dies may be of relatively simple shape (blocker dies) to move metal around, but for maximum utility in manufacture and optimum strength, dies will produce an approximation of the desired final shape. Multiple intermediate shape stages usually are involved when conventional forging is practiced. Isothermal (usually superplastic) forging may go directly from billet to final stage in one step. Dies are very expensive to make and impact the cost of the final forged product. The actual forging temperatures needed will also affect heating costs. A great deal of effort has been expended in attempts to produce net shape forged gas turbine disks but only near-net-shape forgings normally are possible from a technical and economic standpoint. Finish forged products still will need to be machined to final shape.

The resultant strength of forged components is affected by the thermal–mechanical treatments introduced in the forging cycles plus the actual heating cycles given to the forged component as it receives processing to desired dimensions. Grain size is a function of the forging process and in-process heat treatments and can be controlled to fairly precise tolerances. Actual hardening and other phase distribution are a function of forging and final heat treatment. Generally, working a metal by wrought processes followed by final heat treatment produces better strength properties than those achieved by heat treatment alone. Defects in conventional ingot metallurgy forged products are primarily a function of the prior melting history though, under some conditions, they may be a result of the forging and heating process.

In addition to uniaxially operated presses, rotary forging has been applied to produce symmetrical components of extended length such as gas turbine shafts. Such forging practices and machinery have also been employed in the transition of cast ingots to the billet dimensions required for forging of components.

As alloy strengths increase, it becomes increasingly difficult to move the alloy around during forging. When higher pressures are required, defects became more probable. Superplastic forging (isothermal forging) became available in the time frame when the strengths of superalloys were bumping up against metallurgical limits. Simultaneously, the discipline of powder metallurgy (PM) opened the way to create billets of the highest strength alloys without the positive segregation defects (of alloy elements) that made casting and forging of billets to final parts so difficult.

In powder metallurgy, used principally for alloys such as René 95 or IN 100 or similar advanced alloys, a preliminary ingot is remelted and then atomized to small droplets that solidify as “miniature ingots” with limited or no segregation of alloy elements. The powders are transformed to forging billets by HIP and/or by extrusion and processed to achieve 100% density. The aggregates are homogenous and display uniform properties. Sometimes the powder is pressed directly to form a near-net final size/shape, but usually the powder is compacted to an intermediate stage (e.g., extruded billet) and forged (often isothermally) to very near net shape. Powder metallurgy is expensive, but the savings in subsequent machining costs, the ability to control defects, and the ability to use very high strength compositions make a reasonable cost trade. Possible defects in PM include carbide stringers, ceramic inclusions, and “reactive” inclusions (e.g., hair) from the powder production process.

Conventional alloys such as Waspaloy, U 720, IN 718, and IN 718+ are produced by ingot metallurgy and standard forging practices. High-strength alloys such as René 95, IN 100, and René 88 generally are produced using powder metallurgy techniques.

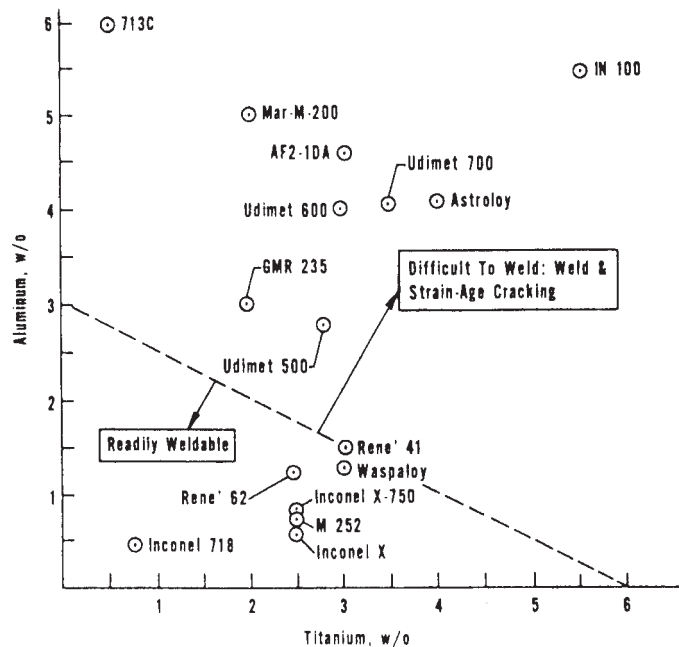
#### **6.4 Wrought Processing—Forging/Working Considerations in Alloy Selection**

The stronger the alloy to be utilized in design, the more difficult it will be to manipulate by mechanical working forces. Limits exist on the capability of an alloy to be worked without cracking, encountering other defects or stalling a forge or extrusion press. Some shaping equipment such as rotary forging devices may be better able than other equipment to change the shape of the stronger superalloys. Powder metallurgy offers an alternative processing route for high-strength alloys used for rotating disks, shafts, hubs, etc., in aircraft and power generation turbines. Powder production reflects an art that is not always directly transferable from one producer or one alloy composition to another. Powder components are best made by producing an ingot from powder and then forging the ingot to component shape. Extensive work with an alloy melt shop and an associated powder producer may be necessary to create a satisfactory metal powder of an alloy selected for design.

#### **6.5 Joining**

Welding and brazing are used to manufacture some superalloy components, but superalloy castings have been employed to reduce component complexity and the need for welding in manufacture.

Components of superalloys often could be repaired by joining processes in the fledgling days of the superalloy industry. That is not necessarily true today for most very high temperature of operation components such as turbine blades. Cobalt-based superalloys, which do not depend on precipitated phases for strength, are generally amenable to fusion welding.



**Figure 8** Weldability diagram for some  $\gamma'$  strengthened nickel-based superalloys showing the influence of total age-hardening elements. Source: *Superalloys*, Vol. 2, Wiley, New York, 1987, p. 152. Used with permission.

Sheet metal structures are routinely fabricated by welding for superalloys. Repair welding of some cobalt-based superalloys is practiced. Wrought iron–nickel-based superalloys can be welded as can solution-hardened (i.e., non-precipitation-hardened) wrought nickel-based superalloys, but precipitation-hardened versions are welded with difficulty. In-process welding may be used to repair surface defects in weldable superalloy components such as large castings. Properties of precipitation-hardened alloys are degraded by the heat of the joining process, and such alloys become increasingly more difficult to weld as the amount of hardener in an alloy increases. Figure 8 shows a relationship between hardener content and weldability for nickel-based superalloys.

Inertia bonding is used to join nickel-based superalloys, but conventional fusion welding is not customarily used, although electron beam welding is possible. Other solid-state joining processes such as transient liquid-phase (TLP) bonding have been used with some measure of success.

The essence of the joining situation for superalloys is that precipitation-hardened nickel-based airfoils generally are not repair welded if cracks appear. Cobalt-based nonrotating airfoils, on the contrary, may be welded to extend life. Sheet metal of cobalt-based, solid-solution-strengthened nickel-based and of lower hardener content nickel-based alloys can be joined as can iron–nickel-based alloys. The higher strength nickel-based alloy of choice for welding is IN 718, which, owing to the unique aspects of its hardening by gamma double prime, can be fusion welded with relative ease.

## 6.6 Summary of Component Production

Figure 9 presents a view of the superalloy manufacturing process. Many producers have been involved in the business of producing superalloys over the years. During the past 70 years of progress, many advances have been made. New companies have formed and others have merged or gone out of business. Some sources of superalloy expertise in ingot melting, component forging, and article casting are listed in the section below.

## 6.7 Some Superalloy Information Sources

This is only a partial list. More information as to websites, locations, etc., is available. Only some of the institutions active in superalloy technology are represented. No recommendation is made or implied by this list.

### *General Information*

ASM International, Materials Park, OH [www.asminternational.org](http://www.asminternational.org)

Nickel Development Institute, Toronto, ON, Canada [www.nidi.org](http://www.nidi.org)

Cobalt Development Institute, Guildford, Surrey, UK [www.cobaltdevinstitute.com](http://www.cobaltdevinstitute.com)

International Chromium Development Institute, Paris, France [www.chromium-assoc.com](http://www.chromium-assoc.com)

Specialty Steel Industry of North America, Washington, DC [www.ssina.com](http://www.ssina.com)

The Minerals, Metals & Materials Society of the American Institute of Mining, Metallurgical and Petroleum Engineers, New York, NY [www.tms.org](http://www.tms.org)

Investment Casting Institute, Montvale, NJ [www.investmentcasting.org](http://www.investmentcasting.org)

### *Industry- or Component-Specific Information*

Information may be found from other more specific sources by searching under headings such as Melting/Ingot Production, Forming and/or Mill Products, Investment Castings, Forgings, Coating and/or Refurbishment/Repair.

No list is provided owing to the frequent ownership and/or name changes of businesses/organizations in the superalloy field.

### *Comments*

The above list may change with time and should only be used as a guide to locate potential suppliers. Most high-end consumers deal with the forging and investment casting vendors who produce the product for subsequent final processing. For best control of properties, many consumers maintain liaison with melters and frequently audit all aspects of the manufacturing process. It is vital to remember in superalloy selection that most superalloys are not off-the-shelf consumer items. They are made to user specifications which may vary from user to user and time to time. Diligence in working with the producers will pay dividends in obtaining optimum properties and reducing difficulties for users of superalloys. This concept is indigenous to the industry and widely followed by superalloy users of components for mission-critical or human-life-critical applications. It is more costly than buying off-the-shelf. For some applications such as in oil development or coal gasification, there may be less stringent controls that permit off-the-shelf purchase of generic mill products. However, no forging or investment casting is an off-the-shelf item.

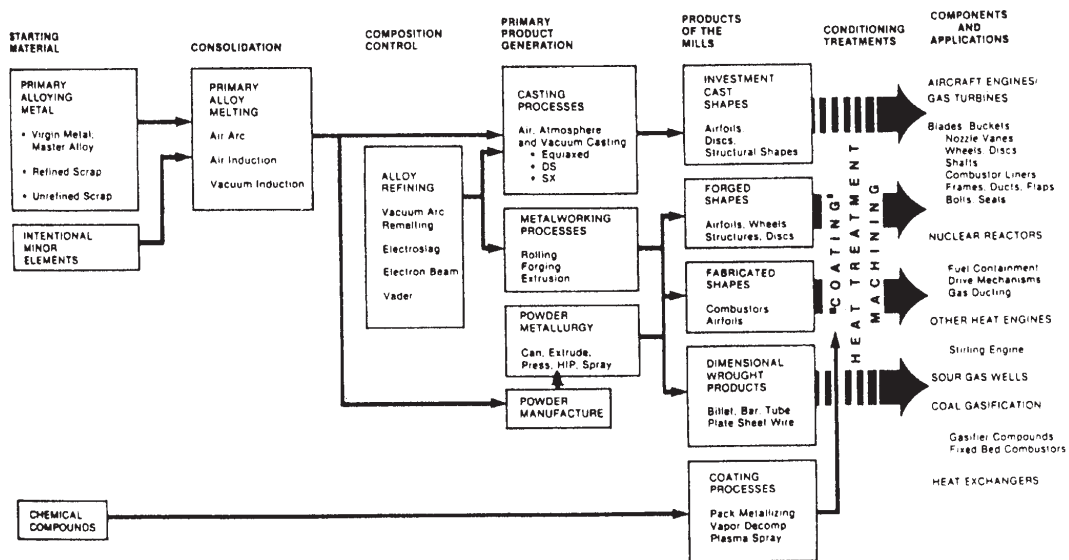


Figure 9 View of the superalloy manufacturing process. Source: *Superalloys*, Vol. 2, Wiley, New York, 1987, p. 23. Used with permission.

## 7 OTHER ASPECTS OF SUPERALLOY SELECTION

### 7.1 Corrosion and Coatings for Protection

Initial superalloys were intended to have both strength and adequate oxidation resistance, and this was accomplished with superalloys which contained upward of 20 wt % chromium. Oxidation resistance up to temperatures around 982°C (1800°F) was excellent. However, as suggested earlier, in order to increase the design flexibility of nickel-based superalloys, chromium content was reduced so that more hardener could be added. Concurrently, some superalloys were put into service in environments (e.g., marine salts) that intensified oxidation or ion-induced attack such as hot corrosion. Also, the operating temperatures (surface environment temperatures) to which the alloys are exposed in the most demanding high-temperature conditions have increased with the strength capability increases of the available alloys.

At higher temperatures, the chromium oxide formed during prior heat treatment is less protective and does not regenerate with exposure to high temperatures. General oxidation and intergranular oxidation along the grain boundaries of superalloys are a problem with chromium-protected superalloys. However, the problem is not as great as initially anticipated owing to the protective nature of aluminum oxide formed in greater amounts by the higher aluminum values of second- and third-generation gamma-prime-hardened superalloys. Nevertheless, general oxidation still occurs and causes reduced cross sections, thus effectively increasing stresses on the remaining material. Grain boundary oxidation creates notches. The combination of these events is of concern, and to protect against them, coatings are applied to superalloys.

The early coatings were diffusion coatings produced by pack aluminizing or slurry application. Chemistry of the coating was determined by the chemistry of the alloy. Later coatings were produced by overlaying a specific chemistry of a protective nature on the surface of the component using physical vapor deposition. Diffusion-type coatings can coat internal (non-line-of-sight) surfaces while the overlay coatings can only coat external surfaces that can be seen by the coating apparatus. Diffusion coatings are cheaper and, for a given thickness, probably nearly as protective as overlay coatings. Diffusion coatings are used to coat internal cooling passages in hot-section airfoils. Some commercial diffusion coating processes are available, but most overlay coating processes are proprietary, having been developed by superalloy users such as the aircraft gas turbine manufacturers. However, overlay coatings can be made nearly twice as thick as the diffusion coatings so overlay coatings often are the coatings of choice for turbine airfoil applications. Overlay coatings also have the advantage of the ability to alloy the coating with various elements that can enhance oxidation behavior. The added thickness of overlay coatings lends itself to better oxidation performance but reduces the component thermal fatigue life.

Overlay coatings are generally more expensive than diffusion coatings. Some diffusion coatings are deposited in conjunction with precious metals such as gold or platinum. There are significant benefits to this incorporation of the noble metals in the coating if the application can justify the increased cost. Overlay coatings can be applied by various processes such as electron beam physical vapor deposition (EBPVD) and plasma spray (PS). In EBPVD, a container of alloy powder or an alloy ingot is vaporized by an electron beam while the part to be coated is suspended above the vapor source. The thickness of coating is determined by the time of part exposure and the temperature of the vessel. In PS, alloy powder is transformed into high-temperature plasma by an electrical arc and propelled toward the component to be coated by a carrier gas. This PS process uses less material than EBPVD. These processes can also be used to apply thermal barrier ceramic coatings which can act as a heat shield onto metallic overlay coatings. Owing to the physics of the deposition processes, the chemistry of the coating ingot or powder may differ from the final deposited coating chemistry.

Coating and corrosion technology are complex and do not lend themselves to a simple overall description and formula for protection. Hot-corrosion phenomena are found below a nominal temperature of 927°C (1700°F). Coatings and higher chromium content in an alloy

inhibit surface attack. Coatings, in general, preserve the surface so that a component may be reused by removing and then restoring the coating.

Coating selection is based on knowledge of oxidation/corrosion behavior in laboratory, pilot plant, and field tests. Attributes that are required for successful coating selection include:

- High resistance to oxidation and/or hot corrosion
- Ductility sufficient to provide adequate resistance to TMF
- Compatibility with the base alloys
- Low rate of interdiffusion with the base alloy
- Ease of application and low cost relative to improvement in component life
- Ability to be stripped and reapplied without significant reduction of base-metal dimensions or degradation of base-metal properties

## 7.2 Special Alloys for Hot-Corrosion Resistance

As temperature decreases below 927°C (1700°F), the amount of hot-corrosion attack decreases until, at a nominal temperature below 760°C (1400°F), attack may begin to increase dramatically with decreasing temperature. In this regime, the province of land-based power gas turbines, attack is resisted best by forming chromium oxide on the surface. Consequently, alloys for this region and application are those such as IN 738, specifically designed to have higher chromium levels, sometimes above 20 wt %. (IN 939 is an alloy in this latter category.) Other alloys have been devised for optimum hot-corrosion resistance at temperatures above 760°C (1400°F). René 80 and IN 792 are such alloys.

## 7.3 Thermal Barrier Coatings

Allied with superalloy protective coating technology is the development of ceramic, so-called thermal barrier, coatings (TBC). TBCs protect components by reducing surface temperature by several hundred degrees, enabling a superalloy to operate at lower temperatures in a region where the superalloy may have higher strength. TBCs have found use on a wide range of alloys. TBCs use overlay coating technology such as EBPVD, chemical vapor deposition, or plasma spray technologies. A thin metallic overlay coat serves as the bond interface between the ceramic of the TBC and the base superalloy. The structure of the deposited layers can enhance the mechanical properties of the coating systems to optimize life.

## 7.4 Postservice Refurbishment and Repair

One important aspect of modern superalloy use is the concern for extending service life of components. Cracking, erosion/corrosion of surfaces, and mechanical property loss are major economic factors in successful component applications. These factors have become of greater interest as the base cost of materials and subsequent components has risen dramatically over the past 40 years. Primary attention to alloy selection has been given with regard to initial producibility and material properties. However, in service, when public safety consideration limits or product integrity design limits are reached after service, costly components may be withdrawn from use. Some components may appear to be unaffected by service time. For economic reasons there may be incentives to return these components to service.

Other components after service may have visible changes in appearance. For example, a high-pressure turbine blade may be missing a coating in the hottest regions of the airfoil or a



crack may develop in a vane airfoil. Seals may be worn. It is highly desirable that such damage can be repaired so that the costly parts can be returned to service.

If possible, superalloys would be selected on the basis of restoration of capability after initial capability has (apparently) been reduced by service exposure of the component. However, most applications do not permit alloy selection on that basis. The best alloy from a property and initial economic viewpoint is usually the choice. However, it is common practice to refurbish or repair many components (usually stationary parts) which have visible external changes. It is not practical to describe most of the varied refurbishment and repair schemes in effect for superalloys, but a brief summary will indicate the range of opportunities possible.

Stripping and recoating of turbine airfoils is one refurbishment and repair practice. Oxidation- and corrosion-resistant coatings and TBCs may be reapplied (after appropriate surface cleaning treatments) to restore resistance of the surface to heat and gaseous environments. In the case of missing, eroded, cracked, and/or routed material, welding traditionally has been used to fill the gaps. Welding of high-strength nickel-based superalloys is very difficult, if not impossible. Welding of solid-solution-hardened nickel-based alloys such as Hastelloy X and of lower strength precipitation-hardened nickel-based alloys is more readily accomplished. However, of the high-strength alloys, only IN 718 precipitation-hardened alloy (cast or wrought) may be considered truly weldable. Welding of (lower strength) cobalt-based turbine airfoil and sheet materials also is accomplished readily. Welding is followed by machining, possible heat treatment, and coating.

Instead of fusion welding, some repair shops have been using HVOF (high-velocity oxy fuel) processes to deposit repair material and methods such as HIP are then used to densify the deposited material. Other processes which rely on laser buildup of material are claimed to be viable as repair processes for eroded surfaces. The main characteristic of refurbishment and repair processes is both the restoration of geometry and the provision of adequate mechanical properties in the repaired area. Care must be taken to assure that no additional alloy degradation occurs owing to the refurbishment and repair practice.

The restoration of mechanical properties degraded by creep and/or fatigue is not as clear cut as stripping and recoating or insertion of material by welding or HVOF or similar deposition processes. Creep degradation of superalloys can occur by changes in microstructure or formation of pores, especially along grain boundaries. Re-heat treatment may restore or nearly restore the original properties to the original microstructure put into service. HIP may close pores. In the laboratory, re-heat treatment, including HIP, has been shown to restore the mechanical properties of some superalloys after service exposure. The degree of restoration is a function of the mechanical history of the component.

Property degradation cannot be measured nondestructively. Extensive records of service operation and a statistical record of how a given alloy performs in a specific service application are required to make an educated guess as to the amount of prior damage a component has received and the potential for recovery of mechanical properties by re-heat treatment. Results of re-heat treatment of service exposed parts are variable. Most post service procedures do not provide specifically for mechanical property restoration.

Selection of refurbishment and repair processes for superalloy components must be as rigorous as the processes followed for original material selection. Indeed, refurbishment and repair processes may have to be held to even higher standards since the material being returned to service may have hidden damage and/or property loss. Development and selection of a particular refurbishment/repair procedure should be undertaken with a suitable supplier of such services. A robust process validated by a comprehensive test program should be followed before approval is granted to use any refurbishment and repair procedure. Appropriate metallurgical assistance should be sought during the development of such procedures.



## 8 ALLOY SELECTION SUMMARY

### 8.1 What Alloys Are Available Off the Shelf for Intermediate Temperature Applications?

Wrought alloys generally are used. Waspaloy, René 41, and Astroloy are standard nickel-based superalloys selected in the past. Waspaloy and René 41 are readily available but Astroloy may not be as readily procured. Wrought U-720 has found use in many applications. IN 718 is the number one choice for intermediate temperature applications such as gas turbine disks but, when a higher temperature capability is required, Waspaloy or similar alloys may be used. IN 718+ offers up to 100°F temperature capability improvement over IN 718 and is claimed to be comparable to Waspaloy in strength capability. Other alloys and techniques exist for more advanced temperature applications. However, proprietary considerations normally make such alloys unavailable for general use.

Castings may be used for some applications of significant physical size. Large case structures for gas turbines are routinely cast of IN 718. However, in other instances, wrought alloys generally are used. Ductilities and fracture toughness of wrought alloys are better than those of cast alloys. Strength in tensile tests usually are better too. Creep may be of concern, but rupture life normally is not an issue. Iron–nickel alloys such as A-286 might be considered as they may have sufficient strength and will be considerably less costly than their nickel-based counterparts. A modification of A-286, 286 LNi, is claimed to have A-286 properties at a reduced cost. The most prominent alloy for intermediate temperature applications continues to be the nickel-based (sometimes called nickel–iron-based) superalloy IN 718.

IN 718 is the most widely used superalloy today. As a wrought alloy, it can be made in various strength levels and in very large ingot sizes. It is the most weldable high-strength superalloy available. As a casting, IN 718's weldability is a significant factor in its application as large cases.

Costs of IN 718 are lower than some other superalloys because of the widespread use of the alloy. As mentioned above, IN 718 is unique in that it contains none of the strategic element cobalt. IN 718 received a significant application boost in the late 1970s when a cobalt “shortage” caused the price of cobalt to soar to astronomical levels. IN 718 at that time faced continued competition from alloys such as Waspaloy and Astroloy. The lack of cobalt in the alloy swung the design pendulum to IN 718, and in the succeeding four decades, IN 718 has solidified its position as the most used superalloy.

In lieu of IN 718, alloys such as Waspaloy, U-720, IN 718+, and others can be and have been adapted to aircraft gas turbine designs. Cost increases are normally obtained for use of such alloys, but they are frequently used in lieu of higher temperature capability powder metal processed high-strength superalloys such as IN 100 or René 95.

### 8.2 Comments on Wrought Alloys for Intermediate-Temperature Applications

Powder metal techniques allow IN 100, René 95, and other high-strength and damage-tolerant alloys to be fabricated and used at the highest temperatures reached by wrought alloys. An important trend in the intermediate-temperature area is the development of dual-material/property gas turbine disks. One of the major concerns for gas turbine disk operation is the difficulty of getting all desired properties in one material. Extensive work has been done to validate the position that a disk may be made of more than one material. Demonstrations have shown that creep-resistant rims can be attached to the brute-strength and fatigue resistance cores of disks. Selection of materials and processes for such an application, however, requires extensive alloy/process development.

An alternate process used to produce dual-property disks is to apply selective heat treatments to the desired alloy such that a creep-resistant rim is created while a high-tensile-strength

and burst-resistant bore is created. Published work shows that such a process can be applied. Production costs for dual material or dual heat treatment of a given material have not been published but certainly will exceed the customary forging and heat treatment costs.

For massive applications such as turbine disks, high tensile yield and ultimate strength are desired. Good tensile ductility is important and good mechanical LCF behavior with acceptable crack propagation rates at expected loads is a must. Massive parts such as disks can benefit from good forgeability but such forgeability does not exist when high-tensile-strength superalloys are required. Powder metallurgy processing enables creation of forged components not otherwise producible. Sonic inspectability of finished shapes is crucial. Cost is a very important factor, but one that may have to be subverted to properties and processing if a desired component is to be made. Of course, use of special processing techniques such as powder metallurgy may enable a part to be formed that could not be made in any other way and so a high cost may be worth paying.

The essence of superalloy selection for intermediate-temperature applications is that there are standard alloys of strength capability up to the levels achieved in Waspaloy and René 41 that can be procured and forged by conventional means. There are specialized powder metallurgy alloys available to achieve the highest strengths possible in wrought nickel-based superalloys for massive applications such as turbine disks. For the highest strength, higher temperature applications, there normally are no easy off-the-shelf technologies or alloys that can just be picked from a catalog and put to work. Selection of alloys is a preliminary step that must be expanded upon to obtain property data and components in a reasonable time frame at acceptable costs.

### 8.3 Comments on Wrought Alloys for Intermediate-Strength Higher Temperature Applications

In the gas turbine industry, sheet metal may be needed to fabricate portions of combustor chambers. If an alloy is to be used as sheet, particularly for very high temperature applications, then reasonable strength coupled with good corrosion resistance will be required. Of course, good formability is a must, coupled with good weldability when considering sheet alloys.

The highest temperature applications invariably require cast superalloys where the requirement of maximum high-temperature strength is concerned. However, some applications, such as combustion chambers where sheet alloys may be used, may require less strength. Nickel- and cobalt-based sheet is available. Hastelloy X, IN 617, HA 188, and others have long experience records. HA 230 also is used extensively. Property data generally are available for these alloys.

### 8.4 What Alloys Are Available for High-Strength, High-Temperature Applications?

Turbine airfoil alloys or some combustor nozzles require stronger alloys than provided by the old standby cobalt-based and early nickel-based PC cast alloys. Many of these highest strength alloys are proprietary to various companies, usually aircraft engine providers. The strongest alloys are the single-crystal nickel-based superalloys.

Cast superalloys for the bottom end of the high-temperature application spectrum may be those standbys such as IN 713 or even cobalt-based alloys such as X-40. These alloys have decades of experience. IN 713 is a good general-purpose PC-equiaxed casting alloy which also happens to have no cobalt. Alloys for higher temperatures include U-700, René 80, IN 792, IN 100 (René 100), Mar-M 246, Mar-M 247, CM 247 LC, Mar-M 200CG (PWA 1422), René 125, CM 186, and single-crystal alloys such as PWA 1480, PWA 1484, René N4, René N6, CMSX-4, and CMSX-486. Some alloys (PWA 1422, René 125) are used only as CGDS components and others only as SCDS components (e.g., PWA 1480, PWA 1484, René N4, René N6, CMSX alloys). Alloys such as René 80 have been available in CGDS as well as

PC-equiaxed form. Others such as IN 792 have been available not only as PC-equiaxed components but also in single-crystal form. A defining feature of the short list above is that nearly half of the alloys mentioned are associated with specific aircraft gas turbine companies. Although non-U.S. alloys were omitted from the list, some non-U.S. alloys also tend to be associated with specific manufacturing company ownership. Thus, many of the alloys that satisfy the most demanding environments may not be available for applications outside of their corporate patent realm.

## 8.5 Comments on Cast Alloys for High-Temperature Applications

Alloys to be used for turbine airfoils require high creep and creep rupture strengths. To maximize strength, the alloys for the most demanding applications in high-pressure turbine (HPT) sections should be SCDS materials. For the ultimate in creep rupture strength, SCDS alloys with special crystallographic orientation (e.g.,  $\langle 111 \rangle$  orientation) may be used. In addition to maximizing creep rupture strength through DS processing, TMF strength is optimized by the reduction in modulus achieved by orienting a specific direction ( $\langle 001 \rangle$  direction) of the superalloy crystal parallel to the airfoil axis. An alloy for the most stringent turbine airfoil applications should have a high melting point and good to excellent oxidation resistance. Additionally, the alloy should be able to accept a coating and have good LCF strength at the temperature where the airfoil attachment is made to a disk. These attachment temperatures are nominally at or below 760°C (1400°F). SCDS processing also will ensure that thin-section properties are optimized. As section thickness is reduced, for a fixed stress load, a superalloy ruptures in less time than a standard thick test bar of the alloy would fail. The order of property reduction is PC equiaxed most reduced, CGDS less, and SCDS least.

For turbine vanes where no centrifugal load exists and TMF properties are acceptable, airfoils may be made from PC-equiaxed high-strength cast cobalt-based alloys instead of DS-processed nickel-based alloys. High incipient melting temperature is desired for first-stage turbine vanes. A special type of superalloy, an oxide-dispersion-strengthened (ODS) alloy, also has been used for turbine vanes in some applications. One such alloy, MA 754, relies on yttria dispersed in a corrosion-resistant nickel–chromium matrix to provide adequate creep rupture capability. ODS alloys are not common. MA 6000 is another such alloy which may have enough strength for a high-pressure turbine blade in aircraft gas turbines. A problem with PC-equiaxed airfoils is that the thermal mechanical stresses are much higher than on CGDS or SCDS parts owing to the higher modulus of PC-equiaxed parts. The modulus of the CGDS and SCDS parts may be only 60 % of the value for the PC-equiaxed nickel-based cast alloys. In the most demanding conditions, TMF problems can be minimized by using oriented grain or crystal structures to reduce stresses.

For low-pressure turbine (LPT) blade airfoils operating at lower temperatures than HPT airfoils, alloys such as IN 100 (René 100) or IN 792 and René 80 PC-equiaxed alloys previously used for HPT airfoils may be chosen. If temperatures or stress conditions are sufficiently relaxed, IN 713, U700, or similar first-generation PC-equiaxed cast nickel-based superalloys might suffice.

It should be recognized that superalloys in some applications may not operate at the high temperatures found in aircraft gas turbine engines but still require high-temperature strength which translates into long lives over 40,000–200,000 h.

## 9 FINAL COMMENTS

Many superalloys have been developed but not so many have been adopted for use. A principal reason for this situation is the high cost of proving the worth and safety of a new material. Within most aircraft engine companies, only a few airfoil alloys and a comparably short list

of disk alloys have ever made it to production. Admittedly this list differs from company to company, but the message is the same. If an existing alloy works and a new alloy does not offer some significant benefit that overrides the development cost of proving up the alloy for its new use, do not change alloys.

If an alloy selector is starting from scratch to pick an alloy for an application, then any commercially available alloy may be fair game. On the other hand, the best alloy may not be available owing to corporate patent protection or cost. Then, selection of another alloy from a superalloy producer may be necessary but may possibly require extensive development costs to get the product in workable form and to determine design properties.

If possible, select a known alloy that has more than one supplier and more than one casting or forging source. Work with the suppliers and others in the manufacturing chain to acquire typical or design properties for the alloy in the form it will be used. Generic alloys owned by superalloy melters or developers are best for the alloy selector not associated with one of the big corporate users of superalloys. Companies with proprietary interests normally have nothing to benefit from giving up a technological advantage by sharing design data or even granting a production release to use a proprietary alloy. However, many alloy/process developers are increasingly willing to lease their inventions.

## BIBLIOGRAPHY

- ASM handbooks online, available: <http://products.asminternational.org/hbk/index.jsp>, ASM International, 2011.
- \*Choose *ASM Handbook* and select *Vol. 1, Properties and Selection: Irons, Steels and High Performance Alloys*. Select category *Specialty Steels and Heat Resistant Alloys*.
- \*Choose *ASM Handbook Supplements* and select category *Superalloys*.
- \*Choose *ASM Desk Editions* and then *Metals Handbook*. Select category *Superalloys*.
- Superalloys Reference Library DVD*, ASM International, Metals Park, OH, 2011.
- Superalloys: Alloying and Performance*, ASM International, Metals Park, OH, 2010.
- High-Temperature Corrosion and Materials Applications*, ASM International, Metals Park, OH, 2007.
- Superalloys: A Technical Guide*, 2nd ed., ASM International, Metals Park, OH, 2002.
- ASM Handbook*, ASM International, Metals Park, OH, publication dates vary by volume.
- Protective Coatings for Turbine Blades*, ASM International, Metals Park, OH, 2002.
- Heat-Resistant Materials*, ASM International, Metals Park, OH, 1995.
- Heat-Resistant Materials*, ASM International, Metals Park, OH, 1991.
- ASM Specialty Handbook: Heat-Resistant Materials*, ASM International, Metals Park, OH, 1997.
- The Superalloys II*, Wiley, New York, 1987.
- Superalloys Source Book*, American Society for Metals, Metals Park, OH, 1984.
- The Nimonic Alloys*, 2nd ed., Crane, Russak and Co., New York, 1974.
- Cobalt-Base Superalloys 1970*, Cobalt Information Center, Brussels, 1970.
- High Temperature Alloys for Gas Turbines*, Applied Science Publishers, 1978.
- See this reference and further proceedings of a continuing series of conferences in Europe, first held in 1978 and at four-year intervals thereafter, with emphasis on gas turbines, power engineering, and other applications.
- International Symposium on Structural Stability in Superalloys*, Vols. I and II, AIME, New York, 1968.
- See this reference and further proceedings of a continuing series of conferences in the United States, first held at Seven Springs Mountain Resort, Champion, PA, in 1968 and at four-year intervals thereafter with emphasis on high-temperature materials.
- Superalloy 718 Metallurgy and Applications*, AIME, New York, 1989.
- See this reference and further proceedings of a continuing series of conferences in the United States, first held in 1989 and at irregular intervals thereafter with emphasis on the metallurgy of IN 718 and related alloys.



# CHAPTER 9

## THERMOPLASTICS, THERMOSETS, AND ELASTOMERS – DESCRIPTIONS AND PROPERTIES

Edward N. Peters

SABIC,

Selkirk, New York

<b>1 INTRODUCTION</b>	<b>354</b>	<b>5 ENGINEERING</b>	<b>370</b>
1.1 Classification of Plastics	354	<b>THERMOPLASTICS</b>	<b>370</b>
1.2 Chemical/Solvent Resistance	355	5.1 Thermoplastic Polyesters	371
1.3 Plastics Additives	355	5.2 Polyamides (Nylon)	374
1.4 Properties	355	5.3 Acetals	378
<b>2 POLYOLEFINIC THERMOPLASTICS</b>	<b>357</b>	5.4 Polycarbonate	379
2.1 Polyethylene	357	5.5 Polycarbonate–ABS Alloys	379
2.2 Polypropylene	358	5.6 Polyester–Carbonates	380
2.3 Polymethylpentane	361	5.7 Polyarylates	381
<b>3 SIDE-CHAIN-SUBSTITUTED VINYL THERMOPLASTICS</b>	<b>361</b>	5.8 Modified Polyphenylene Ether	381
3.1 Polystyrene	361	<b>6 HIGH-PERFORMANCE MATERIALS</b>	<b>383</b>
3.2 Syndiotactic Polystyrene	362	6.1 Polyphenylene Sulfide	383
3.3 Styrene–Acrylonitrile Copolymers	363	6.2 Polyarylsulfones	384
3.4 Acrylonitrile–Butadiene–Styrene Polymers	363	6.3 Polybiphenyldisulfones	385
3.5 Acrylonitrile–Styrene–Acrylate Polymers	365	6.4 Liquid Crystalline Polyesters	386
3.6 Poly(methyl methacrylate)	366	6.5 Polyimides	387
3.7 Styrene–Maleic Anhydride Copolymers	366	6.6 Polyetherimide	387
3.8 Styrene–Methyl Methacrylate Copolymers	367	6.7 Poly(amide imides)	389
3.9 Polyvinyl Chloride	367	6.8 Aromatic Polyketones	389
3.10 Poly(vinylidene chloride)	368	6.9 Modified Poly( <i>p</i> -phenylene)	391
<b>4 POLYURETHANE AND CELLULOSIC RESINS</b>	<b>369</b>	<b>7 FLUORINATED THERMOPLASTICS</b>	<b>392</b>
4.1 Polyurethanes	369	7.1 Poly(tetrafluoroethylene)	392
4.2 Cellulosic Polymers	370	7.2 Poly(chlorotrifluoroethylene)	393
		7.3 Fluorinated Ethylene–Propylene	393
		7.4 Polyvinylidene Fluoride	393
		7.5 Poly(ethylene chlorotrifluoroethylene)	393
		7.6 Poly(vinyl fluoride)	393

Modified from E. N. Peters, "Plastics; Information and Properties of Polymeric Materials," in M. Kutz (Ed.), *Mechanical Engineers' Handbook*, 3rd ed., Wiley, Hoboken, NJ, 2005.

<b>8 THERMOSET RESINS</b>	<b>394</b>	<b>9 GENERAL-PURPOSE ELASTOMERS</b>	<b>396</b>
8.1 Phenolic Resins	394		
8.2 Epoxy Resins	394		
8.3 Unsaturated Polyesters	395	<b>10 SPECIALTY ELASTOMERS</b>	<b>397</b>
8.4 Vinyl Esters	395		
8.5 Alkyd Resins	395	<b>REFERENCES</b>	<b>398</b>
8.6 Diallyl Phthalate	396		
8.7 Amino Resins	396		

## 1 INTRODUCTION

Plastics or polymers are ubiquitous. Through human ingenuity and necessity natural polymers have been modified to improve their utility and synthetic polymers developed. Synthetic polymers in the form of plastics, fibers, elastomers, adhesives, and coatings have come on the scene as the result of a continual search for man-made substances that can perform better or can be produced at a lower cost than natural materials such as wood, glass, and metal, which require mining, refining, processing, milling, and machining. The use of plastics can also increase productivity by producing finished parts and consolidating parts. For example an item made of several metal parts that require separate fabrication and assembly can often be consolidated to one or two plastic parts. Such increases in productivity have led to fantastic growth in macromolecules. Indeed, the use of plastics has increased over 20-fold in the last 40 years. Today there is a tremendous range of polymers and formulated plastics available which offer a wide range of performance. This chapter presents concise information on the synthesis, structure, properties, and applications.

### 1.1 Classification of Plastics

The availability of plastic materials for use in various applications is huge.<sup>1-5</sup> There are various ways to categorize or classify plastics, which facilitates understanding similarities and differences between materials. The two major classifications are thermosetting materials and thermoplastics materials.<sup>5-7</sup> As the name implies, thermosetting plastics or thermosets are set, cured, or hardened into a permanent shape.<sup>5,6</sup> The curing which usually occurs rapidly under heat or UV light leads to an irreversible crosslinking of the polymer. Thermoplastics differ from thermosetting materials in that they do not set or cure under heat.<sup>5</sup> When heated, thermoplastics merely soften to a mobile, flowable state where they can be shaped into useful objects. Upon cooling, thermoplastics harden and hold their shape. Thermoplastics can be repeatedly softened by heat and shaped.

Another major classification of thermoplastics is as amorphous or semicrystalline plastics.<sup>5,6</sup> Most polymers either are completely amorphous or have an amorphous component as part of a semicrystalline polymer. Amorphous polymers are hard, rigid glasses below a fairly sharply defined temperature, which is known as the glass transition temperature, or  $T_g$ . Above the  $T_g$  the amorphous polymer becomes soft and flexible and can be shaped. Mechanical properties show profound changes near the  $T_g$ .

Semicrystalline polymers have crystalline melting points,  $T_m$ , which are above their glass transition temperature. The degree of crystallinity and the morphology of the crystalline phase have an important effect on mechanical properties. Crystalline plastics will become less rigid above their  $T_g$  but will not flow until the temperature is above its  $T_m$ .

Many mechanical and physical properties of plastics are related to their structure. In general, at ambient temperatures, amorphous polymers have greater transparency and greater dimensional stability over a wide temperature range. In semicrystalline plastics the



ordering and packing of the polymer chains make them denser, stiffer, stronger, and harder. Semicrystalline plastics also have better inherent lubricity and chemical resistance and during molding will tend to shrink more and have a greater tendency to warp than amorphous thermoplastics.

Another important class of polymeric resins is elastomers. Elastomeric materials are rubberlike polymers with  $T_g$  below room temperature. Below  $T_g$  an elastomer will become rigid and lose its rubbery characteristics.

## 1.2 Chemical/Solvent Resistance

The solvent or chemical resistance of plastics is a measure of the resin's ability to withstand chemical interaction with minimal change in appearance, weight, dimensions, and mechanical properties and over a period of time.<sup>8</sup> When polymers are exposed to chemical environments, they can dissolve in the solvent, absorb the solvent, become plasticized by the solvent, react with the solvent or chemical, or be stressed cracked.<sup>6</sup> Hence, mechanical properties can be reduced and dimensions of molded parts changed.

Qualitative comments are made in the chapter about the chemical resistance of various plastics. Generally, these comments are based on laboratory screening that the manufacturers have reported. The stress level of the test part has a very significant influence on the performance of the material. When the stress level increases, resistance to chemicals and solvents decreases. Sources of stress can occur from injection molding, applied loads, forming, and assembly operations.

When an application requires exposure to or immersion in chemicals or other harsh environments, it is of prime importance to use prototypes of suitable stressed material for testing under actual operating conditions.<sup>8</sup>

## 1.3 Plastics Additives

The wide variety of synthetic polymers offers a huge range of performance attributes.<sup>9-13</sup> Additives play a key role in optimizing the performance of polymers and transforms them into commercially viable products. Additives are materials that are added to a polymer to produce a desired change in material properties or characteristics. A wide variety of additives are currently used in thermoplastics, to enhance material properties, expand processability, modify aesthetics, or increase environmental resistance. Enhancements of properties include thermal stability, flame retardancy, impact resistance, and UV light stability. Reinforcing fibers, that is, high-strength, inert fibrous material such as glass and carbon fibers, can be incorporated in the polymer matrix to improve modulus and strength while lowering the coefficient of thermal expansion and unusually lowering impact and increasing the density. Particulates of flaked fillers usually increase stiffness as well as lower costs.<sup>13</sup> Plasticizers lower modulus and enhance flexibility. Thus, additives are found in most commercial plastics and are an essential part of the formulation in which performance is tailored for specific applications.<sup>9-13</sup>

This chapter focuses on properties of the base resins with very few additives other than stabilizers. Properties for plastics that contain glass fiber (GF) are listed for those plastics that routinely use such reinforcing fibers.

## 1.4 Properties

Plastic materials can encounter mechanical stress, impact, flexure, elevated temperatures, different environments, etc. Hence, various properties are measured and reported to give an indication of a material's ability to perform under various conditions. Properties are determined on standard test parts and are useful for comparative purposes. Properties used in the chapter would be instructive and are listed below.



*Density.* The mass per unit volume of a material at 73°F (23°C).

*Glass Transition Temperature ( $T_g$ ).* The temperature at which the polymer undergoes a transition from a hard solid to a soft, rubbery, and flexible material.

*Melting Point ( $T_m$ ).* The temperature where the crystalline regions in semicrystalline polymers melt.

*Tensile Modulus.* An indicator of the stiffness of a material. It is basically the applied tensile stress, based on the force and cross-sectional area, divided by the observed strain at that stress level.

*Tensile Strength.* The amount of force required to elongate the plastic by a defined amount. Higher values mean the material is stronger.

*Elongation at Break.* The increase in length of a specimen under tension before it breaks under controlled test conditions. Usually expressed as a percentage of the original length. Also called “strain.”

*Flexural Modulus.* The ratio of applied stress to the deflection caused in a bending test. It is a measure of the stiffness of a material during the first part of the bending process.

*Flexural Strength.* The maximum stress which can be applied to a beam in pure bending before permanent deformation occurs.

*Izod Impact Strength.* The amount of impact energy that is required to cause a test specimen to break completely. The specimen may be notched or unnotched.

*Heat Deflection Temperature.* (HDT, also called deflection temperature under load or DTUL). Gives an indication of a material’s ability to perform at higher temperatures while supporting a load. It shows the temperature at which a test specimen will deflect a given distance under a given load in flexure under specified test conditions, usually at 1.82- or 0.42-MPa loads.

*Vicat Softening Temperature.* A measure of the temperature at which a plastic starts to soften at specified test conditions. It gives an indication of a material’s ability to withstand limited short-term contact with a heated object.

*Relative Thermal Index.* (RTI, formerly called continuous-use temperature). The continuous operating temperature of plastics materials used in electrical applications, as specified by Underwriters’ Laboratories (UL). It is the maximum temperature at which the material retains at least 50% of the original value of all properties tested after the specified amount of time. The RTI tests are important if the final product is to receive UL recognition.

*UL94 V0.* Classification of flammability of plastic materials that follows the UL 94 standard, vertical burning test. The V0 rating is where the total burn time for the five specimens after two 10-s applications of flame is  $\leq 50$  s. Sample thickness on V0 rated test specimens are reported. A rating on thin samples would suggest possible utility in applications requiring thin walls.

*Oxygen Index.* A flammability test that determines the minimum volumetric concentration of oxygen that is necessary to maintain combustion of a specimen after it has been ignited.

*Hardness.* The resistance of a material to indentation under standardized conditions. A hard indenter or standard shape is pressed into the surface of the material under a specified load. The resulting area of indentation or the depth of indentation is measured and assigned a numerical value. For plastics, the most widely used methods are Rockwell and Shore methods and Ball hardness.

*Coefficient of Thermal Expansion (CTE).* A measure of how much a material will lengthen when heated (or shorten upon cooling) based on its original length and the temperature difference to which it is exposed. CTE becomes important when part dimensions are critical or when two different materials with different CTEs are attached to each other.

*Shrinkage.* The percentage of reduction in overall part dimensions during injection molding. The shrinkage occurs during the cooling phase of the process.

*Water Absorption/Moisture Absorption.* The percentage weight gain of a material after immersion in water for a specified time at a specified temperature. Low values are preferred and are important in applications requiring good dimensional stability. As water is absorbed, dimensions of the part tend to increase and physical properties can deteriorate. In addition, low water absorption is very important for most electrical properties.

*Relative Permittivity.* (formerly called dielectric constant). A dielectric is an electrical insulator that can be polarized by an applied electric field. The dielectric polarization is expressed by a number called relative permittivity. Low values suggest less polarization. It is equal to the capacitance of a material divided by the capacitance of a dimensionally equivalent vacuum. This is important for high-frequency or high-power applications in order to minimize power losses. Low values indicate a good insulator. Moisture, frequency, and temperature increases may have adverse effects.

*Loss Tangent.* (also called dissipation factor). A parameter of a dielectric material that quantifies its inherent dissipation of electromagnetic energy. A low loss tangent suggests less power or signal loss into the material. Moisture, frequency, and temperature increases may have adverse effects.

## 2 POLYOLEFINIC THERMOPLASTICS

### 2.1 Polyethylene

Polyethylene (PE) plastics are lightweight, semicrystalline thermoplastics that are prepared by the catalytic polymerization of ethylene.<sup>14–16</sup> Depending on the temperature, pressure, catalyst, and the use of a comonomer, three basic types of polyethylene can be produced: high-density polyethylene (HDPE), low-density polyethylene (LDPE), and linear low-density polyethylene (LLDPE). LDPE and LLDPE contain branching. This branching results in decreased crystallinity and lower density. Most properties of PEs are a function of their density and molecular weight. As density decreases, the strength, modulus, and hardness decrease and flexibility, impact, and clarity increase. Hence, HDPE exhibits greater stiffness and rigidity, improved heat resistance, and increased resistance to permeability than LDPE and LLDPE. LDPE is prepared under more vigorous polymerization conditions, which results in short-chain branching. The amount of branching and the density can be controlled by the polymerization conditions.

LLDPEs are prepared by using an  $\alpha$ -olefin comonomer during polymerization. Hence, branching is introduced in a controlled manner and where the chain length of the branching is uniform. In general, the comonomers are 1-butene, 1-hexene, 1-octene, and 4-methyl-1-pentene (4M1P).

Polyethylene polymers are versatile and inexpensive resins that have become the largest volume use of any plastics. They exhibit toughness, near-zero moisture absorption, excellent chemical resistance, excellent electrical insulating properties, low coefficient of friction, and ease of processing. They are not high-performance resins. Their heat deflection temperatures are reasonable but not high. Specialty grades of PE include very low density (VLDPE), medium-density (MDPE), and ultrahigh molecular weight PE (UHMWPE).

**Table 1** Typical Properties of HDPE, LDPE, LLDPE, and UHMWPE

Property	HDPE	LDPE	LLDPE	UHMWPE
Density (g/cm <sup>3</sup> )	0.94–0.97	0.915–0.935	0.91–0.92	0.93
$T_g$ (°C)	–120	–120	—	—
$T_m$ (°C)	130	105–115	99–105	142
Tensile modulus (GPa)	0.76–1.0	0.14–0.31	0.13–0.19	110
Tensile strength (MPa)	22–32	7–17	14–21	30
Elongation at break (%)	200–1000	100–700	200–1100	300
Flexural modulus (GPa)	0.7–1.6	0.24–0.33	0.25–0.37	—
HDT, 0.45 MPa (°C)	65–90	43	—	79
Vicat softening temperature (°C)	120–130	90–102	80–94	136
Brittle temperature (°C)	<–75	<–75	<–75	—
Hardness (Shore)	D60–D69	D45–60	D45–50	—
CTE (10 <sup>–5</sup> 1/°C)	15	29	18	0.1.6
Shrinkage (in./in.)	0.007–0.009	0.015–0.035	—	—
Water absorption, 24 h (%)	<0.01	<0.01	<0.01	<0.01
Relative permittivity, 1 MHz	2.3	2.2	2.3	2.3
Loss tangent, 1 MHz	0.0003	0.0003	0.0004	0.0005

**Table 2** Typical Properties of LLDPE Copolymers

Property	Comonomer			
	1-Butene	1-Hexene	1-Octene	4M1P
Density (g/cm <sup>3</sup> )	0.919	0.919	0.920	—
$T_m$ (°C)	99	99	98	—
Tensile modulus (GPa)	0.185	0.206	0.200	0.277
Tensile strength (MPa)	41	39	58	42
Elongation at break (%)	430	430	440	510

Some typical properties of PEs are listed in Table 1. Properties of the various copolymers of LLDPE appear in Table 2.

*Uses.* HDPE's major use is in blow-molded containers (milk, water, antifreeze, household chemical bottles), shipping drums, carboys, automotive gasoline tanks; injection-molded material-handling pallets, crates, totes, trash and garbage containers, and household and automotive parts; and extruded pipe products (corrugated, irrigation, sewer/industrial, and gas distribution pipes).

LDPE/LLDPEs find major applications in film form for food packaging as a vapor barrier film which include stretch and shrink wrap; for plastic bags such as grocery, laundry, and dry cleaning bags; for extruded wire and cable insulation; and for bottles, closures, and toys.

## 2.2 Polypropylene

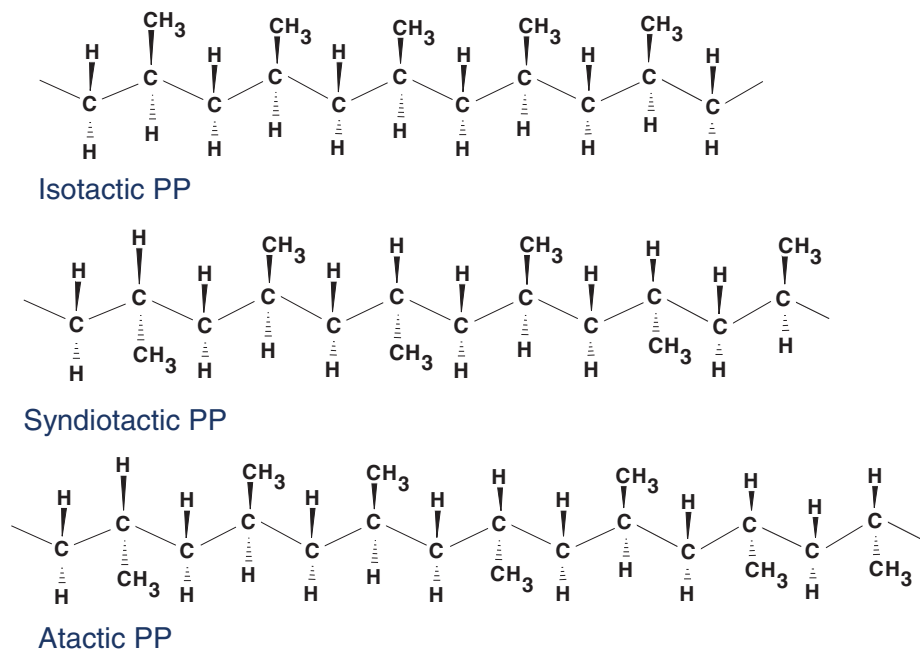
Polypropylene (PP) is a versatile semicrystalline thermoplastic offering a useful balance of properties which are typically higher than HDPE. It is prepared by the catalyzed polymerization of propylene.<sup>17,18</sup> Crystallinity is key to the properties of PP. However, unlike polyethylene, PP polymers can have different stereoisomerisms. The degree of crystallinity is a function of the

degree of geometric orientation (stereoregularity) of the methyl groups on the polymer chain (backbone).

The propylene repeat unit in PP has a  $\text{CH}_2$  part called the head and the  $\text{CH}(\text{CH}_3)$  part called the tail. Generally, the head-to-tail polymer is produced using catalysts that are available. This head-to-tail polymerization leads to a polymer with a methyl group located on every other carbon atom. The carbon atom with the methyl group can adopt different relative orientations with respect to the polymer backbone. This difference in structural orientation or structural isomerism is referred to as stereoisomerism. These differences in stereoisomerism are also called *tacticity*, from the Greek work *taktikos*, meaning “arranging” or “ordering.” Figure 1 depicts models of the three different configurations in polypropylene.

In Fig. 1 the carbon-carbon bonds form the chain backbone, which lies in the plane of the paper, the heavy solid lines represent groups or atoms above the plane, and the dashed line represents groups or atoms below the plane. There are three possible geometric forms of PP. *Isotactic* PP (iPP) has predominantly all the methyl groups aligned on the same side of the chain (shown above the chain). In *syndiotactic* PP (sPP) the methyl groups alternate above and below the polymer chain. Finally *atactic* PP (aPP) has the methyl groups randomly positioned along the chain. Differences in tacticity can play a major role in polymer properties. The tacticity of a polymer can have a dramatic effect on its physical properties. For example, the melting points of iPP, sPP, and aPP are 160–170°C, 125–131°C, and no melting point, respectively.

Both iPP and sPP will crystallize when cooled from the molten states. There are three important crystalline morphologies of iPP. Nucleating agents can control the nature of the crystallinity. Properties can be controlled to some extent by manipulating the amount of these crystalline phases. On the other hand, sPP has very different crystalline morphology and a difference balance of stiffness and toughness. In general, sPP is less crystalline and exhibits greater clarity, elasticity, and impact resistance.



**Figure 1** Stereoregularity of isotactic, syndiotactic, and atactic polypropylene.

Isotactic PP is a highly crystalline thermoplastic that exhibits low density; rigidity; and good chemical resistance to hydrocarbons, alcohols, and oxidizing agents; negligible water absorption; excellent electrical properties; and excellent impact/stiffness balance. PP has the highest flexural modulus of the commercially available polyolefins. In general, PP has poor impact resistance. However, PP–elastomer blends have improved impact strength. Unfilled PP has poor flame resistance and is degraded by sunlight. Flame-retardant and UV-stabilized grades are available.

Catalysts are used to control the stereoregularity of PP by directing incoming monomers to a specific orientation. However, the catalysts are not perfect and there can be small amounts of PP with different tacticity. The classic catalysts are Ziegler–Natta catalysts. However, newer metallocene catalysts offer a much greater ratio of the desired tacticity than Ziegler–Natta catalyst. The proper choice of catalyst can produce isotactic, syndiotactic, atactic, or even a combination of these. Indeed, PP thermoplastic elastomers are made from propylene monomer and have isotactic blocks alternating with atactic blocks. Another area of PP catalyst development is the production of copolymers of PP with higher  $\alpha$ -olefins.

The great variety and versatility of PP mean that their properties can be controlled in several different ways, that is, the tacticity of the monomers (crystallinity), the use of nucleating agents, and the formation of copolymers. PP polymers continue to evolve and new forms continue to be developed in order to get a competitive advantage in the marketplace. Typical properties of iPP, sPP, aPP, and iPP–aPP thermoplastic elastomers (PP–TPEs) are listed in Table 3.

*Uses.* End uses for PP are in blow molding bottles and automotive parts, injection-molded closures, appliances (washer agitators, dishwasher components), housewares, automotive parts, luggage, syringes, storage battery cases, and toys. PP can be extruded into fibers and filaments for use in carpets, rugs, and cordage. In addition, PP can be extruded into film for packaging applications.

**Table 3** Typical Properties of PP

Property	iPP	aPP	PP–TPE	sPP
Density (g/cm <sup>3</sup> )	0.91–0.92	0.86	0.91–0.92	0.89–0.91
$T_g$ (°C)	3–10	–5 to –18	–10	0–5
$T_m$ (°C)	165–180	—	125–145	125–135
Tensile modulus (GPa)	1.4–1.8	—	0.2	110
Tensile strength (MPa)	34.5	1.2	5–8	30
Elongation at yield (%)	10	—	100	300
Elongation at break (%)	—	100–200	1000	—
Flexural modulus (GPa)	1.39	—	—	—
Notched Izod (kJ/m)	0.027	—	—	—
HDT, 1.81 MPa (°C)	60–65	—	—	—
HDT, 0.45 MPa (°C)	107	—	—	—
Vicat softening temperature (°C)	130–148	—	—	—
Oxygen index (%)	17.4	—	—	—
Hardness (Rockwell)	R90	—	—	—
(Shore)	D76	A55–65	A77–85	—
CTE (10 <sup>–5</sup> 1/°C)	9	—	—	—
Shrinkage (in./in.)	0.01–0.02	—	—	—
Water absorption, 24 h (%)	<0.01	<0.01	<0.01	<0.01
Relative permittivity, 1 MHz	2.2–2.3	—	—	—
Dissipation factor, 1 MHz	0.0003	—	—	—

**Table 4** Typical Properties of PMP

Density (g/cm <sup>3</sup> )	0.84
$T_g$ (°C)	35–40
$T_m$ (°C)	245
Tensile modulus (GPa)	1.75
Tensile strength (MPa)	20.5
Elongation at break (%)	18
Flexural modulus (GPa)	1.55
Flexural strength (MPa)	30.0
Notched Izod (kJ/m)	0.150
HDT, 1.81 MPa (°C)	49
HDT, 0.45 MPa (°C)	85
Vicat softening temperature (°C)	173
CTE (10 <sup>-5</sup> 1/°C)	3.8
Hardness (Rockwell)	L85
Relative permittivity, 100 Hz	2.12

### 2.3 Polymethylpentane

Polymethylpentane (PMP) is prepared by the catalytic polymerization of 4-methyl-1-pentene.<sup>14</sup> PMP is a semicrystalline thermoplastic that exhibits transparency (light transmission up to 90%), very low density, chemical resistance, negligible water absorption, and good electrical properties. PMP resins are available as homopolymers and copolymers with higher  $\alpha$ -olefins. The homopolymer is more rigid and the copolymers have increased ductility. PMP is degraded by sunlight and high-energy radiation. Moreover, strong oxidizing acids attack it. PMP grades are available with increased radiation resistance as well as with reinforcing fillers. Properties appear in Table 4.

*Uses.* Applications for PMP resins cover a wide spectrum of end uses. These include medical (hypodermic syringes, disposable cuvettes, blood-handling equipment, respiration equipment, laboratory ware), packaging (microwave and hot-air-oven cookware, service trays, coated paper plates), and miscellaneous (transparent ink cartridges for printers, light covers, slight-glasses, lenses, liquid level and flow indicators, fluid reservoirs).

## 3 SIDE-CHAIN-SUBSTITUTED VINYL THERMOPLASTICS

### 3.1 Polystyrene

The catalytic or thermal polymerization of styrene yields general-purpose or crystal polystyrene (PS).<sup>19,20</sup> The designation of “crystal” refers to its high clarity. PS is an amorphous polymer (atactic geometric configuration) and exhibits high stiffness, good dimensional stability, moderately high heat deflection temperature, and excellent electrical insulating properties. However, it is brittle under impact and exhibits very poor resistance to surfactants and a wide range of solvents.

The three main categories of commercial polystyrene resins are crystal PS, impact PS, and expanded PS foam.

Copolymerization of styrene with a rubber, polybutadiene, results in the PS being grafted onto the rubber. This impact-modified PS has increased impact strength, which is accompanied by a decrease in rigidity and heat deflection temperature. Depending on the levels of rubber, impact polystyrene (IPS) or high-impact polystyrene (HIPS) can be prepared. These materials are translucent to opaque and generally exhibit poor weathering characteristics.

**Table 5** Typical Properties of PS, IPS, and HIPS

Property	PS	IPS	HIPS
Density (g/cm <sup>3</sup> )	1.04	1.04	1.04
$T_g$ , (°C)	100	—	—
Tensile modulus (GPa)	3.14	2.37	1.56
Tensile strength (MPa)	51.1	26.9	15.0
Elongation at break (%)	21	40	65
Flexural modulus (GPa)	3.54	2.61	1.68
Flexural strength (MPa)	102	56.5	30
Notched Izod (kJ/m)	0.021	0.112	0.221
HDT, 1.81 MPa (°C)	77	79	73
HDT, 0.42 MPa (°C)	89	88	79
Vicat softening temperature (°C)	105	104	96
Oxygen index (%)	17.8	—	—
Hardness (Rockwell)	R130	R110	R75
CTE (10 <sup>-5</sup> 1/°C)	9.0	9.0	9.0
Shrinkage (in./in.)	0.005	0.005	0.005
Relative permittivity, 1 kHz	2.53	—	—

PS finds wide use in foamed polystyrene. Typically foamed polystyrene is produced from expandable polystyrene (EPS) beads, which contain a blowing agent. When heated, the blowing agent vaporizes, expands the PS, and forms low-density foam. The density of the foam is controlled by the amount of blowing agent.

Typical properties for PS, IPS, and HIPS appear in Table 5.

*Uses.* Ease of processing, rigidity, clarity, and low cost combine to support applications in toys, displays, consumer goods (television housings), medical (labware, tissue culture flasks), and housewares such as food packaging, audio/video consumer electronics, office equipment, and medical devices.

EPS can readily be prepared and are characterized by excellent low thermal conductivity, high strength-to-weight ratio, low water absorption, and excellent energy absorption. These attributes have made EPS of special interest as insulation boards for construction (structural foam sections for insulating walls), protective packaging materials (foamed containers for meat and produce), insulated drinking cups and plates, and flotation devices.

### 3.2 Syndiotactic Polystyrene

Syndiotactic polystyrene (SPS) is a semicrystalline polymer and is produced via metallocene-catalyzed polymerization of styrene.<sup>21</sup> By comparison to general-purpose, amorphous PS, SPS has stereoregularity in its structure, which facilitates crystallization. In SPS the phenyl groups alternate above and below the polymer chain. Hence, SPS has a high crystalline melting point and good chemical resistance.

The slow rate of crystallization and the high  $T_g$  of SPS typically require an oil-heated tool when injection molding. In addition, longer cycle times are needed in order to maximize physical properties. Typical properties appear in Table 6.

*Uses.* SPS is targeted at automotive under-the-hood and specialty electronic applications. It will compete with polyamides, thermoplastic polyesters, and polyphenylene sulfide (PPS).

**Table 6** Typical Properties of SPS

Property	SPS	SPS + 30% GF
Density (g/cm <sup>3</sup> )	1.05	1.25
$T_g$ (°C)	100	—
$T_m$ (°C)	270	—
Tensile modulus (GPa)	3.44	10.0
Tensile strength (MPa)	41	121
Elongation at break (%)	1	1.5
Flexural modulus (GPa)	3.9	9.7
Flexural strength (MPa)	71	166
Notched Izod (kJ/m)	0.011	0.096
HDT, 1.81 MPa (°C)	99	249
HDT, 0.42 MPa (°C)	—	263
CTE (10 <sup>-5</sup> 1/°C)	9.2	2.5
Water absorption, 24 h (%)	0.04	0.05
Relative permittivity, 1MHz	2.6	2.9
Loss tangent, 1 MHz	< 0.001	< 0.001

### 3.3 Styrene–Acrylonitrile Copolymers

Copolymerization of styrene with a moderate amount of acrylonitrile (AN) provides a clear, amorphous polymer [styrene–acrylonitrile (SAN)].<sup>20</sup> The addition of the polar AN group gives increased heat deflection temperature and chemical resistance compared to PS. Other benefits of SAN are stiffness, strength, and clarity. Like PS the impact resistance is still poor. SAN is chemically resistant to hydrocarbons, bases, most detergents, and battery acid. However, SAN has poor resistance to chlorinated and aromatic solvents, esters, ketones, and aldehydes. The composition and molecular weight can be varied to change properties. An increase in AN will increase SAN physical properties but will make melt processing more difficult and will decrease the transparency. In general, the AN level in SAN does not exceed 30% for molding applications. Typical properties appear in Table 7.

*Uses.* SAN is utilized in typical PS-type applications where a slight increase in heat deflection temperature and/or chemical resistance is needed. Such applications include appliances (refrigerator compartments, knobs, blender and mixer bowls), electronics (cassette cases, tape windows, meter lenses), packaging (bottle jars, cosmetic containers, closures), medical (syringe components, dialyzer housings), and other (glazing, battery cases, pen barrels).

### 3.4 Acrylonitrile–Butadiene–Styrene Polymers

ABS is a generic name for a family of thermoplastics called terpolymers because they are made of three monomers—acrylonitrile, butadiene, and styrene—to create a material that draws on the best properties of all three.<sup>22</sup> Acrylonitrile (“A”) provides chemical resistance, hardness, rigidity, and fatigue resistance and increases the heat deflection temperature. Butadiene rubber (“B”) provides toughness and low-temperature ductility but lowers the heat resistance and rigidity. Styrene (“S”) provides rigidity, hardness, gloss, aesthetics, and processing ease. This three-monomer system offers a lot of flexibility in tailoring ABS resins. Optimization of these monomers can enhance the desired performance profile. Because of the possible variations in composition, properties can vary over a wide range.

Typical resin grades in this product family consist of a blend of an elastomeric component and an amorphous thermoplastic component. Typically the elastomeric component consists of a



**Table 7** Typical Properties of SAN

Property	SAN	SAN + 30% GF
Density (g/cm <sup>3</sup> )	1.07	1.22
$T_g$ (°C)	107	—
Tensile modulus (GPa)	3.45	11.0
Tensile strength (MPa)	76	139
Elongation at break (%)	2.5	1.6
Flexural modulus (GPa)	3.65	9.60
Flexural strength (MPa)	128	—
Notched Izod (kJ/m)	0.016	0.060
HDT, 1.81 MPa (°C)	87	100
HDT, 0.42 MPa (°C)	103	108
Vicat softening temperature (°C)	111	—
Relative thermal index, (°C)	50	74
Oxygen index (%)	19.0	—
Hardness (Rockwell)	R125	R123
6.6	1.9	—
Shrinkage (in./in.)	0.005	—
Water absorption, 24 h (%)	—	0.15
Relative permittivity, 1 MHz	2.9	3.6
Loss tangent, 1 MHz	0.009	0.008

copolymer where SAN was grafted onto polybutadiene base (ABS with very high levels of B). The amorphous thermoplastic component is SAN.

ABS plastics offer a good balance of properties centering on toughness, hardness, high gloss, dimensional stability, and rigidity. Compared to PS, ABS offers good impact strength, improved chemical resistance, and similar heat deflection temperature. ABS is also opaque. ABS has good chemical resistance to acids and bases but poor resistance to aromatic compounds, chlorinated solvents, esters, ketones, and aldehydes. ABS has poor resistance to UV light. Typical properties are shown in Table 8.

**Table 8** Typical Properties of ABS Resins

Property	GP	High Heat	High Impact
Density (g/cm <sup>3</sup> )	1.05	1.05	1.04
Tensile modulus (GPa)	2.28	2.28	2.00
Tensile strength (MPa)	43	47	39
Elongation at break (%)	—	—	26
Flexural modulus (GPa)	2.48	2.41	2.07
Flexural strength (MPa)	77	83	65
Notched Izod (kJ/m)	0.203	0.214	0.454
HDT, 1.81 MPa (°C)	81	99	81
HDT, 0.42 MPa (°C)	92	110	97
Vicat softening temperature (°C)	—	—	99
RTI (°C)	60	—	60
Hardness (Rockwell)	—	R110	—
CTE (10 <sup>-5</sup> 1/°C)	8.82	7.92	9.45
Shrinkage (in./in.)	0.006	0.006	0.006

*Uses.* ABS materials are suitable for tough consumer products (refrigerator door liners, luggage, telephones, business machine housings, power tools, small appliances, toys, sporting goods, personal care devices), automotive (consoles, door panels, various interior trim, exterior grills, and lift gates), medical (clamps, stopcocks, blood dialyzers, check valves), and building and construction (pipes, fittings, faucets, conduit, shower heads, bathtubs).

### 3.5 Acrylonitrile–Styrene–Acrylate Polymers

Acrylonitrile–styrene–acrylate (ASA) terpolymers are amorphous thermoplastics and are similar to ABS resins. However, the butadiene rubber has been replaced by an acrylate-based elastomer, which has excellent resistance to sunlight. Hence ASA offers exceptional durability in weather-related environments without painting. In outdoor applications, ASA resins retain color stability under long-term exposure to UV, moisture, heat, cold, and impact. In addition, ASA polymers offer high gloss and mechanical properties similar to those of ABS resins. ASA has good chemical resistance to oils, greases, and salt solutions. However, resistance to aromatic and chlorinated hydrocarbons, ketones, and esters is poor.

ASA resins exhibit good compatibility with other polymers. This facilitates its use in polymer blends and alloys and as a cost-effective cap-stock (over layer) to protect PS, polyvinyl chloride (PVC), or ABS in outdoor applications.

Various grades are available for injection molding, profile and sheet extrusion, thermoforming, and blow molding. Typical properties appear in Table 9.

*Uses.* ASA resins have applications in automotive/transportation (body moldings, bumper parts, side-view mirror housings, truck trailer doors, roof luggage containers), building/construction (window lineals, door profiles, downspouts, gutters, house siding, windows, mail boxes, shutters, fencing, wall fixtures), sporting goods (snowmobile and all-terrain vehicles, housings, small water craft, camper tops, windsurfer boards), and consumer items (garden hose fittings and reels, lawnmower components, outdoor furniture, telephone handsets, covers for outdoor lighting, spa and swimming pool steps and pumps, housings for garden tractors).

**Table 9** Typical Properties of ASA Resins

	ASA	ASA/PVC	ASA/PC
Density (g/cm <sup>3</sup> )	1.06	1.21	1.15
Tensile modulus (GPa)	1.79	—	—
Tensile strength (MPa)	41	39	62
Elongation at break (%)	40	30	25
Flexural modulus (GPa)	1.79	1.93	2.52
Flexural strength (MPa)	59	48	88
Notched Izod (kJ/m)	0.320	0.961	0.320
Notched Izod, –30°C (kJ/m)	0.059	0.107	0.080
HDT, 1.81 MPa (°C)	77	74	104
HDT, 0.42 MPa (°C)	88	82	116
Vicat softening temperature (°C)	99	—	—
RTI (°C)	50	50	—
Hardness (Rockwell)	R86	R102	R110
CTE (10 <sup>–5</sup> 1/°C)	9.0	8.46	7.2
Shrinkage (in./in.)	0.006	0.004	0.006
Water absorption, 24 h (%)	—	0.11	0.25
Relative permittivity, 1 MHz	3.2	—	—
Loss tangent, 1 MHz	0.026	—	—

### 3.6 Poly(methyl methacrylate)

The catalytic or thermal polymerization of methyl methacrylate yields poly(methyl methacrylate) (PMMA). It is often referred to as acrylic. PMMA is a hard, rigid, transparent, amorphous polymer. The exceptional clarity, rigidity, colorability, and resistance to long-term exposure to sunlight and weathering make PMMA ideal for glass replacement.

In addition, PMMA has low water absorption and good electrical properties.

Acrylics have fair chemical resistance to many chemicals. However, resistance to aromatic and chlorinated hydrocarbons, ketones, and esters is poor. PMMA properties appear in Table 10.

*Uses.* PMMA is used in construction (glazing, lighting diffusers, domed skylights, enclosures for swimming pools and buildings), automotive (exterior lighting lenses in cars and trucks, nameplate, medallions, lenses on instrument panels), household (laboratory, vanity, and counter tops, tubs), medical (filters, blood pumps), and others (appliances, aviation canopies and windows, outdoor signs, display cabinets).

### 3.7 Styrene–Maleic Anhydride Copolymers

SMA resins are copolymers of styrene and maleic anhydride (MA) and offer increased heat deflection temperatures, strength, solvent resistance, and density compared to PS.<sup>20</sup> SMA resins are usually produced via catalyzed bulk polymerization. There is a strong tendency to form the 1:1 styrene–MA copolymer. Random SMA resins containing 5–12% MA are produced via starve feeding, that is, keeping the MA concentration low during the polymerization. SMA resins are brittle and have poor UV resistance. Impact-modified grades and terpolymers (grafting rubber into polymer during polymerization) are available. Typical properties for SMA prepared with 9% MA appear in Table 10.

*Uses.* SMA copolymers have been used in automotive (instrument panels, headliners), food service, plumbing, and electrical applications.

**Table 10** Typical Properties of PMMA, SMMA, and SMA Resins

Property	PMMA	SMMA	SMA
Density (g/cm <sup>3</sup> )	1.19	1.09	1.08
$T_g$ (°C)	109	—	—
Tensile modulus (GPa)	3.10	3.50	—
Tensile strength (MPa)	70	57.2	48.3
Elongation at break (%)	6	2	—
Flexural modulus (GPa)	3.10	3.50	3.61
Flexural strength (MPa)	103	103	115.8
Notched Izod (kJ/m)	0.016	0.020	0.011
HDT, 1.81 MPa (°C)	93	98	96
HDT, 0.42 MPa (°C)	94	—	—
Vicat softening temperature (°C)	103	—	118
RTI (°C)	90	—	—
Hardness (Rockwell)	M91	M64	L108
CTE (10 <sup>-5</sup> 1/°C)	7.6	7.92	6.3
Shrinkage (in./in.)	0.004	0.006	0.005
Water absorption, 24 h (%)	0.3	0.15	0.10
Relative permittivity, 1 kHz	3.3	—	—

### 3.8 Styrene–Methyl Methacrylate Copolymers

Styrene–methyl methacrylate (SMMA) copolymers are prepared by the catalyzed polymerization of styrene and methyl methacrylate (MMA). The advantages of SMMA over PS include improved outdoor weathering and light stability, better clarity, increased chemical resistance, and improved toughness. Properties for SMMA prepared with 30% MMA appear in Table 10.

*Uses.* Applications for SMMA plastics are in small appliances and kitchen and bathroom accessories.

### 3.9 Polyvinyl Chloride

The catalytic polymerization of vinyl chloride yields PVC.<sup>23</sup> It is commonly referred to as PVC or vinyl and is second only to polyethylene in volume use. Normally, PVC has a low degree of crystallinity and good transparency. The high chlorine content of the polymer produces advantages in flame resistance, fair heat deflection temperature, and good electrical properties. The chlorine also makes PVC difficult to process. The chlorine atoms have a tendency to split out under the influence of heat during processing. In addition, heat and light can produce discoloration and embrittlement during end-use conditions. Therefore, special stabilizer systems are often used with PVC to retard degradation.

PVC has good chemical resistance to alcohols, mild acids and bases, and salts. However, halogenated solvents, ketones, esters, aldehydes, ethers, and phenols attack PVC.

There are two major classifications of PVC—rigid and flexible (plasticized). In addition, there are also foamed PVC and PVC copolymers. Typical properties of PVC resins appear in Table 11.

#### *Rigid PVC*

PVC alone is a fairly rigid polymer, but it is difficult to process and has low impact strength. Both of these properties are improved by the addition of elastomers or impact-modified graft copolymers, such as ABS and ASA resins. These improve the melt flow during processing and improve the impact strength without seriously lowering the rigidity or the heat deflection temperature.

**Table 11** Typical Properties for PVC

Property	General Purpose	Rigid	Rigid Foam	Plasticized	Copolymer
Density (g/cm <sup>3</sup> )	1.40	1.34–1.39	0.75	1.29–1.34	1.37
$T_g$ (°C)	98	—	—	—	—
$T_m^g$ (°C)	212	—	—	—	—
Tensile modulus (GPa)	3.45	2.41–2.45	—	—	3.15
Tensile strength (MPa)	56.6	37.2–42.4	>13.8	14–26	52–55
Elongation at break (%)	85	—	>40	250–400	—
Notched Izod (kJ/m)	0.53	0.74–1.12	>0.06	—	0.02
HDT, 1.81 MPa (°C)	77	73–77	65	—	65
Brittle temperature (°C)	—	—	—	–60 to –30	—
Hardness	D85	R107–R122	D55	A71–A96	—
	(Shore)	(Rockwell)	(Shore)	(Shore)	
CTE (10 <sup>–5</sup> 1/°C)	7.00	5.94	5.58	—	—
Shrinkage (in./in.)	0.003	—	—	—	—
Relative permittivity, 1 kHz	3.39	—	—	—	—
Loss tangent, 1 kHz	0.081	—	—	—	—

*Uses.* With this improved balance of properties, rigid PVCs are used in such applications as construction (door and window frames, water supply, pipe, fittings, conduit, building panels and siding, rainwater gutters and downspouts, interior molding, and flooring), packaging (bottles, food containers, films for food wrap), consumer goods (credit cards, furniture parts), and other (agricultural irrigation and chemical processing piping).

#### ***Plasticized PVC***

The rigid PVC is softened by the addition of compatible, nonvolatile, liquid plasticizers. The plasticizers are usually used in >20 parts per hundred resins. It lowers the crystallinity in PVC and acts as an internal lubricant to give clear, flexible plastics. Plasticized PVC is also available in liquid formulations known as plastisols or organosols.

*Uses.* Plasticized PVC is used for construction (wire and cable insulation, interior wall covering), consumer goods (outdoor apparel, rainwear, upholstery, garden hose, toys, shoes, tablecloths, sporting goods, shower curtains), medical (clear tubing, blood and solution bags, connectors), and automotive (seat covers). Plastisols are used in coating fabric, paper, and metal and are rotationally cast into balls, dolls, etc.

#### ***Foamed PVC***

Rigid PVC can be foamed to a low-density cellular material that is used for decorative moldings and trim. Foamed PVC is also available via foamed plastisols. Foamed PVC adds greatly to the softness and energy absorption characteristics already inherent in plasticized PVC. In addition, it gives rich, warm, leatherlike material

*Uses.* Upholstery, clothing, shoe fabrics, handbags, luggage, and auto door panels; energy absorption for quiet and comfort in flooring, carpet backing, auto headliners, etc.

#### ***PVC Copolymers***

Copolymerization of vinyl chloride with 10–15% vinyl acetate gives a vinyl polymer with improved flexibility and less crystallinity than PVC, making such copolymers easier to process without detracting seriously from the rigidity and heat deflection temperature.

*Uses.* These copolymers find primary applications in flooring and solution coatings.

### **3.10 Poly(vinylidene chloride)**

Poly(vinylidene chloride) (PVDC) is prepared by the catalytic polymerization of 1,1-dichloroethylene. This crystalline polymer exhibits high strength, abrasion resistance, high melting point, better than ordinary heat resistance (100°C maximum service temperature), and outstanding impermeability to oil, grease, water vapor, oxygen, and carbon dioxide. It is used in films, coatings, and monofilaments.

When the polymer is extruded into film, quenched, and oriented, the crystallinity is fine enough to produce high clarity and flexibility. These properties contribute to widespread use in packaging film, especially for food products that require impermeable barrier protection.

PVDC and copolymers with vinyl chloride, alkyl acrylate, or acrylonitrile are used in coating paper, paperboard, or other films to provide more economical, impermeable materials. Properties appear in Table 12.

*Uses.* PVDC is used in food packaging where barrier properties are needed. Applications for injection-molding grades are fittings and parts in the chemical industry. PVDC pipe is used in the disposal of waste acids. PVDC is extruded into monofilament and tape that are used in outdoor furniture upholstery.

**Table 12** Typical Properties of Poly(vinylidene chloride)

Density (g/cm <sup>3</sup> )	1.65–1.72
$T_g$ (°C)	–18
$T_m$ (°C)	197
Tensile strength (MPa)	25
Elongation at break (%)	120
Notched Izod (kJ/m)	0.04
Hardness (Rockwell)	M50–65

## 4 POLYURETHANE AND CELLULOSIC RESINS

### 4.1 Polyurethanes

Polyurethanes (PUs) are prepared from polyols and isocyanates.<sup>24,25</sup> The isocyanate groups react with the hydroxyl groups on the polyol to form a urethane bond. The polyol can be a low-molecular-weight, hydroxyl-terminated polyether or polyester. The isocyanate can be aliphatic or aromatic. In the preparation of linear PUs the isocyanate is typically difunctional. However, isocyanates with greater functionality are used in preparing rigid-foam PUs. The family of PU resins is very complex because of the enormous variation in the compositional features of the polyols and isocyanates. This variety results in a large number of polymer structures and performance profiles. Indeed, PUs can be rigid solids, soft and elastomeric, or have a foam (cellular) structure.

The majority of PU resins are thermoset (PUR). However, there are also important thermoplastic polyurethane resins (TPU). Polyurethanes offer high impact strength, even at low temperatures, good abrasion resistance, excellent heat resistance, excellent resistance to non-polar solvents, fuels, and oils, and resistance to ozone, oxidation, and humidity.

TPUs are generally processed by injection-molding techniques. Reaction injection molding (RIM) and various foaming techniques are used to process PURs. A major use of PUR is in the production of flexible, semirigid, and rigid foams. In addition PUs can be used as fibers, sealants, adhesives, and coatings. Typical properties of polyurethanes appear in Table 13.

*Uses.* Typical applications for PUs are in consumer goods (furniture padding, bedding, skateboard and roller blade wheels, shoe soles, athletic shoes, ski booths, backing on carpets and

**Table 13** Typical properties of Polyurethanes

Property	TPU Polyester	TPU Polyether	PUR–RIM Foam	PUR–RIM Solid	PUR–RIM Elastomer
Density (g/cm <sup>3</sup> )	1.21	1.18	0.56	1.13	1.04
Tensile strength (MPa)	41	38	13.8	39	24
Elongation at break (%)	500	250	10	10	250
Flexural modulus (GPa)	0.14	0.54	0.86	0.14	0.36
Flexural strength (MPa)	—	—	27.6	60	—
Notched Izod (kJ/m)	—	—	—	0.05	0.6
HDT, 0.45 MPa (°C)	59	45	70	—	—
Vicat softening temperature (°C)	167	140	—	—	—
Brittle temperature (°C)	<–68	<–70	—	—	—
Hardness (Shore)	D55	D70	D65	D76	D58
CTE (10 <sup>–5</sup> 1/°C)	13	11.5	7.9	10	11
Shrinkage (in./in.)	0.008	0.008	0.8	1.1	1.3

**Table 14** Typical Properties of Cellulosic Materials

Property	CA	CAB	CAP
Density (g/cm <sup>3</sup> )	1.28	1.19	1.19
$T_g$ (°C)	-30	—	—
$T_m$ (°C)	230–237	—	—
Tensile modulus (GPa)	2.17	1.73	1.73
Tensile strength (MPa)	40	34.5	35
Elongation at break (%)	25	50	60
Flexural modulus (GPa)	2.4	1.8	—
Flexural strength (MPa)	66	60	—
Notched Izod (kJ/m)	0.16	0.187	0.41
HDT, 1.81 MPa (°C)	61	65	72
HDT, 0.42 MPa (°C)	72	72	80
Vicat softening temperature (°C)	—	—	100
Hardness (Rockwell)	R82	R75	R70
CTE (10 <sup>-5</sup> 1/°C)	13.5	13.5	14
Relative permittivity, 1 kHz	3.6	3.6	3.6

tiles), automotive (padding, seals, fascias, bumpers, structural door panels), and miscellaneous (tubing, membranes, bearings, nuts, seals, gaskets).

## 4.2 Cellulosic Polymers

Cellulose-based plastics are manufactured by the chemical modification of cellulose.<sup>26–29</sup> Cellulose does not melt and hence is not a thermoplastic material. However, esterification of cellulose gives organic esters of cellulose, which are thermoplastic. These include cellulose acetate (CA), cellulose acetate butyrate (CAB), and cellulose propionate (CP). Cellulosic resins are noted for their wide range of properties, which include clarity (up to 80% light transmission), abrasion resistance, stress crack resistance, high gloss, and good electrical properties. CA offers good rigidity and hardness. CAB and CP offer good weatherability, low-temperature impact strength, and dimensional stability.

In general, cellulosic esters are resistant to aliphatic hydrocarbons, ethylene glycol, bleach, and various oils. However, alkaline materials can attack them. Cellulosic esters have high water absorption and low continuous-use temperatures. Typical properties appear in Table 14.

*Uses.* Typical applications for cellulosic plastics are automotive (steering wheels, trim), films (photographic, audio tape, pressure-sensitive tape), home furnishings (table edging, Venetian blind wands), packaging (tubular containers, thermoformed containers for nuts, bolts, etc.), and miscellaneous (tool and brush handles, toys, filaments for toothbrushes, eye glass frames, lighting fixtures).

## 5 ENGINEERING THERMOPLASTICS

Engineering thermoplastics comprise a special performance segment of synthetic plastics materials that offer enhanced properties.<sup>2,3</sup> A more detailed history of the development of this area of thermoplastics is reviewed elsewhere.<sup>2,3</sup> When properly formulated, they may be shaped into mechanically functional, semiprecision parts or structural components. Mechanical functionality implies that the parts may be subjected to mechanical stress, impact, flexure, vibration, sliding friction, temperature extremes, hostile environments, etc., and continue to function.

As substitutes for metal in the construction of mechanical apparatus, engineering plastics offer advantages such as transparency, light weight, self-lubrication, and economy in fabrication and decorating. Replacement of metals by plastic is favored as the physical properties and operating temperature ranges of plastics improve and the cost of metals and their fabrication increases.

## 5.1 Thermoplastic Polyesters

Thermoplastic polyesters are prepared from the condensation polymerization of a diol and typically a dicarboxylic acid. Usually the dicarboxylic acid is aromatic, that is, terephthalic acid. As a family of polymers thermoplastic polyesters are typically semicrystalline and hence have good chemical resistance. An important attribute of a semicrystalline polymer is a fast rate of crystallization, which facilitates short injection-molding cycles.

### *Poly(butylene terephthalate)*

Poly(butylene terephthalate) (PBT) is prepared from butanediol with dimethyl terephthalate.<sup>29–31</sup> PBT is a semicrystalline polymer which has a fast rate of crystallization and rapid molding cycles. PBT has a unique and favorable balance of properties between polyamides and polyacetals. PBT combines high mechanical, thermal, and electrical properties with low moisture absorption, extremely good self-lubricity, fatigue resistance, very good chemical resistance, very good dimensional stability, and good maintenance of properties at elevated temperatures. Dimensional stability and electrical properties are unaffected by high-humidity conditions.

PBT has good chemical resistance to water, ketones, alcohols, glycols, ethers, and aliphatic and chlorinated hydrocarbons at ambient temperatures. In addition, PBT has good resistance to gasoline, transmission fluid, brake fluid, greases, and motor oil. At ambient temperatures PBT has good resistance to dilute acids and bases, detergents, and most aqueous salt solutions. It is not recommended for use in strong bases or aqueous media at temperatures above 50°C.

PBT grades range from unmodified to glass fiber reinforced to combinations of glass fiber and mineral fillers which enhance strength, modulus, and heat deflection temperature. Both filled and unfilled grades of PBT offer a range of UL and other agency compliance ratings.

A high-density PBT combines the inherent characteristics of PBT with the advantages of high levels of mineral reinforcement. This combination provides a balance of mechanical, thermal, and electrical properties, broad chemical and stain resistance, low water absorption, and dimensional stability. In addition, the smooth, satin finish and heavy weight offer the appearance and quality feel of ceramics while providing design flexibility, injection-molding processing advantages, and recycling opportunities which are common in engineering thermoplastics. Properties appear in Table 15.

*Uses.* Applications of PBT include automotive components (brake system parts, fuel injection modules, grille opening panels), electrical/electronic components (connectors, smart network interface devices, power plugs, electrical components, switches, relays, fuse cases, light sockets, television tuners, fiber optic tubes), medical (check valves, catheter housings, syringes), consumer goods (hair dryer and power tool housings, iron and toaster housings, food processor blades, cooker-fryer handles), and miscellaneous (gears, rollers, bearing, housings for pumps, impellers, pulleys, industrial zippers). High-density PBT is being used in kitchen and bath sinks, countertops, wall tiles, showerheads, speaker housings, medical equipment, and consumer goods.

### *PBT–PC Alloys*

PBT–PC resins are thermoplastic alloys of PBT and polycarbonate (PC). The amorphous PC provides impact resistance and toughness while the PBT provides enhanced chemical resistance



**Table 15** Typical Properties of Poly(butylene terephthalate)

Property	PBT	PBT + 30% GF	PBT + 40% GF
Density (g/cm <sup>3</sup> )	1.31	1.53	1.63
$T_g$ (°C)	40–50	—	—
$T_m$ (°C)	230–235	—	—
Tensile modulus (GPa)	—	—	—
Tensile strength (MPa)	52	119	128
Elongation at break (%)	300	3	—
Flexural modulus (GPa)	2.34	7.58	8.27
Flexural strength (MPa)	83	190	200
Notched Izod (kJ/m)	0.053	0.085	0.096
Unnotched Izod, (kJ/m)	1.602	0.801	0.961
HDT, 1.81 MPa (°C)	54	207	204
HDT, 0.42 MPa (°C)	154	216	216
Vicat softening temperature (°C)	—	—	—
RTI (°C)	—	140	—
Oxygen index (%)	—	—	—
Hardness (Rockwell)	R117	R118	R118
CTE (10 <sup>-5</sup> 1/°C)	8.1	2.5	2.7
Shrinkage (in./in.)	0.006	0.004	0.004
Water absorption, 24 h (%)	0.08	0.06	0.05
Relative permittivity, 1 MHz	3.1	3.7	4.0
Loss tangent, 1 MHz	0.419	0.02	0.02

and thermal stability. Impact modification completes the balanced performance profile by providing both low- and high-temperature durability. Hence, high levels of impact strength are achieved at low temperatures, below  $-40^{\circ}\text{C}$ .

PBT–PC resins offer a balance of performance characteristics unique among engineering thermoplastics with its optimal combination of toughness, chemical resistance, dimensional stability, lubricity, and high heat distortion temperature. In addition, this family of resins offers very good aesthetics, lubricity, UV resistance, and color retention. Originally developed for the automotive industry, PBT–PC resins are designed to provide resistance to various automotive fluids— gasoline, greases, oils, etc. In general, the higher the amounts of PBT in the resin alloy, the higher the resin’s chemical resistance. Hence, resistance to gasoline may vary from grade to grade. PBT–PC resins generally are not very hydrolytically stable. Properties appear in Table 16.

*Uses.* Applications for PBT–PC resins include automotive bumpers/fascia, tractor hoods and panels, components on outdoor recreational vehicles, lawn mower decks, power tool housings, material-handling pallets, and large structural parts.

#### *Poly(ethylene terephthalate)*

Poly(ethylene terephthalate) (PET) is prepared from the condensation polymerization of dimethyl terephthalate or terephthalic acid with ethylene glycol.<sup>29–31</sup> PET is a semicrystalline polymer that exhibits high modulus, high strength, high melting point, good electrical properties, and moisture and solvent resistance. The crystallization rate of PET is relatively slow. This slow crystallization is a benefit in blow molding bottles where clarity is important. Indeed, a small amount of a comonomer is typically added during polymerization of PET. The function of the comonomer is to disrupt the crystallinity and retard an already slow rate of

**Table 16** Typical Properties of PBT–PC Alloys

Property	PBT–PC	PBT–PC + 30% GF
Density (g/cm <sup>3</sup> )	1.21	1.44
Tensile strength (MPa)	59	92
Elongation at break (%)	120	4
Flexural modulus (GPa)	2.04	5.38
Flexural strength (MPa)	85	138
Notched Izod (kJ/m)	0.710	0.171
Notched Izod, -30°C (kJ/m)	3.204	0.112
Unnotched Izod (kJ/m)	0.299	0.641
HDT, 1.81 MPa (°C)	99	149
HDT, 0.42 MPa (°C)	106	204
Hardness (Rockwell)	R112	R109
CTE (10 <sup>-5</sup> 1/°C)	8.4	2.3
Shrinkage (in./in.)	0.009	0.005
Water absorption, 24 h (%)	0.12	0.09
Relative permittivity, 1 MHz	3.04	3.9
Loss tangent, 1 MHz	0.019	0.02

crystallization. However, in injection-molding applications the slow rate of crystallization will increase the molding cycle time.

For most injection-molding applications PET generally contains glass fiber or mineral filler to enhance properties. Typical properties appear in Table 17.

*Uses.* Primary applications of PET include blow-molded beverage bottles; fibers for wash-and-wear, wrinkle-resistant fabrics; and films that are used in food packaging, electrical applications

**Table 17** Typical Properties of Poly(ethylene terephthalate)

Property	PET	PBT + 30% GF
Density (g/cm <sup>3</sup> )	1.41	1.60
$T_g$ (°C)	69	—
$T_m$ (°C)	265	—
Tensile modulus (GPa)	1.71	11.5
Tensile strength (MPa)	50	175
Elongation at break (%)	180	2
Flexural modulus (GPa)	2.0	—
Flexural strength (MPa)	—	225
Notched Izod (kJ/m)	0.090	—
HDT, 1.81 MPa (°C)	63	225
HDT, 0.42 MPa (°C)	71	—
Vicat softening temperature (°C)	—	260
Oxygen index (%)	—	21
Hardness (Rockwell)	R105	—
	2.0	9.1
Shrinkage (in./in.)	—	—
Water absorption, 24 h (%)	—	0.15
Relative permittivity, 1 MHz	3.3	4.2
Loss tangent, 1 MHz	—	0.018

**Table 18** Typical Properties of Poly(trimethylene terephthalate)

Property	PTT	PTT + 30% GF
Density (g/cm <sup>3</sup> )	1.35	1.55
$T_g$ (°C)	40	—
$T_m$ (°C)	230	—
Flexural modulus (GPa)	2.76	10.3
Flexural strength (MPa)	65.1	—
Tensile strength (Mpa)	57	159
Notched Izod (kJ/m)	0.05	0.11
HDT, 1.81 MPa (°C)	59	216
Shrinkage (in./in.)	0.020	0.002
Dielectric constant at 1 MHz	3.0	—
Relative permittivity, 1 MHz	0.02	—

(capacitors, etc.), magnetic recording tape, and graphic arts. Injection-molding application of PET include automotive (cowl vent grills, wiper blade supports) and electrical (computer fan blades, fuse holders and connectors).

#### *Poly(trimethylene terephthalate)*

Poly(trimethylene terephthalate) (PTT) is prepared from 1,3-propanediol and terephthalic acid. PTT is a semicrystalline polymer that exhibits properties between PET and PBT. In particular, it offers high modulus, high strength, good electrical properties, and moisture and solvent resistance. Its crystallization rate is slower than PBT but faster than PET.<sup>32</sup> Properties appear in Table 18.

*Uses.* Initial applications for PTT were in carpet fiber where it offers a softer feel in combination with stain resistance and resiliency. Other fiber markets include textiles and monofilaments. Injection-molding applications would be various automotive parts.

## 5.2 Polyamides (Nylon)

Polyamides, commonly called nylons, are produced by the condensation polymerization of dicarboxylic acids and diamines or the catalytic polymerization of a lactam monomer (a cyclic amide).<sup>33,34</sup> In general, polyamides are semicrystalline thermoplastics. Polyamides are a class of resins characterized by broad chemical resistance, high strength, and toughness. In addition, polyamides absorb high levels of water. Moisture from the atmosphere diffuses into the polymer and hydrogen bonds to the amide groups. This absorbed water causes dimensional changes where the molded part will increase in size and weight. The higher the amount of amide groups in the polymer, the greater the moisture uptake. Furthermore, the absorbed water acts as a plasticizer and lowers the rigidity and strength. Polar solvents such as alcohols are also absorbed into the nylon.

There are numerous dicarboxylic acids and diamines that can be used to make polyamides. The shorthand method for describing the various types of polyamides uses a number to designate the number of carbon atoms in each starting monomer(s). In the case of terephthalic and isophthalic acids, T and I, respectively, are used.

#### *Polyamide 6/6 and 6 (PA6, PA6/6)*

The two major types of polyamides are polyamide 6/6, or nylon 6/6 (PA6/6), and polyamide 6, or nylon 6 (PA6).<sup>33,34</sup> PA6/6 is made from a six-carbon dicarboxylic acid and a six-carbon

**Table 19** Typical Properties of Polyamide 6 and 6/6

Property	PA6	PA6 + 33% Glass Fiber	PA6/6 +	PA6/6 + 40% Glass Fiber
Density (g/cm <sup>3</sup> )	1.13	1.46	1.14	1.44
$T_g$ (°C)	47–57	—	47–57	—
$T_m$ (°C)	220	—	269	—
Tensile modulus (GPa)	—	—	3.30	—
Tensile strength (MPa)	79	200	86	—
Elongation at break (%)	70	3	45	—
Flexural modulus (GPa)	2.83	9.38	2.90	9.3
Flexural strength (MPa)	108	276	—	219
Notched Izod (kJ/m)	0.053	0.117	0.059	0.14
HDT, 1.81 MPa (°C)	64	210	90	250
HDT, 0.45 MPa (°C)	165	220	235	260
RTI (°C)	105	120	—	—
Hardness (Rockwell)	R119	R121	—	M119
CTE (10 <sup>-5</sup> 1/°C)	8.28	2.16	8.10	3.42
Shrinkage (in./in.)	0.013	0.003	0.0150	0.0025
Water absorption, 24 h (%)	1.2	—	1.2	—
Relative permittivity, 1 MHz	3.5	3.8	3.2	—
Loss tangent, 1 MHz	0.023	—	0.025	—

diamine, that is, adipic acid and hexamethylene diamine. PA6 is prepared from caprolactam. Both PA6/6 and PA6 are semicrystalline resins.

Key features of nylons include toughness, fatigue resistance, and chemical resistance. Nylons do exhibit a tendency to creep under applied load. Nylons are resistant to many chemicals, including ketones, esters, fully halogenated hydrocarbons, fuels, and brake fluids. Nylons have a relatively low heat deflection temperature. However, glass fibers or mineral fillers are used to enhance the properties of polyamides. In addition to increasing the heat deflection temperature, the fibers and fillers lessen the effect of moisture and improve the dimensional stability. Properties of PA6/6 and PA6 appear in Table 19.

*Uses.* The largest application of nylons is in fibers. Molded applications include automotive components (electrical connectors, wire jackets, fan blades, valve covers, emission control valves, light-duty gears), electronic (connectors, cable ties, plugs, terminals, coil forms), related machine parts (gears, cams, pulleys, rollers, boat propellers), and appliance parts.

#### **Polyamide–PPE Alloys**

Polyamide–polyphenylene ether (PA–PPE) alloys are compatibilized blends of amorphous PPE and a semicrystalline PA, which has a microstructure in which the PA is the continuous phase and the PPE is the discrete phase.<sup>3,35–37</sup> The PPE acts as an organic reinforcing material. This technology combines the inherent advantages of PPE (dimensional stability, very low water absorption, and high heat resistance) with the chemical resistance and ease of processing of the PA. This combination results in a chemically resistant material with the stiffness, impact resistance, dimensional stability, and heat performance required for an automotive body panel that can undergo on-line painting.

PA–PPE alloys offer broad environmental resistance to commonly used automotive fuels, greases, and oils. In addition, this family of alloys is resistant to detergents, alcohols, aliphatic and aromatic hydrocarbons, and alkaline chemicals.

**Table 20** Typical Properties of PPE–PA6/6 Alloys

Property	Unfilled		10% GF		30% GF	
	PA	PPE–PA	PA	PPE–PA	PA	PPE–PA
Density (g/cm <sup>3</sup> )	1.14	1.10	1.204	1.163	1.37	1.33
Flexural modulus (GPa)						
Dry as molded	2.8	2.2	4.5	3.8	8.3	8.1
100% Relative humidity at 150°C		0.48	0.63	2.3	2.6	4.1
		0.21	0.70	0.9	1.6	3.2
Flexural strength (MPa)						
Dry as molded		96	92	151	146	275
100% Relative humidity		26	60	93	109	200
At 150°C		14	28	55	60	122

Since PPE does not absorb any significant amount of moisture, the effect of moisture on properties is reduced. Indeed, the moisture uptake in PA–PPE alloys is lower. Hence PA–PPE alloys minimize the effect of moisture on rigidity, strength, and dimensional stability vis-à-vis PA.<sup>35,36</sup> In addition, heat deflection temperatures have been enhanced by the PPE. Properties are shown in Table 20.

*Uses.* PA–PPE alloys are used in automotive body panels (fenders and quarter panels); automotive wheel covers, exterior truck parts, and under-the-hood automotive parts (air intake resonators, electrical junction boxes and connectors); and fluid-handling applications (pumps, etc.).

#### ***Polyamide 4/6 (PA4/6)***

Nylon 4/6 is prepared from the condensation polymerization of 1,4-diaminobutane and adipic acid.<sup>33</sup> PA4/6 has a higher crystalline melting point, greater crystallinity, and a faster rate of crystallization than other PAs. In comparison to PA6/6 and PA6, PA4/6 offers high tensile strength and heat deflection temperature; however, it has higher moisture uptake, which can affect properties and dimensional stability. Properties appear in Table 21.

*Uses.* Application for PA4/6 include under-the-hood automotive parts, gears, bearing, and electrical parts.

#### ***Semiaromatic Polyamides (PA6/6T, PA6I/6T)***

Semiaromatic polyamides have been developed in order to increase the performance over that of PA6/6 and PA6.<sup>33</sup> In general, these resins are modified copolymers based on poly (hexamethylene terephthalate) or PA6/T. Pure nylon 6/T exhibits a very high  $T_m$  of 370°C and a  $T_g$  of 180°C. This high  $T_m$  is above its decomposition temperature. PA6/T copolymers have been prepared using additional monomers such as isophthalic acid, adipic acid, caprolactam, or 1,5-hexyl diamine, which lower the crystalline melting point into useful ranges for melt processing. These terpolymers exhibit  $T_m$  from 290 to 320°C and  $T_g$  from 100 to 125°C and offer enhanced performance—i.e., stiffer, stronger, greater thermal and dimensional stability—over PA6/6 and 6. Melt processing requires higher temperatures and often an oil-heated mold (>100°C). These semicrystalline PAs have good chemical resistance, good dielectric properties, lower moisture absorption, and more dimensional stability in the presence of moisture than PA6 and PA6/6. Properties appear in Table 22.

**Table 21** Typical Properties of Nylon 4/6

Property	PA4/6	PA4/6 + 30% GF
Density (g/cm <sup>3</sup> )	1.18	1.41
$T_g$ (°C)	75	—
$T_m$ (°C)	295	—
Tensile modulus (GPa)	3.3	10.0
Tensile strength (MPa)	100	210
Elongation at break (%)	15	4
Flexural modulus (GPa)	3.1	—
Flexural strength (MPa)	149.6	—
Notched Izod (kJ/m)	0.096	0.069
HDT, 1.81 MPa (°C)	190	290
HDT, 0.42 MPa (°C)	280	290
Vicat softening temperature (°C)	290	290
Hardness (Shore)	D85	—
CTE (10 <sup>-5</sup> 1/°C)	9.0	5.0
Water absorption, 24 h (%)	3.7	2.6
Relative permittivity, 1 kHz	3.83	—

**Table 22** Typical Properties of Semiaromatic Polyamides

Property	PA6/6T+35%		PA6T/6I+ 40%	
	PA6/6T	GF	PA6T/6I	GF
Density (g/cm <sup>3</sup> )	1.16	1.43	1.21	1.46
$T_g$ (°C)	200	—	100	—
$T_m$ (°C)	310–340	—	290	—
Tensile modulus (GPa)	3.20	12.0	2.44	11.1
Tensile strength (MPa)	100	210	108	187
Elongation at break (%)	11.5	3	5	2
Flexural modulus (GPa)	—	—	3.43	10.8
Flexural strength (MPa)	—	—	157	284
Notched Izod (kJ/m)	0.070	—	0.049	0.079
Unnotched Izod (kJ/m)	—	—	0.395	0.592
HDT, 1.81 MPa (°C)	100	270	140	295
HDT, 0.45 MPa (°C)	120	—	—	—
RTI (°C)	125	—	120	120
CTE (10 <sup>-5</sup> 1/°C)	7.0	1.5	—	—
Shrinkage (in./in.)	0.0065	0.0035	0.006	0.002
Water absorption, 24 h (%)	1.8	—	0.3	0.2
Relative permittivity, 1 MHz	4.0	4.2	—	—
Loss tangent, 1 MHz	0.030	0.020	—	—

*Uses.* High heat application, automotive (radiator ventilation and fuels supply systems), electrical/electronic ( housings, plugs, sockets, connectors) and recreational (tennis rackets, golf clubs), mechanical (industrial and chemical processing equipment, bearings, gears), appliance and plumbing parts, aerospace components.

#### **Aromatic Polyamides**

Polyamides prepared from aromatic diamines and aromatic dicarboxylic acids give very high heat aromatic nylons or aramids. They are not thermoplastic but are included here

**Table 23** Typical Properties of Aromatic Polyamides

Property	PPTA	MPIA
Density (g/cm <sup>3</sup> )	—	1.38
$T_g$ (°C)	425	280
$T_m$ (°C)	> 550	435
Tensile modulus (GPa)	80–125	—
Tensile strength (MPa)	1500–2500	61
Elongation at break (%)	2	25
Flexural modulus (GPa)	—	3.1
Oxygen index (%)	29	28
CTE (10 <sup>-5</sup> 1/°C)	-0.32	0.62

with other polyamides. Examples are poly (*p*-phenyleneterephthalamide) (PPTA) and poly (*m*-phenyleneisophthalamide) (MPIA). These wholly aromatic PAs have high strength, high modulus, high chemical resistance, high toughness, excellent dimensional stability, and inherent flame resistance. MPIA has a  $T_g$  of 280°C and is difficult to melt process. Typically it is spun into fibers. PPTA has a very high  $T_g$  and  $T_m$  of 425 and 554°C, respectively. In addition, PPTA exhibits liquid crystalline behavior and is spun into highly oriented, very high modulus, crystalline fibers. Properties appear in Table 23.

*Uses.* PPTA fibers have uses in bullet-resistant apparel, composites, brake and transmission parts, gaskets, ropes and cables, sporting goods, tires, belts, and hoses.

MPIA fibers have uses in heat-resistant and flame-retardant apparel, electrical insulation, and composite structures.

### 5.3 Acetals

Polyacetal homopolymer, or polyoxymethylene (POM), is prepared via the polymerization of formaldehyde followed by capping each end of the polymer chain with an ester group for thermal stability. Polyacetal copolymer (POM-Co) is prepared by copolymerizing trioxane with relatively small amounts of a comonomer such as ethylene oxide.<sup>29</sup> The comonomer functions to stabilize the polymer to reversion reactions. POM and POM-Co are commonly referred to as acetals and are semicrystalline polymers.

Polyacetals exhibit rigidity, high strength, excellent creep resistance, fatigue resistance, toughness, self-lubricity/wear resistance, and solvent resistance. Acetals are resistant to gasoline, oils, greases, ethers, alcohols, and aliphatic hydrocarbons. They are not recommended for use with strong acids.

Properties are enhanced by the addition of glass fiber or mineral fillers. Properties of POM and POM-Co appear in Table 24.

*Uses.* Applications of polyacetals include moving parts in appliances and machines (gears, bearings, bushings, rollers, springs, valves, conveying equipment), automobiles (door handles, fasteners, knobs, fuel pumps housings), plumbing and irrigation (valves, pumps, faucet underbodies, shower heads, impellers, ball cocks), industrial or mechanical products (rollers, bearings, gears, conveyer chains, and housings), consumer products (audio/video cassette components, toiletry articles, zippers, pen barrels, disposable lighters, and toy parts), and electronics (key tops, buttons, switches).

**Table 24** Typical Properties of Polyacetals

Property	POM	POM-Co	POM+25% GF	POM-Co+ 30% GF
Density (g/cm <sup>3</sup> )	1.41	1.42	1.58	1.60
$T_g$ (°C)	-75	—	—	—
$T_m$ (°C)	170	165	—	—
Tensile modulus (GPa)	3.12	2.83	9.50	9.20
Tensile strength (MPa)	68.9	60.6	140	135
Elongation at break (%)	50	60	3	2.5
Flexural modulus (GPa)	2.83	2.58	8.00	—
Flexural strength (MPa)	97	90	—	—
Notched Izod (kJ/m)	0.074	0.054	0.096	—
HDT, 1.81 MPa (°C)	136	110	172	160
HDT, 0.45 MPa (°C)	172	158	176	—
Vicat softening point (°C)	—	151	178	158
Hardness (Rockwell)	M94	M80	—	—
CTE (10 <sup>-5</sup> 1/°C)	11.1	8.5	5.6	6.0
Shrinkage (in./in.)	0.02	—	0.008	—
Water absorption, 24 hours (%)	0.25	0.22	0.17	0.17
Relative permittivity, 1 MHz	3.7	4.0	—	4.3
Loss tangent, 1 MHz	—	0.005	—	0.006

## 5.4 Polycarbonate

Most commercial PCs are produced by the interfacial polymerization of bisphenol A and phosgene.<sup>29,38–40</sup> PCs are amorphous resins which have a unique combination of outstanding clarity and high impact strength. In addition, PCs offer high dimensional stability, resistance to creep, and excellent electrical insulating characteristics. Indeed, PCs are among the stronger, tougher, and more rigid thermoplastics available. PC is a versatile material and a popular blend material used to enhance the performance of ABS, ASA, and polyesters (PBT). PCs offer limited resistance to chemicals. PC properties are shown in Table 25.

*Uses.* Applications of PC include glazing (safety glazing, safety shields, nonbreakable windows), automotive parts (lamp housings and lenses, exterior parts, instrument panels), packaging (large water bottles, reusable bottles), food service (mugs, food processor bowls, beverage pitchers), ophthalmic (optical lenses, corrective eyewear, sun wear lenses), medical/laboratory ware (filter housings, tubing connectors, eye ware, health care components), consumer (various appliance parts and housings, power tool housings, cellular phone housings, food processor bowls, lighting), media storage [compact discs (CDs), digital video discs (DVDs)], and miscellaneous (electrical relay covers, aircraft interiors, building and construction). Extruded PC film is used in membrane switches.

## 5.5 Polycarbonate–ABS Alloys

PC–ABS alloys are amorphous blends of PC and ABS resins. They offer a unique balance of properties that combines the most desirable properties of both resins.<sup>41</sup> The addition of ABS improves the melt processing of PC–ABS blends, which facilitates filling large, thin-walled parts. Moreover, the ABS enhances the toughness of PC, especially at low temperatures, while maintaining the high strength and rigidity of the PC. In addition, PC–ABS offers good UV stability, high dimensional stability at ambient and elevated temperatures, and the ability for chlorine/bromine-free flame retardance.



**Table 25** Typical Properties of Polycarbonates

Property	PC	PC + 30% GF
Density (g/cm <sup>3</sup> )	1.20	1.43
$T_g$ , (°C)	150	—
Tensile modulus (GPa)	2.38	8.63
Tensile strength (MPa)	69	131
Elongation at break (%)	130	3
Flexural modulus (GPa)	2.35	7.59
Flexural strength (MPa)	98	158
Notched Izod (kJ/m)	0.905	0.105
Unnotched Izod (kJ/m)	3.20	1.06
HDT, 1.81 MPa (°C)	132	146
HDT, 0.45 MPa (°C)	138	152
Vicat softening point (°C)	154	165
RTI (°C)	121	120
Hardness (Rockwell)	R118	R120
CTE (10 <sup>-5</sup> 1/°C)	6.74	1.67
Shrinkage (in./in.)	0.006	0.002
Water absorption, 24 h (%)	0.15	0.14
Relative permittivity, 1 MHz	2.96	3.31

**Table 26** Typical Properties of Polycarbonate–ABS Blends

Properties	PC–ABS Ratio (wt/wt)			
	0/100	50/50	80/20	100/0
Density (g/cm <sup>3</sup> )	1.06	1.13	1.17	1.20
Tensile modulus (GPa)	1.8	1.9	2.5	2.4
Tensile strength (MPa)	40	57	60	65
Elongation at break (%)	20	70	150	110
Notched Izod, 25°C (kJ/m)	0.30	0.69	0.75	0.86
Notched Izod, –20°C (kJ/m)	0.11	0.32	0.64	0.15
HDT, 1.81 MPa (°C)	80	100	113	132

The properties are a function of the ABS-to-polycarbonate ratio. Properties appear in Table 26.

*Uses.* Automotive (interior and exterior automotive applications as instrument panels, pillar, bezel, grilles, interior and exterior trim), business machines (enclosures and internal parts of products such as lap- and desk-top computers, copiers, printers, plotters, and monitors), telecommunications [mobile telephone housings, accessories, and smart cards (GSM SIM cards)], electrical (electronic enclosures, electricity meter covers and cases, domestic switches, plugs and sockets, and extruded conduits), and appliances (internal and external parts of appliances such as washing machines, dryers, and microwave ovens)

## 5.6 Polyester–Carbonates

Polyester–carbonate (PEC) resins have iso- and terephthalate units incorporated into standard bisphenol A polycarbonate.<sup>38</sup> This modification of the polymer enhances the performance between that of PC and polyarylates. Thus, PECs have properties similar to PC but with higher

**Table 27** Typical Properties of Poly(ester carbonates)

Property	PEC-1	PEC-2
Density (g/cm <sup>3</sup> )	1.20	1.20
Tensile strength (MPa)	71.8	78.0
Elongation at break (%)	120	75
Flexural modulus (GPa)	2.03	2.33
Flexural strength (MPa)	95	96.6
Notched Izod (kJ/m)	0.534	0.534
Unnotched Izod (kJ/m)	3.20	3.22
HDT, 1.81 MPa (°C)	151	162
HDT, 0.42 MPa (°C)	160	174
RTI (°C)	125	130
Hardness (Rockwell)	R122	R127
CTE (10 <sup>-5</sup> 1/°C)	5.1	4.5
Linear mold shrinkage (in./in.)	0.007	0.009
Water absorption, 24 h (%)	0.16	0.19
Relative permittivity, 1 MHz	3.19	3.45

heat deflection temperature and better hydrolytic performance. Increased levels of iso- and terephthalate units result in higher heat deflection temperatures and continuous-use temperatures. Properties of PECs with different heat deflection temperatures appear in Table 27.

*Uses.* PEC is marketed into typical polycarbonate applications that require slightly higher heat deflection temperature and continuous-use temperatures such as consumer goods, electrical/electronic, and automotive parts.

## 5.7 Polyarylates

The homopolymers of bisphenol A and isophthalic acid or terephthalic acids are semicrystalline.<sup>42</sup> The semicrystalline polyarylates (PARs) have high crystalline melting points and very slow crystallization rates. Hence, the need for oil-heated molds and long cycle times would have made commercialization unattractive. However, amorphous PARs prepared from a mixture of isophthalic and terephthalic acids and bisphenol A can be melt processed without difficulty. They are transparent, slightly yellow in color, dimensionally stable, and resistant to creep, have excellent electrical properties, are rigid, and have good impact strength.

PARs have poor chemical resistance to ketones, esters, and aromatic and chlorinated hydrocarbons. Typical properties appear in Table 28.

*Uses.* Polyarylates are marketed into applications requiring a higher heat deflection temperature than PC. These include electrical/electronic and automotive applications.

## 5.8 Modified Polyphenylene Ether

Poly(2,6-dimethylphenylene ether) (PPE) is produced by the oxidative coupling of 2,6-dimethyl phenol.<sup>43–46</sup> PPE is an amorphous thermoplastic. The PPE polymer has a very high heat deflection temperature, good inherent flame resistance, outstanding dimensional stability, and outstanding electrical properties. In addition, PPE has one of the lowest moisture absorption rates found in any engineering plastic.

**Table 28** Typical Properties of Polyarylates

Property	PAR	PAR + 40% GF
Density (g/cm <sup>3</sup> )	1.21	1.40
$T_g$ (°C)	180	—
Tensile modulus (GPa)	2.0	8.28
Tensile strength (MPa)	66	149
Elongation at break (%)	50	0.8
Flexural modulus (GPa)	2.14	7.59
Flexural strength (MPa)	86	220
Notched Izod (kJ/m)	0.22	0.085
HDT, 1.81 MPa (°C)	174	—
Oxygen index (%)	34	—
UL94 VO (mm)	1.60	—
RTI (°C)	120	—
Hardness (Rockwell)	R100	R125
CTE (10 <sup>-5</sup> 1/°C)	5.6	3.0
Shrinkage (in./in.)	0.009	0.002
Water absorption (%)	0.27	0.18
Relative permittivity, 1 MHz	2.62	3.8

PPE by itself is difficult to process; hence, PPE is commonly blended with styrenics (that is, PS and HIPS) to form a family of modified PPE-based resins.<sup>30–32</sup> What is truly unique about the PPE–PS blends is that the PPE and PS form a miscible, single-phase blend. Most polymers have limited solubility in other polymers. Modified PPE resins cover a wide range of compositions and properties.

Modified PPE resins are characterized by ease of processing, high impact strength, outstanding dimensional stability at elevated temperatures, long-term stability under load (creep resistance), and excellent electrical properties over a wide range of frequencies and temperatures. Another unique feature of modified PPE resins is their ability to make chlorine/bromine-free flame-retardant grades.

Modified PPE resins are especially noted for their outstanding hydrolytic stability—they do not contain any hydrolyzable bonds. Their low water absorption rates—both at ambient and elevated temperatures—promote the retention of properties and dimensional stability in the presence of water or high humidity and even in steam environments. In addition, modified PPE resins are also virtually unaffected by a wide variety of aqueous solutions—salts, detergents, acids, and bases.

PPE is a versatile material and is used in alloys with PAs to enhance the performance and decrease the moisture absorbance of the PAs. These alloys were described in Section 5.2 and Table 20 in this chapter.

The chemical compatibility with oils and greases is limited. It is not recommended for contact with ketones, esters, toluene, and halogenated solvents. Typical properties appear in Table 29.

*Uses.* Applications include automotive (instrument panels, trim, spoilers, under-the-hood components, grills), telecommunication equipment (TV cabinets, cable splice boxes, wire board frames, electrical connectors, structural and interior components in electrical/electronic equipment), plumbing/water handling (pumps, plumbing fixtures), consumer goods (microwavable food packaging and appliance parts), medical, and building and construction.

**Table 29** Typical Properties of PPE and Modified PPE Resins

Property	PPE	190 Grade	225 Grade	300 Grade
Density (g/cm <sup>3</sup> )	1.06	1.12	1.11	1.12
$T_g$ (°C)	225	—	—	—
Tensile modulus (GPa)	2.69	2.70	—	—
Tensile strength (MPa)	80	61	67	76
Elongation at break (%)	30	18	17	20
Flexural modulus (GPa)	2.59	2.35	2.49	2.50
Flexural strength (MPa)	114	93	99	110
Notched Izod (kJ/m)	0.064	0.029	0.019	0.023
Unnotched Izod (kJ/m)	—	0.721	—	—
HDT, 1.81 MPa (°C)	174	88	99	145
HDT, 0.42 MPa (°C)	179	96	109	156
Vicat softening temperature (°C)	—	113	129	—
RTI (°C)	—	95	95	105
UL94 V-0 (mm)	—	1.5	1.5	1.5
Oxygen index (%)	29	39	—	—
Hardness (Rockwell)	M78	R120	—	R119
CTE (10 <sup>-5</sup> 1/°C)	8.8	—	5.4	—
Shrinkage (in./in.)	0.006	0.006	0.006	—
Water absorption, 24 h (%)	0.02	0.08	—	0.06
Relative permittivity, 1 MHz	2.56	2.60	2.55	2.63
Loss tangent, 1 MHz	0.0032	0.0055	0.007	0.009

## 6 HIGH-PERFORMANCE MATERIALS

High-performance resins arbitrarily comprise the high end of engineering plastics and offer premium performance. Typically high-performance resins will be used in tough metal replacement applications or replacement of ceramic materials. Such materials offer greater resistance to heat and chemicals, high RTIs, higher strength and stiffness, and inherent flame resistance. These resins have higher cost and the processing can be more challenging.

### 6.1 Polyphenylene Sulfide

The condensation polymerization of 1,4-dichlorobenzene and sodium sulfide yields PPS, a semicrystalline polymer.<sup>47</sup> PPS is characterized by high heat resistance, rigidity, excellent chemical resistance, dimensional stability, low friction coefficient, good abrasion resistance, and electrical properties. PPS has good mechanical properties, which remain stable during exposure to elevated temperatures. Water absorption for PPS is very low and hydrolytic stability is very high. PPS resins are inherently flame resistant.

PPS has excellent chemical resistance to a wide range of chemicals. Indeed, even at elevated temperatures PPS can withstand exposure to a wide range of chemicals such as mineral and organic acids and alkali. However, it is attacked by chlorinated hydrocarbons.

Depending on the polymerization process, PPS can be a linear or branched polymer. The branched polymer is somewhat more difficult to process due to relatively poorer flow characteristics.

PPS resins normally contain glass fibers or mineral fillers. Properties appear in Table 30.

*Uses.* Applications for PPS resins include industrial (parts requiring heat and chemical resistance, submersible, vane, and gear-type pump components), electrical/electronic (high-voltage

**Table 30** Typical Properties of Polyphenylene Sulfide

Property	Branched	Branched+ 40% GF	Linear	Linear+ 40% GF
Density (g/cm <sup>3</sup> )	1.35	1.60	1.35	1.65
$T_g$ (°C)	85	—	90	—
$T_m$ (°C)	270–280	—	285–295	—
Tensile modulus (GPa)	—	14.5	4.0	15.7
Tensile strength (MPa)	65	150	66	150
Elongation at break (%)	2	1.2	12	1.7
Flexural modulus (GPa)	3.85	15.0	3.90	15.0
Flexural strength (MPa)	104	153	130	230
Notched Izod (kJ/m)	0.080	0.578	0.139	0.241
Unnotched Izod (kJ/m)	0.107	0.482	0.167	0.589
HDT, 1.81 MPa (°C)	115	> 260	115	265
RTI (°C)	220	—	220	—
UL94 V-0 (mm)	—	0.8	—	0.6
Oxygen index (%)	44	46.5	44	47
Hardness (Rockwell)	R120	R123	M95	M100
CTE (10 <sup>-5</sup> 1/°C)	4.9	4.0	5.3	4.1
Shrinkage (in./in.)	—	0.004	0	0.004
Water absorption, 24 h (%)	—	0.03	—	0.03
Relative permittivity, 1 MHz	—	3.9	—	4.7
Loss tangent, 1 MHz	—	0.0014	—	0.020

electrical components), automotive (electrical connectors, under-the-hood components), appliance parts (hair dryers, small cooking appliance, range components), medical (hydraulic components, bearing cams, valves), and aircraft/aerospace.

## 6.2 Polyarylsulfones

Polyarylsulfones are a class of amorphous, high-end-use temperature thermoplastics that characteristically exhibit excellent thermo-oxidative stability, good solvent resistance, creep resistance, transparency, and high heat deflection temperatures.<sup>48–51</sup> Polyarylsulfones have excellent hydrolytic stability even in saturated steam; they can be repeatedly steam sterilized. Typically the polyarylsulfone families of resins have low resistance to weathering and are degraded by UV light. There are three major categories of aromatic polyarylsulfone resins—polysulfone (PSU), polyphenylsulfone (PPSU), and polyethersulfone (PES).

Polysulfone is prepared by nucleophilic aromatic displacement of the chloride on bis(*p*-chlorophenyl)sulfone by the anhydrous disodium salt of bisphenol A. This amorphous polymer has a  $T_g$  of 186°C.

Polyphenylsulfone is higher performing than PSU. This wholly aromatic resin is prepared from 4,4'-biphenol and bis(*p*-chlorophenyl)sulfone.<sup>51</sup> The lack of aliphatic groups in this all-aromatic polymer and the presence of the biphenyl moiety impart enhanced chemical/solvent resistance, outstanding toughness, greater resistance to combustion, greater thermo-oxidative stability, and a  $T_g$  of 225°C. PPSU has excellent resistance to mineral acids, caustic, salt solution, and various automotive fluids. Exposure to esters, ketones, and polar aromatic solvents should be avoided.

Polyethersulfone (PES) consists of a diphenyl sulfone unit linked through an ether (oxygen) unit. Again the lack of aliphatic groups results in higher thermo-oxidative stability. PES offers high heat ( $T_g$  of 225°C), chemical/solvent resistance, and improved toughness over PSU.

**Table 31** Typical Properties of Polyarylsulfones

PSU	Property	PES	PPSU
Density (g/cm <sup>3</sup> )	1.24	1.37	1.29
$T_g$ (°C)	186	225	220
Tensile modulus (GPa)	2.48	2.41	2.35
Tensile strength (MPa)	69	82	70
Elongation at break (%)	75	50	60
Flexural modulus (GPa)	2.55	2.55	2.42
Flexural strength (MPa)	102	110	91
Notched Izod (kJ/m)	0.080	0.075	0.694
Notched Izod, -40°C (kJ/m)	0.064	—	0.425
HDT, 1.81 MPa (°C)	174	203	204
HDT, 0.42 MPa (°C)	180	210	—
Vicat softening temperature (°C)	188	226	—
RTI (°C)	160	180	180
UL94 V-0 (mm)	—	0.46	0.58
Oxygen index (%)	—	38	—
Hardness (Rockwell)	M69	M88	—
CTE (10 <sup>-5</sup> 1/°C)	5.1	5.5	5.5
Shrinkage (in./in.)	0.005	0.006	0.006
Water absorption, 24 h (%)	0.3	0.43	0.37
Relative permittivity, 1 MHz	3.19	3.45	3.5
Loss tangent, 1 MHz	—	0.0076	—

PES is chemically resistant to most inorganic chemicals, greases, aliphatic hydrocarbons, and gasoline. However, esters, ketones, methylene chloride, and polar aromatic solvents attack PES.

Typical properties of PSU, PPSU and PES appear in Table 31.

*Uses.* Typical applications of polyarylsulfones include medical/laboratory (surgical equipment, laboratory equipment, life support parts, autoclavable tray systems, suction bottles, tissue culture bottles, and surgical hollow shapes), food handling (microwave cookware, coffee makers, hot-water and food-handling equipment, range components), electrical/electronic (components, multipin connectors, coil formers, printed circuit boards), chemical processing equipment (pump housings, bearing cages), and miscellaneous (radomes, alkaline battery cases).

### 6.3 Polybiphenyldisulfones

Polyetherbiphenyldisulfones are high-temperature sulfone (HTS) polymers. These amorphous polymers are prepared by the nucleophilic displacement of the chlorides on 4,4'-bis(4-chlorophenylsulfonyl)biphenyl with bisphenols under basic conditions in a dipolar aprotic solvent. The more rigid biphenyldisulfone unit results in polymers with noticeably higher  $T_g$  than other sulfone polymers. Indeed, the bisphenol A (BisA-HTS) and hydroquinone (HQ-HTS) based polymers exhibit  $T_g$  of 245 and 265°C, respectively.

These high-temperature sulfone polymers are transparent and completely amorphous and can be melt processed by injection molding and extrusion. They exhibit high thermal performance capabilities; good strength, stiffness, and dielectric properties over a wide temperature range; resistance to hydrolysis by hot water and steam; excellent resistance to acids and bases; and inherent flammability resistance.

**Table 32** Typical Properties of Polybiphenylsulfones

Property	HQ-HTS	BisA-HTS	BisA-HTS + 30% GF
Density (g/cm <sup>3</sup> )	1.31	1.30	1.55
$T_g$ (°C)	265	245	245
Tensile modulus (GPa)	2.30	2.30	9.0
Tensile strength (MPa)	79	76	117
Elongation at break (%)	15	40	2
Flexural modulus (GPa)	2.20	2.30	8.30
Flexural strength (MPa)	93	94	174
Notched Izod (kJ/m)	0.080	0.075	0.694
Unnotched Izod, (kJ/m)	—	—	11.1
HDT, 1.81 MPa (°C)	255	235	240
Hardness (Rockwell)	R127	—	—
Shrinkage (in./in.)	0.007	0.007	0.003
Water absorption, 24 h (%)	0.50	0.40	0.30

The material's thermal performance combined with its good strength and stiffness, dimensional stability, and creep resistance suggests opportunities in high-temperature injection-molding applications that traditionally have been limited to filled, semicrystalline polymers.

Typical properties of HQ-HTS and BisA-HTS appear in Table 32.

*Uses.* Applications for polybiphenylsulfones include opportunities in metal replacement as well as high-performance thermoset resins in a wide range of engineering applications. These include automotive, aerospace, electrical, electronic, and industrial product applications.

## 6.4 Liquid Crystalline Polyesters

Liquid crystalline polymers (LCPs) have a rigid rodlike aromatic structure. The rodlike molecules arrange themselves in parallel domains in both the melt and solid states. In the molten state the molecules readily slide over one another, giving the resin very high flow under shear. Most commercially important polyester LCPs are based on *p*-hydroxy-benzoic acid (HBA). An example would be the copolyester of HBA and hydroxy-naphthanoic acid (HNA) with a molar ratio of 73:27.

LCPs are highly crystalline, thermotropic (melt-orienting) thermoplastics. Because of the possibility of melt orientation during molding, LCPs can have anisotropic properties, that is, properties can differ in the direction of flow and perpendicular to the flow direction. LCPs offer high strength, rigidity, dimensional stability, inherent flame resistance, and high heat resistance. LCPs have high flow and can deliver exceptionally precise and stable dimensions in very thin walled applications.

LCPs are resistant to weathering, burning, gamma radiation, steam autoclaving, and most chemical sterilization methods. They have outstanding strength at elevated temperatures.

LCPs are resistant to most chemicals, including acids, organic hydrocarbons, and boiling water. However, LCPs are attacked by concentrated, boiling caustic but are relatively unaffected by milder solutions. Typical properties of the HBA–HNA LCP appear in Table 33.

*Uses.* Typical applications of LCPs include electrical/electronic (stator insulation, rotors, boards for motors, burn-in sockets, interface connectors, bobbins, switches, chip carriers, and sensors), medical (surgical instruments, needleless syringes, dental tools, sterilizable trays and equipment, drug delivery systems, and diagnostics), industrial (chemical process and oil field equipment), and packaging (food packaging requiring barrier properties).

**Table 33** Typical Properties of LCP Resins (HBA–HNA)

Property	LCP	LCP + 15% GF	LCP + 30% GF
Density (g/cm <sup>3</sup> )	1.40	1.50	1.62
$T_g$ (°C)	120	—	—
$T_m$ (°C)	280	—	—
Tensile modulus (GPa)	10.6	12.0	15.0
Tensile strength (MPa)	182	190	200
Elongation at break (%)	3.4	3.1	2.1
Flexural modulus (GPa)	9.10	12.0	15.0
Flexural strength (MPa)	158	240	280
Notched Izod (kJ/m)	0.75	0.35	0.17
Unnotched Izod (kJ/m)	2.0	0.48	0.23
HDT, 0.45 MPa (°C)	—	250	250
HDT, 1.81 MPa (°C)	187	230	235
Vicat softening point (°C)	145	162	160
Oxygen index (%)	—	—	45
Hardness (Rockwell)	—	M80	M85
CTE (10 <sup>-5</sup> 1/°C)			
Parallel to flow	0.4	1.0	0.6
Perpendicular to flow	3.62	1.8	2.3
Shrinkage (in./in.)			
Parallel to flow	0.0	0.001	0.002
Perpendicular to flow	0.007	0.004	0.004
Water absorption, 24 h (%)	0.03	—	—
Relative permittivity, 1 MHz	3.0	3.0	3.7
Loss tangent, 1 MHz	0.02	0.018	0.018

## 6.5 Polyimides

Polyimides are a class of polymers prepared from the condensation reaction of a dicarboxylic acid anhydride with a diamine.<sup>52</sup> Polyimides are among the most heat resistant polymers. Poly(pyromellitimide-1,4-diphenyl ether) is prepared from pyromellitic anhydride (PMDA) and 4,4'-oxydianiline (ODA). PMDA–ODA has a  $T_g$  of 360°C or higher. This very high  $T_g$  does not lend itself to standard melt processing techniques. PMDA–ODA resins are available as films and direct-formed parts from formulated resin. PMDA–ODA has excellent thermal stability, useful mechanical properties over a very wide temperature range, creep resistance, high toughness, and excellent wear resistance. PMDA–ODA has excellent electrical properties to a broad range of chemicals. However, it will be attacked by 10% and stronger solutions of sodium hydroxide. Typical properties appear in Table 34.

*Uses.* PMDA–ODA films are used as wire and cable wrap, motor-slot liners, flexible printed circuit boards, transformers, and capacitors. Molded parts are used in applications requiring resistance to thermally harsh environments such as automotive transmission parts, thermal and electrical insulators, valve seats, rotary seal rings, thrust washers and discs, bushings, etc.

## 6.6 Polyetherimide

Polyetherimides (PEIs) are prepared from the polymerization of aromatic diamines and ether-dianhydrides.<sup>53,54</sup> PEI is an amorphous thermoplastic which contains repeating aromatic imide and ether units. The rigid aromatic imide units provide PEI with its high-performance



**Table 34** Typical Properties of Polyimide

Property	PMDA-ODA	15% Graphite	40% Graphite
Density (g/cm <sup>3</sup> )	1.43	1.51	1.65
<i>T<sub>g</sub></i> (°C)	360–410	—	—
Tensile strength (MPa)	86.2	65.5	51.7
Elongation at break (%)	7.5	4.5	3.0
Flexural modulus (GPa)	3.10	3.79	4.83
Flexural strength (MPa)	110	110	90
Notched Izod (kJ/m)	0.043	0.043	—
Unnotched Izod (kJ/m)	0.747	0.320	—
HDT, 2 MPa (°C)	360	360	—
Oxygen index (%)	53	49	—
Hardness (Rockwell)		M80	M85
CTE (10 <sup>-5</sup> 1/°C)	5.4	4.9	3.8
Water absorption, 24 h (%)	0.24	0.19	0.14
Relative permittivity, 1 MHz	3.55	13.4	—
Loss tangent, 1 MHz	0.0034	0.0106	—

properties at elevated temperatures, while the ether linkages provide it with the chain flexibility necessary to have good melt flow and processability by injection-molding and other melt-processing techniques.

PEI offers high strength, rigidity, high heat resistance, inherent flame resistance, low smoke generation, excellent processability with very tight molding tolerances, heat resistance up to 200°C, RTI of 170°C, excellent dimensional stability (low creep sensitivity and low coefficient of thermal expansion), superior torque strength and torque retention, stable dielectric constant, and dissipation factor over a wide range of temperatures and frequencies.

PEI has excellent hydrolytic stability, UV stability, and radiation resistance. It is well suited for repeated steam, hot-air, ethylene oxide gas, and cold chemical sterilizations. In addition PEI has proven property retention through over 1000 cycles in industrial washing machines with detergents and compliancy with Food and Drug Administration (FDA), European Union (EU), and national food contact regulations.

In addition, PEI resins are resistant to a wide range of chemicals, including alcohols, hydrocarbons, aqueous detergents and bleaches, strong acids, mild bases, and most automotive fuels, fluids, and oils. Chlorinated hydrocarbons and aromatic solvents can attack PEI resins. Typical properties appear in Table 35.

*Uses.* Automotive (transmission components, throttle bodies, ignition components, sensors, and thermostat housings), automotive lighting (headlight reflectors, fog light reflectors, bezels, and light bulb sockets), telecommunications (molded interconnect devices, electrical control units, computer components, mobile phone internal antennae, RF-duplexers or microfilters, and fiber-optic connectors), electrical (lighting, connectors to reflectors), HVAC/fluid handling (water-pump impellers, expansion valves, hot-water reservoirs, and heat exchange systems), tableware/catering (food trays, soup mugs, steam insert pans or gastronome containers, cloches, microwavable bowls, ovenware, cooking utensils, and reusable airline casseroles), medical (reusable medical devices like sterilization trays, stopcocks, dentist devices, and pipettes), and aircraft (air and fuel valves, food tray containers, steering wheels, interior cladding parts, and semistructural components).

**Table 35** Typical Properties of Polyetherimides

Property	PEI	10% GF+ PEI	20% GF+ PEI	30% GF+ PEI
Density (g/cm <sup>3</sup> )	1.27	1.34	1.42	1.51
$T_g$ (°C)	215	—	—	—
Tensile modulus (GPa)	3.59	4.69	6.89	9.31
Tensile strength (MPa)	110	116	131	169
Elongation at break (%)	60	6	4	3
Flexural modulus (GPa)	3.52	5.17	6.89	8.96
Flexural strength (MPa)	165	200	228	228
Notched Izod (kJ/m)	0.053	0.053	0.064	0.085
Unnotched Izod (kJ/m)	1.335	0.481	0.481	0.427
HDT, 1.81 MPa (°C)	201	209	210	210
HDT, 0.42 MPa (°C)	210	210	210	212
Vicat softening temperature (°C)	219	223	220	228
RTI (°C)	170	170	170	180
UL94 V-0 (mm)	—	0.4	0.4	0.3
Oxygen index (%)	47	47	50	50
Hardness (Rockwell)	M109	M114	M114	M114
CTE (10 <sup>-5</sup> 1/°C)	5.5	3.24	2.52	1.98
Shrinkage (in./in.)	0.006	0.005	0.004	0.003
Water absorption, 24 h (%)	0.25	0.21	0.19	0.16
Relative permittivity, 1 kHz	3.15	3.5	3.5	3.7
Loss tangent, 1 kHz	0.0012	0.0014	0.0015	0.0015

## 6.7 Poly(amide imides)

Poly(amide imides) (PAIs) are prepared from trimellitic anhydride and various aromatic diamines.<sup>55</sup> PAIs are tough, high-modulus thermoplastics capable of high continuous-use temperatures. In addition, they have inherent flame resistance and very high strength. PAIs have very broad chemical resistance but are attacked by aqueous caustic and amines. PAIs have high melting temperatures and require very high processing temperatures. PAIs contain amide groups and hence will absorb moisture, which can affect dimensional stability. Properties appear in Table 36.

*Uses.* Automotive ( housings, connectors, switches, relays, thrust washers, valve seats, bushings, wear rings, rollers, thermal insulators), composites (printed wiring boards, radomes), and aerospace (replacement of metal parts).

## 6.8 Aromatic Polyketones

Aromatic polyketones are a family of semicrystalline high-performance thermoplastics that consist of a combination of ketone, ether, and aromatic units.<sup>56</sup> The absence of aliphatic groups results in outstanding high-temperature performance, exceptional thermal stability, excellent environmental resistance, high mechanical properties, resistance to chemical environments at elevated temperatures, inherent flame resistance, excellent friction and wear resistance, and impact resistance. In addition, aromatic polyketones have high chemical purity suitable for applications in silicon chip manufacturing.

There are two major aromatic polyketone resins—polyetherketone (PEK) and polyetheretherketone (PEEK). Typical properties appear in Table 37.

**Table 36** Typical Properties of PAIs

Property	PAI	PAI + 30% Graphite fiber
Density (g/cm <sup>3</sup> )	1.38	1.42
$T_g$ (°C)	272–287	—
Tensile modulus (GPa)	5.2	20.0
Tensile strength (MPa)	117	207
Elongation at break (%)	15	4
Flexural modulus (GPa)	3.59	17.9
Flexural strength (MPa)	189	316.7
Notched Izod (kJ/m)	0.136	0.07
Unnotched Izod (kJ/m)	1.088	—
HDT, 1.81 MPa (°C)	254	275
RTI (°C)	—	220
Hardness (Rockwell)	E78	E94
Oxygen index (%)	41	49
CTE (10 <sup>-5</sup> 1/°C)	3.6	4.9
Water absorption, 24 h (%)	1.0	0.8
Relative permittivity, 1 MHz	4.0	3.8
Loss tangent, 1 MHz	0.009	—

**Table 37** Typical Properties of Aromatic Polyketones

Property	PEEK	PEEK+ 30% Glass fiber	PEEK+ 30% Carbon Fiber	PEK	PEK+30% Glass fiber
Density (g/cm <sup>3</sup> )	1.32	1.49	1.44	1.30	1.53
$T_g$ (°C)	140	—	—	154	—
$T_m$ (°C)	335–343	—	—	361–367	—
Tensile modulus (GPa)	3.6	9.7	13.0	4.0	10.5
Tensile strength (MPa)	192	157	208	104	160
Elongation at break (%)	50	2.2	1.3	5	4
Flexural modulus (GPa)	3.7	10.3	13.0	3.7	9.0
Flexural strength (MPa)	170	233	318	—	—
Notched Izod (kJ/m)	0.08	0.1	0.09	0.08	0.1
Unnotched Izod (kJ/m)	—	0.73	0.75	—	—
HDT, 1.81 MPa (°C)	160	315	315	165	340
HDT, 0.42 MPa (°C)	—	—	315	—	—
RTI (°C)	—	—	—	260	260
UL94 V-0 (mm)	—	—	—	1.6	1.6
Oxygen index (%)	—	—	—	40	46
Hardness (Rockwell)	M126	R124	R124	R126	R126
CTE (10 <sup>-5</sup> 1/°C)	16	11.5	7.9	5.7	1.7
Shrinkage (in./in.)	0.004	0.005	0.001	0.006	0.004
Water absorption, 24 h (%)	0.5	0.11	0.06	0.11	0.08
Relative permittivity, 1 MHz	3.2	3.7	—	3.4	3.9

*Uses.* Applications are in the chemical process industry (compressor plates, valve seats, pump impellers, thrust washers, bearing cages), aerospace (aircraft fairings, radomes, fuel valves, ducting), and electrical/electronic (wire coating, semiconductor wafer carriers).

## 6.9 Modified Poly(*p*-phenylene)

Poly(*p*-phenylene) is a highly crystalline, rigid rod polymer that is insoluble and infusible. However, modification of poly(*p*-phenylene) can result in an amorphous, transparent, and melt-processible polymer. The structure is based on a string of substituted and unsubstituted benzene rings producing a highly rigid chain structure. The substituted benzene rings have pendant benzoyl groups. These benzoyl-substituted phenylene units along with some *meta*-phenylene units are sufficient to prevent crystallization. These polymers are prepared by carbon–carbon coupling polymerization reactions of 1,4-dichlorobenzene, 2,5-dichloroacetophenone, and 1,3-dichlorobenzene.

The amorphous polymers retain the rigid rod characteristics and are self-reinforcing, which results in very high, isotropic mechanical properties. Indeed, they are the stiffest unreinforced thermoplastics that are commercially available and provide exceptional strength and stiffness without fillers. Hence one no longer has to worry about the orientation of glass or carbon fibers within the plastic matrix—and the resulting directional differences in strength.

Standard melt processing techniques can be used for modified poly(*p*-phenylene). The polymer is soluble in common solvents and can be cast into films and coatings. In addition, machinable stock plastic shapes are available.

These self-reinforcing polyphenylenes are suitable for applications that have historically relied on ceramics, composites, and metals for superior mechanical performance. Mechanical performance is maintained across a wide range of temperatures. For example, mechanical properties are retained all the way down to liquid helium temperatures (4 K). The highly aromatic polymer is inherently flame resistant. Other characteristics include broad chemical resistance and good wear properties, which suggest use as parts in the chemical process industries and for a variety of semiconductor wafer-handling components. Typical properties of modified poly(*p*-phenylene) appear in Table 38.

**Table 38** Typical Properties of Polyphenylene

Density (g/cm <sup>3</sup> )	1.19
$T_g$ (°C)	168
Tensile modulus (GPa)	5.5
Tensile strength (MPa)	152
Elongation at break (%)	6–10
Flexural modulus (GPa)	6.0
Flexural strength (MPa)	234
Notched Izod (kJ/m)	0.059
Unnotched Izod (kJ/m)	1.60
HDT, 1.81 MPa (°C)	159
Hardness (Rockwell)	B32
Oxygen index (%)	55
CTE (10 <sup>-5</sup> 1/°C)	3.1
Shrinkage (in./in.)	0.003–0.005
Water absorption, 24 h (%)	0.14
Water absorption, equilibrium (%)	0.58
Relative permittivity, 1 MHz	3.01
Loss tangent, 1 MHz	0.007

*Uses.* The combination of high strength and light weight makes the material not just a good metal replacement candidate but also a replacement for some reinforced plastics. Market potential includes military equipment, jet engines, missile housings, electronics, chemical processing, oil field components, and medical devices.

## 7 FLUORINATED THERMOPLASTICS

Fluoropolymers or fluoroplastics are a family of fluorine-containing thermoplastics that exhibit some unusual properties.<sup>57,58</sup> These properties include inertness to most chemicals, resistance to high temperatures, extremely low coefficient of friction, weather resistance, and excellent dielectric properties which are relatively insensitive to temperature and frequency. Mechanical properties are normally low but can be enhanced with glass or carbon fiber or fillers such as molybdenum.

In general, their chemical resistance and heat resistance increase with increasing fluoro content. Conversely, their ease of processing and mechanical properties increase with decreasing fluoro content. Properties of various fluoropolymers are shown in Table 39.

### 7.1 Poly(tetrafluoroethylene)

Poly(tetrafluoroethylene) (PTFE) is a highly crystalline polymer produced by the polymerization of tetrafluoroethylene. PTFE offers very high heat resistance (up to 250°C), exceptional chemical resistance, and outstanding flame resistance.<sup>58</sup> The broad chemical resistance includes strong acids and strong bases. In addition, PTFE has the lowest coefficient of friction of any polymer.

PTFE has a high melting point and extremely high melt viscosity and hence cannot be melt processed by normal techniques. Therefore, PTFE has to be processed by unconventional techniques (PTFE powder is usually compacted to the desired shape and sintered).

*Uses.* Typically PTFE is used in applications requiring long-term performance in extreme-service environments. PTFE applications include electrical (high-temperature,

**Table 39** Typical Properties of Fluoropolymers

Property	PTFE	PCTFE	FEP	PVDF	ECTFE	PVF
Density (g/cm <sup>3</sup> )	2.29	2.187	2.150	1.77	1.680	1.368
$T_g$ (°C)	126	150	—	-35	—	64
$T_m$ (°C)	335–345	210–215	—	178	—	197–227
Tensile modulus (GPa)	4.10	14.0	—	1.194	—	1.2–2.3
Tensile strength (MPa)	27.6	40	20.7	44	48.3	40–60
Elongation at break (%)	~275	150	~300	43	200	175
Flexural modulus (GPa)	5.2	1.25	—	—	—	—
Flexural strength (MPa)	—	74	—	—	—	—
Notched Izod (kJ/m)	0.19	0.27	0.15	—	—	—
HDT, 0.45 MPa (°C)	132	126	—	104	116	—
HDT, 1.81 MPa (°C)	60	75	—	71	77	—
RTI (°C)	260	199	204	—	150–170	—
Hardness	D42	D77	D55	D75	R93	—
	(Shore)	(Shore)	(Shore)	(Shore)	(Rockwell)	—
CTE (10 <sup>-5</sup> 1/°C)	12.0	4.8	9.3	11	—	—
Relative permittivity, 10 <sup>2</sup> Hz	2.1	3.0	2.1	9	2.5	—
Loss tangent, 10 <sup>3</sup> Hz	0.0003	—	—	0.03	—	—

high-performance wire and cable insulation, sockets, pins, connectors), mechanical (bushings, rider rings, seals, bearing pads, valve seats, chemically resistant processing equipment and pipe, nonlubricated bearings, pump parts, gaskets, and packings), nonstick coatings (home cookware, tools, food-processing equipment), and miscellaneous (conveyor parts, packaging, flame-retardant laminates)

## 7.2 Poly(chlorotrifluoroethylene)

Poly(chlorotrifluoroethylene) (PCTFE) is less crystalline and exhibits higher rigidity and strength than PTFE.<sup>58</sup> Poly(chlorotrifluoroethylene) has excellent chemical resistance and heat resistance up to 200°C. Unlike PTFE, PCTFE can be molded and extruded by conventional processing techniques.

*Uses.* PCTFE applications include electrical/electronic (insulation, cable jacketing, coil forms), industrial (pipe and pump parts, gaskets, seals, diaphragms, coatings for corrosive process equipment and in cryogenic systems), and pharmaceutical packaging.

## 7.3 Fluorinated Ethylene–Propylene

Copolymerization of tetrafluoroethylene with some hexafluoropropylene produces fluorinated ethylene–propylene (FEP) polymer, which has less crystallinity, lower melting point, and improved impact strength than PTFE. FEP can be molded by normal thermoplastic techniques.<sup>58</sup>

*Uses.* FEP applications include wire insulation and jacketing, high-frequency connectors, coils, gaskets, and tube sockets.

## 7.4 Polyvinylidene Fluoride

Polyvinylidene fluoride (PVDF) is made by emulsion and suspension polymerization of 1,1-difluoroethylene and has better ability to be processed but less thermal and chemical resistance than the FEP, CTFE, and PTFE.<sup>58</sup> PVDF has excellent mechanical properties and resistance to severe environmental stresses and good chemical resistance.

*Uses.* Polyvinylidene fluoride applications include electronic/electrical (wire and cable insulation, films), fluid handling (solid and lined pipes, fittings, valves, seals and gaskets, diaphragms, pumps, microporous membranes), and coatings (metal finishes, exterior wall panels, roof shingles)

## 7.5 Poly(ethylene chlorotrifluoroethylene)

The copolymer of ethylene and chlorotrifluoroethylene is poly(ethylene chlorotrifluoroethylene) (ECTFE) and has high strength and chemical and impact resistance. ECTFE can be processed by conventional techniques.

*Uses.* Poly(ethylene chlorotrifluoroethylene) applications included wire and cable coatings, chemical-resistant coatings and linings, molded lab ware, and medical packing.

## 7.6 Poly(vinyl fluoride)

Poly(vinyl fluoride) (PVF) is the least chemical resistant fluoropolymer.<sup>58</sup> PVF offers weathering and UV resistance, antisoiling, durability, and chemical resistance.

*Uses.* Poly(vinyl fluoride) uses include protective coatings (aircraft interior, architectural fabrics, presurfaced exterior building panels, wall coverings, glazing, lighting).

## 8 THERMOSET RESINS

Thermosetting resins are used in molded and laminated plastics.<sup>59</sup> They are first polymerized into a low-molecular-weight linear or slightly branched polymer or oligomers, which are still soluble, fusible, and highly reactive during final processing. Thermoset resins are generally highly filled with mineral fillers and glass fibers. Thermosets are generally catalyzed and/or heated to finish the polymerization reaction, which crosslinks them to almost infinite molecular weight. This step is often referred to as cure. Such cured polymers cannot be reprocessed or reshaped.

The high filler loading and the high crosslink density of thermoset resins result in high densities, low ductility, high rigidity, and good chemical resistance.

### 8.1 Phenolic Resins

Phenolic resins combine the high reactivity of phenol and formaldehyde to form prepolymers and oligomers called resoles and novolacs. These materials can be used as adhesives and coatings or combined with fibrous fillers to give phenolic resins which when heated undergo a rapid, complete crosslinking to give a cured, highly crosslinked structure. The curing typically requires heat and pressure. Fillers include cellulosic materials, glass, and mineral fibers/fillers. The high crosslinked aromatic structure has high hardness, dimensional stability, rigidity, strength, heat resistance, chemical resistance, and good electrical properties.

Phenolic resins have good chemical resistance to hydrocarbons, phenols, and ethers. However, they can undergo chemical reaction with acids and bases.

*Uses.* Phenolic applications include appliance parts (handles, knobs, bases, end panels), automotive uses (parts in electric motors, brake linings, fuse blocks, coil towers, solenoid covers and housings, ignition parts), electrical/electronic (high-performance connectors and coil bobbins, circuit breakers, terminal switches and blocks, light sockets, receptacles), and miscellaneous (adhesives in laminated materials such as plywood, coatings).

### 8.2 Epoxy Resins

Epoxy resins are materials whose molecular structure contains an epoxide or oxirane ring. The most common epoxy resins are prepared from the reaction of bisphenol A and epichlorohydrin to yield low-molecular-weight resins that are liquid either at room temperature or on warming. Other epoxy resins are available and include novolac and cycloaliphatic epoxy resins. Each epoxy resin usually contains two or more epoxide groups. The high reactivity of the epoxide groups with aromatic and aliphatic amines, anhydrides, carboxylic acids, and other curing agents provides facile conversion into highly crosslinked materials. The large number of variations possible in epoxy structure and curing agent coupled with their ability to be formulated with a wide variety of fillers and additives results in broad application potential. Cured epoxy resins exhibit hardness, strength, heat resistance, good electrical properties, and broad chemical resistance.

Most epoxies are resistant to numerous chemicals, including hydrocarbons, esters, and bases. However, epoxies can exhibit poor resistance to phenols, ketones, ethers, and concentrated acids.

*Uses.* Epoxy resins are used in composites (glass-reinforced, high-strength composites in aerospace, pipes, tanks, pressure vessels), coatings (marine coatings, protective coatings on appliances, chemical scrubbers, pipes), electrical/electronic (encapsulation or casting of various electrical and electronic components, printed wiring boards, switches, coils, insulators, bushings), and miscellaneous (adhesives, solder mask, industrial equipment, and sealants).

### 8.3 Unsaturated Polyesters

Thermoset polyesters are prepared by the condensation polymerization of various diols and maleic anhydride to give a very viscous unsaturated polyester oligomer which is dissolved in styrene monomer. The addition of styrene lowers the viscosity to a level suitable for impregnation and lamination of glass fibers. The low-molecular-weight polyester has numerous maleate/fumarate ester units that provide facile reactivity with styrene monomer. Unsaturated polyesters can be prepared from a variety of different monomers.

Properly formulated glass-reinforced unsaturated polyesters are commonly referred to as sheet-molding compound (SMC) or reinforced plastics. The combination of glass fibers in the cured resins offers outstanding strength, high rigidity, impact resistance, high strength-to-weight ratio, and chemical resistance. SMC typically is formulated with 50% calcium carbonate filler, 25% long glass fiber (typically 1–2 in. in length) and 25% resin (where the resin is 60–40 wt.% unsaturated polyester and 40–50 wt.% styrene). The highly filled nature of SMC results in a high density and a brittle, easily pitted surface.

Bulk molding compounds (BMCs) are formulated similar to SMC except 1/4-in. chopped glass is typically used. The shorter glass length gives easier processing but lower strength and impact.

Thermoset polyesters have good chemical resistance, which includes exposure to alcohols, ethers, and organic acids. They exhibit poor resistance to hydrocarbons, ketones, esters, phenols, and oxidizing acids.

*Uses.* The prime use of unsaturated polyesters is in combination with glass fibers in high-strength composites and in SMC and BMC materials. The applications include transportation markets (large body parts for automobiles, trucks, trailers, buses, and aircraft, automotive ignition components), marine markets (small- to medium-sized boat hulls and associated marine equipment), building and construction (building panels, housing and bathroom components—bathtub and shower stalls), and electrical/electronic (components, appliance housing, switch boxes, breaker components, encapsulation).

### 8.4 Vinyl Esters

Vinyl esters are part of the unsaturated polyester family. They are prepared by the reaction of an epoxy resin with methacrylic acid. Thus, the epoxide group is converted into a methacrylate ester. Vinyl esters offer an enhancement in properties over unsaturated polyesters with greater toughness and better resistance to corrosion by a wide range of chemicals. This chemical resistance includes halogenated solvents, acids, and bases.

*Uses.* Applications for vinyl esters are similar to those for unsaturated polyesters but where added toughness and chemical resistance is required, that is, electrical equipment, flooring, fans, adsorption towers, process vessels, and piping,

### 8.5 Alkyd Resins

Alkyd resins are unsaturated polyesters based on branched prepolymers from polyhydric alcohols (e.g., glycerol, pentaerythritol, ethylene glycol), polybasic acids (e.g., phthalic anhydride, maleic anhydride, fumaric acid), and fatty acids and oils (e.g., oleic, stearic, palmitic, linoleic, linolenic, lauric, and licanic acids). They are well suited for coating with their rapid drying, good adhesion, flexibility, mar resistance, and durability. Formulated alkyd molding resins have good heat resistance, are dimensionally stable at high temperatures, and have excellent dielectric strength, high resistance to electrical leakage, and excellent arc resistance.



Alkyl resins can be hydrolyzed under alkaline conditions.

*Uses.* Alkyd resin applications include coatings (drying oils in paints, enamels, and varnish) and molding compounds when formulated with reinforcing fillers for electrical applications (circuit breaker insulation, encapsulation of capacitors and resistors, coil forms).

## 8.6 Diallyl Phthalate

Diallyl phthalate (DAP) is the most widely used compound in the allylic ester family. The neat resin is a medium-viscosity liquid. These low-molecular-weight prepolymers can be reinforced and compression molded into highly crosslinked, completely cured products.

The most outstanding properties of DAP are excellent dimensional stability and high insulation resistance. In addition, DAP has high dielectric strength and excellent arc resistance. DAP has excellent resistance to aliphatic hydrocarbons, oils, and alcohols but is not recommended for use with phenols and oxidizing acids.

*Uses.* DAP applications include electrical/electronic (parts, connectors, bases and housings, switches, transformer cases, insulators, potentiometers) and miscellaneous (tubing, ducting, radomes, junction bases, aircraft parts). DAP is also used as a coating and an impregnating resin.

## 8.7 Amino Resins

The two main members of the amino resin family of thermosets are the melamine–formaldehyde and urea–formaldehyde resins. They are prepared from the condensation reaction of melamine and urea with formaldehyde. In general, these materials exhibit extreme hardness, inherent flame resistance, heat resistance, scratch resistance, arc resistance, chemical resistance, and light fastness.

*Uses.* Melamine–formaldehyde resins find use in colorful, rugged dinnerware, decorative laminates (countertops, tabletops, and furniture surfacing), electrical applications (switchboard panels, circuit breaker parts, arc barriers, and armature and slot wedges), and adhesives and coatings.

Urea–formaldehyde resins are used in particleboard binders, decorative housings, closures, electrical parts, coatings, and paper and textile treatment.

## 9 GENERAL-PURPOSE ELASTOMERS

Elastomers are polymers that can be stretched substantially beyond their original length and can retract rapidly and forcibly to essentially their original dimensions (on release of the force).<sup>59,60</sup>

The optimum properties and/or economics of many rubbers are obtained through formulating with reinforcing agents, fillers, extending oils, vulcanizing agents, antioxidants, pigments, etc. End-use markets for formulated rubbers include automotive tire products (including tubes, retread applications, valve stems, and inner liners), adhesives, cements, caulks, sealants, latex foam products, hose (automotive, industrial, and consumer applications), belting (V-conveyor and trimming), footwear (heels, soles, slab stock, boots, and canvas), molded, extruded, and calendered products (athletic goods, flooring, gaskets, household products, O-rings, blown sponge,

**Table 40** Properties of General-Purpose Elastomers

Rubber	ASTM Nomenclature	Outstanding Characteristic	Property Deficiency	Temperature Use Range (°C)
Butadiene rubber	BR	Very flexible; resistance to wear	Sensitive to oxidation; poor resistance to fuels and oil	-100-90
Natural rubber	NR	Similar to BR but less resilient	Similar to BR	-50-80
Isoprene rubber	IR	Similar to BR but less resilient	Similar to BR	-50-80
Isobutylene-isoprene rubber (butyl rubber)	IIR	High flexibility; low-permeability air		-45-150
Chloroprene	CR	Flame resistant; fair fuel and oil resistance; increased resistance toward oxygen, ozone, heat, light	Poor low-temperature flexibility	-40-115
Nitrile-butadiene	NBR	Good resistance to fuels, oils, and solvents; improved abrasion resistance	Lower resilience; higher hysteresis; poor electrical properties; poorer low temperature flexibility	-45-80
Styrene-butadiene rubber	SBR	Relatively low cost	Less resilience; higher hysteresis; limited low-temperature flexibility	-45-80
Ethylene-propylene copolymer	EPDM	Resistance to ozone and weathering	Poor hydrocarbon and oil resistance	-50 to <175
Polysulfide	T	Chemical resistance; resistance to ozone and weathering	Creep; low resilience	-45-120

thread, and rubber sundries). A list of general-purpose elastomers and properties is given in Table 40.

## 10 SPECIALTY ELASTOMERS

Specialty rubbers offer higher performance over general-purpose rubbers and find use in more demanding applications.<sup>61</sup> These materials are more costly and hence are produced in smaller volume. Properties and uses are summarized in Table 41.

**Table 41** Features of Specialty Elastomers

Elastomer	ASTM Nomenclature	Temperature Use Range (°C)	Outstanding Characteristic	Typical Applications
Silicones (polydimethylsiloxane)	MQ	−100 to 300	Wide temperature range; resistance to aging, ozone, sunlight; very high gas permeability	Seals, molded and extruded goods; adhesives, sealants; biomedical; personal care products
Fluoroelastomers	CFM	−40 to 200	Resistance to heat, oils, chemical	Seals such as O-rings, corrosion-resistant coatings
Acrylic	AR	−40 to 200	Oil, oxygen, ozone, and sunlight resistance	Seals, hose
Epichlorohydrin	ECO	−18 to 150	Resistance to oil, fuels; some flame resistance; low gas permeability	Hose, tubing, coated fabrics, vibration isolators
Chlorosulfonated	CSM	−40 to 150	Resistance to oil, ozone weathering, oxidizing chemicals	Automotive hose, wire and cable, linings for reservoirs
Chlorinated polyethylene	CM	−40 to 150	Resistance to oils, ozone, chemicals	Impact modifier, automotive applications
Ethylene-acrylic		−40 to 175	Resistance to ozone, weathering	Seals, insulation, vibration damping
Propylene oxide		−6 to 150	Low-temperature properties	Motor mounts

## REFERENCES

1. E. N. Peters, "Thermoplastics, Thermosets, and Elastomers," in M. Kutz (Ed.), *Handbook of Materials Selection*, Wiley-Interscience, New York, 2002, pp. 335–355.
2. D. W. Fox and E. N. Peters, "Engineering Thermoplastics: Chemistry and Technology," in R. W. Tess and G. W. Poehlein (Eds.), *Applied Polymer Science*, 2nd ed., American Chemical Society: Washington, DC, 1985, pp. 495–514.
3. E. N. Peters and R. K. Arisman, "Engineering Thermoplastics," in C. D. Craver and C. E. Carraher (Eds.), *Applied Polymer Science—21st Century*, Elsevier, New York, 2000, pp. 177–196.
4. E. N., Peters, in M. Grayson (Ed.), *Kirk-Othmer Encyclopedia of Chemical Technology*, Vol. 13, 3rd ed., Wiley, New York, 1981.
5. E. N. Peters, "Introduction to Polymer Characterication," in R. F. Brady, Jr. (Ed.), *Comprehensive Desk Reference of Polymer Characterization and Analysis*, Oxford University Press, New York, 2003, pp. 3–29.
6. S. H. Goodman, (Ed.), *Handbook of Thermoset Plastics*, 2nd ed., Plastics Design Library, Brookfield, CT, 1999.
7. O. Olabisi (Ed.), *Handbook of Thermoplastics*, Marcel Dekker, New York, 1998.

8. E. N. Peters, "Behavior in Solvents," in R. F. Brady, Jr. (Ed.), *Comprehensive Desk Reference of Polymer Characterization and Analysis*, Oxford University Press: New York, 2003, pp. 535–554.
9. H. Zweifel (Ed.), *Plastics Additives Handbook*, 5th ed., Hanser/Gardner: Cincinnati, OH, 2001
10. J. Stepek and H. Daoust, *Additives for Plastics*, Springer-Verlag, New York, 1983.
11. G. Pritchard, *Plastics Additives: An A-Z Reference*, Chapman & Hall, London, 1998.
12. J. T. Lutz (Ed.), *Thermoplastic Polymer Additives: Theory and Practice*, Marcel Dekker, New York, 1989.
13. G. Wypych, *Handbook of Fillers: The Definitive User's Guide and Databook on Properties, Effects, and Users*, 2nd ed., Plastics Design Library, Brookfield, CT, 2000.
14. G. M. Benedikt and B. L., Goodall (Eds.), *Metallocene-Catalyzed Polymers—Materials, Properties, Processing and Markets*, Plastics Design Library, Brookfield, CT, 1998.
15. V. Shah (Ed.), *Handbook of Polyolefins*, 2nd ed., revised and expanded, Wiley, New York, 1998.
16. A. J. Peacock, *Handbook of Polyethylene: Structures, Properties, and Applications*, Marcel Dekker, New York, 2000.
17. H. G. Karian (Ed.), *Handbook of Polypropylene and Polypropylene Composites*, Marcel Dekker, New York, 1999.
18. *Polypropylene—The Definitive User's Guide*, Plastics Design Library, Brookfield, CT, 1998.
19. D. A. Smith (Ed.), *Addition Polymers: Formation and Characterization*, Plenum, New York, 1968.
20. J. Scheirs and D. Priddy (Eds.), *Modern Styrenic Polymers*, Wiley, New York, 2003.
21. D. Bank and R. Brentin, *SPS Crystalline Polymer: A New Material for Automotive Interconnect Systems*, SAE Technical Paper 970305, DOI: 10.4271/970305, 1997.
22. H. Vernaleken, "Polycarbonates," in F. Millich and C. Carraher (Eds.), *Interfacial Synthesis*, Vol. II, Marcel Dekker, New York, 1977, pp. 65–124.
23. E. J., Wickson (Ed.), *Handbook of PVC Formulating*, Wiley, New York, 1993.
24. D. Randall and S. Lee (Eds.), *The Polyurethanes Book*, Wiley, New York, 2003.
25. K. Uhlig, *Discovering Polyurethanes*, Hanser Gardner, New York, 1999.
26. W. Pigman and D. Horton (Eds.), *The Carbohydrates*, 2nd ed., Academic, New York, 1970.
27. G. O. Aspinall (Ed.), *The Polysaccharides*, Vol. 1, Academic, New York, 1982.
28. R. Gilbert (Ed.), *Cellulosic Polymers*, Hanser Gardner, Cincinnati, OH, 1993.
29. L. Bottenbruch (Ed.), *Engineering Thermoplastics: Polycarbonates–Polyacetals–Polyesters–Cellulose Esters*, Hanser Gardner, New York, 1996.
30. S. Fakirov (Ed.), *Handbook of Thermoplastic Polyesters*, Wiley, New York, 2002.
31. J. Scheirs and T. E. Long (Eds.), *Modern Polyesters*, Wiley, New York, 2003.
32. B. J. Chisholm and J. G. Zimmer, *J. Appl. Polym. Sci.*, **76**, 1296–1307, 2000.
33. M. I. Kohan (Ed.), *Nylon Plastics Handbook SPE Monograph*, Hanser Gardner, Cincinnati, OH, 1995.
34. S. M. Ahorani, *n-Nylons: Their Synthesis, Structure and Properties*, Wiley, New York, 1997.
35. R. R. Gallucci, "Polyphenylene Ether–Polyamide Blends," in *Conference Proceedings for the Society of Plastics Engineers, Inc., 44th Annual Technical Conference*, Society of Plastics Engineers, Washington, DC, 1986, pp. 48–50.
36. E. N. Peters, "High Performance Polyamides. I. Long Glss PPE/PA66 Alloys," in *Conference Proceedings for the Society of Plastics Engineers, Inc., 55th Annual Technical Conference*, Society of Plastics Engineers, Washington, DC, 1997, pp. 2322–2324.
37. B. Majumdar and D. R. Paul, "Reactive Compatibilization," in D. R. Paul and C. P., Bucknall (Eds.), *Polymer Blends*, Vol. 2, Wiley, New York, 1999, pp. 539–580.
38. D. G. LeGrand and J. T. Bendler (Eds.), *Polycarbonates: Science and Technology*, Marcel Dekker, New York, 1999.
39. W. F. Christopher and D. W. Fox, *Polycarbonates*, Reinhold, New York, 1962.
40. H. Schnell, *Chemistry and Physics of Polycarbonates*, Wiley-Interscience, New York, 1964.
41. E. N. Peters, in M. Kutz (Ed.), "Plastics and Elastomers" in *Mechanical Engineer's Handbook*, 2nd ed., Wiley-Interscience, New York, 1998, pp. 115–129.

42. L. M., Robeson, "Polyarylate," in I. I. Rubin (Ed.), *Handbook of Plastic Materials and Technology*, Wiley-Interscience, New York, 1990, pp. 237–245.
43. A. S. Hay, *J. Polym. Sci.*, **58**, 581, 1962.
44. D. M. White and G. D. Cooper, "Polyethers, Aromatic" in *Kirk-Othmer Encyclopedia of Chemical Technology*, Vol. 18, 3rd ed., Interscience, New York, 1982, pp. 594–615.
45. E. P. Cizek, U.S. Patent 3,338,435, 1968.
46. E. N. Peters, "Polyphenylene Ether Blends and Alloys," in J. M. Margolis (Ed.), *Engineering Plastics Handbook*, McGraw-Hill, New York, 2005, pp. 181–220.
47. J. M. Short and H. W. Hill, *Chemtech*, **2**, 481, 1972.
48. R. N. Johnson, A. G. Farnham, R. A. Clendinning, W. F. Hale, and C. N. Merriam, *J. Polym. Sci., Part A-1*, **5**, 2375, 1967.
49. J. E. Harris, "Polysulfone," in I. I. Rubin (Ed.), *Handbook of Plastic Materials and Technology*, Wiley-Interscience, New York, 1990, pp. 487–510.
50. L. M., Robeson, "Poly(phenyl sulfone)," in I. I. Rubin (Ed.), *Handbook of Plastic Materials and Technology*, Wiley-Interscience, New York, 1990, pp. 385–393.
51. C. E. Sroog, *J. Polym. Sci. Macromol. Rev.*, **11**, 161, 1976
52. D. E. Floryan and I. W. Serfaty, *Modern Plastics*, **59**, 146, 1982.
53. I. W. Serfaty, "Polyetherimide," in I. I. Rubin (Ed.), *Handbook of Plastic Materials and Technology*, Wiley-Interscience, New York, 1990, pp. 263–293.
54. J. L. Thorne, "Polyamide-imide," in I. I. Rubin (Ed.), *Handbook of Plastic Materials and Technology*, Wiley-Interscience, New York, 1990, pp. 225–235.
55. T. W. Haas, "Polyethersulfone," in I. I. Rubin (Ed.), *Handbook of Plastic Materials and Technology*, Wiley-Interscience, New York, 1990, pp. 295–309.
56. S. Ebnesajjad, *Fluoroplastics*, Vol. 1: *Non-Melt Processible Fluoroplastics*, Plastics Design Library, Brookfield, CT, 2000.
57. C. A. Sperati, "Fluoropolymers," in I. I. Rubin (Ed.), *Handbook of Plastic Materials and Technology*, Wiley-Interscience, New York, 1990, pp. 87–136.
58. S. H. Goodman (Ed.); *Handbook of Thermoset Plastics*, 2nd ed., Plastics Design Library, Brookfield, CT, 1999.
59. P. A. Ciullo and N. Hewitt, *The Rubber Formulary*, Plastics Design Library, Brookfield, CT, 1999.
60. M. Morton (Ed.), *Rubber Technology*, Van Nostrand Reinhold, New York, 1973.
61. J. M. Zeigler and F. W. G. Fearon (Eds.), *Silicone-Based Polymer Science: A Comprehensive Resource*, American Chemical Society, Washington, DC, 1990.

# CHAPTER 10

---

## COMPOSITE MATERIALS

**Carl Zweben**  
Zweben Consulting  
Devon, Pennsylvania

<b>1 INTRODUCTION</b>	<b>401</b>	3.3 Properties of Ceramic Matrix Composites	427
1.1 Classes and Characteristics of Composite Materials	402	3.4 Properties of Carbon Matrix Composites	429
1.2 Comparative Properties of Composite Materials	403	3.5 Advanced Thermal Management Materials	430
1.3 Manufacturing Considerations	407	<b>4 APPLICATIONS</b>	<b>432</b>
<b>2 REINFORCEMENTS AND MATRIX MATERIALS</b>	<b>407</b>	4.1 Polymer Matrix Composite Applications	432
2.1 Reinforcements	408	4.2 Metal Matrix Composite Applications	433
2.2 Matrix Materials	411	4.3 Carbon Matrix Composite Applications	434
<b>3 PROPERTIES AND APPLICATIONS OF COMPOSITE MATERIALS</b>	<b>414</b>	4.4 Ceramic Matrix Composite Applications	435
3.1 Polymer Matrix Composites	417	<b>BIBLIOGRAPHY</b>	<b>435</b>
3.2 Mechanical and Physical Properties of Metal Matrix Composites	423		

### 1 INTRODUCTION

The development of composite materials as well as the related design and manufacturing technologies is one of the most important advances in the history of materials. Composites are multifunctional materials having unprecedented mechanical and physical properties which can be tailored to meet the requirements of a particular application. Many composites also exhibit great resistance to wear, corrosion, and high-temperature exposure. These unique characteristics provide the mechanical engineer with design opportunities not possible with conventional monolithic (unreinforced) materials. Composites technology also makes possible the use of an entire class of solid materials, ceramics, in applications for which monolithic versions are unsuited because of their great strength scatter and poor resistance to mechanical and thermal shock. Further, many manufacturing processes for composites are well adapted to the fabrication of large, complex structures, which allows consolidation of parts, reducing manufacturing costs.

Composites are important materials which are now used widely, not only in the aerospace industry, but also in a large and increasing number of commercial mechanical engineering applications, such as internal combustion engines; machine components; thermal management and electronic packaging; automobile, train, and aircraft structures and mechanical components, such as brakes, drive shafts, flywheels, tanks, and pressure vessels; dimensionally stable

components; process industries equipment requiring resistance to high-temperature corrosion, oxidation, and wear; offshore and onshore oil exploration and production; marine structures; sports and leisure equipment; ships and boats; and biomedical devices.

It should be noted that biological structural materials occurring in nature are typically some type of composite. Common examples are wood, bamboo, bone, teeth, and shell. Further, use of artificial composite materials is not new. Straw-reinforced mud bricks were employed in biblical times. Using modern terminology, discussed later, this material would be classified as an organic fiber-reinforced ceramic matrix composite.

In this section, we provide an overview of composite materials. We then consider the properties of reinforcements and matrix materials (Section 2) and properties of composites (Section 3) and applications (Section 4).

## 1.1 Classes and Characteristics of Composite Materials

Perhaps the best definition of a composite is a material consisting of two or more distinct phases bonded together (see *Comprehensive Composite Materials*, Anthony Kelly and Carl Zweben, Editors-in-Chief, Pergamon Press, Elsevier Science, Oxford, 2000). This distinguishes composites from metal alloys in which constituents are dissolved in one another.

Solid materials can be divided into four categories—polymers, metals, ceramics, and carbon, which we consider as a separate class because of its unique characteristics. We find both reinforcements and matrix materials in all four categories. This gives us the ability to create a limitless number of new material systems which have unique properties that cannot be obtained with any single monolithic material. Table 1 shows the types of material combinations which are now in use.

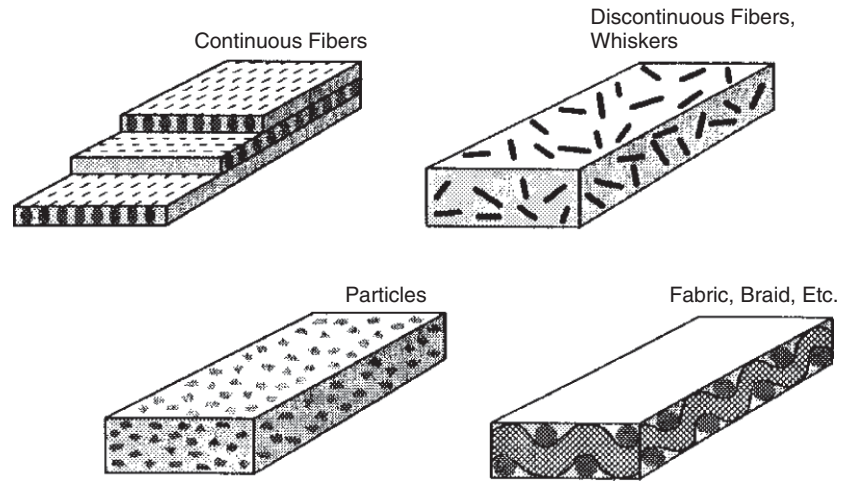
Composites are usually classified by the type of material used for the matrix. The four primary categories of composites are polymer matrix composites (PMCs), metal matrix composites (MMCs), ceramic matrix composites (CMCs), and carbon matrix composites (CAMCs). Carbon-carbon composites (CCCs) are the most important subclass of CAMCs. At this time, PMCs are by far the most widely used type of composites. However, there are important applications of the other types which are indicative of their great potential in mechanical engineering applications.

Figure 1 shows the main types of reinforcements used in composite materials, aligned continuous fibers, discontinuous fibers, whiskers (elongated single crystals), particles, and numerous forms of fibrous architectures produced by textile technology, such as fabrics and braids. Carbon nanotubes are similar to discontinuous fibers. Two-dimensional fabrics are shown. There are also a wide range of three-dimensional woven and braided reinforcements.

A common way to represent fiber-reinforced composites is to show the fiber and matrix separated by a slash. For example, carbon fiber-reinforced epoxy is typically written carbon/epoxy, or in abbreviated form, C/Ep. We represent particle reinforcements by

**Table 1** Types of Composite Materials

REINFORCEMENT	MATRIX			
	Polymer	Metal	Ceramic	Carbon
Polymer	X	X	X	X
Metal	X	X	X	X
Ceramic	X	X	X	X
Carbon	X		X	X



**Figure 1** Reinforcement forms.

enclosing them in parentheses followed by “p.” Using this convention, silicon carbide (SiC) particle-reinforced aluminum appears as (SiC)p/Al.

Composites are strongly heterogeneous materials. That is, the properties of a composite vary considerably from point to point in the material, depending on which material phase the point is located in. Monolithic ceramics and metallic alloys are usually considered to be isotropic materials to a first approximation, although rolled aluminum alloys have anisotropic strength properties.

Many artificial composites, especially those reinforced with fibers, are anisotropic, which means their properties vary with direction (the properties of isotropic materials are the same in every direction). This is a characteristic they share with a widely used natural fibrous composite, wood. As for wood, when structures made from artificial fibrous composites are required to carry load in more than one direction, they are used in laminated form (plywood). Particulate composites can be effectively isotropic if the reinforcements are equiaxed, that is, have roughly the same dimensions in three orthogonal directions (think of sand particles).

Many fiber-reinforced composites, especially PMCs, MMCs, and CAMCs, do not display plastic behavior as metals do, which makes them more sensitive to stress concentrations. However, the absence of plastic deformation does not mean that composites are brittle materials like monolithic ceramics. The heterogeneous nature of composites results in complex failure mechanisms which impart toughness. Fiber-reinforced materials have been found to produce durable, reliable structural components in countless applications. The unique characteristics of composite materials, especially anisotropy, require the use of special design methods.

## 1.2 Comparative Properties of Composite Materials

There are a large and increasing number of materials which fall in each of the four types of composites, so that generalization is difficult. However, as a class of materials, composites tend to have the following characteristics: high strength; high modulus; low density; excellent resistance to fatigue, creep, creep rupture, corrosion, and wear; and low coefficient of thermal expansion (CTE). We also have composites with a wide range of electrical and thermal conductivities.



As for monolithic materials, each of the four classes of composites has its own particular attributes. For example, CMCs tend to have particularly good resistance to corrosion, oxidation, and wear, along with high-temperature capability. Monolithic ceramics are brittle materials with very low fracture toughnesses, because of which their strengths display great scatter. As a result, they are not useful materials for applications that are subjected to significant tension or torsional stress. Reinforcing ceramics with continuous fibers can turn them into attractive materials for high-temperature applications, such as aircraft engines.

In applications for which both mechanical properties and low weight are important, useful figures of merit are specific strength (strength divided by specific gravity or density) and specific stiffness (stiffness divided by specific gravity or density). The advantage of using specific gravity is that it is dimensionless, so that absolute properties and specific properties have the same dimensions. (For all practical purposes, specific gravity has the same numerical value as density expressed in units of grams per cubic centimeters). Figure 2 presents specific stiffness and specific tensile strength of conventional structural metals (steel, titanium, aluminum, magnesium, and beryllium), two engineering ceramics (silicon nitride and alumina), and selected composite materials. The composites are PMCs reinforced with selected continuous fibers—carbon, aramid, E-glass, and boron—and an MMC, aluminum containing silicon carbide particles. Also shown is beryllium–aluminum, which can be considered a type of metal matrix composite rather than an alloy, because the mutual solubility of the constituents at room temperature is low.

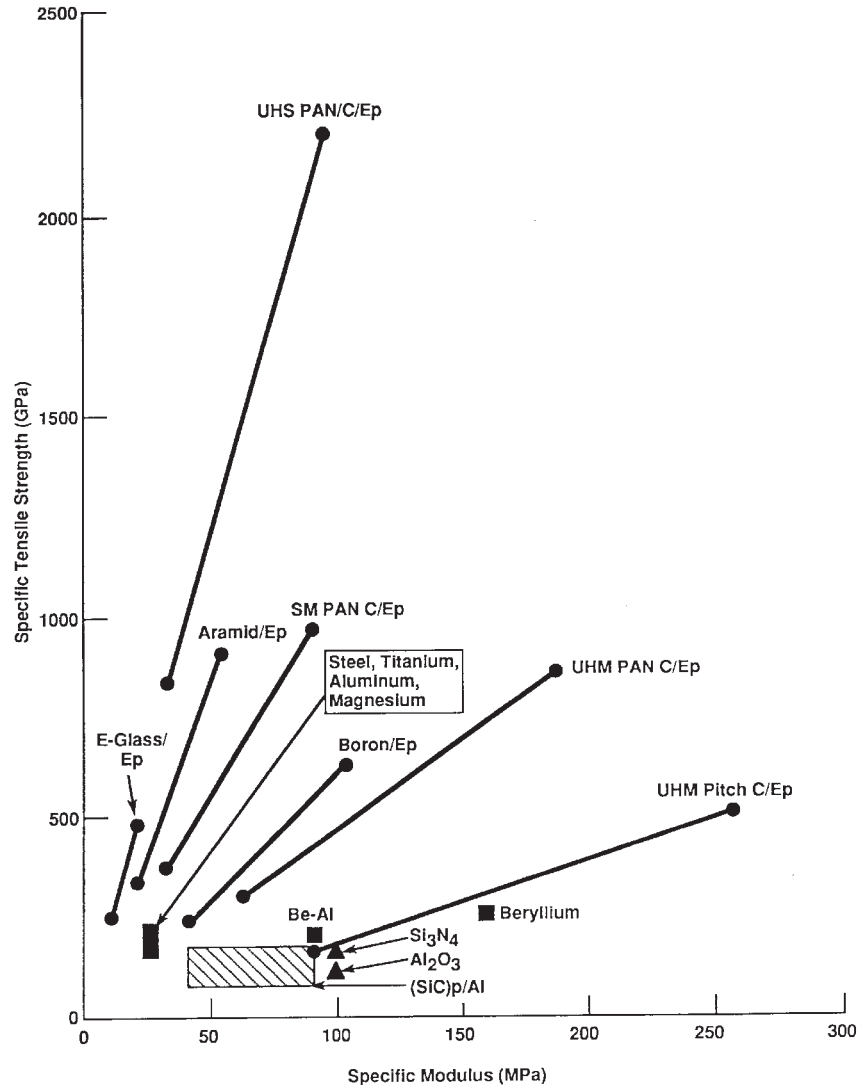
The carbon fibers represented in Fig. 2 are made from several types of precursor materials, polyacrylonitrile (PAN), petroleum pitch, and coal tar pitch. Characteristics of the two types of pitch-based fibers tend to be similar but very different from those made from PAN. Several types of carbon fibers are represented, standard modulus (SM) PAN, ultrahigh-strength (UHS) PAN, ultrahigh-modulus (UHM) PAN, and UHM pitch. These fibers are discussed in Section 2. It should be noted that there are dozens of different kinds of commercial carbon fibers, and new ones are continually being developed. All are proprietary materials having different properties.

Because the properties of fiber-reinforced composites depend strongly on fiber orientation, fiber-reinforced polymers are represented by lines. The upper end corresponds to the axial properties of a unidirectional laminate, in which all the fibers are aligned in one direction. The lower end represents a quasi-isotropic laminate having equal-stiffness and approximately equal-strength characteristics in all directions in the plane of the fibers.

As Fig. 2 shows, composites offer order-of-magnitude improvements over metals in both specific strength and stiffness. It has been observed that order-of-magnitude improvements in key properties can produce revolutionary effects in a technology. Consequently, it is not surprising that composites are having such a dramatic effect on engineering applications.

In addition to their exceptional static strength properties, fiber-reinforced polymers also have excellent resistance to fatigue loading. Figure 3 shows how the number of cycles to failure,  $N$ , varies with maximum stress,  $S$ , for aluminum and selected unidirectional PMCs subjected to tension–tension fatigue. The ratio of minimum stress to maximum stress,  $R$ , is 0.1. The composites consist of epoxy matrices reinforced with key fibers: aramid, boron, SM carbon, high-strength (HS) glass, and E-glass. Because of their excellent fatigue resistance, composites have largely replaced metals in fatigue-critical aerospace applications, such as aircraft structures and helicopter rotor blades. About 50% of the Boeing 787 Dreamliner structure is composed of composite materials. Composites also have been used in commercial fatigue-critical applications, such as automobile leaf springs.

The outstanding mechanical properties of composite materials have been a key reason for their extensive use in structures. However, composites also have important physical properties, especially low, tailorable CTE and high thermal conductivity, which are key reasons for their selection in an increasing number of applications, especially electronics and photonics thermal

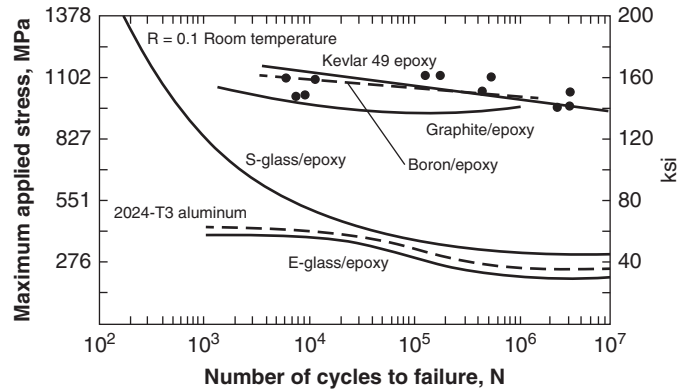


**Figure 2** Specific tensile strength (tensile strength divided by density) as a function of specific modulus (modulus divided by density) of composite materials and monolithic metals and ceramics.

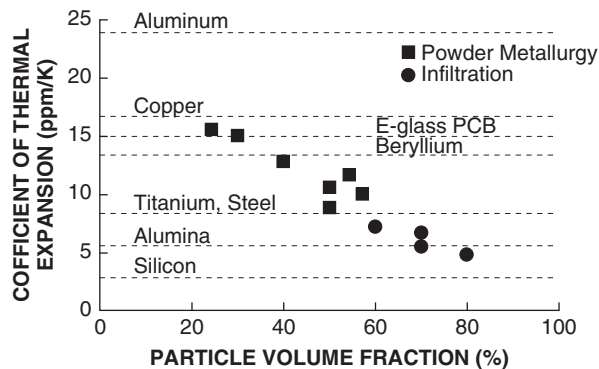
management. For example, composites with thermal conductivities as high as 980 W/m·K have been fabricated. For comparison, the thermal conductivity of copper is about 400 W/m·K.

Many composites, such as PMCs reinforced with carbon and aramid fibers, and silicon carbide particle-reinforced aluminum, have low CTEs, which are advantageous in applications requiring dimensional stability. By appropriate selection of reinforcements and matrix materials, it is possible to produce composites with near-zero CTEs.

Coefficient of thermal expansion tailorability provides a way to minimize thermal stresses and distortions that arise when dissimilar materials are joined. For example, Fig. 4 shows how the CTE of silicon carbide particle-reinforced aluminum varies with particle content.



**Figure 3** Number of cycles to failure as a function of maximum stress for aluminum and unidirectional polymer matrix composites subjected to tension–tension fatigue with a stress ratio  $R = 0.1$ . (Source: L. H. Miner et al., “Fatigue, Creep and Impact Resistance of Kevlar® 49 Reinforced Composites,” in *Composite Reliability*, ASTM STP 580, American Society for Testing and Materials, Philadelphia, PA, 1975, pp. 549–559.)



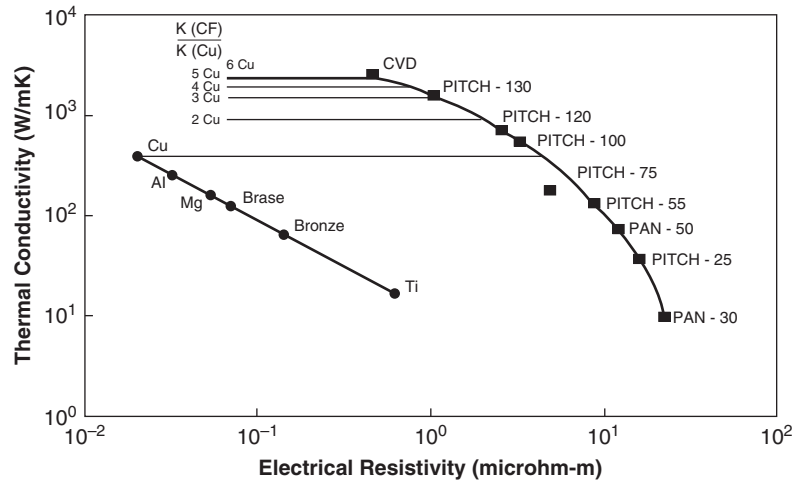
**Figure 4** Variation of CTE with particle volume fraction for silicon carbide particle-reinforced aluminum. (Source: C. Zweben, “Overview of Metal Matrix Composites for Electronic Packaging and Thermal Management,” *JOM*, July 1992.)

By varying the amount of reinforcement, it is possible to match the CTEs of a variety of key engineering materials, such as steel, titanium, and alumina (aluminum oxide), and approach the CTE of silicon.

The ability to tailor CTE is particularly important in applications like electronic and photonic packaging where thermal stresses can cause failure of ceramic substrates, semiconductors, and solder joints.

Another unique and increasingly important property of some composites is their exceptionally high thermal conductivity. This is leading to increasing use of composites in applications for which heat dissipation is a key design consideration. In addition, the low densities of composites make them particularly advantageous in thermal control applications for which weight is important, such as handsets, tablet, laptop computers, avionics, and spacecraft components.

There are a large and increasing number of thermally conductive composites, which are discussed in Chapter 3. Carbon fibers made from petroleum and coal tar pitch precursors and by



**Figure 5** Thermal conductivity as a function of electrical resistivity of metals and carbon fibers (figure adapted from one of Amoco Performance Products).

chemical vapor deposition (CVD) are key reinforcements for these materials. Figure 5 shows how thermal conductivity varies with electrical resistivity for conventional metals and carbon fibers. It can be seen that PAN-based fibers have relatively low thermal conductivities. However, pitch-based fibers with thermal conductivities more than twice that of copper are commercially available. These reinforcements also have very high stiffnesses and low densities. At the upper end of the carbon fiber curve are fibers made by CVD, which have thermal conductivities as high as 2000 W/m·K (1160 Btu/h·ft·°F).

### 1.3 Manufacturing Considerations

Composites also offer a number of significant manufacturing advantages over monolithic metals and ceramics. For example, fiber-reinforced polymers and ceramics can be fabricated in large, complex shapes that would be difficult or impossible to make with other materials. The ability to fabricate complex shapes allows consolidation of parts, which reduces machining, assembly, and fastener costs. Some processes allow fabrication of parts to their final shape (net shape) or close to their final shape (near-net shape), which also produces manufacturing cost savings. The relative ease with which smooth shapes can be made is a significant factor in the use of composites in aircraft, wind turbine blades, and other applications for which aerodynamic considerations are important.

## 2 REINFORCEMENTS AND MATRIX MATERIALS

As discussed in Section 1, we divide solid materials into four classes, polymers, metals, ceramics, and carbon. There are reinforcements and matrix materials in each category. In this section, we consider the characteristics of key reinforcements and matrices.

There are important issues that must be discussed before presenting constituent properties. The conventional materials used in mechanical engineering applications are primarily structural metals for most of which there are industry and government specifications. The situation is very different for composites. Most reinforcements and matrices are proprietary materials

for which there are no industry standards. This is similar to the current status of ceramics. The situation is further complicated by the fact that there are many test methods in use to measure mechanical and physical properties of reinforcements and matrix materials. As a result, there are often conflicting material property data in the usual sources, published papers and manufacturers' literature. The data presented in this chapter represent a carefully evaluated distillation of information from many sources. The principal sources are listed in the bibliography. In view of the uncertainties discussed, the properties presented in this section should be considered approximate values.

Because of the large number of matrix materials and reinforcements, we are forced to be selective. Further, space limitations prevent presentation of a complete set of properties. Consequently, properties cited are room temperature values unless otherwise stated.

## 2.1 Reinforcements

The four key types of reinforcements used in composites are continuous fibers, discontinuous fibers, whiskers (elongated single crystals), and particles (Fig. 1). Continuous, aligned fibers are the most efficient reinforcement form and are widely used, especially in high-performance applications. However, for ease of fabrication and to achieve specific properties, such as improved impact resistance, continuous fibers are converted into a wide variety of reinforcement forms using textile technology. Key among them are two- and three-dimensional fabrics and braids.

### *Fibers*

The great importance of composites and the revolutionary improvements in properties compared to conventional materials that they offer derive to a great extent from the development of fibers with unprecedented properties. The key fibers for mechanical engineering applications are glasses, carbons (also called graphites), several types of ceramics, and high-modulus organics. In recent years, basalt fibers have become commercial.

Most fibers are produced in the form of multifilament bundles, usually called strands or ends in their untwisted forms and yarns when twisted, although definitions vary. Some fibers are produced as monofilaments, which generally have much larger diameters than strand filaments. Table 2 presents properties of key fibers, which are discussed in the following subsections.

Fiber strength requires some discussion. Most of the key fibrous reinforcements are made of brittle glasses, ceramics, or carbon. It is well known that the strengths of monolithic ceramics decrease with increasing material volume because of the increasing probability of finding strength-limiting flaws. This is called size effect. As a result of size effect, mean fiber strength typically decreases monotonically with increasing gage length (and diameter). Flaw sensitivity also results in considerable strength scatter at a fixed test length. Consequently, there is no single value that characterizes fiber strength. This is also true of key organic reinforcements, such as aramid fibers. Consequently, the values presented in Table 1 should be considered approximate values and are useful primarily for comparative purposes. Note that because unsupported fibers buckle under very low compressive stress, it is very difficult to measure their inherent compression strength, and these properties are almost never reported. Instead, composite compression strength is measured directly.

*Glass Fibers.* Glass fibers are used primarily to reinforce polymers. The leading types of glass fibers for mechanical engineering applications are E-glass and HS glass. E-glass fibers, the first important structural composite reinforcements, originally were developed for electrical

**Table 2** Properties of Key Reinforcing Fibers

Fiber	Density g/cm <sup>3</sup> (pci)	Axial Modulus GPa (Msi)	Tensile Strength MPa (ksi)	Axial Coefficient of Thermal Expansion ppm/K (ppm/°F)	Axial Thermal Conductivity W/m-K
E-glass	2.6 (0.094)	70 (10)	2000 (300)	5 (2.8)	0.9
HS glass	2.5 (0.090)	83 (12)	4200 (650)	4.1 (2.3)	0.9
Aramid	1.4 (0.52)	124 (18)	3200 (500)	-5.2 (-2.9)	0.04
Boron	2.6 (0.094)	400 (58)	3600 (520)	4.5 (2.5)	—
SM carbon (PAN)	1.7 (0.061)	235 (34)	3200 (500)	-0.5 (-0.3)	9
UHM carbon (PAN)	1.9 (0.069)	590 (86)	3800 (550)	-1 (-0.6)	18
UHS carbon (PAN)	1.8 (0.065)	290 (42)	7000 (1000)	-1.5 (-0.8)	160
UHM carbon (pitch)	2.2 (0.079)	895 (130)	2200 (320)	-1.6 (-0.9)	640
UHK carbon (pitch)	2.2 (0.079)	830 (120)	2200 (320)	-1.6 (-0.9)	1100
SiC monofilament	3.0 (0.11)	400 (58)	3600 (520)	4.9 (2.7)	—
SiC multifilament	3.0 (0.11)	400 (58)	3100 (450)	—	—
Si-C-O	2.6 (0.094)	190 (28)	2900 (430)	3.9 (2.2)	1.4
Si-Ti-C-O	2.4 (0.087)	190 (27)	3300 (470)	3.1 (1.7)	—
Aluminum oxide	3.9 (0.14)	370 (54)	1900 (280)	7.9 (4.4)	—
High-density polyethylene	0.97 (0.035)	172 (25)	3000 (440)	—	—
Basalt	2.7 (0.099)	100 (15)	2900 (430)	5.5 (3.1)	1.7

insulation applications (that is the origin of the “E”). Corrosion-resistant glass fibers, usually designated CR, are used in the chemical industry.

E-glass is, by many orders of magnitude, the most widely used of all fibrous reinforcements. The primary reasons for this are their low cost and early development compared to other fibers. Glass fibers are produced as multifilament bundles. Filament diameters range from 3 to 20  $\mu\text{m}$  (118–787  $\mu\text{in.}$ ). Table 1 presents representative properties of E-glass and HS glass fibers.

E-glass fibers have relatively low elastic moduli compared to other reinforcements. In addition, E-glass fibers are susceptible to creep and creep (stress) rupture. HS glass is stiffer and stronger than E-glass and has better resistance to fatigue and creep.

The thermal and electrical conductivities of glass fibers are low, and glass fiber-reinforced PMCs are often used as thermal and electrical insulators. The CTE of glass fibers is also low compared to most metals.

*Carbon (Graphite) Fibers.* Carbon fibers, often called graphite fibers in the United States, are used as reinforcements for polymers, metals, ceramics, and carbon. There are dozens of commercial carbon fibers, with a wide range of strengths and moduli. As a class of reinforcements, carbon fibers are characterized by high stiffness and strength and low density and CTE. Fibers with tensile moduli as high as 895 GPa (130 Msi) and with tensile strengths of 7000 MPa (1000 ksi) are commercially available. Carbon fibers have excellent resistance to creep, stress rupture, fatigue, and corrosive environments, although they oxidize at high temperatures.

Some carbon fibers also have extremely high thermal conductivities—many times that of copper—as discussed in Section 1. This characteristic is of considerable interest for electronic packaging and other applications for which heat dissipation and thermal control are important. Carbon fibers are the workhorse reinforcements in high-performance aerospace and commercial PMCs and some CMCs. Of course, as the name suggests, carbon fibers are also the reinforcements in CCCs.

Most carbon fibers are highly anisotropic. Axial stiffness, tension, and compression strength and thermal conductivity are typically much greater than the corresponding properties in the radial direction. Carbon fibers generally have small, negative axial CTEs (which means that they get shorter when heated) and positive radial CTEs. Diameters of common reinforcing fibers, which are produced in the form of multifilament bundles, range from 4 to 10  $\mu\text{m}$  (160 to 390  $\mu\text{in.}$ ). Carbon fiber stress–strain curves tend to be nonlinear. Modulus increases somewhat with increasing strain in tension and decreases with increasing strain in compression. This gives rise to different tensile and compressive moduli when secant values are used.

Carbon fibers are made primarily from three key precursor materials: PAN, petroleum pitch, and coal tar pitch. Rayon-based fibers, once the primary CCC reinforcement, are far less common in new applications. These fibers have relatively poor strength properties. The Space Shuttle Orbiter CCCs were made with rayon-based carbon fibers.

Carbon fibers are also made by CVD. Some of these have reported axial thermal conductivities as high as 2000 W/m-K, five times that of copper.

PAN-based fibers are the most widely used type of carbon fibers. There are dozens on the market. Fiber axial moduli of structural fibers range from about 235 GPa (34 Msi) to 590 GPa (85 Msi). They generally provide composites with excellent tensile and compressive strength properties, although compressive strength tends to drop as modulus increases. Fibers having tensile strengths as high as 7 GPa (1 Msi) are available.

Table 1 presents properties of three types of PAN-based carbon fibers and two types of pitch-based carbon fibers. The PAN-based fibers are SM, UHS, and UHM. SM PAN fibers are the most widely used type of carbon fiber reinforcement. They are one of the first types commercialized and tend to be the least expensive. UHS PAN carbon fibers are the strongest type of another widely used class of carbon fiber, which are usually called intermediate modulus (IM), because their axial modulus falls between those of SM and high-modulus carbon fibers.

A key advantage of pitch-based fibers is that they can be produced with much higher axial moduli than those made from PAN precursors. For example, UHM pitch fibers with moduli as high as 895 GPa (130 Msi) are available. In addition, some pitch fibers, which we designate UHK, have extremely high axial thermal conductivities. There are commercial UHK fibers with a nominal axial thermal conductivity of about 1000 W/m-K, more than twice that of copper. However, composites made from pitch-based carbon fibers generally are somewhat weaker in tension and shear and much weaker in compression than those using PAN-based reinforcements.

*Boron Fibers.* Boron fibers are primarily used to reinforce polymers and metals. Boron fibers are produced as monofilaments (single filaments) by CVD of boron on a tungsten wire. They have relatively large diameters, 100–140  $\mu\text{m}$  (4000–5600  $\mu\text{in.}$ ), which are much greater than those of E-glass and carbon fibers. Table 1 presents representative properties of boron fibers having a diameter of 140  $\mu\text{m}$ . The properties of boron fibers are influenced by the ratio of overall fiber diameter to that of the tungsten core. For example, fiber specific gravity is 2.57 for 100- $\mu\text{m}$  fibers and 2.49 for 140- $\mu\text{m}$  fibers.

*Fibers Based on Silicon Carbide.* Silicon-carbide-based fibers are primarily used to reinforce metals and ceramics. There are a number of commercial fibers based on silicon carbide. One type, a monofilament, like boron fibers, is produced by CVD of high-purity silicon carbide, although the core for these fibers is a carbon monofilament. Some versions use a carbon-rich surface layer which serves as a reaction barrier.

There are a number of multifilament silicon-carbide-based fibers which are made by a variety of processes such as pyrolysis of preceramic polymers. Some of these fibers are far from pure silicon carbide (SiC) and contain varying amounts of silicon, carbon and oxygen,



titanium, nitrogen, zirconium, and hydrogen. Table 1 presents properties of selected silicon-carbide-based fibers.

*Fibers Based on Alumina.* Alumina-based fibers are primarily used to reinforce metals and ceramics, although they have been used to produce polymer matrix composite aircraft firewalls. As for silicon-carbide-based fibers, they have a number of different chemical formulations. The primary constituents, in addition to alumina, are boria, silica, and zirconia. Table 1 presents properties of high-purity alumina fibers.

*Aramid Fibers.* Aramid, or aromatic polyamide fiber, is a high-modulus organic reinforcement primarily used to reinforce polymers and cement and for ballistic protection. There are a number of commercial aramid fibers produced by several manufacturers. “Kevlar” 49 and “Twaron” are examples. As for other reinforcements, they are proprietary materials. Table 1 presents properties of one of the most widely used aramid fibers.

*High-Density Polyethylene Fibers.* High-density polyethylene fibers are primarily used to reinforce polymers and for ballistic protection. Table 1 presents properties of a common reinforcing fiber. The properties of high-density polyethylene tend to decrease significantly with increasing temperature, and they tend to creep significantly under load, even at low temperatures.

*Basalt Fibers.* Basalt fibers are relatively recent additions to the stable of commercially available reinforcements, although the technology goes back many decades. They are made by melting and extruding basalt, a volcanic rock. A key advantage of these fibers is fire resistance because they do not burn and have a high melting point. The mechanical properties of basalt fibers are similar to those of HS glass.

## 2.2 Matrix Materials

As discussed in Section 1, the four classes of matrix materials are polymers, metals, ceramics, and carbon. Table 3 presents representative properties of selected matrix materials in each category. As the table shows, the properties of the four types differ substantially. These differences have profound effects on the properties of the composites using them. In this section, we examine characteristics of key materials in each class.

**Table 3** Properties of Selected Matrix Materials

Material	Class	Density g/cm <sup>3</sup> (pci)	Modulus GPa (Msi)	Tensile Strength MPa (ksi)	Tensile Failure Strain %	Thermal Conductivity W/m·K (Btu/h-ft·°F)	Coefficient of Thermal Expansion ppm/K (ppm/°F)
Epoxy	Polymer	1.8 (0.065)	3.5 (0.5)	70 (10)	3	0.1 (0.06)	60 (33)
Aluminum (6061)	Metal	2.7 (0.098)	69 (10)	300 (43)	10	180 (104)	23 (13)
Titanium (6Al-4V)	Metal	4.4 (0.16)	105 (15.2)	1100 (160)	10	16 (9.5)	9.5 (5.3)
Silicon carbide	Ceramic	2.9 (0.106)	520 (75)	—	<0.1	81 (47)	4.9 (2.7)
Alumina	Ceramic	3.9 (0.141)	380 (55)	—	<0.1	20 (12)	6.7 (3.7)
Glass (borosilicate)	Ceramic	2.2 (0.079)	63 (9)	—	<0.1	2 (1)	5 (3)
Carbon	Carbon	1.8 (0.065)	20 (3)	—	<0.1	5–90 (3–50)	2 (1)



**Polymer Matrix Materials**

Polymer matrices generally are relatively weak, low-stiffness, viscoelastic materials. The strength and stiffness of PMCs come primarily from the reinforcing fibers.

There are two major classes of polymers used as matrix materials, thermosets and thermoplastics. At this time, thermosets are by far the most widely used matrix resins for structural applications, although thermosets are making steady gains. Thermosets tend to be more resistant to solvents and corrosive environments than thermoplastics, but there are exceptions to this rule.

Thermosets are materials which undergo a curing process during part fabrication, after which they are rigid and cannot be reformed. Thermoplastics, on the other hand, can be repeatedly softened and re-formed by application of heat (think of wax). There are numerous types of polymers in both classes.

Resin selection is based on design requirements, and manufacturing and cost considerations. Table 4 presents representative properties of common matrix polymers.

One of the key issues in matrix selection is maximum service temperature. The elastic and strength properties of polymers decrease with increasing temperature. A widely used measure of comparative temperature resistance of polymers is the glass transition temperature,  $T_g$ , which is the approximate measure of the temperature at which a polymer transitions from a relatively rigid material to a rubbery one. Polymers typically suffer significant losses in both strength and stiffness above their glass transition temperatures. New polymers with increasing temperature capability are continually being developed, allowing them to compete with a wider range of metals. For example, carbon fiber-reinforced polyimides have replaced titanium in some aircraft gas turbine engine parts.

An important consideration in the selection of polymer matrices is their moisture sensitivity. Resins tend to absorb water, which causes dimensional changes and reduction of strength, stiffness, and  $T_g$ . The amount of moisture absorption at equilibrium, typically measured as

**Table 4** Properties of Selected Thermosetting and Thermoplastic Matrices

	Density g/cm <sup>3</sup> (pci)	Modulus GPa (Msi)	Tensile Strength MPa (ksi)	Elongation to Break (%)	Thermal Conductivity W/m·K	Coefficient of Thermal Expansion ppm/K (ppm/°F)
Epoxy (1)	1.1–1.4 (0.040–0.050)	3–6 (0.43–0.88)	35–100 (5–15)	1–6	0.1	60 (33)
Thermosetting polyester (1)	1.2–1.5 (0.043–0.054)	2–4.5 (0.29–0.65)	40–90 (6–13)	2	0.2	100–200 (56–110)
Polypropylene (2)	0.90 (0.032)	1–4 (0.15–0.58)	25–38 (4–6)	>300	0.2	110 (61)
Nylon 6-6 (2)	1.14 (0.041)	1.4–2.8 (0.20–0.41)	60–75 (9–11)	40–80	0.2	90 (50)
Polycarbonate (2)	1.06–1.20 (0.038–0.043)	2.2–2.4 (0.32–0.35)	45–70 (7–10)	50–100	0.2	70 (39)
Polysulfone (2)	1.25 (0.045)	2.2 (0.32)	76 (11)	50–100	—	56 (31)
Polyetherimide (2)	1.27 (0.046)	3.3 (0.48)	110 (16)	60	—	62 (34)
Polyamideimide (2)	1.4 (0.050)	4.8 (0.7)	190 (28)	17	—	63 (35)
Polyphenylene sulfide (2)	1.36 (0.049)	3.8 (0.55)	65 (10)	4	—	54 (30)
Polyether etherketone (2)	1.26–1.32 (0.046–0.048)	3.6 (0.52)	93 (13)	50	—	47 (26)

Note: (1) = thermoset, (2) = thermoplastic.

percent weight gain, depends on the polymer and relative humidity. Resins also desorb moisture when placed in a drier atmosphere. The rate of absorption and desorption depends strongly on temperature. The moisture sensitivity of resins varies widely, and some are very resistant when cured.

In a vacuum, resins outgas organic and inorganic chemicals, which can condense on surfaces with which they come in contact. This can be a problem in optical systems and can affect surface properties critical for thermal control, such as absorptivity and emissivity. Outgassing can be controlled by resin selection and baking out the component.

*Thermosetting Resins.* The key types of thermosetting resins used in composites are epoxies, bismaleimides, thermosetting polyimides, cyanate esters, thermosetting polyesters, vinyl esters, benzoxazines, and phenolics. It should be noted that this list is continually expanding.

Epoxies are the workhorse materials for airframe structures and other aerospace applications, with decades of successful flight experience to their credit. They produce composites with excellent structural properties. Epoxies tend to be rather brittle materials, but toughened formulations with greatly improved impact resistance are available. The maximum service temperature is affected by reduced elevated-temperature structural properties resulting from water absorption. A typical airframe limit is about 120°C (250°F).

Bismaleimide resins are used for aerospace applications requiring higher temperature capabilities than can be achieved by epoxies. They are employed for temperatures of up to about 200°C (390°F).

Thermosetting polyimides are being used in applications at temperatures as high as 250–290°C (500–550°F). However, new resins have been developed with even higher temperature limits.

Cyanate ester resins are not as moisture sensitive as epoxies and tend to outgas much less. Formulations with operating temperatures as high as 205°C (400°F) are available.

Thermosetting polyesters are the workhorse resins in commercial applications. They are relatively inexpensive, easy to process, and corrosion resistant.

Vinyl esters are also widely used in commercial applications. They have better corrosion resistance than polyesters but are somewhat more expensive.

Phenolic resins have good high-temperature resistance and produce less smoke and toxic products than most resins when burned. They are used in applications such as aircraft interiors and offshore oil platform structures, for which fire resistance is a key design requirement.

As mentioned earlier, there are an increasing number of high-temperature thermosetting resins.

*Thermoplastic Resins.* Thermoplastics are divided into three main classes, amorphous, crystalline, and liquid crystal. Polycarbonate, acrylonitrile–butadiene–styrene (ABS), polystyrene, polysulfone, and polyetherimide are amorphous materials. Crystalline thermoplastics include nylon, polyethylene, polyphenylene sulfide, polypropylene, acetal, polyethersulfone, and polyether etherketone (PEEK). Amorphous thermoplastics tend to have poor solvent resistance. Crystalline materials tend to be better in this respect. Relatively inexpensive thermoplastics like nylon are extensively used with chopped E-glass fiber reinforcements in countless injection-molded parts. There are an increasing number of applications using continuous fiber-reinforced thermoplastics.

### **Metals**

The metals initially used for MMC matrix materials generally were traditional alloys. As time has progressed, however, special matrix materials, tailored for use in composites, have been

developed. The key metallic matrix materials used for structural MMCs are alloys of aluminum, titanium, and iron. There was a significant amount of research on composites using intermetallic compound matrix materials, such as titanium aluminides, but these were largely unsuccessful.

There have been many other metals used as matrix materials, including copper, lead, magnesium, cobalt, silver, and superalloys. The in situ properties of metals in a composite depend on the manufacturing process and, because metals are elastic–plastic materials, the history of mechanical stresses and temperature changes to which they are subjected.

#### *Ceramic Matrix Materials*

The key ceramics used as CMC matrices are silicon carbide, alumina, silicon nitride, mullite, and various cements. The properties of ceramics, especially strength, are even more process sensitive than those of metals. In practice, it is very difficult to determine the in situ properties of ceramic matrix materials in a composite.

As discussed earlier in the section on fiber properties, ceramics are very flaw sensitive, resulting in a decrease in strength with increasing material volume, a phenomenon called size effect. As a result, there is no single value that describes the tensile strength of ceramics. In fact, because of the very brittle nature of ceramics, it is difficult to measure tensile strength, and flexural strength (often called modulus of rupture) is often reported. It should be noted that flexural strength is also dependent on specimen size and is generally much higher than that of a tensile coupon of the same dimensions. In view of the great difficulty in measuring a simple property like tensile strength, which arises from their flaw sensitivity, it is not surprising that monolithic ceramics are rarely used in applications where they are subjected to significant tensile stresses.

The fracture toughness of ceramics is typically in the range of 3–6 MPa·m<sup>1/2</sup>. Those of transformation-toughened materials are somewhat higher. For comparison, the fracture toughnesses of structural metals are generally greater than 20 MPa·m<sup>1/2</sup>.

#### *Carbon Matrix Materials*

Carbon is a remarkable material. It includes materials ranging from lubricants to diamonds to structural fibers. The forms of carbon matrices resulting from the various carbon–carbon manufacturing processes tend to be rather weak, brittle materials. Thermal conductivities range from very low to high, depending on precursor materials and processes. As for ceramics, in situ matrix properties are difficult to measure.

### 3 PROPERTIES AND APPLICATIONS OF COMPOSITE MATERIALS

There are a large and increasing number of materials in all four classes of composites: PMCs, MMCs, CMCs, and CAMC. CCCs are the most important type of carbon matrix composites at this time. In this section, we present properties of key materials in each class. We also consider the properties of advanced composites and other advanced materials used in electronic and photonic thermal management.

Initially, the excellent mechanical properties of composites were the main reason for their use. However, there are an increasing number of applications for which the unique and tailorable physical properties of composites are key considerations. For example, the extremely high thermal conductivity and tailorability CTE of some composite material systems have led to their increasing use in electronic and photonic thermal management and packaging. Similarly, the extremely high stiffness, near-zero CTE, and low density of carbon fiber-reinforced polymers have made these composites the materials of choice in spacecraft structures, optical systems, antennas, and other applications for which dimensional stability is important.

Composites are complex, heterogeneous material systems. Fiber-reinforced materials are almost always anisotropic. Their properties are affected by many variables, including in situ constituent properties; reinforcement form, volume fraction, and geometry; properties of the interphase, the region where the reinforcement and matrix are joined (also called the interface); and void content. The process by which the composite is made affects many of these variables. The same matrix material and reinforcement, when combined by different processes, can result in composites with very different properties.

There are several other important things that must be kept in mind when considering composite properties. For one, most composites are proprietary material systems made by proprietary processes. There are few industry or government specifications for composites as there are for many, if not most, monolithic structural metals. However, this is also the case for many monolithic ceramics and polymers, which are widely used engineering materials. Despite their inherently proprietary nature, there are some types of composite materials made by a number of manufacturers which have similar properties. Notable examples are some kinds of SM carbon fiber-reinforced epoxy.

Another critical issue is that properties are sensitive to the test methods by which they are measured, and there are many different test methods used throughout the industry. Further, test results are very sensitive to the skill of the technician performing them. Because of these factors, it is very common to find significant differences in reported properties of what is nominally the same composite material.

In Section 2, we discussed the issue of size effect, which is the decrease in strength with increasing material volume which is observed in monolithic ceramics key reinforcing fibers. There is some evidence, which is suggestive but not conclusive, of size effects in composite strength properties, as well. However, if composite strength size effects exist at all, they are much less severe than those of the reinforcing fibers. The reason is that the presence of a matrix results in very different failure mechanisms. However, until the issues are resolved definitively, caution should be used in extrapolating strength data from small coupons to large structures, which may have volumes that are many orders of magnitude greater.

As mentioned earlier, the properties of composites are very sensitive to reinforcement form, volume fraction, and geometry. This is illustrated in Table 5, which presents the properties of several common types of E-glass fiber-reinforced polyester composites. The reinforcement forms are discontinuous fibers, woven roving (a heavy fabric) and straight, parallel continuous fibers. Discontinuous reinforcement is not as efficient as continuous. However, discontinuous fibers allow the composite material to flow during processing, facilitating fabrication of complex molded parts.

Composites using discontinuous fibers can be divided into a number of categories. We consider three of the most significant. The first is bulk molding compound (BMC), also called dough molding compound, in which fibers are relatively short, about 3–12 mm, and are nominally randomly oriented in three dimensions, although it is difficult to achieve this in practice. As a rule, BMC also has a very high loading of mineral particles, such as calcium carbonate,

**Table 5** Effect of Fiber Form and Volume Fraction on Mechanical Properties of E-Glass Reinforced Polyester

	Bulk Molding Compound	Sheet Molding Compound	Chopped Strand Mat	Woven Roving	Unidirectional Axial	Unidirectional Transverse
Glass content (wt. %)	20	30	30	50	70	70
Tensile modulus, GPa (Msi)	9 (1.3)	13 (1.9)	7.7 (1.1)	16 (2.3)	42 (6.1)	12 (1.7)
Tensile strength, MPa (ksi)	45 (6.5)	85 (12)	95 (14)	250 (36)	750 (110)	50 (7)

Source: A. F. Johnson, "Glass-Reinforced Plastics: Thermosetting Resins," in A. Kelly (Ed.), *Concise Encyclopedia of Composite Materials*, rev. ed., Pergamon, Oxford, 1994, pp. 116–123.

which are added for a variety of reasons, including, among others, to reduce dimensional changes from resin shrinkage, to obtain a smooth surface, and to reduce cost. Because it contains both particulate and fibrous reinforcement, BMC can be considered a type of hybrid composite.

The second type of composite is chopped strand mat (CSM), which contains discontinuous fibers, typically about 25 mm long, which are nominally randomly oriented in a plane. The third material is sheet molding compound (SMC), which contains chopped fibers 25–50 mm in length, which also are nominally randomly oriented in two dimensions. Like BMC, SMC also contains particulate mineral fillers, such as calcium carbonate and clay.

The first thing to note in comparing the materials in Table 5 is that fiber content, here presented in the form of weight percent, differs considerably for the four materials. This is significant, because, as discussed in Section 2, the strength and stiffness of polyester and most polymer matrices are considerably lower than those of E-glass, carbon, and other reinforcing fibers. Composites reinforced with randomly oriented fibers tend to have lower volume fractions than those made with aligned fibers or fabrics. There is a notable exception to this. Some composites with discontinuous-fiber reinforcement are made by chopping up composites reinforced with aligned continuous fibers or fabrics that have high fiber contents.

Examination of Table 5 shows that the modulus of SMC is considerably greater than that of CSM, even though they both have the same fiber content. This may be because SMC also has particulate reinforcement. Another possibility is that the fibers are to some extent oriented in the direction of test and are not truly random. Many processes, especially those involving material flow, tend to orient fibers in one or more preferred directions. If so, then one would find that the modulus of the BMC would be much lower than the one presented in the table if measured in other directions. This illustrates one of the limitations of using discontinuous fiber reinforcement; it is often difficult to control fiber orientation.

Note that particulate reinforcement of polymers generally improves modulus but does not increase strength. However, as we will see later, particles often do enhance the strengths of metal matrix composites as well as their moduli.

The moduli and strengths of the composites reinforced with fabrics and aligned fibers are much higher than those with discontinuous fibers when the former two types of materials are tested parallel to fiber directions. For example, the tensile strength of woven roving is more than twice that of CSM. The properties presented are measured parallel to the warp direction of the fabric (the warp direction is the lengthwise direction of the fabric). The elastic and strength properties in the fill direction, which is perpendicular to the warp, typically are similar to but somewhat lower than those in the warp direction, because fill fibers typically are more curved. Here, we assume that the fabric is “balanced,” which means that the number of fibers in the warp and fill directions per unit length are approximately equal. Note, however, that the elastic modulus, tensile strength, and compressive strength at  $45^\circ$  to the warp and fill directions of a fabric are much lower than the corresponding values in the warp and fill directions.

As Table 5 shows, the axial modulus and tensile strength of the unidirectional composite are much greater than those of the fabric. However, the modulus and strength of the unidirectional composite in the transverse direction are considerably lower than the corresponding axial properties. Further, the transverse strength is considerably lower than that of SMC and CSM. In general, the strengths of polymer matrix composites are weak in directions for which there are no fibers. The low transverse moduli and strengths of unidirectional polymer matrix composites are commonly overcome by use of laminates with fibers in several directions. Low through-thickness strength can be improved by use of three-dimensional reinforcement forms or inserting fibers in the through-thickness direction. In most cases, the designer simply assures that through-thickness stresses are within the capability of the material.

In this section, we present representative mechanical and physical properties of key composite materials of interest for a broad range of mechanical engineering applications.

The properties represent a distillation of values from many sources. Because of space limitations and other considerations, it is necessary to be selective in the choice of materials and properties presented.

As discussed earlier, there are many textile forms, such as woven fabrics, used as reinforcements. However, we concentrate on aligned, continuous fibers because they produce the highest strength and stiffness. To do a thorough evaluation of composites, the design engineer should consider alternate reinforcement forms. Unless otherwise stated, room temperature property values are presented.

In this section, we consider mechanical and physical properties of the PMCs, MMCs, CMCs, and CCCs that are of greatest general interest for mechanical engineering applications.

### 3.1 Polymer Matrix Composites

As discussed earlier, polymers are relatively weak, low-stiffness materials. In order to obtain materials with mechanical properties that are acceptable for structural applications, it is necessary to reinforce them with continuous or discontinuous fibers. The addition of ceramic or metallic particles to polymers results in materials which have increased modulus. But, as a rule, strength typically does not increase significantly and often decreases. However, there are many particle-reinforced polymers used in electronic packaging, primarily because of their physical properties, especially increased thermal conductivity compared to monolithic polymers. For these applications, ceramic particles, such as alumina (aluminum oxide), aluminum nitride, boron nitride, and even diamond, are added to obtain an electrically insulating material with higher thermal conductivity and lower CTE than the monolithic base polymer. Metallic particles such as silver and aluminum are added to create materials which are both electrically and thermally conductive. These materials have replaced lead-based solders in some applications. There are also magnetic composites made by incorporating ferrous or permanent magnet particles in various polymers. A common example is magnetic tape used to record audio and video.

#### *Elastic and Strength Properties of Polymer Matrix Composites*

As discussed, composites reinforced with aligned continuous fibers are the most efficient structural materials. Consequently, we focus on them. Table 6 presents room temperature elastic properties of unidirectional polymer matrix composites reinforced with key fibers, E-glass, aramid, boron, SM PAN-based carbon, UHS PAN-based carbon, UHM PAN-based carbon, and UHM pitch-based carbon. We assume that the fiber volume fraction is 60%, a typical value. As discussed in Section 2, UHS PAN-based carbon is the strongest type of IM carbon fiber.

**Table 6** Elastic Properties of Unidirectional Polymer Matrix Composites and 7075-T6 Aluminum

Fiber	Axial Modulus GPa	Transverse Modulus GPa	In-Plane Shear Modulus GPa	Major Poisson's Ratio
7075-T6 aluminum	70	70	27	0.33
E-glass	45	12	5.5	0.28
Aramid	76	5.5	2.1	0.34
Boron	210	19	4.8	0.25
SM carbon (PAN)	145	10	4.1	0.25
UHS(IM) carbon (PAN)	180	9	4.0	—
HM carbon (PAN)	225	7	3.9	—
UHM carbon (PAN)	310	9	4.1	0.20
UHM carbon (pitch)	480	9	4.1	0.25



The properties presented in Table 6 are representative of what can be obtained at room temperature with a well-made PMC employing an epoxy matrix. Epoxies are widely used, provide good mechanical properties, and can be considered a reference matrix material. Properties of composites using other resins may differ from these. This has to be examined on a case-by-case basis.

The properties of polymer matrix composites, especially strengths, depend strongly on temperature. The temperature dependence of polymer properties differs considerably. This is also true for epoxy formulations, which may have different cure and glass transition temperatures. Some polymers, such as polyimides, have good elevated-temperature properties which allow them to compete with titanium. There are aircraft gas turbine engine components employing polyimide matrices which see service temperatures as high as 290°C. Here, again, the effect of temperature on composite properties has to be considered on a case-by-case basis.

The properties shown in Table 6 are axial, transverse, and shear moduli and Poisson's ratio. Properties of 7075-T6 aluminum, a widely used high-strength alloy, is shown for comparison. Poisson's ratio of composites presented is the major Poisson's ratio, which is defined as the ratio of the magnitude of transverse strain divided by axial strain when the composite is loaded in the axial direction. We see that composite transverse and shear moduli are much lower than corresponding axial values.

As discussed in Section 2, carbon fibers display mildly nonlinear stress-strain behavior. Their moduli increase under increasing tensile stress and decrease under increasing compressive stress. This makes the method of calculating modulus important. Various tangent and secant definitions are used throughout the industry, contributing to the confusion in reported properties. The values presented in Table 6, which are approximate, are based on tangents to the stress-strain curves at the origin. Using this definition, tensile and compressive moduli are usually very similar. However, this is not the case for moduli using various secant definitions. Using these definitions typically produces compression moduli which are significantly lower than tension moduli.

Because of the low transverse strengths of unidirectional laminates, they are rarely used in structural applications, except in laminated form. The design engineer selects laminates with layers in several directions to meet requirements for strength, stiffness, buckling, etc. There are an infinite number of laminate geometries that can be selected. For comparative purposes, it is useful to consider quasi-isotropic laminates which have the same elastic properties in all directions in the plane. Laminates are quasi-isotropic when they have the same percentage of layers every  $180/n$  degrees, where  $n \geq 3$ . The most common quasi-isotropic laminates have layers which repeat every 60° or 45° or 30°. We note, however, that strength properties in the plane are not isotropic for these laminates, although they tend to become more uniform as the angle of repetition becomes smaller.

Table 7 presents the elastic properties of quasi-isotropic laminates and 7075-T6 aluminum. Note that the moduli and strengths are much lower than the axial values of unidirectional laminates made of the same material. In most applications, laminate geometry is such that the maximum moduli and tensile and compressive strengths fall somewhere between axial unidirectional and quasi-isotropic values.

Table 8 presents the specific elastic moduli and densities of quasi-isotropic polymer matrix composites and 7075-T6 aluminum. We see that specific moduli of composites reinforced with E-glass and aramid fibers are much lower than that of aluminum. This is a major limitation of these materials. The specific moduli of SM carbon fiber-reinforced epoxy are similar to that of aluminum. Values for composites using UHS (IM) and UHM carbon fibers are significantly greater than that of aluminum.

Table 9 presents strength properties of unidirectional polymer matrix composites and 7075-T6 aluminum. We see that composite transverse and shear strength properties are much lower than those in the axial direction. As for elastic properties, this severe anisotropy

**Table 7** Elastic Properties of Quasi-Isotropic Polymer Matrix Composites and 7075-T6 Aluminum

Fiber	Inplane Extensional Modulus GPa	In-Plane Shear Modulus GPa	In-Plane Poisson's Ratio
7075-T6 aluminum	70	27	0.33
E-glass	23	9.0	0.28
Aramid	29	11	0.32
Boron	80	30	0.33
SM carbon (PAN)	54	21	0.31
UHS(IM) carbon (PAN)	63	21	0.31
UHM carbon (PAN)	110	41	0.32
UHM carbon (Pitch)	165	63	0.32

**Table 8** Specific Modulus (Modulus/Density) and Density of Quasi-Isotropic Polymer Matrix Composites and 7075-T6 Aluminum

Fiber	Specific Gravity (Density, g/cm <sup>3</sup> )	Specific Modulus GPa
7075-T6 aluminum	2.8	26
E-glass	2.1	11
Aramid	1.38	21
Boron	2.0	40
SM carbon (PAN)	1.58	24
UHS (IM) carbon (PAN)	1.61	39
UHM carbon (PAN)	1.66	66
UHM carbon (pitch)	1.80	92

**Table 9** Strength Properties of Unidirectional Polymer Matrix Composites and 7075-T6 Aluminum

Fiber	Axial Tension MPa	Transverse Tension MPa	Axial Compression MPa	Transverse Compression MPa	In-Plane Shear MPa
7075 T-6 aluminum	551 <sup>a</sup>	551 <sup>a</sup>	517 <sup>a</sup>	517 <sup>a</sup>	331 <sup>a</sup>
E-glass	1020	40	620	140	70
Aramid	1240	30	280	140	60
Boron	1240	70	3310	280	90
SM carbon (PAN)	1520	41	1380	170	80
UHS(IM) carbon (PAN)	3500	40	1380	170	80
UHM carbon (PAN)	1380	41	760	170	80
UHM carbon (pitch)	900	20	280	100	41

<sup>a</sup>Military Handbook, Metallic Materials and Elements for Aerospace Vehicle Structures, MIL-HDBK-5H, 1 Dec 1998, Approved for public release: distribution is unlimited.

is a major limitation of unidirectional composites and explains why laminates with fibers in multiple directions are commonly used. Note that the compression strength of carbon fiber-reinforced composites decreases with increasing fiber modulus.

Table 10 presents specific axial strengths of unidirectional composites and 7075-T6 aluminum.

Table 11 presents strength properties of quasi-isotropic polymer matrix composites and 7075-T6 aluminum. We see significant advantages for many of the composites. This benefit is further enhanced by their superior fatigue properties.



**Table 10** Specific Strengths of Unidirectional Polymer Matrix Composites and 7075-T6 Aluminum

Fiber/Metal	Axial Tension MPa	Axial Compression MPa
7075 T-6 aluminum	205 <sup>a</sup>	191 <sup>a</sup>
E-glass	485	300
Aramid	689	200
Boron	620	1660
SM carbon (PAN)	962	870
IM carbon (PAN)	2170	860
UHM carbon (PAN)	831	460
UHM carbon (Pitch)	500	270

<sup>a</sup>Military Handbook, Metallic Materials and Elements for Aerospace Vehicle Structures, MIL-HDBK-5H, 1 Dec 1998, Approved for public release: distribution is unlimited.

**Table 11** Strength Properties of Quasi-Isotropic Polymer Matrix Composites and 7075-T6 Aluminum

Fiber	Tension MPa	Compression MPa	Shear MPa
7075 T-6 aluminum	551 <sup>a</sup>	517 <sup>b</sup>	331 <sup>a</sup>
E-glass	550	330	250
Aramid	460	190	65
Boron	480	1100	360
SM carbon (PAN)	580	580	410
IM carbon (PAN)	1350	580	410
UHM carbon (PAN)	490	270	205
UHM carbon (Pitch)	310	96	73

<sup>a</sup>Ultimate.

<sup>b</sup>Yield.

**Table 12** Specific Strength Properties of Quasi-Isotropic Polymer Matrix Composites and 7075-T6 Aluminum

Fiber/Metal	Tension MPa	Compression MPa
7075 T-6 aluminum	280 <sup>a</sup>	190 <sup>b</sup>
E-glass	260	160
Aramid	330	140
Boron	240	550
SM carbon (PAN)	370	370
IM carbon (PAN)	2210	360
UHM carbon (PAN)	300	160
UHM carbon (Pitch)	170	50

<sup>a</sup>Ultimate.

<sup>b</sup>Yield.

Table 12 presents specific strength properties of quasi-isotropic polymer matrix composites and 7075-T6 aluminum.

### ***Physical Properties of Polymer Matrix Composites***

Tables 13 and 14 present physical properties of unidirectional and quasi-isotropic polymer matrix composites, including density, thermal conductivity, and CTE. In addition to the materials considered in previous tables, we have added composites reinforced with pitch-based

**Table 13** Physical Properties of Unidirectional Polymer Matrix Composites and 7075-T6 Aluminum

Fiber/Metal	Density g/cm <sup>3</sup>	Axial CTE 10 <sup>-6</sup> /K	Transverse CTE 10 <sup>-6</sup> /K	Axial Thermal Conductivity W/m·K	Transverse Thermal Conductivity W/m·K
7075-T6	2.8	24	24	130	130
E-glass	2.1	6.3	22	1.2	0.6
Aramid	1.38	-4.0	58	1.7	0.1
Boron	2.0	4.5	23	2.2	0.7
SM carbon (PAN)	1.58	0.9	27	5	0.5
IM carbon (PAN)	1.61	0.5	27	10	0.5
UHM carbon (PAN)	1.66	-0.9	40	45	0.5
UHM carbon (pitch)	1.80	-1.1	27	380	10
UHK carbon (pitch)	1.80	-1.1	27	600	10

**Table 14** Physical Properties of Quasi-Isotropic Polymer Matrix Composites and 7075-T6 Aluminum

Fiber/Metal	Density g/cm <sup>3</sup>	In-Plane CTE 10 <sup>-6</sup> /K	In-Plane Thermal Conductivity W/m·K	Through- Thickness Thermal Conductivity W/m·K
7075-T6	2.8	24	130	130
E-glass	2.1	10	0.9	0.6
Aramid	1.38	1.4	0.9	0.1
Boron	2.0	6.5	1.4	0.7
SM carbon (PAN)	1.58	3.1	2.8	0.5
IM carbon (PAN)	1.61	2.3	6	0.5
UHM carbon (PAN)	1.66	0.4	23	0.5
UHM carbon (pitch)	1.80	-0.4	195	10
UHK carbon (pitch)	1.80	-0.4	300	10

UHK carbon fibers, which have mechanical properties similar to those of UHM carbon fibers made from pitch, but significantly higher thermal conductivities (about 1000 W/m·K). Note that some composite axial CTEs are negative, which means that they contract in this direction when heated.

We note that the axial thermal conductivity of UHK fiber-reinforced materials is about 50% greater than that of copper (about 400 W/m·K). In addition, their density is much lower than that of aluminum. The density of copper, about 8.9 g/cm<sup>3</sup>, is much greater. The through-thickness thermal conductivities of unidirectional and quasi-isotropic composites are similar to the transverse thermal conductivity of unidirectional composites. The low through-thickness can be a limiting factor for high-through-thickness heat fluxes. This can easily be evaluated by analysis.

Table 15 presents specific in-plane thermal conductivities of quasi-isotropic polymer matrix composites and aluminum. As for modulus and strength, specific thermal conductivity is thermal conductivity divided by density or specific gravity. We use the latter, which is dimensionless. This property is important for applications for which heat transfer and weight (mass) are important, such as spacecraft structures. We see that UHK composites have over three times the specific thermal conductivity of aluminum.

#### *Fatigue Properties of Polymer Matrix Composites*

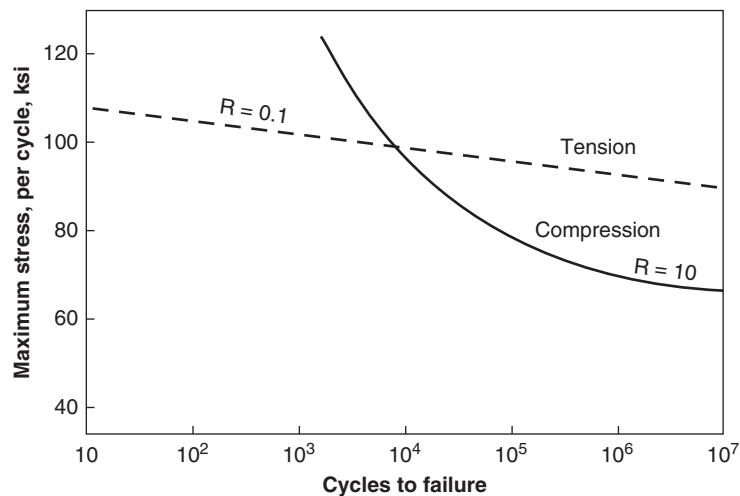
The tension–tension fatigue behavior of unidirectional composites, which was discussed in Section 1, is one of their great advantages over metals (Fig. 3). In general, the tension–tension

**Table 15** Specific thermal conductivity of quasi-isotropic polymer matrix composites and 7075-T6 aluminum

Fiber/Metal	Specific Thermal Conductivity W/m·K
7075-T6	46
E-glass	0.4
Aramid	0.7
Boron	0.7
SM carbon (PAN)	1.8
IM carbon (PAN)	4.8
UHM carbon (PAN)	14
UHM carbon (pitch)	110
UHK carbon (pitch)	170

$S$ – $N$  curves (curves of maximum stress,  $S$ , plotted as a function of cycles to failure,  $N$ ) of polymer matrix composites reinforced with carbon, boron, and aramid fibers are relatively flat. Glass fiber-reinforced composites show a greater reduction in strength with increasing number of cycles. Still, polymer matrix composites reinforced with HS glass are widely used in applications for which fatigue resistance is a critical design consideration, such as helicopter rotors.

Metals are more likely to fail in fatigue when subjected to fluctuating tensile rather than compressive load. This is because they tend to fail by crack propagation under fatigue loading. However, the failure modes in composites are very different and more complex. One consequence is that composites tend to be more susceptible to fatigue failure when loaded in compression than in tension. Figure 6 shows the cycles to failure as a function of maximum stress for carbon fiber-reinforced epoxy laminates subjected to tension–tension and compression–compression fatigue. The laminates have 60% of their layers oriented at  $0^\circ$ , 20% at  $+45^\circ$ , and 20% at  $-45^\circ$ . They are subjected to a fluctuating load in the  $0^\circ$  direction.



**Figure 6** Cycles to failure as a function of maximum stress for carbon fiber-reinforced epoxy laminates loaded in tension–tension ( $R = 0.1$ ) and compression–compression ( $R = -10$ ) fatigue. (Source: After J. Halpin, Lecture Notes, UCLA short course, “Fiber Composites: Design, Evaluation, and Quality Assurance.”)

The ratios of minimum stress to maximum stress,  $R$ , for tensile and compressive fatigue are 0.1 and 10, respectively. We observe that the reduction in strength is much greater for compression–compression fatigue. However, the composite compressive fatigue strength at  $10^7$  cycles is still considerably greater than the corresponding tensile value for aluminum.

#### *Creep and Creep Rupture of Polymer Matrix Composites*

Polymer matrix composites reinforced with carbon and boron are very resistant to deformation and failure under sustained static load when they are loaded in a fiber-dominated direction. (These phenomena are called creep and creep rupture, respectively.) The creep and creep rupture behavior of aramid is not quite as good. Glass fibers display significant creep, and creep rupture is an important design consideration. Polymers are viscoelastic materials which typically display significant creep when they are not constrained with fibers. Therefore, creep should be considered when composites are subjected to significant stresses in matrix-dominated directions, such as the laminate through-thickness direction.

### 3.2 Mechanical and Physical Properties of Metal Matrix Composites

Monolithic metallic alloys are the most widely used materials in mechanical engineering applications. By reinforcing them with continuous fibers, discontinuous fibers, whiskers, and particles, we create new materials with enhanced or modified properties, such as higher strength and stiffness, better wear resistance, and lower CTE. In some cases, the improvements are dramatic.

The greatest increases in strength and modulus are achieved with continuous fibers. However, the relatively high cost of many continuous reinforcing fibers used in metal matrix composites has limited the application of these materials. The most widely used matrix composites are reinforced with discontinuous fibers or particles. This may change as new, lower cost continuous fibers and processes are developed and as cost drops with increasing production volume.

#### *Mechanical Properties of Continuous Fiber-Reinforced Metal Matrix Composites*

One of the major advantages of metal matrix composites reinforced with continuous fibers over unidirectional polymer matrix composites is that many, if not most, of the former have much greater transverse strengths, which allows them to be used in a unidirectional configuration. Table 16 presents representative elastic properties of selected unidirectional metal matrix composites reinforced with continuous boron, alumina, and silicon carbide (SiC) fibers. The values represent a distillation obtained from numerous sources. We see that the axial moduli of the composites are much greater than those of the monolithic base metals used for the matrices.

Table 17 presents the specific axial moduli of unidirectional metal matrix composites, aluminum and titanium. Again, there are clear advantages for the composites.

Tables 18 and 19 present axial tension and compression and specific axial tension and compression strengths of unidirectional metal matrix composites, respectively. We note that the

**Table 16** Elastic Properties of Unidirectional Metal Matrix Composites, 7075-T6 Aluminum and Ti-6Al-4V Titanium

Fiber	Matrix	Density g/cm <sup>3</sup>	Axial Modulus GPa	Transverse Modulus GPa
—	7075-T6	2.8	70	70
—	Ti-6Al-4V	4.4	114	114
Boron	Al	2.6	210	140
Alumina	Al	3.2	240	130
SiC	Ti	3.6	260	170

**Table 17** Specific Axial Modulus of Unidirectional Metal Matrix Composites, 7075-T6 Aluminum and Ti-6Al-4V Titanium

Fiber	Matrix	Specific Axial Modulus
—	7075-T6	26
—	Ti-6Al-4V	26
Boron	Al	81
Alumina	Al	75
SiC	Ti	72

**Table 18** Strength Properties of Unidirectional Metal Matrix Composites, 7075-T6 Aluminum and Ti-6Al-4V Titanium

Fiber	Matrix	Density g/cm <sup>3</sup>	Axial Tension MPa	Transverse Tension MPa	Axial Compression MPa
—	7075-T6	2.8	551 <sup>a</sup>	551 <sup>a</sup>	517 <sup>a</sup>
—	Ti-6Al-4V	4.4	950 <sup>a</sup>	950 <sup>a</sup>	880 <sup>a</sup>
Boron	Al	2.6	1240	140	1720
Alumina	Al	3.2	1700	120	1800
SiC	Ti	3.6	1700	340	2760

<sup>a</sup>Military Handbook, Metallic Materials and Elements for Aerospace Vehicle Structures, MIL-HDBK-5H, 1 Dec 1998, Approved for public release: distribution is unlimited.

**Table 19** Specific Strength Properties of Unidirectional Metal Matrix Composites, 7075-T6 Aluminum and Ti-6Al-4V Titanium

Fiber	Matrix	Axial Tension MPa	Axial Compression MPa
—	7075-T6	200 <sup>a</sup>	190 <sup>a</sup>
—	Ti-6Al-4V	220 <sup>a</sup>	200 <sup>a</sup>
Boron	Al	480	660
Alumina	Al	530	560
SiC	Ti	470	780

<sup>a</sup>Military Handbook, Metallic Materials and Elements for Aerospace Vehicle Structures, MIL-HDBK-5H, 1 Dec 1998, Approved for public release: distribution is unlimited.

absolute and specific composite strengths are significantly greater than those of aluminum and titanium. This is especially true for the compression strength of SiC fiber-reinforced titanium, which is almost four times greater than that of monolithic titanium.

### ***Physical Properties of Unidirectional Metal Matrix Composites***

Table 20 presents physical properties of unidirectional metal matrix composites reinforced with continuous fibers.

### ***Discontinuous Fiber-Reinforced Metal Matrix Composites***

One of the primary mechanical engineering applications of discontinuous fiber-reinforced metal matrix composites is in internal engine components. The primary reason for addition of fibers is to improve the wear resistance and elevated-temperature strength and fatigue

**Table 20** Physical Properties of Unidirectional Metal Matrix Composites

Fiber	Matrix	Density g/cm <sup>3</sup>	Axial CTE 10 <sup>-6</sup> /K	Transverse CTE 10 <sup>-6</sup> /K	Axial Thermal Conductivity W/m-K	Transverse Thermal Conductivity W/m-K
—	7075-T6	2.8	24	24	130	130
—	Ti-6Al-4V	4.4	8.6	8.6	6.7	6.7
Boron	Al	2.6	6	—	—	—
Alumina	Al	3.4	7	16	80	45
SiC	Ti	3.9	5.9	—	—	—

properties of aluminum. The improvement in wear resistance eliminates the need for cast iron sleeves in engine blocks and cast iron inserts in pistons. In addition, fiber-reinforced aluminum composites also have higher thermal conductivities than cast iron, and, when fiber volume fractions are relatively low, their CTEs are closer to that of unreinforced aluminum, reducing thermal stresses.

The key reinforcements used in internal engine components to increase wear resistance are discontinuous alumina and alumina-silica fibers. In one application, Honda Prelude engine blocks, carbon fibers were combined with alumina to tailor both wear resistance and coefficient of friction of cylinder walls. Wear resistance is not an inherent property, so that there is no single value that characterizes a material. However, in engine tests, it was found that ring groove wear for an alumina fiber-reinforced aluminum piston was significantly less than that for one with a cast iron insert.

#### *Properties of Particle-Reinforced Metal Matrix Composites*

Particle-reinforced metals are a particularly important class of metal matrix composites for engineering applications. There are a wide range of materials that fall in this category. A number of them have been used industrially for many years. An important example is a material consisting of tungsten carbide particles embedded in a cobalt matrix which is used extensively in cutting tools and dies. This composite, often referred to as a cermet, cemented carbide, or simply but incorrectly “tungsten carbide,” has much better fracture toughness than monolithic tungsten carbide, which is a brittle ceramic material. Diamond particles embedded in a cobalt matrix, commonly called polycrystalline diamond, are used in rock drill bits and cutting tools. Particle-reinforced metals are now widely used in electronic and photonic thermal management and packaging applications. This is a major growth area, and new materials are continually emerging. These materials are covered in Section 3.5.

Another commercial metal matrix composite, tungsten carbide particle-reinforced silver, has been used as a circuit breaker contact pad material. Here, the composite provides good electrical conductivity and much greater hardness and wear resistance than monolithic silver, which is too soft to be used in this application.

Ferrous alloys reinforced with titanium carbide particles, discussed in the next section, have been used for many years in industrial applications. Compared to the monolithic base metals, they offer greater wear resistance and stiffness and lower density.

*Mechanical Properties of Titanium Carbide Particle-Reinforced Steel.* A number of steel alloys reinforced with titanium carbide (TiC) particles have been used in industrial applications such as cutting blades, tools and dies, and wear parts for many years. They are sold under the trade name “Ferro-Tic.” To illustrate the effect of the particulate reinforcements, we consider

a composite consisting of austenitic stainless steel reinforced with 45% by volume of titanium carbide particles. The modulus of the composite is 304 GPa (44 Msi) compared to 193 GPa (28 Msi) for the monolithic base metal. The specific gravity of the composite is 6.45, about 20% lower than that of monolithic matrix, 8.03. As a result, the specific stiffness of the composite is almost double that of the unreinforced metal. The lower density allows guide rollers to accelerate faster than those made from the base metal, reducing wear. In addition, the composite has higher inherent wear resistance because of the TiC particles.

*Mechanical Properties of Silicon Carbide Particle-Reinforced Aluminum.* Aluminum reinforced with silicon carbide particles is one of the most important metal matrix composites. There are a wide range of materials falling in this category, which are made by a variety of processes, including powder metallurgy, pressure infiltration of particulate preforms, and sintering. Properties depend on the type of particle, particle volume fraction, matrix alloy, and process used to make them. Table 21 presents representative properties of common aluminum, titanium, and steel alloys and composite properties for three volume fractions, 25, 55, and 70%. In general, as particle volume fraction increases, modulus and yield strength increase and fracture toughness and tensile ultimate strain decrease. Particle reinforcement also improves short-term elevated-temperature strength properties and, perhaps surprisingly, fatigue resistance. The moduli and specific moduli of the composites are significantly greater than those of aluminum, titanium, and steel.

*Physical Properties of Silicon Carbide Particle-Reinforced Aluminum.* Silicon carbide particle-reinforced aluminum composites are widely used in thermal management and packaging of electronics and photonics. Table 22 presents physical properties of aluminum, titanium, and steel alloys and composites for three volume fractions, 25, 55, and 70%. We observe that as volume fraction increases, CTE decreases and density increases somewhat and thermal conductivities remain in the range of aluminum alloys. The low CTEs that can be obtained with these materials are a key reason for their widespread use in electronic and photonic thermal management and packaging. We note thermal conductivities as high as 255 W/m·K have been reported for some formulations. This value is greater than that of any common monolithic aluminum alloy.

*Mechanical Properties of Alumina Particle-Reinforced Aluminum.* Alumina particles are used to reinforce aluminum as an alternative to silicon carbide particles because they do not react

**Table 21** Mechanical properties of silicon carbide particle-reinforced aluminum, 6061-T6 aluminum, 6Al-4V titanium and 4340 steel

	Aluminum (6061-T6)	Titanium (6Al-4V)	Steel (4340)	Silicon Carbide Particle-Reinforced Aluminum		
				Particle Volume Fraction		
				25	55	70
Modulus, GPa	69	113	200	114	186	265
Tensile yield strength, MPa	275	1000	1480	400	495	225
Tensile ultimate strength, MPa	310	1100	1790	485	530	225
Elongation (%)	15	5	10	3.8	0.6	0.1
Density, g/cm <sup>3</sup>	2.77	4.43	7.76	2.88	2.96	3.00
Specific modulus, GPa	25	26	26	40	63	88

**Table 22** Physical Properties of Silicon Carbide Particle-Reinforced Aluminum

Property	Aluminum	Titanium	Steel	Composite		
	(6061-T6)	(6Al-4V)	(4340)	Particle Volume Fraction		
				25	55	70
CTE, $10^{-6}/\text{K}$ ( $10^{-6}/^{\circ}\text{F}$ )	23 (13)	9.5 (5.3)	12 (6.6)	16.4 (9.1)	10.4 (5.8)	6.2 (3.4)
Thermal Conductivity, W/m·K (Btu/h·ft·°F)	218 (126)	16 (9.5)	17 (9.4)	160–220 (92–126)	160–220 (92–126)	160–220 (92–126)
Density, $\text{g}/\text{cm}^3$ ( $\text{lb}/\text{in.}^3$ )	2.77 (0.10)	4.43 (0.16)	7.76 (0.28)	2.88 (0.104)	2.96 (0.107)	3.00 (0.108)

as readily with the matrix at high temperatures. Consequently, alumina-reinforced composites can be used in a wider range of processes and applications. However, the stiffness and thermal conductivity of alumina are lower than the corresponding properties of silicon carbide, and these characteristics are reflected in somewhat lower values for composite properties.

### 3.3 Properties of Ceramic Matrix Composites

In general, it is fair to say that ceramic matrix composites are the least developed and most complex class of composites. However, they have great potential for high-temperature and corrosion-resistant applications, especially those for which weight (mass) are important.

Ceramics, in general, are characterized by high stiffness and hardness; resistance to wear, corrosion, and oxidation; and high-temperature operational capability. However, they also have serious deficiencies which have severely limited their use in applications that are subjected to significant tensile stresses. Ceramics have very low fracture toughnesses, which makes them very sensitive to the presence of small flaws. This results in great strength scatter and poor resistance to thermal and mechanical shock. Civil engineers recognized this deficiency long ago, and ceramic materials like stone and concrete are rarely used to carry tensile loads. In concrete, this function has been relegated to reinforcing bars made of steel and, more recently, polymer matrix composites. In lightly loaded structures, concrete reinforced with dispersed asbestos, steel, glass, and carbon fibers allows modest tensile stresses to be supported. These materials are ceramic matrix composites.

#### *Mechanical Properties of Ceramic Matrix Composites*

In ceramic matrix composites, fibers, whiskers, and particles are combined with ceramic matrices to improve fracture toughness, which reduces strength scatter and improves thermal and mechanical shock resistance. By a wide margin, the greatest increases in fracture resistance result from the use of continuous fibers. Table 23 compares fracture toughnesses of structural metallic alloys with those of monolithic ceramics and ceramic matrix composites reinforced with whiskers and with continuous fibers.

The low fracture toughness of monolithic ceramics gives rise to very small critical flaw sizes. For example, the critical flaw sizes for monolithic ceramics corresponding to a failure stress of 700 MPa (about 100 ksi) are in the range of 20–80  $\mu\text{m}$ . Flaws of this size are difficult to detect with conventional nondestructive techniques.

Addition of continuous fibers to ceramics can, if done properly, significantly increase the effective fracture toughness of ceramics. For example, as Table 23 shows, addition of silicon carbide fibers to a silicon carbide matrix results in a ceramic matrix having a fracture toughness in the range of aluminum alloys.

The addition of continuous fibers to a ceramic matrix also changes the failure mode. Figure 7 compares the tensile stress–strain curves for a typical monolithic ceramic with that for

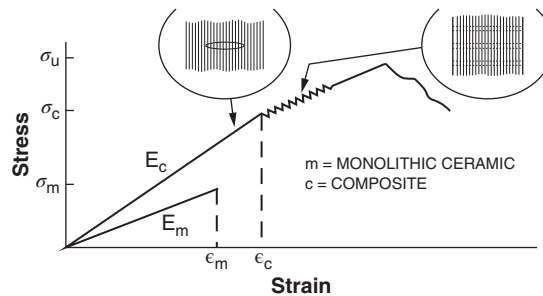


**Table 23** Fracture toughness of structural alloys, monolithic ceramics and ceramic matrix composites

Matrix	Reinforcement	Fracture Toughness MPa·m <sup>1/2</sup>
Aluminum	None	30–45
Steel	None	40–65 <sup>a</sup>
Alumina	None	3–5
Silicon carbide	None	3–4
Alumina	Zirconia particles <sup>b</sup>	6–15
Alumina	Silicon carbide whiskers	5–10
Silicon carbide	Continuous silicon carbide fibers	25–30

<sup>a</sup>The toughness of some alloys can be much higher.

<sup>b</sup>Transformation toughened.



**Figure 7** Stress–strain curves for a monolithic ceramic and ceramic matrix composite reinforced with continuous fibers. (Source: Adapted from NASA Document ID: 19900030246.)

a conceptual continuous fiber-reinforced ceramic matrix composite. The monolithic material has a linear stress–strain curve and fails catastrophically at a low strain level. The composite displays a stress–strain curve that is initially linear. When matrix cracking occurs, the modulus decreases, but there is a significant amount of area under the subsequent curve, indicating that more energy is absorbed during failure and that the material has a less catastrophic failure mode. The fiber–matrix interphase properties must be carefully tailored and maintained over the life of the composite to obtain this desirable behavior.

Although the composite stress–strain curve looks, at first glance, like that of an elastic–plastic metal, this is deceiving. The departure from linearity in the composite results from internal damage mechanisms, such as the formation of microcracks in the matrix. The fibers bridge the cracks, retarding their propagation. However, the internal damage is irreversible. The slope of the stress–strain curve during unloading and subsequent reloading is lower than that of the initial loading. For an elastic–plastic material, the slopes of the unloading and reloading curves are parallel to the initial elastic slope.

There are numerous ceramic matrix composites at various stages of development. One of the most mature types consists of a silicon carbide matrix reinforced with fabric made from silicon carbide-based fibers. These composites are commonly referred to as SiC/SiC. Table 24 the properties of one version, which is composed of an eight-harness satin fabric woven from “Sylramic” silicon carbide fibers embedded in a silicon carbide matrix made by a melt infiltration process. The density is 2.86 g/cm<sup>3</sup>, and the fiber volume fraction is 26%. We observe that the composite retains a significant portion of its room temperature strength up to 1315°C. Long-term strength behavior depends on degradation of the fibers, matrix, and interphase. Because of the continuous fiber reinforcement, SiC/SiC displays excellent resistance to severe thermal shock.

**Table 24** Mechanical Properties of Silicon Carbide Fiber-Reinforced Silicon Carbide

Property	816°C	1038°C	1315°C
Warp tensile modulus (GPa)	208	209	158
Tensile strength (MPa)	362	325	295
Tensile proportional limit (MPa)	177	168	163
In-plane shear strength (MPa)	47.2	—	—

Source: MIL-HDBK-17-5 approved for public distribution.

**Table 25** Comparison of Room Temperature (RT) Densities and Moduli And Strengths at 1038°C of SiC/SiC and Hastelloy X

Material	RT Density g/cc	RT Modulus GPa	Tensile Proportional Limit at 1038°C MPa	Tensile Ultimate Strength at 1038°C MPa
Hastelloy X	8.11	205	74	84
SiC/SiC	2.86	208	168	325

Table 25 compares the room temperature density and moduli and strengths at 1038°C of SiC/SiC and “Hastelloy X,” a nickel–chromium–iron–molybdenum superalloy that is widely used in aerospace and industrial applications. We observe that the composite proportional limit is twice that of the alloy and the ultimate strength about four times as great, while the density is about 65% lower. Properties like these make ceramic matrix composites of great interest for weight-critical high-temperature applications like aircraft gas turbine engines.

### *Physical Properties of Ceramic Matrix Composites*

As discussed earlier, there are many ceramic matrix composites, and they are at various stages of development. One of the more mature systems is silicon carbide fiber-reinforced silicon carbide (SiC/SiC). For a fabric-reinforced composite with a fiber volume fraction of 40%, the density is 2.5 g/cm<sup>3</sup> (0.090 Pci), the CTE is 3 ppm/K (1.7 ppm/°F), the in-plane thermal conductivity is 19 W/m·K (11 Btu/h·ft·°F), and the through-thickness value is 9.5 W/m·K (5.5 Btu/h·ft·°F).

## 3.4 Properties of Carbon Matrix Composites

Carbon matrix composites consist of carbon or ceramic fibers embedded in carbon matrices. The most important subset of carbon matrix composites is carbon–carbon composites, which have carbon fiber reinforcements. As for other composites, there are a wide range of materials that fall in this category. The variables affecting properties include type of fiber, reinforcement form and volume fraction, and matrix characteristics.

Historically, carbon–carbon composites were first used because of their excellent resistance to high-temperature ablation (erosion at high temperature). Strengths and stiffnesses of early materials were low, but these properties have steadily increased over the years.

One of the most significant limitations of carbon–carbon composites is oxidation, which begins at a temperature threshold of approximately 370°C (700°F) for unprotected materials. Addition of oxidation inhibitors in the matrix and ceramic coatings raises the threshold substantially. In inert atmospheres or vacuum, carbon–carbon composites retain their properties to temperatures as high as 1380°C (2500°F).

In recent years, silicon carbide fiber-reinforced carbon has been used in production aircraft gas turbine engine flaps. A significant advantage of this material is that its CTE is closer to that of ceramic coatings like SiC, reducing coating cracking and spallation.

**Table 26** Mechanical Properties of Selected Carbon–Carbon Composites

Material	RCC	ACC-4
Fiber	WCA (rayon)	T300 (PAN)
Fabric	Plain weave	Eight-harness satin
Density, g/cc	1.4–1.7	1.8
<b>In-Plane</b>		
Tensile modulus, GPa	14	110
Compression modulus, GPa	17	110
Tensile strength, MPa	120	330
Compression strength, MPa	88	180
Shear strength, MPa	—	6.9
<b>Through Thickness</b>		
Tensile strength, MPa	5.5	3.4

RCC: Reinforced (reusable) carbon/carbon—Shuttle baseline.

ACC: Advanced carbon/carbon.

### *Mechanical Properties of Carbon Matrix Composites*

Carbon matrices are weak, brittle, low-stiffness materials. As a result, transverse and through-thickness elastic moduli and strength properties of unidirectional carbon–carbon composites are low. Fabric-reinforced materials are weak in the through-thickness direction. Because of this, three-dimensional reinforcement forms are often used. In the direction of fibrous reinforcement, it is possible to obtain moduli as high as 340 GPa (50 Msi), tensile strengths as high as 700 MPa (100 ksi), and compressive strengths as high as 800 MPa (110 ksi). In directions perpendicular to fiber directions, elastic moduli are in the range of 10 MPa (1.5 ksi), tensile strengths 14 MPa (2 ksi), and compressive strengths 34 MPa (5 ksi).

Table 26 presents mechanical properties of selected carbon–carbon composites. The first, the material used on the Space Shuttle Orbiter, was developed decades ago. It is reinforced with carbon fibers made from a rayon precursor, which is relatively weak. This material is called reinforced carbon–carbon (abbreviated RCC), which is redundant. It is sometimes called reusable carbon–carbon. The second material, designated ACC-4, is reinforced with T300, a PAN-based standard modulus fiber. In-plane strength and moduli are much greater for the latter composite.

### *Physical Properties of Carbon Matrix Composites*

There are a wide variety of carbon–carbon composites, which have a wide variety of physical properties. Properties depend on the type of fibers used and the precursor and processes employed to produce the matrix. Densities generally fall in the range of 1.4–1.8 g/cm<sup>3</sup>. In-plane thermal conductivities range from less than 10 to about 350 W/m·K. Through-thickness conductivities are generally very low. CTEs are also very low, generally ranging from -1 to +1 ppm/K.

## 3.5 Advanced Thermal Management Materials

Thermal management is a particularly important consideration in electronic and photonic packaging, because failure rates of semiconductors increase exponentially with temperature. Since conduction is an important method of heat removal, thermal conductivity is a key material property. Because thermal stresses arising from CTE differences between adjacent attached materials are another source of failures, this property is also of great importance. For many

applications, such as spacecraft, aircraft, and portable systems like handsets and notebook computers, weight (mass) and therefore material density are also of concern.

A useful figure of merit for weight-critical applications is specific thermal conductivity, defined as thermal conductivity divided by density. Specific thermal conductivity is analogous to specific modulus and specific strength.

As mentioned, CTE is of great significance in many thermal management applications. For example, semiconductors and ceramic substrates used in electronics and photonics are brittle materials with coefficients of expansion in the range of about 3–7 ppm/K. Semiconductors and ceramic substrates are typically attached to supporting components, such as packages, printed circuit boards (PCBs), and heat sinks with solder, adhesive, or some other type of compliant thermal interface material (TIM). If the CTE of the supporting material is significantly different from that of the ceramic or semiconductor, thermal stresses arise when the assembly is subjected to a change in temperature during manufacture, shipping, storage, or service. These stresses can result in failure of the components or the joint between them.

In some cases, thermal greases are used as a TIM, which eliminate the thermal stress problem. However, greases are messy to apply and are susceptible to dry-out and pump-out. The problem of thermal stresses in solder joints resulting from CTE mismatch is frequently addressed by use of an underfill, which is essentially an adhesive used to reduce stresses on the solder joints.

Table 27 presents physical properties of traditional and advanced thermal management materials, including density, CTE, thermal conductivity, and specific thermal conductivity. For anisotropic materials, in-plane values are shown.

**Table 27** Physical Properties of Monolithic Materials and Composites Used in Electronic and Photonic Thermal Management

Matrix	Reinforcement	Density g/cc	Coefficient of Thermal Expansion ppm/K	Thermal Conductivity W/m·K	Specific Thermal Conductivity W/m·K
Aluminum (6063)	—	2.7	23	218	81
Copper	—	8.9	17	400	45
Epoxy	E-glass	1.6–1.9	12–24	0.3	0.2
Kovar™	—	8.3	5.9	17	2
HOPG	—	2.3	–1	1700	750
Flexible graphite	—	1.1–1.9	–0.4	140–1500	127–780
Beryllium–aluminum	—	2.1	13.9	210	100
Copper–tungsten (10/90)	—	17	6.5	209	12
Copper–molybdenum (15/85)	—	10	6.6	184	18
Aluminum	Silicon	2.5	13.5	126	50
Aluminum	SiC particles	3.0	6.5	120–255	40–85
Aluminum	Graphite platelets	2.3	4–7	650–750	283–326
Beryllium	BeO particles	2.6	6.1	240	92
Copper	Diamond particles	4.6–6.4	4–12	226–800	35–174
Silver	Diamond particles	5.0–6.4	4.5–7.5	350–980	47–217
Aluminum	Diamond particles	2.8–3.3	5.4–10	230–580	70–207
Silicon carbide	Diamond particles	3.3	1.4	600	180
Epoxy	UHK carbon fibers	1.8	–0.7	300	167
Aluminum	UHK carbon fibers	2.6	6.5	290	112
Copper	UHK carbon fibers	7.2	6.5	400	56
Carbon	UHK carbon fibers	1.8	–1	350	194

Before introducing new thermal management materials, it is useful to consider traditional ones that have been used for many decades. These include copper, aluminum, “Kovar,” copper–tungsten, and copper–molybdenum. The properties of E-glass fiber-reinforced printed circuit boards (PCBs) are also shown. Note that there is a wide range of CTEs for these materials found in the literature and manufacturers’ data.

The major problem with copper and aluminum is their high CTEs, about 17 and 23 ppm/K, respectively, which are much greater than the goal range of 3–7 ppm/K. “Kovar,” a nickel–iron alloy, has a low CTE but a very low thermal conductivity. Low-CTE materials like copper–tungsten and copper–molybdenum, both of which are composite materials rather than alloys, have high densities and thermal conductivities no better than those of aluminum alloys.

In response to the limitations of traditional thermal management materials, an increasing number of monolithic carbonaceous materials (various forms of carbon) and composites are being developed that combine high thermal conductivity with low CTE and low density. Some also have excellent mechanical properties.

Table 27 presents properties of the two leading high-performance carbonaceous materials, flexible graphite and highly oriented pyrolytic graphite (HOPG). These materials, which are highly anisotropic, provide in-plane thermal conductivities as high as 1500 and 1700 W/m·K, respectively. Through-thickness thermal conductivities are in the range of 10–20 W/m·K.

We see that there are a significant number of composites with low CTEs and high absolute and specific thermal conductivities. All have densities lower than that of copper.

Thermal management materials in all four classes of composites are being used in electronic and photonic thermal management; however, polymer matrix composites and metal matrix composites dominate at this time, along with flexible graphite and HOPG.

## 4 APPLICATIONS

All four classes of composites are now well established in an increasing number of applications. However, polymer matrix composites are by many orders of magnitude the dominant class of these materials. Despite this, the other types have major advantages in many applications. In this section, we review the key applications of the four classes of composites.

### 4.1 Polymer Matrix Composite Applications

The most important polymer matrix composite reinforcing fibers are E-glass and carbon, followed by aramid and boron. As discussed in Section 3, thermosets are the dominant matrix materials for structural applications. Thermoplastic matrices are most often reinforced with discontinuous fibers, although use of continuous fibers is increasing steadily.

Glass fiber-reinforced polymers (GFRPs) are by orders of magnitude the most widely used polymer matrix composites. Ninety percent of composites manufactured consist of glass fibers in thermosetting polyester and vinyl ester resins. Key reasons for this are their relatively low cost and their position as the first significant structural composite to be developed (the first applications were introduced in the 1940s during World War II). Carbon fiber-reinforced polymers (CFRPs), which are significantly more expensive than GFRPs, are dominant in high-performance applications.

GFRPs reinforced with continuous fibers and fabrics are baseline in numerous commercial, consumer, and aerospace/defense structural applications. Aerospace/defense applications include solid fuel rocket motor cases; rocket launchers; aircraft fairings flooring, interiors, and cargo containers; helicopter rotor blades; patrol boats; mine hunter ships; and ballistic armor.

There are numerous GFRP industrial applications, including trains; truck cabs and trailers; compressed natural gas tanks; wind turbine blades; ships and boats; chemical industry equipment such as tanks and pipes; water treatment equipment; building components; bridges; concrete rebars; concrete forms; transmission line poles; endoscopic surgery equipment; electrical insulation products; oil and gas production; and fire fighter compressed air tank.

Consumer GFRP applications include boats; sports equipment; gliders; shower enclosures and bathtubs; automobile components such as bodies, engine parts, and interior components; and recreational vehicles.

In all of the above applications, continuous unidirectional fibers or fabrics are the key reinforcement forms because of their much greater structural efficiency compared to discontinuous reinforcement, as discussed in Section 3. However, the availability of relatively inexpensive manufacturing processes that use discontinuous fibers makes them a widely used reinforcing form. For example, there are countless injection-molded glass fiber-reinforced parts in consumer products.

The initial applications for CFRP composites were military aircraft and sports equipment. However, industrial applications are now the largest and most rapidly growing market segment.

CFRP aerospace/defense applications include military and commercial aircraft structures; unmanned aerial vehicle (UAV) structures; aircraft gas turbine fan blades; spacecraft structures; satellite antennas; optomechanical systems; and ships.

CFRP industrial applications include compressed natural gas and hydrogen tanks; wind turbine blades; x-ray equipment; robots and other machine components, such as rollers; energy storage flywheels; optomechanical equipment; antennas; uranium centrifuges; fuel cells; fire fighter compressed air tanks; prosthetics and orthotics; oil and natural gas exploration and production; transmission cable cores; train structures and interiors; civil engineering structure repair and reinforcement; and ships.

CFRP consumer applications include sports equipment, such as golf clubs, snowboards, skis, bicycles, softball bats, hockey sticks, bows and arrows, fishing rods, and tennis rackets; musical instruments; head phones; furniture; notebook computer cases; automobile components, such as structural components and drive shafts; and boats. A lightweight electric vehicle with CFRP passenger cell, the BMW i3, is scheduled for serial production. This is a significant milestone in composites.

Boron fiber-reinforced polymer (BFRP) composites are used almost exclusively in aerospace/defense applications. The first advanced composite flight application was the boron fiber-reinforced epoxy F-14 horizontal stabilizer. BFRP was also used in other fighter aircraft and UAVs.

Aramid fiber-reinforced composite (AFRP) applications include ballistic armor, such as helmets; commercial aircraft pressure bottles and freight containers; aircraft engine containment rings; brakes and other friction parts; repair and reinforcement of civil engineering structures; NASCAR racecar bodies; patrol and service boats; and leisure boats, canoes, kayaks, and luxury yachts.

## 4.2 Metal Matrix Composite Applications

As discussed in Section 3, a variety of metal matrix composites have been used commercially for decades, including titanium carbide particle-reinforced ferrous alloys, tungsten carbide particle-reinforced cobalt, and diamond particle-reinforced cobalt.

Metal matrix composites reinforced with continuous fibers are relatively expensive and have had limited but notable application. The Space Shuttle orbiter mid-fuselage section is composed of rib trusses that use boron fiber-reinforced aluminum tubes. The Hubble Space

Telescope high-gain antenna mast/waveguides that project out from the main telescope tubular structure are made of carbon fiber-reinforced aluminum. They have high axial stiffness and low axial CTE, which maintains antenna pointing accuracy. Silicon carbide fiber-reinforced titanium tubes are used in aircraft actuators because of their extremely high axial moduli and strength.

The most notable metal matrix composite commercial material using continuous fibers is alumina fiber-reinforced aluminum, which is being used in transmission lines. The high specific stiffness (stiffness-to-density) and specific strength (strength-to-density) allows support towers to be placed farther apart in new construction and makes it possible to increase current capacity in existing systems.

Automobile and truck engines have used a variety of discontinuous ceramic fibers to improve cylinder bore and piston wear resistance and high-temperature strength, replacing cast iron inserts. Honda combined ceramic and carbon fibers to improve wear resistance and reduce coefficient of friction. Titanium boride particle-reinforced titanium has been used in engine valves.

Silicon carbide particle-reinforced aluminum has been used in a limited number of aerospace, commercial, and optical structural applications. It has become a staple material in electronic and photonic applications. Aerospace/defense applications have included F-16 replacement fuel access doors and ventral fins, gas turbine engine fins, and helicopter rotor blade sleeves. Sports equipment applications have included bicycle structural and mechanical parts, golf clubs, and baseball bats. The high specific stiffness of this material has led to its use in integrated circuit robot end effectors and high-speed machine parts. Other applications include optical systems and high-performance automobile and race car mechanical components.

Silicon particle-reinforced aluminum is used in automobile engine cylinder liners for wear resistance.

Boron carbide particle-reinforced aluminum has been used for spent nuclear fuel containers.

As mentioned, one of the key applications of silicon carbide particle-reinforced aluminum is in electronic and photonic thermal management and packaging applications. In the electronic/photonic packaging industry, these materials are commonly called AlSiC. The main advantages of AlSiC over traditional materials are low CTE and density. One formulation also has a thermal conductivity of 255 W/m·K, which is significantly higher than that of aluminum alloys. To illustrate the benefits of AlSiC, one manufacturer reports that replacement of copper baseplates in power modules essentially eliminates fatigue failure by reducing thermal stresses between the aluminum nitride substrate and base plate.

Silicon–aluminum composites are also used in electronic packaging.

The major limitation of AlSiC composites is that the conductivity of these materials is significantly lower than that of copper. In response, there is continuing development of metal matrix composite materials with higher thermal conductivities. These include aluminum and copper reinforced with carbon fibers and graphite platelets and diamond particle-reinforced aluminum, copper, and silver.

### 4.3 Carbon Matrix Composite Applications

The most important type of carbon matrix composite is carbon–carbon. Carbon–carbon composites are well established in aerospace/defense and commercial applications.

Carbon–carbon composites are widely used in aerospace applications where ablation (resistance to erosion at high temperature) is a key requirement. Examples include reentry vehicle nose tips, rocket nozzles, and exit cones. The Space Shuttle Orbiter used a variety of carbon–carbon components, including leading edges and nose cap.



Carbon-carbon aircraft brakes, which provide significant weight savings over steel, are widely used.

As discussed in Section 3, carbon-carbon composites can be made with a wide range of thermal conductivities. A demonstration high-conductivity carbon-carbon radiator panel was flown on the NASA EO1 Earth Observing Satellite.

The GOCE spacecraft has a carbon-carbon optical bench. Advantages over CFRP include absence of moisture absorption and outgassing.

GE has used silicon carbide fiber-reinforced carbon composites in military aircraft engine flaps. This material has a larger CTE than carbon-carbon, reducing thermal stresses that can cause spalling of protective ceramic coatings.

There are significant industrial carbon-carbon composite applications, including glass-making equipment, heat treatment racks, and wafer-heating elements. Carbon-carbon is also used in racing car and motorcycle brakes and clutches.

#### 4.4 Ceramic Matrix Composite Applications

As discussed in Section 3, reinforcing ceramics with continuous fibers, when done properly, can make them useful structural materials. Discontinuous fibers and whiskers (elongated single crystals) also improve fracture toughness, but to a much smaller degree.

Silicon carbide matrices reinforced with carbon and with silicon carbide fibers (SiC/SiC and C/SiC, respectively) have been used in military aircraft engine flaps, where they provide a significant weight reduction over incumbent nickel-based superalloys. The next generation of aircraft engines from at least one manufacturer are scheduled to make significant use of ceramic matrix composites. Component weight savings as much as 60% over superalloys are reported, and fuel savings of 15% are projected.

C/SiC composites are being used in an increasing number of spacecraft optical systems.

There are a limited number of commercial ceramic matrix composite applications. Silicon carbide whisker-reinforced alumina (aluminum oxide) is used extensively in cutting tools. The advantage is improved fracture toughness over monolithic alumina.

Other applications include heat exchangers for corrosive and high-temperature environments. Silicon carbide particle-reinforced alumina has been used to make parts for abrasive slurry pumps.

C/SiC brakes are being used in high-end automobiles.

Glass-ceramics reinforced with carbon and with SiC fibers are under investigation for a variety of aerospace and commercial applications.

## BIBLIOGRAPHY

- Advanced Materials by Design*, OTA-E-351, U.S. Congress Office of Technology Assessment, U.S. Government Printing Office, Washington, DC, June 1988.
- ASM, *Engineered Materials Handbook*, Vol. 1: *Composites*, ASM International, Materials Park, OH, 1987.
- H. E. Deve and C. McCullough, "Continuous-Fiber Reinforced Al Composites: A New Generation," *JOM*, July 1995, pp. 33-37.
- T. Donomoto et al., "Ceramic Fiber Reinforced Piston for High Performance Diesel Engines," SAE Technical Paper No. 830252, 1983.
- G. F. Hawkins, J. P. Nokes, R. Zaldivar, J. Newman, and C. Zweben, "Measuring the Glass-Transition Temperature of Composites In The Field," in *Proceedings, SAMPE 2002*, Long Beach, CA, May 12-16, 2002.
- T. Hayashi, H. Ushio, and M. Ebisawa, "The Properties of Hybrid Fiber Reinforced Metal and Its Application for Engine Block," SAE Technical Paper No. 890557, 1989.
- A. Kelly (Ed.), *Concise Encyclopedia of Composite Materials*, rev. ed., Pergamon, Oxford, 1994.



- A. Kelly and C. Zweben, Editors-in-Chief, *Comprehensive Composite Materials*, Pergamon, Elsevier Science, Oxford, 2000.
- F. K. Ko, "Three-Dimensional Fabrics for Composites," in T.-W. Chou and F. K. Ko (Eds.), *Textile Structural Composites*, Elsevier Science, Amsterdam, 1989, pp. 129–171.
- F. K. Ko, "Advanced Textile Structural Composites," in J. I. Moran-Lopez and J. M. Sanchez (Eds.), *Advanced Topics in Materials Science and Engineering*, Plenum, New York, 1993.
- A. C. Marshall, *Composite Basics*, 4th ed., Marshall Consulting, Walnut Creek, CA.
- D. B. Marshall and A. G. Evans, "Failure Mechanisms in Ceramic-Fiber/Ceramic-Matrix Composites," *J. Am. Ceramic Soc.*, **68**(5), 225–231, May 1985.
- Military Handbook—5F, *Metallic Materials and Elements for Aerospace Vehicle Structures* (approved for public distribution).
- Military Handbook 17-5, *Composite Materials* (approved for public distribution).
- L. H. Miner, R. A. Wolffe, and C. Zweben, "Fatigue, Creep and Impact Resistance of Kevlar® 49 Reinforced Composites," in *Composite Reliability*, ASTM STP 580, American Society for Testing and Materials, Philadelphia, PA, 1975, pp. 549–559.
- R. Morrell, *Handbook of Properties of Technical & Engineering Ceramics, Part 1: An Introduction for the Engineer and Designer*, Her Majesty's Stationery's Office, London, 1985.
- J. C. Norman and C. Zweben "Kevlar® 49/Thorne1® 300 Hybrid Fabric Composites for Aerospace Applications," *SAMPE Quarterly*, **7**(4), 1–10, July 1976.
- W. H. Pfeifer, J. A. Tallon, W. T. Shih, B. L. Tarasen, and G. B. Engle, "High Conductivity Carbon-Carbon Composites for SEM-E Heat Sinks," paper presented at the Sixth International SAMPE Electronic Materials and Processes Conference, Baltimore, MD, June 22–25, 1992.
- G. Savage, *Carbon-Carbon Composites*, Chapman & Hall, London, 1993.
- K. A. Schmidt and C. Zweben, "Advanced Composite Packaging Materials," *Electronic Materials Handbook*, Vol. 1: *Packaging*, ASM International, Materials Park, OH, 1989, pp. 1117–1131.
- D. L. Smith, K. E. Davidson, and L. S. Thiebert, "Carbon-Carbon Composites (CCC): A Historical Perspective," in *Proceedings, 41st International SAMPE Symposium*, March 24–28, 1996, pp. 32–41.
- W. S. Smith, M. W. Wardle, and C. Zweben, "Test Methods for Fiber Tensile Strength, Composite Flexural Modulus and Properties of Fabric-Reinforced Laminates," in S. W. Tsai (Ed.), *Composite Materials: Testing and Design (Fifth Conference)*, ASTM STP 674, American Society for Testing and Materials, Philadelphia, PA, 1979, pp. 228–262.
- R. Warren (Ed.), *Ceramic-Matrix Composites*, Chapman and Hall, New York, 1992.
- C. Zweben, "Thermomechanical Properties of Fibrous Composite Materials: Theory," in M. B. Bever (Ed.), *Encyclopedia of Materials Science and Engineering*, Pergamon, Oxford, 1986.
- C. Zweben, "Mechanical and Thermal Properties of Silicon Carbide Particle-Reinforced Aluminum," in L. M. Kennedy, H. H. Moeller and W. S. Johnson (Eds.), *Thermal and Mechanical Behavior of Metal Matrix and Ceramic Matrix Composites*, ASTM STP 1080, American Society for Testing and Materials, Philadelphia, PA, 1989.
- C. Zweben, "Is There a Size Effect in Composite Materials and Structures?" *Composites*, **25**(6), 451–454, 1994.
- C. Zweben, "The Future of Advanced Composite Electronic Packaging," in D. D. L. Chung (Ed.), *Materials for Electronic Packaging*, Butterworth-Heinemann, Oxford, 1995a.
- C. Zweben, "Simple, Design-Oriented Composite Failure Criteria Incorporating Size Effects," in *Proceedings, Tenth International Conference on Composite Materials, ICCM-10*, Whistler, British Columbia, Canada, August 1995b.
- C. Zweben, "Overview of Composite Materials for Optomechanical, Data Storage and Thermal Management Systems," in *Proceedings of the SPIE 44th Annual Meeting and Technical Display*, The International Symposium on Optical Science, Engineering, and Instrumentation, Denver, CO, July 18–23, 1999.
- C. Zweben, "Heat Sink Materials for Electronic Packaging," in K. H. J. Buschow et al. (Eds.), *Encyclopedia of Materials: Science and Technology*, Pergamon, Oxford, 2001.

- C. Zweben, "Metal Matrix Composites, Ceramic Matrix Composites, Carbon Matrix Composites and Thermally Conductive Polymer Matrix Composites," in C. A. Harper (Editor-in-Chief), *Handbook of Plastics, Elastomers and Composites*, 4th ed., McGraw-Hill, New York, 2002, Chapter 5.
- C. Zweben, "Materials: Composites," Article 545, in G. Bassani, G. Liedl, and P. Wyder (Eds.), *Encyclopedia of Condensed Matter Physics*, Elsevier (Academic), Oxford, 2005.
- C. Zweben, "Stronger and Lighter—Composites Make Their Mark," *Machine Design*, March 17, 2008.
- C. Zweben, "Thermally Conductive Composites," *JEC Composites Mag.*, January 2009.
- C. Zweben, "Advanced Thermal Management Materials for Electronics and Photonics," *Adv. Microelectron.*, **37**(4), July/August 2010.
- C. Zweben, "Advanced Thermal Management Materials for LED Packaging," *LED Professional Review*, January/February 2010.
- C. Zweben, "Advanced Thermal Management Materials," *Chip Scale Review Tech Monthly*, May 2011



# CHAPTER 11

---

## SMART MATERIALS

**James A. Harvey**  
Under the Bridge Consulting, Inc.  
Corvallis Oregon

1	INTRODUCTION	439	9	pH-SENSITIVE MATERIALS	446
2	PIEZOELECTRIC MATERIALS	440	10	LIGHT-SENSITIVE MATERIALS	446
3	ELECTROSTRICTIVE MATERIALS	443	11	SMART POLYMERS	447
4	MAGNETOSTRICTIVE MATERIALS	443	12	SMART (INTELLIGENT) GELS (HYRDOGELS)	447
5	ELASTORESTRICTIVE MATERIALS	444	13	SMART CATALYSTS	448
6	ELECTRORHEOLOGICAL MATERIALS	445	14	SHAPE MEMORY ALLOYS	448
7	MAGNETORHEOLOGICAL MATERIALS	445	15	UNUSUAL BEHAVIORS OF MATERIALS	449
8	THERMORESPONSIVE MATERIALS	446	16	COMMENTS, CONCERNS, AND CONCLUSIONS	450
			17	FUTURE CONSIDERATIONS	450
				REFERENCES	451

### 1 INTRODUCTION

The world has undergone two materials ages, the plastics age and the composite age, during the past centuries. In the midst of these two ages a new era has developed. This is the smart materials era. According to early definitions, smart materials are materials that respond to their environments in a timely manner.<sup>1-4</sup>

The definition of smart materials has been expanded to materials that receive, transmit, or process a stimulus and respond by producing a useful effect that may include a signal that the materials are acting upon it. Some of the stimuli that may act upon these materials are strain, stress, temperature, chemicals (including pH stimuli), electric field, magnetic field, hydrostatic pressure, different types of radiation, and other forms of stimuli.<sup>5</sup>

The effect can be caused by absorption of a proton, a chemical reaction, integration of a series of events, translation or rotation of segments within the molecular structure, creation and motion of crystallographic defects or other localized conformations, alteration of localized stress and strain fields, and others. The effects produced can be a color change, a change in index of refraction, a change in the distribution of stresses and strains, or a volume change.<sup>5</sup>

Another important criterion for a material to be considered smart is that the action of receiving and responding to stimuli to produce a useful effect must be reversible. Another

important factor in determining if a material is smart pertains to its asymmetrical nature. This is primarily critical for piezoelectric materials. Other types of smart materials exhibit this trait. However, little research has been performed to verify this observation.

Also, it should be pointed out that the word “intelligent” is used to describe smart materials. The notation “smart” has been overused as a means to market materials and products.

From the purist point of view, materials are smart if at some point within their performance history their reaction to a stimulus is reversible. Materials that formally have the label of being smart include piezoelectric materials, electrostrictive materials, electrorheological materials, magnetorheological materials, thermoresponsive materials, pH-sensitive materials, UV-sensitive materials, smart polymers, smart gels (hydrogels), smart catalysts, and shape memory alloys. In this treatment of the subject we will be using some of these classifications; in some cases, however, the classification of a particular material may appear to be in error. This will be done to illustrate the rapid growth of the field of smart materials and the rediscovery of the smart behavior of materials known for centuries. As we continue to better understand smart materials, our definitions will change. In each material section there will be discussions pertaining to the material definition, types of materials that belong to that class, properties of the members, and applications of the materials. In some cases a more detailed discussion of application will be given to both illustrate the benefit of these materials and simulate the use of these materials in new applications.

Another important feature of smart materials is their inclusion in smart structures, which are simply structures with at least one smart material incorporated within its structure and from the effect of the smart material causes an action. A smart structure may have sensors (nerves), actuators (muscles), and a control (brain). Thus, the term *biomimetic* is associated with smart structures. Smart structures are being designed to make our life more productive and easy. With the number of sensors, actuators, and control systems available, coupled with the materials and the genius of scientists and engineers, these structures are becoming more commonplace. Reading nontechnical magazines, watching television, and going to stores can verify this.

In a comical manner the growth of smart structures can be illustrated by an article that appeared in the December 14, 2000, edition of the *New York Times*. This article describes the “Big Mouth Billy Bass,” the singing fish, and how smart this novel toy is.

Examples of technical applications of smart structures are composite materials embedded with fiber optics, actuators, sensors, microelectromechanical systems (MEMSs), vibration control, sound control, shape control, product health or lifetime monitoring, cure monitoring, intelligent processing, active and passive controls, self-repair (healing), artificial organs, novel indicating devices, designed magnets, damping aeroelastic stability, and stress distributions. Smart structures are found in automobiles, space systems, fixed- and rotary-wing aircrafts, naval vessels, civil structures, machine tools, recreation, and medical devices.<sup>5,6</sup>

Another important feature related to smart materials and structures is that they encompass all fields of science and engineering. When searching for information on smart materials and structures, there are numerous sources, websites, and professional societies that deal with this technology.

## 2 PIEZOELECTRIC MATERIALS

The simplest definition of piezoelectric materials can be obtained by first dividing the word into *piezo* and *electric*. *Piezo* is from the Greek word *piezein*, which means “to press tightly or squeeze.” Combining *piezein* with *electric*, we have “squeeze electricity.”

The history of piezoelectric materials is relatively simple and only the highlights will be presented. In 1880, Pierre and Paul-Jean Curie showed the piezoelectric effect in quartz and Rochelle salt crystals. Their first observations were made by placing weights on the faces of

particular crystal cuts, like the X-cut quartz plate, detecting charges on the crystal surfaces, and demonstrating that the magnitude of the charge was proportional to the applied weight. This phenomenon has become known as the direct-pressure piezoelectric effect. In 1881 G. Lippmann predicted that a crystal such as quartz would develop a mechanical strain when an electric field was applied. In the same year the Curies reported the converse pressure piezoelectric effect with quartz and Rochelle salt. They showed that if certain crystals were subjected to mechanical strain, they became electrically polarized and the degree of polarization was proportional to the applied strain. The French inventor Langevin developed the first sonar using quartz crystals in 1920. During the 1940s researchers discovered and developed the first polycrystal line, piezoelectric ceramic, barium titanate. A significant advantage of piezoelectric ceramics over piezoelectric crystals is their ability to be formed in a variety of shapes and sizes. In 1960, researchers discovered a weak piezoelectric effect in whalebone and tendon that led to intense search for other piezoelectric organic materials. And in 1969, Kawai found very high piezoelectric activity in polarized polyvinylidene fluoride (PVDF).<sup>7,8</sup>

The piezoelectric effect exists in a number of naturally occurring crystals, such as quartz, tourmaline, and sodium potassium tartrate. For a crystal to exhibit the piezoelectric effect, it must not have a center of symmetry. When a stress (tensile or compressive) is applied to a crystal with a center of symmetry, it will alter the spacing between the positive and negative sites in each elementary cell unit, thus causing a net polarization at the crystal surface. The effect is approximately linear. The polarization is directly related to the applied stress. It is direction dependent. Thus, compressive and tensile forces will generate electric fields and voltages of opposite polarity. The effect is also reciprocal; thus, when the crystal is exposed to an electric field, it undergoes an elastic strain changing its length based upon the field polarity.

As previously mentioned, the ceramic-type materials play an important role in the area of piezoelectrics. Piezoelectric ceramics are polycrystalline ferroelectric materials with a perovskite-crystal-type structure. The crystal structure is tetragonal/rhombohedral with a close proximity to cubic in nature. Piezoelectric ceramics have the general formula of  $A^{2+}B^{4+}O_3^{2-}$ , where A represents a large divalent metal ion such as barium or lead and B is one or more tetravalent metal ions such as titanium, zirconium, or manganese. These ceramics are considered to be masses of minute crystallites that change crystal forms at the Curie temperature. Above the Curie temperature, the ceramic crystallites have a simple cubic symmetry. This form is centrosymmetric with positive and negative charge sites coinciding; thus there are no dipoles present. The material is considered to be paraelectric. Below the Curie temperature, the ceramic crystallites have a tetragonal symmetry; this form lacks a center of symmetry with the positive and negative charge sites no longer coinciding; thus each unit cell has an electric dipole whose direction may be reversed and switched by the application of an electric field. The material is now considered to be ferroelectric.

The piezoelectric properties of ceramics can be enhanced by applying a large electric field at an elevated temperature, thus generating an internal remnant polarization that continues long after the removal of the electric and thermal fields. This technique is known as poling. The poling of piezoelectric ceramics has eliminated the use of piezoelectric crystals in many applications.

The vinylidene fluoride monomer  $CH_2 = CF$  yields the semicrystalline polymer (PVDF) upon polymerization. This polymer was found to be highly piezoelectric. Polyvinylidene fluoride is manufactured in sheet form from the nonpolar  $\alpha$ -phase film extruded from the melt. The extruded film is uniaxially stretched. This process rotates the long polymer chains and forms the polar  $\beta$ -phase. The  $\beta$ -phase is needed for the high piezoelectricity. The final step consists of reorientation of the randomly directed dipoles associated with the stretched  $\beta$ -phase by applying a poling field in the direction normal to the plane of the film. The resulting piezoelectric PVDF has orthotropic symmetry.

Copolymers and rubber and ceramic blends of PVDF have been prepared for use as piezoelectric materials. The most common copolymer is one based on the polymerization reaction of vinylidene fluoride and trifluoroethylene. Polyvinylidene fluoride and its copolymers with trifluoroethylene have low mechanical quality factors and high hydrostatic-mode responses and their acoustic impedance is similar to water, making them ideal for underwater hydrophone applications.<sup>9</sup>

A series of polyimides has been developed at NASA Langley for use in piezoelectric applications. These polyimides have pendant trifluoromethyl ( $-\text{CF}_3$ ) and cyano ( $-\text{CN}$ ) polar groups. Whenever these polyimides are exposed to applied voltages of the order of 100 MV/m at elevated temperatures, the polar groups develop a high degree of orientation, resulting in polymer films with high piezoelectric and pyroelectric properties. The piezoelectric response for these polyimides is in the same vicinity as those of PVDF at room temperature. However, the piezoelectric response of the polyimides is greater at elevated temperatures.<sup>10</sup>

Multiphase piezoelectric composites have been developed for their synergetic effect between the piezoelectric activity of monolithic ceramics and the low density of non-piezoelectric polymeric materials. One class of piezoelectric composites that has been developed is the smart tagged composites. These piezoelectric composites are PZT-5A (soft piezoelectric ceramic) particles embedded into an unsaturated polyester polymer matrix and are used for structural health monitoring. Conductive metal-filled particles with polyimide films have been explored for microelectronic applications. The use of graphite-filled polymers has shown potential as microsensors and actuators.

Piezoelectric materials have been used in thousands of applications in a wide variety of products in the consumer, industrial, medical, aerospace, and military sectors. When a piezoelectric material is subjected to a mechanical stress, an electric charge is generated across the material. The ability of a material to generate a charge or electric field when subjected to a stress is measured by the piezoelectric voltage coefficient  $g$ .

The converse effect occurs when a piezoelectric material becomes strained when placed in an electric field. Under constant-stress conditions, the general equation for the piezoelectric charge coefficient  $d$  can be expressed as the change in the strain  $S$  of the piezoelectric material as a function of the applied electric field  $E$ .

It should be denoted that piezoelectric materials are also pyroelectric. They generate an electric charge as they undergo a temperature change. Whenever their temperature is increased, a voltage develops having the same orientation as the polarization voltage. Whenever the temperature is decreased, a voltage develops with orientation opposite to the polarization voltage.<sup>11</sup>

Some of the applications of materials that utilize direct and converse piezoelectric effects and the applications of PVDF piezoelectric film follow. Specific applications will be discussed.

One of the uses of piezoelectric ceramics and polymers is in ink-on demand printing. Several commercial available ink-jet printers are based upon this technology.<sup>12,13</sup> In this application the impulse ink jet is produced using a cylindrical transducer that is tightly bound to the outer surface of a cylindrical glass nozzle with an orifice ranging from mils to micrometers in diameter. Several industrious researchers have expanded upon this technique by using a printer as a chemical delivery system for the application of doped polymers for organic light-emitting displays. Researchers from Princeton University have used a color inkjet printer based upon piezoelectric technology with a resolution of 640 dots per line and replaced the inks with polymer solutions.<sup>14</sup> This technique has also been applied to the manufacture of color filters for liquid crystal displays.

Another application of piezoelectric polymer film involves the work of a group of researchers at the Thiokol Company and an earlier work<sup>15,16</sup> to monitor adhesive joints. The Thiokol study showed that during the bonding process, the PVDF piezoelectric film sensors monitored the adhesive cure ultrasonically and qualitatively determined the presence of significant void content. The Thiokol study also indicated that normal bond stresses

were quantified during cyclic loading of single lap joints and electrometric butt joints. The researchers revealed that this was a significant step toward service life predictions. However, more and better understood monitoring techniques are needed.

An interesting application of piezoelectric ceramics can be illustrated by the hundreds of vertical pinball machines popular in the Pachinko parlors of Japan. The machines are assembled with stacks of piezoelectric disks that can act as both sensors and actuators. When a ball falls on the stack, the force of impact generates a piezoelectric voltage pulse that in turn generates a response from the actuator stack through a feedback control system. The stack expands, throwing the ball out of the hole and moving it up a spiral ramp through a sequence of events and then repeating the sequence.<sup>17</sup>

### 3 ELECTROSTRICTIVE MATERIALS

Piezoelectric materials are materials that exhibit a linear relationship between electric and mechanical variables. Piezoelectricity is a third-rank tensor. Electrostrictive materials also show a relationship between these two variables. However, in this case, it is a quadratic relationship between mechanical stress and the square of electrical polarization. Electrostriction can occur in any material and is a small effect. One difference between piezoelectric and electrostrictive materials is the ability of the electrostrictive materials to show a larger effect in the vicinity of its Curie temperature. Electrostriction is a fourth-rank tensor property observed both in centric and acentric insulators. This is especially true for ferroelectric materials such as the members of the perovskite family. Ferroelectrics are ferroic solids whose domain walls have the capability of moving by external forces or fields. In addition to ferroelectrics, the other principal examples of ferroic solids are ferromagnetics and ferroelastics, both of which have potential as smart materials. Other examples of electrostrictive materials include lead manganese niobate–lead titanate (PMN–PT) and lead lanthanum zirconate titanate (PLZT).

An interesting application of electrostrictive materials is in active optical applications. During the Cold War, the satellites that flew over the Soviet Union used active optical systems to eliminate atmospheric turbulence effects. Electrostrictive materials have the advantage over piezoelectric materials of being able to adjust the position of optical components due to the reduced hysteresis associated with the motion. Work on active optical systems has continued. Similar multilayer actuators were used to correct the position of the optical elements in the Hubble telescope. Supermarket scanners use actuators and flexible mirrors to read bar codes optically.<sup>17</sup>

Other examples of this family may be included in the electroactive polymers. This name has appeared in the technical literature for approximately a decade with an increasing interest in the last several years. Electroactive polymers include any polymer that is simulated by electricity and responds to its effect in a reversible manner. This classification is sort of a melting pot of smart materials.<sup>18</sup>

### 4 MAGNETOSTRICTIVE MATERIALS

Magnetostrictive materials are materials that have the material response of mechanical deformation when stimulated by a magnetic field. Shape changes are the largest in ferromagnetic and ferroelastic materials. The repositioning of domain walls that occurs when these solids are placed in a magnetic field leads to hysteresis between magnetization and an applied magnetic field. When a ferromagnetic material is heated above its Curie temperature, these effects disappear. The microscopic properties of a ferromagnetic solid are different than for a ferroelastic solid. The magnetic dipoles of a ferromagnetic solid are aligned parallel. The alignment of dipoles in a ferromagnetic solid can be parallel or in other directions.<sup>5,19,20</sup>



Magnetostrictive materials are usually inorganic in chemical composition and are alloys of iron and nickel and doped with rare earths. The most effective magnetostrictive material is another alloy developed at the Naval Ordnance Laboratory, TERFENOL-D. It is an alloy of terbium, dysprosium, and iron. The full effect of magnetostriction occurs in crystalline materials. One factor preventing magnetostrictive materials from reaching commercial significance has been cost. Over the past three decades there has been a great deal of development of giant magnetostrictive materials, colossal magnetostrictive materials, and organic and organometallic magnets.<sup>5,21</sup>

The giant magnetostrictive effect was first observed in iron–chromium laminates in 1988. These laminates consisted of alternating layers of 50-Å-thick iron with chromium layers of various thicknesses. The iron layers oriented themselves with antiparallel magnetic moments. A magnetic field of 20 kOe applied in the plane of the iron layers will uncouple this antiferromagnetic orientation. Since the magnetic orientation of one layer is controlled, another layer is free to rotate with an applied field; this change in orientation of the two layers produces a magnetostrictive effect. This discovery of giant magnetostrictive materials made the increased sensitivities in hard drive heads more cost effective.

In the 1990s, researchers further enhanced the field of magnetostrictive materials with the development of colossal magnetostrictive materials. Ratios of magnetostrictive effect in excess of 100,000% were observed. These new materials were found to be epitaxial lanthanum–calcium–manganese–oxygen thin films, polycrystalline lanthanum–yttrium–calcium–manganese–oxygen, and polycrystalline lanthanum–barium–manganese–oxygen. These combinations enhanced the product performance at costs below that of original magnetostrictive materials.<sup>21</sup>

Magnets that exhibit commercial potential should have magnetic saturation and coercive field properties that are operational at low temperatures. Magnets are useful below their critical temperature. Most inorganic magnets have critical temperatures well above room temperature. The first organometallic magnet was the ionic salt complex of ferric bis(pentamethylcyclopentadienide) and tetracyanoethylene. This complex was a ferromagnet below its critical temperature of 4.8 K. The highest effective critical temperature of an organometallic magnet was in the vicinity of 400 K.<sup>22</sup>

Organic magnets are different than organometallic magnets for two reasons. The first is obvious: Organic-based magnets contain metal atoms. This results in a rethinking of the principles of magnetism. The second difference refers to the fact that coupled spins of organic magnets reside only in the *p* orbitals while coupled spins of the organometallic magnets can reside in either the *p* orbitals or the *d* orbitals or a combination of the two. A series of organic magnets based upon the nitroxide chemistry was synthesized and their magnetic behavior studied between 0.6 and 1.48 K. The most studied compound of these nitroxide-based magnets is 4-nitrophenylnitronyl nitroxide. This compound showed a saturation magnetization equivalent to one spin per molecule. This is indicative of ferromagnetic behavior.<sup>5,22</sup>

## 5 ELASTORESTRICTIVE MATERIALS

This class of smart materials is the mechanical equivalent to electrostrictive and magnetostrictive smart materials. These smart materials exhibit high hysteresis between stress and strain. The motion of ferroelastic domain walls causes the hysteresis. This motion of the ferroelastic domain walls is very complex near a martensitic-phase transformation. At this phase change, two types of crystal structural changes occur. One is induced by mechanical stress and the other by domain wall motion. Martensitic shape memory alloys have wide, diffuse phase changes and the ability to exist in both high- and low-temperature phases. The domain wall movements disappear with total change to the high-temperature phase.<sup>5,19,20</sup> The elastorestrictive smart material family is in its infancy.

## 6 ELECTORRHEOLOGICAL MATERIALS

Rheological materials comprise an exciting group of smart materials. Electrorheological and magnetorheological materials can change their rheological properties instantly through the application of an electric or a magnetic field. Electrorheological materials (fluids) have been known for several centuries. The rheological or viscous properties of these fluids, which are usually uniform dispersions or suspensions of particles within a fluid, are changed with the application of an electric field. The mechanism of how these electrorheological fluids work is simple. In an applied electric field the particles orient themselves in fiberlike structures (fibrils). When the electric field is off, the fibrils disorient themselves. Another way to imagine this behavior is to consider logs in a river. If the logs are aligned, they flow down the river. If they are disordered, they will cause a log jam, clogging up the river. A typical example of an electrorheological fluid is a mixture of corn starch in silicone oil. Another fluid that has been experimented with as a replacement for silicone oil is chocolate syrup. Another feature of electrorheological systems is that their damping characteristics can be changed from flexible to rigid and vice versa. Electrorheological fluids were evaluated using a single-link flexible-beam test bed. The beam was a sandwich configuration with electrorheological fluids distributed along its length. When the beam was rapidly moved back and forth, the electrorheological fluid was used to provide flexibility during the transient response period of the maneuver for speed and made rigid at the end point of the maneuver for stability. A practical way of viewing this behavior is to compare it with fly fishing.<sup>5</sup> It has been suggested that rheological fluids be used in the construction of fishing rods and golf clubs.

## 7 MAGNETORHEOLOGICAL MATERIALS

Magnetorheological materials (fluids) are the magnetic equivalent of electrorheological fluids. These fluids consist of ferromagnetic particles that are either dispersed or suspended and the applied stimulus is a magnetic field. A simple magnetorheological fluid consists of iron powder in motor oil. The Lord Corporation provided a clever demonstration of magnetorheological fluids. It supplied an interlocking two-plastic-syringe system filled with a magnetorheological fluid and two small magnets. The fluid flows freely, without the magnets placed in the middle of the two syringes. With the two magnets in place, the fluid flows completely.

An interesting adaptation of magnetostrictive fluids is a series of elastomeric matrix composites embedded with iron particles. During the thermal cure of the elastomer, a strong magnetic field was applied to align the iron particles into chains. These chains of iron particles were locked into place within the composite through a crosslinked network of the cured elastomer. If a compressive force stimulated the composite, it was 60% more resistant to deformation in a magnetic field. If the composite was subjected to a shear force, its magnetic-field-induced modulus was an order of magnitude higher than its modulus in a zero magnetic field.<sup>5,23</sup>

Recently attempts to enhance the properties of epoxies with magnetic fields showed that at low conversion rates of the epoxy with a hardener, economically generated magnetic fields had an effect on the properties of the final composite.<sup>24</sup> At the high conversion of the reactants there exists a need to drive the scarce unreacted glycidyl and amine functionalities together. Only magnetic fields generated by superconducting electromagnets are capable of this.<sup>24</sup>

There continues to be a great deal of research into magnets and magnetism. A new area of research involves magnetic nanocomposite films. Magnetic particles exhibit size effects. Below a critical size, magnetic clusters comprise single domains, whereas with bulk materials there are multiple domains. Nanomagnets show unusual properties of magnetism, such as superparamagnetism and quantum tunneling. These unique properties of magnetic nanoclusters can lead to applications in information storage, color imaging, magnetic refrigeration, ferrofluids, cell storage, medical diagnosis, and controlled drug delivery. A nanocomposite

is considered to be the incorporation of these nanoclusters into polymeric matrices such as polyaniline.<sup>25</sup>

## 8 THERMORESPONSIVE MATERIALS

Amorphous and semicrystalline thermoplastic polymeric materials are unique due to the presence of a glass transition temperature. Changes in the specific volume of polymers and their rate of change occur at their glass transition temperatures. This transition affects a multitude of physical properties. Numerous types of indicating devices could be developed based upon the stimulus–response (temperature-specific volume) behavior. This chapter contains several examples of this type of behavior; however, its total impact is beyond the scope of this chapter. To take advantage of this behavior in product development or material selection, it is necessary to consult the many polymer references.

A few unique examples that illustrate thermoresponsive behavior are included in this chapter. One example refers to the polyethylene/poly(ethylene glycol) copolymers that were used to functionalize the surfaces of polyethylene films.<sup>5,26</sup> One may refer to this illustration as being a “smart surface” or functionally gradient surface. When the film is immersed in an aqueous dispersion of the copolymer, the ethylene glycol moieties attach to the polymer film surface, resulting in a film surface having solvation behavior similar to poly(ethylene glycol) itself. Due to the inverse temperature-dependent solubility behavior of poly(alkene oxide)s in water, surface-modified polymers are produced that reversibly change their hydrophilicity and solvation with changes in temperatures.<sup>27</sup> Similar behaviors have been observed as a function of changes in pH.<sup>28–31</sup>

Another interesting example of materials that respond smartly to changes in temperature includes cottons, polyesters, and polyamide/polyurethanes that are modified by poly(ethylene glycol)s. A combination of the thermoresponsiveness of these fabrics with a sensitivity to moisture resulted in a family of fabrics that can serve as smart pressure bandages. When exposed to an aqueous medium such as blood, these fabrics contract and apply pressure. Once the fabric dries, it releases the pressure.<sup>23</sup>

Polymers based upon the monomer vinyl methyl ether have the unique behavior of shrinking upon heating to approximately 40°C. In the right design with normal behaving polymers, one can construct a device that can grasp objects like a hand.

## 9 pH-SENSITIVE MATERIALS

By far, the widely known chemical classes of pH-sensitive materials are the acids, bases, and indicators. The indicators fit the definition of smart materials by changing color as a function of pH and the action is reversible.

Other examples of pH-sensitive materials include some of the smart gels and smart polymers mentioned in this chapter. There are a large number of pH-sensitive polymers and gels that are used in biotechnology and medicine. Usually these materials are prepared from various combinations of such monomers and polymers such as methacrylic acid, methyl methacrylate, carboxymethylethyl cellulose, cellulose acetate, cellulose phthalate, hydroxypropylmethylcellulose phthalate, hydroxypropylmethylcellulose acetate, hydroxypropylmethylcellulose succinate, diethylaminoethyl methacrylate, and butyl methacrylate.<sup>32</sup>

## 10 LIGHT-SENSITIVE MATERIALS

There are several different material families that exhibit different behavior to a light stimulus. Electrochromism is a change in color as a function of an electrical field. Other types of behavior for light-sensitive materials are thermochromism (color change with heat), photochromism

(color change with light), and photostrictism (shape changes caused by changes in electronic configuration due to light).<sup>5,19,20</sup>

Electrochromic smart windows have been intensively researched over the past few decades. There have been over 1800 patents issued for optical switching devices, with the bulk of these being issued in Japan. A typical switchable glass is multilayered with an electrochromic device embedded inside. A window device may have glass with an interior conductive oxide layer both on the top and bottom. Inside the sandwich of glass and conductive oxide is the electrochromic device. This device consists of an electrochromic layer, an ion storage layer, and between these two layers an ion conductor.

An interesting light-sensitive material with both electro- and thermochromism behaviors,  $\text{Li}_x\text{VO}$ , was evaluated for a smart window application.<sup>33</sup>

Materials have been developed to exhibit both photochromic and photographic (irreversible behavior to light) behaviors. One such system is based upon a substituted indolinospirobenzopyran embedded in a polystyrene matrix. This system performs as a photochromic system at low exposure in the UV range and as a photographic system at high exposures. The image can be devisualized by heat and can be restored with UV irradiation many times.<sup>34</sup>

## 11 SMART POLYMERS

The term *smart polymers* was almost dropped as a classification for smart materials in this treatment of the subject. It is very confusing. Each field of science and engineering has its own definition of a smart polymer, each definition can fit in another classification, and its distinction in smartness can be confusing at times. The term is being included in this chapter because several excellent articles on the subject have “smart polymer” in the title.

In medicine and biotechnology, smart polymer systems usually pertain to aqueous polymer solutions, interfaces, and hydrogels. Smart gels, or hydrogels, will be treated separately. Smart polymers refer to polymeric systems that are capable of responding strongly to slight changes in the external medium: a first-order transition accompanied by a sharp decrease in the specific volume of the polymer. If the external medium is temperature, this transition is known as the glass transition temperature of the polymer and several properties of the polymer change. Among these properties are volume, coefficient of thermal expansion, specific heat, heat conductivity, modulus, and permeation. Manipulating the detection around the glass transition temperature of the polymer can develop in smart devices. There are numerous examples of product development that has resulted in failure because the glass transition temperature of the polymer was not considered. It should be noted that as the polymer cools down from high temperatures to below its glass transition temperature its below-glass-transition properties are returned and vice versa.

Smart polymers can respond to stimuli such as temperature, pH, chemical species, light, UV radiation, recognition, electric fields, magnetic fields, and other types of stimuli. The resulting response can be changes in phase, shape, optics, mechanical strength, electrical and thermal properties, reaction rate, and permeation rate.

## 12 SMART (INTELLIGENT) GELS (HYDROGELS)

In the literature you can find these smart materials under a variety of names, as reflected by the title of this section. The concept of smart gels is a combination of the simple concept of solvent-swollen polymer networks in conjunction with the material being able to respond to other types of stimuli. A partial list of these stimuli includes temperature, pH, chemicals, concentration of solvents, ionic strength, pressure, stress, light intensity, electric fields, magnetic

fields, and different types of radiation.<sup>35–39</sup> The founding father of these smart gels, Toyochi Tanaka, first observed this phenomenon in swollen clear polyacrylamide gels. Upon cooling, these gels would cloud up and become opaque. Upon warming these gels regained their clarity. Upon further investigation to explain this behavior, it was found that some gel systems could expand to hundreds of times their original volume or could collapse to expel up to 90% of its fluid content with a stimulus of only a 1°C change in temperature. Similar behavior was observed with a change of 0.1 pH unit.

These types of behaviors led to the development of gel-based actuators, valves, sensors, controlled release systems for drugs and other substances, artificial muscles for robotic devices, chemical memories, optical shutters, molecular separation systems, and toys. Other potential systems for the development of products with smart (intelligent) gels (hydrogels) include paints, adhesives, recyclable absorbents, bioreactors, bioassay systems, and display.

Numerous examples of the commercialization of these smart gels can be found in Ref. 35. This chapter will only include a few examples of smart gels. One such smart gel consists of an entangled network of two polymers, a poly(acrylic acid) (PAA) and a triblock copolymer of poly(propylene oxide) (PPO) and poly(ethylene oxide) (PEO) with a sequence of PEO–PPO–PEO. The PAA portion is a bioadhesive and is pH responsive, the PPO moieties are hydrophobic substances that assist in solubilizing lipophilic substances in medical applications, and the PEO functionalities tend to aggregate, resulting in gelation at body temperatures. Another smart gel system with a fairly complex composition consists of chitosan, a hydrolyzed derivative of chitin (a polymer of *N*-acetylglucosamine that is found in shrimp and crab shells), a copolymer of poly(*N*-isopropylacrylamide) and poly(acrylic acid), and a graft copolymer of poly(methacrylic acid) and poly(ethylene glycol). This gel system was developed for the controlled release of insulin in diabetics.

Polyampholytic smart hydrogels swell to their maximum extent at neutral pH values. When such gels, copolymers of methacrylic acid 2-(*N,N*-dimethylamino)ethyl methacrylate, are subjected to either acidic or basic media, they undergo rapid dehydration.<sup>39</sup>

One very unusual smart gel is based upon the polymerization of *N*-isopropylacrylamide, a derivative of tris(2,2'-bipyridyl)ruthenium(II) that has a polymerizable vinyl group, and *N,N'*-methylenebisacrylamide. It is a self-oscillating gel that simulates the beating of the heart with color changes.<sup>40</sup>

### 13 SMART CATALYSTS

The development of smart catalysts is a new field of investigation and has shown a great deal of activity in universities of the oil-producing states. One such smart catalyst is rhodium based with a poly(ethylene oxide) backbone. Smart catalysts such as this one function opposite to a traditional catalyst; that is, as the temperature increases, they become less soluble, precipitating out of the reaction solution, thus becoming inactive. As the reaction solution cools down, the smart catalyst redissolves and thus becomes active again.<sup>5,23</sup> Other smart catalyst systems are being developed that dissociate at high temperatures (less active) and recombine at low temperatures (more active).<sup>5,27</sup>

### 14 SHAPE MEMORY ALLOYS

The shape memory effect in metals is a very interesting phenomenon. Imagine taking a piece of metal and deforming it completely and then restoring it to its original shape with the application of heat. Taking a shape memory alloy spring and hanging a weight on one end of the spring can easily illustrate this. After the spring has been stretched, heat the spring with a hot-air gun and watch it return to its original length with the weight still attached.

These materials undergo a thermomechanical change as they pass from one phase to another. The crystalline structure of such materials, such as nickel–titanium alloys, enters into the martensitic phase as the alloy is cooled below a critical temperature. In this stage the material is easily manipulated through large strains with a little change in stress. As the temperature of the material is increased above the critical temperature, it transforms into the austenitic phase. In this phase the material regains its high strength and high modulus and behaves normally. The material shrinks during the change from the martensitic to the austenitic phase.<sup>5,19,20</sup>

Nickel–titanium alloys have been the most used shape memory material. This family of nickel–titanium alloys is known as Nitinol, after the laboratory where this material was first observed (Nickel Titanium Naval Ordinance Laboratory). Nitinol has been used in military, medical, safety, and robotics applications. Specific applications include hydraulic lines on F-14 fighter planes, medical tweezers and sutures, anchors for attaching tendons to bones, stents for cardiac arteries, eyeglass frames, and antiscalding valves in water faucets and showers.<sup>5,41,42</sup>

In addition to the family of nickel–titanium alloys there are other alloys that exhibit the shape memory effect. These alloys are silver–cadmium, gold–cadmium, copper–aluminum–nickel, copper–tin, copper–zinc, combinations of copper–zinc with silicon or tin or aluminum, indium–thallium, nickel–aluminum, iron–platinum, manganese–copper, and iron–manganese–silicon.<sup>43</sup> Not all combinations of the two or three elements yield an alloy with the shape memory effect; thus it is recommended to review the original literature.

Several articles from Mitsubishi Heavy Industries describe the room temperature functional shape memory polyurethanes. To this writer, these papers only attest to the behavior of a polymer at its glass transition temperature. Thus, if you wish to describe a polymer's behavior at its glass transition temperature and since the free-volume change is reversible, you may call it a smart polymer, a shape memory material, or a thermoresponsive material. The unique characteristic of these polyurethanes is that their transition occurs in the vicinity of room temperature.<sup>44,45</sup>

## 15 UNUSUAL BEHAVIORS OF MATERIALS

As one researches the field of smart materials and structures, one realizes that there are many smart materials and there are many material behaviors that are reversible. The ability to develop useful products from smart materials is left up to one's imagination. For example, water is a very unique material. It expands upon freezing. As we know, the force generated by this expansion causes sidewalks and highways to crack. Now, what if you surround water pipes with a heating system that consists of a heater and water enclosed in a piezoelectric polymer or elastomer container that is in a fixed space. As the temperature drops to the freezing point of water, it expands and generates a force against the piezoelectric container, which in turn generates electricity, thus powering the heater and keeping the pipes from freezing.

As previously mentioned, sometimes it is difficult to classify the material and its behavior. One such case involves a University of Illinois patent. The title of the patent is "Magnetic Gels Which Change Volume in Response to Voltage Changes for Magnetic Resonance Imaging."<sup>46</sup> The patent teaches the use of a matrix that has a magnetic and preferably superparamagnetic component and the capability of changing its volume in an electric field.

Fullerenes are spherically caged molecules with carbon atoms at the corner of a polyhedral structure consisting of pentagons and hexagons. The most stable of the fullerenes is a C<sub>60</sub> structure known as a buckyball or buckminsterfullerene. The fullerenes have been under commercial development for the past decade. One application of the fullerenes as a smart material consists of embedding the fullerenes into sol–gel matrices for the purpose of enhancing optical limiting properties.<sup>47</sup>



A semiconducting material with a magnetic ordering at 16.1 K was produced from the reaction of buckyball with tetra(dimethylamino)ethylene. This organic-based magnet did not have the coercive or saturation magnetization to function totally as a ferromagnet. The replacement of buckyball with higher carbon number fullerenes in the reaction with tetra(diamethylamino)ethylene did not produce any complexes that showed magnetic ordering.<sup>22</sup>

## 16 COMMENTS, CONCERNS, AND CONCLUSIONS

In dealing with smart materials and structures there is still much confusion over the name of these materials and what makes a material or structure smart. Numerous products with “smart” in the name do not meet the definition of being smart, that is, responding to the environment in a reversible manner. The scientist/engineer should not fault advertising professionals for using the term smart in a product description. But I must admit I chuckle whenever I see the magazine *Smart Money*. Does this mean that I can spend money and it will return to me because it is reversible?

Confusion also exists within the smart materials community with the term smart polymers. Applications of a smart polymer center on the polymer’s glass transition temperature. As design engineers become more familiar with that term and its significance to a design, in some applications the term will be eliminated and replaced with terms like “working smartly with a polymer.”

We have not addressed the versatility of these smart materials. One such example may involve the smart shock absorbers. Two literature sources discuss current research on vibration suppression in automobiles using smart shock absorbers.<sup>3,17</sup> These smart shock absorbers were developed by Toyota and consist of multilayer piezoelectric ceramics. These multilayer stacks are positioned near each wheel. After analyzing the vibration signals, a voltage is fed back to the actuator stack, which responds by pushing on the hydraulic system to enlarge the motion. Signal processors analyze the acceleration signals from road bumps and respond with a motion that cancels the vibration.<sup>3,17</sup> Such active piezoelectric systems are used to minimize excess vibrations in helicopter blades and in the twin tail of F-18 fighter jets. An Internet source<sup>48</sup> has discussed work at the University of Rochester with smart shock absorbers using electrorheological fluids. The electrorheological fluids sense the force of a bump and immediately send an electric signal to precisely dampen the force of the bump, thus providing a smoother ride. In an engine mount, electrorheological fluids damp out the vibrations of the engine, thus reducing wear and tear on the vehicle. Another application of electrorheological fluids is in clutches to reduce the wear between the plates as a driver shifts gears. This can reduce the maintenance costs of high-duty trucks.<sup>47</sup> Or one can dampen the vibrations of the road, engine mounts, and other sources on an automobile or heavy-duty truck with magnetorheological fluids. The Lord Corporation has developed a series of trademarked fluids and systems known as Rheonetic Fluids that are commercially available for vibration control as well as for noise suppression.<sup>49</sup>

## 17 FUTURE CONSIDERATIONS

The future of smart materials and structures is wide open. The use of smart materials in a product and the type of smart structures that one can design are only limited by one’s talents, capabilities, and ability to “think outside the box.”

In an early work<sup>5</sup> and as part of short courses there were discussions pertaining to future considerations. A lot of the brainstorming that resulted from these efforts is now being explored. Some ideas that were in the conceptual stage are now moving forward. Look at the advances in information and comforts provided through smart materials and structures in automobiles.

Automobiles can be taken to a garage for service and be hooked up to a diagnostic computer that tells the mechanic what is wrong with the car. Or a light on the dashboard signals “maintenance required.” Would it not be better for the light to inform us as to the exact nature of the problem and the severity of it? This approach mimics a cartoon that appeared several years ago of an air mechanic near a plane in a hanger. The plane says “Ouch” and the mechanic says “Where do you hurt?”

One application of smart materials is the work mentioned earlier of a piezoelectric inkjet printer that serves as a chemical delivery to print organic light-emitting polymers in a fine detail on various media. Why not take the same application to synthesize smaller molecules? With the right set one could synthesize smaller molecules in significant amounts for characterization and evaluation and in such a way that we could design experiments with relative ease.

A new class of smart materials has appeared in the literature. This is the group of smart adhesives. We previously mentioned that PVDF film strips have been placed within an adhesive joint to monitor performance. Khongtong and Ferguson developed a smart adhesive at Lehigh University.<sup>50</sup> They suggested that this new adhesive could form an antifouling coating for boat hulls or for controlling cell adhesion in surgery. The stickiness of the new adhesive can be switched on and off with changes in temperature. The smart adhesive also becomes water repellent when its tackiness wanes.<sup>50</sup> The term “smart adhesive” is appearing more frequently in the literature.

A topic of research that was in the literature a few years ago was “smart clothes” or “wearable computers” being studied at MIT. The potential of this concept is enormous. This sounds wonderful as long as we learn how to work smarter, not longer.

## REFERENCES

1. I. Amato, *Sci. News*, **137**(10), 152–155, March 10, 1990.
2. O. Port, *Business Week*, No. 3224, 48–55, March 10, 1990.
3. Committee on New Sensor Technologies, Materials and Applications, National Materials Advisory Board, Commission on Engineering and Technical Systems, National Research Council Report, *Expanding the Vision of Sensor Materials*, National Academy Press, Washington, DC, 1995, pp. 33–45.
4. C. A. Rogers, *Sci. Am.*, **273**(3), 122–126, September 1995.
5. J. A. Harvey, *Kirk-Othmer Encyclopedia of Chemical Technology*, 4th ed., Supplement, Wiley, New York, 1998, pp. 502–504.
6. I. Chopra, in *Proceedings of the Smart Structures and Materials 1996—Smart Structures and Integrated Systems Conference for the Society of Photo-Optical Instrumentation Engineers*, Vol. 2717, San Diego, Feb. 26–29, 1996, pp. 20–26.
7. T. Thomas, Portland, OR, private communication, 1999.
8. Technical bulletins and notes, Sensor Technology Limited, Collingwood, Canada.
9. T. T. Wang, J. M. Herbert, and A. M. Glass (Eds.), *Applications of Ferroelectric Polymers*, Blackie and Sons, Glasgow, 1988.
10. J. O. Simpson, available: <http://hsti.larc.nasa.gov/randt/I995/Section131.fm513.html>.
11. Piezo Systems, *Technical Bulletin*, Cambridge, MA, 1993.
12. T. W. DeYoung and V. B. Maltsev, U.S. Patent 4,439,780, 1984.
13. S. D. Howkins, U.S. Patent 4,459,601, 1984.
14. T. R. Hebner, C. C. Wu, D. Marcy, M. H. Lu, and J. C. Sturm, *Appl. Phys. Lett.*, **72**(5), 519–521, 1998.
15. G. L. Anderson, J. Mommaerts, S. L. Tana, J. C. Duke, Jr., and D. A. Dillard, *J. Intell. Mater. Syst. Struct.*, **4**, 425–428, 1993.
16. G. L. Anderson, D. A. Dillard, and J. P. Wightman, *J. Adhesion*, **36**, 213, 1992.
17. R. E. Newnham and A. Amin, *CHEMTECH*, **29**(12), 38–46, December 1999.



18. *Proceedings for a Symposium Entitled Electroactive Polymers (EAP)*, Vol. 600, Boston, November 29– December 1, 1999, Materials Research Society, Warrendale, PA, 2000.
19. R. E. Newnham, *Mater. Res. Soc. Bull.*, **22**(5), 20–34, May 1997.
20. B. Culshaw, *Smart Structures and Materials*, Artech House, Boston, 1996, pp. 43–45, 117–130.
21. K. Derbyshire and E. Korczynski, *Solid State Technol.*, 57–66, September 1995.
22. J. S. Miller and A. J. Epstein, *Chem. Eng. News*, 30–41, October 2, 1995.
23. R. Dagani, *Chem. Eng. News*, 30–33, September 18, 1995.
24. R. H. Gerzeski, *J. Adv. Mater.*, **33**(2), 63–69, April 2001.
25. B. Z. Tang, *CHEMTECH*, **29**(1), 7–12, November 1999.
26. D. E. Bergreiter, B. C. Ponder, G. Aguilar, and B. Srinivas, *Chem. Mater.*, **9**(2), 472–477, 1997.
27. R. Baum, *Chem. Eng. News*, **7**, January 30, 1996.
28. Y. G. Takei, T. Aoki, K. Sanui, N. Ogata, Y. Sakurai, and T. Okano, *Macromolecules*, **27**, 6163–6166, 1994.
29. J. Jhan, R. Pelton, and Y. L. Den, *Langmuir*, **11**, 2301–2302, 1995.
30. J. L. Thomas, H. You, and D. A. Tirrell, *J. Am. Chem. Soc.*, **117**, 2949–2950, 1995.
31. D. H. Carey and G. S. Ferguson, *J. Am. Chem. Soc.*, **118**, 9780–9781, 1996.
32. I. Y. Galaev, *Russ. Chem. Rev.*, **65**(5), 471–489, 1995.
33. M. S. Khan, in *Proceedings of the Metal/Nonmetal Microsystems: Physics, Technology, and Applications Workshop*, Vol. 2780, Polanica Zdroj, Poland, September 11–14, 1996, Society of Photo-Optical Instrumentation Engineers, 1996, pp. 56–59, SPIE, Bellingham, WA.
34. A. Vannikov and A. Kararasev, in *Proceedings of Smart Structures and Materials 1996—Smart Electronics and MEMS Conference*, Vol. 2722, San Diego, February 28–29, 1996, Society of Photo-Optical Instrumentation Engineers, 1996, pp. 252–255, SPIE, Bellingham, WA.
35. R. Dagani, *Chem. Eng. News*, 26–37, June 9, 1997.
36. R. S. Harland and R. K. Prud'homme, *Polyelectrolyte Gels, Properties and Applications*, American Chemical Society, Washington, DC, 1992.
37. D. DeRossi, K. Kajiwaru, Y. Osada, and A. Yamauchi, *Polymer Gels Fundamental and Biomedical Applications*, Plenum, New York, 1991.
38. T. Okano (Ed.), *Biorelated Polymers and Gels—Controlled Release and Applications in Biomedical Engineering*, Academic, Boston, 1998.
39. A. Dupommie, L. Merle-Aubry, Y. Merle, and E. Slany, *Makromolek. Chem.*, **187**, 211, 1986.
40. R. Yoshida, T. Takahashi, T. Yamaguchi, and H. Ichijo, *Adv. Mater.*, **9**, 175, 1997.
41. G. Kauffman and I. Mayo, *Chem. Matters*, 4–7, October 1993.
42. D. Stoeckel and W. Yu, *Superelastic Nickel-Titanium Wire*, Technical Bulletin, Raychem, Menlo Park, CA.
43. K. Shimizu and T. Tadaki, in H. Funakubo (Ed.), *Shape Memory Alloys*, Gordon and Breach, New York, 1987.
44. S. Hayashi, in *Proceedings of the US-Japan Workshop on Smart Materials and Structures*, Minerals, Metals and Materials Society, 1997, pp. 29–38, www.tms.org.
45. S. Hayashi, S. Kondo, P. Kapadia, and E. Ushioda, *Plastics Eng.*, February 29–31, 1995.
46. P. C. Lauterbur and S. Frank, U.S. Patent 5,532,006, July 2, 1996.
47. R. Signorini, M. Zerbetto, M. Meneghetti, R. Bozio, G. Brusatin, E. Menegazzo, M. Guglielmi, M. Maggini, G. Scorrano, and A. Prato, in *Proceedings of the Fullerenes and Photoiniccs III Conference*, Vol. 2854, Society of Photo-Optical Instrumental Engineers, 1996, pp. 130–139, SPIE, Bellingham, WA.
48. T. Jones, available: <http://www.rochester.edu/pr/releases/ce/jones.htm>.
49. Technical bulletins, Lord Corporation, Cary, NC.
50. S. Khongtong and G. Ferguson, *J. Am. Chem. Soc.*, **124**, 7254–7255, 2004.

# CHAPTER 12

## OVERVIEW OF CERAMIC MATERIALS, DESIGN, AND APPLICATION

**R. Nathan Katz**

Department of Mechanical Engineering  
Worcester Polytechnic Institute  
Worcester, Massachusetts

<b>1 INTRODUCTION</b>	<b>453</b>	4.4 Passive Electronics	466
<b>2 PROCESSING OF ADVANCED CERAMICS</b>	<b>454</b>	4.5 Piezoceramics	467
<b>3 BRITTLINESS AND BRITTLE MATERIALS DESIGN</b>	<b>455</b>	4.6 Transparencies	468
<b>4 APPLICATIONS</b>	<b>459</b>	<b>5 INFORMATION SOURCES</b>	<b>469</b>
4.1 Ceramics in Wear Applications	459	5.1 Manufacturers and Suppliers	469
4.2 Thermostructural Applications	464	5.2 Data	469
4.3 Corrosion Resistance	465	5.3 Standards, Test Methods, and Handbooks	469
		<b>6 FUTURE TRENDS</b>	<b>471</b>
		<b>REFERENCES</b>	<b>472</b>

### 1 INTRODUCTION

Engineering ceramics possess unique combinations of physical, chemical, electrical, optical, and mechanical properties. Utilizing the gains in basic materials science understanding and advances in processing technology accrued over the past half century, it is now frequently possible to custom tailor the chemistry, phase content, and microstructure to optimize application-specific combinations of properties in ceramics (which include glasses, single crystals, and coatings technologies, in addition to bulk polycrystalline materials). This capability in turn has led to many important, new applications of these materials. Indeed, in many of these applications the new ceramics and glasses are the key enabling technology.

Ceramics include materials that have the highest melting points, highest elastic moduli, highest hardness, highest particulate erosion resistance, highest thermal conductivity, highest optical transparency, lowest thermal expansion, and lowest chemical reactivity known. Counterbalancing these beneficial factors are brittle behavior and vulnerability to thermal shock and impact. Major progress has been made in learning how to design to mitigate the brittleness and other undesirable behaviors associated with ceramics and glasses. Consequently, many exciting new applications for these materials have emerged over the past several decades. Among the major commercial applications for these materials are:

- Passive electronics (capacitors and substrates)
- Optonics/photronics [optical fibers and light-emitting diodes (LEDs)]

---

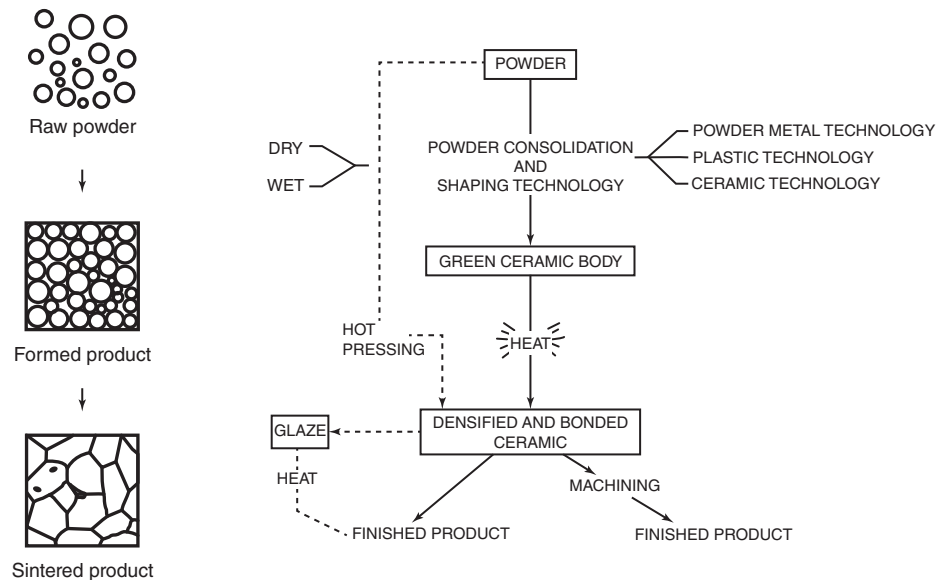
Revised for this edition.

- Piezoceramics (transducers)
- Mechanical (bearings, cutting tools)
- Biomaterials (hard-tissue replacement)
- Refractories (furnace linings, space vehicle thermal protection)
- Electrochemical (sensors, fuel cells)
- Transparencies (visible, radar)

This chapter will provide a brief overview of how ceramics are processed and the ramifications of processing on properties. Next a short discussion of the special issues that one encounters in mechanical design with brittle materials is provided. Short reviews of several of the above engineering applications of ceramics and glasses, which discuss some of the specific combinations of properties that have led design engineers to the selected material(s), follow. A section on how to obtain information on materials sources is provided. Tables listing typical properties of candidate materials for each set of applications are included throughout. Finally, some areas of future potential will be discussed.

## 2 PROCESSING OF ADVANCED CERAMICS

The production of utilitarian ceramic artifacts via the particulate processing route outlined in Fig. 1 actually commenced about 10,000 years ago.<sup>1</sup> Similarly, glass melting technology goes back about 4000 years, and as early as 2000 years ago optical glass was being produced.<sup>1</sup> While many of the basic unit processes for making glasses and ceramics are still recognizable across the millennia, the level of sophistication in equipment, process control, and raw material control has advanced by “light years.” In addition, the past 50 years has created a



**Figure 1** Processing of polycrystalline ceramics via the particulate route.

fundamental understanding of the materials science principles that underlie the processing–microstructure–property relationships. Additionally, new materials have been synthesized that possess extraordinary levels of performance for specific applications. These advances have led to the use of advanced ceramics and glasses in roles that were unimaginable 50 or 60 years ago. For example, early Egyptian glass ca. 2000 B.C. had an optical loss of  $\sim 10^7$  dB/km, compared to an optical loss of  $\sim 10^{-1}$  in mid-1980s glass optical fibers,<sup>2</sup> a level of performance that has facilitated the fiber-optic revolution in telecommunications. Similarly, the invention of barium titanate and lead zirconate titanate ceramics, which have much higher piezoelectric moduli and coupling coefficients than do naturally occurring materials, has enabled the existence of modern sonar and medical ultrasound imaging.<sup>3</sup>

The processing of modern ceramics via the particulate route, illustrated in Fig. 1, is the way that  $\sim 99\%$  of all polycrystalline ceramics are manufactured. Other techniques for producing polycrystalline ceramics, such as chemical vapor deposition<sup>4</sup> or reaction forming,<sup>5</sup> are of growing importance but still represent a very small fraction of the ceramic industry.

There are three basic sets of unit processes in the particulate route (and each of these three sets of processes may incorporate dozens of subprocesses). The first set of processes involves powder synthesis and treatment. The second set of processes involves the consolidation of the treated powders into a shaped preform, known as a “green” body. The green body typically contains about 50 vol. % porosity and is extremely weak. The last set of unit processes utilizes heat, or heat and pressure combined, or more recently heat plus microwave radiation<sup>6</sup> to bond the individual powder particles, remove the free space and porosity in the compact via diffusion, and create a fully dense, well-bonded ceramic with the desired microstructure (see Ref. 4, Chapters 9–11). If only heat is used, this process is called sintering. If pressure is also applied, the process is then referred to as hot pressing (unidirectional pressure) or hot isostatic pressing [(HIP), which applies uniform omnidirectional pressure].

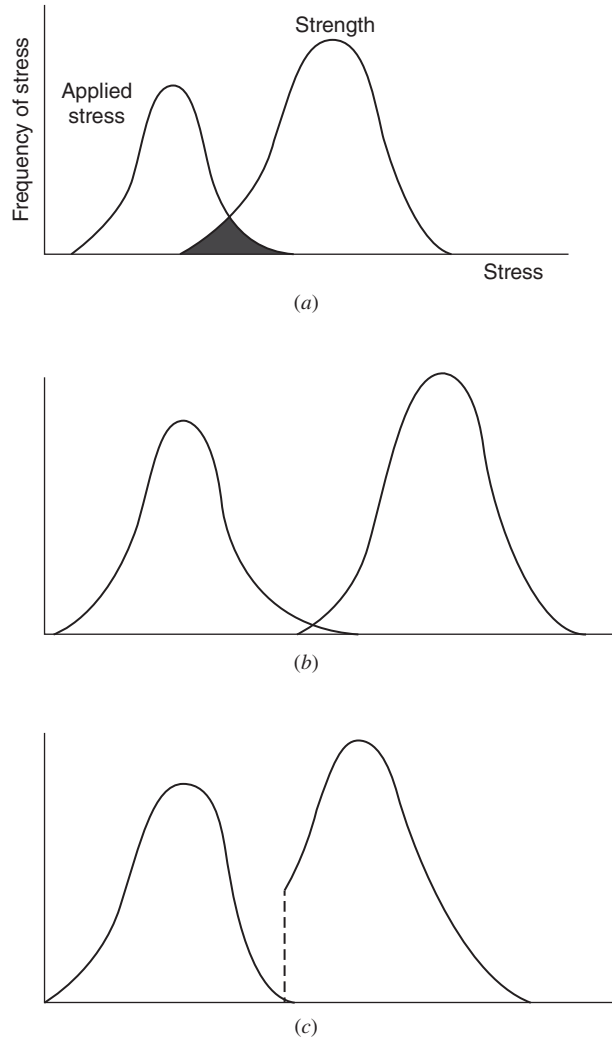
Each of the above steps can introduce processing flaws that can diminish the intrinsic properties of the material. For example, chemical impurities introduced during the powder synthesis and treatment steps may adversely affect the optical, magnetic, dielectric, or thermal properties of the material. Alternatively, the impurities may segregate in the grain boundary of the sintered ceramic and negatively affect its melting point, high-temperature strength, dielectric properties, or optical properties. During green-body formation, platey or high-aspect-ratio powders may align with a preferred orientation, leading to anisotropic properties. Similarly, hot pressing may impose anisotropic properties on a material. Since ceramics are not ductile materials, they can (usually) not be thermomechanically modified after primary fabrication.

Thus, the specific path by which a ceramic component is fabricated can profoundly affect its properties. The properties encountered in a complex shaped ceramic part are often quite different than those encountered in a simply shaped billet of material. This is an important point of which a design engineer specifying a ceramic component needs to be constantly mindful.

### 3 BRITTLENESS AND BRITTLE MATERIALS DESIGN

Even when ceramics are selected for other than mechanical applications, in most cases some levels of strength and structural integrity are required. It is therefore necessary to briefly discuss the issue of brittleness and how one designs with brittle materials before proceeding to discuss applications and the various ceramic and glass materials families and their properties. The main issues in designing with a brittle material are that a very large scatter in strength (under tensile stress), a lack of capacity for mitigating stress concentrations via plastic flow, and relatively low energy absorption prior to failure dominate the mechanical behavior. Each of these issues is a result of the presence of one or more flaw distribution within or at the surface of the

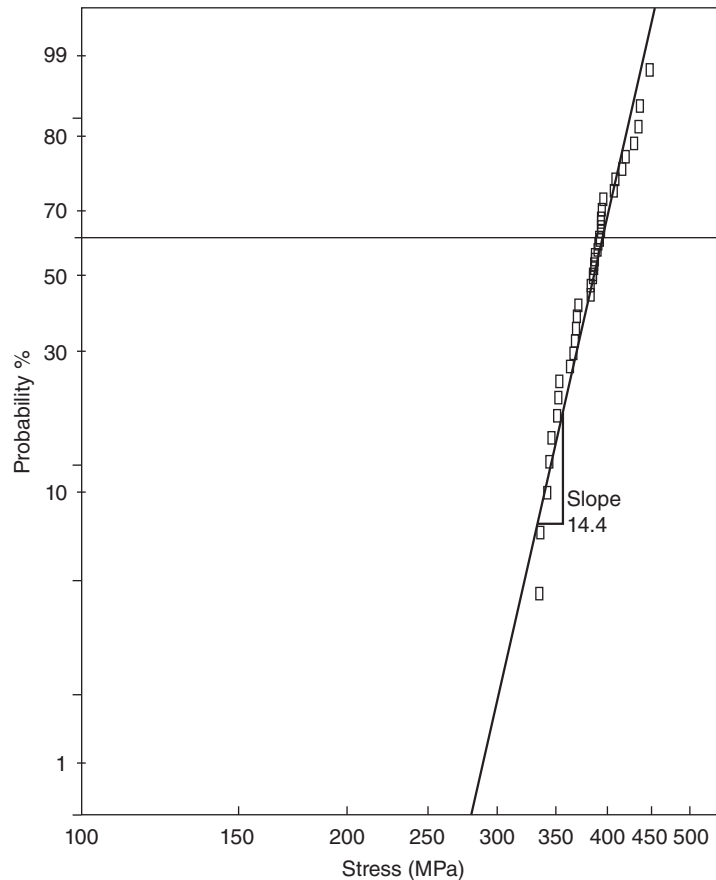
ceramic article and/or the general lack of plastic flow available in ceramics. As a consequence, ceramic and glass components that are subjected to tensile stresses are not designed using a single-valued strength (*deterministic design*) as commonly done with metals. Rather, ceramic components are designed to a specified probability of failure (*probabilistic design*) that is set at acceptably low values. A simplistic way to conceptualize the probabilistic design process is to consider the two distribution curves shown in Figs. 2a through 2c.<sup>7</sup> In each figure the strength distribution of the material is represented by the curve on the right, and the distribution of applied stress (derived from the spectrum of applied loads from all sources) is represented on the left. The overlap of the upper region of the applied stress distribution and the lower region of the strength distribution will define a probability of failure as illustrated by the shaded area in Fig. 2a. Clearly, one wants to minimize or to totally eliminate this region of overlap. The



**Figure 2** Probability of failure of a ceramic component and strategies to reduce it.

ceramic engineer, working on materials and process improvements, will strive to move the strength curve to the right and narrow it. Simultaneously, the design engineer will aim to shift the applied stress distribution to the left by optimizing component geometry and, if possible, reducing applied loads. The goal is to minimize the area of overlap as illustrated in Fig. 2*b*. Finally, the manufacturing or quality control engineer may be able to introduce an overstress “proof test” which will screen out defective components, as illustrated by the truncation of the strength curve in Fig. 2*c*. Such proof testing is frequently utilized with ceramic components. In some cases it can be easily incorporated into the manufacturing process at negligible cost. In other cases proof testing may introduce a major cost. When proof testing is utilized care must be taken to assure that it does not introduce new flaws into the ceramic components.

In practice, engineers executing a probabilistic design do not rely on the simple distribution curves used for illustrative purposes in Fig. 2. Rather the statistics of failure of brittle materials whose strength is determined by a population of varying sized flaws is similar to modeling the statistics of a chain failing at its weakest link. These statistics are known as Weibull statistics (see Ref. 4, Chapter 15).<sup>8</sup> Figure 3 shows a typical Weibull probability-of-failure distribution plot.<sup>9</sup> These plots are characterized by two parameters—the characteristic strength  $\sigma_c$  and the



**Figure 3** Typical Weibull distribution plot for an aluminum oxide material. (After Ref. 9.)

slope  $m$ , referred to as the Weibull modulus. The characteristic strength is not the mean strength, but rather, it is the strength at a probability of failure of 63.2% (where the horizontal line in Fig. 3 is drawn). The use of 63.2% is for reasons having to do with the mathematics of the Weibull distribution. In Fig. 3, the characteristic strength  $\sigma_c$  is 395 MPa and the Weibull modulus  $m$  is 14.4.

Computer programs for incorporating Weibull statistical distributions into finite-element design codes have been developed that facilitate the design of ceramic components optimized for low probabilities of failure.<sup>10</sup> The effectiveness of such a probabilistic design methodology has been demonstrated by the reliable performance of ceramics in many highly stressed structural applications, such as bearings, cutting tools, turbocharger rotors, missile guidance domes, and hip prosthesis. Flaws (strength-limiting features) can be intrinsic or extrinsic to the material and processing route by which a test specimen or a component is made. Intrinsic strength-limiting flaws are generally a consequence of the processing route and may include features such as pores, aggregations of pores, large grains, agglomerates, and shrinkage cracks. While best processing practices will eliminate or reduce the size and frequency of many of these flaws, it is inevitable that some will still persist. Extrinsic flaws can arise from unintended foreign material entering the process stream, i.e., small pieces of debris from the grinding media or damage (cracks) introduced in machining a part to final dimensions. Exposure to a service environment may bring new flaw populations into existence, i.e., oxidation pits on the surface of non-oxide ceramics exposed to high temperatures or may cause existing flaws to grow larger as in the case of static fatigue of glass. In general, one can have several flaw populations present in a component at any time, and the characteristics of each population may change with time. As a consequence of these constantly changing flaw populations, at the present time the state of the art in life prediction of ceramic components for use in extreme environments significantly lags the state of the art in component design. As in most fields of engineering, there are some rules of thumb that one can apply to ceramic design.<sup>11</sup> While these are not substitutes for a carefully executed probabilistic finite-element design analysis, they are very useful in spotting pitfalls and problems when a full-fledged design cannot be executed due to financial or time constraints.

### Rules of Thumb for Design with Brittle Materials

1. Point loads should be avoided to minimize stress where loads are transferred. It is best to use areal loading (spherical surfaces are particularly good); line loading is next best.
2. Structural compliance should be maintained by using compliant layers or springs or radiusing of mating parts (to avoid lockup).
3. Stress concentrators—sharp corners, rapid changes in section size, undercuts, and holes—should be avoided or minimized. Generous radiuses and chamfers should be used.
4. The impact of thermal stresses should be minimized by using the smallest section size consistent with other design constraints. The higher the symmetry, the better (a cylinder will resist thermal shock better than a prism), and breaking up complex components into subcomponents with higher symmetry may help.
5. Components should be kept as small as possible—the strength and probability of failure at a given stress level are dependent on size; thus minimizing component size increases reliability.
6. The severity of impact should be minimized. Where impact (i.e., particulate erosion) cannot be avoided, low-angle impacts ( $20^\circ$ – $30^\circ$ ) should be designed for. Note this is very different than the case of metals, where minimum erosion is at  $90^\circ$ .
7. Avoid surface and subsurface damage. Grinding should be done so that any residual grinding marks are parallel, not perpendicular, to the direction of principal tensile stress during use. Machining-induced flaws are often identified to be the strength-limiting defect.

## 4 APPLICATIONS

The combinations of properties available in many advanced ceramics and glasses provide the designers of mechanical, electronic, optical, and magnetic systems a variety of options for significantly increasing systems performance. Indeed, in some cases the increase in systems performance is so great that the use of ceramic materials is considered an enabling technology. In the applications examples provided below the key properties and combinations of properties required will be discussed, as well as the resultant systems benefits.

### 4.1 Ceramics in Wear Applications

In the largest number of applications where modern ceramics are used in highly stressed mechanical applications, they perform a wear resistance function. This is true of silicon nitride used as balls in rolling element bearings, silicon carbide journal bearings or water pump seals, alumina washers in faucets and beverage dispensing equipment, silicon nitride and alumina-based metal-cutting tools, zirconia fuel injector components, or boron carbide sand blast nozzles, to cite some typical applications and materials.

Wear is a systems property rather than a simple materials property. As a systems property, wear depends upon what material is rubbing, sliding, or rolling over what material, upon whether the system is lubricated or not, upon what the lubricant is, and so forth. To the extent that the wear performance of a material can be predicted, the wear resistance is usually found to be a complex function of several parameters. Wear of ceramic materials is often modeled using an abrasive wear model where the material removed per length of contact with the abrasive is calculated. A wide variety of such models exist, most of which are of the form<sup>12</sup>

$$V \propto P^{0.8} K_{Ic}^{-0.75} H^{-0.5N} \quad (1)$$

where  $V$  is the volume of material worn away,  $P$  is the applied load,  $K_{Ic}$  is the fracture toughness,  $H$  is the indentation hardness, and  $N$  is the number of abrasive particles contacting the wear surface per unit length. Even if there are no external abrasive particles present, the wear debris of the ceramics themselves acts as abrasive particles. The functional relationships that predict that wear resistance should increase as fracture toughness and hardness increase are, in fact, frequently observed in practice.

Even though the point contacts that occur in abrasive wear produce primarily hertzian compressive stresses, in regions away from the hertzian stress field tensile stresses will be present and strength is, thus, a secondary design property. In cases where inertial loading or weight is a design consideration, density may also be a design consideration. Accordingly, Table 1 lists typical values of the fracture toughness, hardness, Young's modulus, four-point modulus of rupture (MOR) in tension, and the density for a variety of advanced ceramic wear materials. Several successful applications of ceramics to challenging wear applications are described below.

**Table 1** Key Properties for Wear-Resistant Ceramics

Material	$K_{Ic}$ (MPa · m <sup>1/2</sup> )	$H$ (kg/mm <sup>2</sup> )	$E$ (GPa)	MOR (MPa)	$\rho$ (g/cm)
Al <sub>2</sub> O <sub>3</sub> 99%	3.5–4.5	1900	360–395	350–560	3.9
B <sub>4</sub> C	2.5	3000	445	300–480	2.5
Diamond	6–10	8000	800–925	800–1400	3.5
SiC	2.6–4.6	2800	380–445	390–550	3.2
Si <sub>3</sub> N <sub>4</sub>	4.2–7	1600	260–320	450–1200	3.3
TiB <sub>2</sub>	5–6.5	2600	550	240–400	4.6
ZrO <sub>2</sub> (Y-TZP)	7–12	1000	200–210	800–1400	5.9



### Bearings

Rolling element bearings, for use at very high speeds or in extreme environments, are limited in performance by the density, compressive strength, corrosion resistance, and wear resistance of traditional high-performance bearing steels. The key screening test to assess a material's potential as a bearing element is rolling contact fatigue (RCF). RCF tests on a variety of alumina, SiC,  $\text{Si}_3\text{N}_4$ , and zirconia materials at loads representative of high-performance bearings demonstrated that only fully dense silicon nitride ( $\text{Si}_3\text{N}_4$ ) could outperform bearing steels.<sup>13</sup> This behavior has been linked to the high fracture toughness of silicon nitride, which results from a unique “self-reinforced” microstructure combined with a high hardness. Additionally, the low density of silicon nitride creates a reduced centrifugal stress on the outer races at high speeds. Fully dense  $\text{Si}_3\text{N}_4$  bearing materials have demonstrated RCF lives 10 times that of high-performance bearing steel. This improved RCF behavior translates into DN (bearing bore diameter in millimeters X shaft rpm) ratings for hybrid ceramic bearings ( $\text{Si}_3\text{N}_4$  balls running in steel races, the most common ceramic bearing configuration) about 50% higher than the DN rating of steel bearings. Other benefits of silicon nitride hybrid bearings include an order-of-magnitude less wear of the inner race, excellent performance under marginal lubrication, survival under lubrication starvation conditions, lower heat generation than comparable steel bearings, and reduced noise and vibration.

Another important plus for  $\text{Si}_3\text{N}_4$  is its failure mechanism. When  $\text{Si}_3\text{N}_4$  rolling elements fail, they do not fail catastrophically; instead they spall—just like bearing steel elements (though by a different microstructural mechanism). Thus, the design community only had to adapt their existing practices, instead of developing entirely new practices to accommodate new failure modes. The main commercial applications of silicon nitride bearing elements are listed in Table 2.

An important new ceramic bearing application has recently been developed. In this case sliding, rather than rolling, elements are utilized, and the material is silicon carbide as opposed to silicon nitride. The new bearings are stacked thrust bearings for the horizontal drilling of oil and gas wells. The bearings are situated between the drilling bit and the motor right at the front of the drilling process. The bearings are subject to mechanical shock, high loads, and abrasion from the drilling mud, which is the lubricant. These hydrodynamically lubricated bearings utilize spring-loaded silicon carbide pads sliding against a continuous opposing ring. During field trials where actual oil or gas boreholes were drilled, the superior wear resistance of the SiC pads significantly reduced the need to pull the motor and drill bit assembly due to bearing wear. In one reported case both the curved and horizontal portions of the borehole were drilled with the same thrust bearing assembly. Significantly, this saved three days of rig time.<sup>14</sup>

**Table 2** Commercial Applications of  $\text{Si}_3\text{N}_4$  Hybrid Bearings

Machine tool spindles	The first and largest application, its main benefits are higher speed and stiffness, hence greater throughput and tighter tolerances
Turbomolecular pump shaft	Presently the industry standard, the main benefits are improved pump reliability and marginal lubrication capability, which provide increased flexibility in pump mounting orientation
Dental drill shaft	The main benefit is sterilization by autoclaving
Aircraft wing flap actuators	Wear and corrosion resistance are the main benefits
In-line skates/mountain bikes	Wear and corrosion resistance are the main benefits
Space Shuttle main engine oxygen fuel pump	Here, the bearing is lubricated by liquid oxygen. Steel bearings are rated for one flight; $\text{Si}_3\text{N}_4$ hybrid bearings are rated for five.

### *Cutting Tool Inserts*

While ceramic cutting tools have been in use for over 70 years, it is only within the past three decades that they have found major application, principally in turning and milling cast iron and nickel-based superalloys and finishing of hardened steels. In these areas ceramics based on aluminum oxide and silicon nitride significantly outperform cemented carbides and coated carbides. High-speed cutting tool tips can encounter temperatures of 1000°C or higher. Thus, a key property for an efficient cutting tool is hot hardness. Both the alumina and  $\text{Si}_3\text{N}_4$  families of materials retain a higher hardness at temperatures between 600 and 1000°C than either tool steels or cobalt-bonded WC cermets. The ceramics are also more chemically inert.

The combination of hot hardness and chemical inertness means that the ceramics can run hotter and longer with less wear than the competing materials. Historic concerns with ceramic cutting tools have focused on low toughness, susceptibility to thermal shock, and unpredictable failure times. Improvements in processing together with microstructural modifications to increase fracture toughness have greatly increased the reliability of the ceramics in recent years. Alumina-based inserts are reinforced (toughened) with zirconia, TiC, or TiN particles or SiC whiskers. The thermal shock resistance of alumina-SiC<sub>w</sub> is sufficiently high, so that cooling fluids can be used when cutting Ni-based alloys. Silicon-nitride-based inserts include fully dense  $\text{Si}_3\text{N}_4$  and SiAlONs, which are solid solutions of alumina in  $\text{Si}_3\text{N}_4$ . Fully dense  $\text{Si}_3\text{N}_4$  can have a fracture toughness of 6–7 MPa·m<sup>1/2</sup>, almost as high as cemented carbides (9 MPa·m<sup>1/2</sup>), a high strength (greater than 1000 MPa), and a low thermal expansion that yields excellent thermal shock behavior. Silicon nitride is the most efficient insert for the turning of gray cast iron and is also used for milling and other interrupted cut operations on gray iron. Because of its thermal shock resistance, coolant may be used with silicon nitride for turning applications. SiAlONs are typically more chemically stable than the  $\text{Si}_3\text{N}_4$  but not quite as tough or thermal shock resistant. They are mainly used in rough turning of Ni-based superalloys.

Ceramic inserts are generally more costly than carbides (1.5–2 times more), but their metal removal rates are 3–4 times greater. However, that is not the entire story. Ceramic inserts also demonstrate reduced wear rates. The combination of lower wear and faster metal removal means many more parts can be produced before tools have to be indexed or replaced. In some cases this enhanced productivity is truly astonishing. In the interrupted single-point turning of the outer diameter counterweights on a gray cast iron crankshaft a SiAlON tool was substituted for a coated carbide tool. This change resulted in the metal removal rate increasing 150% and the tool life increasing by a factor of 10. Each tool now produced 10 times as many parts and in much less time. A gas turbine manufacturer performing a machining operation on a Ni-based alloy using a SiAlON tool for roughing and a tungsten carbide tool for finishing required a total of 5 h. Changing to SiC-whisker-reinforced alumina inserts for both operations reduced the total machining time to only 20 min. This yielded a direct savings of \$250,000 per year, freed up 3000 h of machine time per year, and avoided the need to purchase a second machine tool.

### *Ceramic Wear Components in Automotive and Light-Truck Engines*

Several engineering ceramics have combinations of properties that make them attractive materials for a variety of specialized wear applications in automotive engines.

The use of structural ceramics as wear components in commercial engines began in Japan in the early 1980s. Table 3 lists many of the components that have been manufactured, the engine company that first introduced the component, the material, and the year of introduction. In some of these applications several companies have introduced a version of the component into one or more of their engines. Many of these applications are driven by the need to control

**Table 3** Ceramic Wear Components in Automotive and Light-Truck Engines

Component	Engine Manufacturer	Engine Type	Ceramic	Year of Introduction
Rocker arm insert	Mitsubishi	SI	Si <sub>3</sub> N <sub>4</sub>	1984
Tappet	Nissan	Diesel	Si <sub>3</sub> N <sub>4</sub>	1993
Fuel injector link	Cummins	Diesel	Si <sub>3</sub> N <sub>4</sub>	1989
Injector shim	Yanmar	Diesel	Si <sub>3</sub> N <sub>4</sub>	1991
Cam roller	Detroit Diesel	Diesel	Si <sub>3</sub> N <sub>4</sub>	1992
Fuel injector timing plunger	Cummins	Diesel	ZrO <sub>2</sub>	1995
Fuel pump roller	Cummins Diesel	Diesel	Si <sub>3</sub> N <sub>4</sub>	1996

SI = spark-ignited engine.

the emissions of heavy-duty diesels. Meeting current emissions requirements creates conditions within the engine fuel delivery system that increase wear of lubricated steel against steel. One of these conditions is increased injection pressure; another is an increase in the soot content of engine lubricating oils. Strategic utilization of ceramic components within the fuel delivery systems of many heavy-duty truck engines has enabled the engines to maintain required performance for warranties of 500,000 miles and more. The fuel injector link introduced by Cummins in 1989 is still in production. Well over three million of these components have been manufactured. And many of these have accumulated more than a million miles of service with so little wear that they can be reused in engine rebuilds. In a newer model electronic fuel injector, Cummins introduced a zirconia timing plunger. The part has proved so successful that a second zirconia component was added to the timing plunger assembly several years later.

Increasingly stringent emissions requirements for heavy diesels have increased the market for ceramic components in fuel injectors and valve train components. Many of these heavy-duty engine parts are manufactured at rates of 20,000 up to 200,000 per month.

Perhaps the largest remaining problem for this set of applications is cost. Ceramic parts are still more expensive than generally acceptable for the automotive industry. Reluctance of designers to try ceramic solutions still exists, but it is greatly diminishing thanks to the growing list of reliable and successful applications of structural ceramic engine components.

### **Armor**

Perhaps the ultimate wear application of ceramics is in the area of armor. In recent conflicts most soldiers wear body armor capable of stopping armor piercing projectiles, typically made with hardened steel or tungsten carbide cores. The armor system is made of a hard ceramic face plate and fabric armor backing. This system is inserted into a pocket on a soft armor, fragment protective vest. When the hard armor piercing projectile impacts the even harder ceramic, a compressive elastic wave is generated which propagates to the rear of the ceramic plate and is reflected back to the front face as an elastic tensile wave. This elastic tensile wave interacts with the impacting projectile helping to induce shattering of the projectile. As the fragments of the projectile try to penetrate the armor (which itself is fracturing but is constrained by the material adjacent to the impact area) the projectile fragments are “ground up” by the ceramic rubble. The soldier is protected from injury from the ceramic rubble and projectile fragments, by the soft fabric armor back layer, which acts like a catcher’s mitt. All of these events take place in a time frame of the order of 100 μs. The key ceramic properties for this application are a high hardness (higher than the projectile hardness), a high elastic modulus, and a low mass density. Materials frequently selected for armor application are Al<sub>2</sub>O<sub>3</sub>, B<sub>4</sub>C, and SiC. An excellent overview of the historical development of ceramic armor design and modeling has recently been provided by Anderson.<sup>15</sup>

### ***Water Purification***

As the world's population has grown, the need for potable water has become a critical societal need in arid coastal regions and on many islands. Accordingly, in the past few years many large desalination plants have been built in such areas. Most large desalination plants utilize the "Sea Water Reverse Osmosis" (SWRO) process, in which pressurized sea water is passed through membranes that remove the unwanted ions and impurities in the water. Pressurizing the input water for these types of facilities is an energy intensive endeavor. Consequently, the clean water produced is expensive. To reduce the costs of water, reducing energy costs is a major focus. Many SWRO plants utilize energy recovery devices based on a pressure exchange principle to recover pressure from the effluent water before discharging it (not unlike the use of heat exchangers to recover waste heat). The best way to understand how these devices work is to search "pressure exchange devices" using an Internet browser and view the videos that are available. The key components in the most widely utilized pressure exchange devices are an aluminum oxide cylinder, which houses an aluminum oxide rotor, and two aluminum oxide end caps, which provide a pressure seal and ducting for fresh sea water and the rejected brine to enter and exit the device. The rotor powered by the high pressure brine spins at about 1000 rpm and is the only moving part in the system. Such pressure exchange systems save 50–60% of the energy required to produce a unit of drinkable water. They have been widely utilized in SWRO plants for over a decade and are in use in many of largest SWRO plants in the world. Currently, there are over 15,000 of these devices deployed worldwide. By 2013 these devices were producing over a liter of clean water for every human on earth (~7 billion liters) and saving \$1.4 billion in operating costs. Due to the erosion resistance of the ceramic components, these systems have a projected service life of 25 years justifying the cost of the ceramics. The potential of these devices to reduce energy consumption in other industries where high pressure fluids are used (such as oil, gas, and chemicals) is presently being evaluated.

### ***Bioceramics***

The bones in the human body consist of ~60% hydroxyapatite (HA, a complex calcium phosphate based mineral), a ceramic. Bone replacement materials must bear loads and be able to last decades in highly corrosive body fluids. Joint replacement materials must be capable of the above, with the additional requirement of functioning in an abrasive wear situation with low wear rates and producing fine-sized wear debris. Obviously, the material and/or its reaction products must be nontoxic. In consideration of these requirements ceramics have long been used as dental materials, and it is not surprising that ceramic materials are being utilized in bone or joint replacement applications.

The enamel on the exposed surfaces of our teeth is the hardest mineral in our bodies and is ~92% HA. Historically the most prevalent use of ceramic materials in the body has been in dental restorations. In biting hard objects stresses of up to 100 MPa can be encountered. In chewing and biting, stresses between 20 and 100 MPa are applied from 1000 to 3000 times per day in a water-based liquid that has a pH that can vary from 0 to 8. Temperature excursions vary between 98.6°F (body temperature) and 32°F (ice). Thus, key properties for ceramic dental restorations are high strength, high fracture toughness, wear and thermal shock resistance, and chemical inertness. A wide variety of glass-based restoration materials have been used in the past and continue in wide use today. However, there is a growing trend toward the use of alumina and zirconia ceramics for restorations due to their attractive combination of properties.<sup>16</sup>

Although HA is used as a bone filler and a bone replacement material, the widest use of ceramics in skeletal repair is in joint replacement, principally hip and knee replacement. In the case of hip replacement, ceramics are typically used as one component in a hybrid materials system. The system consists of an ultrahigh-molecular-weight polyethylene acetabular cup, an alumina ball, and a titanium, stainless steel, or vitalium femoral pin, all bathed in a synovial fluid

lubricant. This combination of materials produces the least wear debris compared to alternative systems. (Wear debris will inflame the soft tissue in the joint region and thus accelerate the need for redoing the joint replacement.) Alumina ceramics are also used in knee replacements.

The most comprehensive overview of bioceramics is still the classic paper by Hench.<sup>17</sup>

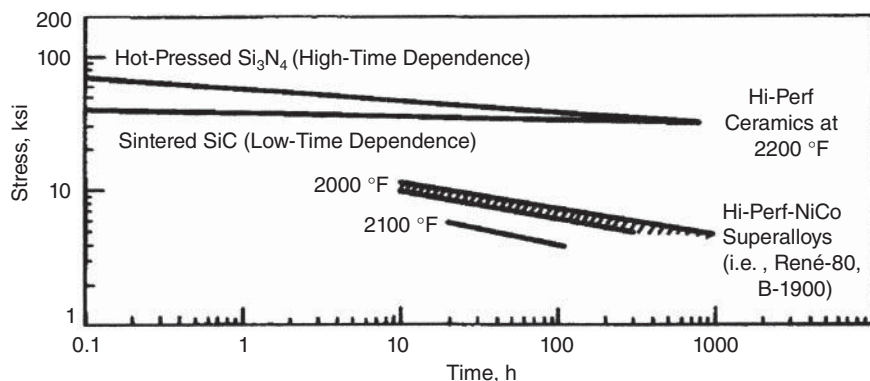
## 4.2 Thermostructural Applications

Due to the nature of their chemical bond, many ceramics maintain their strength and hardness to higher temperatures than metals. For example, at temperatures above 1200°C, silicon carbide and silicon nitride ceramics are considerably stronger than any superalloy. As a consequence, structural ceramics have been considered and utilized in a number of demanding applications where both mechanically imposed tensile stresses and thermally imposed tensile stresses are present. One dramatic example is the ceramic (silicon nitride) turbocharger that has been in commercial production for automobiles in Japan since 1985. Over one million of these have been manufactured and driven with no recorded failure. This is a very demanding application, as the service temperature can reach 900°C, stresses at ~700°C can reach 325 MPa, and the rotor must also endure oxidative and corrosive exhaust gases that may contain erosion-inducing rust and soot particles. Silicon nitride gas turbine nozzle vanes were flown for several years in aircraft auxiliary power units. At that time a corrosion-like problem due to dust and salt terminated plans to go forward.<sup>18</sup> Starting in 2001 a major new application for ceramic matrix composites (CMCs) was introduced on a production sports car. The Porsche implemented CMC rotors for the disk brakes in the 911 GT2.<sup>19</sup> These brakes are still in production, and at least one other manufacturer of high-performance sports cars is starting to implement them. A fascinating short video showing how these brake rotors are made can be viewed on the Web by searching for “How it’s made—ceramic composite disk brakes” on You Tube.

This class of applications requires a focus on the strength, Weibull modulus  $m$  (the higher the  $m$ , the narrower the distribution of observed strength values), thermal shock resistance, and often the stress rupture (strength decrease over time at temperature) and/or creep (deformation with time at temperature) behavior of the materials. Indeed, as shown in Fig. 3, the stress rupture performance of current structural ceramics represents a significant jump in materials performance over superalloys.

The thermal shock resistance of a ceramic is a systems property rather than a fundamental materials property. Thermal shock resistance is given by the maximum temperature change a component can sustain,  $\Delta T$ :

$$\Delta T = \frac{\sigma(1 - \mu)k}{\alpha E r_m h} S \quad (2)$$



**Figure 4** Stress rupture performance of non-oxide structural ceramics compared to superalloys (oxidizing atmosphere). (After ref. 20.)

**Table 4** Calculated Thermal Shock Resistance of Various Ceramics

Material	$\sigma$ (MPa)	$\mu$	CTE (cm/cm K)	E (GPa)	R (K)
Al <sub>2</sub> O <sub>3</sub> (99%)	345	0.22	$7.4 \times 10^{-6}$	375	97
AlN	350	0.24	$4.4 \times 10^{-6}$	350	173
SiC (sintered)	490	0.16	$4.2 \times 10^{-6}$	390	251
PSZ	1000	0.3	$10.5 \times 10^{-6}$	205	325
Si <sub>3</sub> N <sub>4</sub>	830	0.3	$2.7 \times 10^{-6}$	290	742
LAS (glass ceramic)	96	0.27	$0.5 \times 10^{-6}$	68	2061
Al-titanate	41	0.24	$1.0 \times 10^{-6}$	11	2819

Where  $\sigma$  is strength,  $\mu$  is Poisson's ratio,  $\alpha$  is the coefficient of thermal expansion (CTE),  $E$  is Young's modulus,  $k$  is thermal conductivity,  $r_m$  is the half-thickness for heat flow,  $h$  is the heat transfer coefficient, and  $S$  is a shape factor totally dependent on component geometry.<sup>11</sup> Thus it can be seen that thermal shock resistance,  $\Delta T$ , is made up of terms wholly dependent on materials properties and dependent on heat transfer conditions and geometry. It is the role of the ceramic engineer to maximize the former and of the design engineer to maximize the latter two terms. It has become usual practice to report the materials-related thermal shock resistance as the instantaneous thermal shock parameter,  $R$ , which is equal to

$$R = \frac{\sigma(1 - \mu)}{\alpha E} \quad (3)$$

The value of  $R$  for selected ceramics is presented in Table 4. Another frequently used parameter is  $R'$ , the thermal shock resistance where some heat flow occurs:  $R'$  is simply  $R$  multiplied by the thermal conductivity,  $k$ .<sup>21</sup> For cases where heat transfer environments are complex, Ref. 22 lists 22 figures of merit for selecting ceramics to resist thermal stress.

### 4.3 Corrosion Resistance

Many advanced structural ceramics such as alumina, silicon nitride, or SiC have strong atomic bonding that yields materials that are highly resistant to corrosion by acidic or basic solutions at room temperature (the notable exception being glass or glass-bonded ceramics attacked by HF). This corrosion resistance has led to many applications. Carbonated soft drinks are acidic, and alumina valves are used to meter and dispense these beverages at refreshment stands. The chemical industry utilizes a wide variety of ceramic components in pumps and valves for handling corrosive materials. For example, the outstanding corrosion resistance of fully dense SiC immersed in a variety of hostile environments is given in Table 5. There are many cases where corrosion and particulate wear are superimposed, as in the handling of pulp in papermaking or

**Table 5** Weight Loss of Fully Dense SiC in Acids and Bases<sup>a</sup>

Reagent (wt %)	Test Temperature (°C)	Weight Loss (mg/cm <sup>2</sup> · yr)
98% H <sub>2</sub> SO <sub>4</sub>	100	1.5
50% NaOH	100	2.5
53% HF	100	<0.2
85% H <sub>3</sub> PO <sub>4</sub>	100	<0.2
45% KOH	100	<0.2
25% HCl	100	<0.2
10% HF	25	<0.2

<sup>a</sup>All specimens submerged 125–300 h, continuously stirred.  
Source: Data Courtesy of ESK-Wacker, Adrian, MI.



transporting slurries in mineral processing operations, and ceramics find frequent application in such uses.

#### 4.4 Passive Electronics

The role of passive electronics is to provide insulation (prevent the flow of electrons) either on a continuous basis (as in the case of substrates or packages for microelectronics) or on an intermittent basis, as is the case for ceramic capacitors (which store electric charge and hence need a high polarizability). These applications constitute two of the largest current markets for advanced ceramics. For electronic substrates and packages key issues include the minimization of thermal mismatch stresses between the Si (or GaAS) chip and the package material (so the CTE will be important) and dissipation of the heat generated as electrons flow through the millions of transistors and resistors that comprise modern microelectronic chips; hence the thermal conductivity is a key property. All other things being equal, the delay time for electrons to flow in the circuit is proportional to the square root of the dielectric constant of the substrate (or package) material. Additionally, the chip or package must maintain its insulating function, so high resistivities are required. Most high-performance packages for computer chips are alumina. With the advent of microwave integrated circuits (e.g., cell phones) aluminum nitride substrates are beginning to be utilized for high thermal conductivity. The environmental drawbacks to machining BeO have tended to favor the use of AlN to replace or avoid the use of BeO. Synthetic diamond is an emerging substrate material for special applications. Isotopically “pure” synthetic, single-crystal diamond has values of thermal conductivity approaching 10,000 W/m·K. Typical values of the above properties for each of these materials are given in Table 6, along with selected properties of silicon for comparison. For design purposes exact values for specific formulations of the materials should be obtained from the manufacturers.

Over a billion ceramic capacitors or multilayer ceramic capacitors (MLCCs) are made every day.<sup>23</sup> Since electrons do not flow through capacitors, they are considered passive electronic components. However, the insulators from which ceramic capacitors are made polarize, thereby separating electric charge. This separated charge can be released and flow as electrons, but the electrons do not flow through the dielectric material of which the capacitor is composed. Thus, the materials parameter, which determines the amount of charge that can be stored, the dielectric constant  $k$ , is the key parameter for design and application.

Table 7 lists the approximate dielectric constant at room temperature for several families of ceramics used in capacitor technology. The dielectric constant varies with both temperature and frequency. Thus, for actual design precise curves of materials performance over a relevant range of temperatures and frequencies are often utilized. Many ceramics utilized as capacitors are ferroelectrics, and the dielectric constant of these materials is usually a maximum at or near the Curie temperature.

**Table 6** Key Properties for Electronic Substrates and Packages

Material	CTE, $10^{-6}/K$	Thermal Conductivity (W/mK)	Resistivity	Dielectric Constant
Al <sub>2</sub> O <sub>3</sub> (96%)	6.8	26	$>10^{14}$	9.5
Al <sub>2</sub> O <sub>3</sub> (99%)	6.7	35	$>10^{14}$	10
AlN	4.5	140–240	$>10^{14}$	9
BeO	6.4	250	$>10^{14}$	6.5
Diamond	2	2000	$>10^{14}$	5.5
Silicon	2.8	150		

*Note:* CTE and thermal conductivity are at room temperature, and the dielectric constant is at 1 MHz.

**Table 7** Dielectric Constants for Various Ceramics

Material	Dielectric Constant at RT
Tantalum oxide ( $\text{Ta}_2\text{O}_5$ )	25
Barium titanate	5,000
Barium zirconium titanate	20,000
Lead zirconium titanate (PZT)	2,000
PZT with W or Mg additives	9,000
Lead magnesium niobate (PMN)	20,000
Lead zinc niobate (PZN)	20,000

## 4.5 Piezoceramics

Piezoceramics are a multi-billion-dollar market.<sup>24</sup> Piezoceramics are an enabling material for sonar systems, medical ultrasonic imaging, micromotors and micropositioning devices, the timing crystals in our electronic watches, and numerous other applications. A piezoelectric material will produce a charge (or a current) if subjected to pressure (the *direct* piezoelectric effect) or, if a voltage is applied, the material will produce a strain (the *converse* piezoelectric effect). Upon the application of a stress, a polarization charge,  $P$ , per unit area is created that equals  $d\sigma$  where  $\sigma$  is the applied stress and  $d$  is the piezoelectric modulus. This modulus, which determines piezoelectric behavior, is a third-rank tensor<sup>25</sup> that is thus highly dependent on directions along which the crystal is stressed. For example, a quartz crystal stressed in the [100] direction will produce a voltage, but one stressed in the [001] direction will not.

In a polycrystalline ceramic the random orientation of the grains in an as-fired piezoceramic will tend to minimize or zero out any net piezoelectric effects. Thus, polycrystalline piezoceramics have to undergo a postsintering process to align the electrically charged dipoles within the polycrystalline component. This process is known as poling and it requires the application of a very high electric field. If the piezoceramic is taken above a temperature, known as the Curie temperature, a phase transformation occurs and piezoelectricity will disappear. The piezoelectric modulus and the Curie temperature are thus two key materials selection parameters for piezoceramics. The ability of piezoceramics to almost instantaneously convert electrical current to mechanical displacement and vice versa makes them highly useful as transducers. The efficiency of conversion between mechanical and electrical energy (or the converse) is measured by a parameter known as the coupling coefficient. This is a third key parameter that guides the selection of piezoelectric materials.

Although piezoelectricity was discovered by Pierre and Jacques Curie in 1880, piezoceramics were not widely utilized until the development of polycrystalline barium titanate in the 1940s and lead zirconate titanates (PZTs) in the 1950s. Both of these materials have high values of  $d$  and thus develop a high voltage for a given applied stress. PZT has become widely used because, in addition to a high  $d$  value, it also has a very high coupling coefficient.

Sonar, in which ultrasonic pulses are emitted and reflected “echoes” are received, is used to locate ships and fish and map the ocean floor by navies, fishermen, and scientists all over the globe. Medical ultrasound utilizes phased arrays of piezoceramic transducers to image organs and fetuses noninvasively and without exposure to radiation. A relatively new application that has found significant use in the microelectronics industry is the use of piezoceramics to drive micropositioning devices and micromotors. Some of these devices can control positioning to a nanometer or less. Piezoceramic transducers are combined with sophisticated signal detection and generation electronics to create “active” noise and vibration damping devices. In such devices the electronics detect and quantify a noise spectrum and then drive the transducers to provide a spectrum 180° out of phase with the noise, thereby effectively canceling it.



**Table 8** Key Properties for PZT-Based Piezoceramics

Material	Piezoelectric Modulus $d_{33}$	Curie Temperature ( $^{\circ}\text{C}$ )	Coupling Coefficient $k_{33}$
A	$226 \times 10^{-12}$ m/V	320	0.67
B	$635 \times 10^{-12}$ m/V	145	0.68
C	$417 \times 10^{-12}$ m/V	330	0.73

Many of the current high-performance applications of piezoceramics are based on proprietary modifications of PZT, which contain additions of various dopants or are solid solutions with perovskite compounds of Pb with Mg, Mn, Nb, Sn, Mo, or Ni. Table 8 lists the range of several key piezoceramic selection parameters for proprietary PZT compositions from one manufacturer.

## 4.6 Transparencies

Transparent ceramics (which include glasses and single-crystal and polycrystalline ceramics) have been used as optical transparencies or lenses for millennia. Glass windows were in commercial production in first-century Rome, but it was not until the 1800s, with the need for precision optics for microscopes, telescopes, and ophthalmic lenses, that glasses and other optical materials became the object of serious scientific study. As noted in the introduction, progress in glass science and technology, coupled with lasers, has led to the current broadband digital data transmission revolution via optical fibers. Various ceramic crystals are used as laser hosts and specialty optical lenses and windows. A significant fraction of supermarket scanner windows combine the scratch resistance of sapphire (single-crystal alumina) with its ability to transmit the red laser light that we see at the checkout counter. While such windows are significantly more costly than glass, their replacement rate is so low that they have increased profitability for several supermarket chains. For the same reason the crystals in many high-end watches are scratch-resistant man-made sapphire. Sapphire is now used as the protective window for the iPhone 5 and 6 camera lens. Polycrystalline translucent (as opposed to fully transparent) alumina is used as containers (envelopes) for the sodium vapor lamps that light our highways and industrial sites. Not all windows have to pass visible light. Radar or mid- to far-infrared transparencies look opaque to the human eye but are perfectly functional windows at their design wavelengths.

The most demanding application for such transparencies is for the guidance domes of missiles. Materials that can be used for missile radomes include slip-cast fused silica, various grades of pyroceram (glass ceramics), and silicon-nitride-based materials. Infrared (IR) windows and missile domes include  $\text{MgF}_2$  and  $\text{ZnSe}$ . Requirements exist for having missile guidance domes that can transmit in the visible, IR, and radar frequencies (multimode domes). Ceramic materials that can provide such functionality include sapphire and aluminum oxynitride spinel (AlON). In addition to optical properties missile domes must be able to take high aerothermal loading (have sufficient strength) and be thermal shock resistant (a high-speed missile encountering a rain cloud can have an instant  $\Delta T$  of minus several hundred degrees kelvin).

Key properties for visible and IR optical materials include the index of refraction,  $n$  (which will be a function of wavelength), and absorption or loss. For radar transparencies key parameters are dielectric constant (which can be thought of as analogous to the index of refraction) and dielectric loss.

## 5 INFORMATION SOURCES

### 5.1 Manufacturers and Suppliers

There are hundreds of manufacturers of advanced ceramics and glasses. Locating ones that already have the material that is needed and can produce it in the configuration required can be a daunting task. There are two resources published annually that make this task much easier. The American Ceramic Society publishes a directory of suppliers of materials, supplies, and services that can help locate such information quickly. It is called *Ceramic Source*. This directory can also be accessed on the Web at [www.ceramics.org](http://www.ceramics.org). A similar *Buyers Guide* is published by *Ceramic Industry Magazine*, and this can also be viewed online at [www.ceramicindustry.com](http://www.ceramicindustry.com). Once a likely source for your need has been identified, a visit to the supplier's website can often provide a great deal of background information and specific data, which can make further contacts with the supplier much more meaningful and informative.

### 5.2 Data

Manufacturers' literature, both hard copy and posted on the Web, is an invaluable source of data. The handbooks, textbooks, and encyclopedias listed below are also excellent sources of data. However, before committing to a finalized design or to production, it is advisable to develop your own test data in conformance with your organization's design practice. Such data should be acquired from actual components made by the material, processing route, and manufacturer that have been selected for the production item.

Vetted data for many ceramic materials may also be found on the Web. If one goes to the American Ceramics Society's website homepage and clicks on knowledge center (on the menu bar), then clicks on ceramic materials tools, a page will come up that has a list of NIST databases containing property data relevant to ceramics. Google Scholar is a website that can facilitate finding technical papers on a particular topic or by a particular person. It is a great aid in compiling material for library searches, but it does not contain many "free" downloads. Even with the speed and power of the Internet at our fingertips, it is still useful to have some comprehensive handbooks and data collections on our bookshelves. These can facilitate materials comparisons and provide more in-depth overviews of certain areas than most Wikipedia articles.

The following are several ceramic handbooks that are very useful:

*Ceramics and Glasses, Vol. 4: Engineered Materials Handbook*, ASM International, Materials Park, OH, 1991.

J.F. Shackelford, W. Alexander, and J. Park (Eds.), *Materials Science and Engineering Handbook*, 2nd ed., CRC Press, Boca Raton, FL, 1994.

C.X. Campbell and S. K. El-Rahaiby (Eds.), *Databook on Mechanical and Thermophysical Properties of Whisker-Reinforced Ceramic Matrix Composites*, Ceramics Information Analysis Center, Purdue University, W. Lafayette, IN, and The American Ceramic Society, Westerville, OH, 1995.

R.J. Brook (Ed.), *Concise Encyclopedia of Advanced Ceramic Materials*, Pergamon Press, Oxford, 1991.

### 5.3 Standards, Test Methods, and Handbooks

To reliably design, procure materials, and ensure quality, it is necessary to have common, agreed-upon, and authoritative test standards, methods, and practices. Institutions such as

the American Society for Testing and Materials (ASTM, [www.astm.org](http://www.astm.org)), the German Standards Organization (Deutsches Institute für Normung, DIN, [www.din.de](http://www.din.de)), the International Standards Organization (ISO, [www.iso.org](http://www.iso.org)), and the Japanese Standards Association (which produces the Japanese Industrial Standards, JIS, [www.jisa](http://www.jisa)) all provide standards for their various constituencies.

Following is a sample of standards available from the ASTM related to advanced ceramics and ceramic matrix composites:

- C-177-10, Standard Test Method for Steady State Heat Flux and Thermal Transmission by Means of the Gradient-Hot-Plate Apparatus
- C-1145-06, Standard Terminology of Advanced Ceramics
- C-1161-02c, Standard Test Method for Flexural Strength of Advanced Ceramics at Ambient Temperatures
- C-1175-99a (2010), Standard Guide to Test Methods and Standards for Nondestructive Testing of Advanced Ceramics
- C-1198-09, Standard Test Method for Dynamic Young's Modulus, Shear Modulus and Poisson's Ratio for Advanced Ceramics by Sonic Resonance
- C-1211-02(2008), Standard Test Method for Flexural Strength of Advanced Ceramics at Ambient Temperatures
- C-1273-05(2010), Standard Test Method for Tensile Strength of Monolithic Advanced Ceramic at Ambient Temperatures
- C-1292-10, Standard Test Method for Shear Strength of Continuous Fiber-Reinforced Advanced Ceramic Composites at Ambient Temperatures
- C-1337-10, Standard Test Method for Creep and Creep-Rupture of Continuous Fiber-Reinforced Advanced Ceramic Composites under Tensile Loading at Elevated Temperatures
- C-1366-04(2009), Standardized Test Method for Tensile Strength of Monolithic Advanced Ceramics at Elevated Temperatures
- C-1424-10, Standard Test Method for Monotonic Compressive Strength of Advanced Ceramics at Ambient Temperatures
- C-1525-04(2009), Standard Test Method for Determination of Thermal Shock Resistance for Advanced Ceramics by Water Quenching
- C-1683-10, Standard Practice for Size Scaling of Tensile Strengths Using Weibull Statistics for Advanced Ceramics
- E-228-11, Standard Test Method for Linear Thermal Expansion of Solid Materials with a Push-Rod Dilatometer
- F-603-12 Standard Specification for High Purity Aluminum Oxide for Medical Application

The above standards were culled from the current ASTM standards. Anyone who is interested in keeping up with the latest test methodology, which has not yet reached the level of maturity required for acceptance as a standard, can view such work on the ASTM website. In particular, a search for ASTM Committee C28 will bring up their latest activities in advanced ceramics, Committee E37 will address testing thermal properties of solids, and Committee F04 will deal with medical materials and devices including ceramics.

Design handbooks are also useful tools which can provide methodology on how to design with advanced ceramics as well as high-quality design data. The first such handbook was recently created by the U.S. Department of Defense in cooperation with other government

agencies. It is entitled *MIL Handbook 17*, Vol. 5. It provides guidance on how to design with advanced ceramic composites, an area that requires special methodologies.

## 6 FUTURE TRENDS

Future growth in advanced ceramics utilization will be driven by organic growth in many existing applications and by expansion into new ones. These new applications will emerge from opportunities arising from the major societal needs of the next 30 years: energy efficiency, energy security, environmental pollution reduction, quality of life for an aging population, and an aging infrastructure.

The sectors that will likely see the greatest growth are electronics, optronics, and sensors. More extensive implementation of sensors on electrical appliances and power generating equipment will enable “smart” buildings and “smart” homes working with a “smart” grid to minimize and rationalize future electrical power demand. As many of these sensors will require ceramics, this will be an opportunity. Automobiles represent a major growth opportunity for ceramics. Our cars are increasingly electronically controlled and increasingly connected to wireless phone and information networks. Power windows, keyless entry, back-up collision sensors, automatic windshield wiper speed controls, heated seats, etc., are no longer exceptional. This means more ceramic sensors, actuators, motor magnets, passive electronic components, and positive temperature coefficient PTC heater units. Light-emitting diodes (LEDs) are increasingly used in automotive headlights, tail lights, and interior lighting. This is providing scale for LED production, and the cost of LED household lighting (which is already commercially available) will decrease. Both of these trends will increase the market for SiC and sapphire substrates and will significantly reduce household electricity use. The seemingly insatiable demand for bandwidth in the world’s fiber-optic cable networks augers well for long-term growth in the optical fiber area.

One of the largest increases in ceramic use will be in the bioceramic area. The desire to maintain the quality of life for an aging population will result in a significant increase in hip, knee, and shoulder joint replacements. In the near future other joint replacements, such as digital replacements, are certain to become available. Many of these joint replacements will utilize ceramic materials. More bone repair and replacement ceramics and ceramics for dental implants are likely to be utilized. In the area of medical imaging the ceramics in ultrasound imaging will be increasingly important to piezoelectric materials.

The intertwined issues of energy efficiency and environmental protection will see increased use of advanced ceramics in energy systems as diverse as solid oxide fuel cells (SOFCs), batteries, and nuclear reactors. An interesting assessment of the future of nuclear power in the post-Fukushima era, and the potential for the small modular nuclear reactor, which relies on ceramic fuel balls, was recently published.<sup>26</sup> Polycrystalline photovoltaic solar cells are cut from large ingots of very high purity Si. These Si ingots are melted in specially engineered, high-purity, SiO<sub>2</sub> crucibles which can only be used once. The demand for these crucibles will wax and wane with the solar cell market but will grow in the long run. Fresh water produced via SWRO plants will see considerable growth. Thus, demand for the energy-saving ceramic pressure exchangers described previously will also grow.

Silicon nitride and zirconia components for spark-ignited and diesel engines will grow slowly if at all. As heavy-duty diesel engines transition from oil based to clean-burning natural gas fuel (a trend slowly accelerating in the United States), it is likely that the need for ceramic diesel particulate traps will diminish. Ceramic automotive catalyst supports are likely to be minimally affected by natural gas, due to gasoline engines remaining in the vast majority of future cars.

Major opportunities are present for ceramics in the oil and gas industry. The recent success of SiC thrust bearings for deep horizontal drilling was discussed previously. Another important

new application for ceramics are sand filters for deep-water wells used after drilling during the productive life of the well. Ceramic proppants which keep small fissures in fracked wells open so gas and oil can flow through are certain to grow as fracking grows.

Perhaps, surprisingly, ceramic armor and other military applications for advanced ceramics are likely to see an uptick in the near future as military forces around the world absorb the lessons learned in recent conflicts and upgrade and modernize their equipment.

Several years ago, the author was privileged to have toured the Pohang Steel complex in Pohang, ROK. At the entrance was a wonderful sign. It proclaimed: “Resources are Limited—Creativity is Unlimited.” This thought certainly applies to the global future of advanced ceramics. Creatively utilized advanced ceramics will effectively expand our resources, protect our environment, and create new technological opportunities. The potential opportunities go far beyond the few discussed in this chapter.

## REFERENCES

1. P. B. Vandiver, “Reconstructing and Interpreting the Technologies of Ancient Ceramics,” in *Materials Issues in Art and Archaeology, Materials Res. Soc. Symposium Proceed.*, Vol. 123, Materials Research Society, Pittsburgh, PA, 1988, pp. 89–102.
2. *Materials Science and Engineering for the 1990’s*, National Academy Press, Washington, DC, 1989, p. 24.
3. R. N. Katz, “Piezoceramics,” *Ceramic Industry*, August 20, 2000, p. 20.
4. D. W. Richerson, *Modern Ceramic Engineering*, 2nd ed., Marcel Dekker, New York, 1992, pp. 582–588.
5. J. S. Haggerty and Y. M. Chiang, “Reaction-Based Processing Methods for Materials and Composites,” *Ceramic Eng. Sci. Proc.*, **11**(7–8), 757–781, 1990.
6. K. Clerian and M. Kirskey, “Industrial-Scale Microwave Sintering,” *Ceramic Industry*, April 1, 2011.
7. R. N. Katz, *Advanced Materials by Design*, Congress of the United States, Office of Technology Assessment, Washington, DC, June 1988, p. 40.
8. A. F. McLean and D. Hartsock, “Design with Structural Ceramics,” in J. B. Wachtman (Ed.), *Treatise on Materials Science and Technology*, Vol. 29, Academic Press, Boston, 1989, pp. 27–95.
9. G. D. Quinn, “Flexural Strength of Advanced Ceramics—A Round Robin Exercise,” Report MTL-TR 89-62, U.S. Army Materials Technology Laboratory, July 1989, p. 85, Aberdeen, MD.
10. N. N. Nemeth and J. P. Gyekenyesi, “Probabilistic Design of Ceramic Components with the NASA/CAREES Computer Program,” in *Engineered Materials Handbook*, Vol. 4: *Ceramics and Glasses*, ASM International, Metals Park, OH, 1991, pp. 700–708.
11. R. N. Katz, “Application of High Performance Ceramics in Heat Engine Design,” *Mater. Sci. Eng.*, **71**, 227–249, 1985.
12. J. Larsen-Basse, “Abrasive Wear of Ceramics,” in S. Jahanmir (Ed.), *Friction and Wear of Ceramics*, Marcel Dekker, New York, 1994, p. 107.
13. R. N. Katz, “Ceramic Materials for Roller Element Bearing Application,” in S. Jahanmir (Ed.), *Friction and Wear of Ceramics*, Marcel Dekker, New York, 1994, pp. 313–328.
14. R. C. Ide, “Drilling for Oil and Gas, Ceramics Make the Difference,” *Oil Gas Eur. Mag.*, September 3, 2011.
15. C. F. Anderson, Jr., “Review of Computational Ceramic Armor Modeling,” *Ceram. Eng. Sci. Proc.*, **27**(7), 1, 2007.
16. A. Shenoy and N. Shenoy, “Dental Ceramics: An Update,” *J. Conserv. Dent.*, **13**(4), 195–203, 2010.
17. L. L. Hench, “Bioceramics: From Concept to Clinic,” *J. Am. Ceram. Soc.*, **74**(7), 1487–510, 1991.
18. D. W. Richerson, “Historical Review of Addressing the Challenges of Use of Ceramic Components in Gas Turbine Engines,” ASME Proceedings Paper GT2006-90330, presented at ASME Turbo Expo 2006, Barcelona Spain, May 8–11, 2006.
19. R. C. Renz, G. Seifert, and W. Krenkel, “Integration of CMC Brake Disks in Automotive Brake Systems,” *Int. J. Appl. Ceram. Technol.*, **9**(4), 712–724, 2012.

20. R. N. Katz, "Substitution Technology-Advanced Ceramics," *Ceram. Eng. Sci. Proc.*, 4(7-8), 475-484, 1983.
21. W. D. Kingery, H. K. Bowen, and D.R. Uhlmann, *Introduction to Ceramics*, 2nd ed., Wiley, New York, 1976, p. 822ff.
22. D. P. H. Hasselman, "Figures-of-Merit for the Thermal Stress Resistance of High Temperature Brittle Materials: A Review," *Ceramurgica Int.*, 4(4), 147-150, 1978.
23. D. W. Richerson, *The Magic of Ceramics*, American Ceramic Society, Westerville, OH, 2000, p. 141.
24. "Fundamental Research Needs in Ceramics," NSF Workshop Report, Washington, DC, April 1999, p. 9.
25. J. F. Nye, *Physical Properties of Crystals*, Oxford University Press, London, 1964, p. 110ff.
26. P. Wray, "Materials for Nuclear Energy in the Post-Fukushima Era: An Interview with John Marra," *Am. Ceramic Soc. Bull.*, 90(6), 24-28, 2011.



# CHAPTER 13

## ELECTRONIC MATERIALS AND PACKAGING

Warren C. Fackler  
Telesis Systems  
Cedar Rapids, Iowa

<b>1 INTRODUCTION</b>	<b>475</b>	<b>3 ELECTRONIC PACKAGING</b>	<b>499</b>
1.1 Scope	475	3.1 Component Mounting	499
1.2 Overview	475	3.2 Fastening and Joining	500
1.3 Approach	476	3.3 Interconnection	502
1.4 Design Techniques	476	3.4 Shock and Vibration	503
1.5 Availability of Information	477	3.5 Structural Design	506
<b>2 ELECTRONIC MATERIALS PACKAGING</b>	<b>477</b>	3.6 Thermal Design	507
2.1 Material Properties	477	3.7 Protective Packaging	509
2.2 Typical Applications	484	3.8 Software Design Aids	510
2.3 Candidate Materials	490	<b>REFERENCES</b>	<b>512</b>

### 1 INTRODUCTION

#### 1.1 Scope

Electronic packaging is a multidisciplinary process consisting of the physical design, product development, and manufacture required to transform an electronic circuit schematic diagram into functional electronic equipment.<sup>1</sup> The categories of technical knowledge and design emphasis applicable to a given electronic product vary significantly in priority, depending on the intended product application (e.g., aerospace, automotive, computers, consumer goods, medical equipment, industrial equipment, agricultural equipment, military equipment, telephony, test equipment). The key to successful electronic packaging is the ability to identify the applicable field(s) of technology and to select those design approaches most likely to offer solutions to a design problem.

#### 1.2 Overview

There are four basic categories of concern to the electronic packaging engineer, working from the external environment inward:

1. *Exterior Conditions.* Equipment use requirements, service environments, and storage environments define equipment mounting needs, environmental conditions, electrical interconnections, power sources, heat sink availability, surface finishes, repair considerations, and ergonomic human factors requirements.
2. *Internal Conditions.* The equipment enclosure contains and protects internal electronic modules, subassemblies, components, and interconnections and provides thermal and electrical interfaces between the outer environment and the internal environment.



3. *Component Environments.* Module and subassembly housings define the interface between the individual electronic component subenvironment and the equipment's internal environment.
4. *Component Requirements.* Components in modules and subassemblies require protection, which includes limiting temperatures caused by internal heat generation, avoiding excessive mechanical stresses, reducing dynamic shock and vibration loads to below component fragility levels, avoidance of chemical and corrosive agents, and provision for correct mounting methods.

### 1.3 Approach

There are two major considerations in electronic packaging:

1. Correct selection and proper application of materials
2. Physical design of the equipment

#### Materials Selection

The process of materials selection includes the following steps:

1. Identify the desired or dominant material properties for the design application under consideration. See Section 2.1 for a listing of material properties.
2. Define overriding considerations: materials availability, manufacturing process limitations, customer directives, design legacy, and like issues.
3. Review typical applications similar to the design under consideration. See Section 2.2.
4. Compile a list of the most likely candidate materials considering Section 2.3.
5. Select one or more materials that appear to offer the most likely solution.
6. Verify suitability by physically testing the resulting design.

#### Physical Design

The process of physical design includes the following steps:

1. Develop a list of design requirements and restrictions.
2. Using Section 3 and prior experience, select the most probable design approach.
3. Apply the selected design approach.
4. Verify the suitability of the resultant design.
5. Identify and solve the next lower level of design problems.
6. Review the net effect of the combination of solutions considering the interaction between the problem solutions.
7. Iterate until all design requirements and restrictions have been satisfied.

### 1.4 Design Techniques

Several computer-aided design programs address electronic packaging design and development tasks.<sup>2</sup> Most computer algorithms are adaptations of codes generated for other, related purposes (e.g., finite-element techniques for structures, stresses, thermal analysis, fluid flow analysis, and flow visualization; solid-modeling and drafting programs; printed circuit board design programs). In instances other than printed circuit programs and drafting programs, the underlying computational assumptions inherent in the programs sometimes are not thoroughly documented

and may thus produce questionable results. This will provide the opportunity to introduce errors when building a predictive model of a product. The electronic packaging engineer must possess a basic understanding of each physical phenomenon and the underlying assumptions implicit in each analytical model as applied to the specific equipment under analysis. It is always prudent to verify the predicted result by testing and by comparison of the results with one or more known successful designs of a similar nature.

### 1.5 Availability of Information

In addition to the references cited at the end of this chapter, using internet search engines for seeking design and materials properties information cannot be ignored by the Electronic Packaging Engineer.

There are rapidly available, credible materials properties and component specification data posted on web pages by many device manufacturers and materials providers, some providing computer aided design drawing files for download into frequently used mechanical and circuit board design programs. Information found on the web, including user blogs, may uncover ideas for alternate design approaches, pitfalls to avoid, and may be useful for by suggesting ways to reduce the time required to complete and document a design.

## 2 ELECTRONIC MATERIALS PACKAGING

### 2.1 Material Properties

#### *Electrical Conductivity*

A material may be required to conduct electrical currents. This includes metals and some non-metallic elements such as adhesives, greases, and other graphite or metal-powder-loaded compounds. When current flows through the material, electrical resistance creates voltage drop and heat generation, either of which may be a desirable or an undesirable consequence. In screening for electrical conductors, a maximum electrical resistance requirement must be defined; thus materials with equal or lower electrical resistance become candidates for selection. Electrical resistance is temperature sensitive; thus it is necessary to make sure that variances in the material electrical resistance are satisfactory over the temperature range of interest.

Conversely, it may be necessary to electrically isolate a component or current-carrying member to protect from undesired electrical short circuits. Materials used as electrical insulators (dielectrics), such as mica or glass or ceramics and many plastic materials, have very high electrical resistance, are poor conductors of electricity, and are employed to provide electrical isolation.<sup>3</sup> Some high-voltage dielectrics are liquids, which often act as heat transfer media in addition to providing electrical insulation. Examples include mineral oils, silicon oils, polybutanes, fluorocarbons, and organic esters including castor oil. Problems with liquid dielectrics include limited temperature range, chemical decomposition over time, combustibility, and loss of dielectric strength.

#### *Thermal Conductivity*

All materials conduct heat; however, among materials there is a wide range of thermal conductivity. Good conductors of heat include metals, and poor conductors of heat such as ceramic and plastic foam materials are considered to be thermal insulators. The cooling of electronic components and the protection of electronic components from excessive temperatures are managed by employing mounting devices, heat sinks, and thermal insulators using materials of the appropriate thermal conductivity.

### ***Thermal Emissivity***

The thermal emissivity of a material is a measure of the efficiency by which a material will radiate or receive infrared energy. Thermal emissivity is a surface characteristic of a material and to some extent a function of material color. For example, a highly polished light-colored material will have low thermal emissivity and a dark-colored, high-surface-roughness material will exhibit a high thermal emissivity.

When an electronic component is mounted near a high-temperature surface, the heat absorbed by the component may be reduced by using materials and finishes with low thermal emissivity.

Emissivity control is of key importance for electronic equipment used in spacecraft and which may face the sun or be in shadow. Low-emissivity materials, such as plating an equipment case with polished gold, are used to limit the heating from the sun and also to reduce heat loss when the equipment is facing dark space.

If thermal emissivity is a design requirement, the selected material may be chosen for some other dominant criteria and control of thermal emissivity is achieved by surface finish selection, to include application of an electrodeposited highly emissive metal on the exposed surfaces of the part.

Painting a surface with a light-colored paint may slightly lower the emissivity; however, the roughness of a painted surface increases its effective area, which will impact more than the color of the paint. As a result, the emissivity of a painted surface is often essentially the same regardless of paint color, and thus the improvement is minor. Coating a dark, polished surface with a light-colored paint often leads to higher emissivity, not lower emissivity.

### ***Thermal Expansion***

The *coefficient of thermal expansion* is a material property which allows the electronic packaging engineer to predict the linear or volumetric change (expansion or contraction) of a material when the material is exposed to a change in temperature.

It is important to determine the coefficient of thermal expansion for materials which are bonded or mechanically secured together. For example, a ceramic component (very low coefficient of thermal expansion) soldered to a printed circuit board (a higher coefficient of thermal expansion) exposed to repeated temperature cycles, perhaps caused by turning the equipment on and off, can lead to solder joint failure. As another example, when two materials of different thermal expansion characteristics are mechanically joined and exposed to a temperature change, one material will be placed in compression and the other material will be placed in tension. This will result in the composite assembly bending in the direction of the material placed in tension. Also, depending on the relative strength of the materials, one or the other material may fracture or the joining method (adhesive joint, solder joint, weld, rivet, screw, etc.) may fracture or otherwise be degraded. Thermal expansion is a consideration when precise mechanical position is required. Thermal expansion will cause a change in the relative position of parts during a change in temperature. This movement may cause the loss of precise position and improper operation of the assembly.

### ***Chemical Inertness***

Materials may be exposed to potentially damaging chemicals during the life of a product. Such chemicals include fuels and lubricants, cleaning fluids, fluxes, and other chemicals used in industrial processes. Most tables which list material properties also provide limited information regarding chemical resistance. If the material is exposed to conditions not covered by information in the tables, then the designer must contact the provider of the material for additional information. It also may be necessary to experimentally determine and verify the suitability of a material in the presence of chemicals. It is important to note that chemical reactions are affected by temperature and the presence of other chemicals.

**Table 1** Galvanic Series Position of Common Electronic Materials

Most anodic (corroded end) (+) positive end	Magnesium and alloys Zinc Aluminum 1100 alloys Cadmium Aluminum 2024 alloys Steel, iron, cast irons Type 304 and 316 CRES (corrosion-resistant steel) (active) Lead–tin solders Lead Tin Nickel (active) Inconel (active) Brasses, copper, bronze Monel and copper–nickel alloys Monel Silver solder Nickel (passive) Inconel (passive) Type 304 and 316 CRES (corrosion-resistant steel) (passive) Silver, gold, platinum Titanium
Most cathodic (noble end) (-) negative end	Graphite

Source: Ref. 7.

Chemical deterioration may be induced by ionizing radiation (which alters the molecular structure and thus the physical properties of materials) and ultraviolet radiation (such as from sunshine), which may cause depletion of plasticizers from elastomers, such as polyvinyl chloride (PVC) plastic, which is used as wire insulation material, thus eventually rendering the material brittle and weak.

### **Corrosion**

Most tables of material properties provide information of corrosion resistance; however, this information may not be sufficiently complete to give confidence regarding the intended usage of a material. This may (for metals) include susceptibility to intergranular or stress corrosion cracking in the presence of certain acids or bases. For all materials, and especially nonmetals, corrosion deterioration includes processes similar to those identified regarding the chemical inertness of a material.

The process of galvanic corrosion<sup>4</sup> is a primary concern to the electronic packaging engineer. Under certain conditions galvanic corrosion is a leading cause of loss of electrical conductivity or loss of strength in a material or at a riveted, bolted, or welded joint and as failure (perforation or delamination) of electroplated finishes.

Table 1 lists the galvanic series relative position of several materials used in electronic packaging.

Galvanic corrosion is the result of an electrochemical reaction which occurs when a design (which employs mating metals ranking at different levels on the galvanic chart) is in the presence of an electrolyte (i.e., saltwater, contaminated water, or other conducting chemicals). One material acts as an anode and the other as a cathode as in a simple electrical storage cell. The result is ionic migration during which the anodic element suffers sacrificial deterioration. This is

a mechanism for leaching elements from grain boundaries and a corresponding weakening of the affected material and other undesirable effects. This process may be hastened or hindered by passing a small electrical current through the affected area.

### ***Temperature Range***

The operating and storage temperature ranges experienced by a material must be known and the properties of the material must be reviewed for stability over the range of temperatures. This is important for all materials, including metals when the temperatures are very high or very low. Metals and nonmetals will become brittle and stiff at lower temperatures and may soften, lose strength, and creep or flow at elevated temperatures. This is especially true with non-metallic materials, where the operating temperature range is limited due to undesirable changes in material properties.

### ***Strength***

A guide to the load-bearing capacity or strength of a material is its tensile strength, which for many metals is a function of alloy selection and heat treating (i.e., is the material annealed, half hard, or hard?). Strength of nonmetals (plastics) varies significantly with temperature and the rate at which a load is applied (impact strength). Weight reduction is achieved in electronics by using smaller quantities of high-strength materials for forming brackets, structures, and fasteners.

### ***Density***

Density is the weight of a material for a given unit of volume. This property may be used as a guide to reducing weight in a design. Material density establishes the inertia and resonant frequency of mechanical elements and thus the degree to which they are affected by mechanical vibration and mechanical shock loading. Another indicator of the density of a material is its specific gravity, which is a comparative ratio of the weight of a material compared with the weight of an equivalent volume of water.

### ***Electromagnetic and Electrostatic Shielding***

*Electromagnetic shielding* is employed to prevent the imposition of electrical waves from the environment (such as radio waves) on circuit elements, thus inducing currents and voltages and leading to circuit performance failure and possible component damage.

*Electrostatic shielding* is employed to prevent penetration of high-voltage charges on the surface of an electronic enclosure (such as caused by static discharge) from entering the enclosure and therein causing damage to components or circuit performance malfunction.

Protection of equipment from both of these sources of potential performance deterioration involves shielding the equipment, such as preventing radio waves or other electromagnetic noise from entering the enclosure, shielding the equipment to promote the collection of static charges on the surface of the equipment, and dissipating the unwanted energy by providing a conductive path to drain the energy to an appropriate sink (ground).

A circuit may be shielded by housing it in a conductive enclosure, thus creating a Faraday cage, where the imposing electromagnetic waves or static charges cause currents in the skin of the enclosure which do not penetrate into the enclosure. An example would be to shield a high-gain amplifier circuit and avoid malfunction of that circuit when the equipment is exposed to radio waves.

Conversely, essentially identical techniques are used to contain radio wave emissions from a circuit and prevent the radio waves from escaping the enclosure and causing malfunction in other equipment which may be susceptible to such emissions. High-speed digital

circuits at speeds of 10 kHz and above are known to cause such emissions and often require electromagnetic shielding to meet the emission requirements set forth by Part 15 of the Federal Communications Commission Rules and Regulations.<sup>5</sup> Nonmetallic enclosures are sometimes used to shield internal circuits and components from the electromagnetic field by coating the enclosure with an electrically conductive paint.

The primary guide to the effectiveness of a material as an electrostatic shield is the electrical conductivity of the material.

### ***Magnetic Shielding Properties***

Magnetic shielding pertains to protecting a circuit from the presence of fluctuating magnetic field energy which may induce currents in wires and metal structural elements and lead to circuit malfunction or failure. A simple Faraday shield such as used for electromagnetic wave or static discharge protection will not suffice for protection from magnetic fields. It is usually necessary to restrict the shielding materials to alloys of iron. Iron-bearing alloys tend to block penetration of magnetic flux into the equipment. Magnetic flux may induce noise within a circuit, which may cause malfunction of a circuit, including erasure of memory from several classes of memory storage devices or the introduction of false pulses or blockage of pulses in digital circuits.

### ***Fatigue Resistance***

Fatigue is the loss of physical strength and eventual failure of a material due to the material being subjected to repeated loads. Such loads may be the result of thermal expansion stresses which occur during temperature cycles, mechanical loads induced during the operation of the device, shipping and handling stresses, exposure to vibration, and repeated mechanical impact shock loads.

Repetitive loads well below failure-inducing loads are known to cause small incremental damage, and that damage will accumulate until the material fails.<sup>6</sup> Fatigue resistance may be judged on a relative basis by referring to tables of fatigue resistance, which relate stress levels to time to failure for a specific material or alloy under ideal conditions such as rotating beam test data.

The actual ability of a component to withstand fatigue damage is highly sensitive to the loading history, the precise shape of the component (i.e., stress risers), equipment construction details, and variations in temperature. As a result, proof testing is usually required to verify the ability of the selected material and design configuration to avoid excessive fatigue damage.

### ***Hardness***

Hardness is taken as the ability of a material to resist denting as caused by a load bearing on the material using a dimensionally standardized probe. There are different scales by which hardness is measured; the most common are the Brinell hardness number and the Rockwell hardness number for a given Rockwell scale.

Material surfaces are sometimes hardened to reduce wear in mechanical latches, sliding surfaces, and electrical contacts. The lubricity properties of polymers such as nylon and Teflon are used to reduce friction in applications such as drawer slides where a plastic material is used to rub against a hard metal surface.

The hardness of a material is often established by the surface treatment of the material and is not always a bulk property of the base material. That is, the surface of steel and aluminum and many other materials may be chemically or physically hardened to improve the wear of the part under design. The ability of a material to be surface hardened varies widely among materials, with many materials lacking the ability to be surface hardened.

***Ductility***

The ductility of a material refers to the ability of the material to be deformed without breaking. Extreme examples would include tin (very ductile) and glass (brittle and thus not ductile). This is an important property for materials which are to be mechanically formed, which are to be subjected to bending stresses during use, and which must withstand impact shock loading without cracking or shattering.

A guide to ductility of a material is its elongation, which refers to the degree to which a material will deform under load without failing. Elongation is seen to vary with the extent to which a material is heat treated. Ductility in plastic materials is strongly affected by temperature. For example, a plastic gear may work well at room temperature, but at low temperatures it may become brittle and fracture under load. Material ductility often varies widely within a given general class of materials and each individual material must be reviewed for ductility.

Closely related to ductility is the material's malleability, which is the ability of the material (usually metals) to be shaped by stamping, spinning, cold heading, upsetting, rolling, or other physical process involving deformation of the basic material in solid form. A malleable material is one which may be physically formed without tearing, cracking, fracturing, or developing surface defects. Tables of materials properties often provide guidance relative to malleability, and subcontractors who provide metal-shaping services are a good source of information on malleability.

***Wear Resistance***

Wear resistance is a property of materials which does not often appear in tables of material properties. A guide to wear is hardness—the harder and smoother the material, the greater its resistance to wear. Ductility should be considered as a material may become brittle at low temperatures and exhibit surface fractures and fretting under load. Wear life is a function of the magnitude of load-induced localized compressive stresses and the methods, such as lubrication, used to reduce friction. Some nonmetallic materials, such as nylon, are self-lubricating and useful as bearing materials.

***Sublimation***

Sublimation is the loss of material when the material is exposed to low pressures (vacuum) and or elevated temperatures. It involves the conversion from solid form immediately to gaseous form apparently without passing through a liquid phase. Sublimation may occur to the surface of a pure material, or if the material is a more complex matrix, one or more constituent materials may sublime, leaving a residual material possessing poor mechanical or electrical properties.

Sublimation may also result in the deposition of the sublimated material onto other, often cooler surfaces where the presence of the sublimated material is not desired (i.e., perhaps forming a conductive film causing circuit elements to short or reducing visibility through a window). Information on sublimation is limited and may require inquiry to the manufacturer of a material or to experimental test data.

Sublimation is of critical importance when the electronic packaging engineer selects materials which will be subjected to low-pressure and low-vacuum environments such as for electronic equipment for use in test equipment or in space vehicles.

***Combustibility***

Combustibility is the property of a material, under a given set of conditions, to oxidize or burn, which may range from the ability to burn but not sustain flame when the ignition source is removed to burning and sustaining flame after the ignition source is removed. Combustion may lead to the generation of noxious gases and destructive deterioration of the circuit elements in the vicinity of the combustion.



This property is most often associated with plastic and organic materials; however, some metals will burn in the presence of oxidizing gases or chemicals. Many tables of plastic material properties do not include information on combustibility; however, this information is usually available from the manufacturer of the material. If combustibility is to be prevented in a design, it is sometimes necessary to conduct tests to determine if a potential material is suitable for the intended application.

### ***Creep***

Creep is the ongoing deformation (flow) of a material when that material is subjected to a mechanical load. Failure due to creep is often very slow, and creep may occur only during certain conditions (such as a solder-sealed case which is sealed at sea level but operated in an aircraft or the same case operating at seal level but within which the internal pressure is increased due to heating during normal operation of the equipment). It is good design practice to never place such a soldered joint in sustained mechanical stress for the reason that the solder will creep until the stress is relieved or the joint fails. The design of a mechanical joint where solder is employed (e.g., to achieve an enduring electrical connection or to seal a joint) must have the mechanical load taken by structural members without the solder present. Mechanical joints or seals which utilize adhesives, elastomers, and other nonmetallic materials must be treated in the same way to avoid eventual failure.

A creep failure may not become evident for days, weeks, or even years, but it will happen if materials with the known ability to creep are improperly incorporated into a design.

Creep is not only a characteristic of some metals; it is also a property of several inorganic or organic materials. An example would be the loosening of a mechanical joint where the joint consists of metallic elements bolted together and includes a nylon washer. This joint eventually loosens when the nylon washer creeps to relieve the initial clamping stresses. Another example would be when a compressible gasket made of a material which will creep is used in a flanged joint where the joint does not have mechanical stops to control the separation of the flanges when the bolts are tightened. In this case the joint will eventually suffer loosening and possible leakage when the overcompressed gasket creeps to relieve the joint compressive forces. A classic example of a creep-induced failure occurs when an insulated wire presses against a hard metallic object such as the edge of a bracket or panel. In this case, the insulation will creep until the inner conductor of the wire eventually makes contact with (shorts to) the metal object.

### ***Moisture Absorption***

In many instances, when a material is selected for use as an insulator or the material must have dimensional stability in humid environments, the moisture absorption characteristics of the material are important. For metals, moisture absorption is not a significant consideration; however, the presence of moisture will hasten galvanic corrosion when different metals are in intimate contact.

For nonmetals, porous sintered metal structures, and ceramics, moisture absorption is a significant consideration. The absorbed moisture may cause corrosion and lead to failure by expanding within the material at cold temperatures. For materials used as electrical insulators, the insulator may become electrically conductive when moist. Hydrophobic materials (water-resisting materials, the surface tension of which causes water to bead and not wet the surface of the material) are preferred for insulator applications.

Most nonmetallic materials are tested for moisture absorption and the results of these data are found in many listings of material properties. The majority of moisture absorption data relate the absorption of water over a specified period of time.

In some cases, particularly for organic materials, moisture absorption leads to a loss of strength and physical deterioration. If some materials become wet and are subsequently allowed



to dry, they may exhibit permanent shrinkage and the inability to redevelop their original physical characteristics.

The chemical absorption properties of seals, paints, tubing, gasket materials, and plastic materials which are expected to be used in applications involving chemicals (oil, gasoline, fuels, alcohol, cleaning solutions, etc.) most likely have been investigated, and the materials supplier is usually able to provide test data and guidance in the selection of an appropriate material.

During conditions of high humidity and moisture in the presence of inorganic salts, conditions are created which encourage the growth of fungus. Fungus growth can lead to material degradation in appearance and loss of strength and the development of undesirable electrical shorts. Materials are generally categorized as fungus nutrient or fungus resistant. Materials such as metals, glass, ceramics, mica, silicone resins, asbestos, acrylics, diallyl phthalate, and a limited list of plastic resins are fungus resistant. Materials containing organic constituents, rubber, cellulose acetates, epoxy resins, many lubricants, medium- and low-density polyethylene, polyvinyl compounds, formaldehyde compounds, and others are fungus nutrient. The above listing is far from complete, and the designer is cautioned to verify the fungus-nutrient characteristics of any materials used in a design.

## 2.2 Typical Applications

### *General*

An important guide to materials selection is found by considering how materials have been used for similar applications. Electronic packaging applications often fall into one or more of the following categories:

- Equipment attachment
- Equipment racks, frames, and mounting structures
- Equipment and module enclosures
- Temperature control
- Mechanical joints
- Finishes
- Position-sensitive assemblies
- Electrical contacts
- Harsh-environment endurance

### *Equipment Attachment*

Other than desktop and portable equipment, electronic equipment is usually mechanically fastened to an equipment rack, frame, shelf, or mounting structure. These devices may sit on the floor in an equipment room or are bolted [using high-strength Society of Automotive Engineers (SAE) rated fasteners] or welded to the structure of the containing building or vehicle. The attachment may consist of, for relay rack-mounted devices, passing two or more bolts through holes in the equipment front panel into threaded fasteners in the rack frame. For equipment used in aircraft, ships, and vehicles, industry standard ARINC Air Transport Rack (ATR) modular cases are placed on an equipment shelf and are secured thereto. The ATR module mounting usually consists of an engagement device (pins fitting into holes) in the rear of the module and brackets with retained thumbscrews or latching hook arrangements at the lower edge at the front of the module, including a device fastened to the shelf into which the screws or latches engage. Larger equipment used in moving vehicles, such as tanks, battleships, and trucks, where the equipment must be protected from higher levels of vibration and shock loading, mounting often involves bolting the equipment to a frame, which incorporates energy-absorbing dampers, and

bolting the frame to the structure of the vehicle. For consumer goods applications (car radios and CD players, motorcycle and bicycle electronics, etc.) a variety of mounting configurations are employed, some which feature quick release of the attached equipment.

Each application places similar requirements on the materials used for attachment. The dominant considerations are strength, wear resistance, corrosion avoidance, temperature range, and fatigue resistance. The materials are often selected from the steel family to achieve a favorable strength-to-weight ratio. For mounting bolts to fasten commercial goods and other equipment used in relatively benign environments, cadmium- or nickel-plated steel hardware is used. If the mechanical loads are severe, then higher strength SAE-grade steels must be used. For more corrosive environments, stainless steel (usually passivated) is employed. For aggressive high-stress applications where corrosion and wear are a concern, fastening devices and brackets are made from precipitation-hardened stainless steels which are passivated to prevent corrosion.

### ***Equipment Racks, Frames, and Mounting Structures***

Equipment racks, frames, and mounting structures such as an equipment shelf are designed to bear the weight of electronic equipment mounted thereto. The dominant considerations are strength, wear resistance, corrosion, electrical conductivity, and corrosion avoidance. The materials of preference include heat-treated high-strength aluminum (such as 6061-T6) and mild steel materials. The aluminum materials are almost always either anodized or treated (chromate dip or similar) and painted for appearance and protection from the elements. Steel materials are protected from rust by nickel, zinc, or other electroplated finish and often by a rust-resistant paint. Stainless steel parts may be passivated to improve resistance to corrosion.

### ***Equipment and Module Enclosures***

Enclosures are the cases or boxes which house electronic equipment. Dominant considerations include operating temperature range, electromagnetic and electrostatic shielding, magnetic shielding, strength, wear resistance, thermal conductivity, appearance, corrosion resistance, and chemical inertness.

Materials used for enclosures vary with the application and end-user market. They include both metal and plastic materials. Cost containment, ease of fabrication, and appearance are often the overriding considerations.

When electromagnetic, electrostatic, and magnetic shielding protection is not required, plastic materials are often used to fabricate enclosures. Aluminum and steel materials may be utilized to achieve electrostatic and magnetic shielding protection. If magnetic shielding protection is required, iron-based materials are required, and the material of choice is usually steel. Metal cases are almost always protected against corrosion and other environmental damage by a finish treatment, sometimes followed by paint to achieve a suitable appearance.

Plastic materials may be used to build cases for electromagnetic and electrostatic protecting enclosures if they are coated internally with a conductive paint which may bear either silver or nickel powder. Enclosures fabricated from plastic usually do not require application of paint, chemical treatment, or other surface protection. Another dominant consideration for plastic cases is combustibility because many plastics will burn and emit noxious or toxic fumes when exposed to high temperatures.

### ***Temperature Control***

Temperature control is directed at maintaining electronic component temperatures within prescribed limits. This is accomplished by the proper selection and application of materials which are used to conduct heat from or to the components.

The primary modes of heat transfer are conduction, convection, and radiation. The dominant considerations for heat transfer material selection include thermal conductivity,

chemical inertness, resistance to corrosion, and sometimes wear resistance, sublimation, thermal expansion, and the ability to resist ionizing and ultraviolet radiation.

Conduction heat transfer involves the flow of thermal energy through a material from a heat source (component) to a heat sink. The design goal is to reduce the resistance to heat flow between the heat source and the heat sink. The effectiveness of heat transfer within a material is measured by its thermal conductivity. Metals such as silver, copper, and aluminum are good heat conductors; however, aluminum is most often used because it tends not to tarnish, is easy to form, and costs less. Copper or copper alloys are used when large amounts of heat are to be transferred and any small improvement in thermal conductivity is meaningful in the design.

When the design requires electrical insulation and good thermal conduction across a joint between two materials, thin layers of mica, silicon-impregnated cloth, and ceramic materials are often used. The thermal conductivity of these joints may be enhanced by applying a thermal grease to the joining parts to prevent the entrapment of air or other gas (a thermal insulator) between the mating surfaces.

Convection heat transfer involves the movement of heat between one material (usually metal) to a surrounding material such as a gas (air) or a liquid (water, Freon, etc.). A convection design seeks to conduct heat from a heat source into a physical configuration, such as fins, which presents a relatively large area of contact between the metal object and the gas or liquid with which the heat is to be exchanged. Good thermal conductivity is very important; so is strength and resistance to corrosion. Convection heat sinks are often made from high-strength aluminum alloys to meet these requirements. For resistance to corrosion, which may result in the formation of a thermally insulating film between the heat transfer media, the aluminum heat sink is sulfuric acid anodized black in color to also enhance heat transfer by radiation.

Convection heat transfer may be improved by mechanically moving cooling gas over the heat sink fins. This is called forced convection, and by using forced convection, the cooling effects of the heat sink may be greatly improved. Of course, forced convection is only effective when an atmosphere is present, and the ability of the forced convection design to handle a given heat load is strongly affected by the density and pressure of the cooling media.

Radiation heat transfer is the primary mode of heat transfer when considering space applications. Radiation at sea level can contribute 10% or more of the total heat transfer process depending on the temperature gradient and distance between the radiating and receiving objects. Radiation heat transfer applications feature use of thermally conductive materials to transfer heat to radiating surfaces. The effectiveness of the radiation surface emissivity is dependent on the finish applied to those surfaces. For materials which are to reduce the reception or reduce the ability to emit heat, the surfaces are smooth and shiny. Such surfaces are often electroplated with a material such as gold, chromium, or nickel which is chemically inert and may be buffed to a very high gloss. For materials for which the design requires effective heat absorption or emission, the material surface is not smooth (increasing surface area) and is usually black or another dark color. This is achieved on aluminum surfaces by application of a black sulfuric anodize finish such as used on the internal elements of solar collector devices.

Paint on a surface adds a layer of insulation and thus is an impediment to radiation heat transfer. Due to the surface roughness of painted surfaces, the color of the paint usually makes only small differences in surface radiation emissivity; however, a light-colored (white) paint will be somewhat less efficient at radiation heat transfer than a dark (black) paint under extreme thermal loads. Plastic and ceramic materials are not effective radiation heat transfer materials and may be employed as surface insulators to reduce the effectiveness of radiation heat transfer.

### ***Mechanical Joints***

Mechanical joints are structural attachments within an electronic rack, enclosure, case, shelf, or housing and are material sensitive. Mechanical joints may be either permanent or semipermanent. A permanent mechanical joint could be brazed, welded, adhesively bonded,

chemically joined, riveted, or mechanically upset. Semipermanent mechanical joints involve the application of mechanical fasteners and permit the mechanical joint to be attached and detached during service.

Mechanical joints may involve two or more metal elements, two or more nonmetallic elements, or a mixture of both metallic and nonmetallic elements.

For metallic fused joints the metals must be suitable to the joining method, and filler materials which are carefully selected achieve the joint, such as welding rod alloy materials or brazing materials. The dominant considerations include temperature range (will the material properties be altered by the temperatures required by the fusing process?), relative thermal expansion to avoid residual stresses, and avoidance of materials which in combination will lead to galvanic corrosion. If the metals gain their strength properties by being heat treated after forming, the joint materials may require annealing prior to fusing and heat treating after fusing.

Soldering metal parts together using conventional electronic lead-tin or lead-free solders is not a valid method by which to form a mechanical joint. Solder will creep under mechanical load, and if the mechanical load is continuously applied, the soldered joint will eventually creep to failure. Solder is a valid method for electrically bonding and environmentally sealing mechanical joints, such as riveted joints, which are designed to carry mechanical stress without the presence of the solder and where the solder is used for bonding or sealing and is not used to carry mechanical loads.

Nonmetallic (plastic) material joints may be formed by thermal bonding or ultrasonic welding identical formulations together (thermoplastics only) or by chemical fusing agents as recommended by the plastics manufacturer.

Mechanical joints involving a variety of materials (i.e., both metals and plastics) require careful materials selection, and the dominant characteristics of interest include thermal expansion, corrosion, creep, temperature range, and electrical conductivity.

### ***Finishes***

The majority of metallic materials and many plastic materials require the application of a surface finish to enhance resistance to corrosion and to provide an attractive appearance. Dominant considerations regarding application of material finishes include electrical conductivity, thermal conductivity, thermal expansion, chemical inertness, temperature range, wear resistance, emissivity, sublimation, and moisture absorption.

Aluminum materials used inside equipment are usually chemically cleaned and chromate conversion coated. Chromate conversion coating is also used as a surface treatment which promotes improved adhesion of paint to the aluminum. Chemical-film-coated aluminum passes electrical signals and may have an electrical conductivity greater than the base aluminum. These coatings are easily scratched and have poor abrasion resistance.

Anodizing of aluminum creates a wear-resistant and sometimes attractive finish that consists of a thin layer of aluminum oxide. This oxide film is an electrical insulator and may cause a problem if the part is to pass electricity to another component. Sulfuric acid anodize is used to provide protection from corrosion, causes very little thickness growth to the base metal, works well for dyed applications, and is avoided if the design has overlapping surfaces where the acid may be trapped during the anodize process. Chromic acid anodize is preferred when small-dimensional change is necessary for highly stressed parts or on assemblies that could entrap processing solution. Hard anodize provides an extremely hard finish with excellent abrasion resistance and poor electrical conductivity. Hard anodize coating is brittle and will crack should the anodized part be flexed. In addition, hard anodize causes a loss of strength because for 0.04 mm of film thickness, 0.02 mm of the underlying material is lost. In addition, the anodize thickness increases the part dimensions by about half the thickness of the film.

Aluminum may be electroplated to achieve a variety of properties, such as plating with a thin layer of gold over copper to achieve a low thermal emissivity or selective plating of the surface with tin to permit the solder attachment of an electrical conductor to the aluminum part. The entire part should be plated for maximum protection, and voids in the plating will expose the base material and thus may establish conditions for galvanic corrosion.

Steel parts must be protected from oxidizing (rusting) in the presence of even small amounts of moisture or humidity. Steel is usually protected by plating with nickel or zinc for fasteners and with tin when used as an electronic equipment chassis to which electrical connections are required. Nickel plating and chrome plating are used on steel parts to improve resistance to wear and to provide an attractive appearance. Cadmium plating is used extensively to protect steel against corrosion; however, it is limited to use below about 230 and is known to sublimate under vacuum conditions. Other treatments such as black oxide coating and phosphate coating offer alternative approaches to protection of steel surfaces.

Caution is required when a metal is electroplated with another metal. The two materials differ in coefficient of thermal expansion, which may promote delamination of the plating from the base metal when the composite is subjected to thermal cycles. Also, the further apart the materials are listed on the galvanic series, the greater the opportunity for galvanic corrosion to occur. This latter consideration will require the addition of protective coatings (paint, adhesives, etc.) at any location where the plating is removed and both the plating and the base material are exposed to the environment. Aggressive mechanical fastening techniques, such as the use of star-type (shakeproof) lock washers in a bolted joint, may cause local failure of the plating and eventually lead to joint failure (a loss of electrical continuity, mechanical strength, or both) by corrosion.

Stainless steel parts used in electronic applications are passivated to remove surface contamination and to form a uniform protective oxide film that assures that the material delivers maximum resistance to environmental contaminants.

Other commonly used metals, such as beryllium–copper, bronze, and brass, also must be protected and may be treated by processes similar to those used to protect steel.

Plastic materials may require finish treatments such as electroplating to achieve surface electrical conductivity or a metallic finish for appearance purposes such as applying chrome on a knob or bezel or other like application. Not all plastics may be painted due to the inability of commonly used paints to adhere to the plastic surface. The surface texture of thermoplastic parts may be given an attractive matte finish by vapor blasting.

### *Position-Sensitive Assemblies*

Position-sensitive assemblies include devices the operation of which requires an invariant physical relationship between components over the range of temperatures to which the electronic product will be exposed. One example would be an antenna coupler or filter wherein the electrical circuit resonance frequency of the antenna coupler is determined by the length of protrusion of a cylinder (tuning element) into a cavity. The protrusion distance is varied by the equipment operator to be proper for each specific operational frequency and, once set, must be maintained within less than a millimeter over a significant temperature range. A second example would be a variable-frequency tank circuit which after being adjusted must maintain precise values of inductance, capacitance, and resistance over a range of temperature. A third example would be an electronic structure featuring panels or structural elements fabricated from different materials but attached together that must not be allowed to deform when subjected to a change in temperature.

The dominant consideration is the thermal expansion of the materials involved. Some materials, such as Invar, a nickel–steel alloy, and structural ceramics, have a very low coefficient of thermal expansion and are used to facilitate the design of critical positioning mechanisms.

### *Electrical Contacts*

Electrical contacts in electronic applications usually consist of switch contacts and connector contacts. The requirement for each are similar; however, the usage varies in that the switch contacts may be frequently operated and the connector contacts are rarely engaged or disengaged.

Materials selected to make electrical contacts depend substantially upon the amount of electrical energy that the contacts must carry. The dominant considerations for selecting contact materials include electrical conductivity, chemical inertness, corrosion resistance, and wear resistance. Electrical contacts are usually made from metal materials; however, in unusual instances where a low electrical conductivity is not required, conductive plastics (plastics loaded with carbon or metallic particles) are employed. Sometimes a metal contact will ride upon a nonmetallic contact such as in a carbon composition potentiometer.

Connectors which must maintain reliable electrical contact over extended periods of time are often designed to produce high contact forces between the contacting elements. High contact forces result in significant mechanical erosion of the contacting materials whenever the connector is engaged or disengaged and can seriously decrease the number of uses of the connector. Connector engagement is beneficial because the mechanical action of the contacting materials sliding over each other tends to remove surface films and corrosion and thus lead to a lower contact resistance. This lowered contact resistance will last until the contact resistance is increased due to the formation of chemical films or corrosion products.

Contacts which are required to carry (make and break) very low electrical current, such as complementary metal–oxide–semiconductor (CMOS) level signals, are known as “dry contacts.” Dry contacts are fabricated using inert metals or metals plated with an inert metal such as gold or rhodium upon which surface film formation is inhibited. Silver contacts and lead-based metal contacts are not used because they tarnish and the tarnish film is a poor conductor of electricity and thus induces resistance in the switched circuit. Long-term resistance to environmental chemicals is sometimes improved by coating the contacts with protective grease or other media.

Circuit contacts where the circuit carries higher levels of current provide greater freedom in selection of contact materials because the current flow is adequate to dispel the tarnish and other films that may form on the contacts. These contacts are often made from beryllium–copper, silver alloys, lead–tin alloys, nickel, rhodium, and other materials.

Dominant considerations for connectors include electrical conductivity, chemical inertness, prevention of galvanic corrosion, hardness, and wear resistance. Many of the same materials used for switch contacts are used for connector elements, but with more emphasis on wear resistance and chemical resistance. It is necessary to prove electrical contact performance for switches or connectors by extensive life testing with the primary variables being contact force and material hardness.

### *Encapsulation*

Encapsulation or potting of an electronic component or subassembly is utilized to promote ruggedness, resist harsh environments, provide electrical isolation, and promote improved heat transfer for cooling of the encapsulated components. Encapsulation is also used to seal an assembly to protect proprietary design details from the curious.

A variety of material properties must be considered when selecting an encapsulant. Sometimes the requirements are inconsistent with the range of properties offered by any one material. Of interest are the ability of the material to flow freely and not capture or entrain air bubbles; be lightweight; offer acceptable electrical, thermal, and chemical properties; and resist cutting and abrasion after cure. During cure the material should not produce excessive temperatures or excessive stresses on the encapsulated parts. After cure, the material should not absorb moisture, not produce excessive forces during temperature cycles, be stiff enough to support components and connections, and be able to be removed for purposes of repair.



Some properties of the materials may vary during cure and for some duration following cure. An example would be dielectric strength which may not stabilize until several days after cure.

At least three primary groups of material formulations are used for encapsulation:

**Epoxy-Resin-Based Materials.** These materials may be formulated for strength and rigidity. The addition of glass microspheres would reduce density, and addition of metal or other powders will increase thermal and electrical conductivity. Epoxy resins are usually two-part mixtures and require strict control of the mixing, pouring, and curing processes.

**Silicon-Based Materials.** These materials are known for having an extended temperature range over which they do not degrade. They tend to remain flexible and are resistant to water. They are either one- or two-part formulations. Some formulations generate acetic acid during cure and may cause corrosion of parts and conductors. Cure time is a function of the thickness and mass of the encapsulant and may require more than one day to achieve full cure.

**Polyurethane-Based Materials.** These materials generally consist of a catalyst and resin and require mixing prior to pouring. They tend to remain flexible over a useful temperature range and after cure are of a rubberlike consistency; however, they have less tendency to adhere to components, wires entering the potted volume, and potting box surfaces than an epoxy or silicone encapsulant.

Epoxy polymers are used to provide low-cost, high-performance reliability without hermeticity to provide environmental protection for bare circuit chips when used in chip-on-board (COB), ball grid array (BGA), multichip module (MCM), and chip scale packaging (CSP) assemblies.

Data describing the properties of encapsulants may be found on manufacturers' data sheets; however, this information may be incomplete and sometimes does not relate physical properties to the method of cure and the material thickness. It is often necessary to consult with the technical support personnel of the manufacturer and to perform testing to determine suitability for the intended design goals.

### ***Harsh-Environment Endurance***

Environmental endurance is the ability of the selected material(s) to resist degradation when subjected to the service conditions faced by the equipment or device constructed from those materials. Unusually harsh operating conditions may cause the material selection process to focus on the ability of the material to resist the service environment before the designer considers other important desired material properties.

High-temperature environments require the use of metals, ceramics, and temperature-resistant plastics.

A highly corrosive chemical environment possibly involving strong acids or strong alkali vapors or solutions is resisted by some glasses, some ceramics, stainless steels, and some plastics.

Solar radiation creates heating of materials and degrades some plastics, such as nylon and PVC, which lose weight and strength when exposed to ultraviolet radiation.

Glasses, ceramics, and many metals react well in the lower pressures and vacuum conditions of outer space without sublimating or losing strength due to ultraviolet radiation exposure.

## **2.3 Candidate Materials**

### ***General***

With the dominant and overriding design considerations defined, the electronics packaging engineer is ready to survey general classes of materials for the purpose of identifying one or more candidate material for the design task under consideration.

One primary materials selection consideration is often the conductivity of the material, that is, whether the material is a conductor or an insulator of electrical signals and currents. Conductivity is an important characteristic (printed circuit traces, wires, etc.) and is often the reason that metals are the materials of choice. Other important characteristics of metals include strength, durability, thermal conductivity, and ability to work over a wide temperature range.

Nonmetallic elements may exhibit many of the characteristics of metals; however, they are used to provide electrical and thermal insulation. Other properties such as inertness to chemicals, dielectric strength, appearance, low cost, and ease of fabrication may lead to the use of nonmetallic elements.

Semiconductor materials may be employed to achieve, when properly formulated as in transistor junctions, the ability to become either an electrical conductor or an electrical insulator depending on the conditions of use.

Several major categories of materials exist from which the designer may identify subsets and specific materials for detailed review and selection.

### **Metals**

A guide to the electrical conductivity of a metal is its electrical resistance. Table 2 provides examples of materials listed by volume resistivity, where:

- Insulators are considered to have a volume resistivity of  $10 \times 10^6 \Omega \cdot \text{cm}$  or greater.
- Semiconductors have volume resistivity in the range of  $10 \times 10^6 \Omega \cdot \text{cm}$  to about  $10 \times 10^{-3} \Omega \cdot \text{cm}$
- Conductors are materials with volume resistivity of about  $10 \times 10^{-3} \Omega \cdot \text{cm}$  or lower.

Other selected properties of metals used in electronic packaging are provided in Table 3.

*Iron and Its Alloys.* Iron-bearing materials used in electronic packaging include various alloys of steel.<sup>7</sup> Steel materials<sup>8</sup> are strong and durable; however, they are subject to deterioration by oxidation (rust) and relative to other metals such as copper and aluminum are less efficient conductors of electricity and heat.

Steel alloys containing chromium, commonly referred to as “stainless steels” or CRES (corrosion-resistant steel),<sup>9</sup> resist oxidation and tarnishing and are often used in electronic packaging as fastener devices such as screws, nuts, washers, and other hardware. Some alloys of stainless steel are not magnetic, a property which is sometimes useful when used in conjunction with circuits which are sensitive to magnetic fields.

There are a wide variety of properties which may be developed for steel alloys, such as very high strength-to-weight ratios, hardness, wear, selective resistance to chemicals, the ability to be formed by mechanical cutting and shaping, and the ability to be joined by welding and brazing. Consumer goods electronic equipment chassis are sometimes constructed from tin-plated steel, which is a low-cost material that can be easily cut or formed and which may be soldered using conventional lead–tin electronic solders.

**Table 2** Materials Categorized by Resistivity

Conductors	Semiconductors	Insulators
Basic metals	Silicon	Ceramics
Metal alloys	Germanium	Elastomers
Metal-bearing compounds	Gallium arsenide	Gases
Plasma	Selenium	Glass
Some liquids		Solvents
		Thermoplastics
		Thermosets



**Table 3** Typical Properties of Selected Metals

Metal	Melting Point (°C)	Density, $10 \times 10^{-3}$ kg/m <sup>3</sup> (20°C)	Resistivity, $10 \times 10^8 \Omega \cdot \text{m}$ (20°C)	Thermal Conductivity W/m · K (0–100°C)	Thermal Expansion, $10 \times 10^6$ (1°C)
Aluminum	660	2.7	2.7	238	23.5
Antimony	630	6.7	42.0	17.6	8.11
Beryllium	1284	1.8	5.0	167	12.0
Bismuth	271	9.8	116	7.9	13.4
Cadmium	321	8.6	7.4	92.0	31.0
Chromium	1875	7.2	13.0	69.0	6.5
Copper	1491	8.9	1.7	393	17.0
Germanium	937	5.3	$>10 \times 10^6$	59.0	5.8
Gold	1064	19.3	2.3	263	5.8
Indium	156	7.3	9.1	81.9	25.0
Iron	1525	7.9	9.7	71.0	6.8
Lead	328	11.7	21.0	34.3	20.0
Lithium	179	0.5	9.4	71.1	55.0
Magnesium	650	1.7	4.0	167	26.0
Molybdenum	2595	10.2	5.6	142	5.2
Nickel	1254	8.9	6.8	88.0	13.4
Palladium	1550	12.0	10.9	71.0	10.9
Platinum	1770	21.5	10.7	71.0	9.1
Rhodium	1959	12.4	4.7	84.0	8.4
Silicon	1414	2.3	$>10 \times 10^{10}$	83.0	7.5
Silver	961	10.5	1.6	418	19.0
Tantalum	2985	17.0	14.0	54.0	6.5
Tin	232	7.3	12.9	65.0	12.0
Titanium	1670	4.5	55.0	17.0	8.9
Tungsten	3380	19.4	6.0	165	4.5
Uranium <sup>a</sup>	1130	19.0	29.0	29.3	23.0
Zinc	420	7.1	26.0	111	30.0
Zirconium	1860	3.5	45.0	20.0	5.9

<sup>a</sup>This table indicates the relative properties of various metals. Exact properties vary with alloy and temperature.

*Aluminum and Its Alloys.* Aluminum alloys<sup>10</sup> are commonly used in electronic equipment for manufacturing cases, chassis, covers, brackets, and other mechanical parts. Aluminum alloys range from being “dead soft” through alloys for which substantial strength and surface hardness improvements are achieved by heat treatment.

Aluminum alloys are subject to degradation by both acids and bases and are subject to galvanic corrosion when in contact with other metals. Aluminum is a good conductor of both electricity and heat. Common surface protection methods include iridite or chromate dip coating, anodizing, and painting.

Aluminum alloys are easily cut and formed by most mechanical methods. The softer aluminum alloys are very ductile and may be extruded, impact formed, rolled, or mechanically upset. Other alloys may be punched and formed to achieve a defined shape and then heat treated to achieve structural properties. Aluminum has a good strength-to-weight ratio and is used to achieve lightweight products. Commonly used aluminum alloy series include the following:

- 1100: Resists corrosion, good weldability, good conductivity, commonly heat treated, and used for sheetmetal parts, rivets, and other applications without high-strength requirements.

- 3003: Similar to 1100, except higher strength, more corrosion resistant, and used for heat exchanger fins and like applications.
- 5052: Excellent corrosion resistance, especially in marine environments, higher strength than 3003, and used for chassis parts, fan blades, and the like.
- 6061: A heat-treatable high-strength material used for structural parts.
- 356 series alloy: Used for cast aluminum parts. It may be heat treated and is used for sand, permanent mold, and investment casting processes.

*Magnesium.* Magnesium has similarities to aluminum. It is a good but slightly poorer electrical and thermal conductor with a high strength-to-weight ratio and is sometimes used in place of aluminum to effect weight reduction. Care must be taken when using magnesium because magnesium corrodes readily, is highly reactive to oxidizing chemicals, and in shaving and powder form will oxidize (burn).

*Copper and Its Alloys.* The primary attributes of copper are its low electrical resistance and low resistance to the flow of heat (high thermal conductivity). Copper is used for conductive traces on printed circuit boards, in wiring, and in switches and relays. Copper may be machined, formed, and cast. It is easily soldered by conventional lead–tin electronic solders. Copper will tarnish and usually requires surface treatment to avoid tarnishing in service.

Copper is heavy, soft, and ductile and thus is not a good structural material unless used in alloys with other materials such as beryllium. Beryllium–copper alloys are used for electrical contacts (improved wear) and are good materials for constructing springs and spring-type electrical contacts.

*Cadmium, Chromium, Nickel, and Zinc.* These metals are often used as an electroplated finish on iron alloy parts, such as fasteners, to improve the appearance of the parts and to achieve protection against galvanic corrosion.

*Gold and Silver.* Gold and silver are precious metals that exhibit very low electrical resistance and very high thermal conductivity. Both are used to electroplate connector, relay, and switch contacts to achieve low contact resistance, durability, and resistance to corrosion.

Gold is an inert metal and not given to forming nonconductive surface films over time and thus is a good candidate for “dry circuit” switching. (A dry circuit is one in which very low currents are involved, such as signals in a CMOS circuit. The low currents are insufficient to penetrate and dispel the effect of environmental-induced nonconductive films on the contacts. The result is a detrimental increase in contact resistance over time.)

Care must be used when silver is employed in a design as silver will easily tarnish, and when used as a switch or other contacts, this tarnish will create a nonconductive surface film on the silver part. Sulfur, such as found in brown wrapping paper, will quickly cause silver to tarnish. The application of antioxidant grease is used to protect electrical contacts fabricated from silver.

Both gold and silver are easily soldered using conventional electronic solders. When soldering to contacts which are silver plated, the solder will leach the plated silver from the wetted area, resulting in degraded electrical performance. As a result, a “silver solder,” containing approximately 2% silver, is used to prevent leaching.

*Lead and Tin.* Lead is very heavy and may be used to shield electronic components which are subjected to ionizing radiation.

Tin is a soft and ductile material, is substantially inert to the environment, and has lubrication properties. Thus tin may be used to electroplate electrical contacts in connectors to improve the mechanical mating of connector elements.

Used together, lead and tin are the primary constituents in the majority of electronic solder alloys commonly used in the electronic industry. Lead–tin solders vary in the ratio of lead to tin in the alloy, with 63% lead and 37% tin being a eutectic mixture featuring the lowest melting point of solder, and when cooling the entire mixture “freezes” at the same temperature, which leads to improved joint integrity, particularly regarding the attachment of parts to a printed circuit board. Another common solder mixture consists of 60% lead and 40% tin. This mixture melts at a slightly higher temperature; however, it exhibits higher mechanical strength in the solidified form and thus is used to attach wires to connectors and in other general applications.

The presence of lead in solder is believed to cause health risks, and lead-free solders<sup>11</sup> and lead-free conductive adhesives are being used in sensitive applications where lead must be avoided.

*Rhodium.* This metal has very good wear resistance and is used to coat electrical contacts subjected to repetitive usage, such as high-performance relay contacts.

*Titanium.* Heavier than aluminum but lighter than steel, titanium has a melting point comparable to steel, offers a relatively inert structural material with a high strength-to-weight ratio, and is difficult to weld. Titanium electrical resistance is about 20 times that of aluminum, and its thermal conductivity is one-fourth that of aluminum. Its coefficient of thermal expansion is nearly the same as that of steel. Titanium is used for weight reduction when high strength is required for equipment attachments, mounting structures, and cases.

### ***Plastics and Elastomers***

Plastics or organic polymers find extensive use in electronic applications.<sup>12</sup> There are two basic types of plastics: thermoplastics and thermosetting plastics. The difference between thermoplastics and thermosets is whether or not the plastic is completely polymerized at the time of manufacture (i.e., a thermoplastic) or whether the plastic is provided as a resin plus a hardener which must be mixed and polymerized when the plastic is formed into a component (i.e., a thermosetting plastic).

Plastics are commonly used in applications where electrical insulation is required or acceptable. Plastics are unable to operate over the temperature range of metals and are subject to softening at warm temperatures and become brittle at cold temperatures. The physical properties vary widely; however, plastics are used in the construction of many electronic components and may be used for equipment housings and appearance hardware. Care must be taken when soldering near plastic parts, as touching plastic by a soldering iron tip can cause local melting and deformation. Resistance to chemicals varies widely, as does moisture absorption and mechanical load-bearing capacity. Most plastics are subject to creep and must be employed where permanent deformation due to sustained loading is controlled or may be tolerated.

Plastic materials may be formed into component parts by a wide variety of methods, and the cost per unit for large-volume production can be quite low. Typical plastics used in electronic packaging applications are identified in Table 4.

*Thermoplastics.* Thermoplastic materials are available in sheet, granules, and powder and may be fabricated by transfer molding, injection molding, laminating, pultrusion, compression molding, filament winding, and pouring or casting. Thermoplastic materials can be softened by

**Table 4** Plastics Used in Electronic Packaging

Thermoplastics	Thermosets	Elastomers
ABS	Allyl	Natural rubber
Acrylic	Epoxy	Isoprene
Fluoropolymer	Melamine	Chloroprene, neoprene
Nylon	Phenolic	Ethylene-propylene
Polycarbonate	Polyimide	Fluorinated copolymers
Polyetherimide	Polyurethane	Butyl
Polyethylene	Silicone	Nitrile, Buna N
Polyimide		PVC
Polystyrene		Silicone copolymers
PVC		Polysulfide
		Polyurethane

heat and merged or shaped. The properties of thermoplastics may be modified by the addition of fillers or reinforcing fibers.

Acrylonitrile butadiene styrene (ABS) thermoplastics are tough and used to make enclosures, insulators, appearance sheet materials, and a variety of molded parts for electronic applications. They may be varied in color, but the temperature range is limited. Most applications of ABS thermoplastics are in consumer goods and other low-cost applications.

Acrylics may be used for conferral coating and in solid form are optically clear with very good weather resistance. They are temperature sensitive and will readily burn when exposed to flame.

Fluoropolymers are widely used in electronic applications due to the wide range of properties for which they may be formulated. They are high heat resistant, are inert to most chemicals, have essentially zero water absorption, have a low coefficient of friction, have high arc resistance, resist creep, and have low dielectric losses. Teflon, manufactured by DuPont, is an example of a fluoropolymer used for wire insulation, electrical insulation, low load bearings, and dielectric purposes. Fluoropolymers are expensive, relatively soft, and hard to process.

Nylon is a polyamide polymer which is tough and abrasion resistant with good mechanical strength. It is used in fiber form to make fabrics and in solid form to make gears, standoffs, low-pressure unlubricated bearings, wire ties, connectors, wire jackets, and like items. Nylon absorbs water and its dielectric strength and resistivity vary with the humidity of the environment to which it is exposed. Nylon will degrade when subjected to sunlight and will exhibit creep or cold flow under sustained loads.

Polycarbonate materials exhibit high impact strength, are optically clear, are flame resistant, and will perform in higher temperature applications. This material is used to make windows and other functional and appearance-related components. These materials absorb water and when under mechanical stress are degraded by many chemicals and solvents.

Polyetherimide polymer finds usage as fuse blocks, circuit board insulators, chip carriers, equipment housings, switch and circuit breaker housings, and like applications. It exhibits low dielectric losses, functions over a wide temperature range, has high radiation resistance, and withstands boiling water.

Polyethylene is an inert, abrasion-resistant olefin with low weight per unit volume and has very low water absorption. This material is used in molded form for discrete-component enclosures, battery cases, and like applications. In sheet or film form it is used as a dielectric in the manufacture of capacitors. It also is used as a vapor barrier and as insulation and sheath for wires and cables. When exposed to flame, olefins will burn.

Polyimide plastic materials are used for radomes, antenna housings, films, printed circuit boards, and connectors. They have high radiation resistance, have low coefficient of thermal

expansion, have high electrical resistance, are wear resistant, have a low dielectric loss factor, and resist high temperatures. They are chemically resistant but are degraded by hot caustic solutions and highly polar solvents. Hard to mold, polyimide shapes are formed by powder metallurgy and compression molding techniques.

Polystyrene has a very low dissipation factor of about 0.0001 and about a 2.4 dielectric constant and thus is used in foam insulation materials and in radio-frequency (RF) strip lines and similar applications. It is degraded by many solvents and chemicals and by modestly elevated temperatures.

PVC is used to build wire sleeves and jackets, tubing, and insulation due to its flexibility and resistance to most chemicals. It is sensitive to ultraviolet (sunlight) radiation, which causes it to become brittle and shrink. PVC use is restricted to temperatures below about 100°C, and it stiffens at temperatures below 0°C.

*Thermosets.* Thermoset plastic materials are supplied in the form of a resin and hardener, and the final polymerization of the plastic occurs during the final forming process. This final polymerization may be referred to as curing, hardening, vulcanizing, or crosslinking. Sometimes heat is required to complete or hasten the polymerization. The fabricator must be aware that the chemical process of curing involves the generation of heat by an exothermic reaction within the material, and this heat must be shunted away to prevent cracking and other deterioration. The material also shrinks up to 10% by volume during cure, thus having an impact on the configuration of the mold. The addition of fillers, pigments, and lubricants control shrinkage.

The allyl polymer family is characterized by good dimensional stability, having electrical insulation properties, the ability to withstand elevated temperatures, and good moisture resistance. A commonly used allyl is glass-filled diallyl phthalate, which is dimensionally stable and is used to make inserts in connectors, electronic parts, and housings and to form insulating standoff posts.

Epoxy materials adhere well and are used as adhesives as well as for potting, casting, and encapsulation purposes. The properties may be varied from flexible to rigid. The final weight, strength, thermal conduction, and thermal expansion may be modified by inclusion of filler materials. Epoxies are used to encapsulate circuits such as microcircuit chips in MCMs, COB, and conventional components in cordwood array packaging. Epoxy resins are used with glass fabrics and phenolic laminates to fabricate printed circuit boards and also for conformal coating, encapsulation, and adhesives and in forming durable paints and finishes.

Phenolic materials are used for high-temperature, high-mechanical-strength (relative to other plastics), low-cost applications. Phenolics are used to fabricate knobs, handles, connectors, and chip carriers in a laminate form to build small enclosures. Phenolics are not elastic and may fracture upon bending or impact loading.

Polyimide materials exhibit low outgassing and good radiation resistance and have very good high- and low-temperature performance. They must be used with care because they are sensitive to moisture and are degraded by organic acids and alkalis. Applications include bearings, seals, insulators, flexible cable, tapes, sleeving, moldings, wire enamel, chip carriers, and laminates.

Polyurethane materials are often used as paints, wire enamels, conformal coatings, embedding compounds, and foam dielectric and thermal insulation. Some polyurethane materials may be poured and used as an encapsulant to protect circuits from the environment. They exhibit elastomeric properties and have tear resistance, abrasion resistance, and unusual toughness. They can be degraded by strong acids and bases. The operating temperature range is limited and should not exceed 120°C.

Silicone-based materials have a wide range of general-purpose applications in electronic equipment. They may be formulated for use as sealants, elastomers, adhesives, paints,

conformal coatings, and encapsulants. They have a broad temperature range (40–250°C), have excellent arc resistance, are nonburning, and are water resistant when fully cured.

A commonly used silicone family is known as the room temperature vulcanizing (RTV) adhesives and sealants often used to waterproof a component or electrical joint. These products polymerize with water when curing and in the process release acetic acid in some formulations or ethyl alcohol in other formulations. In applications where the presence of acetic acid vapor would degrade circuit elements, such as switch and relay contacts, the RTV should be allowed to fully cure before sealing it within an electronic enclosure. Alternatively, if the presence of acetic acid on a component is a problem and ethyl alcohol may be tolerated, an RTV which does not exude acetic acid may be used in the design.

*Elastomers.* Elastomers are substances such as natural rubber<sup>13</sup> and polymers which have material properties which resemble rubber.<sup>14,15</sup> These substances have the ability to rapidly return to nearly their original shape after sustaining substantial deformation due to the application of mechanical stress and the release of that stress. Elastomers are employed as sealing gaskets and drive belts and find other uses that involve bending and recovery of shape.

Sometimes used for gaskets and power train or drive belts, elastomers are much more vulnerable to aging and environmental degradation than other plastic materials and must be selected with care. The designer is cautioned to consider material properties such as compression set, creep, loss of elasticity, fatigue failure due to repetitive load, loss of elasticity at low temperatures, strength at elevated temperatures, tear resistance, and tensile strength that may be degraded by exposure to ultraviolet and ionizing radiation, elevated temperatures, exposure to some lubricants and chemicals, and continuous mechanical stress.

### *Ceramics and Glasses*

Ceramics and glasses are used in similar ways in electronic packaging applications.<sup>16</sup> They have unique chemical, thermal, and mechanical properties. Both are primarily used as electrical insulators; however, glasses find a wider range of use to include substrates, capacitor and resistor bonding components, and equipment and component enclosure seals.

*Ceramics.* Electronic ceramic materials include electrical porcelains which have varied properties based on the amount of aluminum oxide incorporated into the material. Aluminum oxide is the additive of choice for ceramic materials for it improves mechanical strength, greatly improves thermal conductivity, and improves flexure strength. A concern, however, is that the use of aluminum oxide substantially increases the material coefficient of thermal expansion (about double that of silicon) and elevates the material dielectric constant. Ceramics are often bonded to metal substrates to perform useful electronic functions.

Other oxides may be used, such as beryllium (which is toxic) to achieve high thermal conductivity; aluminum nitride, which has a high thermal conductivity with thermal expansion nearly that of silicon; and boron nitride, which combines high thermal conductivity with machinability in a softer yet durable material.

*Glass.* Glass is an amorphous noncrystalline material that may be heated, even to a liquid phase, and formed into useful shapes. Glass performs like a liquid that has been sufficiently cooled to become substantially stiff and rigid. The inclusions of additives can substantially alter glass melting point, thermal expansion, and electrical properties. Glass may be optically clear, can be fused with other materials to make resistors and capacitor elements, and is vulnerable to impact mechanical loads and thermal shock loads that cause it to exhibit brittle fracture.

Soda–lime glasses are used to seal hermetic packages and to form insulator bushing for feedthrough devices.

Borosilicate glasses have excellent resistance to chemicals, high electrical resistance, and low dielectric constants and are used as binders for compounds associated with component construction.

Lead alkali borosilicate glasses have a lower melting point and are used for adhesive and sealing applications, including semiconductor processing.

Glass ceramics are machinable materials that may have strength twice that of ordinary silicon dioxide glasses. They have a crystalline structure with temperature stability lower than that of other glasses and may be shaped into a variety of useful configurations.

### *Adhesives*

Adhesives are materials that, by adhesion, cohesion, or molecular bonding, cling to the surface of another material. Adhesive materials used for electronic applications are most often derived from elastomers and plastic polymers. Glasses are used to perform adhesive functions when the elastomers and plastics have inadequate temperature range or are insufficiently inert to the product environment. Lead–tin solders are used as conductive adhesives in the application of surface-mounted parts to printed circuit boards.

Adhesives are utilized for structural bonding, to seal enclosures, to bond and protect components from the environment, to seal mechanical joints and thus prevent galvanic corrosion, to join parts for less cost than with mechanical means, and to join materials where the temperatures developed by processes such as brazing or soldering would degrade the bonded elements. The success of an adhesive application is at least as dependent upon proper joint design and application procedures as it is on the selection of a specific adhesive material. The primary requirements for achieving a successful adhesive joint include the following:

- The area of the adhesive overlap must be adequate to withstand the mechanical loads imposed in service.
- The mechanical loading generally should not provide peel or cleavage stresses on the adhesive joint.
- The adhesive must be able to wet and bond to the substrate material to which it is applied.
- The surfaces to be joined must be chemically clean and may require a properly applied primer.
- If the adhesive mixture consists of multiple components, these components must be accurately measured and properly mixed.
- Pressure, elevated temperatures, and positioning fixtures may be needed while curing the adhesive.
- The cure cycle may require several hours for the adhesive to gain full strength.
- The adhesive material must withstand processing and usage environmental temperatures and chemicals.

There are three categories of adhesive materials:

1. Structural adhesives—intended to hold two or more parts together under conditions where the adhesive joint is subjected to high mechanical loads
2. Holding adhesives—intended to permanently or temporarily hold lightweight items in place
3. Sealing adhesives—intended to fill a space between two or more materials and provide a seal without the need to have high structural strength

There are a wide variety of materials utilized as adhesives, including the adhesives identified in Table 5.



**Table 5** Adhesives Used in Electronic Packaging

Thermosetting	Thermoplastic	Elastomeric	Hybrid
Cyanoacrylate	Polyvinyl acetate	Butyl	Epoxy phenolic
Polyester	Polyvinyl acetal	Styrene butadiene	Epoxy polysulfide
Epoxy	Polyamide	Phenolic	Neoprene
Phenolic	Acrylic	Polysulfide	Vinyl phenolic
Polyimide		Silicone	
		Neoprene	

### 3 ELECTRONIC PACKAGING

#### 3.1 Component Mounting

##### *Discrete Components*

Discrete components are circuit elements not incorporated into integrated-circuit-type packaging. Included are components and subassemblies that may or may not be mounted to a printed circuit board. Component specifications provided by the manufacturer usually provide a guide to mounting requirements.

Components not normally mounted to a printed circuit card include disk drives, liquid crystal displays, power relays, panel-mounted switches and controls, connectors, and devices that generate significant amounts of heat.

Small discrete components are often mechanically attached to a structure, lead mounted and soldered to electrical terminals, or soldered to a printed circuit board. Examples include resistors and capacitors in leaded packages, individual transistors, rectifiers, bridges, relays, and light-emitting diodes (LEDs).

##### *Printed Circuit Board Components*

A printed circuit board may consist of one or more patterns of conductive traces separated by an insulator such as FR4 glass epoxy or other suitable rigid or flexible substrate.

Increasingly smaller components and integrated circuits have greater internal complexity with connection point counts which can exceed 400 points per device. Trace widths and spaces between traces of 0.010 in. or wider are common, as are fine-line board traces and spaces of from 0.010 to 0.006 in. Very fine line boards may have traces and spaces 0.001 in. or less; however, these densities are difficult to achieve in production.

The various types of components mounted to a printed circuit board may be classified as either leaded components or surface-mounted components.

Leaded components are mounted by inserting component leads through holes in the printed circuit board and soldering the leads into place followed by lead trimming and cleaning operations. This technology is mature. Leaded components include discrete components and leaded integrated circuits [dual in-line package (DIP) with two rows of pins and single in-line packages (SIPs)].

A variation of leaded components is the pin grid array (PGA), which features a matrix of up to 168 pins protruding from the bottom of the package; another variation is the quad flat pack, which features connection points on all four sides and must be mounted into a suitable chip carrier which is soldered to the circuit board.

Very large scale integrated (VLSI) circuits combine a multiplicity of circuit functions on an often custom-designed integrated circuit.



Surface-mount technology (SMT) consists of component circuit packages which feature conductive pads on the package with no leads protruding. These parts are attached to the printed circuit board by placing the SMT part onto a pattern of circuit board traces which have been coated with a solder paste mixture. Following placement, the assembly is heated to reflow the solder paste and to bond the components to the printed circuit board.

Converting from a through-hole design to an SMT design usually reduces the printed circuit board area to about 40% of the original size. The area reduction is highly dependent on the specific geometry of the components employed, interconnection requirements, and mechanical considerations.

***SMT components include the following:***

- Small-outline integrated circuits (SOICs), similar in appearance to DIP packages, except that the body of the component is smaller and the pins are replaced by gull wing or J-type lead configurations.
- Common SMT discrete packages known as Electronic Industry Association (EIA) sizes 1206, 0805, 0603, and 0402 for resistors, capacitors, and diodes; with EIA sizes A, B, C, D, and MELF packages for various types of capacitors and inductors.
- Plastic or ceramic leaded chip carriers (PLCC or CLCC), rectangular carriers with J leads around all four edges. These components may be directly soldered to the printed circuit board or installed into a socket that in turn is soldered to the printed circuit board.
- Chip-on-board, which consists of adhesive bonding a basic silicon chip die to the printed circuit board, beam welding leads from the die to the printed circuit board, and encapsulating the die and leads in a drop of adhesive potting compound.
- Ball grid array packages, much like PGA packages, except that instead of an array of pins protruding from the bottom of the component, there is an array of solder balls, each affixed to a pad on the component. The component may be either a plastic (PBGA) or a ceramic (CBGA) package. The BGA package is placed onto a corresponding artwork pattern on the printed circuit board and the assembly is heated to reflow the solder balls, thus attaching the BGA to the printed circuit board.
- Flip-chip package, a component package manufactured with small solder balls placed directly on the circuit substrate where electric connections are required. The substrate is then “flipped,” or turned over, so that the solder balls may be fused by reflow directly to pads on a printed circuit board.
- Multichip module, a component package, houses more than one interconnected silicon die within a subassembly. The subassembly is attached to the printed circuit board as a through-hole (DIP or SIP) component or as a SMT component.
- Silicon on silicon (SOS), a component package consisting of silicon die attached to a silicon substrate to create a custom integrated circuit assembly, which is attached to the printed circuit board like a conventional component.

## 3.2 Fastening and Joining

### *Mechanical Fastening*

Conventional machine design techniques apply to the design of mechanical joints employing threaded fasteners, rivets, and pins; they apply when strength and deflection are the primary design criteria. Dynamic loads (shock and vibration) require additional consideration, as does the selection of fastener materials to avoid corrosion.

In many mechanical fastening applications in electronic equipment fastener strength is not an issue and fastener size is selected based on the need to reduce the number of screw sizes used in the design (cost issue), appearance, and space available for tool clearances. For instance, when material compatibility is required between the fastener and aluminum parts with exposure to moisture, weather, and corrosive environments, stainless steel fasteners are advised. In commercial applications where weather exposure and corrosive environments are not a significant issue, zinc- or cadmium-plated steel fasteners are employed. Brass fasteners are used when the electrical resistance must be low to facilitate the flow of electrical current through a joint. Where joint electrical insulation is necessary to prevent electrical current flow through a joint, nylon and machined Teflon fasteners or other nonmetal fasteners are used.

Screw head selection is important in electronic equipment applications. Phillips head screws are preferred over slotted head screws due to the ability to gain increased tightening torque and to avoid marring of nearby surfaces should the screwdriver blade slip out of the screw head slot. Pan-head screws are preferred over round-head screws due to the absence of sharp edges. Flat-head screws are used to bury the screw head within the material thickness of one of the structural elements; however, there is no allowance for tolerances which exist between flat-head screws in a multifastener joint.

When threaded fasteners are used, there is concern that the joint will loosen and become ineffective over time. Such loosening may be caused by thermal cycling, vibration, or repetitive bending of the joint. Techniques used to maintain threaded joint integrity include the following:

- Use of a lock washer between the nut and the base material. To avoid damage to the base material, a flat washer is placed between the lock washer and the base material.
- In the event that an electrical bond must be established through the threaded joint, a toothed-type lock washer without a flat washer must be employed.
- Use of a compression nut (formed as to cause friction between the nut and the screw threads). This device loses effectiveness if frequently removed and may require replacement.
- Use of a nut or screw with a compressible insert (a threaded insert pressed into the base material). This applies to screw sizes of #6 and larger. The same warning on reuse applies as for the compression nut.
- Use of a screw retention adhesive material on the threads prior to making the joint. The adhesive must be reapplied each time the joint is disassembled. Various degrees of hold are available.
- Use of an antirotation wire through a hole in the nut or in the head of the screw. Applicable to larger bolts only.
- Tooth-type lock washers should not be used in contact with printed circuit board (may damage or short to traces) or with nonmetallic base materials (will mar the mating surface).
- Joints where one or more elements are capable of cold flow (creep), e.g., nylon, plastics, and soft metal, require a retention method other than compression-type lock washers.

Rivets are used in electronics assembly to form a permanent joint and may be solid or tubular. One should not depend on a riveted joint to provide long-term electrical connectivity. Cold flow will lead to joint looseness when soft metals or plastic materials are involved. Rivet material must be compatible with other joint materials to avoid corrosion.

Pins pressed into holes in mating parts are sometimes used to make permanent joints. Pin joints may be disassembled; however, a larger diameter pin may be required to achieve full joint strength upon reassembly. Materials selection is important to avoid corrosion.

### ***Welding and Soldering***

Conventional spot welding, inert gas welding, torch welding, and brazing<sup>17,18</sup> are used in the construction of many metal chassis and other mechanical components. Such joints have consistent electrical conductivity. Material properties in the heat-affected zone are often altered and weakened and may cause early mechanical failure of highly stressed joints. Lap joints tend to draw liquids into themselves by capillary action. Lap joints must be carefully cleaned and protected from ingestion of contaminants which may eventually cause corrosion, loss of electrical conductivity, and eventual mechanical failure of the joint.

Lead–tin and no-lead solders are used to make electrical joints<sup>19,20</sup> and to bind components to printed circuit boards. Eutectic 63% lead–37% tin solder has a relatively low melting point and is commonly used, unless there is a no-lead requirement, for attachment of components to circuit boards. No-lead solder is also used; however, the flow temperature is higher by 20°C or more. The manufacturer of the solder should be contacted for recommendations and data on specific no-lead formulations.

In applications where a soldered electrical joint is needed and mechanical stresses will be present, the joint must be designed to accept the mechanical stresses without the solder present. Under load, a solder joint will creep until the loads are eliminated or when the joint fails. As a result, solder is generally used only for electrical connection purposes and not for carrying mechanical loads.

Solder often is the only means of mechanical and electrical support for surface-mounted parts on a circuit board assembly. Due to variations in the coefficient of thermal expansion between the circuit board substrate and the component materials, solder joints will be subjected to thermal cycling-induced stresses caused by environmental or operationally generated temperature changes. Successful surface-mount design requires that the mass of the individual parts is very small and that the circuit board is protected from bending stresses so that solder attachment points will not eventually fail as the result of creep or fatigue failure.

### ***Adhesives***

Adhesives<sup>21</sup> are used in electronic equipment for a variety of purposes, such as component attachment to circuit boards in preparation for wave soldering. Encapsulants are used to encase and protect components and circuits, and adhesives are used to seal mechanical joints to avoid liquid and gas leakage.

Adhesive joints withstand shear loads; however, adhesive joints are much weaker when subjected to peeling loads. The load-bearing properties of cured adhesive joints (creep, stiffness, modulus of elasticity, and shear stresses) may vary significantly over the temperature ranges often experienced in service. Successful joints using adhesives are designed to bear mechanical loads without the adhesive present, with the adhesive applied to achieve seal and environmental protection.

Adhesives may release chemicals and gases during cure which are corrosive to electrical contacts and components and materials used in the construction of electronic equipment. Such adhesives must be avoided or fully cured prior to introduction into a sealed electronic enclosure.

## **3.3 Interconnection**

### ***Discrete Wiring***

Discrete wiring involves the connection from one component to another by use of electronic hookup wire which may or may not be insulated. In either case the individual connections are made mechanically by forming the component leads to fit the support terminals prior to applying solder to the connection. Care must be taken to route wires away from sharp objects and to avoid placing mechanical stresses on the electrical joints.

***Board Level***

Board-level interconnection is accomplished by soldering components to conductive patterns etched onto a printed circuit board. Panel- or bracket-mounted parts may require discrete wiring between the component and the printed circuit board. Board assemblies sometimes consist of two or more individual circuit boards where a smaller board assembly is soldered directly to a host circuit board.

Socket-type connectors may be soldered to a circuit board to receive integrated circuits, relays, memory chips, and other discrete components. Care must be exercised to assure that the socket provides mechanical retention of the part to prevent the part from being dislodged by transportation and service environments.

***Intramodule***

Discrete components and circuit board assemblies located within an electronic subassembly, or module, are interconnected within the module. In addition, the module circuits and components are presented to an interface, such as one or more connectors, to facilitate interconnection with other modules or cable assemblies.

***Intermodule***

Individual modules are interconnected to achieve system-level functions. Modules may be plugged together directly using connectors mounted to each module, be interconnected by cable and wiring harness assemblies, or be plugged into connectors arrayed on a common interconnection circuit board sometimes called a “mother” board.

***Interequipment***

System-level interconnection between electronic equipment may consist of wiring harness assemblies, fiber-optic cables, or wireless interconnection.

***Fiber-Optic Connections***

Fiber-optic<sup>20</sup> links are sometimes employed to interconnect electronic systems instead of conventional metallic conductors. Fiber-optic communication consists of transmitting a modulated light beam through a small-diameter (100- $\mu\text{m}$ ) glass fiber to a receiver where the modulated signal is transformed into a corresponding electrical signal. Used extensively in communications equipment and systems, fiber-optic links are immune to radio and magnetic field interference. Design is centered on methods to provide connectors and splices without inducing signal reflection and attenuation. Also, the design must provide at least the manufacturer-recommended minimum bend radii to avoid reflections and distorting stresses on the fiber. It is important to mechanically support and control fiber cable runs to avoid excessive mechanical stresses.

**3.4 Shock and Vibration*****Fragility***

Fragility refers to the vulnerability of a device to failure. It is necessary for the electronic packaging engineer to understand the most likely modes of failure under dynamic loads and adjust the design to protect against those failures. Fragility not only addresses loads which cause immediate mechanical or electrical malfunctions but also includes failures which result from accumulated damage (fatigue, fretting, or fatiguelike processes) leading to failure early in the expected useful life of a product.

***Shock***

Shock may be defined as a sudden change in momentum of a body. A shock pulse may range from a simple step function or haversine pulse to a brief but complex waveform composed

of several frequencies. The shock pulse may result in operational malfunctions (in operating equipment), breakage of brittle materials, or bending displacement and subsequent (ringing) vibration of elements of the equipment receiving the shock pulse. Shock pulses near the fundamental or harmonic resonance frequency of the structure cause greatly magnified and destructive responses. Shock failures include the following:

- Permanent localized deformation at point of impact
- Permanent deformation of structural elements within an equipment such as distorted mounting brackets
- Secondary impact failures within an equipment should structural deformations cause components to strike adjacent surfaces
- Temporary or permanent malperformance of operating equipment
- Failure of fasteners, structural joints, and mounting attachment points
- Breakage of fragile components and fragile structural elements

Design techniques employed to avoid shock-induced damage<sup>22–24</sup> include the following:

- Characterization of the shock-producing event in terms of impulse waveform, energy, and point of application
- Computation or empirical determination of equipment responses to the shock pulse in terms of acceleration (or  $g$  level) vs. time
- Modifications of the equipment structure to avoid resonant frequencies which coincide with the frequency content of the shock pulse
- Assuring that the strength of structural elements is adequate to withstand the dynamic  $g$  loading without either permanent deformation or harmful displacements due to bending
- Selecting and using components which are known to withstand the internal shock environment to which they are subjected when the local mounting structure responds to the shock pulse transmitted inward from the external blow
- Employing protective measures such as energy-absorbing or resonance-modifying materials between the equipment and the point of shock application or within the equipment as applied to the mounting of fragile components

### ***Vibration***

The response of equipment to vibration may create damage if the equipment or elements thereof are resonant within the passband of the excitation spectra. Vibration failures include the following:

- Fretting, wear, and loosening of mechanical joints, thermal joints, and fasteners and within components such as connectors, switches, and potentiometers
- Fatigue-induced structural failure of brackets, circuit boards, and components
- Physical and operational failure should individual structural element bending displacements produce impact between adjacent objects
- Deviations in the electrical performance of components caused by the relative motion of elements within the component or by the relative motion between a component and other objects which modulate the local electrical and/or magnetic fields

Design techniques employed to avoid vibration-induced damage include the following:

- Characterization of the energy and frequency content of the source of vibration excitation
- Analytical and empirical determination of equipment primary and secondary structural responses and component sensitivity to vibration forces in the passband of the source vibration
- Control of individual resonance frequencies of an equipment structure and internal elements to avoid coincidence of resonance frequencies
- Employing materials which have adequate fatigue life to withstand the cumulative damage predicted to occur over the life of the equipment
- Use of energy-absorbing materials between the equipment and the excitation source and within the equipment for the protective mounting of sensitive components

### ***Testing***

The primary purposes of shock and vibration testing are to evaluate the dynamic response of an equipment and components to the dynamic excitation and to compare these responses with the fragility of the unit under test.

Basic characterization testing is usually performed on an electrodynamic vibration machine with the unit under test hard mounted to a vibration fixture which has no resonance in the passband of the excitation spectrum. The test input is a low-displacement-level sinusoid which is slowly varied in frequency (swept) over the frequency range of interest. Recorded results of sine sweep testing produces a history of the response (displacement or acceleration) as experienced by accelerometers located at selected points on the equipment.

Caution is advised when using a hard-mount vibration fixture because the fixture is very stiff and is capable of injecting more energy into the test specimen at specimen resonance than would be experienced in the actual service environment. For this reason the test input signal should be of low amplitude. In service, the reaction of a less stiff mounting structure to the specimen at specimen resonance could significantly reduce the energy injected into the specimen and lessen the damage thereto. If the specimen response history is known prior to testing, the test system may be programmed to control input levels vs. frequency to reproduce the actual response history. In this case, it is important to assure that the control accelerometer is placed at the exact location on the specimen where the accelerometer was located when the initial response spectrum was recorded.

Vibration test information is used to aid in adjusting the equipment design to avoid unfavorable responses to the serviced excitation, such as the occurrence of coupled resonance (i.e., a component having a resonance frequency coincident with the resonance frequency of its supporting structure or the structure having a significant resonance which coincides with the frequency of an input shock spectra). Individual components are often tested to determine and document the excitation levels and frequencies at which they occur. Finding correlation between the individual resonances and operational failures of the unit under test is fundamental to both shock and vibration design.

For more complex vibration service input spectra, such as multiple sinusoidal or random vibration spectra, additional testing is performed on individual parts of the equipment to ensure that the responses are predictable, which will allow the designer to “tune” the overall equipment to avoid coincident resonances and to limit the responses of sensitive components. The final

equipment testing to the specified dynamic environments and durations, which may be different for each axis of excitation, may be combined with other variables such as temperature, humidity, and altitude environments.

### 3.5 Structural Design

#### *General*

Structural design of an electronic system<sup>24,25</sup> equipment structure, enclosure, module, or bracket involves analytical, empirical, and experimental techniques to predict and thus control mechanical stresses. Structural strength may be defined as the ability of a material to bear both static (sustained) and dynamic (time-varying) loads without significant permanent deformation.

Many nonferrous materials suffer permanent deformation under sustained loads (creep). Ductile materials withstand dynamic loads better than brittle materials, which may fracture under sudden load application. Materials such as plastics often exhibit significant changes in material properties over the temperature range encountered by a product.

Many structural elements require stiffness to control deflection but must be checked to assure that strength criteria are achieved.

#### *Complexity and Mechanical Impedance*

An equipment may be viewed as a collection of individual elements interconnected to achieve an overall systems function. Each element may be individually modeled, but the equipment model becomes complex when the elements are interconnected. The concept of mechanical impedance<sup>6,24</sup> applies to dynamic environments and refers to the reaction between a structural element or component and its mounting points over a range of excitation frequencies. The reaction forces at the structural interface or mounting point are a function of the resonance response of an element and may have an amplifying effect or a dampening effect on the mounting structure. Mechanical impedance design involves control of element resonance frequencies and mounting structural resonance frequencies, so that they do not combine to cause failure.

#### *Degree of Enclosure*

The degree of enclosure is the extent to which the components within electronic equipment are isolated from the surrounding environment.

For vented enclosures the design must provide drain holes to facilitate elimination of induced liquids and condensation. Convection (natural or forced) cooled equipment, when used where dust is present, may require filtration of the air permitted to enter the equipment.

Partially sealed enclosures using permeable sealing materials (e.g., adhesives and plastics) are vulnerable to penetration by water vapor and other gases. Pachen's law states that the total pressure inside an enclosure is the sum of the partial pressures of the constituent gases. When the external partial pressure of a constituent gas is higher than the internal partial pressure of that gas, regardless of the total pressure inside the equipment, the constituent gas will enter through the permeable seal until the internal and external partial pressures are equalized. When water vapor is ingested, condensation may occur inside the enclosure during temperature cycling, resulting in corrosion and perhaps interruption of electrical signals. Permeable seals, which permit gases but not liquids to enter equipment, do not protect against internal moisture damage and corrosion.

Completely (hermetically) sealed equipment enclosures using metal or glass seals permit the internal humidity and pressure to be defined when the unit is sealed. It is necessary to control the dryness of internal gases introduced into the equipment to protect from condensation-induced corrosion. In addition, it is necessary to assure that internal pressures



generated inside of the enclosure due to heating in combination with changes in external ambient pressure (e.g., due to changes in altitude or ambient air pressure) do not exceed the structural deformation limitations and stress-bearing capabilities of the enclosure.

Equipment which operates in the presence of explosive gases or combustible dust mixtures must incorporate components which will not cause ignition, and exposed circuits must operate at low-voltage and low-current conditions so that short-circuit heating and arcing are controlled or eliminated. Vented equipment used in explosive environments may require use of flame propagation barriers, such as a screen mesh, which demonstrate under test should ignition occur inside the equipment that the flame front will not propagate into the outer environment.

### *Thermal Expansion and Stresses*

The coefficient of thermal expansion is a material property which defines the degree to which a material will expand or contract when that material is subjected to a change in temperature. The coefficient of thermal expansion varies widely among the materials available for use in the construction of electronic equipment. When two or more materials are bonded or fastened together and subjected to a change in temperature, they will attempt to expand or contract at different rates. This difference in expansion or contraction leads to bending and shear stresses which may be detrimental to the life and operation of the equipment.

Thermal cycling of mechanically joined materials may lead to failure such as loss of electrical contact in bolted joints, cracking and breaking of ceramic parts bonded to plastic or metal surfaces, solder joint failure, and accelerated fatigue failure when the thermal stresses add to the stresses normally expected during the life cycle of an electronic product. Thermal stresses may be reduced by selecting adjoining materials which have the least difference in coefficient of thermal expansion.

## 3.6 Thermal Design

### *Objectives*

The purpose of thermal design<sup>26–28</sup> is to control component temperatures within acceptable limits and thus to achieve satisfactory product reliability.<sup>29</sup> Newer component fabrication techniques, such as the fabrication of metal–oxide–semiconductors (MOSs) and CMOSs, greatly reduce component input power requirements and thus greatly reduce heat generation within the component. However, components using these and similar techniques of construction are being reduced in size such that the power per unit volume of high-component-density electronic equipment is actually being increased as a result of using these newer fabrication technologies. There are three primary levels of thermal design:

1. Equipment total heat generation and control of how that heat will be dissipated by the equipment enclosure to the local external environment
2. Equipment internal environment, which is the environment experienced by modules and subassemblies, and how heat from the modules and subassemblies will be passed to the equipment enclosure
3. Control of critical component temperatures and how heat is transferred between the components and the internal environment

In addition, the electronic packaging engineer must consider how materials, finishes, and lubricants will behave over the expected range of temperatures.

Heat flow and temperature are analogous to the flow of electrical current and voltage. The term thermal resistance (in degrees Celsius per watt) is employed to relate temperature to the flow of thermal energy in the same manner as Ohm's law relates voltage to the flow of electrical current.



A material or device may be characterized by its thermal resistance. Examples include the thermal resistance of heat sinks, interfaces between components and mounting surfaces, thermal resistance of structural elements, and thermal resistance of mechanical joints.

Thermal design includes the definition of heat flow paths from the component to the ultimate heat sink; for each heat flow path thermal resistances are selected to ensure that component temperatures will be maintained within acceptable levels.

### ***Basis Heat Transfer Modes***

***Conduction...*** Conduction is the transfer of thermal energy directly through a material medium, which may be a solid, liquid, or gas. Conduction of heat from a source to the ultimate heat sink includes as appropriate:

1. Component internal heat transfer from an internal feature, such as a semiconductor junction temperature, to the local mounting surface, liquid or air. Component specifications usually include a thermal resistance which relates an internal critical point temperature to a specified location on the component package.
2. Contact resistance between the component and its mounting surface. Contact resistance depends on contact area, contact pressure, and presence of thermal grease or other materials used to lower contact resistance. Contact resistances are often determined experimentally.
3. Thermal resistance through structural elements (computed based on cross-sectional area and length) using thermal conductivities as defined in tables of material properties.
4. Interface resistance at each structural joint. These may be estimated by calculation and are often defined experimentally.
5. Thermal resistance of heat sinks<sup>30</sup> used to dissipate energy to gas or liquid coolants. Conduction heat sinks include liquid-cooled cold plates, convection (natural and forced) heat sinks, forced-convection heat exchangers, evaporative devices such as heat pipes, and thermoelectric (Peltier effect) cooling devices.

***Free Convection.*** Free convection involves the rejection of thermal energy from a warm object to air or other gas surrounding the object in the absence of mechanically or environmentally induced motion of the gases. Free convection is a continuing process whereby the local warming of surrounding gases in immediate contact with a warm object produces buoyancy and movement of the heated gases away from the warm object. Cooler gases are drawn toward the warm object, replacing the escaping warm gases. In this manner, heat is passed from the warm object to the gas (or liquid) environment.

Free-convection thermal resistance depends on the orientation of warm surfaces relative to gravity, surface area, and surface finish. Free convection is enhanced by providing extended surfaces such as fins to increase the effective contact area between the warm surface and local gases. Manufacturers of commercially available heat sinks are able to provide thermal resistance information for the devices that they market.

Equipment which is to be cooled by natural convection often must be provided with vents to permit the escape of warm gases and the entrance of cooler gases. Warm components must be in the flow path of the cooling gases, and internal obstructions must be avoided which would impede flow of the cooling gases.

Natural-convection cooling is a mass-rate-of-flow process, and cooling effectiveness is decreased by reduction in ambient air pressure (thus lowering the density of the cooling gas) such as occurs at higher altitudes and during hot days when the density of surrounding gases is lower.

*Forced Convection.* Forced convection may be produced mechanically with fans, blowers, and pumps or movement of the equipment during use or by naturally occurring air movement (wind) over unsheltered equipment. Forced-convection thermal resistance values are much lower than those resulting from natural-convection cooling.

Within forced-convection cooled equipment, the cooling media is ducted first to the most temperature sensitive components and then to the less temperature sensitive components located downstream where local temperatures may be higher.

Forced-convection heat sinks<sup>31</sup> and heat exchangers are often used to cool heat-sensitive components and assemblies.

Forced-convection thermal resistance is sensitive to the mass rate of flow and velocity of the cooling medium. Mass rate of flow is pressure dependent and decreases with reductions in ambient pressure. Decreased mass rate of flow causes increased thermal resistance. Increased air velocity past the cooled object reduces the thickness of the boundary layer surrounding the object and thus decreases the effective thermal resistance.

*Radiation.* Radiation heat transfer is the transfer of energy from a warmer object to a cooler object by infrared radiation. Unlike convection cooling, radiation heat transfer is most effective in a vacuum and is not dependent upon the presence of a gaseous media between the objects.

The effectiveness of radiation heat transfer is dependent on the temperature differential between the objects, the distance between the objects, the projected area of each object, and the emissivity of each object. Radiation cooling (or heating) efficiency is reduced if smoke, moisture vapor, dust, or other particulate matter is suspended in the intervening gases.

Radiation is the primary mode of heat transfer in outer space; however, unless large temperature differences and short separation distances are experienced between earthbound objects, radiation involves a small fraction of the total heat flow.

Solar radiation causes heat buildup within an electronic enclosure when ultraviolet rays from the sun strike a closed equipment case adding to the heat load within the equipment. Should solar radiation pass into a device, as through glass or plastic windows or a lens which is transparent to ultraviolet rays, the radiation will heat internal surfaces, which in turn will radiate at infrared frequencies to which the transparent material is usually opaque and will not permit the infrared radiation to leave the enclosure. In this way thermal energy is trapped inside the enclosure and may lead to excessive internal temperatures. Solar-induced heat loading must be considered whenever electronic equipment is exposed to sunlight.

*Evaporation.* Evaporation cooling and condensation cooling techniques utilize the latent heat of vaporization of a heat transfer liquid such as water, alcohol, Freon, or other liquid to cause effective temperature control. Thus, when an object is submerged within a liquid, such as water, the temperature of the object is controlled to the boiling point of the liquid (100°C for water) within which it is submerged.

Heat pipe and evaporation chamber devices utilize evaporation by containing a liquid and providing an internal capillary structure to return condensed liquid from the cool end of the device to the heated end of the device.

### 3.7 Protective Packaging

#### *Definition*

Protective packaging includes the techniques employed to ensure that a product will survive handling, shipping, and storage environments without degradation.

***Storage Environment Protection***

Electronic equipment may be subjected to storage for extended periods of time. The storage environments may be more severe than the equipment will experience after being placed into service.

Protective packaging selected for storage must withstand the storage environments and offer protection to the enclosed product.

The materials from which storage containers and fillers are selected must remain chemically inert and not introduce detrimental effects on the stored equipment. For example, some paper products contain sulfur, the fumes of which accelerate tarnishing, thus increasing contact resistance of silver-plated contacts. Also, some adhesives and wrapping and cushioning materials outgas corrosive fumes at elevated temperatures.

***Shipping Environment Protection***

Protective packaging must withstand transportation environments and the handling associated with movement of the packaged equipment to and from carriers. The transportation and handling environments may include exposure to more severe shock and vibration than the protected product will experience after being placed into service. The shipping containers must tolerate stacking and handling by mechanical lifting devices. When it is predicted that the transportation environment will be severe, the container will need to include packaging materials to cushion the product from mechanical shock and vibration loads.

### 3.8 Software Design Aids

***Selection of Microcomputer Based Design Tools***

A variety of microcomputer design tools are offered on the internet for the purposes of facilitating portions of the electronic packaging design process. The design programs range from freeware and shareware to large and expensive well documented and supported professional programs.

The use of capable but less expensive software package offerings must be handled with care to avoid pitfalls that may be experienced by the user.

For example:

- inadequate documentation
- documentation ineptly translated into English
- unexplained internal algorithms and assumptions that impact output accuracy
- awkward input modeling techniques
- inability to transfer files in a format acceptable other design software programs
- inability to generate output files suitable for use by three-dimensional printers
- lack of customer support
- limited graphics
- limited availability drivers used to handle a variety of input and plotter devices.

There are a variety of intermediate size and supported programs that work well for less complex needs

Full capability, professional programs are used to assure satisfactory results and are applied to multifaceted, large scale project and critical projects for which there is little tolerance for weak results. These professional programs are often able to support multi-user design team activities.

Consultation with users of design software is an excellent source of reference when investigating various programs, and if a program is acquired, the other users may be able to assist in the choice of software specifically appropriate to the needs of the Electronic Packaging Engineer. If a blog is available on the internet for the program of interest, the blog may be a source of helpful information.

It is wise to approach the use of new software packages with caution and to develop confidence in the program by “base lining”, i.e. by the comparing of program output results to the results of an already solved similar problem.

### ***Mechanical Design Tools***

Within the array of mechanical design tools the descriptive marketing rhetoric often minimizes the effort required to achieve efficient productivity. As a general rule, the more versatile the program, the more training and customer support that is required to achieve proficiency. In some cases it becomes necessary to attend initial and annual training courses for the specific program including using consultants who are trained in the use of the specific software package. Finite element modeling including component geometrical mesh development may be needed to achieve refined prediction of static and dynamic deformation information resulting from anticipated service loads.

### ***Circuit Board Design Tools***

A variety of printed circuit (or printed wiring) board design programs are available to aid in the practice of circuit board design. These same programs are often used in the design of flexible circuits, membrane switches, and similar devices.

Available programs range from free (limited, no support), versions offered by board manufacturing houses with output files only useful for the offering board manufacturer; through programs which offer varying degrees of design capabilities, vendor support and documentation. There are also mid-range programs of modest capabilities which are often sufficient to meet the requirements of many circuit board design tasks.

Circuit board programs vary in complexity and the potential user should form a list of minimum requirements and then select a program that best fits the user's needs. Listed below are some of the more important characteristics that may be offered by circuit board design programs:

- the number of components that can be employed
- the number of circuit layers
- the minimum line and space widths
- the ability to provide hidden vias
- the maximum size of a circuit board
- the sophistication of any auto-routing and parts placement features
- the ability to set design rules and to run design rule checking
- the ease with which fabrication files may be generated (Gerber files, drill files, silkscreen files, solder fill patterns)
- The ability to edit Gerber files on existing boards
- the ease with which the designer may create or modify the library of component electrical, mechanical and performance descriptions
- The ability to enter electrical characteristics of components and to employ the descriptions in circuit performance prediction and analysis routines

- the ability to create and revise schematics
- the ability of the program to automatic forward and back-annotate between schematic and artwork files when changes are made
- the ability to view net connectivity and edit nets by splitting, merging, and gate reassignment between nets, and deletion of components
- the generation of materials lists
- the ability to provide assembly drawing graphics.

Regardless of the program employed there are several details that require attention to avoid a ruined board. The design of a board is dependent on the quality of the part device libraries which exist to create, define and store schematic symbols and the associated layout artwork patterns.

It is necessary to have confidence in the device library to avoid surprises such as when a device has a correctly described schematic symbol however the device file (which relates a schematic symbol to a specific layout pattern) contains an incorrect artwork layout pattern in the device library. This is a common error not obvious to the designer when creating a schematic diagram but which becomes apparent when the device file generates a circuit board layout pattern which does not match the physical dimensions of the selected component.

Library information quality can vary greatly within and between the various offered programs. The designer should verify that the electrical symbols and copper patterns are correct for each part used in a design. There are many physical sizes, pin-outs and copper layout patterns available for each industry part definition. This is increasingly true due to the wide variety of surface mount component packages available for any given schematic symbol.

Every new circuit board design may need the designer to create a new device file for every component not previously entered into the device library. Layout pattern information may be found on component manufacturer's websites.

## REFERENCES

1. M. Kutz, *Mechanical Engineers' Handbook*, 3rd ed., John Wiley, Hoboken, NJ, 2006.
2. *The CAD Guidebook*, CRC Press, Boca Raton, FL, 2002.
3. W. T. Shugg, *Handbook of Electrical and Electronic Insulating Materials*, Van Nostrand Reinhold, New York, 1986.
4. B. S. Matisoff, *Handbook of Electronics Packaging*, Van Nostrand Reinhold, New York, 1982
5. Part 15, Federal Communications Rules and Regulations, [www.fcc.gov](http://www.fcc.gov).
6. W. C. Fackler, *Equivalent Techniques for Vibration Testing*, SVM-9, Naval Research Laboratory, Washington, DC, 1972.
7. *Alloy Cross Index*, Mechanical Properties Data Center, Battelle's Columbus Laboratories, Columbus, OH, 1981.
8. *Metals Handbook*, American Society for Metals, Metals Park, OH, 2000.
9. *Stainless Steel Handbook*, Allegheny Ludlum Steel Corporation, Pittsburgh, PA, 1956.
10. *Aluminum and Aluminum Alloys*, American Society for Metals, Metals Park, OH, 1999.
11. [www.Pb-Free.com](http://www.Pb-Free.com), an interactive website dedicated to providing information.
12. C. A. Harper, *Handbook of Plastics and Elastomers*, McGraw-Hill, New York, 1981.
13. M. Morton, *Rubber Technology*, Van Nostrand Reinhold, New York, 1987.
14. R. C. Buchanan, *Ceramic Materials for Electronics*, Marcel Dekker, New York, 1986.
15. C. A. Harper, *Electronic Packaging Handbook*, 3rd ed., McGraw-Hill Professional, New York, 2000.
16. J. B. Wachtman, *Mechanical Properties of Ceramics*, Wiley-Interscience, New York, 1986.
17. R. K. Wassink, *Soldering in Electronics*, 2nd ed., Electrochemical Publications, Isle of Man, British Isles, 1997.

18. A. Rahn, *The Basics of Soldering*, Wiley-Interscience, New York, 1993.
19. R. W. Woodgate, *Handbook of Machine Soldering*, Wiley-Interscience, New York, 1988.
20. M. G. Pecht, *Soldering Processes and Equipment*, Wiley-Interscience, New York, 1990.
21. A. J. Kinloch, *Adhesion and Adhesives*, Chapman and Hall, New York, 1987.
22. J. H. Williams, *Fundamentals of Applied Dynamics*, MIT Press, Cambridge, MA, 1995.
23. P. A. Engle, *Structural Analysis of Printed Circuit Board Systems*, Springer-Verlag, New York, 1993.
24. C. M. Harris and A. G. Piersol, *Harris' Shock and Vibration Handbook*, McGraw-Hill, New York, 2002.
25. G. R. Blackwell, *The Electronic Packaging Handbook*, CRC Press, Boca Raton, FL, 1999.
26. D. J. Dean, *Thermal Design of Electronic Circuit Boards and Packages*, Electrochemical Publications, Isle of Man, British Isles, 1997.
27. A. D. Kraus and A. Bar-Cohen, *Thermal Analysis and Control of Electronic Equipment*, McGraw-Hill, New York, 1993.
28. D. S. Steinberg, *Cooling Techniques for Electronic Equipment*, 2nd ed., Wiley-Interscience, New York, 1991.
29. F. Jensen, *Electronic Component Reliability*, Wiley-Interscience, New York, 1991.
30. A. D. Kraus and A. Bar-Cohen, *Design and Analysis of Heat Sinks*, Wiley, New York, 1995.
31. W. T. Kays and A. L. London, *Compact Heat Exchangers*, McGraw-Hill, New York, 1984.



# CHAPTER 14

## SOURCES OF MATERIAL DATA

**J. G. Kaufman**

Kaufman Associates,  
Lewes, Delaware

<b>1 INTRODUCTION AND SCOPE</b>	<b>515</b>	<b>4 SUBJECTS OF DATA SOURCES</b>	<b>522</b>
<b>2 INTENDED USES FOR DATA</b>	<b>516</b>	<b>5 DATA QUALITY AND RELIABILITY</b>	<b>522</b>
2.1 Modeling Material and/or Product Performance	516	<b>6 PLATFORMS: TYPES OF DATA SOURCES</b>	<b>524</b>
2.2 Materials Selection	516	<b>7 SPECIFIC DATA SOURCES</b>	<b>524</b>
2.3 Analytical Comparisons	517	7.1 ASM International and the Alloy Center	525
2.4 Preliminary Design	517	7.2 STN International	526
2.5 Final Design	518	7.3 knovel.com	527
2.6 Material Specification	518	7.4 The Internet	527
2.7 Manufacturing	519	<b>ACKNOWLEDGMENTS</b>	<b>528</b>
2.8 Quality Assurance	519	<b>REFERENCES</b>	<b>528</b>
2.9 Maintenance	519		
2.10 Failure Analysis	520		
<b>3 TYPES OF DATA</b>	<b>520</b>		
3.1 Textual Data	520		
3.2 Numeric Databases	521		
3.3 Metadata	521		

### 1 INTRODUCTION AND SCOPE

It is the purpose of this chapter to aid engineers and materials scientists in locating reliable sources of high-quality materials property data. While sources in hard-copy form are referenced, the main focus is on electronic sources that provide well-documented searchable property data.

To identify useful sources of materials data, it is important to have clearly in mind at the outset (a) the intended use of data, (b) the type of data required, and (c) the quality of data required. These three factors are key in narrowing a search and improving its efficiency of a search for property data. Therefore, as an introduction to the identification of some specific potentially useful sources of materials data, we will discuss those three factors in some detail and then describe the options available in types of data sources.

Readers interested in a more comprehensive list of sources and of more discussion of the technology of material property data technology and terminology are referred to Westbrook's extensive treatment of these subjects in Refs. 1 and 2 and to the *ASM International Directory of Materials Property Databases*.<sup>3</sup>



## 2 INTENDED USES FOR DATA

Numeric material property data are typically needed for one of the following purposes by individuals performing the respective functions given in parentheses as part of their jobs:

- Modeling material or product performance
- Materials selection (finding candidate materials for specific applications)
- Analytical comparisons (narrowing the choices)
- Preliminary design (initially sizing the components)
- Final design (assuring performance; setting performance specifications)
- Material specification (defining specifications for purchase)
- Manufacturing (assuring processes to achieve desired product)
- Quality assurance (monitoring manufacturing quality)
- Maintenance (repairing deterioration/damage)
- Failure analysis (figuring out what went wrong)

It is useful to note some of the differing characteristics of data needed for these different functions.

### 2.1 Modeling Material and/or Product Performance

To an increasing extent, mathematical modeling is used to establish the first estimates of the required product performance and material behavior and even in some cases the optimum manufacturing processes that should be used to achieve the desired performance. The processes and/or performance analyzed and represented may include any of the issues addressed in the following paragraphs, and so the nature of the types of data described under the various needs is the same as that needed for the modeling process itself.

### 2.2 Materials Selection

The needs of materials specialists and engineers looking for materials data to aid in the selection of a material for some specific application are likely to be influenced by whether they (a) are in the early stages of their process or (b) have already narrowed the options down to two or three candidates and are trying to make the final choice. The second situation is covered in Section 2.3.

If the materials engineers are in the early stages of finding candidate materials for the application, they are likely to be looking for a wide variety of properties for a number of candidate materials. More often, however, they may decide to focus on two or three key properties that most closely define the requirements for that application and search for all possible materials providing relatively favorable combinations of those key properties. In either case, they may not be as much concerned about the quality and statistical reliability of the data at this stage as by the ability to find a wide variety of candidates and to make direct comparisons of the performance of those candidates.

Where there is interest in including relatively newly developed materials in the survey, it may be necessary to be satisfied with only a few representative test results or even educated guesstimates of how the new materials may be expected to perform. The engineers will need to be able to translate these few data into comparisons with the more established materials, but at this stage they are probably most concerned with not missing out on important new materials.

Thus, at this early stage of materials selection, the decision makers may be willing to accept data rather widely ranging in type and quality, with few restrictions on statistical reliability.

They may even be satisfied with quite limited data to identify a candidate that may merit further evaluation.

### 2.3 Analytical Comparisons

If, on the other hand, the task is to make a final decision on which of two or three candidate materials should be selected for design implementation (the process defined here as “analytical comparison”), the quality and reliability of the data become substantially more important, particularly with regard to the key performance requirements for the application. It will be important that all of those key properties, e.g., density, tensile yield strength, and plane-strain fracture toughness, are available for all of the candidate materials make the next cut in the list.

The search will also be for data sources where the background of the data is well defined in terms of the number of tests made, the number of different lots tested, and whether the numbers included in the data source are averages or the result of some statistical calculation, such as that to define three sigma limits. It would not be appropriate at this stage to be uncertain whether the available data represent typical, average values or statistically minimum properties; it may not be important which they are, but the same quality and reliability must be available for all of the final candidates for a useful decision to be made.

In addition, the ability to make direct comparisons of properties generated by essentially the same, ideally standard, methods is very important. The decision maker will want to be able to determine if the properties reported were determined from the same or similar procedures and whether or not those procedures conformed to American Society for Testing and Materials (ASTM), International Organization for Standardization (ISO),<sup>4</sup> or other applicable standard test methods.

One final requirement is added at this stage: The materials for which the data are presented must all represent to the degree possible comparable stages of material production history. It would be unwise to base serious decisions on comparisons of data for a laboratory sample on one hand and a commercial-size production lot on the other. Laboratory samples have a regrettable history of promising performance that is seldom replicated in production-size lots.

Thus, for analytical comparisons for final candidate material selection, specialists need databases for which a relatively complete background of metadata (i.e., data about the data) are included and readily accessible.

Incidentally, it is not unusual at this point in the total process to decide that more data are needed for a particular candidate than are available in any existing database, and so a new series of tests is needed to increase confidence in the comparisons being made.

### 2.4 Preliminary Design

Once a decision is made on a candidate material (or sometimes two) for an application, the task of designing a real component out of that material begins. The requirement for statistical reliability steps up, and the availability of a data source that provides applicable metadata covering quality, reliability, and material history becomes even more important.

At this stage, the statistical reliability required includes not only a minimum value but one based upon a statistically significant sample size, ideally something comparable to the standards required in the establishment of MMPDS-01/MIL-HDBK-5J's A or B values.<sup>5</sup> In MMPDS/MIL-HDBK-5 terminology, an A value is one which would be expected to be equaled or exceeded by 99% of the lots tested with 95% confidence; the B value provides for 90% of lots tested equaling or exceeding the value with 95% confidence. Furthermore, the MIL-HDBK-5 guidelines require that A and B values be based upon predefined sample sizes, representing a minimum number of lots (normally 100 or more) and compositions (normally at least three) of a given alloy. The provision of such statistical levels needs to be a part of data sources used for

design purposes, and the description of the statistical quality needs to be readily available in the data source.

For preliminary design, then, the data sources sought will include both statistically reliable data and well-defined metadata concerning the quality and reliability provided.

## 2.5 Final Design

Setting the final design parameters for any component or structure typically requires not only data of the highest level of statistical reliability but also, in many cases, data that have been sanctioned by some group of experts for use for the given purpose. It is also not unusual that at this stage the need is identified for additional test data generated under conditions as close as possible to the intended service conditions, conditions perhaps not available from any commercial database.

Databases providing the level of information required at this stage often contain what are characterized as “evaluated” or “certified” values. Evaluated data are those that, in addition to whatever analytical or statistical treatment they have been given, have been overviewed by an expert or group of experts who make a judgment as to whether or not the data adequately and completely represent the intended service conditions and if it is necessary to incorporate their own analysis into the final figures. This technique has been widely used in digesting and promulgating representative physical property data for many years; examples are the thermo-physical property data provided by the Thermophysical Properties Research Center (TPRC).<sup>6</sup>

Other databases may be said to provide “certified” data. In this case, the database or set of data going into a database have been evaluated by a group of experts and certified as the appropriate ones to be used for the design of a particular type of structure. Two examples are the aforementioned MMPDS/MIL-HDBK-5 values,<sup>5</sup> which are approved for aircraft design by the MMPDS/MIL-HDBK-5 Coordination Committee consisting of aerospace materials experts, and the American Society of Mechanical Engineers (ASME) Boiler and Pressure Vessel Code,<sup>7</sup> with properties certified by materials experts in that field for the design of pressure vessels and companion equipment for high-temperature chemical processes.

As noted, it is often the case when designers reach this stage (if not the earlier preliminary design stage) that they find it necessary to conduct additional tests of some very specialized type to ensure adequate performance under the specific conditions the component or structure will see service but for which reliable databases have not previously been identified or developed. The net result is the creation of new materials databases to meet highly specialized needs and the need to do so in a manner that provides the appropriate level of statistical confidence.

## 2.6 Material Specification

Material specifications typically include specific property values that must be equaled or exceeded in tests of those materials that are being bought and sold. The properties that one requires in this case may differ from those needed for other purposes in two respects. First and foremost, they must be properties that will ensure that the material has been given the desired mechanical and thermal processing to consistently achieve the desired performance. Second, while in most cases there may be only one or a very few properties required (most often tensile properties), they are required at a very high level of precision and accuracy, similar to or better than that required for the MMPDS/MIL-HDBK-5 A properties defined earlier.

Examples are the material specifications required for the purchase of commercial aluminum alloy products.<sup>8</sup> These are usually only the chemical composition and the tensile properties. So while many of the other properties needed for design are not required as part of the purchase specification, those properties that are required are needed with very high reliability. In the case of aluminum alloys, the requirements for tensile strength, yield strength,

and elongation are normally that 99% of lots produced must have properties that equal or exceed the published purchase specification values with 95% confidence, and they must have been defined from more than 100 different production lots from two or more producers.

In many cases, the databases needed to generate material specification properties are proprietary and are contained within individual companies or within the organizations that set industry specifications. However, the resultant statistically reliable specification properties are resident and more readily available in industry or ASTM material standards.<sup>4,8</sup>

## 2.7 Manufacturing

The properties required for manufacturing purposes may be the most difficult to find in commercially available databases because they typically involve the specialized treatments or processes utilized by specific producers or suppliers of the specific products in question. Sometimes these processes are proprietary and are closely held for competitive advantage. An added complication is that once some semifabricated component (e.g., aircraft sheet) has been purchased, it will require forming to very tight tolerances or finishing at some relatively high temperature. The fabricator may require data to enable the process to be carried through without otherwise damaging or changing the properties of the component but may have difficulty representing the fabricating conditions in meaningful tests. Fabricators may well have to carry out their own tests and build the needed database to provide the desired assurance of quality and to provide a source of information to which their employees can refer to answer specific questions. Typically such databases never become commercially available, and new situations will require compiling new data sources.

Some processing data sources are available, of course. The Aluminum Association, for example, provides to all interested parties a data source defining standard solution heat treating, artificial aging, and annealing treatments for aluminum alloys that will assure the proper levels of properties will be obtained.<sup>8</sup> In some cases, ASTM and American National Standards Institute (ANSI) material specifications will also contain such information.

## 2.8 Quality Assurance

Quality assurance may be considered to be the flip side of material specifications, and so the types of data and the data sources themselves required for the two functions are essentially the same.

Purchasers of materials, for example, may choose to do their own testing of the materials once delivered to their facilities by materials producers. If so, they will use exactly the same tests and refer to exactly the same data sources to determine compliance. The one difference may be that such purchasers may choose to gradually accumulate the results of such tests and build their own databases for internal use, not only by their quality control experts but also by their designers and materials experts, who must establish safe levels of performance of the structures. These types of databases also tend to be proprietary, of course, and are seldom made available to the outside world, especially competitors.

## 2.9 Maintenance

The principal value of material data in connection with maintenance concerns will likely be for reference purposes when problems show up with either deterioration of surface conditions or the suspicion of the development of fatigue cracks at local stress raisers.

In both cases, the important features of the types of data desired to address such issues are more likely to be those based upon individual exposures or prior service experience, and so the user may be more concerned about the degree of applicability than upon data quality and

statistical reliability (though both features would be desired if available). Typically such data are hard to find in any event and once again are more likely to be buried in proprietary files than in published databases.

In the case of engineers and technicians needing databases comprised of service experience, they may well be faced with building their own data sources based upon their organization's production and service experience than expecting to be able to locate applicable external sources.

## 2.10 Failure Analysis

The occurrence of unexpected failure of components in a structure usually calls for some follow-up study to determine the cause and possible ways to avoid further loss. In such cases it is inevitable that such failure analysis will involve both (a) a review of the old databases used to design the part and (b) a search for or the development of new data sources that may shed more light on the material's response to conditions that developed during the life of the structure that had not been anticipated beforehand.

The types of databases sought in this case will likely be those containing statistically reliable data, but recognizing the unexpected nature of some problems, an interest in a wider range of data sources and a willingness to consider a lower level of data quality may result. Databases for failure analysis studies may need to be wider in scope and to cover subjects like corrosion that are not always easily treated by statistical means. In fact, sources covering failure experience may be the most valuable, though hardest to find, because historically engineers and scientists do not publish much detail about their mistakes.

The net result is that when dealing with failure analysis, the search may be quite broad in terms of data quality, and the focus most likely will be more on applicability to the problem than on the quality and structure of the compilation. As in the case of maintenance engineers and technicians needing databases comprised of service experience, failure analysts may well be faced with building new data sources based upon their organization's production and service experience.

## 3 TYPES OF DATA

It is useful at this stage to note that there are several basic types of materials databases, i.e., databases containing significantly different types of information and, hence, different data formats. Note that this is different from the type of platform or presentation format (e.g., hard copy, CD, online); these will be discussed in Section 6.

The two fundamental types of databases that will be discussed here are *textual data* and *numeric data*. In fact, many databases represent a combination of both types, but some basic differences worth noting are presented below.

The concept of metadata will also be described in more detail in this section.

### 3.1 Textual Data

The terminology "textual data" is generally applied to data entries that are purely alphabetic in nature with numbers used only as necessary to complete the thoughts. Textual databases are typically searched with alphabetical strings, e.g., by searching for all occurrences of a term like *aluminum* or *metallurgy* or whatever subject is of interest.

The subjects of textual databases are predominantly bibliographies and abstracts of publications, but they may reflect other specific subjects, such as textual descriptions of failures of components. Bibliographic databases seldom reflect the final answers to whatever inquiry is in mind but rather provide references to sources where the answers may be found.

The majority of all databases in existence in any form (see Section 6) are textual in nature, even many of those purporting to be property databases. Searchers of such textual property databases are searching based upon strings of alphanumeric characters reflecting their interest, not on numeric values of the properties, except as they are expressed as strings. This is quite different from the case for numeric property databases, as we shall see in the next section.

### 3.2 Numeric Databases

Databases classed as numeric (a) have data stored in them in numeric format and (b) are searched numerically. For example, numeric databases may be searched for all materials having a specific property equal to or greater than a certain value or within a certain specific range; this would not be possible in a textual database. To provide such searchability, almost all numeric databases are electronic in nature (see Section 4) though many hard-copy publications also contain extensive amounts of numeric data.

To accommodate numeric searching, the properties must be entered into a database digitally as numbers, not simply as alphanumeric strings. To be useful to material specialists and designers, they must have meaningful precision (i.e., numbers of significant figures) and units associated with each number. The numeric number of a property is of no value if it does not have the applicable unit(s) associated with it.

### 3.3 Metadata

The concept of metadata as “data about data” was introduced earlier, and it is appropriate at this stage to describe the concept and its importance in greater detail.<sup>9</sup> It is vital, especially for numeric databases and independent of their platform, to have ample background information on the numeric properties included in the database and closely associated with the individual properties.

Examples of metadata include the following:

- Original source of data (e.g., from tests at ABC laboratories)
- Test methods by which data were obtained (e.g., ASTM methods, size and type of specimen)
- Production history of the samples for which the data are applicable (e.g., annealed, heat treated, cold worked, special handling?)
- Exposure experienced by the samples tested, if any, prior to the test (e.g., held 1000 h at 500°F)
- Conditions under which the properties were determined (e.g., tested at 300°F, 50% humidity)
- Number of individual tests represented by and statistical precision of the values presented (e.g., individual test results, averages of  $x$  number of tests, statistical basis)
- Any subsequent evaluation or certification of the data by experts (e.g., ASME Boiler and Pressure Vessel Committee)

It should be clear that the value of information in any database, but especially in a numeric database, is greatly diminished by the absence of at least some and potentially all of these types of metadata. For example, a listing of the properties of an alloy is of no value at all if it is not clear at what temperature they were determined. It should be clear that metadata are an integral part of every material property database. Similarly the properties of a material are of virtually no value if it is not clear how the materials were mechanically and thermally processed before they were tested.

## 4 SUBJECTS OF DATA SOURCES

Next it is useful to note some of the major categories of available data and illustrate the manner in which they are likely to be classified or structured. From this point on, the discussion will focus primarily upon numeric materials property data of interest to the engineer and scientist.

The total breadth of properties and characteristics may reasonably be illustrated by the following four categories:

- Fundamental (atomic-level) properties
- Physical properties (atomic and macro/alloy levels)
- Mechanical properties (macro/alloy level)
- Application performance (macro/alloy or component levels)

To provide greater detail on the first three categories, it is helpful to utilize the taxonomy of materials information developed by Westbrook<sup>1</sup> and illustrated in Fig. 1. While the entire list of potential uses of data described above is not included, the taxonomy in Fig. 1 illustrates the variety of subject matter quite well.

The fourth major category identified above involves what is referred to as application performance but which in itself incorporates several areas:

1. Fabrication characteristics (sometimes called the “ilities”)
  - Fabricability (“workability”)
  - Forming characteristics (“formability”)
  - Joining characteristics (“joinability”)
  - Finishing characteristics (“finishability”)
2. Service experience
  - Exposure conditions
  - Service history
  - Failures observed and their causes

It is not necessary to discuss these categories individually; rather one simply needs to recognize that specific databases may focus on only one or a few of these subjects and rarely if ever would all subjects be included in any one database.

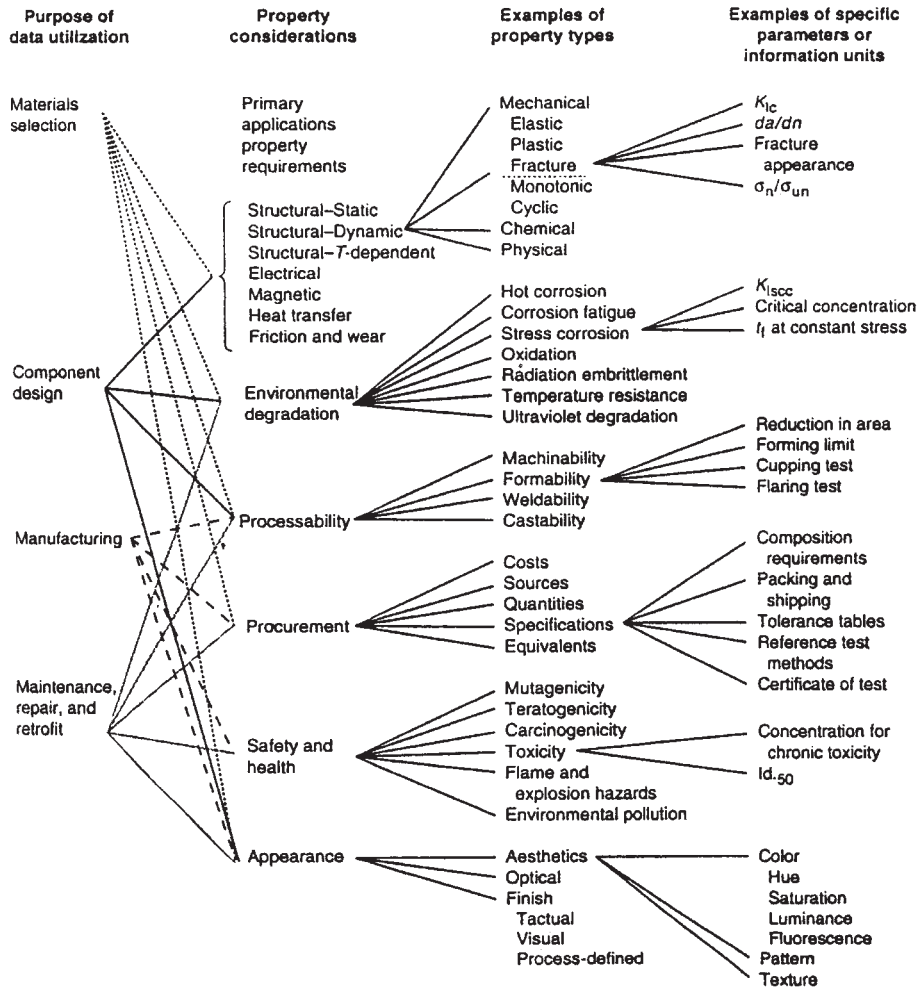
## 5 DATA QUALITY AND RELIABILITY

It was noted in Section 2 that individuals doing preliminary material selection or screening may have different needs with regard to quality and reliability than those doing design functions. It is appropriate at this stage to review the major factors that go into judgments of data quality and reliability.<sup>10</sup> There are two parts to such a discussion: (1) the two major factors affecting the data themselves and (2) the degree to which those factors are reflected in database content.

The two factors affecting quality and reliability include (a) the manner in which the data were obtained and (b) the statistical reliability of the data presented.

First and foremost, the users of a database will want to know that consistent standards were applied in assembling the data for that database and that the properties of one material may reliably be compared with those for another. They will also prefer that those properties have been generated by well-known standard methods such as those prescribed by organizations such as ASTM and ISO.<sup>4</sup> They may also be interested in knowing the specific source of the original data; realistically some laboratories [e.g., the National Institute of Standards and Technology (NIST)] have a more widely recognized reputation than others.





**Figure 1** Taxonomy of materials information. (Source: *ASM Handbook*, Vol. 20: *Materials Selection and Design* (1997), ASM International, Materials Park, OH, 1997, p. 491, Fig. 1.)

The second major factor affecting how the user applies information from a specific database is the statistical reliability of the values included therein. The user will be interested in which of the following categories best describes the values presented:

- Raw data (the results of individual tests)
- Average of multiple tests (how many tests are represented?)
- Statistically analyzed (standard deviation, minimum value at what statistical definition, and with what confidence?)
- Evaluated/certified (by whom and for what purpose?)

Of equal importance to the user of the database is the degree to which those factors affecting quality and reliability as noted above are presented in the database itself and, therefore, are



fully understood by the user. In some instances there may be one or several screens of background information laying out the general guidelines upon which the database was generated. This is particularly effective if the entire database represents properties of a common lineage and character. On the other hand, if the user fails to consult this upfront information, some important delimiters may be missed and the data misinterpreted.

Another means of presenting the metadata concerning quality and reliability is within the database itself. This is especially true for such factors as time–temperature parameters that delimit the applicability of the data and units and other elements of information that may restrict its application (see Section 3.3).

It is also especially important in instances where the individual values may vary with respect to their statistical reliability. While the latter case may seem unlikely, it is actually quite common, as when “design” data are presented: In such cases, the strength values are likely to be statistical minimum values while moduli of elasticity and physical properties are likely to be average values, and the difference should be made clear in the database.

## 6 PLATFORMS: TYPES OF DATA SOURCES

The last feature we will consider before identifying specific data sources is the variety of platforms available for databases today. While it is not necessary to discuss them in detail, it will be obvious that the following choices exist:

- Hard copy (published books, monographs, etc.)
- Self-contained electronic (floppies, CDs, etc.)
- Internet sites (available online; perhaps downloadable)

The only amplification needed on these obvious options is that the last one, the Internet, has become an interesting resource from which to identify and locate specific sources of materials data, and that trend will likely continue to increase. Two large caveats go with the use of Internet sources, however: (1) A great deal of “junk” (i.e., unreliable, undocumented data) may be found on Internet websites and (2) even those containing more reliable data seldom meet all users’ needs with respect to covering the metadata. It is vital that the users themselves apply the guidelines listed earlier to judge the quality and reliability of sources located on the Internet.

## 7 SPECIFIC DATA SOURCES

It is beyond the scope of this chapter to provide an exhaustive list of data sources because there are thousands of them of varying presentation platforms, styles, and content. What we will do here is highlight a few of the potentially most useful sources, in the sense that their coverage is relatively broad and/or they represent good places to go to look for new and emerging sources of materials data.

The sources discussed below representing the variety of types of sources available will include the following:

- The Alloy Center on ASM International’s website; ASM International is a technical society for materials engineers and specialists that produces and provides a wide range of materials databases in hard-copy and electronic form; this service is intended to be used by the engineers and material specialists themselves, the “end users” (see Section 7.1).
- STN International, a service of the American Chemical Society, also provides (for a fee) access to a very wide range of numeric databases as well as a great many

textual/bibliographic databases on materials-related subjects; this service is focused on the professional researcher and technical librarian, not the end user (see Section 7.2).

- The Internet site knovel.com provides full-text searchable handbooks of many disciplines, including materials data (see Section 7.3).
- The Internet as a whole is the most rapidly expanding source for materials data in a variety of forms (see Section 7.4).

For readers interested in more extensive listings, reference is made to the article “Sources of Materials Property Data and Information” by Jack Westbrook in Vol. 20 of the *ASM Handbook*<sup>1</sup> and to the *ASM International Directory of Materials Property Databases*.<sup>3</sup>

## 7.1 ASM International and the Alloy Center

ASM International has emerged as one of the strongest providers of numeric materials data sources, and those sources are generally in three formats or platforms: hard copy, disk (usually CD-ROM), and the Alloy Center on the Internet. As an example, one of the most extensive sources of high- and low-temperature data for aluminum alloys has recently been made available through a collaborative effort of ASM and the Aluminum Association in both the book *Properties of Aluminum Alloys—Tensile, Creep, and Fatigue Data at High and Low Temperatures*<sup>11</sup> and a searchable CD of the same title. Other representative data sources from ASM International include the following:

- *ASM Handbook*,<sup>12</sup> in Hard Copy and CD. Twenty volumes complete or available in a specific set covering material properties; the data sets are available for single workstations and also for local area network (LAN) arrangements. Other CDs are available covering heat treatment, testing and analysis, and manufacturing processes.
- *Alloy Finder CD*. Contains full alloy records from three ASM hard-copy reference standards: *Woldman’s Engineering Alloys*,<sup>13</sup> the *ASM Worldwide Guide to Equivalent Irons and Steels*,<sup>14</sup> and the *ASM Worldwide Guide to Equivalent Nonferrous Metals and Alloys*.<sup>15</sup> The disk is searchable by composition as well as designation, so whether the user requires amplification of an alloy designation or to locate designations within specific composition ranges, the need is addressed.
- *Alloy Digest on CD*. Summaries of recently published data for new and emerging alloys are compiled periodically on disk as well as being made available in hard copy. The advantages include early warning of new materials; the limitation is the inability to provide consistent formats or data scope because such are not available for relatively new materials. More than 4200 data sheets are now available.
- *Binary-Phase Diagrams on CD-ROM*. The world’s most extensive collection of binary-phase diagrams numbering in excess of 4700 is available on CD, in addition to ASM hard-copy publications such *Handbook of Ternary Alloy Phase Diagrams* and the monograph series on specific alloy groupings.
- *Failure Analysis on CD-ROM*. One of the most extensive collection of data expressly developed for failure analysis is available on searchable CD-ROM as well as hard copy.
- *Materials Databases*. Numeric materials databases covering a variety of classes of materials are available from ASM on disk in various formats, including within Mat.DB, MAPP, and Rover search software. The databases are organized and searchable by mechanical and physical property as well as alloy class: steel and stainless steel, aluminum, composites, copper, magnesium, plastics and polymers, nylon, and titanium, plus special disk covering corrosion data.

- *Alloy Center on the ASM International Website.* In collaboration with Granta Design, ASM International has established an extensive Alloy Center on its website [www.asminternational.org](http://www.asminternational.org) that provides searchable access to a wide and growing range of numeric materials property data. Where justified, some are presented in graphical format. The ASM Alloy Center is available for a reasonable subscription fee and, together with the availability of the ASM handbook series online, provides a formidable source of materials information.

## 7.2 STN International

STN International is the online worldwide scientific and technical information network and one of the most extensive sources of numeric materials property data.<sup>16</sup> Built and operated by the American Chemical Society at its Chemical Abstract Service site in Columbus, Ohio, STN International provides about 30 numeric databases, including many developed during the collaboration with the Materials Property Data Network.<sup>17-19</sup> Of great interest to materials data searchers, STN International has the most sophisticated numeric data search software available anywhere online. Thus the data sources may be searched numerically, i.e., using numeric values as ranges or with “greater or less than” types of operators, making it possible to search for alloys that meet required performance needs.

The disadvantages of using STN International to search for numeric data are twofold: (a) The search software is keyed to a command system best known to professional searchers and engineers and scientists will need patience and some training to master the technique and (b) use of the STN International system is billed via a time- and content-based cost accounting system, and so a private account is needed. Outright purchase of databases has not been a policy.

For those able to deal with those conditions, a number of valuable databases exist on STN International, including the following representative sources:

- Aluminium—Aluminum Industry Abstracts (textual; 1868–present)
- ASMDATA—ASM Materials Databases online version
- BEILSTEIN—Beilstein Organic Compound Files (1779–1999)
- COPPERDATA—Copper and Copper Alloy Standards and Data
- DETHERM—Thermophysical Properties Database (1819–present)
- DIPPR—AIChE Design Institute Physical Property Data File
- GMELIN—GMELIN Handbook of Inorganic Chemistry (1817–present)
- ICSD—Inorganic Crystal Structure Database (1912–present)
- NUMERIGUIDE—Property Hierarchy and Directory for Numeric Files
- MDF—Metals Datafile (1982–1993)
- PIRA—PIRA and PAPERBASE Database (1975–present)
- PLASPEC—Plastics Material Selection Database
- RAPRA—Rubber, Plastics, Adhesives, and Polymer Composites (1972–present)

For more information on STN International, readers are referred to the website, [www.stn.org](http://www.stn.org).

### 7.3 knovel.com

A rapidly growing and very useful scientific information website is [www.knovel.com](http://www.knovel.com). Produced by the Knovel subsidiary of William Andrew, Inc., it provides an impressive array of searchable versions of hard-copy engineering and scientific reference publications (e.g., the *Handbook of Chemistry and Physics*) as well as access to a wide range of materials data.

Unlike many online sources where such publications are reproduced only as readable print, Knovel subscription holders may work interactively with the various sources and search them individually, in selected groups, or in total. It is highly unusual to find such an array of highly respected sources accessible through a single site and with a specialized search software that caters to the needs of the searcher.

### 7.4 The Internet

As indicated earlier, there are many websites on the Internet with materials information content in addition to those specifically identified above. In fact, there are so many, the challenge is to determine which have useful, reliable, and relatively easily accessible data.

Here we will focus on guidance on these latter points developed by Fran Cverna, Director of Electronic and Reference Data Sources at ASM International, who recently produced and presented a survey of scope and quality of materials data content provided at Internet websites, and results of the most useful websites screened by Cverna and her ASM resources are referenced here<sup>20</sup>:

<a href="http://www.about.com">www.about.com</a>	Internet search engine—search Materials and Properties
<a href="http://www.nist.gov/public%20affairs/database.htm">www.nist.gov/public affairs/database.htm</a>	NIST Standard Reference Database
<a href="http://www.ecn.purdue.edu/MPHO">www.ecn.purdue.edu/MPHO</a>	TPRL thermophysical properties data
<a href="http://Id.inel.gov/shds">Id.inel.gov/shds</a>	U.S. government solvent database
<a href="http://www.campusplastics.com">www.campusplastics.com</a>	Campus Consortium plastics database
<a href="http://www.copper.org">www.copper.org</a>	Copper Development Association copper alloys database
<a href="http://www.brushwellman.com/homepage.htm">www.brushwellman.com/homepage.htm</a>	Brush Wellman supplier materials database
<a href="http://www.timet.com/overviewframe.html">www.timet.com/overviewframe.html</a>	Timet supplier materials database
<a href="http://www.specialmetals.com">www.specialmetals.com</a>	Special Metals supplier materials database
<a href="http://www.cartech.com">www.cartech.com</a>	Cartech supplier materials database (compositions)
<a href="http://www.macsteel.com/mdb">www.macsteel.com/mdb</a>	McSteel supplier materials database (limited)
<a href="http://www.aluminum.org">www.aluminum.org</a>	Aluminum Association applications, publications' limited data

Of these sources, two merit special mention: the Internet search engine site [www.about.com](http://www.about.com) and the NIST database site [www.nist.gov/public affairs/database.htm](http://www.nist.gov/public%20affairs/database.htm), a part of the Public Affairs menu at NIST's website.

The About.com site provides an excellent means of locating materials data sites and provides a subcategory called Materials Properties and Data if you search for such information. Thirty-two sites are identified, some of which overlap the ASM survey, but to the author's experience others are unique to that site. Many included in the ASM survey are not included here,

so the two are supplementary in scope. Among the specific types of information accessible via about.com are:

- Coefficient of thermal expansion
- Electrical conductivity
- Electrical resistivity
- Hardness conversion charts
- Metal temperature by color
- Metal weight calculator
- Periodic table of elements
- Specific gravity of metals
- Surface roughness comparison charts
- Thermal properties
- Wire gauge conversion tables
- Utilities to simplify tasks such as conversion charts for units, currency conversion, glossaries, and acronym definitions

In addition, About.com has links to many other materials sites, including to Aluminum.com, which also provides materials data for a variety of metals, but often without adequate citation and metadata.

The NIST database site provides direct online access to the highest quality, carefully evaluated numeric data from the following databases:

- Standard Reference Data—reliable scientific and technical data extracted from the world's literature, assessed for reliability and critically evaluated
- Ceramics WebBook—evaluated data and access to data centers as well as tools and resources
- Chemistry WebBook—chemical and physical property data for specific compounds
- Fundamental Physical Constants—internationally recommended values of a wide range of often-used physical constants
- Thermophysical Properties of Gases for the Semiconductor Industry

In summary, there are many sources of numeric materials data available from Internet sites. It remains for the potential users of the data, however, to approach each site with caution, look for the pedigree of the data in terms of quality and reliability, and make certain that the source of interest meets the requirements of the intended use.

## ACKNOWLEDGMENTS

The contributions of Jack Westbrook, of Brookline Technologies, and Fran Cverna, of ASM international, are acknowledged and deeply appreciated.

## REFERENCES

1. J. H. Westbrook, "Sources of Materials Property Data and Information," *ASM Handbook*, Vol. 20, ASM International, Materials Park, OH, 1997.
2. J. H. Westbrook and K. W. Reynard, "Data Sources for Materials Economics, Policy, and Management," in M. B. Bever (Ed.), *Concise Encyclopedia of Materials Economics, Policy, and Management*, Pergamon, New York, 1993.

3. *ASM International Directory of Materials Property Databases*, ASM International, Materials Park, OH, published periodically.
4. ASTM and ANSI / ISO standards, *Annual Book of ASTM Standards*, American Society for Testing and Materials, Conshohocken, PA; American National Standards Institute and International Standards Organization standards, Brussels, published periodically.
5. *Metallic Materials and Elements for Aerospace Vehicle Structures*, MIL-HDBK-5H, U.S. Department of Defense, Washington, DC, published periodically (now known as MMPDS-01).
6. Publications of the Thermophysical Properties Research Center (TPRC, previously known as CINDAS), Lafayette, IN.
7. *ASME Boiler and Pressure Vessel Code*, Section 2, Material—Properties, American Society of Mechanical Engineers, New York, published periodically.
8. *Aluminum Standards and Data, 2000 and Aluminum Standards and Data 1998 Metric SI*, Aluminum Association, Washington, DC, published periodically.
9. J. H. Westbrook and W. Grattidge, "The Role of Metadata in the Design and Operation of a Materials Database," in J. G. Kaufman and J. S. Glazman (Eds.), *Computerization and Networking of Materials Databases*, ASTM STP 1106, American Society for Testing and Materials, Philadelphia, PA, 1991.
10. J. G. Kaufman, "Quality and Reliability Issues in Materials Databases: ASTM Committee E49.05," in T. I. Barry and K. W. Reynard (Eds.), *Computerization and Networking of Materials Databases*, Vol. 3, ASTM STP 1140, American Society for Testing and Materials, Philadelphia, PA, 1992, pp. 64–83.
11. J. G. Kaufman, *Properties of Aluminum Alloys—Tensile, Creep, and Fatigue Data at High and Low Temperatures*, ASM International, Materials Park, OH, 1999.
12. *ASM Handbook*, Vols. 1 and 2: *Properties and Selection*, ASM International, Materials Park, OH, published periodically.
13. *Woldman's Engineering Alloys*, 8th ed., Woldman's, London, published periodically.
14. *Worldwide Guide to Equivalent Irons and Steels*, ASM International, Materials Park, OH, published periodically.
15. *Worldwide Guide to Equivalent Nonferrous Metals and Alloys*, ASM International, Materials Park, OH, published periodically.
16. STN International, the Worldwide Scientific and Technical Information Network, Chemical Abstract Services (CAS), a division of the American Chemical Society, Columbus, OH.
17. J. G. Kaufman, "The National Materials Property Data Network Inc., The Technical Challenges and the Plan," in *Materials Property Data: Applications and Access*, PVP-Vol. 111, J. G. Kaufman, (ed.), MPD-Vol. 1, American Society of Mechanical Engineers, New York, 1986, pp. 159–166.
18. J. G. Kaufman, "The National Materials Property Data Network, Inc.—A Cooperative National Approach to Reliable Performance Data," in *Computerization and Networking of Materials Data Bases*, ASTM STP 1017, J. S. Glazman and J. R. Rumble, Jr., (eds.), American Society for Testing and Materials, Philadelphia, PA, 1989, pp. 55–62.
19. J. H. Westbrook and J. G. Kaufman, "Impediments to an Elusive Dream," in *Modeling Complex Data for Creating Information*, J. E. DuBois and N. Bershon, (eds.), Springer-Verlag, Berlin, 1996.
20. F. Cverna, "Overview of Commercially Available Material Property Data Collections" (on the Internet), presented at the 2000 ASM Materials Solutions Conference on Materials Property Databases, ASM International, St Louis, MO, Oct. 10–12, 2000.



# CHAPTER 15

## QUANTITATIVE METHODS OF MATERIALS SELECTION

**Mahmoud M. Farag**

The American University in Cairo Cairo Egypt

<b>1 INTRODUCTION</b>	<b>531</b>	5.4 Selecting the Optimum Solution	543
<b>2 INITIAL SCREENING OF MATERIALS</b>	<b>532</b>	<b>6 MATERIALS SUBSTITUTION</b>	<b>545</b>
2.1 Analysis of Material Performance Requirements	532	6.1 Pugh Method	546
2.2 Quantitative Methods for Initial Screening	534	6.2 Cost–Benefit Analysis	547
<b>3 COMPARING AND RANKING ALTERNATIVE SOLUTIONS</b>	<b>538</b>	<b>7 CASE STUDY IN MATERIALS SUBSTITUTION</b>	<b>548</b>
3.1 Weighted-Properties Method	538	<b>8 SOURCES OF INFORMATION AND COMPUTER-ASSISTED SELECTION</b>	<b>548</b>
<b>4 SELECTING THE OPTIMUM SOLUTION</b>	<b>540</b>	8.1 Locating Materials Properties Data	548
<b>5 CASE STUDY IN MATERIALS SELECTION</b>	<b>541</b>	8.2 Types of Material Information	549
5.1 Material Performance Requirements	541	8.3 Computerized Materials Databases	549
5.2 Initial Screening of Materials	541	8.4 Computer Assistance in Making Final Selection	550
5.3 Comparing and Ranking Alternative Solutions	542	8.5 Expert Systems	550
		<b>REFERENCES</b>	<b>551</b>

### 1 INTRODUCTION

It is estimated that there are more than 40,000 currently useful metallic alloys and probably close to that number of nonmetallic engineering materials like plastics, ceramics and glasses, composite materials, and semiconductors. This large number of materials and the many manufacturing processes available to the engineer, coupled with the complex relationships between the different selection parameters, often make the selection of a material for a given component a difficult task. If the selection process is carried out haphazardly, there will be the risk of overlooking a possible attractive alternative material. This risk can be reduced by adopting a systematic material selection procedure. A variety of quantitative selection procedures have been developed to analyze the large amount of data involved in the selection process so that a systematic evaluation can be made.<sup>1–11</sup> Several of the quantitative procedures can be adapted to use computers in selection from a data bank of materials and processes.<sup>12–17</sup>

Experience has shown that it is desirable to adopt the holistic decision-making approach of concurrent engineering in product development in most industries. With concurrent



engineering, materials and manufacturing processes are considered in the early stages of design and are more precisely defined as the design progresses from the concept to the embodiment and finally the detail stages. Figure 1 defines the different stages of design and shows the related activities of the material and manufacturing process selection. The figure illustrates the progressive nature of materials and process selection and defines three stages of selection: initial screening, comparing and ranking alternatives, and selecting the optimum solution. Sections 2, 3, and 4 discuss these three stages of material and process selection in more detail and Section 5 gives a case study to illustrate the procedure.

Although the materials and process selection is often thought of in terms of new product development, there are many other incidences where materials substitution is considered for an existing product. Issues related to materials substitution are discussed in Section 6.

Unlike the exact sciences, where there is normally only one single correct solution to a problem, materials selection and substitution decisions require the consideration of conflicting advantages and limitations, necessitating compromises and tradeoffs; as a consequence, different satisfactory solutions are possible. This is illustrated by the fact that similar components performing similar functions but produced by different manufacturers are often made from different materials and even by different manufacturing processes.

## 2 INITIAL SCREENING OF MATERIALS

In the first stages of development of a new product, such questions as the following are posed: What is it? What does it do? How does it do it? After answering these questions, it is possible to specify the performance requirements of the different parts involved in the design and to broadly outline the main materials performance and processing requirements. This is then followed by the initial screening of materials whereby certain classes of materials and manufacturing processes may be eliminated and others chosen as likely candidates.

### 2.1 Analysis of Material Performance Requirements

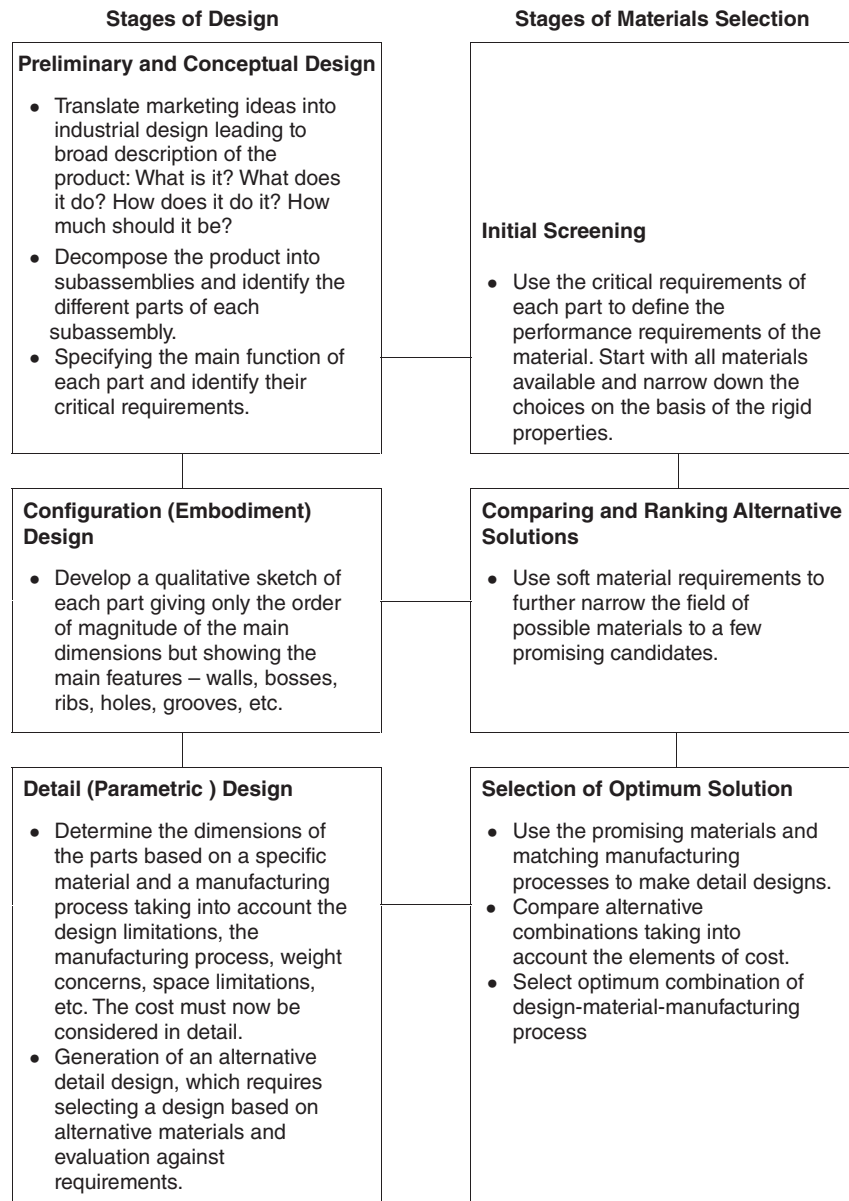
The material performance requirements can be divided into five broad categories: functional requirements, processability requirements, cost, reliability, and resistance to service conditions.<sup>1</sup>

#### *Functional Requirements*

Functional requirements are directly related to the required characteristics of the part or the product. For example, if the part carries a uniaxial tensile load, the yield strength of a candidate material can be directly related to the load-carrying capacity of the product. However, some characteristics of the part or product may not have simple correspondence with measurable material properties, as in the case of thermal shock resistance, wear resistance, reliability, etc. Under these conditions, the evaluation process can be quite complex and may depend upon predictions based on simulated service tests or upon the most closely related mechanical, physical, or chemical properties. For example, thermal shock resistance can be related to the thermal expansion coefficient, thermal conductivity, modulus of elasticity, ductility, and tensile strength. On the other hand, resistance to stress–corrosion cracking can be related to tensile strength and electrochemical potential.

#### *Processability Requirements*

The processability of a material is a measure of its ability to be worked and shaped into a finished part. With reference to a specific manufacturing method, processability can be defined



**Figure 1** Stages of design and the related stages of materials selection.

as castability, weldability, machinability, etc. Ductility and hardenability can be relevant to processability if the material is to be deformed or hardened by heat treatment, respectively. The closeness of the stock form to the required product form can be taken as a measure of processability in some cases.

It is important to remember that processing operations will almost always affect the material properties so that processability considerations are closely related to functional requirements.

***Cost***

Cost is usually an important factor in evaluating materials because in many applications there is a cost limit for a given component. When the cost limit is exceeded, the design may have to be changed to allow for the use of a less expensive material or process. In some cases, a relatively more expensive material may eventually yield a less expensive component than a low-priced material that is more expensive to process.

***Reliability Requirements***

Reliability of a material can be defined as the probability that it will perform the intended function for the expected life without failure. Material reliability is difficult to measure because it is not only dependent upon the material's inherent properties, but it is also greatly affected by its production and processing history. Generally, new and nonstandard materials will tend to have lower reliability than established, standard materials.

Despite difficulties of evaluating reliability, it is often an important selection factor that must be taken into account. Failure analysis techniques are usually used to predict the different ways in which a product can fail and can be considered as a systematic approach to reliability evaluation. The causes of failure of a part in service can usually be traced back to defects in materials and processing, faulty design, unexpected service conditions, or misuse of the product.

***Resistance to Service Conditions***

The environment in which the product or part will operate plays an important role in determining the material performance requirements. Corrosive environments, as well as high or low temperatures, can adversely affect the performance of most materials in service. Whenever more than one material is involved in an application, compatibility becomes a selection consideration. In a thermal environment, for example, the coefficients of thermal expansion of all the materials involved may have to be similar in order to avoid thermal stresses. In wet environments, materials that will be in electrical contact should be chosen carefully to avoid galvanic corrosion. In applications where relative movement exists between different parts, wear resistance of the materials involved should be considered. The design should provide access for lubrication; otherwise self-lubricating materials have to be used.

**2.2 Quantitative Methods for Initial Screening**

Having specified the performance requirements of the different parts, the required material properties can be established for each of them. These properties may be quantitative or qualitative, essential or desirable. For example, the function of a connecting rod in an internal combustion engine is to connect the piston to the crankshaft. The performance requirements are that it should transmit the power efficiently without failing during the expected life of the engine. The essential material properties are tensile and fatigue strengths, while the desirable properties that should be maximized are processability, weight, reliability, and resistance to service conditions. All these properties should be achieved at a reasonable cost. The selection process involves the search for the material or materials that would best meet those requirements. In some cases none of the available materials can meet the requirements or the possible materials are too expensive or environmentally unsafe. In such cases, alternatives must be made possible through redesign, compromise of requirements, or development of new materials.

Generally, the starting point for materials selection is the entire range of engineering materials. At this stage, creativity is essential in order to open up channels in different directions, not let traditional thinking interfere with the exploration of ideas, and ensure that potential materials are not overlooked. A steel may be the best material for one design concept while a plastic is best for a different concept, even though the two designs provide the same function.

After all the alternatives have been suggested, the ideas that are obviously unsuitable are eliminated and attention is concentrated on those that look practical. Quantitative methods can be used for initial screening in order to narrow down the choices to a manageable number for subsequent detailed evaluation. Following are some of the quantitative methods for initial screening of materials.

### ***Limits on Material Properties***

Initial screening of materials can be achieved by first classifying their performance requirements into two main categories<sup>1</sup>:

- Rigid, or go–no go, requirements
- Soft, or relative, requirements

Rigid requirements are those that must be met by the material if it is to be considered at all. Such requirements can be used for the initial screening of materials to eliminate the unsuitable groups. For example, metallic materials are eliminated when selecting materials for an electrical insulator. If the insulator is to be flexible, the field is narrowed further as all ceramic materials are eliminated. Other examples of material rigid requirements include behavior under operating temperature, resistance to corrosive environment, ductility, electrical and thermal conductivity or insulation, and transparency to light or other waves. Examples of process rigid requirements include batch size, production rate, product size and shape, tolerances, and surface finish. Whether or not the equipment or experience for a given manufacturing process exists in a plant can also be considered as a hard requirement in many cases. Compatibility between the manufacturing process and the material is also an important screening parameter. For example, cast irons are not compatible with sheet-metal-forming processes and steels are not easy to process by die casting. In some cases, eliminating a group of materials results in automatic elimination of some manufacturing processes. For example, if plastics are eliminated because service temperature is too high, injection and transfer molding should be eliminated as they are unsuitable for other materials.

Soft, or relative, requirements are those that are subject to compromise and tradeoffs. Examples of soft requirements include mechanical properties, specific gravity, and cost. Soft requirements can be compared in terms of their relative importance, which depends on the application under study.

### ***Cost-per-Unit-Property Method***

The cost-per-unit-property method is suitable for initial screening in applications where one property stands out as the most critical service requirement.<sup>1</sup> As an example, consider the case of a bar of a given length  $L$  to support a tensile force  $F$ . The cross-sectional area  $A$  of the bar is given by

$$A = \frac{F}{S} \quad (1)$$

where  $S$  is the working stress of the material, which is related to its yield strength divided by an appropriate factor of safety.

The cost of the bar ( $C'$ ) is given by

$$C' = C\rho AL = \frac{C\rho FL}{S} \quad (2)$$

where  $C$  = cost of material per unit mass  
 $\rho$  = density of material

Since  $F$  and  $L$  are constant for all materials, comparison can be based on the cost of unit strength, which is the quantity

$$\frac{C\rho}{S} \quad (3)$$

Materials with lower cost per unit strength are preferable. If an upper limit is set for the quantity  $C\rho/S$ , then materials satisfying this condition can be identified and used as possible candidates for more detailed analysis in the next stage of selection.

The working stress of the material in Eqs. (1)–(3) is related to the static yield strength of the material since the applied load is static. If the applied load is alternating, it is more appropriate to use the fatigue strength of the material. Similarly, the creep strength should be used under loading conditions that cause creep.

Equations similar to (2) and (3) can be used to compare materials on the basis of cost per unit stiffness when the important design criterion is deflection in the bar. In such cases,  $S$  is replaced by the elastic modulus of the material. The above equations can also be modified to allow comparison of different materials under loading systems other than uniaxial tension. Table 1 gives some formulas for the cost per unit property under different loading conditions based on either yield strength or stiffness.

### *Ashby's Method*

Ashby's material selection charts<sup>4,5,9,10</sup> are also useful for initial screening of materials. Figure 2 plots the strength versus density for a variety of materials. Depending upon the geometry and type of loading, different  $S$ – $\rho$  relationships apply, as shown in Table 1. For simple axial loading, the relationship is  $S/\rho$ . For a solid rectangle under bending,  $S^{1/2}/\rho$  applies, and for a solid cylinder under bending or torsion the relationship  $S^{2/3}/\rho$  applies. Lines with these slopes are shown in Fig. 2. Thus, if a line is drawn parallel to the line  $S/\rho = C$ , all the materials that lie on the line will perform equally well under simple axial loading conditions. Materials above the line are better and those below it are worse. A similar diagram can be drawn for elastic modulus versus density, and formulas similar to those in Table 1 can be used to screen materials under conditions where stiffness is a major requirement

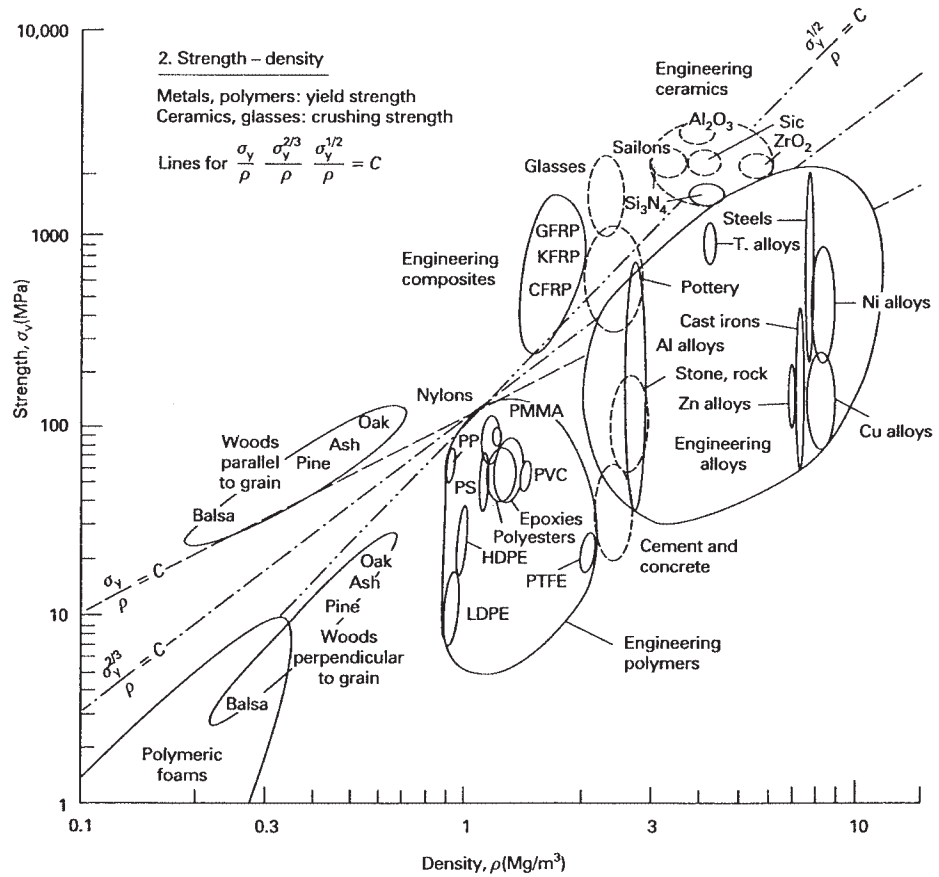
### *Dargie's Method*

The initial screening of materials and processes can be a tedious task if performed manually from handbooks and supplier catalogs. This difficulty has prompted the introduction of several computer-based systems for materials and/or process selection.<sup>12–15</sup> As an illustrative example, the system MAPS 1 proposed by Dargie et al.<sup>15</sup> will be briefly described here. For this system, Dargie et al. proposed a part classification code similar to that used in group technology.

**Table 1** Formulas for Estimating Cost per Unit Property

Cross Section and Loading Condition	Cost per Unit Strength	Cost per Unit Stiffness
Solid cylinder in tension or compression	$C\rho/S$	$C\rho/E$
Solid cylinder in bending	$C\rho/S^{2/3}$	$C\rho/E^{1/2}$
Solid cylinder in torsion	$C\rho/S^{2/3}$	$C\rho/G^{1/2}$
Solid cylindrical bar as slender column	—	$C\rho/E^{1/2}$
Solid rectangle in bending	$C\rho/S^{1/2}$	$C\rho/E^{1/3}$
Thin-walled cylindrical pressure vessel	$C\rho/S$	—

Source: From Ref. 1.



**Figure 2** Example of Ashby's materials selection charts. (From Ref. 10, with permission from The Institute of Materials.)

The first five digits of the MAPS 1 code are related to the elimination of unsuitable manufacturing processes. The first digit is related to the batch size. The second digit characterizes the bulk and depends on the major dimension and whether the part is long, flat, or compact. The third digit characterizes the shape, which is classified on the basis of being prismatic, axisymmetric, cup shaped, nonaxisymmetric, and nonprismatic. The fourth digit is related to tolerance and the fifth digit is related to surface roughness.

The next three digits of the MAPS 1 code are related to the elimination of unsuitable materials. The sixth digit is related to service temperature. The seventh digit is related to the acceptable corrosion rate. The eighth digit characterizes the type of environment to which the part is exposed.

The system uses two types of databases for preliminary selection:

- Suitability matrices
- Compatibility matrix

The suitability matrices deal with the suitability of processes and materials for the part under consideration. Each of the code digits has a matrix. The columns of the matrix correspond

to the value of the digit and the rows correspond to the processes and materials in the database. The elements of the matrix are either 0, indicating unsuitability, or 2, indicating suitability.

The compatibility matrix expresses the compatibility of the different combinations of processes and materials. The columns of the matrix correspond to the materials while the rows correspond to the processes. The elements of the matrix are 0 for incompatible combinations, 1 for difficult or unusual combinations, and 2 for combinations used in usual practice.

Based on the part code, the program generates a list of candidate combinations of materials and processes to produce it. This list helps the designer to identify possible alternatives early in the design process and to design for ease of manufacture.

### *Esawi and Ashby's Method*

Another quantitative method of initial screening is proposed by Esawi and Ashby.<sup>16</sup> The method compares the approximate cost of resources of materials, energy, capital, time, and information needed to produce the component using different combinations of materials and manufacturing processes. The method can be used early in the design process and is capable of comparing combinations of materials and processes such as the cost of a polymer component made by injection molding with that of a competing design in aluminum made by die casting.

According to this method, the total cost of a component has three main elements: material cost, tooling cost, and overhead cost. The material cost is a function of the cost per unit weight of the material and the amount the material needed. Since the cost of tooling (dies, molds, jigs, fixtures, etc.) is normally assigned to a given production run, the tooling cost per component varies as the reciprocal of the number of components produced in that run. The overhead per component varies as the reciprocal of the production rate. Application of this method in initial screening requires a database, such as CES 4, which lists material prices, attributes of different processes, production rates, tool life, and approximate cost of equipment and tooling. CES 4 Software<sup>17</sup> contains records for 112 shaping processes such as vapor deposition, casting, molding, metal forming, machining, and composite forming. The software output can be in the form of graphs giving the variation of cost with the batch size for competing process/material combinations. Another type of output is relative cost per unit when a given component is made by different processing routes.

## 3 COMPARING AND RANKING ALTERNATIVE SOLUTIONS

After narrowing down the field of possible materials using one or more of the quantitative initial screening methods described in Section 2, quantitative methods can then also be used to further narrow the field of possible materials and matching manufacturing processes to a few promising candidates that have good combinations of soft requirements. Several such methods are described in Refs. 1 and 2 and following is a description of one of the methods.

### 3.1 Weighted-Properties Method

In the weighted-properties method each material requirement, or property, is assigned a certain weight, depending on its importance to the performance of the part in service.<sup>1</sup> A weighted-property value is obtained by multiplying the numerical value of the property by the weighting factor ( $\alpha$ ). The individual weighted-property values of each material are then summed to give a comparative materials performance index ( $\gamma$ ). Materials with the higher performance index ( $\gamma$ ) are considered more suitable for the application.

**Table 2** Determination of Relative Importance of Goals Using Digital Logic Method

Goals	Number of Positive Decisions $N = n(n-1)/2$										Positive Decisions	Relative Emphasis Coefficient $\alpha$
	1	2	3	4	5	6	7	8	9	10		
1	1	1	0	1							3	0.3
2	0				1	0	1				2	0.2
3		0			0			1	0		1	0.1
4			1			1		0		0	2	0.2
5				0			0		1	1	2	0.2
	Total positive decisions										10	$\sum \alpha = 1.0$

Note: From Ref. 1.

### Digital Logic Method

In the cases where numerous material properties are specified and the relative importance of each property is not clear, determinations of the weighting factor  $\alpha$  can be largely intuitive, which reduces the reliability of selection. The digital logic approach can be used as a systematic tool to determine  $\alpha$ .<sup>1</sup> In this procedure evaluations are arranged such that only two properties are considered at a time. Every possible combination of properties or goals is compared and no shades of choice are required, only a yes or no decision for each evaluation. To determine the relative importance of each property or goal, a table is constructed, the properties or goals are listed in the left-hand column, and comparisons are made in the columns to the right, as shown in Table 2.

In comparing two properties or goals, the more important goal is given the number 1 and the less important is given a 0. The total number of possible decisions is  $N = n(n-1)/2$ , where  $n$  is the number of properties or goals under consideration. A relative-emphasis coefficient or weighting factor  $\alpha$  for each goal is obtained by dividing the number of positive decisions for each goal ( $m$ ) into the total number of possible decisions ( $N$ ). In this case  $\sum \alpha = 1$ .

To increase the accuracy of decisions based on the digital logic approach, the yes–no evaluations can be modified by allocating gradation marks ranging from 0 (no difference in importance) to 3 (large difference in importance). In this case, the total gradation marks for each selection criterion are reached by adding up the individual gradation marks. The weighting factors are then found by dividing these total gradation marks by their grand total. A simple interactive computer program can be written to help in determining the weighting factors. A computer program will also make it easier to perform several runs of the process in order to test the sensitivity of the final ranking to changes in some of the decisions—sensitivity analysis.

### Performance Index

In its simple form, the weighted-properties method has the drawback of having to combine unlike units, which could yield irrational results. This is particularly true when different mechanical, physical, and chemical properties with widely different numerical values are combined. The property with higher numerical value will have more influence than is warranted by its weighting factor. This drawback is overcome by introducing scaling factors. Each property is so scaled that its highest numerical value does not exceed 100. When evaluating a list of candidate materials, one property is considered at a time. The best value in the list is rated as 100 and the others are scaled proportionally. Introducing a scaling factor facilitates the conversion of normal material property values to scaled dimensionless values. For a given property, the scaled value  $B$  for a given candidate material is equal to

$$B = \text{scaled property} = \frac{\text{numerical value of property} \times 100}{\text{maximum value in list}} \quad (4)$$



For properties like cost, corrosion or wear loss, and weight gain in oxidation, a lower value is more desirable. In such cases, the lowest value is rated as 100 and  $B$  is calculated as

$$B = \text{scaled property} = \frac{\text{maximum value in list} \times 100}{\text{numerical value of property}} \quad (5)$$

For material properties that can be represented by numerical values, application of the above procedure is simple. However, with properties like corrosion, wear resistance, machinability, and weldability, numerical values are rarely given and materials are usually rated as very good, good, fair, poor, etc. In such cases, the rating can be converted to numerical values using an arbitrary scale. For example, corrosion resistance ratings excellent, very good, good, fair, and poor can be given numerical values of 5, 4, 3, 2, and 1, respectively. After scaling the different properties, the material performance index  $\gamma$  can be calculated as

$$\gamma = \sum_{i=1}^n B_i \alpha_i \quad (6)$$

where  $i$  is summed over all the  $n$  relevant properties.

Cost (stock material, processing, finishing, etc.) can be considered as one of the properties and given the appropriate weighting factor. However, if there is a large number of properties to consider, the importance of cost may be emphasized by considering it separately as a modifier to the material performance index  $\gamma$ . In the cases where the material is used for space filling, cost can be introduced on a per-unit-volume basis. A figure of merit  $M$  for the material can then be defined as

$$M = \frac{\gamma}{C\rho} \quad (7)$$

where  $C$  = total cost of material per unit weight (stock, processing, finishing, etc.)

$\rho$  = density of material

When an important function of the material is to bear stresses, it may be more appropriate to use the cost of unit strength instead of the cost per unit volume. This is because higher strength will allow less material to be used to bear the load, and the cost of unit strength may be a better indicator of the amount of material actually used in making the part. In this case, Eq. (7) is rewritten as

$$M = \frac{\gamma}{C'} \quad (8)$$

where  $C'$  is determined from Table 1 depending on the type of loading.

This argument may also hold in other cases where the material performs an important function like electrical conductivity or thermal insulation. In these cases the amount of the material and consequently the cost are directly affected by the value of the property.

When a large number of materials with a large number of specified properties are being evaluated for selection, the weighted properties method can involve a large number of tedious and time-consuming calculations. In such cases, the use of a computer would facilitate the selection process. The steps involved in the weighted-properties method can be written in the form of a simple computer program to select materials from a data bank. The type of material information needed for computer-assisted ranking of an alternative solution is normally structured in the form of databases of properties such as those published by ASM, as will be described in Section 8.

## 4 SELECTING THE OPTIMUM SOLUTION

Candidates that have the most promising performance indices can each now be used to develop a detail design. Each detail design will exploit the points of strength of the material, avoid the weak points, and reflect the requirements of the manufacturing processes needed for the

material. The type of material information needed for detail design is different from that needed for initial screening and ranking. What is needed at this stage is detailed high-quality information about the highest ranking candidates. As will be shown in Section 8, such information is usually unstructured and can be obtained from handbooks, publications of trade organizations, and technical reports in the form of text, pdf files, tables, graphs, photographs, etc. There are instances where some of the desired data may not be available or may be for slightly different test conditions. In such cases educated judgment is required.

After completing the different designs, solutions are then compared, taking the cost elements into consideration in order to arrive at the optimum design–material–process combination, as will be illustrated in the following case study.

## 5 CASE STUDY IN MATERIALS SELECTION

The following case study illustrates the procedure for materials selection as described in Sections 2, 3, and 4 and is based on Ref. 18. The objective is to select the least expensive component that satisfies the requirements for a simple structural component for a sailing-boat mast in the form of a hollow cylinder of length 1000 mm that is subjected to compressive axial forces of 153 kN. Because of space and weight limitations, the outer diameter of the component should not exceed 100 mm, the inner diameter should not be less than 84 mm, and the mass should not exceed 3 kg. The component will be subjected to mechanical impact and spray of water. Assembly to other components requires the presence of relatively small holes.

### 5.1 Material Performance Requirements

Possible modes of failure and the corresponding material properties that are needed to resist failure for the present component include the following:

- Catastrophic fracture due to impact loading, especially near assembly holes, is resisted by the high fracture toughness of the material. This is a rigid-material requirement and will be used for initial screening of materials.
- Plastic yielding is resisted by high yield strength. This is a soft-material requirement, but a lower limit will be determined by the limitation on the outer diameter.
- Local and global buckling are resisted by high elastic modulus. This is a soft-material requirement, but a lower limit will be determined by the limitation on the outer diameter.
- Internal fiber buckling for fiber-reinforced materials is resisted by high modulus of elasticity of the matrix and high volume fraction of fibers in the loading direction. This is a soft-material requirement, but a lower limit will be determined by the limitation on the outer diameter.
- Corrosion, which can be resisted either by selecting materials with inherently good corrosion resistance or by protective coating.
- Reliability of the component in service. A factor of safety of 1.5 is taken for the axial loading, i.e., the working axial force will be taken as 230 kN to improve reliability.

In addition to the above requirements the limitations set on dimensions and weight should be observed.

### 5.2 Initial Screening of Materials

The requirement for fracture toughness of the material is used to eliminate ceramic materials. Because of the limitations set on the outer and inner diameters, the maximum possible cross section of the component is about 2300 mm<sup>2</sup>. To avoid yielding under the axial working load,

the yield strength of the material should be more than 100 MPa, which excludes engineering polymers, woods, and some of the lower strength engineering alloys; see Fig. 2. Corrosion resistance is desirable but will not be considered a factor for screening, since the possibility of protection for less corrosive materials exists but will be considered as a soft requirement.

### 5.3 Comparing and Ranking Alternative Solutions

Table 3 shows a sample of materials that satisfy the conditions set in the initial screening stage. In a real-life situation the list in the table could be much longer, but the intent here is to illustrate the procedure. The yield strength, elastic modulus, specific gravity, corrosion resistance, and cost category are given for each material. At this stage, it is sufficient to classify materials into very inexpensive, inexpensive, etc. A better estimate of the material and manufacturing cost will be needed in making the final decision in selection. Because the weight of the component is important in this application, specific strength and specific modulus would be better indicators of the suitability of the material (Table 4). The relative importance of the material properties is given in Table 5, and the performance indices of the different materials, as determined by the weighted-properties method, are given in Table 6. The seven candidate materials with high-performance indices ( $\gamma > 45$ ) are selected for making actual component designs.

**Table 3** Properties of Sample Candidate Materials

Material	Yield Strength (MPa)	Elastic Modulus (GPa)	Specific Gravity	Corrosion Resistance <sup>a</sup>	Cost Category <sup>b</sup>
AISI 1020 (UNS G10200)	280	210	7.8	1	5
AISI 1040 (UNS G10400)	400	210	7.8	1	5
ASTM A242 type1 (UNS K11510)	330	212	7.8	1	5
AISI 4130 (UNS G41300)	1520	212	7.8	4	3
AISI 316 (UNS S31600)	205	200	7.98	4	3
AISI 416 heat treated (UNS S41600)	440	216	7.7	4	3
AISI 431 heat treated (UNS S43100)	550	216	7.7	4	3
AA 6061 T6 (UNS A96061)	275	69.7	2.7	3	4
AA 2024 T6 (UNS A92024)	393	72.4	2.77	3	4
AA 2014 T6 (UNS A92014)	415	72.1	2.8	3	4
AA 7075 T6 (UNS A97075)	505	72.4	2.8	3	4
Ti-6Al-4V	939	124	4.5	5	1
Epoxy-70% glass fabric	1270	28	2.1	4	2
Epoxy-63% carbon fabric	670	107	1.61	4	1
Epoxy-62% aramid fabric	880	38	1.38	4	1

Source: Based on Ref. 18.

<sup>a</sup>5, Excellent; 4, very good; 3, good; 2, fair; 1, poor.

<sup>b</sup>5, Very inexpensive; 4, inexpensive; 3, moderate price; 2, expensive; 1, very expensive.

**Table 4** Properties of Sample Candidate Materials

Material	Specific Strength (MPa)	Specific Modulus (GPa)	Corrosion Resistance <sup>a</sup>	Cost Category <sup>b</sup>
AISI 1020 (UNS G10200)	35.9	26.9	1	5
AISI 1040 (UNS G10400)	51.3	26.9	1	5
ASTM A242 type 1 (UNS K11510)	42.3	27.2	1	5
AISI 4130 (UNS G41300)	194.9	27.2	4	3
AISI 316 (UNS S31600)	25.6	25.1	4	3
AISI 416 heat treated (UNS S41600)	57.1	28.1	4	3
AISI 431 heat treated (UNS S43100)	71.4	28.1	4	3
AA 6061 T6 (UNS A96061)	101.9	25.8	3	4
AA 2024 T6 (UNS A92024)	141.9	26.1	3	4
AA 2014 T6 (UNS A92014)	148.2	25.8	3	4
AA 7075 T6 (UNS A97075)	180.4	25.9	3	4
Ti-6Al-4V	208.7	27.6	5	1
Epoxy-70% glass fabric	604.8	28	4	2
Epoxy-63% carbon fabric	416.2	66.5	4	1
Epoxy-62% aramid fabric	637.7	27.5	4	1

<sup>a</sup>5, Excellent; 4, very good; 3, good; 2, fair; 1, poor.

<sup>b</sup>5, Very inexpensive; 4, inexpensive; 3, moderate price; 2, expensive; 1, very expensive.

**Table 5** Weighting Factors

Property	Specific Strength (MPa)	Specific Modulus (GPa)	Corrosion Resistance	Relative Cost
Weighting factor, $\alpha$	0.3	0.3	0.15	0.25

## 5.4 Selecting the Optimum Solution

As shown earlier, the possible modes of failure of a hollow cylinder include yielding, local buckling, global buckling, and internal fiber buckling. These four failure modes are used to develop the design formulas for the mast component. For more details on the design and optimization procedure [Eqs. (9)–(12)], refer to Ref. 18:

Condition for yielding:

$$\frac{F}{A} < \sigma_y \quad (9)$$

where  $\sigma_y$  = yield strength of material  
 $F$  = external working axial force  
 $A$  = cross-sectional area

**Table 6** Calculation of Performance Index

Material	Scaled Specific Strength, $\times 0.3$	Scaled Specific Modulus, $\times 0.3$	Scaled Corrosion Resistance, $\times 0.15$	Scaled Relative Cost, $\times 0.25$	Performance Index ( $\gamma$ )
AISI 1020 (UNS G10200)	1.7	12.3	3	25	42
AISI 1040 (UNS G10400)	2.4	12.3	3	25	42.7
ASTM A242 type1 (UNS K11510)	2	12.3	3	25	42.3
AISI 4130 (UNS G41300)	9.2	12.3	6	15	42.5
AISI 316 (UNS S31600)	1.2	11.3	12	15	39.5
AISI 416 heat treated (UNS S41600)	2.7	12.7	12	15	42.4
AISI 431 heat treated (UNS S43100)	3.4	12.7	12	15	43.1
AA 6061 T6 (UNS A96061)	4.8	11.6	9	20	45.4
AA 2024 T6 (UNS A92024)	6.7	11.8	9	20	47.5
AA 2014 T6 (UNS A92014)	7	11.6	9	20	47.6
AA 7075 T6 (UNS A97075)	8.5	11.7	9	20	49.2
Ti-6Al-4V	9.8	12.5	15	5	42.3
Epoxy-70% glass fabric	28.4	12.6	12	10	63
Epoxy-63% carbon fabric	19.6	30	12	5	66.6
Epoxy-62% aramid fabric	30	12.4	12	5	59.4

Condition for local buckling:

$$\frac{F}{A} < \frac{0.121ES}{D} \quad (10)$$

where  $D$  = outer diameter of cylinder  
 $S$  = wall thickness of cylinder  
 $E$  = elastic modulus of material

Condition for global buckling:

$$\sigma_y > \frac{F}{A} \left[ 1 + \left( \frac{LDA}{1000I} \right) \sec \left( \frac{(F/EI)^{1/2}L}{2} \right) \right] \quad (11)$$

where  $I$  = second moment of area  
 $L$  = length of component

Condition for internal fiber buckling:

$$\frac{F}{A} < \left[ \frac{E_m}{4(1 + \nu_m)(1 - V_f^{1/2})} \right] \quad (12)$$

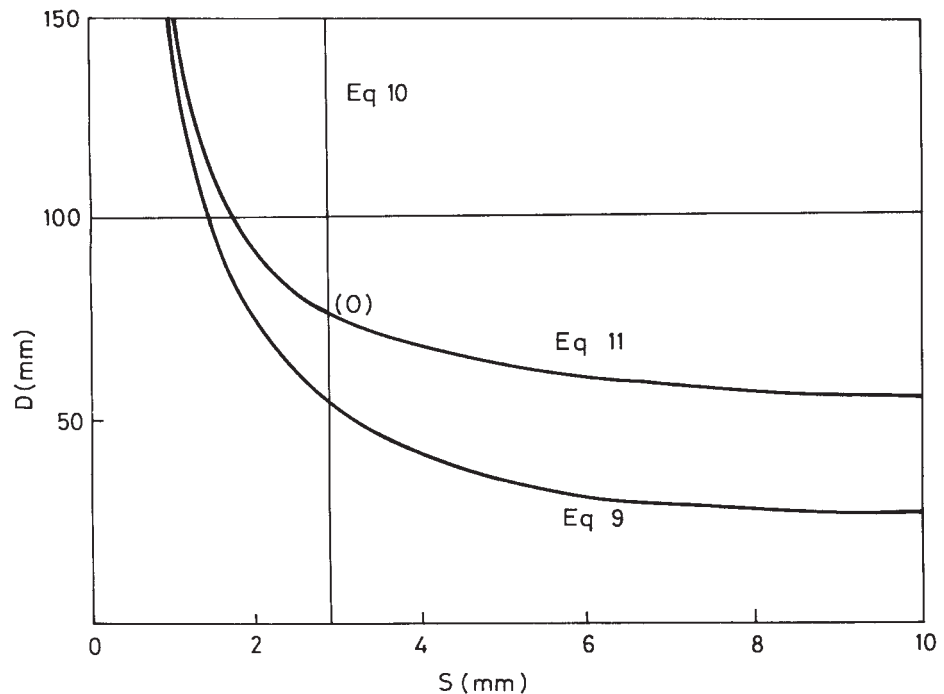
where  $E_m$  = elastic modulus of matrix material  
 $\nu_m$  = Poisson's ratio of matrix material  
 $V_f$  = volume fraction of fibers parallel to loading direction

Figure 3 shows the optimum design range of component diameter and wall thickness as predicted by Eqs. (9)–(11) for AA 7075 aluminum alloy. Point  $O$  represents the optimum design. Similar figures were developed for the different candidate materials in order to determine the most component's optimum design dimensions when made of the materials, and the results are shown in Table 7. Although all the materials in Table 7 can be used to make safe components that comply with the space and weight limitations, AA 2024 T6 is selected since it gives the least expensive solution.

## 6 MATERIALS SUBSTITUTION

Substitution is an activity through which a product, a material, or a process is replaced by a more suitable alternative. An important consideration in making a substitution decision is the relative value, which includes the price ratio, substitution costs, and customer's propensity to substitute. The common reasons for materials substitution include the following:

- Taking advantage of new materials or processes
- Improving service performance, including longer life and higher reliability
- Meeting new legal requirements



**Figure 3** Design range as predicted by Eqs. (9)–(11) for AA 7075 aluminum alloy. (Reprinted from, Ref. 18. © 1992, with permission from Elsevier Science.)

**Table 7** Designs Using Candidate Materials with Highest Performance Indices

Material	$D_a$ (mm)	$S$ (mm)	$A$ (mm <sup>2</sup> )	Mass (kg)	Cost/kg (\$)	Cost of Component (\$)
AA 6061 T6 (UNS A96061)	100	3.4	1065.7	2.88	8	23.2
AA 2024 T6 (UNS A92024)	88.3	2.89	801.1	2.22	8.3	18.4
AA 2014 T6 (UNS A92014)	85.6	2.89	776.6	2.17	9	19.6
AA 7075 T6 (UNS A97075)	78.1	2.89	709.1	1.99	10.1	20
Epoxy–70% glass fabric	78	4.64	1136.3	2.39	30.8	73.6
Epoxy–63% carbon fabric	73.4	2.37	546.1	0.88	99	87.1
Epoxy–62% aramid fabric	75.1	3.99	941.6	1.30	88	114.4

Source: Based on Ref. 18.

- Accounting for changed operating conditions
- Reducing cost and making the product more competitive

Generally, a simple substitution of one material for another does not produce an optimum solution. This is because it is not possible to realize the full potential of a new material unless the component is redesigned to exploit its strong points and manufacturing characteristics. Following is a brief description of some of the quantitative methods that are available for making decisions in materials substitution.

## 6.1 Pugh Method

The Pugh method<sup>19</sup> is useful as an initial screening method in the early stages of design. In this method, a decision matrix is constructed as shown in Table 8. Each of the properties of possible alternative new materials is compared with the corresponding property of the currently used material, and the result is recorded in the decision matrix as + if more favorable, – if less

**Table 8** Example of Use of Pugh Decision Matrix for Materials Substitution

Property	Currently Used Material	New Material 1	New Material 2	New Material 3
1	C1	–	+	+
2	C2	+	+	+
3	C3	+	–	–
4	C4	0	–	–
5	C5	–	0	–
6	C6	0	0	0
7	C7	–	–	0
8	C8	–	+	0
9	C9	–	0	0
Total +		2	5	2
Total –		5	1	3
Total 0		2	3	4

favorable, and 0 if the same. The decision on whether a new material is better than the currently used material is based on the analysis of the result of comparison, i.e., the total number of +', -'s and 0's. New materials with more favorable properties than drawbacks are selected as serious candidates for substitution and are used to redesign the component and for detailed analysis.

## 6.2 Cost–Benefit Analysis

The cost–benefit analysis is more suitable for the detailed analysis involved in making the final material substitution decision.<sup>1</sup> Because new materials are usually more complex and often require closer control and even new technologies for their processing, components made from such materials are more expensive. This means that for materials substitution to be economically feasible, the economic gain as a result of improved performance  $\Delta B$  should be more than the additional cost incurred as a result of substitution  $\Delta C$ :

$$\Delta B - \Delta C > 1 \quad (13)$$

For this analysis it is convenient to divide the cost of materials substitution  $\Delta C$  into the following:

- *Cost Differences in Direct Material and Labor.* New materials often have better performance but are more expensive. When smaller amounts of the new material are used to make the product, the increase in direct material cost may not be as great as it would appear at first. Cost of labor may not be an important factor in substitution if the new materials do not require new processing techniques and assembly procedures. If, however, new processes are needed, new cycle times may result and the difference in productivity has to be carefully assessed.
- *Cost of Redesign and Testing.* Using new materials usually involves design changes and testing of components to ensure that their performance meets the requirements. The cost of redesign and testing can be considerable in the case of critical components.
- *Cost of New Tools and Equipment.* Changing materials can have considerable effect on life and cost of tools, and it may influence the heat treatment and finishing processes. This can be a source of cost saving if the new material does not require the same complex treatment or finishing processes used for the original material. The cost of equipment needed to process new materials can be considerable if the new materials require new production facilities, as in the case of replacing metals with plastics.

Based on the above analysis, the total cost ( $\Delta C$ ) of substituting a new material,  $n$ , in place of an original material,  $o$ , in a given part is

$$\Delta C = (P_n M_n - P_o M_o) + f \left( \frac{C_t}{N} \right) + (T_n - T_o) + (L_n - L_o) \quad (14)$$

- where
- $P_n, P_o$  = price per unit mass of new and original materials used in part
  - $M_n, M_o$  = mass of new and original materials used in part
  - $f$  = capital recovery factor, can be taken as 15% in absence of information
  - $C_t$  = cost of transition from original to new materials
  - $N$  = total number of new parts produced
  - $T_n, T_o$  = tooling cost per part for new and original materials
  - $L_n, L_o$  = labor cost per part using new and old materials



The gains as a result of improved performance  $\Delta B$  can be estimated based on the expected improved performance of the component, which can be related to the increase in performance index of the new material compared with the currently used material. Such increases include the saving gained as a result of weight reduction or increased service life of the component:

$$\Delta B = A(\gamma_n - \gamma_o) \quad (15)$$

where  $\gamma_n, \gamma_o$  = performance indices of new and original materials, respectively  
 $A$  = benefit of improved performance of component expressed in \$  
per unit increase in material performance index  $\gamma$

## 7 CASE STUDY IN MATERIALS SUBSTITUTION

In the case study on materials selection discussed in Section 5, the aluminum alloy AA 2024 T6 was selected since it gives the least expensive solution. Of the seven materials in Table 7, AA 6061 T6, epoxy–70% glass fabric, and epoxy–62% aramid fabric result in components that are heavier and more expensive than those of the other four materials and will be rejected as they offer no advantage. Of the remaining four materials, AA 2024 T6 results in the least expensive but the heaviest component. The other three materials—AA 2014 T6, AA 7075 T6, and epoxy–63% carbon fabric—result in progressively lighter components at progressively higher cost.

For the cases where it is advantageous to have a lighter component, the cost–benefit analysis can be used in finding a suitable substitute for AA 2024 T6 alloy. For this purpose Eq. (15) is used with the performance index  $\gamma$  being considered as the weight of the component and  $\Delta C$  being the difference in cost of component and  $A$  is the benefit expressed in dollars of reducing the mass by 1 kg. Comparing the materials in pairs shows:

For  $A < \$7/\text{kg}$  saved, AA 2024 T6 is the optimum material.

For  $A = \$7\text{--}\$60.5/\text{kg}$  saved, AA 7075 T6 is a better substitute.

For  $A > \$60.5/\text{kg}$  saved, epoxy–63% carbon fabric is optimum.

## 8 SOURCES OF INFORMATION AND COMPUTER-ASSISTED SELECTION

### 8.1 Locating Materials Properties Data

One essential requisite to successful materials selection is a source of reliable and consistent data on materials properties. There are many sources of information, which include governmental agencies, trade associations, engineering societies, textbooks, research institutes, and materials producers. Locating the appropriate type of information is not easy and may require several cycles of iteration until the information needed is gathered. According to Kirkwood,<sup>20</sup> the steps involved in each cycle are: Define the question, set up a strategy to locate the needed information, use the resources you know best, go to less known sources when necessary, evaluate the quality of data/information resources, and start again if needed using the new information to help better define the question. To locate useful sources of materials data, it is important to identify the intended use of data, the type of data required, and the quality of data required.<sup>21</sup> In general, progressively higher quality of data is needed as the selection process progresses from initial screening to ranking and finally to selecting the optimum solution.

ASM International has recently published a directory of materials property databases,<sup>22</sup> which contains more than 500 data sources, including both specific databases and data centers.

For each source, the directory gives a brief description of the available information, address, telephone number, e-mail, website, and approximate cost if applicable. The directory also has indices by material and by property to help the user in locating the most appropriate source of material information. Much of the information is available on CD-ROM or PC disk, which makes it possible to integrate the data source into computer-assisted selection systems. Other useful reviews of the sources of materials property data and information are also available.<sup>23,24</sup>

## 8.2 Types of Material Information

According to Cebon and Ashby,<sup>25</sup> materials information can be classified into structured information either from reference sources or developed in-house and unstructured information either from reference sources or developed in-house. Structured information is normally in the form of databases of properties and is most suited for initial screening (Section 2) and for comparing and ranking of materials (Section 3). Examples of structured reference sources of information material properties include ASM, Materials Universe, and Matweb databases. These databases, in addition to several others, are collected online under the Material Data Network.<sup>26</sup>

Unstructured information gives details about performance of specific materials and is normally found in handbooks, publications of trade organizations, and technical reports in the form of text, pdf files, tables, graphs, photographs, etc. Such information is most suited for detailed consideration of the top-ranking candidates that were selected in the initial screening and the ranking stages, as discussed in Section 4.

## 8.3 Computerized Materials Databases

Computerized materials databases are an important part of any computer-aided system for selection. With an interactive database, as in the case of ASM Metal Selector,<sup>27</sup> the user can define and redefine the selection criteria to gradually sift the materials and isolate the candidates that meet the requirements. In many cases, sifting can be carried out according to different criteria:

1. Specified numeric values of a set of material properties
2. Specified level of processability such as machinability, weldability, formability, availability, processing cost, etc.
3. Class of material, e.g., fatigue resistant, corrosion resistant, heat resistant, electrical materials
4. Forms like rod, wire, sheet, tube, cast, forged, welded
5. Designations: Unified Number System (UNS), American Iron and Steel Institute (AISI), common names, material group, or country of origin
6. Specifications that allow the operator to select the materials that are acceptable to organizations like the American Society for Testing and Materials (ASTM) and the Society of Automotive Engineers (SAE)
7. Composition, which allows the operator to select the materials that have certain minimum and/or maximum values of alloying elements

More than one of the above sifting criteria can be used to identify suitable materials. Sifting can be performed in the AND or OR modes. The AND mode narrows the search since the material has to conform to all the specified criteria. The OR mode broadens the search since materials that satisfy any of the requirements are selected.

The number of materials that survive the sifting process depends on the severity of the criteria used. At the start of sifting, the number of materials shown on the screen is the total in

the database. As more restrictions are placed on the materials, the number of surviving materials gets smaller and could reach zero, i.e., no materials qualify. In such cases, some of the restrictions have to be relaxed and the sifting restarted.

The Material Data Network<sup>26</sup> is an online search engine for materials information and is sponsored by ASM International and Granta Design Limited. Sources of information that are linked to the network (member sites) include ASM International, the Welding Institute, National Physical Laboratory (U.K.), National Institute of Materials Science (Japan), U.K. Steel Association “Steel Specifications,” Cambridge Engineering Selector, MatWeb, and IDES plastics data. Member sites can be searched simultaneously with one search string for all classes of materials. The information provided is both quantitative and qualitative, with tables, graphs, micrographs, etc. Some of the sites are freely available and do not require registration while others require registration in order to access the information.

## 8.4 Computer Assistance in Making Final Selection

Integrating material property database with design algorithms and computer-aided design/manufacturing (CAD/CAM) programs has many benefits, including homogenization and sharing of data in the different departments and decreased redundancy of effort and cost of information storage and retrieval. Several such systems have been cited in Ref. 22:

- The Computerized Application and Reference System (CARS) is developed from the AISI Automotive Steel Design Manual and performs first-order analysis of design using different steels.
- Aluminum Design System (ADS) is developed by the Aluminum Association (U.S.) and performs design calculations and conformance checks of aluminum structural members with the design specifications for aluminum and its alloys.
- Material Selection and Design for fatigue life predictions is developed by ASM International and aids in the design of machinery and engineering structures using different engineering materials.
- Machine Design’s Materials Selection is developed by Penton Media (U.S.) and combines the properties for a wide range of materials and the data set for design analysis.

## 8.5 Expert Systems

Expert systems, also called knowledge-based systems, are computer programs that simulate the reasoning of a human expert in a given field of knowledge. Expert systems rely on heuristics, or rules of thumb, to extract information from a large knowledge base. Expert systems typically consist of three main components:

- Knowledge base, which contains facts and expert-level heuristic rules for solving problems in a given domain. The rules are normally introduced to the system by domain experts through a knowledge engineer.
- Inference engine, which provides an organized procedure for sifting through the knowledge base and choosing applicable rules in order to reach the recommend solutions. The inference engine also provides a link between the knowledge base and the user interface.
- User interface, which allows the user to input the main parameters of the problem under consideration. It also provides recommendations and explanations of how such recommendations were reached.

A commonly used format for the rules in the knowledge base is in the form

IF (condition 1) and/or (condition 2)  
THEN (conclusion 1)

For example, in the case of fiber-reinforced plastic (FRP) selection

IF required elastic modulus, expressed in GPa, is more than 150 and specific gravity less than 1.7  
THEN oriented carbon fibers at 60% by volume

Expert systems are finding many applications in industry, including the areas of design, troubleshooting, failure analysis, manufacturing, materials selection, and materials substitution.<sup>12</sup> When used to assist in materials selection, expert systems provide impartial recommendations and are able to search large databases for optimum solutions. Another important advantage of expert systems is their ability to capture valuable expertise and make it available to a wider circle of users. An example is the Chemical Corrosion Expert System, which is produced by the National Association of Corrosion Engineers (NACE) in the United States.<sup>22</sup> The system prompts the user for information on the environmental conditions and configuration of the component and then recommends candidate materials.

## REFERENCES

1. M. M. Farag, *Materials Selection for Engineering Design*, Prentice-Hall, London, 1997.
2. G. Dieter, "Overview of the Materials Selection Process," in *ASM Metals Handbook*, Vol. 20, *Materials Selection and Design*, Volume Chair G. Dieter, ASM International, Materials Park, OH, 1997, pp. 243–254.
3. J. Clark, R. Roth, and F. Field III, "Techno-Economic Issues in Materials Selection," in *ASM Metals Handbook*, Vol. 20, *Materials Selection and Design*, Volume Chair G. Dieter, ASM International, Materials Park, OH, 1997, pp. 255–265.
4. M. F. Ashby, "Materials Selection Charts," *ASM Metals Handbook*, Vol. 20, *Materials Selection and Design*, Volume Chair G. Dieter, ASM International, Materials Park, OH, 1997, pp. 266–280.
5. M. F. Ashby, "Performance Indices," in *ASM Metals Handbook*, Vol. 20, *Materials Selection and Design*, Volume Chair G. Dieter, ASM International, Materials Park, OH, 1997, pp. 281–290.
6. D. Bourell, "Decision Matrices in Materials Selection," in *ASM Metals Handbook*, Vol. 20, *Materials Selection and Design*, Volume Chair G. Dieter, ASM International, Materials Park, OH, 1997, pp. 291–296.
7. T. Fowler, "Value Analysis in Materials Selection and Design," in *ASM Metals Handbook*, Vol. 20, *Materials Selection and Design*, Volume Chair G. Dieter, ASM International, Materials Park, OH, 1997, pp. 315–321.
8. F. A. Crane and J. A. Charles, *Selection and Use of Engineering Materials*, Butterworths, London, 1984.
9. M. F. Ashby, *Materials Selection in Mechanical Design*, Pergamon, London, 1992.
10. M. F. Ashby, *Mater. Sci. Technol.*, **5**, 517–525, 1989.
11. R. Sandstrom, "An Approach to Systematic Materials Selection," *Mater. Design*, **6**, 328–338, 1985.
12. V. Weiss, "Computer-Aided Materials Selection," in *ASM Metals Handbook*, Vol. 20, *Materials Selection and Design*, Volume Chair G. Dieter, ASM International, Materials Park, OH, 1997, pp. 309–314.
13. P. A. Gutteridge and J. Turner, "Computer Aided Materials Selection and Design," *Mater. Design*, **3**, 504–510, Aug., 1982.
14. L. Olsson, U. Bengtson, and H. Fischmeister, "Computer Aided Materials Selection," in *Computers in Materials Technology*, T. Ericsson (Ed.), Pergamon, Oxford, 1981, pp. 17–25.

15. P. P. Dargie et al., "MAPS 1: Computer Aided Design System for Preliminary Material and Manufacturing Process Selection," *Trans. ASME J. Mech. Design*, **104**, 126–136, 1982.
16. A. M. K. Esawi and M. F. Ashby, "Cost Estimates to Guide Pre-selection of Processes," *Mater. Design*, **24**, 605–616, 2003.
17. CES 4 Software, Granta Design Limited, Cambridge, U.K., [www.Grantadesign.com](http://www.Grantadesign.com), 2002.
18. M. M. Farag and E. El-Magd, "An Integrated Approach to Product Design, Materials Selection, and Cost Estimation," *Mater. Design*, **13**, 323–327, 1992.
19. S. Pugh, *Total Design: Integrated Methods for Successful Product Development*, Addison-Wesley, Reading, MA, 1991.
20. P. E. Kirkwood, "How to Find Materials Properties Data," in *Handbook of Materials Selection*, M. Kutz (Ed.), Wiley, New York, 2002, pp. 441–456.
21. J. G. Kaufman, "Sources of Materials Data," in *Handbook of Materials Selection*, M. Kutz (Ed.), Wiley, New York, 2002, pp. 457–473.
22. B. E. Boardman and J. G. Kaufman, *Directory of Materials Properties Databases*, Special Supplement to Advanced Materials and Processes, ASM International, Materials Park, OH, Aug. 2000.
23. J. H. Westbrook, "Sources of Materials Property Data and Information," in *ASM Metals Handbook*, Vol. 20, *Materials Selection and Design*, Volume Chair G. Dieter, ASM International, Materials Park, OH, 1997, pp. 491–506.
24. D. Price, "A Guide to Materials Databases," *Mat. World*, 418–421, July, 1993.
25. D. Cebon and M. Ashby, "Data Systems for Optimal Materials Selection," *Adv. Mater. Process.*, **161**, 51–54, 2003.
26. [www.matdata.net](http://www.matdata.net).
27. M. E. Heller, *Metal Selector*, ASM International, Materials Park, OH, 1985; also [www.asminternational.org](http://www.asminternational.org).

**PART 2**

---

**ENGINEERING MECHANICS**



# CHAPTER 16

---

## STRESS ANALYSIS

**Franklin E. Fisher**  
Loyola Marymount University,  
Los Angeles, California  
and  
Raytheon Company,  
El Segundo, California

<b>1 STRESSES, STRAINS, AND STRESS INTENSITY</b>	<b>556</b>		
1.1 Fundamental Definitions	556		
1.2 Work and Resilience	563		
<b>2 DISCONTINUITIES, STRESS, AND CONCENTRATION</b>	<b>565</b>		
<b>3 COMBINED STRESSES</b>	<b>566</b>		
<b>4 CREEP</b>	<b>570</b>		
<b>5 FATIGUE</b>	<b>572</b>		
5.1 Modes of Failure	573		
<b>6 BEAMS</b>	<b>574</b>		
6.1 Theory of Flexure	574		
6.2 Design of Beams	584		
6.3 Continuous Beams	586		
6.4 Curved Beams	588		
6.5 Impact Stresses in Bars and Beams	591		
6.6 Steady and Impulsive Vibratory Stresses	595		
<b>7 SHAFTS, BENDING, AND TORSION</b>	<b>596</b>		
7.1 Definitions	596		
7.2 Determination of Torsional Stresses in Shafts	597		
7.3 Bending and Torsional Stresses	601		
<b>8 COLUMNS</b>	<b>601</b>		
8.1 Definitions	601		
8.2 Theory	602		
8.3 Wooden Columns	604		
8.4 Steel Columns	605		
<b>9 CYLINDERS, SPHERES, AND PLATES</b>	<b>608</b>		
9.1 Thin Cylinders and Spheres under Internal Pressure	608		
9.2 Thick Cylinders and Spheres	608		
9.3 Plates	610		
9.4 Trunnion	610		
9.5 Socket Action	615		
<b>10 CONTACT STRESSES</b>	<b>616</b>		
10.1 Contact Stress Theory	616		
<b>11 ROTATING ELEMENTS</b>	<b>616</b>		
11.1 Shafts	616		
11.2 Disks	616		
11.3 Blades	618		
<b>12 SPRINGS</b>	<b>618</b>		
12.1 Helical Compression Springs and Tension Springs	619		
12.2 Torsional Springs under Bending	619		
12.3 Bending Springs under Bending	619		
<b>13 DESIGN SOLUTION SOURCES AND GUIDELINES</b>	<b>619</b>		
13.1 Computers	620		
13.2 Testing	621		
<b>REFERENCES</b>	<b>621</b>		
<b>BIBLIOGRAPHY</b>	<b>622</b>		



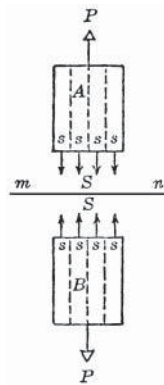
# 1 STRESSES, STRAINS, AND STRESS INTENSITY

## 1.1 Fundamental Definitions

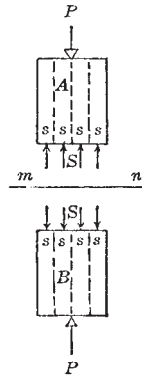
### *Static Stresses*

**TOTAL STRESS** on a section  $mn$  through a loaded body is the resultant force  $S$  exerted by one part of the body on the other part in order to maintain in equilibrium the external loads acting on the part. Thus, in Figs. 1, 2, and 3 the total stress on section  $mn$  due to the external load  $P$  is  $S$ . The units in which it is expressed are those of load, that is, pounds, tons, etc.

**UNIT STRESS**, more commonly called stress  $\sigma$ , is the total stress per unit of area at section  $mn$ . In general it varies from point to point over the section. Its value at any point of a section is the total stress on an elementary part of the area, including the point divided by the elementary area. If in Figs. 1, 2, and 3 the loaded bodies are one unit thick and four units wide, then when the total stress  $S$  is uniformly distributed over the area,  $\sigma = P/A = P/4$ . Unit stresses are expressed in pounds per square inch, tons per square foot, etc.



**Figure 1** Tensile stress.



**Figure 2** Compressive stress.

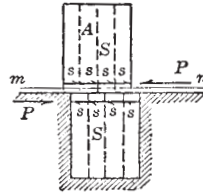


Figure 3 Shear stress.

**TENSILE STRESS OR TENSION** is the internal total stress  $S$  exerted by the material fibers to resist the action of an external force  $P$  (Fig. 1), tending to separate the material into two parts along the line  $mn$ . For equilibrium conditions to exist, the tensile stress at any cross section will be equal and opposite in direction to the external force  $P$ . If the internal total stress  $S$  is distributed uniformly over the area, the stress can be considered as unit tensile stress  $\sigma = S/A$ .

**COMPRESSIVE STRESS OR COMPRESSION** is the internal total stress  $S$  exerted by the fibers to resist the action of an external force  $P$  (Fig. 2) tending to decrease the length of the material. For equilibrium conditions to exist, the compressive stress at any cross section will be equal and opposite in direction to the external force  $P$ . If the internal total stress  $S$  is distributed uniformly over the area, the unit compressive stress  $\sigma = S/A$ .

**SHEAR STRESS** is the internal total stress  $S$  exerted by the material fibers along the plane  $mn$  (Fig. 3) to resist the action of the external forces, tending to slide the adjacent parts in opposite directions. For equilibrium conditions to exist, the shear stress at any cross section will be equal and opposite in direction to the external force  $P$ . If the internal total stress  $S$  is uniformly distributed over the area, the unit shear stress  $\tau = S/A$ .

**NORMAL STRESS** is the component of the resultant stress that acts normal to the area considered (Fig. 4).

**AXIAL STRESS** is a special case of normal stress and may be either tensile or compressive. It is the stress existing in a straight homogeneous bar when the resultant of the applied loads coincides with the axis of the bar.

**SIMPLE STRESS** exists when tension, compression, or shear is considered to operate singly on a body.

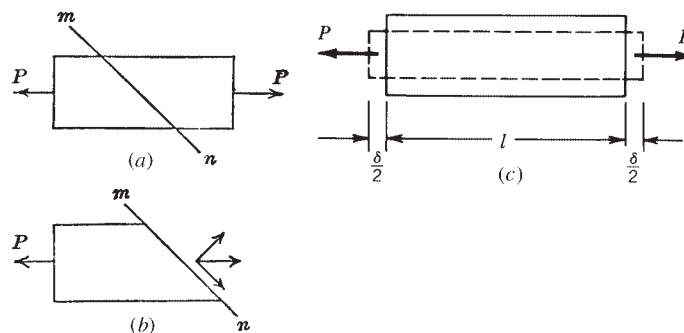


Figure 4 Normal and shear stress components of resultant stress on section  $mn$  and strain due to tension.

**TOTAL STRAIN** on a loaded body is the total elongation produced by the influence of an external load. Thus, in Fig. 4, the total strain is equal to  $\delta$ . It is expressed in units of length, that is, inches, feet, etc.

**UNIT STRAIN**, or deformation per unit length, is the total amount of deformation divided by the original length of the body before the load causing the strain was applied. Thus, if the total elongation is  $\delta$  in an original gauge length  $l$ , the unit strain  $e = \delta/l$ . Unit strains are expressed in inches per inch and feet per foot.

**TENSILE STRAIN** is the strain produced in a specimen by tensile stresses, which in turn are caused by external forces.

**COMPRESSIVE STRAIN** is the strain produced in a bar by compressive stresses, which in turn are caused by external forces.

**SHEAR STRAIN** is a strain produced in a bar by the external shearing forces.

**POISSON'S RATIO** is the ratio of lateral unit strain to longitudinal unit strain under the conditions of uniform and uniaxial longitudinal stress within the proportional limit. It serves as a measure of lateral stiffness. Average values of Poisson's ratio for the usual materials of construction are:

Material	Steel	Wrought iron	Cast iron	Brass	Concrete
Poisson's ratio	0.300	0.280	0.270	0.340	0.100

**ELASTICITY** is that property of a material that enables it to deform or undergo strain and return to its original shape upon the removal of the load.

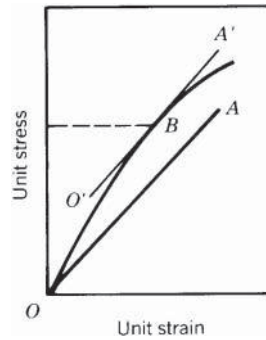
**HOOKE'S LAW** states that within certain limits (not to exceed the proportional limit) the elongation of a bar produced by an external force is proportional to the tensile stress developed. Hooke's law gives the simplest relation between stress and strain.

**PLASTICITY** is that state of matter where permanent deformations or strains may occur without fracture. A material is plastic if the smallest load increment produces a permanent deformation. A perfectly plastic material is nonelastic and has no ultimate strength in the ordinary meaning of that term. Lead is a plastic material. A prism tested in compression will deform permanently under a small load and will continue to deform as the load is increased, until it flattens to a thin sheet. Wrought iron and steel are plastic when stressed beyond the elastic limit in compression. When stressed beyond the elastic limit in tension, they are partly elastic and partly plastic, the degree of plasticity increasing as the ultimate strength is approached.

**STRESS-STRAIN RELATIONSHIP** gives the relation between unit stress and unit strain when plotted on a stress-strain diagram in which the ordinate represents unit stress and the abscissa represents unit strain. Figure 5 shows a typical tension stress-strain curve for medium steel. The form of the curve obtained will vary according to the material, and the curve for compression will be different from the one for tension. For some materials like cast iron, concrete, and timber, no part of the curve is a straight line.

**PROPORTIONAL LIMIT** is that unit stress at which unit strain begins to increase at a faster rate than unit stress. It can also be thought of as the greatest stress that a material can stand without deviating from Hooke's law. It is determined by noting on a stress-strain diagram the unit stress at which the curve departs from a straight line.

**ELASTIC LIMIT** is the least stress that will cause permanent strain, that is, the maximum unit stress to which a material may be subjected and still be able to return to its original form upon removal of the stress.



**Figure 5** Stress–strain relationship showing determination of apparent elastic limit.

**JOHNSON'S APPARENT ELASTIC LIMIT.** In view of the difficulty of determining precisely for some materials the proportional limit, J. B. Johnson proposed as the “apparent elastic limit” the point on the stress–strain diagram at which the rate of strain is 50% greater than at the origin. It is determined by drawing  $OA$  (Fig. 5) with a slope with respect to the vertical axis 50% greater than the straight-line part of the curve; the unit stress at which the line  $O'A'$  that is parallel to  $OA$  is tangent to the curve (point  $B$ , Fig. 5) is the apparent elastic limit.

**YIELD POINT** is the lowest stress at which strain increases without increase in stress. Only a few materials exhibit a true yield point. For other materials the term is sometimes used as synonymous with yield strength.

**YIELD STRENGTH** is the unit stress at which a material exhibits a specified permanent deformation or state. It is a measure of the useful limit of materials, particularly of those whose stress–strain curve in the region of yield is smooth and gradually curved.

**ULTIMATE STRENGTH** is the highest unit stress a material can sustain in tension, compression, or shear before rupturing.

**RUPTURE STRENGTH, OR BREAKING STRENGTH,** is the unit stress at which a material breaks or ruptures. It is observed in tests on steel to be slightly less than the ultimate strength because of a large reduction in area before rupture.

**MODULUS OF ELASTICITY** (Young's modulus) in tension and compression is the rate of change of unit stress with respect to unit strain for the condition of uniaxial stress within the proportional limit. For most materials the modulus of elasticity is the same for tension and compression.

**MODULUS OF RIGIDITY** (modulus of elasticity in shear) is the rate of change of unit shear stress with respect to unit shear strain for the condition of pure shear within the proportional limit. For metals it is equal to approximately 0.4 of the modulus of elasticity.

**TRUE STRESS** is defined as a ratio of applied axial load to the corresponding cross-sectional area. The units of true stress may be expressed in pounds per square inch, pounds per square foot, etc.,

$$\sigma = \frac{P}{A}$$

where  $\sigma$  is the true stress, pounds per square inch,  $P$  is the axial load, pounds, and  $A$  is the smallest value of cross-sectional area existing under the applied load  $P$ , square inches.

**TRUE STRAIN** is defined as a function of the original diameter to the instantaneous diameter of the test specimen:

$$q = 2 \log_e \frac{d_0}{d} \text{ in. / in.}$$

where  $q$  is true strain, inches per inch,  $d_0$  is original diameter of test specimen, inches, and  $d$  is instantaneous diameter of test specimen, inches.

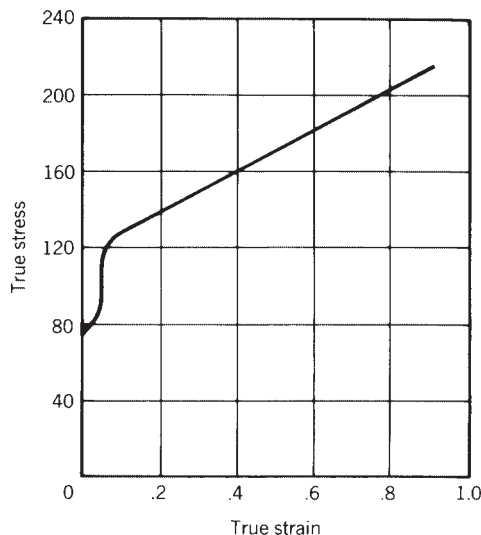
**TRUE STRESS-STRAIN RELATIONSHIP** is obtained when the values of true stress and the corresponding true strain are plotted against each other in the resulting curve (Fig. 6). The slope of the nearly straight line leading up to fracture is known as the coefficient of strain hardening. It, as well as the true tensile strength, appears to be related to the other mechanical properties.

**DUCTILITY** is the ability of a material to sustain large permanent deformations in tension, such as drawing into a wire.

**MALLEABILITY** is the ability of a material to sustain large permanent deformations in compression, such as beating or rolling into thin sheets.

**BRITTLENESS** is that property of a material that permits it to be only slightly deformed without rupture. Brittleness is relative, no material being perfectly brittle, that is, capable of no deformation before rupture. Many materials are brittle to a greater or less degree, glass being one of the most brittle of materials. Brittle materials have relatively short stress-strain curves. Of the common structural materials, cast iron, brick, and stone are brittle in comparison with steel.

**TOUGHNESS** is the ability of the material to withstand high unit stress together with great unit strain without complete fracture. The area  $OAGH$ , or  $OJK$ , under the curve of the stress-strain diagram (Fig. 7), is a measure of the toughness of the material. The distinction between ductility and toughness is that ductility deals only with the ability to deform, whereas toughness considers both the ability to deform and the stress developed during deformation.



**Figure 6** True stress-strain relationship.

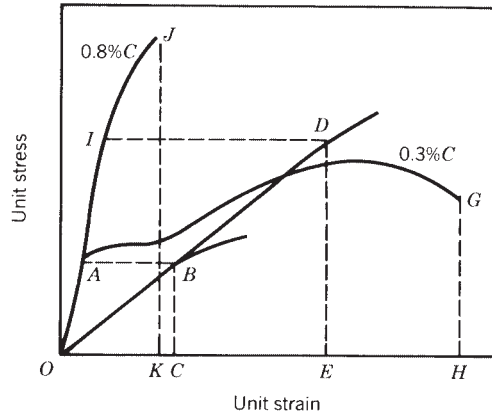


Figure 7 Toughness comparison.

**STIFFNESS** is the ability to resist deformation under stress. The modulus of elasticity is the criterion of the stiffness of a material.

**HARDNESS** is the ability to resist very small indentations, abrasion, and plastic deformation. There is no single measure of hardness, as it is not a single property but a combination of several properties.

**CREEP**, or flow of metals, is a phase of plastic or inelastic action. Some solids, such as asphalt or paraffin, flow appreciably at room temperatures under extremely small stresses; zinc, plastics, fiber-reinforced plastics, lead, and tin show signs of creep at room temperature under moderate stresses. At sufficiently high temperatures, practically all metals creep under stresses that vary with temperature; the higher the temperature, the lower the stress at which creep takes place. The deformation due to creep continues to increase indefinitely and becomes of extreme importance in members subjected to high temperatures, as parts in turbines, boilers, superheaters, etc.

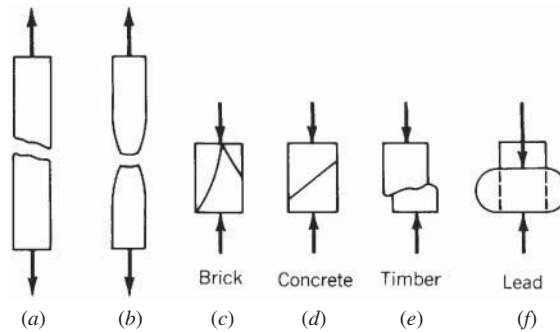
**Creep limit** is the maximum unit stress under which unit distortion will not exceed a specified value during a given period of time at a specified temperature. A value much used in tests and suggested as a standard for comparing materials is the maximum unit stress at which creep does not exceed 1% in 100,000 h.

**TYPES OF FRACTURE.** A bar of brittle material, such as cast iron, will rupture in a tension test in a clean sharp fracture with very little reduction of cross-sectional area and very little elongation (Fig. 8*a*). In a ductile material, as structural steel, the reductions of area and elongation are greater (Fig. 8*b*). In compression, a prism of brittle material will break by shearing along oblique planes; the greater the brittleness of the material, the more nearly will these planes parallel the direction of the applied force. Figures 8*c*, 8*d*, and 8*e*, arranged in order of brittleness, illustrate the type of fracture in prisms of brick, concrete, and timber. Figure 8*f* represents the deformation of a prism of plastic material, such as lead, which flattens out under load without failure.

#### RELATIONS OF ELASTIC CONSTANTS

**Modulus of elasticity,  $E$ :**

$$E = \frac{Pl}{Ae}$$



**Figure 8** (a) Brittle and (b) ductile fractures in tension and compression fractures.

where  $P$  = load, pounds  
 $l$  = length of bar, inches  
 $A$  = cross-sectional area acted on by the axial load  $P$   
 $e$  = total strain produced by axial load  $P$

**Modulus of rigidity,  $G$ :**

$$G = \frac{E}{2(1 + \nu)}$$

where  $E$  is the modulus of elasticity and  $\nu$  is Poisson's ratio.

**Bulk modulus,  $K$ ,** is the ratio of normal stress to the change in volume.

**Relationships.** The following relationships exist between the modulus of elasticity  $E$ , the modulus of rigidity  $G$ , the bulk modulus of elasticity  $K$ , and Poisson's ratio  $\nu$ :

$$E = 2G(1 + \nu) \quad G = \frac{E}{2(1 + \nu)} \quad \nu = \frac{E - 2G}{2G}$$

$$K = \frac{E}{3(1 - 2\nu)} \quad \nu = \frac{3K - E}{6K}$$

**ALLOWABLE UNIT STRESS**, also called allowable working unit stress, allowable stress, or working stress, is the maximum unit stress to which it is considered safe to subject a member in service. The term allowable stress is preferable to working stress since the latter often is used to indicate the actual stress in a material when in service. Allowable unit stresses for different materials for various conditions of service are specified by different authorities on the basis of test or experience. In general, for ductile materials, allowable stress is considerably less than the yield point.

**FACTOR OF SAFETY** is the ratio of ultimate strength of the material to allowable stress. The term was originated for determining allowable stress. The ultimate strength of a given material divided by an arbitrary factor of safety, dependent on material and the use to which it is to be put, gives the allowable stress. In present design practice, it is customary to use allowable stress as specified by recognized authorities or building codes rather than an arbitrary factor of safety. One reason for this is that the factor of safety is misleading in that it implies a greater degree of safety than actually exists. For example, a factor of safety of 4 does not mean that a member can carry a load four times as great as that for which it was designed. It also should be clearly understood that, even though each part of a machine is designed with the same factor of safety, the machine as a whole does not have that factor of safety. When one part is stressed beyond the proportional limit, or particularly the yield point, the load or stress

distribution may be completely changed throughout the entire machine or structure, and its ability to function thus may be changed, even though no part has ruptured.

Although no definite rules can be given, if a factor of safety is to be used, the following circumstances should be taken into account in its selection:

1. When the ultimate strength of the material is known within narrow limits, as for structural steel for which tests of samples have been made, when the load is entirely a steady one of a known amount and there is no reason to fear the deterioration of the metal by corrosion, the lowest factor that should be adopted is 3.
2. When the circumstances of situation 1 are modified by a portion of the load being variable, as in floors of warehouses, the factor should not be less than 4.
3. When the whole load, or nearly the whole, is likely to be alternately put on and taken off, as in suspension rods of floors of bridges, the factor should be 5 or 6.
4. When the stresses are reversed in direction from tension to compression, as in some bridge diagonals and parts of machines, the factor should be not less than 6.
5. When the piece is subjected to repeated shocks, the factor should be not less than 10.
6. When the piece is subjected to deterioration from corrosion, the section should be sufficiently increased to allow for a definite amount of corrosion before the piece is so far weakened by it as to require removal.
7. When the strength of the material or the amount of the load or both are uncertain, the factor should be increased by an allowance sufficient to cover the amount of the uncertainty.
8. When the strains are complex and of uncertain amount, such as those in the crankshaft of a reversing engine, a very high factor is necessary, possibly even as high as 40.
9. If the property loss caused by failure of the part may be large or if loss of life may result, as in a derrick hoisting materials over a crowded street, the factor should be large.

### *Dynamic Stresses*

**DYNAMIC STRESSES** occur where the dimension of time is necessary in defining the loads. They include creep, fatigue, and impact stresses.

**CREEP STRESSES** occur when either the load or deformation progressively varies with time. They are usually associated with noncyclic phenomena.

**FATIGUE STRESSES** occur when type of cyclic variation of either load or strain is coincident with respect to time.

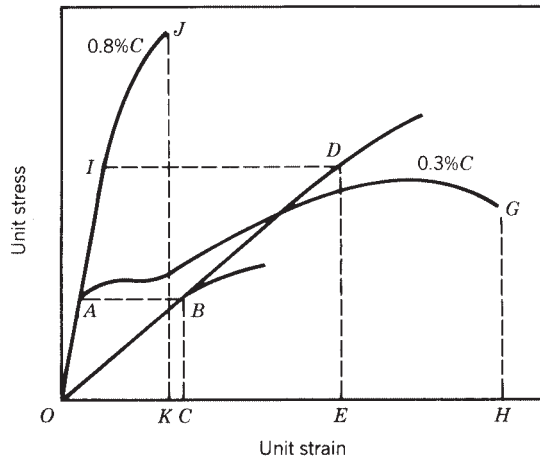
**IMPACT STRESSES** occur from loads that are transient with time. The duration of the load application is of the same order of magnitude as the natural period of vibration of the specimen.

## 1.2 Work and Resilience

**EXTERNAL WORK.** Let  $P$  = axial load, pounds, on a bar, producing an internal stress not exceeding the elastic limit;  $\sigma$  = unit stress produced by  $P$ , pounds per square inch;  $A$  = cross-sectional area, square inches;  $l$  = length of bar, inches;  $e$  = deformation, inches;  $E$  = modulus of elasticity;  $W = \frac{1}{2}Pe$  external work performed on bar, inch-pounds. Then

$$W = \frac{1}{2}A\sigma \left( \frac{\sigma l}{E} \right) = \frac{1}{2} \left( \frac{\sigma^2}{E} \right) Al \quad (1)$$





**Figure 9** Work areas on stress–strain diagram.

The factor  $\frac{1}{2}(\sigma^2/E)$  is the work required per unit volume, the volume being  $Al$ . It is represented on the stress–strain diagram by the area  $ODE$  or area  $OBC$  (Fig. 9), where  $DE$  and  $BC$  are ordinates representing the unit stresses considered.

**RESILIENCE** is the strain energy that may be recovered from a deformed body when the load causing the stress is removed. Within the proportional limit, the resilience is equal to the external work performed in deforming the bar and may be determined by Eq. (1). When  $\sigma$  is equal to the proportional limit, the factor  $\frac{1}{2}(\sigma^2/E)$  is the *modulus of resilience*, that is, the measure of capacity of a unit volume of material to store strain energy up to the proportional limit. Average values of the modulus of resilience under tensile stress are given in Table 1.

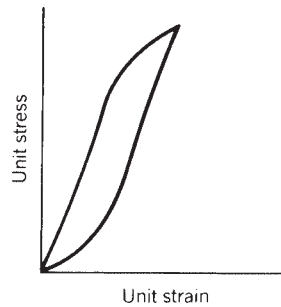
The total resilience of a bar is the product of its volume and the modulus of resilience. These formulas for work performed on a bar and its resilience do not apply if the unit stress is greater than the proportional limit.

**WORK REQUIRED FOR RUPTURE.** Since beyond the proportional limit the strains are not proportional to the stresses,  $\frac{1}{2}P$  does not express the mean value of the force. Equation (1), therefore, does not express the work required for strain after the proportional limit of the material has been passed and cannot express the work required for rupture. The work required per unit volume to produce strains beyond the proportional limit or to cause rupture may be determined from the stress–strain diagram as it is measured by the area under the stress–strain curve up to the strain in question, as  $OAGH$  or  $OJK$  (Fig. 9). This area, however, does not represent the resilience since part of the work done on the bar is present in the form of hysteresis losses and cannot be recovered.

**DAMPING CAPACITY (HYSTERESIS).** Observations show that when a tensile load is applied to a bar, it does not produce the complete elongation immediately, but there is a definite time lapse that depends on the nature of the material and the magnitude of the stresses involved. In parallel with this it is also noted that, upon unloading, complete recovery of energy does not occur. This phenomenon is variously termed *elastic hysteresis* or, for vibratory stresses, damping. Figure 10 shows a typical hysteresis loop obtained for one cycle of loading. The area of this hysteresis loop, representing the energy

**Table 1** Modulus of Resilience and Relative Toughness under Tensile Stress (Average Values)

Material	Modulus of Resilience (in. lb/in. <sup>3</sup> )	Relative Toughness (Area under Curve of Stress Deformation Diagram)
Gray cast iron	1.2	70
Malleable cast iron	17.4	3,800
Wrought iron	11.6	11,000
Low-carbon steel	15.0	15,700
Medium-carbon steel	34.0	16,300
High-carbon steel	94.0	5,000
Ni-Cr steel, hot rolled	94.0	44,000
Vanadium steel, 0.98% C, 0.2% V, heat treated	260.0	22,000
Duralumin, 17 ST	45.0	10,000
Rolled bronze	57.0	15,500
Rolled brass	40.0	10,000
Oak	2.3 <sup>a</sup>	13 <sup>a</sup>

<sup>a</sup>Bending.**Figure 10** Hysteresis loop for loading and unloading.

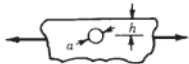
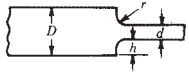
dissipated per cycle, is a measure of the damping properties of the material. While the exact mechanism of damping has not been fully investigated, it has been found that under vibratory conditions the energy dissipated in this manner varies approximately as the cube of the stress.

## 2 DISCONTINUITIES, STRESS, AND CONCENTRATION

The direct design procedure assumes no abrupt changes in cross section, discontinuities in the surface, or holes through the member. In most structural parts this is not the case. The stresses produced at these discontinuities are different in magnitude from those calculated by various design methods. The effect of the localized increase in stress, such as that caused by a notch, fillet, hole, or similar *stress raiser*, depends mainly on the type of loading, the geometry of the part, and the material. As a result, it is necessary to consider a stress concentration factor  $K_t$ , which is defined by the relationship

$$K_t = \frac{\sigma_{\max}}{\sigma_{\text{nominal}}} \quad (2)$$

**Table 2** Stress Concentration Factors

Type		$K_t$ Factors						
Circular hole in plate or rectangular bar		$\frac{h}{a} = 0.67$	0.77	0.91	1.07	1.29	1.56	
		$k = 4.37$	3.92	3.61	3.40	3.25	3.16	
Square shoulder with fillet for rectangular and circular cross sections in bending		$\frac{h}{r} / \frac{L}{d}$	0.05	0.10	0.20	0.27	0.50	1.0
		0.5	1.61	1.49	1.39	1.34	1.22	1.07
		1.0	1.91	1.70	1.48	1.38	1.22	1.08
		1.5	2.00	1.73	1.50	1.39	1.23	1.08
		2.0		1.74	1.52	1.39	1.23	1.09
3.5		1.76	1.54	1.40	1.23	1.10		

Source: Adapted by permission from Ref. 2.

In general  $\sigma_{max}$  will have to be determined by the methods of experimental stress analysis or the theory of elasticity, and  $\sigma_{nominal}$  by a simple theory such as  $\sigma = P/A$ ,  $\sigma = Mc/I$ ,  $\tau = Tc/J$  without taking into account the variations in stress conditions caused by geometrical discontinuities such as holes, grooves, and fillets. For ductile materials it is not customary to apply stress concentration factors to members under static loading. For brittle materials, however, stress concentration is serious and should be considered.

***Stress Concentration Factors for Fillets, Keyways, Holes, and Shafts***

In Table 2 selected stress concentration factors have been given from a complete table in Refs. 1, 2, 3, and 39.

**3 COMBINED STRESSES**

Under certain circumstances of loading, a body is subjected to a combination of tensile, compressive, and/or shear stresses. For example, a shaft that is simultaneously bent and twisted is subjected to combined stresses, namely, longitudinal tension and compression and torsional shear. For the purposes of analysis it is convenient to reduce such systems of combined stresses to a basic system of stress coordinates known as principal stresses. These stresses act on axes that differ in general from the axes along which the applied stresses are acting and represent the maximum and minimum values of the normal stresses for the particular point considered.

***Determination of Principal Stresses***

The expressions for the principal stresses in terms of the stresses along the  $x$  and  $y$  axes are

$$\sigma_1 = \frac{\sigma_x + \sigma_y}{2} + \sqrt{\left(\frac{\sigma_x - \sigma_y}{2}\right)^2 + \tau_{xy}^2} \tag{3}$$

$$\sigma_1 = \frac{\sigma_x + \sigma_y}{2} - \sqrt{\left(\frac{\sigma_x - \sigma_y}{2}\right)^2 + \tau_{xy}^2} \tag{4}$$

$$\tau_1 = \pm \sqrt{\left(\frac{\sigma_x - \sigma_y}{2}\right)^2 + \tau_{xy}^2} \quad (5)$$

where  $\sigma_1$ ,  $\sigma_2$ , and  $\tau_1$  are the principal stress components and  $\sigma_x$ ,  $\sigma_y$ , and  $\tau_{xy}$  are the calculated stress components, all of which are determined at any particular point (Fig. 11).

### Graphical Method of Principal Stress Determination—Mohr's Circle

Let the axes  $x$  and  $y$  be chosen to represent the directions of the applied normal and shearing stresses, respectively (Fig. 12). Lay off to suitable scale distances  $OA = \sigma_x$ ,  $OB = \sigma_y$ , and  $BC = AD = \tau_{xy}$ . With point  $E$  as a center construct the circle  $DFC$ . Then  $OF$  and  $OG$  are the principal stresses  $\sigma_1$  and  $\sigma_2$ , respectively, and  $EC$  is the maximum shear stress  $\tau_1$ . The inverse also holds—that is, given the principal stresses,  $\sigma_x$  and  $\sigma_y$  can be determined on any plane passing through the point.

### Stress–Strain Relations

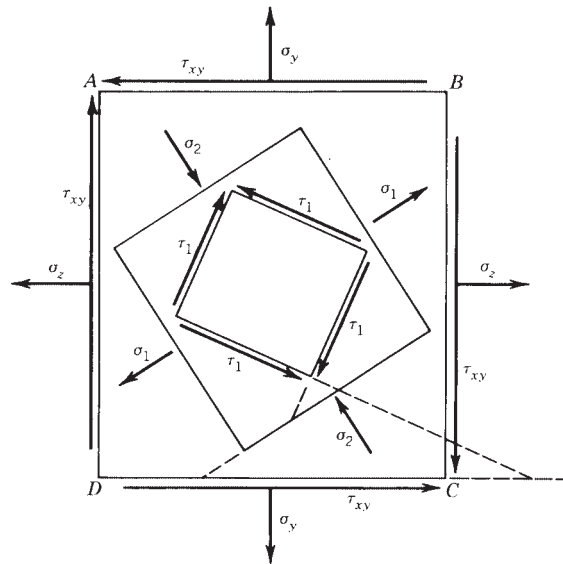
The linear relation between components of stress and strain is known as *Hooke's law*. This relation for the two-dimensional case can be expressed as

$$e_x = \frac{1}{E}(\sigma_x - \nu\sigma_y) \quad (6)$$

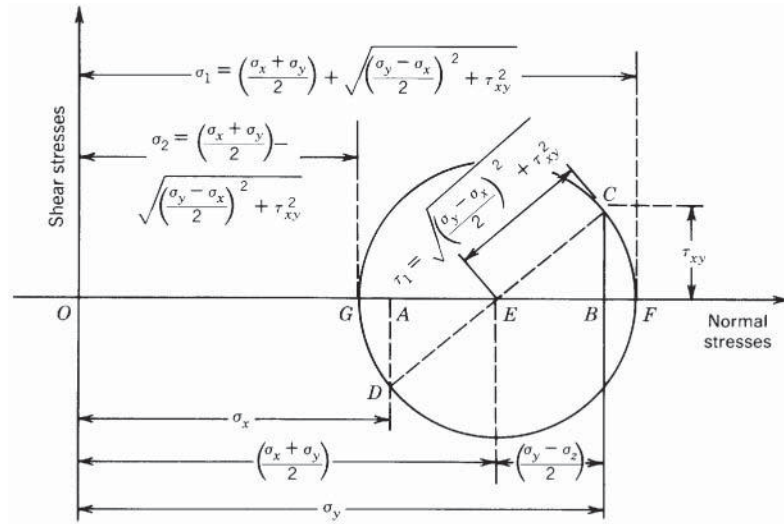
$$e_y = \frac{1}{E}(\sigma_y - \nu\sigma_x) \quad (7)$$

$$\gamma_{xy} = \frac{1}{G}\tau_{xy} \quad (8)$$

where  $\sigma_x$ ,  $\sigma_y$ , and  $\tau_{xy}$  are the stress components of a particular point,  $\nu$  is Poisson's ratio,  $E$  is modulus of elasticity,  $G$  is modulus of rigidity, and  $e_x$ ,  $e_y$ , and  $\gamma_{xy}$  are strain components.



**Figure 11** Diagram showing relative orientation of stresses. (From Ref. 4. Reproduced by permission of McGraw-Hill, New York, 1942.)



**Figure 12** Mohr's circle used for the determination of the principal stresses. (From Ref. 4. Reproduced by permission of McGraw-Hill, New York, 1942.)

The determination of the magnitudes and directions of the principal stresses and strains and of the maximum shearing stresses is carried out for the purpose of establishing criteria of failure within the material under the anticipated loading conditions. To this end several theories have been advanced to elucidate these criteria. The more noteworthy ones are listed below. The theories are based on the assumption that the principal stresses do not change with time, an assumption that is justified since the applied loads in most cases are synchronous.

#### **Maximum Stress Theory (Rankine's Theory)**

This theory is based on the assumption that failure will occur when the maximum value of the greatest principal stress reaches the value of the maximum stress  $\sigma_{\max}$  at failure in the case of simple axial loading. Failure is then defined as

$$\sigma_1 \text{ or } \sigma_2 = \sigma_{\max} \quad (9)$$

#### **Maximum Strain Theory (Saint Venant)**

This theory is based on the assumption that failure will occur when the maximum value of the greatest principal strain reaches the value of the maximum strain  $e_{\max}$  at failure in the case of simple axial loading. Failure is then defined as

$$e_1 \text{ or } e_2 = e_{\max} \quad (10)$$

If  $e_{\max}$  does not exceed the linear range of the material, Eq. (10) may be written as

$$\sigma_1 - \nu\sigma_2 = \sigma_{\max} \quad (11)$$

#### **Maximum Shear Theory (Guest)**

This theory is based on the assumption that failure will occur when the maximum shear stress reaches the value of the maximum shear stress at failure in simple tension. Failure is then defined as

$$\tau_1 = \tau_{\max} \quad (12)$$

**Distortion Energy Theory (Hencky–Von Mises) (Shear Energy)**

This theory is based on the assumption that failure will occur when the distortion energy corresponding to the maximum values of the stress components equals the distortion energy at failure for the maximum axial stress. Failure is then defined as

$$\sigma_1^2 - \sigma_1\sigma_2 + \sigma_2^2 = \sigma_{\max}^2 \quad (13)$$

**Strain Energy Theory**

This theory is based on the assumption that failure will occur when the total strain energy of deformation per unit volume in the case of combined stress is equal to the strain energy per unit volume at failure in simple tension. Failure is then defined as

$$\sigma_1^2 - 2\nu\sigma_1\sigma_2 + \sigma_2^2 = \sigma_{\max}^2 \quad (14)$$

**Comparison of Theories**

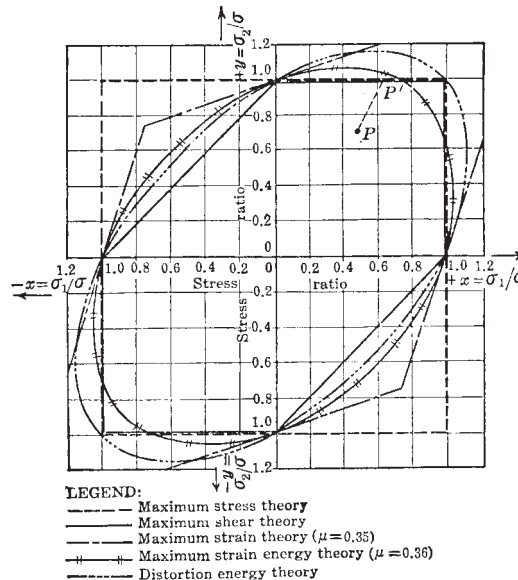
Figure 13 compares the five foregoing theories. In general the distortion energy theory is the most satisfactory for ductile materials and the maximum stress theory is the most satisfactory for brittle materials. The maximum shear theory gives conservative results for both ductile and brittle materials. The conditions for yielding, according to the various theories, are given in Table 3, taking  $\nu = 0.300$  as for steel.

**Static Working Stresses**

*Ductile Materials.* For ductile materials the criteria for working stresses are

$$\sigma_w = \frac{\sigma_{yp}}{n} \quad (\text{tension and compression}) \quad (15)$$

$$\tau_w = \frac{1}{2} \frac{\sigma_{yp}}{n} \quad (16)$$



**Figure 13** Comparison of five theories of failure. (From Ref. 4. Reproduced by permission of McGraw-Hill, New York, 1942.)

**Table 3** Comparison of Stress Theories

$\tau = \sigma_{yp}$	(from the maximum stress theory)
$\tau = 0.77\sigma_{yp}$	(from the maximum strain theory)
$\tau = 0.50\sigma_{yp}$	(from the maximum shear theory)
$\tau = 0.62\sigma_{yp}$	(from the maximum strain energy theory)

*Brittle Materials.* For brittle materials the criteria for working stresses are

$$\sigma_w = \frac{\sigma_{ultimate}}{K_t \times n} \quad (\text{tension}) \quad (17)$$

$$\sigma_w = \frac{\sigma_{compression}}{K_t \times n} \quad (\text{compression}) \quad (18)$$

where  $K_t$  is the stress concentration factor,  $n$  is the factor of safety,  $\sigma_w$  and  $\tau_w$  are working stresses, and  $\sigma_{yp}$  is stress at the yield point.

*Working-Stress Equations for the Various Theories* Stress theory:

$$\sigma_w = \frac{\sigma_x + \sigma_y}{2} \pm \sqrt{\left(\frac{\sigma_x - \sigma_y}{2}\right)^2 + \tau_{xy}^2} \quad (19)$$

Shear theory:

$$\sigma_w = 2\sqrt{\left(\frac{\sigma_x - \sigma_y}{2}\right)^2 + \tau_{xy}^2} \quad (20)$$

Strain theory:

$$\sigma_w = (1 - \nu) \left(\frac{\sigma_x + \sigma_y}{2}\right) + (1 - \nu) \sqrt{\left(\frac{\sigma_x - \sigma_y}{2}\right)^2 + \tau_{xy}^2} \quad (21)$$

Distortion energy theory:

$$\sigma_w = \sqrt{\sigma_x^2 - \sigma_x\sigma_y + \sigma_y^2 + 3\tau_{xy}^2} \quad (22)$$

Strain energy theory:

$$\sigma_w = \sqrt{\sigma_x^2 - 2\nu\sigma_x\sigma_y + \sigma_y^2 + 2(1 + \nu)\tau_{xy}^2} \quad (23)$$

where  $\sigma_x, \sigma_y, \tau_{xy}$  are the stress components of a particular point,  $\nu$  is Poisson's ratio, and  $\sigma_w$  is working stress.

## 4 CREEP

### *Introduction*

Materials subjected to a constant stress at elevated temperatures deform continuously with time, and the behavior under these conditions is different from the behavior at normal temperatures. This continuous deformation with time is called creep. In some applications the permissible creep deformations are critical, in others of no significance. But the existence of creep necessitates information on the creep deformations that may occur during the expected life of the machine. Plastic, zinc, tin, and fiber-reinforced plastics creep at room temperature. Aluminum and magnesium alloys start to creep at around 300°F. Steels above 650°F must be checked for creep.

### Mechanism of Creep Failure

There are generally four distinct phases distinguishable during the course of creep failure. The elapsed time per stage depends on the material, temperature, and stress condition. They are: (1) Initial phase—where the total deformation is partially elastic and partially plastic. (2) Second phase—where the creep rate decreases with time, indicating the effect of strain hardening. (3) Third phase—where the effect of strain hardening is counteracted by the annealing influence of the high temperature, which produces a constant or minimum creep rate. (4) Final phase—where the creep rate increases until fracture occurs owing to the decrease in cross-sectional area of the specimen.

### Creep Equations

In conducting a conventional creep test, curves of strain as a function of time are obtained for groups of specimens; each specimen in one group is subjected to a different constant stress, while all of the specimens in the group are tested at one temperature.

In this manner families of curves like those shown in Fig. 14 are obtained. Several methods have been proposed for the interpretation of such data. (See Refs. 1 and 4.) Two frequently used expressions of the creep properties of a material can be derived from the data in the following form:

$$C = B\sigma^m \quad \epsilon = \epsilon_0 + Ct \quad (24)$$

where  $C$  is the creep rate,  $B$  and  $m$  are experimental constants (where  $B = C/\sigma_1^m$  for  $C = 1\%/1000 \text{ hr}$ ),  $\sigma$  is stress,  $\epsilon$  is creep strain at any time  $t$ ,  $\epsilon_0$  is zero-time strain intercept, and  $t$  is time. See Fig. 15.

### Stress Relaxation

Various types of bolted joints and shrink- or press-fit assemblies and springs are applications of creep taking place with diminishing stress. This deformation tends to loosen the joint and produces a stress reduction or stress relaxation. The performance of a material to be used under diminishing creep–stress condition is determined by a tensile stress relaxation test.

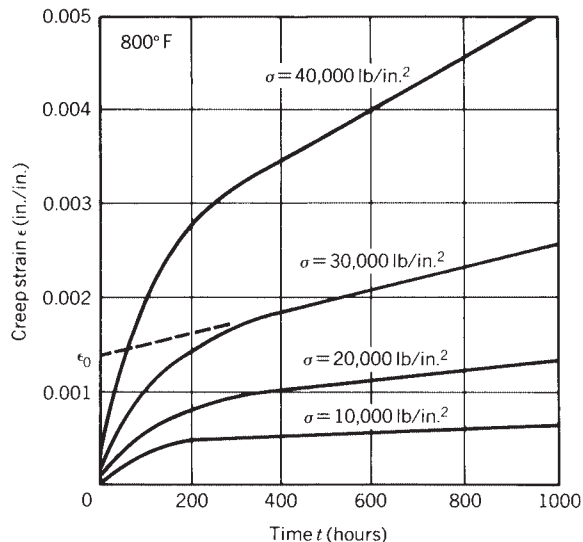


Figure 14 Curves of creep strain for various stress levels.



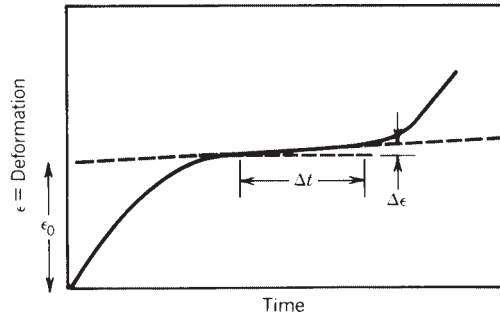


Figure 15 Method of determining creep rate.

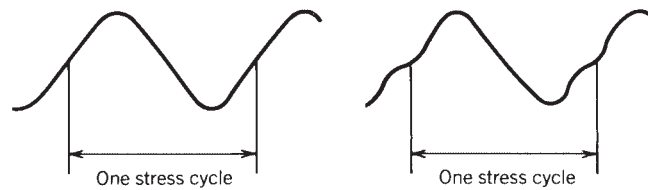


Figure 16 Definition of one stress cycle.

## 5 FATIGUE

### Definitions

**STRESS CYCLE.** A stress cycle is the smallest section of the stress–time function that is repeated identically and periodically, as shown in Fig. 16.

**MAXIMUM STRESS.**  $\sigma_{\max}$  is the largest algebraic value of the stress in the stress cycle, being positive for a tensile stress and negative for a compressive stress.

**MINIMUM STRESS.**  $\sigma_{\min}$  is the smallest algebraic value of the stress in the stress cycle, being positive for a tensile stress and negative for a compressive stress.

**RANGE OF STRESS.**  $\sigma_r$  is the algebraic difference between the maximum and minimum stress in one cycle:

$$\sigma_r = \sigma_{\max} - \sigma_{\min} \quad (25)$$

For most cases of fatigue testing the stress varies about zero stress, but other types of variation may be experienced.

**ALTERNATING-STRESS AMPLITUDE (VARIABLE-STRESS COMPONENT).**  $\sigma_a$  is one-half the range of stress,  $\sigma_a = \sigma_r/2$ .

**MEAN STRESS (STEADY-STRESS COMPONENT).**  $\sigma_m$  is the algebraic mean of the maximum and minimum stress in one cycle:

$$\sigma_m = \frac{\sigma_{\max} + \sigma_{\min}}{2} \quad (26)$$

**STRESS RATIO.**  $R$  is the algebraic ratio of the minimum stress and the maximum stress in one cycle.

## 5.1 Modes of Failure

The three most common modes of failure are\*

$$\text{Soderberg's law: } \frac{\sigma_m}{\sigma_y} + \frac{\sigma_a}{\sigma_e} = \frac{1}{N} \quad (27)$$

$$\text{Goodman's law: } \frac{\sigma_m}{\sigma_u} + \frac{\sigma_a}{\sigma_e} = \frac{1}{N} \quad (28)$$

$$\text{Gerber's law: } \left( \frac{\sigma_m}{\sigma_y} \right)^2 + \frac{\sigma_a}{\sigma_e} = \frac{1}{N} \quad (29)$$

From distortion energy for plane stress

$$\sigma_m = \sqrt{\sigma_{xm}^2 - \sigma_{xm}\sigma_{ym} + \sigma_{ym}^2 + 3\tau_{xym}^2} \quad (30)$$

$$\sigma_a = \sqrt{\sigma_{xa}^2 - \sigma_{xa}\sigma_{ya} + \sigma_{ya}^2 + 3\tau_{xya}^2} \quad (31)$$

The stress concentration factor,<sup>3</sup>  $K_t$  or  $K_f$ , is applied to the individual stress for both  $\sigma_a$  and  $\sigma_m$  for brittle materials and only to  $\sigma_a$  for ductile materials.  $N$  is a reasonable factor of safety.  $\sigma_u$  is the ultimate tensile strength, and  $\sigma_y$  is the yield strength.  $\sigma_e$  is developed from the endurance limit  $\sigma'_e$  and reduced or increased depending on conditions and manufacturing procedures and to keep  $\sigma_e$  less than the yield strength:

$$\sigma_e = k_a k_b \cdots k_n \sigma'_e$$

where  $\sigma'_e$  (Ref. 1) for various materials is

Steel	$0.5\sigma_u$ and never greater than 100 kpsi at $10^6$ cycles
Magnesium	$0.35\sigma_u$ at $10^8$ cycles
Nonferrous alloys	$0.35\sigma_u$ at $10^8$ cycles
Aluminum alloys	$(0.16 - 0.3)\sigma_u$ at $5 \times 10^8$ cycles (Ref. 5)

and where the other  $k$  factors are affected as follows:

*Surface Condition.* For surfaces that are from machined to ground, the  $k_a$  varies from 0.7 to 1.0. When surface finish is known,  $k_a$  can be found<sup>1</sup> more accurately.

*Size and Shape.* If the size of the part is 0.30 in. or larger, the reduction is 0.85 or less, depending on the size.

*Reliability.* The endurance limit and material properties are averages and both should be corrected. A reliability of 90% reduces values 0.897, while one of 99% reduces 0.814.

*Temperature.* The endurance limit at  $-190^\circ\text{C}$  increases 1.54–2.57 for steels, 1.14 for aluminums, and 1.4 for titaniums. The endurance limit is reduced approximately 0.68 for some steels at  $1382^\circ\text{F}$ , 0.24 for aluminum around  $662^\circ\text{F}$ , and 0.4 for magnesium alloys at  $572^\circ\text{F}$ .

*Residual Stresses.* For steel, shot peening increases the endurance limit 1.04–1.22 for polished surfaces, 1.25 for machined surfaces, 1.25–1.5 for rolled surfaces, and 2–3 for forged surfaces. The shot-peening effect disappears above  $500^\circ\text{F}$  for steels and above  $250^\circ\text{F}$  for aluminum. Surface rolling affects the steel endurance limit approximately the same as shot peening, while the endurance limit is increased 1.2–1.3 in aluminum, 1.5 in magnesium, and 1.2–2.93 in cast iron.

\* This section is condensed from Ref. 1, Chapter 12, and expanded for probability from Ref. 44, Chapter 2.

*Corrosion.* A corrosive environment decreases the endurance limit of anodized aluminum and magnesium 0.76–1.00, while nitrided steel and most materials are reduced 0.6–0.8.

*Surface Treatments.* Nickel plating reduces the endurance limit of 1008 steel 0.01 and of 1063 steel 0.77, but, if the surface is shot peened after it is plated, the endurance limit can be increased over that of the base metal. The endurance limit of anodized aluminum is in general not affected. Flame and induction hardening as well as carburizing increase the endurance limit 1.62–1.85, while nitriding increases it 1.30–2.00.

*Fretting.* In surface pairs that move relative to each other, the endurance limit is reduced 0.70–0.90 for each material.

*Radiation.* Radiation tends to increase tensile strength but to decrease ductility.

In discussions on fatigue it should be emphasized that most designs must pass vibration testing. When sizing parts so that they can be modeled on a computer, the designer needs a starting point until feedback is received from the modeling. A helpful starting point is to estimate the static load to be carried, to find the level of vibration testing in  $G$  levels, to assume that the part vibrates with a magnification of 10, and to multiply these together to get an equivalent static load. The stress level should be  $\sigma_u/4$ , which should be less than the yield strength. When the design is modeled, changes can be made to bring the design within the required limits.

## 6 BEAMS

### 6.1 Theory of Flexure

#### *Types of Beams*

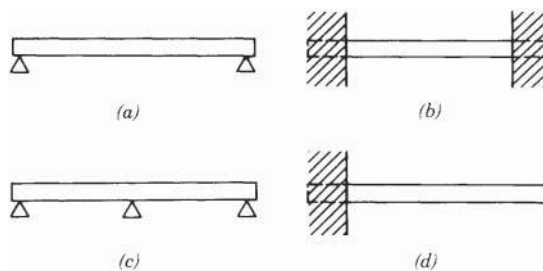
A beam is a bar or structural member subjected to transverse loads that tend to bend it. Any structural member acts as a beam if bending is induced by external transverse forces.

A **simple beam** (Fig. 17a) is a horizontal member that rests on two supports at the ends of the beam. All parts between the supports have free movement in a vertical plane under the influence of vertical loads.

A **fixed beam, constrained beam, or restrained beam** (Fig. 17b) is rigidly fixed at both ends or rigidly fixed at one end and simply supported at the other.

A **continuous beam** (Fig. 17c) is a member resting on more than two supports.

A **cantilever beam** (Fig. 17d) is a member with one end projecting beyond the point of support, free to move in a vertical plane under the influence of vertical loads placed between the free end and the support.



**Figure 17** (a) Simple, (b) constrained, (c) continuous, and (d) cantilever beams.

### *Phenomena of Flexure*

When a simple beam bends under its own weight, the fibers on the upper or concave side are shortened, and the stress acting on them is compression; the fibers on the under or convex side are lengthened, and the stress acting on them is tension. In addition, shear exists along each cross section, the intensity of which is greatest along the sections at the two supports and zero at the middle section.

When a cantilever beam bends under its own weight, the fibers on the upper or convex side are lengthened under tensile stresses; the fibers on the under or concave side are shortened under compressive stresses, the shear is greatest along the section at the support and zero at the free end.

The **neutral surface** is that horizontal section between the concave and convex surfaces of a loaded beam, where there is no change in the length of the fibers and no tensile or compressive stresses acting upon them.

The **neutral axis** is the trace of the neutral surface on any cross section of a beam. (See Fig. 18.)

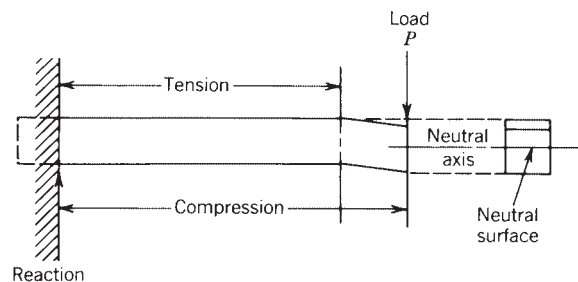
The **elastic curve** of a beam is the curve formed by the intersection of the neutral surface with the side of the beam, it being assumed that the longitudinal stresses on the fibers are within the elastic limit.

### *Reactions at Supports*

The reactions, or upward pressures at the points of support, are computed by applying the following conditions necessary for equilibrium of a system of vertical forces in the same plane: (1) The algebraic sum of all vertical forces must equal zero; that is, the sum of the reactions equals the sum of the downward loads. (2) The algebraic sum of the moments of all the vertical forces must equal zero. Condition (3) applies to cantilever beams and to simple beams uniformly loaded, or with equal concentrated loads placed at equal distances from the center of the beam. In the cantilever beam, the reaction is the sum of all the vertical forces acting downward, comprising the weight of the beam and the superposed loads. In the simple beam each reaction is equal to one-half the total load, consisting of the weight of the beam and the superposed loads. Condition (4) applies to a simple beam not uniformly loaded. The reactions are computed separately, by determining the moment of the several loads about each support. The sum of the moments of the load around one support is equal to the moment of the reaction of the other support around the first support.

### *Conditions of Equilibrium*

The fundamental laws for the stresses at any cross section of a beam in equilibrium are: (1) Sum of horizontal tensile stresses = sum of horizontal compressive stresses. (2) Resisting shear = vertical shear. (3) Resisting moment = bending moment.



**Figure 18** Loads and stress conditions in a cantilever beam.

*Vertical Shear.* At any cross section of a beam the resultant of the external vertical forces acting on one side of the section is equal and opposite to the resultant of the external vertical forces acting on the other side of the section. These forces tend to cause the beam to shear vertically along the section. The value of either resultant is known as the vertical shear at the section considered. It is computed by finding the algebraic sum of the vertical forces to the left of the section; that is, it is equal to the left reaction minus the sum of the vertical downward forces acting between the left support and the section.

A **shear diagram** is a graphic representation of the vertical shear at all cross sections of the beam. Thus in the uniformly loaded simple beam (Table 4) the ordinates to the line represent to scale the intensity of the vertical shear at the corresponding sections of the beam. The vertical shear is greatest at the supports, where it is equal to the reactions, and it is zero at the center of the span. In the cantilever beam (Table 4) the vertical shear is greatest at the point of support, where it is equal to the reaction, and it is zero at the free end. Table 4 shows graphically the vertical shear on all sections of a simple beam carrying two concentrated loads at equal distances from the supports, the weight of the beam being neglected.

*Resisting Shear.* The tendency of a beam to shear vertically along any cross section, due to the vertical shear, is opposed by an internal shearing stress at that cross section known as the resisting shear; it is equal to the algebraic sum of the vertical components of all the internal stresses acting on the cross section.

If  $V$  is the vertical shear, pounds,  $V_r$  is the resisting shear, pounds,  $\tau$  is the average unit shearing stress, pounds per square inch, and  $A$  is the area of the section, square inches, then at any cross section

$$V_r = V = \tau A \quad \tau = \frac{V}{A} \quad (32)$$

The resisting shear is not uniformly distributed over the cross section, but the intensity varies from zero at the extreme fiber to its maximum value at the neutral axis.

At any point in any cross section, the vertical unit shearing stress is

$$\tau = \frac{VA'c'}{I t} \quad (33)$$

where  $V$  is the total vertical shear in pounds for section considered;  $A'$  is the area in square inches of cross section between a horizontal plane through the point where shear is being found and the extreme fiber on the same side of the neutral axis;  $c'$  is the distance in inches from neutral axis to center of gravity of area  $A'$ ;  $I$  is the moment of inertia of the section, inches<sup>4</sup>;  $t$  is the width of section at plane of shear, inches. Maximum value of the unit shearing stress, where  $A$  is the total area, square inches, of cross section of the beam is  $3V$ :

$$\text{For a solid rectangular beam: } \tau = \frac{3V}{2A} \quad (34)$$

$$\text{For a solid circular beam: } \tau = \frac{4V}{3A} \quad (35)$$

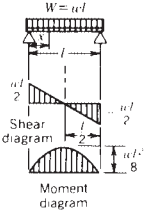
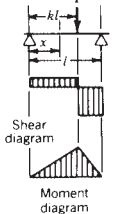
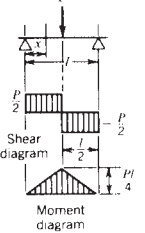
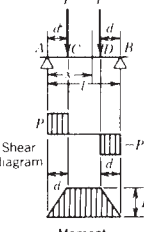
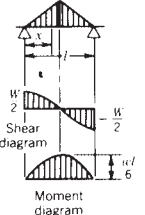
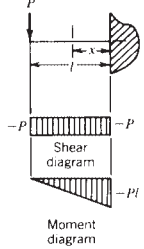
*Horizontal Shear.* In a beam, at any cross section where there is a vertical shearing force, there must be resultant unit shearing stresses acting on the vertical faces of particles that lie at that section. On a horizontal surface of such a particle, there is a unit shearing stress equal to the unit shearing stress on a vertical surface of the particle. Equation (33), therefore, also gives the horizontal unit shearing stress at any point on the cross section of a beam.

**Bending moment**, at any cross section of a beam, is the algebraic sum of the moments of the external forces acting on either side of the section. It is positive when it causes the beam to

**Table 4** Bending Moment, Vertical Shear, and Deflection of Beams of Uniform Cross Section under Various Conditions of Loading<sup>a</sup>

$P$  = concentrated loads, lb  
 $R_1, R_2$  = reactions, lb  
 $w$  = uniform load per unit of length, lb/in.  
 $W$  = total uniform load on beam, lb  
 $l$  = length of beam, in.  
 $x$  = distance from support to any section, in.  
 $E$  = modulus of elasticity, psi

$I$  = moment of inertia, in.<sup>4</sup>  
 $V_x$  = vertical shear at any section, lb  
 $V$  = maximum vertical shear, lb  
 $M_x$  = bending moment at any section, lb-in.  
 $M$  = maximum bending moment, lb-in.  
 $v$  = maximum deflection, in.

<p style="text-align: center;"><b>SIMPLE BEAM—UNIFORM LOAD</b></p>  <p style="text-align: center;"><math>R_1 = R_2 = \frac{wl}{2}</math></p> <p style="text-align: center;"><math>V_x = \frac{wl}{2} - wx</math></p> <p style="text-align: center;"><math>V = \pm \frac{wl}{2}</math> (when <math>\begin{cases} x = 0 \\ x = l \end{cases}</math>)</p> <p style="text-align: center;"><math>M_x = \frac{wx}{2} - \frac{wx^2}{2}</math></p> <p style="text-align: center;"><math>M = \frac{wl^2}{8}</math> (when <math>x = \frac{l}{2}</math>)</p> <p style="text-align: center;"><math>v = \frac{5Wl^3}{384EI}</math> (at center of span)</p>	<p style="text-align: center;"><b>SIMPLE BEAM—CONCENTRATED LOAD AT ANY POINT</b></p>  <p style="text-align: center;"><math>R_1 = P(1 - k)</math>  <math>R_2 = Pk</math></p> <p style="text-align: center;"><math>V_x = R_1</math> (when <math>x &lt; kl</math>)  <math>= R_2</math> (when <math>x &gt; kl</math>)</p> <p style="text-align: center;"><math>V = P(1 - k)</math> (when <math>k &lt; 0.5</math>)  <math>= -Pk</math> (when <math>k &gt; 0.5</math>)</p> <p style="text-align: center;"><math>M_x = Px(1 - k)</math> (when <math>x &lt; kl</math>)  <math>= Pk(l - x)</math> (when <math>x &gt; kl</math>)</p> <p style="text-align: center;"><math>M = Pkl(1 - k)</math> (at point of load)</p> <p style="text-align: center;"><math>v = \frac{Pl^3}{3EI} (1 - k) \times (2/3k - 1/3k^2)^{3/2}</math>  (at <math>x = l\sqrt{2/3k - 1/3k^2}</math>)</p>
<p style="text-align: center;"><b>SIMPLE BEAM—CONCENTRATED LOAD AT CENTER</b></p>  <p style="text-align: center;"><math>R_1 = R_2 = \frac{P}{2}</math></p> <p style="text-align: center;"><math>V_x = V = \pm \frac{P}{2}</math></p> <p style="text-align: center;"><math>M_x = \frac{Px}{2}</math></p> <p style="text-align: center;"><math>M = \frac{Pl}{4}</math> (when <math>x = \frac{l}{2}</math>)</p> <p style="text-align: center;"><math>v = \frac{Pl^3}{48EI}</math> (at center of span)</p>	<p style="text-align: center;"><b>SIMPLE BEAM—TWO EQUAL CONCENTRATED LOADS AT EQUAL DISTANCES FROM SUPPORTS</b></p>  <p style="text-align: center;"><math>R_1 = R_2 = P</math></p> <p style="text-align: center;"><math>V_x = P</math> for AC  <math>= 0</math> for CD  <math>= -P</math> for DB</p> <p style="text-align: center;"><math>V = \pm P</math></p> <p style="text-align: center;"><math>M_x = Px</math> for AC  <math>= Pd</math> for CD  <math>= P(l - x)</math> for DB</p> <p style="text-align: center;"><math>M = Pd</math></p> <p style="text-align: center;"><math>v = \frac{Pd}{24EI} (3l^2 - 4d^2)</math>  (at center of span)</p>
<p style="text-align: center;"><b>SIMPLE BEAM—LOAD INCREASING UNIFORMLY FROM SUPPORTS TO CENTER OF SPAN</b></p>  <p style="text-align: center;"><math>R_1 = R_2 = \frac{W}{2}</math></p> <p style="text-align: center;"><math>V_x = W \left( \frac{1}{2} - \frac{2x^2}{l^2} \right)</math>  (when <math>x &lt; \frac{l}{2}</math>)</p> <p style="text-align: center;"><math>V = \pm \frac{W}{2}</math> (at supports)</p> <p style="text-align: center;"><math>M_x = Wx \left( \frac{1}{2} - \frac{2x^2}{3l^2} \right)</math></p> <p style="text-align: center;"><math>M = \frac{Wl}{6}</math> (at center of span)</p> <p style="text-align: center;"><math>v = \frac{Wl^3}{60EI}</math> (at center of span)</p>	<p style="text-align: center;"><b>CANTILEVER BEAM—LOAD CONCENTRATED AT FREE END</b></p>  <p style="text-align: center;"><math>R = P</math></p> <p style="text-align: center;"><math>V_x = V = -P</math></p> <p style="text-align: center;"><math>M_x = -P(l - x)</math></p> <p style="text-align: center;"><math>M = -Pl</math> (when <math>x = 0</math>)</p> <p style="text-align: center;"><math>v = \frac{Pl^3}{3EI}</math></p>

(continued)

Table 4 (Continued)

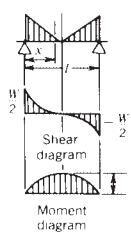
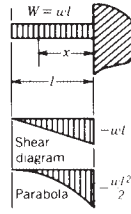
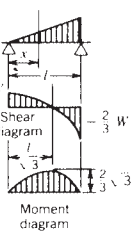
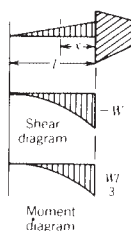
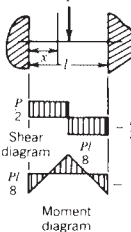
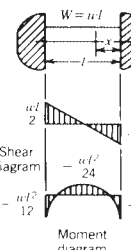
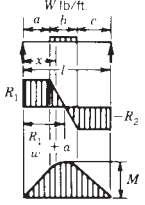
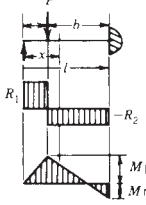
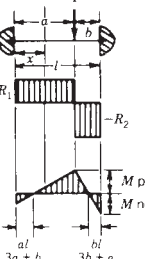
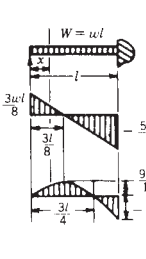
<p><b>SIMPLE BEAM—LOAD INCREASING UNIFORMLY FROM CENTER TO SUPPORTS</b></p>  <p>Shear diagram</p> <p>Moment diagram</p> $R_1 = R_2 = \frac{W}{2}$ $V_x = -W \left( \frac{2x}{l} - \frac{2x^2}{l^2} - \frac{1}{2} \right)$ <p>(when <math>x &lt; \frac{l}{2}</math>)</p> $V = \pm \frac{W}{2}$ $M_x = Wx \left( \frac{1}{2} - \frac{x}{l} + \frac{2x^2}{3l^2} \right)$ <p>(when <math>x &lt; \frac{l}{2}</math>)</p> $M = \frac{Wl}{12}$ (at center of span) $y = \frac{3}{320} \frac{Wl^3}{EI}$ (at center of span)	<p><b>CANTILEVER BEAM—UNIFORM LOAD</b></p>  <p>Shear diagram</p> <p>Parabola</p> <p>Moment diagram</p> $R = W = wl$ $V_x = -w(l - x)$ $V = -wl$ (when $x = 0$ ) $M_x = -w(l - x) \left( \frac{l - x}{2} \right)$ $M = -\frac{wl^2}{2}$ (when $x = 0$ ) $y = \frac{Wl^3}{8EI}$
<p><b>SIMPLE BEAM—LOAD INCREASING UNIFORMLY FROM ONE SUPPORT TO THE OTHER</b></p>  <p>Shear diagram</p> <p>Moment diagram</p> $R_1 = \frac{W}{3}; R_2 = \frac{2}{3}W$ $V_x = W \left( \frac{1}{3} - \frac{x^2}{l^2} \right)$ $V = -\frac{2}{3}W$ (when $x = l$ ) $M_x = \frac{Wx}{3} \left( 1 - \frac{x^2}{l^2} \right)$ $M = \frac{2}{9\sqrt{3}} Wl$ <p>(when <math>x = \frac{l}{\sqrt{3}}</math>)</p> $y = \frac{0.01304}{EI} Wl^3$	<p><b>CANTILEVER BEAM—LOAD INCREASING UNIFORMLY FROM FREE END TO SUPPORT</b></p>  <p>Shear diagram</p> <p>Moment diagram</p> $R = W$ $V_x = -W \frac{(l - x)^2}{l^2}$ $V = -W$ (when $x = 0$ ) $M_x = -\frac{W}{3} \frac{(l - x)^3}{l^2}$ $M = -\frac{Wl}{3}$ (when $x = 0$ ) $y = \frac{Wl^3}{15EI}$
<p><b>FIXED BEAM—CONCENTRATED LOAD AT CENTER OF SPAN</b></p>  <p>Shear diagram</p> <p>Moment diagram</p> $R_1 = R_2 = \frac{P}{2}$ $V_x = V = \pm \frac{P}{2}$ $M_x = P \left( \frac{x}{2} - \frac{l}{8} \right)$ $M_x = -\frac{Pl}{8}$ (when $\begin{cases} x = 0 \\ x = l \end{cases}$ ) $M = +\frac{Pl}{8}$ (at center of span) $y = \frac{Wl^3}{192EI}$	<p><b>FIXED BEAM—UNIFORM LOAD</b></p>  <p>Shear diagram</p> <p>Moment diagram</p> $R_1 = R_2 = \frac{wl}{2} = \frac{W}{2}$ $V_x = \frac{wl}{2} - wx$ $V = \pm \frac{wl}{2}$ (at ends) $M_x = -\frac{wl^2}{2} \left( \frac{1}{6} - \frac{x}{l} + \frac{x^2}{l^2} \right)$ $M = -\frac{1}{12} wl^2$ (when $\begin{cases} x = 0 \\ x = l \end{cases}$ ) $M = \frac{wl^2}{24}$ (when $x = \frac{l}{2}$ ) $y = \frac{Wl^3}{384EI}$

Table 4 (Continued)

	<p style="text-align: center;">SIMPLE BEAM—DISTRIBUTED LOAD OVER PART OF BEAM</p> $R_1 = \frac{wb(2c + b)}{2l}$ $R_2 = \frac{wb(2a + b)}{2l}$ $V_x = \frac{wb(2c + b)}{2l} - w(x - a)$ $V = R_1 \text{ (when } a < c)$ $= R_2 \text{ (when } a > c)$ $M_x = \frac{wbx(2c + b)}{2l} \text{ (when } x < a)$ $= R_1x - \frac{w(x - a)^2}{2}$ <p style="text-align: center;">(when <math>a &lt; x &lt; a + b</math>)</p> $= R_2(l - x)$ <p style="text-align: center;">(when <math>l - x &lt; c</math>)</p> $M = \frac{wb(2c + b)[4al + b(2c + b)]}{8l^2}$		<p style="text-align: center;">BEAM SUPPORTED AT ONE END, FIXED AT OTHER— CONCENTRATED LOAD AT ANY POINT</p> $R_1 = \frac{Pb^2(2l + a)}{2l^3}$ $R_2 = P - R_1$ $V_x = R_1 \text{ (when } x < a)$ $= R_2 \text{ (when } x > a)$ $M_x = \frac{Pb^2x(2l + a)}{2l^3}$ <p style="text-align: center;">(when <math>x &lt; a</math>)</p> $= R_1x - P(x - a)$ <p style="text-align: center;">(when <math>x &gt; a</math>)</p> $M_{\text{positive}} = \frac{Pab^2(2l + a)}{2l^3}$ <p style="text-align: center;">(when <math>x = a</math>)</p> $M_{\text{negative}} = -\frac{Pab(l + a)}{2l^2}$ <p style="text-align: center;">(when <math>x = l</math>)</p>
	<p style="text-align: center;">FIXED BEAM—CON- CENTRATED LOAD AT ANY POINT</p> $a > b$ $R_1 = Pb^2(l + 2a)/l^3$ $R_2 = Pa^2(l + 2b)/l^3$ $V_x = R_1 \text{ (when } x < a)$ $= R_2 \text{ (when } x > a)$ $V = R_2$ $M_x = R_1x - \frac{Pab^2}{l^2}$ <p style="text-align: center;">(when <math>x &lt; a</math>)</p> $= R_2(l - x) - \frac{Pa^2b}{l^2}$ <p style="text-align: center;">(when <math>x &gt; a</math>)</p> $M_{\text{positive}} = \frac{2Pa^2b^2}{l^3}$ $M_{\text{negative}} = -\frac{Pa^2b}{l^2}$ $y = -\frac{2Pa^3b^2}{3EI(3a + b)^2}$		<p style="text-align: center;">BEAM SUPPORTED AT ONE END, FIXED AT OTHER— DISTRIBUTED LOAD</p> $R_1 = \frac{3wl}{8}$ $R_2 = \frac{5wl}{8}$ $V_x = \frac{3wl}{8} - wx$ $V = \frac{3wl}{8} \text{ (at left support)}$ $= \frac{5wl}{8} \text{ (at right support)}$ $M_x = wx \left( \frac{3l}{8} - \frac{x}{2} \right)$ $M_{\text{positive}} = \frac{9wl^2}{128}$ $M_{\text{negative}} = -\frac{wl^2}{8}$ $y = -\frac{0.0054wl^4}{EI} \text{ (at } 0.4215l \text{ from } R_1)$

bend convex downward, hence causing compression in upper fibers and tension in lower fibers of the beam. When the bending moment is determined from the forces that lie to the left of the section, it is positive if they act in a clockwise direction; if determined from forces on the right side, it is positive if they act in a counterclockwise direction. If the moments of upward forces are given positive signs and the moments of downward forces are given negative signs, the bending moment will always have the correct sign, whether determined from the right or left side. The bending moment should be determined for the side for which the calculation will be simplest.

In Table 4 let  $M$  be the bending moment, pound-inches, at a section of a simple beam at a distance  $x$ , inches, from the left support;  $w$  is the weight of beam per 1 in. of length;  $l$  is the length of the beam, inches. Then the reactions are  $1/2wl$ , and  $M = 1/2wlx - 1/2xwx$ . For the sections at the supports,  $x = 0$  or  $x = l$  and  $M = 0$ . For the section at the center of the span  $x = 1/2l$  and  $M = 1/8wl^2 = 1/8Wl$ , where  $W$  is the total weight.



**A moment diagram**, Table 4 shows the bending moment at all cross sections of a beam. Ordinates to the curve represent to scale the moments at the corresponding cross sections. The curve for a simple beam uniformly loaded is a parabola, showing  $M = 0$  at the supports and  $M = 1/8wl^2 = 1/8Wl$  at the center,  $M$  being in pound-inches.

**The dangerous section** is the cross section of a beam where the bending moment is greatest. In a cantilever beam it is at the point of support, regardless of the disposition of the loads. In a simple beam it is that section where the vertical shear changes from positive to negative, and it may be located graphically by constructing a shear diagram or numerically by taking the left reaction and subtracting the loads in order from the left until a point is reached where the sum of the loads subtracted equals the reaction. For a simple beam uniformly loaded, the dangerous section is at the center of the span.

The tendency to rotate about a point in any cross section of a beam is due to the bending moment at that section. This tendency is resisted by the **resisting moment**, which is the algebraic sum of the moments of all the horizontal stresses with reference to the same point.

### *Formula for Flexure*

Let  $M$  be the bending moment,  $M_r$  the resisting moment of the horizontal fiber stresses,  $\sigma$  the unit stress (tensile or compressive) on any fiber, usually that one most remote from the neutral surface, and  $c$  the distance of that fiber from the neutral surface. Then

$$M = M_r = \frac{\sigma I}{c} \quad (36)$$

$$\sigma = \frac{Mc}{I} \quad (37)$$

where  $I$  is the moment of inertia of the cross section with respect to its neutral axis. If  $\sigma$  is in pounds per square inch,  $M$  must be in pound-inches,  $I$  in inches<sup>4</sup>, and  $c$  in inches.

Equation (37) is the basis of the design and investigation of beams. It is true only when the maximum horizontal fiber stress  $\sigma$  does not exceed the proportional limit of the material.

**Moment of inertia** is the sum of the products of each elementary area of the cross section multiplied by the square of the distance of that area from the assumed axis of rotation, or

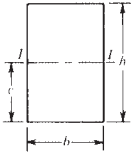
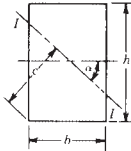
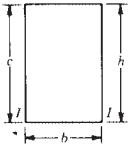
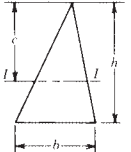
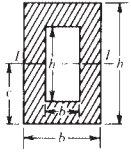
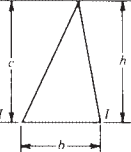
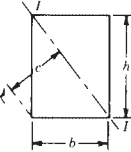
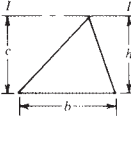
$$I = \sum r^2 \Delta A = \int r^2 dA \quad (38)$$

where  $\Sigma$  is the sign of summation,  $\Delta A$  is an elementary area of the section, and  $r$  is the distance of  $\Delta A$  from the axis. The moment of inertia is greatest in those sections (such as I-beams) having much of the area concentrated at a distance from the axis. Unless otherwise stated, the neutral axis is the axis of rotation considered.  $I$  usually is expressed in inches<sup>4</sup>. See Table 5 for values of moments of inertia of various sections.

**Modulus of rupture** is the term applied to the value of  $\sigma$  as found by Eq. (37), when a beam is loaded to the point of rupture. Since Eq. (37) is true only for stresses within the proportional limit, the value  $\sigma$  of the rupture strength so found is incorrect. However, the equation is used as a measure of the ultimate load-carrying capacity of a beam. The modulus of rupture does not show the actual stress in the extreme fiber of a beam; it is useful only as a basis of comparison. If the strength of a beam in tension differs from its strength in compression, the modulus of rupture is intermediate between the two.

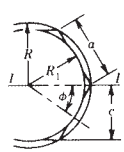
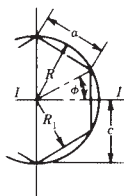
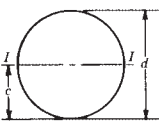
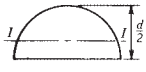
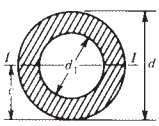
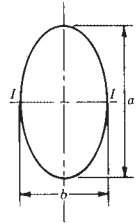
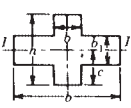
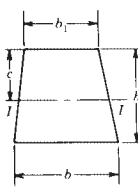
**Section modulus**, the factor  $I/c$  in flexure [Eq. (36)], is expressed in cubic inches. It is the measure of a capacity of a section to resist a bending moment. For values of  $I/c$  for simple shapes, see Table 5. See Refs. 6 and 7 for properties of standard steel and aluminum structural shapes.

Table 5 Elements of Sections<sup>a</sup>

$A$ = area of section $I$ = moment of inertia about axis $I-I$ $c$ = distance from axis $I-I$ to most remote point of section		$I/c$ = section modulus $r$ = radius of gyration	
	<p style="text-align: center;"><b>RECTANGLE</b> Axis through center</p> $A = bh$ $c = h/2$ $I = bh^3/12$ $I/c = bh^2/6$ $r = h/\sqrt{12} = 0.289h$		<p style="text-align: center;"><b>RECTANGLE</b> Axis any line through center of gravity</p> $A = bh$ $c = (b \sin \alpha + h \cos \alpha)/2$ $I = bh(b^2 \sin^2 \alpha + h^2 \cos^2 \alpha)/12$ $I/c = \frac{bh(b^2 \sin^2 \alpha + h^2 \cos^2 \alpha)}{6(b \sin \alpha + h \cos \alpha)}$ $r = \sqrt{(b^2 \sin^2 \alpha + h^2 \cos^2 \alpha)/12}$
	<p style="text-align: center;"><b>RECTANGLE</b> Axis on base</p> $A = bh$ $c = h$ $I = bh^3/3$ $I/c = bh^2/3$ $r = h/\sqrt{3} = 0.577h$		<p style="text-align: center;"><b>TRIANGLE</b> Axis through center of gravity</p> $A = bh/2$ $c = 2/3 h$ $I = bh^3/36$ $I/c = bh^2/24$ $r = h/\sqrt{18} = 0.236h$
	<p style="text-align: center;"><b>HOLLOW RECTANGLE</b> Axis through center</p> $A = bh - b_1h_1$ $c = h/2$ $I = (bh^3 - b_1h_1^3)/12$ $I/c = (bh^3 - b_1h_1^3)/6h$ $r = \sqrt{\frac{bh^3 - b_1h_1^3}{12(bh - b_1h_1)}}$		<p style="text-align: center;"><b>TRIANGLE</b> Axis through base</p> $A = bh/2$ $c = h$ $I = bh^3/12$ $I/c = bh^2/12$ $r = h/\sqrt{6} = 0.408h$
	<p style="text-align: center;"><b>RECTANGLE</b> Axis on diagonal</p> $A = bh$ $c = bh/\sqrt{b^2 + h^2}$ $I = b^3h^3/6(b^2 + h^2)$ $I/c = b^2h^2/6\sqrt{(b^2 + h^2)}$ $r = bh/\sqrt{6(b^2 + h^2)}$		<p style="text-align: center;"><b>TRIANGLE</b> Axis through apex</p> $A = bh/2$ $c = h$ $I = bh^3/4$ $I/c = bh^2/4$ $r = h/\sqrt{2} = 0.707h$

(continued)

Table 5 (Continued)

 <p><b>EQUILATERAL POLYGON</b>                      Axis through center, parallel to one side. <math>n</math> = number of sides</p> $A = nR_1^2 \tan \phi$ $c = a/2 \tan \phi = R_1$ $I = \{A(12R_1^2 + a^2)\}/48$ $I/c = \{A(12R_1^2 + a^2)\}/48R_1$ $r = \sqrt{(12R_1^2 + a^2)/48}$	 <p><b>EQUILATERAL POLYGON</b>                      Axis through center, normal to side. <math>n</math> = number of sides</p> $A = nR_1^2 \tan \phi$ $c = a/(2 \sin \phi) = R$ $I = \{A(6R^2 - a^2)\}/24$ $I/c = \{A(6R^2 - a^2)\}/24R$ $r = \sqrt{(6R^2 - a^2)/24}$
 <p><b>CIRCLE</b>                      Axis through center</p> $A = \pi d^2/4 = 0.7854d^2$ $c = d/2$ $I = \pi d^4/64 = 0.0491d^4$ $I/c = \pi d^3/32 = 0.0982d^3$ $r = d/4$	 <p><b>HALF CIRCLE</b>                      Axis through center of gravity</p> $A = \pi d^2/8 = 0.3927d^2$ $c = \{d(3\pi - 4)\}/6\pi = 0.2878d$ $I = \{d^4(9\pi^2 - 64)\}/1152\pi = 0.0068d^4$ $I/c = \{d^3(9\pi^2 - 64)\}/\{192(3\pi - 4)\} = 0.0238d^3$ $r = \{d\sqrt{(9\pi^2 - 64)}\}/12\pi = 0.1322d$
 <p><b>HOLLOW CIRCLE</b>                      Axis through center</p> $A = \pi(d^2 - d_1^2)/4 = 0.7854(d^2 - d_1^2)$ $c = d/2$ $I = \pi(d^4 - d_1^4)/64 = 0.0491(d^4 - d_1^4)$ $I/c = \pi(d^4 - d_1^4)/32d = 0.0982(d^4 - d_1^4)/d$ $r = \sqrt{(d^2 + d_1^2)/4}$	 <p><b>ELLIPSE</b>                      Axis through center</p> $A = \pi ab/4 = 0.7854ab$ $c = a/2$ $I = \pi a^3b/64 = 0.0491a^3b$ $I/c = \pi a^2b/32 = 0.0982a^2b$ $r = a/4$
 <p><b>CROSSED RECTANGLES</b>                      Axis through center</p> $A = th + t_1(b - t)$ $c = h/2$ $I = \{th^3 + t_1^3(b - t)\}/12$ $I/c = \{th^3 + t_1^3(b - t)\}/6h$ $r = \sqrt{\frac{th^3 + t_1^3(b - t)}{12\{th + t_1(b - t)\}}}$	 <p><b>TRAPEZOID</b>                      Axis through center of gravity</p> $A = \{(b + b_1)h\}/2$ $c = \{(b_1 + 2b)h\}/\{3(b + b_1)\}$ $I = \frac{h^3(b^2 + 4bb_1 + b_1^2)}{36(b + b_1)}$ $I/c = \frac{h^2(b^2 + 4bb_1 + b_1^2)}{12(b_1 + 2b)}$ $r = \frac{h}{6(b + b_1)} \sqrt{2(b^2 + 4bb_1 + b_1^2)}$

### ***Elastic Deflection of Beams***

When a beam bends under load, all points of the elastic curve except those over the supports are deflected from their original positions. The radius of curvature  $\rho$  of the elastic curve at any section is expressed as

$$\rho = \frac{EI}{M} \quad (39)$$

where  $E$  is the modulus of elasticity of the material, pounds per square inch;  $I$  is the moment of inertia, inches<sup>4</sup>, of the cross section with reference to its neutral axis; and  $M$  is the bending moment, pound-inches, at the section considered. Where there is no bending moment,  $\rho$  is infinity and the curve is a straight line; where  $M$  is greatest,  $\rho$  is smallest and the curvature, therefore, is greatest.

If the elastic curve is referred to a system of coordinate axes in which  $x$  represents horizontal distances,  $y$  vertical distances, and  $l$  distances along the curve, the value of  $\rho$  is found, by the aid of the calculus, to be  $d^3l/dx \ d^2y$ . Differential equation (40) of the elastic curve, which applies to all beams when the elastic limit of the material is not exceeded, is obtained by substituting this value in the expression  $\rho = EI/M$  and assuming that  $dx$  and  $dl$  are practically equal:

$$EI \frac{d^2y}{dx^2} = M \quad (40)$$

Equation (40) is used to determine the deflection of any point of the elastic curve by regarding the point of support as the origin of the coordinate axis and taking  $y$  as the vertical deflection at any point on the curve and  $x$  as the horizontal distance from the support to the point considered. The values of  $E$ ,  $I$ , and  $M$  are substituted and the expression is integrated twice, giving proper values to the constants of integration, and the deflection  $y$  is determined for any point. See Table 4.

For example, a cantilever beam in Table 4 has a length  $l$  inches and carries a load  $P$  pounds at the free end. It is required to find the deflection of the elastic curve at a point  $x$  inches from the support, the weight of the beam being neglected.

The moment  $M = -P(l - x)$ . By substitution in Eq. (40), the equation for the elastic curve becomes  $EI(d^2y/dx^2) = -Pl + Px$ . By integrating and determining the constant of integration by the condition that  $dy/dx = 0$  when  $x = 0$ ,  $EI(dy/dx) = -Plx + 1/2Px^2$  results. By integrating a second time and determining the constant by the condition that  $x = 0$  when  $y = 0$ ,  $EIy = -1/2Plx^2 + 1/6Px^3$ , which is the equation of the elastic curve, results. When  $x = l$ , the value of  $y$ , or the deflection in inches at the free end, is found to be  $-Pl^3/3EI$ .

### ***Deflection Due to Shear***

The deflection of a beam as computed by the ordinary formulas is that due to flexural stresses only. The deflection in honeycomb, plastic, and short beams due to vertical shear can be considerable and should always be checked. Because of the nonuniform distribution of the shear over the cross section of the beam, computing the deflection due to shear by exact methods is difficult. It may be approximated by  $y_s = M/AE_s$ , where  $y_s$  = deflection, inches, due to shear;  $M$  = bending moment, pound-inches, at the section where the deflection is calculated;  $E_s$  = modulus of elasticity in shear, pounds per square inch;  $A$  = area of cross section of beam, square inches.<sup>8</sup> For a rectangular section, the ratio of deflection due to shear to the deflection due to bending will be less than 5% if the depth of the beam is less than one-eighth of the length.

## 6.2 Design of Beams

### *Design Procedure*

In designing a beam the procedure is: (1) Compute reactions. (2) Determine position of the dangerous section and the bending moment at that section. (3) Divide the maximum bending moment (expressed in pound-inches) by the allowable unit stress (expressed in pounds per square inch) to obtain the minimum value of the section modulus. (4) Select a beam section with a section modulus equal to or slightly greater than the section modulus required.

### *Web Shear*

A beam designed in the foregoing manner is safe against rupture of the extreme fibers due to bending in a vertical plane, and usually the cross section will have sufficient area to sustain the shearing stresses with safety. For short beams carrying heavy loads, however, the vertical shear at the supports is large, and it may be necessary to increase the area of the section to keep the unit shearing stress within the limit allowed. For steel beams, the average unit shearing stress is computed by  $\tau = V/A$ , where  $V$  is the total vertical shear, pounds;  $A$  is the area of web, square inches.

### *Shear Center*

Closed or solid cross sections with two axes of symmetry will have a shear center at the origin. If the loads are applied here, then the bending moment can be used to calculate the deflections and bending stress, which means there are no torsional stresses. The open section or unsymmetrical section generally has a shear center that is offset on one axis of symmetry and must be calculated.<sup>2,9,10</sup> The load applied at this location will develop bending stresses and deflections. If any sizable torsion is developed, then one must be accounted for torsional stresses and rotations.

### *Miscellaneous Considerations*

Other considerations that will influence the choice of section under certain conditions of loading are: (1) maximum vertical deflection that may be permitted in beams coming in contact with plaster; (2) danger of failure by sidewise bending in long beams, unbraced against lateral deflection; (3) danger of failure by the buckling of the web of steel beams of short span carrying heavy loads; and (4) danger of failure by horizontal shear, particularly in wooden beams.

### *Vertical Deflection*

If a beam is to support or come in contact with materials such as plaster, which may be broken by excessive deflection, it is usual to select such a beam that the maximum deflection will not exceed  $1/360 \times \text{span}$ . It may be shown that for a simple beam supported at the ends with a total uniformly distributed load  $W$  pounds, the deflection in inches is

$$y = \frac{30\sigma L^2}{Ed} \quad (41)$$

where  $\sigma$  is the allowable unit fiber stress, pounds per square inch;  $L$  is the span of beam, feet;  $E$  is the modulus of elasticity, pounds per square inch; and  $d$  is the depth of beam, inches.

If the deflection of a steel beam is to be less than  $1/360$  th of the span, it may be shown from Eq. (41) that, for a maximum allowable fiber stress of 18,000 psi, the limit of span in feet is approximately  $1.8d$ , where  $d$  is the depth of the beam, inches.

For the deflection due to the impact of a moving load falling on a beam, see Section 6.6.

### **Horizontal Shear in Timber Beams**

In beams of a homogeneous material that can withstand equally well shearing stresses in any direction, vertical and horizontal shearing stresses are equally important. In timber, however, shearing strength along the grain is much less than that perpendicular to the grain. Hence, the beams may fail owing to horizontal shear. Short wooden beams should be checked for horizontal shear in order that allowable unit shearing stress along the grain shall not be exceeded. (See Example 1 below.)

### **Restrained Beams**

A beam is considered to be restrained if one or both ends are not free to rotate. This condition exists if a beam is built into a masonry wall at one or both ends, if it is riveted or otherwise fastened to a column, or if the ends projecting beyond the supports carry loads that tend to prevent tilting of the ends, which would naturally occur as the beam deflects. The shears and moments given in Table 4 for fixed-end conditions are seldom, if ever, attained since the restraining elements themselves deform and reduce the magnitude of the restraint. This reduction of restraint decreases the negative moment at the support and increases the positive moment in the central portion of the span. The amount of restraint that exists is a matter that must be judged for each case in the light of the construction used, the rigidity of the connections, and the relative sizes of the connecting members.

### **Safe Loads on Simple Beams**

Equation (42) gives the safe loads on simple beams. This formula is obtained by substituting in the flexure equation (36) the value of  $M$  for a simple beam uniformly loaded, as given in Table 4. Let  $W$  be total load, pounds,  $\sigma$  the extreme fiber unit stress, pounds per square inch,  $S$  the section modulus, inches,<sup>3</sup> and  $L$  the length of span, feet. Then

$$W = \frac{2}{3} \sigma \frac{S}{L} \quad (42)$$

If  $\sigma$  is taken as a maximum allowable unit fiber stress, this equation gives the maximum allowable load on the beam. Most building codes permit a value of  $\sigma = 18,000$  psi for quiescent loads on steel. For this value of  $\sigma$ , Eq. (42) becomes

$$W = \frac{12,000 S}{L} \quad (43)$$

If the load is concentrated at the center of the span, the safe load is one-half the value given by Eq. (43). If the load is neither uniformly distributed nor concentrated at the center of the span, the maximum bending moment must be used. The foregoing equations are for beams laterally supported and are for flexure only. The other factors that influence the strength of the beam, such as shearing, buckling, etc., must also be considered.

### **Use of Tables in Design**

The following is an example in the use of tables for the design of a wooden beam.

#### **Example 1**

Design a southern pine girder of common structural grade to carry a load of 9600 lb distributed uniformly over a 16-ft span in the interior of a building, the beam being a simple beam freely supported at each end.

#### **Solution**

From Table 4, the bending moment of a simple beam uniformly loaded is  $M = wl^2/8$ . Since  $W = wl$  and  $l = 12L$ ,

$$M = 9600 \times 16 \times \frac{1}{8} = 230,400 \text{ lb-in.}$$

If the allowable unit stress on yellow pine is 1200 psi,

$$\frac{I}{c} = \frac{230,400}{1200} = 192 \text{ in.}^3$$

From Table 5, the section modulus of a rectangular section is  $bd^2/6$ . Assume  $b = 8$  in. Then  $8d^2/6 = 192$ , and  $d = \sqrt{144} = 12.0$  in. A beam  $8 \times 12$  in. is selected tentatively and checked for shear.

Maximum shearing stress (horizontal and vertical) is at the neutral surface over the supports. Equation (34) for horizontal shear in a solid rectangular beam is  $\tau = 3V/2A$ ;  $V = 9600/2 = 4800$ , and  $A = 8 \times 12 = 96$ , when  $\tau = (3 \times 4800)/(2 \times 96) = 75$  psi.

If the safe horizontal unit shearing stress for common-grade southern yellow pine is 88 psi and since the actual horizontal unit shearing stress is less than 88 lb, the  $8 \times 12$ -in. beam will be satisfactory.

A **beam of uniform strength** is one in which the dimensions are such that the maximum fiber stress  $\sigma$  is the same throughout the length of the beam. The form of the beam is determined by finding the areas of various cross sections from the flexure formula  $M = \sigma I/c$ , keeping  $\sigma$  constant and making  $I/c$  vary with  $M$ . For a rectangular section of width  $b$  and depth  $d$ , the section modulus  $I/c = 1/6bd^2$ , and, therefore,  $M = 1/6\sigma bd^2$ . By making  $bd^2$  vary with  $M$ , the dimensions of the various sections are obtained. Table 6 gives the dimensions  $b$  and  $d$  at any section, the maximum unit fiber stress  $\sigma$ , and the maximum deflection  $y$  of some rectangular beams of uniform strength. In this table, the bending moment has been assumed to be the controlling factor. On account of the vertical shear near the ends of the beams, the area of the sections must be increased over that given by an amount necessary to keep the unit shearing stress within the allowable unit shearing stress. The discussion of beams of uniform strength, although of considerable theoretical interest, is of little practical value since the cost of fabrication will offset any economy in the use of the material. A plate girder in a bridge or a building is an approximation in practice to a steel beam of uniform strength.

### 6.3 Continuous Beams

As in simple beams, the expressions  $M = \sigma I/c$  and  $\tau = V/A$  govern the design and investigation of beams resting on more than two supports. In the case of continuous beams, however, the reactions cannot be obtained in the manner described for simple beams. Instead, the bending moments at the various sections must be determined, and from these values the vertical shears at the sections and the reactions at the supports may be derived.

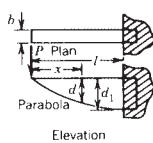
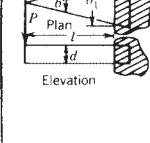
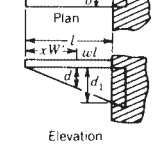
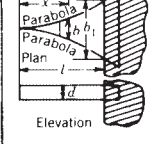
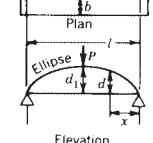
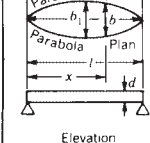
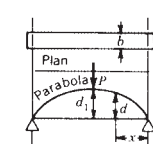
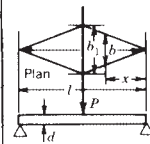
Consider the second span of length  $l_2$  inches of the continuous beam (Fig. 19). Vertical shear  $V_x$  at any section  $x$  inches from the left support of the span is equal to the algebraic sum of all the vertical forces on one side of the section. Thus, if  $V_2$  is the vertical shear at a section to the right of but infinitely close to the left support,  $w_2x$  is the uniform load, and  $\Sigma P_2$  is the sum of the concentrated loads along the distance  $x$  applied at a distance  $kl_2$  from the left support,  $k$  being a fraction less than unity, then

$$V_x = V_2 - w_2x - \Sigma P_2 \quad (44)$$

At any section  $x$  inches from the left support, the bending moment is equal to the algebraic sum of the moments of all forces on one side of the section. If  $M_2$  is the moment in pound-inches at the support to the left,

$$M_x = M_2 + V_2x - \frac{w_2x^2}{2} - \Sigma P_2(x - kl_2) \quad (45)$$

Table 6 Rectangular Beams of Uniform Strength<sup>a</sup>

 <p>I. CANTILEVER BEAM LOADED AT FREE END</p> <p>Width is constant. Depth varies.</p> $d = d_1\sqrt{x/l}$ $\sigma = 6Pl/bd_1^2$ $y = 8Pl^3/Ed_1^3$ <p>Elevation is formed by a straight line and a parabola with its vertex at the loaded end.</p>	 <p>II. CANTILEVER BEAM LOADED AT FREE END</p> <p>Depth constant. Width varies.</p> $b = b_1x/l$ $\sigma = 6Pl/b_1d^2$ $y = 6Pl^3/Eb_1d^3$
 <p>III. CANTILEVER BEAM UNIFORMLY LOADED</p> <p>Width is constant. Depth varies.</p> $d = (x/l)d_1$ $\sigma = 3wl^2/bd_1^2$ $y = 6wl^4/bEd_1^3$	 <p>IV. CANTILEVER BEAM UNIFORMLY LOADED</p> <p>Depth is constant. Width varies.</p> $b = b_1x^2/l^2$ $\sigma = 3wl^2/b_1d^2$ $y = 3wl^4/b_1Ed^3$
 <p>V. SIMPLE BEAM UNIFORMLY LOADED</p> <p>Width varies. Depth is constant.</p> $d = \sqrt{\frac{4d_1^2(lx - x^2)}{l^2}}$ $\sigma = \frac{3wl^2}{4bd_1^2}$ <p>Elevation is formed by a straight line and an ellipse.</p>	 <p>VI. SIMPLE BEAM UNIFORMLY LOADED</p> <p>Depth is constant. Width varies.</p> $b = \frac{4b_1}{l^2}(lx - x^2)$ $\sigma = \frac{3wl^2}{4b_1d^2}$ <p>Plan is two parabolas, with vertices at center of span.</p>
 <p>VII. SIMPLE BEAM LOADED AT CENTER OF SPAN</p> <p>Width varies. Depth is constant.</p> $d = d_1\sqrt{2x/l}$ $\sigma = \frac{3Pl}{2bd_1^2}$ $y = \frac{1}{2} \frac{Pl^3}{Ebd_1^3}$ <p>Elevation is a parabola with vertices at points of support.</p>	 <p>VIII. SIMPLE BEAM LOADED AT CENTER OF SPAN</p> <p>Depth is constant. Width varies.</p> $b = 2b_1x/l$ $\sigma = \frac{3Pl}{2b_1d^2}$ $y = \frac{3Pl^3}{8Eb_1d^3}$ <p>Plan is two triangles with vertices at points of support.</p>

<sup>a</sup> The sections of the beams near the ends must be increased over the amounts shown to resist the vertical shear expressed by the formula  $\tau = 3/2 V/A$ .

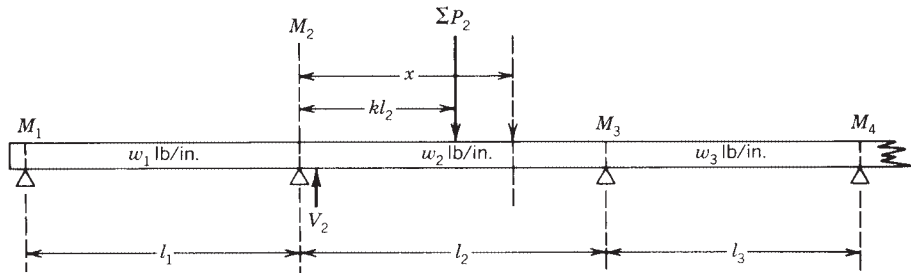


Figure 19 Continuous beam.



Assume that  $x = l_2$ . Then  $M_x$  becomes the moment  $M_3$  at the next support to the right, and the expression may be written

$$V_2 l_2 = M_3 - M_2 + \frac{w_2^2 l_2^2}{2} + \sum P_2(l_2 - kl_2) \quad (46)$$

From Eqs. (44), (45), and (46) it is evident that the bending moment  $M_x$  and the shear  $V_x$  at any section between two consecutive supports may be determined if the bending moments  $M_2$  and  $M_3$  at those supports are known.

To determine bending moments at the supports an expression known as the *theorem of three moments* is used. This gives the relation between the moments at any three consecutive supports of a beam. For beams with the supports on the same level and uniformly loaded over each span, the formula is

$$M_1 l_1 + 2M_2(l_1 + l_2) + M_3 l_2 = 1/4 w_1 l_1^3 - 1/4 w_2 l_2^3 \quad (47)$$

where  $M_1$ ,  $M_2$ , and  $M_3$  are the moments of three consecutive supports;  $l_1$  is the length between first and second support;  $l_2$  is the length between second and third support;  $w_1$  is the uniform load per lineal unit over the first span; and  $w_2$  is the uniform load per lineal unit over the second span. When both spans are of equal length and when the load on each span is the same,  $l_1 = l_2$ ,  $w_1 = w_2$ , and Eq. (47) reduces to

$$M_1 + 4M_2 + M_3 = -1/2 w_1 l^2 \quad (48)$$

which applies to most cases in practice.

Equations (47) and (48) are used as follows: For any continuous beam of  $n$  spans there are  $n + 1$  supports. Assuming the ends of the beam to be simply supported without any overhang, the moments at the end supports are zero, and there are, therefore, to be determined  $n - 1$  moments at the other supports. This may be done by writing  $n - 1$  equations of the form of Eqs. (47) and (48) for each support. These equations will contain  $n - 1$  unknown moments, and their solution will give values of  $M_1, M_2, M_3$ , etc., expressed as coefficients of  $wl^2$ . The shear  $V_1$  at any support may be determined by substituting values of  $M_1$  and  $M_2$  in Eq. (46), and the bending moment at any point in any span may be obtained by Eq. (45). The shear at any point in any span may be determined from Eq. (44).

Figure 20 gives values and diagrams for the reactions, shears, and moments at all sections of continuous beams uniformly loaded up to five spans. Note that the reaction at any support is equal to the sum of the shears to the right and to the left of that support.

## 6.4 Curved Beams

The derivation of the flexure formula,  $\sigma = Mc/I$ , assumes that the beam is initially straight; therefore, any deviation from this condition introduces an error in the value of the stress. If the curvature is slight, the error involved is not large, but in beams with a large amount of curvature, such as hooks, chain links, and frames of punch presses, the error involved in the use of the ordinary flexure formula is considerable. The effect of the curvature is to increase the stress in the inside and to decrease it on the outside fibers of the beam and to shift the position of the neutral axis from the centroidal axis toward the concave or inner side.

The correct value for the unit fiber stress may be found by introducing a correction factor in the flexure formula,  $\sigma = K(P/A \pm Mc/I)$ ; the factor  $K$  depends on the shape of the beam and on the ratio  $R/c$ , where  $R$  is the distance, inches, from the centroidal axis of the section to the center of curvature of the central axis of the unstressed beam and  $c$  is the instance, inches, of centroidal axis from the extreme fiber on the inner or concave side. Reference 9 has an analysis of curved beams, as does Table 7, which gives values of  $K$  for a number of shapes and ratios of  $R/c$ . For slightly different shapes or proportions  $K$  may be found by interpolation.

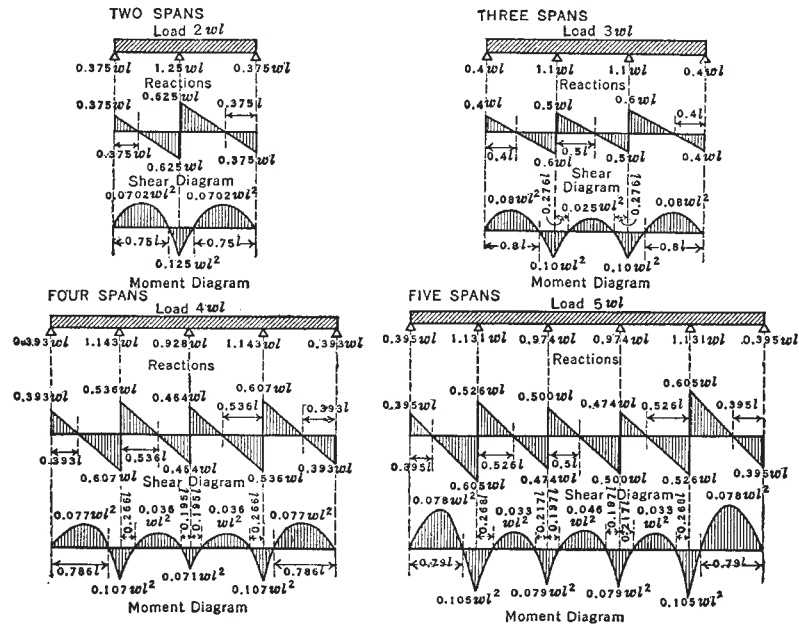


Figure 20 Shear and moment diagrams of continuous beams.

### Deflection of Curved and Slender Curved Beams

The deflection of curved beams<sup>9,10</sup> (Fig. 21) in the curved portion can be found by

$$U = \int \frac{1}{2} \frac{P^2}{EA} ds + \int \frac{\phi V^2}{GA} ds + \int \frac{1}{2} \frac{M^2}{EAy_0 R} ds + \int \frac{MP}{EAR} ds \quad (49)$$

$$\frac{\partial U}{\partial Q} = \delta_Q \quad (50)$$

where  $Q$  is a fictitious load of a couple where the deflection or rotation is desired or can be thought of as a 1-lb load or 1-in.-lb couple;  $y_0$  is from Table 7,  $\phi$  is a shape factor<sup>2</sup> often taken as 1, and  $ds$  is  $R d\theta$ . When  $R/c > 4$ , the last two terms condense to the integral of  $(M^2/2EI) ds$ . When the length of the curved portion to the depth of the beam is greater than 10, the second term of Eq. (49) can be dropped. When in doubt, include all terms.

When beams are not curved (Fig. 22), such as some clamps, the following equations (used by permission of McGraw-Hill from the 4th ed. of Ref. 2) are useful:

$$M = M_0 + HR[\sin(\theta - x) - x] - VR[\cos(\theta - x) - c] + pR^2(1 - u) \quad (51)$$

$$\begin{aligned} \text{Vertical deflection} &= \frac{1}{EI} [M_0 R^2 (s - \theta c) + VR^3 (1/2\theta + c^2\theta - 3/2sc) \\ &+ HR^3 (1/2 - c + sc\theta + 1/2c^2 - s^2) + pR^4 (s + sc - 3/2\theta c - 1/2s^3 - 1/2c^2s)] \quad (52) \end{aligned}$$

$$\begin{aligned} \text{Horizontal deflection} &= \frac{1}{EI} [M_0 R^2 (1 - \theta s - c) + VR^3 (1/2 - c + \theta sc + 1/2c^2 - s^2) \\ &+ HR^3 (-2s + \theta s^2 + 1/2\theta + 3/2sc) + pR^4 (1 - 3/2\theta s + s^2 - c)] \quad (53) \end{aligned}$$

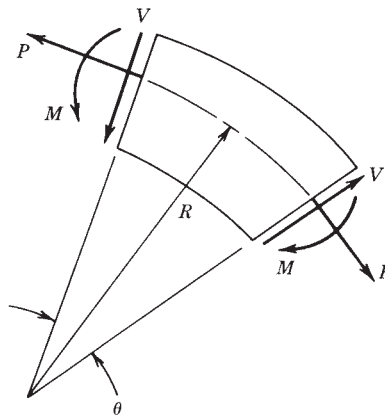
$$\text{Rotation} = \frac{1}{EI} [M_0 R\theta + VR^2 (s - \theta c) + HR^2 (1 - \theta s - c) + pR^3 (\theta - s)] \quad (54)$$

where  $u = \cos x$ ,  $s = \sin \theta$ , and  $c = \cos \theta$ .

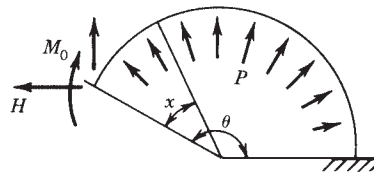
Table 7 Values of Constant  $K$  for Curved Beams

Section	$\frac{R}{c}$	Values of $K$		$\frac{Y_0^a}{R}$	Section	$\frac{R}{c}$	Values of $K$		$\frac{Y_0^a}{R}$
		Inside Fiber	Outside Fiber				Inside Fiber	Outside Fiber	
	1.2	3.41	.54	.224		1.2	2.89	.57	.305
	1.4	2.40	.60	.151		1.4	2.13	.63	.204
	1.6	1.96	.65	.108		1.6	1.79	.67	.149
	1.8	1.75	.68	.084		1.8	1.63	.70	.112
	2.0	1.62	.71	.069		2.0	1.52	.73	.090
	3.0	1.33	.79	.030		3.0	1.30	.81	.041
	4.0	1.23	.84	.016		4.0	1.20	.85	.021
	6.0	1.14	.89	.0070		6.0	1.12	.90	.0093
	8.0	1.10	.91	.0039		8.0	1.09	.92	.0052
	10.0	1.08	.93	.0025		10.0	1.07	.94	.0033
	1.2	3.01	.54	.336		1.2	3.09	.56	.336
	1.4	2.18	.60	.229		1.4	2.25	.62	.229
	1.6	1.87	.65	.168		1.6	1.91	.66	.168
	1.8	1.69	.68	.128		1.8	1.73	.70	.128
	2.0	1.58	.71	.102		2.0	1.61	.73	.102
	3.0	1.33	.80	.046		3.0	1.37	.81	.046
	4.0	1.23	.84	.024		4.0	1.26	.86	.024
	6.0	1.13	.88	.011		6.0	1.17	.91	.011
	8.0	1.10	.91	.0060		8.0	1.13	.94	.0060
	10.0	1.08	.93	.0039		10.0	1.11	.95	.0039
	1.2	3.14	.52	.352		1.2	3.26	.44	.361
	1.4	2.29	.54	.243		1.4	2.39	.50	.251
	1.6	1.93	.62	.179		1.6	1.99	.54	.186
	1.8	1.74	.65	.138		1.8	1.78	.57	.144
	2.0	1.61	.68	.110		2.0	1.66	.60	.116
	3.0	1.34	.76	.050		3.0	1.37	.70	.052
	4.0	1.24	.82	.028		4.0	1.27	.75	.029
	6.0	1.15	.87	.012		6.0	1.16	.82	.013
	8.0	1.12	.91	.0060		8.0	1.12	.86	.0060
	10.0	1.11	.93	.0039		10.0	1.09	.88	.0039
	1.2	3.63	.58	.418		1.2	3.55	.67	.409
	1.4	2.54	.63	.299		1.4	2.48	.72	.292
	1.6	2.14	.67	.229		1.6	2.07	.76	.224
	1.8	1.89	.70	.183		1.8	1.83	.78	.178
	2.0	1.73	.72	.149		2.0	1.69	.80	.144
	3.0	1.41	.79	.069		3.0	1.38	.86	.067
	4.0	1.29	.83	.040		4.0	1.26	.89	.038
	6.0	1.18	.88	.018		6.0	1.15	.92	.018
	8.0	1.13	.91	.010		8.0	1.10	.94	.010
	10.0	1.10	.92	.0065		10.0	1.08	.95	.0065
	1.2	2.52	.67	.408		1.2	2.37	.73	.453
	1.4	1.90	.71	.285		1.4	1.79	.77	.319
	1.6	1.63	.75	.208		1.6	1.56	.79	.236
	1.8	1.50	.77	.160		1.8	1.44	.81	.183
	2.0	1.41	.79	.127		2.0	1.36	.83	.147
	3.0	1.23	.86	.058		3.0	1.19	.88	.067
	4.0	1.16	.89	.030		4.0	1.13	.91	.036
	6.0	1.10	.92	.013		6.0	1.08	.94	.016
	8.0	1.07	.94	.0076		8.0	1.06	.95	.0089
	10.0	1.05	.95	.0048		10.0	1.05	.96	.0057
	1.2	3.28	.58	.269		1.2	2.63	.68	.399
	1.4	2.31	.64	.182		1.4	1.97	.73	.280
	1.6	1.89	.68	.134		1.6	1.66	.76	.205
	1.8	1.70	.71	.104		1.8	1.51	.78	.159
	2.0	1.57	.73	.083		2.0	1.43	.80	.127
	3.0	1.31	.81	.038		3.0	1.23	.86	.058
	4.0	1.21	.85	.020		4.0	1.15	.89	.031
	6.0	1.13	.90	.0087		6.0	1.09	.92	.014
	8.0	1.10	.92	.0049		8.0	1.07	.94	.0076
	10.0	1.07	.93	.0031		10.0	1.06	.95	.0048

<sup>a</sup>  $Y_0$  is distance from centroidal axis to neutral axis, where beam is subjected to pure bending.



**Figure 21** Positive sign convention for curved beams.



**Figure 22** Circular cantilever with end loading and uniform radial pressure  $p$  pounds per linear inch.

## 6.5 Impact Stresses in Bars and Beams

### *Effect of Sudden Loads*

If a sudden load  $P$  is applied to a bar, it will cause a deformation  $el$ , and the work done by the load will be  $Pel$ . Since the external work equals the internal work,  $Pel = \sigma^2 Al/2E$ , and since  $e = \sigma/E$ ,  $P = \sigma A/2$ , or  $\sigma = 2P/A$ . The unit stress and also the unit strain are double those obtained by an equal load applied gradually. However, the bar does not maintain equilibrium at the point of maximum stress and strain. After a series of oscillations, however, in which the surplus energy is dissipated in damping, the bar finally comes to rest with the same strain and stress as that due to the equal static load.

### *Stress Due to Live Loads*

In structural design two loads are considered, the dead load or weight of the structure and the live load or superimposed loads to be carried. The stresses due to the dead load and to the live load are computed separately, each being regarded as a static load. It is obvious that the stress due to the live load may be greatly increased, depending on the suddenness with which the load is applied. It has been shown above that the stress due to a suddenly applied load is double the stress caused by a static load. The term *coefficient of impact* is used extensively in structural engineering to denote the number by which the computed static stress is multiplied to obtain the value of the increased stress assumed to be caused by the suddenness of the application of the live load. If  $\sigma$  is the static unit stress computed from the live load and  $i$  is the coefficient of impact, then the increase of unit stress due to sudden loading is  $i\sigma$ , and the total unit stress due to live load is  $\sigma + i\sigma$ . The value of  $i$  has been determined by empirical methods and varies according to different conditions.

In the building codes of most cities, specified floor loadings for buildings include the impact allowance, and no increase is needed for live loads except for special cases of vibration or other unusual conditions. For railroad bridges, the value of  $i$  depends upon the proportion of the length of the bridge that is loaded. No increase in the static stress is needed when the mass of the structure, as in monolithic concrete, is great. For machinery and for unusual conditions, such as elevator machinery and its supports, each structure should be considered by itself and the coefficient assumed accordingly. It should be noted that the meaning of the word *impact* used above differs somewhat from its strict theoretical meaning and as it is used in the next paragraph. The use of the terms *impact* and *coefficient of impact* in connection with live load stresses is, however, very general.

### ***Axial Impact on Bars***

A load  $P$  dropped from a height  $h$  onto the end of a vertical bar of cross-sectional area  $A$  rigidly secured at the bottom end produces in the bar a unit stress that increases from 0 up to  $\sigma'$ , with a corresponding total strain increasing from 0 up to  $e_1$ . The work done on the bar is  $P(h + e_1)$ , which, provided no energy is expended in hysteresis losses or in giving velocity to the bar, is equal to the energy  $\frac{1}{2}\sigma' Ae_1$  stored in the bar; that is,

$$P(h + e_1) = \frac{1}{2}\sigma' Ae_1 \quad (55)$$

If  $e$  is the strain produced by a static load  $P$  within the proportional limit, then

$$\frac{e}{e_1} = \frac{P/A}{\sigma'} \quad (56)$$

Combining this with Eq. (55) gives

$$\sigma' = \sigma + \sigma \sqrt{1 + 2\frac{h}{e}} \quad (57)$$

$$e_1 = e + e \sqrt{1 + 2\frac{h}{e}} \quad (58)$$

A wrought iron bar 1 in.<sup>2</sup> and 5 ft long under a static load of 5000 lb will be shortened about 0.012 in., assuming no lateral flexure occurs; but, if a weight of 5000 lb drops on its end from a height of 0.048 in., a stress of 20,000 psi will be produced.

Equations (57) and (58) give values of stress and strain that are somewhat high because part of the energy of the applied force is not effective in producing stress but is expended in overcoming the inertia of the bar and in producing local stresses. For light bars they give approximately correct results.

If the bar is horizontal and is struck at one end by a weight  $P$  moving with a velocity  $V$ , the strain produced is  $e_1$ . Then, as before,  $\frac{1}{2}\sigma' Ae_1 = Ph$ . In this case  $h = V^2/2g =$  height from which  $P$  would have to fall to acquire velocity  $V$  ( $g =$  acceleration due to gravity  $= 32.16 \text{ ft/s}^2$ ). Combining with Eq. (56),

$$\sigma' = \sigma \sqrt{2\frac{h}{e}} \quad (59)$$

$$e_1 = e \sqrt{2\frac{h}{e}} \quad (60)$$

**Impact on Beams**

If a weight  $P$  falls on a horizontal beam from a height  $h$  producing a maximum deflection  $y$  and a maximum unit stress  $\sigma'$  in the extreme fiber, the values of  $\sigma'$  and  $y$  are given by

$$\sigma' = \sigma + \sigma \sqrt{1 + 2\frac{h}{y}} \quad (61)$$

$$y_1 = y + y \sqrt{1 + 2\frac{h}{y}} \quad (62)$$

where  $\sigma$  is the extreme fiber unit stress and  $y$  is the deflection due to  $P$ , considered as a static load. The value of  $\sigma$  may be obtained from the flexure formula [Eq. (37)], that of  $y$  from the proper formula for deflection under static load.

If a weight  $P$  moving horizontally with a velocity  $V$  strikes a beam (the ends of which are secured against horizontal movement), the maximum fiber unit stress and the maximum lateral deflection are given by

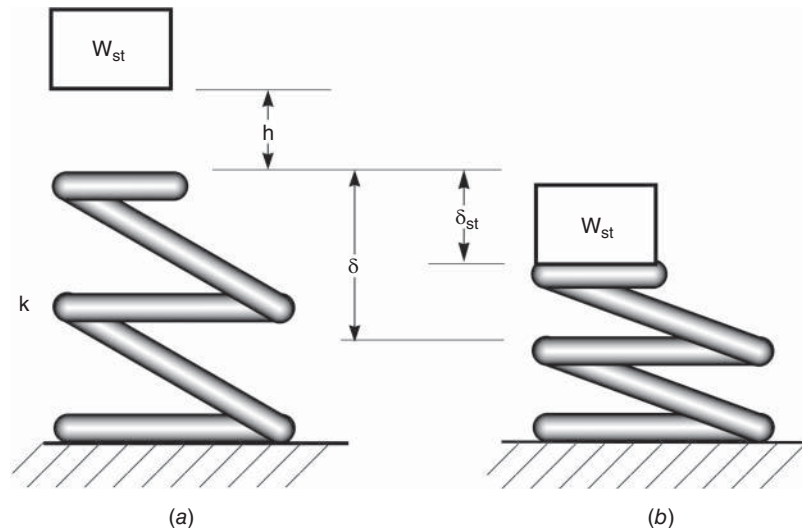
$$\sigma' = \sigma \sqrt{2\frac{h}{y}} \quad (63)$$

$$y_1 = y \sqrt{2\frac{h}{y}} \quad (64)$$

where  $\sigma$  and  $y$  are as before and  $h$  is height through which  $P$  would have to fall to acquire the velocity  $V$ . These formulas, like those for axial impact on bars, give results higher than those observed in tests, particularly if the weight of the beam is great. For further discussion, see Ref. 8 and 9.

**Impact on a Structure**

Fig. 23a is a weight  $W_{st}$  in a 1-G gravity at a height  $h$  above an unloaded structure with a spring constant  $k$ , lb/in. The  $W_{st}$  is released from rest or zero velocity  $v$  and Fig. 23b shows  $W_{st}$  deflection  $\delta$  exceeds  $\delta_{st}$  between the two positions to obtain a maximum deflection and the



**Figure 23** Impact on an unloaded structure.

velocity has again become zero. The energy at the position Fig 23a is  $E_1$  and is potential energy with the zero reference at the maximum spring deflection. At the maximum spring deflection  $\delta$ ,  $E_2$  is the energy in the spring. Then  $E_1 = E_2$  for a spring deflection  $\delta$ .

$$W_{st}(h + \delta) = \frac{1}{2}k\delta^2 \tag{65}$$

Rearranging Eq. (65)

$$k\delta^2 - 2W_{st}\delta - 2W_{st}h = 0 \tag{66}$$

Solving for  $\delta$  using the quadratic equation and noting

$$\frac{W_{st}}{k} = \delta_{st} \tag{67}$$

results in

$$\delta = \delta_{st} \left[ 1 \pm \sqrt{1 + \frac{2h}{\delta_{st}}} \right] \tag{68}$$

If  $h = 0$  and the minus sign ignored

$$\frac{\delta}{\delta_{st}} = 2 = \frac{W/k}{W_{st}/k} \tag{69}$$

Noting that the spring load at  $\delta$  is greater than at  $\delta_{st}$  we have an applied load to the structure of  $W$ . We have the applied structural  $W$  of

$$W = \frac{\delta}{\delta_{st}} W_{st} = 2W_{st} \tag{70}$$

Now take Fig 23b and put a circle around it and accelerate 1G from the equilibrium position of  $\delta_{st}$  in the horizontal direction. A similar form is found from Eqs. (69) and (70) for the horizontal direction.

$$\text{Horizontal } \frac{\delta}{\delta_{st}} = 2$$

$$\text{Horizontal } W = \frac{\delta}{\delta_{st}} W_{st} = 2W_{st} \tag{71}$$

Again use Fig 23b, place a circle around it, and accelerate the circle upwards 1.8Gs.  $W_{st}$  has 1 G downwards all the time making the resultant  $0.8 W_{st}/k = 0.8 \delta_{st}$ , which becomes the gap  $h$  in Eq. (68)

$$\frac{\delta}{\delta_{st}} = \left[ 1 + \sqrt{1 + \frac{2(0.8\delta_{st})}{\delta_{st}}} \right]$$

and

$$\frac{\delta}{\delta_{st}} = 2.6125 = \frac{W}{W_{st}} \tag{72}$$

The applied structural load is

$$W = 2.6125 W_{st} \tag{73}$$

This is the Northridge, California earthquake vertical acceleration.

Now if the circle was accelerated down 1.8G and gravity is 1G down

$$W = 2.8 W_{st} \tag{74}$$

Now consider the plate action during an earthquake Fig. 24 below and the relationships



**Figure 24** Earthquake plate action.

Use again Fig 23b the circled structure and apply a 1.2G Northridge lateral acceleration using Eq. (71)

$$W = 2(1.2 W_{st}) \quad (75)$$

The Japan earthquake  $1.4W_{st}$  would be the lateral acceleration.

An example of a garage, concrete floor with dimensions and height with  $W_{st} = 20 \text{ lb/ft}^2$  (area) could be examined for structural loads and stresses, with considerations for a floor and without.

The previous equations neglect the weight of the structure which are discussed in Refs. 8 and 19.

### ***Rupture from Impact***

Rupture may be caused by impact provided the load has the requisite velocity. The above formulas, however, do not apply since they are valid only for stresses within the proportional limit. It has been found that the dynamic properties of a material are dependent on volume, velocity of the applied load, and material condition. If the velocity of the applied load is kept within certain limiting values, the total energy values for static and dynamic conditions are identical. If the velocity is increased, the impact values are considerably reduced. For further information, see the articles in Ref. 11.

## **6.6 Steady and Impulsive Vibratory Stresses**

For steady vibratory stresses of a weight  $W$  supported by a beam or rod, the deflection of the bar or beam will be increased by the dynamic magnification factor. The relation is given by

$$\delta_{\text{dynamic}} = \delta_{\text{static}} \times \text{dynamic magnification factor}$$

An example of the calculating procedure for the case of no damping losses is 1:

$$\delta_{\text{dynamic}} = \delta_{\text{static}} \times \frac{1}{1 - (\omega/\omega_n)^2} \quad (76)$$

where  $\omega$  is the frequency of oscillation of the load and  $\omega_n$  is the natural frequency of oscillation of a weight on the bar.

For the same beam excited by a single sine pulse of magnitude  $A$  inches per second squared and  $a$  seconds duration, for  $t < a$  a good approximation is

$$\sigma_{\text{dynamic}} = \frac{\delta_{\text{static}}(A/g)}{1 - (\omega/4\pi\omega_n)^2} \left[ \sin \omega t - \frac{1}{4\pi^2} \left( \frac{\omega}{\omega_n} \right) \sin \omega_n t \right] \quad (77)$$

where  $A/g$  is the number of  $g$ 's and  $\omega$  is  $\pi/a$ .



## 7 SHAFTS, BENDING, AND TORSION

## 7.1 Definitions

**TORSIONAL STRESS.** A bar is under torsional stress when it is held fast at one end, and a force acts at the other end to twist the bar. In a round bar (Fig. 25) with a constant force acting, the straight line  $ab$  becomes the helix  $ad$ , and a radial line in the cross section,  $ob$ , moves to the position  $od$ . The angle  $bad$  remains constant while the angle  $bod$  increases with the length of the bar. Each cross section of the bar tends to shear off the one adjacent to it, and in any cross section the shearing stress at any point is normal to a radial line drawn through the point. Within the shearing proportional limit, a radial line of the cross section remains straight after the twisting force has been applied, and the unit shearing stress at any point is proportional to its distance from the axis.

**TWISTING MOMENT,  $T$ ,** is equal to the product of the resultant,  $P$ , of the twisting forces multiplied by its distance from the axis,  $p$ .

**RESISTING MOMENT,  $T_r$ ,** in torsion, is equal to the sum of the moments of the unit shearing stresses acting along a cross section with respect to the axis of the bar. If  $dA$  is an elementary area of the section at a distance of  $z$  units from the axis of a circular shaft (Fig. 23*b*) and  $c$  is the distance from the axis to the outside of the cross section where the unit shearing stress is  $\tau$ , then the unit shearing stress acting on  $dA$  is  $(\tau z/c) dA$ , its moment with respect to the axis is  $(\tau z^2/c) dA$ , and the sum of all the moments of the unit shearing stresses on the cross section is  $\int (\tau z^2/c) dA$ . In this expression the factor  $\int z^2 dA$  is the polar moment of inertia of the section with respect to the axis. Denoting this by  $J$ , the resisting moment may be written  $\tau J/c$ .

**THE POLAR MOMENT OF INERTIA** of a surface about an axis through its center of gravity and perpendicular to the surface is the sum of the products obtained by multiplying each elementary area by the square of its distance from the center of gravity of its surface; it is equal to the sum of the moments of inertia taken with respect to two axes in the plane of the surface at right angles to each other passing through the center of gravity. It is represented by  $J$ , inches<sup>4</sup>. For the cross section of a round shaft,

$$J = \frac{1}{32}\pi d^4 \quad \text{or} \quad \frac{1}{2}\pi r^4 \quad (78)$$

For a hollow shaft,

$$J = \frac{1}{32}\pi (d^4 - d_1^4) \quad (79)$$

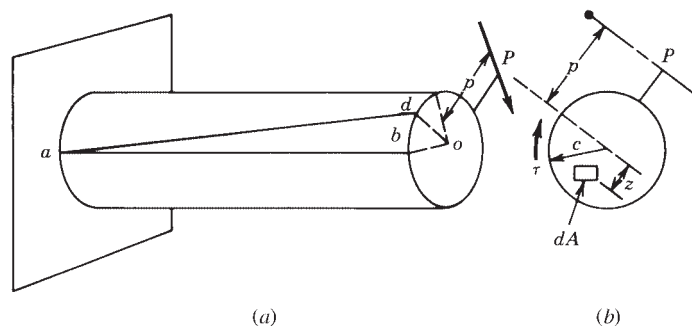


Figure 25 Round bar subject to torsional stress.

where  $d$  is the outside and  $d_1$  is the inside diameter, inches, or

$$J = \frac{1}{2}\pi(r^4 - r_1^4) \quad (80)$$

where  $r$  is the outside and  $r_1$  the inside radius, inches.

**THE POLAR RADIUS OF GYRATION**,  $k_p$ , sometimes is used in formulas; it is defined as the radius of a circumference along which the entire area of a surface might be concentrated and have the same polar moment of inertia as the distributed area. For a solid circular section,

$$k_p^2 = \frac{1}{8}d^2 \quad (81)$$

For a hollow circular section,

$$k_p^2 = \frac{1}{8}(d^2 - d_1^2) \quad (82)$$

## 7.2 Determination of Torsional Stresses in Shafts

### *Torsion Formula for Round Shafts*

The conditions of equilibrium require that the twisting moment,  $T$ , be opposed by an equal resisting moment,  $T_r$ , so that for the values of the maximum unit shearing stress,  $\tau$ , within the proportional limit, the torsion formula for round shafts becomes

$$T_r = T = \tau \frac{J}{c} \quad (83)$$

if  $\tau$  is in pounds per square inch, then  $T_r$  and  $T$  must be in pound-inches,  $J$  is in inches<sup>4</sup>, and  $c$  is in inches. For solid round shafts having a diameter  $d$ , inches,

$$J = \frac{1}{32}\pi d^4 \quad \text{and} \quad c = \frac{1}{2}d \quad (84)$$

and

$$T = \frac{1}{16}\pi d^3 \tau \quad \text{or} \quad \tau = \frac{16T}{\pi d^3} \quad (85)$$

For hollow round shafts,

$$J = \frac{\pi(d^4 - d_1^4)}{32} \quad \text{and} \quad c = \frac{1}{2}d \quad (86)$$

and the formula becomes

$$T = \frac{\tau \pi(d^4 - d_1^4)}{16d} \quad \text{or} \quad \tau = \frac{16Td}{\pi(d^4 - d_1^4)} \quad (87)$$

The torsion formula applies only to solid circular shafts or hollow circular shafts, and then only when the load is applied in a plane perpendicular to the axis of the shaft and when the shearing proportional limit of the material is not exceeded.

### *Shearing Stress in Terms of Horsepower*

If the shaft is to be used for the transmission of power, the value of  $T$ , pound-inches, in the above formulas becomes  $63,030HN$ , where  $H$  is the horsepower to be transmitted and  $N$  is the revolutions per minute. The maximum unit shearing stress, pounds per square inch, then is

$$\text{For solid round shafts:} \quad \tau = \frac{321,000H}{Nd^3} \quad (88)$$

$$\text{For hollow round shafts:} \quad \tau = \frac{321,000Hd}{N(d^4 - d_1^4)} \quad (89)$$

If  $\tau$  is taken as the allowable unit shearing stress, the diameter  $d$ , inches, necessary to transmit a given horsepower at a given shaft speed can then be determined. These formulas give the stress due to torsion only, and allowance must be made for any other loads, as the weight of shaft and pulley, and tension in belts.

**Angle of Twist**

When the unit shearing stress  $\tau$  does not exceed the proportional limit, the angle *bod* (Fig. 25) for a solid round shaft may be computed from the formula

$$\theta = \frac{Tl}{GJ} \quad (90)$$

where  $\theta$  is the angle in radians;  $l$  is the length of shaft in inches;  $G$  is the shearing modulus of elasticity of the material; and  $T$  is the twisting moment in pound-inches. Values of  $G$  for different materials are steel, 12,000,000; wrought iron, 10,000,000; and cast iron, 6,000,000.

When the angle of twist on a section begins to increase in a greater ratio than the twisting moment, it may be assumed that the shearing stress on the outside of the section has reached the proportional limit. The shearing stress at this point may be determined by substituting the twisting moment at this instant in the torsion formula.

**Torsion of Noncircular Cross Sections**

The analysis of shearing stress distribution along noncircular cross sections of bars under torsion is complex. By drawing two lines at right angles through the center of gravity of a section before twisting and observing the angular distortion after twisting, it has been found from many experiments that in noncircular sections the shearing unit stresses are not proportional to their distances from the axis. Thus in a rectangular bar there is no shearing stress at the corners of the sections, and the stress at the middle of the wide side is greater than at the middle of the narrow side. In an elliptical bar the shearing stress is greater along the flat side than at the round side.

It has been found by tests<sup>12,13</sup> as well as by mathematical analysis that the torsional resistance of a section, made up of a number of rectangular parts, is approximately equal to the sum of the resistances of the separate parts. It is on this basis that nearly all the formulas for noncircular sections have been developed. For example, the torsional resistance of an I-beam is approximately equal to the sum of the torsional resistances of the web and the outstanding flanges. In an I-beam in torsion the maximum shearing stress will occur at the middle of the side of the web, except where the flanges are thicker than the web, and then the maximum stress will be at the midpoint of the width of the flange. Reentrant angles, as those in I-beams and channels, are always a source of weakness in members subjected to torsion. Table 8 gives values of the maximum unit shearing stress  $\tau$  and the angle of twist  $\theta$  induced by twisting bars of various cross sections, it being assumed that  $\tau$  is not greater than the proportional limit.

Torsion of thin-wall closed sections (Fig. 26) is derived as

$$T = 2qA \quad (91)$$

$$q = \tau t \quad (92)$$

$$\theta_i = \frac{\theta}{L} = \frac{T}{2A} \frac{1}{2AG} \frac{S}{t} = \frac{T}{GJ} \quad (93)$$


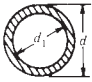

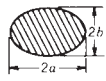
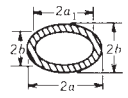

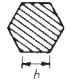
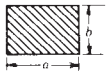
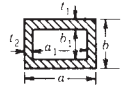

where  $S$  is the arc length around area  $A$  over which  $\tau$  acts for a thin-wall section; shear buckling should be checked. When more than one cell is used<sup>1,14</sup> or if a section is not constructed of a single material,<sup>14</sup> the calculations become more involved:

$$J = \frac{4A^2}{\oint ds/t} \quad (94)$$

In a torsion failure, the outer fibers of a section are the first to shear, and the rupture extends toward the axis as the twisting is continued. The torsion formula for round shafts has no theoretical basis after the shearing stresses on the outer fibers exceed the proportional limit, as the stresses along the section then are no longer proportional to their distances from the axis. It is convenient, however, to compare the torsional strength of various materials by using the

Table 8 Formulas for Torsional Deformation and Stress<sup>a</sup>

General formulas:  $\theta = \frac{TL}{KG}$ ,  $\tau = \frac{T}{Q}$ , where  $\theta$  = angle of twist, radians;  $T$  = twisting moment, in·lb;  $L$  = length, in.;  $\tau$  = unit shear stress, psi;  $G$  = modulus of rigidity, psi;  $K$ , in.<sup>4</sup>, and  $Q$ , in.<sup>3</sup>, are functions of the cross section.

Shape	Formula for $K$ in $\theta = \frac{TL}{KG}$	Formula for Shear Stress
	$K = \frac{\pi d^4}{32}$	$\tau = \frac{16T}{\pi d^3}$
	$K = \frac{1}{32\pi}(d^4 - d_1^4)$	$\tau = \frac{16Td}{\pi(d^4 - d_1^4)}$
	$K = \frac{2}{3}\pi r^3$	$\tau = \frac{3T}{2\pi r^2}$
	$K = \frac{\pi a^3 b^3}{a^2 + b^2}$	$\tau = \frac{2T}{\pi ab^2}$
	$K = \frac{\pi a_1^3 b_1^3}{a_1^2 + b_1^2} [(1+q)^4 - 1]$ $q = \frac{a - a_1}{a_1}$ $q = \frac{b - b_1}{b_1}$	$\tau = \frac{2T}{\pi a_1 b_1^2 [(1+q)^4 - 1]}$
	$K = \frac{b^4 \sqrt{3}}{80}$	$\tau = \frac{20T}{b^3}$
	$K = 2.69b^4$	$\tau = \frac{1.09T}{b^3}$
	$K = \frac{ab^3}{16} \left[ \frac{16}{3} - 3.36 \frac{b}{a} \left( 1 - \frac{b^4}{12a^4} \right) \right]$	$\tau = \frac{(3a + 1.8b)T}{a^2 b^2}$
	$K = \frac{2t_1 t_2 (a - t_2)^2 (b - t_1)^2}{at_2 + bt_1 - t_2^2 - t_1^2}$	$\tau = \frac{T}{2t_2(a - t_2)(b - t_1)}$
	$K = 0.1406b^4$	$\tau = \frac{4.8T}{b^3}$

(continued)

Table 8 (Continued)

General formulas:  $\theta = \frac{TL}{KG}$ ,  $\tau = \frac{T}{Q}$ , where  $\theta$  = angle of twist, radians;  $T$  = twisting moment, in.-lb;  $L$  = length, in.;  $\tau$  = unit shear stress, psi;  $G$  = modulus of rigidity, psi;  $K$ , in.<sup>4</sup>, and  $Q$ , in.<sup>3</sup>, are functions of the cross section.

Shape	Formula for $K$ in $\theta = \frac{TL}{KG}$	Formula for Shear Stress
	$r = \text{fillet radius}$ $D = \text{diameter largest inscribed circle}$ $K = 2K_1 + K_2 + 2\alpha D^4$ $K_1 = ab^3 \left[ \frac{1}{3} - 0.21 \frac{b}{a} \left( 1 - \frac{b^4}{12a^4} \right) \right]$ $K_2 = cd^3 \left[ \frac{1}{3} - 0.105 \frac{d}{c} \left( 1 - \frac{d^4}{192c^4} \right) \right]$ $\alpha = \frac{b}{d} \left( 0.07 + 0.076 \frac{r}{b} \right)$	<p>For all solid sections of irregular form the maximum shear stress occurs at or very near one of the points where the largest inscribed circle touches the boundary, and of these, at the one where the curvature of the boundary is algebraically least. (Convexity represents positive, concavity negative, curvature of the boundary.) At a point where the curvature is positive (boundary of section straight or convex) this maximum stress is given approximately by</p> $\tau = G \frac{\theta}{L} c \quad \text{or} \quad \tau = \frac{T}{K} c$ <p>where</p> $c = \frac{D}{1 + \frac{\tau^2 D^4}{16A^2}}$ $\times \left[ 1 + 0.15 \left( \frac{\tau^2 D^4}{16A^2} - \frac{D}{2r} \right) \right]$ <p>where <math>D</math> = diameter of largest inscribed circle, <math>r</math> = radius of curvature of boundary at the point (positive for this case), <math>A</math> = area of the section.</p>
	$K = 2K_1 + K_2 + 2\alpha D^4$ $K_1 = ab^3 \left[ \frac{1}{3} - 0.21 \frac{b}{a} \left( 1 - \frac{b^4}{12a^4} \right) \right]$ $K_2 = \frac{1}{3} cd^3$ $\alpha = \frac{t}{t_1} \left( 0.15 + 0.1 \frac{r}{b} \right)$ $t = b$ if $b < d$ $t = d$ if $d < b$ $t_1 = b$ if $b > d$ $t_1 = d$ if $d > b$	
	$K = K_1 + K_2 + \alpha D^4$ $K_1 = ab^3 \left[ \frac{1}{3} - 0.21 \frac{b}{a} \left( 1 - \frac{b^4}{12a^4} \right) \right]$ $K_2 = cd^3 \left[ \frac{1}{3} - 0.105 \frac{d}{c} \left( 1 - \frac{d^4}{192c^4} \right) \right]$ $\alpha = \frac{b}{d} \left( 0.07 + 0.076 \frac{r}{b} \right)$	

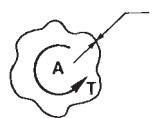


Figure 26 Thin-walled tube.

formula to compute values of  $\tau$  at which rupture takes place. These computed values of the maximum stress sustained before rupture are somewhat higher for iron and steel than the ultimate strength of the materials in direct shear. Computed values of the ultimate strength in torsion are found by experiment to be: cast iron, 30,000 psi; wrought iron, 55,000 psi; medium steel, 65,000 psi; timber, 2000 psi. These computed values of twisting strength may be used in the torsion formula to determine the probable twisting moment that will cause rupture of a given round bar or to determine the size of a bar that will be ruptured by a given twisting moment. In design, large factors of safety should be taken, especially when the stress is reversed, as in reversing engines, and when the torsional stress is combined with other stresses, as in shafting.

### 7.3 Bending and Torsional Stresses

The stress for combined bending and torsion can be found from Eqs. (20) (shear theory) and (22) (distortion energy) with  $\sigma_y = 0$ :

$$\frac{\sigma_w}{2} = \sqrt{\left(\frac{Mc}{2I}\right)^2 + \left(\frac{Tr}{J}\right)^2} \quad (95)$$

For solid round rods, this equation reduces to

$$\frac{\sigma_w}{2} = \frac{16}{\pi d^3} \sqrt{M^2 + T^2} \quad (91)$$

From distortion energy

$$\sigma = \sqrt{\left(\frac{Mc}{I}\right)^2 + 3\left(\frac{Tr}{J}\right)^2} \quad (97)$$

For solid round rods, the equation yields

$$\sigma = \frac{32}{\pi d^3} \sqrt{M^2 + 3/4 T^2} \quad (98)$$

## 8 COLUMNS

### 8.1 Definitions

A **COLUMN OR STRUT** is a bar or structural member under axial compression that has an unbraced length greater than about 8 or 10 times the least dimension of its cross section. On account of its length, it is impossible to hold a column in a straight line under a load; a slight sidewise bending always occurs, causing flexural stresses in addition to the compressive stresses induced directly by the load. The lateral deflection will be in a direction perpendicular to that axis of the cross section about which the moment of inertia is the least. Thus in Fig. 27a the column will bend in a direction perpendicular to  $aa$ , in Fig. 27b it will bend perpendicular to  $aa$  or  $bb$ , and in Fig. 27c it is likely to bend in any direction.

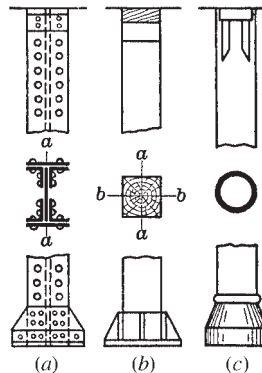


Figure 27 Column end designs.

**RADIUS OF GYRATION** of a section with respect to a given axis is equal to the square root of the quotient of the moment of inertia with respect to that axis divided by the area of the section, that is

$$k = \sqrt{\frac{I}{A}} \quad \frac{I}{A} = k^2 \quad (99)$$

where  $I$  is the moment of inertia and  $A$  is the cross-sectional area. Unless otherwise mentioned, an axis through the center of gravity of the section is the axis considered. As in beams, the moment of inertia is an important factor in the ability of the column to resist bending, but for purposes of computation it is more convenient to use the radius of gyration.

**LENGTH OF A COLUMN** is the distance between points unsupported against lateral deflection.

**SLENDERNESS RATIO** is the length  $l$  divided by the least radius of gyration  $k$ , both in inches.

For steel, a *short column* is one in which  $l/k < 20$  or  $30$ , and its failure under load is due mainly to direct compression; in a *medium-length column*,  $l/k =$  about  $30$ – $175$ , failure is by a combination of direct compression and bending; in a *long column*,  $l/k >$  about  $175$ – $200$ , failure is mainly by bending. For timber columns these ratios are about  $0$ – $30$ ,  $30$ – $90$ , and above  $90$ , respectively. The load that will cause a column to fail decreases as  $l/k$  increases. The above ratios apply to round-end columns. If the ends are fixed (see below), the effective slenderness ratio is one-half that for round-end columns, as the distance between the points of inflection is one-half of the total length of the column. For flat ends it is intermediate between the two.

**CONDITIONS OF ENDS.** The various conditions that may exist at the ends of columns usually are divided into four classes: (1) Columns with round ends: The bearing at either end has perfect freedom of motion, as there would be with a ball-and-socket joint at each end. (2) Columns with hinged ends: They have perfect freedom of motion at the ends in one plane, as in compression members in bridge trusses where loads are transmitted through end pins. (3) Columns with flat ends: The bearing surface is normal to the axis of the column and of sufficient area to give at least partial fixity to the ends of the columns against lateral deflection. (4) Columns with fixed ends: The ends are rigidly secured, so that under any load the tangent to the elastic curve at the ends will be parallel to the axis in its original position.

Experiments prove that columns with fixed ends are stronger than columns with flat, hinged, or round ends and that columns with round ends are weaker than any of the other types. Columns with hinged ends are equivalent to those with round ends in the plane in which they have free movement; columns with flat ends have a value intermediate between those with fixed ends and those with round ends. It often happens that columns have one end fixed and one end hinged or some other combination. Their relative values may be taken as intermediate between those represented by the condition at either end. The extent to which strength is increased by fixing the ends depends on the length of the column, fixed ends having a greater effect on long columns than on short ones.

## 8.2 Theory

There is no exact theoretical formula that gives the strength of a column of any length under an axial load. Formulas involving the use of empirical coefficients have been deduced, however, and they give results that are consistent with the results of tests.

### *Euler's Formula*

Euler's formula assumes that the failure of a column is due solely to the stresses induced by sidewise bending. This assumption is not true for short columns, which fail mainly by direct

compression, nor is it true for columns of medium length. The failure in such cases is by a combination of direct compression and bending. For columns in which  $lk > 200$ , Euler's formula is approximately correct and agrees closely with the results of tests.

Let  $P$  be the axial load, pounds;  $l$  the length of column, inches;  $I$  the least moment of inertia, inches<sup>4</sup>;  $k$  the least radius of gyration, inches;  $E$  the modulus of elasticity; and  $y$  the lateral deflection, inches, at any point along the column that is caused by load  $P$ . If a column has round ends, so that the bending is not restrained, the equation of its elastic curve is

$$EI = \frac{d^2y}{dx^2} = -Py \quad (100)$$

when the origin of the coordinate axes is at the top of the column, the positive direction of  $x$  being taken downward and the positive direction of  $y$  in the direction of the deflection. Integrating the above expression twice and determining the constants of integration give

$$P = \Omega\pi^2 \frac{EI}{l^2} \quad (101)$$

which is Euler's formula for long columns. The factor  $\Omega$  is a constant depending on the condition of the ends. For round ends  $\Omega = 1$ ; for fixed ends  $\Omega = 4$ ; for one end round and the other fixed  $\Omega = 2.05$ .  $P$  is the load at which, if a slight deflection is produced, the column will not return to its original position. If  $P$  is decreased, the column will approach its original position, but if  $P$  is increased, the deflection will increase until the column fails by bending.

For columns with value of  $lk$  less than about 150, Euler's formula gives results distinctly higher than those observed in tests. Euler's formula is now little used except for long members and as a basis for the analysis of the stresses in some types of structural and machine parts. It always gives an ultimate and never an allowable load.

### **Secant Formula**

The deflection of the column is used in the derivation of the Euler formula, but if the load were truly axial, it would be impossible to compute the deflection. If the column is assumed to have an initial eccentricity of load of  $e$  inches (see Ref. 8 for suggested values of  $e$ ), the equation for the deflection  $y$  becomes

$$y_{\max} = e \left( \sec \frac{l}{2} \sqrt{\frac{P}{EI}} - 1 \right) \quad (102)$$

The maximum unit compressive stress becomes

$$\sigma = \frac{P}{A} \left( 1 + \frac{ec}{k^2} \sec \frac{l}{2} \sqrt{\frac{P}{EI}} \right) \quad (103)$$

where  $l$  is the length of column, inches;  $P$  is the total load, pounds;  $A$  is the area, square inches;  $I$  is the moment of inertia, inches<sup>4</sup>;  $k$  is the radius of gyration, inches;  $c$  is the distance from neutral axis to the most compressed fiber, inches; and  $E$  is the modulus of elasticity; both  $I$  and  $k$  are taken with respect to the axis about which bending takes place. The ASCE indicates  $ec/k^2 = 0.25$  for central loading. Because the formula contains the secant of the angle  $\left(\frac{l}{2}\right) \sqrt{P/EI}$ , it is sometimes called the *secant formula*. It has been suggested by the Committee on Steel-Column Research<sup>15,16</sup> that the best rational column formula can be constructed on the secant type, although, of course, it must contain experimental constants.

The secant formula can be used also for columns that are eccentrically loaded if  $e$  is taken as the actual eccentricity plus the assumed initial eccentricity.



***Eccentric Loads on Short Compression Members***

Where a direct push acting on a member does not pass through the centroid but at a distance  $e$  inches from it, both direct and bending stresses are produced. For short compression members in which column action may be neglected, the direct unit stress is  $P/A$ , where  $P$  is the total load, pounds, and  $A$  is the area of cross section, square inches. The bending unit stress is  $Mc/I$ , where  $M = Pe$  is the bending moment, pound-inches;  $c$  is the distance, inches, from the centroid to the fiber in which the stress is desired;  $I$  is the moment of inertia, inches<sup>4</sup>. The total unit stress at any point in the section is  $\sigma = P/A + Pec/I$ , or  $\sigma = (P/A)(1 + ec/k^2)$ , since  $I = Ak^2$ , where  $k$  = radius of gyration, inches.

***Eccentric Loads on Columns***

Various column formulas must be modified when the loads are not balanced, that is, when the resultant of the loads is not in line with the axis of the column. If  $P$  is the load, pounds, applied at a distance  $e$  inches from the axis, bending moment  $M = Pe$ . Maximum unit stress  $\sigma$ , pounds per square inch, due to this bending moment alone is  $\sigma = Mc/I = Pec/Ak^2$ , where  $c$  is the distance, inches, from the axis to the most remote fiber on the concave side;  $A$  is the sectional area, square inches;  $k$  is the radius of gyration in the direction of the bending, inches. This unit stress must be added to the unit stress that would be induced if the resultant load were applied in line with the axis of the column.

The secant formula, Eq. (103), also can be used for columns that are eccentrically loaded if  $e$  is taken as the actual eccentricity plus the assumed initial eccentricity.

***Column Subjected to Transverse or Cross-Bending Loads***

A compression member that is subjected to cross-bending loads may be considered to be (1) a beam subjected to end thrust or (2) a column subjected to cross-bending loads, depending on the relative magnitude of the end thrust and cross-bending loads and on the dimensions of the member. The various column formulas may be modified so as to include the effect of cross-bending loads. In this form the modified secant formula for transverse loads is

$$\sigma = \frac{P}{A} \left[ 1 + (e + y) \frac{c}{k^2} \sec \frac{l}{2k} \sqrt{\frac{P}{AE}} \right] + \frac{Mc}{Ak^2} \quad (204)$$

In the formula,  $\sigma$  is the maximum unit stress on concave side, pounds per square inch;  $P$  is the axial end load, pounds;  $A$  is the cross-sectional area, square inches;  $M$  is the moment due to cross-bending load, pound-inches;  $y$  is the deflection due to cross-bending load, inches;  $k$  is the radius of gyration, inches;  $l$  is the length of column, inches;  $e$  is the assumed initial eccentricity, inches;  $c$  is the distance, inches, from axis to the most remote fiber on the concave side.

**8.3 Wooden Columns*****Wooden Column Formulas***

One of the principal formulas is that formerly used by the American Railroad Engineering Association (AREA),  $P/A = \sigma_1(1 - l/60d)$ , where  $P/A$  is the allowable unit load, pounds per square inch;  $\sigma_1$  is the allowable unit stress in direct compression on short blocks, pounds per square inch;  $l$  is the length, inches; and  $d$  is the least dimension, inches. This formula is being replaced rapidly by formulas recommended by the ASTM and AREA. Committees of these societies, working with the U.S. Forest Products Laboratory, classified timber columns in three groups (ASTM Standards, 1937, D245-37):

1. *Short Columns.* The ratio of unsupported length to least dimension does not exceed 11. For these columns, the allowable unit stress should not be greater than the values given in Table 9 under compression parallel to the grain.

2. *Intermediate-Length Columns.* Where the ratio of unsupported length to least dimension is greater than 10, Eq. (105), of the fourth-power parabolic type, shall be used to determine allowable unit stress until this allowable unit stress is equal to two-thirds of the allowable unit stress for short columns:

$$\frac{P}{A} = \sigma_1 \left[ 1 - \frac{1}{3} \left( \frac{l}{Kd} \right)^4 \right] \quad (105)$$

where  $P$  is the total load, pounds;  $A$  is the area, square inches;  $\sigma_1$  is the allowable unit compressive stress parallel to grain, pounds per square inch (see Table 9);  $l$  is the unsupported length, inches;  $d$  is the least dimension, inches;  $K' = l/d$  at the point of tangency of the parabolic and Euler curves, at which  $P/A = 2/3\sigma_1$ . The value of  $K$  for any species and grade is  $\pi/2\sqrt{E/6\sigma_1}$ , where  $E$  is the modulus of elasticity.

3. *Long Columns.* Where  $P/A$  as computed by Eq. (94) is less than  $2/3\sigma_1$ , Eq. (95) of the Euler type, which includes a factor of safety of 3, shall be used:

$$\frac{P}{A} = \frac{1}{36} \left[ \frac{\pi^2 E}{(l/d)^2} \right] \quad (106)$$

Timber columns should be limited to a ratio of  $l/d$  equal to 50. No higher loads are allowed for square-ended columns. The strength of round columns may be considered the same as that of square columns of the same cross-sectional area.

#### *Use of Timber Column Formulas*

The values of  $E$  (modulus of elasticity) and  $\sigma_1$  (compression parallel to grain) in the above formulas are given in Table 9. Table 10 gives the computed values of  $K$  for some common types of timbers. These may be substituted directly in Eq. (94) for intermediate-length columns or may be used in conjunction with Table 11, which gives the strength of columns of intermediate length, expressed as a percentage of strength ( $\sigma_1$ ) of short columns. In the tables, the term "continuously dry" refers to interior construction where there is no excessive dampness or humidity; "occasionally wet but quickly dry" refers to bridges, trestles, bleachers, and grandstands; and "usually wet" refers to timber in contact with the earth or exposed to waves or tidewater.

## 8.4 Steel Columns

### *Types*

Two general types of steel columns are in use: (1) rolled shapes and (2) builtup sections. The rolled shapes are easily fabricated, accessible for painting, neat in appearance where they are not covered, and convenient in making connections. A disadvantage is the probability that thick sections are of lower strength material than thin sections because of the difficulty of adequately rolling the thick material. For the effect of thickness of material on yield point, see Ref. 16, p. 1377.

### *General Principles in Design*

The design of steel columns is always a cut-and-try method, as no law governs the relation between area and radius of gyration of the section. A column of given area is selected, and the amount of load that it will carry is computed by the proper formula. If the allowable load so computed is less than that to be carried, a larger column is selected and the load for it is computed, the process being repeated until a proper section is found.

**Table 9** Basic Stresses for Clear Material<sup>a</sup>

Species	Extreme Fiber in Bending or Tension Parallel to Grain	Maximum Horizontal Shear	Compression Perpendicular to Grain	Compression Parallel to Grain, $L/d = 11$ or Less	Modulus of Elasticity in Bending
<i>Softwoods</i>					
Bald cypress (Southern cypress)	1900	150	300	1450	1,200,000
Cedars					
Red cedar, Western	1300	120	200	950	1,000,000
White cedar, Atlantic (Southern white cedar) and northern	1100	100	180	750	800,000
White cedar, Port Orford	1600	130	250	1200	1,500,000
Yellow cedar, Alaska (Alaska cedar)	1600	130	250	1050	1,200,000
Douglas fir, coast region	2200	130	320	1450	1,600,000
Douglas fir, coast region, close grained	2350	130	340	1550	1,600,000
Douglas fir, Rocky Mountain region	1600	120	280	1050	1,200,000
Douglas fir, dense, all regions	2550	150	380	1700	1,600,000
Fir, California red, grand, noble, and White	1600	100	300	950	1,100,000
Fir, balsam	1300	100	150	950	1,000,000
Hemlock, Eastern	1600	100	300	950	1,100,000
Hemlock, Western (West Coast hemlock)	1900	110	300	1200	1,400,000
Larch, Western	2200	130	320	1450	1,500,000
Pine, Eastern white (Northern white), ponderosa, sugar, and Western white (Idaho white)	1300	120	250	1000	1,000,000
Pine, jack	1600	120	220	1050	1,100,000
Pine, lodgepole	1300	90	220	950	1,000,000
Pine, red (Norway pine)	1600	120	220	1050	1,200,000
Pine, southern yellow	2200	160	320	1450	1,600,000
Pine, southern yellow, dense	2550	190	380	1700	1,600,000
Redwood	1750	100	250	1350	1,200,000
Redwood, close grained	1900	100	270	1450	1,200,000
Spruce, Engelmann	1100	100	180	800	800,000
Spruce, red, white, and Sitka	1600	120	250	1050	1,200,000
Tamarack	1750	140	300	1350	1,300,000
<i>Hardwoods</i>					
Ash, black	1450	130	300	850	1,100,000
Ash, commercial white	2050	185	500	1450	1,500,000
Beech, American	2200	185	500	1600	1,600,000
Birch, sweet and yellow	2200	185	500	1600	1,600,000
Cottonwood, Eastern	1100	90	150	800	1,000,000
Elm, American and slippery (white or soft elm)	1600	150	250	1050	1,200,000
Elm, rock	2200	185	500	1600	1,300,000
Gums, blackgum, sweetgum (red or sap gum)	1600	150	300	1050	1,200,000
Hickory, true and pecan	2800	205	600	2000	1,800,000
Maple, black and sugar (hard maple)	2200	185	500	1600	1,600,000
Oak, commercial red and white	2050	185	500	1350	1,500,000
Tupelo	1600	150	300	1050	1,200,000
Yellow poplar	1300	120	220	950	1,100,000

<sup>a</sup>These stresses are applicable with certain adjustments to material of any degree of seasoning.

(For use in determining working stresses according to the grade of timber and other applicable factors. All values are in pounds per square inch. U.S. Forest Products Laboratory.)

**Table 10** Values of *K* for Columns of Intermediate Length

Species	ASTM Standards, 1937, D245–37					
	Continuously Dry		Occasionally Wet		Usually Wet	
	Select	Common	Select	Common	Select	Common
Cedar, western red	24.2	27.1	24.2	27.1	25.1	28.1
Cedar, Port Orford	23.4	26.2	24.6	27.4	25.6	28.7
Douglas fir, coast region	23.7	27.3	24.9	28.6	27.0	31.1
Douglas fir, dense	22.6	25.3	23.8	26.5	25.8	28.8
Douglas fir, Rocky Mountain region	24.8	27.8	24.8	27.8	26.5	29.7
Hemlock, west coast	25.3	28.3	25.3	28.3	26.8	30.0
Larch, western	22.0	24.6	23.1	25.8	25.8	28.8
Oak, red and white	24.8	27.8	26.1	29.3	27.7	31.1
Pine, southern	—	27.3	—	28.6	—	31.1
Pine, dense	22.6	25.3	23.8	26.5	25.8	28.8
Redwood	22.2	24.8	23.4	26.1	25.6	28.6
Spruce, red, white, Sitka	24.8	27.8	25.6	28.7	27.5	30.8

**Table 11** Strength of Columns of Intermediate Length, Expressed as a Percentage of Strength of Short Columns<sup>a</sup>

ASTM Standards, 1937, D245–37 Values for Expression  $1 - 1/3(1/Kd)^4$  in Eq. (94)

Ratio of Length to Least Dimension in Rectangular Timbers, *l/d*

***K* 12 13 14 15 16 17 18 19 20 21 22 23 24 25 26 27 28 29 30 31**

22	97	96	95	93	91	88	85	81	77	72	67	.....									
23	98	97	95	94	92	90	87	84	81	77	72	67	.....								
24	98	97	96	95	93	92	89	87	84	80	76	72	67	.....							
25	98	98	97	96	94	93	91	89	86	83	80	76	72	67	.....						
26	99	98	97	96	95	93	92	91	89	86	83	80	76	72	67	.....					
27	99	98	98	97	96	95	93	92	90	88	85	82	79	74	71	67	.....				
28	99	98	98	97	96	95	94	93	91	89	87	85	82	79	75	71	67	.....			
29	99	99	98	98	97	96	95	94	92	91	89	87	84	82	79	75	71	67	.....		
30	99	99	98	98	97	97	96	95	94	92	90	88	86	84	81	78	75	71	67	.....	
31	99	99	99	98	98	97	96	95	94	93	92	90	88	86	84	81	78	75	71	67	.....

<sup>a</sup>This table can also be used for columns not rectangular, the *l/d* being equivalent to  $0.289 l/k$ , where *k* is the least radius of gyration of the section.

A few general principles should guide in proportioning columns. The radius of gyration should be approximately the same in the two directions at right angles to each other; the slenderness ratio of the separate parts of the column should not be greater than that of the column as a whole; the different parts should be adequately connected in order that the column may function as a single unit; the material should be distributed as far as possible from the centerline in order to increase the radius of gyration.

**Steel Column Formulas**

A variety of steel column formulas are in use, differing mostly in the value of unit stress allowed with various values of *l/k*. See Ref. 17 for a summary of the formulas.

**Test on Steel Columns**

After the collapse of the Quebec Bridge in 1907 as a result of a column failure, the ASCE, the AREA, and the U.S. Bureau of Standards cooperated in tests of full-sized steel columns. The results of these tests are reported in Ref. 18, pp. 1583–1688. The tests showed that, for columns of the proportions commonly used, the effect of variation in the steel, kinks, initial stresses, and similar defects in the column was more important than the effect of length. They also showed that the thin metal gave definitely higher strength, per unit area, than the thicker metal of the same type of section.

**9 CYLINDERS, SPHERES, AND PLATES****9.1 Thin Cylinders and Spheres under Internal Pressure**

A cylinder is regarded as thin when the thickness of the wall is small compared with the mean diameter, or  $d/t > 20$ . There are only tensile membrane stresses in the wall developed by the internal pressure  $p$ ,

$$\frac{\sigma_1}{R_1} + \frac{\sigma_2}{R_2} = \frac{p}{t} \quad (107)$$

In the case of a cylinder where  $R_1$ , the curvature, is  $R$  and  $R_2$  is infinite, the hoop stress is

$$\sigma_1 = \sigma_h = \frac{pR}{t} \quad (108)$$

If the two equations are compared, it is seen that the resistance to rupture by circumferential stress [Eq. (108)] is one-half the resistance to rupture by longitudinal stress [Eq. (109)]. For this reason cylindrical boilers are single riveted in the circumferential seams and double or triple riveted in the longitudinal seams.

From the equations of equilibrium, the longitudinal stress is

$$\sigma_2 = \sigma_L = \frac{pR}{2t} \quad (109)$$

For a sphere, using Eq. (107),  $R_1 = R_2 = R$  and  $\sigma_1 = \sigma_2$ , making

$$\sigma_1 = \sigma_2 = \frac{pR}{2t} \quad (110)$$

In using the foregoing formulas to design cylindrical shells or piping, thickness  $t$  must be increased to compensate for rivet holes in the joints. Water pipes, particularly those of cast iron, require a high factor of safety, which results in increased thickness to provide security against shocks caused by water hammer or rough handling before they are laid. Equation (109) applies also to the stresses in the walls of a thin hollow sphere, hemisphere, or dome. When holes are cut, the tensile stresses must be found by the method used in riveted joints.

**Thin Cylinders under External Pressure**

Equations (108) and (109) apply equally well to cases of external pressure if  $P$  is given a negative sign, but the stresses so found are significant only if the pressure and dimensions are such that no buckling can occur.

**9.2 Thick Cylinders and Spheres****Cylinders**

When the thickness of the shell or wall is relatively large, as in guns, hydraulic machinery piping, and similar installations, the variation in stress from the inner surface to the outer surface

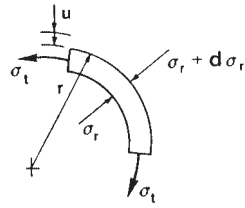


Figure 28 Cylindrical element.

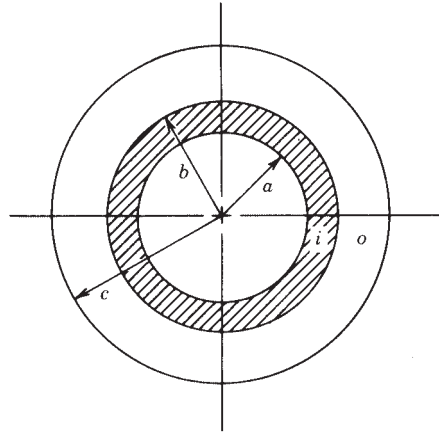


Figure 29 Cylinder press fit.

is relatively large, and the ordinary formulas for thin-wall cylinders are no longer applicable. In Fig. 28 the stresses, strains, and deflections are related<sup>1,19,20</sup> by

$$\sigma_t = \frac{E}{1-\nu^2}(\epsilon_r + \nu\epsilon_t) = \frac{E}{1-\nu^2} \left[ \frac{u}{r} + \nu \frac{\partial u}{\partial r} \right] \quad (111)$$

$$\sigma_r = \frac{E}{1-\nu^2}(\epsilon_t + \nu\epsilon_r) = \frac{E}{1-\nu^2} \left[ \frac{\partial u}{\partial r} + \nu \frac{u}{r} \right] \quad (112)$$

where  $E$  is the modulus and  $\nu$  is Poisson's ratio. In a cylinder (Fig. 29) that has internal and external pressures,  $p_i$  and  $p_o$ ; internal and external radii,  $a$  and  $b$ ;  $K = b/a$ ; the stresses are

$$\sigma_t = \frac{p_i}{K^2 - 1} \left( 1 - \frac{b^2}{r^2} \right) - \frac{p_o K^2}{K^2 - 1} \left( 1 + \frac{a^2}{r^2} \right) \quad (113)$$

$$\sigma_r = \frac{p_i}{K^2 - 1} \left( 1 - \frac{b^2}{r^2} \right) - \frac{p_o K^2}{K^2 - 1} \left( 1 + \frac{a^2}{r^2} \right) \quad (114)$$

if  $p_o = 0$ ,  $\sigma_t, \sigma_r$  are maximum at  $r = a$ ; if  $p_i = 0$ ,  $\sigma_t$  is maximum at  $r = a$  and  $\sigma_r$  is maximum at  $r = b$ .

In shrinkage fits (Fig. 29), a hollow cylinder is pressed over a cylinder with a radial interference  $\delta$  at  $r = b$ .  $p_f$ , the pressure between the cylinders, can be found from

$$\delta = \frac{b p_f}{E_o} \left( \frac{c^2 + b^2}{c^2 - b^2} + \nu_o \right) + \frac{b p_f}{E_i} \left( \frac{a^2 + b^2}{b^2 - a^2} + \nu_i \right) \quad (115)$$

The radial deflection can be found at  $a$ , which shrinks, and  $c$ , which expands, by knowing  $\sigma_r$  is zero and using Eqs. (111) and (112):

$$u_a = \frac{\sigma_t}{E_i} a \quad u_c = \frac{\sigma_t}{E_o} c \quad (116)$$

**Spheres**

The stress, strain, and deflections<sup>20,21</sup> are related by

$$\sigma_t = \frac{E}{1 - \nu - 2\nu^2} [\epsilon + \nu \epsilon_r] = \frac{E}{1 - \nu - 2\nu^2} \left[ \frac{u}{r} + \nu \frac{\partial u}{\partial r} \right] \quad (117)$$

$$\sigma_r = \frac{E}{1 - \nu - 2\nu^2} [2\nu \epsilon_t + (1 - \nu) \epsilon_r] = \frac{E}{1 - \nu - 2\nu^2} \left[ 2\nu \frac{u}{r} + (1 - \nu) \frac{\partial u}{\partial r} \right] \quad (118)$$

The stresses for a thick-wall sphere with internal and external pressures  $p_i$  and  $p_o$  and  $K = b/a$  are

$$\sigma_t = \frac{p_i(1 + b^3/2r^3)}{K^3 - 1} - \frac{p_o K^3(1 - a^3/r^3)}{K^3 - 1} \quad (119)$$

$$\sigma_r = \frac{p_i(1 + b^3/r^3)}{K^3 - 1} - \frac{p_o K^3(1 - a^3/r^3)}{K^3 - 1} \quad (120)$$

If  $p_i = 0$ ,  $\sigma_r = 0$  at  $r = a$ , then

$$u_a = (1 - \nu) \frac{\sigma_t}{E} a \quad (121)$$

Conversely, if  $p_o = 0$ ,  $\sigma_r = 0$  at  $r = b$ , then

$$u_b = (1 - \nu) \frac{\sigma_t}{E} b \quad (122)$$

**9.3 Plates**

The formulas that apply for plates are based on the assumptions that the plate is flat, of uniform thickness, and of homogeneous isotropic material, thickness is not greater than one-fourth the least transverse dimension, maximum deflection is not more than one-half the thickness, all forces are normal to the plane of the plate, and the plate is nowhere stressed beyond the elastic limit. In Table 12 are formulas for deflection and stress for various shapes, forms of load, and edge conditions. For further information see Refs. 14 and 22.

**9.4 Trunnion**

A solid shaft (Fig. 30) on a round or rectangular plate loaded with a bending moment is called a trunnion. The loading generally is developed from a bearing mounted on the solid shaft. For a round, simply supported plate

$$\sigma_r = \frac{\beta M}{at^2} \quad (123)$$

$$\theta = \frac{\gamma M}{Et^3} \quad (113)$$

$$\left. \begin{aligned} \beta &= 10^{(0.7634 - 1.252x)} \\ \log \gamma &= 0.248 - \pi x^{1.5} \end{aligned} \right\} 0 < x = \frac{b}{a} < 1 \quad (124)$$

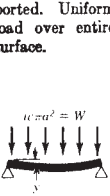

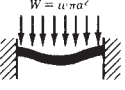
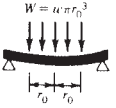
For the fixed-end plate

$$\left. \begin{aligned} \beta &= 10^{(1 - 1.959x)} \\ \log \gamma &= 0.179 - 3.75x^{1.5} \end{aligned} \right\} 0 < x = \frac{b}{a} < 1 \quad (125)$$

The equations for  $\beta, \gamma$  are derived from curve fitting of data (see, for example, Refs. 2, 4th ed., and 23).

Table 12 Formulas for Flat Plates<sup>a</sup>

*Notation:*  $W$  = total applied load, lb;  $w$  = unit applied load, psi;  $t$  = thickness of plate, in.;  $\sigma$  = stress at surface of plate, psi;  $y$  = vertical deflection of plate from original position, in.;  $E$  = modulus of elasticity;  $m$  = reciprocal of  $\nu$ , Poisson's ratio.  $q$  denotes any given point on the surface of plate;  $r$  denotes the distance of  $q$  from the center of a circular plate. Other dimensions and corresponding symbols are indicated on figures. Positive sign for  $\sigma$  indicates tension at upper surface and equal compression at lower surface; negative sign indicates reverse condition. Positive sign for  $y$  indicates upward deflection, negative sign downward deflection. Subscripts  $r, t, a,$  and  $b$  used with  $\sigma$  denote, respectively, radial direction, tangential direction, direction of dimension  $a$ , and direction of dimension  $b$ . All dimensions are in inches. All logarithms are to the base  $e$  ( $\log_e x = 2.3026 \log_{10} x$ ).

TYPE OF LOAD AND SUPPORT	FORMULAS FOR STRESS AND DEFLECTION
<b>CIRCULAR FLAT PLATES</b>	
<p>Outer edges supported. Uniform load over entire surface.</p> 	 <p>At center:  <math>\max \sigma_r = \sigma_t = -\frac{3W}{8\pi mt^2}(3m+1)</math>    <math>\max y = -\frac{3W(m-1)(5m+1)a^2}{16\pi Em^2t^3}</math></p> <p>At <math>q</math>:  <math>\sigma_r = -\frac{3W}{8\pi mt^2} \left[ (3m+1) \left( 1 - \frac{r^2}{a^2} \right) \right]</math>    <math>\sigma_t = -\frac{3W}{8\pi mt^2} \left[ (3m+1) - (m+3) \frac{r^2}{a^2} \right]</math>  <math>y = -\frac{3W(m^2-1)}{8\pi Em^2t^3} \left[ \frac{(5m+1)a^2}{2(m+1)} + \frac{r^4}{2a^2} - \frac{(3m+1)r^2}{m+1} \right]</math></p>
<p>Outer edges fixed. Uniform load over entire surface.</p> 	<p>At center:  <math>\sigma_r = \sigma_t = -\frac{3W(m+1)}{8\pi mt^2}</math>    <math>\max y = -\frac{3W(m^2-1)a^2}{16\pi Em^2t^3}</math></p> <p>At <math>q</math>:  <math>\sigma_r = -\frac{3W}{8\pi mt^2} \left[ (3m+1) \frac{r^2}{a^2} - (m+1) \right]</math>    <math>\sigma_t = \frac{3W}{8\pi mt^2} \left[ (m+3) \frac{r^2}{a^2} - (m+1) \right]</math>  <math>y = -\frac{3W(m^2-1)}{16\pi Em^2t^3} \left[ \frac{(a^2-r^2)^2}{a^2} \right]</math></p>
<p>Outer edges supported. Uniform load over concentric circular area of radius <math>r_0</math>.</p> 	<p>At <math>q, r &lt; r_0</math>:  <math>\sigma_r = -\frac{3W}{2\pi mt^2} \left[ m + (m+1) \log \frac{a}{r_0} - (m-1) \frac{r_0^2}{4a^2} - (3m+1) \frac{r^2}{4r_0^2} \right]</math>  <math>\sigma_t = -\frac{3W}{2\pi mt^2} \left[ m + (m+1) \log \frac{a}{r_0} - (m-1) \frac{r_0^2}{4a^2} - (m+3) \frac{r^2}{4r_0^2} \right]</math>  <math>y = -\frac{3W(m^2-1)}{16\pi Em^2t^3} \left[ 4a^2 - 5r_0^2 + \frac{r^4}{r_0^2} - (8r^2 + 4r_0^2) \log \frac{a}{r_0} - \frac{2(m-1)r_0^2(a^2-r^2)}{(m+1)a^2} + \frac{8m(a^2-r^2)}{m+1} \right]</math></p> <p>At <math>q, r &gt; r_0</math>:  <math>\sigma_r = -\frac{3W}{2\pi mt^2} \left[ (m+1) \log \frac{a}{r} - (m-1) \frac{r_0^2}{4a^2} + (m-1) \frac{r_0^2}{4r^2} \right]</math>  <math>\sigma_t = -\frac{3W}{2\pi mt^2} \left[ (m-1) + (m+1) \log \frac{a}{r} - (m-1) \frac{r_0^2}{4a^2} - (m-1) \frac{r_0^2}{4r^2} \right]</math>  <math>y = -\frac{3W(m^2-1)}{16\pi Em^2t^3} \left[ \frac{(12m+4)(a^2-r^2)}{m+1} - \frac{2(m-1)r_0^2(a^2-r^2)}{(m+1)a^2} - (8r^2 + 4r_0^2) \log \frac{a}{r} \right]</math></p>
	<p>At center:  <math>\max \sigma_r = \sigma_t = -\frac{3W}{2\pi mt^2} \left[ m + (m+1) \log \frac{a}{r_0} - (m-1) \frac{r_0^2}{4a^2} \right]</math>  <math>\max y = -\frac{3W(m^2-1)}{16\pi Em^2t^3} \left[ \frac{(12m+4)a^2}{m+1} - 4r_0^2 \log \frac{a}{r_0} - \frac{(7m+3)r_0^2}{m+1} \right]</math></p>

(continued)



Table 12 (Continued)


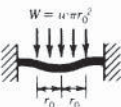
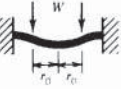
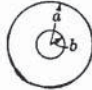

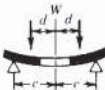
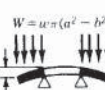
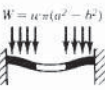
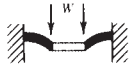

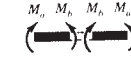
TYPE OF LOAD AND SUPPORT	FORMULAS FOR STRESS AND DEFLECTION
<p>Outer edges supported. Uniform load on concentric circular ring of radius <math>r_0</math>.</p> 	<p style="text-align: center;">CIRCULAR FLAT PLATES</p> <p>At <math>q, r &lt; r_0</math>:</p> $\max \sigma_r = \sigma_t = -\frac{3W}{2\pi mt^2} \left[ \frac{1}{2} (m-1) + (m+1) \log \frac{a}{r_0} - (m-1) \frac{r_0^2}{2a^2} \right]$ $y = -\frac{3W(m^2-1)}{2\pi E m^2 t^3} \left[ \frac{(3m+1)(a^2-r^2)}{2(m+1)} - (r^2+r_0^2) \log \frac{a}{r_0} + (r^2-r_0^2) - \frac{(m-1)r_0^2(a^2-r^2)}{2(m+1)a^2} \right]$ <p>At <math>q, r &gt; r_0</math>:</p> $\sigma_r = -\frac{3W}{2\pi mt^2} \left[ (m+1) \log \frac{a}{r} + (m-1) \frac{r_0^2}{2r^2} - (m-1) \frac{r_0^2}{2a^2} \right]$ $\sigma_t = -\frac{3W}{2\pi mt^2} \left[ (m-1) + (m+1) \log \frac{a}{r} - (m-1) \frac{r_0^2}{2r^2} - (m-1) \frac{r_0^2}{2a^2} \right]$ $y = -\frac{3W(m^2-1)}{2\pi E m^2 t^3} \left[ \frac{(3m+1)(a^2-r^2)}{2(m+1)} - (r^2+r_0^2) \log \frac{a}{r} - \frac{(m-1)r_0^2(a^2-r^2)}{2(m+1)a^2} \right]$
<p>Outer edges fixed. Uniform load over concentric circular area of radius <math>r_0</math>.</p> 	<p>At <math>q, r &lt; r_0</math>:</p> $\sigma_r = -\frac{3W}{2\pi mt^2} \left[ (m+1) \log \frac{a}{r_0} + (m+1) \frac{r_0^2}{4a^2} - (3m+1) \frac{r^2}{4r_0^2} \right]$ $\sigma_t = -\frac{3W}{2\pi mt^2} \left[ (m+1) \log \frac{a}{r_0} + (m+1) \frac{r_0^2}{4a^2} - (m+3) \frac{r^2}{4r_0^2} \right]$ $y = -\frac{3W(m^2-1)}{16\pi E m^2 t^3} \left[ 4a^2 - (8r^2 + 4r_0^2) \log \frac{a}{r_0} - \frac{2r^2 r_0^2}{a^2} + \frac{r^4}{r_0^2} - 3r_0^2 \right]$ <p>At <math>q, r &gt; r_0</math>:</p> $\sigma_r = -\frac{3W}{2\pi mt^2} \left[ (m+1) \log \frac{a}{r} + (m+1) \frac{r_0^2}{4a^2} + (m-1) \frac{r_0^2}{4r^2} - m \right]$ $\sigma_t = -\frac{3W}{2\pi mt^2} \left[ (m+1) \log \frac{a}{r} + (m+1) \frac{r_0^2}{4a^2} - (m-1) \frac{r_0^2}{4r^2} - 1 \right]$ $y = -\frac{3W(m^2-1)}{16\pi E m^2 t^3} \left[ 4a^2 - (8r^2 + 4r_0^2) \log \frac{a}{r} - \frac{2r^2 r_0^2}{a^2} - 4r^2 + 2r_0^2 \right]$ <p>At center:</p> $\sigma_r = \sigma_t = -\frac{3W}{2\pi mt^2} \left[ (m+1) \log \frac{a}{r_0} + (m+1) \frac{r_0^2}{4a^2} \right] = \max \sigma_r \text{ when } r_0 < 0.588a$ $\max y = -\frac{3W(m^2-1)}{16\pi E m^2 t^3} \left[ 4a^2 - 4r_0^2 \log \frac{a}{r_0} - 3r_0^2 \right]$
<p>Outer edges fixed. Uniform load on concentric circular ring of radius <math>r_0</math>.</p> 	<p>At <math>q, r &lt; r_0</math>:</p> $\sigma_r = \sigma_t = -\frac{3W}{4\pi mt^2} \left[ (m+1) \left( 2 \log \frac{a}{r_0} + \frac{r_0^2}{a^2} - 1 \right) \right] = \max \sigma \text{ when } r < 0.31a$ $y = -\frac{3W(m^2-1)}{2\pi E m^2 t^3} \left[ \frac{1}{2} \left( 1 + \frac{r_0^2}{a^2} \right) (a^2 - r^2) - (r^2 + r_0^2) \log \frac{a}{r_0} + (r^2 - r_0^2) \right]$ <p>At <math>q, r &gt; r_0</math>:</p> $\sigma_r = -\frac{3W}{4\pi mt^2} \left[ (m+1) \left( 2 \log \frac{a}{r} + \frac{r_0^2}{a^2} \right) + (m-1) \frac{r_0^2}{r^2} - 2m \right]$ $\sigma_t = -\frac{3W}{4\pi mt^2} \left[ (m+1) \left( 2 \log \frac{a}{r} + \frac{r_0^2}{a^2} \right) - (m-1) \frac{r_0^2}{r^2} - 2 \right]$ $y = -\frac{3W(m^2-1)}{2\pi E m^2 t^3} \left[ \frac{1}{2} \left( 1 + \frac{r_0^2}{a^2} \right) (a^2 - r^2) - (r^2 + r_0^2) \log \frac{a}{r} \right]$ <p>At center:</p> $\max y = -\frac{3W(m^2-1)}{2\pi E m^2 t^3} \left[ \frac{1}{2} (a^2 - r_0^2) - r_0^2 \log \frac{a}{r_0} \right]$

Table 12 (Continued)

TYPE OF LOAD AND SUPPORT	FORMULAS FOR STRESS AND DEFLECTION
Outer edge supported. Uniform load over entire surface.	<p style="text-align: center;">CIRCULAR FLAT PLATES WITH CONCENTRIC CIRCULAR HOLE</p>  <p>At inner edge:</p> $\max \sigma = \sigma_t = -\frac{3w}{4\pi t^2(a^2 - b^2)} \left[ a^4(3m+1) + b^4(m-1) - 4ma^2b^2 - 4(m+1)a^2b^2 \log \frac{a}{b} \right]$ $\max y = -\frac{3w(m^2 - 1)}{2m^2Et^3} \left[ \frac{a^4(5m+1)}{8(m+1)} + \frac{b^4(7m+3)}{8(m+1)} - \frac{a^2b^2(3m+1)}{2(m+1)} + \frac{a^2b^2(3m+1)}{2(m-1)} \log \frac{a}{b} - \frac{2a^2b^4(m+1)}{(a^2 - b^2)(m-1)} \left( \log \frac{a}{b} \right)^2 \right]$
Outer edge supported. Uniform load along inner edge.	 <p>At inner edge:</p> $\max \sigma = \sigma_t = -\frac{3W}{2\pi mt^2} \left[ \frac{2a^2(m+1)}{a^2 - b^2} \log \frac{a}{b} + (m-1) \right]$ $\max y = -\frac{3W(m^2 - 1)}{4\pi Em^2t^3} \left[ \frac{(a^2 - b^2)(3m+1)}{(m+1)} + \frac{4a^2b^2(m+1)}{(m-1)(a^2 - b^2)} \left( \log \frac{a}{b} \right)^2 \right]$
Supported along concentric circle near outer edge. Uniform load along concentric circle near inner edge.	<p>At inner edge:</p> $\max \sigma = \sigma_t = -\frac{3W}{2\pi mt^2} \left[ \frac{2a^2(m+1)}{a^2 - b^2} \log \frac{c}{d} + (m-1) \frac{c^2 - d^2}{a^2 - b^2} \right]$ 
Inner edge supported. Uniform load over entire surface.	<p>At inner edge:</p> $\max \sigma = \sigma_t = \frac{3w}{4\pi t^2(a^2 - b^2)} \left[ 4a^4(m+1) \log \frac{a}{b} + 4a^2b^2 + b^4(m-1) - a^4(m+3) \right]$ <p>At outer edge:</p> $\max y = \frac{3w(m-1)}{16Em^2t^3} \left[ a^4(7m+3) + b^4(5m+1) - a^2b^2(12m+4) - \frac{4a^2b^2(3m+1)(m+1)}{(m-1)} \log \frac{a}{b} + \frac{16a^4b^2(m+1)^2}{(a^2 - b^2)(m-1)} \left( \log \frac{a}{b} \right)^2 \right]$ 
Outer edge fixed and supported. Uniform load over entire surface.	<p>At outer edge:</p> $\max \sigma_r = \frac{3w}{4t^2} \left[ a^2 - 2b^2 + \frac{b^4(m-1) - 4b^4(m+1) \log \frac{a}{b} + a^2b^2(m+1)}{a^2(m-1) + b^2(m+1)} \right] = r \max \sigma$ <p>At inner edge:</p> $\max \sigma_t = -\frac{3w(m^2 - 1)}{4\pi t^2} \left[ \frac{a^4 - b^4 - 4a^2b^2 \log \frac{a}{b}}{a^2(m-1) + b^2(m+1)} \right]$ $\max y = -\frac{3w(m^2 - 1)}{16m^2Et^3} \left[ a^4 + 5b^4 - 6a^2b^2 + 8b^4 \log \frac{a}{b} + \frac{\left\{ [-8b^6(m+1) + 4a^2b^4(3m+1) + 4a^4b^2(m+1)] \log \frac{a}{b} - 16a^2b^4(m+1) \left( \log \frac{a}{b} \right)^2 \right\} + 4a^2b^4 - 2a^4b^2(m+1) + 2b^6(m-1)}{a^2(m-1) + b^2(m+1)} \right]$ 

(continued)

Table 12 (Continued)

TYPE OF LOAD AND SUPPORT	FORMULAS FOR STRESS AND DEFLECTION
<p>Outer edge fixed and supported. Uniform load along inner edge.</p> 	<p>CIRCULAR FLAT PLATES WITH CONCENTRIC CIRCULAR HOLE</p> <p>At outer edge:</p> $\max \sigma_r = \frac{3W}{2\pi t^2} \left[ 1 - \frac{2mb^2 - 2b^2(m+1) \log \frac{a}{b}}{a^2(m-1) + b^2(m+1)} \right] = \max \sigma \text{ when } \frac{a}{b} < 2.4$ <p>At inner edge:</p> $\max \sigma_t = \frac{3W}{2\pi m t^2} \left[ 1 + \frac{ma^2(m-1) - mb^2(m+1) - 2(m^2-1)a^2 \log \frac{a}{b}}{a^2(m-1) + b^2(m+1)} \right]$ <p style="text-align: center;"><math>= \max \sigma \text{ when } \frac{a}{b} &gt; 2.4</math></p> $\max y = -\frac{3W(m^2-1)}{4\pi m^2 E t^3} \times \left[ a^2 - b^2 + \frac{2mb^2(a^2 - b^2) - 8ma^2b^2 \log \frac{a}{b} + 4a^2b^2(m+1) \left( \log \frac{a}{b} \right)^2}{a^2(m-1) + b^2(m+1)} \right]$
<p>Outer edge fixed. Uniform moment along inner edge.</p> 	<p>At inner edge:</p> $\max \sigma_r = \frac{6M}{t^2}$ $\max y = \frac{6M(m^2-1)}{mEt^3} \left[ \frac{a^2b^2 - b^4 - 2a^2b^2 \log \frac{a}{b}}{a^2(m-1) + b^2(m+1)} \right]$ <p>At outer edge:</p> $\sigma_r = -\frac{6M}{t^2} \left[ \frac{2mb^2}{(m+1)b^2 + (m-1)a^2} \right]$
<p>Outer edge supported. Unequal uniform moments along edges.</p> 	<p>At <math>q</math>:</p> $\sigma_r = \frac{6}{t^2(a^2 - b^2)} \left[ a^2M_a - b^2M_b - \frac{a^2b^2}{r^2} (M_a - M_b) \right]$ $\sigma_t = \frac{6}{t^2(a^2 - b^2)} \left[ a^2M_a - b^2M_b + \frac{a^2b^2}{r^2} (M_a - M_b) \right]$ <p>From outer edge level:</p> $y = \frac{12(m^2-1)}{mEt^3(a^2 - b^2)} \left[ \frac{a^2 - r^2}{2} \left( \frac{a^2M_a - b^2M_b}{m+1} \right) + \log \frac{a}{r} \left( \frac{a^2b^2(M_a - M_b)}{m-1} \right) \right]$

<sup>a</sup> By permission from Ref. 22.

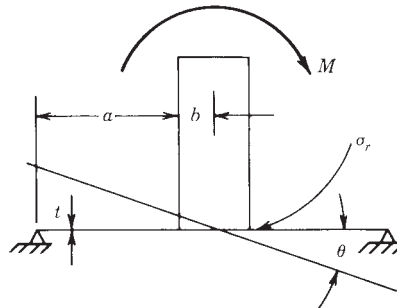


Figure 30 Simply supported trunnion.

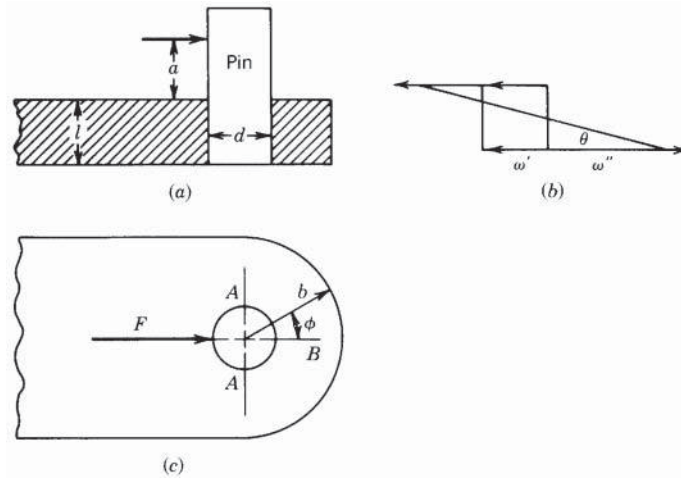


Figure 31 Socket action near an edge.

## 9.5 Socket Action

In Fig. 31a, summation of moments in the middle of the wall yields

$$2 \left[ \left( \frac{\omega''}{2} \frac{l}{2} \right) \left( \frac{2}{3} \frac{l}{2} \right) \right] = F \left( a + \frac{l}{2} \right) \quad (126)$$

$$\omega'' = \frac{6}{l^2} \left[ F \left( a + \frac{l}{2} \right) \right] \quad (127)$$

Summation of forces in the horizontal gives

$$\omega' = \frac{F}{l} \quad (128)$$

At B, the bearing pressure in Fig. 31c is

$$p_i = \frac{\omega' + \omega''}{d} \text{ psi} \quad (129)$$

In Eq. (113)  $p_o = 0$  and

$$\sigma_t = \frac{p_i}{R^2 - 1} \left[ 1 + \left( \frac{b}{d/2} \right)^2 \right]$$

At A in Fig. 31c

$$\sigma = \frac{\phi 8F}{\pi^2 b l}$$

where  $2b/d = 2, 4$  and  $\phi = 4.3, 4.4$ ;

$$F = (\omega' + \omega'')l$$

If a pin is pressed into the frame hole,  $\sigma_t$  created by  $p_f$  [Eq. (115)] must be added. Furthermore, if the pin and frame are different metals, additional  $\sigma_t$  will be created by temperature changes that vary  $p_f$ .

The stress in the pin can be found from the maximum moment developed by  $\omega'$  and  $\omega''$  and then calculating the bending stress.

## 10 CONTACT STRESSES

The stresses caused by the pressure between elastic bodies (Table 13) are of importance in connection with the design or investigation of ball and roller bearings, trunnions, expansion rollers, track stresses, gear teeth, etc.

### 10.1 Contact Stress Theory

H. Hertz<sup>24</sup> developed the mathematical theory for the surface stresses and the deformations produced by pressure between curved bodies, and the results of his analysis are supported by research. Formulas based on this theory give the maximum compressive stresses that occur at the center of the surfaces of contact but do not consider the maximum subsurface shear stresses or the maximum tensile stresses that occur at the boundary of the contact area. In Table 13 formulas are given for the elastic stress and deformation produced by bodies in contact. Numerous tests have been made to determine the bearing strength of balls and rollers, but there is difficulty in interpreting the results for lack of a satisfactory criterion of failure. One arbitrary criterion of failure is the amount of allowable plastic yielding. For further information on contact stresses see Refs. 2, 25, and 26.

## 11 ROTATING ELEMENTS

### 11.1 Shafts

The stress<sup>1</sup> in the center of a rotating shaft or solid cylinder is

$$\sigma_r = \sigma_h = \frac{3 - 2\nu}{8(1 - \nu)} \left( \frac{\gamma\omega^2}{g} \right) r_o^2 \quad (130)$$

$$\sigma_z = \frac{\nu\gamma\omega^2}{4g(1 - \nu)} r_o^2 \quad (131)$$

where  $\nu$  is Poisson's ratio,  $\omega$  is in rad/s,  $\gamma$  is the density in lb/in.<sup>3</sup>, and  $g$  is 386 in./s<sup>2</sup>. The limiting  $\omega$  can be found by using distortion energy; however, most shafts support loads and are limited by critical speeds from torsional or bending modes of vibration. Holzer's method and Dunkerley's equation are used.

### 11.2 Disks

A rotating disk<sup>1,10,20</sup> of inside radius  $a$  and outside radius  $b$  has  $\sigma_r = 0$  at  $a$  and  $b$ , while  $\sigma_t$  is

$$\sigma_{ta} = \frac{3 - \nu}{4g} \gamma\omega^2 \left( b^2 + \frac{1 - \nu}{3 + \nu} a^2 \right) \quad (132)$$

$$\sigma_{tb} = \frac{3 - \nu}{4g} \gamma\omega^2 \left( a^2 + \frac{1 - \nu}{3 + \nu} b^2 \right) \quad (133)$$

Substitution in Eq. (105) gives the outside and inside radial expansions.

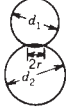
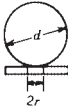
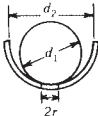
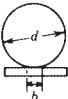

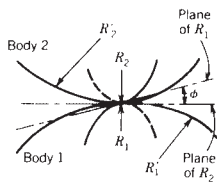
The solid disk of radius  $b$  has stresses at the center,

$$\sigma_t = \sigma_r = \frac{3 + \nu}{8g} \gamma\omega^2 b^2 \quad (134)$$

Substitution into the distortion energy [Eq. (22)] can give one the limiting speed.

**Table 13** Areas of Contact and Pressures with Two Surfaces in Contact<sup>a</sup>

Poisson's ratio = 0.3;  $P$  = load, lb;  $P_1$  = load per in. of length, lb;  $E$  = modulus of elasticity.

Character of Surfaces	Maximum Pressure, $s$ , at Center of Contact, psi	Radius, $r$ , or Width, $b$ , of Contact Area, in.
<p>Two spheres</p> 	$s = 0.616 \sqrt[3]{PE^2 \left(\frac{d_1 + d_2}{d_1 d_2}\right)^2}$	$r = 0.881 \sqrt[3]{\frac{P}{E} \left(\frac{d_1 d_2}{d_1 + d_2}\right)}$
<p>Sphere and plane</p> 	$s = 0.616 \sqrt[3]{\frac{PE^2}{d^2}}$	$r = 0.881 \sqrt[3]{\frac{Pd}{E}}$
<p>Sphere and hollow sphere</p> 	$s = 0.616 \sqrt[3]{PE^2 \left(\frac{d_2 - d_1}{d_1 d_2}\right)^2}$	$r = 0.881 \sqrt[3]{\frac{P}{E} \left(\frac{d_1 d_2}{d_2 - d_1}\right)}$
<p>Cylinder and plane</p> 	$s = 0.591 \sqrt{\frac{P_1 E}{d}}$	$b = 2.15 \sqrt{\frac{P_1 d}{E}}$
<p>Two cylinders</p> 	$s = 0.591 \sqrt{P_1 E \left(\frac{d_1 + d_2}{d_1 d_2}\right)}$	$b = 2.15 \sqrt{\frac{P_1}{E} \left(\frac{d_1 d_2}{d_1 + d_2}\right)}$
<p>General case of two bodies in contact</p> 	$s = \frac{1.5P}{\pi c d}$	$c = \alpha \sqrt[3]{\frac{P\delta}{K}}$ $d = \beta \sqrt[3]{\frac{P\delta}{K}}$ $\delta = \frac{4}{\frac{1}{R_1} + \frac{1}{R_2} + \frac{1}{R_1'} + \frac{1}{R_2'}}$ $K = \frac{8}{3} \frac{E_1 E_2}{E_2(1-\nu_1^2) + E_1(1-\nu_2^2)}$ $\theta = \arccos \frac{1}{4} \delta \sqrt{\left(\frac{1}{R_1} - \frac{1}{R_1'}\right)^2 + \left(\frac{1}{R_2} - \frac{1}{R_2'}\right)^2 + 2\left(\frac{1}{R_1} - \frac{1}{R_1'}\right)\left(\frac{1}{R_2} - \frac{1}{R_2'}\right) \cos 2\phi}$
$\theta$	0° 10° 20° 30° 40° 50° 60° 70° 80° 90°	
$\alpha$	∞ 6.612 3.778 2.731 2.136 1.754 1.486 1.284 1.128 1.00	
$\beta$	0 0.319 0.408 0.493 0.567 0.641 0.717 0.802 0.893 1.00	

11.3 Blades

Blades attached to a rotating shaft will experience a tensile force at the attachment to the shaft. These can be found from dynamics of machinery texts; however, the forces developed from a fluid driven by the blades develop more problems. The blades, if not in the plane, will develop additional forces and moments from the driving force plus vibration of the blades on the shaft.

12 SPRINGS

Tension springs with wires under tension: Wahl proposed a failure line and design line  $s_a - s_m$ , shear amplitude stress – shear mean stress. In Fig.32, where amplitude and mean stress are equal ( $R = 0$ ) or  $45^\circ$  and

$$S_{max} = s_{ms} + s_{as} = 2s_{as} = 2s_{ms} = s_{no} \tag{135}$$

The shear endurance stress  $s_{no}$  for a stress from zero to a maximum and Faires<sup>42</sup> derives a design line for springs whose wires are under torsion.

$$\frac{1}{N} = \frac{s_{ms} - s_{as}}{s_{ys}} + \frac{2s_{as}}{s_{no}} \tag{136}$$

Values have been developed so that

$$s_{ys} = Q/D_w^x \quad s_{no} = Q'/D_w^{x'} \tag{137}$$

where  $Q'$ ,  $Q$  = are constants from tests

$D_w$  = is wire diameter during test

$x'$ ,  $x$  = are constants found from tests

Note:  $s_{ys}$  and  $s_{no}$  will have different equations for the same material with the same  $D_w$ , but the pair will differ for other materials. The values are for room temperature. For cryogenic or high temperatures correlations have to be made from other reference data<sup>34-37</sup>

The temperature ranges for springs<sup>34</sup> are stated in Section 13.1 and thermal expansions<sup>35-38</sup>

The springs using Eq. (136) for solutions to wire diameters are discussed in the following sections.

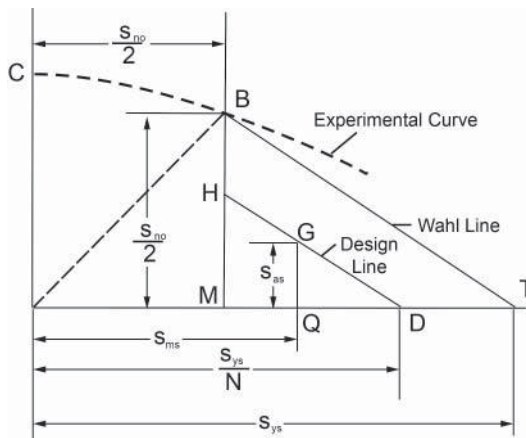


Figure 32 Variable stresses in strings.

### 12.1 Helical Compression Springs and Tension Springs

The torsional stress equations can be found in Refs. 41, 42, 43 and *Springs* magazine.

Bottomed compression springs must be checked for solid stress and for  $D_w/2$  radial clearance on the hole and any guide wire. These springs can buckle, bend and have lateral deflections.

Tension springs must not yield because of permanent set and require detailed calculations for end hooks.

### 12.2 Torsional Springs under Bending

These are springs in torsion which put the normally round or flat wire in bending. Equation (136) must be modified

$$s_{ms} = \frac{\sigma_{ms}}{\sqrt{3}} \quad s_{as} = \frac{\sigma_{as}}{\sqrt{3}} \quad (138)$$

where  $\sigma_{ms}$  and  $\sigma_{as}$  are spring bending stresses for mean and amplitude stresses. Equation (136) becomes with substitution of Eqs. (138).

$$\frac{1}{N} = \frac{\sigma_{ms} - \sigma_{as}}{\sqrt{3} s_{ys}} + \frac{2\sigma_{as}}{\sqrt{3} s_{no}} \quad (139)$$

The bending stresses can be found in Refs. 41, 42, 43 and *Springs Magazine*. Equation (137) can apply to flat wire of thickness (t). The coil can only be wound to a smaller diameter R as wound to a larger diameter could cause the coil to buckle<sup>17,20</sup> or expand binding into a hole.

### 12.3 Bending Springs under Bending

The single or multileaf spring equation with revision of Eq. (139)

$$\frac{1}{N} = \frac{\sigma_{ms} - \sigma_{as}}{\sigma_y} + \frac{2\sigma_{as}}{s_e} \quad (140)$$

where  $s_e$  is reverse bending endurance strength.

Equation (140) is a form of a Soderberg fatigue curve Eq. (27) with  $s_e = \sqrt{3} s_{no}$  the reverse bending developed from zero to maximum loads and Eq. (139) is the Wahl fatigue curve with  $\sqrt{3} s_{no}$  as the endurance in fatigue. They would match if  $s_e = \sqrt{3} s_{no}$  and  $\sigma_{as}$  in the first term of Eq. (140) was zero.

The bending spring under 0 to max load matches Eq. (139)

However, try a cantilever leaf spring flexing  $\pm\delta$  deflection. Use both Eqs. (140) and (27) using the same material and compare solutions.

In all springs one needs to know envelope availability, number of load cycles, temperature range, limitations of materials, and design load deflection or rotation curve. Again, Refs. (41, 42, 43) and *Springs* magazine can be used.

## 13 DESIGN SOLUTION SOURCES AND GUIDELINES

Designs are composed of simple elements, as discussed here. These elements are subjected to temperature extremes, vibrations, and environmental effects that cause them to creep, buckle, yield, and corrode. Finding solutions to model these cases, as elements, can be difficult and when found the solutions are complex to follow, let alone to calculate. See Refs. 2, 23, and 27–33 for the known solutions. Always cross check with another reference. The handbooks of Roark and Young<sup>2</sup> and Blevins<sup>26</sup> have been computerized using a TK solver and are distributed by UTS software. These closed-form solutions would ease some of the more complicated calculations and checks of finite-element solutions using a computer.



### 13.1 Computers

Most computer setups use linear elastic solutions where the analyst supplies mechanical properties of materials such as yield and ultimate strengths and cross-sectional properties like area and area moments of inertia. When solving more complex problems, some concerns to keep in mind:

#### *Questions to Be Asked*

1. Will I know if this model buckles?
2. Can one use a nonlinear stress–strain curve?
3. Is there any provision for creep and buckling?
4. How large and complex a structure can be solved? Look at a solved problem and relate it to future problems.

#### *Things to Watch and Note*

1. Press fit joints, flanges, pins, bolts, welds and bonds, and any connection interface present in modeling problems. The stress analysis of a single loaded weld is not a simple task. The stress solution for a trunnion with more complexity, such as seal grooves in the plate, requires many small finite elements to converge to a closed-form solution [Eq. (112)].
2. Vibration solutions with connection interfaces can give frequency solutions with 50% error with many connections and still have 10–15% error with no connections. The computer solution appears to be always on the high side.
3. Detailed fatigue stresses on elements can be derived out of the loads by printing out the force variation.
4. The materials have good operating range<sup>34</sup> and limitations for spring stress relaxation at higher temperatures or lower limits can be applicable to structural members.

Nickel alloys, Inconels, and similar materials	$-300^{\circ}\text{F} \leq T \leq 1020^{\circ}\text{F}$
300, 400, 17-4, 17-7 stainless or austenitic, martensite, and precipitation-hardening stainless steels	$-110^{\circ}\text{F} \leq T \leq 570^{\circ}\text{F}$
Spring steels	$-5^{\circ}\text{F} \leq T \leq 430^{\circ}\text{F}$
Patented cold-drawn carbon steels	$-110^{\circ}\text{F} \leq T \leq 300^{\circ}\text{F}$
Copper beryllium	$-330^{\circ}\text{F} \leq T \leq 260^{\circ}\text{F}$
Titanium alloys	
Bronzes	$-40^{\circ}\text{F} \leq T \leq 175^{\circ}\text{F}$
Aluminum	$-300^{\circ}\text{F} \leq T \leq 400^{\circ}\text{F}$
Magnesium	$-300^{\circ}\text{F} \leq T \leq 350^{\circ}\text{F}$

The high temperatures are for the onset of creep and stress relaxation and lower mechanical properties with higher temperature. The low temperatures show higher mechanical properties but are shock sensitive. Always examine for the mechanical properties for the temperature range and thermal expansion.<sup>5,35–37</sup> The mechanical properties at room temperature have predictable distributions with ample sample sizes, but if the temperature is varied, similar published results are not readily available.

Rubber, plastics, and elastomers have glassy transition temperatures below which the material is puttylike and above which the material is rocklike and brittle. All material mechanical properties vary a great deal due to temperature. This makes computer solutions much more complex. Testing is the final reliable check.

## 13.2 Testing

Most designs must pass some sets of vibration, environmental, and screen testing before delivery to a customer. It is at this time that design flaws show up and frequencies, stresses, and so on are verified. Some preliminary testing might help:

1. Compare impact hammer frequency test of part of or an entire system to the computer and hand calculations. The physical testing includes the boundary values sometimes difficult to simulate on a computer.
2. Spot bond optical parts to dissimilar-metal structural frame, which must be hot and cold soak tested to see if the bonding fractures the optical parts. Computers cannot predict a failure of this type well.
3. Check test joints and seal surfaces with pressure-sensitive gaskets to see if the developed pressures are sufficient to maintain the design to proper requirements. Then use operational testing to check for thermal warping of these critical surfaces.
4. Pressurize or load braze, weld, or solder part to check the process and its calculations for the pressures and loads.
5. Rapid Prototyping.<sup>38</sup> This method could be used to check a photoelastic model by vibrating it or freezing stresses in the model from static loads. It also could define areas of high stress for a smaller grid finite-element modeling. Stress coating on a regular plastic model could also point out areas of high stress.

## REFERENCES

1. J. H. Faupel and F. E. Fisher, *Engineering Design*, 2nd ed., Wiley, New York, 1981.
2. R. J. Roark and W. C. Young, *Formulas for Stress and Strain*, 6th ed., McGraw-Hill, New York, 1989.
3. R. E. Peterson, *Stress Concentration Factors*, 2nd ed., Wiley, New York, 1974.
4. J. Marin, *Mechanical Properties of Materials and Design*, McGraw-Hill, New York, 1942.
5. *Metallic Materials for Aerospace Structures*, 2 vols., Mil HDBK 5F, Department of Defense, Washington, DC, 1990.
6. *Aluminum Standards and Data*, 3rd ed., Aluminum Association, New York, 1972.
7. *AISC Handbook*, American Institute of Steel Construction, New York, 1989.
8. F. B. Seely and J. O. Smith, *Resistance of Materials*, 4th ed., Wiley, New York, 1957.
9. A. P. Boresi, O. Sidebottom, F. B. Seely, and J. O. Smith, *Advanced Mechanics of Materials*, 3rd ed., Wiley, New York, 1978.
10. S. P. Timoshenko, *Strength of Materials*, 3rd ed., Vols. I and II, Krieger, Melbourne, FL, 1958.
11. (a) H. C. Mann, "Relation of Impact and Tension Testing of Steels," *Metal Prog.*, **27**(3), 36–41, March, 1935. (b) H. C. Mann, "Relation between Tension Static and Dynamic Tests," *Proc. ASTM*, **35**(II), 323–340, 1935. (c) H. C. Mann, "Fundamental Study of Design of Impact Test Specimens," *Proc. ASTM*, **37**(II), 102–118, 1937.
12. C. R. Young, *Bulletin 4*, School of Engineering Research, University of Toronto, 1923.
13. C. R. Bach and R. Baumann, *Elastizität und Festigkeit*, 9th ed., Springer, Berlin, 1924.
14. R. M. Rivello, *Theory Analysis of Flight Structures*, McGraw-Hill, New York, 1969.
15. B. G. Johnston (Ed.), *Structural Research Council, Stability Design Criteria for Metal Structures*, 3rd ed., Wiley, New York, 1976.
16. *Trans. Am. Soc. Civil Eng.*, xcvi, 1933.
17. S. P. Timoshenko and J. M. Gere, *Theory of Elastic Stability*, 2nd ed., McGraw-Hill, New York, 1961.
18. *Trans. Am. Soc. Civil Eng.*, lxxxiii, 1919–20.
19. R. C. Juvinall, *Stress, Strain and Strength*, McGraw-Hill, New York, 1967.

20. S. P. Timoshenko and J. N. Goodier, *Theory of Elastic Stability*, 3rd ed., McGraw-Hill, New York, 1970.
21. M. Hetényi, *Handbook of Experimental Stress Analysis*, Wiley, New York, 1950.
22. R. J. Roark, *Formulas for Stress and Strain*, 2nd ed., McGraw-Hill, New York, 1943.
23. W. Griffel, *Handbook of Formulas for Stress and Strain*, Frederick Ungar, New York, 1966.
24. H. Hertz, *Gesammelte Werke*, Vol. 1, Berth, Leipzig, 1895.
25. R. K. Allen, *Rolling Bearings*, Pitman, London, 1945.
26. A. Palmgren, *Ball and Roller Bearing Engineering*, SKF Industries, Philadelphia, PA, 1945.
27. R. D. Blevins, *Formulas for Natural Frequency and Mode Shapes*, Krieger, Melbourne, FL, 1993.
28. R. D. Blevins, *Flow-Induced Vibration*, 2nd ed., Krieger, Melbourne, FL, 1994.
29. W. Flügge (Ed.), *Handbook of Engineering Mechanics*, McGraw-Hill, New York, 1962.
30. A. W. Leissa, *Vibration of Plates NASA SP-160 (N70-18461)*, NTIS, Springfield, VA.
31. A. W. Leissa, *Vibration of Shells NASA SP-288 (N73-26924)*, NTIS, Springfield, VA.
32. A. Kleinlogel, *Rigid Frame Formulas*, 12th ed., Frederick Ungar, New York, 1958.
33. V. Leontovich, *Frames and Arches*, McGraw-Hill, New York, 1959.
34. M. O'Malley, "The Effect of Extreme Temperature on Spring Performance," *Springs*, May, 1986, p. 19.
35. *Aerospace Structural Metals Handbook*, 5 vols., CINDAS / USAF CRDA, Purdue University, West Lafayette, IN, 1993.
36. *Structural Alloys Handbook*, 3 vols., CINDAS, Purdue University, West Lafayette, IN, 1993.
37. *Thermophysical Properties of Matter*, Vol. 12, *Metallic Expansion*, 1995; Vol. 13, *Non-Metallic Thermoexpansion*, IFI / Phenium, New York, 1977.
38. S. Ashley, "Rapid Prototyping Is Coming of Age," *Mechan. Eng.*, 62–69, July, 1995.
39. W. D. Pilkey, *Petersons Stress Concentration Factors*, 2nd ed., Wiley, Hoboken, NJ, 1997.
40. Forest Products Society, *Wood Handbook*, 2010 ed., Madison Wisconsin.
41. A. W. Wahl, "Mechanical Springs" *ASME Handbook Engineering Tables*, edited by Jesse Huckert, McGraw-Hill, New York, 1956
42. V. M. Faires, *Design of Machine Elements*, 4th ed., MacMillan, New York, 1965
43. *Design Handbook Springs*, Associated Spring Corporation 1967
44. F. E. Fisher and J. R. Fisher, *Probability Applications in Mechanical Design*, Marcel Dekker Inc. 2000 Available through Taylor and Francis Group LLC ENGnet Base <http://www.taylorandfrancis.com>
45. E. B. Haugen, *Probabilistic Mechanical Design*, Wiley, Hoboken, New Jersey, 1980.

## BIBLIOGRAPHY

- J. O. Almen, and P. H. Black, *Residual Stresses and Fatigue in Metals*, McGraw-Hill, New York, 1963.
- M. Di Giovanni, *Flat and Corrugated Diaphragm Design Handbook*, Marcel Dekker, New York, 1982.
- W. R. Osgood, (Ed.), *Residual Stresses in Metals and Metal Construction*, Reinhold, New York, 1954.
- Proceedings of the Society for Experimental Stress Analysis.*
- Symposium on Internal Stresses in Metals and Alloys*, Institute of Metals, London, 1948.
- L. J. Vande Walle, *Residual Stress for Designers and Metallurgists*, 1980 American Society for Metals Conference, American Society for Metals, Metals Park, OH, 1981.

# CHAPTER 17

## FORCE MEASUREMENT

Patrick Collins  
Mecmesin Ltd.  
Slinfold, United Kingdom

<b>1 INTRODUCTION</b>	<b>623</b>	<b>9 FORCE BALANCE TRANSDUCERS</b>	<b>640</b>
<b>2 FORCE TRANSDUCERS</b>	<b>624</b>	<b>10 FORCE TRANSDUCER CHARACTERISTICS</b>	<b>641</b>
<b>3 UNIVERSAL TESTING MACHINES</b>	<b>627</b>	10.1 Capacity	641
3.1 The Strain Gauge Sensor	627	10.2 Output	641
3.2 Strain Gauge Circuit Compensation	630	10.3 Repeatability	642
<b>4 RESONANT ELEMENT TRANSDUCERS</b>	<b>631</b>	10.4 Creep	642
<b>5 SURFACE ACOUSTIC WAVE TRANSDUCERS</b>	<b>634</b>	10.5 Temperature Coefficient	642
<b>6 DYNAMOMETERS</b>	<b>636</b>	10.6 Accuracy	642
<b>7 OPTICAL FORCE TRANSDUCERS</b>	<b>637</b>	<b>11 CALIBRATION</b>	<b>642</b>
<b>8 MAGNETOELASTIC TRANSDUCERS</b>	<b>640</b>	11.1 Uncertainty	644
		11.2 Other Equipment	645
		11.3 Operator Inconsistency	646
		11.4 Conclusion	647
		<b>GLOSSARY</b>	<b>648</b>
		<b>REFERENCES</b>	<b>656</b>

### 1 INTRODUCTION

Force is one of the ubiquitous physical phenomena. From the strong nuclear forces holding subatomic particles together to the weak forces holding the Earth in orbit around the sun and the solar system around the galactic center, forces are an influence in everything we see and do.

Aristotle<sup>1</sup> is credited with an approach that considered the natural phenomena with a combination of observation and philosophical reasoning. He postulated that the relative proportion of Earth, the heaviest element, and Fire, the lightest element, determined the natural motion of a body. Earth tended toward the center of the universe, whereas Fire would like to rise upward away from the center. Terrestrial objects move upward or downward toward their natural place in accordance with their composition of the four elements. His observations were constrained by the technology available at the time. For example, a vacuum was thought to be impossible, but if it did theoretically exist, then motion in a vacuum would be infinitely fast. The ideal speed of an object moving with terrestrial motion (upward or downward) was directly proportional to its weight.

Given the inability to observe a system where friction played only a negligible part, it was thought that the natural state of things was to be at rest. Forced or unnatural motion required the

constant application of force to sustain the motion. Some philosophical thinking was applied to a situation such as the flight of a spear through the air. After an initial impetus, the constant force was thought to be provided by the air as the spear passed through it. The motion of heavenly bodies was considered to be different. The sun, moon, and stars were embedded in crystal spheres that rotated with an unchanging circular motion, with the planets embedded in spheres within spheres to account for their apparently erratic motion.

While we now think that the Aristotelian physics contains some shortcomings, but from a purely practical point of view, it has some resonance. Pushing a cart loaded with bags of rice to the marketplace requires the expenditure of a constant force to keep the cart moving.

In the seventeenth century, Galileo Galilei<sup>2</sup> experimented with cannon balls and inclined slopes to theorize that acceleration due to gravity did not depend on the weight of the object and that the force of friction was responsible for slowing down the motion that would otherwise remain constant.

With the publication of Sir Isaac Newton's *Principia Mathematica*<sup>3</sup> in 1687, a mathematical explanation of the laws of motion was proposed that would last for almost 300 years. Newton realized that the same force of gravity was responsible for items falling toward the Earth and the motion of the moon around the Earth. Newton provided the means to calculate and predict the motion of bodies both terrestrial and celestial based of the forces experienced between the objects. Newton's reasoning was so compelling that when inconsistencies in the orbit of the planet Mercury were observed that could not be fully explained by the Newtonian model, astrophysicists predicted the presence of an unobserved new planet that would account for the discrepancies. No such planet was found, but Albert Einstein<sup>4</sup> sensationally added a correction to his theory of general relativity that precisely accounted for the observed motion.

So, force is a measurement of the interaction between objects. It is a vector quantity with both magnitude and direction. If a body is at equilibrium, the sum of forces acting upon the body is zero. The derived Système International d'Unités (SI) unit of force is named in honor of the aforementioned Sir Isaac Newton with 1 N being the force required to accelerate a mass of 1 kg by 1 m/s/s.

In general, force is calculated using the following formula:

$$F = ma \quad (1)$$

where  $F$  is force in Newton,  $m$  is the mass of the object in kilogram, and  $a$  is its acceleration in meters per second per second.

Because it is not practical to accelerate a mass by  $1 \text{ m/s}^2$  to produce a standard force of 1 N, we tend to use a more readily available and predictable acceleration factor to produce a known force on a transducer, that is, the acceleration due to gravity. This modifies Eq. 2 to become

$$F = mg \quad (2)$$

Local gravity is relatively easy to determine and so when a known mass is applied in any geographical location, the force in Newton is easily determined also. Using such masses, force transducers can be calibrated so that wherever in the world they are used, they will report the correct force.

## 2 FORCE TRANSDUCERS

A transducer is a device that senses a physical parameter and reports it quantitatively as an output of a different type. In the case of a force transducer, the output is most commonly electrical, meaning a change in resistance, capacitance, or voltage, for example. These changes are usually quite small, so associated instrumentation is required to interpret the output quantity and convert it to a display for the operator or user to see.

**Table 1** Common Force Transducers along with Their Typical Uncertainties and Temperature Characteristics

Device Type	Typical Range of Rated Capacities	Typical Total Uncertainty (% fso)	Temperature Sensitivity and Operating Range (% fso per °C)
Strain gauge load cells			
Semiconductor gauges	1 N to 10 kN	0.2–1%	0.2–0.5% (–40°C to +80°C)
Thin-film gauges	0.1 N to 100 N	0.02–1%	0.02% (–40°C to +80°C)
Foil gauges	5 N to 50 MN	0.02–1%	0.0015% (–40°C to +80°C)
Piezoelectric crystal	1.5 mN to 120 MN	0.3–1%	0.02% (–190°C to +200°C)
Hydraulic	500 N to 5 MN	0.25–5%	0.02–0.1% (5–40°C)
Pneumatic	10 N to 500 kN	0.1–2%	0.02–0.1% (5–40°C)
LVDT, capacitive, tuning-fork, vibrating wire, optical	10 mN to 1 MN	0.02–2%	0.02–0.05% (–40°C to +80°C)
Magnetoelastic	2 kN to 50 MN	0.5–2%	0.03–0.05% (–40°C to +80°C)
Gyroscopic	50–250 N	0.001%	0.0001% (–10°C to +40°C)
Force balance	0.25–20 N	1 part in 10 <sup>6</sup>	0.0001% (–10°C to +40°C)

Source: From Ref. 5.

Force transducers take many forms, with some of the more common forms listed in Table 1, along with their approximate ranges and accuracies.

The majority of force measurement devices used in industry fall into the first category, with the others satisfying more specialist applications. This chapter will accordingly emphasize the strain gauge load cell devices, with briefer descriptions of the other transducer types.

In the seventeenth century, British physicist Hooke<sup>6</sup> stated “Ut tensio, sic vis,” roughly translated: “as the extension, so the force,” implying that there is a linear relationship between extension and applied force, and although originally derived for springs, can be applied to most elastic materials. Put another way, when a material is placed under tension, applied force (the stress) is proportional to the amount by which the material deforms (the strain), provided that the elastic limit is not exceeded. This observation is defined by the following equation:

$$F = -kx \quad (3)$$

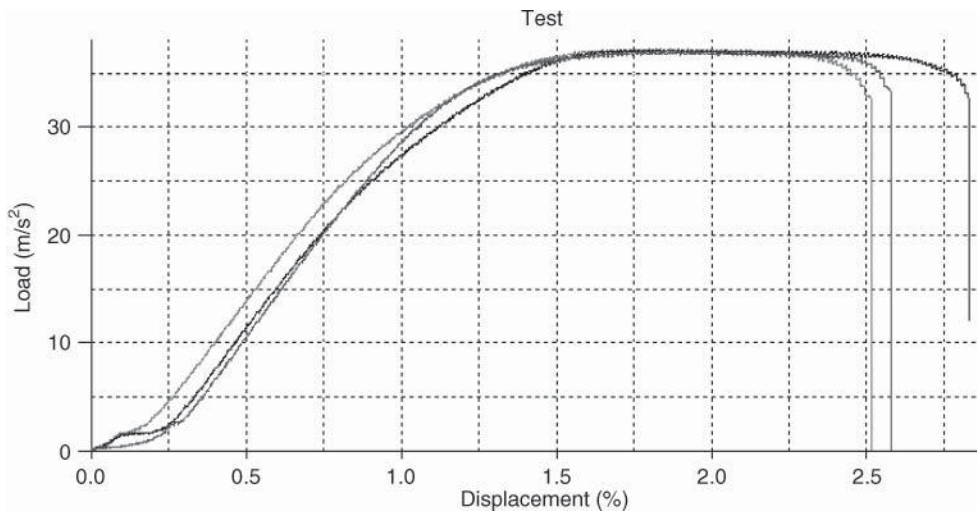
where  $F$  is the restorative force,  $x$  is the displacement, and  $k$  is a force (or spring) constant. Put another way

$$E = \frac{\text{strain}}{\text{stress}} \quad (4)$$

where stress is the force applied to the specimen, and strain is the relative elongation of the specimen from its original length.

Here,  $E$  is also known as Young’s Modulus,<sup>7</sup> represented as the gradient of the stress–strain curve within the initial linear region. This is an extremely useful value to determine because it gives a clear indication of how much the material will deform under applied tensile loading. A bungee rope, for instance, must have a low enough Young’s modulus to guarantee the jumper will achieve a long, thrilling jump without the rope jarring when the slack is taken up, but a high enough Young’s modulus to ensure the rope is sufficiently stiff to bring the jumper springing back skywards prior to hitting the ground.

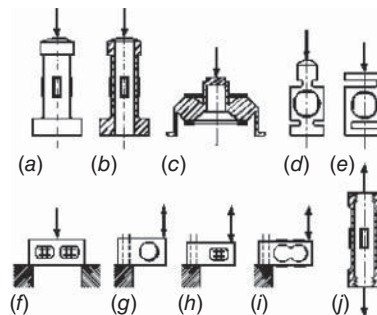
A common stress–strain curve is shown in Fig. 1. The trace shown in Fig. 1 is typical of an aluminum metal plate specimen and shows the linear region, where Hooke’s law is obeyed, followed by a plastic deformation phase indicated by a steady decline in gradient toward the ultimate tensile strength (UTS) point, and then specimen break.



**Figure 1** Typical stress–strain curve for aluminum plate metal. (Courtesy of Mecmesin Ltd.)

Most force transducers consist of a sensing element and an elastic element. The sensing element is the strain gauge, vibrating element or optical sensor, and so on. The elastic element is the bulk medium upon which the sensing element is placed and is designed to operate within the linear region of the stress–strain curve. This ensures that the load cell returns to its zero load position with minimal error.

It is called the elastic element because it is designed so that when a force is applied, it deforms such that the sensing element can report a measurement, and after the applied force is removed, the element returns to its original dimensions. They can be designed to allow measurement in tension and compression or in compression only. Static torque sensors are also constructed using the same principles, although the designs are more complex. Load cells come in many shapes and sizes, but materials tend to remain the same. Steel and aluminum are the most common and are used for their properties as well as their relative abundance. Choice of material depends largely upon the design criteria: Aluminum has better thermal stability, whereas stainless steel has better mechanical stability. Figure 2 shows some of the common forms.<sup>5</sup>



**Figure 2** Load cell types and their common approximate load ranges. (a) Compression on cylinder 50 kN to 50 MN. (b) Compression on cylinder (hollow) 10 kN to 50 MN. (c) Toroidal ring 1 kN to 5 MN. (d) Ring 1 kN to 1 MN. (e) S-beam (bending or shear) 200 N to 50 kN. (f) Double-ended beam (simplified) 500 N to 50 kN. (g) Shear beam 1–500 kN. (h) Double-bending beam 100–10 N. (i) Double-bending beam 100–10 N. (j) Tension cylinder 50 kN to 50 M.



### 3 UNIVERSAL TESTING MACHINES

Load cells are commonly used in materials and product testing applications. This type of testing requires a method of controlling the sometimes complicated test routines. Universal test machines often fulfill this purpose and are available from many manufacturers.

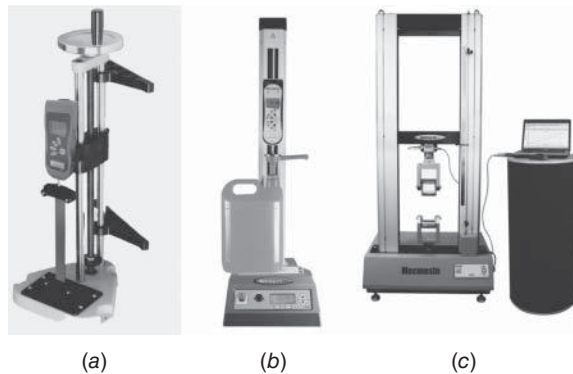
Universal testers provide a means to hold a sample and place it under a compressive or tensile load. They can be simple motorized machines, whereby the speed and direction are controlled using manual controls, hand-operated machines where the operator uses a wheel or pump control to increase the force on the sample, right up to high-end computer-controlled test stands that can run sophisticated multistage test programs. They are available with hydraulic actuation or electromechanical control using electric motors driving a ball screw arrangement, for a wide range of forces from 500 N up to 30 MN. They will perform complex calculations such as Young's modulus and create and print reports. When used in conjunction with other instrumentation, such as extensometers, even more sophistication is possible. With the ever growing library of international test methods, universal testers are required to provide more functionality and more calculations. Figure 3 shows just a few of the range of available universal test machines.

Portable force measurement is catered for by a plethora of handheld instrumentation, from simple gram gauges to advanced force gauges that allow data storage and transmission as well as peak and trough calculations. Some will allow simple control functions for operating some test stands so that no computer is necessary.

Force measurement in this form is used in all industries, from medical and pharmaceutical to food, automotive, and electronics sectors. Both the finished products and the raw materials they are made of are tested for either quality control or to determine basic material properties. Figure 4 shows some examples of force measurement applications in industry, including replacement joint testing, PCB component pull off testing, and food testing.

#### 3.1 The Strain Gauge Sensor

Although Lord Kelvin first reported on the relationship between strain on a metal and its electrical resistance in 1856,<sup>8</sup> it was not until 1936 that a practical implementation of a bonded strain gauge<sup>9</sup> was realized by the eccentric Edward E Simmons, Jr. The invention, which consisted of wires glued to the surface of the object whose stress or strain was to be measured, had an enormous impact on the engineering world and was of great importance during World War II.<sup>10</sup>

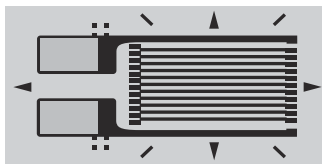


**Figure 3** (a) Manual, (b) motorized, and (c) computerized universal test machines. (Courtesy of Mecmesin Ltd.)





**Figure 4** Some applications of universal test machines and force measurement. (Courtesy of Mecmesin Ltd.)



**Figure 5** A typical strain gauge, complete with mounting guide marks.

In 1952, with the advent of etching technology for electrical components, the first strain gauges were developed using etched metal foil instead of wire.<sup>11</sup> The benefits of this technique are that the resistance of the strain gauge can be more accurately and repeatably achieved, and also a much finer pattern can be achieved, thus increasing the length of resistor in a smaller space allowing for smaller sensors. This revolutionized the strain gauge industry, and now most strain gauges are of the metal foil type (Fig. 5). They are manufactured by photoetching the resistors from a metal coating on a substrate. The substrate has a dual purpose, that of a backing for the strain gauge and as a resistive barrier between the gauge and the item whose strain we want to measure. The gauge on its substrate is adhesively bonded to the component so that strain on the component is transferred efficiently to the gauge. The bonding process is a challenging one given the tolerances that need to be achieved and this is a specialist task, which is highly valued.

As is well known,<sup>12</sup> electrical resistance per unit length,  $L$ , of a metal wire is inversely proportional to its cross-sectional area:

$$R = \rho L / A \quad (5)$$

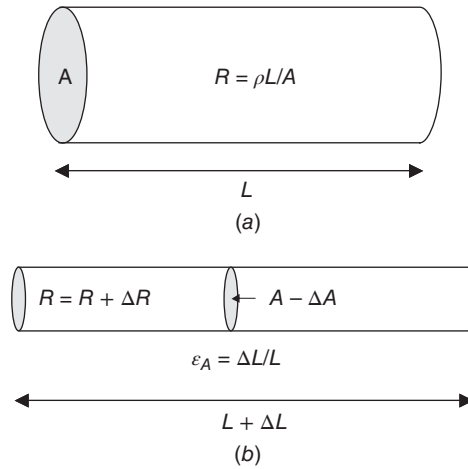
where  $R$  is the resistance,  $\rho$  is the resistivity of the material, and  $A$  is the cross-sectional area.

Figure 6 shows the most basic form of strain gauge, which is a wire of known length,  $L$ , and cross-sectional area,  $A$ . When an external force is applied to the wire, which causes strain,  $\epsilon$  (i.e., it is stretched or compressed), its cross section is also deformed and so a corresponding change in the wire's resistance,  $R$ , can be measured.

By differentiating Eq. (2) and dividing by  $R$ , we get

$$\frac{dR}{R} = \frac{d\rho}{\rho} + \frac{dL}{L} - \frac{dA}{A} \quad (6)$$

We define axial strain by  $\epsilon_a = dL/L$  and transverse strain by  $\epsilon_T = dr/r = -\nu\epsilon_a = -\nu(dL/L)$ ,<sup>13</sup> where  $\nu$  is the Poisson ratio (the ratio between axial and transverse strain) for the wire material.



**Figure 6** (a) Metal wire resistor and (b) metal wire resistor under strain.

The change of radius of the wire under strain is

$$dr = r \left( 1 - \nu \frac{dL}{L} \right) \quad (7)$$

And so the rate of change of the cross-sectional area is given by

$$\frac{dA}{A} = 1 - (1 + \varepsilon_T)^2 = 2\varepsilon_T + \varepsilon_T^2 \approx 2\varepsilon_T \quad (8)$$

And when this is substituted back into Eq. (2), and dividing by axial strain, we get

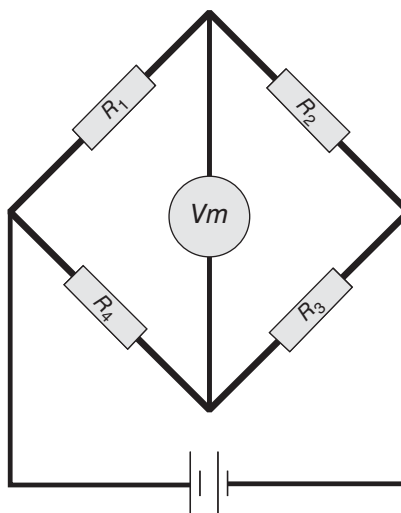
$$S = \frac{dR/R}{\varepsilon_A} = \frac{d\rho/\rho}{\varepsilon_A} + (1 + 2\nu) \quad (9)$$

where  $S$  is the sensitivity of the resistor material to strain—the change of resistance versus strain. This is directly analogous to the sensitivity of the strain gauge to strain and when applied; thus, it is called the gauge factor; a figure of merit for strain gauges. The material that is used to make the strain gauge dictates the gauge factor, the most common being constantan (copper–nickel alloy), nichrome (nickel–chromium alloy), and platinum (normally alloyed with tungsten).<sup>13</sup> For wire and foil strain gauges made from constantan or nichrome, the gauge factor is approximately 2, whereas for Pt-W resistors it is approximately 4. Constantan is a common material for strain gauges as it exhibits a linear response over a large range of strain, and it is relatively stable with changing temperature.

Because the change in resistance is very small, a suitably sensitive circuit is required that can measure it, and the most common circuit configuration used in this type of application is illustrated in Fig. 7, commonly known as a Wheatstone bridge.<sup>14</sup>

In order to be balanced,  $R_1 R_3 = R_2 R_4$ . The simplest form of strain gauge bridge is made by placing a single strain gauge into the circuit in place of  $R_1$  with  $R_2$ ,  $R_3$ , and  $R_4$  chosen to balance the bridge—often equal. It can be shown<sup>13</sup> that the system sensitivity in its simplest form ( $R_1 = R_g$ ) is

$$S_s = \frac{r}{1+r} S_g \sqrt{p_g R_g} \quad (10)$$



**Figure 7** Classic representation of a Wheatstone Bridge circuit.

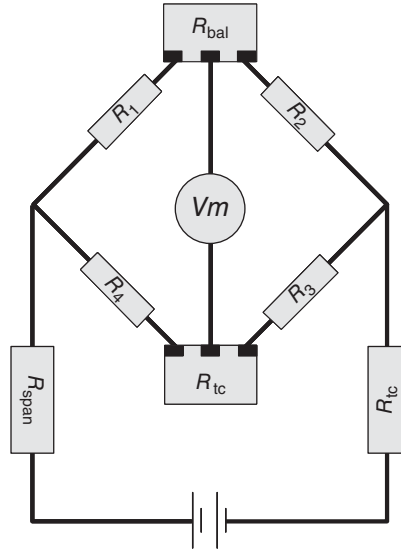
where  $p_g$  is the power dissipation of the gauge, which limits the maximum supply voltage, and  $r$  is the ratio  $R_1/R_2$ . Of course, where  $R_2, R_3,$  and  $R_4$  are chosen to be equal to  $R_g$  then  $r = 1$  although a value of  $r$  in the range 3–5 gives circuit efficiencies of between 75 and 83% while allowing a reasonable supply voltage.

Sensitivity varies with different configurations, with the most sensitive being the use of four gauges in the bridge—normally with the gauges in positions  $R_1$  and  $R_3$  oriented to measure strain in one dimension (tension or compression) and  $R_2$  and  $R_4$  in the other—which roughly doubles the sensitivity over the simplest form. It must be remembered that although sensitivity can be increased by attaching more gauges, the cost will increase accordingly due to the extra work involved in bonding the gauges.

So, the Wheatstone bridge, when properly balanced, is well suited to sensing very small changes in the balance of the bridge, and the output of a strain gauge circuit is measured in mV/V, where  $V$  is the excitation voltage. Most commonly, strain gauge circuits are designed to give an output of 2, 3, or 4 mV/V. The disadvantage here is the need for amplification of the output, which also increases any noise in the system.

### 3.2 Strain Gauge Circuit Compensation

To an extent, the Wheatstone bridge design lends itself to self-compensation for environmental factors such as temperature by virtue of the balanced nature of the resistors—if all resistors are the same, then they will be affected by temperature to the same extent and the net effect is theoretically zero. For more demanding transducer applications, compensation is required for temperature and sometimes zero balance, where, however well balanced the gauges are, their characteristics cannot be identical, and so the balance of the bridge is not exact when under zero load. These things can be compensated for by careful tuning of compensation resistors placed at the vertices of the bridge where the output is read, as shown in Fig. 8. Placing a well-tuned resistor with high thermal conductivity (commonly copper) at the vertex of  $R_4$  and  $R_3$  can compensate for zero drift due to temperature, whereas a temperature stable resistor, commonly constantan, at the vertex of  $R_1$  and  $R_2$  can compensate against bridge imbalance. Span effects can be compensated for by placing resistors either side of the voltage supply.



**Figure 8** Strain gauge bridge with compensation for zero balance ( $R_{bal}$ ), zero temperature compensation ( $R_{tcs}$ ), span adjust ( $R_{span}$ ), and span temperature compensation ( $R_{tcs}$ ).

#### 4 RESONANT ELEMENT TRANSDUCERS

Sometimes also known as tuning fork sensors, these devices are used in a wide variety of applications from measuring pressure, to liquid density and from accelerometers to torque sensors.<sup>14</sup> The principle of operation is similar to a guitar string, which, when plucked, resonates with a tone that is relative to the tension on it. In other words, the resonant frequency of the string is a function of the measurand—tension, the string material property, and its thickness and length. The frequency then increases with increasing axial force.

Similarly in a resonant element force transducer, the structure of the device is a vibrating element, which when excited, vibrates with a natural resonant frequency. When a stress or strain is applied to the device the frequency changes proportionally.

The fundamental frequency of a vibrating beam under tension,  $T$  is governed by the equation

$$T \times \frac{d^2 Y}{dX^2} - E \times I \times \frac{d^4 Y}{dX^4} = \rho \times A \times \frac{d^2 Y}{dt^2} \quad (11)$$

where  $I$  is the second moment of area:  $(b \times h^3) / 12$ ,  $E$  is the Young's modulus of the material,  $r$  is the material density,  $A$  is the cross-sectional area of the beam ( $b \times h$ ),  $b$  and  $h$  are breadth and height of the beam, respectively, and  $t$  is the time.

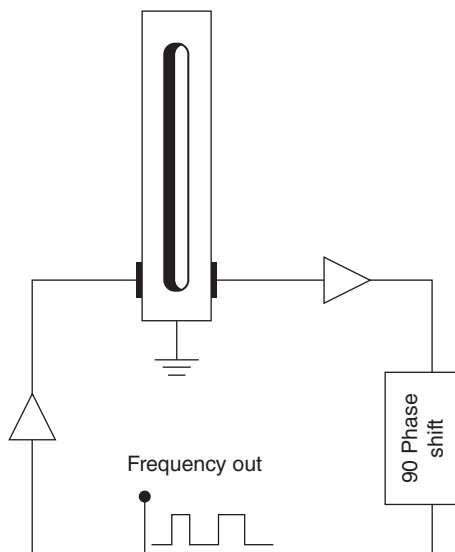
Then, assuming simple harmonic motion and applying the boundary conditions, the natural frequency  $f_{01}$ , when axial force  $T = 0$ , is given by

$$f_{T1} = \frac{a^2}{2\pi \times l^2} \times \sqrt{\frac{E \times I}{\rho \times A}} \quad (12)$$

where  $a$  is the value determined by mode number of vibration  $n_v \approx 0.5 \times \pi \times (1 + 2n)$ , and  $l$  is the beam length.

When the applied tension changes, the natural frequency of the beam under axial force  $f_{T1}$  becomes

$$f_{T1} = f_{01} \times \sqrt{1 + \frac{1}{a^3} \times th \times \frac{a}{2} \times \left( a \times th \times \frac{a}{2} - 2 \right)} \times \frac{l^2 \times T}{2E \times I} \quad (13)$$



**Figure 9** Illustrating the closed-loop circuit that maintains relative oscillation.

These equations can be used to determine the design of a tuning fork sensor with respect to the motion of the device under strain, the nominal frequency of the device, and frequency change at full scale.

An electronic closed-loop circuit such as the one illustrated in Fig. 9.<sup>15</sup> tracks the output of the device and, by also phase shifting the output by 90°, brings the input and output into phase. This keeps the sensor in continuous oscillation, and as the transducer is loaded the resonant frequency is maintained.

Examples of three common forms of resonant element transducer, single, double beam, and triple beam, are illustrated in Fig. 10.<sup>16</sup>

They are manufactured by conventional means, usually by laser cutting the resonant element from steel and then photoetching down to the required thickness.<sup>17</sup> The associated excitation and readout piezoelectric components can then be screen printed on to the element. These are all well-understood manufacturing methods and so volume production can be low, which is attractive commercially.

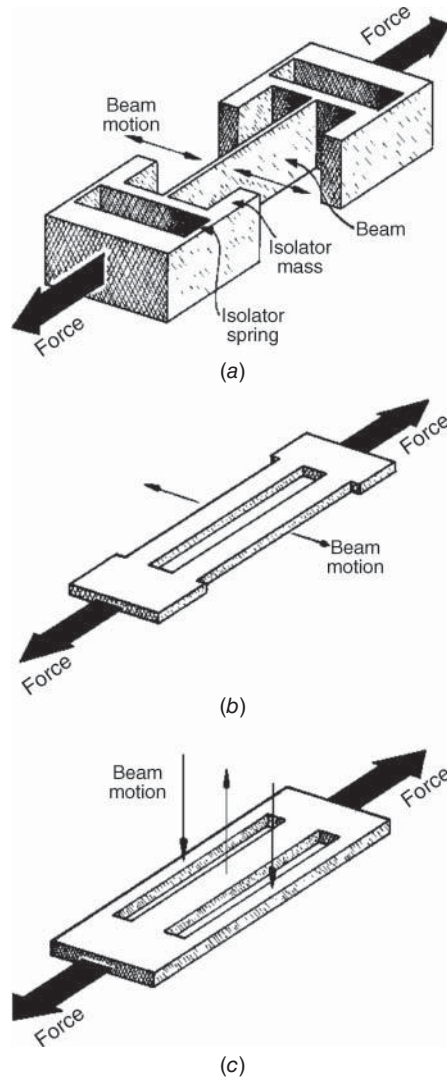
Figure 11 shows a photograph of a triple-beam tuning fork design, as represented in Fig. 10c.<sup>17</sup>

Because the device has a frequency output, it requires no analog-to-digital electronics to read it out. Advantages that are claimed for this type of sensor are:

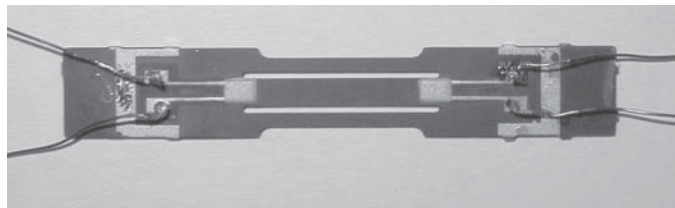
- Long-term stability ( $\pm 3.5 \times 10^{-5}$  over 12 months)
- Easy interface to digital electronics
- Relatively easy manufacturing and cost-effective in quantity

Their disadvantages include a relatively small operating range and design considerations to retrofit into existing applications.

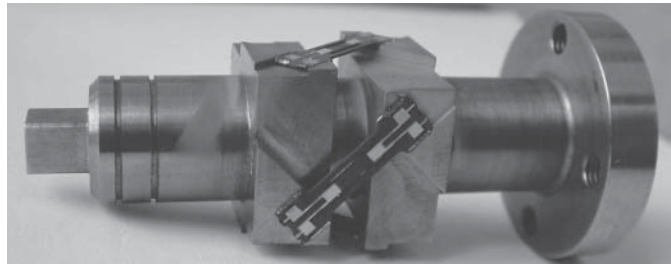
Tuning fork transducers have mostly been used in torque measurement applications as shown in Fig. 12 and described in Intiang et al.<sup>18</sup> and in precision scales, but they are becoming more widely used, with a 50-N load cell based on tuning fork technology, having been



**Figure 10** Three different types of tuning fork sensor: (a) single, (b) double, and (c) triple beam.



**Figure 11** A typical triple-beam tuning fork sensor.



**Figure 12** Resonant sensors mounted in a torque measurement arrangement. (After Ref. 20.)

recently evaluated using the 500-N force standard machine at the National Metrology Institute of Japan.<sup>19</sup> Although they show some good characteristics, such as low hysteresis and good long-term stability, they are large when compared with strain gauge load cells and have only comparable repeatability.

## 5 SURFACE ACOUSTIC WAVE TRANSDUCERS

The existence of surface waves, or Rayleigh waves, was first proposed theoretically in 1885 by, as their name suggests, Lord Rayleigh (John William Strutt)<sup>21</sup> who predicted their presence during earthquakes. However, it would be some 35 years before the development of seismological measurements, which confirmed his theories.

When an earthquake occurs, its energy is propagated in waves of three main types: The primary wave, or P-wave; the secondary wave, or S-wave; and surface waves in the form of Love and Rayleigh waves. The P-wave is analogous to an acoustic, or compression wave. It travels faster than the other two wave types and so is normally detected first. The S-wave is a sinusoid with associated amplitude and frequency. A surface wave is a hybrid of P- and S-waves, which propagates at the interface between two materials, and whose amplitude decreases exponentially with depth beneath—in the context of an earthquake—the surface of the Earth. Rayleigh waves are those surface waves that propagate with particle motion perpendicular in the vertical direction to the direction of propagation. Love waves have particle motion in the transverse direction and perpendicular to the direction of propagation. Diagrams illustrating these wave types can be seen in Fig. 13.<sup>22</sup>

In 1965, the practical implementation of a surface acoustic wave (SAW) on an elastic substrate (quartz) was realized by White and Voltmer,<sup>23</sup> and this paved the way for the subsequent extensive use of SAW devices in telecommunications as bandpass filters and delay components.<sup>24</sup>

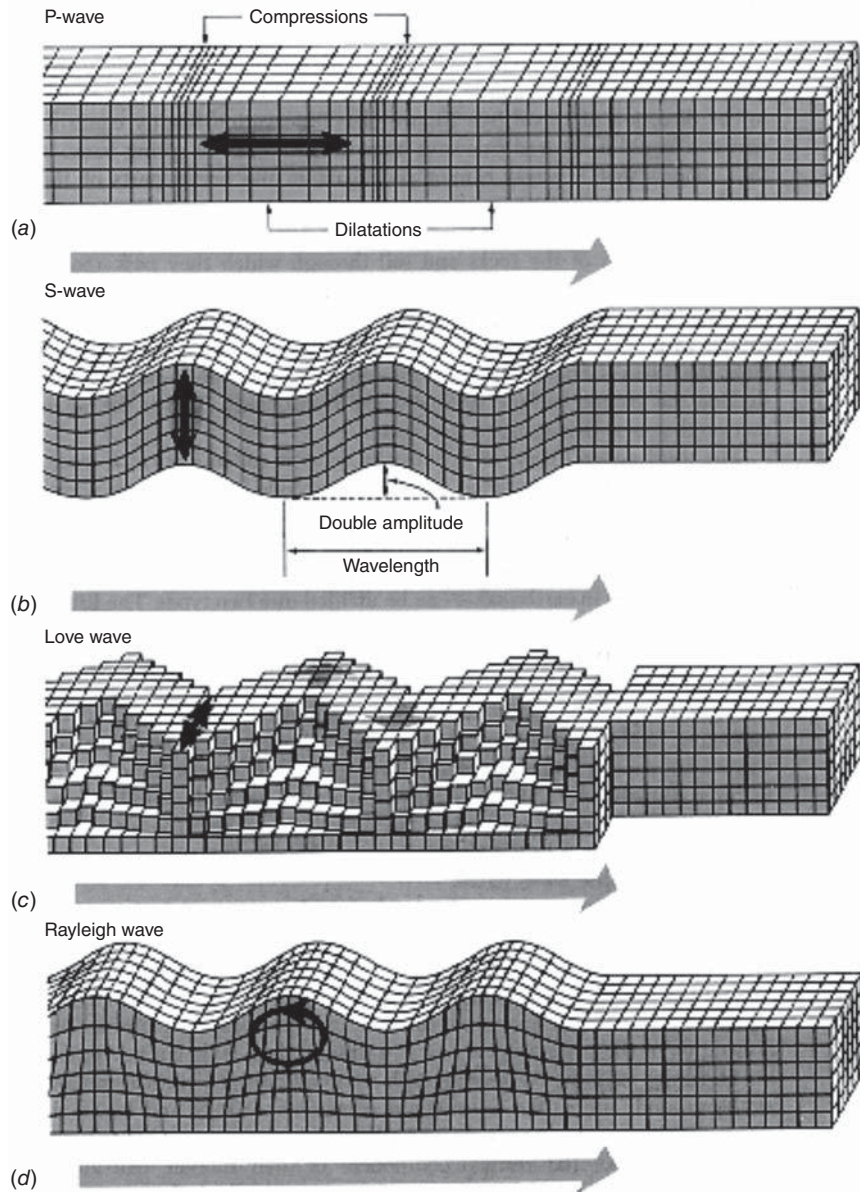
SAW devices such as the one in Fig. 14 consist of an excitation construction made up of “fingers,” spaced at half the resonant wavelength of the desired wave, on a piezoelectric substrate. There are then receivers placed on the substrate, which detects the arrival of SAW’s, and the output frequency is then transmitted as a quasi-digital signal to the processing electronics. The frequency of the SAW is given by<sup>25</sup>

$$f = \frac{(2n\pi - \varphi_{el}) \times v_{SAW}}{L} \quad (14)$$

where  $\varphi_{el}$  is the electrical phase shift of the amplifier circuit,  $n$  is the constant determined by electrode design,  $v_{SAW}$  is the velocity of the SAW, and  $L$  is the distance between transmitter and receiver structures.

This means that frequency is directly dependent on wave velocity and  $L$ , which enables development of SAW devices to measure a range of parameters including acoustic, temperature, and dimensional changes (and hence force and torque) to name but a few.



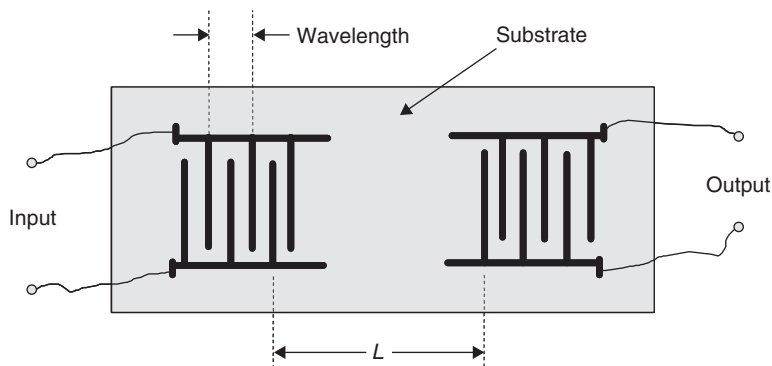


**Figure 13** Illustrating the different wave types observed during earthquakes: (a) P-wave, (b) S-wave, (c) Love wave, and (d) Rayleigh wave.

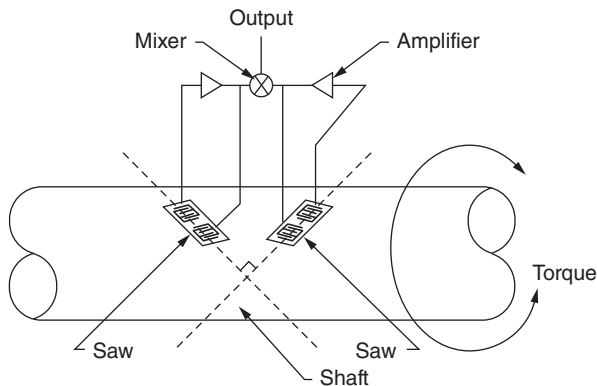
Since then the use of SAW transducers has broadened into other applications, which include temperature<sup>26</sup> and pressure measurement.<sup>27,28</sup> and, of course, force measurement—in particular torque measurement.

In 1990, the first noncontact torque transducer based on a SAW device was patented,<sup>29</sup> and since then the noncontact torque measurement industry has been served mostly by this technology. Applications include Formula 1 vehicle drivetrain monitoring as well as uses in torque monitoring for regenerative braking systems.<sup>30</sup>





**Figure 14** The layout of a typical SAW transducer.



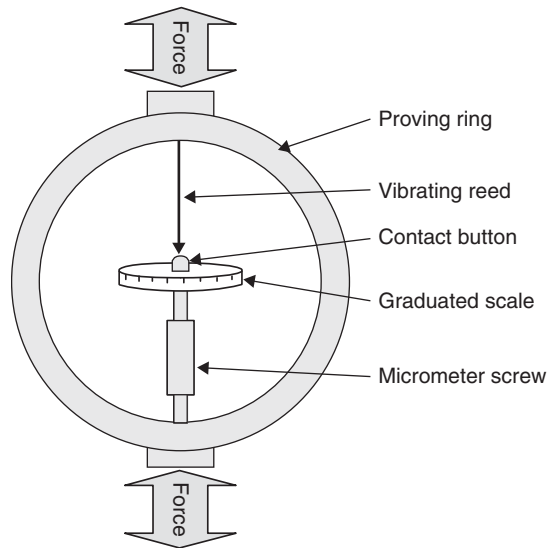
**Figure 15** Configuration of SAW devices on a shaft to measure torque.

If the SAW device is rigidly mounted to a flat spot on a shaft, and the shaft experiences a torque, this torque will stress the sensor and turn it into a wireless passive lightweight torque sensor. As the shaft is rotated one way, the SAW torque sensor is placed in tension. As the shaft is rotated the other way, it is placed in compression. For practical applications, two SAW torque sensors are utilized such that their centerlines are at right angles (Fig. 15).<sup>29</sup> With this system, when one sensor is in compression, the other sensor is in tension. Since both sensors are exposed to the same temperature, the combination of the two signals will act to minimize temperature drift effects.

When compared with other torque sensors, including resistive strain gauges, optical transducers, and torsion bars, SAW torque sensors offer lower cost, higher reliability, and wireless operation.

## 6 DYNAMOMETERS

Strictly speaking, a dynamometer is any force transducer that uses the elastic nature of a material to determine the force causing deformation. This includes load cells, pressure transducers, and so on. A particular type of dynamometer that is encountered in the field of force measurement is a ring dynamometer or “proving ring.”



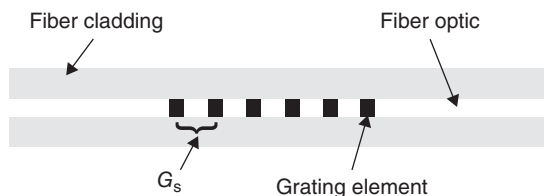
**Figure 16** Schematic of a proving ring with manually adjusted micrometer readout.

The common form, shown in Fig. 16, utilizes a manually adjusted micrometer readout to measure the diameter of the ring under tension and compression. In this configuration, a vibrating reed is set in motion by tapping it with a pencil. The micrometer is then adjusted to move the contact button until it is just in contact with the reed, which will make an audible buzzing noise. The graduated scale is then read off, which will indicate the force applied to the ring. This method was developed in 1946<sup>31</sup> and remains to this day as a proven and reliable method of measuring force with relatively low uncertainty. If a digital readout is required, then the micrometer can be replaced by strain gauges or a LVDT—a linear variable displacement transducer.

Proving rings are used commonly to measure soil compaction but also as calibrating instruments.

## 7 OPTICAL FORCE TRANSDUCERS

There are two main types of optical strain gauges, but both are spectroscopic in nature. One utilizes a change in the arms of an interferometer arrangement of fiber optics. In another, a diffraction grating is incorporated into the fiber with the spacing of the grating being altered by strain upon the fiber through the substrate material. This is otherwise known as a fiber Bragg grating sensor, or FBG sensor, a diagram of which can be seen in Fig. 17.



**Figure 17** Representation of a FBG sensor.

The Bragg condition for constructive interference is a product of the theory of X-ray diffraction by crystals. It is named after father and son physicists, Sir William and Lawrence Bragg who jointly won the Nobel Prize for physics in 1915, and is utilized in fiber-optic sensors that measure, among other things, strain. The condition states<sup>32</sup>

$$2d \times \sin \psi = n\lambda \quad (15)$$

where  $\lambda$  is the wavelength of light,  $n$  is an integer,  $\psi$  is the angle of incidence with respect to the crystal surface, and  $2d$  is the path length difference between two incident light rays.

When this is applied to fiber optic, the isolated wavelength, that is, the one of interest is the one reflected by the grating elements and the equation slightly changes<sup>33</sup>

$$\lambda_B = 2\eta \times G_s \quad (16)$$

where  $\lambda_B$  is the Bragg wavelength,  $\eta$  is the refractive index of the optical fiber, and  $G_s$  is the spacing of the grating elements in the fiber.

In reality, there are thousands of elements in an FBG sensor, which is manufactured by “writing” the elements into a length of germanium-doped optical fiber. The writing is done by exposing the fiber to a spatial pattern of ultraviolet light in the region of 244–248 nm. This fabrication process is based on the photorefractive effect, which was observed in Ge-doped optical fibers in 1978 by Hill et al.<sup>34</sup>

When an FBG sensor is subjected to a strain, the spacing between the grating elements is increased, and the Bragg wavelength is altered according to the equation<sup>35</sup>

$$\Delta\lambda = \lambda_B (k \times \varepsilon + \alpha_\delta \times \Delta T) \quad (17)$$

where  $\Delta\lambda$  is the change in Bragg wavelength,  $k = 1 - p$  ( $p$  is the photoelastic coefficient of the fiber),  $\alpha_\delta$  is the refractive index temperature coefficient, and  $\Delta T$  is the change in temperature.

And so, provided temperature is compensated for (fiber-optic sensors are highly temperature dependent and so are used as temperature sensors also) the change in wavelength can be used as a measurement of the strain on the fiber.

Fiber-optic interferometers such as those illustrated in Fig. 18 constitute the most sensitive of the fiber-optic force sensors and may be based on the many available designs including Michelson, Mach-Zhender, and Fabry-Perot.<sup>36</sup>

In an interferometer, interference between two beams of light is described by the following equation:

$$\Delta\phi = \frac{2\pi}{\lambda} n \times \Delta l \quad (18)$$

where  $\Delta\phi$  is the phase change of the resultant signal,  $n$  is the refractive index,  $\lambda$  is the wavelength, and  $\Delta l$  is the relative path change of the two beams.

In the case of a fiber-optic strain sensor, the path length is introduced when the paths of the interferometer are subjected to a differential strain. When this happens, two changes occur: Its length changes and also the refractive index.

$$\Delta l = \varepsilon_1 \times l_0 \quad (19)$$

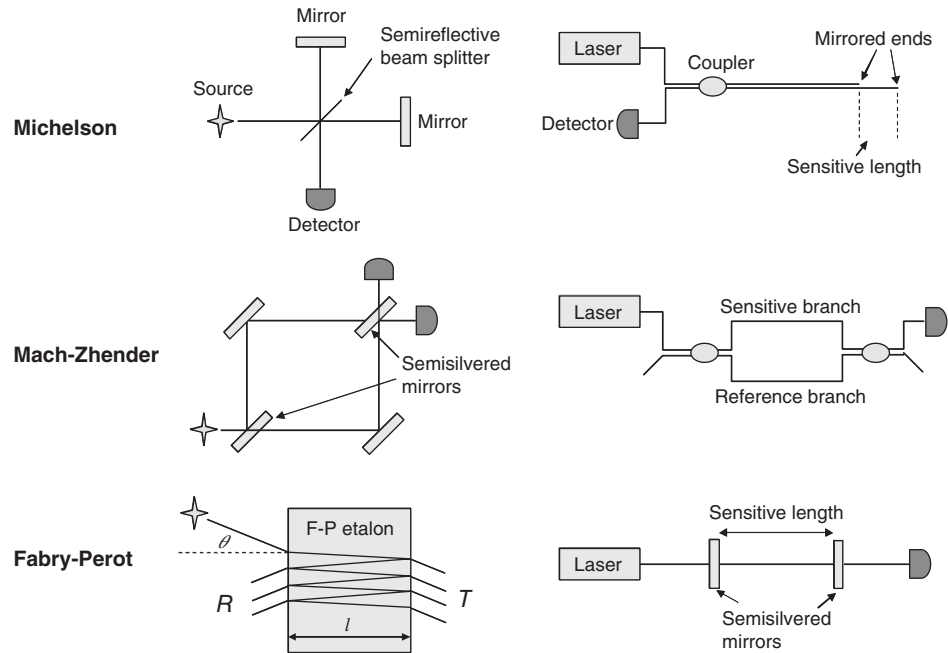
$$n = n_0 \{1 - 1/4n_0^2 [2 \times P_{12}\varepsilon_1 + (P_{11} + P_{12})(\varepsilon_2 + \varepsilon_3)]\} \quad (20)$$

where  $l_0$  and  $n_0$  are the initial (unstrained) length and refractive index, respectively,  $P_{xy}$  are coefficients that depend upon the glass material, and  $\varepsilon_1$ ,  $\varepsilon_2$ , and  $\varepsilon_3$  are strain components acting on the fiber.

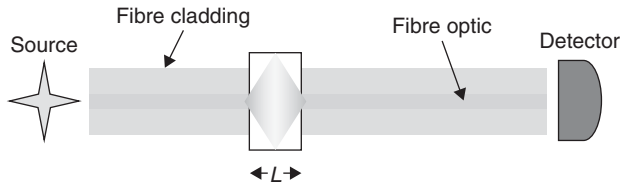
These, when substituted into Eq. (19), and if it is assumed that  $\varepsilon_2 = \varepsilon_3 = -\nu_f \varepsilon_1$ , gives the phase change due to a strain  $\varepsilon_1$  on the fiber.

$$\Delta\Phi(\varepsilon_1) = \frac{2\pi}{\lambda} l_0 \varepsilon_1 n_0 \{1 - 1/2n_0^2 [P_{12}\varepsilon_1 - \nu_f \varepsilon_1 (P_{11} + P_{12})]\} \quad (21)$$

where  $\nu_f$  is Poisson's ratio for the fiber.



**Figure 18** The different interferometer types and their fiber-optic counterparts.



**Figure 19** Representation of a fiber-optic intensity monitoring force sensor.

The intensity at the detector of the resultant signal is given by

$$I = \alpha[1 + V \cos \Delta\phi(\epsilon_1)] \tag{22}$$

where  $\alpha = E^2$  ( $E$  is the optical electric field) and  $V$  is the fringe visibility. Hence, intensity at the detector can be related to strain directly.

Other fiber-optic sensors include intensity monitoring sensors<sup>37</sup> (Fig. 19) where a cavity length is altered by the applied load.

An increase in cavity length induces an intensity drop and vice versa. A detector monitors the output intensity, and this is then converted to a strain. Although simple in their design, they suffer from inefficiencies due to the coupling, alignment, and bending.

Fiber-optic force sensors can be very sensitive and are also immune to electromagnetic interference, and because of this find their applications in challenging environments, such as the measurement of strain in overhead power cables.

## 8 MAGNETOELASTIC TRANSDUCERS

In 1842, Joule<sup>34</sup> discovered that the properties (by which he meant its dimensions) of ferromagnetic material are coupled to its magnetic field flux. It is known as the Joule effect, but more commonly called magnetostriction. He observed that if the material magnetic flux was increased, its length changed and as its length changed, so did its transverse dimension, thus keeping the material volume (approximately) constant. There is a reciprocal effect, known as the Villary effect, whereby subjecting a magnetic material to stress or strain will alter its magnetic flux. There are other magnetoelastic phenomena, such as the Matteucci effect, in which a material exhibits a change in an induced helical magnetic flux when subjected to a torque. Both of these principles are used in force transducers.

Nearly, all ferromagnetic materials will exhibit some magnetostrictive behavior, although much current research involves amorphous alloys,<sup>25</sup>—the so-called giant magnetoelastic materials, such as Terfenol-D—an alloy of terbium, iron, and dysprosium because they give such high values of magnetostriction. An illustration of the effect is shown in Fig. 20.<sup>39</sup>

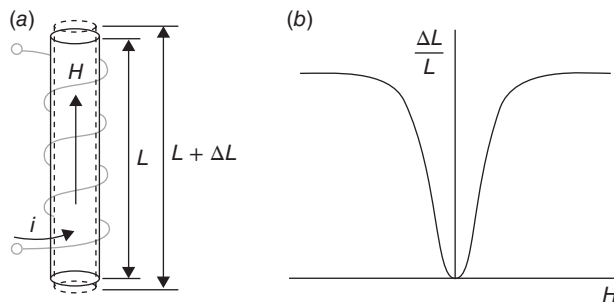
In Fig. 20, a rod of a magnetic material with length  $L$  is surrounded by a coil of wire carrying an electrical current so that a magnetic field,  $H$ , is produced along the rod. When current is flowing, the length of the rod will increase by a small amount  $\Delta L$ . The strain  $\Delta L/L$  is called the magnetostriction, denoted by  $\lambda$ , and normally measured in parts per million. The graph in Fig. 20*b* shows that as the magnetic field,  $H$ , increases,  $\lambda$  also increases but not indefinitely. There is a saturation point, normally denoted  $\lambda_{\text{sat}}$  whereby no matter how intense the magnetic field, the magnetostriction does not change. Also to be noted is that the rod exhibits an increase of length regardless of the sign of the magnetic field increase.

Magnetoelastic force sensors are used in many industrial applications, including as torque sensors in the automotive industry,<sup>40</sup> as sensors and transducers in railway engines<sup>41</sup> and in civil engineering applications,<sup>42</sup> to name but a few.

## 9 FORCE BALANCE TRANSDUCERS

The force balance utilizes one of the oldest forms of weight measurement, the beam balance. If we have ever been weighed by our family doctor, we have seen the beam balance in action. In the balance, an unknown mass is balanced against a known mass, with the distance from the fulcrum giving the value of the weight given by the known mass.

In a modern force balance, the deflection cause by the applied, unknown, mass is used to regulate a current input to an actuator that acts to balance the applied force. This feedback



**Figure 20** (a) The Joule effect. The changes in shape in response to the magnetic field  $H$ . (b) The relationship between  $\Delta L/L$  and  $H$ .

system works to retain the balance in equilibrium, and the current applied to the actuator is directly related to the force applied by the unknown input.

Force balances are widely used as accelerometers in seismographs, aircraft and drilling platform stabilization systems, and so on.<sup>40</sup>

## 10 FORCE TRANSDUCER CHARACTERISTICS

Any force transducer will be supplied with a quoted specification, which places quantitative values on various aspects of the characteristics of a force measurement system. Table 2 lists the typical values in a 1000-N (220-lbf) strain gauge load cell.

So what does all this mean? Next we will discuss these items in turn.

### 10.1 Capacity

This is the maximum force that can be measured reliably using this particular load cell. However, commercially available load cells may have up to 200% overload capacity whereby the load cell can withstand an overload without damage, although it is advisable that load cells that have been overloaded be recalibrated. As with most transducers, it is inadvisable to use load cells within the first or last 10% of their design range. Table 1 shows that there is considerable crossover between device types and their operable ranges, but some will be much better suited to some applications than others, and so care should be taken to specify the device to the application accordingly.

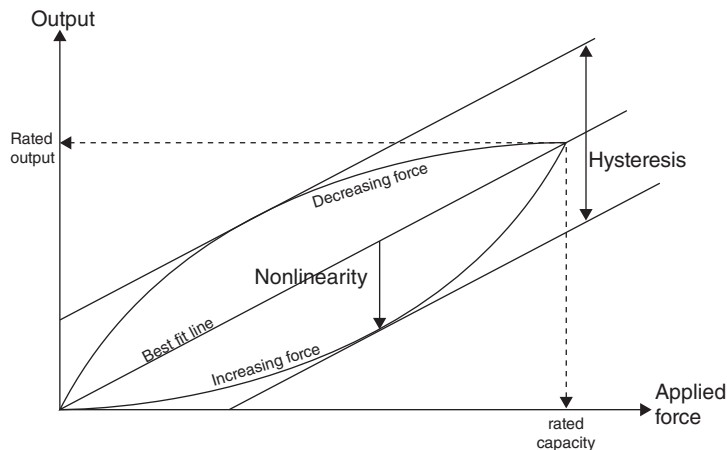
### 10.2 Output

The output of a strain gauge load cell is expressed as mV/V, with the specified output being that at the rated capacity. So, with a specified output of 2 mV/V, the actual output voltage from a strain gauge load cell with a 10-VDC excitation (supply) voltage will be 20 mV.

Figure 21 illustrates the various concepts of nonlinearity and hysteresis as well as rated output and capacity. Load cells by their spring-like nature are linear in their response but with manufacturing inconsistencies and engineering tolerances, there may be some deviation from true linear behavior. When adjusting a load cell prior to calibration, a straight-line fit is made to the device output, and the maximum deviation from this line is calculated and reported as the device nonlinearity. Hysteresis is the maximum difference in output with increasing and decreasing input. Often, load cell manufacturers or suppliers will specify a *combined error*, which is a combination of nonlinearity and hysteresis.

**Table 2** Typical Load Cell Characteristics

Capacity	1000 N
Output	2 mV/V
Creep	±0.01% FS
Nonlinearity	±0.05% FS
Hysteresis	±0.05% FS
Repeatability	±0.05% FS
Temperature coefficient	±0.025% FS
Temperature range	40°C to +60°C
Accuracy	±0.1%
Combined uncertainty	±0.02%



**Figure 21** Illustration of a typical load cell response curve.

### 10.3 Repeatability

Repeatability is the standard deviation of output at any given repeated input, while keeping the measurement conditions the same. In a normal calibration, the repeatability is calculated for all points in the calibration and the specified repeatability is normally the maximum standard deviation. Repeatability should not be confused with reproducibility, which is the measurement of the output variation when the measurement conditions are different each time. This should not be confused with *reproducibility*, which is sometimes also quoted, but is the standard deviation of output at a given input but under differing conditions.

### 10.4 Creep

This is the extent of output change over time after a step change input is given, normally measured over a 30s.

### 10.5 Temperature Coefficient

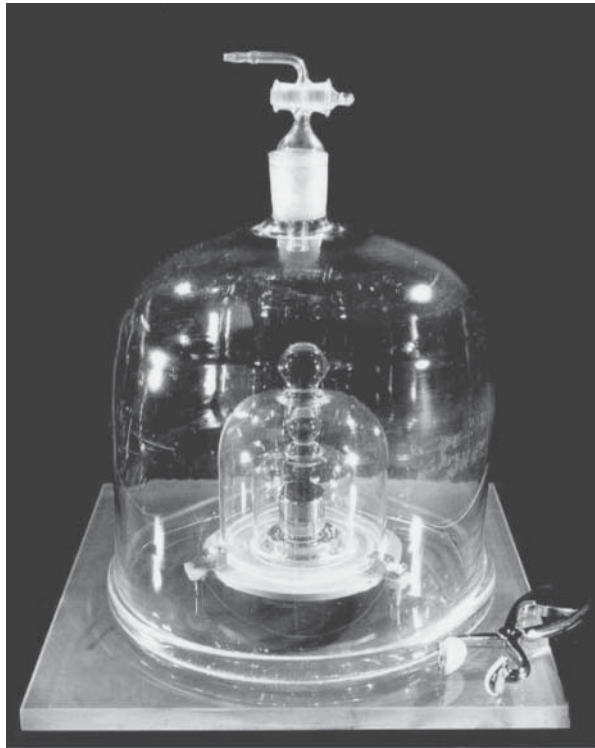
This is a measurement of the load cell susceptibility to temperature change, normally stated as %FSD per degree Celsius.

### 10.6 Accuracy

This is the statement of closeness of the output to the input quantity, taking into account uncertainty of measurement. This value is determined during calibration. Accuracy should not be confused with *precision* or *resolution*, these being closeness of repeated output values and the minimum observable output change, respectively.

## 11 CALIBRATION

The importance of having traceable calibration records for your force transducer is not to be underestimated. All calibrated load cells can be traced back to primary mass standards, which are in turn directly traceable to the international prototype kilogram (IPK) (Fig. 22).



**Figure 22** A photograph of the IPK in Paris.

The IPK and its six sister copies are stored at the International Bureau of Weights and Measures in an environmentally monitored vault in Sèvres on the outskirts of Paris. Official copies of the IPK, which are measured against the IPK every 50 years, are held by other nations and constitute the national standard kilogram. Masses used in calibration laboratories to calibrate other masses are calibrated against the national standard. Those masses are called primary standards and are used to calibrate the so-called secondary standards, which may be either masses or very accurate force transducers. The key to any acceptable calibration is traceability to the primary standard. That is to say that a documentation trail can be followed back to the national primary standard.

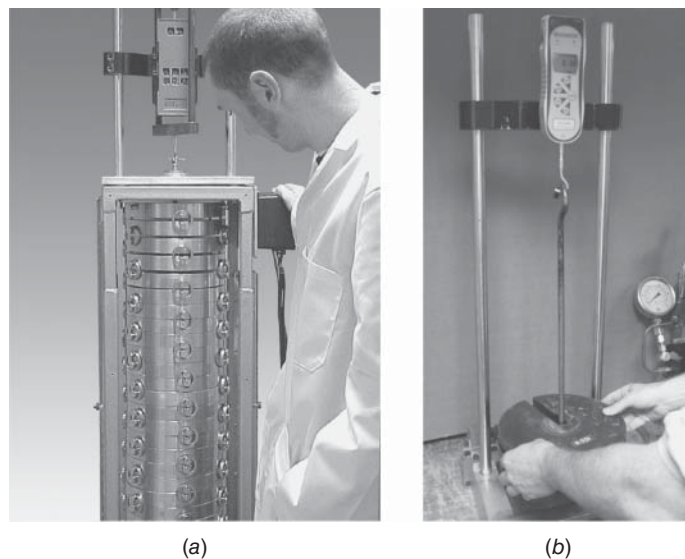
Of course, it is not enough to know that your mass is the equivalent of a kilogram when measuring force: Equation 2 states  $F = mg$ , where  $g$  is the acceleration due to gravity. So, to measure static forces on Earth, we need to know what the acceleration due to gravity is at our location. Because  $g$  decreases radially from the center of the Earth according to the inverse square law, the acceleration due to gravity at the Earth's surface very much depends on the altitude and latitude of your measurement position according to the equation<sup>43</sup>

$$g = 9.80613(1 - 0.0026325 \cos 2L)(1 - 3.92 \cdot 10^{-7}H) \quad (23)$$

where  $L$  is the latitude of the measurement position in degrees and  $H$  is the altitude, or height.

The force applied by an adjusted 1-kg mass measured with a force transducer in a laboratory in Mexico a local  $g$  is  $9.77954 \text{ ms}^{-2}$ , would be approximately 0.4% different from an identical measurement made in Oslo a local  $g$  is  $9.825 \text{ ms}^{-2}$ .





**Figure 23** (a) A small 2500-N weight stack and (b) a basic frame for hanging calibrated masses onto a force gauge. (Courtesy of Mecmesin Ltd.)

Load cells are calibrated using a force application system, which can be as simple as a calibrated mass hung by a hook, normally for smaller force ranges for health and safety reasons, or a so-called weight stack, which may be manually or computer controlled, where a set of calibrated masses can be applied sequentially to measure a load cell's output at regular intervals across its range. Weight stacks can range from small ( $< 1$  kN) through to the very large ( $> 1$  MN). The largest weight stack in Europe has a capacity of 1.2 MN and is at the National Physical Laboratory in London (Fig. 23). The largest weight stack in the world resides in the United States and is rated at 4.45 MN (1000,000 lbf)!

## 11.1 Uncertainty

There are many texts<sup>44–46</sup> that cover uncertainty of measurement in much more detail than is given here, but we will give a brief overview.

In all measurements, there is never absolute certainty of the result. However, we can estimate the level of uncertainty in a measurement in order to communicate the likelihood of a result being accurate. We can also design our measurement systems in such a way as to minimize uncertainty. This is especially important in calibration because whoever is providing the calibration service is making a statement about a device's accuracy that customers will use in their analysis of the measurements they make. Given that some applications are safety critical, it is vitally important that the customer is provided with accurate estimations of calibration measurement uncertainty. Using masses calibrated against primary standards ensures that the uncertainties related to the masses are minimized, but there are many other contributing factors.

*Temperature.* Because load cells (and the systems that hold them) are made of metal (aluminum or steel mostly), temperature will have an effect on performance. Temperature stability during calibration is therefore vital.

*Humidity.* Humidity affects the buoyancy of the air, thereby affecting the applied force, and so should be kept as constant as possible during calibration.

*Gravity.* The local value for gravitational acceleration ( $g$ ) should be taken into account when calibrating and using masses. If a calibrated mass is taken elsewhere to be used to verify a measurement, then a simple correction factor should be calculated for the new location depending on its value for  $g$ . An example follows that illustrates this.

For example, say we want to calibrate a device at our laboratory using a mass that applies a force of 1000 N. Previously,  $g$  at our location has been calculated to be  $9.81 \text{ ms}^{-2}$ . A mass is then manufactured and adjusted to our specification, and it is delivered with its certificate confirming traceability to the primary standard, so that if an instrument is then calibrated in our lab using the mass, we will know that exactly 1000 N (with a small uncertainty) is being applied to our device. The instrument is then sold to a customer in a different location with a local  $g$  value of 9.8120000, and 12 months later the customer requires a recalibration at her premises. The following options are presented: We could purchase a mass that is adjusted to the  $g$  value at the customer premises, which could be costly and of limited use, or we could use our own adjusted masses and apply a correction factor taking into account the  $g$  value where the customer is. The correction factor would be evaluated as follows.

A mass is calibrated and adjusted to apply a specific force according to Eq. (2), so if that mass is transported elsewhere and applied to an instrument previously calibrated in the laboratory, the resultant measurement will read

$$F' = m(g + \Delta g) \quad (24)$$

Taking  $m$  out of the equation

$$F' = F \left( 1 + \frac{\Delta g}{g} \right) \quad (25)$$

And so

$$F' \left( 1 + \frac{\Delta g}{g} \right)^{-1} = F \quad (26)$$

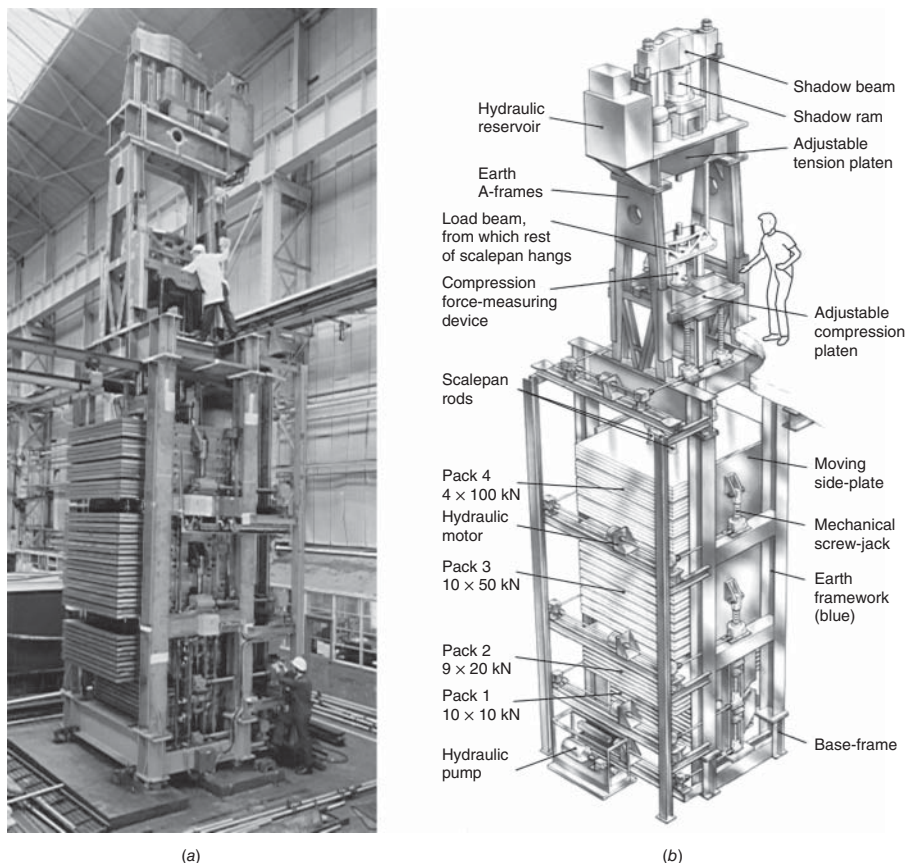
Substituting the  $g$  values from the example, a correction factor of 0.9997962 should be used to correct the displayed force. Without using  $g$  correction, at 1000 N the error would be approximately 0.2 N.

For the 1.2-MN calibration stack in Fig. 24, in order to reduce uncertainties associated with the force application, it is constructed on top of 40-m piles for stability and each mass in the stack is trimmed to its own value of  $g$  depending upon its altitude in the stack!

In minimizing uncertainties, providing the correct mechanical linkage is also vital, that is, the means to connect your load cell to the applied force. Because strain gauges are positioned very carefully on an elastic element of a specific shape, which is designed to measure force in a specific direction, and which as a whole is calibrated to measure axially, any off-axis loading (i.e., side loading) will result in an erroneous measurement. For this reason, it is vital that when using the load cell that it is mounted correctly, as incorrect fixturing can cause off-axis loading that will introduce errors, sometimes significant. Axial alignment of force vectors is easier in tension than in compression because in tension, provided that no part of the system is rigidly fixed, the system will have a tendency to self-align. In compression though, it is easy to end up in a situation where you are trying to “push a rope” so to speak, and in doing so can introduce significant alignment errors, and so a reliable method of linking the system components needs to be devised.

## 11.2 Other Equipment

If other equipment is used in the calibration, for example, voltmeters, thermometers, and so on, then the uncertainties of these instruments should be considered in the uncertainty budget.



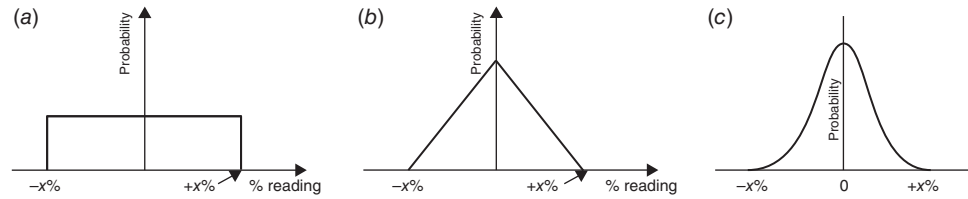
**Figure 24** (a) Photograph of the trial assembly of a 1.2 MN deadweight force standard machine, now located at NPL in Teddington. and (b) A schematic of the design. (© Crown Copyright, Courtesy of the National Physical Laboratory, London, UK.)

### 11.3 Operator Inconsistency

Finally, in a laboratory with more than one operator, results of calibrations can vary depending on the operator. Laboratory procedures may be in place that minimize the uncertainties introduced when different operators perform the same function, but there may be random errors introduced that should be considered.

The list could go on, but the contributions made become smaller until they are no longer significant—it is also important to retain a sense of proportion! While it may be commendable to calculate the uncertainty contribution of a given item to the eighth decimal place, this is hardly significant to a device with a required accuracy of 0.5%.

When preparing your uncertainty budget, it is important to note that, because uncertainties are not precisely known, they are normally quoted as  $\pm x\%$  along with a confidence limit. We must, therefore, understand the probability distribution associated with it. Taking the contributing factor of resolution as an example: If, say, a force gauge is reading a nominal value of 1.55 N but the last significant digit of the display is fluctuating between 1.54 and 1.56 N, then, because we only know the upper and lower bounds of the error, the true value could be anywhere between these limits with an equal probability of any one true value in that range. If we plotted the probability distribution it would look like the diagram in Fig. 25a).



**Figure 25** (a) Rectangular, (b) triangular, and (c) normal probability distribution.

The uncertainty of this type of contributing factor has what we call a rectangular distribution. A combination of two rectangle distributions gives, by the process of convolution, a triangle distribution as shown in Fig. 25*b*. Triangular distributions are rare but could apply to the process of interpolation between two known values, for example, and this is unlikely in the case of an uncertainty budget of a measurement process. If many probability distributions are combined or where random factors are involved, then the result will be a normal distribution—Fig. 25*c*. Normal distributions are assigned to uncertainties given in calibration certificates, for example, the “calibration of adjusted masses” entry in Table 3. In force measurement, the majority of uncertainty budget contributors have rectangle or normal distributions.

Once all contributions have been accounted for and their values calculated, a divisor is applied, which is dependent upon the probability distribution function. Uncertainties are combined by quadrature addition, that is

$$\text{Combined}_U = \sqrt{\sum u^2} \quad (27)$$

In order to quote a confidence level of 95%, the combined uncertainty is multiplied by a factor of 2. If a value,  $k = 3$  were to be used, the confidence level would rise to 99.7%, but this is rarely used in force measurement. A typical uncertainty analysis table for a deadweight frame such as the ones in Fig. 19 is shown in Table 3.

Looking at the table, we can see the contributors that have been considered in the overall uncertainty budget along with their probability distribution functions. There was one contributor in this particular analysis that was not included, which was the effect of temperature on the deadweight frame. Because of thermal fluctuations, the metal frame will undergo a dimensional change due to expansion and contraction. After analysis it was seen that the overall effect on the application of mass was approximately 0.0000001% and so was not included.

## 11.4 Conclusion

There are many ways to measure force and torque, and this chapter has given a review of but a few of the more common methods, along with an overview of calibration and traceability

**Table 3** A Typical Uncertainty Budget for a Deadweight Calibration System

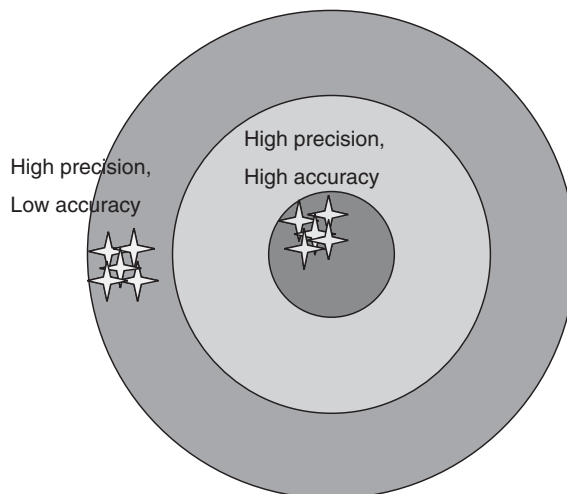
Source of Uncertainty	Value $\pm\%$	Distribution	Divisor	$c_i$	$u_{iT}$
Static frame alignment	0.001	Rectangle	1.73	1	0.00058
Frame flex under load	0.0001	Rectangle	1.73	1	0.000058
Calibration of adjusted masses	0.01	Normal	2	1	0.005
Drift of adjusted masses	0.01	Rectangle	1.73	1	0.0058
Random	0.001	Normal	2	1	0.0005
Combined uncertainty normal		Normal			0.011
Expanded uncertainty		Normal ( $k = 2$ )			0.022

Source: Courtesy of Mecmesin Ltd.

considerations. Which method is used will depend on many factors including range, application, environment, life requirement of the sensor, instrumentation availability, and, of course, cost.

## GLOSSARY

**Accuracy** This is an expression of how close a measurement is to the actual value. Not to be confused with precision.



**Analogue Output** An analogue output is a continuous signal, from a transducer, given usually as a voltage or a current. The output from a load cell is an analogue one, but it is put through an analog-to-digital converter so that it can be manipulated and stored in a useful form for computers.

**Axial Strain** Axial, meaning “on axis.” This is the extent of sample deformation in the direction in which the force is applied.

**Band Pass** In filtering, a filter that allows a given range of frequencies to pass unhindered, while frequencies above and below the filter band limits are blocked.

**Bridge Resistance (Load Cell)** The nominal electrical resistance of the load cell circuit measured at the excitation connections of the load cell with zero load applied to the load cell and the output connections open circuit. Expressed in ohms ( $\Omega$ ).

**Calibration** The comparison of transducer output against input quantities that are traceable to international standards. Calibration would normally be carried out by a recognized authority and should result in the issue of a calibration certificate. If there is any change in transducer performance or damage to the transducer or if there is any unusual behavior exhibited by the transducer, it should be recalibrated.

**Capacity (of Load Cell)** The maximum axial load a load cell is designed to measure within its specifications.

**Compression** The application of a force, the end result of which is to reduce the sample height. Applying pressure to a sample in order to deform or flatten it.

**Creep** When a change in load is applied to a specimen, the new stress and/or strain reading can drift by a small amount over time. This is termed creep.

- Deflection** The degree to which a structural element is displaced under a load. In Mecmesin systems, this is measured from the cross-head position as standard, but where more accurate measurement of deflection is required an extensometer should be used.
- Deformation** A change in the dimensions of a material under stress or strain.
- Displacement** The total driven movement of a test stand. Linear displacement is usually measured in millimeters or inches, whereas rotary displacement is usually measured in revolutions (revs) or degrees. Note that displacement may differ from specimen deformation.
- Drift** The change in transducer output when zero input is given. Not to be confused with creep, which is the change in transducer output under a load.
- Ductility** The amount of plastic deformation exhibited by a material before it ruptures.
- Eccentricity** The difference between the direction of load application to the true axial direction.
- Elastic/Elasticity** A material is said to be elastic if it deforms under stress (e.g., external forces), but then returns to its original shape when the stress is removed. The amount of deformation is called the strain. Elasticity is the ability of a material to return to its original dimensions subsequent to the application of stress or strain. The linear portion of the stress–strain curve of a Hookean material is called the elastic region because if applied force is removed within this region, the material will return to its original shape and size.
- Elastic Limit** This is the stress value during a tensile or compression test after which the sample suffers permanent deformation. For Hookean materials, it is roughly equal to the limit of proportionality (LOP).
- Energy** The work done on a sample during a tensile or compression test. It is calculated as the area under the stress–strain curve and is measured in joules, the SI-derived unit for energy.
- Equilibrium** Achieved when the sum of all forces acting upon a body is zero.
- Extension** The amount by which an object is increased in length.
- Extensometer** An instrument used to measure extension.
- Extrinsic** Extrinsic properties are characteristics of a test specimen as a whole, rather than the material from which it is made. Examples of extrinsic properties are mass and volume. Opposite of intrinsic, examples of which include temperature, density, and melting point.
- Force** The classic definition of force is any action that alters or tends to alter a body's state of rest or of uniform motion in a straight line. Force has both magnitude and direction, making it a vector quantity. Newton's second law states that an object with a constant mass will accelerate in proportion to the net force acting upon and in inverse proportion to its mass. Equivalently, the net force on an object equals the rate at which its momentum changes. Force is measured in newton, which is an SI-derived unit. One Newton is the force required to accelerate 1 kg to  $1 \text{ m/s}^2$ . Forces acting on three-dimensional objects may also cause them to rotate or deform or result in a change in pressure and/or volume in some cases. The tendency of a force to cause changes in rotational speed about an axis is called torque.
- Frequency** The number of times an event occurs per unit time. Rate. Measured in hertz (Hz), kilohertz (kHz), or megahertz (MHz).
- Frequency Response** This is the ability of a system output to replicate the input. Most electrical systems have limited frequency response (bandwidth), which allows the elimination of noise from the measurement. It is important for a system to have a bandwidth sufficient to capture significant events of the test, for example, details at sample break. Mecmesin Emperor driven systems have a sampling frequency of 2000 Hz, which means that a reading is taken every 0.5 ms.



**Friction** Static friction is the force required to start one surface sliding against another. Dynamic friction is the force required to keep one surface sliding over another.

**Full Scale (FSD)** This is the capacity of a sensor, in this context, the load measurement system or load cell. FSD stands for full-scale deflection and is derived from old analogue displays, which used a needle against a background scale.

**Gauge Factor** A figure of merit for strain gauges. A sensitivity ratio that describes the relative ability of a strain gauge to measure strain.

**Gauge Length** Used to calculate elongation. This is often stated in industry standards as the distance between the grips on a universal testing machine.

**Grating** An optical device that allows spectroscopic analysis of incident light.

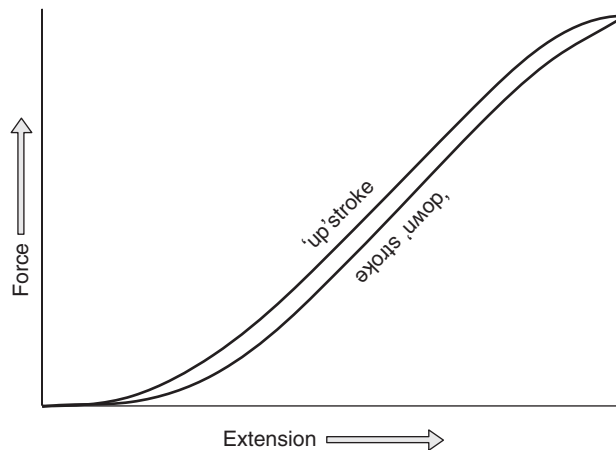
**Gravity** The relatively weak force that is measured between two masses.

**Grips/Fixtures** A mechanical device that grasps and holds the test specimen. Mecmesin grips include mechanical, pneumatic, vice grips, textile attachments, and specialist fixtures.

**Guide to the Expression of Uncertainty in Measurement** The resolution corresponds to the smallest two digits/values that can be read from a measurement device. Resolution should in no way be confused with accuracy.

**Hooke's Law** Assuming perfectly elastic behavior, stress is linearly related to strain: Robert Hooke, in the seventeenth century, stated "As the extension, so the force."  $F = -kx$ , where  $x$  is the displacement,  $F$  is the restoring force required, and  $k$  is the force or spring constant. Materials that exhibit near ideal elastic behavior are sometimes called "Hookean" materials.

**Hysteresis** When a material is cycled from zero stress to a peak stress and then back to zero again, the stress–strain curve follows a closed loop. This is because the material does not have perfect elasticity and is slightly stretched on the "up" stroke. The maximum difference between stress on the upward and downward strokes of the cycle is quoted as the hysteresis, normally in terms of % FSD.



**Intrinsic** The fundamental properties of a material. Melting point, density, heat capacity, and so on.

**Joule** The SI-derived unit of work, energy, and heat. It is the work done when a force of 1 N moves through a distance of 1 m. The area under a stress–strain curve gives the measurement of work done on a sample during a test.

**Kilogram Force (kgf)** The kilogram force is 9.80665 N. The practice of expressing force in kgf arose from the historical confusion that existed between "mass" and that particular force with which we are all familiar and that we refer to as "weight." Although not adopted as a

unit by the International System of Units (SI), kgf may be defined as “the force that produces an acceleration of  $9.80665 \text{ m/s}^2$  (this is the internationally adopted value of the acceleration due to gravity) on a mass of one kilogram.” A kgf may sometimes be written as “kp” and referred to as a “kilopond.”

**Kilopascal (kPa)** The SI-derived unit of pressure and stress is the pascal (force per unit area:  $1 \text{ Pa} = 1 \text{ N/m}^2$ ). The “kilopascal” is  $1000 \text{ N/m}^2$  or  $1 \text{ mN/mm}^2$ .

**lbf** The true imperial unit of force is the poundal (the force that produces an acceleration of one foot per second per second on a mass of one pound), but this is no longer used. Instead the term “pound force” is in widespread use and is a curious mixture of imperial and metric measurements. One lbf is about  $4.44822 \text{ N}$ , the force required to accelerate  $1 \text{ lb}$  by  $9.80665 \text{ m/s}^2$ .

**Load** An alternative term to mean force. The two are used interchangeably.

**Load Cell** The transducer used in Mecmesin Universal testing machines. Load cells are based on strain gauge technology. This is a tried and tested method of measuring force using a change in electrical resistance brought about by dimensional changes in a metal block caused by increasing and decreasing force.

**Load at Yield** The load reported at the point at which a specified deviation from proportionality of stress and strain occurs.

**LOP (Limit of Proportionality)** This is the point on the stress–strain curve beyond which the stress does not increase proportionally with strain.

**LVDT** Linear variable differential transformer. A type of electrical transformer used to measure linear displacement. Three coils are used, with the central coil being the primary. When an alternating current is present in the primary coil, a voltage is induced in the secondary coils, which is proportional to the inductance between them and the primary. As the coils are moved along a tube, their mutual inductances change and a voltage change is seen in the secondary coils. The difference between the two secondary coil voltages is proportional to the linear displacement along the tube.

**Mass** Mass is related to force by the equation,  $F = mg$ , where mass is effectively constant, subject to the special theory of relativity where the mass of a body is measured in terms of its total energy content.

**Magnetostriction** The effect seen when a change in the strain on a magnetic object produces a change in the measured magnetic flux in the object.

**Measuring Range** The difference between maximum and minimum loads in a specific test or application. It must not exceed load cell capacity.

**Median Force** This is the central value in a group of values, when placed in order. If there is an even number of values, then the median is halfway between the two central values.

**Minimum Load** The lowest load in a specific test or application. This is not necessarily zero load, but includes the weight of any fixtures that are attached plus any intentional preload that is applied.

**Modulus of Elasticity** Rate of change of strain as a function of stress. The slope line portion of a stress–strain diagram.

**MPa** The SI-derived unit of stress is the pascal ( $1 \text{ N/m}^2$ ). The “megapascal” is  $1 \text{ N/mm}^2$ .

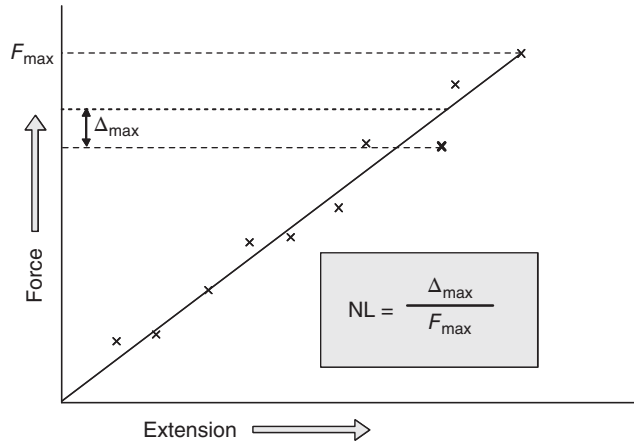
**Newton** The SI-derived unit of force is the newton (the force that produces an acceleration of  $1 \text{ m/s}^2$  on a mass of  $1 \text{ kg}$ ).

**Nonlinearity** Nonlinearity can be evaluated for either an individual data point or for a measurement run.

For an individual point it is the difference between measured output at a specific load and the corresponding point on the straight-line fit to the output data. Normally expressed in units of %FSD.



The nonlinearity for a measurement is usually defined as the maximum deviation between the measured output and straight-line fit to the output data. This can be expressed in terms of the measurement units or %FSD.



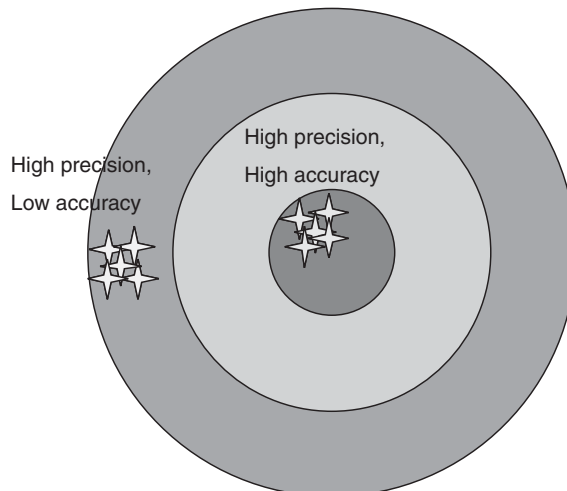
**Nonrepeatability** Sometimes used to mean the same as repeatability.

**Overload** Applying a force that exceeds the capacity of the load cell. Repeated overload, or significant overload, can damage the load cell and require a recalibration or replacement. It is important to ensure that there is headroom built in to your system, that is, use a load cell that has a capacity of approximately 120% of the expected maximum load.

**Photo Etch** A manufacturing process utilizing light upon a photochemically sensitive layer to create a template pattern on very thin material.

**Piezoelectric Effect** Whereby a material exhibits a voltage created when its dimensions are changed. Conversely, a piezoelectric material will exhibit a dimensional change if an electric field is applied.

**Precision** The expression of how close multiple measurements of the same quantity are to each other. Not to be confused with accuracy.



**psi** “Pounds per square inch,” the imperial unit of stress.

**Quasi-digital** An output signal that is time based, for example, a frequency, that can be then coupled directly to a digital circuit with time measurement capability.

**Refractive Index** The ratio of speed of light in a material to the speed of light in a vacuum

**Repeatability** The closeness of agreement between independent results obtained with the same method on identical test material, under the same conditions (same operator, same apparatus, same laboratory and after short intervals of time). Traditionally, repeatability is expressed as the standard deviation of results from repeated measurements of loadings under identical loading and environmental conditions using the same operator. When using this method, quoting 2 times the standard deviation gives approximately 95% confidence. Sometimes the maximum difference between output readings is used. Normally expressed in units of %RO or %FSD.

In some contexts repeatability may be defined as the value below which the absolute difference between two single test results obtained under the above conditions may be expected to lie with a specified probability.

**Reproducibility** Reproducibility, although similar, should not be confused with repeatability. It is the closeness of agreement between independent results obtained with the same method on identical test material, under the same conditions but with different operators.

**Resonance** Resonance occurs when the frequency of an input signal coincides with the natural resonant frequency of a material or object.

**Sensitivity** The response of a device to a unit change input.

**SI Units** In 1960, the Syst me International d’Unit s (SI) was introduced to replace systems of units based upon the meter/kilogram/second (mks), the centimeter/gram/second (cgs), and the foot/pound/second (fps). It is based on seven basic units:

- Length, meter (m)
- Mass, kilogram (kg)
- Time, second (s)
- Electrical current, ampere (A)
- Temperature, Kelvin (K)
- Amount of a substance, mole (mol)
- Luminosity, candela (cd)

All other measurement units can be derived by a combination of these basic units.

**Signa** The absolute level of the measurable quantity into which a force input has been converted. Normally expressed as a displacement (as in a dial-type force gauge), or a voltage or current in electrical gauges and load cells.

**Standard Deviation** This is the root mean square deviation from the mean of a random distribution.

**Standard Uncertainty** A component of uncertainty in a measurement, expressed as a standard deviation  $S$ .

All components of an uncertainty will be combined to form the uncertainty of measurement as quoted on a calibration certificate.

**Static Force** In door closing applications: This is the average force from the end of the dynamic time until data acquisition stops, that is, at 6 s.

**Strain** Usually used to denote the engineering strain. Quantitatively, it is the change in length of a specimen (as a result of an applied load) divided by the original length of the specimen; it is usually expressed as a percentage.

**Strain Gauge** A device with electrical resistance that is a function of the applied strain; normally in a Wheatstone bridge configuration.

**Stress** Usually used to denote the engineering stress. It is the load applied to a specimen, divided by the cross-sectional area of the specimen. Pressure. Can be measured in  $\text{N}/\text{mm}^2$ ,  $\text{N}/\text{m}^2$ , psi, MPa, or kPa.

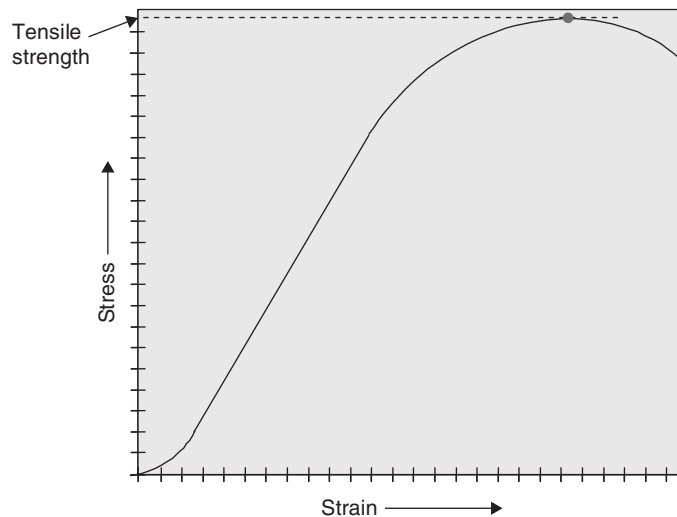
**Tare** To automatically subtract either the weight of a container, fixture, or specimen or the residual force being exerted by the specimen. Subsequent readings correspond either to the weight of the contents of a container or to the force being exerted (through the fixturing) by a specimen under tensile or compressive load.

**Temperature Range, Compensated** The range of temperature over which the load cell is compensated to maintain output and zero balance within specified limits.

**Temperature Range, Operating** The extremes of ambient temperature within which the load cell will operate without permanent adverse change to any of its performance characteristics.

**Tension** A force tending to stretch or elongate a specimen or material.

**Tensile Strength** The ultimate strength of a material subjected to tensile loading. It is the maximum stress developed in a material during a tensile test.



**Tensile Test** A tensile test is a way of determining how something will react when it is being pulled apart, or more correctly, when a force is applied to it in tension. Also known as a pull test.

**Torque** A twisting effect, or moment, exerted by a force acting at a distance on a body, equal to the force multiplied by the perpendicular distance between the line of action of the force and the center of rotation at which it is exerted. Torque is often expressed in units: N m, kgf m, kgf cm, lbf ft, and lbf in.

**Torsion Test** Method for determining behavior of materials subjected to twisting loads. Shear properties are often determined in a torsion test (ASTM E-143).

**Torsional Modulus** AKA torsional modulus of elasticity, it is usually equal to the shear modulus. It is the modulus of elasticity of a material subjected to a twisting force.

**Traceability** Traceability is the property of a measured result or value of a standard, whereby it can be related to stated references, usually national or international primary or secondary standards, through an unbroken chain of comparisons and all having stated uncertainties.

**Transducer** Device that converts a physical input into an output of a different form.

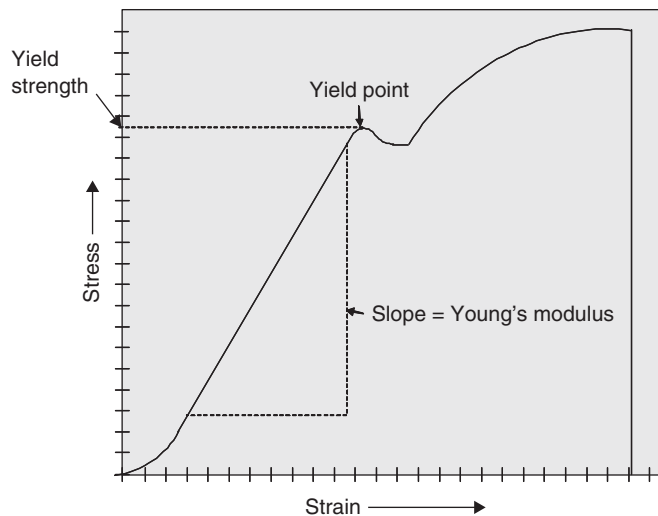
**True Strain** This differs from engineering strain in that it is determined from the rate of change in gauge length with respect to the instantaneous gauge length. It is expressed as a natural logarithm of engineering strain.

**True Stress** True stress is the load divided by the instantaneous area of the specimen.

**Ultimate Strength** The highest engineering stress developed in material during a test and prior to rupture or break. Normally, changes in area due to changing load and necking are disregarded in determining ultimate strength.

**Wave** Consisting of amplitude and frequency, a wave is a disturbance through a material or vacuum that is normally accompanied by a transfer of energy.

**Yield Point/Yield Strength** The point during a tensile test when a specimen ends elastic deformation and begins plastic deformation. There is an increase in strain with no corresponding increase in stress.



Yield strength is an indication of maximum stress that can be developed in a material without causing plastic deformation. It is the stress at which a material exhibits a specified permanent deformation and is a practical approximation of elastic limit.

**Young's Modulus** Hooke's law states

$$F = -kx$$

where  $F$  is the restorative force,  $x$  is the displacement, and  $k$  is a force (or spring) constant. Put another way

$$E = \frac{\text{strain}}{\text{stress}}$$

where stress is the force applied to the specimen and strain is the relative elongation of the specimen from its original length.  $E$  is known as Young's Modulus, represented as the gradient of the stress–strain curve within the initial linear region.

## REFERENCES

1. Aristotle (4th century BC) *Physics: Bks. 1-4—Loeb Classical Library* No. 228, Vol 2. Harvard University Press, Cambridge, 1934.
2. G. Galileo, *Dialogue Concerning the Two Chief World Systems (1632)*—Translated by Drake, 1953 (abridged).
3. I. Newton, *Principia Mathematica*, 1685.
4. A. Einstein, "Die Grundlage der allgemeinen Relativitätstheorie," *Ann. Phys.*, **354**, 769–822, 1916.
5. Institute of Measurement and Control (London), *Force Measurement Guide*, Institute of Measurement and Control (London), 1996.
6. R. Hooke, *Lectures de potentia restitutiva, or, Of Spring [microform]: Explaining the Power of Springing Bodies: To Which Are Added Some Collections*, Martyn, London, 1678.
7. T. Young, *Lectures on Natural Philosophy*, Vol. 1. London, 1807, pp. 78–79.
8. W. Thomson "On the Electro-dynamic Qualities of Metals," *Phil. Trans. Roy. Soc. London*, 1 **146**, 649–751, 1856.
9. E. E. Simmons Jr., "Material Testing Apparatus," U. S. patent no. 2292549, 1942.
10. J. Dietrich, "Simmons and the Strain Gage," *Eng. Sci.*, **50**, 19–23, 1986.
11. P. G. S. Jackson, "The Early Days of the Saunders-Roe Foil Strain Gauge," *Strain*, **26**, 61–66, 1990.
12. Young and Freedman, *University Physics with Modern Physics*, 10th ed., 2000, p. 806; Young and Freedman, *Instrumentation for Engineering Measurements*, 2nd ed., pp. 129–135.
13. C. Wheatstone, "The Bakerian Lecture: An Account of Several New Instruments and Processes for Determining the Constants of a Voltaic Circuit," *Phil. Trans. Roy. Soc. London*, **133**, 303–327, 1843.
14. R. M. Langdon, "Resonator Sensors—A Review," *Jo. Phys. E: Sci. Instrum.* **18**, 103, 1985.
15. A. Cheshmehdoost and B.E. Jones, "A New Cylindrical Structure Load Cell with Integral Resonators, *Proceedings SENSORS VI: Technology, Systems and Applications*, IOP Publishing, Bristol, 1993, pp. 429–434.
16. E. P. Eernisse, R. W. Ward, R. B. Wiggins, et al., "Survey Quartz Bulk Resonator Sensor Technologies," *Proceedings IEEE International Frequency Control Symposium*, pp. 24–32, 1996.
17. T. Yan, et al., "Metallic Triple Beam Resonator with Thick-Film Printed Drive and Pickup." 17th European Conference on Solid State Transducers, pp. 10–13, 2003.
18. J. Intiang, et al., "Characteristics of 9mm Metallic Triple-Beam Tuning Fork Resonant Sensor," *Proceedings Sensors and Their Applications XIV (SENSORS07)*, *Jo. Phys.: Confe. Series*, **76**, 2007.
19. H. Toshiyuki, et al., "Development and Evaluation of Tuning Fork Type Force Transducers," XVIII Imeko World Congress, Metrology for a Sustainable Development, Sept. 17–22, 2006, Rio de Janeiro, Brazil, 2006.
20. Forcensys Ltd., Printed Tuning Fork Sensors, Application Whitepaper, Summer, 2007.
21. L. Rayleigh, "On Waves Propagating along the Plane Surface of an Elastic Solid," *Proc. London Math. Soc.*, **7**, 4–11, 1885.
22. L. T. Ikelle and L. Amundsen, "Introduction to Petroleum Seismology: 12 (investigations in Geophysics)," *Soci. Explor. Geophys.* 2005.
23. R. M. White and F. W. Voltmer, "Direct Piezoelectric Coupling to Surface Elastic Waves," *Appl. Phys. Lett.* **7**, 314–316, 1965.
24. C. K. Campbell, "Applications of Surface Acoustic and Shallow Bulk Acoustic Wave Devices," *Proc IEEE*, **77**(10), 1453–1484, 1989.
25. P. Hauptmann, *Sensors, Principles and Applications*, Prentice Hall, Engelwood Cliffs, NJ, 1991.
26. C. Wold, et al., "Temperature Measurement Using Surface Skimming Bulk Waves," *Proc. Ultrason. Symp.*, **1**, 441–444, 1991.

27. D. Cullen and T. Reeder, "Measurement of SAW Velocity versus Strain for YX and ST Quartz," *Pro. Ultrason. Symp.*, 519–522, 1975.
28. D. Cullen, and T. Montress, "Progress in the Development of SAW Resonator Pressure Transducers", *Proc. Ultrason. Symp.* **2**, 519–522, 1980.
29. A. Lonsdale and B. Lonsdale, Method and Apparatus for Measuring Strain, International patent public. No. WO91/13832, 19 Sept. 1991, Int. Applic. No. PCT/GB91/00328, Int. filing date: 4 March 1991, Priority: 9004822.4, 3 March 1990, GB.
30. V. Kalinin et al., High-Speed High Dynamic Range Resonant SAW Torque Sensor for Kinetic Energy Recovery System, Proceedings ETFT 2010, Session 5,
31. Bruce et al. 1946.
32. M. Born, and E. Wolf, *Principles of Optics*, 7th ed., Cambridge University Press, Cambridge, UK, 1999.
33. R. Yun-Jiang, "In Fibre Bragg Grating Sensors, *Measure. Scie. Tech.* **8**; 355–375, 1997.
34. K. O. Hill, et al. "Photosensitivity in optical fiber Waveguides: Application to Reflection Filter Fabrication, *Appl. Phys. Lett.* **32**, 647–649.
35. M. Kreuzer, White Paper. *Strain Measurement with Fiber Bragg Grating Sensors*. HBM, Darmstadt, Germany, 2007; available at: <http://www.HBM.com>.
36. M. Tatti, et al., Production and Use of an Interferometric Optical Strain Gauge with Comparison to Conventional Techniques," *Optics Lasers Eng.* **27**, 269–284, 1997.
37. B. Gholamzadeh and H. Nabovati, "Fiber Optic Sensors," *World Acad. Sci., Eng. Tech.*, **42**, 297–307, 2008.
38. J. P. Joule, "On the Effects of Magnetism upon the Dimensions of Iron and Steel Bars. *Phil. Mag. J. Sci.* **30** (Third Series: 76–87), 225– 241, 1847.
39. N. B. Ekreem, A. G. Olabi, T. Prescott, A. Rafferty, and M. S. J. Hashmi "An Overview of Magnetostriction, Its Use and Methods to Measure These Properties," *Jou. Mate. Proc. Tech.* **191**(1–3), 96–101, 2007.
40. S. Dan Mihai, *Handbook of Force Transducers Principles and Components*, Springer Berlin, 2011.
41. A. Bienkowski, R. Szewczyk, and J. Salach, Industrial Application of Magnetoelastic Force and Torque Sensors, *Acta Phys. Polon. A*, **118**(5); 1008–1009, 2010.
42. G. Ausanio et al. "Magnetoelastic sensor application in Civil Buildings Monitoring," *Sensors Actuators A: Phys.*, **123–124**, 290–295, 2005.
43. R. Boynton, *Precise Measurement of Mass*, Sawe Paper. No. 3147, S.A.W.E., Arlington TX, 2001.
44. International Organization for Standardization (ISO). *Guide to the Expression of Uncertainty in Measurement*, International Organization for Standardization; 1995.
45. M3003, *The Expression of Uncertainty and Confidence in Measurement*, 2nd ed., UKAS, 2007.
46. "European Co-operation for Accreditation," *Expression of the Uncertainty of Measurement in Calibration*, Publication reference EA-4/02, 1999.



# CHAPTER 18

## RESISTIVE STRAIN MEASUREMENT DEVICES

**Mark Tuttle**  
University of Washington  
Seattle, Washington

<b>1 PRELIMINARY DISCUSSION</b>	<b>659</b>	2.4 Strain Gauge Rosettes	670
1.1 Scope	659	2.5 The Wheatstone Bridge	673
1.2 Definition of Strain	659	<b>3 SEMICONDUCTOR STRAIN GAUGES</b>	<b>676</b>
1.3 Practical Implications	664	<b>4 LIQUID METAL STRAIN GAUGES</b>	<b>678</b>
<b>2 RESISTANCE METAL STRAIN GAUGES</b>	<b>664</b>	<b>REFERENCES</b>	<b>679</b>
2.1 General Description	664		
2.2 Strain Sensitivity	665		
2.3 Strain Gauge Alloys and Calibration Parameters	666		

### 1 PRELIMINARY DISCUSSION

#### 1.1 Scope

The measurement of strain is a fundamental necessity in many engineering disciplines and related industries. Consequently, many strain measurement techniques have been developed. Methods of measurement can be roughly grouped into two major categories: those based on the behavior of light and those based on electronic devices. Examples of the former include reflection photoelasticity, geometric moiré, moiré interferometry, holographic interferometry, and digital image correlation (DIC). Examples of the latter include techniques that infer strain based on some change in an electrical characteristic of a strain measurement device, such as changes in resistance, inductance, or capacitance.

A significant discussion of all of these techniques would require a major treatise and is beyond the scope of this chapter. Rather, discussion is focused herein on one subcategory: strain measurements obtained by monitoring resistance changes. This focus is appropriate because at present strain measurement via resistance strain gauges is by far the most widely used technique, although other methods (particularly DIC) are gaining in popularity. The reader interested in strain measurement methods beyond those described here is referenced to one of several excellent books devoted to these topics, including Refs.1–5.

#### 1.2 Definition of Strain

In this chapter, strain is discussed within the framework of continuum mechanics. In continuum mechanics, matter is studied at a physical scale large enough such that existence of individual atoms or molecules is not perceptible. That is, continuum mechanics analyses treat matter as a



continuous substance, rather than as an assembly of discrete particles. This forms the basis of two major fields of study, *solid* mechanics and *fluid* mechanics. A solid substance is one that can resist deformation due to shear stress, whereas a fluid substance cannot. This chapter is devoted to strains encountered in solid mechanics.

*Strain* is essentially a description of the deformations that have occurred at a point in a solid body. Many different factors may have caused the deformation, including application of surface forces, gravity effects, electromagnetic forces, temperature changes, and so on or some combination thereof. The mechanisms that caused the deformations are immaterial to this discussion. It is sufficient to say that the deformation has occurred, and hence a nonzero *state of strain* may exist at any point in the solid body. The definition used to describe strain depends on the magnitudes of the deformation. *Finite strain theory* is used when the deformation is arbitrarily large, whereas *infinitesimal strain theory* is used when the magnitude of the deformation is small. Throughout this chapter it will be assumed that deformations are small, such that infinitesimal strain theory can be applied. This is usually the case for structures encountered in civil, mechanical, and aerospace structural engineering.

Displacements of a solid body in the  $x$ ,  $y$ , and  $z$  directions are typically denoted  $u(x, y, z)$ ,  $v(x, y, z)$ , and  $w(x, y, z)$ , respectively. Infinitesimal strains are related to displacements as follows:

$$\begin{aligned}\epsilon_{xx} &= \frac{\partial u}{\partial x} & \gamma_{xy} &= \gamma_{yx} = \left( \frac{\partial v}{\partial x} + \frac{\partial u}{\partial y} \right) \\ \epsilon_{yy} &= \frac{\partial v}{\partial y} & \gamma_{yz} &= \gamma_{zy} = \left( \frac{\partial w}{\partial y} + \frac{\partial v}{\partial z} \right) \\ \epsilon_{zz} &= \frac{\partial w}{\partial z} & \gamma_{zx} &= \gamma_{xz} = \left( \frac{\partial u}{\partial z} + \frac{\partial w}{\partial x} \right)\end{aligned}\quad (1)$$

Strain components  $\epsilon_{xx}$ ,  $\epsilon_{yy}$ , and  $\epsilon_{zz}$  are called *normal strains*, whereas  $\gamma_{xy} = \gamma_{yx}$ ,  $\gamma_{yz} = \gamma_{zy}$ , and  $\gamma_{zx} = \gamma_{xz}$  are called *engineering shear strains*. To fully describe the state of strain at a point, the numerical values of all six independent strain components must be specified.

Although strains occur in three dimensions, most strain measurements are limited to strains that occur on the surface of a solid. Let the surface of interest lie in the  $x - y$  plane. Therefore, the three strain components to be measured are  $\epsilon_{xx}$ ,  $\epsilon_{yy}$ , and  $\gamma_{xy}$ .

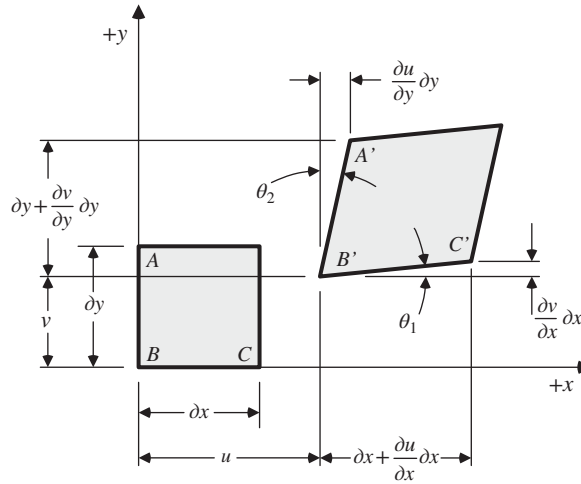
A physical interpretation of normal and engineering shear strains that occur in the  $x - y$  plane can be developed based on the two-dimensional sketch shown in Fig. 1. Imagine that a rectangle with dimensions  $dx$  and  $dy$  has been drawn on a flat surface. Three corners of the rectangle are labeled as  $A$ ,  $B$ , and  $C$ . Initially, the angle  $ABC$  is precisely  $\pi/2$  radians (i.e., initially  $ABC = 90^\circ$ ). Now assume some mechanism(s) causes a displacement of the surface, and consequently the rectangle displaces as shown. The sides of the rectangle have increased in length and rotated, such that  $A'B'C' < \pi/2$ .

Normal strains in the  $x$  and  $y$  directions,  $\epsilon_{xx}$  and  $\epsilon_{yy}$ , respectively, are defined as change in length divided by the original length of the rectangle sides in the  $x$  and  $y$  directions. From Fig. 1, and assuming small displacements and displacement gradients, we have

$$\epsilon_{xx} = \frac{[\partial_x + (\partial_u / \partial_x)\partial_x] - (\partial x)}{\partial_x} = \frac{\partial u}{\partial x}$$

and

$$\epsilon_{yy} = \frac{[\partial_y + (\partial v / \partial_y)\partial_y] - (\partial y)}{\partial_y} = \frac{\partial v}{\partial y}$$



**Figure 1** Sketch used to visualize infinitesimal strain.

These results are among those listed in Eq. (2). A normal strain corresponding to an increase in length is called a *tensile strain* and is algebraically positive. Conversely, a normal strain corresponding to a decrease in length is called a *compressive strain* and is algebraically negative. Note that normal strain is a unitless quantity since it is a ratio of two lengths.

Referring again to Fig. 1, engineering shear strain  $\gamma_{xy}$  is defined as the *change* in  $ABC$ , expressed in radians. That is, engineering shear strain equals the *sum* of angles  $\theta_1$  and  $\theta_2$ :

$$\gamma_{xy} = \gamma_{yx} = \theta_1 + \theta_2$$

The tangent of angle  $\theta_1$  is given by

$$\tan \theta_1 = \frac{(\partial v / \partial x) dx}{dx + (\partial u / \partial x) dx} = \frac{\partial v / \partial x}{1 + (\partial u / \partial x)}$$

Assuming small displacement gradients, the denominator in this expression is very close to unity, and hence

$$\tan \theta_1 \approx \frac{\partial v}{\partial x}$$

An identical process leads to

$$\tan \theta_2 \approx \frac{\partial u}{\partial y}$$

Again assuming small displacements and displacement gradients, which in the present context implies that both  $\theta_1$  and  $\theta_2$  are small angles expressed in radians, we have

$$\tan \theta_1 \approx \theta_1 \quad \text{and} \quad \tan \theta_2 \approx \theta_2$$

Combining the above, we find

$$\gamma_{xy} = \gamma_{yx} = \theta_1 + \theta_2 = \frac{\partial v}{\partial x} + \frac{\partial u}{\partial y}$$

This result is among those listed in Eq. (2). A shear strain is positive if  $ABC$  has *decreased* (thus, Fig. 1 illustrates a *positive* engineering shear strain). Since shear strain is an angle

measured in radians, and since radians are defined as the ratio of two lengths and are, therefore, unitless, shear strain is a unitless quantity.

In passing, the reader should contrast the definition of engineering shear strain described earlier to the definition of *tensoral shear strain*, usually denoted  $\epsilon_{xy} = \epsilon_{yx}$ . Tensoral shear strains are defined as the *average* of angles  $\theta_1$  and  $\theta_2$ , rather than the sum:

$$\epsilon_{xy} = \epsilon_{yx} = \frac{\theta_1 + \theta_2}{2}$$

Hence, engineering shear strain differs from tensoral shear strain by a factor of 2:

$$\gamma_{xy} = \gamma_{yx} = 2\epsilon_{xy} = 2\epsilon_{yx}$$

Although the use of tensoral shear strain is mathematically elegant, engineering shear strains are far more commonly used in practice. The use of engineering shear strain will be assumed throughout the remainder of this chapter. In the following discussion, the phrase “engineering shear strain” will be abbreviated as “shear strain.”

Consider the tensile member shown in Fig. 2*a*. A square grid pattern referenced to the  $x$ - $y$  coordinate system is printed on the surface of the member. An axial tensile load is applied, causing both an increase in length and decrease in width (Fig. 2*b*). It is apparent that the initially square grids will deform into rectangles. Qualitatively, the following strains are induced

$$\epsilon_{xx} < 0 \text{ (compressive)}$$

$$\epsilon_{yy} > 0 \text{ (tensile)}$$

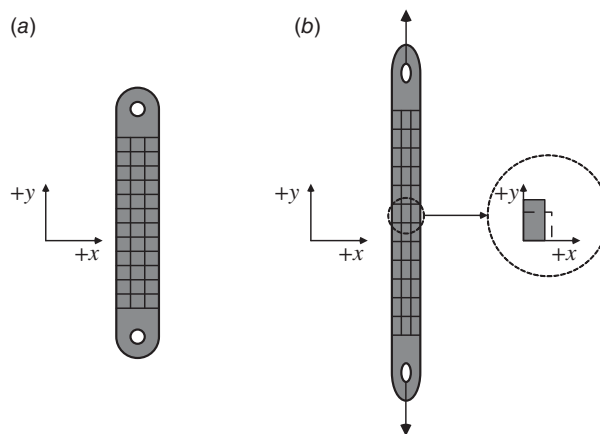
$$\gamma_{yy} = 0 \text{ (no change in angle)}$$

Now consider the identical tensile member shown in Fig. 3*a*. In this case, the square grid pattern is referenced to a  $x'$ - $y'$  coordinate system oriented  $\theta$  degrees counterclockwise from the longitudinal axis. An identical axial load is applied, causing an identical increase in length and decrease in width. However, the initially square grids now deform into a rhombus. The insert in Fig. 3*b* implies that the following strains have been induced:

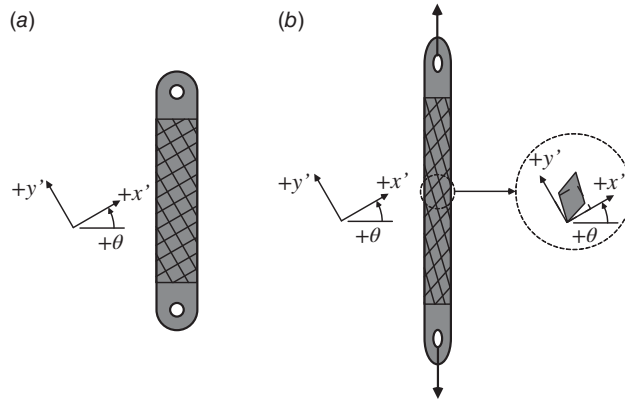
$$\epsilon_{x'x'} < 0 \text{ (compressive)}$$

$$\epsilon_{y'y'} > 0 \text{ (tensile)}$$

$$\gamma_{y'y'} > 0 \text{ (decrease in corner angle)}$$



**Figure 2** Beam with a square grid pattern parallel to beam axis: (a) undeformed and (b) deformed.



**Figure 3** Beam with a square grid pattern inclined  $\theta$  degrees from the beam axis: (a) undeformed and (b) deformed.

Figures 2 and 3 illustrate two important points. First, although strain is a description of deformation, the numerical values of the individual strain components that (collectively) describe the deformation depend on the coordinate system used. For example, the numerical values of the strain components illustrated in Fig. 2. differ from the numerical values of the strain components illustrate in Fig. 3, even though the tensile member deformation is identical in both cases. The description of the deformation, that is, the strains, can be rotated from one coordinate system to another using the *strain transformation equations*. Recall that the present discussion has been limited to strains within a plane. For this case, if strain components relative to the  $x$ - $y$  coordinate system are known ( $\epsilon_{xx}$ ,  $\epsilon_{yy}$ ,  $\gamma_{xy}$ ), then strain components referenced to a new  $x'$  -  $y'$  coordinate system-oriented  $\theta$  degree from the  $x$ - $y$  coordinate system are given by

$$\begin{aligned}\epsilon_{x'x'} &= \epsilon_{xx} \cos^2 \theta + \epsilon_{yy} \sin^2 \theta + \gamma_{xy} \sin \theta \cos \theta \\ \epsilon_{y'y'} &= \epsilon_{xx} \sin^2 \theta + \epsilon_{yy} \cos^2 \theta - \gamma_{xy} \sin \theta \cos \theta \\ \gamma_{x'y'} &= 2 \sin \theta \cos \theta (\epsilon_{yy} - \epsilon_{xx}) + \gamma_{xy} (\cos^2 \theta - \sin^2 \theta)\end{aligned}\quad (2)$$

The algebraic sign of angle  $\theta$  is defined in accordance with the right-hand rule. For example, in Fig. 3 angle  $\theta$  is a positive angle since axis  $x'$  is rotated *from* the  $x$  axis *toward* the  $y$  axis.

The second important point illustrated by Fig. 2 and 3 is that there is always a particular coordinate system, called the *principal strain coordinate system*, in which shear strains are zero. Obviously, the coordinate system used in Fig. 2 is a principal strain coordinate system, whereas the coordinate system used in Fig. 3 is not. The normal strains that exist in the principal coordinate system are called the *principal strains* and are denoted  $\epsilon_1$ ,  $\epsilon_2$ , and  $\epsilon_3$ . Since in this discussion it has been assumed that out-of-plane shear strains  $\gamma_{yz} = \gamma_{zx} = 0$ , one of the principal strains is the out-of-plane normal strain  $\epsilon_{zz}$ . The other two principal strains lie within the  $x$ - $y$  plane. Ordinarily, the three principal strains are ordered such that  $\epsilon_1 > \epsilon_2 > \epsilon_3$ . However, since in the present case  $\epsilon_{zz}$  is always a principal strain, the convention adopted here is that  $\epsilon_3 = \epsilon_{zz}$ , and the two in-plane strains will be labeled  $\epsilon_1$  and  $\epsilon_2$ . If strain components ( $\epsilon_{xx}$ ,  $\epsilon_{yy}$ ,  $\gamma_{xy}$ ) are known, then the in-plane principal strains are given by

$$\epsilon_{1,2} = \frac{\epsilon_{xx} + \epsilon_{yy}}{2} \pm \sqrt{\left(\frac{\epsilon_{xx} - \epsilon_{yy}}{2}\right)^2 + \left(\frac{\gamma_{xy}}{2}\right)^2}\quad (3)$$

The angle  $\theta_p$  from the  $x$  axis to the 1 axis is given by

$$\theta_p = \tan^{-1} \left[ \frac{2(\epsilon_1 - \epsilon_x)}{\gamma_{xy}} \right] = \tan^{-1} \left[ \frac{\gamma_{xy}}{2(\epsilon_1 - \epsilon_y)} \right] \quad (4)$$

### 1.3 Practical Implications

As is evident from the preceding discussion, strain measurement involves two types of measurements. Normal strains require measurement of a change in length, and shear strains require measurement of a change in angle. Conceptually, these could be made with a simple ruled scale and protractor. For two reasons, these simple measurement devices are usually inadequate. First, the changes in lengths and angles involved are exceedingly small and difficult to measure precisely with simple measurement devices. A numerical example will serve to illustrate this difficulty. Many steel alloys will yield at a strain level of about 0.0012 m/m, or about  $1200 \times 10^{-6}$  m/m =  $1200 \mu\epsilon$  (read: “1200 microstrain”). This implies a steel element with an initial length of 10 mm will increase to a length of 10.012 mm at yielding. Recognizing that structural engineers are required to measure strains well below yielding, it is obvious that ruled scales do not provide the resolutions required. Similarly, many steel alloys subjected to a pure shear strain will yield at a shear strain level of about 0.0016 rad, or about  $1600 \times 10^{-6}$  rad =  $1600 \mu\epsilon$  (about  $0.09^\circ$ ). Once again, simple protractors cannot be used to measure such small angular changes.

Second, since strains generally vary throughout a structure, the goal is usually to measure strains “at a point.” Thus, not only must very small changes in length and angle be measured, but also these changes must be measured over as small an initial area as possible.

Finally, for a simple isotropic structure such as that shown in Fig. 2 the orientation of the principal axis is known by inspection. In contrast, for the complex structural shapes and loadings typically encountered in practice, the orientation of the principal coordinate system is rarely known a priori.

## 2 RESISTANCE METAL STRAIN GAUGES

### 2.1 General Description

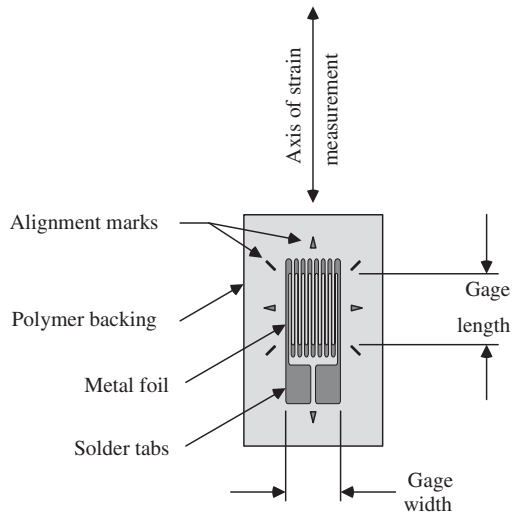
Nowadays, the most widely used strain measurement device is certainly the resistance metal strain gauge and is originally known as “bonded wire strain gauges,” they are based on a phenomenon first noticed by William Thomson (later named Lord Kelvin) in 1856: The resistance of an electrically conductive metal wire is increased if the wire is stretched and decreased if the wire is compressed. This phenomenon has since come to be known as the piezoresistive effect.\*

Based on this observation and working independently, Edward Simmons (in about 1937) and Arthur Ruge (in 1938) bonded small metal wires to structures they were studying and monitored the resistance change as the structures were loaded. The change in resistance provided an indirect measure of the change in wire length and hence strain. Simmons and Ruge are considered to be the coinventors of resistance strain gauges. The first resistance strain gauges became commercially available in 1941 and were marketed under the trade name “SR-4 gauge,” in honor of Simmons, Ruge, and two colleagues who helped perfect and market the gauge.

The next major development occurred in 1952, when engineers at Saunders-Roe Ltd. used the photoetch process to produce strain-sensing elements from thin metal foil rather than wire. The etching process makes it possible to produce large numbers of very small and complex

---

\* The piezoresistive effect should not be confused with the piezoelectric effect. In the former, a mechanical strain results in a resistance change. In the latter, a mechanical strain causes an electrical potential to occur.



**Figure 4** Basic elements of a metal foil strain gauge.

sensing elements from a single parent sheet of metal foil. Although wire gauges are still used in some circumstances, today most resistance metal strain gauges are produced using the photoetch process.

The basic construction of a metal foil strain gauge is summarized in Fig. 4. The sensing element is etched from a parent metal foil in the desired pattern and bonded to a thin and flexible polymeric backing film. Backing films of polyimide or glass-reinforced epoxy are most commonly used, and serve to stabilize the delicate foil pattern during handling and also to electrically isolate the metal foil from the underlying substrate. The metal foil/backing film is subsequently adhesively bonded to the surface of interest. A good bond between the surface and the gauge assembly is critically important since the strain being measured must be transferred through the adhesive bond line and backing film to the metal foil. Detailed strain gauge bonding instructions are provided by strain gauge manufacturers, and the user is well advised to follow these instructions precisely.

The gauge pattern is designed such that strain is sensed primarily in the axial direction of the grid. Alignment marks are included as an alignment aid during the bonding process. Traditionally, leadwires are soldered to the solder tabs of the gauge after it has been bonded to the surface, although it is possible to attach the leadwires prior to bonding, and in fact most strain gauge manufacturers now offer gauges with preattached leadwires.

## 2.2 Strain Sensitivity

Strain sensitivity is a measure of how much resistance changes per unit strain and is defined as

$$S = \frac{\partial R/R}{\epsilon} \quad (5)$$

Strain sensitivity for pure metals ranges from about  $-12 < S < 6$ . Alloys commonly used in strain gauges have strain sensitivities ranging from about 2 to 4. Note that a positive strain sensitivity implies that a tensile strain ( $\epsilon > 0$ ) causes an increase in resistance ( $\partial R > 0$ ).

Strain sensitivity is often equated to the “gauge factor” of the strain gauge. In reality, there is a subtle difference between strain sensitivity, as defined by Eq. (6), and the gauge

factor measured for a strain gauge. The difference arises because of differences in the strain field present during measurement of strain sensitivity versus the strain field present during measurement of the gauge factor. That is, strain sensitivity of an alloy is measured by applying uniaxial stress to an unconstrained metal specimen (typically a wire with circular cross section) with initial resistance  $R$ . The resulting normal strain in the direction of loading  $\epsilon$  and change in resistance  $\partial R$  are measured and used to calculate the strain sensitivity. Since the specimen is unconstrained, due to the Poisson effect a transverse strain equal to  $-\nu\epsilon$  also occurs, where  $\nu$  is the Poisson ratio of the wire. The definition of strain sensitivity implies that this transverse strain is allowed to occur.

If the transverse strain actually differs from  $-\nu\epsilon$ , which is a common occurrence for a strain gauge bonded to a structure, then the resistance change of the bonded strain gauge may not correspond to the strain sensitivity. This situation is described in greater detail in a following section titled “Gauge Factor and Transverse Sensitivity Coefficient.”

### 2.3 Strain Gauge Alloys and Calibration Parameters

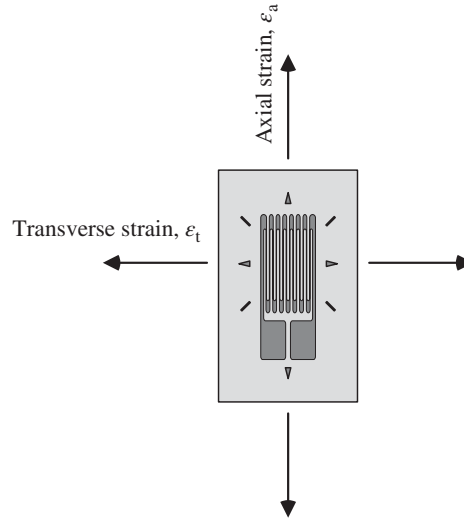
Strain gauges have been produced using many different metal alloys since their introduction in 1941. The most common gauge alloys are summarized in Table 1. These alloys have become preferred for various reasons, including the ability to roll the alloy into thin metal foils, ease of soldering lead wires to the alloy, linear change in resistance with strain, high strain to failure, good fatigue life, and thermal stability. Calibration parameters provided by the manufacturer include the gauge resistance, the gauge factor and transverse sensitivity coefficient, and the self-temperature compensation (STC) number.

*Gauge Resistance:* In principle, a strain gauge with any initial resistance can be used.

In practice, 120-, 350-, or 1000- $\Omega$  gauges are most common since most commercial strain gauge amplifiers and data acquisition systems are designed to accept one of these resistances. The primary reason for selecting one gauge resistance over another is the self-heating effect. That is, during the measurement process, a voltage is applied to the gauge, and the associated electrical current passing through the gauge will cause an increase in gauge temperature. Unstable temperature fluctuations may occur if a relatively high voltage is applied and the gauge is bonded to a substrate that is a poor

**Table 1** Common Resistance Strain Gauge Alloys

Alloy	Nominal Composition	Gauge Factor ( $S_g$ )	Comments
Constantan (or advance)	45% Ni, 55% Cu	2.1	Most widely used general-purpose gauge alloy Max strain $\sim 3\text{--}5\%$ (30,000–50,000 $\mu\epsilon$ )
Karma	74% Ni, 20% Cr, 3% Al, 3% Fe	2.0	Excellent long-term stability More difficult to solder than Constantan Max strain $\sim 1.5\%$ (15,000 $\mu\epsilon$ )
Isoelastic	36% Ni, 8% Cr, 0.5% Mo, 55.5% Fe	3.6	High thermal output Max strain $\sim 1.5\%$ , but nonlinear at strains above 0.5% (5000 $\mu\epsilon$ ) Excellent fatigue life
Nichrome V	80% Ni, 20% Cr	2.1	Used for high-temperature strain gauges
Armour D	70% Fe, 20% Cr, 10% Al	2.0	Difficult to solder using standard methods
Alloy 479	92% Pt, 8% W	4.0	



**Figure 5** Strain gauge subjected to a biaxial strain field.

thermal conductor. The manufacturer provides recommendations on the maximum voltage (i.e., power) that can be safely applied based on the thermal properties of the substrate.

*Gauge Factor and Transverse Sensitivity Coefficient.* A strain gauge subjected to a biaxial strain field is shown in Fig. 5. The resistance of the gauge will be changed due to *both* the axial and the transverse strain components,  $\epsilon_a$  and  $\epsilon_t$ , respectively. This is an undesirable characteristic since it would be ideal if the gauge would respond *only* to the axial strain component. The gauge factor and transverse sensitivity coefficient are calibration parameters that allow the user to remove the undesirable response to transverse strains from the strain signal.

Suppose a gauge is subjected to an axial strain *only* (i.e., assume  $\epsilon_t = 0$ ). The axial strain sensitivity of the gauge,  $S_a$ , is defined under this condition:

$$S_a = \frac{\Delta R_a / R_g}{\epsilon_a} \quad (6)$$

where  $R_g$  = original gauge resistance;

$\Delta R_a$  = change in gauge resistance due to axial strain

Note that the definition of the axial strain sensitivity is similar to the expression used to calculate the strain sensitivity of an alloy [Eq. (6)]. However, a requirement associated with Eq. (7) is that the transverse strain is zero, whereas this restriction is not imposed during measurement of the strain sensitivity of an alloy.

Now consider a case in which the gauge is subjected to a transverse strain *only* (i.e.,  $\epsilon_a = 0$ ). For this condition the transverse strain sensitivity of the gauge can be defined as

$$S_t = \frac{\Delta R_t / R_g}{\epsilon_t} \quad (7)$$

where  $\Delta R_t$  is the change in gauge resistance due to transverse strain  $\epsilon_t$ .

Gauge manufacturers measure both the axial and the transverse strain sensitivities by subjecting a gauge to pure axial or pure transverse strain, using a fixture specially designed for



this purpose and described in an ASTM standard.<sup>6</sup> The *transverse sensitivity coefficient*,  $K_t$ , is defined as the ratio of the transverse and axial strain sensitivities:

$$K_t = \frac{S_t}{S_a} \quad (8)$$

The measured  $K_t$  is included in the calibration materials provided with each gauge and is customarily defined as a percentage. For example, if a transverse sensitivity of 0.010 is measured for a particular gauge, the manufacturer will report a value  $K_t = 1.0\%$ .

Now consider the case in which the gauge is subjected to *both* the axial and transverse strains simultaneously. The total change in gauge resistance  $\Delta R$  in this case equals the sum of Eq. (7) and (8):

$$\frac{\Delta R_g}{R_g} = \left( \frac{\Delta R_a}{R_g} \right) + \left( \frac{\Delta R_t}{R_g} \right) = S_a \varepsilon_a + S_t \varepsilon_t \quad (9)$$

Substituting the definition of  $K_t$ , this equation can be written as

$$\frac{\Delta R_g}{R_g} = S_a (\varepsilon_a + K_t \varepsilon_t) \quad (10)$$

During calibration, the strain gauge is subjected to a *biaxial* strain field with a known ratio of  $\varepsilon_t / \varepsilon_a$ .<sup>6</sup> This is achieved by mounting a gauge in the axial direction on a tensile specimen with known Poisson ratio  $\nu_o$  and applying an axial load (usually,  $\nu_o = 0.285$ ). The resulting uniaxial state of stress causes a biaxial strain field, where the transverse strain is caused by the Poisson effect:

$$\varepsilon_t = -\nu_o \varepsilon_a \quad (11)$$

Substituting Eq. (12) into Eq. (11), the change in resistance for these conditions is

$$\frac{\Delta R_g}{R_g} = S_a (1 - \nu_o K_t) \varepsilon_a \quad (12)$$

The *gauge factor*  $S_g$  is defined as

$$S_g = S_a (1 - \nu_o K_t) \quad (13)$$

Substituting this definition into Eq. (13), we have

$$\frac{\Delta R_g}{R_g} = S_g \varepsilon_a \quad (14)$$

Through careful design of the gauge grid, strain gauge manufacturers has successfully reduced transverse strain sensitivities to near-zero levels for many gauge alloys and styles. If transverse strain sensitivity is reduced to a negligibly small value, then  $K_t \approx 0$ ,  $S_g \approx S_a$ , and Eq. (15) reduced to Eq. (6). If transverse strain sensitivity is not negligibly small, then a strain gauge measurement must be corrected for transverse sensitivity effects. Methods to correct for transverse sensitivity effects will be described in Section 2.4.

The strain sensitivity of an alloy, and consequently the gauge factor of a strain gauge, exhibits a modest temperature dependency. The magnitude and linearity of gauge factor variation with temperature depends on the alloy used. As a rough rule of thumb, the gauge factor for most commercial strain gauges changes by 1–2% for a 100°C temperature change.

*Self-Temperature Compensation Number.* Consider a structure that is subjected to both external loading and to a temperature change  $\Delta T$ . Some fraction of the strains induced in the structure is due to the external loading, while a fraction is due to thermal expansion or contraction caused by the temperature change. For modest temperature changes, strains associated with thermal expansion/contraction ( $\varepsilon^T$ ) can be calculated using the linear thermal expansion coefficient,  $\alpha$ :

$$\varepsilon^T = \alpha (\Delta T) \quad (15)$$

The linear thermal expansion coefficient has been measured for most structural materials and is available in reference handbooks. For example, the thermal expansion coefficient for steel alloys is about  $11 \mu\epsilon / ^\circ\text{C}$  ( $6\mu\epsilon / ^\circ\text{F}$ ).\*

A strain measurement is said to be “temperature compensated” if that portion of the strain associated with free thermal expansion or contractions is subtracted from the total strain measurement. If this can be achieved, then only strains associated with stress will be measured.

A straightforward method of strain gauge temperature compensation is to mount a gauge on a small coupon of the material of interest and to subject the unconstrained coupon to uniform temperature changes under carefully controlled laboratory conditions. The obtained measurements are plotted against temperature, generating a so-called thermal apparent strain curve. An identical strain gauge is now bonded to a structure made from the same material, and the structure is subjected to the loads and temperature changes that occur in service. Apparent strains at a given temperature are subtracted from the strains measured in service, thereby compensating the strain measurements for temperature.

Initially, one might suppose that apparent strains would simply reflect the difference in thermal expansion of substrate and gauge,  $(\alpha_s - \alpha_g)\Delta T$ . However, a change in the resistance of an *unbonded* strain gauge also occurs with a change in temperature. Consequently even if the thermal expansion coefficients of the substrate and gauge are identical, such that no mismatch exists, the resistance of a strain gauge will change with temperature and an apparent strain will be measured. The change in resistance caused by a uniform temperature change  $\Delta T$  can be written as

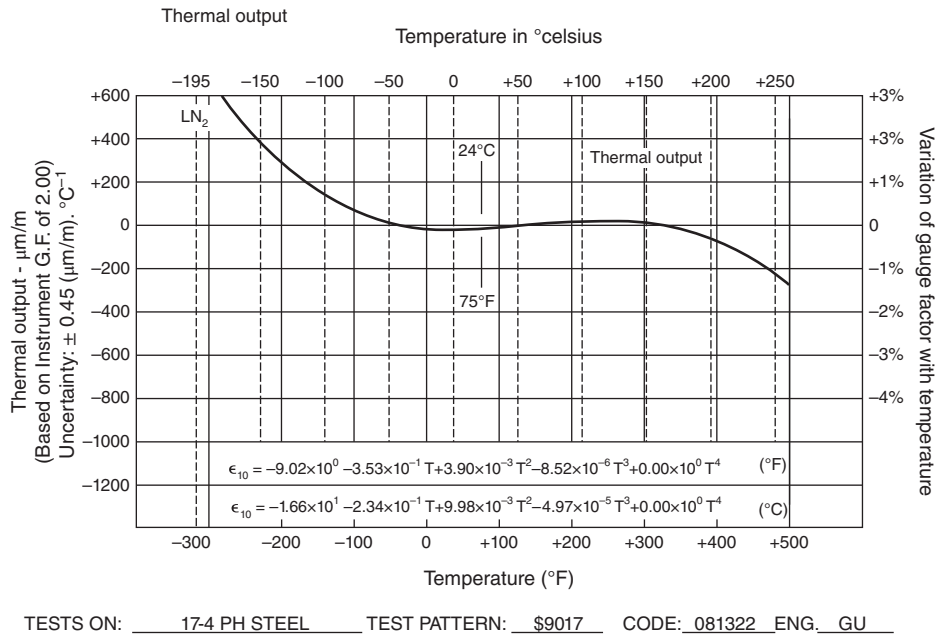
$$\left. \frac{\partial R}{R} \right|_{T_o} = \left[ \beta_g + S_g \left( \frac{1 + K_t}{1 - \nu_o K_t} \right) (\alpha_s - \alpha_g) \right] \Delta T \quad (16)$$

where  $\beta_g$  is called the temperature coefficient of resistance of the gauge alloy and is a measure of the change in gauge resistance with temperature. In general,  $\beta_g$  is a highly nonlinear function of temperature and can be algebraically negative or positive depending on temperature. For most alloys  $\beta_g$  can be manipulated over a wide range, through the use of cold-working and heat treatment processes. This gives rise to the concept of a self-temperature-compensated strain gauge. The gauge manufacturer manipulates  $\beta_g$  such that the change in gauge resistance due to a temperature change is equal and opposite to resistance changes due to the mismatch in thermal expansion coefficients. Because  $\beta_g$  is highly nonlinear compensation, it is not exact and can only be approximated over a limited temperature range. The *self-temperature compensation* number of a strain gauge corresponds roughly to the thermal expansion coefficient of the test material to which the strain gauge is intended to be bonded. The system of temperature measurement used by the gauge manufacturer is reflected in the STC number. That is, some manufacturers define the STC number in  $^\circ\text{F}$ , whereas others define the STC number in  $^\circ\text{C}$ . For example, a gauge produced by manufacturer A and intended for use on steel could have an STC number of 06 (corresponding to  $6 \mu\epsilon / ^\circ\text{F}$ ), whereas a similar gauge offered by manufacturer B may have an STC number of 11 (corresponding to  $11 \mu\epsilon / ^\circ\text{C}$ ).

A typical apparent strain is shown in Fig. 6. In this case, a self-temperature-compensated gauge has been mounted to a sample of 17-4PH (a precipitation-hardened stainless steel alloy), and the self-temperature compensated gauge exhibits an apparent strain of less than  $\pm 100 \mu\epsilon$  over the range  $-75^\circ\text{C} \leq T \leq 200^\circ\text{C}$ . The gauge manufacturer typically fits the entire apparent structure curve to a fourth-order polynomial and provides this curve-fit to the user. Curve fits

---

\* This discussion assumes that the material is isotropic. Anisotropic materials, such as composites, usually exhibit three different thermal expansion coefficients, which are measured along the principal material coordinate system. This added complexity will not be addressed here. Suffice it to say that temperature-compensated strain gauges can be used to measure strains in anisotropic materials, although extra care is needed to account for different thermal expansion coefficients in different material directions.



**Figure 6** Apparent strain curve obtained for a strain gauge with STC number 06, mounted in a coupon of 17-4 precipitation-hardened stainless steel.

based on temperatures measured in °C and °F are provided below the apparent strain curve shown in Fig. 6.

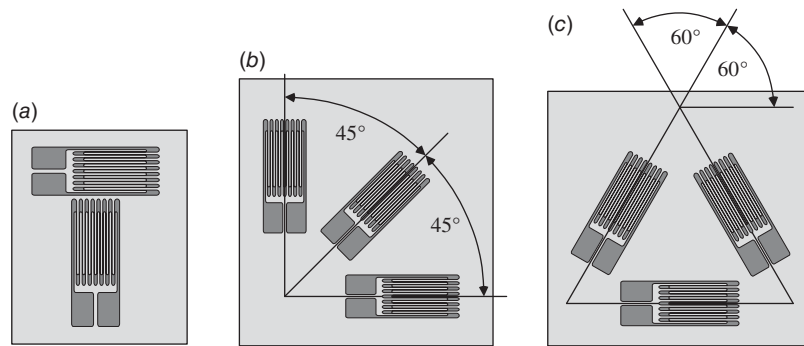
### 2.4 Strain Gauge Rosettes

The strain gauge shown in Fig. 4 and 5 is called a “uniaxial” strain gauge, since it is intended to measure strain in only one direction. As discussed in Section 11.2, in practice three components of strain must be measured to determine the state of strain within a plane:  $\epsilon_{xx}$ ,  $\epsilon_{yy}$ , and  $\gamma_{xy}$ . Once these strain components are known, the principal strains  $\epsilon_1$  and  $\epsilon_2$  and the orientation angle  $\theta$  of the principal strain coordinate system can be calculated using Eq. (4) and (5), respectively.

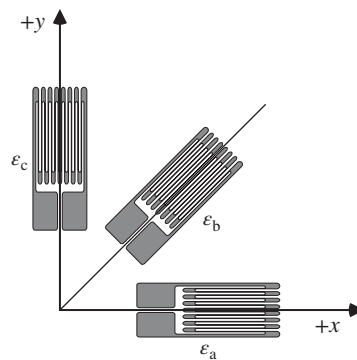
Since there are in general three unknowns ( $\epsilon_{xx}$ ,  $\epsilon_{yy}$ , and  $\gamma_{xy}$ , or equivalently,  $\epsilon_1$ ,  $\alpha_2$ , and  $\theta$ ), three independent strain measurements are normally required to determine the state of strain within a plane. An exception occurs when the orientation angle  $\theta$  is known a priori due to specimen geometry and loading (as in Fig. 2, for example), in which case there are only two unknowns ( $\epsilon_1$  and  $\epsilon_2$ ), and only two independent strain measurements are required.

Conceptually, three uniaxial strain gauges (or two uniaxial gauges, if there are only two unknowns) could be used to measure strains in three (or two) different directions. However, as a practical matter it is easier to precisely align the gauges in the intended orientation if three (or two) strain gauges are bonded to the same backing by the gauge manufacture. Strain gauges produced in this manner are called *strain gauge rosettes*.

Strain gauge rosettes are commonly available in three forms, as shown in Fig. 7. A biaxial rosette (also known as a T-rosette) consists of two perpendicular and electrically independent gauge elements. Two types of three-element rosettes are available: the rectangular rosette,



**Figure 7** Common strain gauge rosettes. (a) biaxial rosette, (b) rectangular rosette, and (c) delta rosette.



**Figure 8** Rectangular rosette relative to an  $x$ - $y$  coordinate system.

where the three gauge elements are orientated in  $45^\circ$  increments, and the delta rosette, where the three gauge elements are orientated in  $60^\circ$  increments.\*

### **Rosette Equations**

Three strain gauges oriented at distinct angles  $\theta_a$ ,  $\theta_b$ , and  $\theta_c$  relative to the  $x$  axis are shown in Fig. 8. Applying the first of Eq. (3) to each of these gauges in turn, we have

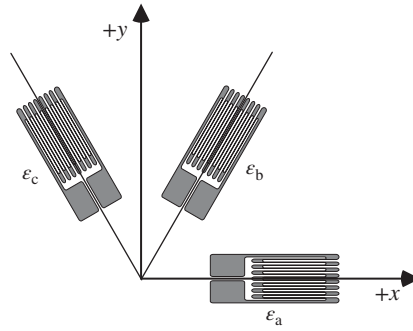
$$\begin{aligned}\epsilon_a &= \epsilon_{xx} \cos^2 \theta_a + \epsilon_{yy} \sin^2 \theta_a + \gamma_{xy} \sin \theta_a \cos \theta_a \\ \epsilon_b &= \epsilon_{xx} \cos^2 \theta_b + \epsilon_{yy} \sin^2 \theta_b + \gamma_{xy} \sin \theta_b \cos \theta_b \\ \epsilon_c &= \epsilon_{xx} \cos^2 \theta_c + \epsilon_{yy} \sin^2 \theta_c + \gamma_{xy} \sin \theta_c \cos \theta_c\end{aligned}\quad (17)$$

The equations in (18) are called the *general rosette equations*. Since  $\epsilon_a$ ,  $\epsilon_b$ ,  $\epsilon_c$ ,  $\theta_a$ ,  $\theta_b$ , and  $\theta_c$  are all measured, we have three equations involving three unknowns,  $\epsilon_{xx}$ ,  $\epsilon_{yy}$ , and  $\gamma_{xy}$ .

A rectangular rosette is shown relative to an  $x$ - $y$  coordinate system in Fig. 8. In this case,

$$\theta_a = 0^\circ \quad \theta_b = 45^\circ \quad \theta_c = 90^\circ$$

\* As is evident in Fig. 7c, delta rosettes are so named because the pattern of the three strain gauges often resembles the uppercase Greek letter  $\Delta$ .



**Figure 9** Delta rosette relative to an  $x$ - $y$  coordinate system.

Substituting these angles into Eq. (18) and solving for the unknown strains, we have

$$\begin{aligned}\epsilon_{xx} &= \epsilon_a \\ \epsilon_{yy} &= \epsilon_c \\ \gamma_{xy} &= 2\epsilon_b - (\epsilon_a + \epsilon_c)\end{aligned}\quad (18)$$

Equation (19) is the rosette equations for use with rectangular rosettes.

A delta rosette is shown relative to an  $x$ - $y$  coordinate system in Fig. 9. In this case,

$$\theta_a = 0 \quad \theta_b = 60 \quad \theta_c = 120$$

Substituting these angles into Eq. (18) and solving for the unknown strains, we have

$$\begin{aligned}\epsilon_{xx} &= \epsilon_a \\ \epsilon_{yy} &= \left(\frac{1}{3}\right) [2(\epsilon_b + \epsilon_c) - \epsilon_a] \\ \gamma_{xy} &= \left(\frac{2}{\sqrt{3}}\right) (\epsilon_b - \epsilon_c)\end{aligned}\quad (19)$$

Equation (20) is the rosette equations for use with delta rosettes.

### ***Corrections for Transverse Sensitivity Effects***

As previously discussed, strain gauges generally respond to both axial and transverse strains. Therefore, a measured axial strain is generally in error due to transverse sensitivity effects. The transverse sensitivity coefficient  $K_t$  provided by the manufacturer indicates the severity of this problem for a given strain gauge. Gauge manufacturers have been successful in reducing  $K_t$  to low levels; for modern metal foil gauges  $K_t$  is usually less than  $\pm 5\%$  (i.e.,  $|K_t| < 0.05$ ). At these low levels transverse sensitivity can often be ignored, depending on the level of accuracy needed in a given application. Nevertheless, for the highest accuracy strain gauges measurements should be corrected for transverse effects. At least two orthogonal strain measurements are required to correct for transverse sensitivity, which means that a 2- or 3-element strain gauge rosette must be used.

Consider first the correction of strains measured using a biaxial rosette. Referring to Fig. 7a, denote the uncorrected strains measured by the two gauge elements as  $\epsilon_{m0}$  and

$\varepsilon_{m90}$ . Strain measurements corrected for transverse sensitivity effects,  $\varepsilon_0$  and  $\varepsilon_{90}$ , are then given by

$$\begin{aligned}\varepsilon_0 &= \frac{(1 - \nu_o K_t)(\varepsilon_{m0^\circ} - K_t \varepsilon_{m90^\circ})}{1 - K_t^2} \\ \varepsilon_{90^\circ} &= \frac{(1 - \nu_o K_t)(\varepsilon_{m90^\circ} - K_t \varepsilon_{m0^\circ})}{1 - K_t^2}\end{aligned}\quad (20)$$

where  $\nu_o$  is the Poisson's ratio of the calibration material used by the gauge manufacturer during measurement of  $K_t$  (usually  $\nu_o = 0.285$ ).

In the case of a 3-element rectangular rosette (Fig. 7b), denote the uncorrected strain measurements as  $\varepsilon_{m0}$ ,  $\varepsilon_{m45}$ , and  $\varepsilon_{m90}$ . The corrected strain measurements are given by

$$\begin{aligned}\varepsilon_0 &= \frac{(1 - \nu_o K_t)(\varepsilon_{m0^\circ} - K_t \varepsilon_{m90^\circ})}{1 - K_t^2} \\ \varepsilon_{45^\circ} &= \frac{1 - \nu_o K_t}{1 - K_t^2} [\varepsilon_{m45^\circ} - K_t (\varepsilon_{m0^\circ} + \varepsilon_{m90^\circ} - \varepsilon_{m45^\circ})] \\ \varepsilon_{90^\circ} &= \frac{(1 - \nu_o K_t)(\varepsilon_{m90^\circ} - K_t \varepsilon_{m0^\circ})}{1 - K_t^2}\end{aligned}\quad (21)$$

Finally, for the case of a 3-element delta rosette (Fig. 7c), denote the uncorrected strains as  $\varepsilon_{m0}$ ,  $\varepsilon_{m60}$ , and  $\varepsilon_{m120}$ . The corrected strain measurements are given by

$$\begin{aligned}\varepsilon_0 &= \frac{1 - \nu_o K_t}{1 - K_t^2} \left[ \left(1 + \frac{K_t}{3}\right) \varepsilon_{m0^\circ} - \frac{2}{3} K_t (\varepsilon_{m60^\circ} + \varepsilon_{m120^\circ}) \right] \\ \varepsilon_{60^\circ} &= \frac{1 - \nu_o K_t}{1 - K_t^2} \left[ \left(1 + \frac{K_t}{3}\right) \varepsilon_{m60^\circ} - \frac{2}{3} K_t (\varepsilon_{m0^\circ} + \varepsilon_{m120^\circ}) \right] \\ \varepsilon_{120^\circ} &= \frac{1 - \nu_o K_t}{1 - K_t^2} \left[ \left(1 + \frac{K_t}{3}\right) \varepsilon_{m120^\circ} - \frac{2}{3} K_t (\varepsilon_{m0^\circ} + \varepsilon_{m60^\circ}) \right]\end{aligned}\quad (22)$$

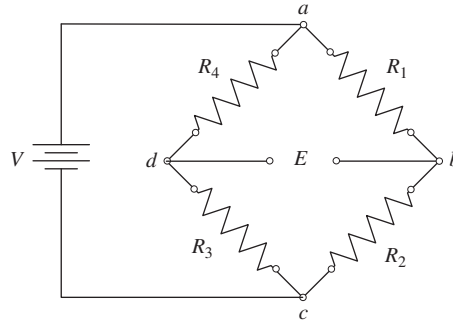
Equations (20) and (21) are based on the assumption that all gauge elements exhibit the same transverse sensitivity coefficient, which is usually the case. Analogous expressions that account for different transverse sensitivities for different gauge elements are available.<sup>7</sup>

## 2.5 The Wheatstone Bridge

In practice, strain gauges are routinely used to measure strains to a resolution of  $1 \mu\varepsilon$ . The change in gauge resistance caused by  $1 \mu\varepsilon$  is very small. Using Eq. (15) and assuming a gauge factor  $S_g = 2.0$

$$\frac{\Delta R}{R} = S_g \mu_a = (2)(1e) = 2 \times 10^{-6}$$

This shows that the change in resistance caused by  $1 \mu\varepsilon$  is only about 2 parts per million. For example, a strain gauge with an initial resistance of precisely  $120 \Omega$  will exhibit a resistance of about  $119.9998 \Omega$  if subjected to a tensile strain of  $1 \mu\varepsilon$ . It is very difficult to measure these small resistance changes directly. Consequently strain gauges are usually wired into special electrical circuits that convert the small resistance change into a relatively larger voltage change that is easier to accurately measure. The Wheatstone bridge is the most widely applied circuit of this type and will be reviewed here.



**Figure 10** Wheatstone bridge circuit.

A basic Wheatstone bridge circuit is shown in Fig. 10. Four resistances ( $R_1 - R_4$ ) are wired into a four-arm pattern. An excitation voltage ( $V$ ) is applied across junctions  $a$  and  $c$ , and an output voltage ( $E$ ) is monitored between junctions  $b$  and  $d$ .

Output voltage  $E$  is related to the excitation voltage  $V$  as follows:

$$E = \left[ \frac{R_1 R_3 - R_2 R_4}{(R_1 + R_2)(R_3 + R_4)} \right] V \quad (23)$$

The bridge is said to be “balanced” if the output voltage is  $E = 0$ . From Eq. (24) it is seen that this occurs if  $R_1 R_3 = R_2 R_4$ . That is, the bridge is balanced if

$$\frac{R_2}{R_1} = \frac{R_3}{R_4} \quad (24)$$

In strain gauge applications, the bridge is initially balanced. Often (but not always) the four resistances are initially identical ( $R_1 = R_2 = R_3 = R_4$ ). As discussed later, one or more of the resistances may be a strain gauge. If any of the four resistances change, the bridge may become unbalanced ( $E \neq 0$ ). Suppose that all four resistances are strain gauges, that the initial resistance of all gauges is identical ( $R_1 = R_2 = R_3 = R_4 = R$ , say), and that all four gauges experience a strain and consequently exhibit a change in resistance. It can be shown 1–3 that the resulting output voltage is given by

$$E = \left( \frac{V}{4R} \right) (\Delta R_1 - \Delta R_2 + \Delta R_3 - \Delta R_4)(1 - \eta) \quad (25)$$

The quantity  $\eta$  represents a nonlinear term. That is, rigorously speaking, the output voltage of the Wheatstone bridge is a nonlinear function of the change(s) in resistance. In most cases, the nonlinearity is very small and can be ignored, although if the bridge is initially unbalanced, then errors due to nonlinearities can be significant. As a rule of thumb, in practical strain measurements, the percent error due to bridge nonlinearities is roughly equal to the measured strain expressed as a percentage. Wheatstone bridge nonlinearities can usually be safely ignored and will not be further considered here.

Ignoring the nonlinear term  $\eta$ , Eq. (26) becomes

$$E = \left( \frac{V}{4R} \right) (\Delta R_1 - \Delta R_2 + \Delta R_3 - \Delta R_4) \quad (26)$$

Equation (27) shows that the effects of resistance changes in adjacent arms ( $\Delta R_1$  and  $\Delta R_2$ , for example) are subtractive, whereas changes in opposite arms ( $\Delta R_1$  and  $\Delta R_3$ , for example) are additive. In fact, if  $\Delta R_1 = \Delta R_2 = \Delta R_3 = \Delta R_4$ , the output voltage is  $E = 0$ , and the bridge remains balanced.

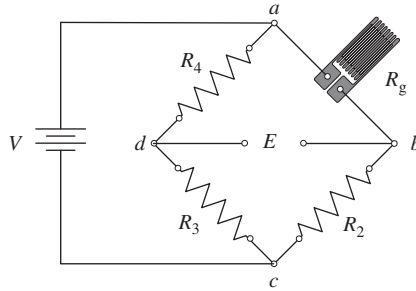


Figure 11 Quarter Wheatstone bridge circuit.

In general-purpose strain analysis each strain gauge is monitored using a separate Wheatstone bridge circuit, as shown in Fig. 11, rather than placing four gauges in a single bridge. This is called a quarter-bridge circuit, since resistances  $R_2 - R_4$  are now fixed, and only the gauge resistance  $R_g$  changes as strain is applied. Eq. (27) becomes

$$E = \left( \frac{\Delta R_g}{R_g} \right) \frac{V}{4} \tag{27}$$

Combining Eq. (15) and (27), we find

$$\epsilon = \frac{4E}{S_g V} \tag{28}$$

Equation (29) summarizes how a resistance strain gauge is used to measure strain. A strain gauge with known gauge factor  $S_g$  is bonded to a surface of interest. The gauge is then wired into a quarter-bridge Wheatstone circuit, a known voltage  $V$  is applied, and the circuit is initially balanced. If the strain gauge subsequently experiences a strain, the resistance will change, the bridge becomes unbalanced, and the resulting output voltage  $E$  is measured and interpreted in terms of strain using Eq. (29).

**The Three-Lead-Wire System**

During practical implementation of the Wheatstone circuit fixed resistors  $R_2 - R_4$  are incorporated into a strain gauge amplifier and lead wires of the appropriate length are used to connect the strain gauge to the rest of the circuit and complete the bridge. The situation that exists if only two lead wires are used is shown schematically in Fig. 12a. Note that the lead wires

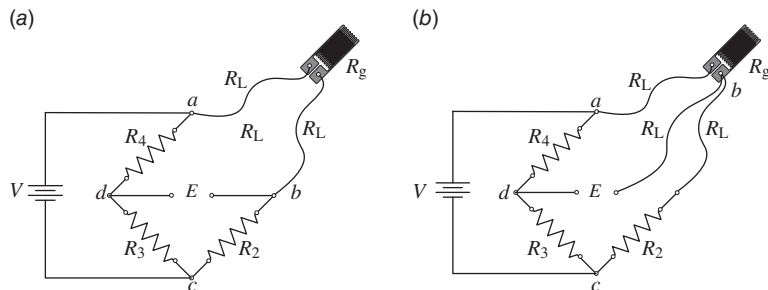


Figure 12 Illustration of the two-lead-wire circuit versus three-lead-wire Wheatstone bridge circuit. (a) Two-lead-wire circuit, resulting in an increase of  $2R_L$  in resistance of arm  $a-b$ . (b) Three-lead-wire circuit, where an equal resistance of  $R_L$  is added to arms  $a-b$  and  $b-c$ .



possess a measurable resistance  $R_L$ , so the total resistance in arm  $a-b$  is  $(R_g + 2R_L)$ . The magnitude of  $R_L$  depends, in part, on the length of the lead wire and is often a few ohms. Assuming  $R_2 = R_3 = R_4 = R_g$ , the resistance of the lead wires will cause an initial imbalance of the Wheatstone bridge. For this reason commercial strain gauge amplifiers often incorporate variable resistors that allow the resistance of adjacent arms to be varied, so that the bridge can be initially balanced in accordance with Eq. (25). However, if a temperature change occurs during the course of a strain measurement the *lead-wire* resistance will change since the resistance of the lead wires is governed in part by the temperature coefficient of resistivity of the lead wire alloy. A change in resistance due to lead-wire effects is interpreted as strain, so changes in lead wire resistance results in an erroneous apparent strain measurement.

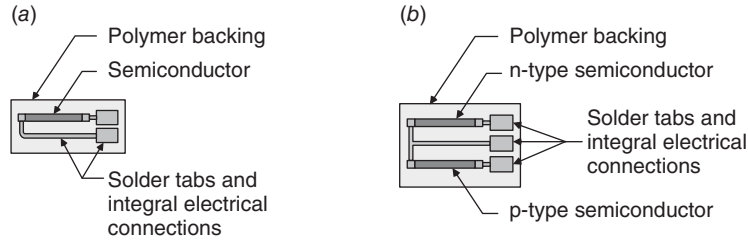
Due to the characteristics of the Wheatstone bridge, this situation can be remedied through the use of three lead wires. A three-lead-wire circuit is shown in Fig. 12b. Note that use of three lead wires effectively places an additional resistance  $R_L$  in adjacent arms  $a-b$  and  $b-c$  and moves junction  $b$  to one of the strain gauge solder tabs. The voltmeter used to measure the output voltage  $E$  has very high impedance (on the order of megaohms), so adding a small resistance of  $R_L$  between junctions  $b-d$  has no effect on measurement of the output voltage. The resistance of arm  $a-b$  is  $(R_g + R_L)$ , whereas the resistance of arm  $b-c$  is  $(R_2 + R_L)$ . All three lead wires are kept physically as close as possible so that the temperature along the length of the lead wires is essentially identical (this is easily achieved in practice since in most cases all three lead wires are encased in the same sheathing). Therefore, identical lead-wire resistance changes occur in adjacent arms and are canceled, as per Eq. (27).

### 3 SEMICONDUCTOR STRAIN GAUGES

Like metals, semiconductors exhibit the piezoresistive effect; their resistance changes when subjected to strain. In fact, the piezoresistive effect is much more pronounced in semiconductors than in metals or metal alloys, and consequently semiconductor strain gauges have much higher gauge factors than metal foil gauges. Despite this advantage semiconductor gauges are not widely used for general-purpose strain measurement. Two major drawbacks have limited their use. First, although the gauge factor of semiconductors is very high, it is also a nonlinear function of strain. The gauge factor of semiconductor strain gauges varies substantially over the strain range of interest to structural engineers (often by a factor of 2–3), and this nonlinearity must be accounted for when interpreting the measured change in resistance. Second, the resistivity of semiconductors is far more sensitive to temperature changes than that of metals, so temperature compensation of semiconductor strain gauges is generally less exact than for metal gauges.

Semiconductor gauges were first developed in the 1950s<sup>8,9</sup> and were commercially available by about 1960. Most semiconductor gauges are based on doped silicon. The two most common doping agents are phosphorous and boron. Silicon doped with phosphorous results in an n-type semiconductor, in which electrical conduction occurs due to the flow of electrons (a negative charge carrier). In contrast, silicon doped with boron results in a p-type semiconductor, where electrical conduction occurs due to vacancies in the atomic lattice (also called “holes,” a positive charge carrier).

The available literature and technologies describing semiconductor strain gauges is not as detailed as for metal foil gauges. The basic elements of uniaxial semiconductor gauges are shown schematically in Fig. 13. Since the piezoelectric effect exhibited by semiconductors is high, there is no need for the undulating grid pattern that is characteristic of a metal foil gauge (as shown in Fig. 4, for example). Semiconductor gauges are commercially available with or without a polymer backing. Backings are usually made of phenolic resin and serve to stabilize the gauge element and as an aid during handling and bonding. Gauges are often provided



**Figure 13** Typical semiconductor strain gauges with polymer backing. (a) uniaxial gauge with a single sensing element and (b) uniaxial gauge with two sensing elements, providing thermal compensation.

with preattached lead wires or lead-wire ribbons. Both uniaxial and biaxial (T-rosettes) gauges are available. Three-element rosettes are apparently not commercially available, at least as an off-the-shelf product. The uniaxial gauge with two semiconductor elements shown in Fig. 13b is a particularly interesting configuration because, as will be discussed later, the combined use of one n-type semiconductor and one p-type semiconductor in a Wheatstone bridge results in self-temperature compensation.

The transverse sensitivity of semiconductor strain gauges has apparently not been measured, or at least a transverse sensitivity coefficient is not provided with commercially available semiconductor strain gauges. The gauge factor for semiconductor gauges is simply equated to the strain sensitivity:

$$S_g = S = \frac{\partial R/R}{\epsilon}$$

The *magnitude* of gauge factors of n- and p-type silicon semiconductors are similar and range from about 40 to 200, compared with only 2 to 3 for metallic foil gauges. Interestingly, the gauge factor of p- and n-type semiconductor gauges differ in algebraic sign. That is, the resistance of p-type silicon increases with a tensile strain (as do metal conductors); therefore, p-type semiconductor strain gauges have a positive gauge factor. In contrast, the resistances of n-type silicon decrease with tensile strain; therefore, n-type semiconductor gauges have a negative gauge factor.

The change of resistance of a semiconductor gauge bonded to an unconstrained test sample and subjected to a change in temperature is given by Eq. (17), except that it is now assumed that  $K_T = 0$ :

$$\left. \frac{\partial R}{R} \right|_{T_0} = [\beta_g + S_g(\alpha_s - \alpha_g)]\Delta T \quad (29)$$

It would be ideal if a semiconductor gauge could be produced for which  $\beta_g = -S_g(\alpha_s - \alpha_g)$ , which would eliminate the resistance change due solely to free expansion or contraction due to  $\Delta T$  and allow development of a self-temperature-compensated semiconductor gauge using a single semiconductor element. Unfortunately, the temperature coefficient of resistance  $\beta_g$  for semiconductors is established strictly by the level of doping employed and cannot be modified by cold-working or thermal treatments. However, thermal compensation can be achieved using the configuration shown in Fig. 13b. This configuration placed sensing elements in two arms of a half-bridge Wheatstone circuit, where the p- and n-type gauge elements are placed in adjacent arms. Compensation is achieved because the gauge factor of p-type semiconductors is positive, whereas the gauge factor of n-type semiconductors is negative, and because resistance changes in adjacent arms of a Wheatstone bridge are subtractive. As long as  $\beta_g$  and  $\alpha_g$  for both elements are the same, resistance changes associated with the thermal coefficient of resistance and the mismatch in thermal expansion coefficients occur in adjacent arms and cancel. Since gauge factors of p- and n-type silicon have opposite algebraic signs, resistance changes

due to mechanically induced strains do not cancel, and in fact the overall strain sensitivity is increased. A practical requirement is that both gauge elements must experience the same strain and temperature change. This requirement is generally satisfied since the gauge elements are small and bonded to the same backing.

#### 4 LIQUID METAL STRAIN GAUGES

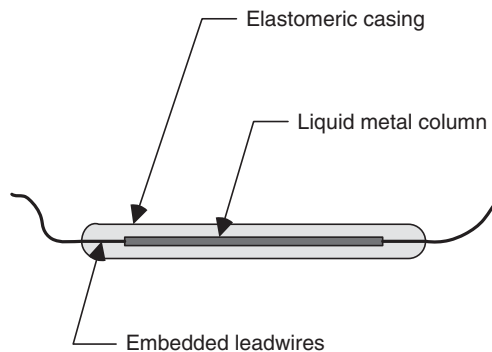
Liquid metal strain gauges can be used to measure very large strains (in excess of 150% or more). They are often used to measure strain in biological tissues such as ligaments or tendons and are also used in engineered structures that experience large deformations during service such as automobile, truck, or aircraft tires.

The first liquid metal strain gauge was developed and applied to the study of biological structures by Whitney in the late 1940s.<sup>10,11</sup> Various applications have been described in the literature since that time, and design and fabrication guidelines appeared in 1983.<sup>12</sup> The demand for these devices has never been large enough to warrant commercialization, so liquid metal gauges are usually custom-made and calibrated by the user. A typical configuration is shown in Fig. 14. The gauge consists of a column(s) of liquid metal, usually mercury, encased in an elastomeric casing capable of large extensions, often silicon rubber. Lead wires in contact with the liquid metal and embedded within the elastomeric body are connected to external instrumentation. The method of attachment to the structure varies according to application; in biological studies, the gauge is often sutured to the tissue of interest.

The resistance of the gauge is established by the liquid metal used and by length and diameter of the liquid metal column. Initial resistance is often very low, on the order of a few ohms. If a tensile strain is applied, the length is increased and diameter is decreased (due to the Poisson effect), resulting in an increase in gauge resistance. A gauge factor is defined as normal and is determined by measuring the resistance change as a function of strain:

$$S = \frac{\Delta R/R}{\epsilon}$$

A typical gauge factor for liquid metal gauges cannot be defined since these devices are custom-made. In general, gauge factors are about 2, at least at small strain levels. Although these gauges can sustain very high strain levels repeatedly and without failure, a cautionary note is that the gauge factor often becomes nonlinear at high strain levels. The strain level at which nonlinear effects become pronounced cannot be specified, again because these gauges are custom-made, but in general substantial nonlinearities occur at strain levels greater than about 40%.



**Figure 14** Typical configuration of a liquid metal strain gauge.

## REFERENCES

1. W. N. Sharpe, Jr. (Ed.), *Handbook of Experimental Solids Mechanics*, Springer, 2008, p. 1098.
2. A. Shukla and J. W. Dally, *Experimental Solid Mechanics*, College House Enterprises, 2010, p. 668.
3. J. R. Dally, and W. F. Riley, *Experimental Stress Analysis*, 4th ed., College House Enterprises, 2005, p. 686.
4. G. Cloud, *Optical Methods of Engineering Analysis*, Cambridge University, Cambridge, UK, 1995, p. 503.
5. M. A. Sutton, J.-J. Orteu, and H. Schreier, Image Correlation for Shape, Motion and Deformation Measurements: Basic Concepts, *Theory and Applications*, Springer New York, 2009, p. 344.
6. ASTM Standard E251, *Standard Test Methods for Performance Characteristics of Metallic Bonded Resistance Strain Gages*, ASTM International, West Conshohocken, PA, 2009.
7. Errors Due to Transverse Sensitivity in Strain Gauges. Appendix, Tech Note TN-509, Micro- Measurements, Raleigh, NC, 1982. Available at: [www.vishaypg.com/docs/11059/tn509tn5.pdf](http://www.vishaypg.com/docs/11059/tn509tn5.pdf).
8. C. S. Smith, "Piezoresistive Effect in Germanium and Silicon," *Phys. Rev.*, **94**(1), 42–49, 1954.
9. W. P. Mason and R. N. Thurston, "Piezoresistive Materials in Measuring Displacement, Force, and Torque," *J. Acoustic Soc Ame.*, **29**(10), 1096–1101, 1957.
10. R. J. Whitney, "The Measurement of Changes in Human Limb Volume by Means of a Mercury-in-Rubber Strain Gauge," *Proceedings of Physical Society, March* **26**, 1949.
11. R. J. Whitney, "The Measurement of Volume Change in Human Limbs," *J. Physiol.*, **121**, 1–27, 1953.
12. J. E. Stone, N. H. Madsen, J. L. Milton, W. F. Swinson, J. L. Turner, "Developments in the Design and Use of Liquid-Metal Strain Gauges," *Exp. Mech.*, **23**(2), 129–139, 1983.



# CHAPTER 19

## AN INTRODUCTION TO THE FINITE-ELEMENT METHOD

Tarek I. Zohdi  
University of California  
Berkeley, California

1	DEFORMATION OF A SOLID	682	7	GLOBAL/LOCAL TRANSFORMATIONS	692
2	EQUILIBRIUM	684	8	DIFFERENTIAL PROPERTIES OF SHAPE FUNCTIONS	693
3	INFINITESIMAL LINEARLY ELASTIC CONSTITUTIVE LAWS	686	9	DIFFERENTIATION IN REFERENTIAL COORDINATES	695
4	FOUNDATIONS OF THE FINITE-ELEMENT METHOD	689	10	POSTPROCESSING	698
5	HILBERTIAN SOBOLEV SPACES	690	11	ONE-DIMENSIONAL EXAMPLE	699
6	FINITE-ELEMENT FORMULATION IN THREE DIMENSIONS	690	12	SUMMARY	701
				REFERENCES	702

The finite-element method (FEM), which has become a dominant numerical method in mathematical physics, applied mathematics, and engineering analysis, is a huge field of study. This chapter is intended to provide a concise review of basic field equations in solid mechanics and then illustrate how the FEM can be employed to solve them. The implementation, theory, and application of FEM is a subject of immense literature. We will not attempt to review this huge field.

To motivate the use of the FEM, we derive the classical equations of mechanical equilibrium. Throughout this analysis, boldface symbols imply vectors or tensors. The inner product of two vectors  $\mathbf{u}$  and  $\mathbf{v}$  is denoted  $\mathbf{u} \cdot \mathbf{v}$ . At the risk of oversimplification, we ignore the distinction between second-order tensors and matrices. Furthermore, we exclusively employ a Cartesian basis. Readers may consult the texts of Malvern<sup>1</sup> and Marsden and Hughes<sup>2</sup> for more background information. Hence, if we consider the second-order tensor  $\mathbf{A}$  with its matrix representation

$$[\mathbf{A}] \stackrel{\text{def}}{=} \begin{bmatrix} A_{11} & A_{12} & A_{13} \\ A_{21} & A_{22} & A_{23} \\ A_{31} & A_{32} & A_{33} \end{bmatrix} \quad (1)$$

then the product of two second-order tensors  $\mathbf{A} \cdot \mathbf{B}$  is defined by the matrix product  $[\mathbf{A}][\mathbf{B}]$ , with components of  $A_{ij}B_{jk} = C_{ik}$ . The second-order inner product of two tensors or matrices is  $\mathbf{A} : \mathbf{B} = A_{ij}B_{ij} = \text{tr}([\mathbf{A}]^T[\mathbf{B}])$ . Finally, the divergence of a vector  $\mathbf{u}$  is defined by  $\nabla \cdot \mathbf{u} = u_{i,i}$ ; whereas for a second-order tensor  $\mathbf{A}$ ,  $\nabla \cdot \mathbf{A}$  describes a contraction to a vector with components  $A_{ij,j}$ .

## 1 DEFORMATION OF A SOLID

The term *deformation* refers to a change in the shape of the continuum between a reference configuration and current configuration. In the reference configuration, a representative particle of the continuum occupies a point  $\mathbf{P}$  in space and has the position vector  $\mathbf{X} = X_1\mathbf{e}_1 + X_2\mathbf{e}_2 + X_3\mathbf{e}_3$  (Fig. 1), where  $(\mathbf{e}_1, \mathbf{e}_2, \mathbf{e}_3)$  is a Cartesian reference triad and  $X_1, X_2, X_3$  (with center  $\mathbf{O}$ ) can be thought of as labels for the point. Sometimes the coordinates or labels  $(X_1, X_2, X_3, t)$  are called the referential coordinates. In the current configuration the particle originally located at point  $\mathbf{P}$  is located at point  $\mathbf{P}'$  and can be expressed also in terms of another position vector  $\mathbf{x}$ , with the coordinates  $(x_1, x_2, x_3, t)$ . These are called the current coordinates. It is obvious with this arrangement that the displacement is  $\mathbf{u} = \mathbf{x} - \mathbf{X}$  for a point originally at  $\mathbf{X}$  and with final coordinates  $\mathbf{x}$ . When a continuum undergoes deformation (or flow), its points move along various paths in space. This motion may be expressed by  $\mathbf{x}(X_1, X_2, X_3, t) = \mathbf{u}(X_1, X_2, X_3, t) + \mathbf{X}(X_1, X_2, X_3, t)$ , which gives the present location of a point that occupied the position  $(X_1, X_2, X_3, t)$  at time  $t = t_0$ , written in terms of the labels  $X_1, X_2, X_3$ . The previous position vector may be interpreted as a mapping of the initial configuration onto the current configuration. In classical approaches, it is assumed that such a mapping is one to one and continuous, with continuous partial derivatives to whatever order that is required. The description of motion or deformation expressed previously is known as the Lagrangian formulation. Alternatively, if the independent variables are the coordinates  $\mathbf{x}$  and  $t$ , then  $\mathbf{x}(x_1, x_2, x_3, t) = \mathbf{u}(x_1, x_2, x_3, t) + \mathbf{X}(x_1, x_2, x_3, t)$ , and the formulation is denoted as Eulerian (Fig. 1).

Partial differentiation of the displacement vector  $\mathbf{u} = \mathbf{x} - \mathbf{X}$  produces the following displacement gradients:  $\nabla_{\mathbf{x}}\mathbf{u} = \mathbf{F} - \mathbf{1}$  and  $\nabla_{\mathbf{x}}\mathbf{u} = \mathbf{1} - \bar{\mathbf{F}}$ , where

$$\nabla_{\mathbf{x}}\mathbf{x} \stackrel{\text{def}}{=} \frac{\partial \mathbf{x}}{\partial \mathbf{X}} = \mathbf{F} \stackrel{\text{def}}{=} \begin{bmatrix} \frac{\partial x_1}{\partial X_1} & \frac{\partial x_1}{\partial X_2} & \frac{\partial x_1}{\partial X_3} \\ \frac{\partial x_2}{\partial X_1} & \frac{\partial x_2}{\partial X_2} & \frac{\partial x_2}{\partial X_3} \\ \frac{\partial x_3}{\partial X_1} & \frac{\partial x_3}{\partial X_2} & \frac{\partial x_3}{\partial X_3} \end{bmatrix} \quad (2)$$

$$\nabla_{\mathbf{x}}\mathbf{X} \stackrel{\text{def}}{=} \frac{\delta \mathbf{X}}{\delta \mathbf{x}} = \bar{\mathbf{F}} \stackrel{\text{def}}{=} \begin{bmatrix} \frac{\partial X_1}{\partial x_1} & \frac{\partial X_1}{\partial x_2} & \frac{\partial X_1}{\partial x_3} \\ \frac{\partial X_2}{\partial x_1} & \frac{\partial X_2}{\partial x_2} & \frac{\partial X_2}{\partial x_3} \\ \frac{\partial X_3}{\partial x_1} & \frac{\partial X_3}{\partial x_2} & \frac{\partial X_3}{\partial x_3} \end{bmatrix} \quad (3)$$

where  $\mathbf{F}$  is known as the material deformation gradient and  $\bar{\mathbf{F}}$  is known as the spatial deformation gradient. Now, consider the length of a differential element in the reference configuration  $d\mathbf{X}$  and  $d\mathbf{x}$  in the current configuration,  $d\mathbf{x} = \nabla_{\mathbf{x}}\mathbf{x} \cdot d\mathbf{X} = \mathbf{F} \cdot d\mathbf{X}$ . Taking the

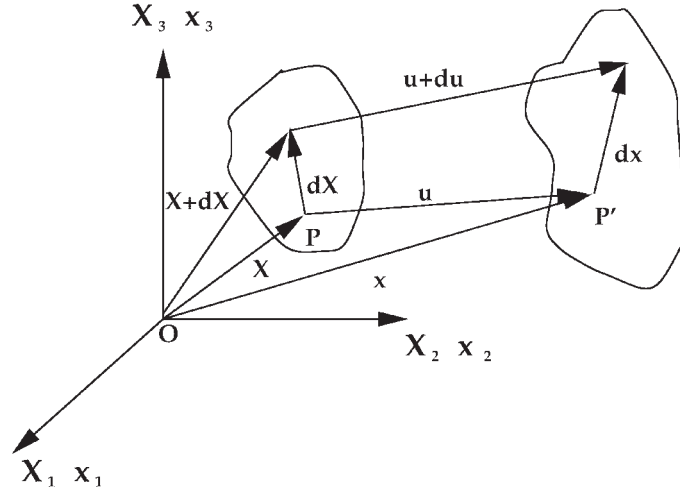


Figure 1 Different descriptions of a deforming body.

difference in the magnitudes of these elements yields

$$\begin{aligned} d\mathbf{x} \cdot d\mathbf{x} - d\mathbf{X} \cdot d\mathbf{X} &= (\nabla_{\mathbf{x}}\mathbf{X} \cdot d\mathbf{X}) \cdot (\nabla_{\mathbf{x}}\mathbf{X} \cdot d\mathbf{X}) - d\mathbf{X} \cdot d\mathbf{X} \\ &= d\mathbf{X} \cdot (\mathbf{F}^T \cdot \mathbf{F} - 1) \cdot d\mathbf{X} \stackrel{\text{def}}{=} 2 \, d\mathbf{X} \cdot \mathbf{E} \cdot d\mathbf{X} \end{aligned} \quad (4)$$

Alternatively, we have with  $d\mathbf{X} = \nabla_{\mathbf{x}}\mathbf{X} \cdot d\mathbf{x} = \bar{\mathbf{F}} \cdot d\mathbf{x}$  and

$$\begin{aligned} d\mathbf{x} \cdot d\mathbf{x} - d\mathbf{X} \cdot d\mathbf{X} &= d\mathbf{x} \cdot d\mathbf{x} - (\nabla_{\mathbf{x}}\mathbf{X} \cdot d\mathbf{X}) \cdot (\nabla_{\mathbf{x}}\mathbf{X} \cdot d\mathbf{X}) \\ &= d\mathbf{x} \cdot (1 - \bar{\mathbf{F}}^T \cdot \bar{\mathbf{F}}) \cdot d\mathbf{x} \stackrel{\text{def}}{=} 2 \, d\mathbf{x} \cdot \mathbf{L} \cdot d\mathbf{x} \end{aligned} \quad (5)$$

Therefore, we have the so-called *Lagrangian* strain tensor

$$\mathbf{E} \stackrel{\text{def}}{=} \frac{1}{2} (\mathbf{F}^T \cdot \mathbf{F} - 1) = \frac{1}{2} \left[ \nabla_{\mathbf{x}}\mathbf{u} + (\nabla_{\mathbf{x}}\mathbf{u})^T + (\nabla_{\mathbf{x}}\mathbf{u})^T \cdot \nabla_{\mathbf{x}}\mathbf{u} \right] \quad (6)$$

Frequently, the Lagrangian strain tensor is defined in terms of the so-called right Cauchy–Green strain,  $\mathbf{E} \stackrel{\text{def}}{=} \frac{1}{2}(\mathbf{C} - 1)$ ,  $\mathbf{C} = \mathbf{F}^T \cdot \mathbf{F}$ . The Eulerian strain tensor is defined as

$$\mathbf{L} \stackrel{\text{def}}{=} \frac{1}{2} (1 - \bar{\mathbf{F}}^T \cdot \bar{\mathbf{F}}) = \frac{1}{2} \left[ \nabla_{\mathbf{x}}\mathbf{u} + (\nabla_{\mathbf{x}}\mathbf{u})^T - (\nabla_{\mathbf{x}}\mathbf{u})^T \cdot \nabla_{\mathbf{x}}\mathbf{u} \right] \quad (7)$$

In a similar manner as for the Lagrangian strain tensor, the Eulerian strain tensor can be defined in terms of the so-called left Cauchy–Green strain,  $\mathbf{L} \stackrel{\text{def}}{=} \frac{1}{2}(1 - \mathbf{b}^{-1})$ ,  $\mathbf{b} = \mathbf{F} \cdot \mathbf{F}^T$ .

REMARK. It should be clear that  $d\mathbf{x}$  can be reinterpreted as the result of a mapping  $\mathbf{F} \cdot d\mathbf{X} \rightarrow d\mathbf{x}$ , or a change in configuration (reference to current), while  $\bar{\mathbf{F}} \cdot d\mathbf{x} \rightarrow d\mathbf{X}$  maps the current to the reference system. For the deformations to be invertible and physically realizable,  $\bar{\mathbf{F}}(\mathbf{F} \cdot d\mathbf{X}) = d\mathbf{x}$  and  $\mathbf{F}(\bar{\mathbf{F}} \cdot d\mathbf{x}) = d\mathbf{X}$ . We note that  $(\det \bar{\mathbf{F}})(\det \mathbf{F}) = 1$  and the following obvious relation  $(\partial \mathbf{X} / \partial \mathbf{x})(\partial \mathbf{x} / \partial \mathbf{X}) = \bar{\mathbf{F}}\mathbf{F} = 1$ . It should be clear that  $\bar{\mathbf{F}} = \mathbf{F}^{-1}$ .

We now employ infinitesimal deformation theory. In infinitesimal deformation theory, the displacement gradient components being “small” implies that higher order terms like  $(\nabla_{\mathbf{x}}\mathbf{u})^T \cdot \nabla_{\mathbf{x}}\mathbf{u}$  and  $(\nabla_{\mathbf{x}}\mathbf{u})^T \cdot \nabla_{\mathbf{x}}\mathbf{u}$  can be neglected in the strain measure



$\mathbf{L} = \frac{1}{2} [\nabla_{\mathbf{x}}\mathbf{u} + (\nabla_{\mathbf{x}}\mathbf{u})^T - (\nabla_{\mathbf{x}}\mathbf{u})^T \cdot \nabla_{\mathbf{x}}\mathbf{u}]$  and  $\mathbf{E} = \frac{1}{2} (\nabla_{\mathbf{x}}\mathbf{u} + (\nabla_{\mathbf{x}}\mathbf{u})^T + (\nabla_{\mathbf{x}}\mathbf{u})^T \cdot \nabla_{\mathbf{x}}\mathbf{u})$ , leading to  $\mathbf{L} \approx \boldsymbol{\varepsilon}^E \stackrel{\text{def}}{=} \frac{1}{2} [\nabla_{\mathbf{x}}\mathbf{u} + (\nabla_{\mathbf{x}}\mathbf{u})^T]$  and  $\mathbf{E} \approx \boldsymbol{\varepsilon}^L \stackrel{\text{def}}{=} \frac{1}{2} [\nabla_{\mathbf{x}}\mathbf{u} + (\nabla_{\mathbf{x}}\mathbf{u})^T]$ . If the displacement gradients are small compared with unity,  $\boldsymbol{\varepsilon}^E$  and  $\boldsymbol{\varepsilon}^L$  coincide closely to  $\mathbf{L}$  and  $\mathbf{E}$ , respectively. If we assume that  $\partial/\partial X \approx \partial/\partial x$ , we may use  $\boldsymbol{\varepsilon}^E$  or  $\boldsymbol{\varepsilon}^L$  interchangeably. Usually  $\boldsymbol{\varepsilon}$  is the symbol used for infinitesimal strains. Furthermore, to avoid confusion, when using models employing the geometrically linear infinitesimal strain assumption, we use the symbol of  $\nabla$  with no  $\mathbf{X}$  or  $\mathbf{x}$  subscript.

REMARK. The Jacobian of the deformation gradient,  $\mathbf{F}$ , is defined as

$$J \stackrel{\text{def}}{=} \det \mathbf{F} = \begin{vmatrix} \frac{\partial x_1}{\partial X_1} & \frac{\partial x_1}{\partial X_2} & \frac{\partial x_1}{\partial X_3} \\ \frac{\partial x_2}{\partial X_1} & \frac{\partial x_2}{\partial X_2} & \frac{\partial x_2}{\partial X_3} \\ \frac{\partial x_3}{\partial X_1} & \frac{\partial x_3}{\partial X_2} & \frac{\partial x_3}{\partial X_3} \end{vmatrix} \quad (8)$$

To interpret the Jacobian in a physical way, consider a reference differential volume given by  $dS^3 = d\omega$ , where  $d\mathbf{X}^{(1)} = dS\mathbf{e}_1$ ,  $d\mathbf{X}^{(2)} = dS\mathbf{e}_2$ , and  $d\mathbf{X}^{(3)} = dS\mathbf{e}_3$ . The current differential element is described by  $d\mathbf{x}^{(1)} = (\partial x_k / \partial X_1) dS\mathbf{e}_k$ ,  $d\mathbf{x}^{(2)} = (\partial x_k / \partial X_2) dS\mathbf{e}_k$  and  $d\mathbf{x}^{(3)} = (\partial x_k / \partial X_3) dS\mathbf{e}_k$ , where  $\mathbf{i}$  is a unit vector and

$$\underbrace{d\mathbf{x}^{(1)} \cdot (d\mathbf{x}^{(2)} \times d\mathbf{x}^{(3)})}_{\stackrel{\text{def}}{=} d\omega} = \begin{vmatrix} dx_1^{(1)} & dx_2^{(1)} & dx_3^{(1)} \\ dx_1^{(2)} & dx_2^{(2)} & dx_3^{(2)} \\ dx_1^{(3)} & dx_2^{(3)} & dx_3^{(3)} \end{vmatrix} = \begin{vmatrix} \frac{\partial x_1}{\partial X_1} & \frac{\partial x_2}{\partial X_1} & \frac{\partial x_3}{\partial X_1} \\ \frac{\partial x_1}{\partial X_2} & \frac{\partial x_2}{\partial X_2} & \frac{\partial x_3}{\partial X_2} \\ \frac{\partial x_1}{\partial X_3} & \frac{\partial x_2}{\partial X_3} & \frac{\partial x_3}{\partial X_3} \end{vmatrix} dS^3 \quad (9)$$

Therefore,  $d\omega = J d\omega_0$ . Thus, the Jacobian of the deformation gradient must remain positive definite; otherwise we obtain physically impossible “negative” volumes.

## 2 EQUILIBRIUM

We start with the following postulated balance law for an arbitrary part of a body,  $\Omega$ ,  $\omega$ , around a point  $P$ , with boundary  $\partial\omega$ :

$$\underbrace{\int_{\partial\omega} \mathbf{t} \, da}_{\text{surface forces}} + \underbrace{\int_{\omega} \mathbf{f} \, d\omega}_{\text{body forces}} = \underbrace{\frac{d}{dt} \int_{\omega} \rho \dot{\mathbf{u}} \, d\omega}_{\text{inertial forces}} \quad (10)$$

where  $\rho$  is the material density,  $\mathbf{b}$  is the body force per unit mass ( $\mathbf{f} = \rho\mathbf{b}$ ), and  $\dot{\mathbf{u}}$  is the time derivative of the displacement. When the actual molecular structure is considered on a sub-microscopic scale, the force densities,  $\mathbf{t}$ , which we commonly refer to as “surface forces,” are taken to involve short-range intermolecular forces. Tacitly, we assume that the effects of radiative forces, and others that do not require momentum transfer through a continuum, are negligible. This is a so-called local action postulate. As long as the volume element is large, our resultant body and surface forces may be interpreted as sums of these intermolecular forces. When we pass to larger scales, we can justifiably use the continuum concept.

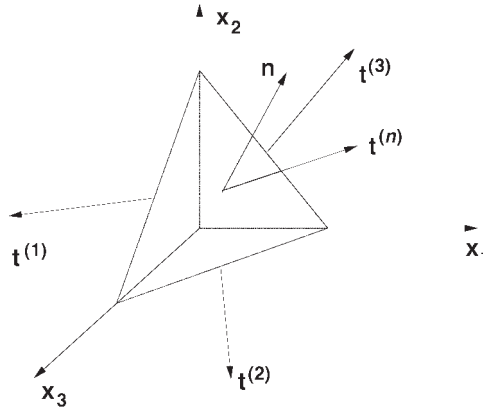


Figure 2 Cauchy tetrahedron: a “sectioned material point.”

Now consider a tetrahedron in equilibrium, as shown in Fig. 2. From Newton’s laws,  $\mathbf{t}^{(n)} \Delta A^{(n)} + \mathbf{t}^{(1)} \Delta A^{(1)} + \mathbf{t}^{(2)} \Delta A^{(2)} + \mathbf{t}^{(3)} \Delta A^{(3)} + \mathbf{f} \Delta \Omega = \rho \Delta \Omega \ddot{\mathbf{u}}$ , where  $\Delta A^{(n)}$  is the surface area of the face of the tetrahedron with normal  $\mathbf{n}$  and  $\Delta \Omega$  is the tetrahedron volume. Clearly, as the distance between the tetrahedron base [located at  $(0,0,0)$ ] and the surface center, denoted  $h$ , goes to zero, we have  $h \rightarrow 0 \Rightarrow \Delta A^{(n)} \rightarrow 0 \Rightarrow \Delta \Omega / \Delta A^{(n)}$ . Geometrically, we have  $\Delta A^{(i)} / \Delta A^{(n)} = \cos(x_i, x_n) \stackrel{\text{def}}{=} -n_i$ , and therefore  $\mathbf{t}^{(n)} = \mathbf{t}^{(1)} \cos(x_1, x_n) = \mathbf{t}^{(2)} \cos(x_2, x_n) + \mathbf{t}^{(3)} \cos(x_3, x_n) = \mathbf{0}$ . It is clear that forces on the surface areas could be decomposed into three linearly independent components. It is convenient to express the concept of stress at a point, representing the surface forces there, pictorially represented by a cube surrounding a point. The fundamental issue that must be resolved is the characterization of these surface forces. We can represent the force density vector, the so-called traction, on a surface by the component representation:  $\mathbf{t}^{(i)} \stackrel{\text{def}}{=} (\sigma_{i1}, \sigma_{i2}, \sigma_{i3})^T$ , where the second index represents the direction of the component and the first index represents the normal to the corresponding coordinate plane. From this point forth, we will drop the superscript notation of  $\mathbf{t}^{(n)}$ , where it is implicit that  $\mathbf{t} \stackrel{\text{def}}{=} \mathbf{t}^{(n)} \boldsymbol{\sigma}^T \cdot \mathbf{n}$  or explicitly

$$\mathbf{t}^{(n)} = \mathbf{t}^{(1)} n_1 + \mathbf{t}^{(2)} n_2 + \mathbf{t}^{(3)} n_3 = \boldsymbol{\sigma}^T \cdot \mathbf{n} = \begin{bmatrix} \sigma_{11} & \sigma_{12} & \sigma_{13} \\ \sigma_{21} & \sigma_{22} & \sigma_{23} \\ \sigma_{31} & \sigma_{32} & \sigma_{33} \end{bmatrix}^T \begin{bmatrix} n_1 \\ n_2 \\ n_3 \end{bmatrix} \quad (11)$$

where  $\boldsymbol{\sigma}$  is the so-called Cauchy stress tensor.\*

Substitution of Eq. (11) into Eq. (10) yields ( $\omega \subset \Omega$ )

$$\underbrace{\int_{\partial \omega} \boldsymbol{\sigma} \cdot \mathbf{n} \, da}_{\text{surface forces}} + \underbrace{\int_{\omega} \mathbf{f} \, d\omega}_{\text{body forces}} = \underbrace{\frac{d}{dt} \int_{\omega} \rho \ddot{\mathbf{u}} \, d\omega}_{\text{inertial forces}} \quad (12)$$

A relationship can be determined between the densities in the current and reference configurations,  $\int_{\omega} \rho \, d\omega = \int_{\omega_0} \rho_0 J \, d\omega = \int_{\omega_0} \rho_0 \, d\omega$ . Therefore, the Jacobian can also be interpreted as the

---

\* Some authors follow the notation of the first index representing the direction of the component and the second index representing the normal to corresponding coordinate plane. This leads to  $\mathbf{t} \stackrel{\text{def}}{=} \mathbf{t}^{(n)} = \boldsymbol{\sigma} \cdot \mathbf{n}$ . In the absence of couple stresses, a balance of angular momentum implies a symmetry of stress,  $\boldsymbol{\sigma} = \boldsymbol{\sigma}^T$ , and thus the difference in notations becomes immaterial.

ratio of material densities at a point. Since the volume is arbitrary, we can assume that  $\rho J = \rho_0$  holds at every point in the body. Therefore, we may write

$$\frac{d}{dt}(\rho_0) = \frac{d}{dt}(\rho J) = 0$$

when the system is mass conservative over time. This leads to writing the last term in Eq. (12) as

$$\frac{d}{dt} \int_{\omega} \rho \dot{\mathbf{u}} \, d\omega = \int_{\omega_0} \frac{d(\rho J)}{dt} \dot{\mathbf{u}} \, d\omega_0 + \int_{\omega} \rho \ddot{\mathbf{u}} \, d\omega = \int_{\omega} \rho \ddot{\mathbf{u}} \, d\omega$$

From Gauss’s divergence theorem and an implicit assumption that  $\sigma$  is differentiable, we have  $\int_{\omega} (\nabla_x \cdot \sigma + \mathbf{f} - \rho \ddot{\mathbf{u}}) \, d\omega = 0$ . If the volume is argued as being arbitrary, then the relation in the integral must hold pointwise, yielding

$$\nabla_x \cdot \sigma + \mathbf{f} + \rho \ddot{\mathbf{u}} \tag{13}$$

*Note:* Invoking an angular momentum balance, under the assumptions that no infinitesimal “micromoments” or so-called couple stresses exist, it can be shown that the stress tensor must be symmetric,<sup>1</sup> i.e.,

$$\int_{\partial\omega} \mathbf{x} \times \mathbf{t} \, da + \int_{\omega} \mathbf{x} \times \mathbf{f} \, d\omega = \frac{d}{dt} \int_{\omega} \mathbf{x} \cdot \rho \dot{\mathbf{u}} \, d\omega$$

which implies  $\sigma^T = \sigma$ . It is somewhat easier to consider a differential element, such as in Fig. 3, and to simply sum moments about the center. Doing this one immediately obtains  $\sigma_{12} = \sigma_{21}$ ,  $\sigma_{23} = \sigma_{32}$ , and  $\sigma_{13} = \sigma_{31}$ . Therefore

$$\mathbf{t}^{(n)} = \mathbf{t}^{(1)}n_1 + \mathbf{t}^{(2)}n_2 + \mathbf{t}^{(3)}n_3 = \sigma \cdot \mathbf{n} = \begin{bmatrix} \sigma_{11} & \sigma_{12} & \sigma_{13} \\ \sigma_{21} & \sigma_{22} & \sigma_{23} \\ \sigma_{31} & \sigma_{32} & \sigma_{33} \end{bmatrix} \begin{bmatrix} n_1 \\ n_2 \\ n_3 \end{bmatrix} = \sigma^T \cdot \mathbf{n} \tag{14}$$

### 3 INFINITESIMAL LINEARLY ELASTIC CONSTITUTIVE LAWS

The fundamental mechanism that produces forces in elastic deformation is the stretching of atomic bonds. If the deformations are small, then one can argue that we are dealing with only the linear portion of the response. Ultimately, this allows us to usually use linear relationships for models relating forces to deformations. The usual procedure to determine tensile properties of materials is to place samples of material in testing machines, apply the loads, and then measure the resulting deformations, such as lengths and changes in diameter in a portion of the specimen,

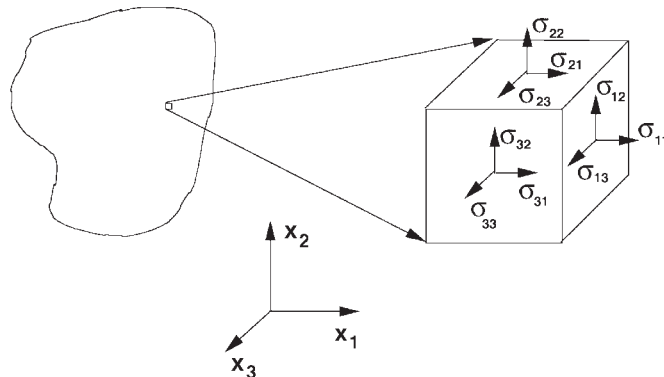


Figure 3 Stress at a point.

of circular cross section, called the gauge length. The location of the gauge length is away from the attachments to the testing machine. The ends where the samples are attached to the machine are larger so that failure will not occur there first, which would ruin the experimental measurements. Slow rates of deformation are applied, and the response is usually measured with strain gauges or extensometers. For a metal, samples are usually 1.25 cm in diameter and 5 cm in length.

The immediate result of a tension test is the axial force ( $F$ ) divided by the original area ( $A_0$ ), denoted, loosely speaking, the “stress,” and change in length ( $\Delta L = L - L_0$ ) per unit length ( $\epsilon_0$ ), or “engineering strain,” measured by strain gauges. As a first approximation we define the tensile stiffness of the material, known as Young’s modulus, denoted  $E$ , by  $\sigma_0 \stackrel{\text{def}}{=} F/A_0 = E(\Delta L/L) \stackrel{\text{def}}{=} E\epsilon_0$ . As we know, the terms  $\sigma_0$  and  $\epsilon_0$  are, strictly speaking, not the true stress and strain but simply serve our presentation purposes. Clearly, what we have presented is somewhat ad hoc; therefore, next we present the classical theory of isotropic elastic material responses for three-dimensional states of stress and strain.

We now discuss relationships between the stress and strain, so-called material laws or constitutive relations for geometrically linear problems (infinitesimal deformations).<sup>\*</sup> The starting point to develop a constitutive theory is to assume a stored elastic energy function exists, a function denoted  $W$ , that depends only on the mechanical deformation. The simplest function that fulfills  $\sigma = \partial W/\partial \epsilon$  is  $W = \frac{1}{2} \epsilon : \mathbb{E} : \epsilon$ . Such a function satisfies the intuitive physical requirement that, for any small strain from an undeformed state, energy must be stored in the material. Alternatively, a small-strain material law can be derived from  $\sigma = \partial W/\partial \epsilon$  and  $W \approx \mathbf{c}_0 + \mathbf{c}_1 : \epsilon + \frac{1}{2} \epsilon : \mathbb{E} : \epsilon + \dots$ , which implies  $\sigma \approx \mathbf{c}_1 + \mathbb{E} : \epsilon + \dots$ . We are free to set  $\mathbf{c}_0 = \mathbf{0}$  (it is arbitrary) to have zero strain energy at zero strain, and furthermore we assume that no stresses exist in the reference state ( $\mathbf{c}_1 = \mathbf{0}$ ); we obtain the familiar relation  $\sigma \approx \mathbb{E} : \epsilon$ . This is a linear (tensorial) relation between stresses and strains. The existence of a strictly positive stored energy function at the reference configuration implies that the linear elasticity tensor must have positive eigenvalues at every point in the body. Typically, different materials are classified according to the number of independent constants in  $\mathbb{E}$ . A general material has 81 independent constants, since it is a fourth-order tensor relating nine components of stress to strain. However, the number of constants can be reduced to 36 since the stress and strain tensors are symmetric. This is easily seen from the matrix representation of  $\mathbb{E}$ :

$$\underbrace{\begin{Bmatrix} \sigma_{11} \\ \sigma_{22} \\ \sigma_{33} \\ \sigma_{12} \\ \sigma_{23} \\ \sigma_{31} \end{Bmatrix}}_{\stackrel{\text{def}}{=} \{\sigma\}} = \underbrace{\begin{bmatrix} E_{1111} & E_{1122} & E_{1133} & E_{1112} & E_{1123} & E_{1113} \\ E_{2211} & E_{2222} & E_{2233} & E_{2212} & E_{2223} & E_{2213} \\ E_{3311} & E_{3322} & E_{3333} & E_{3312} & E_{3323} & E_{3313} \\ E_{1211} & E_{1222} & E_{1233} & E_{1212} & E_{1223} & E_{1213} \\ E_{2311} & E_{2322} & E_{2333} & E_{2312} & E_{2323} & E_{2313} \\ E_{1311} & E_{1322} & E_{1333} & E_{1312} & E_{1323} & E_{1313} \end{bmatrix}}_{\stackrel{\text{def}}{=} \{\mathbb{E}\}} = \underbrace{\begin{Bmatrix} \epsilon_{11} \\ \epsilon_{22} \\ \epsilon_{33} \\ 2\epsilon_{12} \\ 2\epsilon_{23} \\ 2\epsilon_{31} \end{Bmatrix}}_{\stackrel{\text{def}}{=} \{\epsilon\}} \quad (15)$$

The symbol  $[\cdot]$  is used to indicate standard matrix notation equivalent to a tensor form, while  $\{\cdot\}$  indicates vector representation. The existence of a scalar energy function forces  $\mathbb{E}$  to be symmetric since the strains are symmetric, in other words  $W = \frac{1}{2} \epsilon : \mathbb{E} : \epsilon = \frac{1}{2} (\epsilon : \mathbb{E} : \epsilon)^T = \frac{1}{2} \epsilon^T : \mathbb{E}^T : \epsilon = \frac{1}{2} \epsilon : \mathbb{E}^T : \epsilon$ , which implies  $\mathbb{E}^T = \mathbb{E}$ . Consequently,  $\mathbb{E}$  has only 21 free constants. The nonnegativity of  $W$  imposes the restriction that  $\mathbb{E}$  remain positive definite. At this point, based on many factors that depend on the material microstructure, it can be shown that the components of  $\mathbb{E}$  may be written in terms of anywhere between 21 and 2 independent parameters. Specifically, if there are an infinite number of planes where the material properties

<sup>\*</sup> Furthermore, we neglect all thermal effects.

are equal in all directions, there are two free constants, the Lamé parameters, and the material is of the familiar *isotropic* variety. An isotropic body has material properties that are the same in every direction at a point in the body, i.e., the properties are not a function of orientation at a point in a body. Accordingly, for isotropic materials, with two planes of symmetry and an infinite number of planes of directional independence (two free constants),

$$\mathbb{E} \stackrel{\text{def}}{=} \begin{bmatrix} \kappa + \frac{4}{3}\mu & \kappa - \frac{2}{3}\mu & \kappa - \frac{2}{3}\mu & 0 & 0 & 0 \\ \kappa - \frac{2}{3}\mu & \kappa + \frac{4}{3}\mu & \kappa - \frac{2}{3}\mu & 0 & 0 & 0 \\ \kappa - \frac{2}{3}\mu & \kappa - \frac{2}{3}\mu & \kappa + \frac{4}{3}\mu & 0 & 0 & 0 \\ 0 & 0 & 0 & \mu & 0 & 0 \\ 0 & 0 & 0 & 0 & \mu & 0 \\ 0 & 0 & 0 & 0 & 0 & \mu \end{bmatrix} \quad (16)$$

In this case we have

$$\mathbb{E} : \boldsymbol{\varepsilon} = 3\kappa \frac{\text{tr } \boldsymbol{\varepsilon}}{3} \mathbf{1} + 2\mu \boldsymbol{\varepsilon}' \Rightarrow \boldsymbol{\varepsilon} : \mathbb{E} : \boldsymbol{\varepsilon} = 9\kappa \left( \frac{\text{tr } \boldsymbol{\varepsilon}}{3} \right)^2 + 2\mu \boldsymbol{\varepsilon}' : \boldsymbol{\varepsilon}' \quad (17)$$

where  $\text{tr } \boldsymbol{\varepsilon} = \varepsilon_{ii}$  and  $\boldsymbol{\varepsilon}' = \boldsymbol{\varepsilon} - \frac{1}{3}(\text{tr } \boldsymbol{\varepsilon})\mathbf{1}$ . The eigenvalues of an isotropic elasticity tensor are  $(3, 2\mu, 2\mu, \mu, \mu, \mu)$ . Therefore, we must have  $\kappa > 0$  and  $\mu > 0$  to retain positive definiteness of  $\mathbb{E}$ .

It is sometimes important to split infinitesimal strains into two physically meaningful parts  $\boldsymbol{\varepsilon} = (\text{tr } \boldsymbol{\varepsilon}/3)\mathbf{1} + [\boldsymbol{\varepsilon} - (\text{tr } \boldsymbol{\varepsilon}/3)\mathbf{1}]$ . The Jacobian,  $J$ , of the deformation gradient  $\mathbf{F}$  is  $\det(\mathbf{1} + \nabla_{\mathbf{x}} \mathbf{u})$  and can be expanded as  $J = \det \mathbf{F} = \det(\mathbf{1} + \nabla_{\mathbf{x}} \mathbf{u}) \approx \mathbf{1} + \text{tr } \nabla_{\mathbf{x}} \mathbf{u} + \mathcal{O}(\nabla_{\mathbf{x}} \mathbf{u}) = \mathbf{1} + \text{tr } \boldsymbol{\varepsilon} + \dots$ , and therefore with infinitesimal strains  $(\mathbf{1} + \text{tr } \boldsymbol{\varepsilon}) d\omega_0 = d\omega \Rightarrow \text{tr } \boldsymbol{\varepsilon} = (d\omega - d\omega_0)/d\omega_0$ . Hence,  $\text{tr } \boldsymbol{\varepsilon}$  is associated with the volumetric part of the deformation. Furthermore, since  $\text{tr}[\boldsymbol{\varepsilon} - (\text{tr } \boldsymbol{\varepsilon}/3) \mathbf{1}] = 0$ , the so-called strain deviator can only affect the shape of a differential element. *In other words, it describes distortion in the material.*

The stress  $\boldsymbol{\sigma}$  can be split into two parts (dilatational and a deviatoric part):  $\boldsymbol{\sigma} = (\text{tr } \boldsymbol{\sigma}/3) \mathbf{1} + [\boldsymbol{\sigma} - (\text{tr } \boldsymbol{\sigma}/3) \mathbf{1}] - p\mathbf{1} + \boldsymbol{\sigma}'$ , where we call the symbol  $p$  the hydrostatic pressure and  $\boldsymbol{\sigma}'$  the stress deviator. This is one form of Hooke's law. The resistance to change in the volume is measured by  $\kappa$ . We note that  $[(\text{tr } \boldsymbol{\sigma}/3)\mathbf{1}]' = 0$ , which indicates that this part of the stress produces no distortion. Another fundamental form of Hooke's law is

$$\boldsymbol{\sigma} = \frac{E}{1 + \nu} \left( \boldsymbol{\varepsilon} + \frac{\nu}{1 - 2\nu} \text{tr } \boldsymbol{\varepsilon} \mathbf{1} \right)$$

which implies  $\boldsymbol{\varepsilon} = [(1 - \nu)/E]\boldsymbol{\sigma} - (\nu/E) \text{tr } \boldsymbol{\sigma} \mathbf{1}$ . To interpret the constants, consider a uniaxial test where  $\sigma_{12} = \sigma_{13} = \sigma_{23} = 0 \Rightarrow \varepsilon_{12} = \varepsilon_{13} = \varepsilon_{23} = 0, \sigma_{22} = \sigma_{33} = 0$ . Under these conditions we have  $\sigma_{11} = E\varepsilon_{11}$  and  $\varepsilon_{22} = \varepsilon_{33} = \nu\varepsilon_{11}$ . Therefore, Young's modulus  $E$  is the ratio of the uniaxial stress to the corresponding strain component. The Poisson ratio is the ratio of the transverse strains to the uniaxial strain.

Another commonly used set of stress-strain forms are the Lamé relations,  $\boldsymbol{\sigma} = \lambda \text{tr } \boldsymbol{\varepsilon} \mathbf{1} + 2\mu \boldsymbol{\varepsilon}$  or

$$\boldsymbol{\varepsilon} = \frac{\lambda}{2\mu(3\lambda + 2\mu)} \text{tr } \boldsymbol{\sigma} \mathbf{1} + \frac{\boldsymbol{\sigma}}{2\mu}$$

To interpret the constants, consider a pressure test where  $\sigma_{12} = \sigma_{13} = \sigma_{23} = 0$  and  $\sigma_{11} = \sigma_{22} = \sigma_{33}$ . Under these conditions we have

$$\kappa = \lambda + \frac{2}{3} \mu = \frac{E}{3(1 - 2\nu)} \quad \mu = \frac{E}{2(1 + \nu)} \quad \frac{\kappa}{\mu} = \frac{2(1 + \nu)}{3(1 - 2\nu)}$$

We observe that  $\kappa/\mu \rightarrow \infty$ , which implies that  $\nu \rightarrow \frac{1}{2}$ , and  $\kappa/\mu \rightarrow 0$  implies  $\nu \rightarrow -1$ . Therefore, from the fact that both  $\kappa$  and  $\mu$  must be positive and finite, this implies  $-1 < \nu < 0.5$

and  $0 < E < \infty$ . For example, some polymeric foams exhibit  $\nu < 0$ , steels  $\nu \approx 0.3$ , and some forms of rubber have  $\nu \rightarrow 0.5$ . However, *no restrictions arise on  $\lambda$ , i.e., it could be positive or negative.*

#### 4 FOUNDATIONS OF THE FINITE-ELEMENT METHOD

In most problems of mathematical physics the true solutions are nonsmooth, i.e., not continuously differentiable. For example, in the equation of static mechanical equilibrium,\*

$$\nabla \cdot \boldsymbol{\sigma} + \mathbf{f} = \mathbf{0} \tag{18}$$

there is an implicit requirement that the stress  $\boldsymbol{\sigma}$  is differentiable in the classical sense. Virtually the same mathematical structure holds for other partial differential equations of mathematical physics describing diffusion, heat conduction, etc. *In many applications, differentiability is too strong a requirement.* Therefore, when solving such problems we have two options: (1) enforcement of jump conditions at every interface or (2) weak formulations (weakening the regularity requirements). Weak forms, which are designed to accommodate irregular data and solutions, are usually preferred. *Numerical techniques employing weak forms, such as the FEM, have been developed with the essential property that whenever a smooth classical solution exists, it is also a solution to the weak-form problem.* Therefore, we lose nothing by reformulating a problem in a weaker way.

The FEM starts by rewriting the field equations in so-called weak form. To derive a direct weak form for a body, we take the equilibrium equations (denoted the strong form) and form a scalar product with an arbitrary smooth vector-valued function  $\mathbf{v}$  and integrate over the body,  $\int_{\Omega} (\nabla \cdot \boldsymbol{\sigma} + \mathbf{f}) \cdot \mathbf{v} \, d\Omega = \int_{\Omega} \mathbf{r} \cdot \mathbf{v} \, d\Omega = 0$ , where  $\mathbf{r}$  is called the residual. We call  $\mathbf{v}$  a “test” function. If we were to add a condition that we do this for all ( $\stackrel{\text{def}}{=} \forall$ ) possible test functions, then  $\int_{\Omega} (\nabla \cdot \boldsymbol{\sigma} + \mathbf{f}) \cdot \mathbf{v} \, d\Omega = \int_{\Omega} \mathbf{r} \cdot \mathbf{v} \, d\Omega = 0 \forall \mathbf{v}$  implies  $\mathbf{r} = \mathbf{0}$ . Therefore, if every possible test function was considered, then  $\mathbf{r} = \nabla \cdot \boldsymbol{\sigma} + \mathbf{f} = \mathbf{0}$  on any finite region in  $\Omega$ . Consequently, the weak and strong statements would be equivalent provided the true solution is smooth enough to have a strong solution. Clearly,  $\mathbf{r}$  can never be zero over any finite region in the body because the test function will “find” them. Using the product rule of differentiation,  $\nabla \cdot (\boldsymbol{\sigma} \cdot \mathbf{v}) = (\nabla \cdot \boldsymbol{\sigma}) \cdot \mathbf{v} + \nabla \mathbf{v} : \boldsymbol{\sigma}$  leads to,  $\forall \mathbf{v}$ ,  $\int_{\Omega} (\nabla \cdot (\boldsymbol{\sigma} \cdot \mathbf{v}) - \nabla \mathbf{v} : \boldsymbol{\sigma}) \, d\Omega + \int_{\Omega} \mathbf{f} \cdot \mathbf{v} \, d\Omega = 0$ , where we choose the  $\mathbf{v}$  from an admissible set, to be discussed momentarily. Using the divergence theorem leads to,  $\forall \mathbf{v}$ ,  $\int_{\Omega} \nabla \mathbf{v} : \boldsymbol{\sigma} \, d\Omega = \int_{\Omega} \mathbf{f} \cdot \mathbf{v} \, d\Omega + \int_{\partial\Omega} \boldsymbol{\sigma} \cdot \mathbf{n} \cdot \mathbf{v} \, dA$ , which leads to  $\int_{\Omega} \nabla \mathbf{v} : \boldsymbol{\sigma} \, d\Omega = \int_{\Omega} \mathbf{f} \cdot \mathbf{v} \, d\Omega + \int_{\Gamma_t} \mathbf{t} \cdot \mathbf{v} \, dA$ . If we decide to restrict our choices of  $\mathbf{v}$ ’s to those such that  $\mathbf{v}|_{\Gamma} = \mathbf{0}$ , we have, where  $\mathbf{d}$  is the applied boundary displacement on  $\Gamma_u$ , for infinitesimal strain linear elasticity,

Find  $\mathbf{u}$ ,  $\mathbf{u}|_{\Gamma_u} = \mathbf{d}$  such that,  $\forall \mathbf{v}$ ,  $\mathbf{v}|_{\Gamma_u} = \mathbf{0}$ :

$$\underbrace{\int_{\Omega} \nabla \mathbf{v} : \boldsymbol{\varepsilon} : \nabla \mathbf{u} \, d\Omega}_{\stackrel{\text{def}}{=} \mathcal{B}(\mathbf{u}, \mathbf{v})} = \underbrace{\int_{\Omega} \mathbf{f} \cdot \mathbf{v} \, d\Omega + \int_{\Gamma_t} \mathbf{t} \cdot \mathbf{v} \, dA}_{\stackrel{\text{def}}{=} \mathcal{F}(\mathbf{v})} \tag{19}$$

This is called a weak form because it does not require the differentiability of the stress  $\boldsymbol{\sigma}$ . In other words, the differentiability requirements have been *weakened*. It is clear that we are able to consider problems with quite irregular solutions. We observe that if we test the solution with all possible test functions of sufficient smoothness, then the weak solution is equivalent to the

---

\* Here  $\mathbf{f}$  are the body forces.

strong solution. We emphasize that provided the true solution is smooth enough, the weak and strong forms are equivalent, which can be seen by the above constructive derivation.

### 5 HILBERTIAN SOBOLEV SPACES

A key question is the selection of the sets of functions in the weak form. Somewhat naively, the answer is simple, the integrals must remain finite. Therefore, the following restrictions hold  $(\forall \mathbf{v}), \int_{\Omega} \mathbf{f} \cdot \mathbf{v} \, d\Omega < \infty, \int_{\partial\Omega} \boldsymbol{\sigma} \cdot \mathbf{n} \cdot \mathbf{v} \, d\Omega < \infty$  and  $\int_{\Omega} \nabla \mathbf{v} : \boldsymbol{\sigma} \, d\Omega < \infty$ , and govern the selection of the approximation spaces. These relations simply mean that the functions must be square integrable. To make precise statements, one must have a method of bookkeeping. Such a system is to employ so-called Hilbertian Sobolev spaces. We recall that a norm has three main characteristics for any vectors  $\mathbf{u}$  and  $\mathbf{v}$  such that  $\|\mathbf{u}\| < \infty$  and  $\|\mathbf{v}\| < \infty$  and (1)  $\|\mathbf{u}\| > 0, \|\mathbf{u}\| = 0$  if and only if  $\mathbf{u} = 0$ , (2)  $\|\mathbf{u} + \mathbf{v}\| \leq \|\mathbf{u}\| + \|\mathbf{v}\|$ , and (3)  $\|\alpha \mathbf{u}\| \leq |\alpha| \|\mathbf{u}\|$ , where  $\alpha$  is a scalar. Certain types of norms, so-called Hilbert space norms, are frequently used in solid mechanics. Following standard notation, we denote  $H^1(\Omega)$  as the usual space of scalar functions with generalized partial derivatives of order  $\leq 1$  in  $L^2(\Omega)$ , i.e., square integrable, in other words

$$u \in H^1(\Omega) \quad \text{if} \quad \|u\|_{H^1(\Omega)}^2 \stackrel{\text{def}}{=} \int_{\Omega} \frac{\partial u}{\partial x_j} \frac{\partial u}{\partial x_j} \, d\Omega + \int_{\Omega} uu \, d\Omega < \infty$$

We define  $\mathbf{H}^2(\Omega) \stackrel{\text{def}}{=} [H^1(\Omega)]^3$  as the space of vector-valued functions whose components are in  $H^1(\Omega)$ , i.e.,

$$\mathbf{u} \in \mathbf{H}^1(\Omega) \quad \text{if} \quad \|\mathbf{u}\|_{H^1(\Omega)}^2 \stackrel{\text{def}}{=} \int_{\Omega} \frac{\partial u_i}{\partial x_j} \frac{\partial u_i}{\partial x_j} \, d\Omega + \int_{\Omega} u_i u_i \, d\Omega < \infty \tag{20}$$

and we denote  $\mathbf{L}^2(\Omega) \stackrel{\text{def}}{=} [L^2(\Omega)]^3$ . Using these definitions, a complete boundary value problem can be written as follows. The data (loads) are assumed to be such that  $\mathbf{f} \in \mathbf{L}^2(\Omega)$  and  $\mathbf{t} \in \mathbf{L}^2(\Gamma_t)$ , but less smooth data can be considered without complications. Implicitly we require that  $\mathbf{u} \in \mathbf{H}^1(\Omega)$  and  $\boldsymbol{\sigma} \in \mathbf{L}^2(\Omega)$  without continually making such references. Therefore, in summary, we assume that our solutions obey these restrictions, leading to the following infinitesimal strain linear elasticity weak form:

Find  $\mathbf{u} \in \mathbf{H}^1(\Omega), \mathbf{u}|_{\Gamma_u} = \mathbf{d}$ , such that,  $\forall \mathbf{v} \in \mathbf{H}^1(\Omega), \mathbf{v}|_{\Gamma_u} = \mathbf{0}$  :

$$\int_{\Omega} \nabla \mathbf{v} : \mathbb{E} : \nabla \mathbf{u} \, d\Omega = \int_{\Omega} \mathbf{f} \cdot \mathbf{v} \, d\Omega + \int_{\Gamma_t} \mathbf{t} \cdot \mathbf{v} \, dA \tag{21}$$

We note that if the data in (21) are smooth and if (21) possesses a solution  $\mathbf{u}$  that is sufficiently regular, then  $\mathbf{u}$  is the solution of the classical linear elastostatic problem in strong form:

$$\begin{aligned} \nabla \cdot (\mathbb{E} : \nabla \mathbf{u}) + \mathbf{f} &= 0, & \mathbf{x} &\in \Omega \\ \mathbf{u} &= \mathbf{d} & \mathbf{x} &\in \Gamma_u \\ (\mathbb{E} : \nabla \mathbf{u}) \cdot \mathbf{n} &= \mathbf{t} & \mathbf{x} &\in \Gamma_t \end{aligned} \tag{22}$$

### 6 FINITE-ELEMENT FORMULATION IN THREE DIMENSIONS

Consider the following general form:

Find  $\mathbf{u} \in \mathbf{H}^1(\Omega)$  such that,  $\forall \mathbf{v} \in \mathbf{H}^1(\Omega)$ ,

$$\int_{\Omega} \nabla \mathbf{v} : \mathbb{E} : \nabla \mathbf{u} \, d\Omega = \int_{\Omega} \mathbf{f} \cdot \mathbf{v} \, d\Omega + \int_{\Gamma_t} \mathbf{t} \cdot \mathbf{v} \, dA \tag{23}$$

It is convenient to write the bilinear form in the following (matrix) manner:

$$\int_{\Omega} ([\mathbf{D}]\{\mathbf{v}\})^T [E]([\mathbf{D}]\{\mathbf{u}\}) d\Omega = \int_{\Omega} \{\mathbf{v}\}^T \{\mathbf{f}\} d\Omega + \int_{\Gamma_t} \{\mathbf{v}\}^T \{\mathbf{t}\} dA \quad (24)$$

where  $[\mathbf{D}]$ , the deformation tensor, is

$$[\mathbf{D}] \stackrel{\text{def}}{=} \begin{bmatrix} \frac{\partial}{\partial x_1} & 0 & 0 \\ 0 & \frac{\partial}{\partial x_2} & 0 \\ 0 & 0 & \frac{\partial}{\partial x_3} \\ \frac{\partial}{\partial x_2} & \frac{\partial}{\partial x_1} & 0 \\ 0 & \frac{\partial}{\partial x_3} & \frac{\partial}{\partial x_2} \\ \frac{\partial}{\partial x_3} & 0 & \frac{\partial}{\partial x_1} \end{bmatrix} \quad \{\mathbf{u}\} \stackrel{\text{def}}{=} \begin{Bmatrix} u_1 \\ u_2 \\ u_3 \end{Bmatrix} \quad \{\mathbf{f}\} \stackrel{\text{def}}{=} \begin{Bmatrix} f_1 \\ f_2 \\ f_3 \end{Bmatrix} \quad \{\mathbf{t}\} \stackrel{\text{def}}{=} \begin{Bmatrix} t_1 \\ t_2 \\ t_3 \end{Bmatrix} \quad (25)$$

It is clear that in an implementation of the FEM, the sparsity of  $\mathbf{D}$  should be taken into account. It is also convenient to write

$$\begin{aligned} u_1^h(x_1, x_2, x_3) &= \sum_{i=1}^N a_i \phi_i(x_1, x_2, x_3) \\ u_2^h(x_1, x_2, x_3) &= \sum_{i=1}^N a_{i+N} \phi_i(x_1, x_2, x_3) \\ u_3^h(x_1, x_2, x_3) &= \sum_{i=1}^N a_{i+2N} \phi_i(x_1, x_2, x_3) \end{aligned} \quad (26)$$

or  $\{\mathbf{u}^h\} = [\phi]\{\mathbf{a}\}$ , where, for example, for trilinear shape functions

$$[\phi] \stackrel{\text{def}}{=} \begin{bmatrix} \phi_1 & \phi_2 & \phi_3 & \phi_4 & \phi_5 & \phi_6 \cdots \phi_N & 0 & 0 & 0 & 0 & 0 & 0 \cdots & 0 & 0 & 0 & 0 & 0 \cdots \\ 0 & 0 & 0 & 0 & 0 & 0 & \phi_1 & \phi_2 & \phi_3 & \phi_4 & \phi_5 & \phi_6 \cdots \phi_N & 0 & 0 & 0 & 0 & 0 \cdots \\ 0 & 0 & 0 & 0 & 0 & 0 & 0 & 0 & 0 & 0 & 0 & 0 \cdots & \phi_1 & \phi_2 & \phi_3 & \phi_4 & \phi_5 & \phi_6 \cdots \phi_N \end{bmatrix} \quad (27)$$

where  $\mathbf{u}^h$  is the discrete (approximate) solution.

It is advantageous to write

$$\{\mathbf{a}\} \stackrel{\text{def}}{=} \begin{Bmatrix} a_1 \\ a_2 \\ a_3 \\ \vdots \\ \vdots \\ a_{3N} \end{Bmatrix} \quad \underbrace{\{\phi_i\} \stackrel{\text{def}}{=} \begin{Bmatrix} \phi_i \\ 0 \\ 0 \end{Bmatrix}}_{\text{for } 1 \leq i \leq N} \quad \underbrace{\{\phi_i\} \stackrel{\text{def}}{=} \begin{Bmatrix} 0 \\ \phi_i \\ 0 \end{Bmatrix}}_{\text{for } N+1 \leq i \leq 2N} \quad \underbrace{\{\phi_i\} \stackrel{\text{def}}{=} \begin{Bmatrix} 0 \\ 0 \\ \phi_i \end{Bmatrix}}_{\text{for } 2N+1 \leq i \leq 3N} \quad (28)$$

and  $\{\mathbf{u}^h\} = \sum_{i=1}^N \mathbf{a}_i \{\phi_i\}$ . If we choose  $\mathbf{v}$  with the same basis but a different linear combination  $\{\mathbf{v}\} = [\phi]\{\mathbf{b}\}$ , then we may write

$$\underbrace{\int_{\Omega} ([\mathbf{D}][\phi]\{\mathbf{b}\})^T [E]([\mathbf{D}][\phi]\{\mathbf{a}\}) d\Omega}_{\{\mathbf{b}\}^T [\mathbf{K}]\{\mathbf{a}\} \text{ stiffness}} = \underbrace{\int_{\Omega} ([\phi]\{\mathbf{b}\})^T \{\mathbf{f}\} d\Omega}_{\text{body load}} + \underbrace{\int_{\Gamma_t} ([\phi]\{\mathbf{b}\})^T \{\mathbf{t}\} dA}_{\text{traction load}} \quad (29)$$



Since  $\{\mathbf{b}\}$  is arbitrary, i.e., the weak statement implies  $\forall \mathbf{v} \Rightarrow \nabla\{\mathbf{b}\}$ , therefore

$$\begin{aligned} \{\mathbf{b}\}^T \{[\mathbf{K}]\{\mathbf{a}\} - \{\mathbf{R}\}\} &= \mathbf{0} \Rightarrow [\mathbf{K}]\{\mathbf{a}\} = \{\mathbf{R}\} \\ [\mathbf{K}] &\stackrel{\text{def}}{=} \int_{\Omega} ([\mathbf{D}][\phi])^T [\mathbf{E}]( [\mathbf{D}][\phi]) \, d\Omega \\ [\mathbf{R}] &\stackrel{\text{def}}{=} \int_{\Omega} [\phi]^T \{\mathbf{f}\} \, d\Omega + \int_{\Gamma_t} [\phi]^T \{\mathbf{t}\} \, dA \end{aligned} \quad (30)$$

This is the system of equations that is to be solved.

## 7 GLOBAL/LOCAL TRANSFORMATIONS

One strength of the FEM is that most of the computations can be done in an element-by-element manner. We define the entries of  $[\mathbf{K}]$ ,

$$K_{ij} = \int_{\Omega} ([\mathbf{D}][\phi_i])^T [\mathbf{E}]( [\mathbf{D}][\phi_j]) \, d\Omega \quad (31)$$

and

$$R_i = \int_{\Omega} [\phi_i]^T \{\mathbf{f}\} \, d\Omega + \int_{\Gamma_t} [\phi_i]^T \{\mathbf{t}\} \, dA \quad (32)$$

Breaking the calculations into elements,  $K_{ij} = \sum_e K_{ij}^e$ , where

$$K_{ij}^e = \int_{\Omega_e} ([\mathbf{D}][\phi_i])^T [\mathbf{E}]( [\mathbf{D}][\phi_j]) \, d\Omega \quad (33)$$

To make the calculations systematic, we wish to use the generic or master element defined in a local coordinate system  $(\zeta_1, \zeta_2, \zeta_3)$  (Fig. 4). Accordingly, we need the

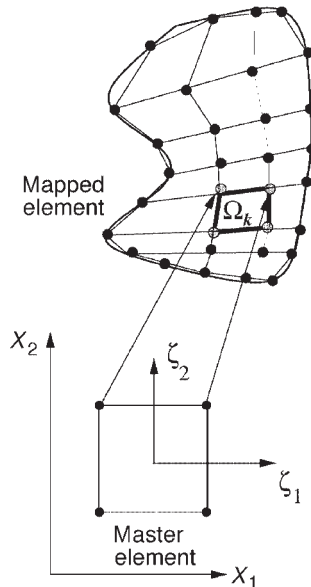


Figure 4 Two-dimensional finite-element mapping.

following mapping functions, from the master coordinates to the real space coordinates,  $M : (x_1, x_2, x_3) \mapsto (\zeta_1, \zeta_2, \zeta_3)$  (for example, trilinear bricks):

$$\begin{aligned} x_1 &= \sum_{i=1}^8 X_{1i} \hat{\phi}_i \stackrel{\text{def}}{=} M_{x_1}(\zeta_1, \zeta_2, \zeta_3) \\ x_2 &= \sum_{i=1}^8 X_{2i} \hat{\phi}_i \stackrel{\text{def}}{=} M_{x_2}(\zeta_1, \zeta_2, \zeta_3) \\ x_3 &= \sum_{i=1}^8 X_{3i} \hat{\phi}_i \stackrel{\text{def}}{=} M_{x_3}(\zeta_1, \zeta_2, \zeta_3) \end{aligned} \quad (34)$$

where  $(X_{1i}, X_{2i}, X_{3i})$  are true spatial coordinates of the  $i$ th node and where  $\hat{\phi}(\zeta_1, \zeta_2, \zeta_3) \stackrel{\text{def}}{=} \phi(x_1(\zeta_1, \zeta_2, \zeta_3), x_2(\zeta_1, \zeta_2, \zeta_3), x_3(\zeta_1, \zeta_2, \zeta_3))$ . These types of mappings are usually termed parametric maps. If the polynomial order of the shape functions is as high as the element, it is an isoparametric map; lower, then a subparametric map; higher, then a superparametric map.

## 8 DIFFERENTIAL PROPERTIES OF SHAPE FUNCTIONS

The master element shape functions form a nodal base of trilinear approximation given by

$$\begin{aligned} \hat{\phi}_1 &= \frac{1}{8}(1 - \zeta_1)(1 - \zeta_2)(1 - \zeta_3) & \hat{\phi}_2 &= \frac{1}{8}(1 + \zeta_1)(1 - \zeta_2)(1 - \zeta_3) \\ \hat{\phi}_3 &= \frac{1}{8}(1 + \zeta_1)(1 + \zeta_2)(1 - \zeta_3) & \hat{\phi}_4 &= \frac{1}{8}(1 - \zeta_1)(1 + \zeta_2)(1 - \zeta_3) \\ \hat{\phi}_5 &= \frac{1}{8}(1 - \zeta_1)(1 - \zeta_2)(1 + \zeta_3) & \hat{\phi}_6 &= \frac{1}{8}(1 + \zeta_1)(1 - \zeta_2)(1 + \zeta_3) \\ \hat{\phi}_7 &= \frac{1}{8}(1 + \zeta_1)(1 + \zeta_2)(1 + \zeta_3) & \hat{\phi}_8 &= \frac{1}{8}(1 - \zeta_1)(1 + \zeta_2)(1 + \zeta_3) \end{aligned} \quad (35)$$

- For trilinear elements we have a nodal basis consisting of 8 nodes, and since it is vector valued, 24 total degrees of freedom, or 3 shape functions for each node. See Fig. 5.
- For triquadratic elements we have a nodal basis consisting of 27 nodes, and since it is vector valued, 81 total degrees of freedom, or three shape functions for each node. The nodal shape functions can be derived quite easily by realizing that it is a nodal basis, e.g., they are unity at the corresponding node and zero at all other nodes.

We note that the  $\phi_i$ 's are never really computed; we actually start with the  $\hat{\phi}_i$ 's. Therefore in the stiffness matrix and right-hand-side element calculations, all terms must be defined in terms of the local coordinates. With this in mind we lay down some fundamental relations, which are directly related to the concepts of deformation presented in our discussion in continuum mechanics. It is not surprising that a deformation gradient reappears in the following form:

$$|\mathbf{F}| \stackrel{\text{def}}{=} \left| \frac{\partial \mathbf{x}(x_1, x_2, x_3)}{\partial \zeta(\zeta_1, \zeta_2, \zeta_3)} \right| \quad \text{where} \quad \mathbf{F} \stackrel{\text{def}}{=} \begin{bmatrix} \frac{\partial x_1}{\partial \zeta_1} & \frac{\partial x_1}{\partial \zeta_2} & \frac{\partial x_1}{\partial \zeta_3} \\ \frac{\partial x_2}{\partial \zeta_1} & \frac{\partial x_2}{\partial \zeta_2} & \frac{\partial x_2}{\partial \zeta_3} \\ \frac{\partial x_3}{\partial \zeta_1} & \frac{\partial x_3}{\partial \zeta_2} & \frac{\partial x_3}{\partial \zeta_3} \end{bmatrix} \quad (36)$$

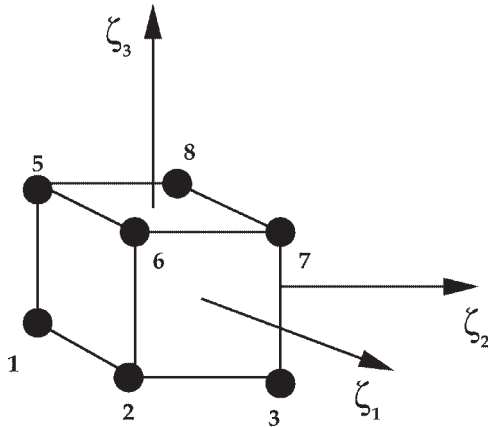


Figure 5 Trilinear hexahedron or “brick.”

The corresponding determinant is

$$\begin{aligned}
 |\mathbf{F}| &= \frac{\partial x_1}{\partial \zeta_1} \left( \frac{\partial x_2}{\partial \zeta_2} \frac{\partial x_3}{\partial \zeta_3} - \frac{\partial x_3}{\partial \zeta_2} \frac{\partial x_2}{\partial \zeta_3} \right) - \frac{\partial x_1}{\partial \zeta_2} \left( \frac{\partial x_2}{\partial \zeta_1} \frac{\partial x_3}{\partial \zeta_3} - \frac{\partial x_3}{\partial \zeta_1} \frac{\partial x_2}{\partial \zeta_3} \right) \\
 &\quad + \frac{\partial x_1}{\partial \zeta_3} \left( \frac{\partial x_2}{\partial \zeta_1} \frac{\partial x_3}{\partial \zeta_2} - \frac{\partial x_3}{\partial \zeta_1} \frac{\partial x_2}{\partial \zeta_2} \right)
 \end{aligned} \tag{37}$$

The differential relations  $\zeta \rightarrow \mathbf{x}$  are

$$\begin{aligned}
 \frac{\partial}{\partial \zeta_1} &= \frac{\partial}{\partial x_1} \frac{\partial x_1}{\partial \zeta_1} + \frac{\partial}{\partial x_2} \frac{\partial x_2}{\partial \zeta_1} + \frac{\partial}{\partial x_3} \frac{\partial x_3}{\partial \zeta_1} \\
 \frac{\partial}{\partial \zeta_2} &= \frac{\partial}{\partial x_1} \frac{\partial x_1}{\partial \zeta_2} + \frac{\partial}{\partial x_2} \frac{\partial x_2}{\partial \zeta_2} + \frac{\partial}{\partial x_3} \frac{\partial x_3}{\partial \zeta_2} \\
 \frac{\partial}{\partial \zeta_3} &= \frac{\partial}{\partial x_1} \frac{\partial x_1}{\partial \zeta_3} + \frac{\partial}{\partial x_2} \frac{\partial x_2}{\partial \zeta_3} + \frac{\partial}{\partial x_3} \frac{\partial x_3}{\partial \zeta_3}
 \end{aligned} \tag{38}$$

The inverse differential relations  $\mathbf{x} \rightarrow \zeta$  are

$$\begin{aligned}
 \frac{\partial}{\partial x_1} &= \frac{\partial}{\partial \zeta_1} \frac{\partial \zeta_1}{\partial x_1} + \frac{\partial}{\partial \zeta_2} \frac{\partial \zeta_2}{\partial x_1} + \frac{\partial}{\partial \zeta_3} \frac{\partial \zeta_3}{\partial x_1} \\
 \frac{\partial}{\partial x_2} &= \frac{\partial}{\partial \zeta_1} \frac{\partial \zeta_1}{\partial x_2} + \frac{\partial}{\partial \zeta_2} \frac{\partial \zeta_2}{\partial x_2} + \frac{\partial}{\partial \zeta_3} \frac{\partial \zeta_3}{\partial x_2} \\
 \frac{\partial}{\partial x_3} &= \frac{\partial}{\partial \zeta_1} \frac{\partial \zeta_1}{\partial x_3} + \frac{\partial}{\partial \zeta_2} \frac{\partial \zeta_2}{\partial x_3} + \frac{\partial}{\partial \zeta_3} \frac{\partial \zeta_3}{\partial x_3}
 \end{aligned} \tag{39}$$

and

$$\begin{Bmatrix} dx_1 \\ dx_2 \\ dx_3 \end{Bmatrix} = \begin{bmatrix} \frac{\partial x_1}{\partial \zeta_1} & \frac{\partial x_1}{\partial \zeta_2} & \frac{\partial x_1}{\partial \zeta_3} \\ \frac{\partial x_2}{\partial \zeta_1} & \frac{\partial x_2}{\partial \zeta_2} & \frac{\partial x_2}{\partial \zeta_3} \\ \frac{\partial x_3}{\partial \zeta_1} & \frac{\partial x_3}{\partial \zeta_2} & \frac{\partial x_3}{\partial \zeta_3} \end{bmatrix} \begin{Bmatrix} d\zeta_1 \\ d\zeta_2 \\ d\zeta_3 \end{Bmatrix} \quad (40)$$

and the inverse form

$$\begin{Bmatrix} d\zeta_1 \\ d\zeta_2 \\ d\zeta_3 \end{Bmatrix} = \begin{bmatrix} \frac{\partial \zeta_1}{\partial x_1} & \frac{\partial \zeta_1}{\partial x_2} & \frac{\partial \zeta_1}{\partial x_3} \\ \frac{\partial \zeta_2}{\partial x_1} & \frac{\partial \zeta_2}{\partial x_2} & \frac{\partial \zeta_2}{\partial x_3} \\ \frac{\partial \zeta_3}{\partial x_1} & \frac{\partial \zeta_3}{\partial x_2} & \frac{\partial \zeta_3}{\partial x_3} \end{bmatrix} \begin{Bmatrix} dx_1 \\ dx_2 \\ dx_3 \end{Bmatrix} \quad (41)$$

Noting the following relationship

$$\mathbf{F}^{-1} = \frac{\text{adj } \mathbf{F}}{|\mathbf{F}|} \quad \text{where} \quad \text{adj } \mathbf{F} \stackrel{\text{def}}{=} \begin{bmatrix} A_{11} & A_{12} & A_{13} \\ A_{21} & A_{22} & A_{23} \\ A_{31} & A_{32} & A_{33} \end{bmatrix}^T \quad (42)$$

where

$$\begin{array}{ll} A_{11} = \left[ \frac{\partial x_2}{\partial \zeta_2} \frac{\partial x_3}{\partial \zeta_3} - \frac{\partial x_3}{\partial \zeta_2} \frac{\partial x_2}{\partial \zeta_3} \right] = |\mathbf{F}| \frac{\partial \zeta_1}{\partial x_1} & A_{12} = \left[ \frac{\partial x_2}{\partial \zeta_1} \frac{\partial x_3}{\partial \zeta_3} - \frac{\partial x_3}{\partial \zeta_1} \frac{\partial x_2}{\partial \zeta_3} \right] = |\mathbf{F}| \frac{\partial \zeta_2}{\partial x_1} \\ A_{13} = \left[ \frac{\partial x_2}{\partial \zeta_1} \frac{\partial x_3}{\partial \zeta_2} - \frac{\partial x_3}{\partial \zeta_1} \frac{\partial x_2}{\partial \zeta_2} \right] = |\mathbf{F}| \frac{\partial \zeta_3}{\partial x_1} & A_{21} = \left[ \frac{\partial x_1}{\partial \zeta_2} \frac{\partial x_3}{\partial \zeta_3} - \frac{\partial x_3}{\partial \zeta_2} \frac{\partial x_1}{\partial \zeta_3} \right] = |\mathbf{F}| \frac{\partial \zeta_1}{\partial x_2} \\ A_{22} = \left[ \frac{\partial x_1}{\partial \zeta_1} \frac{\partial x_3}{\partial \zeta_3} - \frac{\partial x_3}{\partial \zeta_1} \frac{\partial x_1}{\partial \zeta_3} \right] = |\mathbf{F}| \frac{\partial \zeta_2}{\partial x_2} & A_{23} = \left[ \frac{\partial x_1}{\partial \zeta_1} \frac{\partial x_3}{\partial \zeta_2} - \frac{\partial x_3}{\partial \zeta_1} \frac{\partial x_1}{\partial \zeta_2} \right] = |\mathbf{F}| \frac{\partial \zeta_3}{\partial x_2} \\ A_{31} = \left[ \frac{\partial x_1}{\partial \zeta_2} \frac{\partial x_2}{\partial \zeta_3} - \frac{\partial x_2}{\partial \zeta_2} \frac{\partial x_1}{\partial \zeta_3} \right] = |\mathbf{F}| \frac{\partial \zeta_1}{\partial x_3} & A_{32} = \left[ \frac{\partial x_1}{\partial \zeta_1} \frac{\partial x_2}{\partial \zeta_3} - \frac{\partial x_2}{\partial \zeta_1} \frac{\partial x_1}{\partial \zeta_3} \right] = |\mathbf{F}| \frac{\partial \zeta_2}{\partial x_3} \\ A_{33} = \left[ \frac{\partial x_1}{\partial \zeta_1} \frac{\partial x_2}{\partial \zeta_2} - \frac{\partial x_2}{\partial \zeta_1} \frac{\partial x_1}{\partial \zeta_2} \right] = |\mathbf{F}| \frac{\partial \zeta_3}{\partial x_3} & \end{array} \quad (43)$$

With these relations, one can then solve for the components of  $\mathbf{F}$  and  $\mathbf{F}^{-1}$ .

## 9 DIFFERENTIATION IN REFERENTIAL COORDINATES

We now need to express  $[\mathbf{D}]$  in terms of  $(\zeta_1, \zeta_2, \zeta_3)$  via

$$[\mathbf{D}(\phi(x_1, x_2, x_3))] = [\hat{\mathbf{D}}(\hat{\phi}(M_{x_1}(\zeta_1, \zeta_2, \zeta_3), M_{x_2}(\zeta_1, \zeta_2, \zeta_3), M_{x_3}(\zeta_1, \zeta_2, \zeta_3)))] \quad (44)$$

Therefore we write for the first column of  $[\hat{\mathbf{D}}]^*$

$$\begin{bmatrix} \frac{\partial}{\partial \zeta_1} \frac{\partial \zeta_1}{\partial x_1} + \frac{\partial}{\partial \zeta_2} \frac{\partial \zeta_2}{\partial x_1} + \frac{\partial}{\partial \zeta_3} \frac{\partial \zeta_3}{\partial x_1} \\ 0 \\ 0 \\ \frac{\partial}{\partial \zeta_1} \frac{\partial \zeta_1}{\partial x_2} + \frac{\partial}{\partial \zeta_2} \frac{\partial \zeta_2}{\partial x_2} + \frac{\partial}{\partial \zeta_3} \frac{\partial \zeta_3}{\partial x_2} \\ 0 \\ \frac{\partial}{\partial \zeta_1} \frac{\partial \zeta_1}{\partial x_3} + \frac{\partial}{\partial \zeta_2} \frac{\partial \zeta_2}{\partial x_3} + \frac{\partial}{\partial \zeta_3} \frac{\partial \zeta_3}{\partial x_3} \end{bmatrix} \quad (45)$$

for the second column

$$\begin{bmatrix} 0 \\ \frac{\partial}{\partial \zeta_1} \frac{\partial \zeta_1}{\partial x_2} + \frac{\partial}{\partial \zeta_2} \frac{\partial \zeta_2}{\partial x_2} + \frac{\partial}{\partial \zeta_3} \frac{\partial \zeta_3}{\partial x_2} \\ 0 \\ \frac{\partial}{\partial \zeta_1} \frac{\partial \zeta_1}{\partial x_1} + \frac{\partial}{\partial \zeta_2} \frac{\partial \zeta_2}{\partial x_1} + \frac{\partial}{\partial \zeta_3} \frac{\partial \zeta_3}{\partial x_1} \\ \frac{\partial}{\partial \zeta_1} \frac{\partial \zeta_1}{\partial x_3} + \frac{\partial}{\partial \zeta_2} \frac{\partial \zeta_2}{\partial x_3} + \frac{\partial}{\partial \zeta_3} \frac{\partial \zeta_3}{\partial x_3} \\ 0 \end{bmatrix} \quad (46)$$

and for the last column

$$\begin{bmatrix} 0 \\ 0 \\ \frac{\partial}{\partial \zeta_1} \frac{\partial \zeta_1}{\partial x_2} + \frac{\partial}{\partial \zeta_2} \frac{\partial \zeta_2}{\partial x_3} + \frac{\partial}{\partial \zeta_3} \frac{\partial \zeta_3}{\partial x_3} \\ 0 \\ \frac{\partial}{\partial \zeta_1} \frac{\partial \zeta_1}{\partial x_2} + \frac{\partial}{\partial \zeta_2} \frac{\partial \zeta_2}{\partial x_2} + \frac{\partial}{\partial \zeta_3} \frac{\partial \zeta_3}{\partial x_2} \\ \frac{\partial}{\partial \zeta_1} \frac{\partial \zeta_1}{\partial x_1} + \frac{\partial}{\partial \zeta_2} \frac{\partial \zeta_2}{\partial x_1} + \frac{\partial}{\partial \zeta_3} \frac{\partial \zeta_3}{\partial x_1} \end{bmatrix} \quad (47)$$

For an element, our shape function matrix ( $\stackrel{\text{def}}{=} [\hat{\phi}]$ ) has the following form for linear shape functions; for the first eight columns

$$\begin{bmatrix} \hat{\phi}_1 & \hat{\phi}_2 & \hat{\phi}_3 & \hat{\phi}_4 & \hat{\phi}_5 & \hat{\phi}_6 & \hat{\phi}_7 & \hat{\phi}_8 \\ 0 & 0 & 0 & 0 & 0 & 0 & 0 & 0 \\ 0 & 0 & 0 & 0 & 0 & 0 & 0 & 0 \end{bmatrix} \quad (48)$$

for the second eight columns

$$\begin{bmatrix} 0 & 0 & 0 & 0 & 0 & 0 & 0 & 0 \\ \hat{\phi}_1 & \hat{\phi}_2 & \hat{\phi}_3 & \hat{\phi}_4 & \hat{\phi}_5 & \hat{\phi}_6 & \hat{\phi}_7 & \hat{\phi}_8 \\ 0 & 0 & 0 & 0 & 0 & 0 & 0 & 0 \end{bmatrix} \quad (49)$$

---

\* This is for illustration purposes only. For computational efficiency, one should not program such operations in this way. Clearly, the needless multiplication of zeros is to be avoided.

and for the last eight columns

$$\begin{bmatrix} 0 & 0 & 0 & 0 & 0 & 0 & 0 & 0 \\ 0 & 0 & 0 & 0 & 0 & 0 & 0 & 0 \\ \hat{\phi}_1 & \hat{\phi}_2 & \hat{\phi}_3 & \hat{\phi}_4 & \hat{\phi}_5 & \hat{\phi}_6 & \hat{\phi}_7 & \hat{\phi}_8 \end{bmatrix} \quad (50)$$

which in total is a  $3 \times 24$  matrix. Therefore, the product  $[\hat{\mathbf{D}}][\hat{\phi}]$  is a  $6 \times 24$  matrix of the form for the first eight columns

$$\begin{bmatrix} \frac{\partial \hat{\phi}_1}{\partial \zeta_1} \frac{\partial \zeta_1}{\partial x_2} + \frac{\partial \hat{\phi}_1}{\partial \zeta_2} \frac{\partial \zeta_2}{\partial x_1} + \frac{\partial \hat{\phi}_1}{\partial \zeta_3} \frac{\partial \zeta_3}{\partial x_1}, \dots 8 \\ 0 & 0 & 0 & 0 & 0 & 0 & 0 & 0 \\ 0 & 0 & 0 & 0 & 0 & 0 & 0 & 0 \\ \frac{\partial \hat{\phi}_1}{\partial \zeta_1} \frac{\partial \zeta_1}{\partial x_2} + \frac{\partial \hat{\phi}_1}{\partial \zeta_2} \frac{\partial \zeta_2}{\partial x_2} + \frac{\partial \hat{\phi}_1}{\partial \zeta_3} \frac{\partial \zeta_3}{\partial x_2}, \dots 8 \\ 0 & 0 & 0 & 0 & 0 & 0 & 0 & 0 \\ \frac{\partial \hat{\phi}_1}{\partial \zeta_1} \frac{\partial \zeta_1}{\partial x_3} + \frac{\partial \hat{\phi}_1}{\partial \zeta_2} \frac{\partial \zeta_2}{\partial x_3} + \frac{\partial \hat{\phi}_1}{\partial \zeta_3} \frac{\partial \zeta_3}{\partial x_3}, \dots 8 \end{bmatrix} \quad (51)$$

and for the second eight columns

$$\begin{bmatrix} 0 & 0 & 0 & 0 & 0 & 0 & 0 & 0 \\ \frac{\partial \hat{\phi}_1}{\partial \zeta_1} \frac{\partial \zeta_1}{\partial x_2} + \frac{\partial \hat{\phi}_1}{\partial \zeta_2} \frac{\partial \zeta_2}{\partial x_2} + \frac{\partial \hat{\phi}_1}{\partial \zeta_3} \frac{\partial \zeta_3}{\partial x_2}, \dots 8 \\ 0 & 0 & 0 & 0 & 0 & 0 & 0 & 0 \\ \frac{\partial \hat{\phi}_1}{\partial \zeta_1} \frac{\partial \zeta_1}{\partial x_1} + \frac{\partial \hat{\phi}_1}{\partial \zeta_2} \frac{\partial \zeta_2}{\partial x_1} + \frac{\partial \hat{\phi}_1}{\partial \zeta_3} \frac{\partial \zeta_3}{\partial x_1}, \dots 8 \\ \frac{\partial \hat{\phi}_1}{\partial \zeta_1} \frac{\partial \zeta_1}{\partial x_3} + \frac{\partial \hat{\phi}_1}{\partial \zeta_2} \frac{\partial \zeta_2}{\partial x_3} + \frac{\partial \hat{\phi}_1}{\partial \zeta_3} \frac{\partial \zeta_3}{\partial x_3}, \dots 8 \\ 0 & 0 & 0 & 0 & 0 & 0 & 0 & 0 \end{bmatrix} \quad (52)$$

and for the last eight columns

$$\begin{bmatrix} 0 & 0 & 0 & 0 & 0 & 0 & 0 & 0 \\ 0 & 0 & 0 & 0 & 0 & 0 & 0 & 0 \\ \frac{\partial \hat{\phi}_1}{\partial \zeta_1} \frac{\partial \zeta_1}{\partial x_3} + \frac{\partial \hat{\phi}_1}{\partial \zeta_2} \frac{\partial \zeta_2}{\partial x_3} + \frac{\partial \hat{\phi}_1}{\partial \zeta_3} \frac{\partial \zeta_3}{\partial x_3}, \dots 8 \\ 0 & 0 & 0 & 0 & 0 & 0 & 0 & 0 \\ \frac{\partial \hat{\phi}_1}{\partial \zeta_1} \frac{\partial \zeta_1}{\partial x_2} + \frac{\partial \hat{\phi}_1}{\partial \zeta_2} \frac{\partial \zeta_2}{\partial x_2} + \frac{\partial \hat{\phi}_1}{\partial \zeta_3} \frac{\partial \zeta_3}{\partial x_2}, \dots 8 \\ \frac{\partial \hat{\phi}_1}{\partial \zeta_1} \frac{\partial \zeta_1}{\partial x_1} + \frac{\partial \hat{\phi}_1}{\partial \zeta_2} \frac{\partial \zeta_2}{\partial x_1} + \frac{\partial \hat{\phi}_1}{\partial \zeta_3} \frac{\partial \zeta_3}{\partial x_1}, \dots 8 \end{bmatrix} \quad (53)$$

Finally, with Gaussian quadrature for each element

$$K_{ij}^e = \underbrace{\sum_{q=1}^g \sum_{r=1}^g \sum_{s=1}^g w_q w_r w_s ([\hat{\mathbf{D}}]\{\hat{\phi}_i\})^T [\hat{\mathbf{E}}]([\hat{\mathbf{D}}]\{\hat{\phi}_j\})|\mathbf{F}|}_{\text{standard}} \quad (54)$$

and

$$R_i^e = \underbrace{\sum_{q=1}^g \sum_{r=1}^g \sum_{s=1}^g w_q w_r w_s \{\hat{\phi}_i\}^T \{\mathbf{f}\} |\mathbf{F}|}_{\text{standard}} + \underbrace{\sum_{q=1}^g \sum_{r=1}^g w_q w_r \{\hat{\phi}_i\}^T \{\mathbf{t}\} |\mathbf{F}_s|}_{\text{for } \Gamma_i \cap \Omega_e \neq \emptyset} \quad (55)$$

where  $w_q, w_r, w_s$  are Gauss weights and where  $|\mathbf{F}_s|$  represents the (surface) Jacobians of element faces on the exterior surface of the body, where, depending on the surface on which it is to be evaluated, one of the  $\zeta$  components will be +1 or -1. These surface Jacobians can be evaluated in a variety of ways, for example, using the Nanson formulas frequently encountered in the field of continuum mechanics.

### 10 POSTPROCESSING

Postprocessing for the stress, strain, and energy from the existing displacement solution, i.e., the values of the nodal displacements, the shape functions, is straightforward, namely,  $[\mathbf{D}]\{\mathbf{u}^h\} = \{\boldsymbol{\epsilon}^h\}$ . Therefore, for each element

$$\begin{Bmatrix} \boldsymbol{\epsilon}_{11}^h \\ \boldsymbol{\epsilon}_{22}^h \\ \boldsymbol{\epsilon}_{33}^h \\ 2\boldsymbol{\epsilon}_{12}^h \\ 2\boldsymbol{\epsilon}_{23}^h \\ 2\boldsymbol{\epsilon}_{13}^h \end{Bmatrix} = \begin{bmatrix} \frac{\partial}{\partial x_1} & 0 & 0 \\ 0 & \frac{\partial}{\partial x_2} & 0 \\ 0 & 0 & \frac{\partial}{\partial x_3} \\ \frac{\partial}{\partial x_2} & \frac{\partial}{\partial x_1} & 0 \\ 0 & \frac{\partial}{\partial x_3} & \frac{\partial}{\partial x_2} \\ \frac{\partial}{\partial x_3} & 0 & \frac{\partial}{\partial x_1} \end{bmatrix} \underbrace{\begin{Bmatrix} \sum_{i=1}^8 u_{1i}^h \phi_i \\ \sum_{i=1}^8 u_{2i}^h \phi_i \\ \sum_{i=1}^8 u_{3i}^h \phi_i \end{Bmatrix}}_{\text{known values}} \quad (56)$$

where the global coordinates must be transformed to the master system in both the deformation tensor and the displacement representation. At each Gauss point, we add all eight contributions for each of the six components, then multiply by the corresponding nodal displacements that have previously been calculated. The following expressions must be evaluated at the Gauss points, multiplied by the appropriate weights and added together:

$$\begin{array}{ccc} \frac{\partial u_1^h}{\partial x_1} = \sum_{i=1}^8 u_{1i}^h \frac{\partial \phi_i}{\partial x_1} & \frac{\partial u_2^h}{\partial x_1} = \sum_{i=1}^8 u_{1i}^h \frac{\partial \phi_i}{\partial x_1} & \frac{\partial u_3^h}{\partial x_1} = \sum_{i=1}^8 u_{1i}^h \frac{\partial \phi_i}{\partial x_1} \\ \frac{\partial u_1^h}{\partial x_2} = \sum_{i=1}^8 u_{1i}^h \frac{\partial \phi_i}{\partial x_2} & \frac{\partial u_2^h}{\partial x_2} = \sum_{i=1}^8 u_{2i}^h \frac{\partial \phi_i}{\partial x_2} & \frac{\partial u_3^h}{\partial x_2} = \sum_{i=1}^8 u_{2i}^h \frac{\partial \phi_i}{\partial x_2} \\ \frac{\partial u_1^h}{\partial x_3} = \sum_{i=1}^8 u_{1i}^h \frac{\partial \phi_i}{\partial x_3} & \frac{\partial u_2^h}{\partial x_3} = \sum_{i=1}^8 u_{1i}^h \frac{\partial \phi_i}{\partial x_3} & \frac{\partial u_3^h}{\partial x_3} = \sum_{i=1}^8 u_{1i}^h \frac{\partial \phi_i}{\partial x_3} \end{array} \quad (57)$$

where  $u_{1i}^h$  denotes the  $x_1$  component of the displacement of the  $i$ th node. Combining the numerical derivatives to form the strains, we obtain  $\boldsymbol{\epsilon}_{11}^h = \partial u_1^h / \partial x_1$ ,  $\boldsymbol{\epsilon}_{22}^h = \partial u_2^h / \partial x_2$ , and  $\boldsymbol{\epsilon}_{33}^h = \partial u_3^h / \partial x_3$  and  $2\boldsymbol{\epsilon}_{12}^h = \gamma_{12} = \partial u_1^h / \partial x_2 + \partial u_2^h / \partial x_1$ ,  $2\boldsymbol{\epsilon}_{23}^h = \gamma_{23} = \partial u_2^h / \partial x_3 + \partial u_3^h / \partial x_2$ , and  $2\boldsymbol{\epsilon}_{13}^h = \gamma_{13} = \partial u_1^h / \partial x_3 + \partial u_3^h / \partial x_1$ .

## 11 ONE-DIMENSIONAL EXAMPLE

Consider the general form

$$\boxed{\text{Find } u \in H^1(\Omega) \text{ such that, } \forall v \in H^1(\Omega), v|_{\Gamma_u} = 0,} \\ \int_{\Omega} \frac{dv}{dx} E \frac{du}{dx} dx = \int_{\Omega} f v dx + vt|_{\Gamma_t} \quad (58)$$

It is convenient to write the bilinear form in the following manner:

$$\int_{\Omega} \frac{dv}{dx} E \frac{du}{dx} dx = \int_{\Omega} v f dx + vt|_{\Gamma_t} \quad (59)$$

We write

$$u^h(x) \sum_{j=1}^N a_j \phi_j(x) \quad (60)$$

If we choose  $v$  with the same basis but a different linear combination,

$$v(x) \sum_{i=1}^N b_i \phi_i(x) \quad (61)$$

then we may write

$$\underbrace{\int_{\Omega} \left( \frac{d}{dx} \sum_{i=1}^N b_i \phi_i(x) \right) E \frac{d}{dx} \left( \sum_{j=1}^N a_j \phi_j(x) \right) dx}_{\{b\}^T \{K\} \{a\} \text{ stiffness}} \\ = \underbrace{\int_{\Omega} \left( \sum_{i=1}^N b_i \phi_i(x) \right) f dx}_{\text{body load}} + \underbrace{\left( \left( \sum_{i=1}^N b_i \phi_i(x) \right) t \right) \Big|_{\Gamma_t}}_{\text{traction load}} \quad (62)$$

Since the  $b_i$  are arbitrary, i.e., the weak form implies  $\forall v \Rightarrow \forall b_i$ , therefore

$$\boxed{\sum_{i=1}^N b_i \left( \sum_{j=1}^N K_{ij} a_j - R_i \right) = 0 \Rightarrow [K] \{a\} = \{R\} \\ K_{ij} \stackrel{\text{def}}{=} \int_{\Omega} \frac{d\phi_i}{dx} E \frac{d\phi_j}{dx} dx \\ R_i \stackrel{\text{def}}{=} \int_{\Omega} \phi_i f dx + \phi_i t|_{\Gamma_t}} \quad (63)$$

This is the system of equations that is to be solved.

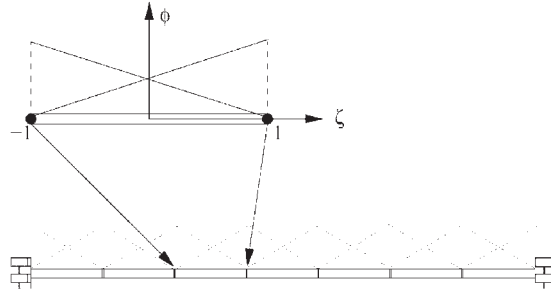
One strength of the FEM is that most of the computations can be done in an element-by-element manner. Accordingly, we define the entries of  $[K]$ ,

$$K_{ij} = \int_{\Omega} \frac{d\phi_i}{dx} E \frac{d\phi_j}{dx} dx \quad (64)$$

and

$$R_i = \int_{\Omega} \phi_i f dx + \phi_i t|_{\Gamma_t} \quad (65)$$





**Figure 6** One-dimensional linear finite-element mapping.

We can break the calculations into elements,  $K_{ij} = \sum_e K_{ij}^e$ , where

$$K_{ij}^e = \int_{\Omega_e} \frac{d\phi_i}{dx} E \frac{d\phi_j}{dx} dx \tag{66}$$

To make the calculations systematic, we wish to use the generic or master element defined in a local coordinate system ( $\zeta$ ). Accordingly, we need the following mapping functions, from the master coordinates to the real space coordinates,  $M(x) \mapsto (\zeta)$  (Fig. 6):

$$x = \sum_{i=1}^2 X_i \hat{\phi}_i \stackrel{\text{def}}{=} M_x(\zeta) \tag{67}$$

where the  $X_i$  are true spatial coordinates of the  $i$ th node and where  $\hat{\phi}(\zeta) \stackrel{\text{def}}{=} \phi(x(\zeta))$ .

The master element shape functions form a nodal bases of linear approximation given by

$$\hat{\phi}_1 = \frac{1}{2}(1 - \zeta) \quad \hat{\phi}_2 = \frac{1}{2}(1 + \zeta) \tag{68}$$

- For linear elements we have a nodal basis consisting of two nodes and thus two degrees of freedom.
- The nodal shape functions can be derived quite easily by realizing that it is a nodal basis, e.g., they are unity at the corresponding node and zero at all other nodes.

We note that the  $\phi_i$ 's are never really computed; we actually start with the  $\hat{\phi}_i$ 's and then map them into the actual problem domain. Therefore, in the stiffness matrix and right-hand-side element calculations, all terms must be defined in terms of the local coordinates. With this in mind, we introduce some fundamental quantities, such as the deformation gradient

$$F \stackrel{\text{def}}{=} \frac{dx}{d\zeta} \tag{69}$$

The corresponding “determinant” is  $|F| = |dx/d\zeta|$ . The differential relations  $\zeta \rightarrow x$  are

$$\frac{d}{d\zeta} = \frac{d}{dx} \frac{dx}{d\zeta} \tag{70}$$

The inverse differential relations  $x \rightarrow \zeta$  are

$$\frac{d}{dx} = \frac{d}{d\zeta} \frac{d\zeta}{dx} \tag{71}$$

We can now express  $d/dx$  in terms of  $\zeta$  via

$$\frac{d\phi}{dx} = \frac{d}{dx}\phi(M(\zeta)) \quad (72)$$

Finally with quadrature for each element

$$K_{ij}^e = \underbrace{\sum_{q=1}^g w_q \left( \frac{d}{d\zeta} (\phi_i(M(\zeta))) \right) \frac{d\zeta}{dx} E \left( \frac{d}{d\zeta} (\phi_j(M(\zeta))) \right) \frac{d\zeta}{dx} |F|}_{\text{evaluated at } \zeta=\zeta_q}$$

and

$$R_i^e = \underbrace{\sum_{q=1}^g w_q \phi_i(M(\zeta)) f |F|_{\zeta}}_{\text{evaluated at } \zeta=\zeta_q} + \underbrace{\phi_i(M(\zeta)) t}_{\text{evaluated on traction endpoints}}$$

where the  $w_q$  are Gauss weights.

Postprocessing for the stress, strain, and energy from the existing displacement solution, i.e., the values of the nodal displacements, the shape functions, is straightforward. Essentially, the process is the same as the formation of the virtual energy in the system. Therefore, for each element

$$\frac{du}{dx} = \frac{d}{dx} \sum_{i=1}^2 a_i \phi_i = \left( \frac{d}{d\zeta} \sum_{i=1}^2 a_i \hat{\phi}_i \right) \frac{d\zeta}{dx} \quad (73)$$

REMARKS. On the implementation level, the system of equations to be solved are  $[K]\{u^h\} = \{R\}$ , where the stiffness matrix is represented by  $K(I, J) = k(ELEM, i, j)$ , where  $I, J$  are the global entries and  $i, j$  are the local entries. Here a global/local index relation must be made to connect the local entry to the global entry when solution time begins. This is a relatively simple and efficient storage system to encode. The element-by-element strategy has other advantages with regard to element-by-element system solvers. This is trivial in one dimension; however, it can be extremely complicated in three dimensions. Major software exists that can automate these procedures. Some of the most widely used are:

- Abaqus, located at <http://www.hks.com/>
- Adina, located at <http://www.adina.com/>
- Ansys, located at <http://www.ansys.com/>
- LS-Dyna, located at <http://www.lstc.com/>
- Nastran, located at <http://www.mscsoftware.com/>

This is by no means a comprehensive list.

## 12 SUMMARY

Classical older techniques construct approximations from globally kinematically admissible functions. Two main obstacles arise: (1) It may be very difficult to find a kinematically admissible function over the entire domain and (2) if such functions are found, they lead to be large, strongly coupled, and complicated systems of equations. These problems have been overcome by the fact that local approximations, i.e., over a very small portion of the domain, are possible that deliver adequate solutions and simultaneously lead to systems of equations that have an advantageous structure amenable to large-scale computation by high-speed computers. This piecewise or “elementwise” approximation technique was recognized at least 60 years ago by Courant.<sup>3</sup> There have been a variety of such approximation methods to solve equations of

mathematical physics. The most popular is the finite-element method. The central feature of the method is to reduce the field equations in a physically sound and systematic manner to an assembly of discrete subdomains, or “elements.” The process is designed to keep the resulting algebraic systems as computationally manageable and memory efficient as possible.

The implementation, theory, and application of the FEM is a subject of immense literature. We have not attempted to review this huge field. For general references on the subject see the standard books by Bathe,<sup>4</sup> Becker et al.,<sup>5</sup> Hughes,<sup>6</sup> Szabo and Babuska,<sup>7</sup> and Zienkiewicz and Taylor.<sup>8</sup>

## REFERENCES

1. L. Malvern, *Introduction to the Mechanics of a Continuous Medium*, Prentice-Hall, Englewood Cliffs, NJ, 1968.
2. J. E. Marsden and T. J. R. Hughes, *Mathematical Foundations of Elasticity*, Prentice-Hall, Englewood Cliffs, NJ, 1983.
3. R. Courant, “Variational Methods for the Solution of Problems of Equilibrium and Vibrations,” *Bull. Am. Math. Soc.*, **49**, 1–23, 1943.
4. K. J. Bathe, *Finite Element Procedures*, Prentice-Hall, Englewood Cliffs, NJ, 1996.
5. E. B. Becker, G. F. Carey, and J. T. Oden, *Finite Elements: An Introduction*, Prentice-Hall, Englewood Cliffs, NJ, 1980.
6. T. J. R. Hughes, *The Finite Element Method*, Prentice-Hall, Englewood Cliffs, NJ, 1989.
7. B. Szabo, and I. Babúska, *Finite Element Analysis*, Wiley-Interscience, New York, 1991.
8. O. C. Zienkiewicz and R. L. Taylor, *The Finite Element Method*, Vols. I and II, McGraw-Hill, New York, 1991.

# CHAPTER 20

## FAILURE MODELS: PERFORMANCE AND SERVICE REQUIREMENTS FOR METALS

**J. A. Collins**  
The Ohio State University,  
Columbus, Ohio

**G. P. Potirniche**  
University of Idaho,  
Moscow, Idaho

**S. R. Daniewicz**  
Mississippi State University,  
Starkville, Mississippi

<b>1</b>	<b>CRITERIA OF FAILURE</b>	<b>703</b>	6.2	Prediction of Long-Term Creep Behavior	739
<b>2</b>	<b>FAILURE MODES</b>	<b>704</b>	6.3	Creep under a Uniaxial State of Stress	740
<b>3</b>	<b>ELASTIC DEFORMATION AND YIELDING</b>	<b>710</b>	6.4	Creep under a Multiaxial State of Stress	742
<b>4</b>	<b>FRACTURE MECHANICS AND UNSTABLE CRACK GROWTH</b>	<b>711</b>	6.5	Mechanisms of Creep–Fatigue Failure	743
<b>5</b>	<b>FATIGUE</b>	<b>718</b>	<b>7</b>	<b>FRETTING AND WEAR</b>	<b>744</b>
5.1	Fatigue Loading and Laboratory Testing	719	7.1	Fretting Phenomena	745
5.2	Stress–Life Approach to Fatigue	723	7.2	Wear Phenomena	753
5.3	Strain–Life Approach to Fatigue	730	<b>8</b>	<b>CORROSION AND STRESS CORROSION</b>	<b>759</b>
5.4	Fatigue Crack Propagation	732	8.1	Types of Corrosion	759
<b>6</b>	<b>CREEP AND STRESS RUPTURE</b>	<b>736</b>	8.2	Stress Corrosion Cracking	765
6.1	Basic Mechanisms of Creep Deformation	737	<b>9</b>	<b>FAILURE ANALYSIS AND RETROSPECTIVE DESIGN</b>	<b>765</b>
			<b>REFERENCES</b>	<b>766</b>	

### 1 CRITERIA OF FAILURE

Any change in the size, shape, or material properties of a structure, machine, or machine part that renders it incapable of performing its intended function must be regarded as a mechanical failure of the device. It should be carefully noted that the key concept here is that *improper functioning* of a machine part constitutes failure. Thus, a shear pin that does *not* separate into two or more pieces upon the application of a preselected overload must be regarded as having failed as surely as a drive shaft has failed if it *does* separate into two pieces under normal expected operating loads.

Failure of a device or structure to function properly might be brought about by any one or a combination of many different responses to loads and environments while in service. For example, too much or too little elastic deformation might produce failure. A fractured load-carrying structural member or a shear pin that does not shear under overload conditions each would constitute failure. Progression of a crack due to fluctuating loads or aggressive environment might lead to failure after a period of time if resulting excessive deflection or fracture interferes with proper machine function.

A primary responsibility of any mechanical designer is to ensure that his or her design functions as intended for the prescribed design lifetime and, at the same time, that it be competitive in the marketplace. Success in designing competitive products while averting premature mechanical failures can be achieved consistently only by recognizing and evaluating all potential modes of failure that might govern the design. To recognize potential failure modes, a designer must be acquainted with the array of failure modes observed in practice and with the conditions leading to these failures. The following section summarizes the mechanical failure modes most commonly observed in practice followed by a brief description of each one.

## 2 FAILURE MODES

A failure mode may be defined as the physical process or processes that take place or that combine their effects to produce a failure. In the following list of commonly observed failure modes, it may be noted that some failure modes are unilateral phenomena, whereas others are combined phenomena. For example, fatigue is listed as a failure mode, corrosion is listed as a failure mode, and corrosion fatigue is listed as still another failure mode. Such combinations are included because they are commonly observed, important, and often *synergistic*. In the case of corrosion fatigue, for example, the presence of active corrosion aggravates the fatigue process and at the same time the presence of a fluctuating load accelerates the corrosion process.

The following list is not presented in any special order, but it includes all commonly observed modes of mechanical failure<sup>1</sup>:

1. Force- and/or temperature-induced elastic deformation
2. Yielding
3. Brinnelling
4. Ductile rupture
5. Brittle fracture
6. Fatigue
  - a. High-cycle fatigue
  - b. Low-cycle fatigue
  - c. Thermal fatigue
  - d. Surface fatigue
  - e. Impact fatigue
  - f. Corrosion fatigue
  - g. Fretting fatigue
7. Corrosion
  - a. Direct chemical attack
  - b. Galvanic corrosion

- c. Crevice corrosion
  - d. Pitting corrosion
  - e. Intergranular corrosion
  - f. Selective leaching
  - g. Erosion corrosion
  - h. Cavitation corrosion
  - i. Hydrogen damage
  - j. Biological corrosion
  - k. Stress corrosion
8. Wear
- a. Adhesive wear
  - b. Abrasive wear
  - c. Corrosive wear
  - d. Surface fatigue wear
  - e. Deformation wear
  - f. Impact wear
  - g. Fretting wear
9. Impact
- a. Impact fracture
  - b. Impact deformation
  - c. Impact wear
  - d. Impact fretting
  - e. Impact fatigue
10. Fretting
- a. Fretting fatigue
  - b. Fretting wear
  - c. Fretting corrosion
11. Creep
12. Thermal relaxation
13. Stress rupture
14. Thermal shock
15. Galling and seizure
16. Spalling
17. Radiation damage
18. Buckling
19. Creep buckling
20. Stress corrosion
21. Corrosion wear
22. Corrosion fatigue
23. Combined creep and fatigue

As commonly used in engineering practice, the failure modes just listed may be defined and described briefly as follows. It should be emphasized that these failure modes only produce failure when they generate a set of circumstances that interfere with the proper functioning of a machine or device.

*Force and/or temperature-induced elastic deformation* failure occurs whenever the elastic (recoverable) deformation in a machine member, induced by the imposed operational loads or temperatures, becomes large enough to interfere with the ability of the machine to perform its intended function satisfactorily.

*Yielding* failure occurs when the plastic (unrecoverable) deformation in a ductile machine member, brought about by the imposed operational loads or motions, becomes large enough to interfere with the ability of the machine to perform its intended function satisfactorily.

*Brinnelling* failure occurs when the static forces between two curved surfaces in contact result in local yielding of one or both mating members to produce a permanent surface discontinuity of significant size. For example, if a ball bearing is statically loaded so that a ball is forced to permanently indent the race through local plastic flow, the race is brinnelled. Subsequent operation of the bearing might result in intolerably increased vibration, noise, and heating; and, therefore, failure would have occurred.

*Ductile rupture* failure occurs when the plastic deformation in a machine part that exhibits ductile behavior is carried to the extreme so that the member separates into two pieces. Initiation and coalescence of internal voids slowly propagate to failure, leaving a dull, fibrous rupture surface.

*Brittle fracture* failure occurs when the elastic deformation in a machine part that exhibits brittle behavior is carried to the extreme so that the primary interatomic bonds are broken and the member separates into two or more pieces. Pre-existing flaws or growing cracks form initiation sites for very rapid crack propagation to catastrophic failure, leaving a granular, multifaceted fracture surface.

*Fatigue* failure is a general term given to the sudden and catastrophic separation of a machine part into two or more pieces as a result of the application of fluctuating loads or deformations over a period of time. Failure takes place by the initiation and propagation of a crack until it becomes unstable and propagates suddenly to failure. The loads and deformations that typically cause failure by fatigue are far below the static or monotonic failure levels. When loads or deformations are of such magnitude that more than about 10,000 cycles are required to produce failure, the phenomenon is usually termed *high-cycle fatigue*. When loads or deformations are of such magnitude that less than about 10,000 cycles are required to produce failure, the phenomenon is usually termed *low-cycle fatigue*. When load or strain cycling is produced by a fluctuating temperature field in the machine part, the process is usually termed *thermal fatigue*. *Surface fatigue* failure, usually associated with rolling surfaces in contact, manifests itself as pitting, cracking, and spalling of the contacting surfaces as a result of the cyclic Hertz contact stresses that result in maximum values of cyclic shear stresses slightly below the surface. The cyclic subsurface shear stresses generate cracks that propagate to the contacting surface, dislodging particles in the process to produce surface pitting. This phenomenon is often viewed as a type of wear. Impact fatigue, corrosion fatigue, and fretting fatigue are described later.

*Corrosion* failure, a very broad term, implies that a machine part is rendered incapable of performing its intended function because of the undesired deterioration of the material as a result of chemical or electrochemical interaction with the environment. Corrosion often interacts with other failure modes such as wear or fatigue. The many forms of corrosion include the following. *Direct chemical attack*, perhaps the most common type of corrosion, involves corrosive attack of the surface of the machine part exposed to the corrosive media, more or less uniformly over the entire exposed surface. *Galvanic corrosion* is an accelerated electrochemical corrosion that occurs when two dissimilar metals in electrical contact are made part of a circuit completed by a connecting pool or film of electrolyte or corrosive medium, leading

to current flow and ensuing corrosion. *Crevice corrosion* is the accelerated corrosion process highly localized within crevices, cracks, or joints where small-volume regions of stagnant solution are trapped in contact with the corroding metal. *Pitting corrosion* is a localized attack that leads to the development of an array of holes or pits that penetrate the metal. *Intergranular corrosion* is the localized attack occurring at grain boundaries of certain copper, chromium, nickel, aluminum, magnesium, and zinc alloys when they are improperly heat treated or welded. Formation of local galvanic cells that precipitate corrosion products at the grain boundaries seriously degrades the material strength because of the intergranular corrosive process. *Selective leaching* is a corrosion process in which one element of a solid alloy is removed, such as in dezincification of brass alloys or graphitization of gray cast irons. *Erosion corrosion* is the accelerated chemical attack that results when abrasive or viscid material flows past a containing surface, continuously baring fresh, unprotected material to the corrosive medium. *Cavitation corrosion* is the accelerated chemical corrosion that results when, because of differences in vapor pressure, certain bubbles and cavities within a fluid collapse adjacent to the pressure vessel walls, causing particles of the surface to be expelled, baring fresh, unprotected surface to the corrosive medium. *Hydrogen damage*, while not considered to be a form of direct corrosion, is induced by corrosion. Hydrogen damage includes hydrogen blistering, hydrogen embrittlement, hydrogen attack, and decarburization. *Biological corrosion* is a corrosion process that results from the activity of living organisms, usually by virtue of their processes of food ingestion and waste elimination, in which the waste products are corrosive acids or hydroxides. *Stress corrosion*, an extremely important type of corrosion, is described separately later.

*Wear* is the undesired cumulative change in dimensions caused by the gradual removal of discrete particles from contacting surfaces in motion, usually sliding, predominantly as a result of mechanical action. Wear is not a single process, but a number of different processes that can take place by themselves or in combination, resulting in material removal from contacting surfaces through a complex combination of local shearing, plowing, gouging, welding, tearing, and others. *Adhesive wear* takes place because of high local pressure and welding at asperity contact sites, followed by motion-induced plastic deformation and rupture of asperity functions, with resulting metal removal or transfer. *Abrasive wear* takes place when the wear particles are removed from the surface by the plowing, gouging, and cutting action of the asperities of a harder mating surface or by hard particles entrapped between the mating surfaces. When the conditions for either adhesive wear or abrasive wear coexist with conditions that lead to corrosion, the processes interact synergistically to produce *corrosive wear*. As described earlier, *surface fatigue wear* is a wear phenomenon associated with curved surfaces in rolling or sliding contact, in which subsurface cyclic shear stresses initiate microcracks that propagate to the surface to spall out macroscopic particles and form wear pits. *Deformation wear* arises as a result of repeated *plastic* deformation at the wearing surfaces, producing a matrix of cracks that grow and coalesce to form wear particles. Deformation wear is often caused by severe impact loading. *Impact wear* is impact-induced repeated *elastic* deformation at the wearing surface that produces a matrix of cracks that grows in accordance with the surface fatigue description just given. Fretting wear is described later.

*Impact* failure results when a machine member is subjected to nonstatic loads that produce in the part stresses or deformations of such magnitude that the member no longer is capable of performing its function. The failure is brought about by the interaction of stress or strain waves generated by dynamic or suddenly applied loads, which may induce local stresses and strains many times greater than would be induced by the static application of the same loads. If the magnitudes of the stresses and strains are sufficiently high to cause separation into two or more parts, the failure is called *impact fracture*. If the impact produces intolerable elastic or plastic deformation, the resulting failure is called *impact deformation*. If repeated impacts induce cyclic elastic strains that lead to initiation of a matrix of fatigue cracks, which grows to failure by the surface fatigue phenomenon described earlier, the process is called *impact wear*.



If fretting action, as described in the next paragraph, is induced by the small lateral relative displacements between two surfaces as they impact together, where the small displacements are caused by Poisson strains or small tangential “glancing” velocity components, the phenomenon is called *impact fretting*. *Impact fatigue* failure occurs when impact loading is applied repetitively to a machine member until failure occurs by the nucleation and propagation of a fatigue crack.

*Fretting* action may occur at the interface between any two solid bodies whenever they are pressed together by a normal force and subjected to small-amplitude cyclic relative motion with respect to each other. Fretting usually takes place in joints that are not intended to move but, because of vibrational loads or deformations, experience minute cyclic relative motions. Typically, debris produced by fretting action is trapped between the surfaces because of the small motions involved. *Fretting fatigue* failure is the premature fatigue fracture of a machine member subjected to fluctuating loads or strains together with conditions that simultaneously produce fretting action. The surface discontinuities and microcracks generated by the fretting action act as fatigue crack nuclei that propagate to failure under conditions of fatigue loading that would otherwise be acceptable. Fretting fatigue failure is an insidious failure mode because the fretting action is usually hidden within a joint where it cannot be seen and leads to premature, or even unexpected, fatigue failure of a sudden and catastrophic nature. *Fretting wear* failure results when the changes in dimensions of the mating parts, because of the presence of fretting action, become large enough to interfere with proper design function or large enough to produce geometrical stress concentration of such magnitude that failure ensues as a result of excessive local stress levels. *Fretting corrosion* failure occurs when a machine part is rendered incapable of performing its intended function because of the surface degradation of the material from which the part is made, as a result of fretting action.

*Creep* failure results whenever the plastic deformation in a machine member accrues over a period of time under the influence of stress and temperature until the accumulated dimensional changes interfere with the ability of the machine part to satisfactorily perform its intended function. Three stages of creep are often observed: (1) transient or primary creep during which time the rate of strain decreases, (2) steady-state or secondary creep during which time the rate of strain is virtually constant, and (3) tertiary creep during which time the creep strain rate increases, often rapidly, until rupture occurs. This terminal rupture is often called creep rupture and may or may not occur, depending on the stress–time–temperature conditions.

*Thermal relaxation* failure occurs when the dimensional changes due to the creep process result in the relaxation of a prestrained or prestressed member until it no longer is able to perform its intended function. For example, if the prestressed flange bolts of a high-temperature pressure vessel relax over a period of time because of creep in the bolts, so that, finally, the peak pressure surges exceed the bolt preload to violate the flange seal, the bolts will have failed because of thermal relaxation.

*Stress rupture* failure is intimately related to the creep process except that the combination of stress, time, and temperature is such that rupture into two parts is ensured. In stress rupture failures the combination of stress and temperature is often such that the period of steady-state creep is short or nonexistent.

*Thermal shock* failure occurs when the thermal gradients generated in a machine part are so pronounced that differential thermal strains exceed the ability of the material to sustain them without yielding or fracture.

*Galling* failure occurs when two sliding surfaces are subjected to such a combination of loads, sliding velocities, temperatures, environments, and lubricants that massive surface destruction is caused by welding and tearing, plowing, gouging, significant plastic deformation of surface asperities, and metal transfer between the two surfaces. Galling may be thought

of as a severe extension of the adhesive wear process. When such action results in significant impairment to intended surface sliding or in seizure, the joint is said to have failed by galling. *Seizure* is an extension of the galling process to such severity that the two parts are virtually welded together so that relative motion is no longer possible.

*Spalling* failure occurs whenever a particle is spontaneously dislodged from the surface of a machine part so as to prevent the proper function of the member. Armor plate fails by spalling, for example, when a striking missile on the exposed side of an armor shield generates a stress wave that propagates across the plate in such a way as to dislodge or spall a secondary missile of lethal potential on the protected side. Another example of spalling failure is manifested in rolling contact bearings and gear teeth because of the action of surface fatigue as described earlier.

*Radiation damage* failure occurs when the changes in material properties induced by exposure to a nuclear radiation field are of such a type and magnitude that the machine part is no longer able to perform its intended function, usually as a result of the triggering of some other failure mode and often related to loss in ductility associated with radiation exposure. Elastomers and polymers are typically more susceptible to radiation damage than are metals, whose strength properties are sometimes enhanced rather than damaged by exposure to a radiation field, although ductility is usually decreased.

*Buckling* failure occurs when, because of a critical combination of magnitude and/or point of load application, together with the geometrical configuration of a machine member, the deflection of the member suddenly increases greatly with only a slight change in load. This nonlinear response results in a buckling failure if the buckled member is no longer capable of performing its design function.

*Creep buckling* failure occurs when, after a period of time, the creep process results in an unstable combination of the loading and geometry of a machine part so that the critical buckling limit is exceeded and failure ensues.

*Stress corrosion* failure occurs when the applied stresses on a machine part in a corrosive environment generate a field of localized surface cracks, usually along grain boundaries, that render the part incapable of performing its function, often because of triggering some other failure mode. Stress corrosion is a very important type of corrosion failure mode because so many different metals are susceptible to it. For example, a variety of iron, steel, stainless steel, copper, and aluminum alloys are subject to stress corrosion cracking if placed in certain adverse corrosive media.

*Corrosion wear* failure is a combination failure mode in which corrosion and wear combine their deleterious effects to incapacitate a machine part. The corrosion process often produces a hard, abrasive corrosion product that accelerates the wear, while the wear process constantly removes the protective corrosion layer from the surface, baring fresh metal to the corrosive medium and thus accelerating the corrosion. The two modes combine to make the result more serious than either of the modes would have been otherwise.

*Corrosion fatigue* is a combination failure mode in which corrosion and fatigue combine their deleterious effects to cause failure of a machine part. The corrosion process often forms pits and surface discontinuities that act as stress raisers that in turn accelerate fatigue failure. Furthermore, cracks in the usually brittle corrosion layer also act as fatigue crack nuclei that propagate into the base material. On the other hand, the cyclic loads or strains cause cracking and flaking of the corrosion layer, which bares fresh metal to the corrosive medium. Thus, each process accelerates the other, often making the result disproportionately serious.

*Combined creep and fatigue* failure is a combination failure mode in which all of the conditions for both creep failure and fatigue exist simultaneously, each process influencing the other to produce failure. The interaction of creep and fatigue is complex and synergistic in nature and is less well understood.

### 3 ELASTIC DEFORMATION AND YIELDING

Small changes in the interatomic spacing of a material, induced by applied forces or changing temperatures, are manifested macroscopically as elastic strain. Although the maximum elastic strain in crystalline solids, including engineering metals, is typically very small, the force required to produce the small strain is usually large; hence, the accompanying stress is large. For uniaxial loading of a machine or structural element, the total elastic deformation of the member may be found by integrating the elastic strain over the length of the element. Thus, for a uniform bar subjected to uniaxial loading, the total deformation of the bar in the axial direction is

$$\Delta l = l\varepsilon \quad (1)$$

where  $\Delta l$  is total axial deformation of the bar,  $l$  is the original bar length, and  $\varepsilon$  is the axial elastic strain. If  $\Delta l$  exceeds the design-allowable axial deformation, failure will occur. For example, if the axial deformation of an aircraft gas turbine blade, due to the centrifugal force field, exceeds the tip clearance gap, failure will occur because of force-induced elastic deformation. Likewise, if thermal expansion of the blade produces a blade-axial deformation that exceeds the tip clearance gap, failure will occur because of temperature-induced elastic deformation.

When the state of stress is more complicated, it becomes necessary to calculate the elastic strains induced by the multiaxial states of stress in three mutually perpendicular directions through the use of the generalized Hooke's law equations for isotropic materials:

$$\begin{aligned} \varepsilon_x &= \frac{1}{E}[\sigma_x - \nu(\sigma_y + \sigma_z)] \\ \varepsilon_y &= \frac{1}{E}[\sigma_y - \nu(\sigma_x + \sigma_z)] \\ \varepsilon_z &= \frac{1}{E}[\sigma_z - \nu(\sigma_x + \sigma_y)] \end{aligned} \quad (2)$$

where  $\sigma_x$ ,  $\sigma_y$ , and  $\sigma_z$  are the normal stresses in the three coordinate directions,  $E$  and  $\nu$  are Young's modulus and Poisson's ratio, respectively, and  $\varepsilon_x$ ,  $\varepsilon_y$ , and  $\varepsilon_z$  are the elastic strains in the three coordinate directions. Again, total elastic deformation of a member in any of the coordinate directions may be found by integrating the strain over the member's length in that direction. If the change in length of the member in any direction exceeds the design-allowable deformation in that direction, failure will occur. The use of commercial finite-element analysis software packages is one commonly used means of determining both the elastic strains produced in a structural element and the subsequent elastic deformations produced.

If applied loads reach certain critical levels, the atoms within the microstructure may be moved into new equilibrium positions and the induced strains are not fully recovered upon release of the loads. Such permanent strains, usually the result of slip, are called plastic strains, and the macroscopic permanent deformation due to plastic strain is called yielding. If applied loads are increased even more, the plastic deformation process may be carried to the point of instability where *necking* begins: Internal voids form and slowly coalesce to finally produce a ductile rupture of the loaded member.

After plastic deformation has been initiated, Eqs. (2) are no longer valid, and the predictions of plastic strains and deformations under multiaxial states of stress are more difficult. If a designer can tolerate a prescribed plastic deformation without experiencing failure, these plastic deformations may be determined using plasticity theory. Nowadays, commercial finite-element analysis software packages possess the capability to compute both plastic strains and deformations for a prescribed nonlinear elastic-plastic constitutive relation.

For the case of simple uniaxial loading, the onset of yielding may be accurately predicted to occur when the uniaxial normal stress reaches a value equal to the yield strength of the

material read from an engineering stress–strain curve. If the loading is more complicated and a multiaxial state of stress is produced by the loads, the onset of yielding may no longer be predicted by comparing any one of the normal stress components with uniaxial material yield strength, not even the maximum principal normal stress. Onset of yielding for multiaxially stressed critical points in a machine or structure is more accurately predicted through the use of a *combined stress theory of failure*, which has experimentally been validated for the prediction of yielding. The two most widely accepted theories for predicting the onset of yielding are the distortion energy theory (also called the octahedral shear stress theory or the von Mises criterion) and the maximum shearing stress theory (also called the Tresca criterion). The distortion energy theory is somewhat more accurate while the maximum shearing stress theory may be slightly easier to use and is more conservative.

In words, the distortion energy theory may be expressed as follows: *Failure is predicted to occur in the multiaxial state of stress when the distortion energy per unit volume becomes equal to or exceeds the distortion energy per unit volume at the time of failure in a simple uniaxial stress test using a specimen of the same material.*

Mathematically, the distortion energy theory may be formulated as: *Failure is predicted by the distortion energy theory to occur if*

$$[(\sigma_1 - \sigma_2)^2 + (\sigma_1 - \sigma_3)^2 + (\sigma_2 - \sigma_3)^2] \geq 2\sigma_f^2 \quad (3)$$

The maximum shearing stress theory may be stated in words as: *Failure is predicted to occur in the multiaxial state of stress when the maximum shearing stress magnitude becomes equal to or exceeds the maximum shearing stress magnitude at the time of failure in a simple uniaxial stress test using a specimen of the same material.*

Mathematically, the maximum shearing stress theory becomes: *Failure is predicted by the maximum shearing stress theory to occur if*

$$\sigma_1 - \sigma_3 \geq \sigma_f \quad (4)$$

where  $\sigma_1$ ,  $\sigma_2$  and  $\sigma_3$  are the principal stresses at a point ordered such that  $\sigma_1 \geq \sigma_2 \geq \sigma_3$  and  $\sigma_f$  is the uniaxial failure strength in tension.

Comparisons of these two failure theories with experimental data on yielding are shown in Fig. 1 for a variety of materials and different biaxial states of stress.

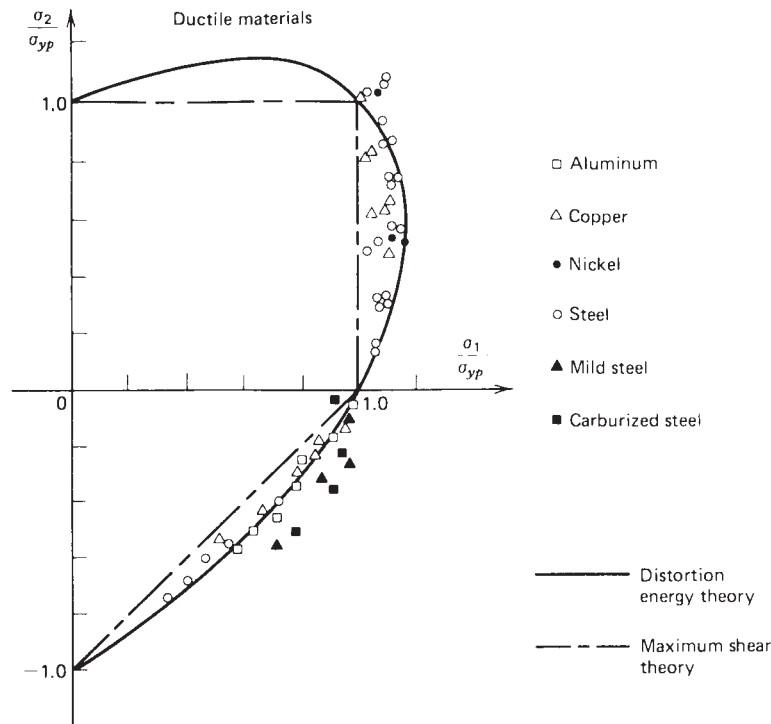
## 4 FRACTURE MECHANICS AND UNSTABLE CRACK GROWTH

When the material behavior is brittle rather than ductile, the mechanics of the failure process are very different. Instead of the slow coalescence of voids associated with ductile rupture, brittle fracture proceeds by the high-velocity propagation of a crack across the loaded member. If the material behavior is clearly brittle, fracture may be predicted with reasonable accuracy through use of the maximum normal stress theory of failure. In words, the maximum normal stress theory may be expressed as follows: *Failure is predicted to occur in the multiaxial state of stress when the maximum principal normal stress becomes equal to or exceeds the maximum normal stress at the time of failure in a simple uniaxial stress test using a specimen of the same material.*

Mathematically, the maximum normal stress theory becomes: *Failure is predicted by the maximum normal stress theory to occur if*

$$\sigma_1 \geq \sigma_t \quad |\sigma_3| \geq \sigma_c \quad (5)$$

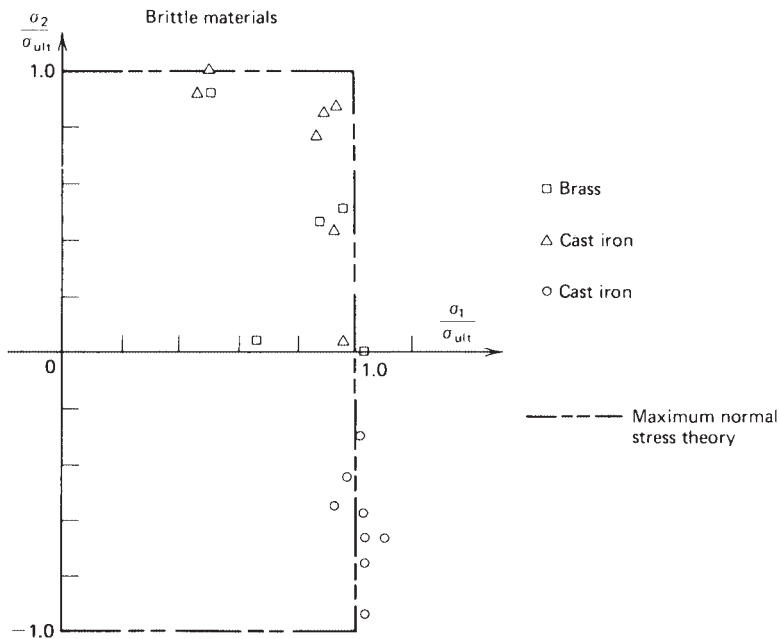
where  $\sigma_t$  is the uniaxial failure strength in tension, and  $\sigma_c$  is the uniaxial failure strength in compression. Comparison of this failure theory with experimental data on brittle fracture for different biaxial states of stress is shown in Fig. 2.



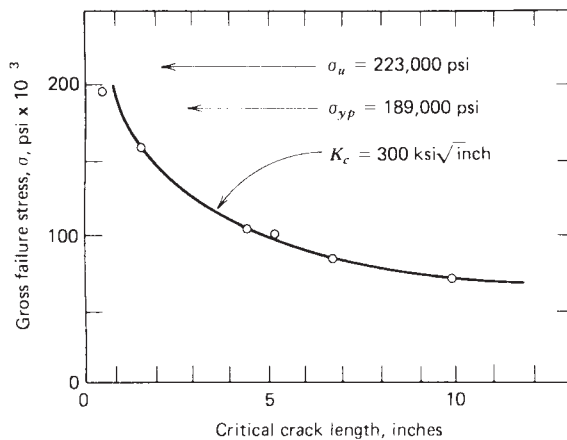
**Figure 1** Comparison of biaxial yield strength data with theories of failure for a variety of ductile materials.

On the other hand, more recent experience has led to the understanding that nominally ductile materials may also fail by a brittle fracture response in the presence of cracks or flaws if the combination of crack size, geometry of the part, temperature, and/or loading rate lies within certain critical regions. Furthermore, the development of higher strength structural alloys, the wider use of welding, and the use of thicker sections in some cases have combined their influence to reduce toward a critical level the capacity of some structural members to accommodate local plastic strain without fracture. At the same time, fabrication by welding, residual stresses due to machining, and assembly mismatch in production have increased the need for accommodating local plastic strain to prevent failure. Fluctuating service loads of greater severity and more aggressive environments have also contributed to unexpected fractures.

An important observation in studying fracture behavior is that the magnitude of the nominal applied stress that causes fracture is related to the size of the crack or cracklike flaw within the structure.<sup>2-4</sup> For example, observations of the behavior of central through-the-thickness cracks, oriented normally to the applied tensile stress in steel and aluminum plates, yielded the results shown in Figs. 3 and 4. In these tests, as the tensile loading on the precracked plates was slowly increased, the crack initially extended slowly for a time and then abruptly extended to failure by rapid crack propagation. The slow stable crack growth or tearing was characterized by speeds of the order of fractions of an inch per minute. The rapid crack propagation was characterized by speeds of the order of hundreds of feet per second. The data of Figs. 3 and 4 indicate that for longer initial crack lengths the fracture stress (the stress corresponding to the

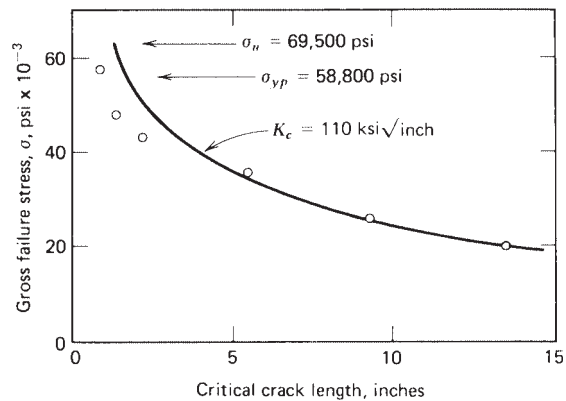


**Figure 2** Comparison of biaxial brittle fracture strength data with maximum normal stress theory for several brittle materials.



**Figure 3** Influence of crack length on gross failure stress for center-cracked steel plate. (After Ref. 5. Copyright ASTM, adapted with permission.)

onset of stable tearing) was lower. For the aluminum alloy the fracture stress was less than the yield strength for cracks longer than about 0.75 in. For the steel alloy the fracture stress was less than the yield strength for cracks longer than about 0.5 in. In both cases, for shorter cracks the fracture stress approaches the ultimate strength of the material determined from a conventional uniaxial tension test.



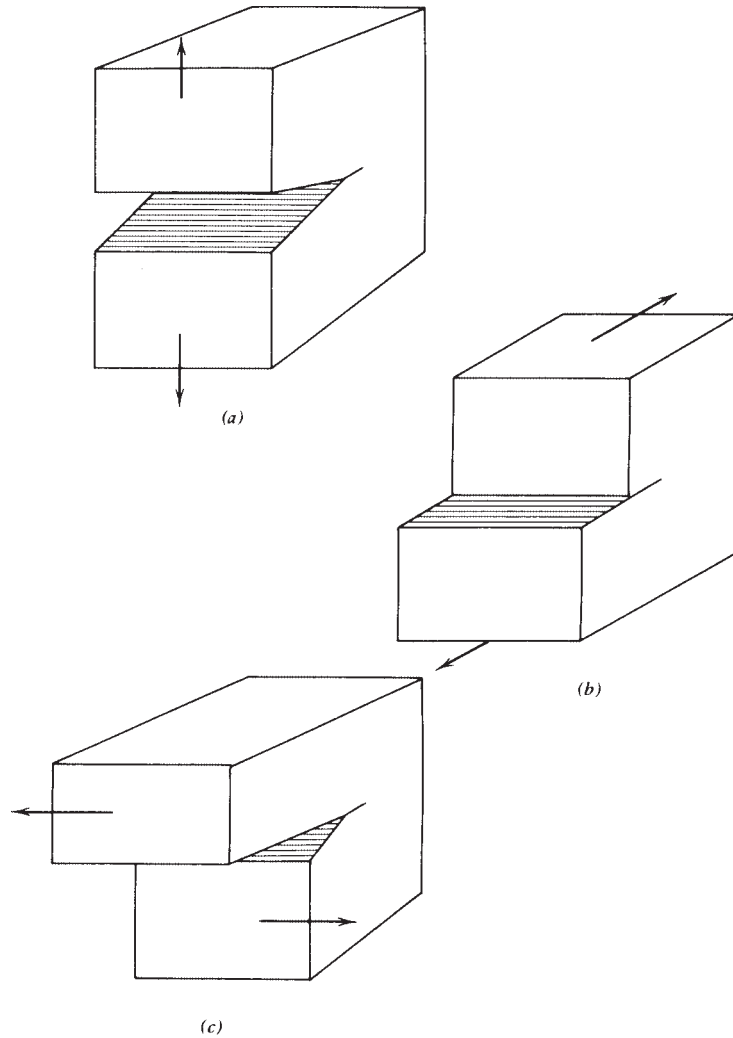
**Figure 4** Influence of crack length on gross failure stress for center-cracked aluminum plate. (After Ref. 5. Copyright ASTM, adapted with permission.)

Experience has shown that the onset of stable tearing establishes an important material property termed *fracture toughness*. The fracture toughness may be used as a design criterion in fracture prevention, just as the yield strength is used as a design criterion in prevention of yielding of a ductile material under static loading. It should be noted that not all materials and/or specimen types exhibit stable tearing. Many materials and/or specimen configurations exhibit rapid crack propagation without any evidence of prior stable tearing.

In many cases slow crack propagation occurs by means other than stable tearing, especially under conditions of fluctuating loads and/or aggressive environments. In analyses and predictions involving fatigue failure phenomena, characterization of the rate of slow crack extension and the initial flaw size, together with critical crack size, are used to determine the useful life of a component or structure subjected to fluctuating loads. The topic of fatigue crack propagation is discussed further in Section 5.

The simplest useful model for the stresses near the tip of a crack is based on the assumptions of linear elastic material behavior and a two-dimensional analysis; thus, the procedure is often referred to as linear elastic fracture mechanics. Although the validity of the linear elastic assumption may be questioned in view of plastic zone formation at the tip of a crack in any real engineering material, as long as *small-scale yielding* occurs, that is, as long as the plastic zone size remains small compared to the dimensions of the crack, the linear elastic model gives good engineering results. Thus, the small-scale yielding concept implies that the small plastic zone is confined within a linear elastic field surrounding the crack tip. If the material properties, section size, loading conditions, and environment combine in such a way that large-scale plastic zones are formed, the basic assumptions of linear elastic fracture mechanics are violated, and elastic plastic fracture mechanics methods must be employed.<sup>4</sup>

Three basic types of stress fields can be defined for crack-tip stress analysis, each one associated with a distinct mode of crack deformation, as illustrated in Fig. 5. The opening mode, mode I, is associated with local displacement in which the crack surfaces move directly apart, as shown in Fig. 5a. The sliding mode, mode II, is developed when crack surfaces slide over each other in a direction perpendicular to the leading edge of the crack, as shown in Fig. 5b. The tearing mode, mode III, is characterized by crack surfaces sliding with respect to each other in a direction parallel to the leading edge of the crack, as shown in Fig. 5c. Superposition of these three modes will fully describe the most general three-dimensional case of local crack-tip deformation and stress field, although mode I is most common.



**Figure 5** Basic modes of crack displacement: (a) mode I, (b) mode II, and (c) mode III.

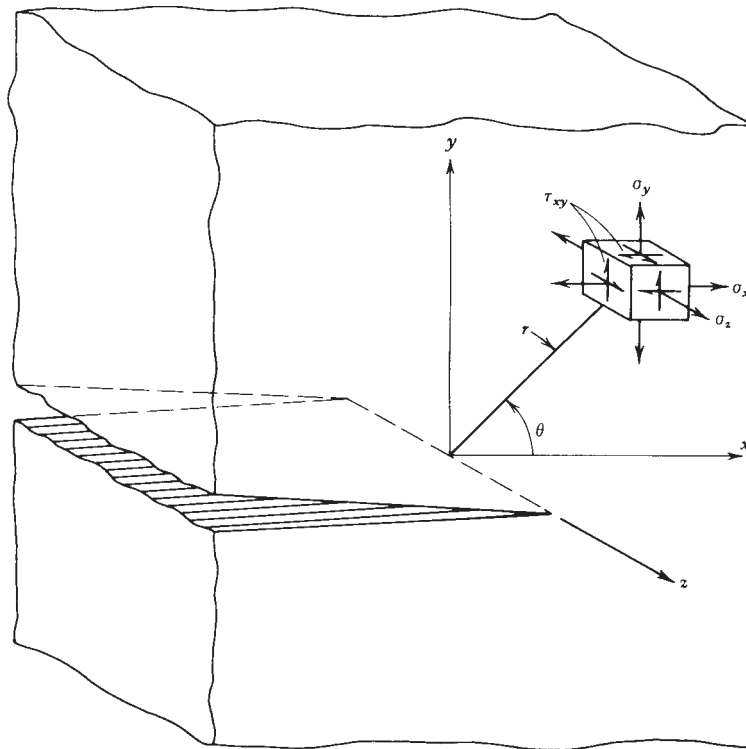
In terms of the coordinates shown in Fig. 6, the stresses near the crack tip for mode I loading may be written as

$$\sigma_x = \frac{K_I}{\sqrt{2\pi r}} \cos \frac{\theta}{2} \left[ 1 - \sin \frac{\theta}{2} \sin \frac{3\theta}{2} \right] \quad (6)$$

$$\sigma_y = \frac{K_I}{\sqrt{2\pi r}} \cos \frac{\theta}{2} \left[ 1 + \sin \frac{\theta}{2} \sin \frac{3\theta}{2} \right] \quad (7)$$

$$\tau_{xy} = \frac{K_I}{\sqrt{2\pi r}} \sin \frac{\theta}{2} \cos \frac{\theta}{2} \cos \frac{3\theta}{2} \quad (8)$$





**Figure 6** Coordinates measured from leading edge of a crack.

The parameter  $K_I$  is known as the mode I stress intensity factor. This parameter represents the strength of the stress field surrounding the tip of the crack. Since fracture is induced by the crack-tip stress field, the stress intensity factor is the primary correlation parameter used in current practice.

In general, the expressions for the stress intensity factor are of the form

$$K_I = C\sigma\sqrt{\pi a} \quad (9)$$

where  $a$  is the crack size,  $\sigma$  is the gross-section stress, and  $C$  is dependent on the type of loading and the geometry away from the crack. Much work has been completed in determining values of  $C$  for a wide variety of conditions. (See, for example, Ref. 5.)

Many commercial finite-element analysis software packages possess special crack-tip elements allowing the numerical computation of stress intensity factors. A discussion of some of the techniques employed within these software packages is given by Anderson.<sup>4</sup> Through the use of weight functions,<sup>6,7</sup> stress intensity factors may also be computed easily using numerical integration and the stresses that would exist in the uncracked body.

From Eq. (9), the stress intensity factor increases proportionally with gross nominal stress  $\sigma$  and also is a function of the crack length  $a$ . The value of  $K_I$  associated with the onset of fracture has been designated the *critical stress intensity*,  $K_C$ . As noted earlier in Figs. 3 and 4, the fracture of specimens with different crack lengths occurs at different values of gross-section stress but at a constant value of  $K_C$ . Thus,  $K_C$  provides a single-parameter fracture criterion that allows the prediction of fracture based on (9). That is, *fracture is predicted to occur if*

$$K_I \geq K_C \quad (10)$$

**Table 1** Yield Strength and Plane-Strain Fracture Toughness Data for Selected Engineering Alloys<sup>9,10</sup>

Alloy	Form	Test Temperature		$\alpha / y_p$		$K_{I,C}$	
		F	C	ksi	MPa	ksi $\sqrt{\text{in.}}$	MPa $\sqrt{\text{m}}$
4340 (500 °F temper) steel	Plate	70	21	217–238	1495–1640	45–57	50–63
4340 (800 °F temper) steel	Forged	70	21	197–211	1360–1455	72–83	79–91
D6AC (1000 °F temper)	Plate	170	21	217	1495	93	102
D6AC (1000 °F temper)	Plate	65	54	228	1570	56	62
A 538 steel				250	1722	100	111
2014-T6 aluminum	Forged	75	24	64	440	28	31
2024-T351 aluminum	Plate	80	27	54–56	370–385	28–40	31–44
7075-T6 aluminum				85	585	30	33
7075-T651 aluminum	Plate	70	21	75–81	515–560	25–28	27–31
7075-T7351 aluminum	Plate	70	21	58–66	300–455	28–32	31–35
Ti-6Al-4V titanium	Plate	74	23	119	820	96	106

In studying material behavior, one finds that for a given material, as the specimen thickness is increased, the critical stress intensity  $K_C$  decreases to a lower limiting value. This lower limiting value defines a basic material property  $K_{I,C}$  the *plane-strain fracture toughness* for the material. Standard test methods have been established for the determination of  $K_{I,C}$  values.<sup>8</sup> A few data are shown in Table 1. Useful compilations of fracture toughness values have been prepared by several organizations and individuals. These include Refs. 10–16.

For the plane-strain fracture toughness  $K_{I,C}$  to be a valid failure prediction criterion for a specimen or a machine part, plane-strain conditions must exist at the crack tip; that is, the material must be thick enough to ensure plane-strain conditions. It has been estimated<sup>8</sup> empirically that for plane-strain conditions the minimum material thickness  $B$  must be

$$B \geq 2.5 \left( \frac{K_{I,C}}{\sigma_{yp}} \right) \quad (11)$$

where  $\sigma_{yp}$  is the material yield strength.

If the material is not thick enough to meet the criterion of (11), plane stress is a more likely state of stress at the crack tip; and  $K_C$ , the critical stress intensity factor for failure prediction under plane-stress conditions, may be estimated using a semiempirical relationship<sup>17</sup>:

$$K_C = K_{I,C} \left[ 1 + \frac{1.4}{B^2} \left( \frac{K_{I,C}}{\sigma_{yp}} \right)^4 \right]^{1/2} \quad (12)$$

As long as the crack-tip plastic zone remains in the regime of small-scale yielding, this estimation procedure provides a good design approach. For conditions that result in large crack-tip plastic zones (large applied stresses, large crack lengths), performing a failure assessment using linear elastic fracture mechanics (LEFM) is invalid and potentially nonconservative. A general rule of thumb is that plasticity effects become significant when the applied stresses approach 50% of the yield stress, but this is by no means a universal rule.<sup>4</sup> When small-scale yielding is not generated at the crack tip, a better design approach would involve the implementation of an appropriate elastic–plastic fracture mechanics (EPFM) procedure.

## 5 FATIGUE

Static or quasi-static loading is rarely observed in modern engineering practice, making it essential for the designer to address himself or herself to the implications of repeated loads, fluctuating loads, and rapidly applied loads. By far, the majority of engineering design projects involve machine parts subjected to fluctuating or cyclic loads. Such loading induces fluctuating or cyclic stresses that often result in failure by fatigue.

Fatigue failure investigations over the years have led to the observation that the fatigue process actually embraces two domains of cyclic stressing or straining that are significantly different in character and in each of which failure is probably produced by different physical mechanisms. One domain of cyclic loading is that for which significant plastic strain occurs during each cycle. This domain is associated with high loads and short lives, or low numbers of cycles to produce fatigue failure, and is commonly referred to as *low-cycle fatigue*. The other domain of cyclic loading is that for which the strain cycles are largely confined to the elastic range. This domain is associated with lower loads and long lives, or high numbers of cycles to produce fatigue failure, and is commonly referred to as *high-cycle fatigue*. Low-cycle fatigue is typically associated with cycle lives from 1 up to about  $10^4$  cycles. Fatigue may be characterized as a progressive failure phenomenon that proceeds by the *initiation* and *propagation* of cracks to an unstable size. Numerous experimental tests over the years have concluded that there is no single microscopic feature that controls the initiation and propagation of fatigue cracks. Nowadays, it is widely accepted that, in pure metals, fatigue cracks nucleate from persistent slip bands (PSBs) at the surface of the material. A PSB is a dislocation structure caused by the reversed slip of dislocations along crystallographic planes. The intersection of a PSB with the surface of the material creates small ledges on the surface acting as microscopic stress concentration factors. Fatigue cracks nucleate and grow from these microscopic surface features inward along PSBs. In alloys, crack initiation and growth within the microstructure is mainly controlled by other microstructural features such as inclusions, second-phase particles, impurities, or grain boundaries. Fatigue crack nucleation and growth can be also caused by mechanical defects, such as surface cracks or voids at or near the surface. Once a fatigue crack reaches a critical length, one additional loading cycle causes complete failure. The final failure region will typically show evidence of plastic deformation produced just prior to final separation. For ductile materials the final fracture area often appears as a shear lip produced by crack propagation along the planes of maximum shear.

Although designers find these basic observations of great interest, they must be even more interested in the macroscopic phenomenological aspects of fatigue failure and in avoiding fatigue failure during the design life. Some of the macroscopic effects and basic data requiring consideration in designing under fatigue loading include:

1. The effects of a simple, completely reversed alternating stress on the strength and properties of engineering materials
2. The effects of a steady stress with a superposed alternating component, that is, the effects of cyclic stresses with a nonzero mean
3. The effects of alternating stresses in a multiaxial state of stress
4. The effects of stress gradients and residual stresses, such as imposed by shot peening or cold rolling
5. The effects of stress raisers, such as notches, fillets, holes, threads, riveted joints, and welds
6. The effects of surface finish, including the effects of machining, cladding, electroplating, and coating
7. The effects of temperature on fatigue behavior of engineering materials

8. The effects of size of the structural element
9. The effects of accumulating cycles at various stress levels and the permanence of the effect
10. The extent of the variation in fatigue properties to be expected for a given material
11. The effects of humidity, corrosive media, and other environmental factors
12. The effects of interaction between fatigue and other modes of failure, such as creep, corrosion, and fretting

## 5.1 Fatigue Loading and Laboratory Testing

Faced with the design of a fatigue-sensitive element in a machine or structure, a designer is very interested in the fatigue response of engineering materials to various loadings that might occur throughout the design life of the machine under consideration. That is, the designer is interested in the effects of various *loading spectra* and associated *stress spectra*, which will in general be a function of the design configuration and the operational use of the machine.

Perhaps the simplest fatigue stress spectrum to which an element may be subjected is a zero-mean sinusoidal stress–time pattern of constant amplitude and fixed frequency, applied for a specified number of cycles. Such a stress–time pattern, often referred to as a completely reversed cyclic stress, is illustrated in Fig. 7*a*. Utilizing the sketch of Fig. 7*b*, we can conveniently define several useful terms and symbols; these include

$\sigma_{\max}$  = maximum stress in the cycle

$\sigma_{\min}$  = minimum stress in the cycle

$\sigma_m$  = mean stress, =  $(\sigma_{\max} + \sigma_{\min})/2$

$\sigma_a$  = alternating stress, =  $(\sigma_{\max} - \sigma_{\min})/2$

$\Delta\sigma$  = range of stress, =  $(\sigma_{\max} - \sigma_{\min})/2$

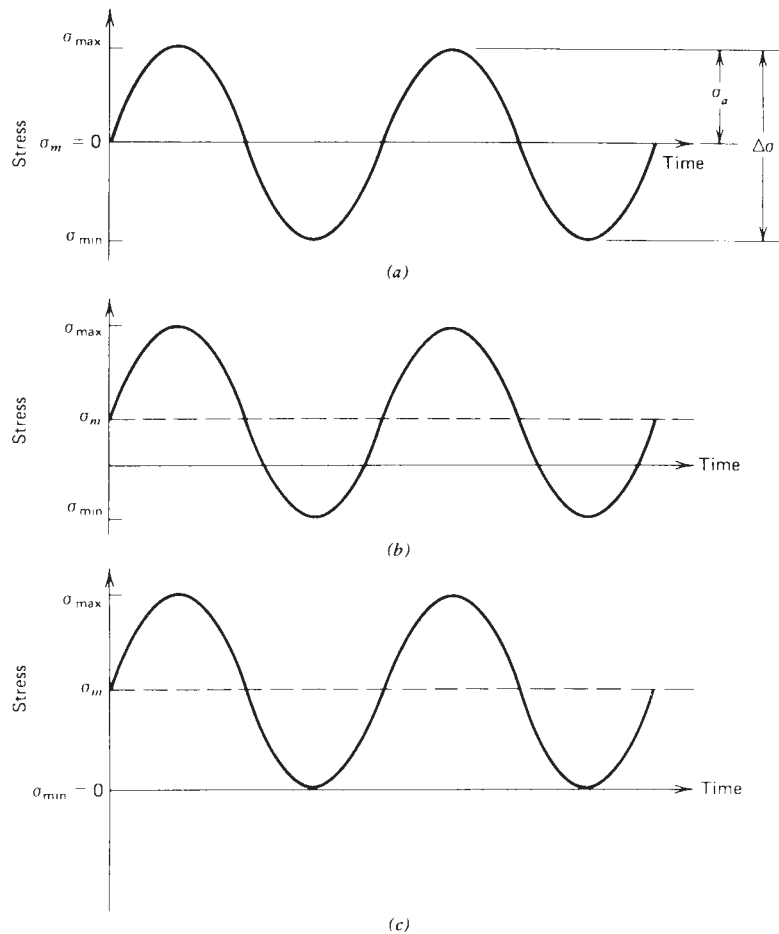
$R$  = stress ratio, =  $\sigma_{\min}/\sigma_{\max}$

Any two of the quantities just defined, except the combinations  $\sigma_a$  and  $\Delta\sigma$ , are sufficient to describe completely the stress–time pattern.

More complicated stress–time patterns are produced when the mean stress, the stress amplitude, or both change during the operational cycle, as illustrated in Fig. 8. It may be noted that this stress–time spectrum is beginning to approach a degree of realism. Finally, in Fig. 9 a sketch of a realistic stress spectrum is given. This type of quasi-random stress–time pattern might be encountered in an airframe structural member during a typical mission including refueling, taxi, takeoff, gusts, maneuvers, and landing. The obtaining of useful, realistic data is a challenging task in itself. Instrumentation of existing machines, such as operational aircraft, provide some useful information to the designer if his or her mission is similar to the one performed by the instrumented machine. Recorded data from accelerometers, strain gauges, and other transducers may in any event provide a basis from which a statistical representation can be developed and extrapolated to future needs if the fatigue processes are understood.

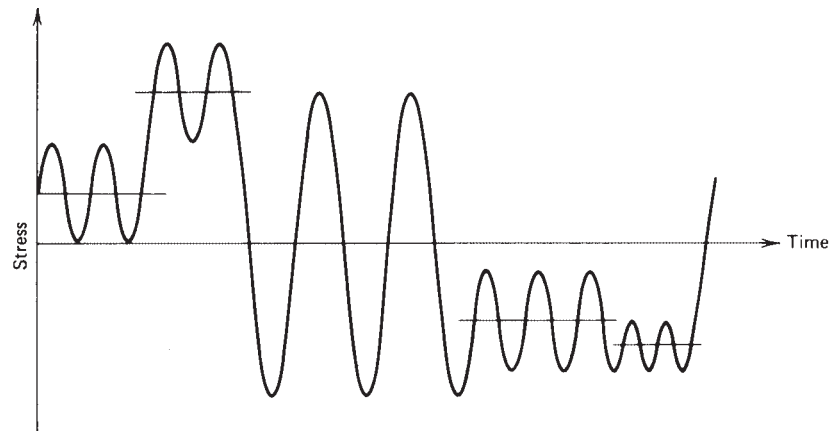
Basic data for evaluating the response of materials, parts, or structures are obtained from carefully controlled laboratory tests. Various types of testing machines and systems commonly used include:

1. Rotating-bending machines
  - a. Constant bending moment type
  - b. Cantilever bending type

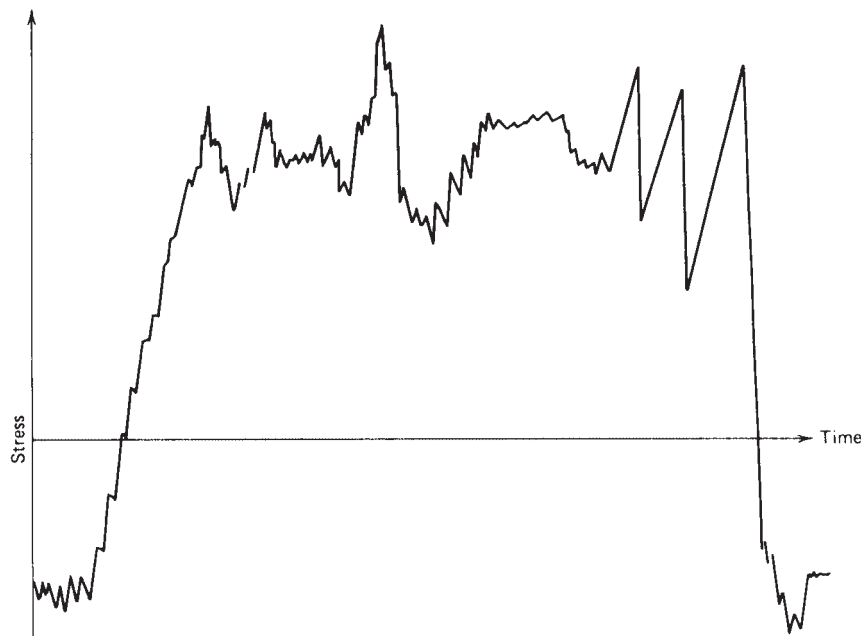


**Figure 7** Several constant-amplitude stress–time patterns of interest: (a) completely reversed,  $R = -1$ , (b) nonzero mean stress, and (c) released tension,  $R = -0$ .

2. Reciprocating-bending machines
3. Axial direct-stress machines
  - a. Brute-force type
  - b. Resonant type
4. Vibrating shaker machines
  - a. Mechanical type
  - b. Electromagnetic type
5. Repeated torsion machines
6. Multiaxial stress machines
7. Computer-controlled closed-loop machines
8. Component testing machines for special applications
9. Full-scale or prototype fatigue testing systems

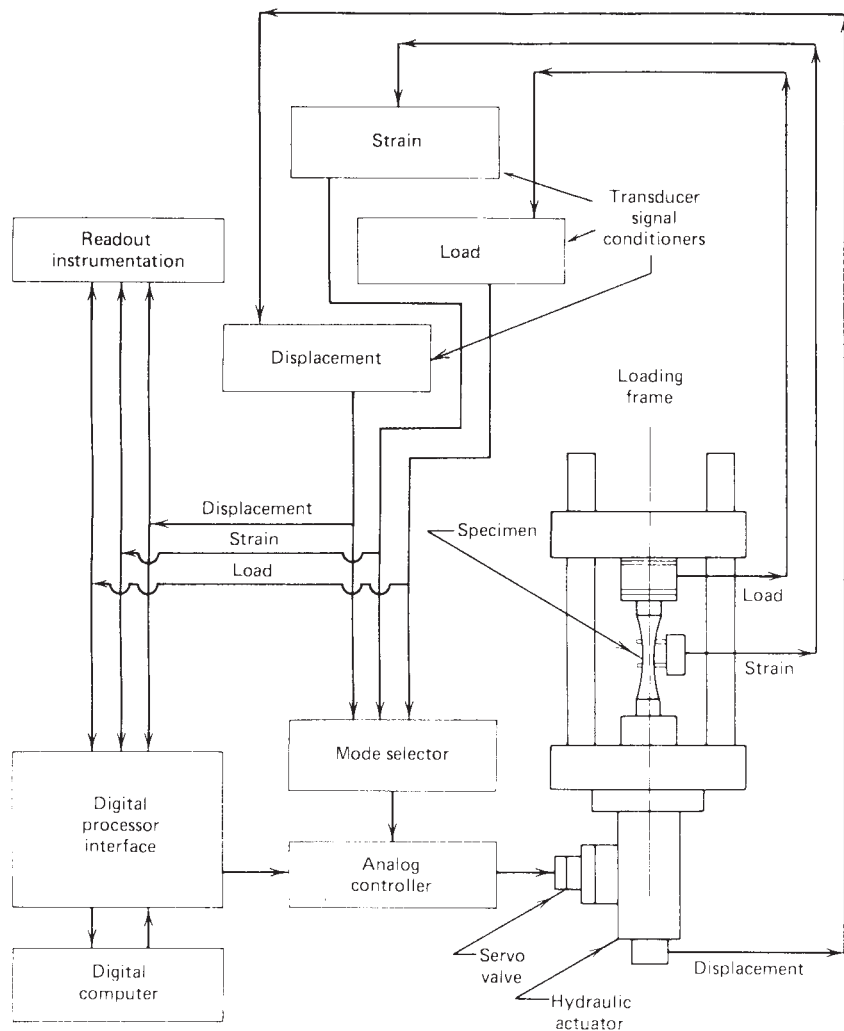


**Figure 8** Stress-time pattern in which both mean and amplitude change to produce a more complicated stress spectrum.



**Figure 9** A quasi-random stress-time pattern typical of an aircraft during a given mission.

Computer-controlled fatigue testing machines are widely used in all modern fatigue testing laboratories. Usually such machines take the form of precisely controlled hydraulic systems with feedback to electronic controlling devices capable of producing and controlling virtually any strain-time, load-time, or displacement-time pattern desired. A schematic diagram of such a system is shown in Fig. 10.



**Figure 10** Schematic diagram of a computer-controlled closed-loop fatigue-testing machine.

Special testing machines for component testing and full-scale prototype testing are not found in the general fatigue-testing laboratory. These systems are built up especially to suit a particular need, for example, to perform a full-scale fatigue test of a commercial jet aircraft.

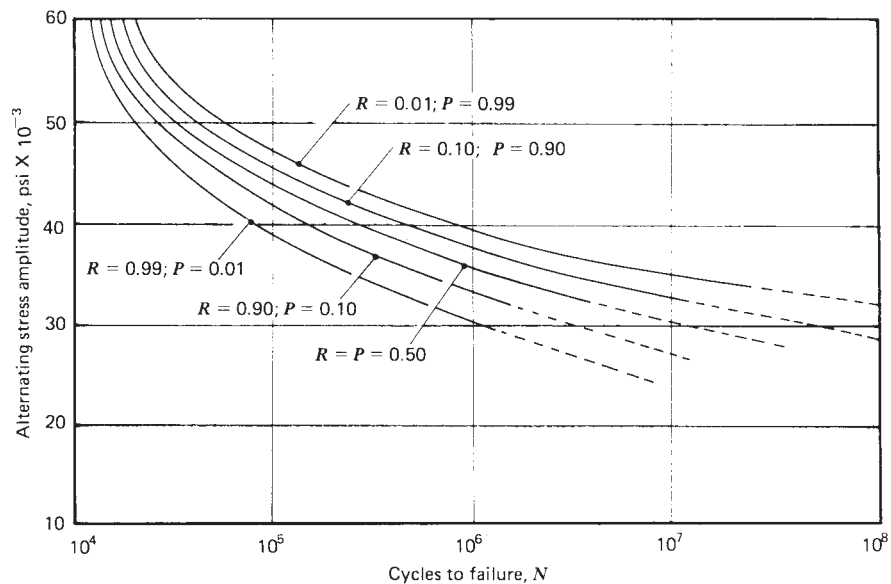
It may be observed that fatigue-testing machines range from very simple to very complex. The very complex testing systems, used, for example, to test a full-scale prototype, produce very specialized data applicable only to the particular prototype and test conditions used; thus, for the particular prototype and test conditions the results are very accurate, but extrapolation to other test conditions and other pieces of hardware is difficult, if not impossible. On the other hand, simple smooth-specimen laboratory fatigue data are very general and can be utilized in designing virtually any piece of hardware made of the specimen material. However, to use such data in practice requires a quantitative knowledge of many pertinent differences between the laboratory and the application, including the effects of nonzero mean stress, varying stress amplitude,

environment, size, temperature, surface finish, residual stress pattern, and others. Fatigue testing is performed at the extremely simple level of smooth-specimen testing, the extremely complex level of full-scale prototype testing, and everywhere in the spectrum between. Valid arguments can be made for testing at all levels.

## 5.2 Stress–Life Approach to Fatigue

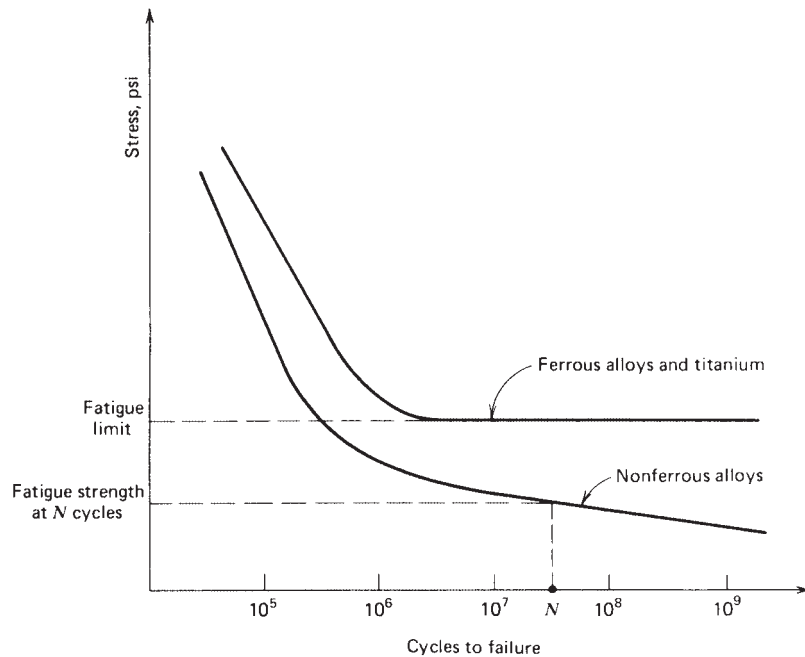
Basic fatigue data in the high-cycle life range can be conveniently displayed on a plot of cyclic stress level versus the logarithm of life or, alternatively, on a log-log plot of stress versus life. These plots, called  $S-N$  curves, constitute design information of fundamental importance for machine parts subjected to repeated loading. Because of the scatter of fatigue life data at any given stress level, it must be recognized that there is not only one  $S-N$  curve for a given material, but a family of  $S-N$  curves with probability of failure  $P$  as the parameter. These curves are called the  $S-N-P$  curves, or curves of constant probability of failure on a stress-versus-life plot. A representative family of  $S-N-P$  curves is illustrated in Fig. 11. It should also be noted that references to the “ $S-N$  curve” in the literature generally refer to the mean curve unless otherwise specified. Details regarding fatigue testing and the experimental generation of  $S-N-P$  curves may be found in Ref. 1.

The mean  $S-N$  curves sketched in Fig. 12 distinguish two types of material response to cyclic loading commonly observed. The ferrous alloys and titanium exhibit a steep branch in the relatively short life range, leveling off to approach a stress asymptote at longer lives. This stress asymptote is called the *fatigue limit* or *endurance limit*, and is the stress level below which an infinite number of cycles can be sustained without failure. The nonferrous alloys do not exhibit an asymptote, and the curve of stress versus life continues to drop off indefinitely. For such alloys there is no fatigue limit, and failure as a result of cyclic load is only a matter of applying enough cycles. All materials, however, exhibit a relatively flat curve in the long-life range. The



**Figure 11** Family of  $S-N-P$  curves or  $R-S-N$  curves, for 7075-T6 aluminum alloy. Note:  $P$  = probability of failure;  $R$  = reliability =  $1 - P$ . (Adapted from Ref. 18. Reprinted with permission from John Wiley & Sons.)





**Figure 12** Two types of material response to cyclic loading.

linear portion of the  $S$ - $N$  curve at applied stress amplitudes greater than the endurance limit is described by the Basquin equation<sup>19</sup>

$$\sigma_a = \frac{\Delta\sigma}{2} = \sigma'_F (2N_f)^b \quad (13)$$

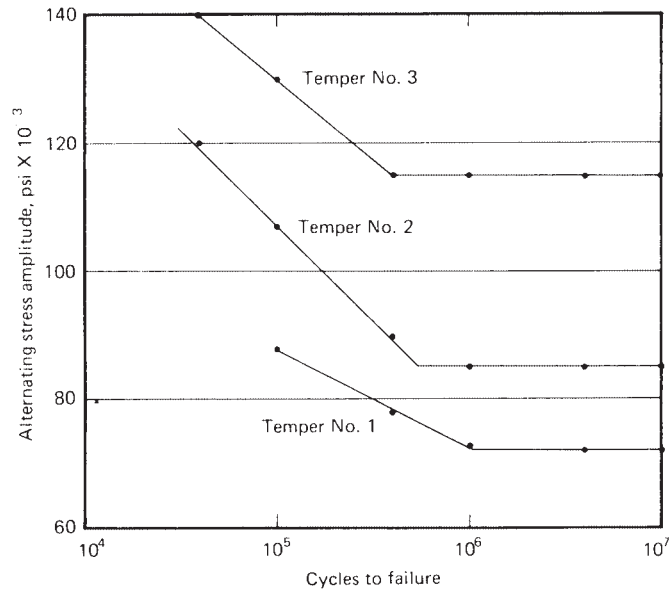
where  $\sigma'_F$  is the fatigue strength coefficient,  $b$  is the fatigue strength exponent, and  $N_f$  is the number of cycles to failure, thus  $2N_f$  is the number of load reversals to failure. This equation describes the fatigue life of a mechanical component experiencing relatively long fatigue life under low stresses. For these low stress levels, the strains are within the elastic range, and the elastic strain amplitude is calculated from Eq. (13) and the Hooke's law when the modulus of elasticity  $E$  is known

$$\varepsilon_a^e = \frac{\Delta\sigma}{2E} = \frac{\sigma'_F}{E} (2N_f)^b \quad (14)$$

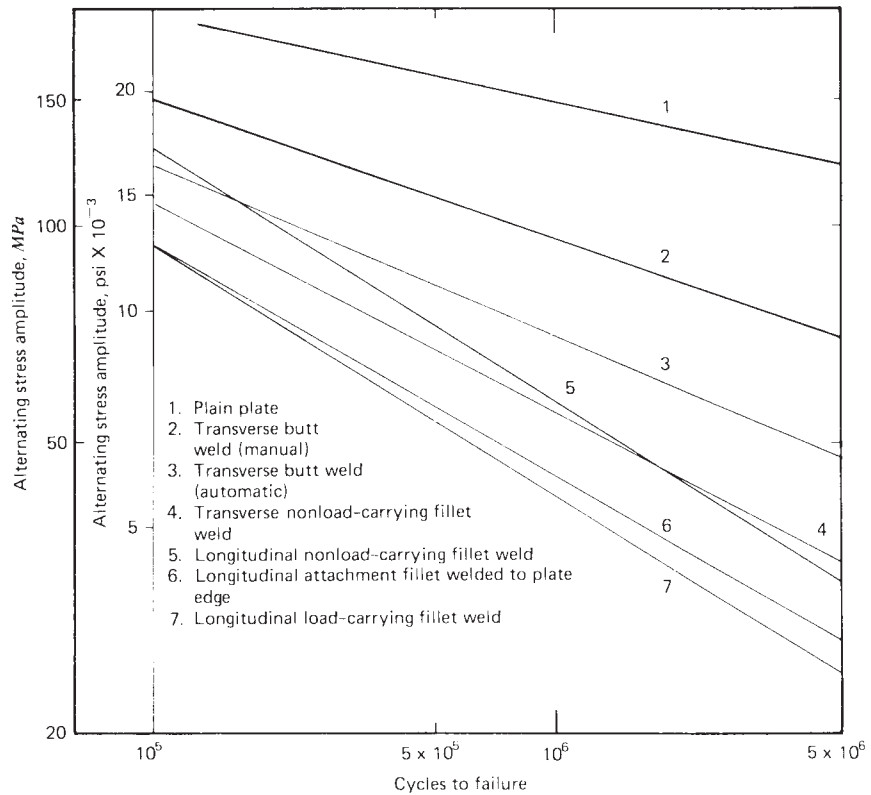
To characterize the failure response of nonferrous materials and of ferrous alloys in the finite-life range, the term *fatigue strength at a specified life*,  $\sigma_N$ , is used. The term fatigue strength identifies the stress level at which failure will occur at the specified life. The specification of *fatigue strength* without specifying the corresponding life is meaningless. The specification of a *fatigue limit* always implies infinite life.

#### **Factors That Affect S–N–P Curves**

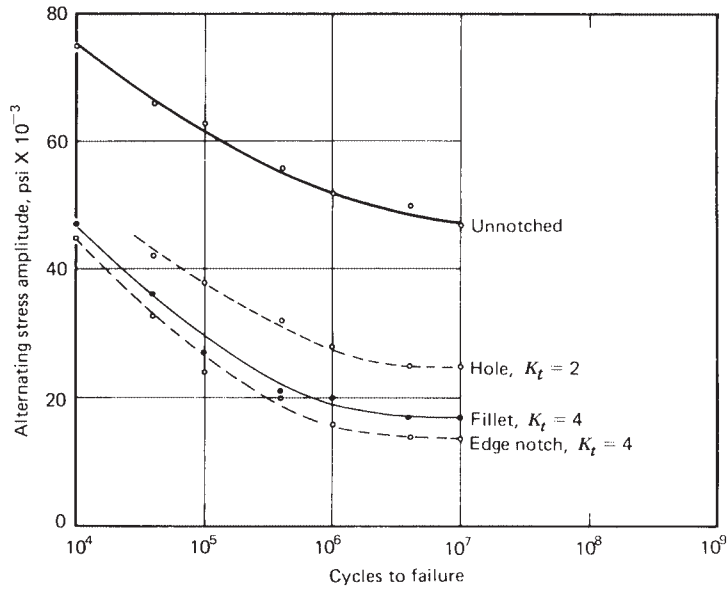
There are many factors that may influence the fatigue failure response of machine parts or laboratory specimens, including material composition, grain size and grain direction, heat treatment, welding, geometrical discontinuities, size effects, surface conditions, residual surface stresses, operating temperature, corrosion, fretting, operating speed, configuration of the stress–time pattern, nonzero mean stress, and prior fatigue damage. Typical examples of how some of these factors may influence fatigue response are shown in Figs. 13–19. It is usually necessary



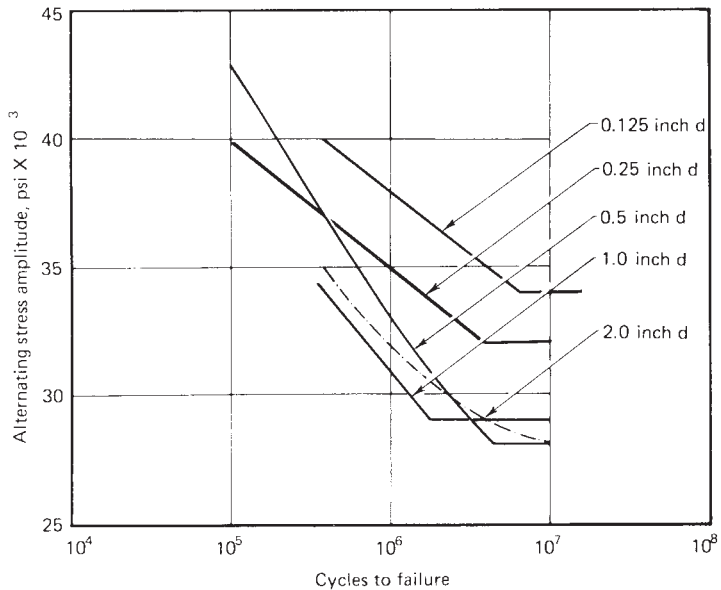
**Figure 13** Effects of heat treatment on the S–N curve of oil-quenched SAE 4130 steel. Temper No. 1:  $S_u = 129$  ksi; temper No. 2:  $S_u = 150$  ksi; temper No. 3:  $S_u = 206$  ksi.



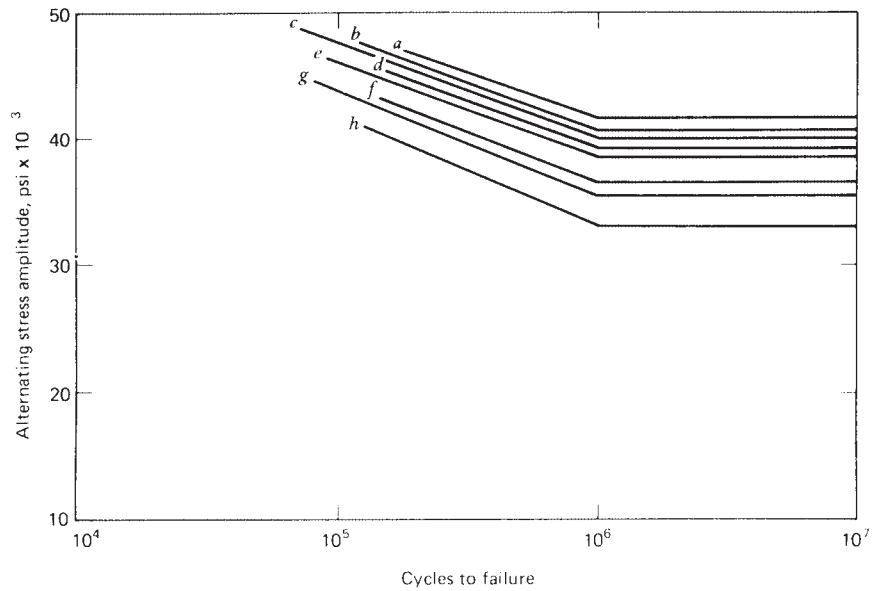
**Figure 14** Effects of welding detail on the S–N curve of structural steel, with yield strength in the range of 30–52 ksi. Tests were released tension ( $R = 0$ ). (Data from Ref. 20.)



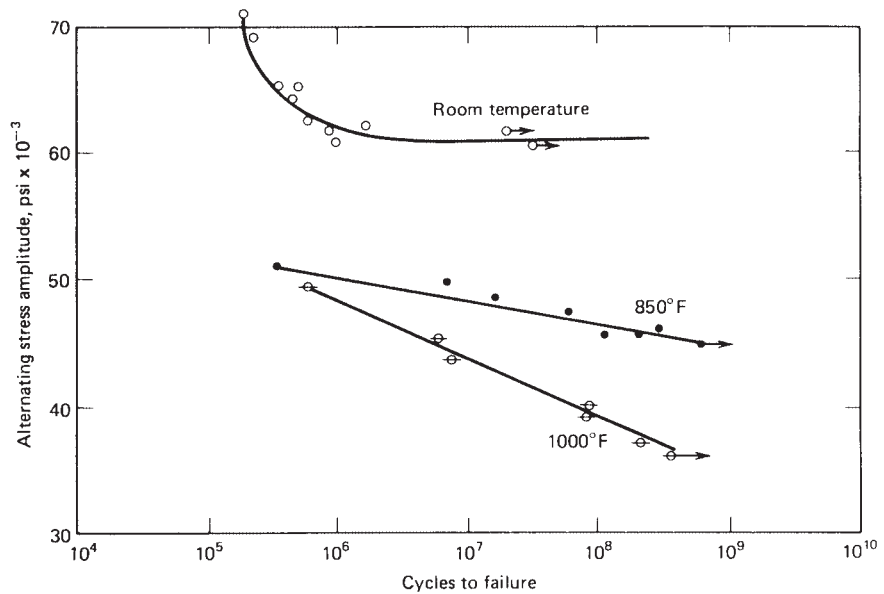
**Figure 15** Effects of geometrical discontinuities on the S–N curve of SAE 4130 steel sheet, tested under completely reversed axial loading. Specimen dimension ( $t$  = thickness,  $w$  = width,  $r$  = notch radius); unnotched:  $t$  = 0.075 in.,  $w$  = 1.5 in.; hole:  $t$  = 0.075 in.,  $w$  = 4.5 in.,  $r$  = 1.5 in.; fillet:  $t$  = 0.075 in.,  $w_{\text{net}}$  = 1.5 in.,  $w_{\text{gross}}$  = 2.25 in.,  $r$  = 0.0195 in.; edge notch:  $t$  = 0.075 in.,  $w_{\text{net}}$  = 1.5 in.,  $w_{\text{gross}}$  = 2.25 in.,  $r$  = 0.057 in. (Data from Ref. 21.)



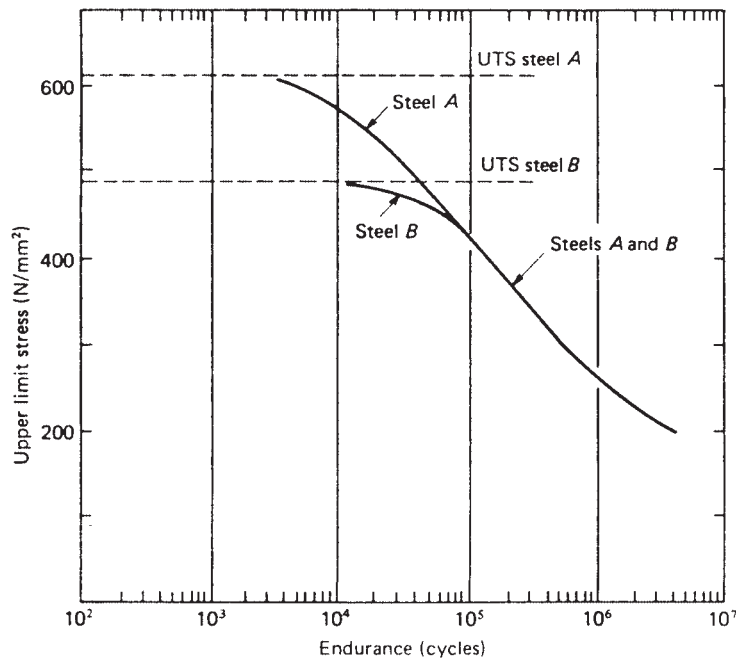
**Figure 16** Size effects on the S–N curve of SAE 1020 steel specimens cut from a 3.5-in.-diameter hot-rolled bar, testing in rotating bending. (Data from Ref. 22.)



**Figure 17** Effect of surface finish on the S-N curve of carbon steel specimens, testing in rotating bending: (a) high polish, longitudinal direction; (b) FF emery finish: (c) No. 1 emery finish; (d) coarse emery finish; (e) smooth file; (f) as-turned; (g) bastard file; and (h) coarse file. (Data from Ref. 23.)



**Figure 18** Effect of operating temperature on the S-N curve of a 12% chromium steel alloy. (Data from Ref. 24.)



**Figure 19** Effect of ultimate strength on the S–N curve for transverse butt welds in two steels. (Data from Ref. 25.)

to search the literature and existing databases to find the information required for a specific application, and it may be necessary to undertake experimental testing programs to produce data where they are unavailable.

### ***Nonzero Mean Stress***

Most basic fatigue data collected in the laboratory are for completely reversed alternating stresses, that is, zero mean cyclic stresses. Most service applications involve nonzero mean cyclic stresses. It is therefore very important to a designer to know the influence of mean stress on fatigue behavior so that he or she can utilize basic completely reversed laboratory data in designing machine parts subjected to nonzero mean cyclic stresses.

If a designer is fortunate enough to find test data for his or her proposed material under the mean stress conditions and design life of interest, the designer should, of course, use these data. Such data are typically presented on so-called *master diagrams* or *constant life diagrams* for the material. A master diagram for a 4340 steel alloy is shown in Fig. 20. An alternative means of presenting this type of fatigue data is illustrated in Fig. 21 for a 4130 steel alloy.

If data are not available to the designer, he or she may estimate the influence of nonzero mean stress by any one of several empirical relationships that relate failure at a given life under nonzero mean conditions to failure at the same life under zero mean cyclic stresses.

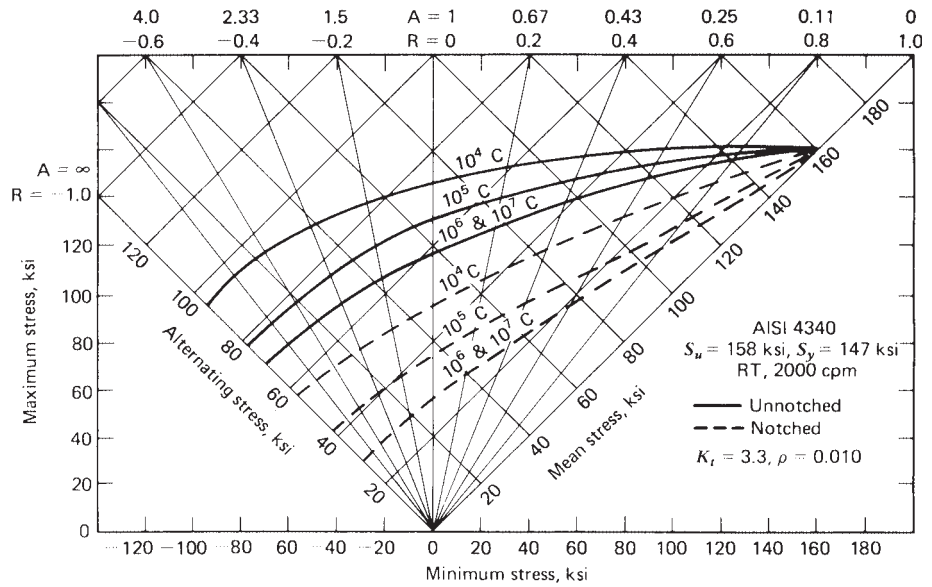


Figure 20 Master diagram for 4340 steel. (Reprinted from Ref. 26, p. 37.)

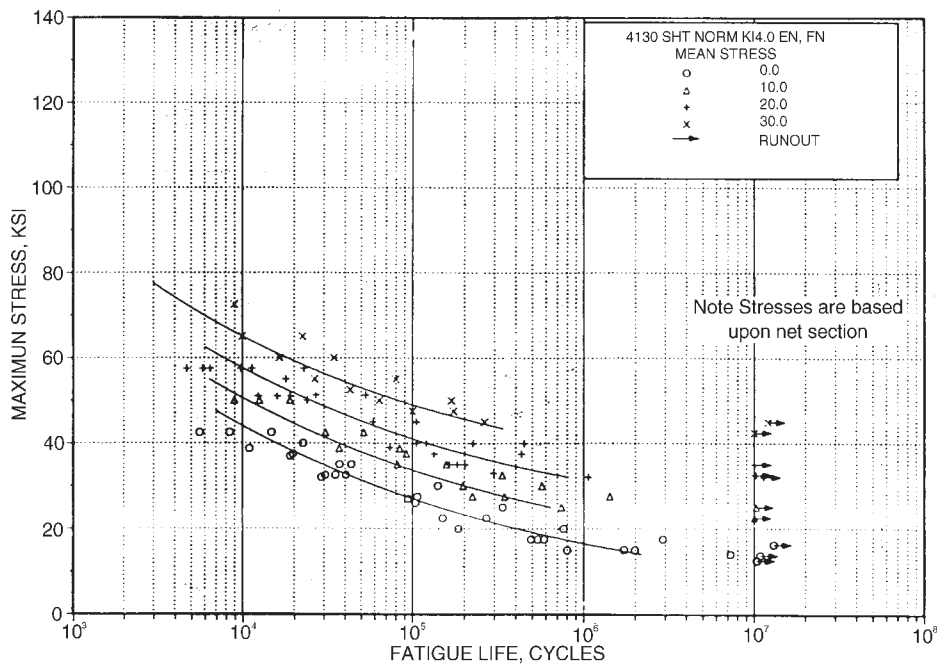


Figure 21 Best-fit S-N curves for notched 4130 alloy steel sheet,  $K_t = 4.0$ . (From Ref. 11. Courtesy of U.S. Dept. of Defense, Naval Publications and Forms Center.)

Historically, the plot of alternating stress amplitude  $\sigma_a$  versus mean stress  $\sigma_m$  has been the object of numerous empirical curve-fitting attempts. The more successful attempts have resulted in four different relationships:

1. Goodman's linear relationship
2. Gerber's parabolic relationship
3. Soderberg's linear relationship
4. The elliptic relationship

A modified form of the Goodman relationship is recommended for general use under conditions of high-cycle fatigue. For tensile mean stress ( $\sigma_m > 0$ ), this relationship may be written

$$\frac{\sigma_a}{\sigma_N} + \frac{\sigma_m}{\sigma_u} = 1 \quad (15)$$

where  $\sigma_u$  is the material ultimate strength, and  $\sigma_N$  is the zero mean stress fatigue strength for a given number of cycles  $N$ . For a given alternating stress, compressive mean stresses ( $\sigma_m < 0$ ) have been empirically observed to increase fatigue resistance. However, for conservatism, it is typically assumed that compressive mean stress exerts no influence on fatigue life.

Thus, for  $\sigma_m < 0$ , the fatigue response is identical to that for  $\sigma_m = 0$  with  $\sigma_a = \sigma_N$ . The modified Goodman relationship is illustrated in Fig. 22. This curve is a failure locus for the case of *uniaxial* fatigue stressing. Any cyclic loading that produces an alternating stress and mean stress that exceeds the bounds of the locus will cause failure in fewer than  $N$  cycles. Any alternating stress–mean stress combination that lies within the locus will result in more than  $N$  cycles without failure. Combinations on the locus produce failure in  $N$  cycles. The modified Goodman relationship shown in Fig. 22 considers fatigue failure exclusively.

The reader is cautioned to ensure that the maximum and minimum stresses produced by the cyclic loading do not exceed the material yield strength  $\sigma_{yp}$  such that failure by yielding would be predicted to occur.

### 5.3 Strain–Life Approach to Fatigue

An alternate approach to fatigue design is the strain–life methodology. The strain-based approach is applicable in situations when mechanical components are loaded under a known fluctuating strain range. Fatigue testing machines are capable of applying prescribed strain-controlled fatigue loads. For a component subjected to large plastic strain amplitudes, the fatigue life can be calculated using the Coffin–Manson<sup>27,28</sup> equation

$$\epsilon_a^p = \frac{\Delta \epsilon^p}{2} = \epsilon'_F (2N_f)^c \quad (16)$$

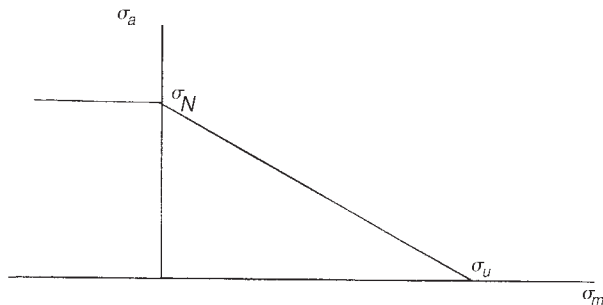


Figure 22 Modified Goodman relationship.

where  $\Delta\varepsilon^p$  is the plastic strain range,  $\varepsilon_a^p$  is the plastic strain amplitude, and  $2N_f$  is the number of load reversals to failure. The material parameters  $\varepsilon'_F$  and  $c$  are called the fatigue ductility coefficient and fatigue ductility exponent, respectively. Since plastic strain amplitudes are quite large for the range of applicability of Eq. (16), the ensuing fatigue life is short (i.e., low-cycle fatigue). In situations where the total applied strain range is given, the number of cycles to failure  $N_f$  can be computed by expanding the above strain-life equation to include the low-cycle fatigue regime. The total strain can be decomposed into its elastic and plastic components either in terms of amplitude or range,

$$\varepsilon_a = \varepsilon_a^e + \varepsilon_a^p = \frac{\Delta\varepsilon^e + \Delta\varepsilon^p}{2} \quad (17)$$

where  $\Delta\varepsilon^e$  is the elastic strain range. By combining Eqs. (14) and (15), one obtains the widely used strain-life equation

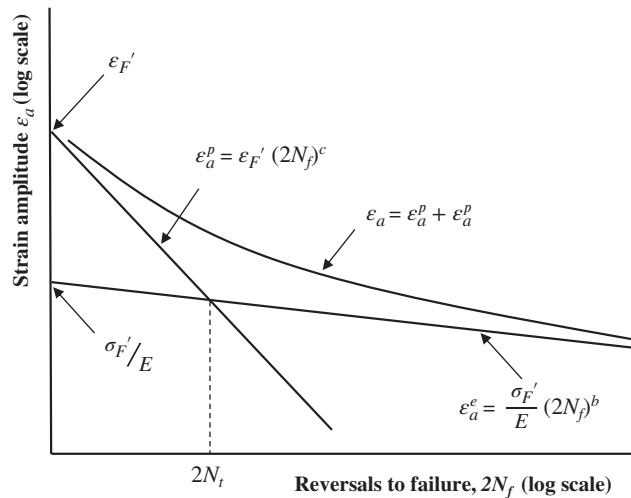
$$\varepsilon_a = \frac{\Delta\varepsilon}{2} = \frac{\sigma'_F}{E}(2N_f)^b + \varepsilon'_F(2N_f)^c \quad (18)$$

Figure 23 shows the superposition of Eqs. (14) and (16) on a log-log strain-life plot. The transition life  $N_t$  between the low-cycle and high-cycle fatigue regimes is easily obtained as the intersection point between the two straight lines, and can be calculated as

$$N_t = \frac{1}{2} \left( \frac{\sigma'_F}{E\varepsilon'_F} \right)^{1/b-c} \quad (19)$$

Klesnil and Lukáš<sup>29</sup> cited several studies performed on steels, aluminum alloys, and nickel alloys and focused on the relationship between the fatigue ductility coefficient  $\varepsilon'_F$  and the true fracture strain under monotonic loading  $\varepsilon_F$ . Depending on the material tested, the relation between the two properties was found as  $\varepsilon'_F = k\varepsilon_F$  where  $k$  is a material constant.

In situations when fatigue constants in Eq. (18) are lacking, the universal slope method originally proposed by Manson<sup>30</sup> can be employed to produce strain-life predictions. This method assumed that the two straight lines in Fig. 23 have the same slope for all materials. Then, one only needs to know the monotonic tensile test data  $\sigma_{ut}$ ,  $\varepsilon_f$  and  $E$  for a particular material, and also the values of  $b$  and  $c$ . The original method of universal slopes was later



**Figure 23** Strain-life diagram illustrating the combined effect of the elastic and plastic strain amplitudes on the fatigue life.



modified by Muralidharan and Manson,<sup>31</sup> and they expressed the strain–life equation as

$$\Delta \epsilon = 1.17 \left( \frac{\sigma_{ut}}{E} \right)^{0.832} N_f^{-0.09} + 0.0266 \epsilon_f^{0.155} \left( \frac{\sigma_{ut}}{E} \right)^{-0.53} N_f^{-0.56} \quad (20)$$

Other methods for the estimation of fatigue properties from known data from monotonic tensile tests include the fictive stress method,<sup>32</sup> the uniform material law method,<sup>33</sup> and the four-point correlation method.<sup>30,34</sup> A review of some of these methods along with an analysis of their accuracy on 138 metallic alloys was performed by Park and Song.<sup>35</sup>

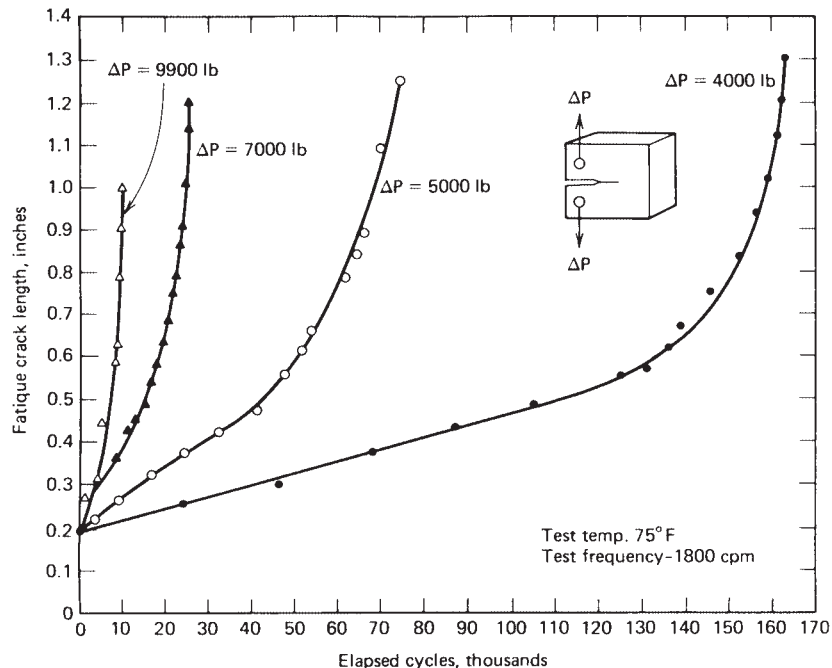
## 5.4 Fatigue Crack Propagation

A fatigue crack that has been initiated by cyclic loading, or any other pre-existing flaw in the structure or material, may be expected to grow under sustained cyclic loading until it reaches the critical size from which it will propagate rapidly to catastrophic failure in accordance with the principles of fracture mechanics. For many structures or machine elements, the time required for a fatigue-initiated crack or a pre-existing flaw to grow to critical size is a significant portion of the total life.

The fatigue crack growth rate  $da/dN$  has been found to often correlate with the crack-tip stress intensity factor range such that

$$\frac{da}{dN} = f(\Delta K) \quad (21)$$

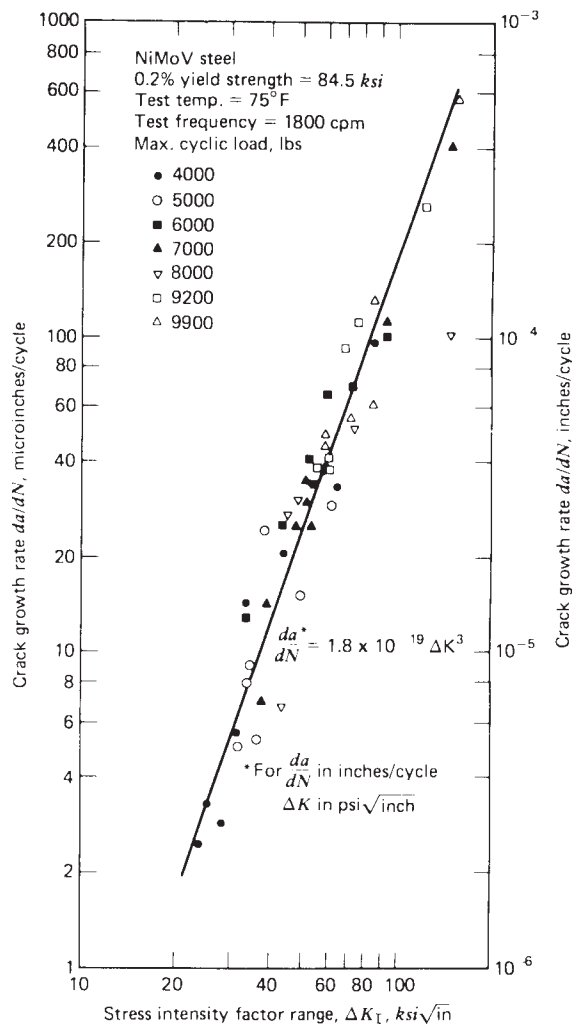
where  $a$  is the crack length,  $N$  is the number of cycles,  $f$  is a function of the stress intensity factor range  $\Delta K$ , computed using the maximum and minimum applied stresses with  $\Delta K = K_{\max} - K_{\min}$ . Most crack growth rate data produced have been characterized in terms of  $\Delta K$ . For example, Fig. 24 illustrates indirectly the dependence of fatigue crack growth on the



**Figure 24** Effect of cyclic-load range on crack growth in Ni–Mo–V alloy steel for released tension loading. (From Ref. 36. Reprinted with permission of the Society for Experimental Mechanics, www.sem.org.)

stress intensity factor. The crack growth rate, indicated by the slope of the  $a$ -versus- $N$  curves, increases with both the applied load and crack length. Since the crack-tip stress intensity factor range also increases with applied load and crack length, it is clear that the crack growth rate is related to the applied stress intensity factor range.

To plot the data of Fig. 24 in terms of the stress intensity factor range and crack growth rate, the crack growth rate is estimated from a numerically determined slope of the  $a$ -versus- $N$  curves between successive data points. Corresponding values of  $\Delta K$  are then computed from the applied load range and mean crack length for each interval. The results of this procedure are shown in Fig. 25 for the data presented in Fig. 24. It should be noted that all the curves of Fig. 24 are incorporated into the single curve shown in Fig. 25 through use of the stress intensity factor, and the curve of Fig. 25 is therefore applicable to any combination of cyclic stress range and crack length for released loading ( $R = 0$ ) on specimens of this geometry. Different geometries under different applied stresses will exhibit identical crack-tip stress fields if the stress intensity



**Figure 25** Crack growth rate as a function of stress-intensity range for Ni-Mo-V steel. (From Ref 36. Reprinted with permission of the Society for Experimental Mechanics, www.sem.org.)

factors are equal. Thus, because the stress intensity factor characterizes the state of stress near the crack tip, the fatigue crack growth rate correlation shown in Fig. 25 is applicable to any cyclically loaded component with  $R = 0$  manufactured using the same material. This allows crack growth data generated from simple laboratory specimens to be utilized for approximate crack growth predictions in more complex geometries.

Fatigue crack growth rate data similar to that shown in Fig. 25 have been reported for a wide variety of engineering metals. The linear behavior observed using log-log coordinates suggests that Eq. (21) may be generalized as follows:

$$\frac{da}{dN} = C\Delta K^n \quad (22)$$

where  $n$  is the slope of the plot of  $\log da/dN$  versus  $\log \Delta K$  and  $C$  is the  $da/dN$  value found by extending the straight line to a  $\Delta K$  value of unity. This relationship was first proposed by Paris and Erdogan.<sup>37</sup> The empirical parameters  $C$  and  $n$  are a function of material,  $R$  ratio, thickness, temperature, environment, and loading frequency.

Standard methods have been established for conducting fatigue crack growth tests,<sup>38</sup> and fatigue crack growth rate data may be found in Refs. 10, 11, and 13–16. Many other fracture mechanics–based empirical correlations other than Eq. (22) have been proposed, some of which are discussed by Schijve.<sup>39</sup> An extensive overview of the fatigue crack propagation problem is provided by Pook.<sup>40</sup>

Given an initial crack of length  $a_i$ , Eq. (22) may be integrated to give the number of cycles  $N$  required to propagate a crack to a size  $a_N$  such that

$$N = \int_{a_i}^{a_f} \frac{da}{C\Delta K^n} \quad (23)$$

Given that  $\Delta K$  is a function of crack length  $a$ , numerical integration techniques will in general be required to compute  $N$ . An approximate procedure and several idealized examples are presented by Parker.<sup>7</sup>

It must be emphasized that Eqs. (22) and (23) are applicable only to region II crack growth, as illustrated in Fig. 26. Region I of Fig. 26 exhibits a threshold  $\Delta K_{th}$  below which the crack will not propagate. Region III corresponds to the transition into the unstable regime of rapid crack extension. In this region, crack growth rates are large and the number of cycles associated with growth in this region is small.

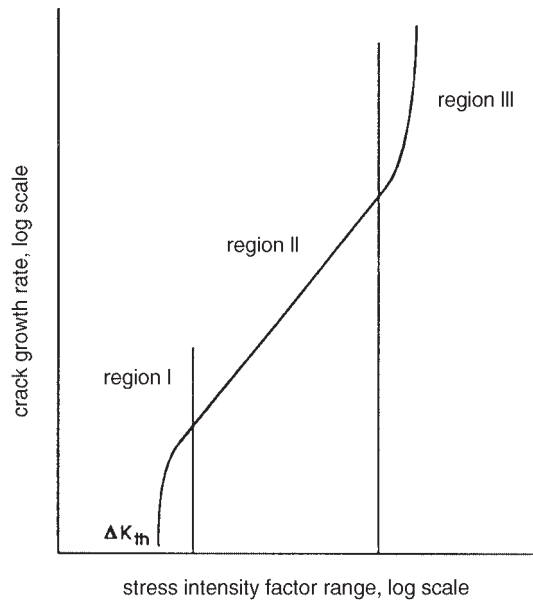
With an initial crack of length  $a_i$ , from Eq. (23), the number of cycles required to grow a crack to a critical length  $a_c$  such that rapid crack extension would be predicted may be approximated as

$$N_p = \int_{a_i}^{a_c} \frac{da}{C\Delta K^n} \quad (24)$$

Assuming an initial crack that has been initiated by cyclic loading, the crack propagation life  $N_p$  given by Eq. (24) may then be added to the crack initiation life  $N_i$  to obtain an estimate of the total fatigue life  $N$  with

$$N = N_i + N_p \quad (25)$$

Such estimates are highly sensitive to the length of the initial crack  $a_i$ . While the local stress–strain approach<sup>1,41</sup> may be used to compute the number of cycles  $N_i$  required to initiate a crack, the corresponding length of this initiated crack is not defined specifically. No consensus has yet been reached regarding the length of this initiated crack. A size of between 0.25 and 5.0 mm has been suggested,<sup>41</sup> as cracks of this size normally exist at fracture in the small laboratory specimens used to generate the strain-versus-cycles-to-failure data required for the local stress–strain approach. An alternative approach would involve the assumption of a pre-existing material or manufacturing defect such that  $N_i = 0$ . For example, such an assumption is often made during the analysis of welded joints.<sup>42</sup> If nondestructive techniques are employed, a



**Figure 26** Schematic representation of fatigue crack growth rate data.

reasonable assumption for the size of this initial defect would be the largest flaw that could avoid detection.

Crack growth rates determined from constant-amplitude cyclic loading tests are approximately the same as for random loading tests in which the maximum stress is held constant but mean and range of stress vary randomly. However, in random loading tests where the maximum stress is also allowed to vary, the sequence of loading cycles may have a marked effect on crack growth rate, with the overall crack growth being significantly higher for random loading spectra.

Many investigations have shown a significant delay in crack propagation following intermittent application of high stresses. That is, fatigue damage and crack extension are dependent on preceding cyclic load history. This dependence of crack extension on preceding history and the effects upon future damage increments are referred to as *interaction* effects. Most of the interaction studies conducted have dealt with *retardation* of crack growth as a result of the application of occasional tensile overload cycles. Retardation may be characterized as a period of reduced crack growth rate following the application of a peak load or loads higher and in the same direction as those peaks that follow.

The modeling of interaction effects requires consideration of crack-tip plasticity and its subsequent influence. In metals of all types, cracks will remain closed or partially closed for a portion of the applied cyclic load as a consequence of plastically deformed material left in the wake of the growing crack. Under cyclic loading, crack growth will occur during the loading portion of the cycle. Given that a plastic zone exists at the crack tip prior to crack extension, as the material at the crack tip separates, the newly formed crack surfaces will exhibit a layer of plastically deformed material along the newly formed crack faces. Subsequent unloading will compress this plastically deformed material, closing the crack while the applied stress remains tensile. This phenomenon is known as plasticity-induced fatigue crack closure and was first discussed by Elber.<sup>43</sup> Upon reloading during the following cycle, crack growth will not continue unless the applied load is sufficiently large such that the compressive stresses acting

along the crack surfaces are overcome and the crack is fully opened. This load is known as the crack opening load and has been demonstrated to be a key parameter in determining fatigue crack growth rates under both constant amplitude and spectrum loading. Further information regarding crack closure may be found in Refs. 1, 4, 17, 39, and 44.

Discussion to this point has been limited to the growth of through-thickness cracks under mode I loading. While mode I loading is often dominant, under the most general circumstances the applied cyclic loads will generate stress intensity factor ranges  $\Delta K_I$ ,  $\Delta K_{II}$ , and  $\Delta K_{III}$  at the crack tip, and *mixed-mode* fatigue crack growth must be considered. Modeling methodologies for mixed-mode fatigue crack growth are discussed in Refs. 7 and 45. In addition, fatigue cracks in machine elements and structures are often not through-thickness cracks but rather surface cracks that extend partially through the thickness.

Such surface cracks are often semielliptical in shape and the analysis of these cracks is considerably more complicated. Information regarding surface cracks may be found in Refs. 4 and 46.

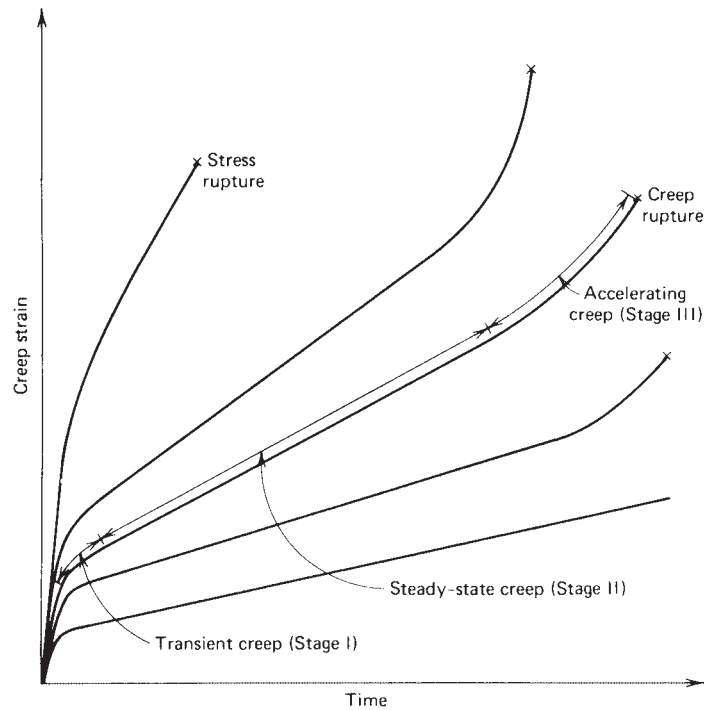
Research has suggested that when fatigue cracks are small, crack growth rates are larger than would be predicted using Eq. (22) for a given  $\Delta K$ .<sup>47</sup> Small-crack behavior is often important, as a significant portion of the fatigue life may be spent in the small-crack regime.

The fatigue crack propagation life  $N_p$  will also be influenced by the presence of residual stresses such as might exist as a consequence of welding, heat treatment, carburizing, grinding, or shot peening. Compressive residual stresses are beneficial, decreasing the rate of fatigue crack growth and increasing propagation life. While approximate methodologies exist for incorporating the effects of residual stress within fatigue crack growth predictions,<sup>7</sup> residual stress distributions are often difficult to characterize.

Reasonable design estimates for the fatigue crack propagation life may be obtained using Eq. (24). However, the many uncertainties typically associated with fatigue life predictions emphasize the essential requirement to conduct full-scale fatigue tests to provide acceptable reliability.

## 6 CREEP AND STRESS RUPTURE

Structural components in steam and gas turbines, coal-fired or gas-fired power plants, reactor internals or pressure vessels are loaded at high temperatures with constant or variable stresses. The combination of elevated temperature and stress creates the condition for creep deformation and fracture. In its simplest form, *creep* is the progressive accumulation of plastic strain in a specimen or machine part under stress at elevated temperature over a period of time. Creep failure occurs when the accumulated creep strain results in a deformation of the machine part that exceeds the design limits. *Creep rupture* is an extension of the creep process to the limiting condition where the stressed member actually separates into two parts. *Stress rupture* is a term used interchangeably by many with creep rupture; however, others reserve the term stress rupture for the rupture termination of a creep process in which steady-state creep is never reached and use the term creep rupture for the rupture termination of a creep process in which a period of steady-state creep has persisted. Figure 27 illustrates a typical creep process, which is divided in three stages. An initial instantaneous elastic loading is followed by the primary stage I in which the creep strain rate decreases with increasing deformation or time. The secondary stage II creep is a steady-state phase in which the rate of deformation, i.e., the slope of the strain versus time curve, is constant. In a creep process driven by dislocation climb or glide, the constant strain rate is the result of a balance between the generation and annihilation of dislocations. Stage II records the minimum deformation strain during the entire creep process. In stage III, the creep rate increases rapidly as a result of crack and/or void nucleation and growth. This stage eventually leads to rupture or failure.



**Figure 27** Illustration of creep and stress rupture.

Creep strains of engineering significance are not usually encountered until the operating temperatures reach a range of approximately 35–70% of the melting temperature  $T_m$  (in Kelvins). The approximate melting temperature for several substances is shown in Table 2.

Not only is excessive deformation due to creep an important consideration, but other consequences of the creep process may also be important. These might include creep rupture, thermal relaxation, dynamic creep under cyclic loads or cyclic temperatures, creep and rupture under multiaxial states of stress, cumulative creep effects, and effects of combined creep and fatigue.

## 6.1 Basic Mechanisms of Creep Deformation

Creep deformation and rupture are initiated in the grain boundaries and proceed by sliding and separation. Thus, creep failures are intercrystalline, in contrast, for example, to the transcrystalline failure surface exhibited by room temperature fatigue failures. Diffusion plays a major role in creep deformation. It has been observed that the activation energies for diffusion and creep are similar for a large number of metals,<sup>49</sup> and diffusion is significant in creep deformation for wide ranges of temperature and stress.

Several mechanisms can cause creep deformation, depending on temperature and stress. In metals, creep deformation can be caused by vacancy diffusion, dislocation climb and/or glide, and grain boundary sliding. For temperatures below  $0.5T_m$ , the diffusion occurs along dislocations as opposed to bulk diffusion. This phenomenon is called pipe diffusion. For temperatures above  $0.5T_m$ , the creep mechanism can operate either at the boundary or in the crystalline lattice,

**Table 2** Melting Temperatures<sup>48</sup>

Material	°F	°C
Hafnium carbide	7030	3887
Graphite (sublimes)	6330	3500
Tungsten	6100	3370
Tungsten carbide	5190	2867
Magnesia	5070	2800
Molybdenum	4740	2620
Boron	4170	2300
Titanium	3260	1795
Platinum	3180	1750
Silica	3140	1728
Chromium	3000	1650
Iron	2800	1540
Stainless steels	2640	1450
Steel	2550	1400
Aluminum alloys	1220	660
Magnesium alloys	1200	650
Lead alloys	605	320

depending on the stress level.<sup>50</sup> Between  $0.7$  and  $0.8T_m$  the difference between the secondary creep activation energy and the bulk diffusion activation energy decreases significantly.<sup>51</sup>

*Diffusion creep* occurs at low stresses and high temperatures. In diffusion-controlled creep, the strain rate is linearly proportional to stress, thus in a typical creep strain rate equation  $\dot{\epsilon} \propto \sigma^n$ , where the creep exponent is  $n = 1$ . It has been observed that creep deformation by vacancy diffusion occurs in three distinct ways: the Nabarro–Herring creep,<sup>52,53</sup> Cobble creep,<sup>54</sup> or the Harper–Dorn creep.<sup>55</sup>

*Nabarro–Herring creep* is a bulk diffusion process in which the flux of vacancies is directed from the source grain boundaries oriented perpendicularly to the loading direction toward sink grain boundaries oriented perpendicularly to that direction. The atoms migrate in the direction opposed to that of vacancies, thus leading to an increase in the grain length parallel to the loading direction, and decrease of length in a direction perpendicular to the loading direction. The migration of vacancies and atoms is through the bulk of the lattice. Consequently, the grain elongates in the loading direction, proportionally with the influx of vacancies, given by the number of vacancies and the volume of each vacancy. The elongation of the grain with time results in the macroscopically observed creep rate.

*Cobble creep* is a boundary diffusion process, which also results in grain boundary sliding. In this case, vacancies migrate along grain boundaries. With increasing temperature, the ratio of Cobble to Nabarro–Herring creep increases because the activation energy for boundary-controlled creep is lower than that for lattice-controlled creep.

*Harper–Dorn creep* is activated by dislocation climb facilitated by vacancy diffusion. Under compressive or tensile applied stresses, vacancies can migrate to a dislocation line, and cause it to move up or down, perpendicularly to its Burgers vector.

The grain size dictates which of the *Nabarro–Herring* or *Cobble* creep mechanisms become operative. In the case of *Harper–Dorn creep*, the grain boundaries and grain size are not influential in determining the creep process, thus they become irrelevant. This mechanism is more likely to dominate in materials with large grain sizes. In materials with small grains, the predominance of grain boundaries facilitates the activation of the other two diffusion-based creep mechanisms.<sup>50</sup>

*Dislocation creep* is activated at intermediate and elevated stresses. Creep deformation is caused by dislocation climb or glide. At intermediate stresses, vacancy diffusion can aid dislocations climb over obstacles, according to a mechanism proposed by Weertman.<sup>56</sup> At higher stress levels than those that activate dislocation climb, the creep deformation manifests itself predominantly by dislocation glide, without facilitation from vacancy diffusion. The rate of deformation in a dislocation creep is given by the balance between hardening and recovery, i.e., between the generation and annihilation of dislocations.

*Grain boundary sliding* is a creep mechanism that involves the relative sliding of grains against each other.

## 6.2 Prediction of Long-Term Creep Behavior

Much time and effort has been expended in attempting to develop good short-time creep tests for accurate and reliable prediction of long-term creep and stress rupture behavior. It appears, however, that really reliable creep data can be obtained only by conducting long-term creep tests that duplicate actual service loading and temperature conditions as nearly as possible. Unfortunately, designers are unable to wait for years to obtain design data needed in creep failure analysis. Therefore, certain useful techniques have been developed for approximating long-term creep behavior based on a series of short-term tests. Data from creep testing may be plotted in a variety of different ways. The basic variables involved are stress, strain, time, temperature, and, perhaps, strain rate. Any two of these basic variables may be selected as plotting coordinates, with the remaining variables treated as parametric constants for a given curve. Three commonly used methods for extrapolating short-time creep data to long-term applications are the abridged method, the mechanical acceleration method, and the thermal acceleration method. In the abridged method of creep testing the tests are conducted at several different stress levels and at the contemplated operating temperature. The data are plotted as creep strain versus time for a family of stress levels, all run at constant temperature. The curves are plotted out to the laboratory test duration and then extrapolated to the required design life. In the mechanical acceleration method of creep testing, the stress levels used in the laboratory tests are significantly higher than the contemplated design stress levels, so the limiting design strains are reached in a much shorter time than in actual service. The data taken in the mechanical acceleration method are plotted as stress level versus time for a family of constant-strain curves all run at a constant temperature. The thermal acceleration method involves laboratory testing at temperatures much higher than the actual service temperature expected. The data are plotted as stress versus time for a family of constant temperatures where the creep strain produced is constant for the whole plot.

It is important to recognize that such extrapolations are not able to predict the potential of failure by creep rupture prior to reaching the creep design life. In any testing method it should be noted that creep-testing guidelines usually dictate that test periods of less than 1% of the expected life are not deemed to give significant results. Tests extending to at least 10% of the expected life are preferred where feasible.

Several different theories have been proposed to correlate the results of short-time elevated-temperature tests with long-term service performance at more moderate temperatures. One of the more accurate and useful of these proposals is the Larson–Miller theory.

The Larson–Miller theory<sup>57</sup> postulates that for each combination of material and stress level there exists a unique value of a parameter  $P$  that is related to temperature and time by the equation

$$P = (\theta + 460)(C + \log_{10}t) \quad (26)$$



where  $P$  = Larson–Miller parameter, constant for a given material and stress level  
 $\theta$  = temperature, °F  
 $C$  = constant, usually assumed to be 20  
 $t$  = time in hours to rupture or to reach a specified value of creep strain

This equation was investigated for both creep and rupture for some 28 different materials by Larson and Miller with good success. By using Eq. (26) it is a simple matter to find a short-term combination of temperature and time that is equivalent to any desired long-term service requirement. For example, for any given material at a specified stress level the test conditions listed in Table 3 should be equivalent to the operating conditions.

### 6.3 Creep under a Uniaxial State of Stress

Many relationships have been proposed to relate stress, strain, time, and temperature in the creep process. If one investigates experimental creep–strain-versus-time data, it will be observed that the data are close to linear for a wide variety of materials when plotted on log strain–log time coordinates. Such a plot is shown, for example, in Fig. 28 for three different materials. An equation describing this type of behavior is

$$\epsilon^{cr} = At^a \quad (27)$$

where  $\epsilon^{cr}$  = true creep strain

$t$  = time

$A, a$  = empirical constants

Differentiating Eq. (27) with respect to time gives

$$\dot{\epsilon}^{cr} = Aat^{a-1} \quad (28)$$

or, setting  $aA = b$  and  $1 - a = n$ ,

$$\dot{\epsilon}^{cr} = bt^{-n} \quad (29)$$

This equation represents a variety of different types of creep–strain-versus-time curves, depending on the magnitude of the exponent  $n$ . If  $n$  is zero, the behavior, characteristic of high temperatures, is termed *constant creep rate*, and the creep strain is given as

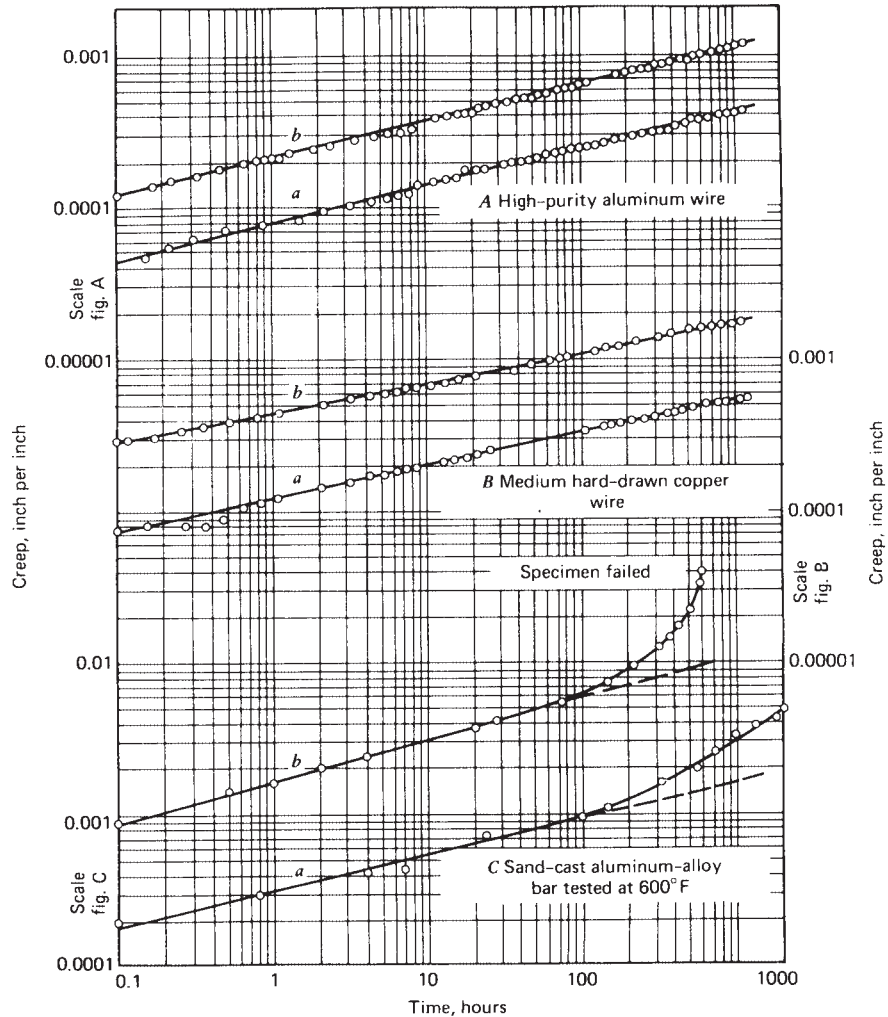
$$\epsilon^{cr} = b_1t + C_1 \quad (30)$$

If  $n$  lies between 0 and 1, the behavior is termed *parabolic creep*, and the creep strain is given by

$$\epsilon^{cr} = b_3t^m + C_3 \quad (31)$$

**Table 3** Equivalent Conditions Based on Larson–Miller Parameter

Operating Condition	Equivalent Test Condition
10,000 h at 1000°F	13 h at 1200°F
1,000 h at 1200°F	12 h at 1350°F
1,000 h at 1350°F	12 h at 1500°F
1,000 h at 300°F	2.2 h at 400°F



**Figure 28** Creep curves for three materials. (From Ref. 60. Reprinted with permission of John Wiley & Sons.)

This type of creep behavior occurs at intermediate and high temperatures. The coefficient  $b_3$  increases exponentially with stress and temperature, and the exponent  $m$  decreases with stress and increases with temperature. The influence of stress level  $\sigma$  on creep rate can often be represented by the empirical expression

$$\dot{\epsilon}^{\text{cr}} = b\sigma^N \quad (32)$$

A time-hardening equation of the creep strain rate is obtained by taking the time derivative in Eq. (31). On the other hand, a strain-hardening equation is an equation in which the creep strain rate is a function of accumulated strain.<sup>58</sup>

Assuming the stress  $\sigma$  to be independent of time, we may integrate Eq. (32) to yield the creep strain

$$\epsilon^{\text{cr}} = Bt\sigma^N + C' \quad (33)$$

If the constant  $C'$  is small compared with  $Bt\sigma^N$ , as it often is, the result is called the *log-log stress-time creep law*, given as

$$\epsilon^{\text{cr}} = Bt\sigma^N \quad (34)$$

As long as the instantaneous deformation on load application and the stage I transient creep are small compared to stage II steady-state creep, Eq. (34) is useful as a design tool.

If it is necessary to consider all stages of the creep process, the creep strain expression becomes much more complex. The most general expression for the creep process is<sup>59</sup>

$$\epsilon^{\text{cr}} = \frac{\sigma}{E} + k_1\sigma^m + k_2(1 - e^{-qt})\sigma^n + k_3t\sigma^p \quad (35)$$

where  $\delta$  = total creep strain  
 $\sigma/E$  = initial elastic strain  
 $k_1\sigma^m$  = initial plastic strain  
 $k_2(1 - e^{-qt})\sigma^n$  = anelastic strain  
 $k_3t\sigma^p$  = viscous strain  
 $\sigma$  = stress  
 $E$  = modulus of elasticity  
 $m$  = reciprocal of strain-hardening exponent  
 $k_1$  = reciprocal of strength coefficient  
 $q$  = reciprocal of Kelvin retardation time  
 $k_2$  = anelastic coefficient  
 $n$  = empirical exponent  
 $k_3$  = viscous coefficient  
 $p$  = empirical exponent  
 $t$  = time

To utilize this empirical nonlinear expression in a design environment requires specific knowledge of the constants and exponents that characterize the material and temperature of the application. In all cases it must be recognized that stress rupture may intervene to terminate the creep process, and the prediction of this occurrence is difficult.

## 6.4 Creep under a Multiaxial State of Stress

Oftentimes, components operating at elevated temperatures are loaded under a multiaxial state of stress. Let  $\sigma_{ij}$  be such a stress state in three dimensions, with  $i, j = 1, 2, 3$ . Creep deformation is a volume preserving deformation, that is

$$\dot{\epsilon}_1^{\text{cr}} + \dot{\epsilon}_2^{\text{cr}} + \dot{\epsilon}_3^{\text{cr}} = 0 \quad (36)$$

Moreover, it has been observed that the principal shear strain rates are proportional to the shear stresses during creep<sup>61,62</sup>

$$\frac{\dot{\gamma}_1}{\tau_1} + \frac{\dot{\gamma}_2}{\tau_2} + \frac{\dot{\gamma}_3}{\tau_3} = 0 \quad (37)$$

where  $\dot{\gamma}$  = shear strain rate  
 $\tau$  = shear stress

A common approach to modeling creep under multiaxial stresses is by using the formulation of classical plasticity theory based upon the von Mises yield function, or  $J_2$  potential.<sup>63</sup> In this model, the creep strains are proportional with the deviatoric stresses, as expressed in the flow rule for creep deformation:

$$\dot{\epsilon}_{ij}^{\text{cr}} = \lambda S_{ij} \quad (38)$$

where  $\dot{\epsilon}_{ij}^{\text{cr}} = ij$  component of the creep strain rate tensor  
 $\lambda =$  material constant  
 $S_{ij} = ij$  component of deviatoric stress tensor

The deviatoric stresses are computed with the equation

$$S_{ij} = \sigma_{ij} - \sigma_m \delta_{ij} \quad (39)$$

where  $\sigma_m = (\sigma_{11} + \sigma_{22} + \sigma_{33})/3$  is the hydrostatic stress  
 $\delta_{ij} =$  Kronecker delta function, equal to one for  $i = j$ , and zero for  $i \neq j$

According to the von Mises theory, the equivalent strain rate is defined as

$$\dot{\bar{\epsilon}}^{\text{cr}} = \frac{\sqrt{2}}{3} \{ (\dot{\epsilon}_{11}^{\text{cr}} - \dot{\epsilon}_{22}^{\text{cr}})^2 + (\dot{\epsilon}_{22}^{\text{cr}} - \dot{\epsilon}_{33}^{\text{cr}})^2 + (\dot{\epsilon}_{11}^{\text{cr}} - \dot{\epsilon}_{33}^{\text{cr}})^2 + 6 [(\dot{\epsilon}_{12}^{\text{cr}})^2 + (\dot{\epsilon}_{23}^{\text{cr}})^2 + (\dot{\epsilon}_{13}^{\text{cr}})^2] \}^{1/2} \quad (40)$$

where  $\dot{\bar{\epsilon}}^{\text{cr}}$  is the equivalent strain rate. Substituting Eq. (38) into Eq. (40), the equivalent creep strain rate is obtained as

$$\dot{\bar{\epsilon}}^{\text{cr}} = \frac{\sqrt{2}}{3} \lambda \{ (S_{11} - S_{22})^2 + (S_{22} - S_{33})^2 + (S_{11} - S_{33})^2 + 6 [S_{11}^2 + S_{22}^2 + S_{33}^2] \}^{1/2} \quad (41)$$

The equivalent von Mises stress  $\bar{\sigma}$  is given as

$$\bar{\sigma} = \frac{1}{\sqrt{2}} \{ (S_{11} - S_{22})^2 + (S_{22} - S_{33})^2 + (S_{11} - S_{33})^2 + 6 [S_{11}^2 + S_{22}^2 + S_{33}^2] \}^{1/2} \quad (42)$$

Using the flow rule in Eq. (38) and Eqs. (41) and (42), the creep strain multiplier  $\lambda$  results in

$$\lambda = \frac{3\dot{\bar{\epsilon}}^{\text{cr}}}{2\bar{\sigma}} \quad (43)$$

## 6.5 Mechanisms of Creep–Fatigue Failure

Although creep is a plastic flow phenomenon, the intercrystalline failure path gives a rupture surface that has the appearance of brittle fracture. Creep rupture typically occurs without necking and without warning. Current state-of-the-art knowledge does not permit a reliable prediction of creep or stress rupture properties on a theoretical basis. Furthermore, there seems to be little or no correlation between the creep properties of a material and its room temperature mechanical properties. Therefore, test data and empirical methods of extending these data are relied on heavily for prediction of creep behavior under anticipated service conditions.

Metallurgical stability under long-time exposure to elevated temperatures is mandatory for good creep-resistant alloys. Prolonged time at elevated temperatures acts as a tempering process, and any improvement in properties originally gained by quenching may be lost. Resistance to oxidation and other corrosive media are also usually important attributes for a good creep-resistant alloy. Larger grain size may also be advantageous since this reduces the length of grain boundary, where much of the creep process resides.

The mechanisms of a creep failure depend on temperature. For instance, in stainless steels at temperatures up to  $0.3\text{--}0.4 T_m$ , creep failure is characterized by intergranular fracture caused by microcracks.<sup>64</sup> At median temperatures, between  $0.4\text{--}0.5 T_m$ , the fracture process has a transgranular aspect. Microcracks often originate at the interface between grains, and initially grow along a random path dictated by the microstructure. At higher temperatures, the failure occurs predominantly by ductile failure, characterized by nucleation, growth, and coalescence of intergranular voids or cavities. Cavity nucleation takes place at grain boundaries by several mechanisms:

1. From impurity particle decohesion or cracking
2. Dislocation pile-up breaking through grain boundaries
3. Grain boundary sliding, and the inability of the surrounding grains to accommodate such motion

While cavity nucleation was shown to occur predominantly during stages I and II creep, while their growth and coalescence leads to the tertiary stage III in which fracture occurs.<sup>65</sup> Cavity growth is classified in plasticity-induced, diffusion-controlled, or constrain-controlled growth. The dominant growth mechanism is by diffusion in the case of small cavities. With increasing size, the plastic deformation becomes the controlling mechanism. Stress level also plays a major role in determining the dominant growth mechanism. At high stresses, cavity growth is plasticity controlled, resulting in high creep rates and short rupture times. At low stresses, cavity growth is constraint controlled, resulting in low creep rates and long rupture times. At intermediate stresses cavity growth is diffusion controlled. Numerous models have been developed over the years for each of the mechanisms of cavity growth: plasticity controlled,<sup>66-68</sup> diffusion controlled<sup>69,70</sup> and cavity controlled.<sup>71-75</sup>

## 7 FRETTING AND WEAR

Fretting and wear share many common characteristics but, at the same time, are distinctly different in several ways. Basically, fretting action has, for many years, been defined as a combined mechanical and chemical action in which contacting surfaces of two solid bodies are pressed together by a normal force and are caused to execute oscillatory sliding relative motion, wherein the magnitude of normal force is great enough and the amplitude of the oscillatory sliding motion is small enough to significantly restrict the flow of fretting debris away from the originating site.<sup>76</sup> More recent definitions of fretting action have been broadened to include cases in which contacting surfaces periodically separate and then reengage as well as cases in which the fluctuating friction-induced surface tractions produce stress fields that may ultimately result in failure. The complexities of fretting action have been discussed by numerous investigators, who have postulated the combination of many mechanical, chemical, thermal, and other phenomena that interact to produce fretting. Among the postulated phenomena are plastic deformation caused by surface asperities plowing through each other, welding and tearing of contacting asperities, shear and rupture of asperities, friction-generated subsurface shearing stresses, dislodging of particles and corrosion products at the surfaces, chemical reactions, debris accumulation and entrapment, abrasive action, microcrack initiation, and surface delamination.<sup>77-92</sup>

Damage to machine parts due to fretting action may be manifested as corrosive surface damage due to fretting corrosion, loss of proper fit or change in dimensions due to fretting wear, or accelerated fatigue failure due to fretting fatigue. Typical sites of fretting damage include interference fits; bolted, keyed, splined, and riveted joints; points of contact between wires in wire ropes and flexible shafts; friction clamps; small-amplitude-of-oscillation bearings of all kinds; contacting surfaces between the leaves of leaf springs; and all other places where the conditions of fretting persist. Thus, the efficiency and reliability of the design and operation of a wide range of mechanical systems are related to the fretting phenomenon.

Wear may be defined as the undesired cumulative change in dimensions caused by the gradual removal of discrete particles from contacting surfaces in motion, due predominantly to mechanical action. It should be further recognized that corrosion often interacts with the wear process to change the character of the surfaces of wear particles through reaction with the environment. Wear is, in fact, not a single process but a number of different processes that may take place by themselves or in combination. It is generally accepted that there are at least five

major subcategories of wear (see p. 120 of Ref. 93; see also Ref. 94), including adhesive wear, abrasive wear, corrosive wear, surface fatigue wear, and deformation wear. In addition, the categories of fretting wear and impact wear<sup>89,95,96</sup> have been recognized by wear specialists. Erosion and cavitation are sometimes considered to be categories of wear as well. Each of these types of wear proceeds by a distinctly different physical process and must be separately considered, although the various subcategories may combine their influence either by shifting from one mode to another during different eras in the operational lifetime of a machine or by simultaneous activity of two or more different wear modes.

## 7.1 Fretting Phenomena

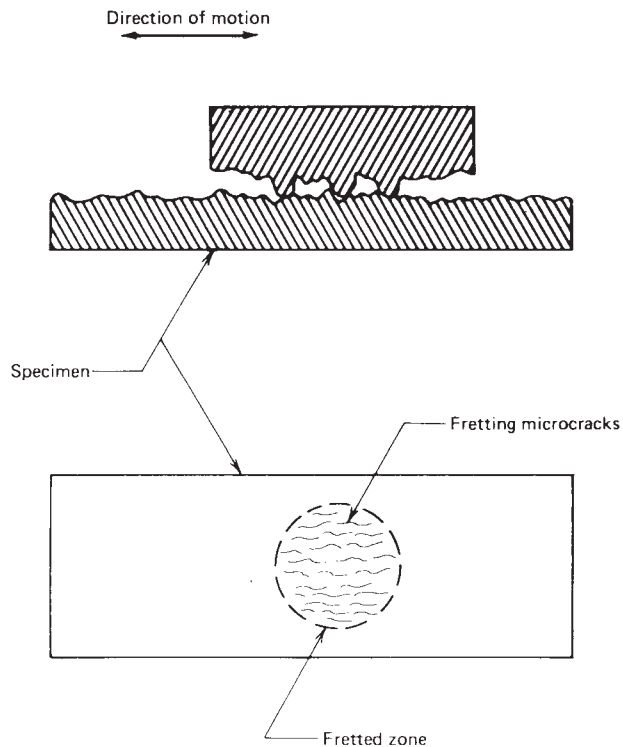
Although fretting fatigue, fretting wear, and fretting corrosion phenomena are potential failure modes in a wide variety of mechanical systems, and much research effort has been devoted to the understanding of the fretting process, there are very few quantitative design data available, and no generally applicable design procedure has been established for predicting failure under fretting conditions. However, even though the fretting phenomenon is not fully understood and a good general model for prediction of fretting fatigue or fretting wear has not yet been developed, significant progress has been made in establishing an understanding of fretting and the variables of importance in the fretting process. It has been suggested that there may be more than 50 variables that play some role in the fretting process.<sup>97</sup> Of these, however, there are probably only 8 that are of major importance:

1. The magnitude of relative motion between the fretting surfaces
2. The magnitude and distribution of pressure between the surfaces at the fretting interface
3. The state of stress, including magnitude, direction, and variation with respect to time in the region of the fretting surfaces
4. The number of fretting cycles accumulated
5. The material, and surface condition, from which each of the fretting members is fabricated
6. Cyclic frequency of relative motion between the two members being fretted
7. Temperature in the region of the two surfaces being fretted
8. Atmospheric environment surrounding the surfaces being fretted

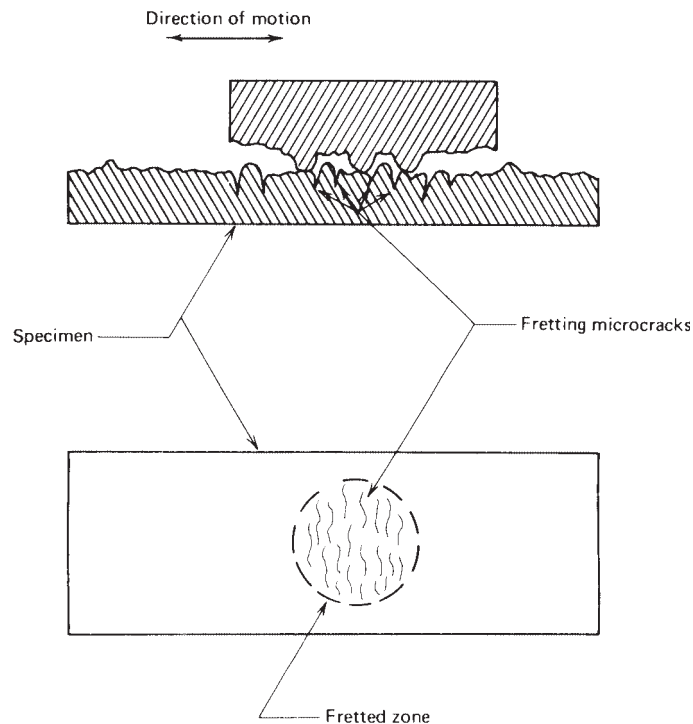
These variables interact so that a quantitative prediction of the influence of any given variable is very dependent on all the other variables in any specific application or test. Also, the combination of variables that produce a very serious consequence in terms of fretting fatigue damage may be quite different from the combinations of variables that produce serious fretting wear damage. No general techniques yet exist for quantitatively predicting the influence of the important variables of fretting fatigue and fretting wear damage, although many special cases have been investigated. However, it has been observed that certain trends usually exist when the variables just listed are changed. For example, fretting damage tends to increase with increasing contact pressure until a nominal pressure of a few thousand pounds per square inch is reached, and further increases in pressure seem to have relatively little direct effect. The state of stress is important, especially in fretting fatigue. Fretting damage accumulates with increasing numbers of cycles at widely different rates, depending on specific operating conditions. Fretting damage is strongly influenced by the material properties of the fretting pair surface hardness, roughness, and finish. No clear trends have been established regarding frequency effects on fretting damage, and although both temperature and atmospheric environment are important influencing factors, their influences have not been clearly established. A clear presentation relative to these various parameters is given in Ref. 89.

Fretting fatigue is fatigue damage directly attributable to fretting action. It has been suggested that premature fatigue nuclei may be generated by fretting through either abrasive pit-digging action, asperity-contact microcrack initiation,<sup>98</sup> friction-generated cyclic stresses that lead to the formation of microcracks,<sup>99</sup> or subsurface cyclic shear stresses that lead to surface delamination in the fretting zone.<sup>92</sup> Under the abrasive pit-digging hypothesis, it is conjectured that tiny grooves or elongated pits are produced at the fretting interface by the asperities and abrasive debris particles moving under the influence of oscillatory relative motion. A pattern of tiny grooves would be produced in the fretted region with their longitudinal axes all approximately parallel and in the direction of fretting motion, as shown schematically in Fig. 29.

The asperity-contact microcrack initiation mechanism is postulated to proceed due to the contact force between the tip of an asperity on one surface and another asperity on the mating surface as the surfaces move back and forth. If the initial contact does not shear one or the other asperity from its base, the repeated contacts at the tips of the asperities give rise to cyclic or fatigue stresses in the region at the base of each asperity. It has been estimated<sup>85</sup> that under such conditions the region at the base of each asperity is subjected to large local stresses that probably lead to the nucleation of fatigue microcracks at these sites. As shown schematically in Fig. 30, it would be expected that the asperity-contact mechanism would produce an array of microcracks whose longitudinal axes would be generally perpendicular to the direction of fretting motion.



**Figure 29** Idealized schematic illustration of the stress concentrations produced by the abrasive pit-digging mechanism.



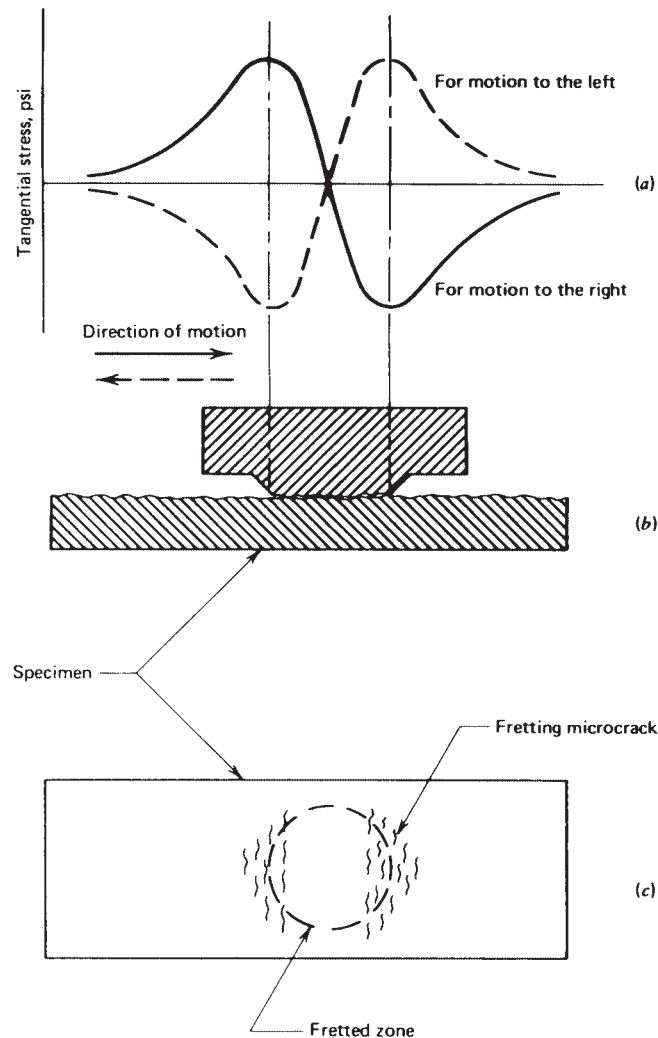
**Figure 30** Idealized schematic illustration of the stress concentrations produced by the asperity-contact microcrack initiation mechanism.

The friction-generated cyclic stress fretting hypothesis<sup>87</sup> is based on the observation that when one member is pressed against the other and caused to undergo fretting motion, the tractive friction force induces a compressive tangential stress component in a volume of material that lies ahead of the fretting motion and a tensile tangential stress component in a volume of material that lies behind the fretting motion, as shown in Fig. 31a. When the fretting direction is reversed, the tensile and compressive regions change places. Thus, the volume of material adjacent to the contact zone is subjected to a cyclic stress that is postulated to generate a field of microcracks at these sites. Furthermore, the geometrical stress concentration associated with the clamped joint may contribute to microcrack generation at these sites.<sup>88</sup> As shown in Fig. 31c, it would be expected that the friction-generated microcrack mechanism would produce an array of microcracks whose longitudinal axes would be generally perpendicular to the direction of fretting motion. These cracks would lie in a region adjacent to the fretting contact zone.

In the delamination theory of fretting<sup>92</sup> it is hypothesized that the combination of normal and tangential tractive forces transmitted through the asperity-contact sites at the fretting interface produces a complex multiaxial state of stress, accompanied by a cycling deformation field, which produces subsurface peak shearing stress and subsurface crack nucleation sites. With further cycling, the cracks propagate approximately parallel to the surface, as in the case of the surface fatigue phenomenon, finally propagating to the surface to produce a thin wear sheet, which “delaminates” to become a particle of debris.

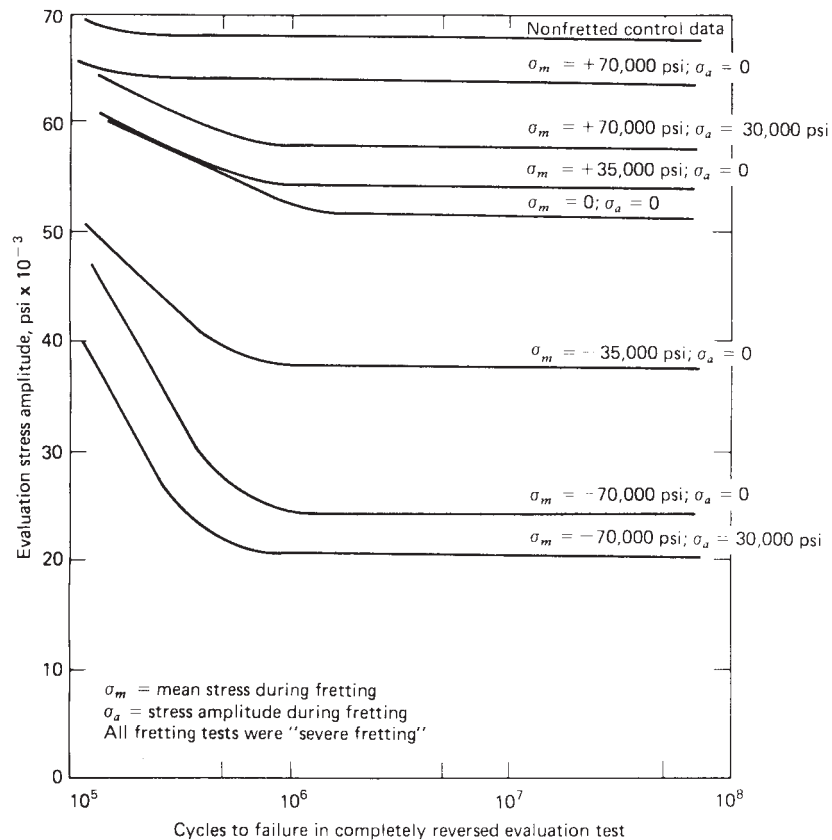
Supporting evidence has been generated to indicate that under various circumstances each of the four mechanisms is active and significant in producing fretting damage.





**Figure 31** Idealized schematic illustration of the tangential stress components and microcracks produced by the friction-generated microcrack initiation mechanism.

The influence of the state of stress in the member during the fretting is shown for several different cases in Fig. 32, including static tensile and compressive mean stresses during fretting. An interesting observation in Fig. 32 is that fretting under conditions of compressive mean stress, either static or cyclic, produces a drastic reduction in fatigue properties. This, at first, does not seem to be in keeping with the concept that compressive stresses are beneficial in fatigue loading. However, it was deduced<sup>100</sup> that the compressive stresses during fretting shown in Fig. 32 actually resulted in local residual tensile stresses in the fretted region. Likewise, the tensile stresses during fretting shown in Fig. 32 actually resulted in local residual compressive stresses in the fretted region. The conclusion, therefore, is that local compressive stresses are beneficial in minimizing fretting fatigue damage.

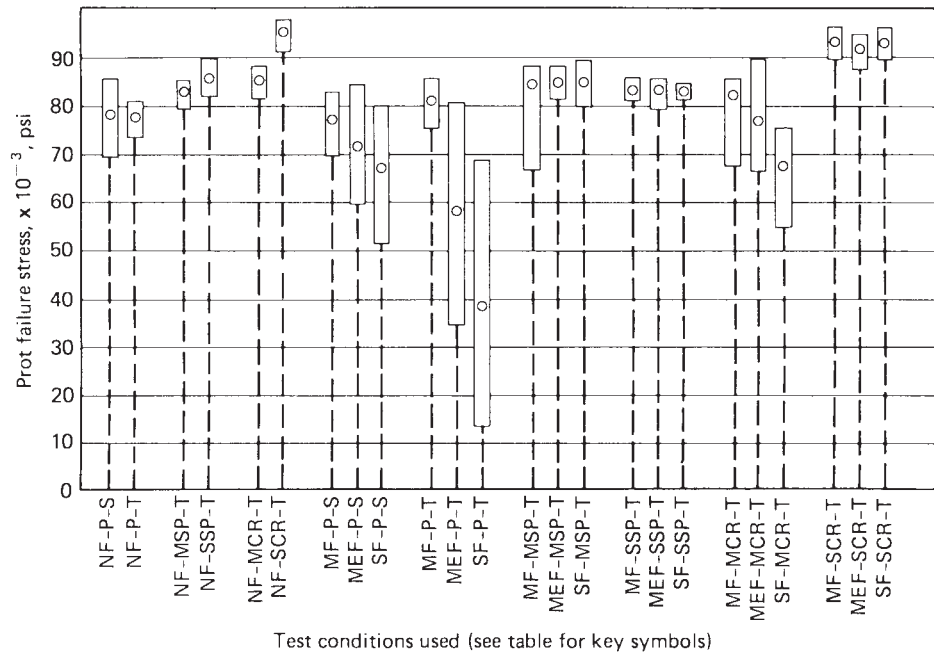


**Figure 32** Residual fatigue properties subsequent to fretting under various states of stress.

Further evidence of the beneficial effects of compressive residual stresses in minimizing fretting fatigue damage is illustrated in Fig. 33, where the results of a series of Prot (fatigue limit) tests are reported for steel and titanium specimens subjected to various combinations of shot peening and fretting or cold rolling and fretting. It is clear from these results that the residual compressive stresses produced by shot peening and cold rolling are effective in minimizing the fretting damage. The reduction in scatter of the fretted fatigue properties for titanium is especially important to a designer because design stress is closely related to the lower limit of the scatter band.

In the final analysis, it is necessary to evaluate the seriousness of fretting fatigue damage in any specific design by running simulated service tests on specimens or components. Within the current state-of-the-art knowledge in the area of fretting fatigue, there is no other safe course of action open to the designer.

Fretting wear is a change in dimensions through wear directly attributable to the fretting process between two mating surfaces. It is thought that the abrasive pit-digging mechanism, the asperity contact microcrack initiation mechanism, and the wear sheet delamination mechanism may all be important in most fretting wear failures. As in the case of fretting fatigue, there has been no good model developed to describe the fretting wear phenomenon in a way useful for



Test Condition Used	Code Designation	Sample Size	Mean Prot Failure Stress, psi	Unbiased Standard Deviation, psi
Nonfretted, polished, SAE 4340 steel	NF-P-S	15	78,200	5,456
Nonfretted, polished, Ti-140-A titanium	NF-P-T	15	77,800	2,454
Nonfretted, mildly shot-peened, Ti-140-A titanium	NF-MSP-T	15	83,100	1,637
Nonfretted, severely shot-peened, Ti-140-A titanium	NF-SSP-T	15	85,700	2,398
Nonfretted, mildly cold-rolled, Ti-140-A titanium	NF-MCR-T	15	85,430	1,924
Nonfretted, severely cold-rolled, Ti-140-A titanium	NF-SCR-T	15	95,400	2,120
Mildly fretted, polished, SAE 4340 steel	MF-P-S	15	77,280	4,155
Medium fretted, polished, SAE 4340 steel	MeF-P-S	15	71,850	5,492
Severely fretted, polished, SAE 4340 steel	SF-P-S	15	67,700	6,532
Mildly fretted, polished, Ti-140-A titanium	MF-P-T	15	81,050	3,733
Medium fretted, polished, Ti-140-A titanium	MeF-P-T	15	58,140	15,715
Severely fretted, polished, Ti-140-A titanium	SF-P-T	15	38,660	19,342
Mildly fretted, mildly shot-peened, Ti-140-A titanium	MF-MSP-T	15	84,520	5,239
Medium fretted, mildly shot-peened, Ti-140-A titanium	MeF-MSP-T	15	84,930	2,446
Severely fretted, mildly shot-peened, Ti-140-A titanium	SF-MSP-T	15	84,870	2,647
Mildly fretted, severely shot-peened, Ti-140-A titanium	MF-SSP-T	15	83,600	1,474
Medium fretted, severely shot-peened, Ti-140-A titanium	MeF-SSP-T	15	83,240	1,332
Severely fretted, severely shot-peened, Ti-140-A titanium	SF-SSP-T	15	83,110	1,280
Mildly fretted, mildly cold-rolled, Ti-140-A titanium	MF-MCR-T	15	82,050	4,313
Medium fretted, mildly cold-rolled, Ti-140-A titanium	MeF-MCR-T	15	76,930	8,305
Severely fretted, mildly cold-rolled, Ti-140-A titanium	SF-MCR-T	15	67,960	5,682
Mildly fretted, severely cold-rolled, Ti-140-A titanium	MF-SCR-T	15	93,690	1,858
Medium fretted, severely cold-rolled, Ti-140-A titanium	MeF-SCR-T	15	91,950	2,098
Severely fretted, severely cold-rolled, Ti-140-A titanium	SF-SCR-T	15	93,150	1,365

Figure 33 Fatigue properties of fretted steel and titanium specimens with various degrees of shot peening and cold rolling. (See Ref. 86. Reprinted with permissions of ASME.)

design. An expression for weight loss due to fretting has been proposed<sup>82</sup> as

$$W_{\text{total}} = (k_0 L^{1/2} - k_1 L) \frac{C}{F} + k_2 S L C \quad (44)$$

where  $W_{\text{total}}$  = total specimen weight loss  
 $L$  = normal contact load  
 $C$  = number of fretting cycles  
 $F$  = frequency of fretting  
 $S$  = peak-to-peak slip between fretting surfaces  
 $k_0, k_1, k_2$  = constants to be empirically determined

This equation has been shown to give relatively good agreement with experimental data over a range of fretting conditions using mild steel specimens. However, weight loss is not of direct use to a designer. Wear depth is of more interest. Prediction of wear depth in an actual design application must in general be based on simulated service testing.

Some investigators have suggested that estimates of fretting wear depth may be based on the classical adhesive or abrasive wear equations in which wear depth is proportional to load and total distance slid, where the total distance slid is calculated by multiplying relative motion per cycle by number of cycles. Although there are some supporting data for such a procedure,<sup>101</sup> more investigation is required before it could be recommended as an acceptable approach for general application.

If fretting wear at a support interface, such as between tubes and support plates of a steam generator or heat exchanger or between fuel pins and support grids of a reactor core, produces loss of fit at a support site, impact fretting may occur. Impact fretting is fretting action induced by the small lateral relative displacements between two surfaces when they impact together, where the small displacements are caused by Poisson strains or small tangential “glancing” velocity components. Impact fretting has only recently been addressed in the literature,<sup>102</sup> but it should be noted that under certain circumstances impact fretting may be a potential failure mode of great importance.

Fretting corrosion may be defined as any corrosive surface involvement resulting as a direct result of fretting action. The consequences of fretting corrosion are generally much less severe than for either fretting wear or fretting fatigue. Note that the term *fretting corrosion* is not being used here as a synonym for fretting, as in much of the early literature on this topic. Perhaps the most important single parameter in minimizing fretting corrosion is proper selection of the material pair for the application. Table 4 lists a variety of material pairs grouped according to their resistance to fretting corrosion.<sup>103</sup> Cross comparisons from one investigator’s results to another’s must be made with care because testing conditions varied widely. The minimization or prevention of fretting damage must be carefully considered as a separate problem in each individual design application because a palliative in one application may significantly accelerate fretting damage in a different application. For example, in a joint that is designed to have no relative motion, it is sometimes possible to reduce or prevent fretting by increasing the normal pressure until all relative motion is arrested. However, if the increase in normal pressure does not completely arrest the relative motion, the result may be significantly increasing fretting damage instead of preventing it.

Nevertheless, there are several basic principles that are generally effective in minimizing or preventing fretting. These include:

1. Complete separation of the contacting surfaces.
2. Elimination of all relative motion between the contacting surfaces.

**Table 4** Fretting Corrosion Resistance of Various Material Pairs<sup>103</sup>

<i>Material Pairs Having Good Fretting Corrosion Resistance</i>		
Sakmann and Rightmire	Lead	on Steel
	Silver plate	on Steel
Gray and Jenny	Silver plate	on Silver plate
	“Parco-lubrized” steel	on Steel
	Grit blasted steel plus lead plate	on Steel (very good)
	$\frac{1}{16}$ in. nylon insert	on Steel (very good)
McDowell	Zinc and iron phosphated (bonderizing) steel	on Steel (good with thick coat)
	Laminated plastic	on Gold plate
	Hardtool steel	on Tool steel
	Cold-rolled steel	on Cold-rolled steel
	Cast iron	on Cast iron with phosphate coating
	Cast iron	on Cast iron with rubber cement
	Cast iron	on Cast iron with tungsten sulfide coating
	Cast iron	on Cast iron with rubber insert
	Cast iron	on Cast iron with Molykote lubricant
Cast iron	on Stainless steel with Molykote lubricant	
<i>Material Pairs Having Intermediate Fretting Corrosion Resistance</i>		
Sakmann and Rightmire	Cadmium	on Steel
	Zinc	on Steel
	Copper alloy	on Steel
	Zinc	on Aluminum
	Copper plate	on Aluminum
	Nickel plate	on Aluminum
	Silver plate	on Aluminum
	Iron plate	on Aluminum
Gray and Jenny	Sulfide-coated bronze	on Steel
	Cast bronze	on “Parco-lubrized” steel
	Magnesium	on “Parco-lubrized” steel
McDowell	Grit-blasted steel	on Steel
	Cast iron	on Cast iron (rough or smooth surface)
	Copper	on Cast iron
	Brass	on Cast iron
	Zinc	on Cast iron
	Cast iron	on Silver plate
	Cast iron	on Copper plate
Sakmann and Rightmire	Magnesium	on Copper plate
	Zirconium	on Zirconium
	Steel	on Steel
	Nickel	on Steel
	Aluminum	on Steel
	Al-Si alloy	on Steel
	Antimony plate	on Steel
	Tin	on Steel
	Aluminum	on Aluminum
	Zinc plate	on Aluminum

**Table 4** (Continued)

Gray and Jenny	Grit blast plus silver plate	on Steel <sup>a</sup>
	Steel	on Steel
	Grit blast plus copper plate	on Steel
	Grit blast plus in plate	on Steel
	Grit blast and aluminum foil	on Steel
	Be-Cu insert	on Steel
	Magnesium	on Steel
	Nitrided steel	on Chromium-plated steel <sup>b</sup>
<i>Material Pairs Having Poor Fretting Corrosion Resistance</i>		
McDowell	Aluminum	on Cast iron
	Aluminum	on Stainless steel
	Magnesium	on Cast iron
	Cast iron	on Chromium plate
	Laminated plastic	on Cast iron
	Bakelite	on Cast iron
	Hardtool steel	on Stainless steel
	Chromium plate	on Chromium plate
	Cast iron	on Tin plate
Gold plate	on Gold plate	

<sup>a</sup>Possibly effective with light loads and thick (0.005-in.) silver plate.

<sup>b</sup>Some improvement by heating chromium-plated steel to 538°C for 1 h.

3. If relative motion cannot be eliminated, it is sometimes effective to superpose a large unidirectional relative motion that allows effective lubrication. For example, the practice of driving the inner or outer race of an oscillatory pivot bearing may be effective in eliminating fretting.
4. Providing compressive residual stresses at the fretting surface; this may be accomplished by shot peening, cold rolling, or interference fit techniques.
5. Judicious selection of material pairs.
6. Use of interposed low-shear-modulus shim material or plating, such as lead, rubber, or silver.
7. Use of surface treatments or coatings as solid lubricants.
8. Use of surface grooving or roughening to provide debris escape routes and differential strain matching through elastic action.

Of all these techniques, only the first two are completely effective in preventing fretting.

The remaining concepts, however, may often be used to minimize fretting damage and yield an acceptable design.

## 7.2 Wear Phenomena

The complexity of the wear process may be better appreciated by recognizing that many variables are involved, including the hardness, toughness, ductility, modulus of elasticity, yield strength, fatigue properties, and structure and composition of the mating surfaces, as well as geometry, contact pressure, temperature, state of stress, stress distribution, coefficient of friction, sliding distance, relative velocity, surface finish, lubricants, contaminants, and ambient atmosphere at the wearing interface. Clearance versus contact time history of the wearing surfaces may also be an important factor in some cases. Although the wear processes are complex,

progress has been made toward development of quantitative empirical relationships for the various subcategories of wear under specified operating conditions.

Adhesive wear is often characterized as the most basic or fundamental subcategory of wear since it occurs to some degree whenever two solid surfaces are in rubbing contact and remains active even when all other modes of wear have been eliminated. The phenomenon of adhesive wear may be best understood by recalling that all real surfaces, no matter how carefully prepared and polished, exhibit a general waviness upon which is superposed a distribution of local protuberances or asperities. As two surfaces are brought into contact, therefore, only a relatively few asperities actually touch, and the *real* area of contact is only a small fraction of the *apparent* contact area. (See Chap. 1 of Ref. 78 and Chap. 2 of Ref. 104.) Thus, even under very small applied loads, the local pressures at the contact sites become high enough to exceed the yield strength of one or both surfaces, and local plastic flow ensues. If the contacting surfaces are clean and uncorroded, the very intimate contact generated by this local plastic flow brings the atoms of the two contacting surfaces close enough together to call into play strong adhesive forces. This process is sometimes called *cold welding*. Then if the surfaces are subjected to relative sliding motion, the cold-welded junctions must be broken. Whether they break at the original interface or elsewhere within the asperity depends on surface conditions, temperature distribution, strain-hardening characteristics, local geometry, and stress distribution. If the junction is broken away from the original interface, a particle of one surface is transferred to the other surface, marking one event in the adhesive wear process. Later sliding interactions may dislodge the transferred particles as loose wear particles or they may remain attached. If this adhesive wear process becomes severe and large-scale metal transfer takes place, the phenomenon is called *galling*. If the galling becomes so severe that two surfaces adhere over a large region so that the actuating forces can no longer produce relative motion between them, the phenomenon is called *seizure*. If properly controlled, however, the adhesive wear rate may be low and self-limiting, often being exploited in the “wearing-in” process to improve mating surfaces such as bearings or cylinders so that full film lubrication may be effectively used.

One quantitative estimate of the amount of adhesive wear is given as follows (see Ref. 93 and Chapters 2 and 6 of Ref. 105):

$$d_{\text{adh}} = \frac{V_{\text{adh}}}{A_a} = \left( \frac{k}{9\sigma_{\text{yp}}} \right) \left( \frac{W}{A_a} \right) L_s \quad (45)$$

or

$$d_{\text{adh}} = k_{\text{adh}} p_m L_s \quad (46)$$

where  $d_{\text{adh}}$  is the average wear depth,  $A_a$  is the apparent contact area,  $L_s$  is the total sliding distance,  $V_{\text{adh}}$  is the wear volume,  $W$  is the applied load,  $p_m = W/A_a$  is the mean nominal contact pressure between bearing surfaces, and  $k_{\text{adh}} = k/9\sigma_{\text{yd}}$  is a wear coefficient that depends on the probability of formation of a transferred fragment and the yield strength (or hardness) of the softer material. Typical values of the wear constant  $k$  for several material pairs are shown in Table 5, and the influence of lubrication on the wear constant  $k$  is indicated in Table 6. Noting from Eq. (46) that

$$k_{\text{adh}} = \frac{d_{\text{adh}}}{p_m L_s} \quad (47)$$

it may be observed that if the ratio  $d_{\text{adh}}/p_m L_s$  is experimentally found to be constant, Eq. (46) should be valid. Experimental evidence has been accumulated (see pp. 124–125 of Ref. 93) to confirm that for a given material pair this ratio is constant up to mean nominal contact pressures approximately equal to the uniaxial yield strength. Above this level the adhesive wear coefficient increases rapidly, with attendant severe galling and seizure.

In the selection of metal combinations to provide resistance to adhesive wear, it has been found that the sliding pair should be composed of mutually insoluble metals and that at least one

**Table 5** Archard Adhesive Wear Constant  $k$  for Various Unlubricated Material Pairs in Sliding Contact

Material	Wear Constant $k$
Zinc on zinc	$160 \times 10^{-3}$
Low-carbon steel on lowcarbon steel	$45 \times 10^{-3}$
Copper on copper	$32 \times 10^{-3}$
Stainless steel on stainless steel	$21 \times 10^{-3}$
Copper (on low-carbon steel)	$1.5 \times 10^{-3}$
Low-carbon steel (on copper)	$0.5 \times 10^{-3}$
Bakelite on bakelite	$0.02 \times 10^{-3}$

Source: From Ref. 105, with permission of John Wiley & Sons.

**Table 6** Order-of-Magnitude Values for Adhesive Wear Constant  $k$  under Various Conditions of Lubrication

Lubrication Condition	Metal (on Metal)		Nonmetal (on Metal)
	Like	Unlike	
Unlubricated	$5 \times 10^{-3}$	$2 \times 10^{-4}$	$5 \times 10^{-6}$
Poorly lubricated	$2 \times 10^{-4}$	$2 \times 10^{-2}$	$5 \times 10^{-6}$
Average lubrication	$2 \times 10^{-5}$	$2 \times 10^{-5}$	$5 \times 10^{-6}$
Excellent lubrication	$2 \times 10^{-6}$ to $10^{-7}$	$2 \times 10^{-6}$ to $10^{-7}$	$2 \times 10^{-6}$

Source: From Ref. 105, with permission of John Wiley & Sons.

of the metals should be from the B subgroup of the periodic table. (See p. 31 of Ref. 106.) The reasons for these observations are that the number of cold-weld junctions formed is a function of the mutual solubility, and the strength of the junction bonds is a function of the bonding characteristics of the metals involved. The metals in the B subgroup of the periodic table are characterized by weak, brittle covalent bonds. These criteria have been verified experimentally, as shown in Table 7, where 114 of 123 pairs tested substantiated the criteria.

In the case of abrasive wear, the wear particles are removed from the surface by the plowing and gouging action of the asperities of a harder mating surface or by hard particles trapped between the rubbing surfaces. This type of wear is manifested by a system of surface grooves and scratches, often called *scoring*. The abrasive wear condition in which the hard asperities of one surface wear away the mating surface is commonly called *two-body wear*, and the condition in which hard abrasive particles between the two surfaces cause the wear is called *three-body wear*.

An average abrasive wear depth  $d_{abr}$  may then be estimated as

$$d_{adh} = \frac{V_{abr}}{A_a} = \left( \frac{(\tan \theta)_m}{3\pi\sigma_{yp}} \right) \left( \frac{W}{A_a} \right) L_s \quad (48)$$

$$d_{abr} = k_{abr} p_m L_s \quad (49)$$

where  $W$  is total applied load,  $\theta$  is the angle a typical conical asperity makes with respect to the direction of sliding,  $(\tan \theta)_m$  is a weighted mean value for all asperities,  $L_s$  is a total distance of sliding,  $\sigma_{yp}$  is the uniaxial yield point strength for the softer material,  $V_{abr}$  is abrasive wear volume,  $p_m = W/A_a$  is the mean nominal contact pressure between bearing surfaces, and



$k_{\text{abr}} = (\tan \theta)_m / 3\pi\sigma_{yp}$  is an abrasive wear coefficient that depends on the roughness characteristics of the surface and the yield strength (or hardness) of the softer material.

Comparing Eq. (48) for abrasive wear volume with Eq. (45) for adhesive wear volume, we note that they are formally the same except the constant  $k/3$  in the adhesive wear equation is replaced by  $(\tan \theta)_m / \pi$  in the abrasive wear equation. Typical values of the wear constant  $3(\tan \theta)_m / \pi$  for several materials are shown in Table 8. As indicated in Table 8, experimental evidence shows that  $k_{\text{abr}}$  for three-body wear is typically about an order of magnitude smaller than for the two-body case, probably because the trapped particles tend to roll much of the time and cut only a small part of the time.

**Table 7** Adhesive Wear Behavior of Various Pairs<sup>a</sup>

Description of Metal Pair	Material Combination				Remarks
	Al Disk	Steel Disk	Cu Disk	Ag Disk	
Soluble pairs with poor adhesive wear resistance	Be	Be	Be	Be	These pairs substantiate the criteria of solubility and B subgroup metals
	Mg	—	Mg	Mg	
	Al	Al	Al	—	
	Si	Si8	Si	Si	
	Ca	—	Ca	—	
	Ti	Ti	Ti	—	
	Cr	Cr	—	—	
	—	Mn	—	—	
	Fe	Fe	—	—	
	Co	Co	Co	—	
	Ni	Ni	Ni	—	
	Cu	—	Cu	—	
	—	Zn	Zn	—	
	Zr	Zr	Zr	Zr	
	Nb	Nb	Nb	—	
	Mo	Mo	Mo	—	
	Rh	Rh	Rh	—	
	—	Pd	—	—	
	Ag	—	Ag	—	
	—	—	Cd	Cd	
—	—	In	In		
Sn	—	Sn	—		
Ce	Ce	Ce	—		
Ta	Ta	Ta	—		
W	W	W	—		
—	Ir	—	—		
Pt	Pt	Pt	—		
Au	Au	Au	Au		
Th	Th	Th	Th		
U	U	U	U		
Soluble pairs with fair or good adhesive wear resistance.	—	Cu(F)	—	—	These pairs do not substantiate the stated criteria
	Zn(F)	—	—	—	
	—	—	Sb(F)	—	
Insoluble pairs, neither from the B subgroup, with poor adhesive wear resistance	—	Li	—	—	These pairs substantiate the stated criteria
	—	Mg	—	—	
	—	Ca	—	—	
—	—	Ba	—	—	

**Table 7** (Continued)

Description of Metal Pair	Material Combination				Remarks
	A1 Disk	Steel Disk	Cu Disk	Ag Disk	
Insoluble pairs, one from the B subgroup, with fair or good adhesive wear resistance.	—	C(F)	—	—	These pairs substantiate the stated criteria
	—	—	—	Ti(F)	
	—	—	Cr(F)	Cr(F)	
	—	—	—	Fe(F)	
	—	—	—	Co(F)	
	—	—	Ge(F)	—	
	—	Se(F)	Se(F)	—	
	—	—	—	Nb(F)	
	—	Ag	—	—	
	Cd	Cd	—	—	
	Ln	In	—	—	
	—	Sn(F)	—	—	
	—	Sb(F)	Sb	—	
	Te(F)	Te(F)	Te(F)	—	
	Ti	Ti	Ti	—	
Pb(F)	Pb	Pb	—		
Bi(F)	Bi	Bi(F)	—		
Insoluble pairs, one from the B subgroup, with poor adhesive wear resistance	—	—	C	C	These pairs do not substantiate the stated criteria
	—	—	—	Ni	
	—	—	—	—	
	—	—	—	Mo	

<sup>a</sup>See pp. 34–35 of Ref. 106.

**Table 8** Abrasive Wear Constant  $3(\tan\theta)_m/\pi$  for Various Materials in Sliding Contact as Reported by Different Investigators

Materials	Wear Type	Particle ( $\tau_m$ )	$3(\tan\theta)_m/\beta$
Many	Two body	—	$180 \times 10^{-3}$
Many	Two body	110	$150 \times 10^{-3}$
Many	Two body	40–150	$120 \times 10^{-3}$
Steel	Two body	260	$80 \times 10^{-3}$
Many	Two body	80	$24 \times 10^{-3}$
Brass	Two body	70	$16 \times 10^{-3}$
Steel	Two body	150	$6 \times 10^{-3}$
Steel	Two body	80	$4.5 \times 10^{-3}$
Many	Two body	40	$2 \times 10^{-3}$

Source: See p. 169 of Ref. 105. Reprinted with permission from John Wiley & Sons.

In selecting materials for abrasive wear resistance, it has been established that both hardness and modulus of elasticity are key properties. Increasing wear resistance is associated with higher hardness and lower modulus of elasticity since both the amount of elastic deformation and the amount of elastic energy that can be stored at the surface are increased by higher hardness and lower modulus of elasticity.

Table 9 tabulates several materials in order of descending values of (hardness)/(modulus of elasticity). Well-controlled experimental data are not yet available, but general experience

**Table 9** Values of (Hardness/Modulus of Elasticity) for Various Materials

Material	Condition	BHN <sup>a</sup> ( $E \times 10^{-6}$ ) (in mixed units)
Alundum (Al <sub>2</sub> O <sub>3</sub> )	Bonded	143
Chrome plate	Bright	83
Gray iron	Hard	33
Tungsten carbide	9% Co	22
Steel	Hard	21
Titanium	Hard	17
Aluminum alloy	Hard	11
Gray iron	As cast	10
Structural steel	Soft	5
Malleable iron	Soft	5
Wrought iron	Soft	3.5
Chromium metal	As cast	3.5
Copper	Soft	2.5
Silver	Pure	2.3
Aluminum	Pure	2.0
Lead	Pure	2.0
Tin	Pure	0.7

<sup>a</sup>Brinell hardness number.

Source: Reprinted from Ref. 93 with permission from Elsevier Science.

would provide an ordering of materials for decreasing wear resistance compatible with the array of Table 9. When the conditions for adhesive or abrasive wear exist together with conditions that lead to corrosion, the two processes persist together and often interact synergistically. If the corrosion product is hard and abrasive, dislodged corrosion particles trapped between contacting surfaces will accelerate the abrasive wear process. In turn, the wear process may remove the “protective” surface layer of corrosion product to bare new metal to the corrosive atmosphere, thereby accelerating the corrosion process. Thus, the corrosion wear process may be self-accelerating and may lead to high rates of wear.

On the other hand, some corrosion products, for example, metallic phosphates, sulfides, and chlorides, form as soft lubricative films that actually improve the wear rate markedly, especially if adhesive wear is the dominant phenomenon.

Three major wear control methods have been defined, as follows (see p. 36 of Ref. 106): *principle of protective layers*, including protection by lubricant, surface film, paint, plating, phosphate, chemical, flame-sprayed, or other types of interfacial layers; *principle of conversion*, in which wear is converted from destructive to permissible levels through better choice of metal pairs, hardness, surface finish, or contact pressure; and *principle of diversion*, in which the wear is diverted to an economical replaceable wear element that is periodically discarded and replaced as “wear-out” occurs.

When two surfaces operate in rolling contact, the wear phenomenon is quite different from the wear of sliding surfaces just described, although the “delamination” theory<sup>107</sup> is very similar to the mechanism of wear between rolling surfaces in contact as described here. Rolling surfaces in contact result in Hertz contact stresses that produce maximum values of shear stress slightly below the surface. (See, for example, Ref. 108.) As the rolling contact zone moves past a given location on the surface, the subsurface peak shear stress cycles from zero to a maximum value and back to zero, thus producing a cyclic stress field. Such conditions may lead to fatigue failure by the initiation of a subsurface crack that propagates under repeated cyclic loading and that

may ultimately propagate to the surface to spall out a macroscopic surface particle to form a wear pit. This action, called *surface fatigue wear*, is a common failure mode in antifriction bearings, gears, and cams and all machine parts that involve rolling surfaces in contact.

## 8 CORROSION AND STRESS CORROSION

Corrosion may be defined as the undesired deterioration of a material through chemical or electrochemical interaction with the environment or destruction of materials by means other than purely mechanical action. Failure by corrosion occurs when the corrosive action renders the corroded device incapable of performing its design function. Corrosion often interacts synergistically with another failure mode, such as wear or fatigue, to produce the even more serious combined failure modes, such as corrosion wear or corrosion fatigue. Failure by corrosion and protection against failure by corrosion has been estimated to cost in excess of \$276 billion annually in the United States alone.<sup>109</sup>

The complexity of the corrosion process may be better appreciated by recognizing that many variables are involved, including environmental, electrochemical, and metallurgical aspects. For example, anodic reactions and rate of oxidation; cathodic reactions and rate of reduction; corrosion inhibition, polarization, or retardation; passivity phenomena; effect of oxidizers; effect of velocity; temperature; corrosive concentration; galvanic coupling; and metallurgical structure all influence the type and rate of the corrosion process.

Corrosion processes have been categorized in many different ways. One convenient classification divides corrosion phenomena into the following types<sup>110,111</sup>:

1. Direct chemical attack
2. Galvanic corrosion
3. Crevice corrosion
4. Pitting corrosion
5. Intergranular corrosion
6. Selective leaching
7. Erosion corrosion
8. Cavitation corrosion
9. Hydrogen damage
10. Biological corrosion
11. Stress corrosion cracking

Depending on the types of environment, loading, and mechanical function of the machine parts involved, any of the types of corrosion may combine their influence with other failure modes to produce premature failures. Of particular concern are interactions that lead to failure by corrosion wear, corrosion fatigue, fretting fatigue, and corrosion-induced fracture.

### 8.1 Types of Corrosion

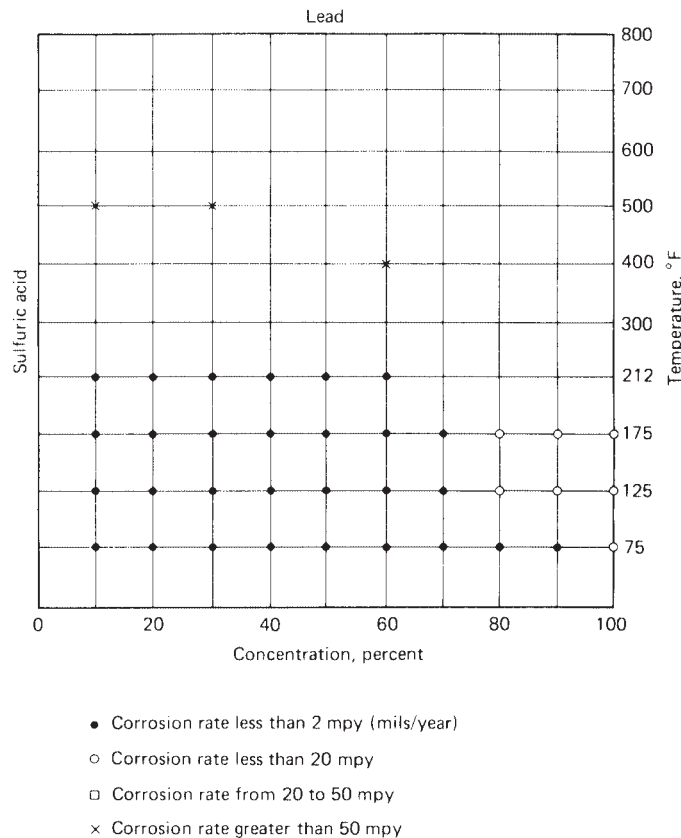
Direct chemical attack is probably the most common type of corrosion. Under this type of corrosive attack the surface of the machine part exposed to the corrosive media is attacked more or less uniformly over its entire surface, resulting in a progressive deterioration and dimensional reduction of sound load-carrying net cross section. The rate of corrosion due to direct attack can usually be estimated from relatively simple laboratory tests in which small specimens of the selected material are exposed to a well-simulated actual environment, with frequent weight

change and dimensional measurements carefully taken. The corrosion rate is usually expressed in mils per year (mpy) and may be calculated as<sup>110</sup>

$$R = \frac{534W}{\gamma At} \quad (50)$$

where  $R$  is rate of corrosion penetration in mils (1 mil = 0.001 in.) per year (mpy),  $W$  is weight loss in milligrams,  $A$  is exposed area of the specimen in square inches,  $\gamma$  is density of the specimen in grams per cubic centimeter, and  $t$  is exposure time in hours. Use of this corrosion rate expression in predicting corrosion penetration in actual service is usually successful if the environment has been properly simulated in the laboratory. Corrosion rate data for many different combinations of materials and environments are available in the literature.<sup>112-114</sup> Figure 34 illustrates one presentation of such data.

Direct chemical attack may be reduced in severity or prevented by any one or a combination of several means, including selecting proper materials to suit the environment; using plating, flame spraying, cladding, hot dipping, vapor deposition, conversion coatings, and organic coatings or paint to protect the base material; changing the environment by using lower temperature or lower velocity, removing oxygen, changing corrosive concentration, or adding corrosion inhibitors; using cathodic protection in which electrons are supplied to the metal surface to be



**Figure 34** Nelson's method for summarizing corrosion rate data for lead in sulfuric acid environment as a function of concentration and temperature. (After Ref. 112, G. Nelson, *Corrosion Data Survey*, ©NACE International 1972.)

protected either by galvanic coupling to a sacrificial anode or by an external power supply; or adopting other suitable design modifications.

Galvanic corrosion is an accelerated electrochemical corrosion that occurs when two dissimilar metals in electrical contact are made part of a circuit completed by a connecting pool or film of electrolyte or corrosive medium. Under these circumstances, the potential difference between the dissimilar metals produces a current flow through the connecting electrolyte, which leads to corrosion, concentrated primarily in the more anodic or less noble metal of the pair. This type of action is completely analogous to a simple battery cell. Current must flow to produce galvanic corrosion, and, in general, more current flow means more serious corrosion. The relative tendencies of various metals to form galvanic cells and the probable direction of the galvanic action are illustrated for several commercial metals and alloys in seawater in Table 10.<sup>110,111</sup>

**Table 10** Galvanic Series of Several Commercial Metals and Alloys in Seawater

↑	Platinum
Noble or cathodic (protected end)	Gold
	Graphite
	Titanium
	Silver
	[Chlorimet 3 (62 Ni, 18 Cr, 18 Mo)]
	[Hastelloy C (62 Ni, 17 C, 15 Mo)]
	[18-8 Mo stainless steel (passive)]
	[18-8 stainless steel (passive)]
	[Chromium stainless steel 11–30% Cr (passive)]
	[Inconel (passive) (80 Ni, 13 Cr, 7 Fe)]
	[Nickel (passive)]
	Silver solder
	[Monel (70 Ni, 30 Cu)]
	[Cupronickels (60-90 Cu, 40-10 Ni)]
	[Bronzes (Cu–Sn)]
	[Copper]
	[Brasses (Cu–Zn)]
	[Chlorimet 2 (66 Ni, 32 Mo, 1 Fe)]
	[Hastelloy B (60 Ni, 30 Mo, 6 Fe, 1 Mn)]
	[Inconel (active)]
	[Nickel (active)]
	Tin
	Lead
Lead–tin solders	
[18-8 Mo stainless steel (active)]	
[18-8 stainless steel (active)]	
Ni-Resist (high-Ni cast iron)	
Chromium stainless steel, 13% Cr (active)	
[Cast iron]	
[Steel or iron]	
Active or anodic (corroded end)	2024 aluminum (4.5 Cu, 1.5 Mg, 0.6 Mn)
↓	Cadmium
	Commercially pure aluminum (1100)
	Zinc
	Magnesium and magnesium alloys

Source: Ref. 110. Reprinted with permission of McGraw-Hill Book Company.

Ideally, tests in the actual service environment should be conducted; but, if such data are unavailable, the data of Table 10 should give a good indication of possible galvanic action. The farther apart the two dissimilar metals are in the galvanic series, the more serious the galvanic corrosion problem may be. Material pairs within any bracketed group exhibit little or no galvanic action. It should be noted, however, that there are sometimes exceptions to the galvanic series of Table 10, so wherever possible, corrosion tests should be performed with actual materials in the actual service environment.

The accelerated galvanic corrosion is usually most severe near the junction between the two metals, decreasing in severity at locations farther from the junction. The ratio of cathodic area to anodic area exposed to the electrolyte has a significant effect on corrosion rate. It is *desirable* to have a *small ratio* of cathode area to anode area. For this reason, if only *one* of two dissimilar metals in electrical contact is to be coated for corrosion protection, the more noble or more corrosion-resistant metal should be coated. Although this at first may seem the wrong metal to coat, the area effect, which produces anodic corrosion rate of  $10^2 - 10^3$  times cathodic corrosion rates for equal areas, provides the logic for this assertion.

Galvanic corrosion may be reduced in severity or prevented by one or a combination of several steps, including the selection of material pairs as close together as possible in the galvanic series, preferably in the same bracketed group; electrical insulation of one dissimilar metal from the other as completely as possible; maintaining as small a ratio of cathode area to anode area as possible; proper use and maintenance of coatings; the use of inhibitors to decrease the aggressiveness of the corroding medium; and the use of cathodic protection in which a third metal element anodic to both members of the operating pair is used as a sacrificial anode that may require periodic replacement.

Crevice corrosion is an accelerated corrosion process highly localized within crevices, cracks, and other small-volume regions of stagnant solution in contact with the corroding metal. For example, crevice corrosion may be expected in gasketed joints; clamped interfaces; lap joints; rolled joints; under bolt and rivet heads; and under foreign deposits of dirt, sand, scale, or corrosion product. Until recently, crevice corrosion was thought to result from differences in either oxygen concentration or metal ion concentration in the crevice compared to its surroundings. More recent studies seem to indicate, however, that the local oxidation and reduction reactions result in oxygen depletion in the stagnant crevice region, which leads to an excess positive charge in the crevice due to increased metal ion concentration. This, in turn, leads to a flow of chloride and hydrogen ions into the crevice, both of which accelerate the corrosion rate within the crevice. Such accelerated crevice corrosion is highly localized and often requires a lengthy incubation period of perhaps many months before it gets under way. Once started, the rate of corrosion accelerates to become a serious problem. To be susceptible to crevice corrosion attack, the stagnant region must be wide enough to allow the liquid to enter but narrow enough to maintain stagnation. This usually implies cracks and crevices of a few thousandths to a few hundredths of an inch in width.

To reduce the severity of crevice corrosion or prevent it, it is necessary to eliminate the cracks and crevices. This may involve caulking or seal welding existing lap joints; redesign to replace riveted or bolted joints by sound, welded joints; filtering foreign material from the working fluid; inspection and removal of corrosion deposits; or using nonabsorbent gasket materials.

Pitting corrosion is a very localized attack that leads to the development of an array of holes or pits that penetrate the metal. The pits may be widely scattered or so heavily concentrated that they simply appear as a rough surface. The mechanism of pit growth is virtually identical to that of crevice corrosion described, except that an existing crevice is not required to initiate pitting corrosion. The pit is probably initiated by a momentary attack due to a random variation in fluid concentration or a tiny surface scratch or defect. Some pits may become inactive because of a stray convective current, whereas others may grow large enough to provide a stagnant region of stable size, which then continues to grow over a long period of time at an accelerating rate. Pits

usually grow in the direction of the gravity force field since the dense concentrated solution in a pit is required for it to grow actively. Most pits, therefore, grow downward from horizontal surfaces to ultimately perforate the wall. Fewer pits are formed on vertical walls, and very few pits grow upward from the bottom surface.

Measurement and assessment of pitting corrosion damage is difficult because of its highly local nature. Pit depth varies widely and, as in the case of fatigue damage, a statistical approach must be taken in which the probability of a pit of specified depth may be established in laboratory testing. Unfortunately, a significant size effect influences depth of pitting, and this must be taken into account when predicting service life of a machine part based on laboratory pitting corrosion data.

The control or prevention of pitting corrosion consists primarily of the wise selection of material to resist pitting or, since pitting is usually the result of stagnant conditions, imparting velocity to the fluid. Increasing its velocity may also decrease pitting corrosion attack.

Because of the atomic mismatch at the grain boundaries of polycrystalline metals, the stored strain energy is higher in the grain boundary regions than in the grains themselves. These high-energy grain boundaries are more chemically reactive than the grains. Under certain conditions depletion or enrichment of an alloying element or impurity concentration at the grain boundaries may locally change the composition of a corrosion-resistant metal, making it susceptible to corrosive attack. Localized attack of this vulnerable region near the grain boundaries is called intergranular corrosion. In particular, the austenitic stainless steels are vulnerable to intergranular corrosion if *sensitized* by heating into the temperature range from 950 to 1450°F, which causes depletion of the chromium near the grain boundaries as chromium carbide is precipitated at the boundaries. The chromium-poor regions then corrode because of local galvanic cell action, and the grains literally fall out of the matrix. A special case of intergranular corrosion, called “weld decay,” is generated in the portion of the weld heat-affected zone, which is heated into the sensitizing temperature range.

To minimize the susceptibility of austenitic stainless steels to intergranular corrosion, the carbon content may be lowered to below 0.03%, stabilizers may be added to prevent depletion of the chromium near the grain boundaries, or a high-temperature solution heat treatment, called quench annealing, may be employed to produce a more homogeneous alloy.

Other alloys susceptible to intergranular corrosion include certain aluminum alloys, magnesium alloys, copper-based alloys, and die-cast zinc alloys in unfavorable environments.

The corrosion phenomenon in which one element of a solid alloy is removed is termed selective leaching. Although the selective leaching process may occur in any of several alloy systems, the more common examples are *dezincification* of brass alloys and *graphitization* of gray cast iron. Dezincification may occur as either a highly local “plug-type” or a broadly distributed layer-type attack. In either case, the dezincified region is porous, brittle, and weak. Dezincification may be minimized by adding inhibitors such as arsenic, antimony, or phosphorus to the alloy; by lowering oxygen in the environment; or by using cathodic protection.

In the case of graphitization of gray cast iron, the environment selectively leaches the iron matrix to leave the graphite network intact to form an active galvanic cell. Corrosion then proceeds to destroy the machine part.

Use of other alloys, such as nodular or malleable cast iron, mitigates the problem because there is no graphite network in these alloys to support the corrosion residue. Other alloy systems in adverse environments that may experience selective leaching include aluminum bronzes, silicon bronzes, and cobalt alloys.

Erosion corrosion is an accelerated, direct chemical attack of a metal surface due to the action of a moving corrosive medium. Because of the abrasive wear action of the moving fluid, the formation of a protective layer of corrosion product is inhibited or prevented, and the corroding medium has direct access to bare, unprotected metal. Erosion corrosion is usually characterized by a pattern of grooves or peaks and valleys generated by the flow pattern of the



corrosive medium. Most alloys are susceptible to erosion corrosion, and many different types of corrosive media may induce erosion corrosion, including flowing gases, liquids, and solid aggregates. Erosion corrosion may become a problem in such machine parts as valves, pumps, blowers, turbine blades and nozzles, conveyors, and piping and ducting systems, especially in the regions of bends and elbows.

Erosion corrosion is influenced by the velocity of the flowing corrosive medium, turbulence of the flow, impingement characteristics, concentration of abrasive solids, and characteristics of the metal alloy surface exposed to the flow. Methods of minimizing or preventing erosion corrosion include reducing the velocity, eliminating or reducing turbulence, avoiding sudden changes in the direction of flow, eliminating direct impingement where possible, filtering out abrasive particles, using harder and more corrosion-resistant alloys, reducing the temperature, using appropriate surface coatings, and using cathodic protection techniques.

Cavitation often occurs in hydraulic systems, such as turbines, pumps, and piping, when pressure changes in a flowing liquid give rise to the formation and collapse of vapor bubbles at or near the containing metal surface. The impact associated with vapor bubble collapse may produce high-pressure shock waves that may plastically deform the metal locally or destroy any protective surface film of corrosion product and locally accelerate the corrosion process. Furthermore, the tiny depressions so formed act as a nucleus for subsequent vapor bubbles, which continue to form and collapse at the same site to produce deep pits and pockmarks by the combined action of mechanical deformation and accelerated chemical corrosion. This phenomenon is called cavitation corrosion. Cavitation corrosion may be reduced or prevented by eliminating the cavitation through appropriate design changes. Smoothing the surfaces, coating the walls, using corrosion-resistant materials, minimizing pressure differences in the cycle, and using cathodic protection are design changes that may be effective.

Hydrogen damage, although not considered to be a form of direct corrosion, is often induced by corrosion. Any damage caused in a metal by the presence of hydrogen or the interaction with hydrogen is called hydrogen damage. Hydrogen damage includes hydrogen blistering, hydrogen embrittlement, hydrogen attack, and decarburization.

Hydrogen blistering is caused by the diffusion of hydrogen atoms into a void within a metallic structure where they combined to form molecular hydrogen. The hydrogen pressure builds to a high level that, in some cases, causes blistering, yielding, and rupture. Hydrogen blistering may be minimized by using materials without voids, by using corrosion inhibitors, or by using hydrogen-impervious coatings.

Hydrogen embrittlement is also caused by the penetration of hydrogen into the metallic structure to form brittle hydrides and pin dislocation movement to reduce slip. Hydrogen embrittlement is more serious at the higher strength levels of susceptible alloys, which include most of the high-strength steels. Reduction and prevention of hydrogen embrittlement may be accomplished by “baking out” the hydrogen at relatively low temperatures for several hours, use of corrosion inhibitors, or use of less susceptible alloys.

Decarburization and hydrogen attack are both high-temperature phenomena. At high temperatures hydrogen removes carbon from an alloy, often reducing its tensile strength and increasing its creep rate. This carbon-removing process is called *decarburization*. It is also possible that the hydrogen may lead to the formation of methane in the metal voids, which may expand to form cracks, another form of hydrogen attack. Proper selection of alloys and coatings is helpful in prevention of these corrosion-related problems.

Biological corrosion is a corrosion process or processes that result from the activity of living organisms. These organisms may be microorganisms, such as aerobic or anaerobic bacteria, or they may be macroorganisms, such as fungi, mold, algae, or barnacles. The organisms may influence or produce corrosion by virtue of their processes of food ingestion and waste elimination. There are, for example, sulfate-reducing anaerobic bacteria, which produce iron sulfide when in contact with buried steel structures, and aerobic sulfur-oxidizing bacteria, which

produce localized concentrations of sulfuric acid and serious corrosive attack on buried steel and concrete pipelines. There are also iron bacteria, which ingest ferrous iron and precipitate ferrous hydroxide to produce local crevice corrosion attack. Other bacteria oxidize ammonia to nitric acid, which attacks most metals, and most bacteria produce carbon dioxide, which may form the corrosive agent carbonic acid. Fungi and mold assimilate organic matter and produce organic acids. Simply by their presence, fungi may provide the site for crevice corrosion attacks, as does the presence of attached barnacles and algae. Prevention or minimization of biological corrosion may be accomplished by altering the environment or by using proper coatings, corrosion inhibitors, bactericides or fungicides, or cathodic protection.

## 8.2 Stress Corrosion Cracking

Stress corrosion cracking is an extremely important failure mode because it occurs in a wide variety of different alloys. This type of failure results from a field of cracks produced in a metal alloy under the combined influence of tensile stress and a corrosive environment. The metal alloy is not attacked over most of its surface, but a system of intergranular or transgranular cracks propagates through the matrix over a period of time.

Stress levels that produce stress corrosion cracking are well below the yield strength of the material, and residual stresses as well as applied stresses may produce failure. The lower the stress level, the longer is the time required to produce cracking, and there appears to be a threshold stress level below which stress corrosion cracking does not occur.<sup>110</sup>

The chemical compositions of the environments that lead to stress corrosion cracking are highly specific and peculiar to the alloy system, and no general patterns have been observed. For example, austenitic stainless steels are susceptible to stress corrosion cracking in chloride environments but not in ammonia environments, whereas brasses are susceptible to stress corrosion cracking in ammonia environments but not in chloride environments. Thus, the “season cracking” of brass cartridge cases in the crimped zones was found to be stress corrosion cracking due to the ammonia resulting from decomposition of organic matter. Likewise, “caustic embrittlement” of steel boilers, which resulted in many explosive failures, was found to be stress corrosion cracking due to sodium hydroxide in the boiler water.

Stress corrosion cracking is influenced by stress level, alloy composition, type of environment, and temperature. Crack propagation seems to be intermittent, and the crack grows to a critical size, after which a sudden and catastrophic failure ensues in accordance with the laws of fracture mechanics. Stress corrosion crack growth in a statically loaded machine part takes place through the interaction of mechanical strains and chemical corrosion processes at the crack tip. The largest value of plane-strain stress intensity factor for which crack growth does not take place in a corrosive environment is designated  $K_{ISCC}$ . In many cases, corrosion fatigue behavior is also related to the magnitude of  $K_{ISCC}$ .<sup>9</sup>

Prevention of stress corrosion cracking may be attempted by lowering the stress below the critical threshold level, choice of a better alloy for the environment, changing the environment to eliminate the critical corrosive element, use of corrosion inhibitors, or use of cathodic protection. Before cathodic protection is implemented, care must be taken to ensure that the phenomenon is indeed stress corrosion cracking because hydrogen embrittlement is accelerated by cathodic protection techniques.

## 9 FAILURE ANALYSIS AND RETROSPECTIVE DESIGN

In spite of all efforts to design and manufacture machines and structures to function properly without failure, failures do occur. Whether the failure consequences simply represent an annoying inconvenience or a catastrophic loss of life and property, it is the responsibility of the

designer to glean all of the information possible from the failure event so that similar events can be avoided in the future. Effective assessment of service failures usually requires the intense interactive scrutiny of a team of specialists, including at least a mechanical designer and a materials engineer trained in failure analysis techniques. The team might often include a manufacturing engineer and a field service engineer as well. The mission of the failure analysis team is to discover the initiating cause of failure, identify the best solution, and redesign the product to prevent future failures. Although the results of failure analysis investigations may often be closely related to product liability litigation, the legal issues will not be addressed in this discussion.

Techniques utilized in the failure analysis effort include the inspection and documentation of the event through direct examination, photographs, and eyewitness reports; preservation of all parts, especially failed parts; and pertinent calculations, analyses, and examinations that may help establish and validate the cause of failure. The materials engineer may utilize macroscopic examination, low-power magnification, microscopic examination, transmission or scanning electron microscopic techniques, energy-dispersive X-ray techniques, hardness tests, spectrographic analysis, metallographic examination, or other techniques of determining the failure type, failure location, material abnormalities, and potential causes of failure. The designer may perform stress and deflection analyses, examine geometry, assess service loading and environmental influences, reexamine the kinematics and dynamics of the application, and attempt to reconstruct the failure scenario. Other team members may examine the quality of manufacture, the quality of maintenance, the possibility of unusual or unconventional usage by the operator, or other factors that may have played a role in the service failure. Piecing all of this information together, it is the objective of the failure analysis team to identify as accurately as possible the probable cause of failure.

As undesirable as service failures may be, the results of a well-executed failure analysis may be transformed directly into improved product reliability by a designer who capitalizes on service failure data and failure analysis results. These techniques of retrospective design have become important working tools of the profession and are likely to continue to grow in importance.

## REFERENCES

1. J. A. Collins, *Failure of Materials in Mechanical Design; Analysis, Prediction, Prevention*, 2nd ed., Wiley, New York, 1993.
2. K. Hellan, *Introduction to Fracture Mechanics*, McGraw-Hill, New York, 1984.
3. H. Tada, P. C. Paris, and G. R. Irwin, *The Stress Analysis of Cracks Handbook*, 3rd ed., ASME, New York, 2000.
4. T. L. Anderson, *Fracture Mechanics, Fundamentals and Applications*, 3rd ed., CRC Press, Boca Raton, FL, 2004.
5. "Progress in Measuring Fracture Toughness and Using Fracture Mechanics," *Mat. Res. Stand.*, March, 103–119, 1964.
6. X. Wu and A. J. Carlsson, *Weight Functions and Stress Intensity Factor Solutions*, Pergamon Press, Oxford, 1991.
7. A. P. Parker, *The Mechanics of Fracture and Fatigue*, E. & F. N. Spon, New York, 1981.
8. E 399-90, "Standard Test Method for Plane-Strain Fracture Toughness of Metallic Materials," *Annual Book of ASTM Standards*, Vol. 03.01, ASTM, Philadelphia, 1991.
9. R. W. Hertzberg, *Deformation and Fracture Mechanics of Engineering Materials*, 3rd ed., Wiley, New York, 1989.
10. J. P. Gallagher (Ed.), *Damage Tolerant Design Handbook*, 4 vols., Metals and Ceramics Information Center, Battelle Columbus Labs., Columbus, OH, 1983.

11. *Metallic Materials and Elements for Aerospace Vehicle Structures*, MIL-HDBK-5F, 2 vols., U.S. Dept. of Defense, Naval Publications and Forms Center, Philadelphia, 1987.
12. W. T. Matthews, *Plane Strain Fracture Toughness (K<sub>IC</sub>) Data Handbook for Metals*, Report No. AMMRC MS 73-6, U.S. Army Materiel Command, NTIS, Springfield, VA, 1973.
13. C. M. Hudson and S. K. Seward, "A Compendium of Sources of Fracture Toughness and Fatigue Crack Growth Data for Metallic Alloys," *Int. J. Fracture*, **14**, R15, 1978.
14. C. M. Hudson and S. K. Seward, "A Compendium of Sources of Fracture Toughness and Fatigue Crack Growth Data for Metallic Alloys—Part II," *Int. J. Fracture*, **20**, R59, 1982.
15. C. M. Hudson and S. K. Seward, "A Compendium of Sources of Fracture Toughness and Fatigue Crack Growth Data for Metallic Alloys—Part III," *Int. J. Fracture*, **39**, R43, 1989.
16. C. M. Hudson and J. J. Ferrainolo, "A Compendium of Sources of Fracture Toughness and Fatigue Crack Growth Data for Metallic Alloys—Part IV," *Int. J. Fracture*, **48**, R19, 1991.
17. M. F. Kanninen and C. H. Popelar, *Advanced Fracture Mechanics*, Oxford University Press, New York, 1985.
18. A. F. Madayag, *Metal Fatigue, Theory and Design*, Wiley, New York, 1969.
19. O. H. Basquin, "The Exponential Law of Endurance Tests," *Proc. ASTM*, **10**, 625–630, 1910.
20. *Proceedings of the Conference on Welded Structures*, Vols. **I and II**, Welding Institute, Cambridge, England, 1971.
21. H. J. Grover, S. A. Gordon, and L. R. Jackson, *Fatigue of Metals and Structures*, GPO, Washington, DC, 1954.
22. H. F. Moore, "A Study of Size Effect and Notch Sensitivity in Fatigue Tests of Steel," *ASTM Proc.*, **45**, 507, 1945.
23. W. N. Thomas, "Effect of Scratches and Various Workshop Finishes upon the Fatigue Strength of Steel," *Engineering*, **116**, 449ff, 1923.
24. G. V. Smith, *Properties of Metals at Elevated Temperatures*, McGraw-Hill, New York, 1950.
25. N. E. Frost and K. Denton, "The Fatigue Strength of Butt Welded Joints in Low Alloy Structural Steels," *Brit. Welding J.*, **14**(4), 1967.
26. H. J. Grover, *Fatigue of Aircraft Structures*, GPO, Washington, DC, 1966.
27. L. F. Coffin, "A Study of the Effects of Cyclic Thermal Stresses on a Ductile Metal," *Trans. ASME*, **76**, 931–950, 1954.
28. S.S. Manson, "Behavior of Materials under Conditions of Thermal Stress," National Advisory Commission on Aeronautics: Report 1170, Lewis Flight Propulsion Laboratory, Cleveland, 1954.
29. M. Klesnil and P. Lukáš, "Fatigue of Metallic Materials," *Mat. Sci. Mono.* **71**, Elsevier, 1992.
30. S. S. Manson, "Fatigue—A Complex Subject—Some Simple Approximations," *Exp. Mech.*, **5**, 193–226, 1965.
31. U. Muralidharan and S. S. Manson, "Modified Universal Slopes Equations for Estimation of Fatigue Characteristics," *J. Eng. Mat. Tech., Trans. ASME*, **110**, 55–58, 1988.
32. B. F. Langer, "Design of Pressure Vessels for Low-Cycle Fatigue," *J. Basic Eng.*, **84**, 389–399, 1962.
33. A. Bäümel, Jr., and T. Seeger, *Materials Data for Cyclic Loading*, Supplement 1, Elsevier Science, Amsterdam, 1990.
34. J. H. Ong, "Evaluation of Existing Methods for the Prediction of Axial Fatigue Life from Tensile Data," *Int. J. Fatigue*, **15**, 13–19, 1993.
35. J.-H. Park and J.-H. Song, "Detailed Evaluation of Methods for Estimation of Fatigue Properties," *Int. J. Fatigue*, **17**, 365–373, 1995.
36. W. G. Clark, Jr., "Fracture Mechanics in Fatigue," *Exp. Mech.*, Sep., 1971.
37. P. C. Paris and F. Erdogan, "A Critical Analysis of Crack Propagation Laws," *Trans. ASME, J. Basic Eng.*, **85**, 528–534, 1963.
38. ASTM E 647-88a, "Standard Test Method for Measurement of Fatigue Crack Growth Rates," ASTM, Philadelphia, 1988.
39. J. Schijve, "Four Lectures on Fatigue Crack Growth," *Eng. Fracture Mech.*, **11**, 167–221, 1979.
40. L. P. Pook, *The Role of Crack Growth in Metal Fatigue*, Metals Society, London, 1983.

41. R. I. Stephens, A. Fatemi, R. R. Stephens, and H. O. Fuchs, *Metal Fatigue in Engineering*, 2nd ed., Wiley, New York, 2001.
42. S. J. Maddox, *Fatigue Strength of Welded Structures*, 2nd ed., Abington, Cambridge, England, 1991.
43. W. Elber, "Fatigue Closure under Cyclic Loading," *Eng. Fracture Mech.*, **2**, 37–45, 1970.
44. J. C. Newman and W. Elber (Eds.), *Mechanics of Fatigue Crack Closure*, STP-982, ASTM, Philadelphia, 1988.
45. D. Broek, *Elementary Engineering Fracture Mechanics*, 4th ed., Kluwer, London, 1986.
46. W. G. Reuter, J. H. Underwood, and J. C. Newman (Eds.), *Surface-Crack Growth: Models, Experiments and Structures*, STP-1060, ASTM, Philadelphia, 1990.
47. R. D. Ritchie and J. Lankford (Eds.), *Small Fatigue Cracks*, Metallurgical Society, Warrendale, PA, 1986.
48. R. C. Juvinall, *Engineering Considerations of Stress, Strain, and Strength*, McGraw-Hill, New York, 1967.
49. O. D. Sherby, R. L. Orr, and J. E. Dorn, "Creep Correlations of Metals at Elevated Temperatures," *J. Metals*, **6**, 71–80, 1954.
50. M. A. Meyers and K. K. Chawla, *Mechanical Behavior of Materials*, 2nd ed. Cambridge University Press, Cambridge, UK, 2009.
51. O. D. Sherby and A. K. Miller, "Combining Phenomenology and Physics in Describing the High Temperature Mechanical Behavior of Crystalline Solids," *J. Eng. Mat. Tech., Trans. ASME*, **101**, 387–395, 1979.
52. F. R. Nabarro, *Report of a Conference on Strength of Solids*, Physical Society, London, 75, 1948.
53. C. Herring, "Diffusional Viscosity of a Polycrystalline Solid," *Jo. Appl. Phys.*, **21**, 437–445, 1950.
54. R. L. Coble, "A Model for Boundary Diffusion Controlled Creep in Polycrystalline Materials," *Jo. Appl. Phys.*, **34**, 1679–1682, 1963.
55. L. Harper and J. E. Dorn, "Viscous Creep of Aluminum near Its Melting temperature," *Acta Metall*, **5**, 654–665, 1957.
56. J. Weertman, "Steady-State Creep of Crystals," *J. Appl. Phys.*, **28**, 1185–1189, 1957.
57. F. R. Larson and J. Miller, "Time-Temperature Relationships for Rupture and Creep Stresses," *ASME Trans.*, **74**, 765, 1952.
58. B. Josef, *Creep Mechanics*, Springer, Berlin, 2003.
59. N. H. Polakowski and E. J. Ripling, *Strength and Structure of Engineering Materials*, Prentice-Hall, Englewood Cliffs, NJ, 1966.
60. R. G. Sturm, C. Dumont, and F. M. Howell, "A Method of Analyzing Creep Data," *ASME Trans.*, **58**, A62, 1936.
61. H.-T. Yao, F.-Z. Xuan, Z. Wang, and S.T. Tu, "A Review of Creep Analysis and Design under Multiaxial Stress States," *Nucl. Eng. Design*, **237**, 1969–1986, 2007.
62. J. T. Boyle and J. Spence, *Stress Analysis for Creep*, Camelot Press, London, 1983.
63. K. Kraus, *Creep Analysis*, J Wiley, New York, 1980.
64. K. Yagi, K. Kubo, O. Kamemaru, and C. Tanaka, "Damage Evaluation and Life Prediction under Creep-Fatigue Loading Condition for Austenitic Stainless Steel and Low Alloy Steel," in *High Temperature Creep-Fatigue*, London, 1988, pp. 115–135.
65. M. E. Kassner and T. A. Hayes, "Creep Cavitation in Metals," *Int. J. Plasticity*, **19**, 1715–1748, 2003.
66. J. R. Rice and D. M. Tracey, "On Ductile Enlargement of Voids in Triaxial Stress Fields," *J. Mech. Phys Solids*, **17**, 201–217, 1969.
67. A. L. Gurson, "Continuum Theory of Ductile Rupture by Void Nucleation and Growth. Part I: Yield Criteria and Flow Rules for Porous Ductile Media," *J. Eng. Mat. Tech.*, **99**, 2–15, 1977.
68. F. A. McClintock, "A Criterion for Ductile Fracture by Growth of Holes," *J. Appl. Mech.*, **35**, 363–371, 1968.
69. D. Hull and E. Rimmer, "The Growth of Grain Boundary Voids under Stress," *Phil. Mag.*, **4**, 673–687, 1959.
70. M. V. Speight and W. Beere, "Vacancy Potential and Void Growth on Grain Boundaries," *Metal Sci. J.*, **9**, 190–191, 1975.

71. A. C. F. Cocks and M. F. Ashby, "Intergranular Fracture During Power-Law Creep under Multiaxial Stresses," *Metal Sci.*, **14**, 395–402, 1980.
72. A. C. F. Cocks and M. F. Ashby, "On Creep Fracture by Void Growth," *Prog. Mat. Sci.*, **27**, 189–244 1982.
73. A. C. F. Cocks and M. F. Ashby, "Creep Fracture by Coupled Power-Law Creep and Diffusion under Multi-axial Stress," *Metal Sci.*, **16**, 465–474, 1982.
74. B. F. Dyson, "Constraints on Diffusional Cavity Growth Rates," *Metal Sci.*, **10**, 349–353 (1976).
75. T. J. Delph, "Some Selected Topics in Creep Cavitation," *Metall. Mat. Trans.*, **33A**, 383–390, 2002.
76. J. A. Collins, "Fretting-Fatigue Damage-Factor Determination," *J. Eng. Ind.*, **87**(8), 298–302, 1965.
77. D. Godfrey, "Investigation of Fretting by Microscopic Observation," NACA Report 1009, Cleveland, OH, 1951 (formerly TN-2039, Feb. 1950).
78. F. P. Bowden and D. Tabor, *The Friction and Lubrication of Solids*, Oxford University Press, Amen House, London, 1950.
79. D. Godfrey and J. M. Baily, "Coefficient of Friction and Damage to Contact Area During the Early Stages of Fretting; I-Glass, Copper, or Steel Against Copper," NACA TN-3011, Cleveland, OH, Sept., 1953.
80. M. E. Merchant, "The Mechanism of Static Friction," *J. Appl. Phys.*, **11**(3), 232, 1940.
81. E. E. Bisson, R. L. Johnson, M. A. Swikert, and D. Godfrey, "Friction, Wear, and Surface Damage of Metals as Affected by Solid Surface Films," NACA TN-3444, Cleveland, OH, May, 1955.
82. H. H. Uhlig, "Mechanisms of Fretting Corrosion," *J. Appl. Mech.*, **76**, 401–407, 1954.
83. I. M. Feng and B. G. Rightmire, "The Mechanism of Fretting," *Lubrication Eng.*, **9**, 134ff, June, 1953.
84. I. M. Feng, "Fundamental Study of the Mechanism of Fretting," Final Report, Lubrication Laboratory, Massachusetts Institute of Technology, Cambridge, MA, 1955.
85. H. T. Corten, "Factors Influencing Fretting Fatigue Strength," T. & A. M. Report No. 88, Department of Theoretical and Applied Mechanics, University of Illinois, Urbana, IL, June, 1955.
86. W. L. Starkey, S. M. Marco, and J. A. Collins, "Effects of Fretting on Fatigue Characteristics of Titanium-Steel and Steel-Steel Joints," Paper 57-A-113, ASME, New York, 1957.
87. W. D. Milestone, "Fretting and Fretting-Fatigue in Metal-to-Metal Contacts," Paper 71-DE-38, ASME, New York, 1971.
88. G. P. Wright and J. J. O'Connor, "The Influence of Fretting and Geometric Stress Concentrations on the Fatigue Strength of Clamped Joints," *Proc. Inst. Mech. Eng.*, **186**, 1972.
89. R. B. Waterhouse, *Fretting Corrosion*, Pergamon, New York, 1972.
90. "Fretting in Aircraft Systems," AGARD Conference Proceedings CP161, distributed through NASA, Langley Field, VA, 1974.
91. "Control of Fretting Fatigue," Report No. NMAB-333, National Academy of Sciences, National Materials Advisory Board, Washington, DC, 1977.
92. N. P. Suh, S. Jahanmir, J. Fleming, and E. P. Abrahamson, "The Delamination Theory of Wear-II," Progress Report, Materials Processing Lab, Mechanical Engineering Dept., MIT Press, Cambridge, MA, Sept. 1975.
93. J. T. Burwell, Jr., "Survey of Possible Wear Mechanisms," *Wear*, **1**, 119–141, 1957.
94. M. B. Peterson, M. K. Gabel, and M. J. Derine, "Understanding Wear"; K. C. Ludema, "A Perspective on Wear Models"; E. Rabinowicz, "The Physics and Chemistry of Surfaces"; J. McGrew, "Design for Wear of Sliding Bearings"; R. G. Bayer, "Design for Wear of Lightly Loaded Surfaces," *ASTM Standard. News*, **2**(9), 9–32, 1974.
95. P. A. Engel, "Predicting Impact Wear," *Mach. Design*, May, 100–105, 1977.
96. P. A. Engel, *Impact Wear of Materials*, Elsevier, New York, 1976.
97. J. A. Collins, "A Study of the Phenomenon of Fretting-Fatigue with Emphasis on StressField Effects," Dissertation, Ohio State University, Columbus, OH, 1963.
98. J. A. Collins and F. M. Tovey, "Fretting Fatigue Mechanisms and the Effect of Direction of Fretting Motion on Fatigue Strength," *J. Mat.*, **7**(4), Dec. 1972.



99. W. D. Milestone, "An Investigation of the Basic Mechanism of Mechanical Fretting and Fretting-Fatigue at Metal-to-Metal Joints, with Emphasis on the Effects of Friction and Friction-Induced Stresses," Dissertation, Ohio State University, Columbus, 1966.
100. J. A. Collins and S. M. Marco, "The Effect of Stress Direction During Fretting on Subsequent Fatigue Life," *ASTM Proc.*, **64**, 547, 1964.
101. H. Lyons, "An Investigation of the Phenomenon of Fretting-Wear and Attendant Parametric Effects towards Development of Failure Prediction Criteria," Ph.D. Dissertation, Ohio State University, Columbus, OH, 1978.
102. P. L. Ko, "Experimental Studies of Tube Fretting in Steam Generators and Heat Exchangers," ASME/CSME Pressure Vessels and Piping Conference, Nuclear and Materials Division, Montreal, Canada, June 1978.
103. R. B. Heywood, *Designing against Fatigue of Metals*, Reinhold, New York, 1962.
104. F. P. Bowden and D. Tabor, *Friction and Lubrication*, Methuen, London, 1967.
105. E. Rabinowicz, *Friction and Wear of Materials*, Wiley, New York, 1966.
106. C. Lipson, *Wear Considerations in Design*, Prentice-Hall, Englewood Cliffs, NJ, 1967.
107. N. P. Suh, "The Delamination Theory of Wear," *Wear*, **25**, 111–124, 1973.
108. J. E. Shigley and C. R. Mischke, *Mechanical Engineering Design*, 5th ed., McGraw-Hill, New York, 1989.
109. "Corrosion Costs and Preventive Strategies in the United States," NACE Report; available at: <http://www.nace.org/uploadedFiles/Publications/ccsupp.pdf>.
110. M. G. Fontana and N. D. Greene, *Corrosion Engineering*, 2nd ed., McGraw-Hill, New York, 1978.
111. L. S. Seabright and R. J. Fabian, "The Many Faces of Corrosion," *Mat. Design Eng.*, **57**(1), 1963.
112. G. Nelson, *Corrosion Data Survey*, National Association of Corrosion Engineers, Houston, TX, 1972.
113. H. H. Uhlig (Ed.), *Corrosion Handbook*, Wiley, New York, 1948.
114. E. Rabald, *Corrosion Guide*, Elsevier, New York, 1951.

# CHAPTER 21

## FAILURE ANALYSIS OF PLASTICS

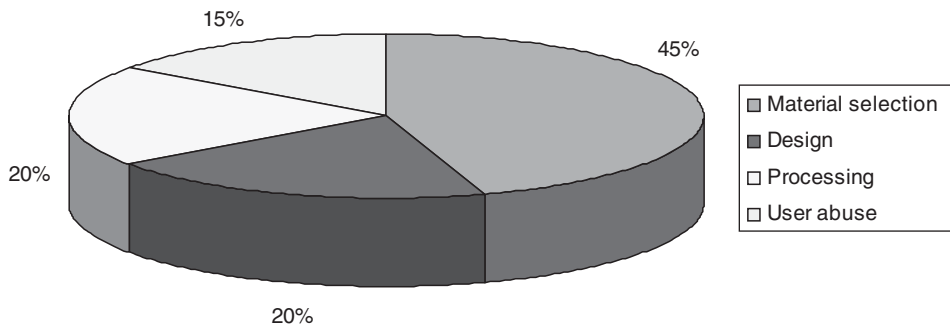
**Vishu Shah**  
Consultek Consulting Group  
Diamond Bar, California

<b>1 INTRODUCTION</b>	<b>771</b>	3.3 Stress Analysis	780
1.1 Material Selection	772	3.4 Heat Reversion (ASTM F1057)	782
1.2 Design	773	3.5 Microtoming (Microstructural Analysis)	783
1.3 Process	775	3.6 Mechanical Testing	784
1.4 Service Conditions	775	3.7 Thermal Analysis	785
<b>2 TYPES OF FAILURES</b>	<b>776</b>	3.8 Nondestructive Testing Techniques	785
2.1 Mechanical Failure	776	3.9 Fractography (ASTM C1145)	785
2.2 Thermal Failure	777	3.10 Simulation Testing	785
2.3 Chemical Failure	777		
2.4 Environmental Failure	777	<b>BIBLIOGRAPHY</b>	<b>786</b>
<b>3 ANALYZING FAILURES</b>	<b>777</b>		
3.1 Visual Examination	779		
3.2 Identification Analysis	779		

### 1 INTRODUCTION

The fundamental problem concerning the failures of parts made out of plastics materials is a lack of understanding of the difference between the nature of relatively new polymeric materials and traditional materials such as metal, wood, and ceramics. Designers, processors, and end users are all equally responsible in contributing to the problem. Merely copying a metal or wood product with some minor aesthetic changes can lead to premature and sometimes catastrophic failures. Designers are generally most familiar with metals and their behavior under load and varying conditions of temperature and environment. While designing metal parts, a designer can rely on instantaneous stress–strain properties and for most applications can disregard the effect of temperature, environment, and long-term load (creep). Plastics materials are viscoelastic in nature, and unlike other materials, properties can vary considerably under the influence of temperature, load, environment, and presence of chemicals. For example, a well-designed part may perform its intended function for a very long time at room temperature environment and under normal load. The same part may fall apart quickly when exposed to extreme cold or hot environment and the process can accelerate if it is subjected to mechanical loading or exposed to a chemical environment. Most often overlooked is the synergistic effect of all the conditions, such as temperature, creep, chemicals, ultraviolet (UV), and other environmental factors, on plastic parts. During processing, plastic materials are subjected to severe physical conditions involving elevated temperatures, high pressures, and high-shear-rate flow as well as chemical changes. The processor must follow the proper procedures and guidelines set forth by material suppliers and make sure that the material is processed optimally in well-maintained equipment. Lastly, end users must be educated by product manufacturers in the proper use of the plastics





**Figure 1** Major reasons for plastics product failures. Reprinted with permission from Rapra Technology Ltd.

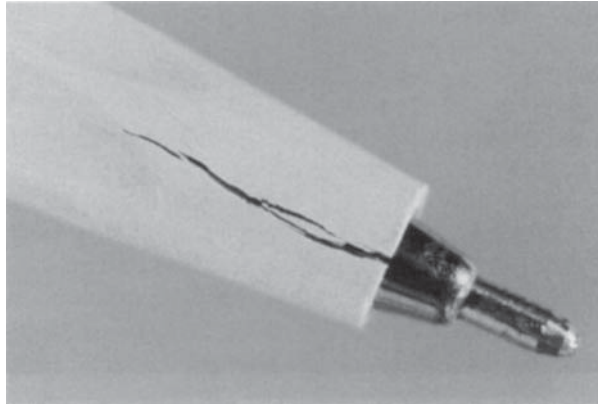
products and make sure that they are used for the intended purpose. Plastic parts often fail prematurely because of intentional or unintentional abuse by consumers.

Part failure is generally related to one of four key factors: material selection, design, process, and service conditions. Figure 1 shows reasons for plastic product failures.

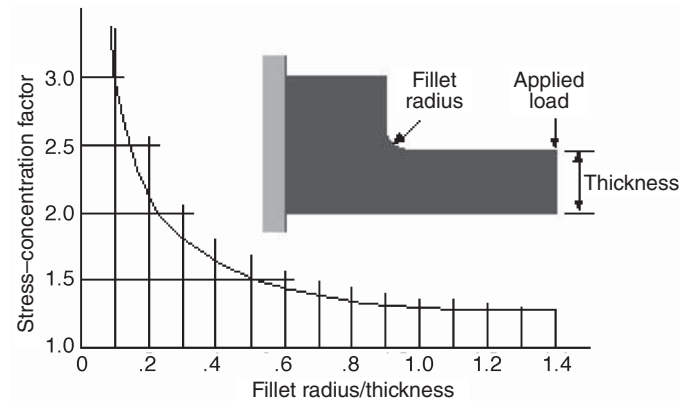
### 1.1 Material Selection

Failures arising from hasty material selection are not uncommon in the plastics or any other industry. In an application that demands high-impact resistance, a high-impact material must be specified. If the material is to be used outdoors for a long period, a UV-resistant material must be specified. For proper material selection, careful planning, a thorough understanding of plastic materials, and reasonable prototype testing are required. The material selection should not be based solely on cost. A systematic approach to the material selection process is necessary to select the best material for any application. The proper material selection technique starts with carefully defining the application requirements in terms of mechanical, thermal, environmental, electrical, and chemical properties. In many instances, it makes sense to design a thinner wall part, taking advantage of the stiffness-to-weight ratio offered by higher priced, fast-cycling engineering materials. All special needs such as outdoor UV exposure, light transmission, fatigue, creep and stress relaxation, and regulatory requirements must be considered. Processing techniques and assembly methods play a key role in selecting the appropriate material and should be given consideration. Many plastic materials are susceptible to chemical attack, and therefore the behavior of plastic material in a chemical environment is one of the most important considerations in selecting the material. No single property defines a material's ability to perform in a given chemical environment, and factors such as external or molded-in stresses, length of exposure, temperature, and chemical concentration should be carefully scrutinized. Many companies, including material suppliers, have developed software to assist in material selection simply by selecting the application requirement in the order of importance.

Some common pitfalls in the material selection process are relying on published material property data, misinterpretation of data sheets, and blindly accepting the material supplier's recommendations. Material property data sheets should only be used for screening various types and grades of materials and not for ultimate selection or engineering design. The reported data are generally derived from short-term tests and single-point measurements under laboratory conditions using standard test bars. The published values are generally higher and do not correlate well with actual-use conditions. Such data do not take into account the effect of time, temperature, environment, and chemicals. Figure 2 shows a typical failure arising from improper material selection.



**Figure 2** Failure arising from improper material selection.




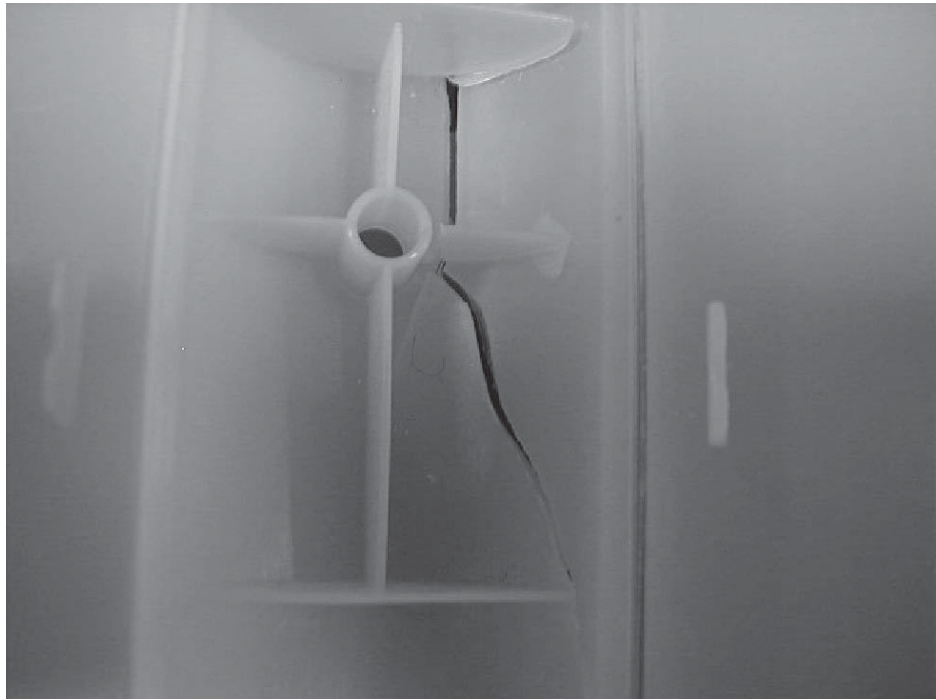
**Figure 3** Influence of fillet radius on stress concentration.

## 1.2 Design

Proper material selection alone will not prevent a product from failing. While designing a plastic product, the designer must use the basic rules and guidelines provided by the material supplier for designing a particular part in that material. One must remember that with the exception of a few basic rules in designing plastic parts, the design criteria change from material to material as well as from application to application. The most common mistakes made by designers when working in plastics are related to wall thickness, sharp corners, creep, draft, environmental compatibility, and placement of ribs. Failure arising from designing parts with sharp corners (insufficient radius) by far exceeds all other reasons for part failures. Stresses build rapidly in internal sharp corners of the part, as shown in Fig. 3, which illustrates the influence of fillet radius on stress concentration. Maintaining uniform wall thickness is essential in keeping sink marks, voids, warpage, and more importantly areas of molded-in stresses to a minimum. The viscoelastic nature of plastic materials as opposed to metals requires designers to pay special attention to creep and stress relaxation data. Plastic parts will deform under load over time depending upon the type of material, amount of load, length of time, and temperature. Design guides for proper plastic part design are readily available from material suppliers. Table 1 shows a typical part design checklist. Figure 4 illustrates a typical part failure arising from improper design.

Table 1 Part Design Checklist

<b>Part Design Checklist</b> for injection molded engineering thermoplastics		<b>MILES</b>  <b>Polymers Division</b>
<b>Material Selection Requirements</b>		
<input type="checkbox"/> <b>LOADS</b>	___ Magnitude	___ Duration ___ Impact ___ Fatigue ___ Wear
<input type="checkbox"/> <b>ENVIRONMENT</b>	___ Temperature	___ Chemicals ___ Humidity ___ Cleaning agents
	___ Lubricants	___ U.V. light
<input type="checkbox"/> <b>SPECIAL</b>	___ Transparency	___ Paintability ___ Warpage/Shrinkage
	___ Plateability	___ Flammability ___ Cost ___ Agency test
<b>Part Details Review</b>		
<input type="checkbox"/> <b>RADII</b>	___ Sharp corners	___ Ribs ___ Bosses ___ Lettering
<input type="checkbox"/> <b>WALL THICKNESS</b>		
	• Material ___ Strength	___ Electrical ___ Flammability
	• Flow ___ Flow length	___ Too thin ___ Thin to thick
	___ Picture framing	___ Orientation
	• Uniformity ___ Thick areas	___ Thin areas ___ Abrupt changes
<input type="checkbox"/> <b>RIBS</b>	___ Radii	___ Draft ___ Height ___ Spacing
	___ Base thickness	
<input type="checkbox"/> <b>BOSSSES</b>	___ Radii	___ Draft ___ Inside diameter/outside diameter
	___ Base thickness	___ Length/diameter
<input type="checkbox"/> <b>WELD LINES</b>	___ Proximity to load	___ Strength vs. load ___ Visual area
<input type="checkbox"/> <b>DRAFT</b>	___ Draw polish	___ Texture depth ___ 1/2 degree (minimum)
<input type="checkbox"/> <b>TOLERANCE</b>	___ Part geometry	___ Material
	___ Tool design (across parting line, slides)	
<b>Assembly Considerations</b>		
<input type="checkbox"/> <b>PRESS FIT</b>	___ Tolerances	___ Long-term retention ___ Hoop stress
<input type="checkbox"/> <b>SNAP FIT</b>	___ Allowable strain	___ Assembly force
	___ Tapered beam	___ Multiple assembly
<input type="checkbox"/> <b>SCREWS</b>	___ Thread-cutting vs. forming	___ Avoid countersinks
<input type="checkbox"/> <b>MOLDED THREAD</b>	___ Avoid feather-edges, sharp corners and pipe threads	
<input type="checkbox"/> <b>ULTRASONICS</b>	___ Energy director	___ Shear joint interference
	___ Wall thickness	___ Hermetic seal
<input type="checkbox"/> <b>ADHESIVE &amp; SOLVENT BONDS</b>	___ Shear vs. butt joint	___ Compatibility
	___ Trapped vapors	
<input type="checkbox"/> <b>GENERAL</b>	___ Interfit tolerances	___ Stack tolerances ___ Thermal expansion
	___ Care with rivets and molded-in inserts	___ Component compatibility
<b>Mold Concerns</b>		
<input type="checkbox"/> <b>WARPAGE</b>	___ Cooling (corners)	___ Ejector placement
<input type="checkbox"/> <b>GATES</b>	___ Type	___ Size ___ Location
<input type="checkbox"/> <b>RUNNERS</b>	___ Size and shape	___ Sprue size ___ Balanced flow
	___ Cold slug well	___ Sharp corners
<input type="checkbox"/> <b>GENERAL</b>	___ Draft	___ Part ejection ___ Avoid thin/long cores



**Figure 4** Brittle failure due to sharp corner (lack of radius) on part.

### 1.3 Process

After proper material selection and design, the responsibility shifts from the designer to the plastic processor. The most innovative design and a very careful material selection cannot make up for poor processing practices. Molded-in stresses, voids, weak weld lines, and moisture in the material are some of the most common causes for premature product failures.

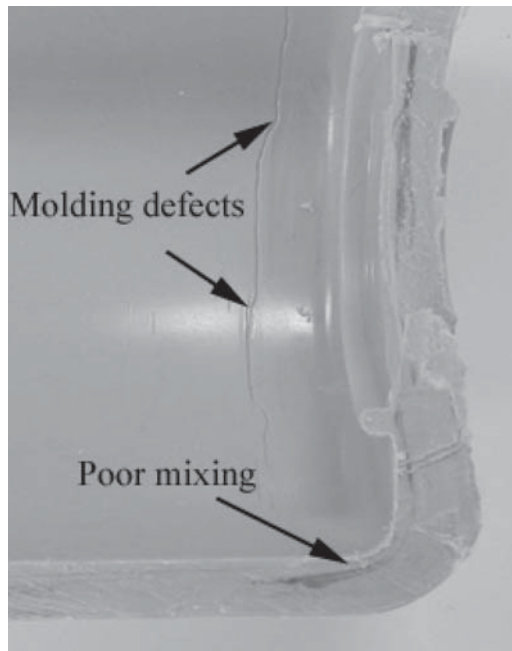
The latest advancement in process control technology not only allows the processors to control the process with a high degree of reliability but also helps in recordkeeping should a product fail at a later date. Such records of processing parameters are invaluable to a person conducting failure analysis. Any assembly or secondary operation on a processed part must be evaluated carefully to avoid premature failures. Failures arising from stress cracking around metal inserts, drilled holes, and welded joints are quite common. Part failure resulting from poor processing practices is shown in Fig. 5.

### 1.4 Service Conditions

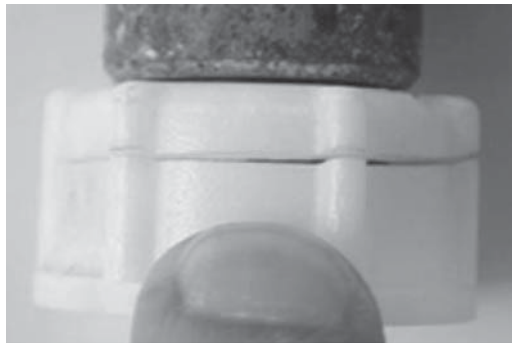
In spite of warning labels and user's instructions, failures arising from service conditions are quite common in the plastics industry. Five categories of unintentional service conditions are as follows:

1. Reasonable misuse
2. Use beyond intended lifetime
3. Unstable service conditions
4. Beyond reasonable misuse
5. Simultaneous application of two stresses operating synergistically

Figure 6 shows a failed nut due to overtightening by the consumer.



**Figure 5** Failure as result of poor processing practices. Courtesy of The Madison Group.



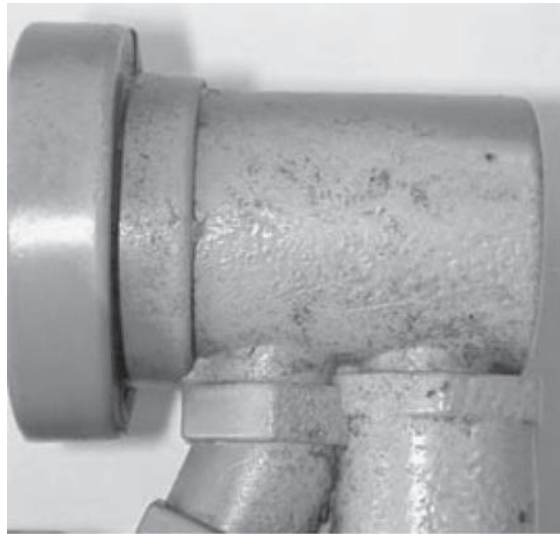
**Figure 6** Failed nut due to overtightening nut from a water supply line. Courtesy of The Madison Group.

Most stresses imposed on plastic products in service can be grouped under thermal, chemical, physical, biological, mechanical, and electrical.

## 2 TYPES OF FAILURES

### 2.1 Mechanical Failure

Mechanical failure arises from applied external forces which, when they exceed the yield strength of the material, cause the product to deform, crack, or break into pieces. The force



**Figure 7** Polystyrene (PS) degraded by prolonged contact with gasoline. Courtesy of The Madison Group.

may have been applied in tension, compression, and impact for a short or a long period of time at varying temperatures and humidity conditions.

## 2.2 Thermal Failure

Thermal failures occur from exposing products to an extremely hot or extremely cold environment. At abnormally high temperatures the product may warp, twist, melt, or even burn. Plastics tend to get brittle at low temperatures. Even the slightest amount of load may cause the product to crack or even shatter.

## 2.3 Chemical Failure

Very few plastics are totally impervious to all chemicals. Failure occurring from exposing the products to certain chemicals is quite common. Residual or molded-in stress, high temperatures, and external loading tend to aggravate the problem. Figure 7 illustrates failure of a product from chemical attack.

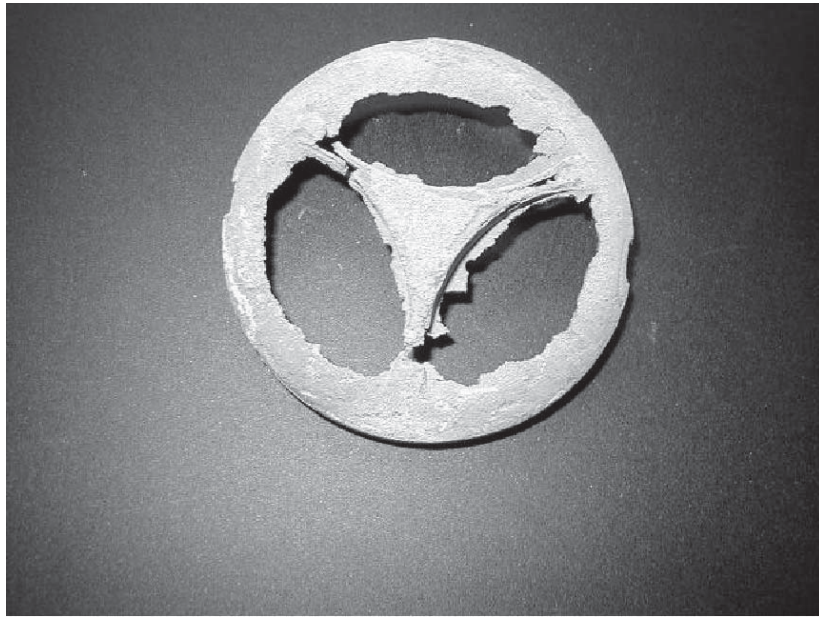
## 2.4 Environmental Failure

Plastics exposed to outdoor environments are susceptible to many types of detrimental factors. Ultraviolet rays, humidity, microorganisms, ozone, heat, and pollution are major environmental factors that seriously affect plastics. The effect can be a mere loss of color, slight crazing and cracking, or complete breakdown of the polymer structure. A typical product failure arising from weathering effects is shown in Fig. 8.

# 3 ANALYZING FAILURES

The first step in analyzing any type of failure is to determine the cause of the failure. Before proceeding with elaborate tests, some basic information regarding the product must be gathered.





**Figure 8** Failure occurring in plastics part due to prolonged exposure and resulting degradation from UV rays.

If the product is returned from the field, the district manager or consumer should be asked for basic information such as the date of purchase, date of installation, date when the first failure encountered, geographic location, types of chemicals used with or around the product, and whether the product was used indoors or outdoors. This information is vital if one is to analyze the defective product proficiently. For example, if the report from the field indicates a certain type of chemical was used with the product, one can easily check the chemical compatibility of the product or go one step further and simulate the actual-use condition with that chemical. Recordkeeping also simplifies the task of failure analysis. A simple date code or cavity identification number will enhance the traceability. Many types of checklists to help analyze the failures have been developed. Ten basic methods are employed to analyze product failure:

1. Visual examination
2. Identification analysis
3. Stress analysis
4. Heat reversion technique
5. Microtoming (microstructural analysis)
6. Mechanical testing
7. Thermal analysis
8. Nondestructive testing (NDT) techniques
9. Fractography
10. Simulation testing

By zeroing in on the type of failure, one can easily select the appropriate method of failure analysis.

### 3.1 Visual Examination

A careful visual examination of the returned part can reveal many things. Excessive splay marks indicate that the materials were not adequately dried before processing. The failure to remove moisture from hygroscopic materials can lower the overall physical properties of the molded article and in some cases even cause them to become brittle. The presence of foreign material and other contaminants is also detrimental and could have caused the part to fail. Burn marks on molded articles are easy to detect. They are usually brown streaks and black spots. These marks indicate the possibility of material degradation during processing, causing the breakdown of molecular structure and leading to overall reduction in the physical properties. Sink marks and weak weld lines, readily visible on molded parts, represent poor processing practices and may contribute to part failure.

A careful visual examination will also reveal the extent of consumer abuse. The presence of unusual chemicals, grease, pipe dope, and other substances may give some clues. Heavy marks and gouges could be the sign of excessively applied external force.

The defective part should also be cut in half using a sharp saw blade. The object here is to look for voids caused by trapped gas and excessive shrinkage, especially in thick sections during molding. A reduction in wall thickness caused by such voids could be less than adequate for supporting compressive or tensile force or withstanding impact load and may cause a part to fail. Lastly, if the product has failed because of exposure to UV rays and other environmental factors, a slight chalking, microscopic cracks, large readily visible cracks, or loss of color will be evident.

### 3.2 Identification Analysis

One of the main reasons for product failure is use of the wrong material. When a defective product is returned from the field, material identification tests must be carried out to verify that the material used in the defective product is, in fact, the material specified on the product drawing. However, identifying the type of material is simply not enough. Since all plastic materials are supplied in a variety of grades with a broad range of properties, the grade of material must also be determined. A simple technique such as the melt index test can be carried out to confirm the grade of a particular type of material. The percentage of regrind material mixed with virgin material has a significant effect on the physical properties. Generally, the higher the level of regrind material mixed with virgin, the lower the physical properties. If during processing higher than recommended temperature and long residence time are used, chances are the material will degrade. This degraded material, when reground and mixed with virgin material, can cause a significant reduction in overall properties. Unfortunately, the percentage of regrind used with virgin material is almost impossible to determine by performing tests on the molded parts. However, a correlation between the melt index value and the part failure rate can be established by conducting a series of tests to determine the minimum or maximum acceptable melt index value.

Part failures due to impurities and contamination of virgin material are quite common. Material contamination usually occurs during processing. A variety of purging materials are used to purge the previous material from the extruder barrel before using the new material. Not all of these purging materials are compatible. Such incompatibility can cause the loss of properties, brittleness, and delamination. In the vinyl compounding operation, failure to add key ingredients, such as an impact modifier, can result in premature part failure. Simple laboratory techniques cannot identify such impurities, contamination, or the absence of a key ingredient. More sophisticated techniques, such as Fourier transform infrared (FTIR) analysis and gel permeation chromatography (GPC), must be employed. These methods can not only identify the basic material but also point out the type and level of impurities in most cases. Plastic materials



are rarely manufactured without some type of additives. These additives play an important role in thermally or environmentally stabilizing the base polymer. Antioxidants, flame retardants, UV stabilizers, heat stabilizers, and lubricants are routinely added for enhancement. If for some reason these important additives are left out or depleted due to poor processing practices, plastic parts may fail prematurely. Techniques such as deformation or reverse engineering a product are employed for separation, identification, and quantification of ingredients.

### 3.3 Stress Analysis

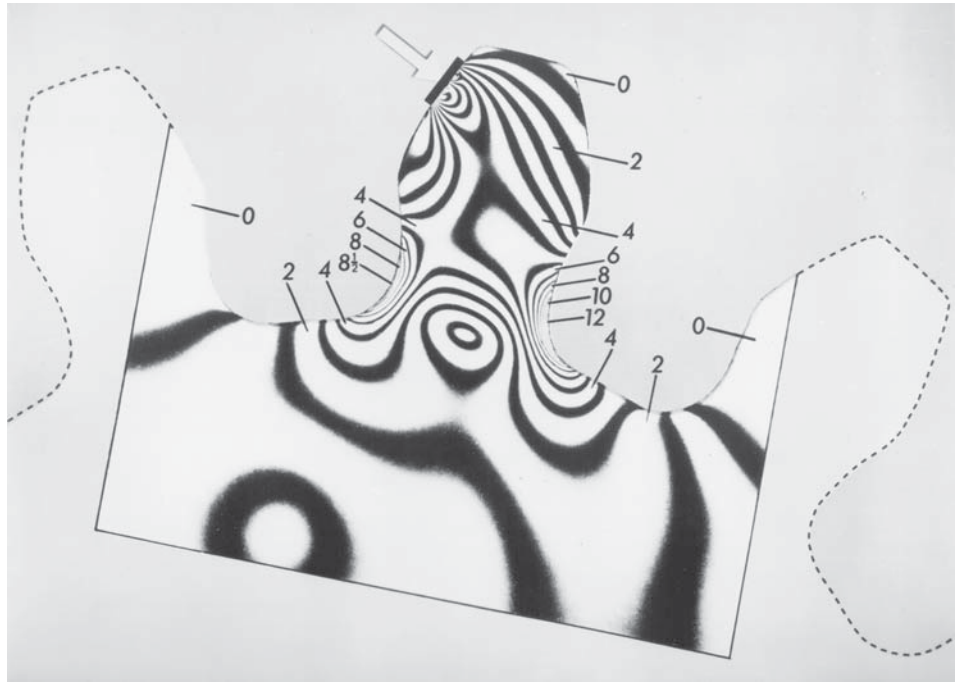
Once the part failure resulting from poor molding practices or improper material usage through visual examination and material identification is ruled out, the next logical step is to carry out an experimental stress analysis. Experimental stress analysis is one of the most versatile methods for analyzing parts for possible failure. The part can be externally stressed or can have residual or molded-in stresses. External stresses or molded-in stresses or a combination of both can cause a part to fail prematurely. Stress analysis is an important part of failure identification. Detection of residual stresses has a different meaning than evaluation of stresses due to applied forces. It is possible of course to see failure due to poor design or underestimating forces. These failures are usually detected in proof testing or in early production. Residual stresses are different: A molding process can generate residual stress just about anywhere, anytime. Here, ongoing photoelastic inspection can prove extremely helpful, allowing detection of defective molded parts or identification of failures in clear plastic products. Experimental stress analysis can be conducted to determine the actual levels of stress in the part. Five methods are used to conduct stress analysis: photoelastic method, brittle-coating method, strain gauge method, chemical method, and heat reversion.

#### *Photoelastic Method*

The photoelastic method for experimental stress analysis is quite popular among design engineers and has proven to be an extremely versatile, yet simple technique.

If the parts to be analyzed are made of one of the transparent materials, stress analysis is simple. All transparent plastics, being birefringent, lend themselves to photoelastic stress analysis. The transparent part is placed between two polarizing media and viewed from the opposite side of the light source. The fringe patterns are observed without applying external stress. This allows the observer to study the molded-in or residual stresses in the part. High fringe order indicates the area of high stress level whereas low fringe order represents an unstressed area. Also, close spacing of fringes represents a high stress gradient. A uniform color indicates uniform stress in the part. Next, the part should be stressed by applying external force and simulating actual-use conditions. The areas of high stress concentration can be easily pinpointed by observing changes in fringe patterns brought forth by external stress. Figure 9 illustrates a typical stress pattern in a part. This type of evaluation is useful as a regular part of product inspection for quality control of transparent parts for any manufacturer to maintain product quality and consistency and to prevent failures. The method often reveals problems associated with many other process control parameters, such as temperature, material, fill rate, design, etc.

Another technique known as the photoelastic coating technique can be used to photoelastically stress analyze opaque plastic parts. The part to be analyzed is coated with a photoelastic coating, service loads are applied to the part, and the coating is illuminated by polarized light from the reflection polariscope. Molded-in or residual stresses cannot be observed with this technique. However, the same part can be fabricated using one of the transparent plastic materials. In summary, photoelastic techniques can be used successfully for failure analysis of a defective product.



**Figure 9** Typical photoelastic stress pattern. Courtesy of Micro-Measurements, Raleigh, NC, a brand of Vishay Precision Group.

#### ***Brittle-Coating Method***

The brittle-coating method is another technique of conveniently measuring the localized stresses in a part. Brittle coatings are specially prepared lacquers that are usually applied by spraying on the actual part. The part is subjected to stress after air drying the coating. The location of maximum strain and the direction of the principal strain is indicated by the small cracks that appear on the surface of the part as a result of external loading. Thus, the technique offers valuable information regarding the overall picture of the stress distribution over the surface of the part. The data obtained from the brittle coating method can be used to determine the exact areas for strain gauge location and orientation, allowing precise measurement of the strain magnitude at points of maximum interest. They are also useful for the determination of stresses at stress concentration points that are too small or inconveniently located for installation of strain gauges. The brittle-coating technique, however, is not suitable for detailed quantitative analysis such as photoelasticity. Sometimes it is necessary to apply an undercoating prior to the brittle coating to promote adhesion and to minimize compatibility problems. Further discussion on this subject is found in the literature (see the Bibliography).

#### ***Strain Gauge Method***

The electrical resistance strain gauge method is the most popular and widely accepted method for strain measurements. The strain gauge consists of a grid of strain-sensitive metal foil bonded to a plastic backing material. When a conductor is subjected to a mechanical deformation, its electrical resistance changes proportionally. This principle is applied in the operation of a strain

gauge. For strain measurements, the strain gauge is bonded to the surface of a part with a special adhesive and then connected electrically to a measuring instrument. When the test part is subjected to a load, the resulting strain produced on the surface of the part is transmitted to the foil grid. The strain in the grid causes a change in its length and cross section and produces a change in the resistivity of the grid material. This change in grid resistance, which is proportional to the strain, is then measured with a strain gauge recording instrument. In using strain gauges for failure analysis, care must be taken to test the adhesives for compatibility with particular plastics to avoid stress cracking problems.

Residual or molded-in stresses can be directly measured with strain gauges using the hole-drilling method. This method involves measuring a stress at a particular location, drilling a hole through the part to relieve the frozen-in stresses, and then remeasuring the stress. The difference between the two measurements is calculated as residual stress.

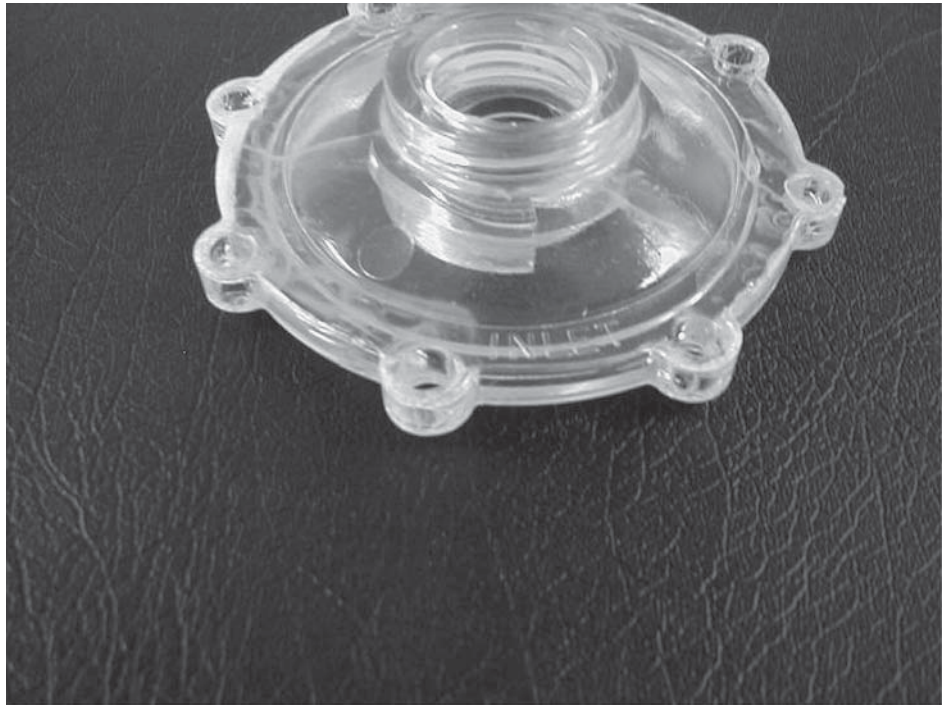
### ***Chemical Method***

When exposed to certain chemicals while under stress, most plastics show stress cracking. This phenomenon is used in the stress analysis of molded parts. The level of molded-in or residual stress can be determined by this method. The part is immersed in a mixture of glacial acetic acid and water for 2 min at 73°F and later inspected for cracks that occur where tensile stress at the surface is greater than the critical stress. The part may also be externally stressed to a predetermined level and sprayed with the chemical to determine critical stresses. Stress cracking curves for many types of plastics have been developed by material suppliers. If a defective product returned from the field appears to have stress cracked, similar tests should be carried out to determine molded-in stresses as well as the effect of external loading by simulating end-use conditions. Failures of such types are seen often in parts where metal inserts are molded in or inserted after molding. Three other tests— stain resistance test, solvent stress cracking resistance, and environmental stress cracking resistance (ESCR)—are also employed to analyze failed parts. The acetone immersion test to determine the quality of rigid polyvinyl chloride (PVC) pipe and fittings as indicated by their reaction to immersion in anhydrous acetone is very useful. An unfused PVC compound attacked by an anhydrous acetone causes the material to swell, flake, or completely disintegrate. A properly fused PVC compound is impervious to anhydrous acetone and only a minor swelling, if any, is observed. Defective PVC pipe or fittings returned from the field are subjected to this test for failure analysis.

Solvent stress analysis provides a quantitative means of determining stress levels in parts molded from various plastic materials. The test is primarily used in evaluating residual molded-in stress. The test is also very useful in determining the effect of external stress such as the ones induced by the screw, rivet, or insert used in assembly. Inherent stresses develop in molded parts as a result of injecting hot molten plastic material into a relatively cold mold. Such molecular orientation develops during the mold-filling phase as the melt is injected through the nozzle, runners, gates, and cavity. Internal stresses related to molecular orientation can lead to warpage or remain as internal stresses, reducing the durability and environmental stress crack resistance of the molded part. Highly stressed parts are attacked by solvents above its critical stress level. The net effect is crazing and cracking, which can be visually seen on the part. Figure 10 illustrates the result of solvent attack in terms of crazing and cracking around the highly stressed mounting holes.

## **3.4 Heat Reversion (ASTM F1057)**

All plastics manufacturing processes introduce some degree of stress in the finished product. The stresses in molded parts are commonly referred to as molded-in (residual) stresses. By reversing the process, by reheating the molded or extruded product, the presence of stress can



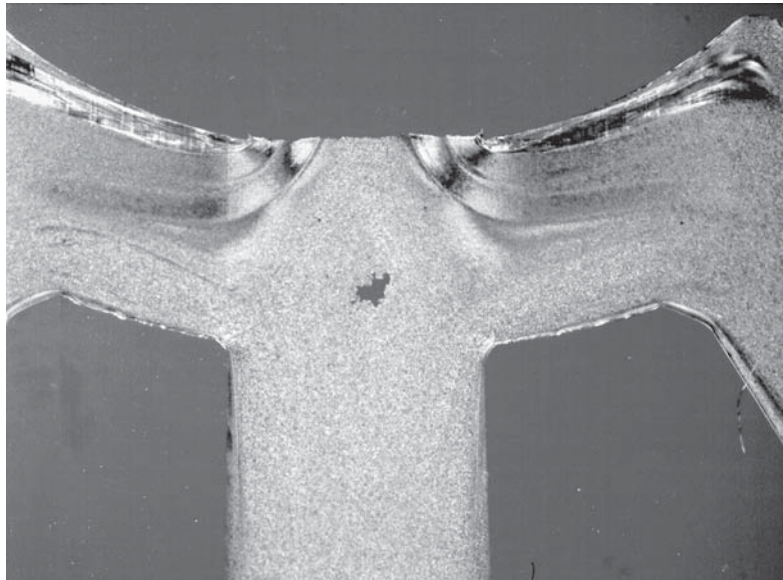
**Figure 10** Result of solvent attack in terms of crazing and cracking around highly stressed mounting holes.

be determined. The test is conducted by simply placing the entire specimen or a portion of the specimen in a thermostatically controlled, circulating air oven and subjecting to a predetermined temperature for a specified time. The specimens are visually examined for a variety of attributes. The degree and severity of warpage, blistering, wall separation, fish scaling, and distortion in the gate area of molded parts indicate the stress level. Stresses and molecular orientation effects in the plastic material are relieved, and the plastic starts to revert to a more stable form. The temperature at which this begins to occur is important. If changes start below the heat distortion temperature of the material, high levels of stress and flow orientation are indicated. The test has been significantly improved by new methods, including the attachment of strain gauges to critical regions of the part to carefully monitor initial changes in the shape. The American Society for Standards and Materials (ASTM) F1057 describes the standard practice for estimating the quality of extruded PVC pipe by heat reversion.

### 3.5 Microtoming (Microstructural Analysis)

Microtoming is a technique of slicing an ultrathin section from a molded plastic part for microscopic examination. This technique has been used by biologists and metallurgists for years, but only in the last decade has this technique been used successfully as a valuable failure analysis tool.

Microtoming begins with the skillful slicing of an 8–10- $\mu\text{m}$ -thick section from a part and mounting the slice on a transparent glass slide. The section is then examined under a light transmission microscope equipped with a polarizer for photoelastic analysis. A high-power



**Figure 11** Shrinkage voids created by insufficient time and pressure to freeze the gates during injection-molding process. Courtesy of BASF Corp.

(1000 $\times$ ) microscope which will permit photographic recording of the structure in color is preferred. By examining the microstructure of a material, much useful information can be derived. For example, microstructural examination of a finished part that is too brittle may show that the melt temperature was either nonuniform or too low. The presence of unmelted particles is usually evident in such cases. Another reason for frequent failures of the injection-molded part is failure to apply sufficient time and pressure to freeze the gates. This causes the parts to be underpacked, which creates center-wall shrinkage voids. Figure 11 illustrates such shrinkage voids. Voids tend to reduce the load-bearing capabilities and toughness of a part through the concentration of stress in a weak area. Contamination, indicated by abnormality in the microstructure, almost always creates some problems. Contamination caused by the mixing of different polymers can be detected through such analysis by carefully studying the differences in polymer structures. Quite often, a poor pigment dispersion also causes parts to be brittle. This is readily observable through the microtoming technique. To achieve optimum properties, additives such as glass fibers and fillers must disperse properly. Microtoming a glass-fiber-reinforced plastic part reveals the degree of bonding of the glass fiber to the resin matrix as well as the dispersion and orientation of glass fibers. Molded-in stresses as well as stresses resulting from external loading are readily observed under cross-polarized light because of changes in birefringence when the molecular structure is strained. Microtoming can also be applied to check the integrity of spin and ultrasonic or vibration welds.

### 3.6 Mechanical Testing

Defective product returned from the field is often subjected to a variety of mechanical tests to determine the integrity of the product. Two basic methods are employed. The first one involves conducting mechanical tests such as tensile, impact, or compression on the actual part or a small sample cut from the part. The test results are then compared to the test results obtained



from the retained samples. The second method requires grinding the defective parts and either compression or injection molding standard test bars and conducting mechanical tests. The test results are compared to the published data for the virgin material. The amount of material available for molding the test bars quite often precludes injection molding. The test data obtained from compression-molded samples are generally lower than for injection-molded samples. Fatigue failure tests such as flexural fatigue or tensile fatigue can be employed to determine premature failure from cyclic loading.

### 3.7 Thermal Analysis

Thermal analysis techniques are used extensively in failure analysis. Three of the most popular techniques are differential scanning calorimetry (DSC), thermogravimetric analysis (TGA), and thermomechanical analysis (TMA). DSC is a technique in which the heat flow rate to the sample (differential power) is measured while the temperature of the sample, in a specified atmosphere, is programmed. Because all materials have a finite heat capacity, heating or cooling a sample specimen results in a flow of heat in or out of the sample. TGA is a test procedure in which changes in weight of a specimen are monitored as the specimen is progressively heated. The sample weight is continuously monitored as the temperature is increased either at a constant rate or through a series of steps. The components of a polymer or elastomer formulation volatilize or decompose at different temperatures. This leads to a series of weight loss steps that allow the components to be quantitatively measured. TMA is a thermal analysis technique consisting of measuring physical expansion or contraction of a material or changes in its modulus of viscosity as a function of temperature.

### 3.8 Nondestructive Testing Techniques

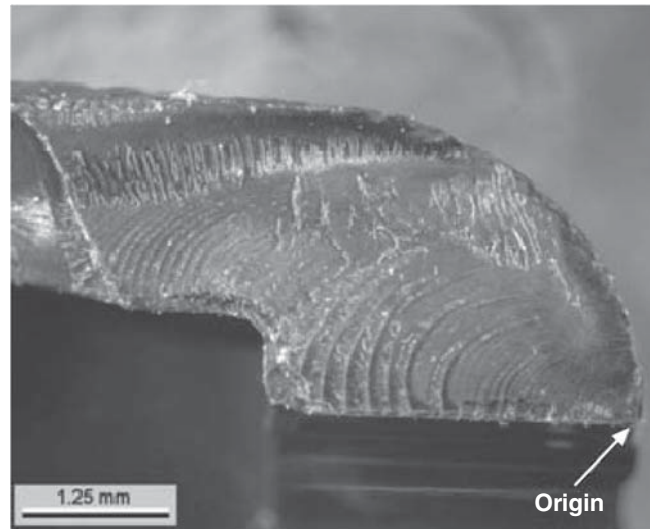
NDT techniques are useful in determining the flaws, discontinuities, and joints. In its simplest form, NDT involves measurement, weighing, visual examination, and looking for surface imperfections, weak knit lines, etc. Ultrasonic testing and acoustic emission are the most common techniques used for failure analysis.

### 3.9 Fractography (ASTM C1145)

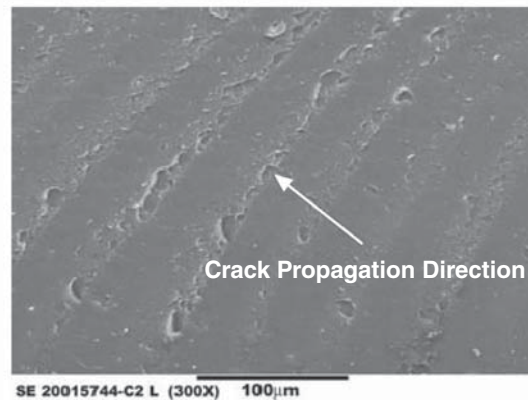
Fractography is one of the most valuable tools available for failure analysis. It differs from microstructural analysis techniques using a microtome, an instrument which slices a very thin section from a part for microscopic examination. Fractography is defined as the means and methods for characterizing a fractured specimen or component. By examining the exposed fractured surface and interpreting the crack pattern and fracture markings, one can determine the origin of the crack, direction of the crack propagation, failure mechanism, and stresses involved. On the microscopic scale, all fractures fall into one of the two categories: ductile and brittle. Ductile fractures are characterized by material tearing and exhibit gross plastic deformation. Brittle fractures display little or no microscopically visible plastic deformation and require less energy to form. Fracture analysis usually involves the unexpected brittle failure of normally ductile material. The scanning electron microscope (SEM) is the most widely used instrument for fractographic analysis. Figure 12 shows a micrograph of a failed specimen.

### 3.10 Simulation Testing

In many instances, by simulating certain conditions such as exposing a part similar to the one that has failed to chemicals and/or other environment, valuable knowledge concerning possible cause of failure can be gained.



(a)



(b)

**Figure 12** (a) Fatigue striations emanating from fracture origin of polycarbonate latch handle. (b) SEM micrograph of fatigue striations shown in (a). Courtesy of IMR Test Labs.

## BIBLIOGRAPHY

- A. J. Durelli, E. A. Phillips, and C. H. Tsao, *Introduction to the Theoretical and Experimental Analysis of Stress and Strain*, McGraw-Hill, New York, 1958.
- M. Ezrin, *Plastics Failure Guide Causes and Prevention*, Hanser Gardner, 1996, p. 154.
- J. P. Holman, *Experimental Methods for Engineers*, McGraw-Hill, New York, 1971, pp. 333–334.
- “Introduction to Stress Analysis by the Photoelastic Coating Technique,” Technical Bulletin IDCA-I, Photo-Elastic Division, Vishay Intertechnology, Raleigh, NC.
- S. Levy, “Product Testing, Insurance against Failure,” *Plastics Design Forum*, July–August 1984, p. 83.
- Measurements Group, Technical Bulletin, Vishay Intertechnology, Raleigh, NC.
- E. Miller, *Plastics Products Design Handbook*, Marcel Dekker, New York, 1981, p. 4

- D. R. Morita, "QC Tests That Can Help Pin Point Material or Design Problems," *Plastics Design Forum*, May–June 1980, pp. 51–55.
- R. Perrington, "Fractography of Metals and Plastics," available: [www.imrtest.com](http://www.imrtest.com).
- "Reflection Polariscopes," Technical Bulletin S-103-A, Photoelastic Division, Vishay Intertechnology, Raleigh, NC.
- M. L. Sessions, "Microtoming, Engineering Design with Dupont Plastics," E. I. Dupont Co., Wilmington, DE, Spring 1977, p. 12.
- I. M. Spier, "The Most Common Mistakes Made by Design Engineer Working in Plastics," *Plastic Design Forum*, March–April 1986, p. 24.
- W. Tobin, "Why Products Fail," *Plastic Design Forum*, January–February 1987, p. 48.
- J. P. Vogt, "Testing for Mechanical Integrity Assures Service Life of Plastic Parts," *Plast. Design Process.*, March 1976, pp. 12–13.





# CHAPTER 22

## FAILURE MODES: PERFORMANCE AND SERVICE REQUIREMENTS FOR CERAMICS

Dietrich Munz  
University of Karlsruhe  
Karlsruhe, Germany

1	OVERVIEW	789	7.1	Strength under Compression Loading	799
2	FLAWS	791	7.2	Global Multiaxial Fracture Criterion	799
3	FRACTURE MECHANICS	791	7.3	Local Multiaxiality Criterion	800
4	STRENGTH	793	8	MATERIALS SELECTION FOR THERMAL SHOCK CONDITIONS	803
5	DELAYED FAILURE	794	9	FAILURE AT HIGH TEMPERATURES	804
6	SCATTER OF STRENGTH AND LIFETIME	795	9.1	Creep Strain	805
6.1	Scatter of Strength	795	9.2	Creep Rupture	806
6.2	Scatter of Lifetime	798	REFERENCES		807
7	DESIGN APPLYING MULTIAXIAL WEIBULL STATISTICS	799			

### 1 OVERVIEW

A reliable design of components requires the knowledge of the possible failure modes under service conditions and knowledge of the material properties describing these failure modes. These material properties are characterized by specific material parameters, such as strength, fracture toughness, hardness, and relations between loading parameters and materials response, e.g., the stress–strain curve or the  $S$ – $N$  curve for fatigue loading. A reliable design has to incorporate the uncertainties in the loading parameters and in the material response. Therefore, a correct description of the scatter of the material properties is an important part in any design procedure. Material properties usually are determined under simple loading conditions: uniaxial loading, homogeneous stress state, constant temperature, simple load–time variations, such as constant load, cyclic loading, or constant loading rate. The loading conditions of components are more complex: multiaxial and inhomogeneous stress state, complex load, and temperature variation. Therefore, methods to transform results from simple loading conditions to complex situations in components have to be developed and applied.

For metals, a good knowledge of failure modes, design rules following from these failure modes, and criteria for materials selection exists. Ceramics are brittle materials that fail without preceding plastic deformation. Only at high temperatures may creep deformation occur before fracture. The brittle failure mode requires specific design rules and criteria for material

Reprinted from *Handbook of Materials Selection*, Wiley, New York, 2002, by permission of the publisher.

selection. Whereas in metals high local stresses lead to local plastic deformation only and not to failure of the component in ceramics, these high local stresses can lead to failure at relatively low global stresses. High local stresses can occur under different situations: sharp notches, thermal shock, contact loading. Tension stresses under these conditions are dangerous because of the lower tensile strength compared to compressive strength. From this behavior general design rules follow:

- Avoid sharp notches.
- Avoid surface damage, e.g., scratches.
- Avoid sudden changes in temperature.
- Avoid point or line loading of ceramic components.

The failure in ceramics starts from flaws introduced during fabrication or surface treatment. These flaws may be pores, inclusions, cracks, or surface scratches. Due to the scatter in the size of the flaws, the strength also shows a large scatter, which is much larger than in metals. This requires special statistical design criteria. This large scatter is associated with a large effect of the size of the component on the strength, which has to be included in the statistical design criteria.

Under mechanical or thermal loading, different failure modes are possible:

- Unstable fracture
- Subcritical extension of flaws under constant loading (static fatigue)
- Subcritical extension of flaws under cyclic loading (cyclic fatigue)
- Creep deformation and creep fracture at high temperatures
- Corrosion, especially oxidation
- Wear in components under sliding contact

The different failure modes are characterized by material properties and relations between the applied loading in terms of stresses or stress intensity factors and the materials response in terms of lifetime or plastic deformation. The material properties are:

- Tensile strength  $\sigma_c$  or, to be more specific,  $\sigma_{ct}$
- Compressive strength  $\sigma_c^c$
- Fracture toughness  $K_{IC}$
- Hardness  $H$

The failure relations are:

- Relation between stress  $\sigma$  and lifetime  $t_f$
- Relation between stress amplitude  $\sigma_a$  or stress range  $\Delta\sigma = 2\sigma_a$  and number of cycles to failure  $N_f$
- Relation between creep strain and time

The flaws leading to failure can be described as cracks. Therefore, the methods of fracture mechanics can be applied to describe the flaw extension behavior. The corresponding relations are:

- Relation between flaw size and strength
- Relation between crack growth rate and stress intensity factor for static fatigue
- Relation between crack extension for one load cycle and the range of the stress intensity factor for cyclic fatigue

Because of the scatter in strength and in the lifetime, the failure cannot be described by a unique strength or a fixed lifetime. For a given load, only the probability of failure can be specified. This failure probability depends not only on the maximum load in the component but also on the size of the component and the stress distribution in the component.

## 2 FLAWS

Looking on a fracture surface of a ceramic, one very often can find the origin of the fracture. An example is shown in Fig. 1. It can distinguish between intrinsic and extrinsic flaws. Intrinsic flaws are generated during the fabrication process. They can be pores, shrinkage cracks, or areas of low density. Inclusions of other materials and specific grain configurations, especially large grains, may lead to high microstructural residual stresses after cooling from the sintering temperature. These stresses may cause cracks during the application of a small mechanical load. Phase transformation during cooling or under an applied load, accompanied by a change in volume, e.g., in zirconia, is another cause of crack nucleation. All these flaws are primarily volume flaws that, however, may extend to the surface. Extrinsic flaws are surface flaws caused by surface treatment, such as machining or grinding. Oxidation at high temperature may introduce surface pits.

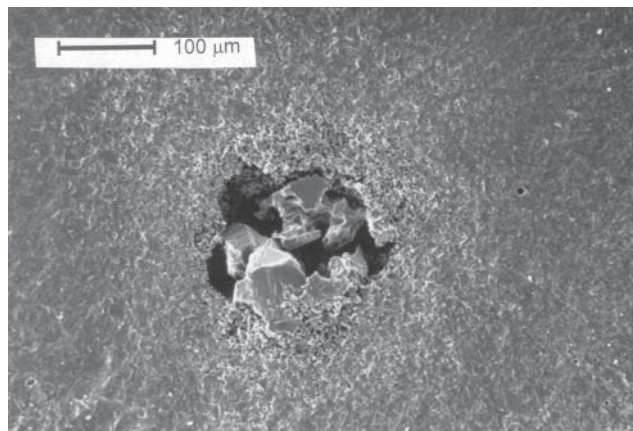
## 3 FRACTURE MECHANICS

The flaws that cause failure are described as cracks. Consequently, the methods of linear elastic fracture mechanics can be applied. The relation between the size of the flaw  $a$  and the strength  $\sigma_c$  is

$$\sigma_c = \frac{K_{IC}}{\sqrt{aY}} \quad (1)$$

where  $K_{IC}$  is the fracture toughness and  $Y$  a constant that depends on the shape of the crack. For a semicircular surface flaw  $Y = 1.28$ .

The fracture toughness is a material property. In Table 1 typical values of fracture toughness are listed. They range from less than  $1 \text{ MPa} \cdot \sqrt{\text{m}}$  for glass to  $8 \text{ MPa} \cdot \sqrt{\text{m}}$  for silicon



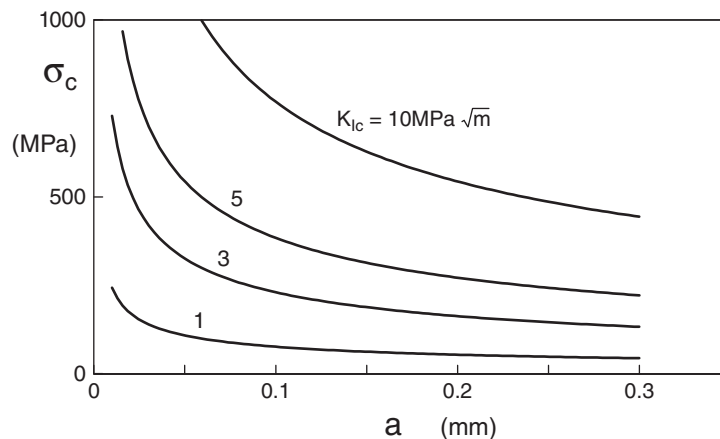
**Figure 1** Flaw origin in a silicon carbide.

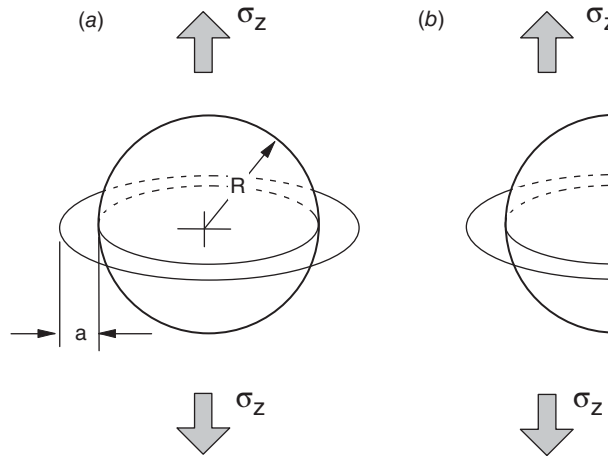
**Table 1** Fracture Toughness and Strength of Different Ceramics

	Fracture Toughness (MPa $\sqrt{\text{m}}$ )	Tensile Strength (MPa)	Compressive Strength (MPa)
AlN	3–4.5	300–500	
Al <sub>2</sub> O <sub>3</sub>	3–4.5	300–500	2500
Al <sub>2</sub> TiO <sub>5</sub>		10–50	
B <sub>4</sub> C	3.5	300–500	2900
BeO		200–400	1500
MoSi <sub>2</sub>		300	2500
SiC hot pressed	4.6	500–850	460
Si <sub>3</sub> N <sub>4</sub> dense reaction bonded	4–8	500–1200	
	1.5–2.8	150–350	
SiO <sub>2</sub> fused quartz	0.8	50–100	1300
			2000
TiB <sub>2</sub>		300–400	1600
TiC		400	
ZrB <sub>2</sub>		300	
ZrO <sub>2</sub>	8–12	800–1000	2000
Glass	0.6–1.0		

nitride and 12 MPa $\cdot\sqrt{\text{m}}$  for zirconia. For a given material the fracture toughness depends on the specific microstructure and density. Therefore, a large variation of  $K_{IC}$  is observed.

In Fig. 2 the strength  $\sigma_c$  according to Eq. (1) is plotted versus the crack size  $a$  for different values of  $K_{IC}$ . A flaw of a size of 100 $\mu\text{m}$  leads to a strength of 391 MPa for a material with  $K_{IC} = 5 \text{ MPa}\cdot\sqrt{\text{m}}$  (e.g., alumina) and to a strength of 781 MPa for a material with  $K_{IC} = 10 \text{ MPa}\cdot\sqrt{\text{m}}$  (e.g., zirconia). For a flaw size of 20 $\mu\text{m}$  the corresponding values are 873 and 1747 MPa. In view of this large effect of the flaw size on the strength, a process technique that

**Figure 2** Strength as a function of flaw size for materials with different fracture toughness.



**Figure 3** Pores with annular crack.

leads to a reduction of the processing flaws is desirable. Fracture may also be caused by surface flaws, introduced by grinding. Therefore, polishing the surface may also increase the strength.

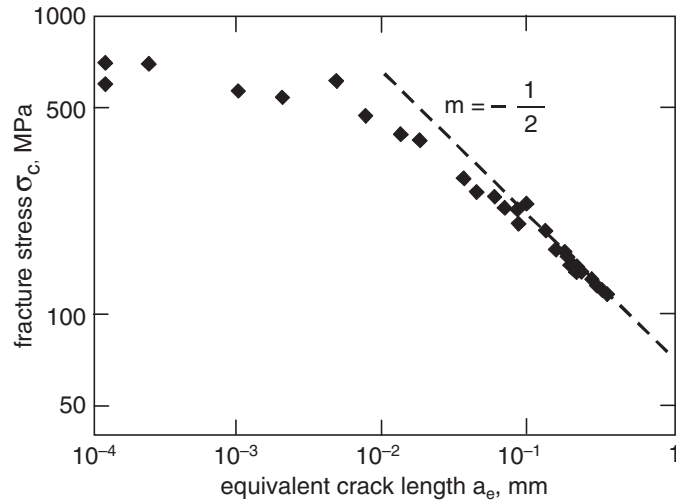
The type of flaws also affects the strength. Applying Eq. (1) requires the existence of a crack. Three-dimensional flaws such as pores are described as spheres with a surrounding annular crack (Fig. 3). The stress intensity factor then depends on the ratio of the size of the crack  $a$  to the radius of the sphere  $R$ . The size of the crack may be on the order of the grain size.

## 4 STRENGTH

Equation (1) can be applied to predict the strength if the crack size is known. In metals this relation is used, for instance, to predict the remaining strength of a component with a fatigue crack, whose size has been determined by a nondestructive testing method and is on the order of millimeters. In ceramic materials the flaws are small, on the order of  $10\text{--}100\mu\text{m}$ , and difficult to detect. Therefore Eq. (1) has not yet been used to predict the strength or to reject components after a nondestructive testing procedure. However, the relation shows the potential of a material. A material with a high fracture toughness and a low strength may have a potential for higher strength by a reduction in the flaw size.

In Fig. 4 the strength of SiC is plotted versus the crack size in a log-log plot. For cracks larger than about  $100\mu\text{m}$  a straight line with a slope of  $-\frac{1}{2}$  is obtained according to Eq. (1). For smaller cracks a deviation with an upper limit is observed. The equivalent crack size is a length transformed to an internal crack in a plate. The reasons for the deviation from Eq. (1) for small flaw sizes will not be discussed here.

Because of the large dependence of the strength on the flaw size for a given material, the strength exhibits a large variation, depending on the processing method of the material. Strength also can be varied for a given material by varying the grain size and the microstructure in multiphase materials because this may change the fracture toughness and the processing flaw size. The values given in Table 1 are typical values of dense materials. Generally, the tensile strengths of ceramics are lower than those of high-strength metals. Silicon nitride and some zirconia materials, however, have strength values of up to 1000 MPa.



**Figure 4** Strength of silicon carbide vs. crack size. (From Ref. 1.)

## 5 DELAYED FAILURE

Under cyclic loading, but also under constant loading, ceramic materials may fail after some time. This is called static fatigue for constant loading and cyclic fatigue for cyclic loading. This designation contrasts with that in metals, where the designation of fatigue is restricted to the damage under cyclic loading. The failure behavior is described by an  $S$ - $N$  curve, where the stress is plotted versus the lifetime under static loading and the stress range  $\Delta\sigma$  (twice the amplitude) versus the number of cycles to failure under cyclic loading. In a log-log plot straight lines are observed, which correspond to the relations

$$t_f = \frac{A}{\sigma^n} \quad (2a)$$

$$N_f = \frac{A}{(\Delta\sigma)^n} \quad (2b)$$

The phenomenon of delayed failure is caused by subcritical extension of the flaws. For static loading the crack growth rate depends on the stress intensity factor  $K$  and for cyclic loading on the range of the stress intensity factor  $\Delta K$ . In a large range of crack growth rate, the subcritical crack extension can be described by the relations

$$\frac{da}{dt} = CK^n \quad (3a)$$

$$\frac{da}{dN} = C(\Delta K)^n \quad (3b)$$

where  $da/dN$  is the crack extension for one load cycle. Equation (3) can be obtained by integration of Eq. 4 from an initial crack size  $a_i$  to a critical crack size  $a_c$ . Because of the high values of  $n$ , the critical crack size can be set to infinity. The values of  $n$  in Eqs. (3) and (4) are the same for corresponding loading situations (static or cyclic). The parameters  $A$ ,  $C$ , and  $n$  are different for static and cyclic loading,  $n_{\text{cyclic}}$  being always somewhat smaller than  $n_{\text{static}}$ . For cyclic loading  $A$  and  $C$  depend on the mean stress, which conveniently is expressed by the ratio  $R = \sigma_{\min}/\sigma_{\max} = K_{\min}/K_{\max}$ .

**Table 2** Some Values of  $n$  and  $p^2$ 

Material	$n$	$p^2$
ZrO <sub>2</sub> (Y - TZP)	19	3
Si <sub>3</sub> N <sub>4</sub>	29	1.3
SiC <sub>w</sub> /Al <sub>2</sub> O <sub>3</sub>	10.2	4.8

The following relation was found:

$$\frac{da}{dN} = \frac{C}{(1-R)^{n-p}} (\Delta K)^n \quad (4)$$

Integration leads to

$$N_f = C^* \frac{(1-R)^{n-p}}{(\Delta\sigma)^n} = C^* \frac{1}{(\Delta\sigma)^p (\sigma_m + \Delta\sigma/2)^{n-p}} \quad (5)$$

Some values are given in Table 2. High values of  $n$  mean a large effect of the stress or the stress range on the lifetime.

### Summary

- Delayed failure is described by a power law relation between crack growth rate and the stress intensity factor for constant loading and by a power law relation between crack extension for one load cycle and the range of the stress intensity factor for cyclic loading.

## 6 SCATTER OF STRENGTH AND LIFETIME

### 6.1 Scatter of Strength

Because of the statistical distribution of the flaw size, the strength is subjected to considerable scatter. As a consequence, the design of ceramic components cannot be based on an average strength and the application of a safety factor, as is usually done for metallic components. The scatter is associated with an effect of the size of a component and the stress distribution in the component on the strength. Therefore, a statistical treatment of the scatter and a design according to prescribed failure probability is necessary. In this section the method of applying Weibull statistics to uniaxial loading is described. The design applying multiaxial Weibull statistics will be presented in Section 7.

The scatter in the strength is described by the two-parameter Weibull distribution. The failure probability, i.e., the probability of failure occurring below the stress  $\sigma = \sigma_c$ , is given by

$$F = 1 - \exp \left[ - \left( \frac{\sigma_c}{\sigma_0} \right)^m \right] \quad (6)$$

The Weibull parameter  $m$  is called the Weibull modulus and is a measure of the scatter. The Weibull parameter  $\sigma_0$  is related to the strength. Whereas  $m$  is a material parameter,  $\sigma_0$  depends on the material as well as the size of the component and the stress distribution in the component.

From Eq. (6) it follows that failure is possible also at very low stresses. Therefore, a three-parameter Weibull distribution with a lower limit  $\sigma_u$  is considered sometimes:

$$F = 1 - \exp \left[ - \left( \frac{\sigma_c - \sigma_u}{\sigma_0} \right)^m \right] \quad \sigma_c > \sigma_u \quad (7)$$



It is, however, not possible to determine  $\sigma_u$  with sufficient accuracy when applying a limited number of test specimens. Hence, the two-parameter distribution is used usually.

Failure can be caused by surface flaws or volume flaws. For a homogeneous stress distribution in a component and failure by volume flaws, Eq. (6) can be replaced by

$$F = 1 - \exp \left[ -\frac{V}{V_0} \left( \frac{\sigma_c}{\sigma_V} \right)^m \right] \tag{8}$$

where  $V$  is the volume and  $V_0$  is the unit volume, which is introduced for normalization. Now  $\sigma_V$  is a quantity independent of the size of the component. An inhomogeneous stress distribution in a component is described by the relation

$$\sigma(x, y, z) = \sigma^* g(x, y, z) \tag{9}$$

where  $\sigma^*$  is a characteristic stress in the component and  $g(x, y, z)$  a geometry function. The failure probability then is given by

$$F = 1 - \exp \left[ -\frac{1}{V_0} \left( \frac{\sigma_c^*}{\sigma_V} \right)^m \int g^m dV \right] = 1 - \exp \left[ -\frac{V_{\text{eff}}}{V_0} \left( \frac{\sigma_c^*}{\sigma_V} \right)^m \right] \tag{10}$$

where  $\sigma_c^*$  is the value of  $\sigma^*$  at fracture and

$$V_{\text{eff}} = \int g^m dV \tag{11}$$

is the effective volume.

For surface flaws the volume in Eqs. 8–11 has to be replaced by the surface area.

If Eq. 6 is used to calculate the failure probability for a component,  $\sigma_{0,C}$  of the component can be calculated from  $\sigma_{0,SP}$  of the specimen by

$$\sigma_{0,C} = \sigma_{0,SP} \left( \frac{V_{\text{eff,SP}}}{V_{\text{eff,C}}} \right)^{1/m} \tag{12}$$

Experimental results are presented in a Weibull diagram, where  $\ln \ln 1/(1 - F)$  is plotted versus  $\ln \sigma_c$ . To correlate the measured strength values with the failure probabilities, the strength values are ranked in increasing order and numbered from 1 to  $n$ . Then, the strength values  $\sigma_{ci}$  are related to the failure probability  $F_i$  according to

$$F_i = \frac{i - 0.5}{n} \tag{13}$$

The slope of the Weibull plot is  $m$ ;  $\sigma_0$  is the strength  $F = 0.632$ . Examples are shown in Fig. 5.

The average strength  $\bar{\sigma}_c$  and the median strength for  $\sigma_{\text{med}}(\sigma_c$  for  $F = 0.5)$  are related to  $m$  and  $\sigma_0$  by

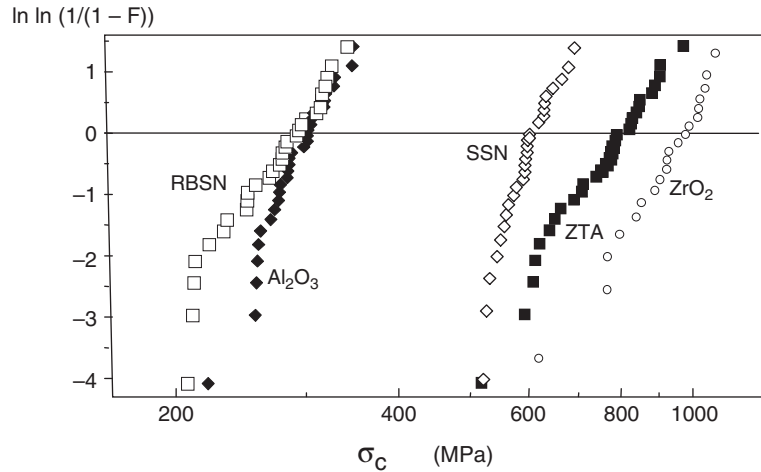
$$\bar{\sigma}_c = \sigma_0 \Gamma \left( 1 + \frac{1}{m} \right) \quad \sigma_{\text{med}} = (0.693)^{1/m} \tag{14}$$

where  $\Gamma$  is the gamma function. In Table 3 the ratios  $\bar{\sigma}_c/\sigma_0$  and  $\sigma_{\text{med}}/\sigma_0$  are given for different values of  $m$ .

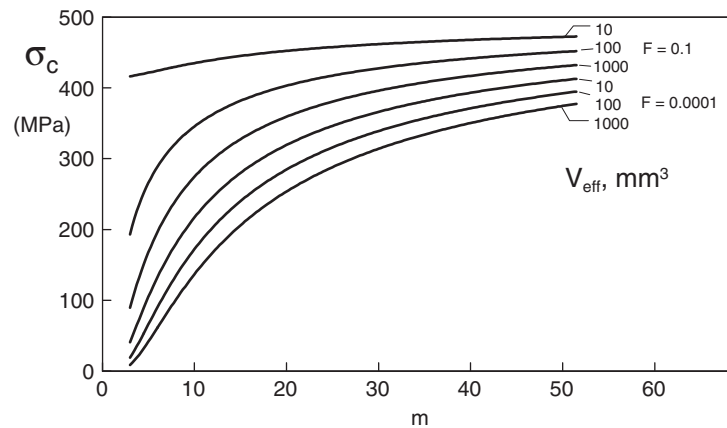
Equations (8) and (10) lead to a large effect of the size of the component on the strength, which depends on the Weibull modulus  $m$ . They also show a large effect of  $m$  on the failure

**Table 3** Ratios  $\bar{\sigma}_c/\sigma_0$  and  $\sigma_{\text{med}}/\sigma_0$

	$m = 5$	$m = 10$	$m = 20$	$m = 30$	$m = 50$
$\bar{\sigma}_c/\sigma_0$	0.918	0.951	0.974	0.982	0.989
$\sigma_{\text{med}}/\sigma_0$	0.929	0.964	0.982	0.988	0.993



**Figure 5** Weibull plots of strength for several materials (RBSN: reaction-bonded silicon nitride, SSN: sintered silicon nitride, ZTA: zirconia-toughend alumina).



**Figure 6** Effect of Weibull modulus  $m$  and effective volume on the strength for two different failure probabilities for materials with the same average strength of 500 MPa.

probability. This effect is illustrated in Fig. 6 by the strength at different failure probabilities, Weibull parameters  $m$ , and different effective volumes. For a material with a mean strength  $\bar{\sigma}_c = 500$  MPa determined with four-point specimens having an inner span  $L = 20$  mm, width  $W = 4.5$  mm, and height  $H = 3.5$  mm, the effective volume is

$$V_{\text{eff}} = \frac{LWH}{2(m+1)} \quad (15)$$

In Table 4 the parameter  $\sigma_0$  and the effective volume are given for different failure probabilities and different values of  $m$ .

**Table 4** Strength at Different Failure Probabilities and Effective Volumes (Materials with the Same Average Strength in Bending Tests)

$m$	$V_{\text{eff}}(\text{mm}^3)$	$\sigma_0$	$F = 0.0001$	$F = 0.001$	$F = 0.01$	$F = 0.1$	$F = 0.5$
5	10	661	105	166	264	4222	615
	100	417	66	105	168	266	388
	1000	263	42	66	195	168	245
10	10	545	217	273	435	435	526
	100	433	172	217	346	346	417
	1000	349	137	172	275	275	332
20	10	506	319	358	402	452	496
	100	451	284	319	358	403	442
	1000	402	253	284	319	359	394
50	10	495	411	431	451	473	491
	100	473	393	412	431	452	470
	1000	452	376	394	412	432	449

### 6.2 Scatter of Lifetime

The scatter of the lifetime under constant or cyclic loading is much larger than that of the strength and can also be described by a Weibull distribution. For static fatigue the failure probability is

$$F = 1 - \exp \left[ - \left( \frac{t_f}{t_0} \right)^{m^*} \right] \tag{16a}$$

and for cyclic fatigue

$$F = 1 - \exp \left[ - \left( \frac{N_f}{N_0} \right)^{m^*} \right] \tag{16b}$$

If the strength and lifetime are caused by the same flaws, then the Weibull parameters  $m^*$ ,  $t_0$ , and  $N_0$  can be related to the Weibull parameters  $m$  and  $\sigma_0$  of the strength:

$$m^* = \frac{m}{n - 2} \tag{17}$$

$$t_0 = \frac{B\sigma_0^{n-2}}{\sigma^n} \tag{18a}$$

$$N_0 = \frac{B\sigma_0^{n-2}}{(\Delta\sigma)^n} \tag{18b}$$

where  $n$  is the crack growth exponent for static and cyclic crack extension, respectively;  $B$  is given by

$$B = \frac{2}{(n - 2)CY^2K_{IC}^{n-2}} \tag{19}$$

with  $C$  from Eq. 4.

In Eq. (18)  $\sigma_{0,C}$  of the component has to be used. If  $\sigma_{0,SP}$  as obtained from the specimens is known, the parameters  $t_0$  and  $N_0$  in Eqs. (16) are

$$t_{0,C} = \frac{B\sigma_{0,SP}^{n-2}}{\sigma^n} \left( \frac{V_{\text{eff},SP}}{V_{\text{eff},C}} \right)^{(n-2)/m} \tag{20a}$$

$$N_{0,C} = \frac{B\sigma_{0,SP}^{n-2}}{(\Delta\sigma)^n} \left( \frac{V_{\text{eff, SP}}}{V_{\text{eff, C}}} \right)^{(n-2)/m} \quad (20b)$$

### Summary

- The scatter of the strength is described by the two-parameter Weibull distribution with the Weibull modulus  $m$ .
- The average strength and the strength at given failure probability depend on the size of the component and the stress distribution in the component.
- The lifetime is described by a Weibull distribution; the parameters can be obtained from the Weibull parameters of the strength, if strength and lifetime are caused by the same flaws.

## 7 DESIGN APPLYING MULTIAXIAL WEIBULL STATISTICS

### 7.1 Strength under Compression Loading

The strength of ceramic materials under compressive loading is much higher than under tension loading. Usually compression tests are performed applying cylindrical specimens. The cylinders are loaded with parallel stamps. Due to the different lateral expansion of the specimen and the stamp under compressive loading, radial stresses occur in the loaded specimen, which may lead to premature failure. Therefore the compressive strength measured may depend on the loading conditions. A detailed description of the compressive test is given in Ref. 2. Some compressive strength results are presented in Table 1. The ratio between compressive and tensile strength ranges between 2.5 and 18 depending on the material and the porosity. Dense materials have a higher ratio than porous materials.

### 7.2 Global Multiaxial Fracture Criterion

Whereas the strength of materials is measured under uniaxial tension or compression loading, multiaxial stresses very often occur in components. This is the case for uniaxial loading of notched components, components under internal pressure, or components under inhomogeneous temperature distribution. The degree of multiaxiality is described by the ratios

$$\alpha = \frac{\sigma_2}{\sigma_1} \quad \beta = \frac{\sigma_3}{\sigma_1} \quad (21)$$

where  $\sigma_1$ ,  $\sigma_2$ , and  $\sigma_3$  are the principal stresses. Two different approaches exist to assess multiaxial stresses: global multiaxiality and local multiaxiality criteria.

A global multiaxiality criterion is a relation between the principal stresses and one or two material properties. The most reliable criterion is Mohr's hypothesis, which is presented here for a plane stress situation. It is based on the tensile strength  $\sigma_{ct}$  and compressive strength  $\sigma_{cc}$ . The criterion is shown in Fig. 7 and reads

$$\begin{aligned} \sigma_1 &= \sigma_{ct} \quad \text{for } \sigma_1 > 0, \sigma_2 > 0 \\ \sigma_2 &= -\sigma_{cc} \quad \text{for } \sigma_1 < 0, \sigma_2 < 0 \\ \sigma_1 &= \sigma_{ct} \left( 1 + \frac{\sigma_2}{\sigma_{cc}} \right) \quad \text{for } \sigma_1 > 0, \sigma_2 < 0 \end{aligned} \quad (22)$$

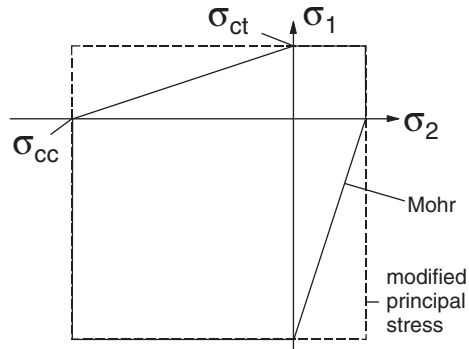


Figure 7 Mohr's hypothesis for biaxial loading.

### 7.3 Local Multiaxiality Criterion

The local multiaxiality criterion starts with a flaw type that may be a pore or a crack. The local fracture criterion is a critical tensile stress for a pore or a critical stress intensity factor for a crack. Details can be found in Ref. 3. In the pore models only the tensile strength appears as a material property. For a spherical pore the failure relation is

$$\sigma_1 + \frac{15\nu - 3}{27 - 15\nu} \sigma_2 - \frac{3 + 15\nu}{27 - 15\nu} \sigma_3 = \sigma_{ct} \tag{23}$$

From this relation the compressive strength follows as

$$\sigma_{cc} = \frac{27 - 15\nu}{3 + 15\nu} \sigma_{ct} = \begin{cases} 4\sigma_{ct} & \text{for } \nu = 0.2 \\ 3\sigma_{ct} & \text{for } \nu = 0.3 \end{cases} \tag{24}$$

Under triaxial compression, no failure is expected because the stresses at the pore are negative. In Fig. 8 the failure diagram for plane stress is shown. Results for an ellipsoidal pore are

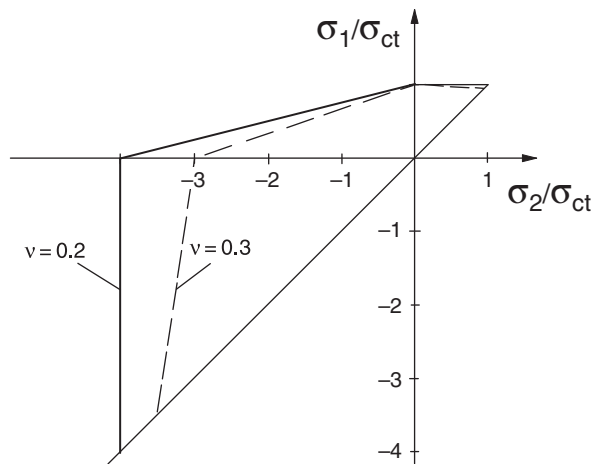


Figure 8 Failure diagram for a spherical pore.

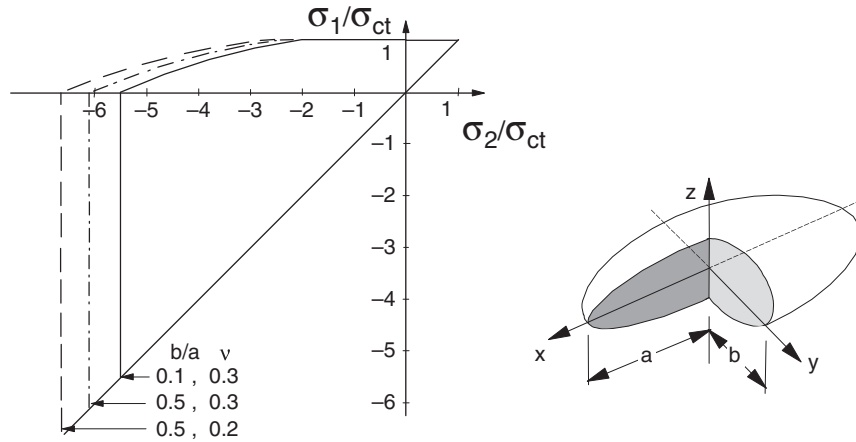


Figure 9 Failure diagram for an elliptical pore. (From Ref. 3.)

represented in Fig. 9. From these results it can be concluded that the ratio of compressive to tensile strength may vary between about 3 and 6, depending on the shape of the pore and the Poisson ratio. It also shows that Mohr's hypothesis is a good approximation to the more detailed pore models.

For a given pore geometry (spherical or ellipsoidal with a given ratio of  $b/a$ ), the strength is independent of the size of the pore. Consequently, it is not possible to derive a statistical multiaxial failure relation. Such a relation can be obtained for a crack model. In this model the flaws are described as cracks with a given shape, e.g., as circular cracks or semicircular surface cracks. Then, a statistical multiaxial failure criterion can be developed in the following steps. The cracks are assumed to be randomly orientated and have a size distribution that leads to the Weibull distribution of the strength under uniaxial loading. Depending on the orientation of the flaw with respect to the principal stress axis and the ratios of the principal stresses  $\alpha$  and  $\beta$ , the stresses at the crack tip are described by the mixed-mode stress intensity factors  $K_I$ ,  $K_{II}$ , and  $K_{III}$ :  $K_I$  is caused by the normal stress on the crack area  $\sigma_n$ ;  $K_{II}$  and  $K_{III}$  are caused by the shear stress  $\tau$  acting on the crack plane. The local failure criterion is a relation between these three stress intensity factors and the fracture toughness  $K_{IC}$ . Different relations are discussed in the literature, some of them also include the fracture toughness  $K_{II,C}$  for mode II loading. An example is the criterion of constant-energy release rate:

$$K_I^2 + K_{II}^2 + \frac{1}{1-\nu} K_{III}^2 = K_{IC}^2 \quad (25)$$

For any local stress state a critical orientation of the crack exists. If the normal stress is compressive ( $\sigma_n < 0$ ), then  $K = 0$  and  $K_{II}$  and  $K_{III}$  have to be calculated with an effective shear stress:

$$\tau_{\text{eff}} = \begin{cases} |\tau| + \mu\sigma_n & \text{for } |\mu\sigma_n| < \tau \\ 0 & \text{for } |\mu\sigma_n| > \tau \end{cases} \quad (26)$$

with the friction coefficient  $\mu$ . As an example, the resulting failure criterion is shown for circular cracks and a specific mixed-mode failure criterion in Fig. 10.

If the scatter of the strength is included in the calculation procedure, the resulting failure criterion also depends on the Weibull parameter  $m$ . For details see Ref. 3.

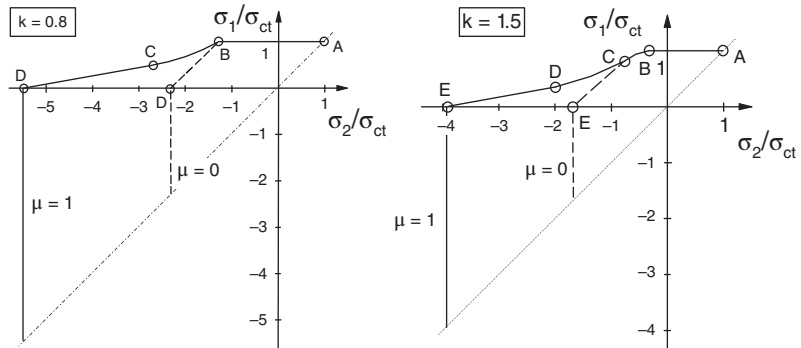


Figure 10 Failure diagram for circular cracks ( $k$  characterizes the mixed-mode criterion). (From Ref. 3.)

For an inhomogeneous stress distribution the failure probability of a component is given by the integral

$$F = 1 - \exp \left[ -\frac{1}{2\pi} \left( \frac{\sigma_c^*}{\sigma_{I0}} \right)^m \iint h^m \sin \Phi \, d\Phi \, d\Psi \int g^m \, dV \right] \quad (27)$$

The angles  $\Phi$  and  $\Psi$  characterize the orientation of the crack normal to the principal stress axis. The quantity  $h$  depends on the stress ratios  $\alpha$  and  $\beta$  and on the mixed-mode fracture criterion;  $\sigma_{I0}$  is a material-dependent critical stress.

The flowchart for the computation of the failure probability is presented in Fig. 11. It shows the necessary input information:

- The stress state in the component (usually from finite-element calculation)
- A crack model

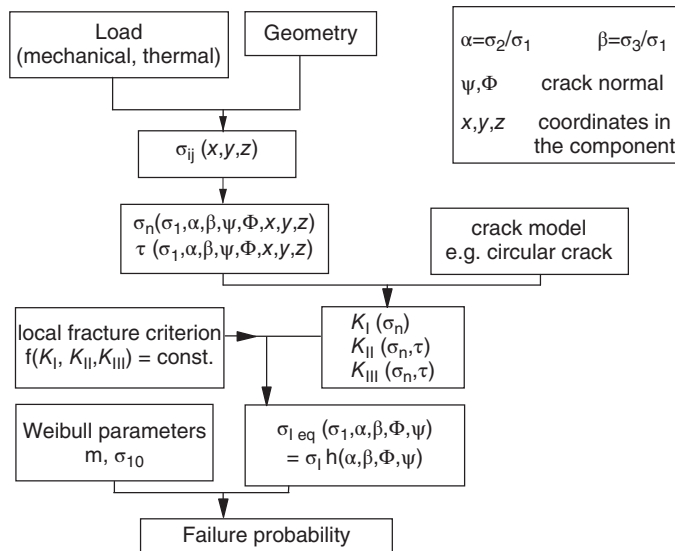


Figure 11 Flowchart for computation of failure probability for multiaxially loaded components. (From Ref. 3.)

- A local failure criterion
- The material properties  $m$  and  $\sigma_{I0}$

Postprocessor programs are available for the calculation of failure properties.

### Summary

- The failure probability of components under multiaxial loading can be calculated applying multiaxial Weibull theory, where the flaws are described as randomly orientated cracks.
- As a global multiaxial fracture criterion Mohr's hypothesis can be applied.

## 8 MATERIALS SELECTION FOR THERMAL SHOCK CONDITIONS

Ceramic materials may fail during rapid cooling or rapid heating. Due to the time-dependent transient temperature distribution in a component, the thermal expansion depends on the location and has to be compensated for by mechanical deformation. Whereas in metals these strains lead to small local plastic deformation, they may cause high local stresses in ceramics that may exceed the local strength. The failure probability of a component under thermal shock conditions can be calculated applying the multiaxial Weibull statistics described in Section 7.

The resistance against thermal shock varies for different materials. It depends on the following material properties: thermal expansion coefficient  $\alpha$ , elastic properties Young's modulus  $E$ , Poisson's ratio  $\nu$ , thermal conductivity  $\lambda$ , density  $\rho$ , heat capacity  $C_p$ , and strength  $\sigma_c$ . Under different thermal conditions different thermal shock parameters have been defined that characterize the thermal shock sensitivity.

For perfect heat transfer from the medium to the component, the thermal stress at the surface after a thermal shock by  $\Delta T$  is

$$\sigma_{\max} = \frac{E\alpha \Delta T}{1 - \nu} \quad (28)$$

The critical temperature for fracture under thermal shock therefore is

$$R = \frac{\sigma_c(1 - \nu)}{E\alpha} \quad (29)$$

For cooling with a constant heat transfer coefficient  $h$  the maximum stress at the surface increases with time and decreases after passing a maximum. The maximum stress is given by

$$\sigma_{\max} = \frac{E\alpha \Delta T}{1 - \nu} f(B) \quad (30)$$

where  $f$  is a function of the Biot modulus

$$B = \frac{hd}{\lambda} \quad (31)$$

where  $\lambda$  is the thermal conductivity and  $d$  a characteristic size parameter of the component. For small values of  $B$  the maximum stress is proportional to  $B$ . Hence the critical temperature for failure is proportional to

$$R' = \frac{\sigma_c \lambda (1 - \nu)}{E\alpha} \quad (32)$$

For a constant heating rate at the surface, the maximum stress is

$$\sigma_{\max} = -C \frac{\alpha E \rho C_p}{\lambda(1 - \nu)} \frac{dT}{dt} \quad (33)$$



where  $\rho$  is the density,  $C_p$  the heat capacity, and  $C$  a constant depending on the geometry. The critical heating rate therefore is proportional to

$$R'' = \frac{\sigma_c \lambda (1 - \nu)}{E \alpha \rho C_p} \tag{34}$$

Whereas under mechanical loading a crack extends unstably after initiation, a crack stops after some extension under thermal shock conditions. The remaining strength, however, decreases considerably. If the strength of the component is not of importance, a limited amount of crack extension may be tolerable. Then, the condition for materials selection may be a small extension of an existing crack. It can be shown that the amount of crack extension during thermal shock increases with increasing crack size. Consequently a material with a large initial crack may be of advantage. The initial crack size follows from

$$\alpha_i = \left( \frac{K_{IC}}{\sigma_c Y} \right)^2 \tag{35}$$

leading to another thermal shock parameter

$$R''' = \frac{K_{IC}^2}{\sigma_c^2} \tag{36}$$

( $R^m$  is not considered here).

In Table 5 typical values of the thermal shock parameters are given.

**Summary**

- The sensitivity to failure by thermal shock increases with increasing Young’s modulus, increasing thermal expansion coefficient, decreasing strength, and decreasing thermal conductivity.
- For a constant heating rate at the surface the sensitivity decreases further with increasing density and increasing heat capacity.

**9 FAILURE AT HIGH TEMPERATURES**

Failure at high temperatures is caused by creep elongation and creep rupture. Another failure mode is oxidation. Different mechanisms may contribute to creep and creep damage. In many

**Table 5** Thermal Shock Parameters for Different Materials

	Al <sub>2</sub> O <sub>3</sub>	MgO	ZrO <sub>2</sub>	SiC	Si <sub>3</sub> N <sub>4</sub>		BeO	Al <sub>2</sub> TiO <sub>5</sub>
					HPSN	RBSN		
$\alpha(10^{-6}K^{-1})$	8	12	11	4	3.2	2.5	8	1.8
$E(\text{GPa})$	400	270	200	350	300	180	360	30
$\nu$	0.22	0.17	0.25	0.2	0.28	0.23	0.25	0.2
$\lambda(\text{W m}^{-1}\text{K}^{-1})$	30	30	2.5	100	35	10	300	2.5
$\rho(\text{g cm}^{-3})$	3.9	3.5	6.0	1.0	0.7	0.7	1.3	0.7
$C(\text{J g}^{-1}\text{K}^{-1})$	1.0	1.0	0.5	1.0	0.7	0.7	1.3	0.7
$\sigma_c(\text{MPa})$	300	180	950	360	660	200	180	65
$K_{IC}(\text{MPa} \cdot \text{m}^{1/2})$	4.5	3.0	10	4	7	2	4.8	—
$R(\text{K})$	73	46	324	206	495	342	47	962
$R'(\text{kW m}^{-1})$	2.19	1.38	0.81	20.6	17.3	3.42	14.1	2.41
$R''(\text{W cm}^2\text{g}^{-1}\text{K})$	5.6	3.9	2.7	66	75	20	36	9.6
$R'''(\text{mm})$	0.23	0.28	0.11	0.12	0.11	0.10	0.71	

cases, creep is caused by grain boundary effects, such as viscous flow of an amorphous grain boundary phase, diffusion of vacancies along grain boundaries, formation and extension of cavities at grain boundaries or dissolution, and reprecipitation of material through the glassy phase. Creep within the grain is caused by the motion of dislocations or vacancies.

Damage mechanisms leading to the rupture of a component can be the formation of grain boundary cavities, coalescence to cracks, and growth of the cracks until final failure.

## 9.1 Creep Strain

After application of a load to a specimen, the same variation of strain with time as in metals is observed. After an instantaneous strain  $\epsilon_0$ , the creep curve can be subdivided into three stages. In stage I—the primary creep—the strain rate decreases and reaches in stage II—secondary creep—a constant value. Afterwards, in stage III—tertiary creep—the strain rate increases.

Primary creep can be described by one of the following relations:

$$\epsilon_p = At^m \text{ with } m < 1 \quad (36a)$$

$$\epsilon_p = A[1 - \exp(-mt)] \quad (36b)$$

The effect of the stress on the creep rate is often described by Norton's law:

$$\dot{\epsilon} = B\sigma^n \quad (37)$$

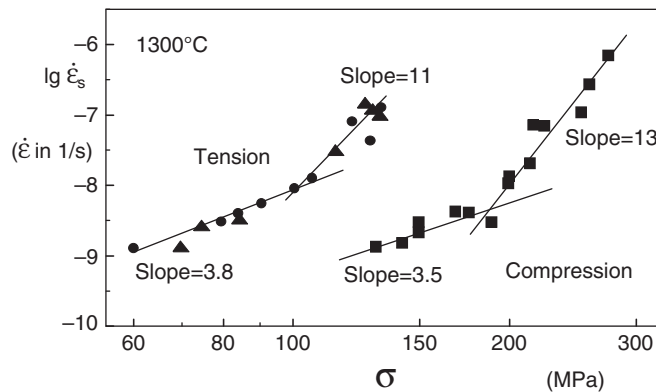
Other proposed relations are

$$\dot{\epsilon} = B[\exp(\alpha\sigma) - 1] \quad (38)$$

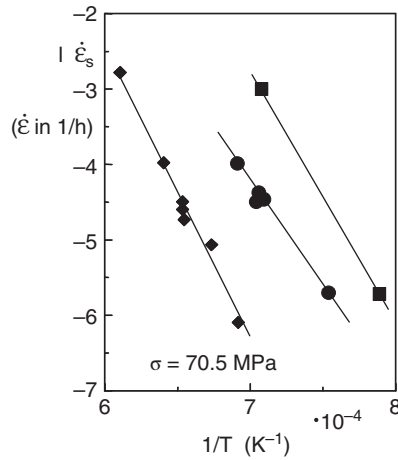
$$\dot{\epsilon} = B \sinh(\alpha\sigma) \quad (39)$$

These relations can be applied for the primary and secondary creep range with possibly different parameters  $\alpha$  and  $n$ .

Creep under compression differs from creep in tension, especially for secondary creep, where the creep rate in compression is lower than under tension. An example is shown in Fig. 12. In this case the exponent  $n$  in Eq. 37 is similar in tension and compression; the constant  $B$ , however, is different. Figure 12 also shows that Eq. 37 cannot be applied for the whole range of the stress: The exponent  $n$  for small stresses is lower than at higher stresses.



**Figure 12** Stress dependence of the secondary creep rate for reaction-bonded siliconized silicon carbide tested under tension and compression. (From Ref. 4.)



**Figure 13** Secondary creep rate as a function of temperature for three hot-pressed silicon nitrides. (From Ref 5.)

The effect of temperature usually can be described by

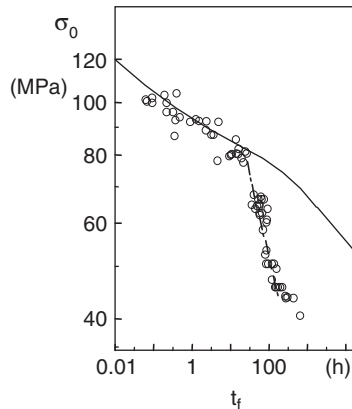
$$\dot{\epsilon} = C \exp\left(-\frac{Q}{RT}\right) \quad (40)$$

where  $R$  is the gas constant and  $Q$  the activation energy for the leading creep process. An example of Eq. 40 is shown in Fig. 13.

The problem of these relations is that the lowest creep rates measured are usually higher than the allowable creep rate in a component. It is obvious from Fig. 12 that the lowest creep rates measured in these investigations are on the order of  $10^{-9}/s$ . For this creep rate the creep strain is 3% in one year. Therefore an extrapolation to lower creep rates often is necessary.

## 9.2 Creep Rupture

The mechanism of creep rupture differs from the mechanism of subcritical crack extension at low temperatures. This can be seen in Fig. 14, where the stress is plotted versus the lifetime for



**Figure 14** Lifetime as a function of the (elastically calculated) outer fiber bending stress for static bending tests on  $\text{Al}_2\text{O}_3$  with 4% glass content. Solid line predictions from subcritical crack growth.

an alumina at 1100°C in a log-log plot. Two ranges can be distinguished. At high stresses, the failure is caused by the extension of preexisting flaws. The relation between stress and failure strain can be described by Eq. 3a with  $n = 12$  [the slightly curved line in Fig. 14 is obtained by applying Eq. 3a for the bending tests taking into account small stress redistribution due to creep]. At lower stresses, the observed lifetime is much lower than predicted from Eq. (3).

### Summary

- Creep at high temperatures is described by relations between creep rate, stress, and temperature.
- The time to failure in the creep range is less stress dependent than at lower temperatures.

## REFERENCES

1. S. Usami, I. Takahashi, and T. Machida, "Static Fatigue Limit of Ceramic Materials Containing Small Flaws," *Eng. Fract. Mech.*, **25**, 483–495, 1986.
2. G. Sines and M. Adams, *Compression Testing of Ceramics, Fracture Mechanics of Ceramics*, Vol. **3**, Plenum, New York, 1978, pp. 403–434.
3. D. Munz and T. Fett, *Ceramics—Mechanical Properties, Failure Behaviour, Materials Selection*, Springer, Berlin, 1999.
4. D. F. Carroll and S. M. Wiederthorn, "High Temperature Creep Testing of Ceramics," in *Mechanical Testing of Engineering Ceramics at High Temperatures*, Elsevier Applied Science, London, 1989, pp. 135–149.
5. R. Kossowsky, D. G. Miller, and E. S. Diaz, "Tensile Creep Strength of Hot-Pressed  $\text{Si}_3\text{N}_4$ ," *J. Mater. Sci.*, **10**, 983–997, 1975.



# CHAPTER 23

## VISCOSITY MEASUREMENT

Ann M. Anderson, Bradford A. Bruno, and Lilla Safford Smith

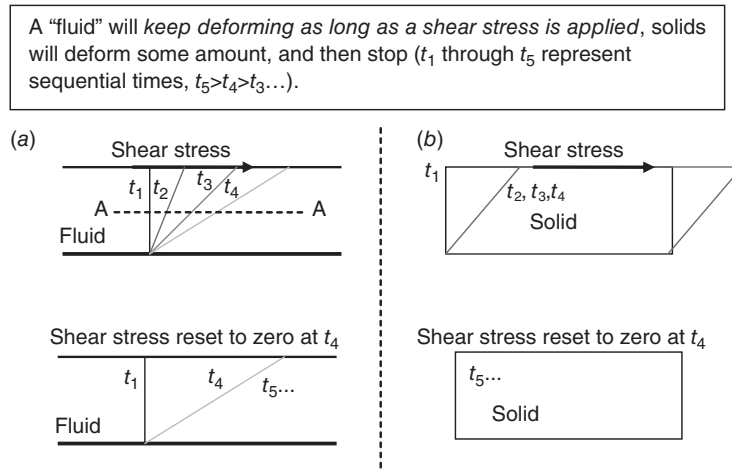
Union College

Schenectady, New York

<b>1</b>	<b>VISCOSITY BACKGROUND</b>	<b>809</b>	<b>3</b>	<b>MAJOR VISCOSITY MEASUREMENT METHODS</b>	<b>819</b>
<b>2</b>	<b>COMMON UNITS OF VISCOSITY</b>	<b>811</b>	3.1	Drag-Type Viscometers	820
2.1	Absolute Viscosity, $\mu$	811	3.2	Bubble (Tube) Viscometers	823
2.2	Kinematic Viscosity, $\nu$	811	3.3	Rotational Viscometers	824
2.3	Nonstandard Units	811	3.4	Flow-Type Viscometers	827
2.4	Distinction between Rheology and Viscometry	812	3.5	Orifice-Type (Cup) Viscometers	829
2.5	Mathematical Formalism	813	3.6	Vibrational (Resonant) Viscometers	831
2.6	Relation of Viscosity to Molecular Theory	815	<b>4</b>	<b>ASTM STANDARDS FOR MEASURING VISCOSITY</b>	<b>832</b>
2.7	Effect of Pressure and Temperature on Viscosity	816	<b>5</b>	<b>QUESTIONS TO ASK WHEN SELECTING A VISCOSITY MEASUREMENT TECHNIQUE</b>	<b>833</b>
2.8	Correlations of Viscosity with Temperature for Gases	818	<b>REFERENCES</b>	<b>835</b>	
2.9	Correlations of Viscosity with Temperature for Liquids	818			
2.10	Effect of Pressure on Viscosity	819			

### 1 VISCOSITY BACKGROUND

The most significant mechanical difference between materials classified as “fluids” and those classified as solids is in their reaction to shear stresses. (Recall that a shear stress is a distributed force, or force per unit area, whose direction of action is within the plane of application. If you slide your open hand over a desk top, the friction between your hand and the desk will create a shear stress on your hand.) As illustrated in Fig. 1, a solid (within its elastic limit) will deform through some limited angle while a shear stress is applied and will then return to its original configuration when the stress is removed. A fluid on the other hand will deform continuously as long as a shear stress is applied and will not return to its original shape when the stress is removed. For a fluid the *rate* of shear deformation is related to the magnitude of the shear stress applied, while for a solid the *amount* of shear deformation is related to the magnitude of the shear stress applied. This seemingly innocuous mechanical difference in reaction to shear stresses gives rise to the large difference in character between solids and fluids. In fact it gives rise to all of the behaviors that one thinks of as inherently “fluid”: the ability to flow, the ability to fill volumes of arbitrary shape, the ability to spread out and “wet” certain surfaces, etc. It also gives rise to the complex nature of fluid mechanics because it allows for the very large material deformations that in turn give rise to phenomena like turbulence.



**Figure 1** Fluid (viscous) versus solid (elastic) behavior. (a) Fluid (viscous) behavior: A thin layer of fluid held between two parallel plates, the top plate caused to move relative to the bottom plate by application of a shear stress, will continue to deform (experience shear strain) as long as the shear stress is applied. The rate of shear strain is related to the magnitude of the shear stress. When the shear stress is removed the fluid will remain in its deformed state. (b) Solid (elastic) behavior: A solid will deform (experience shear strain) through some fixed angle when a shear stress is applied. The amount of shear strain is related to the magnitude of the shear stress. When the shear stress is released the solid will return to its original.

Viscosity (or more precisely the *shear viscosity*, defined below) is the material property that defines the quantitative relation between the applied shear stress and the shear deformation rate in a fluid. Qualitatively the viscosity indicates the “thickness” or resistance to flow of a fluid. Since viscosity is the property that controls and quantifies the shear stress/shear rate behavior that is definitional to fluids, it is in many regards the most important physical property of a fluid.

Unfortunately, as alluded to above, the term *viscosity* is actually used to denote several related, *but different*, physical properties. It is important to understand these distinctions in terms from the outset. First, the term viscosity is most commonly used in conjunction with effects arising from *shear* forces and *shear* deformations in fluids. When used in this context, the most common one, the property is more precisely called the shear viscosity or the “first coefficient of viscosity.” However, when used in this sense, it is almost always simply referred to as “viscosity.” This is contrasted with the *bulk viscosity*, associated with volume dilatation. Bulk viscosity is rarely an important parameter and hence is not as well known or understood as the more common shear viscosity. Bulk viscosity is discussed briefly in Section 2.5. Second, it should be noted that even the shear viscosity described above is often stated in two different forms, the *absolute* or *dynamic* viscosity,  $\mu$ , and the *kinematic* viscosity or *momentum diffusivity*,  $\nu$ , where  $\nu = \mu/\rho$  and  $\rho$  is the fluid’s density. Although the dynamic and kinematic viscosities are clearly related properties, they are dimensionally dissimilar, and it is critically important to always distinguish between them. More is said on the distinction between dynamic and kinematic viscosity in the following section on common viscosity units.

The remainder of this chapter begins by discussing the units by which viscosity is measured. Then the distinction between the larger field of rheology and its subfield viscometry is made in the context of differentiating between the so-called Newtonian and non-Newtonian fluids. After that the chapter provides a brief theoretical and mathematical overview of viscosity.

Finally, the majority of the chapter provides detailed and practical information on methods for measuring viscosity.

## 2 COMMON UNITS OF VISCOSITY

There are several systems of units used with viscosity; many of them are archaic and/or closely tied to one specific viscosity measuring technique (e.g., the Saybolt cup and the Saybolt universal second, and the Krebs unit) or one particular industry (e.g., SAE oil grade and the automotive industry). It is impossible to capture all of these systems in one document, but an attempt is made below to define and relate the most common and standard units associated with viscosity measurement.

### 2.1 Absolute Viscosity, $\mu$

In terms of the SI (Le Système Internationale d'Unités) system of fundamental units, the derived units for absolute viscosity,  $\mu$ , are  $\text{kg}/\text{m} \times \text{s}$ , which is equivalent to  $\text{Pa} \cdot \text{s}$  (Pascal-seconds). This grouping of units has not received a name of its own. In the closely related cgs (centimeter, gram, and second) system of units, the derived unit of  $\text{g}/\text{cm} \times \text{s}$  or  $\text{dyne} \times \text{s}/\text{cm}^2$  is called a Poise (after Poiseuille). More commonly a centipoise,  $\text{cP} = 1/100\text{th}$  of a Poise is used. In the fps (foot, pound, and second) system of units, the units of absolute viscosity are  $\text{lb}_F \cdot \text{s}/\text{in}^2$ , which is called the reyn (after Osbourne Reynolds). Refer to Table 1 for a collection of units of absolute viscosity.

### 2.2 Kinematic Viscosity, $\nu$

Recall that the dynamic (kinematic) viscosity,  $\nu$ , is defined as the absolute viscosity divided by the fluid density,  $\rho$ . In the SI system of fundamental units the units for kinematic viscosity are meter square per second, which is not a named grouping. It should be noted that the units of kinematic viscosity ( $\text{m}^2/\text{s}$ ) are identical to the units of thermal diffusivity used in heat transfer, and mass (species) diffusivity used in diffusion. This leads to the kinematic viscosity being referred to as the coefficient of momentum diffusivity by analogy. In the cgs system the unit of kinematic viscosity is the centimeter square per second called the stokes (after G.G. Stokes). More commonly the kinematic viscosity is given in centistokes (cSt) where  $100 \text{ cSt} = 1 \text{ stokes}$ . In the fps system kinematic viscosity would be foot square per second or inch square per second, neither of which is a named unit.

### 2.3 Nonstandard Units

Kinematic viscosity is also often given in Saybolt universal seconds, or SUS (also sometimes SSU, "Saybolt seconds universal, or SUV, Saybolt universal viscosity), which is directly related to the Saybolt viscosity cup measuring system (see Section 2.2). Of course, the unit of seconds is

**Table 1** Units for Absolute/Dynamic Viscosity,  $\mu$

Units System	Derived Viscosity Unit	Unit Name	Equivalence
SI	$\text{kg}/\text{m} \times \text{s}$ or $\text{Pa} \times \text{s}$	none	$1 \text{ Pa} \cdot \text{s} = 10 \text{ poise} = 1000 \text{ centipoise}$
cgs	$\text{g}/\text{cm} \times \text{s}$ or $\text{dyne} \times \text{s}/\text{cm}^2$	Poise	$100 \text{ centipoise} = 1 \text{ poise}$
English (fps)	$\text{lb}_F \times \text{s}/\text{in}^2$	Reyn	$1 \text{ reyn} = 68,948 \text{ poise}$



not a dimensionally correct unit for the physical quantity of kinematic viscosity, so this system is problematic. The Saybolt measurement system is based on American Society for Testing and Materials (ASTM) method D88, and measurements in SUS can be converted into more standard (dimensionally correct) viscosity units using procedures provided in ASTM 2161. There are countless other such “legacy” scales of viscosity associated with different industries, and unfortunately there is often no standard method for converting these legacy measures into dimensionally correct viscosity units. A number of online viscosity converters exist (see [www.coleparmer.com](http://www.coleparmer.com), [www.gardco.com](http://www.gardco.com), or [www.cannon.com](http://www.cannon.com), for example) (Table 2).

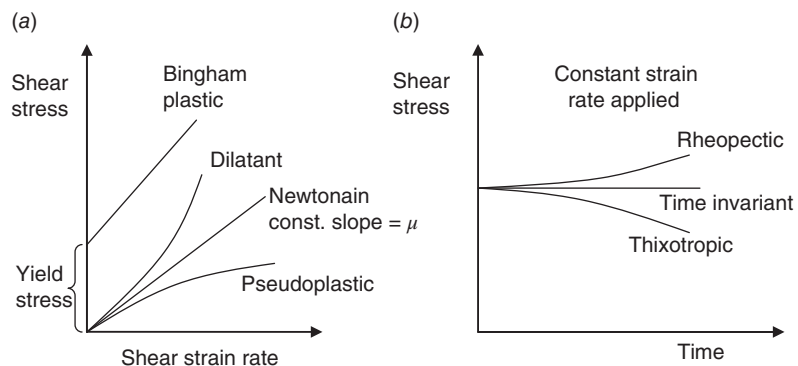
## 2.4 Distinction between Rheology and Viscometry

A simple linear relationship between shear stress and shear strain rate is observed in a wide variety of fluids (Fig. 2a). The constant slope of the line labeled Newtonian is the (shear) viscosity of the fluid. Fluids demonstrating such a relationship are known as *Newtonian fluids*. Many common fluids like air, gases in general, water, or simple oils demonstrate Newtonian behavior meaning constant viscosity with respect to strain rate over a very wide range (many orders of magnitude) of strain rates. The measurement of the shear viscosity of Newtonian fluids is referred to as *viscometry* and is the focus of this chapter.

Fluids with more complicated molecular structures (e.g., polymers) or fluids with other phases suspended in them (e.g., mixtures, slurries, and colloids) often demonstrate more complicated shear stress to strain rate behaviors (see Fig. 2a). Fluids exhibiting such behaviors are broadly characterized as “non-Newtonian” fluids. Non-Newtonian fluids can be further classified according to how they react to changes in shear deformation rates, to the duration of application of the applied loading, and to whether or not they exhibit a threshold elastic (solid-like) shear resistance prior to deforming like a fluid.

**Table 2** Units for Kinematic Viscosity,  $\nu$

Units System	Derived Viscosity Unit	Unit Name	Equivalence
SI	$\text{m}^2/\text{s}$	None	$1 \text{ m}^2/\text{s} = 10,000 \text{ Stokes}$
cgs	$\text{cm}^2/\text{s}$	Stokes	$100 \text{ centistokes} = 1 \text{ stokes}$
English (fps)	$\text{in.}^2/\text{s}, \text{ft}^2/\text{s}$	None	$1 \text{ in.}^2/\text{s} = 645.16 \text{ centistokes} = 0.00694 \text{ ft}^2/\text{s}$



**Figure 2** Newtonian and non-Newtonian fluid behavior (a) shear stress versus strain rate (b) shear stress versus duration of applied strain rate.

Fluids that show increasing *apparent viscosity* (the *apparent viscosity* is the local slope of the stress versus strain rate curve, see Fig. 2a) as the applied strain rate increases are called “shear thickening” or *dilatant* fluids. The classic example of a shear thickening fluid is a mixture of cornstarch in water. If one attempts to shear this fluid quickly (e.g., hit it with a hammer), the viscosity will rise to such a level that the fluid seems almost solid, the hammer blow will bounce off the surface. Yet at lower shear rates the mixture will act like a “normal” fluid (e.g., a hammer set on its surface would sink right into the fluid). Fluids that show the opposite behavior (decrease in apparent shear viscosity with increasing strain rate) are called “shear thinning” or *pseudoplastic* fluids. A common example of a shear thinning fluid would be “no-drip” paint, which behaves as a fairly thick (viscous) fluid while adhering to a paintbrush (a low shear rate circumstance) but that spreads easily (i.e., exhibits lower viscosity) when the paintbrush is dragged along a surface thereby increasing the shear strain rate applied to the fluid.<sup>1</sup>

Some fluids will “thin” (produce a lower shear stress resisting the motion) or some will “thicken” (produce a higher shear stress resisting the motion) as the *duration* for which a constant strain rate is applied increases (see Fig. 2b). Fluids exhibiting the former behavior are referred to as “thixotropic,” the latter as “rheopectic.” Such fluids are also sometimes referred to as “time-thinning” or “time-thickening” fluids. Examples of thixotropic fluids include yogurt and some classes of paint. Rheopectic behavior is much rarer. Examples include gypsum paste and printers ink. Newtonian fluids exhibit constant strain rate with regard to loading duration for a constant applied shear stress.

Newtonian fluids will exhibit constant strain rate to shear stress behavior down to very low (theoretically zero) applied shear stresses. However, some fluids, called “Bingham plastic” fluids will initially show “solidlike” behavior until a threshold shear stress (called the “yield stress”) is applied; after which they will show “fluidlike” behavior (continuously deforming while the shear stress is applied) (see Fig. 2a). A common example of this type of fluid is toothpaste, which will not flow at all until a threshold shear value is exceeded. Broadly speaking, this kind of behavior is described as viscoelasticity. Bingham plastic materials can show dilatant, Newtonian, or pseudoplastic behavior after their yield point. It is also worth noting that these terms are often not consistently applied.

The study and measurement of these more complicated, non-Newtonian, shear stress/shear strain rate behaviors is a subset of the larger science referred to as rheology and is largely beyond the scope of this chapter.

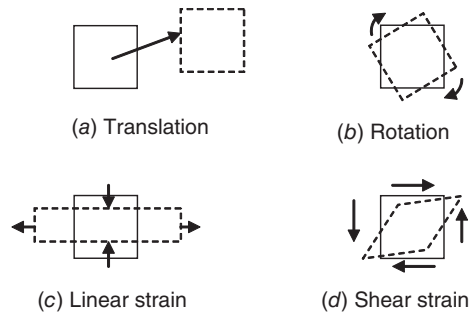
## 2.5 Mathematical Formalism

In this section we develop the mathematical formulations governing viscosity, and explain the roles and relations between “shear” viscosity and “bulk” viscosity. The discussion begins with the consideration of a very simple one-dimensional (1D) flow situation and then introduces the more general 3D form of the equations.

Shear viscosity is defined mathematically by Newton’s law of viscosity. Newton’s law defines viscosity as the physical property that relates the shear stress produced as a reaction to an applied strain deformation rate. If one considers the simple flow shown in Fig. 1a, a thin layer of fluid confined between two infinite parallel flat plates, the upper moving within its own plane relative to the lower, the total *shear strain rate* on any layer in the fluid is given by  $\partial u/\partial y$ , which is the rate of change of *x*-direction velocity in the perpendicular (*y*) direction. Newton’s law states that the shear stress experienced on the lower face of such a layer is given by

$$\tau = -\mu \frac{du}{dy} \quad (1)$$

where  $\mu$  is the (shear) viscosity of the fluid at the applied strain rate. If the shear viscosity is constant with regard to strain rate, then the fluid is said to be “Newtonian.” If the fluid



**Figure 3** Types of fluid motion and deformation illustrated in 2-D.

exhibits a more complex relationship between shear stress and strain rate, the fluid is defined as “non-Newtonian.” Distinctions between Newtonian and non-Newtonian behavior is discussed in greater detail in Section 2.4.

The viscosity picture becomes more complicated if we allow for more complex (3D) motions of the fluid. Any motion that a “particle” of fluid can undertake can be constructed from a superposition of the following four simpler types of motion: pure translation (movement without rotation or deformation), pure rotation (rotation without movement or deformation), pure linear strain (deformation without motion that does not disturb angles within the fluid particle), and pure shear strain (deformation without motion that does change angles within the fluid particle). Figure 3 illustrates these types of motions in two dimensions. In a fully general flow any combination of these motions can occur in any or all of the three coordinate directions. In such cases independent shear deformations (Fig. 3*d*) can occur on any or all of three orthogonal planes. The fluid can also undergo purely extensional deformations (i.e., elongations without shear, Fig. 3*c*) in any or all of the three dimensions. These extensional deformations will in some circumstances also contribute to the stress response of the fluid, for example, if they combine in such a way that the volume of the fluid element changes, then the bulk viscosity described below will also be important. Thus for general 3D deformations it is necessary to use tensors (a branch of mathematics that describes vectors pointing in several directions) to describe the full relation between the stress at a point in the fluid and the resulting strain.

The stress response of a Newtonian fluid element in response to a fully general deformation is given in White<sup>2</sup> as

$$\tau_{ij} = -P\delta_{ij} + \mu \left( \frac{\partial u_i}{\partial x_j} + \frac{\partial u_j}{\partial x_i} \right) + \delta_{ij}\gamma(\nabla \cdot \vec{V}) \quad (2)$$

Here  $\mu$  is the shear viscosity,  $\gamma$  is the bulk viscosity coefficient, and  $\delta_{ij}$  is the Kronecker delta function (i.e.,  $\delta = 1$  when  $i = j$ , and  $\delta = 0$  when  $i \neq j$ ), and  $i$  and  $j$  are indices used to refer to the three orthogonal planes. Those interested in the derivation of this relation are directed to White or any other graduate-level fluids text<sup>5</sup>.

One important point to note arising from Eq. (2) is that the stress response to purely extensional strains is described by the bulk viscosity,  $\gamma$ , or through the closely related “second coefficient of viscosity”  $\mu'$  (the bulk viscosity,  $\gamma$  is equal to the second coefficient of viscosity,  $\mu'$ , plus  $\frac{2}{3}\mu$ ; see Owczarek,<sup>3</sup> for example, for a more thorough discussion). The topic of bulk viscosity is largely beyond the scope of this chapter, but these few comments are made to inform the reader of when it may be safely ignored, and when it may become important. First it is important to note that the bulk viscosity is not as well understood or characterized as the more common shear viscosity. Fortunately, for Newtonian fluids, the bulk viscosity coefficient occurs

only in combination with the divergence of the velocity field ( $\nabla \cdot \vec{V}$ ); and for incompressible fluids conservation of mass (i.e., continuity) requires that  $\nabla \cdot \vec{V} = 0$ . Hence the bulk viscosity will play no role in a truly incompressible fluid.

Of course, no substance is truly 100% incompressible, so if one is concerned with acoustic issues (which are inherently a compressibility phenomenon) or flows at significant Mach number, the bulk viscosity may play a role. One way to gain insight on when the bulk viscosity may play a significant role is to examine its role in viscous dissipation. Ultimately, the role of viscosity (shear or bulk) is to irreversibly convert the mechanical energy in a flow into thermal energy (heat). This effect is known as “viscous dissipation.” Hence the magnitude of the dissipation caused by the viscosity can give one indication of the qualitative importance of viscosity in the flow. The dissipation ( $\Phi$ ) caused by the bulk viscosity is given by Shaughnessy et al.<sup>4</sup> as

$$\Phi_{\text{bulk}} = \frac{\gamma}{\rho^3} \left( \frac{d\rho}{dt} \right)^2 \quad (3)$$

where  $\gamma$  is the bulk viscosity and  $\rho$  is the density. In order to be significant, either large changes in density are required, or the changes in density must occur over very short time scales. Thus, due to the relative magnitudes of the extensional strains typically involved, the dissipation due to bulk viscosity (and indeed the bulk viscosity itself) may safely be ignored for almost all practical applications except shock waves (which involve large changes in density) and attenuation of high-frequency (small  $dt$ ) sound or “ultrasound.” Henceforth in this chapter the term viscosity shall refer to shear viscosity only.

## 2.6 Relation of Viscosity to Molecular Theory

As discussed above, ultimately the role of viscosity is to dissipate the ordered kinetic energy associated with the macroscopic motions of a flow to disordered, randomly distributed, microscopic molecular energy (i.e., thermal energy). As such it becomes clear that the quantity that we refer to as viscosity is the macroscopic manifestation of molecular-level effects, much in the same way that the macroscopic quantity of “pressure” represents the average net force per unit area caused by countless individual molecular collisions on a surface. That is to say that viscosity, like pressure, temperature, and density, is a “continuum property” of a substance. It makes no more sense to talk about the viscosity of a single molecule than it does to talk about the density of a single atom of a gas. The fact that the viscosity is an emergent property arising only for large collections of molecules places an important limitation on the concept of fluid viscosity, namely the continuum limit. Essentially the (continuum) concept of viscosity breaks down when applied on length scales that are comparable to the mean free path of the molecules in the fluid, or when applied on time scales that are comparable to the mean time period between molecular collisions in the fluid. For ordinary macroscopically sized flows at ordinary pressures, the continuum limit is not a concern. However, in applications such as nanotechnology (where the length scales of concern become very small) or rarefied gas dynamics (where the mean free path of molecules in very low density gases becomes very large), this limit should be kept in mind.

Examining how the macroscopically observed property of viscosity arises from molecular effects can provide insight and physical intuition about viscosity. If we examine how momentum is transported by the thermal (random) motions of molecules within a flow, we can come to understand the molecular basis for viscosity.

First, let us consider the physics qualitatively. To do so, consider again the simple 1D shear flow shown in Fig. 1. Specifically, consider the molecules near a plane parallel to the top plate and half way between the top plate and the bottom plate. All of these molecules will have

velocities that are composed of their individual, random (thermal) velocities (which average out to zero bulk velocity), plus a small extra velocity component that depends on the local value of the bulk velocity. Those molecules slightly above the plane will, on average, have slightly larger values of velocity in the  $x$  direction and therefore also have slightly higher values of  $x$ -direction momentum. Similarly, on average, those below the plane will have slightly lower values of  $x$  velocity and momentum. All of the molecules (above and below the plane) will have random thermal velocities with components in all three directions. The  $y$  component of these random velocities will occasionally carry molecules across the plane in both directions. But because of the asymmetry in velocity above and below the plane (i.e., because of the gradient of velocity perpendicular to the plane) the net effect of these random cross-plane exchanges will be to transport  $x$  momentum from above the plane to below the plane. That is, there will be a net flux of  $x$  momentum in the negative  $y$  direction.

In fact the quantity we call viscosity is precisely defined by this “diffusive” transport (i.e., transport caused by random molecular motions rather than bulk macroscopic fluid motions) of momentum in the direction opposite to a velocity gradient. A simple dimensional analysis will convince the reader that a stress, such as shear stress (measured in  $(\text{Pa} = \text{kg}/\text{m s}^2)$ , is dimensionally identical to a flux of momentum (transport of momentum per second per unit area  $= \text{kg}/\text{m s}^2$ ). Thus, referring back to Eq. (1), we can consider viscosity to be the fluid property that relates the diffusive momentum flux ( $\tau$ ) to the velocity gradient driving it.

## 2.7 Effect of Pressure and Temperature on Viscosity

### *Low-Density Gases*

We can make this relationship more quantitative by examining the actual molecular interactions occurring in the fluid. The following development parallels that given by Bird et al.,<sup>5</sup> but similar developments can be found in any text covering the kinetic theory of gases. The simplest model of viscosity arises from a consideration of simple kinetic theory of a low-density gas where we assume that the gas molecules are rigid spheres with diameter  $d$  that only interact through collisions (i.e., there are no forces causing “action at a distance” between molecules). Thus molecules will exchange momentum and come into equilibrium with their surroundings only through collisions. Kinetic theory for rigid sphere molecules also provides these other important results that will be used in this development:

The average random (thermal) velocity of the molecules in the gas will be

$$\bar{V} = \sqrt{\frac{8kT}{\pi m}} \quad (4)$$

where  $k$  is Boltzman’s constant,  $m$  is the mass of the individual molecules, and  $T$  is the absolute temperature.

The mean free path of a molecule between collisions,  $\lambda$ , will be

$$\lambda = \frac{1}{\sqrt{2}\pi d^2 n} \quad (5)$$

where  $n$  is the number density (number per unit volume) of the gas molecules.

The average frequency of collision per unit area (from one side) on any plane in the flow

$$Z = \frac{1}{4} n \bar{V} \quad (6)$$

If one again considers the situation of a plane between the two plates in Fig. 1, it can be shown that a molecule will travel an average vertical distance of  $\frac{2}{3} \lambda$  between collisions. The flux of  $x$  momentum transferred across the plane from below is then  $Zm v_{x,y=2/3\lambda}$  where  $v_{x,y=2/3\lambda}$  is the average excess (nonthermal)  $x$  velocity component at a  $y$  location “one collision distance”

below the plane (i.e., at  $y - \frac{2}{3}\lambda$ ). Similarly the flux of  $x$  momentum transferred across the plane from above is,  $Zmv_{x,y+2/3\lambda}$ . Thus the net  $x$  momentum flux is

$$\tau = Zmv_{x,y-2/3\lambda} - Zmv_{x,y+2/3\lambda} \quad (7)$$

And, if the  $x$  velocity gradient in the vicinity of  $y$  is linear, we can replace the  $v_x$  at locations above and below the plane with a first-order Taylor series in terms of the gradient at the plane, yielding

$$\tau = Zm \left[ \left( v_{x,y} - \frac{2}{3}\lambda \frac{dv_x}{dy} \right) - \left( v_{x,y} + \frac{2}{3}\lambda \frac{dv_x}{dy} \right) \right] \quad (8)$$

Simplifying and substituting in the definition of  $Z$  gives

$$\tau = \frac{-1}{3}nm\bar{V}\lambda \frac{dv_x}{dy}. \quad (9)$$

Comparing back to Eq. (1) we can see that

$$\mu = \frac{1}{3}nm\bar{V}\lambda \quad (10)$$

Further substitution for  $\bar{V}$  and  $\lambda$  yields

$$\mu = \frac{2}{3} \frac{1}{\pi^{3/2}} \frac{\sqrt{mkT}}{d^2} \quad (11)$$

Thus if the molecules are considered as perfectly rigid spheres (the simplest model), then  $\mu \sqrt{T}$ . Note also that the viscosity of such a gas is not expected to be a function of pressure based on this very simple molecular model. This is an important result that is largely borne out by experimental observations of real low-density gases; their dynamic viscosity is observed to depend only very weakly on pressure.

Of course, molecules are not perfectly rigid spheres for that would imply no force whatsoever between molecules until they come into contact (when their center-to-center distance equals  $d$ ) and then an infinite repulsion force. Clearly the idea of an infinite repulsion force is unphysical. In fact all molecules will show some “action at a distance” and, more importantly, act as if they have some “give” or flexibility when they “collide,” which will eliminate the unphysical infinite forces inherent in the simple rigid sphere model. Typically, these interactions are modeled as an intermolecular “potential” function from which the magnitudes of attractive and/or repulsive forces as a function of center-to-center distance can be calculated, as can an effective molecular diameter. The exact nature of these intermolecular potential functions is complicated and has received extensive study but is largely beyond the scope of this chapter. The interested reader is directed to Kogan<sup>6</sup> or Vicenti and Kruger,<sup>7</sup> for example. Here it is sufficient to make a few points. First, as more complex and precise relations for the potential theory are used, the predictions of macroscopic properties such as viscosity improve markedly. Second, the “action at a distance” effects associated with these potentials allow for pressure to have an effect on the viscosity of gases. But, as stated above, this is typically found to be a weak effect for common gases. And finally, the functional relation between the viscosity and the temperature in low-density gases depends critically on the details of this potential function.

The next simplest model of intermolecular relations (after the rigid sphere model) is one proposed by Maxwell. In such a model the potential function drops off as  $1/s^4$  where  $s$  is the center-to-center distance between the molecules. With such a model it can be shown that the “effective molecular diameter” will vary as:  $d^2 \propto 1/\sqrt{T}$  and so, referring back to Eq. (11),  $\mu \propto T$ . That is, a gas composed of “Maxwellian” molecules will have a viscosity that will increase linearly with temperature, as opposed to with the square root of temperature predicted from the rigid sphere model.

## 2.8 Correlations of Viscosity with Temperature for Gases

In reality, gases typically exhibit behaviors between the two extremes discussed in the section above (rigid and “Maxwellian”) and so their viscosity’s dependence on temperature is commonly correlated with a power-type law, as given by White:<sup>2</sup>

$$\frac{\mu}{\mu_0} = \left(\frac{T}{T_0}\right)^n \quad (12)$$

where the parameters  $n$ ,  $T_0$ , and  $\mu_0$  are specific to the particular gas. Values for  $n$  for most simple gas molecules fall between 0.5 and 1, as predicted by the above discussion. Some values for  $n$ ,  $T_0$ , and  $\mu_0$  can be found in White.

Another common correlation technique for gas viscosities is based on the work of Sutherland (1893) (as covered in Vicenti and Kruger<sup>7</sup>. Here viscosity is correlated as

$$\frac{\mu}{\mu_0} = \left(\frac{T}{T_0}\right)^{\frac{3}{2}} \left(\frac{T_0 + S}{T + S}\right) \quad (13)$$

where  $S$  is the so-called Sutherland parameter and  $T_0$ , and  $\mu_0$  are reference values. A completely equivalent form of this equation:

$$\mu = \left(\frac{C_1 T^{\frac{3}{2}}}{T + S}\right) \quad (14)$$

where

$$C_1 = \left(\frac{\mu_0}{T_0^{\frac{3}{2}}}\right)(T_0 + S) \quad (15)$$

is often used as well. Poling et al.<sup>8</sup> provided a detailed discussion of several much more detailed methods for estimating the variation of viscosity of both pure gases and mixtures of gases at various temperatures.

## 2.9 Correlations of Viscosity with Temperature for Liquids

In real (higher density, more complex molecular structure) gases and especially in liquids intermolecular forces (beyond the “collisional” forces discussed previously) play a critically important role. Molecules in such substances can exert significant force (and hence transfer significant momentum) “at a distance” without colliding. Since viscosity as a property arises from transfers of momentum, these “actions at a distance” must be accounted for in any physical model that hopes to adequately predict a material’s viscosity. The nature and magnitude of these noncollisional interactions are so complex and so large in liquids that currently no one general model exists that will adequately predict the viscosity of all liquids. Instead many specialized empirical and semiempirical relations are available. Some general trends, however, are observed for liquids, the most important being that *the viscosity of liquids falls off strongly with increasing temperatures*. One type of curve fit that is recommended for liquid viscosity, recommended by White,<sup>2</sup> is

$$\ln \frac{\mu}{\mu_0} \cong a + b \left(\frac{T_0}{T}\right) + c \left(\frac{T_0}{T}\right)^2 \quad (16)$$

where  $a$ ,  $b$ , and  $c$  are curve fit parameters and  $T_0$  and  $\mu_0$  are reference values. Another, slightly simpler, empirical correlation often used is “Andrade’s equation”<sup>9</sup>

$$\mu = D e^{BT} \quad (17)$$



which is often presented in the alternate form

$$\ln \mu = A + \frac{B}{T} \quad (18)$$

Viswanath et al.<sup>10</sup> provide a lengthy discussion of such correlation methods and coefficients  $A$  and  $B$  for a wide variety of liquids.

## 2.10 Effect of Pressure on Viscosity

The effects of pressure on viscosity are not nearly as significant as the effects of temperature. In many practical circumstances it is entirely sufficient to simply neglect the effect of pressure on viscosity. This has led to pressure effects being much less studied, and to data on viscosity at different pressures being much more sparse.

For low-density gases, the molecular dynamics models discussed above [refer to Eq. (10)] indicate that the absolute viscosity,  $\mu$ , should not depend on pressure at all; due to the competing effects of increasing number density ( $n$ ) and decreasing mean free path ( $\lambda$ ) as pressure is increased. Of course, the value of the kinematic viscosity,  $\nu = \mu/\rho$ , of gases will decrease with increasing pressure due to the increase in density,  $\rho$ , of the gas as the pressure increases. These predictions are largely borne out by experimental data for common low-density (ideal) gases. Poling et al.<sup>8</sup> provide a detailed discussion of several methods for estimating the viscosities of both pure gases and mixtures of gases at higher pressures.

Viscosity data for liquids at high pressure is sparse when compared to the quantity of data available at or near atmospheric pressures. In general, as pressure increases, so does the viscosity of most liquids. Both Viswanath et al.<sup>10</sup> and Poling et al.<sup>8</sup> recommend a method for estimating the effect of pressure on liquid viscosity attributed to Lucas<sup>11</sup>:

$$\frac{\mu}{\mu_{SL}} = \frac{1 + D(\Delta P_r/2.118)^A}{1 + C\omega \Delta P_r} \quad (19)$$

where  $\mu$  is the viscosity of the liquid at pressure  $P$ ;  $\mu_{SL}$  is the viscosity of the liquid at vapor pressure  $P_{vp}$ ;  $P_{vp}$  is the the vapor pressure;  $\Delta P_r = (P - P_{vp})/P_c$ ;  $T_r = T/T_c$ ;  $P_c, T_c$  are the critical pressure and temperature; and  $\omega$  is the acentric factor:

$$A = 0.9991 - \left[ \frac{4.674 \times 10^{-4}}{1.0523T_r^{-0.03877} - 1.0513} \right] \quad D = \left[ \frac{0.3257}{(1.0039 - T_r^{2.573})^{0.2906}} \right] - 0.2086$$

$$C = -0.07921 + 2.1616T_r - 13.4040T_r^2 + 44.1706T_r^3 - 84.8291T_r^4 + 96.1209T_r^5 - 59.8127T_r^6 + 15.6719T_r^7$$

In spite of the theory and correlation techniques described above, in many practical situations one must resort to simply measuring viscosity. The following section describes the different measurement techniques available.

## 3 MAJOR VISCOSITY MEASUREMENT METHODS

Viscometers are designed to make use of the theoretical relationship between shear stress and strain rate to measure viscosity. They do this using simple flows (1D, steady, fully developed) in which both the shear stress and strain rate can be measured. There are three primary types of viscometers: flow, drag, and resonant. The flow-type viscometers measure the rate of flow of the fluid in a tube or through an orifice. The shear stress can be calculated from theory (e.g., capillary tube viscometer) or estimated based on theory (e.g., orifice cup viscometers). Use of these



types of viscometers yields values for kinematic viscosity. Design parameters for flow-type viscometers include minimizing entrance and exit effects, maintaining a constant pressure head (which drives the flow), minimizing surface tension effects, and mitigating effects of temperature variation. Drag-type viscometers measure either the force on an object as it moves at a specified rate in the fluid (rotational viscometers) or measure the time it takes for an object to move a specified distance through the fluid (falling object and bubble tube viscometers). Use of these types of viscometers yields values for absolute viscosity (except for the bubble tube, which measures kinematic viscosity). Design parameters for drag-type viscometers include minimizing the effects of turbulence and flow separation through the specification of a flow condition (generally a low relevant Reynolds number), controlling for transients, minimizing surface tension effects, and mitigating effects of temperature variation. The third type of viscometer is the resonant or vibrational viscometer, which is most commonly used in in-line process applications. These are designed so that changes in the viscous damping bring about significant changes in the resonance behavior of the instrument. Use of these viscometers yields values for kinematic viscosity.

This section presents information on each of the three major viscometer types. It begins with the drag-type viscometers (falling object, bubble tube, and rotational) followed by the flow-type viscometers (capillary and orifice) and concludes with a discussion of vibrational viscometers. Each section includes information on the theory of operation, a description of the types of viscometers available, a list of available manufacturers, and the capabilities and advantages/limitations. This chapter focuses on the use of laboratory-type viscometers; however, some information is included on the use of process viscometers. This list of viscometers is not intended to be exhaustive but includes many of those that are most readily available commercially. There are other specialized methods for measuring viscosity, and the reader is referred to Viswanath et al.<sup>10</sup> for more information.

### 3.1 Drag-Type Viscometers

#### *Falling-Object Viscometers*

##### *Theory of Operation*

Falling-object viscometers determine viscosity ( $\mu$ ) by measuring the drag force acting on a falling object under specific flow conditions. Use of the falling-object viscometer requires a separate measurement of density to calculate kinematic viscosity. Figure 4 illustrates the forces acting on a falling object. This case shows a spherical object (a ball); however, there are a variety of falling objects that can be used such as needles and cylinders. There are three forces acting on the object:  $F_B$  the buoyancy force and  $F_D$  the drag force act upwards while  $F_G$  the gravitation force (weight) acts down. The buoyancy force is calculated using Archimedes principle and is equal to the weight of the fluid displaced by the object:

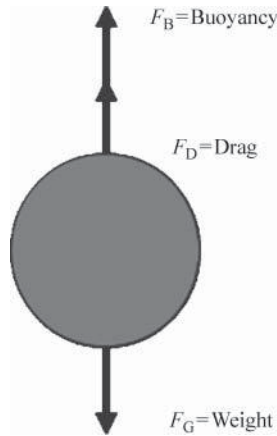
$$F_B = \forall_B \rho_f g \quad (20)$$

where  $\forall_B$  is the volume of the object,  $\rho_f$  is the density of the fluid, and  $g$  is the gravitational constant. The weight of the object is simply:

$$F_G = \forall_B \rho_B g \quad (21)$$

where  $\rho_B$  is the density of the object. If the object is traveling at terminal speed, the acceleration will be zero and application of Newton's second law yields an equation relating the three forces:

$$F_D = F_G - F_B = \forall_B (\rho_B - \rho_f) g \quad (22)$$



**Figure 4** Schematic showing the forces acting on a falling object.

The drag force is composed of a shearing force (due to the fluid) and a pressure force (due to flow separation). Falling-object viscometers are generally designed to operate in the Stokes (creeping) flow regime, which is characterized by a lack of flow separation and occurs for very low Reynolds numbers ( $Re < 0.1$ ). In this case the drag force is due only to the shearing force. For example, if the object is a sphere, then the Reynolds number is calculated as

$$Re = \frac{\rho_f V D}{\mu} \quad (23)$$

where  $V$  is the terminal speed of the object,  $D$  is the diameter of the sphere, and  $\mu$  is the viscosity. For the low Reynolds number situation, the drag force is related to Reynolds number by Stokes' Law:

$$F_D = \frac{3\pi\mu V D}{Re} \quad (24)$$

Combination of these equations yields an equation for viscosity in terms of the speed, diameter, and density difference:

$$\mu = \frac{g D^2}{18V} (\rho_{obj} - \rho_{fluid}) \quad (25)$$

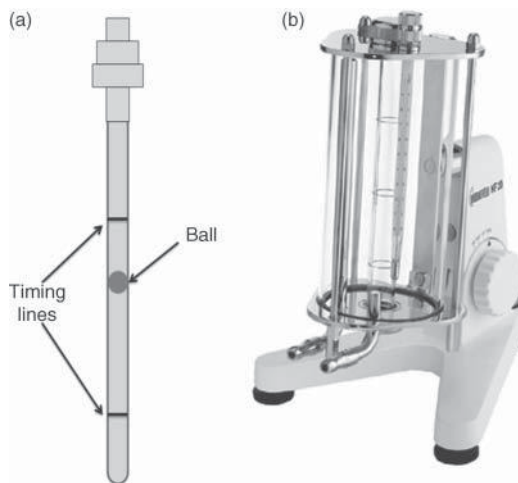
This theory applies to balls moving at low Reynolds number in an infinite media (see Brizard et al.<sup>12</sup> for development of the theory accounting for more realistic conditions). In many commercial applications, the falling object is placed in a tube of specified diameter (see Fig. 5). The object, typically a ball, will fall or slide down the tube, and the user measures the time it takes for the ball to travel between two timing lines. The first timing line is placed sufficiently far from the top of the viscometer to allow the ball to reach terminal velocity. The manufacturer supplies a calibration equation of the sort:

$$\mu = Kt(\rho_{obj} - \rho_{fluid}) \quad (26)$$

where  $K$  is a calibration constant and  $t$  is the measured time to fall the specified distance. To obtain the calibration constant the manufacturer measures the fall time of the ball in a series of liquids of known viscosity.

### ***Types of Viscometers/Options***

Falling-object viscometers use a variety of objects including spheres, needles, and cylinders. Falling-object viscometers often come with a set of objects, each with different mass/density,



**Figure 5** Falling ball viscometers (a) Gilmont and (b) Haake type. (Courtesy of Brookfield Engineering Labs)

which allows one to measure viscosity over a range of values. The most readily available commercial falling object viscometers are the relatively inexpensive Gilmont-type falling-ball viscometers and the more expensive, more accurate Haake-type falling-ball viscometers as shown in Figs. 5a and 5b. The Haake viscometers include a mounting mechanism and an outer chamber that can be used for temperature control of the sample during testing. Falling-needle viscometers use thin needlelike objects that are designed to minimize wall effects and are more stable as they fall (see Davis and Brenner<sup>13</sup>. They can be used to measure viscosity of non-Newtonian fluids. Falling cylinder viscometers involve a more complex flow field subject to significant end effects; however, they are useful for measuring viscosity at high pressure (Cristescu et al.<sup>14</sup>. Table 3 provides further information about suppliers of falling-object viscometers.

### Summary

Although falling-object viscometers are relatively inexpensive, the use of one requires some skill and is labor intensive. The tubes must be carefully cleaned before use and when filling the tube with the fluid of interest, care needs to be taken to avoid air bubbles. They cannot be used with opaque liquids. After setup, each individual measurement can take 1–2 min to complete.

**Table 3** Sampling of Common Falling-Ball Viscometer Types

Type	Name	Manufacturer/Vendor	Range (cP)	Price
Falling ball	Gilmont falling-ball viscometers	Gilmont; Cole Parmer/Thermo Scientific; Gardco	0.2–200	\$ (\$200)
Falling ball	HAAKE falling ball viscometer	HAAKE/Therm. Scientific	0.5–10 (up to 7500)	\$\$\$ (\$3500)
Falling ball	Brookfield falling ball viscometer	Brookfield/Gardco	0.5–70,000	\$\$\$ (\$3000)
Falling needle	PDV-100 portable field viscometer	Stony Brook Scientific/Gardco; Cole Parmer	5–106	\$\$ (\$700)

Gilmont-type viscometers must be mounted or held vertically, and care needs to be taken when handling them to avoid heating up the fluid in the viscometer. Haake-type viscometers are premounted at a specified angle, and the falling-ball tube is located inside an outer glass tube that can be easily connected to a circulating water bath for temperature control. They are not automated and require manual timing. However, it is relatively easy to compare the viscosity of different fluids by using multiple viscometers. The primary sources of error that arise in the use of a falling-ball viscometer are related to temperature effects, handling, and contamination.

### 3.2 Bubble (Tube) Viscometers

#### *Theory of Operation*

Although most drag-type viscometers measure absolute viscosity and require a separate measurement of density to calculate kinematic viscosity, bubble viscometers measure kinematic viscosity ( $\nu$ ) by measuring the drag on a rising bubble of air, which has low density compared to the fluid. The bubble tube consists of a glass tube (see Fig. 6a), which is filled with the liquid of interest (leaving space for a bubble to form). The tube is marked with timing lines, and the time for the bubble to rise is measured and compared to times for liquids with known viscosities.

The theory in this case is similar to that for a falling object, except that here one measures the time for the bubble to rise a specific distance (see Goldsmith et al.<sup>15</sup> for more information on the theory). If we ignore the effect of bubble viscosity the same equation for viscosity applies:

$$\mu = \frac{gD^2}{18V}(\rho_{\text{obj}} - \rho_{\text{fluid}}) \quad (27)$$

However, in the case of a rising gas bubble one can assume that the object (air) density is much less than that of the fluid and the calibration equation becomes

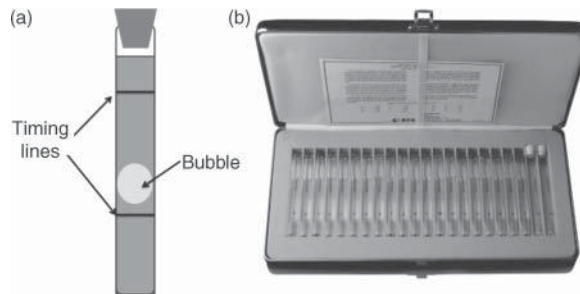
$$\mu = \frac{gD^2}{18V}(\rho_{\text{fluid}}) \quad (28)$$

Or in terms of kinematic viscosity

$$\nu = \frac{\mu}{\rho_{\text{fluid}}} = \frac{gD^2}{18V} \quad (29)$$

In practical applications, bubble viscometers use carefully manufactured precision tubes, which are calibrated using known viscosity standards. The kinematic viscosity is then calculated as

$$\nu = kt \quad (30)$$



**Figure 6** (a) Schematic of a bubble tube viscometer and (b) BYK-Gardner Bubble Viscometer Set. (Courtesy of BYK Gardner USA)

**Table 4** Sampling of Common Bubble Tube Viscometer Types

Type	Name	Manufacturer/Vendor	Range (St)	Price
Bubble viscometers	Gardner Standard Bubble Viscometers	Gardner/Gardco	0.5–5.5	\$\$
Bubble viscometers	Bubble Viscometer Kits	Cole Parmer	0.005–0.320	\$–\$\$

where  $k$  is the calibration constant for the tube and  $t$  is the time for the bubble to rise a specific distance. The faster the bubble travels, the lower the viscosity.

### *Types of Viscometers/Options*

Bubble tube viscometers are used to measure viscosity using either a direct measurement method or a comparison method. In the direct method, a single tube (like that shown in Fig. 6a) is used to measure the bubble rise time, and that time is converted to viscosity using information from the manufacturer. In the comparison method, the user selects reference tubes of known viscosity (see Fig. 6b) and directly compares the bubble rise time in the fluid of interest to the rise time in the reference tubes. The fluid of interest is then assumed to have the same viscosity as that of the reference tube with the closest rise time. Table 4 includes a list of suppliers for bubble tube viscometers.

### *Summary*

Bubble tube viscometers are relatively inexpensive. Their use requires some skill and measuring viscosity is labor intensive. The tubes must be carefully cleaned before use. After setup, each individual measurement typically takes 1–2 min to complete. The viscometer needs to be held in a vertical position during measurement (some manufacturers supply a stand to hold and flip the tubes) and care must be taken not to heat the liquid in the tube when handling. They are not suitable for use with opaque liquids. They are not automated and require manual timing; however, one can easily use multiple tubes to compare the viscosity of different fluids. The primary sources of error that arise in the use of a falling ball viscometer are related to temperature effects (it is not easy to supply external temperature control), handling, and contamination.

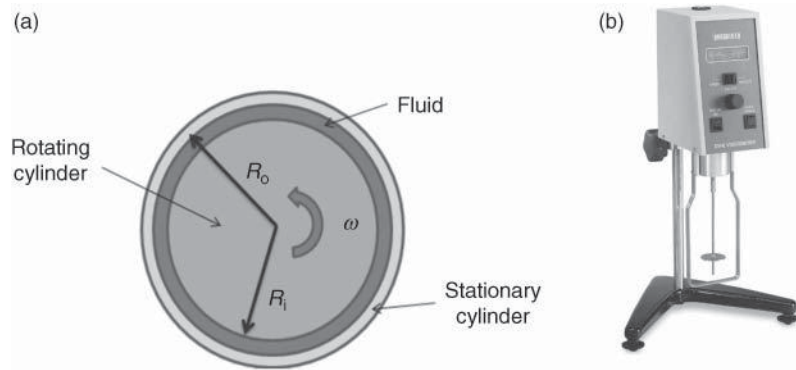
## 3.3 Rotational Viscometers

### *Theory of Operation*

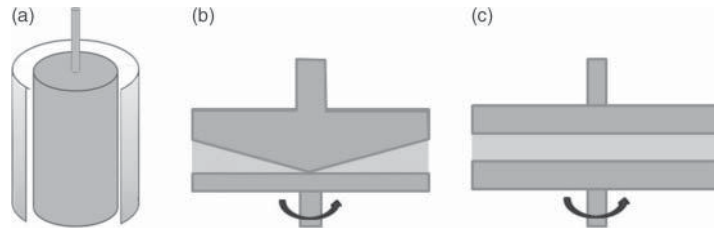
Rotational viscometers determine viscosity by measuring the resistance on a shaft rotating in the liquid of interest. They are designed to make a direct measurement of the absolute viscosity  $\mu$ . A schematic of a rotational viscometer is shown in Fig. 7a and 8a. Fig. 7b shows a commercially available Brookfield rotational viscometer. The viscometer includes a spindle (cylinder), attached to a rotating shaft. The spindle is placed in the liquid of interest and rotated at constant speed. The torque required to rotate the spindle is measured and then related to the fluid viscosity. Although their setup is somewhat more elaborate than that of the falling-ball or capillary viscometers, they can be used to study the behavior of non-Newtonian fluids.

The theory of operation of a rotational viscometer is based on the Couette flow model for fully developed, steady, incompressible laminar flow between two surfaces, one of which is moving. If we model a viscometer as a rotating cylinder inside a stationary cylinder as shown in Fig. 7a, the Couette flow solution for the wall shear  $\tau$ , assuming the gap between the two cylinders is small and the velocity varies linearly, is given as

$$\tau = \mu \frac{du}{dy} = \mu \frac{\omega R_i}{R_o - R_i} \quad (31)$$



**Figure 7** (a) Schematic of a cylinder in cylinder rotational viscometer and (b) spindle-type viscometer. (Courtesy of Brookfield Engineering Labs)



**Figure 8** Geometries typically used in rotational viscometer (a) cylindrical, (b) cone and plate, and (c) parallel plate.

where  $\omega$  is the rotational speed of the cylinder,  $R_i$  is the radius of the rotating cylinder, and  $R_o$  is the radius of the outer, stationary cylinder. The torque due to this wall shear is then equal to the shear force times the area over which the shear acts times the moment arm (in this case the inner radius):

$$T = \tau A R_i = \mu \frac{\omega R_i}{R_o - R_i} (2\pi R_i L) R_i \quad (32)$$

where  $T$  is the torque and  $A$  is the area of the rotating cylinder ( $2\pi R_i L$ ). Under steady-state conditions the torque due to the viscous forces equals that which is applied to keep the cylinder rotating. Therefore, the viscosity can be measured using the measured torque value and the geometry of the system:

$$\mu = T \frac{R_o - R_i}{2\pi\omega R_i^3 L} \quad (33)$$

In practice, rotational viscometers come with a variety of rotating spindles and calibration information that allows one to relate the torque measurement to viscosity. A typical calibration equation is in a form such as

$$\mu = \frac{T}{c\omega} \quad (34)$$

where  $T$  is the measured torque at a given rotation rate, and  $w$  and  $c$  are the calibration constants used to account for geometry and end effects. Some viscometers are equipped with a digital readout.

*Types of Viscometers/Options*

There are three main types of rotational viscometers: Concentric cylinders, cone and plate, and parallel plate. The concentric cylinder theory is described above for a rotating inner cylinder, which is more common. Systems are also designed to have a rotating outer cylinder to minimize the centrifugal forces, which lead to the formation of Taylor vortices. A variation on the concentric cylinder-type viscometer uses a rotating spindle in an infinite medium.

Cone and plate viscometers (see Fig. 8*b*) are designed to provide a uniform shear rate across the rotating plate. They consist of a conical surface and a flat plate, separated by a small gap that is filled with the liquid of interest. One of the plates is rotated and the torque required to hold the other in place is measured. The theory of operation is similar to that described above for the concentric cylinder viscometer, although the geometry is different. The cone angle in Fig. 8*b* is designed to provide the uniform shear rate.

Parallel-plate viscometers provide a nonuniform shear rate. They consist of two parallel plates (see Fig. 8*c*) separated by a gap filled with the liquid of interest. The shear rate acting on the fluid depends on the radial location. One plate typically rotates and the torque required to hold the other is measured. Again, the theory is similar to that described above; however, in this case the shear rate varies with radial distance. Table 5 presents a listing of types and manufacturers of rotational viscometers.

*Summary*

Rotational viscometers are more expensive than the other drag-type viscometers, but they are somewhat easier to use. Measurements can be made rapidly. Rotational speed can be altered to vary shear rates and test non-Newtonian fluids. The spindles, cones, and plates must be carefully cleaned before use so the testing of multiple fluids is more complex. The primary sources of error that arise in the use of a rotational viscometer are related to temperature effects, setup errors (the system must be level and care must be taken to avoid end effects and eccentricity), and calibration of the torque measurement system. Some rotational viscometers have built in temperature control. Process versions exist that can be used in-line (see Table 5).

**Table 5** Sampling of Common Rotational Viscometer Types

Type	Name	Manufacturer/Vendor	Range (cP)	Price
Cylindrical	Dial Reading	Brookfield Eng./Gardco	1–64 M	
Cylindrical	DV-E; DV-I Prime; DV-II+ Pro; DV-II+ Pro EXTRA	Brookfield Eng./Gardco	1–320 M	\$\$–\$\$\$\$
Cylindrical	HAAKE Rotational Plus Viscometer	Thermo Scientific; Cole Parmer	0.3–4000	\$\$\$\$
Cylindrical	Thomas Stormer Viscometers	Thomas Stormer/Gardco	332–2000	\$
Cylindrical	KU-2	Brookfield Eng./Gardco	27–5,274	
Cylindrical in-line	VTA Pneumatic Viscosel; VTE Electric Viscosel	Brookfield Eng.	0–10,000	
Cylindrical in-line	TT Series In-Line PV Process	Brookfield Eng.	2–10,000,000	
Cone and plate	LV, RV, HA and HB Series Viscometers	Wells-Brookfield/Brookfield Eng.; Gardco	0.3–7,864,000	
Cone and plate	High Shear CAP-1000+, CAP-2000+	Wells-Brookfield/Brookfield Eng.; Gardco	20–1,500,000	\$\$\$\$

### 3.4 Flow-Type Viscometers

#### *Capillary Viscometers*

##### *Theory of Operation*

Capillary viscometers determine viscosity through measurement of the flow rate of the liquid traveling through a capillary tube. A capillary tube is one with a large length to diameter ratio (i.e., long and skinny). A schematic of a capillary tube viscometer is shown in Fig. 9. Capillary viscometers are typically made of glass and consist of a bulb reservoir connected to the capillary tube. The theory of operation for a capillary tube viscometer is based on the Poiseuille model of laminar flow, which describes flow through a round pipe. The volume flow rate  $Q$  in a pipe can be derived from the Navier–Stokes equations for steady, laminar, and fully developed, incompressible flow as

$$Q = -\frac{\pi R^4}{8\mu} \frac{dP}{dy} \quad (35)$$

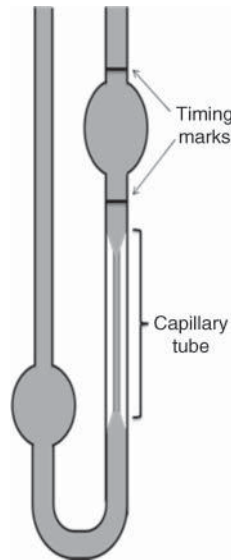
where  $R$  is the pipe radius,  $\mu$  is the viscosity and  $dP/dy$  is the pressure gradient (i.e., the change in pressure over the length of the pipe), which is the driving head for the flow. In the case of a vertical tube with both ends open to the ambient, the pressure gradient is caused by the hydrostatic pressure gradient:

$$\frac{dP}{dy} = -\rho g \quad (36)$$

where  $\rho$  is the density and  $g$  is the gravitational constant. Combining equations and rearranging

$$\frac{\mu}{\rho} = \nu = \frac{\pi R^4 g}{8Q} \quad (37)$$

which allows for calculation of the kinematic viscosity,  $\nu$ , from the measured flow rate and the geometry of the capillary tube. In practical applications, capillary viscometers are carefully calibrated and the manufacturer supplies a calibration constant. The user is instructed to



**Figure 9** Capillary tube viscometer (Ostwald type).



measure the time for the fluid to travel a specified distance and then the kinematic viscosity is calculated as:

$$v = Kt \quad (38)$$

where  $K$  is the manufacturer-supplied calibration constant and can be a function of temperature depending on the viscometer type.

### *Types of Viscometers/Options*

There are four primary types of capillary tube viscometers. They are the original Ostwald, the modified Ostwald, the suspended level (Ubbelohde), and the reverse-flow capillary viscometers. Each is described below.

The Ostwald viscometer is one of the simplest capillary tube viscometers. As shown in the schematic (Fig. 9), the viscometer consists of a bulb connected to a long capillary tube. To use the viscometer, one partially fills it and then draws the fluid to the upper mark above the right-side bulb (typically using a syringe system). The fluid is released to flow through the capillary tube and the time for the upper bulb to (fluid level at upper marks to lower marks) is measured. Some of the problems associated with the use of the Ostwald viscometer include the need to keep the viscometer vertical, the requirement for a specific volume of fluid and the effect of temperature on the viscosity measurement.

A number of modified Ostwald-type viscometers exist. These include the Cannon–Fenske routine viscometer, the Pinkevitch viscometer, and the Zeitfuchs (see Viswanath et al.<sup>10</sup>). Each is designed to address some of the sources of error found in the Ostwald type. For example, the Cannon–Fenske routine viscometer is designed to minimize the effect of tilt angle by placing the upper and lower bulbs along the same vertical axis.

Suspended-level viscometers are designed to address loading issues by using a constant pressure gradient (driving head) during measurement of viscosity. They do this by suspending the test liquid above the capillary tube and using a pressure equalization tube. They include the Ubbelohde and Cannon–Ubbelohde type of viscometers. To determine viscosity, the test liquid is loaded into the upper bulb and then released. The liquid flowing through the capillary is separated from the reservoir bulb at the bottom. The third tube, which connects the bottom of the capillary tube to the ambient, ensures that the only pressure difference between the top of the bulb and the bottom of the capillary is that due to the hydrostatic pressure, that is, the weight of the liquid.

Reverse-flow viscometers are used to measure the viscosity of opaque fluids (although they can also be used to measure that of transparent liquids). They measure the flow rate through a “dry” capillary tube so that the leading edge of the opaque fluid can be easily identified. Reverse-flow viscometers must be cleaned between each measurement.

There are a number of variations on the standard capillary tube viscometer, including small-volume (micro or semimicro) viscometers requiring 1 mL or less of fluid (useful in the measurement of the viscosity of blood and plasma), dilution viscometers with extra large reservoirs for dilution of the sample and vacuum viscometers for fluids with high viscosities such as asphalt. There also exist more rugged capillary tube viscometers that are used under continuous flow conditions in industrial applications, and disposable capillary models to avoid the labor (and error potential) associated with cleaning. Table 6 provides a sampling of the various capillary tube viscometers.

### *Summary*

Capillary tubes are used to measure viscosity for a wide range of fluids from oils to blood/plasma and even asphalt. They are relatively inexpensive (although generally more costly than the falling-ball and bubble tube viscometers). They require skill to use and can

**Table 6** Sampling of Common Capillary Viscometer Types

Type	Name	Manufacturer/Vendor	Range (St)	Price
Cannon-Fenske routine	Cannon-Fenske Routine	Cannon	0.5–100,000	\$
Ubbelohde	Cannon-Ubbelohde; Ubbelohde	Cannon	0.5–100,000	\$
Reverse flow	BS/U-Tube; Zeitfuchs Cross-Arm; Cannon-Fenske Opaque	Cannon	0.5–100,000	\$
Small volume	Cannon-Manning; Cannon-Ubbelohde Semi-Micro	Cannon	0.5–20,000	\$
Dilution	Cannon-Ubbelohde Four-Bulb Shear; Cannon-Ubbelohde Dilution	Cannon	0.5–20,000	\$
Vacuum	Asphalt Institute; Cannon-Manning; Modified Koppers Vacuum; and Zeitfuchs Cross-Arm	Cannon	0.036–5,800,000 P	\$
In-line viscometer	KV100 Capillary Viscometer	Brookfield Eng.	0–500 cP	

be labor intensive. Measurements take 1–5 min. Use requires manual timing and a method for filling the viscometer (a syringe system is typically used). The glass tubes are fragile. The tubes must be carefully cleaned before use, but the viscosity of different fluids is easily measured using different tubes. The primary sources of error that arise in the use of a capillary viscometer are related to temperature effects, setup errors (the tubes must be mounted vertically), and contamination. The tubes can be mounted in a temperature-controlled bath to minimize temperature effects and care must be taken not to affect the fluid temperature when handling. The calibration constant can be sensitive to temperature. Process versions exist that can be used in-line.

### 3.5 Orifice-Type (Cup) Viscometers

#### *Theory of Operation*

Orifice-type viscometers measure kinematic viscosity by comparing the time it takes the fluid to pass through an orifice (the efflux time) to the time that it takes a fluid of known viscosity to pass through the same orifice. They generally consist of a fluid reservoir from which the fluid flows, an orifice and a capturing reservoir (see Fig. 10). Although they were originally designed using the Poiseuille flow model, it was determined that entrance and exit effects in this type of device are significant. Therefore, cup methods only provide a relative measurement. Absolute values of viscosity cannot be measured using this type of viscometer.

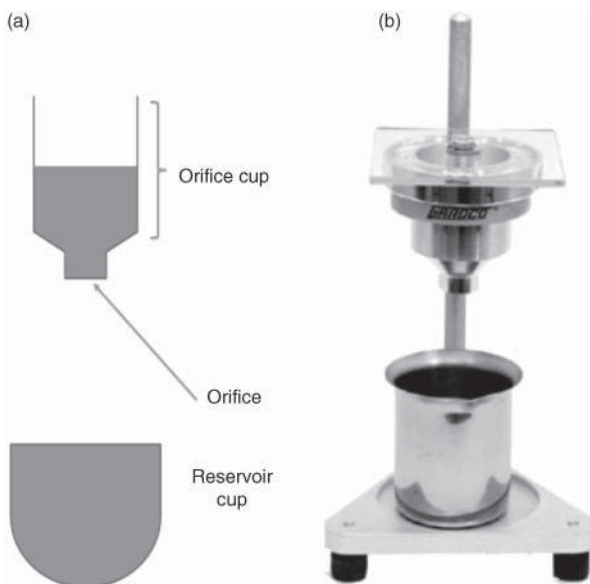
In practice, a “cup” or reservoir is filled with a specified quantity of the fluid of interest and allowed to equilibrate thermally. Then a valve is opened at the bottom of the cup and the time for the cup to is measured. Viscosity is then calculated using an *empirical* equation:

$$v = kt \quad (39)$$

where  $k$  is supplied by the manufacturer. These types of viscometers are commonly used to measure the viscosity of oils, varnishes, and paints. Specifications in certain industries or for certain industrial processes are often closely tied to one particular type of cup measurement, and thus it may be difficult to use or generalize viscosity information found with other viscosity measuring methods to these industrial applications.

#### *Types of Viscometers/Options*

Cup viscometers are commonly used in field measurements. There are a variety of cup types, including the early models used in the petroleum industry such as the Saybolt, Redwood, and



**Figure 10** (a) Schematic of cup viscometer and (b) image of a Ford cup viscometer. (Courtesy of Paul N. Gardner Company, Inc.)

**Table 7** Sampling of Common Cup Viscometer Types

Type	Name	Manufacturer/Vendor	Range (cSt)	Price
Dip viscosity cups	EZ (Equivalent Zahn) Viscosity Cups	Zahn/Gardco	10–1401	\$
Dip viscosity cups	S90 Zahn Signature Cups	Zahn/Gardco; Spectrum Chemical	15–1627	\$
Dip viscosity cups	Gardco/DIN 4mm Dip Viscosity Cups	DIN/Gardco	38–545	\$
Dip viscosity cups	Ford Dip Viscosity Cups	Ford/Gardco	2–1413	\$
Dip viscosity cups	Gardco/Fisher Dip Viscosity Cups	Fisher/Gardco	11–1125	\$
Dip viscosity cups	Gardco/ISO Mini Dip and Orifices	ISO/Gardco	4.6–823	\$
Dip viscosity cups	Norcross® Shell Viscosity Cup	Gardco	3.3–400	\$
Laboratory or “ring stand” viscosity cups	Ford Standard Viscosity Cups	Gardco	29–1413	\$
Laboratory or “ring stand” viscosity cups	Gardco/ISO Viscosity Cups	Gardco	4.6–2611	\$

Engle cups. The Ford, Zahn, and Shell viscosity cups (to name just a few) are more commonly used for measuring the viscosity of paints, varnishes, and lacquers. A sampling of cup viscometer types is listed in Table 7.

### Summary

Cup viscometers are relatively inexpensive but generally not very accurate. In fact cup “viscometers” do not produce true viscosity measurements, only relative ones. Their primary drawback is that information gained using them is not directly translatable or comparable to information obtained by other methods (although empirical relations making comparisons to other methods abound). In practice this leads to significant “legacy” effects, necessitating

the continued use of the same exact cup method if comparisons to historical data are desired. Thus a particular type of cup's use is typically closely tied to a certain industry, industrial process, or product, and the primary benefit of using such an "industry standard cup" is that their measurements can be directly compared to previous industrial knowledge or standards developed using the same method. Cup viscometers also require some skill to use (the cup requires steady holding during measurement) and can be labor intensive. Some models include a ring stand, others have handles, to hold the cup still and improve accuracy. Typical measurements are made in the field and each can take 1–2 min. The primary sources of error that arise in the use of a cup viscometer are related to temperature effects, setup errors, unsteadiness, and contamination. Most cups do not come with temperature control, and this can affect the measurement although Saybolt-type cup viscometers do include temperature control. Cups must be properly cleaned because even slight clogging of the orifice can cause significant error.

### 3.6 Vibrational (Resonant) Viscometers

#### *Theory of Operation*

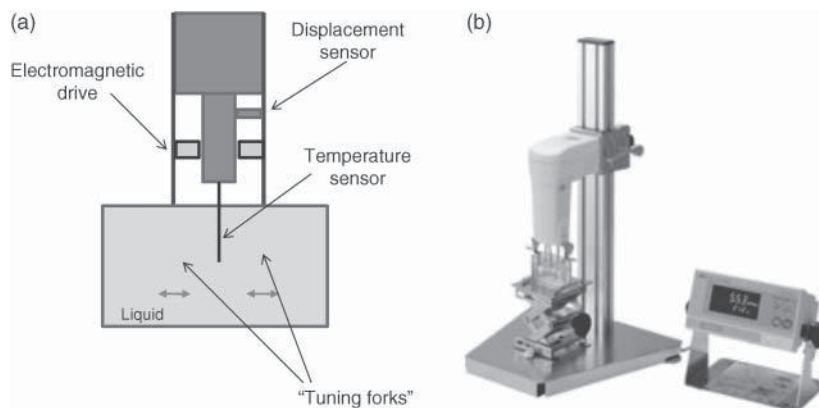
Vibrational viscometers determine viscosity by forcing a resonator to vibrate in the fluid of interest and then measuring the damping that is associated with fluid viscosity. This dampening effect is measured by one of three methods: (a) through measurement of the power required to maintain a constant vibration (the higher the viscosity of the fluid, the higher the power need); (b) measurement of the signal decay time upon halting the vibration (higher viscosity fluids will have a shorter decay time); or (c) looking at the frequency of the resonator as a function of the phase angle between the excitation and response signals.

#### *Types of Viscometers/Options*

Vibrational viscometers are commonly used in in-line process measurement applications, although lab versions exist. Table 8 presents information on a sampling of commercially available vibrational viscometers. The most common vibrational viscometers are configured as a tuning fork, an oscillating sphere, or a vibrating rod. Tuning fork vibrational viscometers have two sensor plates that are immersed in the liquid of interest. The plates (which have the same natural frequency) are made to vibrate at the same amplitude using an electromagnetic

**Table 8** Sampling of Common Vibrational Viscometer Types

Type	Name	Manufacturer/Vendor	Range (cP)	Price
Vibrational	Process viscometers	Vindum Eng.		
Vibrational	Portable viscometers	Vindum Eng.		
Vibrational	Special viscometers	Vindum Eng.		
Vibrational	Reactor viscometer	Vindum Eng.		
Vibrational	SV-A100	Gardco; Spectrum Chemical	1,000–100,000	\$\$\$\$
Vibrational	SV-10	Gardco	0.3–10,000	\$\$\$\$
Vibrational	SV-100	Gardco	1,000–100,000	\$\$\$\$
Vibrational	In-line viscometer	Nametre/Galvanic Applied Sciences		
Tuning fork vibrational	SV-A1 tuning fork vibration viscometer	Gardco; Spectrum Chemical; Cole Parmer	0.3–1,000	\$\$\$\$–\$\$\$\$\$
Tuning fork vibrational	SV-A10 tuning fork vibration viscometer	Gardco; Spectrum Chemical; Cole Parmer	0.3–10,000	\$\$\$\$\$–\$\$\$\$\$



**Figure 11** (a) Schematic of a vibrational viscometer and (b) Image of an SV-A Series Sine Wave Vibro Viscometer. (Courtesy of A&DWeighing)

force. The viscosity of the liquid is determined by measuring the current required to maintain the constant amplitude motion. Figure 11 shows a schematic of one type of tuning fork viscometer.

The oscillating sphere viscometers use the dampening associated with the torsional motion of a sphere immersed in the fluid of interest to measure viscosity. Vibrating rod viscometers do the same with a rod-shaped sensor. Tuning fork vibrational viscometers are capable of simultaneously measuring density and viscosity; however, the oscillating spheres and rod types require separate measurement of density (see Retsina et al.<sup>16</sup> for more details).

### Summary

Vibrational viscometers are more expensive than the other types of viscometers but they are much easier to use. Once they are installed in-line they require minimal skill and measurements can be made quickly. Their fundamental lack of moving parts makes them more robust and resilient, and thus better suited for use in harsh environments. The primary sources of error that arise in the use of a vibrational viscometer are related to calibration and drift errors.

*Viscosity Calibration Fluids.* Viscosity standards are standard fluids of known viscosity that are used to calibrate a viscometer. Most manufacturers recommend three or more fluids specified by the National Institute of Standards and Technology (NIST) that can be used to calibrate a viscometer. Viscosity standard oils can be found through Sigma–Aldrich, Gardco, Cole–Parmer, or other similar companies.

## 4 ASTM STANDARDS FOR MEASURING VISCOSITY

There are a variety of published standards available. In this section we focus on the standards put out by ASTM. Many industries adhere to specific guidelines provided by these or similar standards.

The ASTM viscosity standards come in two types: (a) standards focused on methods (method standards) and (b) standards based on materials (material standards). A method standard describes a viscosity measurement method that can be applied in a variety of circumstances. An example of this would be the Standard Test Method for High-Shear Viscosity

**Table 9** ASTM Standards

Material/ Method	Rotational Viscometers	Capillary Viscometers	Falling Object Viscometers	Cup-Type Viscometers	Bubble Viscometer	Tapered Plug/Bearing Viscometer
Iron and steel products	D562; D2196					
Construction	D4016-08; D7226-06e1; D4402-06; D7496-09; D562; D2196	D2171M-10; D2170M-10; D4957-08; D4603-03	D1823			
Petroleum products, lubricants and fossil fuels	D2983-09; D7042-04; D6896-03; D2161-05e1; D7279-08	D5481-10; D446-07; D445-09	D7483-08		D1545-07	D6616-07; D4683-09; D4741-06
Paints, related coatings and aromatics	D2196-10; D7394-08; D562-10; D4287; D6606; D7395-07	D5478-09; D6606-00; D4040-10; D1343-95	D1200-10; D4212-10; D5125-10;		D1725-04	
Plastics	D1824-95	D5225-09; D4603-03; D446	D1823			

Using a Cone/Plate Viscometer, D-4287, which specifies a method for using a cone-and-plate viscometer and in particular applies this to paint. Because such standards specify the method, they can be applied beyond the particular material discussed in the standard. A material standard outlines multiple techniques that can be used to measure the viscosity of one specific material. For example, the Standard Test Methods for Viscosity of Adhesives, D1084, provides four different methods to test free-flowing adhesives with a viscosity range from 50 to 20 k cP. One limitation of the material standards is that they have a narrow focus.

Table 9 provides a starting point for finding both types of standards. In this table the different methods (viscometer type) are listed by column and the material types are listed by row. For example, if one wishes to use a cup-type viscometer to measure the viscosity of paints ASTM D1200-10, D4212-10, and D5125-10 apply. One can also utilize the ASTM website to search for standards. The bolded standards in Table 9 are the recommend starting standards as they are the most general and provide a good list of referenced documents.

## 5 QUESTIONS TO ASK WHEN SELECTING A VISCOSITY MEASUREMENT TECHNIQUE

This section is intended as a guide to the practicing engineer on how to choose the appropriate viscometer. It is structured as a series of nonhierarchical questions. Table 10 also provides a summary comparison of the different viscometer types.

**1. Do you need an online/process measurement or an offline measurement?** If you need to continuously monitor the viscosity of an industrial process stream online or in situ, your choices of available technique will be limited, and the cost of your system will be higher. On the positive side, very little operator labor will be required once the system is installed, and there will be no need to remove and handle samples from the process stream. Measurements

**Table 10** Comparison of Viscometer Types

Type	Falling Object	Bubble Tube	Rotational	Capillary	Cup	Vibrational
Viscosity range	0.2–70 k cP	0.005–5.5 cSt	0.3–320 M cP	0.5–100 k cSt (general), 0.5–20 k cSt (small volume) up to 5.8 MP (vacuum)	4–2600 cSt	4–2600 cSt
Labor/skill level	High	High	Med	High	Med	Low
Automated?	No	No	Yes	Some	No	Yes
In-line?	No	No	Some	Some	No	Yes
Expense	\$100–\$200 Gilmont \$1000 Haake	(\$50–100 each or \$400–1000 for a kit)	Expensive	\$200–\$300		Expensive

can be taken at much shorter time intervals, and the viscosity will be known at exactly the conditions (temperature, pressure) associated with the process. The main viscometry techniques available for online measurement are resonant, capillary, and rotational. More information on the measurement range and suppliers of these viscometers can be found in Tables 5, 6, and 8.

**2. What is the viscosity range that you will be measuring?** Matching the viscometer to the viscosity range to be measured is one of the most important tasks associated with selecting a viscometer. Since many techniques measure the time for a certain amount of fluid to flow (e.g., cup or capillary types), or for an object to fall through the fluid (e.g., falling-ball or rising bubble types), if the fluid viscosity is higher than optimal for a given viscometer, the measurements may take an exceedingly long time to conduct. On the other hand, if the viscosity is too low, key assumptions related to the operation of the viscometer (e.g., the low Reynolds number assumption) may be violated and accuracy will be lost. Rotational-type viscometers simply will not give a reading and may in fact be damaged if the fluid being measured is too viscous for the instrument and settings selected. On the other hand if the viscosity is such that the reading is less than 10% of the instrument's full range (for a given setting), the uncertainty of the measurement will become unacceptably high. Thus good results necessitate careful matching of the viscosity range and the instrument. Operating ranges for many common types of viscometers are listed in Tables 3–8.

**3. What other characteristics of the fluid must be considered?** Other physical properties of the fluid beyond viscosity are also important to consider. For example, certain techniques or instruments lend themselves to use with opaque fluids (e.g., the reverse-flow viscometer) while others cannot be used because the technique depends on being able to see through the fluid (e.g., falling ball). Likewise, chemical compatibility of the fluid with the exposed viscometer surfaces is important to consider, as are any issues associated with safe handling of the fluid. Also various properties such as how difficult the fluid will be to clean off of the viscometer surfaces, and how likely the fluid is to solidify and clog are critical. Certain specialized fluids, like blood, have specific viscosity instruments designed specifically for use with them.

**4. Do you wish to measure kinematic or dynamic viscosity?** Each type of viscometer fundamentally measures either the absolute viscosity of a fluid ( $\mu$ ) or the kinematic viscosity ( $\nu$ ). In order to convert between the two a separate measurement of the fluid's density is required. Thus care must be exercised in selecting a viscometer if one wishes to avoid the need for this additional measurement.



5. *How much and what type of labor is required?* The quantity of labor (time) and skill level required to make accurate viscosity measurements varies significantly among different viscometer types. Broadly speaking, the lower cost viscosity measurement instruments (falling ball, rising bubble, and capillary tube) are more labor intensive to use and require significantly more skill (operator training) than the more expensive viscometer types (rotating disk, vibrating rod, etc.). The frequency of measurements required, as well as the labor associated with maintenance, calibration, and cleaning of the viscometer should be carefully considered in this context.

6. *What is the required accuracy?* Another major factor influencing the type of viscometer to chose is the required accuracy. Here some of the simplest models (e.g., capillary and falling ball) compare quite well on the basis of accuracy with more expensive techniques, assuming a sufficiently skilled and careful operator. However, the old truism that increased accuracy leads to increased expense does generally hold within a given class of viscometer. As discussed in point 5, labor costs may be significant in regards to the cost/accuracy decision.

7. *Are there standard methods associated with your industry or fluid?* Viscosity measurements for many substances, for many industries, and for the use of many types of viscometers are the subject of government or industrial standards. For example, the ASTM standards governing viscosity measurement are discussed at length in Section 3. Likewise many industries or industrial processes are closely tied to particular viscosity measurement techniques, even if these are outmoded. In such cases there may be a considerable body of industrial or process control knowledge that is not readily translatable to more standard viscosity measurements (e.g., the use of the “Stein–Hall cup” measurement with starch-based adhesives used in corrugated box manufacturing). In such cases sticking with the “standard method” may be the most desirable approach.

8. *Is temperature control needed? Is viscosity as a function of temperature needed?* The viscosities of liquids and gases are a strong function of temperature, and this should always be kept in mind when collecting and reporting viscosity data. Some viscosity measurement techniques lend themselves more readily to maintaining temperature control of the fluid during the measurement (e.g., the Haake falling-ball viscometer has a built-in temperature bath capability, for other types that capability must be added ad hoc). Likewise some viscometers (e.g., Brookfield rotational viscometer with small sample adapter) lend themselves to measuring the viscosity of a fluid over a wide range of temperatures.

9. *Quantity of fluid needed for the measurement.* This is an important factor to consider when dealing with scarce or expensive fluids (e.g., blood). Viscosity measurement techniques can vary by more than an order of magnitude in the amount of liquid required to make a measurement.

10. *Specialized needs.* If your process involves specialized needs or requirements, that is, measurements at high pressure or measurements at temperature extremes, there are viscometers available specifically for those purposes.

## REFERENCES

1. Y. A. Cengel and J. M. Cimbala *Fluid Mechanics, Fundamentals and Applications*, 2nd ed., McGraw-Hill, New York, 2010.
2. F. M. White, *Viscous Fluid Flow*, 3rd ed, McGraw-Hill, New York 2006.
3. J. A. Owczarek, *Fundamentals of Gas Dynamics*, International Textbook, Scranton, PA, 1964.
4. J. Shaughnessy, Jr. M. Katz, and J. P. Schaffer, *Introduction to Fluid Mechanics*, Oxford University Press, New York, 2005.
5. R. B. Bird, W. E. Stewart, and E. N. Lightfoot, *Transport Phenomena*, Wiley, New York, 1960.



6. M. N. Kogan, *Rarefied Gas Dynamics*, Plenum New York, 1969.
7. W. G. Vicenti and C. H. Kruger, *Introduction to Physical Gas Dynamics*, Wiley, New York, 1965.
8. B. E. Poling, J. M. Prausnitz, and J. P. O'Connell, *The Properties of Gases and Liquids*, 5th ed., McGraw-Hill, New York, 2004.
9. B. R. Munson, D. F. Young, T. H. Okiishi, and W. W. Huebsch, *Fundamentals of Fluid Mechanics*, 6th ed., Wiley, Hoboken, NJ, 2009.
10. D. S. Viswanath T. K. Ghosh D. H. Prasad N. V. K. Dutt and K. Rani *Viscosity of Liquids. Theory, Estimation, and Data*, Springer, New York 2007.
11. K. Lucas, Die Druckabhängigkeit der Viskosität von Flüssigkeiten eine einfache Abschätzung, *Chem. Ing. Tech.* **53**, 959, 1981.
12. M. Brizard et al., "Design of a High Precision Falling-Ball Viscometer," *Rev. Scient. Instru.*, **76**, 025 109, 2005.
13. A. M. J. Davis and H. Brenner "The Falling-Needle Viscometer," *Phys. Fluids*, **13**, 3086, 2001.
14. N. D. Cristescu B. P. Conrad, and R. Tran-Son-Tay, "A Closed Form Solution for Falling Cylinder Viscometers," *Int. Jo. Eng. Sci.* **40**,(6), 605–20, 2002.
15. H. L. Goldsmith and S. G. Mason, "The Movement of Single Large Bubbles in Closed Vertical Tubes," *J. Fluid Mech.* **14**(01), 42–58, 1962.
16. T. Retsina, S. M. Richardson and W. A. Wakeham, "The Theory of a Vibrating-Rod Viscometer," *Appl. Scien. Res.* **43**, 325–346, 1987.

# CHAPTER 24

## TRIBOLOGY MEASUREMENTS

**Prasanta Sahoo**  
Jadavpur University  
Kolkata, India

<b>1 INTRODUCTION</b>	<b>837</b>	5.8 Measurement of Oxygen and Other Gauges	852
<b>2 MEASUREMENT OF SURFACE ROUGHNESS</b>	<b>839</b>	<b>6 MEASUREMENT OF MATERIAL CHARACTERISTICS</b>	<b>852</b>
2.1 Surface Profilometer	839	6.1 Hardness	852
2.2 Optical Microscopy	840	6.2 Young's Modulus and the Elasticity Limit	854
2.3 Advanced Techniques for Surface Topography Evaluation	840	6.3 Fracture Toughness	854
<b>3 MEASUREMENT OF FRICTION</b>	<b>844</b>	6.4 Residual Stresses	854
3.1 Inclined-Plane Rig	845	6.5 Chemical Composition of a Surface	855
3.2 Pin-on-Disc Rig	845	<b>7 MEASUREMENT OF LUBRICANT CHARACTERISTICS</b>	<b>855</b>
3.3 Conformal and Nonconformal Geometry Rig	846	7.1 Analysis of Chemical Changes	856
3.4 Environment Control	846	7.2 Viscosity Measurement	856
3.5 Techniques for Friction Force Measurement	846	7.3 Lubricant Oxidation Tests	858
<b>4 MEASUREMENT OF WEAR</b>	<b>847</b>	<b>8 WEAR PARTICLE ANALYSIS</b>	<b>858</b>
<b>5 MEASUREMENT OF TEST ENVIRONMENT</b>	<b>849</b>	8.1 Chemical Analysis of Particles in Lubricant	858
5.1 Temperature Measurement	849	8.2 Analysis Based on Separation of Wear Particles	859
5.2 Thermocouples	849	<b>9 INDUSTRIAL MEASUREMENTS</b>	<b>859</b>
5.3 Thin-Film Sensors	850	<b>10 SUMMARY</b>	<b>859</b>
5.4 Radiation Detectors	850		
5.5 Metallographic Observation	850		
5.6 Liquid Crystals	852		
5.7 Humidity Measurement	852		

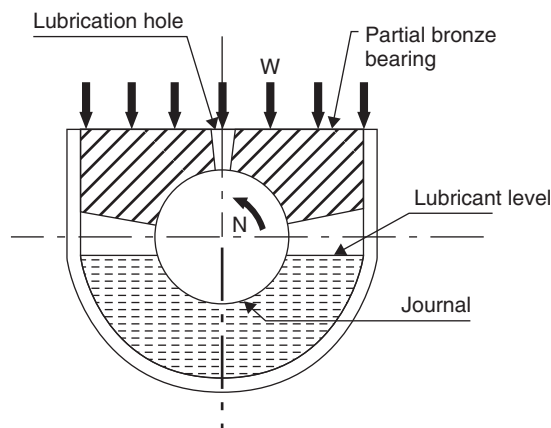
### 1 INTRODUCTION

Tribology as a subject is relatively new, but the practice of tribological principles is older than recorded history. Tribology is defined as the science and technology of interacting surfaces in relative motion and of related subjects and practices. It deals with the technology of lubrication, control of friction, and prevention of wear. Successful design of machine elements depends essentially on the understanding of tribological principles. During contact of two nominally flat surfaces, contact occurs at discrete spots due to surface roughness and adhesion occurs due

to intimate contact. When one solid body moves over another, it experiences the resistance to motion called friction. The surface damage or material removal that takes place in a moving contact is termed as wear. Surface coatings and treatments are provided to monitor friction and to control wear. The most effective way of friction and wear control is by using proper lubricants either liquid, solid, or gas. The lubricant properties and the mechanisms of lubrication constitute the essence of optimum performance and reliability of bearings. The recent emergence of proximal probes and high-capability computational techniques has stimulated systematic investigations of interfacial problems with high resolution in micro- and nanocomponents leading to the development of the new field of micro-/nanotribology.

Tribology is different from other science branches, for example, fundamental physics, where theoretical predictions are made long before the experimental validation of the same. Tribology uses a more empirical methodology based on experimental observation and theoretical concepts follow the findings later. A classical example of experimental observation leading to the development of the basic tribological concept of a hydrodynamic pressure field operating in a lubricated bearing is Tower's friction experiments. The railway axle bearings were fitted with numerous oil holes in order to supply oil to the bearing. However, during operations, oil leaked through the holes and even wooden plugs were unable to prevent the leakage. Tower fitted pressure gauge at the oil holes to find that the oil pressure was capable of supporting the bearing load. Figure 1 is a schematic representation of the partial bearing used by Tower. Tower's results led to development of the hydrodynamic theory of lubrication by Osborne Reynolds.

Most tribological phenomena, for example, friction, wear, and frictional heating, are not intrinsic material properties. These depend on a number of competing factors. For example, to evaluate load capacity of a hydrodynamic bearing one needs to consider viscous heating of the lubricant, cavitation and turbulent lubricant flow, elastic deformation of bearing structure, and so on. Friction and wear being chaotic processes, these are described in terms of specific experimental findings that are systematically analyzed to get an engineering model of friction, wear, and lubrication. Tribological investigation may be categorized into two groups: fundamental research for understanding of basic mechanisms of friction and wear and applied research for resolving specific industrial friction and wear issues. On both counts, tribological measurements mainly include surface roughness, friction, wear, test environment, material characteristics, and lubricant characteristics. Wear particle analysis and industrial tribology form an important part of tribological measurement.



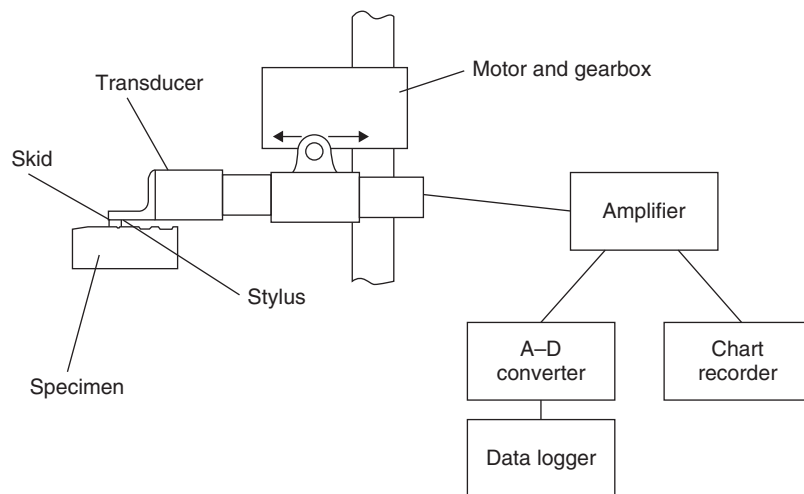
**Figure 1** Schematic representation of the partial bearing used by Tower.

## 2 MEASUREMENT OF SURFACE ROUGHNESS

The surfaces of any engineering component contain a vast number of peaks and valleys and it is not possible to measure the height and location of each of the peaks. So what is done is to take measurements from a small and representative sample of the surface so chosen that there is a high probability for the surface lying outside the sample to be statistically similar to that lying within the sample. Over the years different methods have been devised to study the topography of surfaces. A brief outline of some of the methods is presented here.

### 2.1 Surface Profilometer

The most common method of studying surface texture features is the stylus profilometer, the essential features of which are illustrated in Fig. 2. A fine, very lightly loaded stylus is dragged smoothly at a constant speed across the surface under examination. The transducer produces an electrical signal, proportional to displacement of the stylus, which is amplified and fed to a chart recorder that provides a magnified view of the original profile. But this graphical representation differs from the actual surface profile because of difference in magnifications employed in vertical and horizontal directions. Surface slopes appear very steep on the profilometric record though they are rarely steeper than  $10^\circ$  in actual cases. The shape of the stylus also plays a vital role in incorporating error in measurement. The finite tip radius (typically  $1\text{--}2.5\ \mu\text{m}$  for a diamond stylus) and the included angle (of about  $60^\circ$  for pyramidal or conical shape) result in preventing the stylus from penetrating fully into deep and narrow valleys of the surface, and thus some smoothing of the profile is done. Some error is also introduced by the stylus in terms of distortion or damage of a very delicate surface because of the load applied on it. In such cases a noncontacting optical profilometer having optical heads replacing the stylus may be used. Reflection of infrared radiation from the surface is recorded by arrays of photodiodes, and analysis of the same in a microprocessor results in the determination of the surface topography. Vertical resolution of the order of  $0.1\ \text{nm}$  is achievable though maximum height of measurement is limited to a few micrometers. This method is clearly advantageous in the case of very fine surface features.



**Figure 2** Component parts of a typical stylus surface-measuring instrument.

## 2.2 Optical Microscopy

In this method, the surface of interest is held to reflect a beam of visible light and then these are collected by the objective of the optical microscope. An image of the surface is produced and is analyzed at very high rates of resolution (up to  $0.01\ \mu\text{m}$ ) by optical interferometers. Depth of field achievable is up to  $5\ \mu\text{m}$ . However, success of the method depends on the reflective property of the material, which limits the use of the same.

Optical methods may be divided into two groups: geometric methods and physical methods. Geometric methods include light-sectioning and taper-sectioning methods. Physical methods include specular reflection, diffuse reflection, speckle pattern, and optical interference.

In the *light-sectioning method*, the image of a slit is thrown onto the surface at an incident angle of  $45^\circ$ . The reflected image appears as a straight line if the surface is smooth and as an undulating line if the surface is rough. In the *taper-sectioning method*, a section is cut through the surface to be examined at an angle of  $\theta$ , thus effectively magnifying the height variation by a factor of  $\cot \theta$  and is subsequently examined by an optical microscope. The surface is supported with an adherent coating that prevents smearing of the contour during the sectioning process. The taper section is lapped, polished, and lightly heat tinted to provide good contrast for optical examination. The process suffers from the disadvantages, e.g., destruction of test surface and tedious specimen preparation.

In the *specular reflection method*, gloss or specular reflectance, which is a surface property of the material and a function of reflective index and surface roughness, is measured by a gloss meter. Surface roughness scatters the reflected light and affects the specular reflectance. Thus a change in specular reflectance provides a measure for surface roughness.

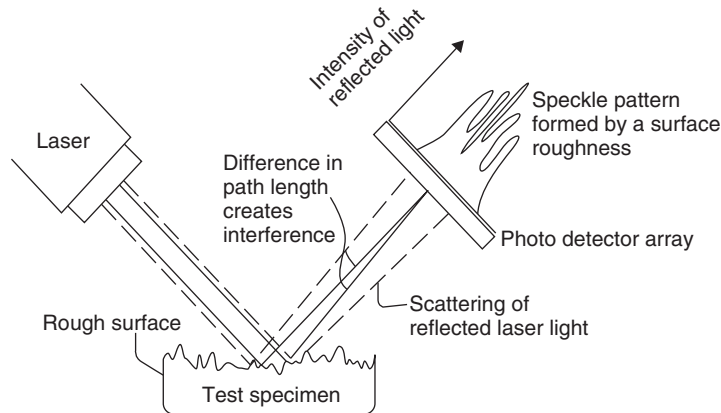
The *diffuse reflection method* is particularly suitable for online roughness measurement during manufacture since it is continuous, fast, noncontacting, and nondestructive. This method employs three varieties of approaches. In the total integrated scatter (TIS) approach, one measures the total intensity of the diffusely scattered light and the same is used to generate the maps of asperities, defects, and particles rather than microroughness distribution. The diffuseness of scattered light (DSL) approach measures a parameter that characterizes the diffuseness of the scattered radiation pattern and relates the same to the surface roughness. In the angular distribution (AD) approach, the scattered light provides roughness height, average wavelength, or average slope. With rougher surfaces, this may be useful as a comparator for monitoring both amplitude and wavelength surface properties.

In the *speckle pattern method*, surface roughness is related to speckle, which is basically the local intensity variation between neighboring points in the reflected beam when a surface is illuminated with partially coherent light. The principle of the laser speckle roughness measuring system is schematically shown in Fig. 3.

The *optical interference technique* involves looking at the interference fringes and characterizing the surface with suitable computer analysis. Common interferometers include the Nomarski polarization interferometer and the Tolanski multiple beam interferometer.

## 2.3 Advanced Techniques for Surface Topography Evaluation

A further improvement in the resolution of surface topographic examination is possible by the use of electron microscopes. Two basic types of electron microscopes are available: scanning electron microscopes and transmission electron microscopes. In scanning electron microscopy (SEM) a focused beam of high-energy electrons is incident on the surface at a point resulting in the emission of secondary electrons. These are then collected and fed to an amplifier to send an electric signal to a cathode ray tube (CRT). The electron beam is scanned over the surface

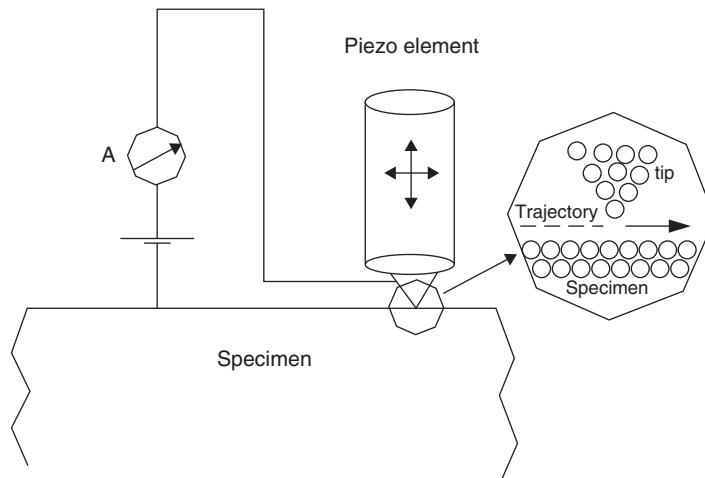


**Figure 3** Schematic of laser speckle roughness-measuring system.

to have a complete picture. The CRT screen gives a topographical image of the entire area of interest. Depth of field is up to  $1000\ \mu\text{m}$ , which acts as a primary advantage of this method over the optical method. The requirement on size of the specimen to be placed within the vacuum chamber of the instrument raises a drawback of the method. This can be overcome by preparing a replica of the surface.

In transmission electron microscopy (TEM), the focused beam of high-energy electrons is made to transmit through a very thin specimen. Then the deflection and scattering of the electrons is recorded to analyze the surface topography. Preparation of a specimen thin enough to transmit electrons plays a vital role. Sometimes a replica of the surface retaining all the texture features but of a material having greater electron transparency is produced for the same purpose.

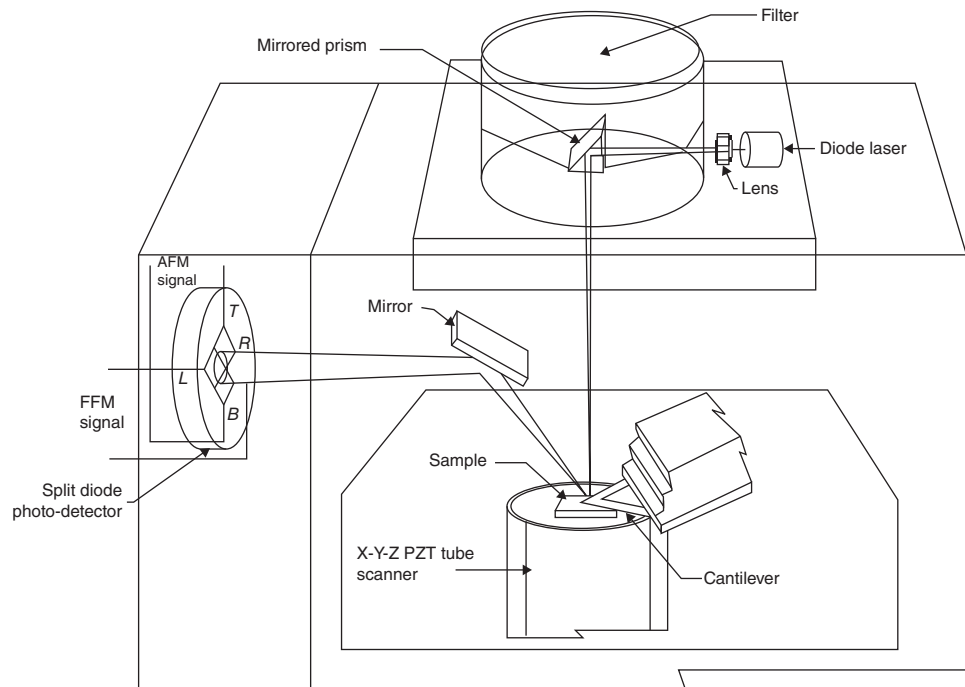
Recently, a different type of electron microscopy called scanning tunneling electron microscopy (STM) is in use. It incorporates the electron-tunneling phenomenon through an insulating layer separating two conductors. The sharp pointed tip of a probe forms one electrode and the surface of the specimen the other. The probe is moved by a highly precise positional controller to keep the tunneling current at a steady value. The probe provides an image of the surface under examination. The method is superior to the earlier ones in the sense that it does not require any vacuum. The only disadvantage is the proper design of the controller mechanism. The principle of STM is very simple. Just like in a record player, the instrument uses a sharp needle, referred to as the tip, to investigate the shape of the surface. But the STM tip does not touch the surface. The schematic of the method is shown in Fig. 4. A voltage is applied between the metallic tip and the specimen, typically between a few millivolts and volts. The tip touching the surface of the specimen results in a current and when the tip is far away from the surface, the current is zero. STM operates in the regime of extremely small distances between the tip and the surface of only  $0.5\text{--}1.0\ \text{nm}$ , which are typically  $2\text{--}4$  atomic diameters. At these distances, the electrons can jump from the tip to the surface or vice versa. This jumping is necessarily a quantum mechanical process known as “tunneling” and hence the name scanning tunneling microscopy. STM usually operates at tunneling currents between a few picoamperes and a few nanoamperes. The tunneling current depends critically on the precise distance between the last atom of the tip and the nearest atom or atoms of the underlying specimen. When this distance is increased a little bit, the tunneling current decreases



**Figure 4** Schematic of STM.

heavily. As a rule of thumb, for each extra atom diameter that is added to the distance, the current becomes a factor of 1000 lower. Thus the tunneling current provides a highly sensitive measure of the distance between the tip and the surface. The tunneling electron microscope tip is attached to a piezoelectric element, which changes its length a little bit when it is put under an electrical voltage. The distance between the tip and the surface can be regulated by adjusting the voltage on the piezoelement. In most STM, the voltage on the piezoelements is adjusted in a manner that the tunneling current always has the same value, say 1 nA. Thus the distance between the last atom on the tip and the nearest atoms on the surface is kept constant. Using the so-called electronics; the distance regulation is done automatically. The feedback electronics continually measures the deviation of the tunneling current from the desired value and accordingly adjusts the position of the tip. While this feedback system is active, two other parts of the piezoelements are used to move the tip in a plane parallel to the surface to scan over the surface. In the scanning process, every time that the last atom of the tip is precisely over a surface atom, the tip needs to be retracted a little bit, while it has to be brought slightly closer when the tip atom is between the surface atoms. This automatically leads the tip to follow a bumpy trajectory, which replicates the atoms of the surface. Then this information about the trajectory, available in the form of the voltages that have been applied by the feedback electronics, is then finally visualized in the form of a collection of individual height lines, in the form of grey scale/color scale representation, or in the form of some three-dimensional (3D) perspective views.

More recently AFM (atomic force microscopy) has been developed to investigate surfaces of both conductors and insulators on an atomic scale. Like STM, AFM relies on a scanning technique to produce very high resolution, 3D images of sample surfaces. In AFM, the ultra-small forces (less than 1 nN) present between the atomic force microscope tip and sample surface are measured by measuring the motion of a very flexible cantilever beam having an ultrasmall mass. AFM combines the principles of STM and the stylus profiler. The important difference between AFM and STM is that in AFM the tip gently touches the surfaces. AFM records not the tunneling current but the small force between the tip and the surface. The atomic force microscope tip is attached to a tiny leaf spring, known as the cantilever, which has a low



**Figure 5** Schematic operation of AFM/FFM.

spring constant. The bending of the cantilever is detected with the use of a laser beam, which is reflected from the cantilever. AFM thus measures contours of constant attractive or repulsive force. The detection is made very sensitive such that forces as small as a few piconewtons can be detected. Forces below 1 nN are usually sufficiently low to avoid damage to either the tip or the surface. Since AFM does not rely on the presence of a tunneling current, it can also be used on nonconductive materials. Soon after the introduction of AFM, it was realized that the same instrument could be used to also measure forces in the direction parallel to the surface, that is, the friction forces. When modifications are incorporated for atomic-scale and microscale studies of friction, it is termed friction force microscopy (FFM) or the lateral force microscopy (LFM). FFM usually detects not only the deflection of the cantilever perpendicular to the surface but also the torsion of the cantilever, resulting from one lateral force. A schematic of the AFM/FFM commonly used for measurements of surface roughness, friction, adhesion, wear, scratching, indentation, and boundary lubrication from the micro- to the atomic scales is shown in Fig. 5.

In all surface profilometric methods, roughness (small-scale irregularities) and form error (deviation from its intended shape) remain coupled in the recorded data. Form error may be subtracted from the recorded data to provide only the roughness features by different means. The two most common methods used in a stylus profilometer are (a) use of datum-generating attachments and (b) use of large radius skids or flat shoes. With these the average local level is used as datum and form error or waviness is not recorded. Other methods include the use of filtering the displacement signal corresponding to waviness. Table 1 summarizes the comparison of the different roughness-measuring methods.

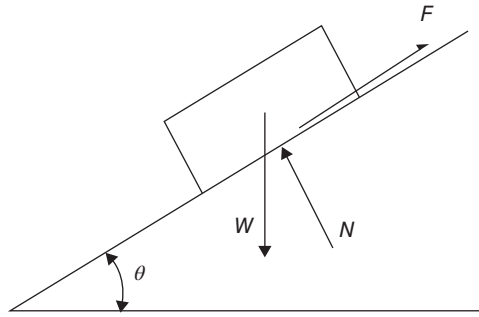


**Table 1** Summary and Comparison of Roughness Measurement Methods

Method	Quantitative Data	Three-Dimensional Data	Resolution at Maximum Magnification, nm		On-Line Measurement Capability	Limitations/Comments
			Horizontal	Vertical		
Stylus method	Yes	Yes	15–100	0.1–1	No	Operates along linear track, contact type can damage sample, slow speed in 3D mapping
Optical methods						
Light sectioning	Limited	Yes	500	0.1–1	No	Qualitative
Taper sectioning	Yes	No	500	25	No	Destructive, tedious specimen preparation
Specular reflection	No	No	$10^5$ – $10^6$	0.1–1	Yes	Semiquantitative
Diffuse reflection	Limited	Yes	$10^5$ – $10^6$	0.1–1	Yes	Smooth surfaces (<100 nm)
Speckle pattern	Limited	Yes			Yes	Smooth surfaces (<100 nm)
Optical interference	Yes	Yes	500–1000	0.1–1	No	
SEM	Limited	Yes	10	0.1	No	Operates in vacuo, limits on specimen size
TEM	Limited	Yes	0.5	0.02	No	Operates in vacuo, requires replication of surface
STM	Yes	Yes	0.2	0.02	No	Requires a conducting surface, scans small areas
AFM	Yes	Yes	0.2–1	0.02	No	Scans small areas

### 3 MEASUREMENT OF FRICTION

Friction is defined as the force of resistance to motion that occurs when a solid body moves tangentially with respect to the surface of another body that it touches. The friction force acts in a direction opposite to that of motion. Even when an attempt is made to initiate the motion, the friction force exists. The friction force required to initiate the sliding is called the static friction force and that required to maintain sliding is called the kinetic friction force, the value of which is usually lower than the former for the same combination of material and other parameters. The basic principle of any friction-measuring instrument is to place two specimens together under a specified normal load and in relative motion while the tangential force resisting motion



**Figure 6** Measuring friction by an inclined-plane test rig.

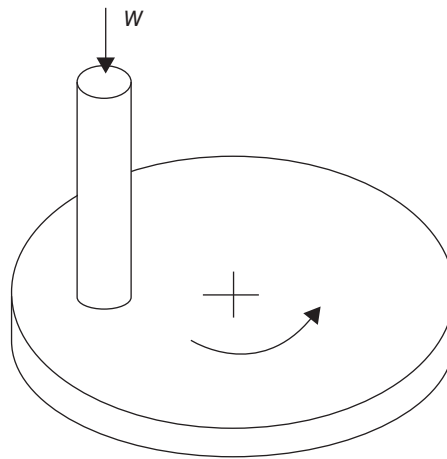
is measured. Many methods of varying specimen geometry, loading condition, and resisting force measurement are available. Different researchers use many ingenious setups to investigate different specific cases.

### 3.1 Inclined-Plane Rig

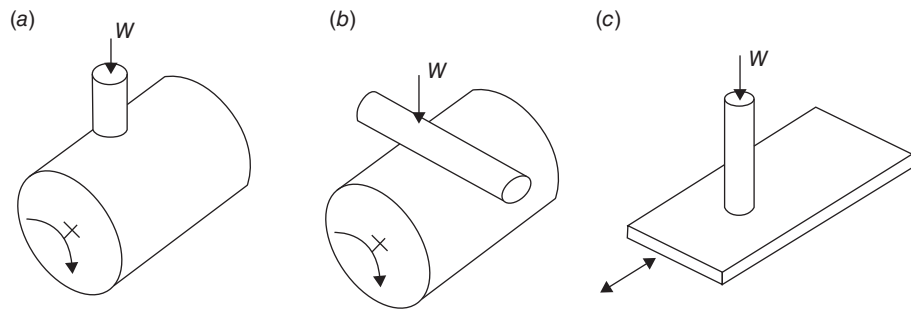
The simplest arrangement is the inclined-plane test shown in Fig. 6. A specimen is placed on a flat plane whose inclination with the horizontal is gradually increased until the specimen on it starts sliding. If the inclination at this moment is  $\theta$ , then  $\mu s = \tan \theta$ . Obviously, this method is not capable of evaluating friction in continuous sliding.

### 3.2 Pin-on-Disc Rig

In continuous-sliding cases, the rig based on pin-on-disc configuration (Fig. 7) is used. The pin is held stationary under a normal load while the disc is made to rotate. The loading can be provided by simple dead weight or by spring loading or hydraulic or pneumatic pressure.



**Figure 7** Pin-on-disk friction-measuring device.



**Figure 8** Friction-measuring devices: (a) pin-on-cylinder, (b) crossed cylinder, and (c) reciprocating rig.

The friction force is measured with the help of the calibrated tangential movement of a capacitive or inductive transducer mounted on the stationary specimen. For a multiple-pass arrangement the pin is held at a constant radial distance from the center of the disc, but in a single-pass arrangement it is moved radially during the experiment. Other standard arrangements such as pin-on-cylinder, crossed cylinder, and reciprocating arrangement are shown in Fig. 8.

### 3.3 Conformal and Nonconformal Geometry Rig

The test rigs can be classified into two groups depending on the test geometry: conformal and nonconformal. In the conformal geometry test, the profiles of the two contacting surfaces are matched carefully before the experiment is started. In this case the contact pressure is moderate and normally held constant throughout the experiment. The test may then be used to simulate the situations such as brakes, thrust bearings, plane bearings, face seals, and clutches. On the other hand, in the nonconformal geometry test (with spherically profiled pin) contact pressure is initially high because on first loading contact is made at a single point and with time pressure reduces due to development of small wear scars. This can be used to simulate the heavily loaded contacts such as gear teeth or to provide accelerated tests of friction and wear of a number of candidate material pairs for specified applications.

### 3.4 Environment Control

For accurate investigation the friction test must be carried out in an enclosed environment having simulated environmental conditions. Different friction pairs are susceptible to the presence of liquid lubricants, water vapor, gases, and so on. If pin-on-disc tests are carried out in the presence of liquid lubricant, the results vary due to poorly controlled hydrodynamic conditions at the interface. Sometimes the small deformations of the rig caused by the thermal loading or pressure loading may give rise to experimental scatter. So many other forms of test rigs have been developed for specific applications involving different environmental conditions. For example, space environments are simulated by the use of high-vacuum conditions where the entire test rig is installed inside the vacuum chamber.

### 3.5 Techniques for Friction Force Measurement

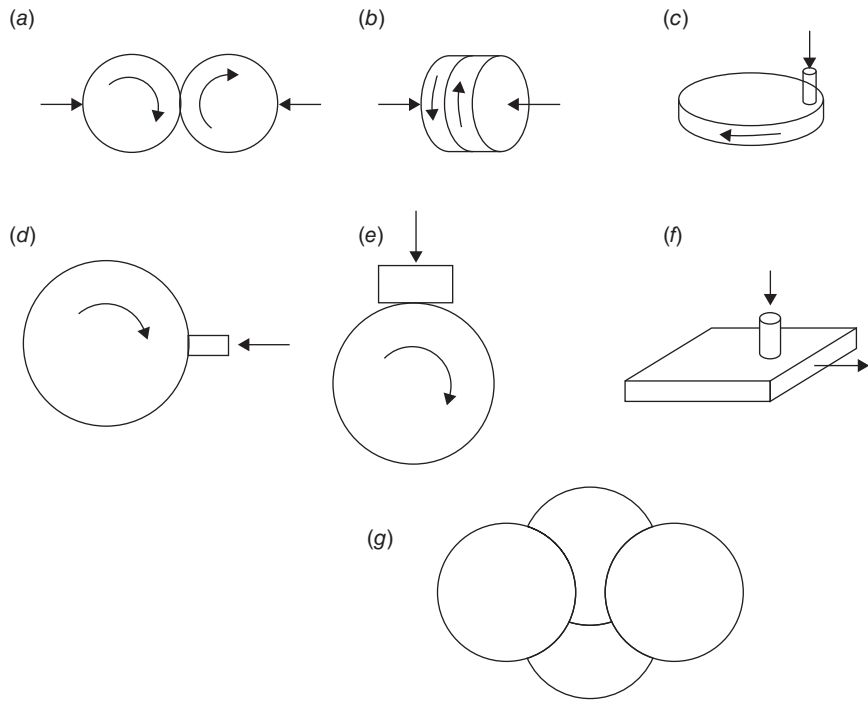
Two basic types of devices are commonly used for the measurement of friction force, viz., the piezoelectric force gauge and strain gauge transducer. Piezoelectric force gauges give a direct measurement of friction force as an electrical impulse that is recorded electronically. Piezoelectric gauges operate by elastic deflection of a piezoelectric crystal and are sensitive to

temperature, vibration, and corrosive agents. Piezoelectric gauges are also relatively expensive. Strain gauge beams are comparatively cheaper. In this case, friction force is usually measured from the bending of a beam arranged perpendicular to the direction of the friction force and strain gauges are mounted on the beam to record the deflection of the beam. Strain gauge beams are effective in recording steady friction forces where piezoelectric force gauges are unsuitable. The only difficulty with the strain gauge beam is its failure to record rapid change in friction force.

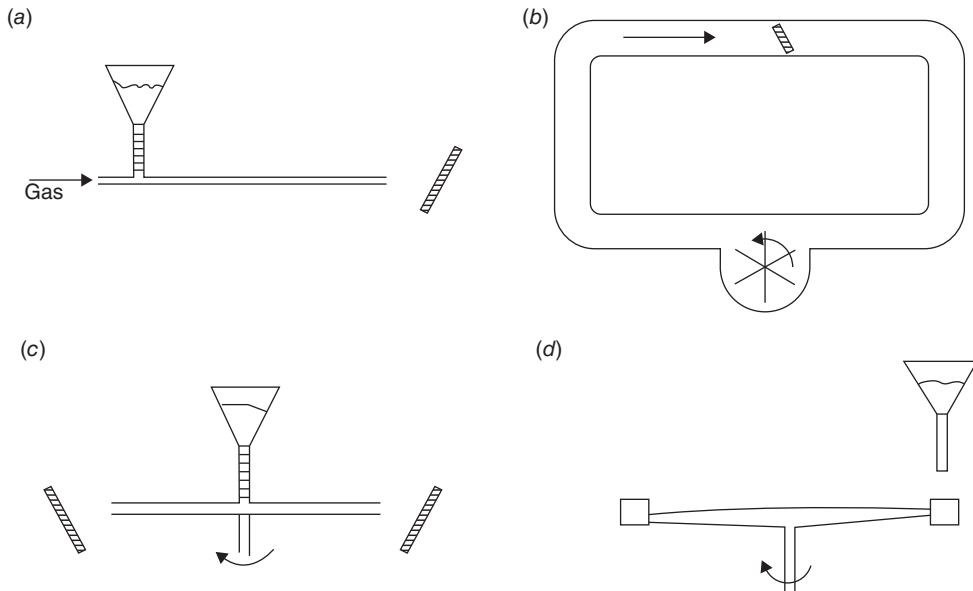
#### 4 MEASUREMENT OF WEAR

Wear is the removal of material from one or both of two solid surfaces in relative motion (sliding, rolling, or impact). Wear occurs as a natural consequence and mostly through surface interactions at asperities. Though wear generally refers to material removal, surface damage due to material displacement with no net change in volume or weight is also termed as wear. Wear is a system response; it is not a material property. Interface wear is strongly dominated by operating conditions. Thus the measurement of wear is mainly influenced by the definition of wear that is considered. For the definition of loss of mass, it is possible to measure wear by simply weighing the worn object before and after a wear test. But this does not allow to measure wear if material displaced by wear gets attached to the worn object. Thus there are three basic methods of measuring wear, viz., detection of change in mass, measurement of reduction in the dimension of a worn specimen, and profilometry of the worn object. Measurement of mass change is usually done using a sensitive analytical balance since mass changes in wear are usually small. Reduction in dimensions of the worn object is usually measured by connecting a displacement transducer to the surface of the worn object that is directly above the wear spot. Linear variable differential transformer (LVDT) transducers or noncontact inductive proximity probes along with an electronic amplifier are commonly used. The other commonly used technique for evaluation of the worn volume from the wear scar is profilometry where an optical profile projector or a stylus profilometer or a laser scanning profilometer is used. The optical profile projector is based on projecting an image of the object on a screen and measuring the change in dimensions of the worn specimen. In stylus profilometry, a picture of the wear scar is taken and compiled by using several evenly spaced traverses of the stylus over the scar. Then wear is determined from the deepest wear scar profile. In scanning profilometry, light from a laser is focused on the surface to measure the dimensions of the wear scar. Other specialized techniques for wear measurement are thin-layer activation by radioactivity and ultrasonic interference measurements of dimensional changes. Noise emission and thermal emission from a dynamic contact can also be used for recording changes in wear condition.

Many different experimental arrangements are used to study sliding wear. These are usually carried out either to examine the process by which wear takes place or to simulate practical situations to generate design data on wear rates and coefficients of friction. Close control and monitoring of all the variables which may influence wear are essential if the results of a test are to be useful for wider scientific purposes. Figure 9 shows the geometric arrangements in several common types of wear testing apparatus. For adhesive wear between identical materials, the two surfaces are made of the same material. For abrasive wear testing, one of the surfaces, generally the larger one, is made of abrasive material. Changes in geometries and arrangements are done for testing different mechanisms of wear. For two-body abrasive wear, commercial bonded-abrasive paper or cloth is usually used for the counterface, carrying evenly distributed grit particles of narrow-size distribution, bonded to the substrate by a strong resin. In simulating three-body abrasion, silica (quartz) particles of a narrow-size distribution and from a specified source are fed at a constant rate into the contact region. Figure 10 shows schematic diagrams of four types of testing methods for erosive wear. In the jet impingement method (Fig. 10a),



**Figure 9** Sliding wear test arrangements: (a) roller/roller, (b) disk/disk, (c) pin on disk, (d) pin on roller, (e) disk on roller, (f) pin on flat, and (g) four ball.



**Figure 10** Schematic of erosive wear test arrangements: (a) jet impingement method, (b) recirculating loop, (c) centrifugal accelerator, and (d) whirling arm rig.

particles are accelerated in a fluid stream along a nozzle to strike the target material, which is held some distance from the end of the nozzle at a fixed angle. In the recirculating loop test (Fig. 10*b*), a two-phase flow of particles and fluid is driven around a loop of pipe-work where the specimen is kept completely immersed in the flow. In the centrifugal accelerator (Fig. 10*c*), a continuous stream of particles, generated by circular motion of a rotor, strikes the stationary specimens arranged around the rim after the rotor. In the whirling arm rig (Fig. 10*d*), two specimens at the ends of a balanced rotor move at high speed through a slowly falling stream of particles, striking them at the peripheral speed of the rotor.

## 5 MEASUREMENT OF TEST ENVIRONMENT

Many experiments often omit the measurement of environmental factors such as temperature, humidity, and oxygen and lead to apparent conflict in experimental data. Careful measurement and control of these environmental factors are necessary for tribology experiments.

### 5.1 Temperature Measurement

In a dynamic contact situation, most of the frictional energy input is generally used up in plastic deformation which is directly converted to heat in the material close to the interface with a consequent rise in temperature. Since the heat is produced as a continuous process, temperature gradients will develop in the contacting bodies with the highest temperature occurring at the point of heat release (heat source), that is, the contact surface. In the absence of lubricants, this heat is conducted into the two sliding bodies through contact spots. Contact between two bodies may be approximated as a single contact or as multiple contacts depending on the stress situation. For high-contact stress situations, the real area of contact approaches the apparent area of contact and a single contact may be assumed to occur during sliding. Contact of two very smooth surfaces, even at low load, may be assumed as a single contact. For a low-contact stress-sliding situation, most engineering contacts of interest are of this type; asperity interaction results in numerous high, transient temperature flashes of as high as several hundred degrees Celsius over a very small area within a few nanoseconds to a few microseconds. As the sliding continues, these temperature flashes shift from one place to another. Measurement of temperature rise over isolated microcontacts is very difficult. A number of techniques have been used to measure the transient temperature rise in a sliding contact, but with limited success.

Techniques for interface temperature measurement include thermocouples, thin-film sensors, radiation detectors, metallographic observation, and liquid crystals. Thermocouples are most commonly used but do not measure true flash temperature. Radiation detectors come close to true measurement while liquid crystals and metallographic observations provide a rough estimate of flash temperature.

### 5.2 Thermocouples

A thermocouple uses wires of two dissimilar metals connected together at the two ends and gives rise to a thermal electromotive force (EMF) which depends on the difference in the temperature between two junctions; while one junction is kept at a known reference temperature (cold), the temperature of the other measuring junction (hot) can be obtained from measured EMF using a calibration chart. Two types of thermocouples are in use: embedded thermocouples and dynamic thermocouples. In the embedded type, a small hole is drilled through the stationary component of a sliding pair and a small thermocouple is held within the hole such that its measuring junction rests just beneath the sliding surface. In the dynamic variety, a thermocouple junction is created at the sliding interface of the contacting bodies. Schematics of

both types are shown in Fig. 11. While the embedded type cannot measure true flash temperature because of its position and the finite mass of the measuring junction, the dynamic variety gives a good measure of an average surface temperature rise. Dynamic thermocouples are found to give higher values of measured temperatures and faster transient response than embedded thermocouples. The major disadvantage with dynamic type is that it can only be used for metallic pairs of dissimilar metals and requires electrical contact with a moving body.

### 5.3 Thin-Film Sensors

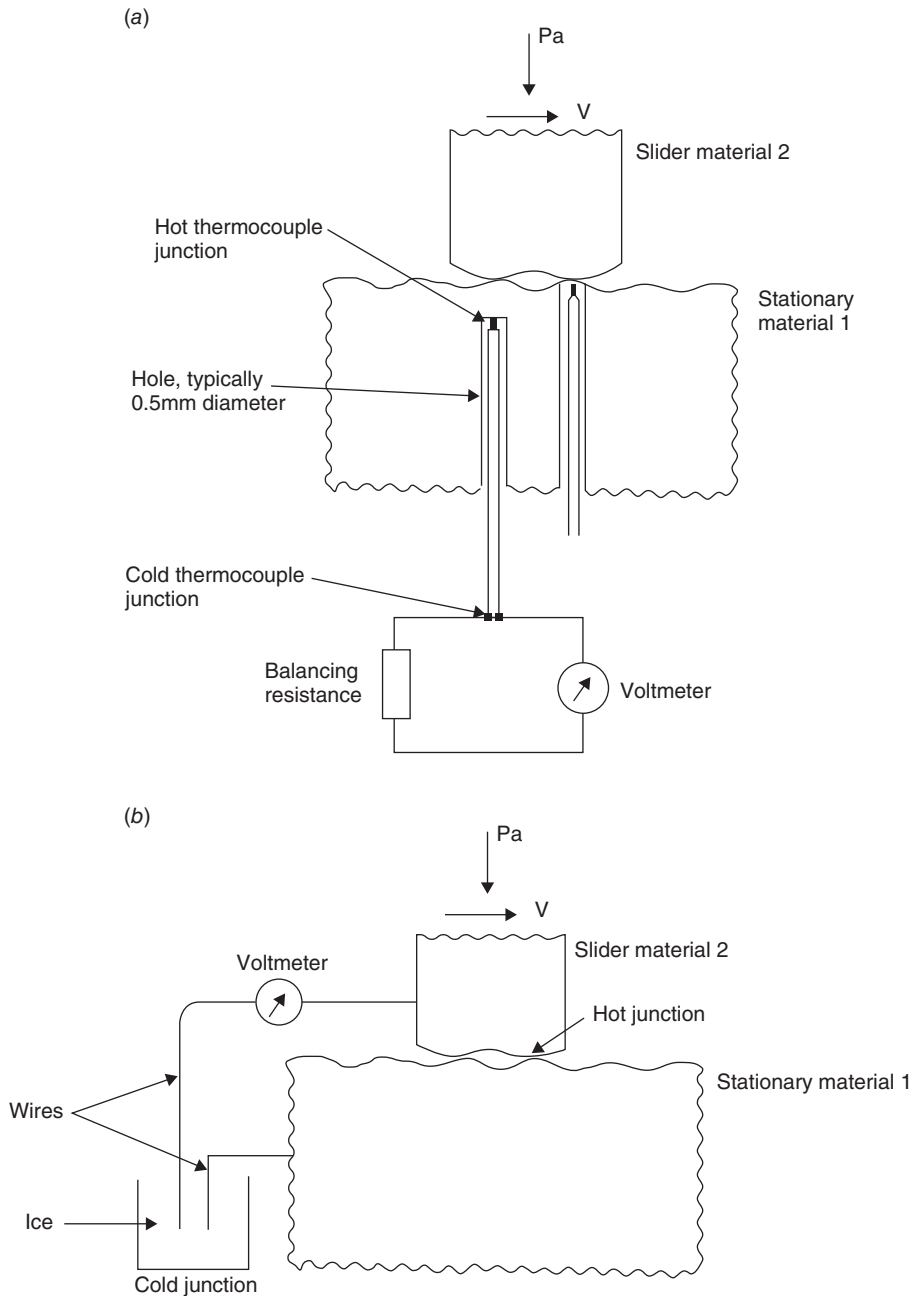
Thin-film temperature sensors are used on surfaces to measure temperature rise on a small region and on a very small mass. One of the first of its kind was the thermistor used to measure surface temperature on gear teeth. The resistance of titanium being sensitive to temperature and pressure, measurement of any change in resistance indicates the change in temperature and pressure. Magnetoresistive (MR) sensors are used to measure interface flash temperature at magnetic head-medium interfaces. Thin-film thermocouples produced by vapor deposition techniques are also used for measurement of sliding interface temperatures.

### 5.4 Radiation Detectors

All materials emit thermal radiation that depends on the surface temperature and structure of the material. It is concentrated in the infrared region if the temperature of the material lies between 10 and 5000 K. Knowing the radiation characteristics of the material and radiant heat transfer properties of a particular geometry configuration, the temperature of the material may be determined. This method has been successfully used to measure the transient flash temperature. However, it requires one of the bodies to be transparent to the radiation to be detected and sapphire is a useful material in this respect. Different radiation measurement techniques have been successfully used to measure surface temperatures. These methods include photography, pyrometry, photon detection, and thermal imaging. In infrared (IR) detection technique, an IR radiometric microscope is used for local surface temperature measurements where the detector is equipped with optics to limit the field of view to a small spot size in order to permit a small spatial resolution. In the photon detection technique, a photomultiplier is used to collect photons emitted by a hot contact spot. The response time of the photomultiplier being very small (less than 30 ns), the technique can be used for detecting flash temperatures of very short duration (2  $\mu$ s or less). In the thermal imaging technique, a charge-coupled device (CCD) camera with an IR pass filter is used. The IR radiation emitted at the contact surface is detected through the sapphire material by the CCD camera, which is linked to a computer-based image processing system. The IR pass filter permits only IR radiation to reach the CCD camera. The video signal is then processed for thermal imaging and the contact temperature rise may be obtained by suitable transformation through calibration.

### 5.5 Metallographic Observation

Microstructure of many materials undergoes changes due to surface and near-surface frictional heating. Using scanning electron microscopic examination of the cross section of the sliding body in a perpendicular plane to the sliding direction, these changes can be detected and may give a rough estimate of the temperature rise. For some material, this can be done by microhardness measurements. In metal cutting, the flash temperatures during contact can be determined from the microstructural changes in the metal chips, but with limited accuracy. The major limitation of the method is that the microstructural changes may occur due to plastic deformation in surface or near-surface regions in addition to being due to the temperature rise.



**Figure 11** Schematics of thermocouples: (a) embedded type and (b) dynamic type.



## 5.6 Liquid Crystals

Cholesteric liquid crystals are also used in surface temperature measurements because these crystals undergo changes in color with very small changes in temperature. When a surface of a body is coated with a specific liquid crystal and subjected to body temperature changes, the color change occurring in the liquid crystal material estimates the temperature change. Liquid crystals can be sprayed or applied by brush. These are used to measure the bulk temperature of bodies rather than flash temperatures.

## 5.7 Humidity Measurement

The routine measurement of humidity and its control at a constant level are necessary as it has a strong influence on friction and wear. Conventionally wet- and dry-bulb thermometers are used for humidity measurement during tribological studies.

## 5.8 Measurement of Oxygen and Other Gauges

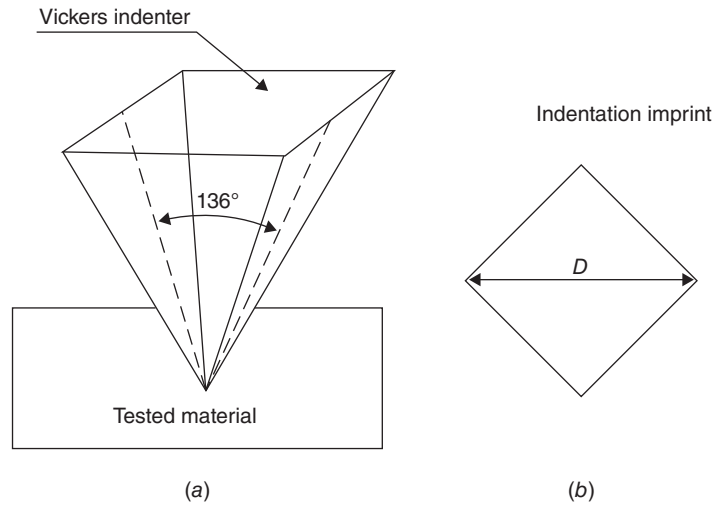
The variation in concentration of oxygen and other gauges in the atmosphere affect the friction and wear processes to a large extent. Thus there is a need to observe their concentration during tribological tests for effective conclusion of the tests. For this purpose, gas chromatography is commonly used. Gas chromatography is a technique for separating different components of a mixture for analysis by diffusing a gaseous or vaporized sample through a column of liquid. This is based on the principle that different substances are transported at different speeds through a medium. A carrier gas, usually nitrogen, hydrogen, or helium, transports the sample through the chromatograph. The mixture of sample and carrier gas is transferred to a long capillary tube filled with liquid, usually a hydrocarbon fluid such as silicone oil or squalene, which acts as the separating medium. The components of the sample pass through the capillary tubes at different speeds and are then detected on leaving the capillary to obtain the composition of the sample. Oxygen analysis electrodes are readily available for direct measurement of oxygen concentration in water.

# 6 MEASUREMENT OF MATERIAL CHARACTERISTICS

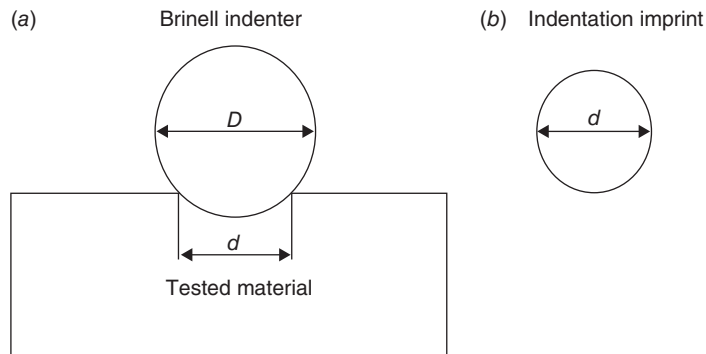
The tribological behavior of any material depends on its material characteristics. Each type of material, metal, polymer, or ceramic, requires different material properties. For metals, the chemical composition and metallurgical phases are significant. For polymers, the organic components, additives, and degree of crystallinity are essential. For ceramics, apart from composition, grain size and material toughness are usually important parameters. Accurate measurements of hardness and microhardness are essential for analysis of surface contact and deformation in friction and wear. The materials are in general characterized using four quantities: (a) hardness, which describes the resistance to plastic deformation; (b) Young's modulus and the elasticity limit, which describe the materials' elastic properties; (c) toughness, which accounts for the relative brittleness of the material; and (d) residual stresses, which play an important role in the resistance to wear and cracking.

## 6.1 Hardness

Hardness tests use indenters to make an impression on a sample of a material under a normal load ( $F$ ) and measure the surface area ( $S$ ) of the residual impression left after removal of the load. Then hardness is expressed as  $F/S$ . Indenters can be of various shapes. For the Vickers test, a square-based pyramid is used, while for the Brinell test, spherical indenters are used. For the Rockwell test, either conical or spherical indenters are used, while Shore hardness tests use two types of cones.



**Figure 12** Vickers hardness test: (a) Vickers indenter and (b) residual square indentation of diagonal  $D$ .



**Figure 13** Brinell hardness test: (a) indenter and (b) residual impression.

In the Vickers test, the indenter used is a diamond square-based pyramid with an angle of  $136^\circ$  between opposite faces, as shown in Fig. 12.

Vickers hardness is given by the formula

$$HV = 1.854 \frac{F}{D^2}$$

where  $F$  is the applied load (kg) and  $D$  is the diagonal of the residual indentation (mm).

Brinell hardness is determined using tungsten carbide spherical indenters of 10, 5, 2.5, or 1 mm in diameter (shown in Fig. 13). Brinell hardness can be expressed as

$$HB = \frac{0.204F}{\pi D \left( D - \sqrt{D^2 - d^2} \right)}$$

where  $F$  is in newtons and both the diameter of the spherical indenter ( $D$ ) and the diameter of the residual impression ( $d$ ) are in millimeters.

In the Rockwell hardness test, the depth of the residual impression,  $h$ , is measured instead of its diameter. First a preliminary (minor) load of 98 N is applied and it forces the indenter into

the surface to a depth of  $l$  (say). This depth of penetration is not taken into account in hardness measurement but is used as the zero-penetration reference point. Then a major normalized load is applied to the surface for a few seconds leading to a total depth of penetration  $t$  (say). The major load is then reduced to the minor load and the depth of the residual impression  $h$  is measured in millimeters. In the Rockwell B test, a steel spherical indenter of diameter 1.58 mm is used with a normal load of 980 N. In the Rockwell C test, the load is 1470 N and the indenter is a conical diamond indenter with radius of curvature of 0.2 mm and apex angle of  $120^\circ$ . Rockwell B and Rockwell C hardness can be expressed as

$$\text{HRB} = 130 - \frac{h}{0.002}$$

and

$$\text{HRC} = 100 - \frac{h}{0.002}$$

The Shore hardness test is suitable specifically for polymers and is conducted with an apparatus called a durometer and a calibrated spring that generates a known force on the indenter. The penetration depth is recorded and the corresponding value of Shore hardness is obtained in a scale of 0–100 with these values corresponding to maximum penetration and zero penetration, respectively. For the Shore A test, a truncated cone with an apex angle of  $35^\circ$  is used, while for the Shore D test, a sharp cone with an apex angle of  $30^\circ$  is used.

## 6.2 Young's Modulus and the Elasticity Limit

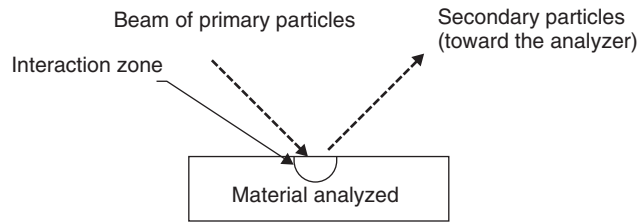
For an isotropic material, Young's modulus is the constant of proportionality between the stress applied to a specimen rod and its elastic deformation. Generally uniaxial tensile tests are carried out to determine Young's modulus as well as the elasticity limit. However, the same can be determined from indentation tests also.

## 6.3 Fracture Toughness

Different modes of fracture can occur within a brittle material. Brittleness is characterized using a parameter known as fracture toughness (denoted  $K_{Ic}$ ), which describes the resistance of the material to fracture propagation and is generally determined from impact tests on a single-edge notch bend specimen. It can also be obtained using Vickers indentation tests by measuring the length of the radial crack during indentation.

## 6.4 Residual Stresses

Machining methods and surface production processes incorporate strains on the surface layers of materials that in turn induce internal residual stresses. These may be either tensile or compressive. Tensile stresses are dangerous as they help fracture propagation while compressive stresses are beneficial and often added deliberately to harden the surface of a material in order to increase its resistance to wear. Measurement of residual stresses is done by either destructive techniques or nondestructive techniques. The destructive method relies on the cutting away of some stressed material and measuring of the resulting deformation in the adjacent material that has occurred due to the relaxation of the residual stresses. The nondestructive method relies on the analysis of the changes of the physical and crystallographic properties of the material due to residual stresses. These include the ultrasound method, which uses the effect of residual stresses on the variation of speed of ultrasound waves; the Barkhausen technique, which uses the interaction between elastic strain and magnetization in ferromagnetic materials; and x-ray diffraction.



**Figure 14** Principle of spectroscopic surface analysis.

## 6.5 Chemical Composition of a Surface

The chemical composition of a surface can be determined using a number of methods. Generally, a primary particle beam (electronic, optical, or ionic) is directed at the surface under investigation and it produces the emission of secondary particles (photons, electrons, or ions). The characterization of these secondary particles allows the identification of the composition of the surface under study (Fig. 14). The most widely used techniques include energy dispersive x-ray analysis (EDX), x-ray photoelectron spectroscopy (XPS), Auger electron spectroscopy (AES), glow discharge optical emission spectroscopy (GDOS), Rutherford backscattering spectroscopy (RBS), secondary ion mass spectroscopy (SIMS), and IR spectroscopy. In EDX, the primary particle is the electron and the secondary particle is the photon. EDX helps in elemental analysis of materials to a depth of a few micrometers, but this is not suitable for light element analysis. EDX is generally used in the analysis of precipitation and segregation in metallurgical materials, characterization of thermal oxide films, and hard coatings. In XPS, the primary particle is the photon and the secondary particle is the electron. It helps in elemental analysis of materials along with the information of the environment of the atoms and nature of chemical bonds. In AES, both primary and secondary particles are electrons. It helps in elemental analysis of the top few-atom layers of a solid. It is generally used for analysis of adsorbed layers, thermal or anodic oxide films, and thin deposits. In GDOS, the primary particle is an ion and the secondary particle is a photon. It can provide simultaneous elemental analysis of dozens of elements and in-depth sample analysis over large areas. In RBS, both primary and secondary particles are ions. In this technique, the analysis of the energy of backscattered helium ions after elastic collision with the sample surface atoms allows the determination of their mass. In SIMS, both primary and secondary particles are ions. It provides elemental and isotopic analysis of all elements in the periodic table. It can be used to obtain ionic images providing elemental distribution. In IR spectroscopy, both primary and secondary particles are photons. This is primarily used for the analysis of organic materials and allows the determination of functional groups present in the material and the nature of the different bonds.

## 7 MEASUREMENT OF LUBRICANT CHARACTERISTICS

Characterization of a lubricant is an essential part of any study related to lubricated wear and friction. Lubricant characterization requires both chemical and physical parameters. Hence different techniques of rheometry and chemical analysis are used for this purpose. The significance of lubricant parameters varies widely depending on the tribological function for which the same is used. For hydrodynamic and elastohydrodynamic lubrication, the parameters of significance are viscosity, Barus pressure–viscosity coefficient, temperature dependence of viscosity, limiting shear stress, glass transition, compressibility, and thermal conductivity. For boundary lubricants, the significant parameters are composition and concentration of surfactants and corrosive compounds, temperature of lubricant failure, corrosivity, solubility, and diffusivity

of dissolved gases. A sample of a used lubricant can provide much information regarding the prevailing wear taking place within the tribological system or the quality of lubrication. Also the oxidation or chemical decomposition of a lubricant can easily be detected from the actual lubricant sample.

## 7.1 Analysis of Chemical Changes

Chemical changes occurring in lubricants are directly analyzed using IR spectroscopy. The only difficulty in this technique is the interpretation of complex spectra obtained from degraded lubricants. Specialized numerical analysis of IR spectra is done to extract proper analytical information from overlapping absorption peaks. The most popular one used to detect small changes in the IR spectra is Fourier transform IR (FTIR) spectroscopy. Typical IR spectra are displayed as a standard graph of IR transmittance or absorbance within the sample versus the wavenumber of the IR radiation.

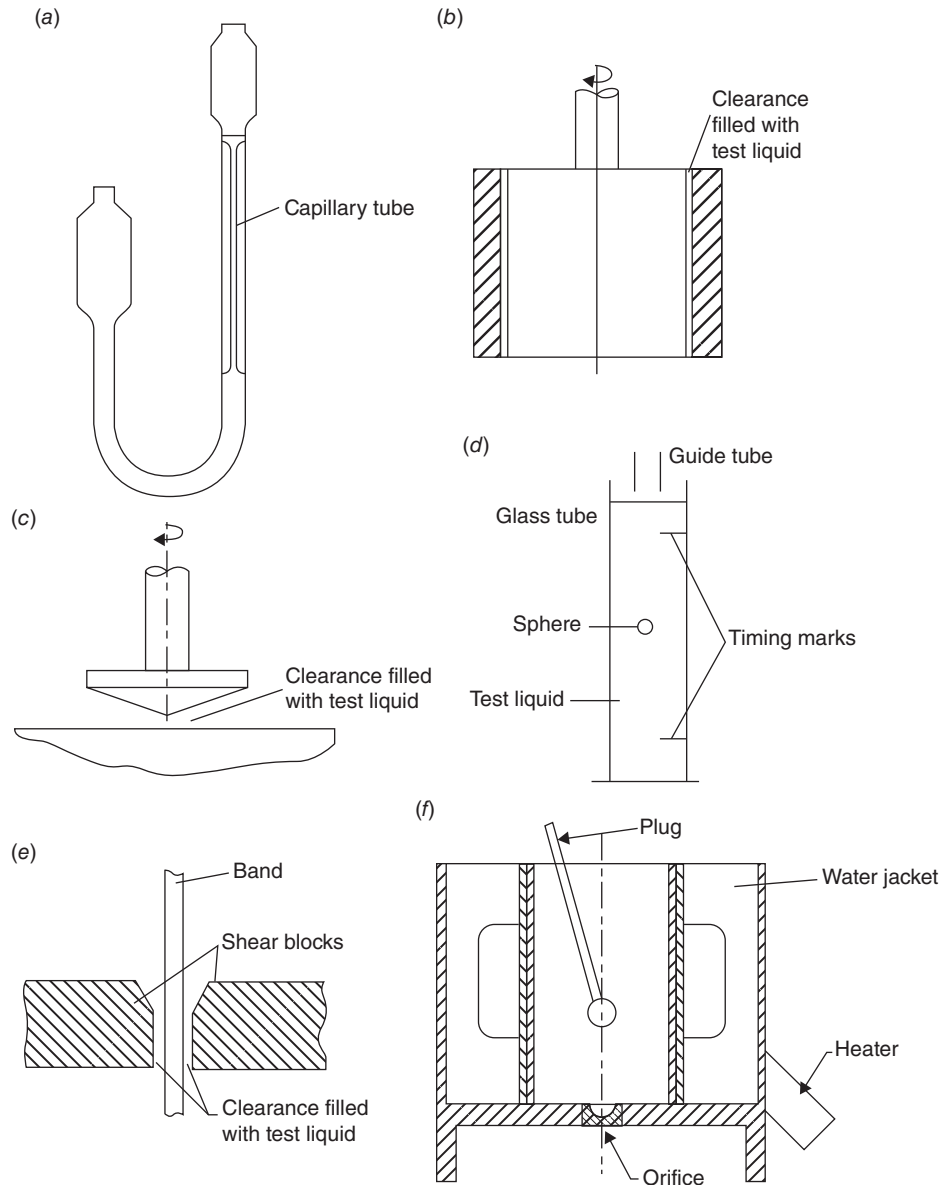
## 7.2 Viscosity Measurement

The viscosity of lubricants can be measured by many methods based on different principles. Most commonly used instruments typically fall into four categories depending on geometry: capillary, rotational, and falling sphere and efflux viscometers.

The capillary viscometer is based on measuring the rate at which a fluid flows through a small-diameter tube and this takes the form of measuring the time taken to discharge a given quantity of liquid for an applied pressure difference and tube dimensions. In capillary viscometers direct measurement of absolute viscosity is not possible and kinematic viscosity is measured. The kinematic viscosity is given as  $\nu = ct$ , where  $c$  is a constant for a given viscometer and  $t$  is the time required for a given volume of liquid to flow through the tube. By using some liquid of known viscosity and density, the time required for a given volume to flow through the capillary is determined and the constant for the instrument is found. The sketch of one such viscometer is shown in Fig. 15.

In rotational viscometers the absolute viscosity of oil is measured. Three different types of rotational viscometers are used: cylindrical, cone-plate type, and parallel-plate type. The cylindrical type is in the form of two concentric cylinders of which one rotates in the oil whose viscosity is to be measured. The viscosity measurements are made either by applying a fixed torque and measuring the speed of rotation or by driving the rotating element at a constant speed and measuring the torque required. The cone-plate and parallel-plate rotational viscometers are variations of the same technique. For viscosity measurements of non-Newtonian fluids, rotational viscometers involving shearing of the fluid are used. These instruments are usually calibrated with fluids of known viscosity and the viscosities of test samples are taken from the calibration chart. Basic arrangements of cylindrical and cone-plate rotational viscometers are shown in Fig. 15.

In the falling-sphere viscometer, the time taken for a ball to fall through a measured height of fluid in a tube is measured. The time required is a measure of absolute viscosity. Other variations of this type are also available. In the rolling-sphere viscometer, a ball rolls down an inclined tube filled with test fluid. The falling coaxial cylinder viscometer consists of two coaxial cylinders with their axes vertical. The outer cylinder is clamped and the clearance space between the cylinders is filled with the test fluid. In operation, the inner cylinder is released and falls under gravity. The viscosity is determined from the speed of descent of the cylinder whose motion is opposed by the shear stresses induced in the test fluid. Another variety is the band viscometer where a thin band is located in a narrow gap between two parallel shear blocks filled with the test fluid. The band is released to fall under gravity, its motion being opposed by the shear stresses induced in the test fluid. The viscosity is determined from the speed of descent



**Figure 15** (a) U-tube viscometer, (b) rotating-cylinder viscometer, (c) cone and plate viscometer, (d) falling-sphere viscometer, (e) band viscometer, and (f) efflux viscometer.

of the band. These types of instruments are useful for non-Newtonian measurements and for high-viscosity fluids.

In efflux viscometers the viscosity is measured by the time taken for a given volume of liquid to discharge under gravity through a short tube orifice placed in the base of the instrument. Three types are common: Redwood, Saybolt, and Engler. The first one is commonly used in the United Kingdom, while the second one is mainly used in Europe and the United States. In all

three instruments, the viscosities are quoted in terms of the efflux time, for example, Redwood sec, Saybolt sec or Engler sec. These measurements are then converted to kinematic viscosity using conversion tables.

### 7.3 Lubricant Oxidation Tests

Hydrocarbon lubricants oxidize readily as a result of low-temperature acidification. Thus it is important to know the remaining useful life (RUL) of lubricant before the uncontrolled oxidation of the base oil occurs. This is done by conducting laboratory oxidation stability tests where the lubricant is oxidized under various conditions of temperature, pressure, and catalysts. Then lubricant characteristics such as viscosity, antioxidant depletion, total acid number, sludge content, and so on, are evaluated to measure oil degradation and oxidation stability and finally to determine the remaining useful life of the lubricant. Lubricant oxidation stability tests can be grouped into three categories: bulk oxidation tests, microscale oxidation tests, and nonstandard tests. The bulk oxidation test is done to see if excessive oil oxidation takes place when lubricating oil is stored in a storage tank. These methods include open-vessel tests and bomb oxidation tests. Microscale oxidation tests involve small amounts of lubricant and are carried out to accurately simulate oxidation of oil when it is present as a thin layer so that all parts of the oil are in close contact with atmospheric oxygen. These methods include thin-layer oxidation tests and gel permeation chromatography. Nonstandard tests are done to reduce the test duration in comparison to standard tests. These methods include differential scanning calorimetry, differential thermal analysis, thermogravimetric balance, and chemiluminescence tests.

## 8 WEAR PARTICLE ANALYSIS

Wear particles are produced during almost every tribological operation and are an important source of information about wear processes. The composition, size, and morphology of wear particles are indicative of the wear mechanism involved in their formation. Wear particle analysis helps to assess the condition of the machinery and reliability in mechanical systems. Two basic types of analysis are widely used. One is based on the analysis of the chemical composition of the lubricant to reveal the presence and quantity of metallic wear particles in hydrocarbon-based lubricating oil. The other method involves an extraction of wear particles from a used lubricant and then assessment of their number, size, shape, and morphology.

### 8.1 Chemical Analysis of Particles in Lubricant

The common method used to analyze the chemical composition of particles present in lubricating oil is flame spectroscopy. This is based on the principle of emission or absorption of characteristic color by an individual chemical element when heated in a flame or arc. Systematic analysis of the colors so produced by a lubricant sample provides complete data of the chemical elements present therein. The concentration of different elements can also be assessed. The technique of flame spectroscopy is commonly known as the Spectroscopic Oil Analysis Program (SOAP) and is used in machine condition monitoring. SOAP is used to specify whether to continue operating a machine or to go for any maintenance based on the concentration of contaminant metals and water in the lubricating oil beyond acceptable limits. In tribological experiments on lubricated wear, SOAP is used to determine if oil is functioning at desired conditions. SOAP provides the information about very small wear particles that remain suspended in the oil but fails to capture large wear particles. Thus, as the size of the wear particles increases, the SOAP accuracy decreases, and it becomes insensitive to particles larger than 10  $\mu\text{m}$ .

## 8.2 Analysis Based on Separation of Wear Particles

To avoid the limitations of SOAP analysis, a technique called “ferrography” is developed. In this method, wear particles are separated from the lubricating oil according to their size based on the application of a strong magnetic field. A sample of lubricating oil or oil diluted by solvent is allowed to flow over an inclined glass slide suspended above a magnetic field. The fluid sample flows by gravity along the slide. The combination of viscous and magnetic forces acting on the wear particles helps in separation and settlement of the particles on the glass slide. Large particles of iron and steel get deposited near the entry region due to strong attraction of the magnetic field and fine particles are deposited away from the entry region on the slide. Then the slide containing the thin streak of wear particles is subjected to either analytical ferrography or direct-reading ferrography. In the former method, the slide is examined under a microscope to study the morphology of wear particles. In the other method, the change in transmission of light through wear particles deposited in a glass tube is measured.

The shape and surface morphology of wear particles provide the information of how the wear particles are formed. Wear particle morphology is in general described by two sets of parameters: particle boundary descriptors, e.g., aspect ratio, shape factor, convexity, curl, roundness, and fractal dimension, and surface topography descriptors, e.g., perspective view, color stereo, and contour map image.

## 9 INDUSTRIAL MEASUREMENTS

Measurements in an industrial context are performed to confirm the performance of a component or system. This is usually different from scientific tribological measurement where the basic objective is to develop a model of friction, wear, or related phenomena. Industrial measurements are primarily empirical and differ from scientific investigation with respect to specifications. Industrial testing usually relates to commercial products, where the test specification is either confidential or incompletely specified. For example, oil additives are marketed without publicly available specification. In many cases, the complexity of the phenomena occurring inside the system hinders direct tribological investigation in a simple tribometer. The interaction between the lubricating oil and combustion cycles of an internal combustion engine is extremely difficult to simulate with the help of a tribometer. Thus, direct testing of the engines and gearboxes is the only means to evaluate the performance of the system. Similarly, metalworking involves many frictional situations that cannot be simulated in a tribometer and the same requires special tests that are significantly different from common tribological tests with respect to the controlling factors. In metalworking the significant parameters are surface finish, precision, tool life, power consumption, and so on. The complexity of service conditions inside a synovial joint in orthopedic implants is always a challenge to tribologists and designers of tribometers. All these fields of testing ranging from lubricants to orthopedic implants are known as “industrial tribology” where the major concern is to overcome the difficulties in identifying the controlling parameters to have a comprehensive understanding of the system.

## 10 SUMMARY

Tribologists for generations have faced a unique problem; predictions and designs are based on a continuum- and scale-independent phenomenon. Though tribological interactions often occur in very small scales and volumes, the observations are related to large-scale dimensions and volumes. As an example, Bowden and Tabor’s junction growth model may be cited. It is a very small volume phenomenon at the asperity level that involves molecular-level interactions. However, due to unavailability of instrumentation that makes it possible to observe directly



the phenomenon and the related small-volume deformations, the model was based on continuum plasticity theory to provide a phenomenological view of adhesive wear and friction. The situation has undergone a dramatic change in the last two decades. With a virtual revolution in materials technology and electronics, reliable measurements down to nano- and picometric levels are now possible. This advancement coupled with recent advances in noncontinuum modeling at the molecular level has opened up a new horizon for the tribologists and scientists. These advances have opened up the new field of nanotribology. It involves experimental and theoretical investigations of interfacial processes on scales ranging from the atomic/molecular- to the microscale that occur during adhesion, friction, wear, indentation, and thin-film lubrication at sliding surfaces.

# CHAPTER 25

## VIBRATION AND SHOCK

Singiresu S. Rao  
University of Miami  
Coral Gables, Florida

<b>1 INTRODUCTION</b>	<b>861</b>	6.1 Transverse Vibration of a String	873
<b>2 MODELING OF PHYSICAL SYSTEMS</b>	<b>862</b>	6.2 Longitudinal Vibration of a Bar	874
<b>3 SINGLE DEGREE OF FREEDOM SYSTEM</b>	<b>865</b>	6.3 Torsional Vibration of a Shaft	874
3.1 Equation of Motion	865	6.4 Flexural Vibration of a Beam	875
3.2 Free Vibration	866	6.5 Free Vibration Solution	875
3.3 Forced Harmonic Vibration	867	<b>7 VIBRATION AND SHOCK ISOLATION</b>	<b>877</b>
3.4 Forced Nonharmonic Vibration	868	7.1 Vibration Isolation	878
<b>4 SHOCK SPECTRUM</b>	<b>868</b>	7.2 Shock Isolation	880
<b>5 MULTIDEGREE OF FREEDOM SYSTEM</b>	<b>870</b>	<b>8 STANDARDS FOR VIBRATION OF MACHINES</b>	<b>881</b>
5.1 Equations of Motion	871	<b>NOMENCLATURE</b>	<b>882</b>
5.2 Free Vibration Response	872	<b>REFERENCES</b>	<b>883</b>
5.3 Forced Vibration Response	872	<b>BIBLIOGRAPHY</b>	<b>883</b>
<b>6 VIBRATION OF CONTINUOUS SYSTEMS</b>	<b>873</b>		

### 1 INTRODUCTION

The subject of vibrations is a specialized area of dynamics. Dynamics is concerned with the motion of physical systems. Vibrations are concerned with the motion of a system in the form of oscillation or repetitive motion relative to a reference state. The reference state, in most cases, denotes the static equilibrium position of the system (as in the case of buildings). The reference state, in some cases, denotes the steady motion of the system (as in the case of spinning of a satellite). In vibrations, the motion is induced by a disturbing force. If the disturbing force acts only initially (at time zero), the resulting vibration is known as free vibration. On the other hand, if the disturbing force acts for some time (even after time zero), the resulting vibration is called forced vibration. Shock is a somewhat loosely defined term that implies a degree of suddenness and severity. It denotes a nonperiodic excitation in the form of a pulse of short duration. For the analysis and design of mechanical and structural systems, it is essential that the analyst or the designer have a thorough understanding of the basic principles of vibration and shock.

Some common sources of vibration and shock to equipment include handling, transportation by trucks, trains, airplanes, ships, and other vehicles, and blasts from explosions. Vibrations can be observed in the following typical situations:

An automobile traveling over a rough surface, earthquakes, motion of an airplane in turbulence, and a washing machine during spin cycle. The objectives of study of vibration and shock are:

- To explain, predict, and control the oscillatory behavior or response of systems
- To avoid fatigue damage in structures and machines
- To avoid physical discomfort to humans operating/working near vibrating equipment
- To safely design buildings, bridges, mechanical equipment and machinery
- To avoid noise generated by vibration

The study of vibration requires the following mathematical and computational tools:

1. Linear algebra: Matrix operations, solution of simultaneous equations, and solution of algebraic eigenvalue problem
2. Complex algebra: Representation and manipulation of harmonic and periodic functions in complex form
3. Ordinary differential equations: Solution by Laplace transforms and other techniques
4. Partial differential equations: Solution by method of separation of variables and other techniques
5. Approximate analytical methods: Solution by Rayleigh, Rayleigh–Ritz, Galerkin, least squares, and other variational and weighted residual approaches
6. Numerical methods: Solution of continuous systems as equivalent discrete systems using finite difference and finite element methods

## 2 MODELING OF PHYSICAL SYSTEMS

A physical system is to be replaced by a mathematical model in order to predict its vibration behavior. The accuracy of the predicted behavior depends on the level of difficulty associated with the mathematical model. The model must account for the four basic phenomena associated with the physical system, namely, the elasticity, inertia, excitation or input energy, and damping or dissipation of energy. The mathematical model should not be too complex and overly sophisticated to include more details of the system than are necessary. An overly sophisticated model will require more computational effort than necessary. In some cases, it may not be possible to find the solution of an overly complicated model. Based on the nature of the mathematical model used, the system may be called a discrete (or lumped) system or a continuous (or distributed) system<sup>1</sup>. In the discrete model, the physical system is assumed to consist of several rigid bodies (usually considered as point masses) connected by springs and dampers. The springs denote restoring forces that tend to return the masses to their respective undisturbed (or equilibrium) states. The dampers provide resistance to velocity and dissipate the energy of the system. In the continuous model, the mass, elasticity, and damping are assumed to be distributed throughout the system. The equations of motion of a discrete system are in the form of a system of  $n$  coupled second-order ordinary differential equations where  $n$  denotes the number of masses (discrete masses or rigid bodies). The number of independent coordinates needed to describe the configuration of a system at any time during vibration defines the degrees of freedom of the system. For example, Figs. 1, 2 and 3 denote typical 1, 2, and 3 degrees of freedom systems, respectively. A point mass can have three translational degrees of freedom while a rigid body can have three translational and three rotational degrees of freedom. Many mechanical and structural components and systems such as bars, beams, plates, and shells have

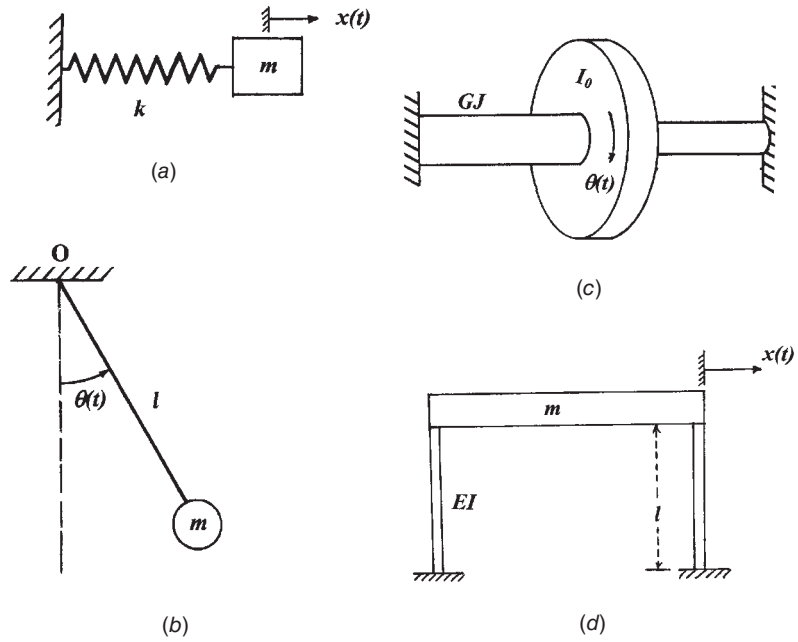


Figure 1 Typical 1 degree of freedom systems.

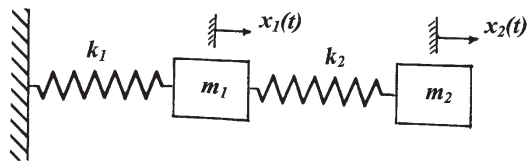


Figure 2 A two degree of freedom system.

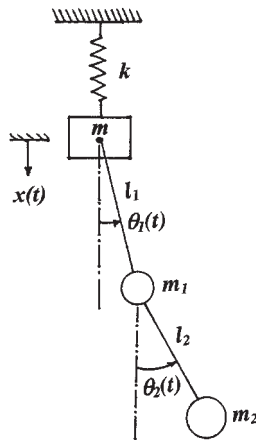
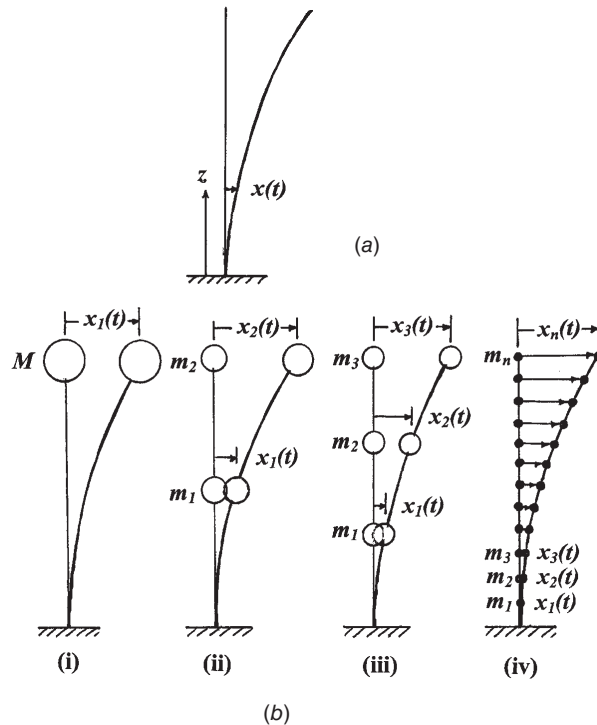


Figure 3 A three degree of freedom system.



**Figure 4** Modeling of a continuous system: (a) as a continuous system and (b) as a discrete system.

distributed mass, elasticity, and damping. The equation of motion of a continuous system is in the form of a partial differential equation. A continuous system can be modeled either as a discrete or lumped parameter system with varying number of degrees of freedom or as a continuous system with infinite number of degrees of freedom as illustrated for a cantilever beam in Fig. 4.

The oscillatory motion of a body may be harmonic, periodic, or non-periodic in nature. If the time variation of the displacement of the mass is sinusoidal, the motion will be harmonic. The number of cycles of motion per unit time defines the frequency, and the maximum magnitude of motion is called the amplitude of vibration. If the periodic variation of motion is not harmonic, the motion will be periodic. In this case, the periodic motion can be expressed as a sum of harmonic motions of different frequencies. If the time variation of the displacement of the mass is arbitrary (non-periodic), the motion is said to be non-periodic. If the non-periodic motion can be described either by an equation or by a set of tabulated values, the motion is considered to be deterministic. On the other hand, if the motion cannot be described by any equation or tabulated values, it is said to be random or probabilistic. When an external force or excitation is applied to a mechanical or structural system, the amplitude of the resulting vibration can become very large when a frequency component of the applied force or excitation approaches one of the natural frequencies of the system, particularly the fundamental one. Such a condition, known as resonance, and the attendant stresses and strains might cause a failure of the system. Because of this reason, designers should have a means of determining the natural frequencies of mechanical and structural systems using analytical or experimental approaches.

### 3 SINGLE DEGREE OF FREEDOM SYSTEM

A study of the vibration characteristics of a single degree of freedom system is extremely important in the study of vibration and shock because the approximate or qualitative response of most systems can be determined by using a single degree of freedom model for the system. A general single degree of freedom system consists of a mass  $m$ , spring of stiffness  $k$ , and a viscous damper with a damping constant  $c$  as shown in Fig. 5. The significance of the quantities  $m$ ,  $c$ , and  $k$  for different types of systems is given in Table 1.

#### 3.1 Equation of Motion

The equation of motion is given by

$$m\ddot{x} + c\dot{x} + kx = f(t) \quad (1)$$

where a dot (two dots) above  $x$  denotes the first (second) derivative with respect to time.

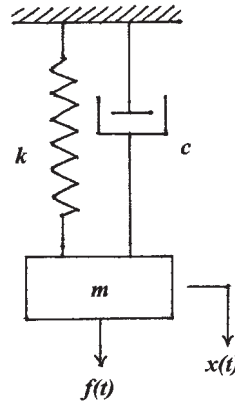


Figure 5 A mass–spring–damper system.

Table 1 Significance of  $m$ ,  $c$ , and  $k$  in Different Systems

Vibrating System	$m$	$c$	$k$	Variable $x$
1. Translatory spring–mass–damper system (Fig. 5)	Mass (kg)	Viscous damping constant (N – s/m)	Spring stiffness (N/m)	Linear displacement (m)
2. Rotational spring–mass–damper system (Fig. 1c)	Mass moment of inertia (kg – m <sup>2</sup> )	Torsional damping constant (m – N – s/rad)	Torsional spring stiffness (m – N/rad)	Angular displacement (rad)
3. Swinging pendulum (Fig. 1b)	Moment of inertia of bob (kg – m <sup>2</sup> )	Damping constant of surrounding medium (m – N – s/rad)	Angular stiffness constant due to gravity (N – m/rad)	Angular displacement (rad)
4. Transversely vibrating cantilever beam (Fig. 4a)	Mass at the end of beam (kg)	Damping constant due to surrounding medium (N – s/m)	Flexural stiffness of beam (N/m)	Transverse displacement of mass at end of cantilever (m)

### 3.2 Free Vibration

The free vibration response of the system, corresponding to  $f(t) = 0$  in Eq. (1), is given by

$$x(t) = e^{-\zeta\omega_n t} (C_1 e^{\omega_n \sqrt{\zeta^2-1} t} + C_2 e^{-\omega_n \sqrt{\zeta^2-1} t}) \quad (2)$$

where  $C_1$  and  $C_2$  are constants, and  $\omega_n$  is the undamped natural frequency of vibration:

$$\omega_n = \sqrt{\frac{k}{m}} \quad (3)$$

and  $\zeta$  is the damping ratio:

$$\zeta = \frac{c}{c_{\text{cri}}} = \frac{c}{2m\omega_n} = \frac{c}{2\sqrt{km}} \quad (4)$$

with  $c_{\text{cri}}$  denoting critical damping:

$$c_{\text{cri}} = 2m\omega_n = 2\sqrt{km} \quad (5)$$

Equation (2) indicates that the physical behavior of a system depends primarily upon the magnitude of the damping ratio  $\zeta$ . There are three distinct damping cases: (i)  $\zeta > 1$ , (ii)  $\zeta = 1$ , and (iii)  $\zeta < 1$ .

*Case 1.* When  $\zeta > 1$ , the system is said to be overdamped and will not oscillate when displaced from its static equilibrium position. A typical displacement–time curve of the system, when the mass is given an initial displacement  $x_0$  from its static equilibrium position and released with nonzero initial velocity, is shown in Fig. 6a. It can be seen that an overdamped system takes an extremely long time (theoretically infinite time) to return to its static equilibrium position.

*Case 2.* When  $\zeta = 1$ , the system is said to be critically damped and the free vibration solution becomes

$$x(t) = (C_1 + C_2 t) e^{-\omega_n t} \quad (6)$$

In this case, the system will not oscillate when given an initial displacement but returns to its static equilibrium position similar to that of an overdamped system. Here also it takes an infinite time for the system to return to its static equilibrium position as shown in Fig. 6b. However, the critically damped system returns to its static equilibrium position in minimum possible time without oscillation.

*Case 3.* When  $\zeta < 1$ , the system is said to be underdamped and the free vibration solution can be expressed as

$$x(t) = e^{-\zeta\omega_n t} (C_1 e^{i\omega_d t} + C_2 e^{-i\omega_d t}) \quad (7)$$

or

$$x(t) = X_0 e^{-\zeta\omega_n t} \sin(\omega_d t + \phi) \quad (8)$$

where

$$\omega_d = \omega_n \sqrt{1 - \zeta^2} \quad (9)$$

denotes the damped frequency of vibration and  $C_1$  and  $C_2$  or  $X_0$  and  $\phi$  are constants that can be determined from the initial conditions. If the initial displacement and initial velocity of the system are specified as

$$x(t=0) = x_0 \quad \dot{x}(t=0) = \dot{x}_0 \quad (10)$$

Equations (7) and (8) can be expressed in equivalent form as

$$x(t) = e^{-\zeta\omega_n t} \left( x_0 \cos \omega_d t + \frac{\dot{x}_0 + \zeta \omega_n x_0}{\omega_d} \sin \omega_d t \right) \quad (11)$$

A typical response of the system, when given an initial displacement  $x_0$  with nonzero initial velocity, is shown in Fig. 6c.

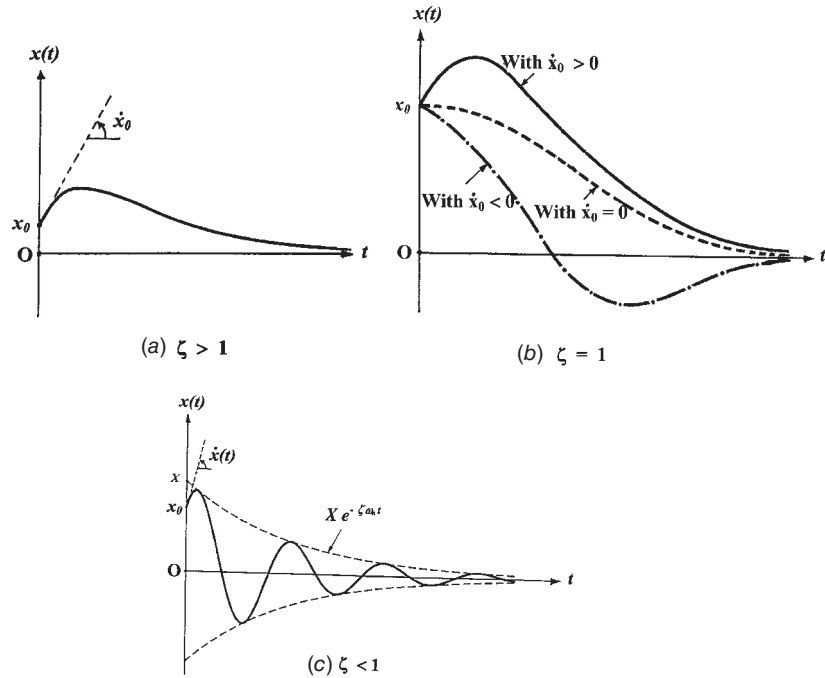


Figure 6 Free vibration response.

### 3.3 Forced Harmonic Vibration

When a single degree of freedom system is subjected to a harmonic force in addition to the initial conditions, the equation of motion and its solution are given by

$$m\ddot{x} + c\dot{x} + kx = f_0 \sin \omega t \quad (12)$$

$$x(t) = e^{-\zeta \omega_n t} (C_1 \cos \omega_d t + C_2 \sin \omega_d t) + X \sin(\omega t - \phi) \quad (13)$$

where  $f_0$  is the magnitude and  $\omega$  is the frequency of the applied force. In Eq. (13), the first term denotes the transient vibration ( $x_h$ ) while the second term indicates the steady-state solution ( $x_p$ ) with  $X$  indicating the amplitude and  $\phi$  the phase angle. The amplitude  $X$  and the phase angle  $\phi$  are given by

$$X = \frac{(f_0/k)}{\sqrt{[1 - (\omega/\omega_n)^2]^2 + [2\zeta \omega/\omega_n]^2}} = \frac{\delta_{st}}{\sqrt{(1-r^2)^2 + (2\zeta r)^2}} \quad (14)$$

and

$$\phi = \tan^{-1} \left[ \frac{2\zeta (\omega/\omega_n)}{1 - (\omega/\omega_n)^2} \right] = \tan^{-1} \left( \frac{2\zeta r}{1-r^2} \right) \quad (15)$$

with

$$\delta_{st} = \frac{f_0}{k} = \text{static deflection under the force } f_0 \quad (16)$$

$$r = \frac{\omega}{\omega_n} = \text{frequency ratio} \quad (17)$$



### 3.4 Forced Nonharmonic Vibration

When  $f(t)$  is nonharmonic, the steady-state response or the particular integral of Eq. (1),  $x_p(t)$ , is given by the Duhamel or convolution integral:

$$x_p(t) = \frac{1}{m \omega_d} \int_0^t f(\eta) e^{-\zeta \omega_n (t-\eta)} \sin \omega_d (t-\eta) d\eta \quad (18)$$

Unless the forcing function  $f(t)$  is a simple analytical function, such as a step function, the integral in Eq. (18) needs to be evaluated by some numerical method. The solution given by Eq. (18) for a step function,  $f(t) = f_0, t > 0$ , can be expressed as

$$x_p(t) = \frac{f_0}{k} \left\{ 1 - \frac{e^{-(\zeta 2\pi t / \tau_n)}}{\sqrt{1-\zeta^2}} \left[ \cos \left( \frac{2\pi \sqrt{1-\zeta^2} t}{\tau_n} - \phi \right) \right] \right\} \quad (19)$$

where

$$\phi = \tan^{-1} \frac{\zeta}{\sqrt{1-\zeta^2}} \quad (20)$$

and

$$\tau_n = \frac{2\pi}{\omega_n} = 2\pi \sqrt{\frac{m}{k}} \quad (21)$$

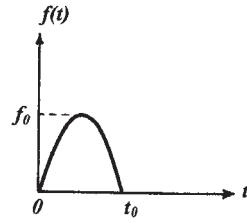
If the initial conditions of the system are not zero, the homogeneous solution of the differential equation, Eq. (1),  $x_h(t)$  is to be added to the particular integral so that the complete solution becomes

$$\begin{aligned} x(t) &= x_h(t) + x_p(t) \\ &= e^{-\zeta \omega_n t} \left( x_0 \cos \omega_d t + \frac{\dot{x}_0 + \zeta \omega_n x_0}{\omega_d} \sin \omega_d t \right) \\ &\quad + \frac{1}{m\omega_d} \int_0^t f(\eta) e^{-\zeta \omega_n (t-\eta)} \sin \omega_d (t-\eta) d\eta \end{aligned} \quad (22)$$

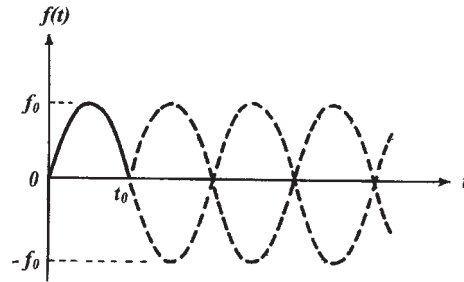
## 4 SHOCK SPECTRUM

Many mechanical and structural systems are subjected, on occasion, to sudden large forces acting for short periods of time that are small compared to the natural time period of the system. Such forces, known as shock, can cause damage to the system and can induce undesirable vibration of the system. Hence the prediction of the response of a system to shock is of great importance in mechanical and structural design. Generally, the severity of a shock is measured in terms of the maximum value of the response. It is customary to use the response of an undamped single degree of freedom system for comparison purposes. A plot of the maximum response of an undamped single degree of freedom system to a given shock as a function of the natural time period (or natural frequency) of the system is known as the shock spectrum or response spectrum. These plots help in finding the ratio of the maximum dynamic stress to the corresponding static stress in a mechanical or structural system. In most practical cases, the time at which the maximum response of the system occurs is also of interest; hence such plots are also given along with the shock spectrum. It is known that the maximum response of a single degree of freedom system subjected to a force depends upon the characteristics of the system as well as the nature of the applied force. For an undamped system, the natural period or frequency is the characteristic that determines the response for any specified forcing function. The shape and duration of the force  $f(t)$  also plays an important role in determining the response.

For example, if the half sine wave shown in Fig. 7 denotes a shock pulse where  $f_0$  denotes the peak value of the force and  $t_0$  indicates the duration of the pulse. This force can be regarded



(a)



(b)

**Figure 7** Half sine wave.

as the superposition of two one-sided sine functions—one starting at  $t = 0$  and the other starting at  $t = t_0 = \pi/\omega$  as shown in Fig. 7b. Defining the unit step function applied at  $x = a$  as  $u(t-a)$ :

$$u(t-a) = \begin{cases} 0 & t < a \\ 1 & t > a \end{cases} \quad (23)$$

The shock pulse of Fig. 7a can be described as

$$f(t) = f_0 \{ \sin \omega t u(t) + \sin \omega(t-t_0) u(t-t_0) \} \quad (24)$$

The response of an undamped spring-mass system to the forcing function given by Eq. (24) can be expressed as

$$\begin{aligned} x(t) = & \frac{f_0}{k} \frac{1}{1 - (\omega/\omega_n)^2} \\ & \times \left[ \left( \sin \omega t - \frac{\omega}{\omega_n} \sin \omega_n t \right) u(t) \right. \\ & \left. + \left\{ \sin \omega(t-t_0) - \frac{\omega}{\omega_n} \sin \omega_n(t-t_0) \right\} u(t-t_0) \right] \quad (25) \end{aligned}$$

It is to be noted that the first term in the square brackets on the right side of Eq. (25) gives the response of the system for  $0 < t < \pi/\omega$  (during the time of application of the pulse), while the response of the system for any time after the termination of the pulse ( $t > \pi/\omega$ ) can be expressed in a compact form as

$$x(t) = \frac{f_0 (\omega_n/\omega)}{k \{ 1 - (\omega_n/\omega)^2 \}} [\sin \omega_n t + \sin \omega_n(t-t_0)] \quad (26)$$

To determine the maximum response of the system, we need to first find the time,  $t_{\max}$ , at which the maximum response,  $x_{\max}$ , occurs by solving the equation  $\dot{x} = dx/dt = 0$ , and then substitute the value of  $t_{\max}$  for  $t$  in the expression of  $x(t)$  to find  $x_{\max}$ . The time derivatives of  $x(t)$  are given by

$$\dot{x}(t) = \frac{f_0 \omega}{k \{1 - (\omega/\omega_n)^2\}} (\cos \omega t - \cos \omega_n t) \quad 0 < t < \frac{\pi}{\omega} \quad (27)$$

and

$$\dot{x}(t) = \frac{f_0 (\omega_n^2/\omega)}{k \{1 - (\omega_n/\omega)^2\}} (\cos \omega_n t + \cos \omega_n \{t - t_0\}) \quad t > \frac{\pi}{\omega} \quad (28)$$

By setting  $\dot{x} = 0$ , Eqs. (27) and (28) yield

$$t_{\max} = \frac{2j\pi}{\omega_n + \omega} \quad j = 1, 2, 3, \dots \quad (29)$$

$$x_{\max} = \frac{f_0 (\omega_n/\omega)}{k \{(\omega_n/\omega) - 1\}} \sin \frac{2j\pi}{\{1 + (\omega_n/\omega)\}} \quad j < \frac{1}{2} (1 + \omega_n/\omega) \quad \text{for } 0 < t < \frac{\pi}{\omega} \quad (30)$$

and

$$t_{\max} = (2j - 1) \frac{\pi}{2 \omega_n} + \frac{t_0}{2} \quad j = 1, 2, 3, \dots \quad (31)$$

$$x_{\max} = \frac{2f_0 (\omega_n/\omega)}{k \{1 - (\omega_n/\omega)^2\}} \cos \frac{\pi \omega_n}{2\omega} \quad \text{for } t > \frac{\pi}{\omega} \quad (32)$$

Thus the shock spectrum can be obtained by plotting  $x_{\max}$  versus  $\omega_n/\omega$  using both Eqs. (30) and (32). The shock spectrum is shown in nondimensional form in Fig. 8.

### 5 MULTIDEGREE OF FREEDOM SYSTEM

Most mechanical and structural systems have distributed mass, elasticity, and damping. These systems are modeled as multi-( $n$ )-degree-of-freedom systems to facilitate analysis of their vibration behavior. Several methods are available to construct an degree-of-freedom model from a continuous system. These include the physical lumping or modeling method, the finite-element method, finite-difference method, modal analysis method, Rayleigh–Ritz method, Galerkin method, and many others. In most cases, the number of degrees of freedom ( $n$ ) to be used in the model depends on the frequency range. If the system is expected to undergo significant deformations at higher frequencies, the model should include enough

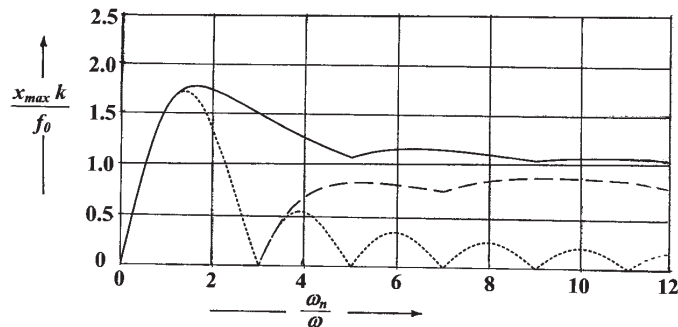


Figure 8 Shock spectrum.

number of degrees of freedom to cover all the important frequencies. Most vibration characteristics of a  $n$ -degree-of-freedom system are similar to those of a single degree of freedom system. An  $n$ -degree of freedom system will have  $n$  natural frequencies, its free vibrations denote exponentially decaying motions, its forced vibrations exhibit resonance behavior, etc. However, there are some vibration characteristics that are unique to an  $n$ -degree-of-freedom system that are absent in single-degree-of-freedom systems. For example, the existence of normal modes, orthogonality of normal modes, and decomposition of the response of the system (free or forced) in terms of normal modes are unique to multidegree of freedom systems.

## 5.1 Equations of Motion

Consider a three-degree-of-freedom system consisting of three masses  $m_1$ ,  $m_2$  and  $m_3$ , three springs with stiffnesses  $k_1$ ,  $k_2$  and  $k_3$ , and three viscous dampers with damping constants  $c_1$ ,  $c_2$ , and  $c_3$  as shown in Fig. 9. The mass  $m_i$ , subjected to the force  $f_i(t)$ , undergoes a displacement  $x_i(t)$ ,  $i = 1, 2, 3$ . The equations of motion, derived from the free-body diagrams of the masses, can be expressed in matrix form as

$$\begin{bmatrix} m_1 & 0 & 0 \\ 0 & m_2 & 0 \\ 0 & 0 & m_3 \end{bmatrix} \begin{Bmatrix} \ddot{x}_1 \\ \ddot{x}_2 \\ \ddot{x}_3 \end{Bmatrix} + \begin{bmatrix} c_1 + c_2 & -c_2 & 0 \\ -c_2 & c_2 + c_3 & -c_3 \\ 0 & -c_3 & c_3 \end{bmatrix} \begin{Bmatrix} \dot{x}_1 \\ \dot{x}_2 \\ \dot{x}_3 \end{Bmatrix} + \begin{bmatrix} k_1 + k_2 & -k_2 & 0 \\ -k_2 & k_2 + k_3 & -k_3 \\ 0 & -k_3 & k_3 \end{bmatrix} \begin{Bmatrix} x_1 \\ x_2 \\ x_3 \end{Bmatrix} = \begin{Bmatrix} f_1(t) \\ f_2(t) \\ f_3(t) \end{Bmatrix} \quad (33)$$

Equation (33) can be generalized to an  $n$ -degree-of-freedom system as

$$[m] \ddot{\mathbf{x}} + [c] \dot{\mathbf{x}} + [k] \mathbf{x} = \mathbf{f}(t) \quad (34)$$

where  $[m]$ ,  $[c]$ , and  $[k]$  are called the mass, damping, and stiffness matrices, respectively,  $\mathbf{x}$ ,  $\dot{\mathbf{x}}$ , and  $\ddot{\mathbf{x}}$  are called the displacement, velocity, and acceleration vectors, respectively, and  $\mathbf{f}(t)$  is the vector of forces with

$$\mathbf{x}(t) = \begin{Bmatrix} x_1(t) \\ x_2(t) \\ \vdots \\ x_n(t) \end{Bmatrix} \quad \mathbf{f}(t) = \begin{Bmatrix} f_1(t) \\ f_2(t) \\ \vdots \\ f_n(t) \end{Bmatrix} \quad (35)$$

The mass matrix  $[m]$  is a symmetric positive definite matrix,  $[c]$  is a symmetric nonnegative matrix, and  $[k]$  is a symmetric nonnegative matrix. The symmetry of the matrices  $[m]$ ,  $[c]$ , and  $[k]$  implies that the Maxwell–Betti reciprocity theorem<sup>2</sup> is valid for the system.

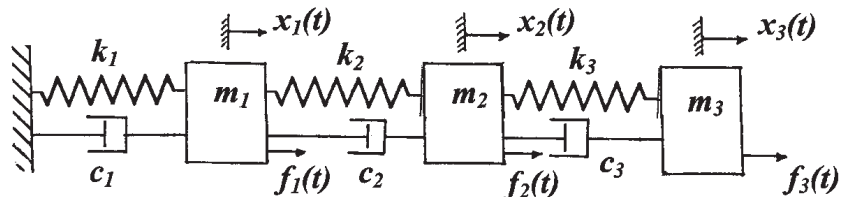


Figure 9 A three-degree-of-freedom system.

## 5.2 Free Vibration Response

When  $\mathbf{f}(t) = 0$ , Eq. (34) gives the free vibration equation. For the undamped free vibration of the system, harmonic solution is assumed as

$$\mathbf{x}(t) = \mathbf{X} \cos \omega t \quad (36)$$

where  $\mathbf{X}$  is the vector of amplitudes of the masses (or mode shape) and  $\omega$  is the natural frequency. By substituting  $[c] = [0]$  and Eq. (36) into the free vibration equation, we obtain

$$\omega^2 [m] \mathbf{X} = [k] \mathbf{X} \quad (37)$$

The solution of the eigenvalue problem of Eq. (37) gives the natural frequencies  $\omega_1, \omega_2, \dots, \omega_n$  and the corresponding mode shapes, natural modes or eigenvectors  $\mathbf{X}^{(1)}, \mathbf{X}^{(2)}, \dots, \mathbf{X}^{(n)}$ . The mode shapes  $\mathbf{X}^{(i)}$  are orthogonal with respect to the mass and stiffness matrices. When the mode shapes are normalized with respect to the mass matrix, we obtain

$$\mathbf{X}^{(i)T} [m] \mathbf{X}^{(j)} = \delta_{ij} \quad (38)$$

$$\mathbf{X}^{(i)T} [k] \mathbf{X}^{(i)} = [\omega_i^2] \quad (39)$$

where  $\delta_{ij}$  is the Kronecker delta defined by

$$\delta_{ij} = \begin{cases} 1 & \text{if } i = j \\ 0 & \text{if } i \neq j \end{cases} \quad (40)$$

and  $[\omega_i^2]$  is a diagonal matrix consisting of  $\omega_1^2, \omega_2^2, \dots, \omega_n^2$  in the diagonal locations. For the free vibration of the undamped system, a procedure known as modal analysis, can be used. In this procedure, the free vibration solution is assumed as

$$\mathbf{x}(t) = \sum_{i=1}^n \eta_i(t) \mathbf{X}^{(i)} \quad (41)$$

where  $\eta_i(t)$  is the generalized coordinate corresponding to the mode  $i$ . Using the initial conditions

$$\mathbf{x}(t=0) = \mathbf{x}_0 \quad \dot{\mathbf{x}}(t=0) = \dot{\mathbf{x}}_0 \quad (42)$$

The generalized coordinates can be found as

$$\eta_i(t) = \eta_i(0) \cos \omega_i t + \frac{\dot{\eta}_i(0)}{\omega_i} \sin \omega_i t \quad i = 1, 2, \dots, n \quad (43)$$

where the initial values of the generalized displacements,  $\eta_i(0)$ , and the generalized velocities,  $\dot{\eta}_i(0)$ , can be found using Eqs. (42). Finally the free vibration solution of the multidegree of freedom system can be determined using Eq. (41).

## 5.3 Forced Vibration Response

The forced vibration of the system, given by the solution of Eq. (34), can be found using the modal analysis. For simplicity, we assume the damping to be proportional, and the matrix  $[c]$  is assumed to be given by a linear combination of the mass and stiffness matrices:

$$[c] = \alpha [m] + \beta [k] \quad (44)$$

where  $\alpha$  and  $\beta$  are constants. By using a solution of the form of Eq. (42) and using the orthogonality properties of the normal modes, the generalized coordinates can be found as

$$\eta_i(t) = a_i e^{-\zeta_i \omega_i t} \sin(\omega_{d_i} t + \phi_i) + \frac{1}{\omega_{d_i}} e^{-\zeta_i \omega_i t} \int_0^t F_i(\tau) e^{\zeta_i \omega_i \tau} \sin \omega_{d_i} (t - \tau) d\tau \quad (45)$$

where

$$\omega_{d_i} = \omega_i \sqrt{1 - \zeta_i^2} \quad (46)$$

and  $a_i$  and  $\phi_i$  can be determined from the initial values of the modal coordinates,  $\eta_i(0)$  and  $\dot{\eta}_i(0)$ , and  $\zeta_i$  is the damping ratio determined from the relation

$$\zeta_i = \frac{1}{2\omega_i} (\alpha + \beta \omega_i^2) \quad i = 1, 2, \dots, n \quad (47)$$

where  $\omega_i$  denotes the  $i$ th natural frequency of the system. Once the generalized coordinates are known, the forced vibration response of the multidegree of freedom system can be found from Eq. (42).

## 6 VIBRATION OF CONTINUOUS SYSTEMS

Some practical mechanical and structural systems with uniform or regular geometry can be modeled as simple continuous vibratory systems. In these models, the inertial and elastic properties are distributed in terms of mass density and elastic moduli. A continuous vibratory system will have infinite degrees of freedom. Examples of continuous systems include strings, bars, shafts, beams, membranes, plates, and shells. The vibration of simple undamped continuous systems due to only initial conditions is considered in this section. The responses of undamped continuous systems due only to nonzero initial conditions are sinusoidal transient responses and denote free vibrations.

### 6.1 Transverse Vibration of a String

A string is geometrically a line and hence will support only tensile load. Each point of the string is assumed to have only transverse motion (Fig. 10). We assume that the transverse displacement of the string ( $w$ ) is small so that the tension,  $T(x)$ , may be assumed to be a constant independent of the position along the curve of the string. In the free-body diagram of a differential length ( $dx$ ) of the string shown in Fig. 10b, the horizontal components of the tension  $T(x)$  and  $T(x + dx)$  are approximately equal to each other but are opposite in sign:

$$T(x)|_x = -T(x + dx)|_x \quad (48)$$

According to Newton's second law, the sum of the vertical components of the tensile forces causes the time rate of change of the linear momentum of the element of string in the transverse direction:

$$T(x)|_z + T(x + dx)|_z = \mu dx \frac{\partial^2 w}{\partial t^2} \quad (49)$$

where  $\mu$  is the mass per unit length and  $\partial^2 w / \partial t^2$  is the acceleration of the differential element of the string. Using

$$\begin{aligned} T(x)|_z &= T \sin \theta(x), & \sin \theta(x) &\cong -\frac{\partial w(x)}{\partial x} \\ T(x + dx)|_z &= T \left( \frac{\partial w}{\partial x} + \frac{\partial^2 w}{\partial x^2} dx \right) \end{aligned} \quad (50)$$

Equation (49) yields the equation of motion as

$$\frac{\partial^2 w}{\partial x^2} = \frac{1}{\alpha^2} \frac{\partial^2 w}{\partial t^2} \quad (51)$$

where

$$\alpha = \sqrt{\frac{T}{\mu}} \quad (52)$$

Equation (51) is called the wave equation and  $\alpha$  denotes the wave velocity.

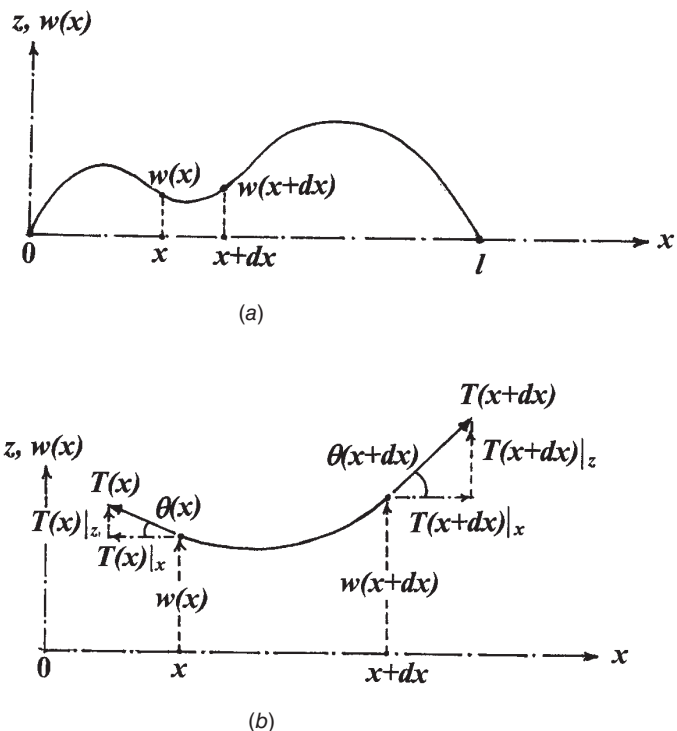


Figure 10 Vibrating string.

### 6.2 Longitudinal Vibration of a Bar

By proceeding as in the case of the transverse vibration of a string, the free-body diagram of an element of the bar yields the equation of motion for the longitudinal vibration of a bar as

$$\frac{\partial^2 u}{\partial x^2} = \frac{1}{\alpha^2} \frac{\partial^2 u}{\partial t^2} \tag{53}$$

where  $u$  is the axial displacement of the cross section of the bar at  $x$  and

$$\alpha = \sqrt{\frac{E}{\mu}} \tag{54}$$

with  $E$  denoting Young's modulus and  $\mu$  the mass density of the bar. If the bar is nonuniform, the cross-sectional area,  $A(x)$ , varies with  $x$  and the equation of motion becomes

$$\frac{\partial^2 u}{\partial x^2} + \frac{1}{A(x)} \frac{\partial A}{\partial x} \frac{\partial u}{\partial x} = \frac{\mu}{E} \frac{\partial^2 u}{\partial t^2} \tag{55}$$

### 6.3 Torsional Vibration of a Shaft

Denoting the angular displacement of the cross section of the shaft at  $x$  as  $\theta(x, t)$ , the equation of motion can be derived as

$$\frac{\partial^2 \theta}{\partial x^2} = \frac{1}{\alpha^2} \frac{\partial^2 \theta}{\partial t^2} \tag{56}$$

where

$$\alpha = \sqrt{\frac{G}{\mu}} \tag{57}$$

with  $\mu$  denoting the mass density and  $G$  the shear modulus of the material. If the cross-sectional area of the shaft,  $A(x)$ , varies with  $x$ , the equation of motion becomes

$$G \left( J \frac{\partial^2 \theta}{\partial x^2} + \frac{\partial J}{\partial x} \frac{\partial \theta}{\partial x} \right) = \mu J \frac{\partial^2 \theta}{\partial t^2} \quad (58)$$

It is to be noted that the equations of motion of a string, bar, and shaft, Eqs. (51), (53), and (56), have the same form and hence their solutions will be similar.

## 6.4 Flexural Vibration of a Beam

The bending moment–deflection relation of the beam is given by

$$M(x) = EI \frac{\partial^2 w}{\partial x^2} \quad (59)$$

where  $E$  is Young's modulus and  $I$  is the area moment of inertia of the cross section of the beam. The equation of motion of the beam is given by

$$EI \frac{\partial^4 w}{\partial x^4} + \mu A \frac{\partial^2 w}{\partial t^2} = 0 \quad (60)$$

where  $\mu$  is the density and  $A$  is the area of cross section of the beam. If an external force  $f(x, t)$  per unit length acts on the beam, the equation of motion takes the form

$$EI \frac{\partial^4 w}{\partial x^4} + \mu A \frac{\partial^2 w}{\partial t^2} = f(x, t) \quad (61)$$

For a nonuniform beam, the cross section varies along the length and the equation of motion for forced vibration becomes

$$\frac{\partial^2}{\partial x^2} \left( EI \frac{\partial^2 w}{\partial x^2} \right) + \mu A \frac{\partial^2 w}{\partial t^2} = f(x, t) \quad (62)$$

## 6.5 Free Vibration Solution

The free vibration solution of a continuous system depends on its boundary conditions and initial conditions. The free vibration solution can be determined either in the form of wave solution or in the form of superposition of normal modes of vibration. Both these methods are indicated in the following sections.

### Wave Solution

We shall consider the free vibration equation of strings, bars, and shafts to illustrate the wave solution. The one-dimensional wave equation can be expressed in the general form

$$\frac{\partial^2 f}{\partial x^2} = \frac{1}{\alpha^2} \frac{\partial^2 f}{\partial t^2} \quad (63)$$

where  $\alpha$  indicates the wave propagation velocity, and  $f(x, t)$  denotes the transverse displacement in the case of strings, longitudinal displacement in the case of bars, and angular displacement in the case of shafts. The solution of Eq. (63) is

$$f(x, t) = f_1(x - \alpha t) + f_2(x + \alpha t) \quad (64)$$

where  $f_1$  and  $f_2$  are arbitrary functions of the arguments  $x - \alpha t$  and  $x + \alpha t$ , respectively;  $f_1(x - \alpha t)$  denotes a displacement wave of arbitrary shape  $f_1$  traveling in the positive  $x$  direction with a constant velocity  $\alpha$  and without a change in shape. Similarly,  $f_2(x + \alpha t)$  represents a displacement wave of arbitrary shape  $f_2$  traveling in the negative  $x$  direction. Thus a general type of motion consists of a superposition of two waves of arbitrary shape traveling in opposite directions as shown in Fig. 11.



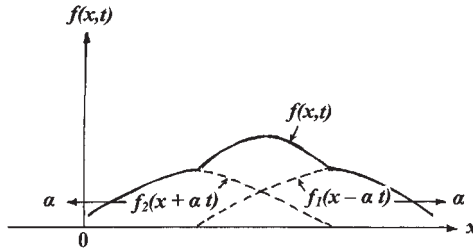


Figure 11 Wave solution.

**Normal Mode Solution**

We shall consider the free vibration equation of beams to illustrate the normal mode solution. The governing equation is

$$\alpha^2 \frac{\partial^4 w}{\partial x^4} + \frac{\partial^2 w}{\partial t^2} = 0 \tag{65}$$

where

$$\alpha = \sqrt{\frac{EI}{\rho A}} \tag{66}$$

The solution of Eq. (65) is assumed to be harmonic with frequency  $\omega$  as

$$w(x, t) = W(x) \cos \omega t \tag{67}$$

where  $W(x)$  is a function of  $x$  indicating the deflection (normal mode) of the beam during vibration at frequency  $\omega$ . Substitution of Eq. (67) into Eq. (65) yields

$$\frac{d^4 W}{dx^4} - \beta^4 W = 0 \tag{68}$$

where

$$\beta^4 = \frac{\omega^2}{\alpha^2} \tag{69}$$

The solution of Eq. (68) can be expressed as

$$W(x) = C_1 \sinh \beta x + C_2 \cosh \beta x + C_3 \sin \beta x + C_4 \cos \beta x \tag{70}$$

where the constants  $C_1, C_2, C_3,$  and  $C_4$  are evaluated using the boundary conditions of the beam. To indicate the procedure, consider a beam simply supported at both ends. The boundary conditions can be expressed as

$$w(0, t) = \frac{\partial^2 w(0, t)}{\partial x^2} = 0 \quad \text{or} \quad W(0) = \frac{d^2 W(0)}{dx^2} = 0 \tag{71}$$

$$w(l, t) = \frac{\partial^2 w(l, t)}{\partial x^2} = 0 \quad \text{or} \quad W(l) = \frac{d^2 W(l)}{dx^2} = 0 \tag{72}$$

Substitution of the solution, Eq. (70), into Eqs. (71) and (72) leads to

$$C_2 + C_4 = 0 \tag{73}$$

$$\beta^2(C_2 - C_4) = 0 \tag{74}$$

$$C_1 \sinh \beta l + C_2 \cosh \beta l + C_3 \sin \beta l + C_4 \cos \beta l = 0 \tag{75}$$

$$\beta^2 (C_1 \sinh \beta l + C_2 \cosh \beta l - C_3 \sin \beta l - C_4 \cos \beta l) = 0 \tag{76}$$

By setting the determinant of the coefficient matrix of  $C_1$ ,  $C_2$ ,  $C_3$ , and  $C_4$  in Eqs. (73)–(76) equal to zero, we obtain the frequency equation

$$\sin \beta l = 0 \quad (77)$$

The roots of Eq. (77) are given by

$$\beta l = n \pi \quad n = 1, 2, \dots \quad (78)$$

which, in view of Eq. (69), gives

$$\omega_n = (\beta_n l)^2 \sqrt{\frac{EI}{\rho A l^4}} \quad (79)$$

The free vibration response of the simply supported beam can be determined by superposing the normal modes as

$$w(x, t) = \sum_{n=1}^{\infty} \sin \frac{n \pi x}{l} (A_n \sin \omega_n t + B_n \cos \omega_n t) \quad (80)$$

where  $A_n = C_2 A$  and  $B_n = C_2 B$ . The constants  $A_n$  and  $B_n$  are evaluated by applying the initial conditions. The frequency equations and the first three natural frequencies of beams with some simple boundary conditions are given in Table 2.

## 7 VIBRATION AND SHOCK ISOLATION

Vibration and shock isolation denotes the storage of energy temporarily and its release in a different time relation. Isolation may be either for force or for motion. Isolation of motion involves the reduction of the deflections and stresses in systems whose supports experience motion due to vibration or shock. The concept of isolation of motion can be explained with reference to the system shown in Fig. 12. First consider a system that consists of a precision instrument of mass  $m$  connected to a larger mass  $M$  by a spring  $k$ . The mass  $M$  rests on a support (without the spring  $K$ ) that is subjected to vibration and shock. In order to reduce the motion of mass  $m$  relative to  $M$ , an isolator, in the form of a spring  $K$ , is inserted between the mass  $M$  and the support  $S$  as shown in Fig. 12. The characteristics of the isolator  $K$  depend on the type of system or equipment to be protected and the nature of the disturbing motion,  $y(t)$ . Force isolation involves the forces developed by the operation of machinery. For example, in an internal combustion engine, forces are generated by the firing of the fuel–air mixture. Additional forces result from the inertia of the unbalanced rotating and reciprocating members. All these forces are transmitted to the support or base or foundation of the engine. These forces may cause unacceptably high stresses in the support or the motion of the support may cause annoyance to

**Table 2** Frequency Equations and Natural Frequencies<sup>a</sup> of Uniform Beams

Boundary Conditions of the Beam	Frequency Equation	$\beta_1 l$	$\beta_2 l$	$\beta_3 l$
Simply supported at both ends	$\sin \beta l = 0$	3.1416	6.2832	9.4248
Fixed at both ends	$\cos \beta l \cosh \beta l = 1$	4.7300	7.8532	10.9956
Free at both ends	$\cos \beta l \cosh \beta l = 1$	4.7300	7.8532	10.9956
Fixed—free beam	$\cos \beta l \cosh \beta l = -1$	1.8751	4.6941	7.8548
Fixed—simply supported beam	$\tan \beta l = \tanh \beta l$	3.9266	7.0686	10.2102
Simply supported—free beam	$\tan \beta l = \tanh \beta l$	3.9266	7.0686	10.2102

<sup>a</sup> $\omega_n = (\beta_n l)^2 \sqrt{\frac{EI}{\rho A l^4}}$ .

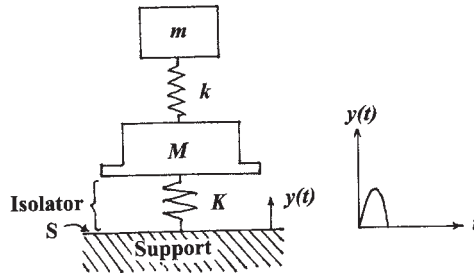


Figure 12 Isolation of motion.

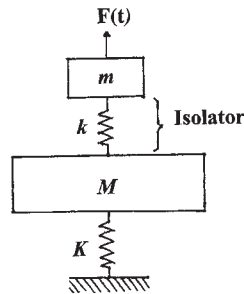


Figure 13 Isolation of force.

the personnel working nearby. The forces created by the operation of the engine can be isolated from the support by mounting the engine on a properly designed isolation system.

The concept of force isolation can be explained with reference to the system shown in Fig. 13 where the engine of mass  $m$  is placed on a support or foundation that can be represented by a mass  $M$  and a spring  $K$  (with no spring  $k$ ). Here  $f(t)$  indicates the force developed due to gas pressure and inertia force. Since the engine is directly attached to the foundation, both the engine and the foundation experience a common deflection in response to the force  $f(t)$ . By inserting a properly designed isolator  $k$  in between the engine and its support as shown in Fig. 13, the motion of the support  $M$  can be reduced. This will reduce the stress in the spring  $K$  and will reduce the disturbance experienced by the personnel working on or near the engine support.

## 7.1 Vibration Isolation

As stated earlier, two aspects of vibration isolation are to be considered—one for the isolation of forces and the other for the isolation of motions. The isolation of forces is required for rotating and reciprocating machinery such as fans, electric motors, compressors, and diesel engines. In these cases, the objective of isolation is to reduce the magnitude of the force transmitted to the support, base, or foundation of the machine. The isolation of motion is required for automobiles, trucks, trains, airplanes, and ships. In this case, the objective of isolation is to reduce the amplitude of vibration so that the mounted equipment is subjected to less severe vibration compared to the supporting structure, base, or foundation.

Consider a system consisting of a concentrated mass  $m$  supported by a spring of stiffness  $k$  and moves only in the vertical direction. When a harmonic force  $F(t) = F_0 \sin \omega t$  is applied

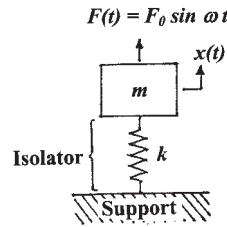


Figure 14 Isolation of forced transmitted to the support.

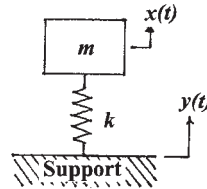


Figure 15 Isolation of displacement transmitted to the mass.

to the mass as shown in Fig. 14, the steady-state response or displacement of the mass  $m$  is given by

$$x(t) = \frac{F_0/k}{1 - \omega^2/\omega_n^2} \sin \omega t \quad (81)$$

where  $\omega_n = \sqrt{k/m}$  is the natural frequency of the system. The applied force,  $F(t)$ , is often due to the unbalanced rotating or reciprocating members. The spring  $k$  acts as an isolator. The purpose of the isolator is to ensure that the force transmitted to the support is less than the force  $F(t)$  applied to the mass  $m$ . The force transmitted to the support is equal to  $kx(t)$ . The effectiveness of the isolator is measured in terms of a quantity known as force transmissibility,  $T_F$ , which is defined as the ratio of the force transmitted by the isolator to the force applied to the mass:

$$T_F = \frac{kx}{F} = \frac{1}{1 - \omega^2/\omega_n^2} \quad (82)$$

It can be seen that the transmissibility,  $T_F$ , becomes negative when the frequency ratio,  $\omega/\omega_n$ , is larger than unity. Thus, for  $\omega/\omega_n < 1$ , the mass  $m$  moves downward if  $F(t)$  acts downward. The maximum downward force exerted on the support occurs at the same instant when the downward force  $F(t)$  is maximum. On the other hand, for  $\omega/\omega_n > 1$ , the maximum downward force on the support occurs at the same instant when the force  $F(t)$  is maximum upward.

Next, consider a system consisting of a concentrated mass  $m$  supported by a spring of stiffness  $k$  in which the support is subjected to a harmonic disturbance (or motion) as shown in Fig. 15:

$$y(t) = y_0 \sin \omega t \quad (83)$$

In this case also, the spring acts as an isolator. The purpose of the isolator is that the displacement (motion) transmitted to the mass  $m$  is less than the displacement applied to the support. The displacement transmissibility,  $T_D$ , is defined as the ratio of the maximum displacement of the mass  $m$  to the maximum displacement of the support:

$$T_D = \frac{x_0}{y_0} = \frac{1}{1 - \omega^2/\omega_n^2} \quad (84)$$

It can be seen that the expression of the displacement transmissibility is identical to that of the force transmissibility. In the design of vibration isolators, a quantity, isolation, is used to denote the complement of transmissibility. Thus a system with a transmissibility of 0.25 (or 25%) is said to have an isolation of 0.75 (or 75%).

## 7.2 Shock Isolation

Consider a shock to equipment that occurs due to a sudden change in velocity caused, for example, by the dropping of a package from a height. The equipment can be modeled, for a simple analysis, by a mass  $m$  and a spring of stiffness  $k$  as shown in Fig. 16. Here the equipment is originally assumed to be attached to a chassis of mass  $M$ , which, in turn, is secured rigidly to a support  $S$  (with no spring  $K$ ). Under a velocity shock, the support experiences a sudden velocity

$$\dot{z} = \frac{dz}{dt} = V = \sqrt{2gh} \quad (85)$$

where  $h$  is the height from which the chassis and equipment is dropped and  $g$  is the acceleration due to gravity. Since the chassis is rigidly attached to the support, it experiences the same velocity so that

$$\dot{y} = \dot{z} = V \quad (86)$$

and hence the displacement of the mass  $M$  is given by

$$y(t) = Vt \quad (87)$$

The displacement of the equipment (mass  $m$ ) can be expressed as

$$x(t) = V \left( t - \frac{1}{\omega_n} \sin \omega_n t \right) \quad (88)$$

where

$$\omega_n = \sqrt{\frac{k}{m}} \quad (89)$$

is the natural frequency of the equipment. The severity of the shock is usually measured by the maximum deformation of the spring,  $\delta_{\max}$ . The deformation of the spring,  $\delta$ , is given by

$$\delta = y - x = \frac{V}{\omega_n} \sin \omega_n t \quad (90)$$

and hence

$$\delta_{\max} = \frac{V}{\omega_n} \quad (91)$$

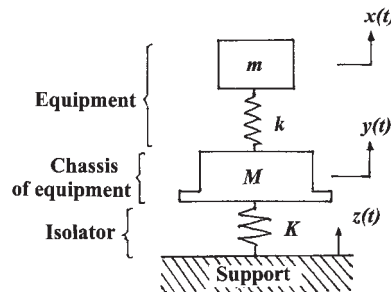


Figure 16 Shock to equipment due to sudden change in velocity.

In some cases, the severity of the shock experienced by the equipment or one of its components is measured by the acceleration experienced by the mass  $m$ . The acceleration of the equipment,  $\ddot{x}(t)$ , is given by

$$\ddot{x}(t) = V \omega_n \sin \omega_n t \quad (92)$$

and hence

$$\ddot{x}(t) |_{\max} = V \omega_n \quad (93)$$

In order to isolate the equipment from shock, an isolator, in the form of a spring of stiffness  $K$ , is inserted between the chassis of the equipment and the support as shown in Fig. 16. When the support is subjected to a velocity shock  $\dot{z} = V$ , the displacement of the support will be

$$z(t) = Vt \quad (94)$$

The equation of motion of the chassis is given by

$$M\ddot{y} + K(y - z) = 0 \quad (95)$$

with the solution

$$y(t) = V \left( t - \frac{1}{\Omega_n} \sin \Omega_n t \right) \quad (96)$$

where

$$\Omega_n = \sqrt{\frac{K}{M}} \quad (97)$$

is the natural frequency of the chassis–isolator system. The equation of motion of the equipment (mass  $m$ ) can be expressed as

$$m\ddot{x} + k(x - y) = 0 \quad (98)$$

Using Eq. (96), the solution of Eq. (98) can be determined as

$$x(t) = V \left\{ t - \frac{\sin \omega_n t}{\omega_n (1 - \omega_n^2/\Omega_n^2)} - \frac{\sin \Omega_n t}{\Omega_n (1 - \Omega_n^2/\omega_n^2)} \right\} \quad (99)$$

where  $\omega_n$  is the natural frequency of the equipment:

$$\omega_n = \sqrt{\frac{k}{m}} \quad (100)$$

The maximum acceleration of the equipment,  $m$ , is given by

$$\ddot{x} |_{\max} = \frac{V \omega_n}{1 - \omega_n/\Omega_n} \quad (101)$$

The shock transmissibility,  $T_s$ , is defined as the ratio of maximum accelerations of the equipment with and without the isolator:

$$T_s = \frac{\ddot{x} |_{\max} \text{ with isolator, Eq. (101)}}{\ddot{x} |_{\max} \text{ without isolator, Eq. (93)}} = \frac{1}{1 - \omega_n/\Omega_n} \quad (102)$$

The effectiveness of the shock isolator is measured in terms of the shock transmissibility, which can be seen to be a function of the characteristics of both the isolator and the equipment.

## 8 STANDARDS FOR VIBRATION OF MACHINES

Standards are established for vibration of machines by international organizations such as International Organization for Standardization (ISO), which works in cooperation with national organizations such as American National Standards Institute (ANSI) in the United States and the British Standards Institute (BSI) in the United Kingdom, the Deutsches Institut für Normung (DIN) in Germany, the Danish Standards Association (DS) in Denmark, the

Indian Standards Institute (ISI) in India. Vibration standards are intended to establish criteria for rating or classifying the performance of machines and equipment, provide a basis for selection of machines, and establish procedures for the calibration of machines. Vibration standards are developed by classifying machinery into four categories as follows:

1. Reciprocating machinery having both rotating and reciprocating components such as diesel engines, compressors, and pumps. In these machines, the amplitude of vibration is measured on the main structure of the machine at low frequencies in order to establish the severity of vibration.

2. Rotating machinery having rigid rotors such as electric motors and single-stage pumps. For these machines, vibration is measured on the main structure such as a pedestal or bearing cap to determine the severity of vibration.

3. Rotating machinery having flexible rotors such as large steam turbine generators, compressors, and multistage pumps. For these machines, vibration is measured on the shaft (rotor) directly to assess the severity of vibration.

4. Rotating machinery having quasi-rigid rotors such as low-pressure steam turbines, fans, and axial-flow compressors. In these cases, vibration amplitude is measured on the bearing cap of the flexible rotor to establish the severity of vibration.

The classification of severity of machine vibration is based on the amplitude of the motion variable, namely, the displacement, velocity, or acceleration. The particular motion variable used depends on the type of standard, frequency range, and other factors. For example, the rms (root mean square) value of velocity in the frequency range 10–1000 Hz is commonly used in many standards. The vibration velocity can be converted to vibration displacement for a single-frequency component as

$$S_f = \frac{V_f}{\omega_f} \sqrt{2} = \frac{V_f}{2\pi f} \sqrt{2} = 0.225 \frac{V_f}{f} \quad (103)$$

where  $S_f$  is the peak displacement amplitude,  $V_f$  is the rms value of the vibration velocity,  $f$  is the linear frequency (Hz), and  $\omega_f$  is the angular frequency (rad/s).

The ISO standards, for example, specifying the allowable vibration severity of rotating machinery are given in the references.

## NOMENCLATURE

$A$	cross-sectional area
$A_n, B_n$	constants
$c$	damping constant
$c_{\text{cri}}$	critical damping constant
$C_1, \dots, C_4$	constants
$E$	Young's modulus
$f(t)$	external force
$f_0$	amplitude of force
$f_1, f_2$	arbitrary functions
$G$	shear modulus
$I$	area moment of inertia
$k, K$	spring stiffness
$l$	length of beam
$m$	mass

$M$	mass, bending moment
$r$	frequency ratio
$t$	time
$T$	tension in string
$T_D(T_F)$	displacement (force) transmissibility
$T_s$	shock transmissibility
$u$	axial displacement of bar, unit step function
$V$	velocity
$w$	transverse displacement of string or beam
$x$	displacement
$x_h(x_p)$	homogeneous solution (particular integral)
$x_0(\dot{x}_0)$	initial displacement (velocity)
$X, X_0$	amplitude of displacement
$\mathbf{X}^{(i)}$	$i$ th modal vector
$\alpha$	constant, wave velocity
$\beta$	constant, frequency parameter in beam vibrations
$\phi$	phase angle
$\theta$	angular displacement of shaft
$\zeta$	damping ratio
$\mu$	mass density, mass per unit length
$\omega$	frequency of applied force
$\omega_n, \Omega_n$	natural frequency of vibration
$\eta_i(t)$	$i$ th generalized (modal) coordinate
$\delta_{st}$	static deflection
$\delta_{ij}$	Kronecker delta
$\omega_n$	natural frequency, $n$ th frequency
$\omega_d$	damped frequency
$( )_{\max}$	maximum value of ( )
$\vec{(\ )}$	vector of ( )
$[ \ ]$	matrix
$\dot{x} = \frac{dx}{dt}$ $\ddot{x} = \frac{d^2x}{dt^2}$	

## REFERENCES

1. S. S. Rao, *Mechanical Vibrations*, 5th ed., Pearson Prentice-Hall, Upper Saddle River, NJ, 2011.
2. E. Volterra and E. C. Zachmanoglou, *Dynamics of Vibrations*, C. E. Merrill Books, Columbus, OH, 1965.

## BIBLIOGRAPHY

- S. G. Braun, D. J. Ewins, and S. S. Rao (Eds.), *Encyclopedia of Vibration*, 3 Vol., Academic Press, San Diego, CA, 2002.
- C. E. Crede, *Vibration and Shock Isolation*, J Wiley, New York, 1951.
- B. K. Donaldson, *Analysis of Aircraft Structures: An Introduction*, McGraw-Hill, New York, 1993.
- C. M. Harris, *Shock and Vibration Handbook*, 4th ed., McGraw-Hill, New York, 1996.
- International Standards Organization, *ISO Standards Handbook – Mechanical Vibration and Shock. Volume 1: Terminology and Symbols; Tests and Test Equipment; Balancing and Balancing Equipment; Volume 2: Human Exposure to Vibration and Shock, Vibration in Relation to Vehicles, Specific Equipment and Machines, Buildings*. International Standards Organization, Geneva, 1995.



- International Standards Organization, ISO 2372, *Mechanical Vibration of Machines with Operating Speeds from 10 to 200 rps – Basis for Specifying Evaluation Standards*, International Standards Organization, Geneva, 1995.
- International Standards Organization, ISO 2954, *Mechanical Vibration of Rotating and Reciprocating Machinery – Requirements for Instruments for Measuring Vibration Severity*, International Standards Organization, Geneva, 2012.
- International Standards Organization, ISO 3945, *The Measurement and Evaluation of Vibration Severity of Large Rotating Machines, in Situ; Operating at Speeds from 10 to 200 rps*, International Standards Organization, Geneva, 1977.
- International Standards Organization, ISO/DIS 10816 Series, ISO/DIS 10816/1: *General Guidelines, Mechanical Vibration – Evaluation of Machine Vibration by Measurements on Non-Rotating Parts*, International Standards Organization, Geneva, 2009.
- S. G. Kelly, *Fundamentals of Mechanical Vibrations*, McGraw-Hill, New York, 2000.
- L. Meirovitch, *Fundamentals of Vibrations*, McGraw-Hill, New York, 2001.
- S. S. Rao, *Vibration of Continuous Systems*, J Wiley, Hoboken, NJ, 2007.
- R. F. Steidel, *An Introduction to Mechanical Vibrations*, 3rd ed., Wiley, New York, 1989.
- J. W. Tedesco, W. G. McDougal, and C. A. Ross, *Structural Dynamics: Theory and Applications*, Addison-Wesley, Menlo Park, CA, 1999.
- R. K. Vierck, *Vibration Analysis*, 2nd ed., Thomas Y. Crowell Harper & Row, New York, 1979.

# CHAPTER 26

## ACOUSTICS

Jonathan D. Blotter, Scott D. Sommerfeldt, and Kent L. Gee

Brigham Young University

Provo, Utah

<b>1 INTRODUCTION</b>	<b>886</b>	9.7 Single- and Double-Leaf Partitions	914
<b>2 SOUND POWER, SOUND INTENSITY, AND SOUND PRESSURE</b>	<b>886</b>	9.8 Enclosures	915
2.1 Sound Power	886	<b>10 ACTIVE NOISE CONTROL</b>	<b>916</b>
2.2 Sound Intensity	887	10.1 Control Architectures	917
2.3 Sound Pressure	888	10.2 Attenuation Limits	919
<b>3 DECIBEL AND OTHER SCALES</b>	<b>889</b>	10.3 Filtered-x Algorithm	919
<b>4 WEIGHTING FILTERS</b>	<b>891</b>	10.4 System Identification	920
<b>5 IMPEDANCE</b>	<b>893</b>	10.5 Control Applications	921
<b>6 THEORY OF SOUND</b>	<b>894</b>	<b>11 ARCHITECTURAL ACOUSTICS</b>	<b>922</b>
6.1 Constitutive Equations	895	<b>12 COMMUNITY AND ENVIRONMENTAL NOISE</b>	<b>922</b>
6.2 Wave Equation	896	12.1 Outdoor Sound Propagation	923
6.3 Absorptive Processes	898	12.2 Representations of Community Noise Data	926
<b>7 REFLECTION, TRANSMISSION, AND ABSORPTION</b>	<b>900</b>	12.3 Community Noise Criteria	929
7.1 Reflection/Transmission from a Single Interface	900	12.4 Community Response to Noise	930
7.2 Reflection/Transmission from a Solid Surface	902	<b>13 SOUND QUALITY ANALYSIS</b>	<b>930</b>
7.3 Reflection/Transmission at Discontinuities in Pipes	904	13.1 Mathematical Metrics Procedures	932
<b>8 HEARING LOSS</b>	<b>905</b>	13.2 Critical Band Rate	933
8.1 Hearing Protection	905	13.3 Loudness	934
8.2 Hearing Protection Devices	906	13.4 Sharpness	935
<b>9 PASSIVE NOISE CONTROL</b>	<b>906</b>	13.5 Fluctuation Strength	935
9.1 Source/Path/Receiver Considerations	907	13.6 Roughness	936
9.2 Definitions	908	13.7 Tonality	936
9.3 Impedance Considerations: Vibration Isolation Mounts	909	13.8 Sensory Pleasantness	937
9.4 Transmission Loss for Isolation Mounts	909	13.9 Limitations	937
9.5 Acoustic Filters	910	<b>14 NONLINEAR ACOUSTICS</b>	<b>937</b>
9.6 Lined Ducts	913	14.1 Theory	938
		14.2 Radiation Pressure and Streaming	940
		14.3 Applications of Nonlinear Acoustics	940

<b>15 THE HUMAN EAR AND HEARING</b>	<b>942</b>	<b>REFERENCES</b>	<b>949</b>
15.1 Psychoacoustic Effects	944	<b>SUGGESTIONS FOR FURTHER READING</b>	<b>951</b>
<b>16 MICROPHONES AND LOUDSPEAKERS</b>	<b>946</b>		

## 1 INTRODUCTION

Acoustics is the term used to describe the science of sound. It is derived from the Greek word *akoustos*, which means “hearing.” Acoustics is a very broad field of science that covers the generation, reduction, control, transmission, and reception aspects of sound. The earliest known studies of sound were made by Pythagoras during the sixth century bc. Pythagoras was the first to identify the musical consonances described as the octave, the fifth, and the fourth. He also initiated the theory of the inverse proportionality between pitch and the length of a vibrating string. In the Renaissance era of the late fifteenth century, the famous artist Leonardo da Vinci (1452–1519) also made many significant contributions to the theory of mechanics and wave motion. The works of Galileo Galilei (1564–1642) have had a larger impact on theoretical mechanics than any other before Newton. Galileo is recognized as having built on Leonardo’s speculative work and developed it into quantitative logic. Some likely consider Galileo as formalizing the science of sound. However, most generally recognized as the first significant contributor to the quantitative study of acoustics is Marin Mersenne (1588–1648). Mersenne performed and developed significant experimental techniques that laid foundations in many areas of acoustics. From the time of Mersenne to the twentieth century, many significant contributions to the area of acoustics were made by Newton, Euler, Green, Stokes, Helmholtz, Kirchhoff, Rayleigh, and Sabine. However, recent contributions during the twentieth century have also had a tremendous impact in the area of acoustics today. One of these developments was active noise control by Paul Leug in Germany in 1932. Other developments include computational sound field modeling, measurement methods, and measurement hardware, including computers, digital signal processors, and various transducers.<sup>1–3</sup>

## 2 SOUND POWER, SOUND INTENSITY, AND SOUND PRESSURE

In this section we discuss three fundamental measures of sound. These are sound power, sound intensity, and sound pressure. These three terms are discussed in most books on acoustics.<sup>1,3</sup>

### 2.1 Sound Power

Sound power is the term that describes the rate at which sound energy is radiated per unit time. The units of sound power are joules per second or watts. As an example of sound power, assume that there is a small spherical sound source. The sound power is a measure of the total amount of sound that the source can produce. Assuming that the source has constant sound power output and that unobstructed radiation occurs, the sound power output of the source is the same at any radius away from the source. A balloon analogy is often used to describe sound power. A balloon has the same amount of material surrounding the internal gas whether the balloon is partially or fully inflated. This is the same concept in that the sound power radiating from the source is a constant independent of distance from the source.

The range of sound powers encountered can be extremely large. For example, the sound power of a large rocket engine is on the order of 1,000,000 W while the sound power of a

soft whisper is approximately 0.000,000,001 W. Because of this large range in power values, a logarithmic scale known as the decibel scale is widely used in acoustic applications.

When sound power is expressed in terms of decibels, it is called a sound power level and is computed as

$$L_w = 10 \log \left( \frac{W}{W_{\text{ref}}} \right) \quad (1)$$

In Eq. (1),  $L_w$  represents the sound power level,  $W$  is the power of the sound energy source, and  $W_{\text{ref}}$  is the standard reference power, usually taken to be  $1 \times 10^{-12}$  W, or 1 pW. Table 1 provides an example of the range of sound power and sound power levels.

Sound power may be measured in various ways depending on the environment in which the measurements are to be made (free field, diffuse field, hemianechoic, etc.). The two basic techniques of measuring sound power consist of using an array of pressure microphones placed around the source or by using a sound intensity probe. Other comparative techniques also exist where measurements are compared to calibrated sources. The international standards that outline the processes for measuring sound power are International Organization for Standardization (ISO) 3741, 3742, 3744, 3745.<sup>4</sup>

## 2.2 Sound Intensity

Sound intensity is defined as the amount of sound power for a given area of the wave front. Relating this back to the balloon analogy, sound intensity would be a measure of the balloon wall thickness. For a given balloon there will be more balloon material due to the thickness of the balloon wall if the balloon is partially inflated as compared to fully inflated where a thinner balloon wall will occur. This is the same as sound intensity, in that the closer to the source, the higher the intensity for a given area. As previously mentioned, sound power and sound intensity are related by an area. For a spherical wave front, the relationship is expressed as

$$I = \frac{W}{4\pi r^2} \quad (2)$$

where  $I$  represents the sound intensity,  $W$  represents the sound power, and  $4\pi r^2$  is the surface area of the sphere where  $r$  is the radius of the sphere. From Eq. (2), it should be noted that the

**Table 1** Sound Power and Sound Power Level

Sound Source	Sound Power (W)	Sound Power Level, $L_w$ (dB re $1 \times 10^{-12}$ W)
Saturn rocket	25–40 million	195
Rocket engine	1,000,000	180
Turbojet engine	10,000	160
Siren	1,000	150
Heavy-truck engine/rock concert	100	140
75-Piece orchestra pipe organ	10	130
Piano/small aircraft, jackhammer	1	120
Excavator/trumpet	0.3	115
Chain saw/blaring radio	0.1	110
Helicopter	0.01	100
Auto on highway, loud speech/shouting	0.001	90
Normal speech	$1 \times 10^{-5}$	70
Refrigerator	$1 \times 10^{-7}$	50
Auditory threshold	$1 \times 10^{-12}$	0

decay of the sound intensity is directly proportional to the square of the radius of the sphere. This relationship is often referred to as the inverse-square law.

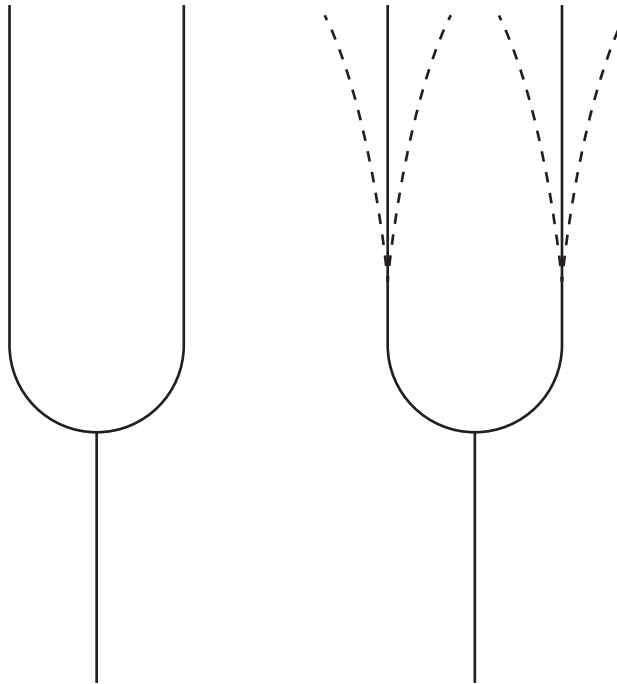
Sound intensity values are directly related to sound power values by an area term and hence also have a very wide range of values. It is therefore again common to express the sound intensity using a decibel scale and then refer to it as a sound intensity level. Sound intensity level is expressed as shown by Eq. (3), where  $L_I$  is the sound intensity level,  $I$  is the measured intensity at some distance from the source, and  $I_{\text{ref}}$  is the reference sound intensity usually taken as  $1 \times 10^{-12} \text{W/m}^2$ :

$$L_I = 10 \log \left( \frac{I}{I_{\text{ref}}} \right) \quad (3)$$

Sound intensity is the time-averaged product of the pressure and particle velocity. The pressure can simply be measured with a pressure microphone. However, the particle velocity is somewhat more difficult to measure. One common method of measurement is to place two similar microphones a known distance apart. By doing this, the pressure gradient can be measured. Then using Euler's equation the pressure gradient can be used to compute the particle velocity.

### 2.3 Sound Pressure

Sound pressure refers to the small deviations of pressure from the ambient value that are propagated by sound waves. To better understand this wave phenomenon, take, for example, a U-shaped tuning fork as shown in Fig. 1a. The tuning fork is a device used to create a tone at a specific frequency that can then be used to tune various musical instruments. The tone is



**Figure 1** (a) Static position and (b) vibrating motion showing tine motion.

**Table 2** Sound Pressure and Sound Pressure Level

Sound Source	Sound Pressure (Pa)	Sound Pressure Level, $L_p$ (dB re 20 $\mu$ Pa)
Krakatoa (at 160 km)	20,000	180
M1 Garand being fired	12,000	176
Jet engine (at 30 m)	630	150
Threshold of pain	100	130
Hearing damage (short-term exposure)	20	120
Jet (at 100 m)	6–200	110–140
Jack hammer (at 1 m)	2	100
Major road (at 10 m)	0.2–0.6	80–90
Passenger car (at 10 m)	0.02–0.2	60–80
Normal talking (at 1 m)	0.002–0.02	40–60
Very calm room	0.0002–0.0006	20–30

created by striking one of the tines with a hammer, causing the forks to freely vibrate, as shown in Fig. 1*b*. As the tine moves outward from equilibrium, the air adjacent to the outward moving tine is compressed and forced outward. As the air adjacent to the tine is pushed outward, the pressure at that point increases as does the density of the air molecules. As the tine returns back to equilibrium and displacement in the opposite direction, the air molecules spread back out, leaving a lower pressure and air molecule density as they return to their original position. The expansion and subsequent return to equilibrium are commonly called rarefaction.

As with sound power and sound intensity, sound pressures encountered also have a very wide range of values. For example, a typical jet engine is on the order of 630 Pa, while the threshold of hearing is approximately  $2 \times 10^{-5}$  Pa at 2 kHz. Therefore, as with sound power and sound intensity, sound pressure level  $L_p$  has been developed as

$$L_p = 20 \log \left( \frac{p}{p_{\text{ref}}} \right) \quad (4)$$

where  $p$  is the measured root-mean-square (rms) sound pressure and  $p_{\text{ref}}$  is the reference sound pressure usually taken as 20  $\mu$ Pa ( $2 \times 10^{-5}$  Pa), which is the threshold of hearing for an undamaged ear and also corresponds closely with the reference power of  $1 \times 10^{-12}$  W. Table 2 shows the relationship between sound pressure and sound pressure level.

### 3 DECIBEL AND OTHER SCALES

The decibel scale is a unitless logarithmic scale that is widely used in many fields of science, including acoustics, electronics, signals, and communication. The decibel scale is used to describe a ratio of values that among others may be sound power, sound intensity, sound pressure, and voltage. One main advantage of a logarithmic scale is that a very wide range of values can be reduced to a much smaller range that provides the user with a better feel for the particular values of interest.

In the field of acoustics, the decibel (dB), which is one-tenth of a bel, is almost exclusively used. Decibels are used over bels to simply increase the sensitivity of the values, similar to using inches instead of feet or centimeters instead of meters. The term bel (in honor of Alexander Graham Bell) refers to the basic logarithm of the ratio of two values. The definition of the base 10 logarithm is shown as

$$10^{\log p} = p \quad (5)$$

The log of  $p$  is the value to which 10 must be raised in order to obtain the value  $p$ . The decibel equation can then be expressed as

$$N(\text{dB}) = 10 \log \frac{A}{A_{\text{ref}}} \quad (6)$$

Two examples using the decibel scale are now provided to better illustrate the significance of the relationship.

### Example 1

An increase in sound power of a ratio of 2 : 1 results in what gain in decibels?

*Solution.*

$$N(\text{dB}) = 10 \log 2/1 = 10 \times (0.3010) = 3.01 \text{ dB}$$

Therefore, a doubling of the sound power results in an increase of 3 dB.

### Example 2

The noise level at a factory property line caused by 12 identical air compressors running simultaneously is 60 dB. If the maximum sound pressure level permitted at this location is 57 dB, how many compressors can run simultaneously?

*Solution.* For 1 compressor the  $L_p$  is  $L_{p1} = 20 \log(P_{\text{rms1}}/P_{\text{ref}})$ . For 12 compressors the  $L_p$  is  $P_{\text{rms12}}^2 = 12P_{\text{rms1}}^2$ ; therefore  $P_{\text{rms12}} = \sqrt{12}P_{\text{rms1}}$ :

$$L_{p12} = 20 \log \left( \frac{\sqrt{12}P_{\text{rms1}}}{P_{\text{ref}}} \right) = 20 \log \left( \frac{P_{\text{rms1}}}{P_{\text{ref}}} \right) + 20 \log \sqrt{12}$$

Therefore,

$$L_{p12} - L_{p1} = 20 \log \sqrt{12} = 10.79 \quad \text{and} \quad L_{p1} = L_{p12} - 10.79 = 60 - 10.79 = 49.21 \text{ dB}$$

Now for  $x$  compressors

$$L_{p,\text{max}} = 20 \log \sqrt{x} + L_{p1}$$

Therefore,

$$\log \sqrt{x} = \frac{L_{p,\text{max}} - L_{p1}}{20} = \frac{57 - 49.21}{20} = 0.3895$$

$$x = (10^{(0.3895)^2})^2 = 6.01$$

Therefore, six compressors, at most, can be operated in order to meet the 57-dB limit.

Besides the conventional decibel scale, there are other scales that have been developed that filter or weight the sound. This chapter continues by presenting and discussing several of these filtered scales.

In 1933, Fletcher and Munson<sup>5</sup> presented what is typically called the equal-loudness curves (see Fig. 2). This set of curves represents what is considered to be tones of equal loudness over the frequency range from 20 Hz to 15 kHz. The unit of measure for loudness is the phon. A phon is a unit of apparent loudness. The value for the unit of phon comes from the intensity level in decibels of a 1-kHz tone with the same perceived loudness. Therefore, a decibel value and a phon value are the same for a 1-kHz tone. These curves were determined experimentally. The experiment consisted of playing pure tones at a specific intensity level along with a 1-kHz reference signal. The intensity of the reference signal was increased until the two tones were perceived to be of the same loudness by the listener. Other work on the development of equal-loudness curves has been generated since Fletcher and Munson. The most recent standards can be found in ISO 226:2003.<sup>4</sup>

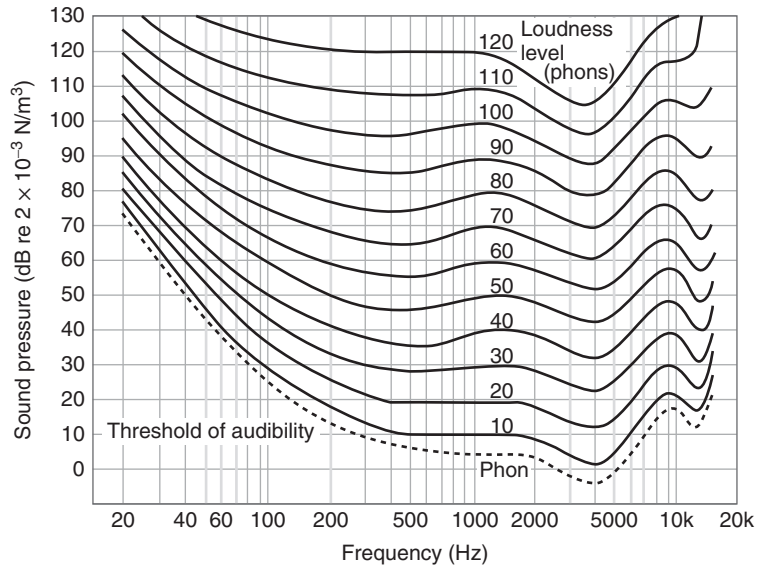


Figure 2 Equal-loudness curves.

#### 4 WEIGHTING FILTERS

The first weighting filter to be discussed is called A weighting and usually carries the associated symbol dBA or dB(A). This weighting was developed to apply the same filter to a tone that the human ear applies. As a result, this weighting is based on the 40-phon pure-tone equal-loudness curve. The 40-phon pure tone is a relatively quiet tone. It should be noted that the A-weighted curve roughly corresponds to the inverse of the 40-phon equal-loudness curve. The A-weighted curve tends to amplify signals in the region of 1–6 kHz. Sound outside this frequency range is reduced by the A weighting. The A-weighted filter is shown in Fig. 3.

The A-weighted scale is very popular and is used in many applications. These include environmental noise, noise control, construction noise, and community noise standards. The main violation of usage of the A-weighted scale is that it was developed for relatively quiet pure tones.

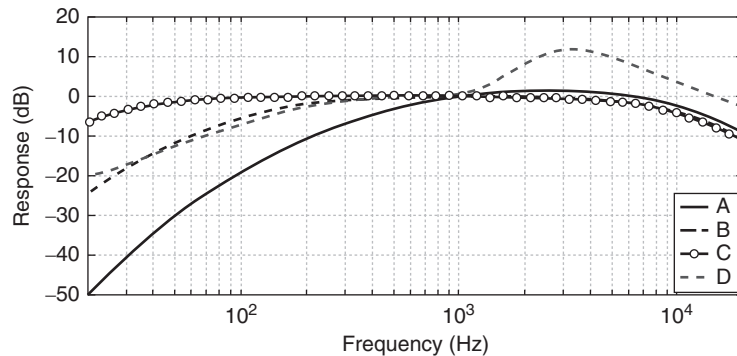


Figure 3 A, B, C, and D weighting filters.



The dB(B) and dB(C) scales were developed along similar methods as the dB(A) scale except that they were developed for tones with higher sound pressure levels. The dB(B) scale is seldom used but was developed for tones between the low sound pressure level of the A-weighted scale and the high sound pressure level of the C-weighted scale. The dB(C) scale is used for the highest sound pressure levels and, as shown in Fig. 3, is nearly linear over a large frequency range. The dB(D) scale is often used for aircraft noise. The equations for the weighting scales are shown in Eqs. (7), where  $s = j\omega, j = \sqrt{-1}$ , and  $\omega$  is the frequency:

$$\begin{aligned}
 G_A(s) &= \frac{k_A s^1}{(s + 129.4)^2 (s + 676.7)(s + 4636)(s + 76,655)^2} \\
 G_B(s) &= \frac{k_B s^3}{(s + 129.4)^2 (s + 995.9)(s + 76,655)^2} \\
 G_C(s) &= \frac{k_C s^2}{(s + 129.4)^2 (s + 76,655)^2} \\
 G_D(s) &= \frac{k_D s(s^2 + 6532s + 4.0975 \times 10^7)}{(s + 1776.3)(s + 7288.5)(s^2 - 21,514s + 3.8836 \times 10^8)} \tag{7}
 \end{aligned}$$

where  $k_A \approx 7.39705 \times 10^9, k_B \approx 5.99185 \times 10^9, k_C \approx 5.91797 \times 10^9$ , and  $k_D \approx 91104.32$ .

Another unit of measure for perceived loudness is the sone. The sone was developed experimentally to relate perceived loudness to phons. In the experiment, volunteers were asked to adjust the loudness of a tone until it was perceived to be twice as loud as the original tone. As a result, 1 sone is arbitrarily equal to 40 phons, and a doubling of the loudness (in sones) corresponds to a doubling of the perceived loudness. A graph relating sones and phons is shown in Fig. 4.

**Octave Bands in Audio Range**

In reference to the audio range, the term *octave* corresponds to a doubling or a halving of a frequency. For example, 200 Hz is one octave above 100 Hz and 4000 Hz is one octave above 2000 Hz. The 400 Hz would be considered to be two octaves above 100 Hz and so on.

In audio acoustics, the term *octave band* is commonly used to represent a range of frequencies where the highest frequency is twice the lowest frequency. These octave bands are commonly used to represent what is going on in the acoustic signal over a band or range of frequencies as compared to discrete frequencies. Most sound-level meters will output the data in some form of a standardized octave band.

Octave bands are typically defined by a center frequency  $f_C$ . The upper frequency  $f_U$  and the lower frequency  $f_L$  of the band are computed as

$$f_L = \frac{f_C}{\sqrt{2}} \quad f_U = \sqrt{2}f_C \quad \text{where} \quad f_C = \sqrt{f_L f_U} \tag{8}$$

Furthermore, the bandwidth for a given octave can be computed as

$$\text{Bandwidth} = f_U - f_L = f_C \left( \sqrt{2} - \frac{1}{\sqrt{2}} \right) \tag{9}$$

In the field of acoustics standard octave bands have been defined. The lower frequency, center frequency, and upper frequency for the standard acoustic octave bands are given in Table 3

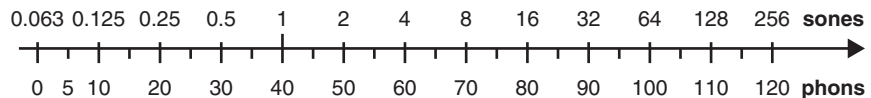


Figure 4 Relationship of sones and phons.

**Table 3** Octave-Band Lower, Center, and Upper Band Frequencies (Hz)

Lower Band Frequency, $f_L$	Center Band Frequency, $f_C$	Upper Band Frequency, $f_U$
22.4	31.5	45
45	63	90
90	125	180
180	250	355
355	500	710
710	1,000	1,400
1,400	2,000	2,800
2,800	4,000	5,600
5,600	8,000	11,200
11,200	16,000	22,400

In many applications, a higher resolution on the frequency axis is desired. In these cases, the octave band is split into smaller groups. Another very common scale is the one-third octave band, in which each of the octave bands is split into three smaller bands. The one-third-octave-band scale is commonly used for environmental, noise control, and building acoustics, among others. The lower, center, and upper frequencies for the one-third octave bands are given in Table 4 and calculated using the equations

$$f_L = \frac{f_C}{\sqrt[6]{2}} \quad f_U = \sqrt[6]{2}f_C \quad \text{where} \quad f_C = \sqrt{f_L f_U} \quad (10)$$

$$\text{Bandwidth} = f_C \left( \sqrt[6]{2} - \frac{1}{\sqrt[6]{2}} \right)$$

## 5 IMPEDANCE

Mathematical models for mechanical, electrical, fluid, and thermal systems can be developed essentially independent of the discipline based on concepts of system similarity. In each discipline, the variables that are used to express the differential equations can be classified as either effort, flow, or combinations of effort and flow variables.<sup>6</sup>

Effort variables describe the effort that is put on a component. Typical effort variables are force, voltage, pressure, and temperature. Flow variables are those that describe the rate of change, such as velocity, current, volume flow rate, and heat flow. Impedance of a component is defined as the ratio of the effort variable to the flow variable. For a mechanical system this is force divided by velocity.

In acoustic systems, the effort variable is pressure  $p$  and the flow variable is velocity. However, there are two velocities often considered in acoustics: volume velocity  $U$  and particle velocity  $u$ . With these two velocities there are two acoustic impedance terms. Acoustic impedance is defined as the acoustic pressure divided by the volume velocity as

$$Z = \frac{P}{U} \quad (11)$$

Specific acoustic impedance is defined as the acoustic pressure divided by the particle velocity as

$$z = \frac{p}{u} \quad (12)$$

Radiation impedance is a term often used to represent the coupling between acoustic waves and a driving source or driven load. The radiation impedance for a vibrating surface with area  $A$  is given by the equation

$$Z_r = zA \quad (13)$$

**Table 4** One-Third-Octave-Band Lower, Center, and Upper Band Frequencies (Hz)

Lower Band Frequency, $f_L$	Center Band Frequency, $f_C$	Upper Band Frequency, $f_U$
18.0	20	24.4
22.4	25	28.0
28.0	31.5 <sup>a</sup>	35.5
35.5	40	45
45	50	56
56	63 <sup>1</sup>	71
71	80	90
90	100	112
112	125 <sup>a</sup>	140
140	160	180
180	200	224
224	250 <sup>a</sup>	280
280	315	355
355	400	450
450	500 <sup>a</sup>	560
560	630	710
710	800	900
900	1,000 <sup>a</sup>	1,120
1,120	1,250	1,400
1,400	1,600	1,800
1,800	2,000 <sup>a</sup>	2,240
2,240	2,500	2,800
2,800	3,150	3,550
3,550	4,000 <sup>a</sup>	4,500
4,500	5,000	5,600
5,600	6,300	7,100
7,100	8,000 <sup>a</sup>	9,000
9,000	10,000	11,200
11,200	12,500	14,000
14,000	16,000 <sup>a</sup>	18,000
18,000	20,000	22,400

<sup>a</sup>Octave-band center frequencies.

This can also be computed as the ratio of the force  $f$  acting on the fluid and the particle velocity:

$$Z_r = \frac{f}{u} \quad (14)$$

The radiation impedance is part of the overall mechanical impedance of the system. The magnitude of the contribution of the radiation impedance to the overall mechanical impedance is generally small but is, of course, related to the magnitudes of the values in the impedance equations.

## 6 THEORY OF SOUND

In this section, some of the fundamental theoretical developments of acoustics in a fluid are summarized. For theoretical developments of acoustic propagation in solids, see Ref. 7. Of foremost importance in this section is a discussion of the acoustic wave equation and forms of solutions.

## 6.1 Constitutive Equations

Acoustic disturbances are ultimately an unsteady portion of the overall dynamics of the fluid. Consequently, the equations that describe the motion of a fluid—the equations of continuity, force, state, and so on—can be applied to describe acoustic pressure fluctuations. However, with the exception of Section 14 on nonlinear acoustics, we will consider the fluctuating pressure term in the overall description of the fluid to be “small.” In terms of the acoustic Mach number, which is a dimensionless quantity that describes the velocity of acoustic fluctuations,  $\mathbf{u}$ , relative to the speed of sound in the fluid,  $c_0$ , this assumption of “smallness” may be expressed as  $|\mathbf{u}|/c_0 \gg 1$ . This assumption applies to the vast majority of applications of acoustics and allows for considerable simplification of the constitutive equations of fluid mechanics to first-order accuracy.

The constitutive equations of the wave equation in fluid acoustics are used to relate the acoustic pressure  $p$ , the acoustic density  $\rho$ , and the acoustic “particle” velocity  $\mathbf{u}$ , which despite its name, describes the motion of a small volume or continuum of fluid. These acoustic variables describe the unsteady fluctuations in the fluid that are acoustic waves. On the other hand, variables that describe the ambient pressure or density will be denoted with the subscript 0. Note that both the mean velocity of the fluid and losses (e.g., thermoviscous) are considered to be zero in the equations that follow.

The first equation is the equation of continuity, which relates  $\rho$  to  $\mathbf{u}$  and connects the compression of the fluid with its motion. In its linearized form, the equation of continuity may be written as

$$\frac{\partial \rho}{\partial t} + \rho_0 \nabla \cdot \mathbf{u} = 0 \quad (15)$$

where the first term,  $\partial \rho / \partial t$ , describes the time rate of change of the acoustic density for a small volume fixed in space. For continuity of the fluid to hold,  $\partial \rho / \partial t$  must be equal to the net flux of fluid into the volume, approximated by  $-\rho_0 \nabla \cdot \mathbf{u}$ . (The minus sign is needed because the divergence operator describes flow of fluid away from the volume.)

The second equation relates  $\mathbf{u}$  to  $p$  and is an expression of Newton’s second law,  $\sum F = ma$ . For a fluid element that moves with the surrounding fluid, the linearized Euler equation (a lossless form of the Navier–Stokes equation) is written as

$$\rho_0 \frac{\partial \mathbf{u}}{\partial t} = -\nabla p \quad (16)$$

Note that because  $\mathbf{u}$  is a vector that describes the velocity of the fluid in three-dimensional space, Eq. (16) is a composite vector equation.

The third constitutive equation necessary in the development of a small-amplitude wave equation relates the two scalars  $p$  and  $\rho$ . If we neglect losses and treat the acoustic processes in air as perfectly adiabatic, the equation of state between  $p$  and  $\rho$  may be approximated to first order as

$$p = c_0^2 \rho \quad (17)$$

where

$$c_0^2 = \frac{\mathbf{B}}{\rho_0} \quad (18)$$

where  $\mathbf{B}$  is the adiabatic bulk modulus of the fluid. In air,  $\mathbf{B} = \gamma p_0$ , where  $\gamma$  is the ratio of specific heats ( $\gamma = 1.402$ ). By use of the ideal gas law, the sound speed in air may be expressed as a function of temperature as

$$c_0^2 = \gamma r T \quad (19)$$

where  $r$  is the specific gas constant (287 J/kg·K) and  $T$  is the temperature in kelvin. An alternative expression is to write the sound speed relative to some reference value, which is 331 m/s

at 0°C (273.15 K). Relative to 331 m/s,  $c_0$  is expressed as

$$c_0 = 331 \sqrt{\frac{T}{273.15}} \quad \text{m/s} \quad (20)$$

Equation (19) may be used to calculate sound speed in other gases given the appropriate values of  $\gamma$  and  $r$ , whereas in fluids that cannot be considered ideal gases, Eq. (18) can be used. For the sake of completeness, the speed of compressional waves in solids may be calculated as

$$c_0 = \sqrt{\frac{Y}{\rho}} \quad (21)$$

where  $Y$  is Young's modulus and, in this case,  $\rho$  is the density of the solid in kilograms per meters cubed. A list of sound speed values in different media is given in Table 5. A more complete listing may be found in the literature.<sup>7</sup>

## 6.2 Wave Equation

Although not repeated here, the constitutive equations may be manipulated to form a wave equation for any of the acoustic variables,  $p$ ,  $\rho$ , and  $\mathbf{u}$ . The acoustic wave equation for the pressure  $p$  may be expressed as

$$\nabla^2 p - \frac{1}{c_0^2} \frac{\partial^2 p}{\partial t^2} = 0 \quad (22)$$

If we assume a one-dimensional wave equation in the  $x$  direction, Eq. (22) may be divided up as

$$\left( \frac{\partial}{\partial x} - \frac{1}{c_0} \frac{\partial}{\partial t} \right) \left( \frac{\partial}{\partial x} + \frac{1}{c_0} \frac{\partial}{\partial t} \right) p = 0 \quad (23)$$

Equation (23) demonstrates that the wave equation may be viewed as right-going and left-going wave operators that act on  $p$ . In fact, the general solution to the one-dimensional wave equation for  $p$  is

$$p(x, t) = p_1 \left( t - \frac{x}{c_0} \right) + p_2 \left( t + \frac{x}{c_0} \right) \quad (24)$$

**Table 5** Speed of Sound in Various Media

Medium	Sound Speed (m/s)	
Gases (20°C and 1 atm)		
Air	343	
Helium	1007	
Oxygen (O <sub>2</sub> )	317	
Carbon dioxide	258	
<i>Liquids</i>		
Freshwater	1481	
Seawater	1500	
Glycerin	1980	
<i>Solids</i>		
	Bar	Bulk
Aluminum	5150	6300
Steel	5050	6100
Hard rubber	1450	2400
Glass (Pyrex)	5200	5600
Lead	1200	2050

where the function  $p_1$  is a wave that travels in the  $+x$  direction and  $p_2$  is a wave that travels in the  $-x$  direction. The forms of functions  $p_1$  and  $p_2$  depend on source, boundary, and initial conditions. Specific types of solutions to the acoustic wave equation are now discussed.

### Plane Waves

One possible solution to the wave equation is a monofrequency plane wave with angular frequency  $\omega$ . A plane wave's amplitude and phase are constant on any plane perpendicular to the direction of travel. The most common application of plane wave propagation is in ducts at low frequencies, where the acoustic wavelength is much greater than the cross-sectional dimensions of the duct. In addition, at large distances from an acoustic source, spherical waves look locally planar. Expressed in complex exponential form, the plane wave solution for the acoustic pressure in one dimension ( $x$ ) is

$$p(x, t) = \mathbf{A}e^{j(\omega t - kx)} + \mathbf{B}e^{j(\omega t + kx)} \quad (25)$$

where the boldface italic text denotes a complex quantity and  $k$  is the wavenumber, where  $k = \omega/c_0$ . Complex notation is frequently used for mathematical convenience in this section and throughout the remainder of this section. The actual scalar pressure is

$$p(x, t) = \mathbf{Re}\{p(x, t)\} \quad (26)$$

The above result may be extended for a plane wave of frequency  $\omega$  that is propagating in an arbitrary direction. If we consider just a single forward-propagating plane wave, the solution to the wave equation may be expressed as

$$p(\mathbf{r}, t) = \mathbf{A}e^{j(\omega t - \mathbf{k} \cdot \mathbf{r})} \quad (27)$$

where  $\mathbf{r}$  is the position vector from the origin and  $\mathbf{k}$ , the wavenumber propagation vector with magnitude  $k = \omega/c_0$ , is written as

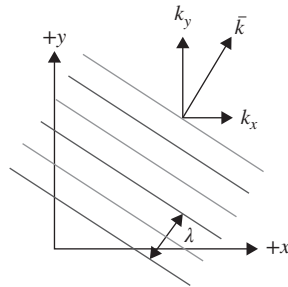
$$k = k_x \hat{x} + k_y \hat{y} + k_z \hat{z} \quad (28)$$

An example of a two-dimensional plane wave is shown in Fig. 5.

One final point regarding plane waves is the relationship between  $p$  and  $\mathbf{u}$ . Use of the linearized Euler equation for a wave traveling in the positive direction results in the expression

$$\frac{p}{|\mathbf{u}|} = \rho_0 c_0 \quad (29)$$

which has units of specific acoustic impedance. This quantity is referred to as the characteristic impedance of the medium and is approximately equal to 415 Pa · s/m in air.



**Figure 5** Representation of plane wave propagation perpendicular to  $z$  axis. The lines represent surfaces of constant phase.

### Spherical Waves

For sources of sound whose dimensions are much less than a wavelength or for distances much greater than the source dimensions, the acoustic radiation in free space is spherically diverging. For radial symmetry, the wave equation in spherical coordinates may be written as

$$\frac{\partial^2 p}{\partial r^2} + \frac{2}{r} \frac{\partial p}{\partial r} = \frac{1}{c_0^2} \frac{\partial^2 p}{\partial t^2} \quad (30)$$

A different form of Eq. (30) lends insight into the physical behavior of spherical waves. Rather than  $p$  as the dependent variable, rewriting Eq. (30) in terms of  $rp$  results in

$$\frac{\partial^2(rp)}{\partial r^2} = \frac{1}{c_0^2} \frac{\partial^2(rp)}{\partial t^2} \quad (31)$$

Comparison of Eq. (31) with the general wave equation (24) shows that the general solution to this wave equation for spherical waves can be written as

$$p(r, t) = \frac{1}{r} p_1 \left( t - \frac{r}{c_0} \right) + \frac{1}{r} p_2 \left( t + \frac{r}{c_0} \right) \quad (32)$$

The first term in Eq. (32) represents outgoing waves and the second term incoming waves. For diverging monofrequency waves of frequency  $\omega$ , the solution to Eq. (30) in complex form is

$$p(r, t) = \frac{A}{r} e^{j(\omega t - kr)} \quad (33)$$

From this expression for  $p$ , particle velocity, intensity, and sound power can all be calculated. However, of particular interest are the ratios of acoustic pressure between  $r_1$  and  $r_2$ . For spherical spreading between  $r_1$  and  $r_2$ ,

$$\frac{p(r_1)}{p(r_2)} = \frac{r_2}{r_1} e^{-jk(r_2 - r_1)} \quad (34)$$

For  $r_2 = 2 r_1$ ,

$$\left| \frac{p(r_2)}{p(r_1)} \right| = \frac{1}{2} \quad (35)$$

## 6.3 Absorptive Processes

Although losses were neglected in the theoretical development of the wave equation, they are essential to everyday acoustic analyses. Losses may be readily incorporated into the solution of a propagating wave by making the wavenumber  $k$  complex:

$$k = k - j\alpha \quad (36)$$

The variable  $\alpha$  is known as the absorption coefficient, with units of nepers per meter, and its value depends on both frequency and the propagation environment (the neper is a dimensionless unit). The solution for a traveling plane wave takes the form

$$p(\mathbf{r}, t) = A e^{-\alpha r} e^{j(\omega t - \mathbf{k} \cdot \mathbf{r})} \quad (37)$$

The term  $e^{-\alpha r}$  represents an exponential decay in amplitude as a function of distance. The absorption coefficient can also be directly considered with regards to its impact on sound pressure level. For plane wave propagation from the source ( $x = 0$ ) to some distance  $x$ ,

$$L_p(x) = L_p(0) - 8.686\alpha x \quad (38)$$

Two types of absorption are briefly considered, atmospheric absorption and boundary layer absorption in pipes. Note that the absorptive processes in the atmosphere and near pipe walls

give rise to not only absorption but dispersion as well. However, because dispersion does not affect amplitude at a given frequency, the phenomenon is not discussed further in this section. Instead the reader is referred to Refs. 8 and 9, which contain more in-depth discussions on the absorptive processes.

The absorption of sound by the atmosphere is dominated by thermoviscous (tv) losses and vibrational relaxation losses due to the diatomic molecules of oxygen ( $O_2$ ) and nitrogen ( $N_2$ ). The combined effects of these processes represent the total atmospheric absorption coefficient

$$\alpha = \alpha_{tv} + \alpha_{O_2} + \alpha_{N_2} \quad (39)$$

To calculate atmospheric absorption as given below, values of  $p_0$  in atmospheres, ambient temperature ( $T_0$ ) in kelvin, and relative humidity (RH) in percent are needed as inputs. Although other units are possible, they result in different expressions for  $\alpha$ . With ambient pressure, temperature, and relative humidity expressed in the appropriate units  $\alpha$  is calculated as

$$\alpha = p_0 F^2 \left\{ 1.84 \times 10^{-11} \left( \frac{T_0}{293.15} \right)^{1/2} + \left( \frac{T_0}{293.15} \right)^{-5/2} \right. \\ \left. \times \left[ 0.01275 \frac{e^{-2239.1/T_0}}{F_{r,O} + F^2/F_{r,O}} + 0.1068 \frac{e^{-3352/T_0}}{F_{r,N} + F^2/F_{r,N}} \left\{ 1.84 \times 10^{-11} \left( \frac{T_0}{293.15} \right)^{1/2} \right\} \right] \right\} \quad (40)$$

where

$$F = \frac{f}{p_0} \quad F_{r,O} = \frac{f_{r,O}}{p_0} \quad F_{r,N} = \frac{f_{r,N}}{p_0} \quad (41)$$

The normalized relaxation frequencies  $F_r$  for oxygen and nitrogen are, respectively,

$$F_{r,O} = 24 + 4.04 \times 10^4 h \frac{0.02 + h}{0.391 + h} \quad (42)$$

and

$$F_{r,N} = \left( \frac{293.15}{T_0} \right)^{1/2} \times \left( 9 + 280h \exp \left\{ -4.17 \left[ \left( \frac{293.15}{T_0} \right)^{1/3} - 1 \right] \right\} \right) \quad (43)$$

where  $h$  is the absolute humidity, or molar concentration of water vapor, in percent. Absolute humidity can be calculated from relative humidity as

$$h = RH \frac{p_{sat}}{p_0} \quad (44)$$

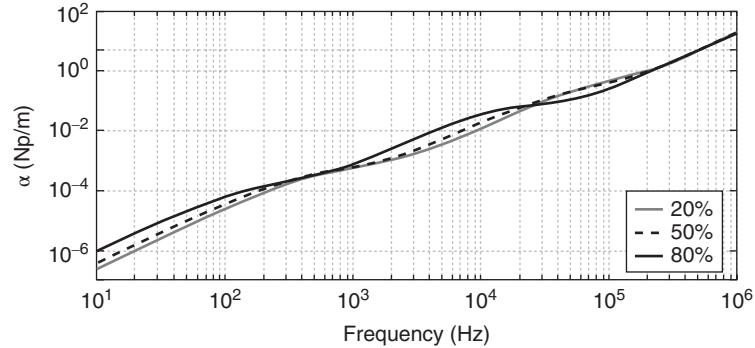
Finally, the saturation vapor pressure  $p_{sat}$  can be calculated from

$$\log_{10}(p_{sat}) = -6.8346 \left( \frac{273.16}{T_0} \right)^{1.261} + 4.6151 \quad (45)$$

In Fig. 6, curves of the absorption coefficient for 1 atm and 20°C (293.15 K) are displayed as a function of frequency for three values of relative humidity. The figure shows that variation in water vapor content in the atmosphere can significantly affect the absorption over the audio range (20 Hz–20 kHz). At low frequencies, the dominant absorption mechanism is due to nitrogen relaxation. Above a few hundred hertz, oxygen relaxation becomes the dominant process. It is not until high frequencies (50–100 kHz) that the diatomic molecules are considered frozen and thermoviscous processes dominate.

The second type of absorption is boundary layer absorption, which is relevant to propagation in pipes or ducts. The additional absorption near the walls of the duct is due to the viscous and thermal boundary layers. For a duct with a given hydraulic diameter ( $HD = 4S/C$ ,





**Figure 6** Atmospheric absorption coefficient as function of frequency for 1 atm, 20°C, and various values of relative humidity.

where  $S$  is the area and  $C$  is the perimeter of the cross section),  $\alpha$  for an air-filled pipe may be calculated as

$$\alpha = \frac{2}{HD} \sqrt{\frac{\pi f \mu}{\rho_0 c_0^2}} \left( 1 + \frac{\gamma - 1}{\sqrt{Pr}} \right) \quad (46)$$

where  $\mu$  is the shear viscosity coefficient,  $\gamma$  is the ratio of specific heats, and  $Pr$  is the Prandtl number. Unlike atmospheric absorption, which approaches an  $f^2$  dependence well above the relaxation frequencies, boundary layer absorption only increases as  $\sqrt{f}$ .

## 7 REFLECTION, TRANSMISSION, AND ABSORPTION

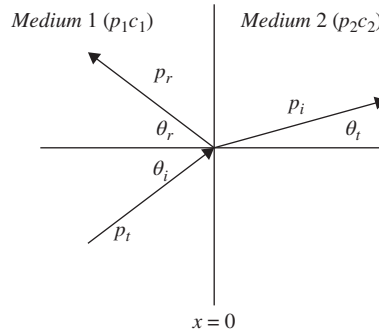
When a wave propagating in a medium encounters a change in the impedance presented to the wave, reflection and transmission of the wave occur. There are two general ways in which this could occur: (i) the medium could change, such as when a wave propagates from air into water, or (ii) the geometry could change even though the medium does not, such as when a wave propagates from a pipe into an expansion chamber.

The physical concepts that govern the reflection and transmission are not difficult to understand, although the algebra that results in analyzing the situation can quickly become very cumbersome. Thus, for all but the simplest cases, one would typically solve the resulting expressions with the aid of a computer.

There are several reflection and transmission coefficients of interest. The *pressure* reflection and transmission coefficients ( $\mathbf{R}$ ,  $\mathbf{T}$ ) provide the ratio of the reflected and transmitted pressure to the incident pressure. The *intensity* reflection and transmission coefficients ( $R_I$ ,  $T_I$ ) provide the ratio of the reflected and transmitted acoustic intensity to the incident acoustic intensity. Note that these two sets of coefficients are not generally the same, as they involve two different physical quantities. Finally, the *power* reflection and transmission coefficients ( $R_{\Pi}$ ,  $T_{\Pi}$ ) provide the ratio of the reflected and transmitted acoustic power to the incident acoustic power. These coefficients will, in general, be different than the intensity reflection and transmission coefficients, except in the case of normal incidence.

### 7.1 Reflection/Transmission from a Single Interface

Consider first the case of a plane wave impinging on an interface between two fluid media. One of the most common examples considered for this case is that of sound propagating from



**Figure 7** Reflection and transmission at interface of two fluid media. The vectors represent the propagation directions of the incident, reflected, and transmitted waves.

air into water (or vice versa), although it can be used for any two fluids in contact with each other. The general configuration can be seen in Fig. 7. There are two physical conditions that must be met. First, the pressure in fluid 1 at the interface will be the same as the pressure in fluid 2 at the interface. Second, the displacement normal to the interface (or equivalently, the particle velocity) in fluid 1 will be the same as the normal displacement (particle velocity) in fluid 2 at the boundary. If the interface lies in the  $y$ - $z$  plane, the waves in the two media can be expressed as

$$\begin{aligned} p_i &= p_i e^{j(\omega t - k_1 x \cos \theta_i - k_1 y \sin \theta_i)} \\ p_r &= p_r e^{j(\omega t + k_1 x \cos \theta_r - k_1 y \sin \theta_r)} \\ p_t &= p_t e^{j(\omega t - k_2 x \cos \theta_t - k_2 y \sin \theta_t)} \end{aligned} \quad (47)$$

where,  $\theta_i$  is the angle of incidence of the wave,  $\theta_r$  is the angle of reflection, and  $\theta_t$  is the angle of transmission. The wavenumber  $k$  is specific to the medium of interest and will differ for the two media since the phase speed  $c$  differs in the two media. Analysis of the conditions at the boundary leads to the following important result:

$$\theta_i = \theta_r \quad (48)$$

This result is known as the law of reflection and simply indicates that the angle of reflection must equal the angle of incidence. This is the same result as for light reflecting from a plane mirror.

Equation (49) is known as Snell's law and governs the refraction of sound waves as they propagate from one medium into another. Note that the refraction depends on the speed of sound in the two media. This is also manifest in the atmosphere when there is a temperature gradient in the air. In this case, there is a continuous rather than a discrete change in the sound speed, and as a result the sound waves bend either upward or downward as the wave propagates. This phenomenon is responsible for being able to clearly hear a cricket that is a long distance away on a cool evening, for example:

$$\frac{\sin \theta_i}{c_1} = \frac{\sin \theta_t}{c_2} \quad (49)$$

Equations (50) are the pressure reflection and transmission coefficients. In these expressions,  $\mathbf{Z}_n$  refers to the normal specific acoustic impedance of either medium 1 or medium 2. For a fluid, this is given by  $\mathbf{Z}_n = \rho c / \cos \theta$ , where the angle  $\theta$  is the angle of incidence in medium 1 and the transmitted angle in medium 2 and the  $\rho c$  of the appropriate medium is used. For normal incidence,  $\cos \theta = 1$ . It is also of note that  $\mathbf{T} = 1 + \mathbf{R}$  for the pressure coefficients, but

for the power coefficients (and intensity for normal incidence),  $R_{\text{II}} + T_{\text{II}} = 1$  (conservation of energy). Equations are the intensity and power reflection and transmission coefficients:

$$\mathbf{R} = \frac{\mathbf{Z}_{n2} - \mathbf{Z}_{n1}}{\mathbf{Z}_{n2} + \mathbf{Z}_{n1}} \quad \mathbf{T} = 1 + \mathbf{R} = \frac{2\mathbf{Z}_{n2}}{\mathbf{Z}_{n1} + \mathbf{Z}_{n2}} \quad (50)$$

$$R_I = R_{\text{II}} = \left( \frac{\mathbf{Z}_{n2} - \mathbf{Z}_{n1}}{\mathbf{Z}_{n2} + \mathbf{Z}_{n1}} \right)^2$$

$$T_I = \frac{\rho_1 c_1}{\rho_2 c_2} \left( \frac{2\mathbf{Z}_{n2}}{\mathbf{Z}_{n2} + \mathbf{Z}_{n1}} \right)^2$$

$$T_{\text{II}} = \frac{4\mathbf{Z}_{n1}\mathbf{Z}_{n2}}{(\mathbf{Z}_{n2} + \mathbf{Z}_{n1})^2} \quad (51)$$

An analysis of these results yields several important special cases:

1. **Angle of Intromission.** This occurs when  $\mathbf{R}$  in Eq. (50) equals zero and corresponds to complete transmission through the interface. Although the material properties of density and speed of sound change, the normal specific impedance does not so that the wave does not “see” any discontinuity.
2. **Grazing Incidence.** In this case,  $\theta_i$  goes to  $90^\circ$  and  $\mathbf{Z}_{n1}$  goes toward infinity, resulting in a pressure reflection coefficient of  $\mathbf{R} = -1$ . Thus, the boundary between the two fluids acts as a pressure release boundary.
3. **Critical Angle for  $c_1 < c_2$ .** If  $c_1 < c_2$ , there is an angle of incidence  $\theta_i$  where  $\sin \theta_i = 1$  [using Eq. (49)]. This gives  $\theta_i = 90^\circ$ . For angles of incidence greater than this,  $\theta_i$  must become complex to satisfy the mathematical condition. Physically, this means that the transmitted waves become “evanescent,” meaning that the waves decay exponentially in the  $x$  direction, propagate in the  $y$  direction, and cannot effectively penetrate into the second medium.

## 7.2 Reflection/Transmission from a Solid Surface

In the case of a wave in a fluid impinging upon a solid surface, the nature of the reflection/transmission phenomena depends upon the properties of the solid. If the solid has properties consistent with a bulk isotropic solid (no significant elastic response), the transmission of the wave into the solid will obey the equations given above, and the analysis can proceed as if the solid behaved as a fluid. If the solid behaves as a *locally reacting* material, the analysis must be modified slightly. One example of such a material would be an anisotropic solid, where waves propagate much faster in a direction perpendicular to the solid surface than they do in a direction parallel to the surface. Examples of such materials include many sound absorption materials such as acoustic tile, perforated panels, and other materials with a honeycomb structure. In these cases, the expressions given above can be used if one lets the transmission angle  $\theta_t$  go to zero, that is,  $\mathbf{Z}_{n2} = \rho_2 c_2$ .

### *Reflection/Transmission through a Fluid Layer*

One can often encounter situations where sound waves propagate through one or more fluid layers. These fluid layers may be small or large relative to an acoustic wavelength. The expressions will be developed here for a single layer with normal incidence. The methods can be extended in a straightforward manner to multiple layers and/or oblique incidence, but the algebra is such that use of a computer would be desirable. Use of these techniques can allow one to design a single or multilayer to have desired reflection/transmission characteristics. It also can be used for the analysis needed for noise control problems such as transmission through walls and other barriers.

The general configuration for understanding transmission through a layer can be seen in Fig. 8. With normal incidence, the acoustic waves involved can be represented as

$$\begin{aligned} p_i &= P_i e^{j(\omega t - k_1 x)} \\ p_r &= P_r e^{j(\omega t + k_1 x)} \\ p_{2r} &= P_{2r} e^{j(\omega t - k_2 x)} \\ p_{2l} &= P_{2l} e^{j(\omega t + k_2 x)} \\ p_t &= P_t e^{j(\omega t - k_3 x)} \end{aligned} \quad (52)$$

The new terms in these equations represent the right- and left-going waves in the fluid layer. Again using continuity of acoustic pressure and acoustic particle velocity at the two interfaces ( $x = 0$  and  $x = L$ ) leads to the following result for the pressure reflection coefficient:

$$\mathbf{R} = \frac{[1 - \rho_1 c_1 / (\rho_3 c_3)] \cos(k_2 L) + j[\rho_2 c_2 / (\rho_3 c_3) - \rho_1 c_1 / (\rho_2 c_2)] \sin(k_2 L)}{[1 + \rho_1 c_1 / (\rho_3 c_3)] \cos(k_2 L) + j[\rho_2 c_2 / (\rho_3 c_3) + \rho_1 c_1 / (\rho_2 c_2)] \sin(k_2 L)} \quad (53)$$

For transmission through the layer, the intensity transmission coefficient is given by

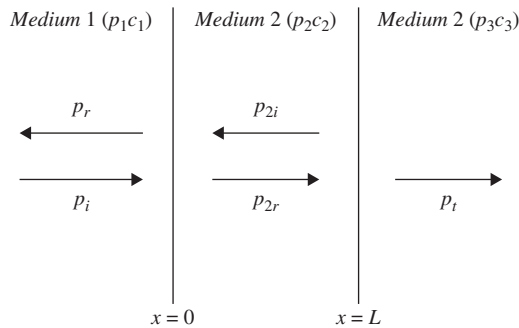
$$T_I = \frac{4}{2 + [\rho_3 c_3 / (\rho_1 c_1) + \rho_1 c_1 / (\rho_3 c_3)] \cos^2(k_2 L) + [(\rho_2 c_2)^2 / (\rho_1 c_1 \rho_3 c_3) + \rho_1 c_1 \rho_3 c_3 / (\rho_2 c_2)^2] \sin^2(k_2 L)} \quad (54)$$

It is of note that this expression is symmetric, implying that the same energy propagates through the layer regardless of the direction of incidence. Many specific cases could be analyzed. However, one case that is often of practical interest is when fluid 1 is the same as fluid 3, such as transmission through a wall with air on both sides. In this case,

$$T_I = \frac{1}{1 + \left(\frac{1}{4}\right) [\rho_2 c_2 / (\rho_1 c_1) - \rho_1 c_1 / (\rho_2 c_2)]^2 \sin^2(k_2 L)} \quad (55)$$

From this expression, it can be seen that for low frequencies and/or thin walls ( $k_2 L \gg 1$ ) there will be nearly perfect transmission through the layer. There will also be perfect transmission at discrete frequencies where  $\sin(k_2 L) = 0$ . Also, if the specific acoustic impedance of the layer ( $\rho_2 c_2$ ) is large (as is the case with most walls, for example) and  $k_2 L \gg 1$ , the expression in Eq. (55) reduces to the well-known mass law, expressed as

$$T_I = \left( \frac{2\rho_1 c_1}{\omega \rho_2 L} \right)^2 \quad (56)$$



**Figure 8** Reflection and transmission through a fluid layer. The vectors represent the propagation directions of the incident, reflected, and transmitted waves in the three fluids.

Thus, at low frequencies, one must increase the mass per unit area of the intermediate layer in order to reduce transmission for this case.

### 7.3 Reflection/Transmission at Discontinuities in Pipes

Another important class of problems involves the reflection and transmission that occurs when waves propagating in pipes or vents encounter a geometric discontinuity, such as a branch in the pipe or an expansion chamber or constriction, as shown in Fig. 9. For this analysis, continuity of pressure still holds at the discontinuity. However, instead of continuity of particle velocity, there is now continuity of volume velocity, given as the product of the particle velocity and the cross-sectional area ( $\mathbf{U} = \mathbf{u}S$ ). For this case, the pressure reflection coefficient is given by

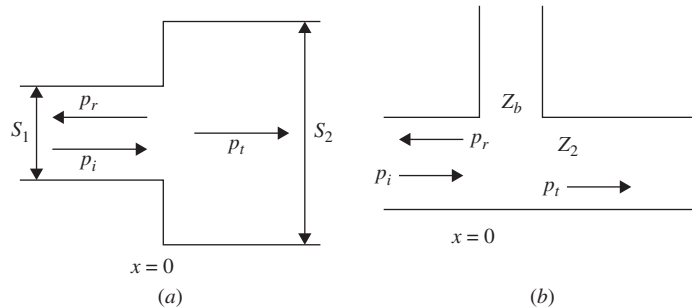
$$\mathbf{R} = \frac{\mathbf{Z}_0 - \rho c/S_1}{\mathbf{Z}_0 + \rho c/S_1} \tag{57}$$

where  $\mathbf{Z}_0$  is the acoustic impedance at  $x = 0$  and  $S_1$  is the cross-sectional area of the pipe for  $x > 0$ . The power reflection and transmission coefficients are given by  $R_{\Pi} = |\mathbf{R}|^2$  and  $T_{\Pi} = 1 - R_{\Pi}$ . For the case of a single pipe with a different cross-sectional area, for  $x > 0$ ,  $\mathbf{Z}_0 = \rho c/S_2$ . For branches in the pipe or for more complex impedances such as expansion chambers and constrictions, the measured or calculated acoustic impedance at  $x = 0$  should be used.

#### Side Branch

A special case of practical interest is where a side branch exists at  $x = 0$ . This could be a branching of the pipe or it could be a noise reduction device such as a Helmholtz resonator (see Section 9). Let the acoustic impedance of the side branch be given by  $\mathbf{Z}_b = R_b + jX_b$  and the impedance of the continuing pipe be  $\rho c/S_1$ . Using these values leads to the power reflection coefficient, the power transmission coefficient for waves propagating further down the pipe, and the power transmission coefficient for waves propagating into the side branch:

$$\begin{aligned} R_{\Pi} &= \frac{(\rho c/2S_1)^2}{(\rho c/2S_1 + R_b)^2 + X_b^2} \\ T_{\Pi} &= \frac{R_b^2 + X_b^2}{(\rho c/2S_1 + R_b)^2 + X_b^2} \\ T_{\Pi b} &= \frac{(\rho c/2S_1)R_b}{(\rho c/2S_1 + R_b)^2 + X_b^2} \end{aligned} \tag{58}$$



**Figure 9** Reflection and transmission from geometric discontinuities: (a) pipe expansion and (b) side branch with impedance  $Z_b$ .

## 8 HEARING LOSS

### 8.1 Hearing Protection

Because excess noise can be damaging to the human ear, precautions must be taken to protect one's hearing. Sensorineural hearing loss, or permanent damage to the inner ear, can occur through sudden trauma, for example, caused by an explosion at close range. It can also occur if chemicals that are damaging to the cilia (called ototoxic chemicals) are not handled properly. However, the most common cause of sensorineural hearing loss is prolonged exposure to significant noise levels. To help workers safeguard their hearing, the Occupational Safety and Health Administration (OSHA) act (see <http://www.osha.gov/dts/osta/otm/noise/standards.html>) sets forth permissible exposure limits in the workplace. Table 6 summarizes daily exposure limits for various A-weighted sound levels. Note that if noise exposure occurs at various levels throughout the day, in order to be under the cumulative noise exposure limit, the condition of  $\sum t_i/T_i \leq 1$ , where  $t_i$  is the exposure time at the  $i$ th level and  $T_i$  is the daily limit for that level that must be met. However, because a typical workday may consist of many different sound levels for as many different exposure periods, a noise dosimeter, which consists of a microphone and a sound level logger, can be worn by workers to track total daily noise exposure. Other noise and vibration exposure criteria are summarized by von Gierke and Ward.<sup>10</sup>

There are underlying assumptions regarding the OSHA act that should be made clear. First, the act is only intended to protect hearing for the purposes of understanding speech. Hearing loss above 4 kHz is likely to occur and is deemed acceptable. Second, an 8-h workday and a 5-day workweek are assumed. It is further assumed that leisure time is not spent in high-noise-level activities that could be damaging to the ear. Finally, and perhaps most importantly, the OSHA criteria are designed to protect only 85% of the population exposed at the limits. The remaining, more damage-prone 15% are to be financially compensated for the hearing loss suffered as part of their jobs.

The risk of hearing impairment can be summarized another way, as a function of both frequency and level. Shown in Fig. 10 are different zones that represent different amounts of potential for damage to the ear. In zone I, sounds are inaudible. The levels in zone II are everyday audible sounds that present no risk. In zone III, there is a qualified risk, especially for prolonged exposure periods, and in zone IV, there is a high risk of hearing damage. The division between zones II and III roughly follows the equal-loudness contours, meaning the ear is most susceptible to damage at those frequencies where it is most sensitive.

**Table 6** Daily Noise Exposure Limits ( $L_{pA}$ ) in dBA

Hours	dBA
8	90
6	92
4	95
3	97
2	100
1.5	102
1	105
0.5	110
< 0.25	115

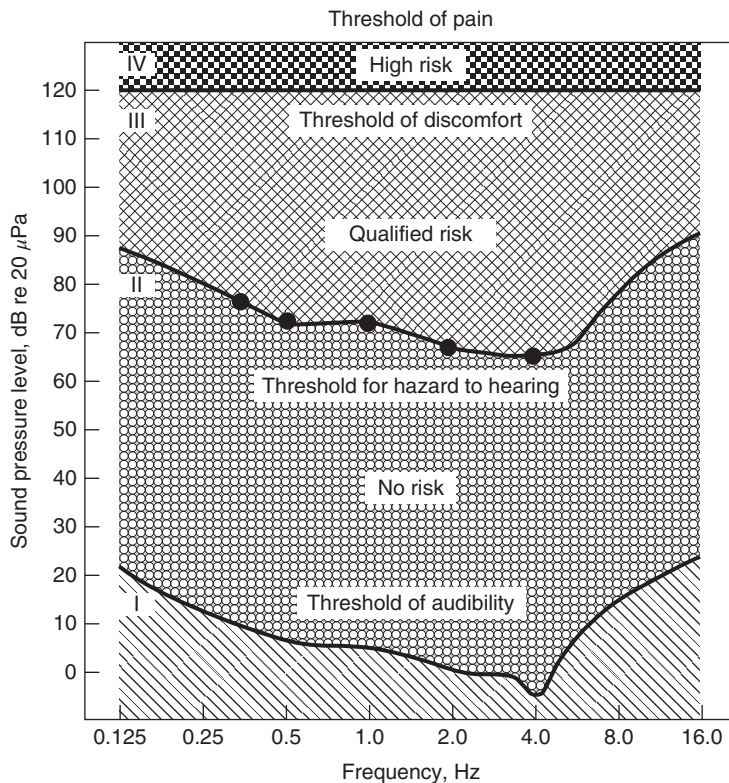


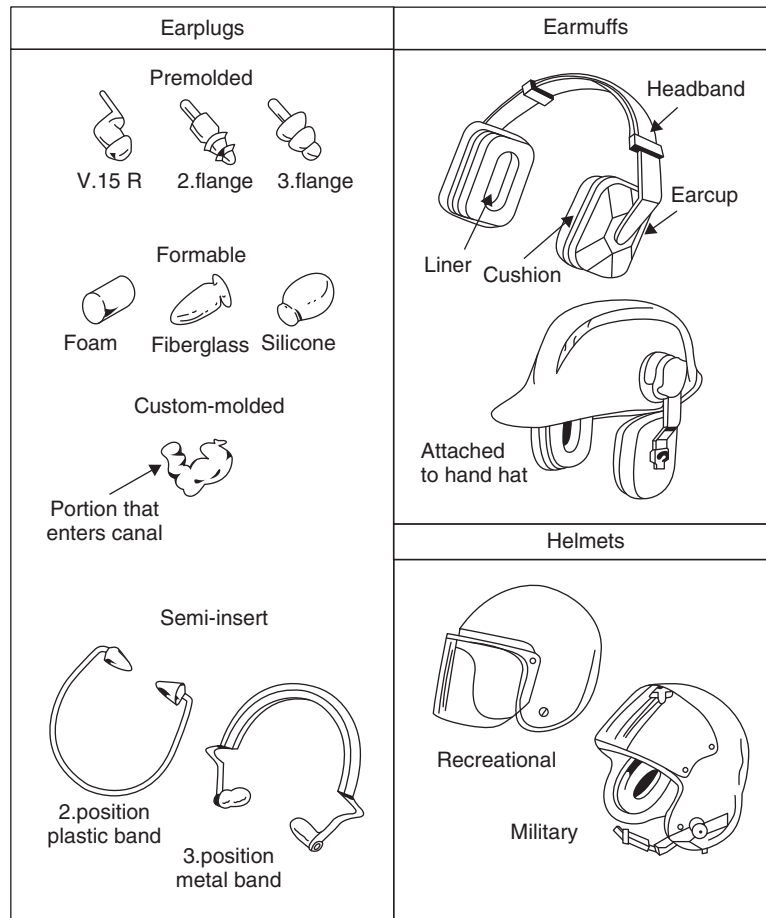
Figure 10 Graphical representation of hearing damage risk as function of frequency and level.<sup>11</sup>

## 8.2 Hearing Protection Devices

To preserve hearing, in addition to limiting exposure time, hearing protectors can be worn to reduce the noise levels to which the ear is exposed. Figures 11 and 12 summarize many classes of hearing protectors and ranges for attenuation provided by each type as a function of frequency. In general, the effectiveness of hearing protectors increases as a function of frequency, but to achieve sufficient attenuation, the user should take care to wear them properly. For simple formable earplugs, the attenuation can be quite high, but care must be taken to insert them sufficiently deep into the ear canal. For ear muffs to provide the proper attenuation, the wearer needs to ensure that the cushioned cups that enclose the pinnae (outer ears) fit snugly enough that an airtight seal is formed.

## 9 PASSIVE NOISE CONTROL

There are numerous situations where it is desirable to reduce unwanted sound, or noise. There are many approaches for accomplishing this, with some approaches being more appropriate for a given situation than others. This section will outline some general concepts associated with the use of passive noise control for reducing unwanted noise and the next section will outline concepts associated with active noise control. Much more information regarding these control methods can be found using the references at the end of the chapter (see particularly Refs. 13 and 14). The distinguishing feature between these two approaches is that passive noise



**Figure 11** Various types of hearing protectors.<sup>12</sup>

control relies on the inherent acoustic properties of the noise control material or device being used to reduce the unwanted noise, while active noise control involves the active generation of additional sound or vibration to interact with the existing noise or vibration in a manner that attenuates the field.

## 9.1 Source/Path/Receiver Considerations

For any given noise control application, one should consider that three components exist: (a) there is an acoustic source that is responsible for generating the noise, (b) there is an acoustic path that the sound energy propagates through, and (c) there is a receiver (often the human ear) that receives the acoustic energy. Where possible, this also gives the hierarchy of how to most effectively attenuate unwanted noise. The most effective solution is to modify the source characteristics so that less acoustic energy is generated. If that is not possible, the next most effective approach would be to modify the acoustic path. This can be done, for example, by using walls, barriers, absorptive materials, acoustic mufflers, and so forth. The final possibility is to modify the receiver. There is little possibility for doing much in this regard when the receiver is the












Type of protection	One-third-octave-band center frequencies, Hz						
	125	250	500	1000	2000	4000	8000
 Earplugs (premolded, user formable)	10–30	10–30	15–35	20–35	20–40	30–45	25–45
 Foam earplugs (attenuation varies with depth of insertion)	20–35	20–35	25–40	25–40	30–40	40–45	35–45
 Earplugs (custom-molded)	5–20	5–20	10–25	10–25	20–30	25–40	25–40
 Semi-insert earplugs (also called semiaural devices or canal caps)	10–25	10–25	10–30	10–30	20–35	25–40	25–40
 Earmuffs (with or without communications components)	5–20	10–25	15–30	25–40	30–40	30–40	25–40
 Earplugs and earmuffs (in combination)	20–40	25–45	25–50	30–50	35–45	40–50	40–50
 Active noise reduction headsets	15–25	15–30	20–45	Identical to earmuffs above 1000 Hz			
 Military helmets	0–15	5–15	15–25	15–30	25–40	30–50	20–50
 Motorcycle helmets	0–5	0–5	0–10	0–15	5–20	10–30	15–35

Figure 12 Expected attenuation (dB) for various types of hearing protectors.<sup>12</sup>

human ear (except that the ear has a protective mechanism that reduces the sensitivity of the ear when exposed to loud sounds; however, this mechanism has a finite response time, and one should never rely on this ear protection as a means of making noise exposure acceptable). (Depending on one's point of view, hearing protectors such as earmuffs could be viewed as part of the receiver or part of the acoustic path.) If the receiver is not the human ear, there may be the possibility of modifying its response characteristics. Most typical noise control approaches are based on the assumption that the source has been optimized and the receiver characteristics are fixed. Thus, the focus then needs to be on modifying the acoustic path.

## 9.2 Definitions

A number of terms are commonly used in the context of noise control, and an understanding of their meaning is beneficial:

**Transmission Coefficient ( $\tau$ ):** The fraction of incident energy that is transmitted through a noise control element.

**Transmission Loss (TL):** Expresses the transmission coefficient on a logarithmic scale and is obtained as  $TL = -10 \log_{10} \tau$  (dB).

**Insertion Loss (IL):** The decrease in sound power level measured at a receiver location after a noise control element is inserted into the acoustic transmission path.

**Absorption Coefficient ( $\alpha$ ):** The fraction of energy that is randomly incident on a given material that is absorbed.

**Noise Reduction Coefficient (NRC):** Given by the arithmetic mean of the sound absorption coefficients for a material at 250, 500, 1000, and 2000 Hz and used as a single-number rating of the absorption characteristics of the material.

### 9.3 Impedance Considerations: Vibration Isolation Mounts

Many noise control situations involve a source that converts mechanical vibration energy into acoustic energy. Such examples could be a vibrating motor or generator that transmits energy to a support structure which then radiates acoustic energy or a vibrating wall or casing, which in turn radiates acoustic energy. In general, there are three properties of the source that can be modified to attenuate the noise: mass, stiffness, and damping. Modifying each of these properties will be effective under certain conditions but completely ineffective under other conditions. This can best be seen by considering a vibration isolation mount, such as might be used for mounting a motor or generator. The general configuration is shown in Fig. 13. The mechanical impedance of this mount is given by

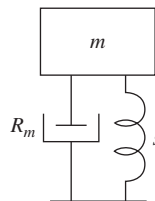
$$\mathbf{Z}_m = R_m + j \left( \omega m - \frac{s}{\omega} \right) \quad (59)$$

Looking at this expression in various frequency regions indicates how to most effectively modify the vibration response. At low frequencies, the stiffness term dominates, and the impedance is given as  $\mathbf{Z}_m \approx -j s/\omega$ . This is referred to as the stiffness-controlled region, and one should alter the stiffness of the mount to most effectively modify the response of the structure. Around the resonance frequency of the mount, the impedance is given as  $\mathbf{Z}_m \approx R_m$ . This is referred to as the damping-controlled region, and increased damping will be most effective in this frequency region. At higher frequencies above the resonance frequency, the impedance is given by  $\mathbf{Z}_m \approx j\omega m$ . This is referred to as the mass-controlled region, and one should alter the mass to most effectively modify the response of the structure.

Although this was developed for a vibration isolation mount, the same concepts hold for all vibrating sources—at any given frequency the system response will be dominated by the stiffness, damping, or mass properties of the structure. An investigation of the phase of the impedance can reveal which property is dominant. The stiffness-controlled region exhibits an impedance phase near  $-90^\circ$ , the damping-controlled region has a phase near  $0^\circ$ , and the mass-controlled region has a phase near  $90^\circ$ .

### 9.4 Transmission Loss for Isolation Mounts

Isolation mounts are normally designed for operation above the resonance frequency of the mount. For the single-stage isolation mount shown in Fig. 13, the resonance frequency is



**Figure 13** Single-stage vibration isolation mount showing mass  $m$  to be isolated, spring element with stiffness  $s$ , and mechanical damping  $R_m$ .

given by

$$f_r = \frac{1}{2\pi} \sqrt{\frac{s}{m}} \quad (60)$$

The transmission loss for the mount is given by

$$\text{TL} = -10 \log_{10} \left[ \frac{1 + \left[ 2 \left( \frac{R}{4\pi m f_r} \right) \left( \frac{f}{f_r} \right) \right]^2}{\left[ 1 - \left( \frac{f}{f_r} \right)^2 \right]^2 + \left[ 2 \left( \frac{R}{4\pi m f_r} \right) \left( \frac{f}{f_r} \right) \right]^2} \right] \quad (61)$$

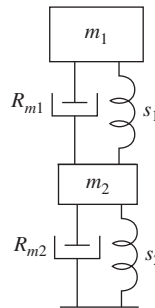
In this expression, the quantity  $4\pi m f_r$  is commonly called “critical damping” and represents the damping that results in the fastest decay time for a disturbance with no oscillation. It can be seen that at frequencies above the resonance frequency the transmission loss increases by 12 dB/octave (doubling of frequency). If additional isolation is required, a two-stage isolation mount can be implemented, as shown in Fig. 14. For this type of mount, the transmission loss increases by 24 dB/octave above the resonance frequencies of the mount. The tradeoff is that an additional resonance frequency is introduced at lower frequencies, so the isolation performance is degraded at lower frequencies. However, if operation will always be at frequencies above the resonance frequencies, this type of mount design can be desirable when greater isolation is required.

## 9.5 Acoustic Filters

Acoustic filters can be designed effectively when the wavelength at the frequencies of interest is significantly larger than the dimensions of the acoustic elements used to construct the acoustic filters. It can be shown that a tube whose length is small relative to a wavelength behaves as a mass, and a cavity (enclosed volume of fluid) behaves as a spring. These, along with damping materials, allow one to develop low-pass, high-pass, and bandstop filters in much the same way as one designs *LRC* electrical circuits. These three types of filters are reviewed briefly.

### *Bandstop Filter*

The design of a bandstop filter is typically dependent on the use of a Helmholtz resonator. A Helmholtz resonator consists of a tube connected to a cavity, typically with some damping included. A common example we are familiar with is a soda bottle, where the neck of the



**Figure 14** Two-stage vibration isolation mount showing mass  $m_1$  to be isolated, spring elements with stiffness  $s_1$  and  $s_2$ , mechanical damping  $R_{m1}$  and  $R_{m2}$ , and intermediate mass (raft)  $m_2$ .

bottle behaves as a tube and the portion below the neck behaves as the cavity. A Helmholtz resonator has a resonance frequency associated with it, and when used as a filter, it is capable of attenuating that frequency. The use of such a filter is shown in Fig. 15. The reactance of the side branch (Helmholtz resonator) is given by

$$X_b = \rho_0 \left( \frac{\omega L_{\text{eff}}}{S_b} - \frac{c^2}{\omega V} \right) \quad (62)$$

where  $L_{\text{eff}}$  is the effective length of the tube (including end corrections),  $S_b$  is the cross-sectional area of the tube, and  $V$  is the volume of the cavity. The effective length is given by

$$L_{\text{eff}} = \begin{cases} L + 1.7a & \text{(outer end flanged)} \\ L + 1.4a & \text{(outer end unflanged)} \end{cases} \quad (63)$$

where  $a$  is the radius of the tube. This configuration will give a stopband centered at the frequency

$$\omega_{\text{sb}} = c \sqrt{\frac{S_b}{L_{\text{eff}} V}} \quad (64)$$

and the power transmission coefficient for this filter is given by

$$T_{\Pi} = \frac{1}{1 + [(c/2S)/(\omega L_{\text{eff}}/S_b - c^2/\omega V)]^2} \quad (65)$$

where  $S$  is the cross-sectional area of the main duct. Figure 16 shows the characteristics of the power transmission coefficient for a typical bandstop filter.

### Low-Pass Filter

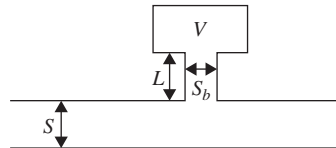
An acoustic low-pass filter can be constructed using an enlarged section of pipe or a constriction in the pipe. An enlarged section of pipe is used, for example, in the basic design of mufflers and will be considered here, as shown in Fig. 17. The enlarged section behaves acoustically as a cavity, and the acoustic impedance of the cavity is given by

$$Z_c \approx \frac{-j\rho_0 c^2}{\omega(S_1 - S)L} \quad (66)$$

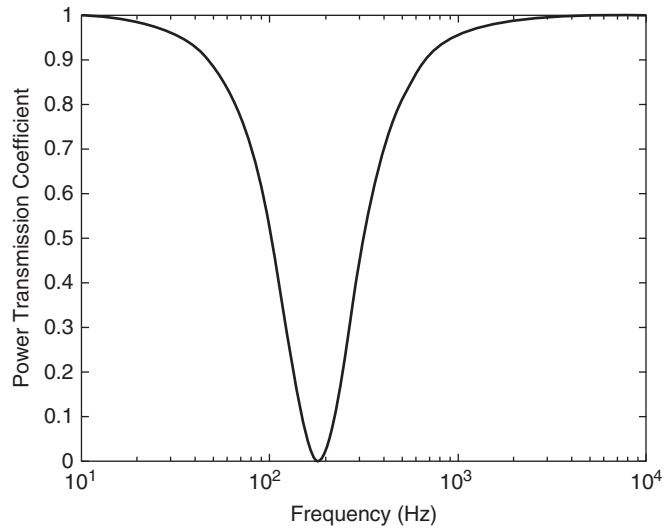
The resulting power transmission coefficient is given by

$$T_{\Pi} \approx \frac{1}{1 + \{[(S_1 - S)/2S]/kL\}^2} \quad (67)$$

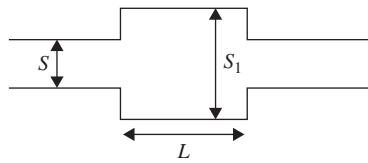
A typical response for this low-pass filter is shown in Fig. 18. It should be remembered that this acoustic response is only valid for low frequencies (wavelength significantly larger than the acoustic elements), and the response shown in Fig. 18 will not be valid for  $kL > 1$ .



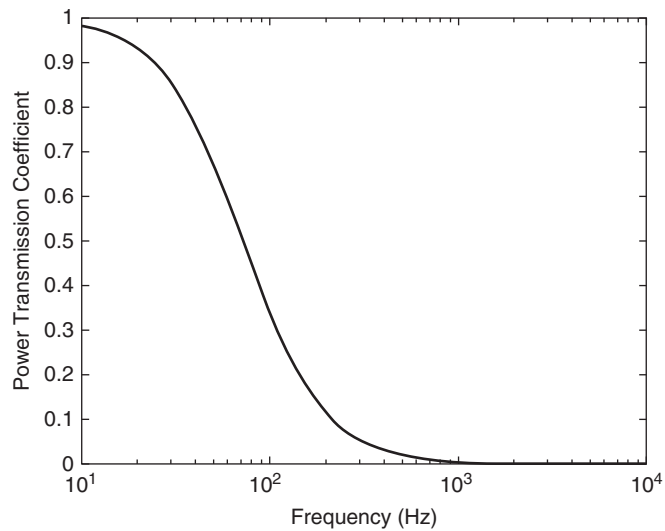
**Figure 15** Bandstop filter using Helmholtz resonator as side branch. The stopband is centered at the resonance frequency of the Helmholtz resonator.



**Figure 16** Power transmission coefficient for bandstop filter using Helmholtz resonator. The resonator has a volume of  $2000 \text{ cm}^3$ , a neck length of  $0.8 \text{ cm}$ , and a cross-sectional area of  $7.5 \text{ cm}^2$ . The main pipe has a cross-sectional area of  $28 \text{ cm}^2$ .



**Figure 17** Low-pass filter using expansion chamber.



**Figure 18** Power transmission coefficient for low-pass filter using enlarged section of pipe. The main pipe has a radius of  $2.54 \text{ cm}$ , and the enlarged section has a length of  $30.5 \text{ cm}$  and an area six times that of the main pipe.

**High-Pass Filter**

An acoustic high-pass filter can be constructed using a side branch consisting of a short length of unflanged pipe (with radius  $a$ ), such as is used for toneholes in musical instruments like a flute or clarinet, as shown in Fig. 19. The acoustic impedance of the side branch is given by

$$\mathbf{Z}_{\text{sb}} = \frac{\rho_o c k^2}{4\pi} + j\omega \left( \frac{\rho_o L_{\text{eff}}}{\pi a^2} \right) \quad (68)$$

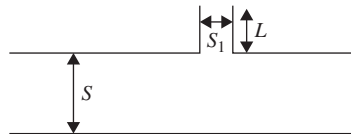
The resulting power transmission coefficient is given by

$$T_{\Pi} = \frac{1}{1 + [S_1 / (2SL_{\text{eff}}k)]^2} \quad (69)$$

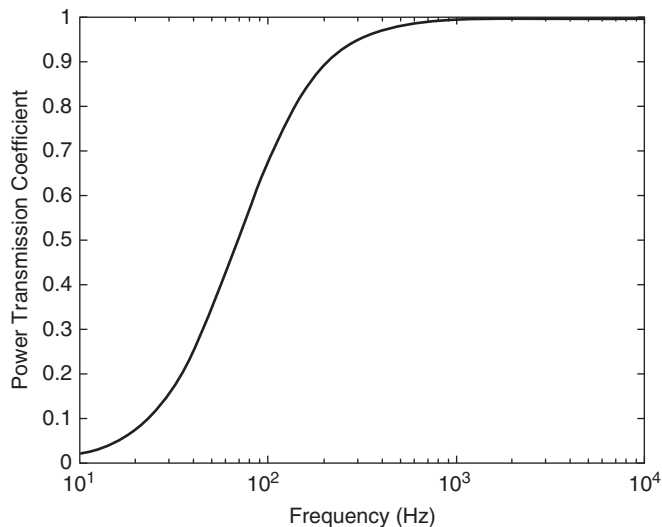
A typical response for this high-pass filter is shown in Fig. 20. It should again be remembered that this acoustic response is only valid for frequencies where the wavelength is significantly larger than the side branch.

**9.6 Lined Ducts**

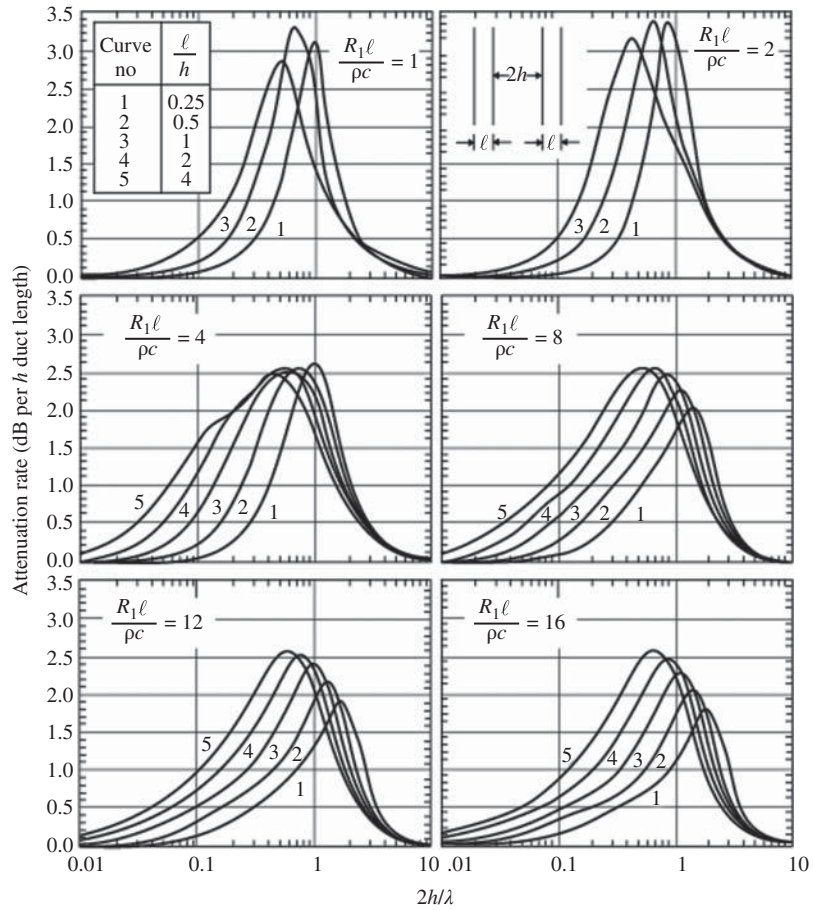
Ducts lined with absorbing material are often used as dissipative muffling devices to muffle fans in heating and air-conditioning systems. The liner material generally consists of a porous material such as fiberglass or rockwool, usually covered with a protective facing. The protective facing may be a thin layer of acoustically transparent material, such as a lightweight plastic



**Figure 19** High-pass filter using open side branch.



**Figure 20** Power transmission coefficient for high-pass filter using open side branch. The main pipe has a cross-sectional area of  $28 \text{ cm}^2$ , and the side branch has a length of  $8 \text{ cm}$  and a cross-sectional area of  $7.5 \text{ cm}^2$ .



**Figure 21** Predicted octave-band attenuations for rectangular duct lined on two opposite sides. Lined circular ducts or square ducts lined on all four sides give twice the attenuation shown here. The quantity  $\rho$  is the density of fluid flowing in the duct,  $c$  is the speed of sound in the duct,  $\ell$  is the liner thickness,  $h$  is the half-width of the airway, and  $R_1$  is the liner flow resistivity. For these results, a bulk reacting liner with no limp membrane covering and zero mean flow is assumed.<sup>14</sup>

sheet, or it may be a perforated heavy-gauge metal facing. If a perforated facing is used, it should have a minimum open area of 25% to ensure proper performance.

The performance of a lined duct with liner thickness  $l$  and airway width  $2h$  is shown in Fig. 21 for the case of zero mean flow. This figure shows some of the dependencies on the ratio of liner thickness to airway width as well as the flow resistivity.

### 9.7 Single- and Double-Leaf Partitions

Partitions (such as walls) are often used to separate a noise source from a receiving space. When partitions are used, it is important to check for flanking paths and leakage. Small openings or flanking paths with low impedance can easily reduce the effectiveness of partitions significantly. Single-leaf partitions exist when there is a single surface or when both surfaces of the wall vibrate as a unit. Double-leaf partitions consist of two unconnected walls separated by a cavity.

At low frequencies for single-leaf partitions, the transmission through the partition is governed by the mass of the partition, and the mass law governs this behavior. The intensity transmission coefficient is given in Eq. (56), and the resulting transmission loss can be expressed as

$$TL = 20\log(f\rho_s) - 47(\text{dB}) \quad (70)$$

where  $\rho_s$  is the surface density of the partition, given as the product of the density and thickness of the partition. Thus, at low frequencies, one must increase the density of the partition in order to increase the transmission loss; doubling the density of the partition increases the transmission loss by 6 dB.

For a single-leaf partition, wave effects in the partition lead to a coincidence frequency, which corresponds to the condition where the flexural wavelength in the partition matches the acoustic wavelength along the direction of the partition. When this condition is met, the transmission loss drops significantly, with the decrease being governed by the damping in the partition. Above the coincidence frequency, the partition becomes stiffness controlled, and the transmission loss increases at a rate higher than the mass law (theoretically 18 dB/octave for a single angle of incidence or about 9 dB/octave for diffuse-field incidence). The coincidence frequency separates these two behaviors and is given by

$$f_{\text{co}} = \frac{1}{2\pi} \sqrt{\frac{\rho_p h}{D}} \left( \frac{c}{\sin \phi} \right)^2 \quad (71)$$

In this equation,  $c$  is the speed of sound in the fluid,  $\rho_p$  is the density of the partition,  $h$  is the thickness of the partition, and  $D$  is the bending rigidity of the partition, given by  $D = Eh^3/[12(1 - \nu^2)]$ , where  $E$  is Young's modulus of the partition and  $\nu$  is Poisson's ratio for the partition.

The transmission loss through a double-leaf partition is noticeably higher than through a single-leaf partition with the same mass density. While the behavior is too complex to be covered extensively here, the following characteristics are generally associated with double-leaf partitions. (a) At low frequencies, the transmission loss follows the mass law, with the combined mass of the two leaves being used to determine the surface density. (b) A mass–air–mass resonance exists where the air cavity between the two leaves behaves as a spring between two masses. (c) Above the mass–air–mass resonance, the transmission loss increases sharply (18 dB/octave) until resonance effects in the cavity become important. (d) The transmission loss oscillates as the cavity resonance effects become important. At resonances of the cavity (cavity depth  $\approx n\lambda/2$ ), the transmission loss drops to values consistent with the mass law, while the peaks in the transmission loss occur at antiresonances of the cavity and continue to rise at about 12 dB/octave. Experimental transmission loss measurements typically show some variation from these predicted trends, but the results are generally consistent with predicted behavior.

## 9.8 Enclosures

For noisy equipment, one can install an enclosure around the piece of equipment. The insertion loss of the enclosure can be estimated using

$$IL = TL - C \quad (\text{dB}) \quad (72)$$

where TL is the transmission loss associated with the walls of the enclosure and

$$C = 10\log \left[ 0.3 + \frac{S_E (1 - \bar{\alpha}_i)}{S_i \bar{\alpha}_i} \right] \quad \text{dB} \quad (73)$$

$\bar{\alpha}_i$  is the mean Sabine absorption coefficient of the interior of the enclosure,  $S_i$  is the interior surface area of the enclosure, and  $S_E$  is the external surface area of the enclosure.



## 10 ACTIVE NOISE CONTROL

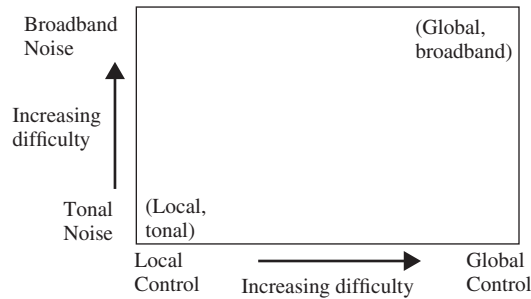
Over the last couple of decades, there has been considerable interest in the use of active noise control to address noise control applications. In many cases, it has been a technology that has not been well understood. There are many applications for which active noise control is not a good solution. In such cases, active noise control will be quite ineffective, and as a result, people can be easily disappointed. Thus, active noise control as a noise control solution should be chosen with care. However, for applications where active noise control is appropriate, it works *very* well and can produce impressive results. While active noise control can be very effective for proper applications, it is generally not a straightforward “off-the-shelf” solution. Thus, the focus of this section is to give an overview of how active noise control works and the direction in identifying proper applications. If active noise control is a viable solution, expertise should be sought in implementing the solution.

In deciding whether active noise control is a viable solution, there are several characteristics of active noise control that should be understood. First, active noise control is inherently a low-frequency solution. Implementation at high frequencies has several difficulties associated with it. First, effective control requires precise phase and amplitude matching. For example, if one wishes to achieve 20 dB of attenuation, the control signal must have a phase error of less than  $4.7^\circ$  (assuming perfect amplitude matching) or a magnitude error of less than 0.9 dB (assuming perfect phase matching). This tight tolerance in phase and magnitude matching is significantly easier to achieve at lower frequencies than at higher frequencies.

It is also easier to achieve significant spatial control of the acoustic field at lower frequencies than it is at higher frequencies. In active noise control, one can achieve localized control or global control of the field, depending on the physical configuration of the problem. In those cases where local control is achieved, the spatial volume where significant attenuation occurs scales according to the wavelength. The diameter of the sphere where at least 10 dB of attenuation is achieved is about one-tenth of a wavelength. Thus, lower frequencies result in larger volumes of control. If global control is to be achieved, good spatial matching must be achieved, which is also easier to achieve at lower frequencies than at higher frequencies.

In a number of applications, it is desirable to achieve global control of the acoustic field. In order to accomplish this, there must be a good acoustic coupling between the primary noise source and the secondary control source used to control the field. This can be achieved using one of two mechanisms. The first is to have the spacing between the primary noise source and the secondary control source be significantly less than an acoustic wavelength. For an extended noise source, this would require multiple control sources that will acoustically couple to the primary noise source. For an enclosed noise field (such as in rooms or cabs), it is also possible to achieve acoustic coupling without the control source being less than a wavelength away from the noise source. Instead, the coupling occurs through the acoustic modes of the enclosed field. The acoustic modes have a distinct spatial response, and by exciting the secondary control source properly, it is possible to achieve the same spatial (modal) response but with opposite phase, thus resulting in global attenuation of the field. However, it should be noted that this approach is effective only for low modal density fields. If too many modes are excited, global control can rarely be achieved and local control is the result.

It is also important to understand that discrete tonal noise is significantly easier to control than broadband noise. When multiple frequencies must be controlled, it is necessary to control the precise phase and amplitude matching at all frequencies. This is easier to accomplish with a small number of discrete tones than it is with many frequencies or broadband noise. In addition, when controlling broadband noise, *causality* also becomes an important issue. When controlling tonal noise, if it is not possible to generate the control signal to arrive with the noise signal at the error sensor at exactly the same time, it is still possible to achieve effective control by delaying the control signal to match the noise signal one period later. However, with broadband



**Figure 22** Level of difficulty for various classes of noise control problems.

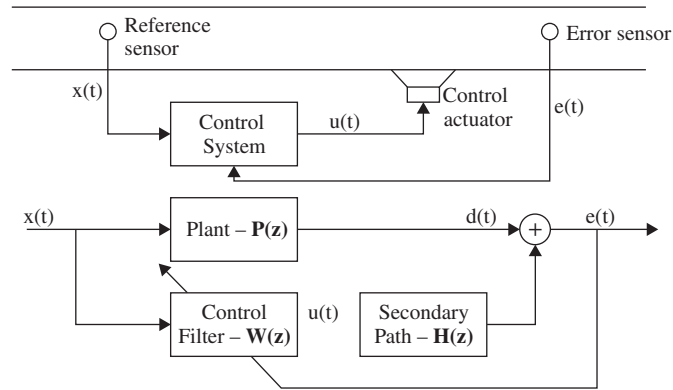
noise, this approach is not possible. If broadband control is to be achieved, the control signal and the noise signal must be temporally aligned, which cannot occur if it takes longer for the control signal to get to the error sensor than the primary noise signal.

To summarize, when considering a particular application, the lower the frequencies involved, the more effective the control can be, in general. In addition, the difficulty of the solution depends on the frequency content of the noise and the spatial extent of the control needed, as shown in Fig. 22.

## 10.1 Control Architectures

Active control can be implemented in either an adaptive mode or a nonadaptive mode. In a nonadaptive mode, the control filter is fixed such that if the filter is designed properly, good attenuation results. However, if the acoustic system changes, reduced effectiveness can result. In adaptive mode, the control filter has the ability to adjust itself to a changing acoustic environment, based on the response of one or more error sensors. Most active noise control solutions are based on an adaptive mode solution that is based on a digital signal processing (DSP) platform.

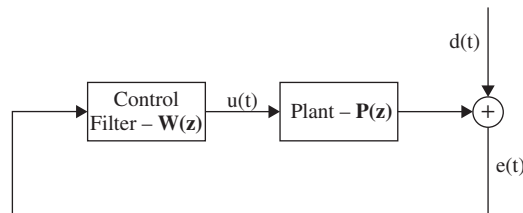
There are two general architectures that can be implemented with an active noise control system. These are referred to as feedforward and feedback. While both adaptive control and nonadaptive control have been used with both architectures, adaptive control has generally been used for feedforward control systems. To understand the basic working of an adaptive feedforward control system, consider the control of a plane wave propagating in a duct, as shown in Fig. 23. This is a prototypical application and allows one to understand the basic configuration in a straightforward manner. The noise to be controlled is detected by a “reference sensor,” which could be a microphone in the duct or some other sensor whose output is correlated to the noise to be attenuated. It should be understood that the control system will only be capable of attenuating noise that is correlated with the signal from this reference sensor. This signal is then used as the input to an adaptive control filter that determines the control signal output. The output signal is passed to a control actuator (such as one or more loudspeakers), where it generates an acoustic response that combines with the uncontrolled field and is measured by one or more error sensors. The error sensor response is then used to update the adaptive control filter. For implementation of a feedforward control system, care must also be taken to account for any possible response from the control output at the reference sensor. In our example, not only does the control signal propagate “downstream” in the duct to provide the desired attenuation, but it also propagates “upstream” in the duct where it can alter the reference signal if a microphone is being used. This can be accounted for either by using a nonacoustic reference signal (such as a tachometer signal if the noise is being created by some piece of rotating equipment such as a fan) or by modeling the feedback contribution from the control output to the reference sensor and compensating for that feedback component in the control system.



**Figure 23** Adaptive feedforward control for a duct. The upper figure shows the physical layout of the system, while the lower figure shows a block diagram of the control system implementation.

Causality is a potentially important issue in implementing feedforward control. There is an acoustic delay that exists as the noise to be controlled propagates from the reference sensor to the error sensor. If the reference signal can be processed and the response from the control actuator can arrive at the error sensor at the same time as the uncontrolled noise, the system will be causal. In this case, both random and periodic noise could be effectively controlled since it will be possible to achieve the precise time alignment needed. If the noise to be controlled is periodic, the causality constraint can be relaxed. If the control signal does not arrive in time to be perfectly aligned in time, the DSP will adjust itself to effectively line up the signal properly one cycle later, thus still achieving the desired attenuation.

Feedback control systems have used both adaptive and nonadaptive control configurations. Perhaps the most common example involving feedback control is with active headsets that are commercially available to reduce noise (although some headsets are now also implementing feedforward control). For a feedback control system (Fig. 24), the noise to be controlled is detected by a reference sensor that is used as the input to the control filter. The output of the control filter is again sent to a control actuator, and the sound generated combines with the uncontrolled field. The result is measured at the reference sensor and thus creates the “feedback loop.” Feedback control systems are generally more tolerant of model errors in the control system implementation. Thus, implementation of feedforward control in a nonadaptive mode is rarely effective in a practical application. However, feedback control systems can also easily become unstable if designed improperly. Staying within stability constraints often leads to a solution that does not achieve as much attenuation as with feedforward control. The stability constraint also often determines the frequency bandwidth that can be effectively controlled.



**Figure 24** Block diagram of feedback control implementation. The uncontrolled signal is given by  $d(t)$ .

It should also be understood that there is inherently an acoustic delay present in the feedback loop when implementing feedback control. This delay results from the finite response time of the control actuator, the acoustic propagation time from the control actuator to the reference sensor, and any delays associated with the electronics of the system. As a result, it is impossible to achieve perfect time alignment of the uncontrolled noise and the noise generated by the active control system. In general, the shorter the delay time in the feedback loop, the greater the attenuation that can be achieved and the wider the frequency bandwidth that can be controlled.

## 10.2 Attenuation Limits

Good estimates of the maximum attenuation achievable can be determined for both feedforward and feedback control implementations. Because of the structure of feedforward systems, the control system will only attenuate noise that is correlated with the reference sensor signal. Thus, it is imperative that the error signal sensor and the reference signal sensor be correlated. This is embodied in the expression that gives the maximum obtainable attenuation,

$$\Delta L_{\max} = 10 \log[1 - \gamma_{xd}^2(\omega)] \quad (74)$$

where  $\Delta L_{\max}$  is the maximum obtainable attenuation and  $\gamma_{xd}^2(\omega)$  is the coherence (frequency dependent) between the reference signal,  $x(t)$ , and the uncontrolled error signal,  $d(t)$ . A quick method of determining if active noise control would be effective would be to measure the coherence between a proposed reference sensor and a proposed error sensor. It should be remembered that this gives a prediction of the attenuation at the error sensor. If local control is being achieved, this will give no indication as to how effective the control will be at locations removed from the error sensor location.

For feedback control, the autocorrelation of the reference signal can be used to predict the attenuation that can be achieved if the time delay associated with the feedback loop is known. Conversely, if the desired attenuation is known, this autocorrelation can also be used to determine how short the time delay must be. The predicted attenuation is given by

$$\Delta L_{\max} = -10 \log \left( 1 - \frac{E_p}{E_0} \right) \quad (75)$$

where  $E_0$  is the autocorrelation level at zero delay and  $E_p$  is the largest magnitude of the autocorrelation that exists in the autocorrelation at any time greater than the group delay of the feedback loop.

## 10.3 Filtered-x Algorithm

The most common adaptive algorithm in current use for active noise control is the filtered-x algorithm or some variation of that algorithm. A brief review of the algorithm is helpful in understanding the general architecture of most active noise control systems. In the DSP architecture, the control filter is implemented as a finite impulse response filter, whose response can be represented by a vector of the filter coefficients. Thus,

$$\mathbf{W} = [w_0, w_1, w_2, \dots, w_{I-1}]^T \quad (76)$$

Similarly, the secondary path transfer function (represented by  $\mathbf{H}$  in Fig. 23) can be represented by a vector of filter coefficients:

$$\mathbf{H} = [h_0, h_1, h_2, \dots, h_{J-1}]^T \quad (77)$$

The output of a digital filter is the convolution sum of the input signal with the filter response vector. Thus, if the reference input and control output signals are represented as vectors,

$$\begin{aligned}\mathbf{X}(t) &= [x(t)x(t-1)x(t-2)\cdots x(t-I+1)]^T \\ \mathbf{U}(t) &= [u(t)u(t-1)u(t-2)\cdots u(t-J+1)]^T\end{aligned}\quad (78)$$

the control output signal is given by  $u(t) = \mathbf{W}^T \mathbf{X}(t)$  and the error signal is given by  $e(t) = d(t) + \mathbf{H}^T \mathbf{U}(t)$ . Most active noise control systems are based on quadratic minimization techniques. For the filtered- $x$  algorithm, the algorithm updates its coefficients according to the negative gradient (with respect to the control filter coefficients) of the squared instantaneous error signal. Calculating the gradient of the squared error signal leads to

$$\mathbf{W}(t+1) = \mathbf{W}(t) - \mu \mathbf{R}(t)e(t) \quad (79)$$

which gives the control filter coefficients for the next iteration of the algorithm. In this expression,  $\mu$  is a convergence parameter chosen to maintain stability and  $\mathbf{R}(t)$  is the “filtered- $x$ ” signal vector, whose components are given by

$$r(t) = \hat{\mathbf{H}}^T \mathbf{X}(t) \quad (80)$$

where  $\hat{\mathbf{H}}$  is a vector of filter coefficients that models the physical secondary path transfer function  $\mathbf{H}$ .

## 10.4 System Identification

In order to achieve stable, effective control, it is necessary to have a reasonable model of the secondary path transfer function  $\mathbf{H}$ . It has been shown that the phase of the model is the primary concern in achieving good control. While phase errors of up to  $\pm 90^\circ$  can be tolerated in order to maintain stability, the performance of the control system degrades seriously as the phase errors approach this limit. Thus, an accurate model with minimal phase errors will result in substantially improved control results.

There are several methods that have been used to obtain a good model of  $\mathbf{H}$ . The most straightforward method is to obtain a model of  $\mathbf{H}$  a priori. This is done by injecting broadband noise into the secondary path (typically from the DSP used for the control) and measuring the response at the error signal with the primary noise source turned off. In this manner, a straightforward adaptive system identification routine can be used to obtain the coefficients of  $\mathbf{H}$ .

A second method implements an adaptive online secondary-path estimation technique by injecting low-level broadband noise,  $n(t)$ , along with the control signal,  $u(t)$ . This broadband signal is uncorrelated with the primary noise,  $d(t)$ , and with the control signal,  $u(t)$ . Thus, the error signal can be used as an output, with the noise signal  $n(t)$  as an input in a typical adaptive system identification routine. Since the primary noise and control signal are not correlated with  $n(t)$ , they do not affect the system identification and the process proceeds similar to the offline approach. The difficulty with this approach is that the injected noise must be high enough in level to achieve good system identification and yet kept low enough in level to not affect the overall noise level at the error sensor. In many cases, this can involve adaptive gain control to maintain the correct balance between the control signal and the injected noise.

A final method that has been used is also adaptive in nature. This method performs system identification not only for the secondary path but also for the plant,  $P$ . In other words, it implements a model of the entire system that is unlike the previous two methods. One of the results of this approach is that the model of the secondary path is not unique, unless the excitation of the system can be characterized as “persistent excitation,” which essentially means broadband excitation. For excitation signals that are narrowband in nature, although there is not a unique solution for the secondary path, it has been shown that the solution obtained leads to stable, effective control. For more information on both adaptive system identification methods, the reader is referred to Refs. 15 and 16.

## 10.5 Control Applications

This section briefly outlines application areas where active noise control may be applicable:

- 1. Active Control in Ducts:** Active control of ducts has been implemented in a number of commercial applications, such as in exhaust stacks at industrial plants and in heating, ventilation, and air-conditioning (HVAC) ducts. The most successful applications have been at low frequencies, where only plane waves propagate in the duct. At higher frequencies, higher order modes propagate in the duct. While control of such fields can be effective, it requires sensing and actuating configurations that are able to sense and control those higher order modes. Another consideration is that even in the frequency range where only plane waves propagate, the control actuator will generate evanescent higher order modes. Thus, the control system must be configured so that all evanescent modes have effectively decayed by the time they reach the error sensor and/or the reference sensors.
- 2. Active Control of Free-Field Radiation:** Active control has been investigated for applications such as radiation from transformers and even as part of noise barriers for highways. For these applications, the control configuration significantly impacts the amount of control that can be achieved and whether the control is local or global. The control source configuration must be carefully selected for these applications if control in a desired direction or even global control is to be achieved.
- 3. Active Control in Enclosures:** The most successful application currently is for active headsets. These implement control in a small confined volume surrounding the ears, and a number of active headsets are commercially available. Other applications include active control in automobile cabins, aircraft fuselages, other vehicles, and rooms. The active control will be more effective at lower frequencies and is dependent to a large extent on the modal density in the enclosure. In a number of applications, local control is achieved, although if the modal density is low, it can be possible to achieve global control, or at least control extended over a much broader portion of the volume. In general, if global control is desired, the number of control actuators used must be at least as great as the number of modes to be controlled.
- 4. Active Vibration Isolation Mounts:** This approach uses active vibration control to minimize the transmission of vibration energy through isolation mounts associated with engines, generators, and so forth. Active mounts have been investigated for automobile engine mounts and aircraft engine mounts, among others. Depending on the mount configuration, it may be necessary to control multiple degrees of freedom in the mount in order to achieve the desired isolation, and it may be necessary to use active mounts on most, if not all, of the engine mounts.
- 5. Active Control of Transmission Loss:** This approach is focused on increasing the transmission loss through a partition, such as an aircraft fuselage or a partition in a building. There are multiple possible approaches, including controlling the structural response of the partition using structural actuators or directly controlling the acoustic field (on either the source or receiver side) through the use of acoustic actuators. For these applications, a thorough understanding of the physics associated with the structural response of the partition and its coupling with the incident and transmitted acoustic fields is essential in developing an effective solution.

With all of these applications, it is important to do a careful analysis of the noise reduction requirements in order to assess whether active noise control is an appropriate solution. Several applications using active noise control are currently commercially available and others are nearing commercialization. Nonetheless, if one does not carefully consider the application, it is easy to be disappointed in active noise control when it is not as effective as hoped.

In review, active noise control is better suited for low frequencies. It is easier to achieve success for tonal noise than it is for broadband noise. It will generally be more effective for compact noise sources than for complex extended sources. If these criteria are met, active noise control could be a very effective and viable solution, although currently it would still generally require the involvement of someone knowledgeable in the field.

## 11 ARCHITECTURAL ACOUSTICS

This section defines the four principal, physical measures used to determine performance hall listening quality. Several perceptual attributes correlated with a physical measure are also listed.

The four main measures used to qualify concert halls are the binaural quality index (BQI), the early decay time (EDT), the strength ( $G$ ), and the initial time delay gap (ITDG). The BQI is defined as  $BQI = 1 - IACC$ , where IACC is the average of the interaural cross correlation in octave bands of 500, 1000, and 2000 Hz. The BQI and IACC are measures of the relative sound reached at each ear. If a listener's two ears receive identical reflections such as from a ceiling, floor, or back wall, the BQI would equal zero and the IACC would equal unity. If reflection at both ears are received from side walls or such that the reflections at both ears are not identical, the BQI would be greater than zero and the IACC would be less than unity. BQI values of 0.65–0.71 are representative of the best concert halls.

The second measure is EDT. This is a measure of the time required for a 10-dB decay to occur in the signal. This time is then multiplied by a factor of 6 that provides an extrapolated comparison to a 60-dB decay time that is a similar measure of the reverberation time ( $T/60$ ). Because of the 10-dB decay, the abbreviation of EDT10 is often used. EDT typically has a linear relationship in frequency between occupied and unoccupied halls. This can simplify the process of gathering data. The better concert halls have EDT values in the range from 1.7 to 2.1 s.

The third measure is  $G$ , defined as  $G = L_p - L_w + 31$  dB, where  $L_p$  is the sound pressure level measured at the point of interest and  $L_w$  is the power level of the source. Typically,  $L_p$  will decrease as the room volume and room absorption increase. However, if the reverberation time (RT) also increases with room volume, the  $L_p$  can be held constant. The better concert halls have  $G$  values that range from 3–6 dB, while relatively large concert halls with less sound quality have  $G$  values in the range of 0–3 dB.

The fourth measure is the ITDG, which is defined as the time interval in milliseconds from the direct sound to the first reflected sound. ITDG values are functions of walls, balconies, and other obstacles that provide a reflective surface for the sound. ITDG values should not exceed 35 ms for best results.

There are also several perceptual attributes that are used to describe concert halls. These attributes are listed and defined by providing a measure in Table 7. This table was produced from class notes provided by William Strong at Brigham Young University.<sup>17</sup> It is important to note that halls that provide good speech intelligibility are not necessarily the best halls for music.

## 12 COMMUNITY AND ENVIRONMENTAL NOISE

Measurement and analysis of the impact of noise on both individuals and communities represent a major subfield within acoustics. They are also topics inherently fraught with debate because human perception of noise is ultimately a subjective phenomenon. To introduce this section, some of the basic principles of outdoor sound propagation are summarized. This is done to demonstrate the impact the propagation environment can have on the noise at a receiver.



**Table 7** Perceptual Attributes, Physical Measures, and Optimal Values for Concert Halls

Perceptual Attribute	Physical Measure	Optimal Values
Spaciousness	Binaural quality index, lateral fraction	BQI > 0.64
Reverberance	Early decay time	EDT and RT depend on type of music
Dynamic loudness	Strength	$G > 3$ dB, low background level
Intimacy	Initial time delay gap	ITDG (15–35 ms)
Clarity	Early/late ratio	Large early/late ratio for speech, depends on music
Envelopment	Highly diffuse, reverberant sound	Similarity of EDT and RT
Warmth	Frequency dependence of EDT	$EDT_{low} > EDT_{high}$
Ensemble	Early (15–35-ms) stage reflections, at frequencies above 500 Hz	Stage with ample reflecting surfaces

## 12.1 Outdoor Sound Propagation

Many phenomena can affect the propagation of noise from source to receiver and therefore have a direct impact on community noise issues. Some of these phenomena are:

- Geometric spreading
- Atmospheric absorption
- Ground effect
- Refraction
- Atmospheric turbulence
- Barriers

The effects that each of these can have on sound pressure level are now reviewed.

Geometric spreading for distances much larger than the characteristic dimensions of the source will be spherical. For every doubling of distance,  $\Delta L_p$  will be  $-6$  dB. There are situations, such as supersonic aircraft or steady traffic near a roadway, where the spreading will be cylindrical, which reduces  $\Delta L_p$  to  $-3$  dB for every doubling of distance.

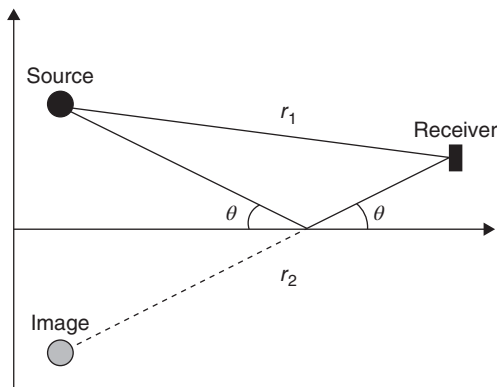
Because of its frequency-dependent nature, absorption causes high-frequency energy to decay much more rapidly than low-frequency energy. In addition to overall level, absorption can play an important role in changing spectral shape and therefore community response to the noise.

Another effect is that of reflections of nonplanar waves off a finite-impedance ground. If we consider the basic setup in Fig. 25, where the distance from the source to the receiver is  $r_1$  and the distance from the image source to the receiver is  $r_2$ , the complex pressure amplitude at the receiver may be expressed as

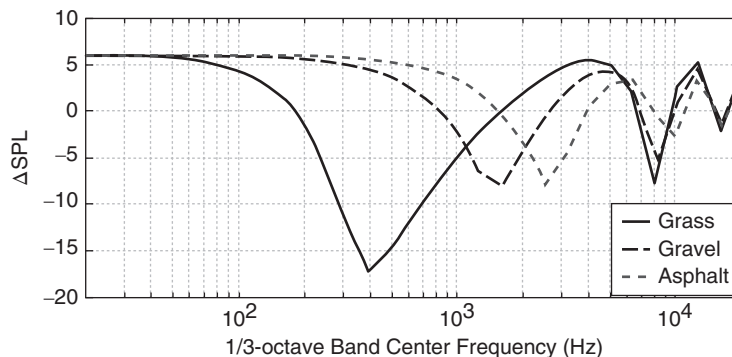
$$p = \frac{Ae^{-jkr_1}}{r_1} + Q \frac{Ae^{-jkr_2}}{r_2} \quad (81)$$

where the quantity  $Q$  is the spherical wave reflection coefficient and may be calculated from Appendix D.4 in Ref. 18. This coefficient is generally complex and accounts for the amplitude and phase changes encountered when the nonplanar sound wave reflects off the finite-impedance ground.





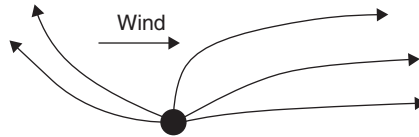
**Figure 25** Direct and ground-reflected paths from source to receiver.



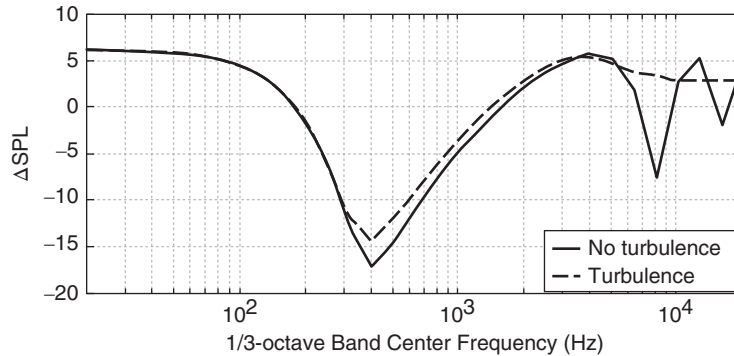
**Figure 26** Change in sound pressure level relative to free-field propagation due to ground reflections. The source and receiver are both at a height of 6 ft and the distance between them is 500 ft.

An example of the significant effect that the impedance of the ground can have is shown in Fig. 26, where the impedance values chosen are representative of grass, gravel, and asphalt. In this example, for which one-third octave bands are displayed, the source and receiver are both at a height of 6 ft (1.8 m) and are separated by a distance of 500 ft (152 m). At low frequencies, the wavelengths of sound are such that the direct and reflected sound waves arrive in phase, resulting in constructive interference and a doubling of pressure (+6 dB  $\Delta L_p$ ). The first interference null varies significantly in frequency for the three surfaces. Note that asphalt begins to approximate a rigid ground surface.

Atmospheric refraction can also have a significant impact on the propagation of sound from source to receiver. Refraction is caused by variations in sound speed. The first cause of a variable sound speed is wind. For sound propagation upwind, upward refraction occurs. For sound propagation downwind, downward refraction occurs, as illustrated in Fig. 27. The second cause of sound speed variation is a temperature gradient. During the day, solar radiation causes the ground to warm up and a temperature lapse to occur, meaning that the temperature decreases as a function of height. This condition causes upward refraction to occur as the sound waves bend toward where the sound speed is slower and can create a “shadow region” near the ground where the sound (theoretically) does not reach. At night, however, temperature inversions can occur as the ground cools more quickly than the surrounding air. In this case,



**Figure 27** Effect of wind on direction of sound rays radiating from a source.



**Figure 28** Change in sound pressure level for propagation over grass with and without atmospheric turbulence.

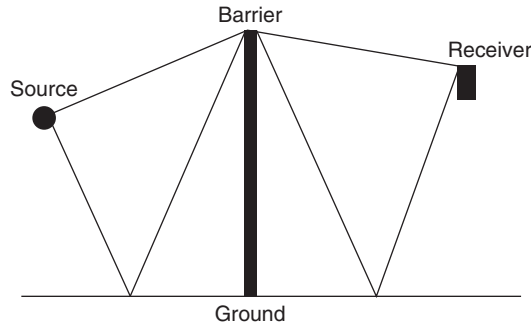
downward refraction occurs. This also occurs at the surface of a body of water, where the air temperature just above the water is cooler than the surrounding air. This condition makes sound propagated over large distances near the ground more readily audible and can greatly impact community noise issues.

Atmospheric turbulence may be viewed as small-scale refraction. Small-scale inhomogeneities in temperature or air velocity can cause sound to be scattered (diffracted). The main effect of turbulence is to generally lessen the impact of other propagation effects. For example, in Fig. 28,  $\Delta L_p$  has been calculated for propagation over grass with and without atmospheric turbulence. Turbulence minimizes the interference nulls at high frequencies because the scattered sound takes slightly different paths to the receiver. The effect for a refracting atmosphere is similar. Although the shadow zone can readily occur near the ground for upward refraction, turbulence causes some sound to be scattered into the region.

The final phenomenon in outdoor sound propagation that is discussed is the behavior of acoustic waves when a barrier is encountered. For the case of natural barriers, such as hills, acoustic propagation over a hill can often be treated as propagation through an upward-refracting atmosphere over a flat plane. For the case of man-made barriers, such as sound walls, analytical methods may be used to account for the sound that reaches a receiver. If the length of the barrier is much greater than the height, there are four basic paths that need to be accounted for, which are depicted in Fig. 29. The first path is a direct path from the source to barrier and then, due to diffraction, from the top of the barrier to the receiver. The other paths involve one or two ground reflections before reaching the receiver.

Although more sophisticated analytical methods exist (e.g., Ref. 18), the basic effects of the multipath problem can be included in the following equation,<sup>19</sup> which describes the insertion loss, in decibels, of a thin barrier for a point source and for ranges less than 100 m, where atmospheric effects are ignored:

$$IL = -\Delta SPL = 10 \log_{10} [3 + 10N] - A_{\text{ground}} \quad (82)$$



**Figure 29** Four different paths that the barrier-diffracted sound can take between the source and receiver.

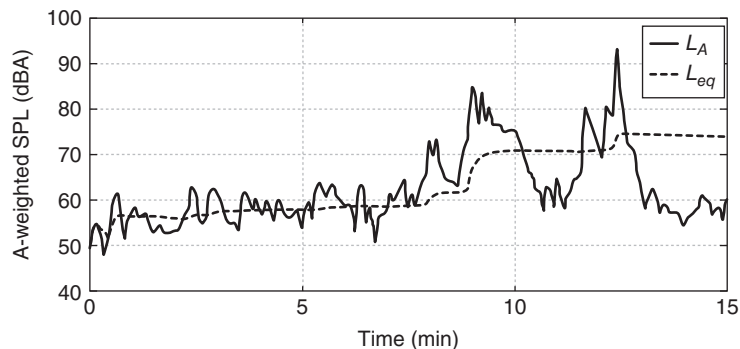
where  $A_{\text{ground}}$  is the absorption due to the ground (in decibels) before the barrier is installed, SPL stands for sound pressure level, and  $N$  is the Fresnel number, which for sound of wavelength  $\lambda$  can be calculated as

$$N = \frac{2}{\lambda}(d_{\text{SB}} + d_{\text{BR}} - d_{\text{SR}}) \quad (83)$$

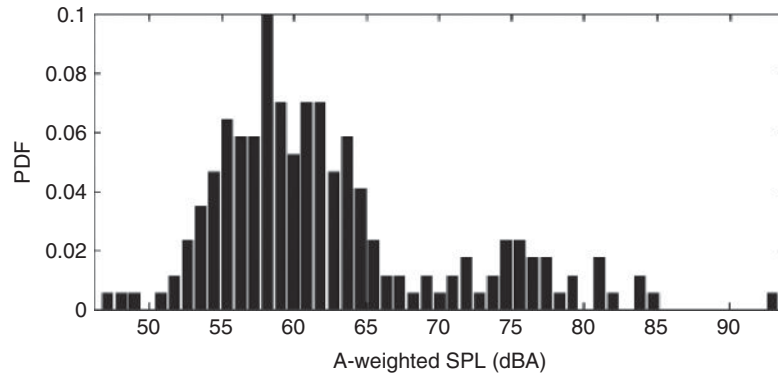
The distances are the distances from the source to the top of the barrier (SB), from the barrier to the receiver (BR), and the direct line-of-sight distance from the source to the receiver (SR). One point to make is that although the barrier effectiveness does generally increase as a function of frequency, the diffraction from the top of the barrier can play a significant role and result in diminished performance. This is especially true for path lengths for which the interference is constructive. More general analytical techniques, applicable to thick barriers or diffraction due to gradual structures like hills, do exist and can be found in Refs. 14 and 18. However, explicit inclusion of atmospheric effects (e.g., refraction) is usually accomplished with numerical models.

## 12.2 Representations of Community Noise Data

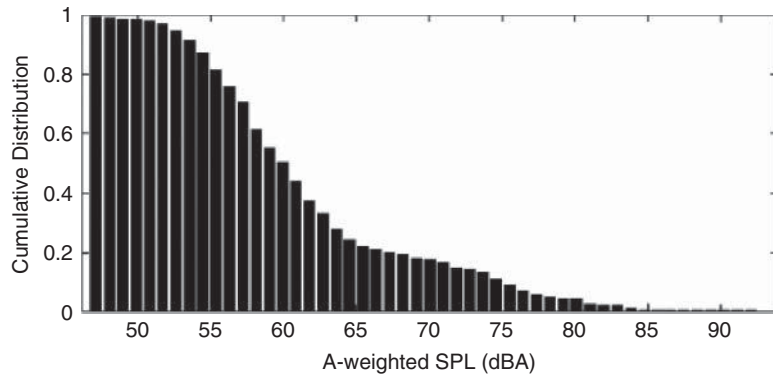
There are numerous ways of representing the noise to which communities are subjected. One way is to simply display the A-weighted sound pressure level ( $L_A$ ) as a function of time. One example, displayed in Fig. 30, is the emptying of several trash dumpsters during the early morning at an apartment complex in Provo, Utah. Before the garbage truck arrived, major noise sources were due to intermittent traffic from the nearby street. The most significant noise events



**Figure 30** A-weighted  $L_p$  and  $L_{\text{eq}}$  as function of time before, during, and after garbage truck arrival.



**Figure 31** Probability density function (PDF) of  $L_p$  for time series shown in Fig. 30.



**Figure 32** Cumulative distribution of time series in Fig. 30 showing fraction of time sound level exceeds given  $L_p$ .

were due to the dumpsters being shaken by the hydraulic arms on the truck before being noisily set back down.

Other representations of community noise are statistical in nature. Using the same garbage truck example, the estimated probability density function of the A-weighted level is displayed in Fig. 31. The broad tail of large values is caused primarily by the garbage truck noise events. Another statistical representation is a cumulative distribution, which displays the percentage of time that the noise levels exceed a given value. This is shown for the same garbage truck data in Fig. 32. Finally, statistical moments can also be calculated from the time series. For example, the mean level during the 15-min sampling period was 62.4 dBA and the skewness of the data was 1.1. This latter moment emphasizes the non-Gaussian characteristics of the noise distribution because skewness is zero for Gaussian distributions.

In addition to A-weighted sound pressure level, there are many other single-number metrics that are used to describe community noise. These metrics have been the result of attempts to correlate subjective response with objective, albeit empirical measures. Some of the commonly used metrics are as follows:

- **Equivalent Continuous Sound Level ( $L_{eq}$ ):** The A-weighted level of the steady sound that has the same time-averaged energy as the noise event. Common averaging times include hourly levels, day levels (7 AM–10 PM), evening levels (7–10 PM), and night

levels (10 PM–7 AM). For the time interval  $T$ , which runs between  $T_1$  and  $T_2$ ,  $L_{eq}$  is calculated as

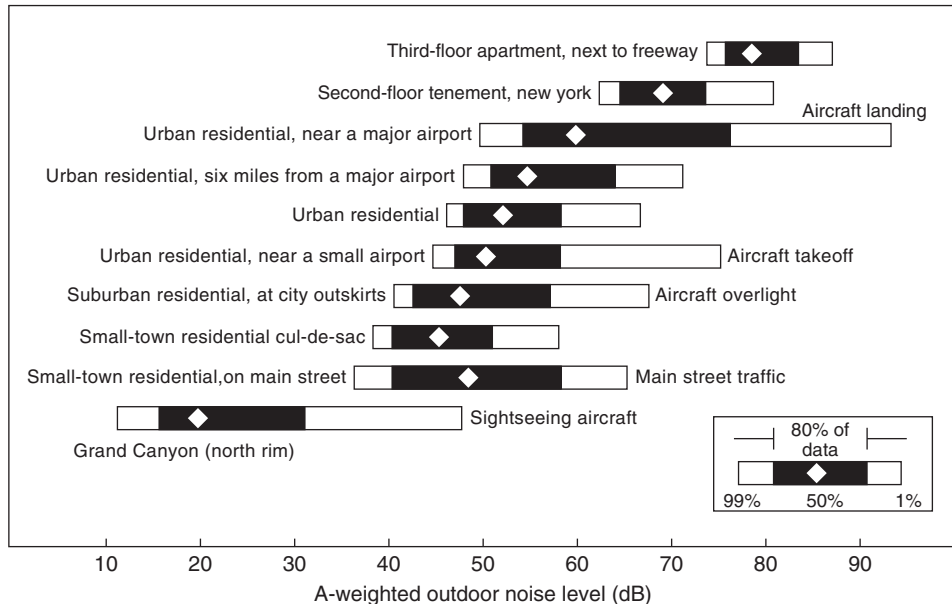
$$L_{eq} = 10 \log_{10} \left[ \frac{1}{4 \times 10^{-10}} \frac{1}{T} \int_{T_1}^{T_2} p_A^2(t) dt \right] \quad (84)$$

where  $p_A$  is the instantaneous A-weighted sound pressure. The  $L_{eq}$  as a function of time was shown for the previous garbage truck example in Fig. 30.

- **Day–Night Level (DNL or  $L_{dn}$ ):** The  $L_{eq}$  obtained for a 24-h period after a 10-dBA penalty is added to the night levels (10 PM–7 AM). For individual  $L_{eq}$  calculations carried out over 1-h intervals ( $L_{1h}$ ),  $L_{dn}$  may be expressed as

$$L_{dn} = 10 \log_{10} \left\{ \frac{1}{24} \left[ \sum_{i=0100}^{0700} 10^{0.1[L_{1h}(i)+10]} + \sum_{i=0800}^{2200} 10^{0.1L_{1h}(i)} + \sum_{i=2300}^{2400} 10^{0.1[L_{1h}(i)+10]} \right] \right\} \quad (85)$$

- **Community Noise Equivalent Level (CNEL):** The  $L_{eq}$  obtained for a 24-h period after 5 dBA is added to the evening levels (7–10 PM) and 10 dBA is added to the night levels. It can be calculated similar to  $L_{dn}$ , with the appropriate penalty given during the evening (between 8 and 10 PM).
- **X-Percentile-Exceeded Sound Level ( $L_X$ ):** Readily calculated from the cumulative distribution (e.g., see Fig. 32),  $L_X$  is the level exceeded  $X$  percent of the time. Common values are  $L_{10}$ ,  $L_{50}$ , and  $L_{90}$ . In Fig. 33,  $L_X$  values are shown as bars for  $L_{99}$ ,  $L_{10}$ ,  $L_{50}$ ,  $L_{90}$ , and  $L_1$  for representative noise environments.
- **C-Weighted Sound Pressure Level (LC):** Similar to A weighting, but designed to mimic the 90-phon equal-loudness contour. Consequently, C weighting is more appropriate than A weighting for louder sounds. The equation for the C-weighting filter was given previously in Eq. (7).



**Figure 33** Community noise data showing  $L_{99}$ ,  $L_{90}$ ,  $L_{50}$ ,  $L_{10}$ , and  $L_1$  data points for various noise events.

- **D-Weighted Sound Pressure Level (LD):** Developed for assessing the auditory impact of aircraft noise. The weighting curve heavily penalizes high frequencies to which the ear is most sensitive (see Fig. 3). The equation for the D-weighting filter was given previously in Eq. (7).
- **Effective Perceived Noise Level (EPNL).** This metric was designed for characterizing aircraft noise impact and is used by the Federal Aviation Administration (FAA; see FAR Part 36, Sec. A.36) in the certification of commercial aircraft. The metric accounts for (a) the nonuniform response of the human ear as a function of frequency (i.e., the perceived noise level), (b) the additional annoyance due to significant tonal components of the spectrum (the tone-corrected perceived noise level), and (c) the change in perceived noisiness due to the duration of the flyover event. Too involved to be repeated here, calculation procedures for EPNL may be found in FAR Part 36, Sec. A.36.4, or Ref. 20.

### 12.3 Community Noise Criteria

Because of increased awareness regarding community noise issues, city noise ordinances are becoming more commonplace. Many of these ordinances are based on maximum allowable A-weighted sound pressure level, broken down into land usage and day or night. In addition, consideration can be given to the nature of the noise source (e.g., is it essential to commerce/industry) and its duration (e.g., is it intermittent or continuous). As an example, portions of the Provo, Utah, noise ordinance, which is representative of many cities, are summarized in Table 8. Continuous sounds are those that have a duration greater than 6 min, intermittent sounds last between 2 s and 6 min, and impulse sounds last less than 2 s. The level listed is not to be exceeded at the property line of interest.

Noise levels are an important consideration when considering land use. Guidelines for outdoor DNL (for structures in 24-h/day use) or  $L_{eq}$  (for structures being used only part of the day) have been put forth in a land-use compatibility report published by the FAA. If the appropriately measured outdoor levels for a yearly average are < 65 dB, then the land is compatible for

**Table 8** Summary of A-Weighted Level Limits (dBA) in Provo, Utah

District	Day	Night
<i>Continuous and Intermittent Sounds of Industry and Commerce</i>		
Residential/agricultural	85	55
Commercial	85	65
Industrial	85	85
<i>Continuous Public Disturbances</i>		
Residential/agricultural	65	55
Commercial	70	65
Industrial	75	75
<i>Intermittent Public Disturbances</i>		
Residential/agricultural	70	60
Commercial	75	65
Industrial	80	80
<i>Impulse Noises</i>		
Residential/agricultural	75	60
Commercial	80	65
Industrial	85	85

**Table 9** Land-Use Compatibility<sup>a</sup>

Structure	Outdoor DNL or $L_{eq}$ (dB)				
	65–70	70–75	75–80	80–85	<85
Home	25	30	N	N	N
Church, school, hospital, library	25	30	N	N	N
Business offices, retail, restaurant	Y	25	30	N	N
Manufacturing	Y	25 <sup>b</sup>	30 <sup>b</sup>	35 <sup>b</sup>	N
Agriculture	Y	Y	Y <sup>NB</sup>	Y <sup>NB</sup>	Y <sup>NB</sup>
Livestock breeding	Y	Y	N	N	N
Mining	Y	Y	Y	Y	Y
Nature exhibits/zoos	Y	N	N	N	N
Amusement parks	Y	Y	N	N	N
Outdoor music, amphitheaters	N	N	N	N	N
Outdoor sports arenas	Y <sup>SR</sup>	Y <sup>SR</sup>	N	N	N

<sup>a</sup>NB denotes residential buildings not permitted and SR means sound reinforcement may be required.

<sup>b</sup>Applies to areas sensitive to noise.

Source: Adapted from FAA AC 150/2050-1, “Noise Control and Compatibility Planning for Airports.”

all the uses listed below. In Table 9, if a number is listed, then the guidelines indicate that the transmission loss between outdoors and indoors needs to meet the value listed.

In the case of airports, DNL contour maps showing community noise impact are used to make land usage decisions. Shown in Fig. 34 is an example of a DNL map for the Colorado Springs Airport superimposed on a photograph of the area. The figure shows appropriate land usage in that urban development has occurred outside the 65-dB DNL contour. The land usage that occurs closest to the airport is not a residential district, but rather an Air Force base.

## 12.4 Community Response to Noise

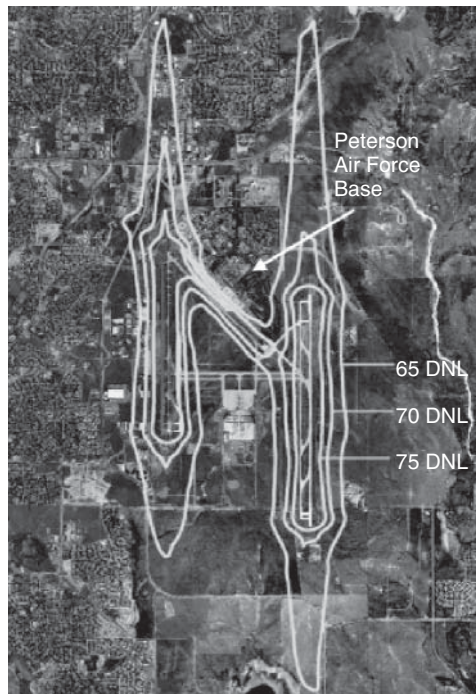
The response of an individual to a given noise event is a highly subjective, variable measure. Noise surveys are conducted to obtain the average response of citizens to different noise sources. For transportation noise (e.g., traffic, aircraft), these surveys have resulted in an empirical relationship between transportation noise events and the percentage of people that were highly annoyed (HA).<sup>21</sup> If this percentage is defined as %HA, it may be expressed in terms of the DNL ( $L_{dn}$ ) as

$$\%HA = 0.0360L_{dn}^2 - 3.265L_{dn} + 78.9 \quad (86)$$

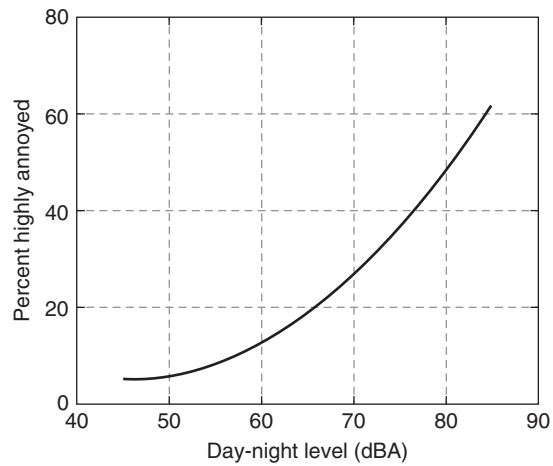
The uncertainty for this measure is approximately  $\pm 5$  dBA between 45 and 85 dBA. The percent highly annoyed is plotted as a function of DNL in Fig. 35. Note that for 65-dB DNL 20% of the population will still be highly annoyed. This curve suggests the difficulty that noise control engineers and land-use planners encounter when trying to balance the needs and desires of the community and industry.

## 13 SOUND QUALITY ANALYSIS

Good sound quality has traditionally been synonymous with quiet sounds. However, over the last three decades, the definition of sound quality has changed. Blauert and JeKosch<sup>22</sup> define sound quality as “the adequacy of a sound in the context of a specific technical goal and/or task.” The term “compatibility” has also been used in this context, especially with regard to sounds accompanying actions of product users.<sup>23</sup> With this definition in mind, sound quality



**Figure 34** DNL contour map for Colorado Springs Airport. Urban development has occurred outside the 65-dB DNL contour.



**Figure 35** Percentage of people highly annoyed for given DNL. Calculated from Eq. (86).



now represents the “sensory pleasantness” of the sound, which is a combination of the perceived loudness, roughness, and pitch.<sup>24</sup> The difference in definition contrasts the one-dimensional approach initially used to the current multifaceted technique that includes aspects of psychology and anatomy as well as the physical parameters engineers are accustomed to using.

While much of what is now considered sound quality analysis originated in the automotive industry, there are a myriad of applications in nearly all consumer products and industrial processes. Sound quality analysis has generally focused on many automotive aspects, including exterior vehicle passing noise,<sup>25</sup> holistic vehicle sounds and research,<sup>26,27</sup> engine noise, and exhaust noise.<sup>28,29</sup> Sound quality analysis techniques have also been used to improve the acoustic signatures of everything from helicopter main rotor blades and aircraft interior noise<sup>30,31</sup> to hairdryers and vacuum cleaners.<sup>32,33</sup> Computer hard drives, HVAC systems in buildings,<sup>34</sup> construction machinery, and boxes at Italian opera houses<sup>35</sup> have also been improved through psychoacoustic studies.

As sound quality is dependent on the opinions of consumers, a common and effective approach is to form listening juries and survey their responses to different sounds. The primary reason for this method is the disparity between what a sound level meter measures and what an individual reports regarding the loudness of a given sound as well as the instrument’s inability to describe other parameters of sound that a consumer hears and recognizes. This inconsistency results from the nonlinear nature of the human auditory system and the inability of traditional sound measurement techniques to approximate this behavior. A significant drawback to this technique is the requirement of large groups of research subjects to perform the listening tests. However, approximations using empirical equations have allowed the calculation of metrics that closely approximate the human subject responses.

These metrics are grouped into four categories: loudness, sharpness, grating, and tonality. Loudness characterizes the response of the cochlea given the sound’s frequency, bandwidth, and amplitude in decibels. Sharpness is a metric that describes the amount of high-frequency energy present in a sound. It is a weighted average, or area moment, of the loudness with more weight given to frequencies above  $\sim 3000$  Hz. Grating describes two metrics: fluctuation strength and roughness. Fluctuation strength is a metric that characterizes amplitude modulation of the sound that is partially to entirely audibly perceptible. The modulation frequencies that cause the sensation of fluctuation strength are frequencies up to  $\sim 20$  Hz. Roughness represents amplitude modulation of the sound that is too rapid to be even partially audibly perceptible; that is, it is perceived that the sound is modulated but the degree of modulation is unclear to the human ear. Frequencies of modulation that cause a sensation of roughness fall between  $\sim 20$  and 300 Hz. Tonality characterizes the tonal presence in a sound. The questions it answers is: Are there distinct tones present in a seemingly broadband sound? If so, how strong are they? These five metrics can then be combined into a relative-pleasantness measure when comparing two or more sounds. This pleasantness metric, called sensory pleasantness, is convenient as it consolidates these five independent metrics into a single response in the same way a juror does subconsciously.

### 13.1 Mathematical Metrics Procedures

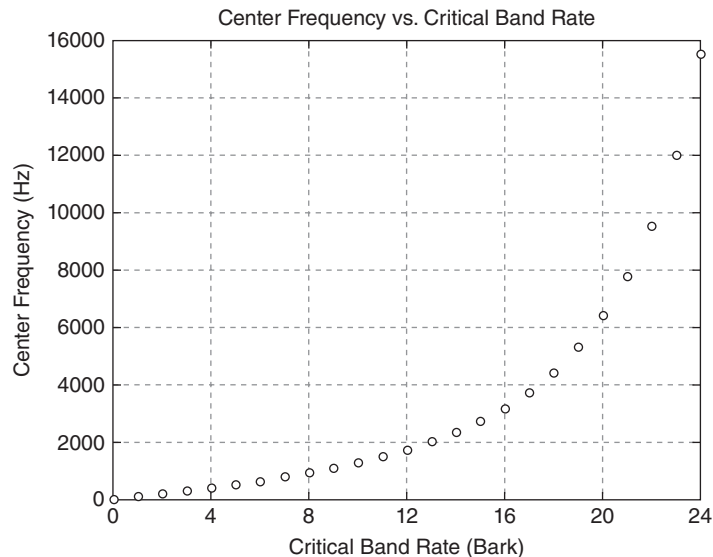
This section continues by presenting an overview of the procedures developed for using mathematical metrics to assess sound quality. The complexity of using humans as instruments for sound quality evaluation has inspired several attempts to quantify human responses, hence creating parameters representing the acts of auditory perception, cognition, and judgment. These parameters can be measured using traditional sound analysis instruments and are quantified based on empirical equations to represent a juror’s response regarding the quality of a sound. The process consists of using standard microphone recordings in either a free field (with frontal

incidence from the noise source) or a binaural field (microphones set up in a dummy head to approximate how the ears receive sound). The measured sound is then processed mathematically to calculate the sound quality metrics. These results can then be compared to jury listener tests and correlated for the given sound source. The result is a process that can accurately predict the sensory pleasantness of a sound with a minimum of human subjects, allowing sound quality analysis to be performed earlier in the product development and often with fewer jurors during the product life cycle. To better understand the mathematical metric method, a few common terms and each of the sound quality metrics will be briefly reviewed (see Refs. 36–38 for more details).

### 13.2 Critical Band Rate

The human auditory systems response is dependent on both the frequency and amplitude of a given sound. Therefore, it is useful to alter the frequency scaling used in sound quality metric calculations. Characteristic frequency bands are defined as bandwidths that produce the same perceived loudness in a tone and in narrowband noise spectrum within that band when the tone is just masked. This scale of critical band rates is used to approximate the frequency dependence of each of the metrics, as it represents the bandpass nature of the auditory system. These critical band rates are given the name *barks*, named after Heinrich Barkhausen, an acoustician whose pioneering work in loudness approximations has produced two subjective-loudness amplitude scales. Figure 36 and Table 10 illustrate the relationship between barks (critical band rate) and center frequencies in hertz. All of the metrics will use critical band rate as the abscissa in all of their plots and calculations.

The following sections give derivations as to the method for calculating each metric as well as examples to help clarify the necessity for each of the individual metrics. The overall combination metric is called sensory pleasantness. Sensory pleasantness describes the holistic result similar to the response a juror would give when evaluating a sound.



**Figure 36** Frequency versus critical band rate.

**Table 10** Frequency to Critical Band Rate for Selected Frequency Values

Frequency (Hz)	Critical Band Rate
100	1
510	5
1,000	8.5
2,000	13
4,800	18.5
10,500	22.5
15,500	24

### 13.3 Loudness

The loudness of a sound is a perceptual measure of the effect of the energy content of sound on the ear. It is related to but not the same as the sound pressure level ( $L_p$ ), a logarithmic scale used to quantify the pressure amplitude of a sound. Loudness, however, is also dependent on the frequency content of a sound. For example, a low-frequency sound such as a 100-Hz tone at 40 dB would be perceived to be significantly quieter to a normal-hearing person than a 1-kHz tone at 40 dB; in fact, the 1-kHz tone would sound nearly four times as loud.

The fundamental assumption of this model of loudness is that it is not a product of spectral lines or obtained from the spectral distribution of the sound directly but that the total loudness is the sum of the specific loudness from each critical band. Empirical studies have shown that this process yields the best equivalent psychoacoustic values.

Hence, using the threshold of quiet as a base or minimum level of excitation, the specific loudness ( $N'$ ) of a sound can be determined as

$$N' = N'_0 \left( \frac{E_{TQ}}{sE_0} \right)^k \left[ \left( 1 + \frac{sE}{E_{TQ}} \right)^k - 1 \right] \quad (87)$$

where  $E_{TQ}$  is the excitation level at the threshold of quiet,  $E_0$  is the excitation level that corresponds to the reference intensity  $I_0 = 10^{-12} \text{ W/m}^2$ , and  $N_0$  is a reference-specific loudness. The variable  $s$ , which is the ratio between the intensity of a just audible test tone and the intensity of broadband noise appearing within the same critical band as the test tone, is determined experimentally. The exponent  $k$  is also determined experimentally.

The result of numerous jury tests using specific tones and broadband noise yields an approximation for the specific loudness in each critical band formulated by Zwicker and Fastl<sup>36</sup> and presented here as

$$N' = 0.08 \left( \frac{E_{TQ}}{E_0} \right)^{0.23} \left[ \left( 0.5 + \frac{E}{2E_{TQ}} \right)^{0.23} - 1 \right] \times \text{sone/bark} \quad (88)$$

The calculation of the total loudness is then a summation of all of the specific loudnesses across all of the critical bands, as shown in the equation

$$N = \sum_{z=1}^{24\text{bark}} N'_z \quad (89)$$

This results in a mathematical representation of the sensation of loudness in the human auditory system. This model accounts for the effects of masking as well as the nonlinear relationship between loudness and frequency. Extensive empirical studies have verified the accuracy of this model and provided a foundation for its use in many applications.

The process for calculating the loudness of a given sound is as follows. Assuming this is being done digitally in a computer, the first step is to convert the amplitude from volts to

a calibrated decibel value. The array of sound pressure levels is subsequently multiplied by a series of 24 one-third-octave filters to decompose the spectral response into the critical bands. The only unknown in the above equations is the excitation level ( $E$ ) of the sound in a particular critical band, where  $E$  is approximated using the sound pressure level. The result is an array that can be interpreted to represent the excitation level of the cochlear duct over the audible spectrum. This array is then summed to give a value representing the total loudness that a listener would perceive when exposed to this sound.

### 13.4 Sharpness

Sharpness is a measure of the high-frequency energy content of a sound. Sharpness is therefore very similar to a weighted loudness ratio, with emphasis on the high-frequency sounds. A plot of the weighting function versus critical band rate is shown in Fig. 37. The unit of measure for sharpness is the *acum*, which is the Latin word for sharp.

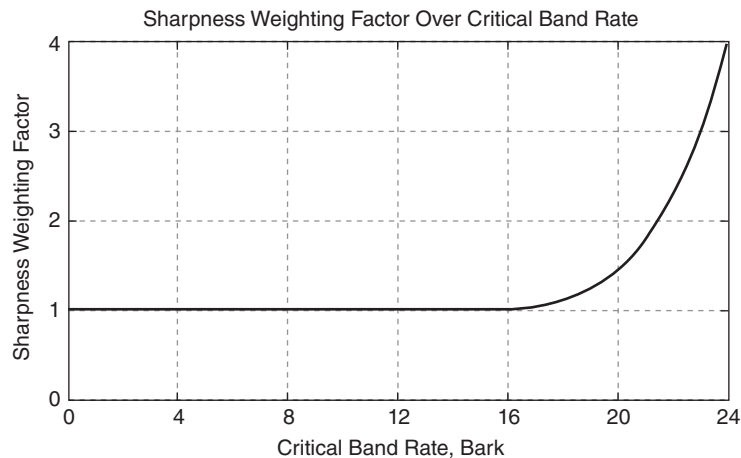
This metric is normalized to the sound pressure level and frequency scales by the following relationship; 1 acum corresponds to a narrowband noise with a bandwidth of one critical band bandwidth wide at a center frequency of 1 kHz with a level of 60 dB. The model for sharpness is simply a weighted first moment of the critical band rate distribution of specific loudness, as seen in Eq. (90), where  $g(z)$  is the weighting function given in Fig. 37:

$$S = 0.11 \frac{\int_0^{24\text{bark}} N'_0 g(z) z dz}{\int_0^{24\text{bark}} N' dz} \quad (90)$$

This model of sharpness takes into account that the sharpness of a narrowband noise increases significantly at high center frequencies. Although the model is relatively simple, empirical data show that the agreement between the model and test subject responses is very good.

### 13.5 Fluctuation Strength

Modulated sounds cause two different kinds of hearing sensations. At low modulation frequencies, fluctuation strength is produced. At higher modulation frequencies, a sensation of roughness is produced. The sensation of fluctuation strength occurs for modulation



**Figure 37** Sharpness weighting factor versus critical band rate.

frequencies between 0 and about 20 Hz. This metric represents the modulation of the sound that is strongly audible.

This leads to a relationship for fluctuation strength. Empirical studies have shown that the total fluctuation for a fluctuating sound is approximated by Zwicker's model, given here as

$$F = \frac{0.008 \cdot \int_0^{24\text{bark}} [4 \log(N'_{\max}/N'_{\min}) \text{ dB}(\text{dB}/\text{bark})] dz}{f_{\text{mod}}/4 \text{ Hz} + 4 \text{ Hz}/f_{\text{mod}}} \quad (91)$$

where  $f_{\text{mod}}$  is the modulation frequency, which is determined for a given sound by examining its spectral content and evaluating what frequency is modulating the sound. The unit for fluctuation strength is *vacil*, which is Latin for oscillate. The relationship describing vacils is that 1 vacil corresponds to a 60-dB, 1-kHz tone that is 100% amplitude modulated at a frequency of 4 Hz.

### 13.6 Roughness

Roughness is similar to fluctuation strength. However, it quantifies the subjective perception of rapid (15–300-Hz) amplitude modulation of a sound. This metric is often considered to be the property of a sound that would be described as grating, as the temporal masking effects of the human auditory system do not allow the total recognition of changes in amplitude at these frequencies. Roughness, like fluctuation strength, is therefore influenced by two main factors: frequency resolution and temporal resolution of the human auditory system.

For very low frequencies of modulation, roughness is also small. For midfrequencies, around 70 Hz, roughness is at its maximum. At very high frequencies, due to the restrictions of the temporal resolution of the human auditory system, roughness falls off. As the value of  $\Delta L$  is also dependent on the critical band rate, a more accurate approximation of roughness would include this dependence, which leads to a fairly accurate proportionality, given as

$$R \sim f_{\text{mod}} \int_0^{24\text{bark}} \Delta L(z) dz \quad (92)$$

Using the boundary conditions of one *asper* (a Latin word meaning rough, which will be the unit for this metric), corresponding to a 60-dB, 1-kHz tone that is 100% amplitude modulated at a frequency of 70 Hz, Zwicker and Fastl<sup>36</sup> propose the following model of roughness, again based on significant empirical data:

$$R = 0.3 \frac{f_{\text{mod}}}{1 \text{ kHz}} \int_0^{24\text{bark}} \frac{20 \log(N'_{\max}/N'_{\min}) \text{ dB}}{\text{dB}/\text{bark}} dz \quad (93)$$

where  $z$  is the critical band rate variable and the parameter dB/bark is simply a unit conversion factor. Similar to the rest of the metrics, roughness is a summation of effects across all of the critical bands.

### 13.7 Tonality

Tonality is concerned with the tonal prominence of a sound (i.e., are there tones present/absent in the sound). Several models of tonality have been developed, each with unique strengths and weaknesses. However, there is one common weakness with each of the currently accepted models of tonality. As the noise floor around the tone is increased in bandwidth to values greater than 100 Hz, the model for describing the tonality falls off at such a rate that it becomes inaccurate. Tonality can also be estimated using fast Fourier transform (FFT) analysis, where a time-aliased (frequency-averaged) FFT versus a non-time-aliased FFT are compared. Plotting the two FFTs in the same window, the position and amplitude of peaks can be compared versus

averaging. If the peaks move, they are not tonal; however, if they remain the same, there is a tone at that frequency. The magnitude of tonality can be estimated from a comparison in amplitude of the “noise floor” versus the peak amplitude of the tone. This estimate is expressed in Eq. (94) as the ratio of amplitudes of the tone and the broadband noise. This is, however, a subjective approach to determining tonality:

$$T \approx \frac{\text{amplitude of tone}}{\text{amplitude of noise floor}} \quad (94)$$

### 13.8 Sensory Pleasantness

The relationship between sensory pleasantness and the sensations of loudness, sharpness, roughness, fluctuation, and tonality can be modeled based on relative values of each of the metrics. The resulting relationship proposed by Zwicker and Fastl<sup>36</sup> is presented in Eq. (95). It should be noted that because the influence of tonality  $T$  is small, the tonality term [the term in the parenthesis in Eq. (95)] reduces to an approximate value of 0.24:

$$\frac{P}{P_0} = e^{-[0.023(N/N_0)]^2} e^{-1.08(S/S_0)} e^{-0.7(R/R_0)} \times \left(1.24 - e^{-2.43(T/T_0)}\right) \quad (95)$$

where  $P_0$ ,  $N_0$ ,  $S_0$ ,  $R_0$ , and  $T_0$  represent the sensory pleasantness, loudness, sharpness, roughness, and tonality of the reference sound to which the current sound is being compared. In other words, the model is a model of relative sensory pleasantness measured against a benchmark sound.

One of the key factors of Eq. (95) is that sensory pleasantness is not dominated by loudness. In fact, the effect of loudness on pleasantness is only strongly evident for sounds with significantly strong loudness values. Zwicker and Fastl<sup>36</sup> suggest that the role of loudness in sensory pleasantness is only important when a sound has a calculated loudness greater than 15 sones.

### 13.9 Limitations

Each sound quality metric is based on using “curve-fit” functions designed around sets of tests using jury listening evaluation of specific tones and developing empirical equations to match the juror response in each of the five categories. They are based on assumptions that approximations for each of the immeasurable factors can be made using one-third-octave filters and weighting functions to represent the cochlear response to auditory inputs. The question then arises as to whether this method can be applied to other sounds in general as they are not specific tones well defined by their frequency and amplitude. This brings to light the importance of at least some jury testing to compare with the results from the sound quality metrics.

## 14 NONLINEAR ACOUSTICS

This section provides an overview of nonlinear acoustics. All the theory and applications treated in this chapter thus far have relied on the fundamental assumption put forth in the wave equation section, which was that the acoustic perturbations are very small ( $|\mathbf{u}|/c_0 \ll 1$ ). This supposition allowed us to keep only the first-order terms in the constitutive equations. However, there are certain situations in which this small-amplitude assumption breaks down and second-order (nonlinear) phenomena result. This section is a brief introduction into nonlinear acoustics theory and applications. It concludes with the description of data analysis tools that can be used to help in characterizing nonlinear phenomena.

14.1 Theory

It is first relevant to consider the basic effects of nonlinearity. In a linear system, an amplitude and phase change may occur, as is shown in Fig. 38, but the acoustic excitation remains at frequency  $\omega$ . In a quadratically nonlinear system, however, such as  $y = x + x^2$  shown in Fig. 39, the output contains energy not only at  $\omega$  but also at zero frequency [direct current (dc)] and at  $2\omega$ . If an input waveform that contains energy at  $\omega_1$  and at a greater frequency  $\omega_2$  is passed through  $y = x + x^2$ , trigonometric relationships demonstrate that the output of the nonlinear system will contain energy at dc,  $\omega_1, \omega_2, 2\omega_1, 2\omega_2, \omega_1 + \omega_2$ , and  $\omega_2 - \omega_1$ . The nonlinear generation of harmonics is called harmonic distortion and generation of sum and difference frequencies is called intermodulation distortion.

There are other classes of nonlinearities (e.g., cubic), but quadratic nonlinearities are emphasized here because they appear in the constitutive equations for sound propagation before they are neglected in first-order (i.e., linear) approximations. These nonlinearities culminate in an amplitude-dependent sound speed, expressed for one-dimensional propagation as

$$c = c_0 + \beta u \tag{96}$$

where  $u$  is the particle velocity,  $c_0$  is the small-signal sound speed, and  $\beta$  is the coefficient of nonlinearity in the fluid ( $\beta = 1.201$  in air). For general fluids or biological tissues,  $\beta = 1 + B/2A$ , where  $B/A$  is the “parameter of nonlinearity” of the medium. Measured values of  $B/A$  in a few other media are listed in Table 11. The tabulated values reveal that most media are significantly more nonlinear than air.

The significance of Eq. (96) is that the portions of the waveforms with positive particle velocities (or pressures) travel faster than those with negative particle velocities or pressures. For  $|\mathbf{u}/c_0| \ll 1$ ,  $c \approx c_0$  and the linear approximation is recovered. If we consider an initially sinusoidal waveform that propagates as a plane wave, the waveform will eventually steepen

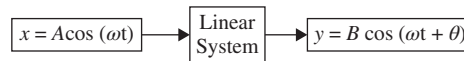


Figure 38 Example of linear system that induces amplitude and phase change.

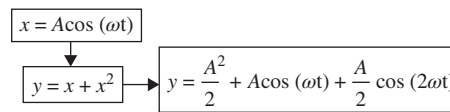


Figure 39 Example of quadratic nonlinear system that produces dc and  $2\omega$ .

Table 11 Parameter of Nonlinearity for Selected Media

Medium	$B/A$
Distilled water, 20°C	5.0
Seawater, 20°C	5.25
Liquid nitrogen, 90 K	9.00
Human liver, 30°C	7.6 ( $\pm 0.8$ )

to the point that an acoustic shock forms. This distance is known as the shock formation or discontinuity distance and may be written as

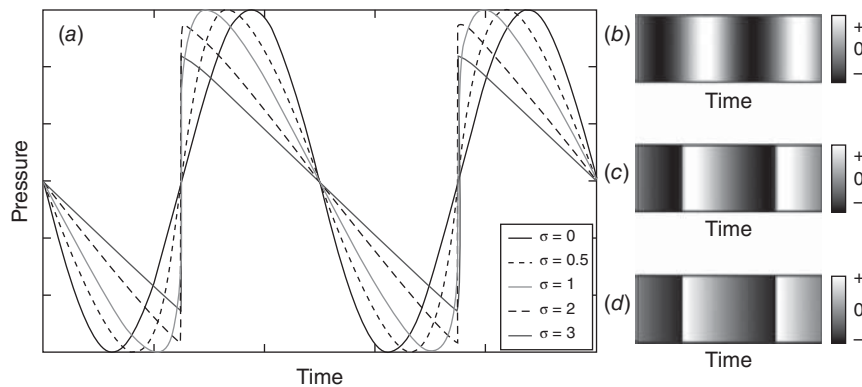
$$\bar{x} = \frac{\rho_0 c_0^2}{\beta p_{\text{init}} k} \quad (97)$$

where  $p_{\text{init}}$  is the pressure amplitude of the initial sinusoid. We can also express propagation distance in terms of  $\bar{x}$  and define a dimensionless distance,  $\sigma = x/\bar{x}$ . The nonlinear evolution of an initially sinusoidal waveform is shown in Fig. 40 between  $\sigma = 0$  and  $\sigma = 3$ . The time waveforms are expressed both as traditional pressure waveform traces in Fig. 40a and as longitudinal wave representations in Figs. 40b–d. At  $\sigma = 1$  a discontinuity has just formed, and by  $\sigma = 3$  the wave is essentially a fully developed sawtooth wave. The waveform steepening represents a transfer of energy from  $\omega$  to higher harmonics that can eventually be expressed as the Fourier series of a sawtooth waveform that, in principle, contains an infinite number of harmonics to account for the discontinuous slope at the shock front.

The shock formation distance is an important parameter in determining the degree of nonlinearity of the propagation. However, another essential phenomenon to consider is the absorptive losses that occur in the propagation. The losses, which increase as a function of frequency, would “compete” with the nonlinear steepening that transfers energy to high harmonics. The importance of nonlinearity relative to absorption is expressed in the Gol’dberg number, a dimensionless quantity that can be written for an initially sinusoidal plane wave in a thermoviscous medium as

$$\Gamma = \frac{1}{\alpha \bar{x}} \quad (98)$$

If  $\Gamma \gg 1$ , absorption and/or the shock formation distance is very small, which means that the propagation is highly nonlinear and that shocks will form. On the other hand, if  $\Gamma \ll 1$ , absorption and/or  $\bar{x}$  is very large, which means that nonlinear waveform steepening is negligible. Finally,  $\Gamma \sim 1$  represents an intermediate case, where steepening is likely, but an acoustic shock may not develop as the higher harmonic energy is absorbed. As a final note, the above description of the Gol’dberg number is only qualitative for any acoustic waveform besides a pure sinusoid in a thermoviscous medium; however,  $\Gamma$  demonstrates qualitatively the processes (e.g., amplitude, frequency, absorption) that determine when nonlinearity plays a significant



**Figure 40** (a) Nonlinear evolution of sinusoidal waveform into sawtooth wave. Longitudinal wave representation at (b)  $\sigma = 0$ , (c)  $\sigma = 1$ , and (d)  $\sigma = 3$ .



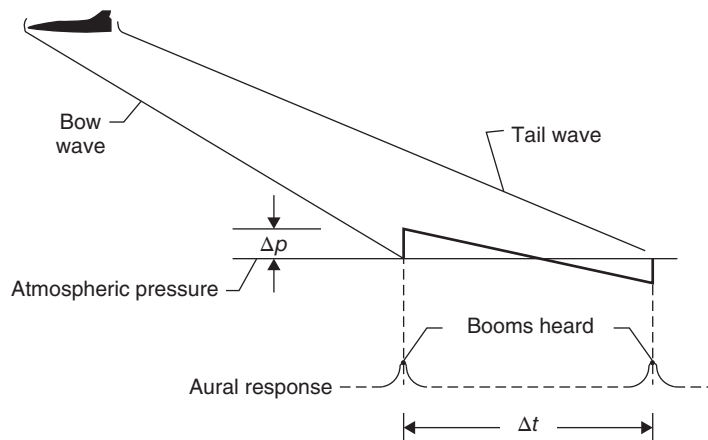
role in sound propagation. In all cases, as propagation occurs, the effective Gol'dberg number gradually lessens as a function of distance as acoustic amplitudes are reduced through losses and possibly geometric spreading. This will eventually cause steepened waveforms to gradually unsteepen as the rate of absorption at high frequencies begins to exceed the nonlinear energy transfer rate.

## 14.2 Radiation Pressure and Streaming

Although their derivations are beyond the scope of this discussion, there are physical phenomena directly related with the nonlinear energy transfer to dc. The first is called acoustic streaming, which is a mean velocity that is set up in the fluid by the acoustic fluctuations. The second phenomenon is radiation pressure, which is a time-averaged pressure exerted on an object in the fluid or on a boundary. (Acoustic radiation pressure is analogous to the radiation pressure exerted by light waves.) One or both of these phenomena can be very relevant to applications of nonlinear acoustics, particularly in enclosed systems. For more detailed discussions, see Refs. 39 and 40.

## 14.3 Applications of Nonlinear Acoustics

Nonlinearity is often a factor in the atmospheric propagation of high-amplitude sources. For example, the nonlinear evolution of sonic boom waveforms is a problem that has been investigated in a variety of ways. The pressure fluctuations created by the supersonic aircraft travel at different speeds, and the shocks that form often coalesce into two single shocks that form a wave called an N wave (see Fig. 41). The propagation of noise from explosions is also nonlinear, but unlike the sonic boom, there is typically a single shock front associated with the blast waveform. The last example of nonlinear atmospheric propagation is the noise radiated by military fighter jets and by rockets. The nonlinear interactions between spectral components as the shaped broadband noise waveform propagates result in a transfer of energy to high frequencies. The waveform steepening can lead to the formation of significant acoustic shocks. The excess high-frequency energy (relative to that linearly predicted) and its arrival in the form of shocks at discrete instances in time appear to have a significant impact on human perception of these sounds.<sup>41</sup>



**Figure 41** N wave, characteristic of sonic booms.<sup>42</sup>

Ultrasound is used in many applications of nonlinear acoustics that include the fields of audio, biomedical, and industrial acoustics. Parametric arrays have been investigated for audio applications for several decades. In its simplest form, the parametric array uses high-intensity ultrasonic transducers configured so as to produce a narrow primary beam of sound (in general, the larger the dimensions of the array, the narrower the beam). The array is driven at two closely spaced ultrasonic frequencies,  $\omega_1$  and  $\omega_2$ , at high enough amplitudes to produce the difference frequency,  $\omega_2 - \omega_1$ . For proper selection of source frequencies,  $\omega_2 - \omega_1$  will be in the audio range. Harmonics and sum frequencies are also generated, but atmospheric absorption at any of these ultrasonic frequencies is much greater than at the difference frequency. Consequently, the parametric array is unique in its ability to generate a narrow beam of low-frequency sound. Potential applications include audio complements to displays in museums, individualized stereo systems in vehicles, and other situations where spatially narrow audio is desired.

Applications of nonlinear acoustics in biomedical ultrasound are many, but a few are briefly summarized. The harmonic imaging technique in diagnostic ultrasound relies on harmonic distortion as waves propagate through human tissue (which is generally a nonlinearity-prone medium). The ultrasonic transducer transmits a wave at  $\omega$ , but then the ultrasonic sensors “listen” for the scattered signal at  $2\omega$ . The result is better spatial resolution of the tissue to be imaged. Other applications of nonlinear ultrasound include for high-intensity focused ultrasound (HIFU). Shock wave lithotripsy uses focused ultrasonic waves that nonlinearly steepen into a shock wave to break up kidney stones. Although the physical mechanisms by which this occurs are still being researched, it is believed that cavitation, or the formation and subsequent violent collapse of bubbles due to large pressure changes in a fluid, plays a significant role in breaking up of the stones. Because HIFU can lead to significant heating of internal tissue (which is ordinarily avoided), other applications of HIFU that are being investigated include ultrasonic treatment for cancer and stoppage of internal bleeding by wound cauterization.

Industrial applications of high-intensity ultrasound include ultrasonic cleaning, ultrasonic welding, and nondestructive evaluation (NDE).<sup>43</sup> There is a wealth of information on each of these topics that can be consulted. However, due to the brevity of the discussion, general principles of operation will be given. An ultrasonic cleaner is a fluid-filled chamber that is activated using one or more ultrasonic transducers. Although all the physical mechanisms behind the cleaning are not totally understood, microjets created by cavitating bubbles are believed to be largely responsible for the cleaning. One principal advantage of ultrasonic cleaning is that milder chemicals may be used in the cleaning process than other cleaning techniques. The use of ultrasonic cleaning is widespread and can be readily found in, for example, automotive, pharmaceutical, and medical applications.

Ultrasonic welding, which has been around since the 1960s, utilizes directional, high-intensity sound energy with typical frequencies ranging from 20 to 40 kHz. Although ultrasonic welding is most extensively used in the welding of plastics, it is also used in small-scale welding of metals (e.g., wires). The principle of ultrasonic welding is different for thermoplastics and metals. In thermoplastics, as the materials are pressed together and ultrasound is applied, the acoustic energy absorbed by the materials is transformed into heat, resulting in high temperatures in a localized area. This causes localized melting of the plastic surfaces and the formation of a bond. In ultrasonic welding of metal surfaces, studies have shown that the heat generated is insufficient to melt the metals at the interface. Rather, the mechanism is due to abrasive shear forces excited at the interface between the metals that disperse oxides and other contaminants. If the exposed metal surfaces are held together with sufficient pressure, a solid-state bonding takes place. Because the temperatures involved in an ultrasonic weld are relatively low, embrittlement of the metals, which can occur with other welding techniques, is avoided.

Finally, ultrasound is a viable method within the broad field of NDE for testing material properties. Although some ultrasonic NDE, which typically involves frequencies in the megahertz range, employ linear acoustic techniques and processing, nonlinear phenomena can

be used to readily identify defects in solids. Cracks and other defects exhibit high nonlinearity such that the amount of harmonic and intermodulation distortion increases significantly. Therefore, harmonic imaging or measurements of the amount of harmonic and intermodulation distortion in the scattered wave can be used to assess the properties of the solid. Examples of ultrasonic NDE include weld inspection, pipe wall inspection, assessment of concrete strength, and even recent examinations of the space shuttle wings and external fuel tanks.

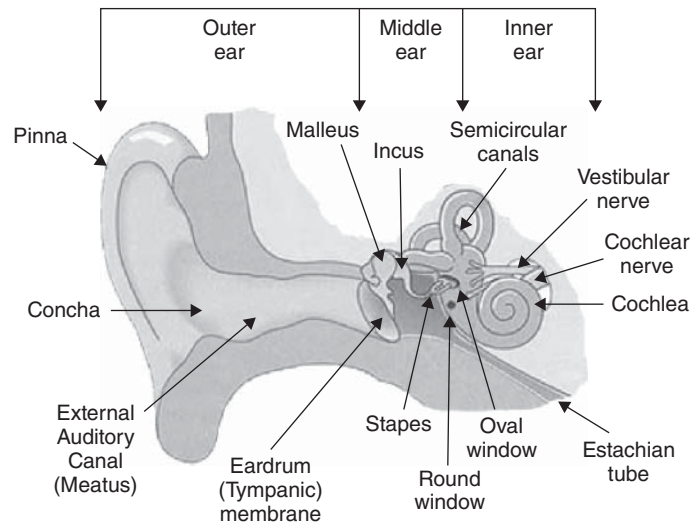
## 15 THE HUMAN EAR AND HEARING

The human auditory system is complex from the standpoint of both how the nervous system responds to auditory inputs and the physical makeup of the human ear. This section first will discuss the structure of the ear, outlining the physical aspects of how humans hear, followed by a brief discussion of the nervous system response to auditory inputs and the role of the brain in hearing.<sup>44</sup>

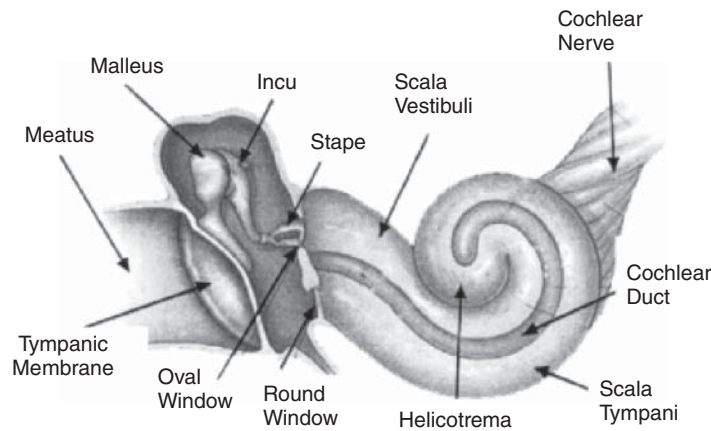
The human ear can be subdivided into three main parts, as illustrated in Fig. 42: the outer, middle, and inner ear. The outer ear consists of the pinna, which serves as a horn that collects sound and directs it into the auditory canal. The pinna is comparatively ineffective in humans. The auditory canal is essentially a straight tube about 0.7 cm in diameter and 2.5 cm long, open at one end and closed at the other, as seen in Fig. 43 in the section labeled outer ear.

There are resonances associated with this tube, the lowest resonance occurring at about 3 kHz. At this resonance frequency, the sound pressure level is about 10 dB higher at the closed end than at the open end. This is the most sensitive frequency region of the ear. Above this frequency, resonance phenomena can be observed, but resonance peaks tend to be relatively broad and flat.

The outer ear is connected to the middle ear by the tympanic membrane, commonly known as the eardrum. This membrane forms a flattened cone with its apex facing inward. It is flexible in the center and attached to the end of the auditory canal at its edges. The middle ear is an air-filled cavity, with a volume of approximately 2 cm<sup>3</sup>, which contains three ossicles (bones): the malleus (hammer), the incus (anvil), and the stapes (stirrup). These bones form a mechanical linkage to amplify the force transmitted to the inner ear from the outer ear. The stapes is



**Figure 42** Diagram of human ear.

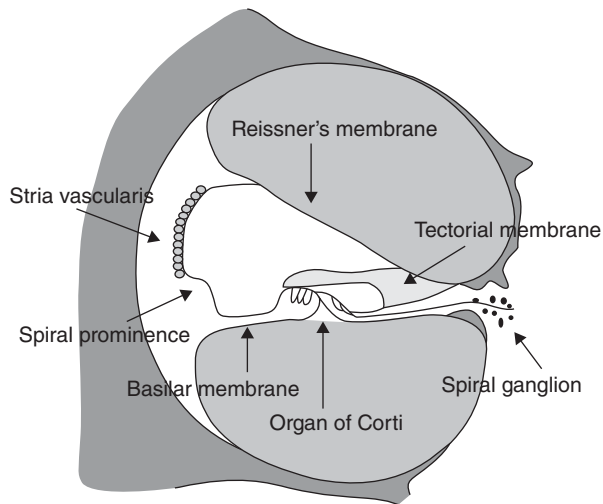


**Figure 43** Middle-to-inner-ear transition.

connected to the inner ear via the “oval window.” The area ratio of the eardrum to the oval window is about 30:1. This system combines to create an approximate impedance match between the auditory canal and the inner ear. This is controlled to some extent to protect the ear from high-intensity sounds, known as the acoustic reflex. Acoustic reflex takes about one-half of a millisecond to respond. Therefore, it is ineffective at protecting the ear from impulsive noise, for example, explosions, sonic booms, and gunshots. The middle ear is connected to the throat via the eustachian tube, also shown in Fig. 42. The purpose of the eustachian tube is to equalize the pressure on both sides of the eardrum. Normally it is closed, but it opens during yawning and swallowing.

The inner ear contains three significant parts, the vestibule (entrance chamber), semicircular canals, and the cochlea, as illustrated in Fig. 43. The semicircular canals give humans their sense of balance and do not affect hearing. The vestibule is connected to the middle ear through the oval window and the round window. Both windows are sealed to prevent the inner ear fluids from escaping. Bone surrounds the remainder of the inner ear. The cochlea is a tube with an approximately circular cross section, which is curled in a shape similar to a snail shell. The tube makes approximately two and one-half turns with a length of approximately 3.5 cm. The total volume of the cochlear tube is approximately  $0.05 \text{ cm}^3$ , with the cross section decreasing from entrance to termination. However, the average diameter is approximately 1.3 mm. The cochlear tube is divided by the cochlea partition into two channels, the upper gallery (scala vestibule) and the lower gallery (scala tympani). The two galleries are joined at the apex by the helicotrema. The other ends of the galleries are connected to the oval (upper gallery) and round (lower gallery) windows.

The cross section of the cochlear duct is presented in Fig. 44. There is a “bony ledge” that projects (from the right in the figure) into the fluid-filled tube, which carries the auditory nerve. At the termination of the bony ledge, the nerve fibers enter the basilar membrane, which continues across the tube and is attached to the spiral ligament on the opposite side of the tube. Above the basilar membrane is the tectorial membrane, which projects into the fluid in the scala media. Reissner’s membrane (vestibular membrane) runs diagonally across the tube from the bony ledge to the opposite wall, forming the pie-shaped cochlea sack, which is completely sealed. The cochlea sack is filled with endolymphatic fluid and the two galleries are filled with perilymphatic fluid. The organ of Corti is attached to the top of the basilar membrane. It contains four rows of hair cells, which span the entire length of the cochlear duct, giving roughly 30,000 cells. Several small hairs extend from each hair cell to the undersurface of the tectorial membrane.



**Figure 44** Cross section of cochlear ducts.

When the ear is exposed to a sound, the eardrum's vibration is transmitted to the inner ear via the bones in the middle ear. The fluid of the inner ear in the upper gallery is disturbed by the motion of the stapes against the oval window. This fluid disturbance travels down the length of the upper gallery, through the helicotrema, then back down the lower gallery to the round window. The round window acts like a pressure release termination to the tube. The basilar membrane is driven by this fluid motion into highly damped motion with the peak amplitude increasing slowly with distance from the oval window. Once it reaches a maximum, it decreases rapidly. The location of the maximum amplitude is a function of frequency, with low frequencies causing the peak to occur close to the helicotrema and high frequencies reaching a peak much closer to the oval window. It is because of this behavior that low frequencies mask higher frequencies better than vice versa. As the organ of Corti is attached to the basilar membrane and the tectorial membrane is attached to the bony ledge, relative motion between the two flex the hair follicles, which excite the nerve endings attached to these hair cells. This in turn creates an electrical impulse that is sent up the nerve fibers. As may be implicated by the complex physical nature of the inner ear, the individual nerves do not fire at the same frequency as that of the excitation sound. In fact, the nerves tend to fire in a quasi-random frequency that is dependent upon the stress on the individual hair cells, which is more closely related to the sound intensity. These pulses then travel to the auditory center in the brain. Here a complex decoding and processing process formulates the mental "picture" of the sound.

### 15.1 Psychoacoustic Effects

From the previous discussion, it is apparent that when a sound excites the basilar membrane, a small group of cells at the point of maximum deviation has the maximum excitation, causing it to send the largest electrical impulse up the nerve, whereas the neighboring cells to either side of this point are also disturbed but to a lesser degree. As a result, they also fire impulses, but not as strongly. Each point of the basilar membrane is the point of maximum excitation for some frequency but will also join in the excitation when a different frequency excites one of its neighbors. Therefore, a sound at a given frequency excites nerves belonging to a range of frequencies. Any sound at a high level centered at a given frequency raises the hearing level threshold for

frequencies in its vicinity. This phenomenon of some sounds rendering other sounds inaudible (or less audible) is termed masking. Studies have shown that tones or narrowband noise at a given frequency raise the audibility threshold of tones at neighboring frequencies. A broadband noisy sound, like a vacuum, a loud ventilation system, or a jet airplane engine, can therefore raise the hearing threshold of just about everything.<sup>44</sup>

The segment of the basilar membrane that joins the excitement is called the critical band. The frequency range spanned by this section is called the critical bandwidth. It is important to note the difference between the two because they do not maintain a constant relationship. A frequency of 350 Hz stimulates a band of cells having a bandwidth of 100 Hz (300–400 Hz). However, a frequency of 4 kHz excites a critical band of cells having a bandwidth of 700 Hz (3.7–4.4 Hz). Thus, the critical bandwidth is much wider for higher frequencies than it is for lower frequencies.

Precisely where along the membrane this point of excitement occurs is another important aspect of the auditory system. As the frequencies of single-tone or narrowband noise are doubled, the point of excitement moves in equal increments. An equal length of basilar membrane is traversed to reach the points excited by 500 Hz, 1 kHz, 2 kHz, 4 kHz, 8 kHz, and so on. This corresponds to the human perception of pitch; individuals hear doubling of frequencies as a change of an octave. Other musical intervals are also based on the ratio of any two given frequencies, not the absolute distance between them. For example, a perfect fifth above some note is always a frequency ratio of 3 : 2: the E above A (440 Hz) is 660 Hz, an increase of 220 Hz and a ratio of 3 (660 Hz) to 2 (440 Hz). An additional fifth above 660 Hz is not, however, at 880 Hz (660 + 220), but rather at 990 Hz ( $660 \times \frac{3}{2}$ ). Such a relationship, based on multiplication rather than addition, is logarithmic rather than linear.

From the example above, it is evident that the logarithmic relationship of the basilar membrane to the spectrum applies to the perception of pitch for human beings. A logarithmic relationship is also behind the changes in the sensitivity to frequency differences over the frequency spectrum. When two tones are played consecutively, the minimum frequency difference they must have in order for listeners to notice that difference is called the “just noticeable difference.” The just noticeable difference depends on a variety of factors, including frequency range and suddenness of the change. However, the just noticeable difference below 1 kHz is about 3 Hz, with the just noticeable difference for tones from 1 to about 4 kHz being 0.5% of the frequency. The just noticeable difference becomes larger above 5 kHz. Sine wave melodies transposed into that range tend to melt into a bunch of screaming, high beeps.

The auditory system is not completely egalitarian, however. Thus, the minimum sound pressure level required for a sound to be audible, called the threshold of audibility, is different for different frequencies. Lower frequencies must be produced at much greater sound pressure levels than higher frequencies in order for them to be perceived as having equal loudness, if perceived at all. The threshold is lowest for frequencies in the region of greatest importance for speech—hence giving the finest resolution of amplitude differences in this range. High frequencies excite the basilar membrane at points near the oval window, leaving points that are more distant relatively undisturbed. Low frequencies, however, excite the membrane at points more distant from the oval window, creating waves in the membrane that have to travel past those closer points excited by higher frequencies. Therefore, when high and low frequencies are heard together, the low frequencies can, in some circumstances, interfere with the high frequencies.

In review, the main psychoacoustic effects are masking, critical bands, critical bandwidths, pitch, threshold of audibility, and just noticeable differences. Masking is caused by a high level of excitation at a particular point along the basilar membrane. This high level of excitation results in a change in the threshold of audibility for frequencies in the neighborhood of the masking tone. Critical bands are the bands of frequencies that humans recognize as an interference zone, which is nominally one-third-octave frequency band spacing. Pitch is related to the critical bands and the location along the basilar membrane where the maximum excitation



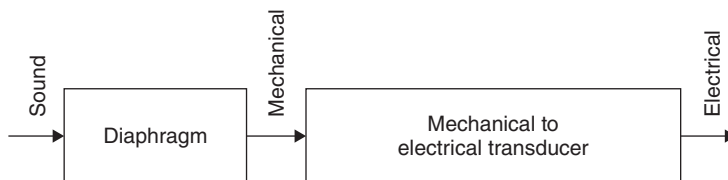
occurs. Threshold of audibility is the sound pressure level where a tone is just audible; it is important to reiterate that it is not equal for all frequencies. This, however, is good because it prevents humans from hearing their own heartbeat and other low-frequency, low-amplitude sounds that would be disturbing but allows them to hear the spoken word very well. Just noticeable differences are the distances between two frequencies that are perceivable. It is this psychoacoustic effect, as well as that of masking, that is the basis of the principles of music compression for the MP3 format. The tones that would be masked or are not noticeably different from another simultaneously played tone are removed, allowing the file size to be greatly reduced without sacrificing acoustic quality.

## 16 MICROPHONES AND LOUDSPEAKERS

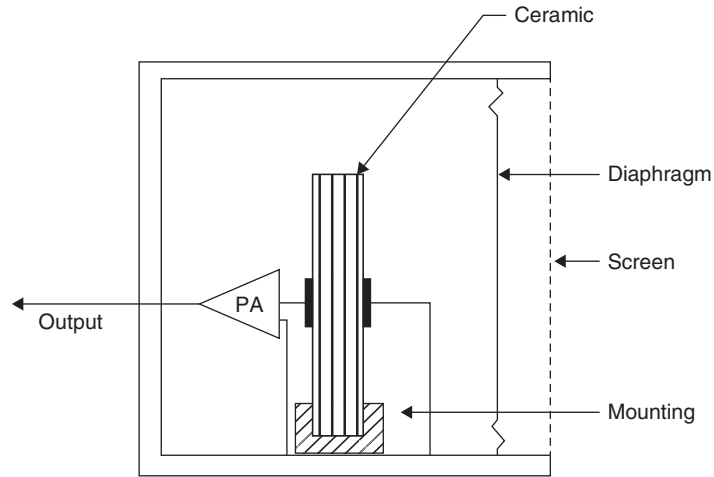
A microphone is a transducing device that converts acoustic energy into electrical energy in the form of a time-varying voltage. The voltage should fluctuate so as to accurately represent the vibration of the air. The basic operation of a microphone can be represented as shown in Fig. 45. Sound impinging on a diaphragm causes the diaphragm to vibrate. The mechanical motion of the diaphragm is coupled to the transducer, producing the varying voltage. The original acoustic vibrations are thus preserved in the form of a time-varying voltage.

A microphone can be classified as pressure sensing, velocity sensing, or some combination of these two types. In the pressure sensing type sound is allowed to strike only one side of the diaphragm. Thus, the diaphragm is sensitive to pressure changes. Pressure microphones are said to be omnidirectional or nondirectional because they respond to sound coming from any direction. In velocity microphones both sides of the diaphragm are exposed to the sound. Velocity microphones respond mostly to sounds striking one side or the other of the diaphragm in a head-on fashion. Sound approaching the edge of the diaphragm exerts equal but oppositely directed pressures on each side of the diaphragm so that no motion is produced. A velocity microphone is said to be bidirectional.

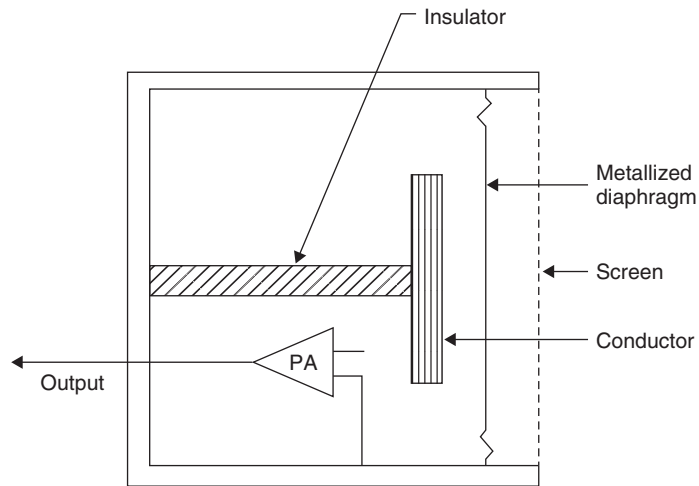
The piezoelectric effect is the transducing principle employed in crystal microphones and ceramic microphones. Ceramic materials are more commonly used because they are less sensitive than crystal materials to mechanical shock, humidity, and temperature. Typical elements of a ceramic microphone are shown in Fig. 46. One end of the ceramic is attached to the microphone casing and the other end is coupled to the diaphragm by a drive pin. Conducting material is deposited on the two surfaces of the ceramic. When the diaphragm moves, the ceramic element is bent and a positive or negative (depending on the direction of bending) voltage appears on the electrical lead attached to one side of the ceramic. The principal disadvantage of a ceramic microphone is that relatively small output voltages are obtained for normal acoustic pressures. However, in modern designs this disadvantage is usually overcome by mounting a small preamplifier in the microphone casing. Microphones of this type have a fairly wide (20 Hz–10 kHz) but somewhat uneven frequency response. They are small and relatively inexpensive and are widely used in hearing aids, public address systems, portable sound equipment, and tape recorders.



**Figure 45** Basic processes in a microphone.



**Figure 46** Elements of a ceramic microphone.

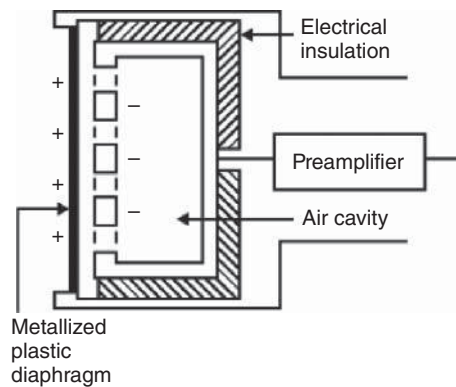


**Figure 47** Elements of a condenser microphone.

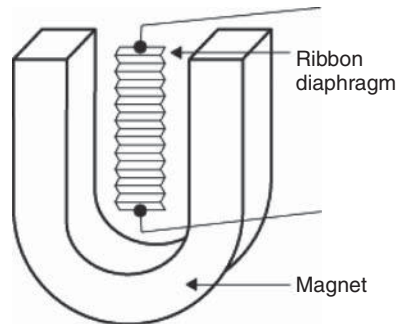
Typical elements of a *condenser microphone* are shown in Fig. 47. One conducting plate is fixed to the microphone casing, although it is electrically isolated from the casing. A metal or metallized plastic diaphragm is used and acts as the second (and movable) conducting plate of the capacitor. When the diaphragm vibrates, an oscillating voltage appears on the electrical leads attached to the plates. The principal disadvantage of these microphones is the need to have a bias voltage (200–400 V) across the plates and a preamplifier in close proximity to the plates. Condenser microphone designs have typically incorporated a preamplifier in the microphone casing. Condenser microphones are used in research, to produce high-fidelity recordings, and in hearing aids and portable sound equipment.

*Electret condenser microphones* (see Fig. 48) are now in wide use because they offer the advantages of a condenser microphone without the disadvantage of needing a polarizing





**Figure 48** Elements of an electret condenser microphone.



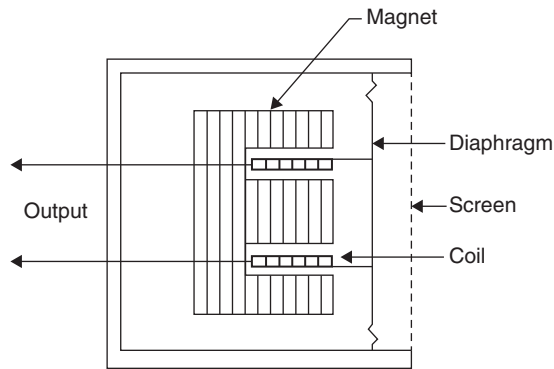
**Figure 49** Elements of a ribbon microphone.

voltage. The diaphragm consists of an electret plastic foil that has been permanently electrically charged and overlaid with a thin metallic layer. The electret condenser microphone typically employs a preamplifier. It is slightly less sensitive than the condenser microphone.

A *ribbon microphone* (see Fig. 49) consists of a very thin metallic ribbon set in a magnetic field. A current is caused to flow in the ribbon as it is pushed and pulled back and forth in the magnetic field by acoustic pressures. Maximum response occurs when the pressure is perpendicular to the face of the ribbon. Pressure coming from the edge pushes oppositely on the two sides of the ribbon and so little response results. A ribbon microphone is bidirectional in response and is an example of a velocity microphone.

A *dynamic microphone* has a coil of wire attached to its diaphragm as shown in Fig. 50. The transducing element is a coil that is free to move between the poles of a magnet. The electrons in the coil move with the coil and experience a force (as described by the magnetic force law) that produces a varying electric voltage across the ends of the coil. Dynamic microphones are capable of a relatively high power output. They are rugged and capable of a broad frequency response over a wide dynamic range. Because they are able to withstand the high-intensity sound levels often associated with popular music, they are widely used for live performances and for recording sessions.

A *loudspeaker* is a transducing device that converts electrical energy into acoustic energy. One common type of loudspeaker is the direct radiator dynamic loudspeaker. It operates on the same principle as the dynamic microphone, only in the opposite sense. Figure 50 illustrates



**Figure 50** Elements of a dynamic microphone.

a dynamic loudspeaker as well as a dynamic microphone. A voltage source is connected to a coil of wire situated in the magnetic field of a permanent magnet. A varying voltage produces a varying current in the coil. The coil experiences a force (because a magnetic field is present) that causes the coil to vibrate. The coil is attached to a diaphragm so the motion of the coil “drives” the diaphragm, causing the air to vibrate. Because of the simplicity of construction, the small space requirements, and the fairly uniform frequency response, this type of speaker is the most widely used.

## REFERENCES

1. F. V. Hunt, *Origins in Acoustics, The Science of Sound from Antiquity to the Age of Newton*, Acoustical Society of America, Woodbury, NY, 1992.
2. C. E. Speaks, *Introduction to Sound: Acoustics for the Hearing and Speech Sciences*, 3rd ed., Singular Publications Group, San Diego, CA, 1999.
3. D. R. Raichel, *The Science and Applications of Acoustics*, Springer, New York, 2000.
4. International Organization for Standardization (ISO), Geneva, Switzerland.
5. H. Fletcher, and N. A. Munson, “Loudness; Its Definition, Measurement, and Calculation,” *J. Acoust. Soc. Am.*, **5**, 82–108, 1933.
6. R. L. Woods, and K. L., Lawrence, *Modeling and Simulation of Dynamic Systems*, Prentice-Hall, Englewood Cliffs, NJ, 1997.
7. L. E. Kinsler, A. R. Frey, A. R. Coppens, and J. V. Sanders, *Fundamentals of Acoustics*, 4th ed., Wiley, New York, 2000.
8. O. Blackstock, *Fundamentals of Physical Acoustics*, Wiley, New York, 2000.
9. A. D. Pierce, *Acoustics: An Introduction to Its Physical Principles and Applications*, Acoustical Society of America, Woodbury, NY, 1989.
10. H. E. von Gierke, and W. Dixon, “Criteria for Noise and Vibration Exposure,” in *Handbook of Acoustical Measurements and Noise Control*, 3rd ed., C. M. Harris (Ed.), Acoustical Society of America, Woodbury, NY, 1998.
11. W. Melnick, “Hearing Loss from Noise Exposure,” in *Handbook of Acoustical Measurements and Noise Control*, 3rd ed., C. M. Harris (Ed.), Acoustical Society of America, Woodbury, NY, 1998.
12. C. W. Nixon, and E. W. Berger, “Hearing Protection Devices,” in *Handbook of Acoustical Measurements and Noise Control*, 3rd ed., C. M. Harris (Ed.), Acoustical Society of America, Woodbury, NY, 1998.
13. Harris, C. M. (Ed.), *Handbook of Acoustical Measurements and Noise Control*, Acoustical Society of America, Woodbury, NY, 1998.
14. C. Hansen, *Noise Control: From Concept to Application*, Taylor & Francis, London, 2005.

15. S. M. Kuo, and D. R. Morgan, *Active Noise Control Systems: Algorithms and DSP Implementations*, Wiley, New York, 1996.
16. S. D. Sommerfeldt, "Multi-Channel Adaptive Control of Structural Vibration," *Noise Control Eng. J.*, **37**(2), 77–89, 1991.
17. W. J. Strong, and G. R. Plitnik, *Music Speech High-Fidelity*, 2nd ed., Soundprint, Provo, UT, 1983.
18. E. M. Salomons, *Computational Atmospheric Acoustics*, Kluwer Academic, Dordrecht, 2001.
19. J. E. Piercy, and G. A. Daigle, "Sound Propagation in the Open Air," in *Handbook of Acoustical Measurements and Noise Control*, 3rd ed., C. M. Harris (Ed.), Acoustical Society of America, Woodbury, NY, 1998.
20. J. P. Raney, and J. M. Cawthorn, "Aircraft Noise," in *Handbook of Acoustical Measurements and Noise Control*, 3rd ed., C. M. Harris (Ed.), Acoustical Society of America, Woodbury, NY, 1998.
21. S. Fidell, D. S. Barber, and T. J. Schultz, "Updating a Dosage Effect Relationship for the Prevalence of Annoyance Due to General Transportation Noise," *J. Acoust. Soc. Am.*, **89**, 221–233, 1991.
22. J. Blauert, and U. Jekosch, "Sound–Quality Evaluation—A Multi-Layered Problem," *Acustica*, **83**(5), 747–753, 1997.
23. J. Blauert, "Product-Sound Assessment: An Enigmatic Issue from the Point of View of Engineering," *Proc. Internoise*, **94**(2), 857–862, 1994.
24. R. Guski, "Psychological Methods for Evaluating Sound-Quality and Assessing Acoustic Information," *Acustica*, **83**(5), 765–774, 1997.
25. J. Blauert, and U. Jekosch, "A Semiotic Approach towards Product Sound Quality," *Proc. Internoise*, **96**, 2283–2286, 1996.
26. R. H. Lyon, "Designing for Sound-Quality," *Proc. Internoise 94J-Yokohama*, **2**, 863–868, 1994.
27. D. Vastfjall, M. A. Gulbol, and M. Kleiner, "Wow, What Car Is That?": Perception of Exterior Vehicle Sound Quality," *Noise Control Eng. J.*, **51**(4), 253–261, 2003.
28. N. C. Otto, B. J. Feng, and G. H. Wakefield, "Sound Quality Research at Ford—Past, Present and Future," *Sound Vib.*, **32**(5), 20–24, 1998.
29. M. Ishihama, "Sound Quality R and D in the Japanese Automotive Industry," *Noise Control Eng. J.*, **51**(4), 191–194, 2003.
30. N. C. Otto, and G. H. Wakefield, "Design of Automotive Acoustic Environments. Using Subjective Methods to Improve Engine Sound Quality," *Proc. Human Factors Soc.*, **1**, 475–479, 1992.
31. A. Gonzalez, M. Ferrer, M. DeDiego, G. Pinero, and J. J. Barcia-Bonito, "Sound Quality of Low-Frequency and Car Engine Noises after Active Noise Control," *J. Sound Vib.*, **265**(3), 663–679, 2003.
32. K. S. Brentner, B. D. Edwards, R. Riley, and J. Schillings, "Predicted Noise for a Main Rotor with Modulated Blade Spacing," *J. Am. Helicopter Soc.*, **50**(1), 18–25, 2005.
33. A. Vecchio, T. Polito, K. Janssens, and H. Van Der Auweraer, "Real-Time Sound Quality Evaluation of Aircraft Interior Noise," *Acustica*, **89**(Suppl.), S53, 2003.
34. S. N. Y. Gerges, and T. R. L. Zmijewski, "Hairdryer Sound Quality," *Acustica*, **89**(Suppl.), S90, 2003.
35. L. Jiang, and P. Macioce, "Sound Quality for Hard Drive Applications," *Noise Control Eng. J.*, **49**(2), 65–67, 1996.
36. E. Zwicker, and H. Fastl, *Psychoacoustics Facts and Models*, Springer, Berlin, 1990.
37. A. Hastings, and P. Davies, "An Examination of Aures's Model of Tonality," *Proc. Internoise 02*, Dearborn, MI, 2002.
38. A. Hastings, K. H. Lee, P. Davies, and A. M. Surprenant, "Measurement of the Attributes of Complex Tonal Components Commonly Found in Product Sound," *Noise Control Eng. J.*, **51**(4), 195–209, 2003.
39. R. T. Beyer, *Nonlinear Acoustics*, Acoustical Society of America, Woodbury, NY, 1997.
40. M. F. Hamilton, and D. T. Blackstock, *Nonlinear Acoustics*, Academic, San Diego, 1998.
41. K. L. Gee, S. H. Swift, V. W. Sparrow, K. P. Plotkin, and J. M. Downing, "On the Potential Limitations of Conventional Sound Metrics in Quantifying Perception of Nonlinearly Propagated Noise," *J. Acoust. Soc. Am.*, **121**, EL1–EL7, 2007.
42. D. J. Maglieri, and K. J. Plotkin, *Aeroacoustics of Flight Vehicles: Theory and Practice, Vol. 1: Noise Sources*, H. H. Hubbard (Ed.), NASA Reference Publication 1258, 1991.

43. A. Shoh, "Industrial Applications of Ultrasound—A Review: I. High Power Ultrasound," *IEEE Trans. Sonics Ultrasonics*, **SU-22**, 60–71, 1975.
44. M. Kawaguchi, and M. Nishimura, "Sound Quality Evaluation, Based on Hearing Characteristics, for Construction Machinery, Nippon Kikai Gakkai Ronbunshu," *C Hen/Trans. Jpn. Soc. Mech. Eng., Pt. C*, **61**(584), 1509–1515, 1995.

## SUGGESTIONS FOR FURTHER READING

- W. E. Blazier, Jr., "Sound Quality Considerations in Rating Noise from Heating, Ventilating, and Air-Conditioning (HVAC) Systems in Buildings," *Noise Control Eng. J.*, **43**(3), 53–63, 1995.
- A. Cocchi, M. Garai, and C. Tavernelli, "Boxes and Sound Quality in an Italian Opera House," *J. Sound Vib.*, **232**(1), 171–191, 2000.
- F. J. Fahy, *Sound and Structural Vibration: Radiation, Transmission, and Response*, Academic, San Diego, 1985.
- M. F. Hamilton, and D. T. Blackstock, *Nonlinear Acoustics*, Academic, San Diego, 1998.
- J. G. Ih, D. H. Lim, S. H. Shin, and Y. Park, "Experimental Design and Assessment of Product Sound Quality: Application to a Vacuum Cleaner," *Noise Control Eng. J.*, **51**(4), 244–252, 2003.
- M. C. Junger, and D. Feit, *Sound Structures and Their Interaction*, Massachusetts Institute of Technology, Cambridge, MA, 1986.
- T. R. Letowski, "Guidelines for Conducting Listening Tests on Sound Quality," in Proc. National Conference on Noise Control Engineering, Fort Lauderdale, FL, May 1–4, 1994, pp. 987–992.
- P. A. Nelson, and S. J. Elliot, *Active Control of Sounds*, Academic, London, 1992.
- S. D. Snyder, *Active Noise Control Primer*, Springer, New York, 2000.
- S. D. Sommerfeldt, *Fundamentals of Acoustics Course Notes*, Brigham Young University, Provo, UT, 2003.
- P. Susini, S. McAdams, S. Winsberg, I. Perry, S. Vieillard, and X. Rodet, "Characterizing the Sound Quality of Air-Conditioning Noise," *Appl. Acoust.*, **65**(8), 763–790, 2004.
- D. Vastfjall, "Contextual Influences on Sound Quality Evaluation," *Acustica*, **90**(6), 1029–1036, 2004.
- I. C. Whitfield, *The Auditory Pathway*, Edward Arnold, London, 1967.
- W. A. Yost, *Fundamentals of Hearing: An Introduction*, Academic, San Diego, 2000.



# CHAPTER 27

## ACOUSTICAL MEASUREMENTS

**Brian E. Anderson,  
Jonathan D. Blotter,  
Kent L. Gee, and  
Scott D. Sommerfeldt**

**Brigham Young University,  
Provo, UTAH**

<b>1 INTRODUCTION</b>	<b>954</b>	<b>6 ROOM ACOUSTICS</b>	
1.1 Acoustical Measurement Standards	954	<b>MEASUREMENTS</b>	<b>975</b>
<b>2 FUNDAMENTAL MEASURES</b>	<b>954</b>	6.1 Reverberation	975
2.1 Sound Pressure	955	6.2 Room Resonances	977
2.2 Sound Power	957	6.3 Critical Distance	979
2.3 Sound Intensity	958	<b>7 COMMUNITY AND ENVIRONMENTAL NOISE</b>	<b>980</b>
2.4 Decibel Scale	958	7.1 Representations of Community Noise Data	980
2.5 Frequency Weightings	959	7.2 Noise Surveys	982
2.6 Octave Frequency Bands	962	<b>8 SOUND INTENSITY MEASUREMENTS</b>	<b>982</b>
<b>3 MICROPHONES</b>	<b>962</b>	8.1 Sound Intensity via the “p-p” Principle	982
3.1 Condenser Microphone	964	8.2 Intensity Probes	984
3.2 Electret Condenser Microphones	965	8.3 Systematic Measurement Errors	985
3.3 Dynamic Microphone	965	8.4 Transducer Mismatch	985
3.4 Microphone Selection	965	8.5 Sound Intensity Applications	987
3.5 Microphone Accuracy	967	<b>9 SOUND POWER MEASUREMENTS</b>	<b>988</b>
3.6 Calibration	967	9.1 Measurement of the Sound Power Level in a Free Field	989
3.7 Pistonphone Calibration	967	9.2 The Reverberation Method	991
3.8 Reciprocity Calibration	968	9.3 Comparison Method	992
3.9 Relative Calibration	968	<b>10 SOUND EXPOSURE MEASUREMENTS</b>	<b>992</b>
3.10 Switching Calibration	968	10.1 Sound Exposure Level	992
<b>4 SOUND PRESSURE LEVEL MEASUREMENTS</b>	<b>969</b>	10.2 Noise Dosage	993
4.1 Sound Level Meters	969	10.3 Equipment	993
4.2 Sound Pressure Level Metrics	970	<b>REFERENCES</b>	<b>995</b>
<b>5 MEASUREMENT OF SOUND ISOLATION</b>	<b>971</b>		
5.1 Transmission Loss	972		
5.2 Insertion Loss	973		
5.3 Noise Reduction	973		
5.4 Sound Isolation of Partitions	973		
5.5 Sound Transmission Class	974		

## 1 INTRODUCTION

As noise continues to grow as a significant design concern, the importance of proper measurement techniques is becoming more crucial. The focus of this chapter is to provide a working knowledge of the basic acoustical or sound measurements and measurement techniques for the practicing engineer. The chapter will also provide a broad overview and introduction to more advanced acoustical measurement methods. There are several published documents including tutorials on the proper methods for measuring sound. This chapter is heavily referenced pointing the reader to these excellent sources of information.

The chapter first provides a discussion of the acoustical quantities that are typically measured. Definitions of the terms, measurement units, and weighting filters are presented. The hardware used to make the measurements is then explained along with principles of calibration and data acquisition. Detailed steps to the measurement of sound pressure are then given. Acoustical measurements important in the areas of sound isolation and room acoustics are then discussed. We then move to measurements of sound intensity and sound power, which are the most advanced measures of a sound field. The chapter is then concluded with a discussion of sound exposure and noise dosage measurements.

### 1.1 Acoustical Measurement Standards

An important source of additional information beyond this chapter is the national and international standards that cover acoustical instruments, measurements, and calculations. These standards are written by committees of experts on particular topics and represent recommended best practices. Some of the information in this chapter is drawn directly from these standards.

Three organizations that have developed standards related to acoustics instrumentation and measurements are the International Electrotechnical Commission (IEC), the International Organization for Standardization (ISO), and the American National Standards Institute (ANSI). Because these organizations deal with standardization well beyond the scope of acoustics, the specific technical committees that treat acoustical measurement standards are provided. Subcommittees SC1 and SC2 within ISO TC 43 deal with noise and building acoustics, respectively. IEC TC 29 treats the development of instrumentation under the topic of electroacoustics. ANSI Accredited Standards Committees (ASC) S1 (Acoustics) and S12 (Noise) deal specifically with acoustical hardware and measurements. ISO TC 108 and ANSI ASC S2 both treat mechanical vibration and shock, topics related to acoustical measurements. Numerous other organizations related to standardization and regulation of acoustic testing and the development of test codes are provided in Lang and Nobile.<sup>1</sup>

Standards generally begin with an introduction, explanation of the scope, and, in some cases, areas of application. The introductory sections are then usually followed by a list of normative references and definitions that aid in understanding the standardized hardware specifications or measurement procedures. Some example standards from ISO, IEC, and ANSI are described in Table 1.

## 2 FUNDAMENTAL MEASURES

This section outlines some of the fundamental measures commonly encountered in acoustical measurements. First, the three fundamental measures of sound pressure, sound power, and sound intensity will be discussed. These three terms are discussed in most texts on acoustics.<sup>2-5</sup> We will then discuss the decibel scale, frequency weightings, and octave frequency bands. It is crucial that the reader understand these basic fundamental measures before progressing to advanced topics in acoustical measurements.

**Table 1** Various Standards Related to Acoustical Measurements

Standard Number	Standard Name	Description
ANSI S1.1-1994 (R2004)	Acoustical Terminology	Provides definitions for a wide variety of terms, abbreviations, and symbols used in acoustics
ANSI S12.19— 1996 (R2006)	Measurement of Occupational Noise Exposure	Presents methods that can be used to measure a person's noise exposure in the workplace
ANSI S12.54— 1999/ISO 3744— 1994 (R2004)	Acoustics—Determination of Sound Power Levels of Noise Sources Using Sound Pressure—Engineering Method in an Essentially Free Field over a Reflecting Plane	Method for measuring sound pressure levels on a measurement surface enveloping a noise source in order to calculate sound power level produced by the source
ISO 2923:1996	Acoustics—Measurement of Noise on Board Vessels	Techniques and conditions for measurement of noise on board vessels. Results may be used to compare various vessels and, for example, assess audibility of acoustical alarms
ISO 9295:1988	Measurement of High-Frequency Noise Emitted by Computer and Business Equipment	Details four methods for determining sound power levels in the 11.2–22.4 kHz range
IEC 61260 (1995-2008)	Electroacoustics—Octave-Band and Fractional-Octave-Band Filters	Performance requirements and methods for various implementations of bandpass filters that comprise a filter set or spectrum analyzer
IEC 61672-1 (2002-2005)	Electroacoustics—Sound Level Meters—Part 1: Specifications	Performance specifications for three kinds of sound measuring instruments

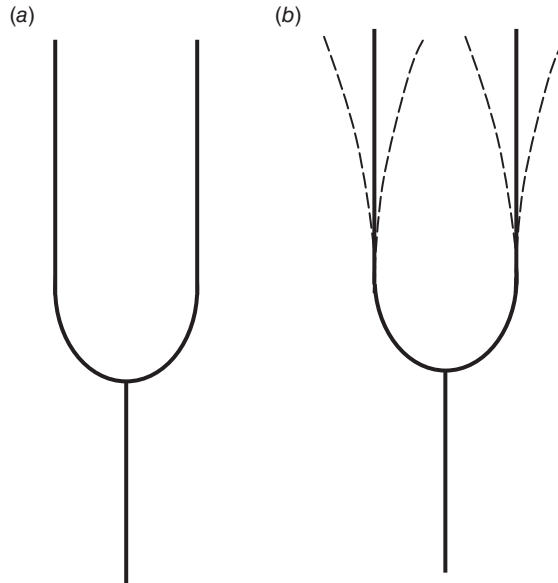
## 2.1 Sound Pressure

Sound pressure, or acoustic pressure, refers to the small deviations of pressure from the ambient generated by sound waves. To better understand this wave phenomenon, take, for example, a U-shaped tuning fork as shown in Fig. 1*a*. The tuning fork is a device used to create a tone at a specific frequency that can then be used to tune various musical instruments. The tone is created by striking one of the tines with a hammer, causing the forks to freely vibrate as shown in Fig. 1*b*. As the tine moves outward from equilibrium, the air adjacent to the outward moving tine is compressed and accelerated outward. As the air adjacent to the tine is pushed outward, the pressure at that location increases slightly above atmospheric pressure as the density of the air molecules also increases. This local increase in air density is commonly called a condensation. After the tine passes back through equilibrium and displaces in the opposite direction, the adjacent air molecules spread out, leaving a pressure slightly lower than atmospheric pressure along with a decreased density of air molecules. This local decrease in air density is commonly called a rarefaction. These deviations above and below atmospheric pressure are sound pressure fluctuations.

Everyday sound pressures may take on a very wide range of values (see Table 2). For example, the sound pressure from a typical jet engine is on the order of 630 Pa, while the threshold of hearing is approximately  $2 \times 10^{-5}$  Pa at 1 kHz. Therefore, the term sound pressure level ( $L_p$ ) or also referred to as SPL as defined by Eq. (1) has been developed:

$$L_p = 20 \log \left( \frac{p}{p_{\text{ref}}} \right) \quad (1)$$





**Figure 1** Illustration of the vibration of a tuning fork: (a) static position and (b) vibrating motion showing tine motion.

**Table 2** Relationship of Sound Pressure and Sound Pressure Level for Various Examples

Sound Source	Sound Pressure (Pa)	Sound Pressure Level ( $L_p$ ) (dB re 20 $\mu$ Pa)
Krakatoa (at 160 km)	20,000	180
M1 Garand being fired	12,000	176
Jet engine (at 30 m)	630	150
Threshold of pain	100	130
Hearing damage (short-term exposure)	20	120
Jet (at 100 m)	6–200	110–140
Jack hammer (at 1 m)	2	100
Hearing damage (8-h exposure)	0.5	88
Major road (at 10 m)	0.2–0.6	80–90
Passenger car (at 10 m)	0.02–0.2	60–80
Normal talking (at 1 m)	0.002–0.02	40–60
Very calm room	0.0002–0.0006	20–30

where  $p$  is the measured root-mean-square (rms) sound pressure,  $p_{\text{ref}}$  is the reference rms sound pressure usually taken as 20  $\mu$ Pa ( $2 \times 10^{-5}$  Pa), which is the threshold of hearing for an undamaged ear and also corresponds closely with the reference power of  $1 \times 10^{-12}$  W as shown in a following section. Table 2 shows the relationship between sound pressure and sound pressure level for several acoustic environments. Sound pressure level measurements are the most common acoustical measurement made. The measurement can be made with a simple low-cost

microphone or an expensive, comprehensive sound-level meter. Procedures and methods for sound pressure measurements are discussed in Section 4.

## 2.2 Sound Power

Sound power is the term that describes the rate at which sound energy is radiated per unit time. The units of sound power are joules/second or watts. As an example of sound power, assume that there is a small spherical sound source. The sound power is a measure of the total amount of sound that the source can produce. Assuming that the source has constant sound power output and that unobstructed radiation occurs, the sound power output of the source is the same at any radius away from the source. A balloon analogy is often used to describe sound power. A balloon has the same amount of material surrounding the internal gas whether the balloon is partially or fully inflated. This is the same concept in that the sound power radiating from the source is constant and is independent of distance from the source.

The range of sound powers encountered can be extremely large. For example, the sound power of a large rocket engine is on the order of 1,000,000 W, whereas the sound power of a soft whisper is approximately 0.000000001 W. Because of this large range in power values, a logarithmic scale known as the decibel scale is widely used in acoustic applications.

When sound power,  $W$ , is expressed in terms of decibels, it is called a sound power level,  $L_w$ , and is computed as

$$L_w = 10 \log \left( \frac{W}{W_{\text{ref}}} \right) \quad (2)$$

where  $W_{\text{ref}}$  is the standard reference power usually taken to be  $1 \times 10^{-12}$  W or 1 pW. Table 3 provides an example of the range of sound power and sound power levels.

Sound power may be measured in various ways depending on the environment in which the measurements are to be made (free field, diffuse field, hemianechoic, etc.). The two basic

**Table 3** Relationship between Sound Power and Sound Power Level for Various Examples

Sound Source	Sound Power (W)	Sound Power Level ( $L_w$ ) (dB re $1 \times 10^{-12}$ W)
Saturn rocket	25–40 million	195
Rocket engine	1,000,000	180
Turbojet engine	10,000	160
Siren	1,000	150
Heavy truck engine/ rock concert	100	140
75-Piece orchestra pipe organ	10	130
Piano/small aircraft/ jackhammer	1	120
Excavator/trumpet	0.3	115
Chain saw/blaring radio	0.1	110
Helicopter	0.01	100
Auto on highway/ loud speech/shouting	0.001	90
Normal speech	$1 \times 10^{-5}$	70
Refrigerator	$1 \times 10^{-7}$	50
Auditory threshold	$1 \times 10^{-12}$	0

techniques of measuring sound power consist of using an array of pressure microphones placed around the source or using a sound intensity probe. Other comparative techniques also exist where measurements are compared with calibrated sources. The international standards that outline the processes for measuring sound power are ISO 3741, 3742, 3744, and 3745.

### 2.3 Sound Intensity

Sound intensity is defined as the amount of sound power per unit area of a given wave front. Relating this back to the balloon analogy, sound intensity would be a measure of the balloon wall thickness at a certain location. The thickness of the balloon material will depend on how much the balloon is inflated, with the thickness decreasing as the balloon is further inflated. By analogy, sound intensity decreases as the distance from the source is increased, and vice versa. As previously mentioned, sound power and sound intensity are related by an area. For a spherical wave front, the relationship is expressed as

$$I = \frac{W}{4\pi r^2} \quad (3)$$

where  $I$  represents sound intensity,  $4\pi r^2$  is the surface area of the sphere, and  $r$  is the radius of the sphere. From Eq. (3), it should be noted that the decay of the sound intensity is directly proportional to the square of the radius of the sphere. This relationship is often referred to as the inverse square law.

Sound intensity values are directly related to sound power values by an area term and hence also have a very wide range of values. Again, it is therefore common to express the sound intensity using a decibel scale referred to as a sound intensity level. Sound intensity level is expressed as shown in Eq. (4), where  $L_I$  is the sound intensity level,  $I$  is the measured intensity at some distance from the source, and  $I_{\text{ref}}$  is the reference sound intensity usually taken as  $1 \times 10^{-12} \text{ W/m}^2$ :

$$L_I = 10 \log \left( \frac{I}{I_{\text{ref}}} \right) \quad (4)$$

Sound intensity is the time-averaged product of the pressure and particle velocity. The pressure can simply be measured with a standard microphone. However, the particle velocity is somewhat more difficult to measure. One common method of measurement is to place two similar microphones a known distance apart. By doing this, the pressure gradient can be measured. Then using Euler's equation, the pressure gradient can be used to compute the particle velocity. This topic is expounded upon in Section 8.

### 2.4 Decibel Scale

The decibel scale is a unitless logarithmic scale that is widely used in many fields of science, including acoustics, electronics, signals, and communication. The decibel scale is used to describe a ratio of values, which among others may be sound power, sound intensity, sound pressure, and voltage. One main advantage of a logarithmic scale is that a very wide range of values can be reduced to a much smaller range, which provides the user with a better feel for the particular values of interest.

In the field of acoustics, the decibel (dB), which is  $\frac{1}{10}$  of a bel, is almost exclusively used. Decibels are used over bels to simply increase the sensitivity of the values, similar to using inches instead of feet or centimeters instead of meters when a pencil-sized object is measured. The term bel (in honor of Alexander Graham Bell) refers to the basic logarithm of the ratio of two values. The definition of the base 10 logarithm is shown in Eq. (5):

$$10^{\log p} = p \quad (5)$$

The log of  $p$  is the value to which 10 must be raised in order to obtain the value  $p$ . The decibel equation can then be expressed as

$$N(\text{dB}) = 10 \log \frac{A}{A_{\text{ref}}} \quad (6)$$

Two examples using the decibel scale are now provided to better illustrate the significance of the relationship.

### Example

An increase in sound power of a ratio of 2:1 results in what gain in decibels?

### Solution

$$N(\text{dB}) = 10 \log 2 / 1 = 10 \times (0.3010) = 3.01 \text{ dB}$$

Therefore, a doubling of the sound power results in an increase of approximately 3 dB.

### Example

The noise level at a factory property line caused by 12 identical air compressors running simultaneously is 60 dB (assuming they are incoherent noise sources). If the maximum sound pressure level permitted at this location is 57 dB, how many compressors can run simultaneously?

### Solution

For 1 compressor:  $L_{p1} = 20 \log(P_{\text{rms1}} / P_{\text{ref}})$

For 12 compressors:  $P_{\text{rms12}}^2 = 12P_{\text{rms1}}^2$ ,

Therefore,

$$P_{\text{rms12}} = \sqrt{12} P_{\text{rms1}}$$

$$P_{\text{rms1}} \cdot L_{p12} = 20 \log \left( \frac{\sqrt{12} P_{\text{rms1}}}{P_{\text{ref}}} \right) = 20 \log(P_{\text{rms1}} / P_{\text{ref}}) + 20 \log \sqrt{12}$$

Therefore,

$$L_{p12} - L_{p1} = 20 \log \sqrt{12} = 10.79 \text{ and } L_{p1} = L_{p12} - 10.79 = 60 - 10.79 = 49.21 \text{ dB}$$

Now for  $x$  compressors:

$$L_{p \text{ max}} = 20 \log \sqrt{x} + L_{p1}$$

Therefore,

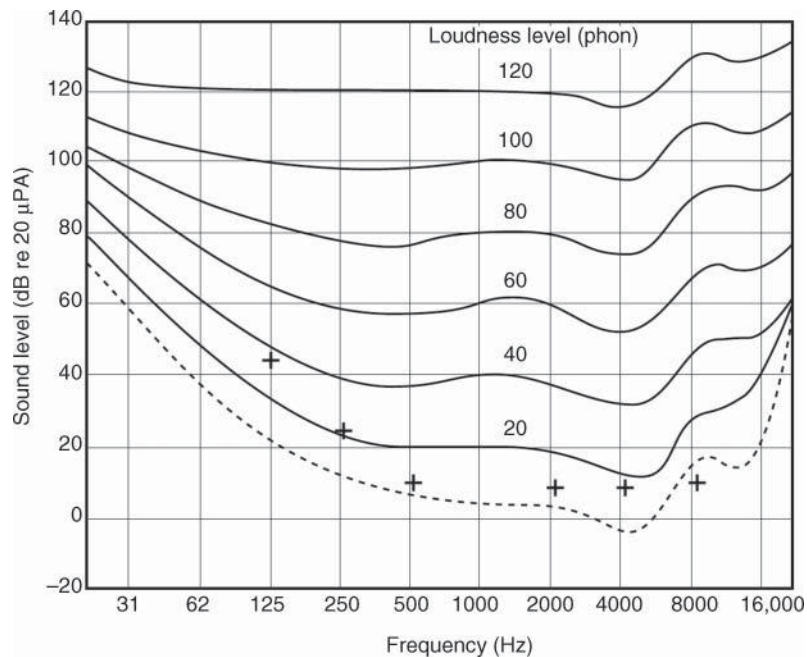
$$\log \sqrt{x} = \frac{L_{p \text{ max}} - L_{p1}}{20} = \frac{57 - 49.21}{20} = 0.3895x = (10^{(0.3895)})^2 = 6.01$$

Therefore, six compressors, at most, can be operated in order to meet the 57-dB limit.

## 2.5 Frequency Weightings

Besides the conventional decibel scale, other scales have been developed that filter or weight the sound according to how human ears respond to amplitudes at different frequencies. This chapter continues by presenting and discussing several of these filtered scales.

Fletcher and Munson<sup>6</sup> presented what is typically called the equal loudness contours (see Fig. 2). This set of contours represents how human ears perceive tones of equal loudness over

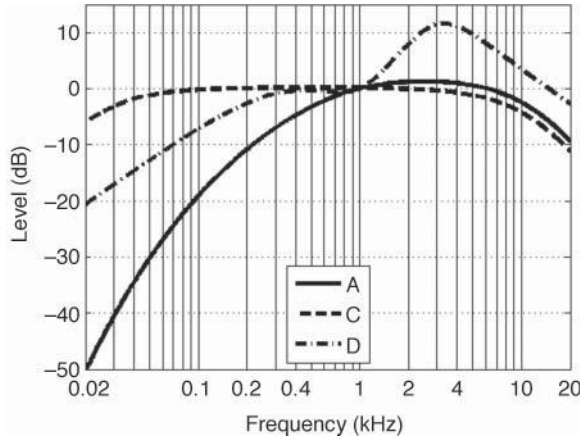


**Figure 2** Equal loudness level contours for sinusoidal sounds. Dashed contour represents the threshold of hearing. (After Refs. 7 and 8.)

the frequency range from 20 Hz to 15 kHz. Apparent loudness is given in units of phons. The magnitude for the phon unit comes from the intensity level in decibels of a 1-kHz tone with the same perceived loudness as other tones at different frequencies and intensity levels. Therefore, a decibel value and a phon value are the same only for a 1-kHz tone. These contours were determined experimentally in an anechoic chamber. The experiment consisted of playing pure tones at a specific intensity level, along with a 1-kHz reference signal. The intensity of the reference signal was increased until the two tones were perceived to be of the same loudness by the listener. Other work, by Robinson and Dadson<sup>7</sup> and Davis and Silverman,<sup>8</sup> on the development of equal loudness contours has been generated since Fletcher and Munson.<sup>6</sup> The most recent standards can be found in ISO 226:2003.

Weighting filters have been developed to adjust sound pressure levels measured by microphones to mimic how our ears respond according to these equal loudness contours. The first weighting filter to be discussed is called A weighting and usually carries the associated symbol dBA or dB(A). This weighting was developed to nominally apply the same filter to an incident sound that the human ear applies for tones that lie on the 40-phon equal loudness contour. The 40-phon contour represents relatively quiet tones. It should be noted that the A-weighting curve roughly corresponds to the inverse of the 40-phon equal loudness contour developed by Fletcher and Munson.<sup>6</sup> The A-weighting curve tends to amplify signals in the 1–6-kHz region. Sound outside this frequency range is reduced by the A weighting. The A-weighting filter is shown in Fig. 3.

The A-weighting filter is very popular and is used in many applications. Some of these include environmental noise, noise control, construction noise, community noise standards, and so on. The usage of the A-weighting filter for such a wide range of sound pressure levels is



**Figure 3** Common frequency weighting curves based on equal loudness contours.

in spite of the fact that the A-weighting filter is only appropriate for relatively quiet pure tones (the 40-phon contour).

The dB(B) and dB(C) scales were developed along similar methods of the dB(A) scale except that they were developed for tones with higher sound pressure levels. The dB(B) scale is seldom used but was developed for tones between the low sound pressure level of the A-weighted scale and the high sound pressure level of the C-weighted scale. The dB(C) scale is used for the high sound pressure levels (based off of the 90-phon curve) and as shown in Fig. 3 is nearly flat over a large frequency range. The dB(D) scale has been developed for aircraft noise and is depicted in Fig. 3. The D-weighting curve heavily penalizes high frequencies to which the ear is most sensitive. The equations for the weighting scales are shown in Eq. (7) where  $s = j\omega$ ,  $j = \sqrt{-1}$ , and  $\omega$  is the angular frequency:

$$G_A(s) = \frac{k_A \times s^4}{(s + 129.4)^2 (s + 676.7)(s + 4636)(s + 76,655)^2}$$

$$G_B(s) = \frac{k_B \times s^3}{(s + 129.4)^2 (s + 995.9)(s + 76,655)^2}$$

$$G_C(s) = \frac{k_C \times s^2}{(s + 129.4)^2 (s + 76,655)^2}$$

$$G_D(s) = \frac{k_D \times s \times (s^2 + 6532s + 4.0975 \times 10^7)}{(s + 1776.3)(s + 7288.5)(s^2 + 21,514s + 3.8836 \times 10^8)}$$

where  $k_A \approx 7.39705 \times 10^9$ ,  $k_B \approx 5.99185 \times 10^9$ ,  $k_C \approx 5.91797 \times 10^9$ , and  $k_D \approx 91104.32$ .

Another unit of measure for perceived loudness is the sone. The sone was developed to relate a perceived doubling of loudness in phons to a sone number that doubles. Experiments found that when volunteers were asked to adjust the loudness of a tone until it was perceived to be twice as loud as the original tone that the doubling corresponded to an increase of 10 phons. One sone is arbitrarily equal to 40 phons, and a doubling of the loudness (in sones) corresponds to a doubling of the perceived loudness. The relationship between sones and phons is given in Table 4.

**Table 4** Table of Phons to Sones Conversion

Loudness Level (Phons)	Loudness (Sones)
20	0.12
30	0.4
40	1
50	2
60	4
70	8
80	16
90	32
100	64

## 2.6 Octave Frequency Bands

In reference to music theory, the term *octave* corresponds to a doubling or a halving of frequency. For example, 200 Hz is one octave above 100 Hz and is one octave below 400 Hz. 400 Hz; would be considered to be two octaves above 100 Hz and so on.

In acoustics, the term *octave band* is commonly used to represent a range of frequencies where the highest frequency is twice the lowest frequency. These octave bands are commonly used to represent what is going on in the acoustic signal over a band or range of frequencies as compared to discrete frequencies. Many sound level meters will output sound pressure level data in standardized octave bands.

Octave bands are typically specified by a center frequency  $f_C$ . The upper frequency limit,  $f_U$ , and the lower frequency limit,  $f_L$ , of the band are computed as

$$f_L = \frac{f_C}{\sqrt{2}} \quad f_U = \sqrt{2}f_C \quad \text{where} \quad f_C = \sqrt{f_L f_U} \quad (8)$$

Furthermore, the bandwidth for a given octave can be computed by

$$\text{Bandwidth} = f_U - f_L = \frac{f_C}{\sqrt{2}} \quad (9)$$

In the field of acoustics, standard octave bands have been defined. The lower frequency, center frequency, and upper frequency for the standard acoustical octave bands are shown in Table 5.

In many applications, a higher resolution on the frequency axis is desired. In these cases, the octave band is split into smaller groups. A common way to do this is to split up the octave band into three smaller bands called one-third-octave bands. The one-third-octave band scale is commonly used for environmental, noise control, and building acoustics among others. The lower, center, and upper frequencies for the one-third-octave bands are shown in Table 6 and calculated using Eq. (10):

$$f_L = \frac{f_C}{\sqrt[3]{6}} \quad f_U = \sqrt[3]{6}f_C \quad \text{where} \quad f_C = \sqrt{f_L f_U} \quad \text{Bandwidth} = f_C \left( \sqrt[3]{6} - \sqrt[3]{-6} \right) \quad (10)$$

## 3 MICROPHONES

This section will discuss various types of microphones. It will then cover important considerations in microphone selection, including the sound field in which the microphone will be used and how the physical characteristics of a microphone affect measurements. We will then

**Table 5** Octave Band Lower, Center, and Upper Band Frequencies (Hz)

Lower Band Frequency $f_L$	Center Band Frequency $f_C$	Upper Band Frequency $f_U$
22.4	31.5	45
45	63	90
90	125	180
180	250	355
355	500	710
710	1,000	1,400
1,400	2,000	2,800
2,800	4,000	5,600
5,600	8,000	11,200
11,200	16,000	22,400

**Table 6** One-Third-Octave Band Lower, Center, and Upper Band Frequencies (Hz)

Lower Band Frequency $f_L$	Center Band Frequency $f_C$	Upper Band Frequency $f_U$
18.0	20.0	24.4
22.4	25.0	28.0
28.0	31.5 <sup>a</sup>	35.5
35.5	40	45
45	50	56
56	63 <sup>a</sup>	71
71	80	90
90	100	112
112	125 <sup>a</sup>	140
140	160	180
180	200	224
224	250 <sup>a</sup>	280
280	315	355
355	400	450
450	500 <sup>a</sup>	560
560	630	710
710	800	900
900	1,000 <sup>a</sup>	1,120
1,120	1,250	1,400
1,400	1,600	1,800
1,800	2,000 <sup>a</sup>	2,240
2,240	2,500	2,800
2,800	3,150	3,550
3,550	4,000 <sup>a</sup>	4,500
4,500	5,000	5,600
5,600	6,300	7,100
7,100	8,000 <sup>a</sup>	9,000
9,000	10,000	11,200
11,200	12,500	14,000
14,000	16,000 <sup>a</sup>	18,000
18,000	20,000	22,400

<sup>a</sup>Octave band center frequencies.



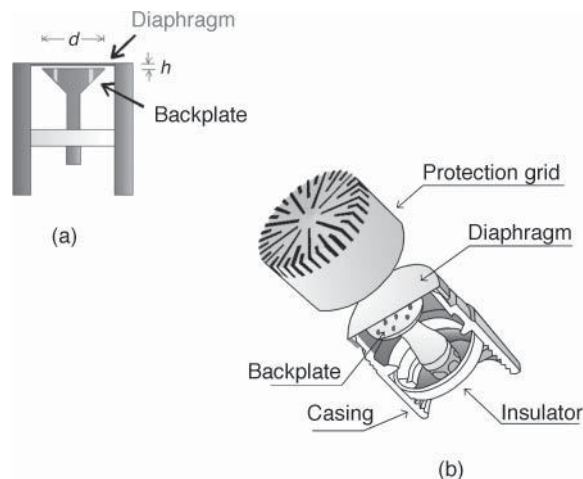
discuss microphone accuracy specifications. The section will then conclude by discussing various calibration techniques.

A microphone is a device that converts acoustical energy in the form of a compression wave into electrical energy in the form of a time-varying voltage. There are several types of microphones and some of these will be discussed in this section. The most common types of microphones use a thin membrane referred to as a diaphragm to sense the incident wave energy. The compression and expansion of sound waves impinging on the diaphragm causes the diaphragm to vibrate. The mechanical motion of the diaphragm is coupled to a transducer, which then produces a varying voltage proportional to the diaphragm deflection. The coupling mechanism between the diaphragm and the transducer is what distinguishes different types of microphones.

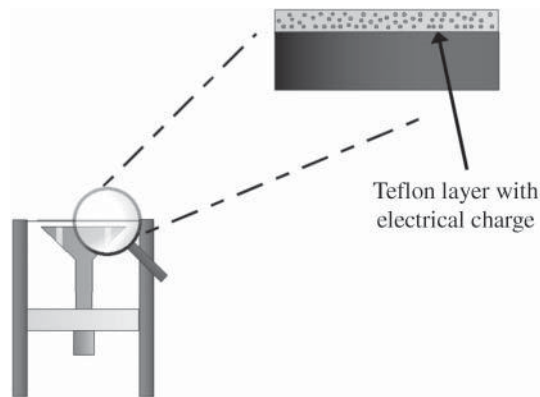
The most common microphones as based on the transducing components are the condenser, electret, and dynamic microphones. This section provides a brief overview of these different microphones, and the reader is also referred to the vast amount of information available on the Internet.

### 3.1 Condenser Microphone

Typical elements of a condenser microphone (also called a capacitor microphone or electrostatic microphone) are shown in Fig. 4. One conducting plate, often referred to as the back plate, is fixed to the microphone casing, although it is electrically isolated from the casing. A metal or metallized plastic diaphragm is placed a small distance away from the back plate and acts as the second (and movable) conducting plate of a dynamic capacitor. When the diaphragm vibrates, an oscillating voltage appears on the electrical leads attached to the plates. The principal advantage of this type of microphone is that it possesses a uniform frequency response over a wide band of frequencies. The principal disadvantage of these microphones is the need to have a direct-current (dc) bias voltage (e.g., 200 V) across the plates (in order to produce an electrical output signal and to linearize the response of the microphone) and a preamplifier in close proximity to the plates. Condenser microphone designs have typically incorporated a preamplifier in the microphone casing. Condenser microphones are used in research, to produce high-fidelity recordings, and in hearing aids and portable sound equipment.



**Figure 4** Cross section of a condenser microphone. (Courtesy of G.R.A.S. Sound and Vibration.)



**Figure 5** Illustration of the electrical charge applied to the diaphragm of an electret microphone. (Courtesy of G.R.A.S. Sound and Vibration.)

### 3.2 Electret Condenser Microphones

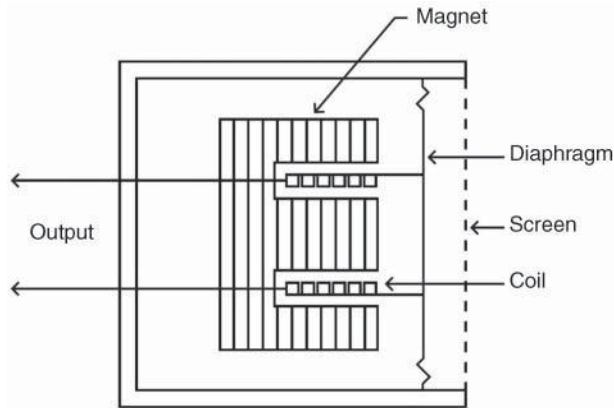
Technically a subset of condenser microphones, electret microphones (sometimes called a pre-polarized microphone) are now in wide use because they offer the advantages of a condenser microphone without the disadvantage of needing a large polarizing dc voltage. Figure 5 depicts an illustration of an electret microphone with an electrically charged Teflon diaphragm. The diaphragm consists of an electret plastic foil that has been permanently electrically charged and overlaid with a thin metallic layer. The electret condenser microphone typically employs a preamplifier. It is slightly less sensitive than the condenser microphone, and the “permanent” electric charge has a finite life span (e.g., 5 years, but this depends on the design). One should note here that sometimes certain preamplifiers, used in conjunction with electret microphones, require a polarization voltage (e.g., 24 VDC drawing approximately 4 mA of current).

### 3.3 Dynamic Microphone

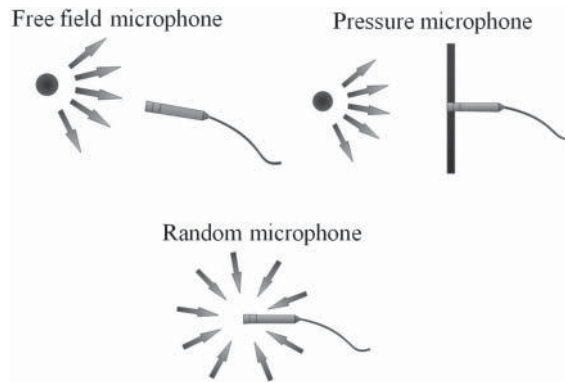
A dynamic microphone (also called an electrodynamic microphone or a moving-coil microphone) has a coil of wire attached to its diaphragm as shown in Fig. 6. The transduction in a dynamic microphone is induced when the diaphragm moves its attached coil between the poles of a magnet, inducing an electromotive force (emf) and a corresponding electrical voltage signal (this is known as Faraday’s law of induction). Dynamic microphones are capable of a relatively high gain before feedback. They are rugged and capable of a broad frequency response over a wide dynamic range. Because they are able to withstand the high-intensity sound levels often associated with popular music, they are widely used for live performances and for recording sessions. The principal disadvantage of dynamic microphones is that their frequency response is not as uniform as for condenser microphones.

### 3.4 Microphone Selection

Most microphones are designed to work in one of three sound fields. These sound fields are typically classified as free field, diffuse field, and pressure field. The different microphone designs have been developed to minimize the effect of the microphone in the particular field of measurement. Because the correction for the influence of the microphone in the sound field can be



**Figure 6** Illustration of the parts of a dynamic microphone.



**Figure 7** Illustrations of how (a) free-field, (b) pressure, and (c) random incidence microphones are intended to be used. (Courtesy of G.R.A.S. Sound and Vibration.)

built into the microphone body, care should be taken when selecting microphones for a particular sound field. Using the wrong microphone in a particular field may result in errors of several decibels.

Free-field conditions exist when the sound waves propagate in a specific direction without the effects of any reflections. These conditions could exist in an anechoic chamber, outdoors, or in other places where reflecting surfaces are not present (or provide minimal reflection). The microphone is typically placed in this field with the diaphragm perpendicular to the sound wave as shown in Fig. 7. When the sound wave is not perpendicular to the diaphragm, corrections can be made if the angle of incidence is known.

A diffuse field, or random field, is created when sound waves from many different directions pass through a point. Statistically, in a diffuse field, sound waves have equal probability of arriving from any direction, and the sound field is considered to be spatially uniform in amplitude for a particular frequency (but not in general equal in amplitude across all frequencies). These sound waves may or may not be generated from the same source but typically multiple reflections are part of the sound field as well. These microphones, sometimes referred to as random incidence microphones (depicted in Fig. 7a), are designed to be direction insensitive.

This is achieved by designing their response to compensate for the fact that the presence of the microphone perturbs the sound field. This type of sound field would exist with a steady-state noise source in a closed room with reflecting walls.

Pressure-field conditions exist in enclosures where the dimensions are much smaller than the wavelength of the sound. This is typically achieved with a single source and the resulting field has the same magnitude and phase at all locations. The microphone, sometimes termed a pressure microphone, is typically placed such that the end of the microphone is flush with the enclosure surface (as depicted in Fig. 7*b*). These microphones are often used to measure the sound waves inside a duct or on a surface. As with the other microphones, pressure-field microphones are designed to account for the changes they make in the sound field.

### 3.5 Microphone Accuracy

Measurement microphones are also rated on a standard scale as given by ANSI S1.12-1967 (R1977).<sup>9</sup> This particular standard rates the microphone on its calibration and type of application. This standard is summarized below and was taken from the Measurement Microphone primer by Brüel and Kjær, which can be found on their website (<http://www.bksv.com/library/primers.aspx>; last viewed on February 2, 2011).

*Type L*: Precisely calibrated reference standard with a closely specified outer diameter (to enable use in couplers).

*Type XL*: As above, but with no specified outside diameter.

*Type M*: For measuring sound-pressure magnitudes of the order  $0.1 \text{ N/m}^2$  or higher. Better high-frequency and high sound pressure performance than for types L and XL. Copes with relatively large ambient pressure changes.

*Type H*: For applications in which diffraction errors in the measurements must be small or in which the sound pressure magnitude is of the order of  $0.5 \text{ N/m}^2$  or higher. Copes with relatively large ambient pressure changes.

### 3.6 Calibration

Proper calibration is a vital process when making acoustic measurements. ANSI S1.10-1966 (R1986)<sup>10</sup> gives the standard method for the calibration of microphones, although there are many different methods of microphone calibration. In this section, we provide an overview of the following types of microphone calibration: pistonphone, reciprocity, relative, and switching calibrations. Good resources for further reading on calibration is provided by ANSI S1.12-1967—R1977,<sup>9</sup> ANSI S1.10-1966—R1986,<sup>10</sup> Burnett and Nedzelnitsky,<sup>11</sup> Torr and Jarvis,<sup>12</sup> Kinsler et al.,<sup>5</sup> pp. 428–430, Maclean,<sup>13</sup> pp. 140–146, and Bobber.<sup>14</sup>

### 3.7 Pistonphone Calibration

A pistonphone calibrator has an enclosed volume in which the microphone to be calibrated is inserted with an airtight seal. In the pistonphone, a mechanical cam drives a piston, or a pair of pistons, in a sinusoidal motion to create a pressure field at a steady frequency and at steady amplitude. The pressure in the enclosure can be accurately determined by knowing the internal dimensions of the enclosure, the ratio of the specific heats for the gas in the coupler (1.402 for air at  $20^\circ\text{C}$  and 1 atm), the atmospheric pressure, the cross-section area of the piston(s), and the peak motion of the piston(s). The microphone recordings may then be calibrated by knowing this pressure field inside the pistonphone either electronically within a sound level meter or in the postprocessing phase of data analysis.

Pistonphones are commercially available from most major microphone manufacturing companies. Given that the sound field is generated with a rotating cam and a moving piston, most pistonphones calibrate at low frequencies at or near 250 Hz (though some operate at 1 kHz). There is a little more variation on the level of pressure generated by a pistonphone but most commercial pistonphones calibrate at levels from 114 dB re 20  $\mu$ Pa to 134 dB re 20  $\mu$ Pa. One of the main sources of error with a pistonphone calibration is an accurate barometric pressure reading. However, depending on the barometer, pistonphones can be very robust and can be used to calibrate class 0 and class 1 systems following IEC standard 942, 1988 Sound Calibrators.

### 3.8 Reciprocity Calibration

Reciprocity calibration has become a very common primary calibration process. The calibration can be performed using an anechoic chamber or in an environment that can be considered to be a free-field environment. The calibration process consists of using three transducers (1–3). The first is the microphone to be calibrated, the second any reversible transducer that may act as both a transmitter or a receiver, and the third a source. The three transducers are organized into three pairs (3–2, 3–1, and 2–1). Each of the three pairs is tested separately. During the first test, the source is placed a distance,  $r$ , from the reversible transducer and the open-circuit voltage response is measured at the reversible transducer's terminals,  $V_2$ . The distance  $r$  must be sufficiently large so that these measurements are made in the acoustic far field of the transducers used as sources. In the second test, the source outputs the same signal as in the first test and the microphone is put in the place of the reversible transducer. The open-circuit voltage response at the microphone's terminals,  $V_1$ , is then measured. Finally in the third test, the reversible transducer is used in place of the source and is now operated as a source, while the current through the reversible transducer is measured,  $I_2$ . The open-circuit voltage response is now measured at the microphone's terminals,  $V'_1$ . The open-circuit receiving sensitivity of the microphone,  $M_{O1}$ , is then

$$M_{O1} = \sqrt{\frac{2r}{\rho_0 f} \frac{|V_1||V'_1|}{|V_2||I_2|}} \quad (11)$$

where  $\rho_0$  is the ambient air density.

### 3.9 Relative Calibration

In cases where one cannot afford expensive precision microphones, one may use lower quality microphones and calibrate them against a microphone with a known sensitivity,  $M_{KS}$ . In this method, sometimes referred to as a substitution technique, the precision microphone is placed in a repeatable broadband sound field and its open-circuit voltage response as a function of frequency is then measured,  $V_{KS}$ . The microphone of unknown calibration is then put in place of the precision microphone and its open-circuit voltage response is measured,  $V_{UM}$ . The sensitivity of the unknown microphone,  $M_{UM}$ , may then be determined as

$$M_{UM} = M_{KS} \frac{V_{UM}}{V_{KS}} \quad (12)$$

### 3.10 Switching Calibration

In some sound fields it may be desirable to employ multiple microphones. One need not possess multiple precision microphones if a switching calibration is employed, however, the microphones must be stable over the period in which the measurements are made. In the switching

calibration technique, the microphones are placed in their desired locations in a sound field and a complex, frequency-dependent transfer function is measured between the two microphones,  $H_{I,12}$ . The microphones' positions are then interchanged and a second transfer function is measured,  $H_{II,12}$ . The calibration transfer function,  $H_{CAL,12}$ , between these two microphones is then

$$H_{CAL,12} = \sqrt{H_{I,12} \times H_{II,12}} \quad (13)$$

This calibration transfer function can then be used to determine the open-circuit voltage response of one of the two microphones used for the calibration if the other one is used by dividing the measured open-circuit voltage response by  $H_{CAL,12}$ .

Another example where the switching calibration technique is useful is in absorption coefficient measurements of acoustic ceiling tiles using a plane wave tube. The absorption properties are measured in a plane wave tube through a measurement of a complex frequency response between two microphones. This complex frequency response must be calibrated by the measured frequency response by dividing the measured frequency response by  $H_{CAL,12}$ .

## 4 SOUND PRESSURE LEVEL MEASUREMENTS

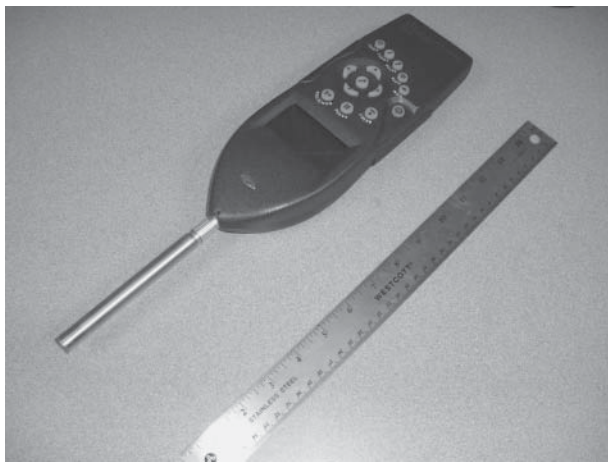
Since there is an extremely large range of pressure measurements, the results are often presented as a logarithmic measure with units of decibels (reported in terms of decibels) as previously discussed. This chapter will discuss the basics of sound level meters and then describe various types of typical quantities measured in field tests that are then used for community noise standards, and to determine worker sound exposure, as will be described in more detail later in this chapter.

### 4.1 Sound Level Meters

Sound pressure level measurements are typically made with a sound pressure level meter or sound level meter, SLM. Many manufacturers provide SLMs that have a fast and simple method of making sound pressure level measurements. An SLM typically consists of a condenser microphone, preamplifier, data acquisition hardware and software, a display to present the results, and a storage system to save the recorded data. The microphone is typically mounted on a rod extending out past the data acquisition box to minimize sound reflections from the user and system during the test. A photograph of a typical SLM is shown in Fig. 8.

There is a large range of quality and price on SLMs. A significant cost of the system is associated with the quality of microphone. Another significant cost factor is the capability of the system hardware and software. For example, storage space, real-time spectral analysis, averaging, sample rate, automatic data logging, filtering, and weighting are some of the capabilities to consider when selecting an SLM.

To help the user select the appropriate SLM, a classification known as types or classes of sound level meters has been set. The two main classes of SLM classifications are class 1 and class 2. The basic difference between the two classes is the tolerance limit with which the specifications are met. Class 1 meters are designed to be used for laboratory and field applications where the highest accuracy is required. Class 2 meters can be considerably less expensive but do not provide the same high accuracy and precision, especially in the high-frequency range. In general, specifications for class 1 and class 2 SLMs have the same design goals and differ mainly in the tolerance limits and the range of operational temperatures. Tolerance limits for class 2 specifications are greater than, or equal to, those for class 1 specifications. The details of these classifications can be found in International Standard IEC 61672-1. There are also class 0 and class 3 transducers. The class 0 transducers are used in laboratory applications for the calibration of other meters. Class 3 transducers are used primarily in field studies where accuracy



**Figure 8** Photograph of a typical sound level meter.

**Table 7** Sound Pressure Level Measurement Standards

- 
1. ISO 2204: 1979—Acoustics—Guide to International Standards on the measurement of airborne acoustical noise and evaluation of its effects on human beings. This standard provides a very good introduction to various acoustic terms and measuring methods
  2. ANSI S1.4-1983 (R2006)/ANSI S1.4A-1985 (R2006)—American National Standard Specification for Sound Level Meters
  3. IEC 61672 : 2003—International Standard for Sound Level Meter Performance
- 

is not of extreme importance. ANSI S1.4-183 is another standard that discusses classifications 0–2. Some manufacturers will designate their microphone, preamp, or filter as a certain type or to meet a particular standard. In order to conform, the complete system must be reviewed. The whole system is what must meet the standard, not just one component.

National and international standards exist for making sound pressure level measurements. The ANSI and the IEC are two organizations responsible for developing and maintaining these standards. The standards state both the measurement process that should be followed and the specifications of the equipment required to make the measurements. Several of the standards for sound pressure measurements are listed in Table 7.

## 4.2 Sound Pressure Level Metrics

There are numerous ways of representing measured noise. One way is to simply display the A-weighted sound pressure level ( $L_A$ ) as a function of time. In addition to A-weighted sound pressure level, there are many other single-number metrics that are used to describe noise.

Perhaps, the most common metric is the equivalent continuous sound level ( $L_{eq}$ ). The  $L_{eq}$  is commonly determined from A-weighted sound pressures, but it may in general be expressed using other types of weightings (though the weighting used should always be specified, for example, the C-weighted sound pressure level would be  $L_C$ ). Further it is the level of the steady sound that has the same time-averaged energy as the noise event. For the time interval,  $T$ , which



runs between  $T_1$  and  $T_2$ ,  $L_{\text{eq}}$  is calculated as

$$L_{\text{eq}} = 10 \log_{10} \frac{1}{4 \times 10^{-10}} \frac{1}{T} \int_{T_1}^{T_2} p_A^2(t) dt \quad (14)$$

where  $p_A$  is the instantaneous A-weighted sound pressure (a time-domain A-weighting filter must be applied to an instantaneous pressure versus time waveform to obtain  $p_A[t]$ ). A running, live update on a sound level meter of  $L_{\text{eq}}$  is often called a running  $L_{\text{eq}}$ . The  $\frac{1}{4} \times 10^{-10}$  is the reciprocal of the reference sound pressure squared ( $20 \mu\text{Pa}$ )<sup>2</sup>. The  $L_{\text{eq}}$  gives equal weighting to all noise summed over  $T$  irrespective of the time at which it is present. Common values for  $T$  include 1 s, 1 min, 1 h, 8 h, and 24 h.

If one has a set of A-weighted,  $L_{\text{eq}}$  measurements, each taken over a 1-h period of time [expressed as  $L_{A,1h}(n)$ ], for the 24 h of a given day, then we may average these values to arrive at the average  $L_{\text{eq},24h}$  for that day:

$$L_{\text{eq},24h} = 10 \log_{10} \frac{1}{4 \times 10^{-10}} \frac{1}{24} \sum_{n=1}^{24} 10^{0.1L_{A,1h}(n)} \quad (15)$$

Therefore,  $L_{\text{eq}}$  measurements are useful to determine average noise exposures over a given period of time.

In order to obtain live readings of sound pressure levels, for example, with a handheld sound level meter in the field, exponential time weightings have been developed. Various exponential time weightings have been standardized including slow, fast, and impulse. Often a slow exponential time weighting is called a slow detector for short. Slow and fast exponential-time-weighted sound pressure levels,  $L_{A,t_w}$ , are given by

$$L_{A,t_w} = 10 \log_{10} \frac{1}{4 \times 10^{-10}} \frac{1}{\tau} \int_{T_1}^{T_2} p_A^2(\xi) e^{-(t-\xi)/\tau} dt \quad (16)$$

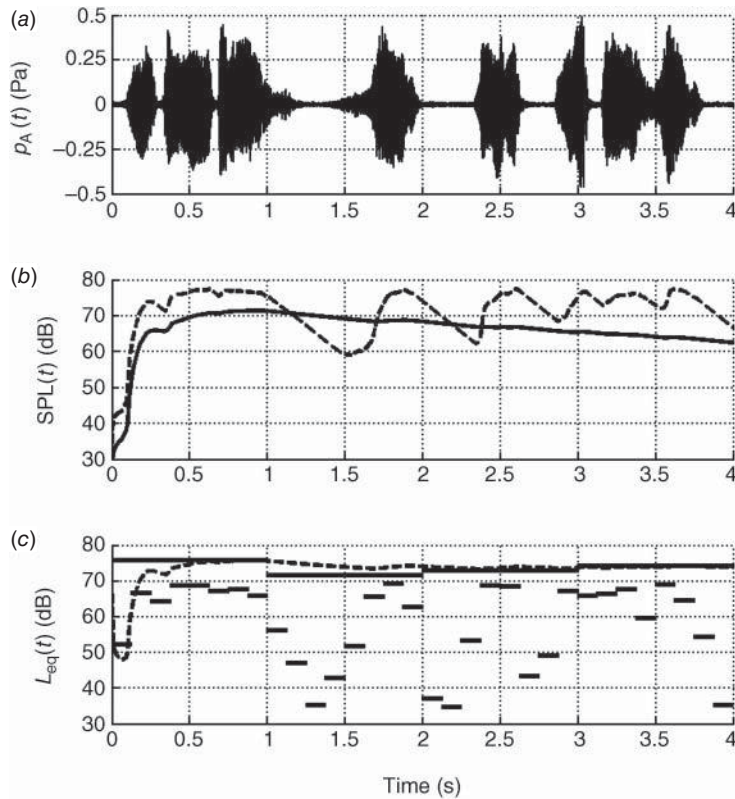
where  $\tau = 1$  s for slow, and  $\tau = 0.125$  s for fast weightings. Thus, a slow detector has a longer “memory” than does a fast detector since it gives a higher weighting to previous sound pressures than a fast detector does. The impulse detector is similar in nature to slow and fast detectors, but it has a different time constant depending on whether the sound pressures are rising ( $\tau = 0.035$ ) or falling ( $\tau = 1.5$ ). Thus, the impulse detector responds well to impulsive changes in sound pressure and holds that level fairly constant on the meter so that it can be noted by the operator.

Figure 9a displays pressure versus time for an example sound recording that has had a time-domain A-weighting filter applied to it. Figure 9b shows the instantaneous sound pressure levels using a slow detector and a fast detector. Note the differences in the trailing slopes of the slow and fast detectors when the sound pressures drop suddenly, indicating the respective memories of each type of detector. Figure 9c shows a running  $L_{\text{eq}}$ , and  $L_{\text{eq}}$  measurements at intervals of 0.125 and 1 s. Recall that, in general, an  $L_{\text{eq}}$  measurement represents a summation without any time weighting applied.

## 5 MEASUREMENT OF SOUND ISOLATION

There are numerous applications where it is desired to measure the isolation that is achieved by placing an acoustic treatment between a source and a receiver location. Such applications include noise barriers, enclosures, partitions or walls, and mufflers among others. While the concepts presented here are applicable to all of these applications, the development will focus specifically on sound isolation in a room or cabin and transmission between two such adjacent spaces. Several metrics have been developed to quantify the effectiveness of such treatments.





**Figure 9** (a) A sample microphone recording displayed in A-weighted sound pressure versus time. (b) Instantaneous sound pressure levels with a slow (solid line) and a fast detector (dashed line) for the waveform in (a). (c) Equivalent continuous sound level measurements,  $L_{eq}$ , for the waveform in (a) (dashed line represents the running  $L_{eq}$ , the solid lines of long and short duration are  $L_{eq}$  measurements over the time intervals of 1 s and  $\frac{1}{8}$  s, respectively).

## 5.1 Transmission Loss

Conceptually, the ideal metric to quantify the effectiveness of an acoustic treatment is often the *transmission loss*. The transmission loss (TL) is defined as

$$TL = 10 \log_{10} \left( \frac{W_i}{W_t} \right) \quad (17)$$

where  $W_i$  is the total acoustic power incident on the treatment of interest and  $W_t$  is the total acoustic power transmitted through the treatment. In practice, this metric can often be difficult to measure, as it requires one to be able to measure the incident power with the treatment in place. A common measurement error encountered occurs when the user measures the sound power radiated by the source without the treatment in place, then puts the treatment in place and measures the sound power radiated through the treatment, and calls the difference between the two measurements the transmission loss. This approach would be correct if the sound power radiated by the source does not change with a changing acoustic load. However, it is often the case that inserting the acoustic treatment also alters the acoustic load on the source and as a result alters the acoustic power radiated from the source. Thus, for an accurate measurement of transmission loss, the incident power must be measured with the acoustic treatment in place.

## 5.2 Insertion Loss

As a result of this difficulty, alternative metrics have also been developed. One of those is the *insertion loss*. The insertion loss (IL) is defined as

$$\text{IL} = 20 \log_{10} \left( \frac{p_w}{p_{w/o}} \right) \quad (18)$$

where  $p_{w/o}$  is the pressure at a field point without the treatment in place, and  $p_w$  is the pressure at the same field point with the treatment in place.

## 5.3 Noise Reduction

A third metric used when the application of interest is transmission of noise from one reverberant room to a second reverberant room is the *noise reduction* (NR), defined as

$$\text{NR} = 10 \log_{10} \left( \frac{I_1}{I_2} \right) = L_{p1} - L_{p2} \quad (19)$$

Here,  $I_1$  and  $I_2$  are the acoustic intensities in the source and receiving rooms, respectively, and  $L_{p1}$  and  $L_{p2}$  are the sound pressure levels in the source and receiving rooms. For Eq. 19 to be accurate, the sound field in the two rooms must be diffuse—a condition that is approximated in a reverberation chamber. For a more accurate measurement, a spatially averaged sound pressure response should be obtained using an array of microphones (as described in ISO 3741, for example) to reduce the effects of nonuniform distribution of sound energy.

For the case of two coupled reverberant rooms, the noise reduction in Eq. 19 can be related to the transmission loss in Eq. 17. The sound power incident on the partition between the rooms can be expressed as  $W_i = I_2 A$ , where  $S$  is the area of the partition. The power transmitted (and subsequently absorbed) in the receiving room can be expressed as  $W_t = I_2 A$ , where  $A$  is the total sound absorption of the receiving room. This leads to

$$\text{TL} = \text{NR} + 10 \log_{10} \left( \frac{S}{A} \right) \quad (20)$$

## 5.4 Sound Isolation of Partitions

A single-leaf partition is a partition where both faces of the partition are connected together in a manner such that the cross section moves as a rigid body. Solid panels would be the simplest example of such a partition. At low frequencies, the transmission loss associated with a single-leaf partition placed between two acoustic spaces is governed by the mass per unit area of the partition. The mass law predicts the attenuation of a rigid single leaf partition as

$$\text{TL} = 20 \log_{10}(f \rho_s) - 47 \text{ dB} \quad (21)$$

where  $f$  is the frequency (Hz), and  $\rho_s$  is the surface density of the solid partition ( $\text{kg}/\text{m}^2$ ). The mass law predicts that the transmission loss increases by 6 dB with a doubling of frequency or with a doubling of the surface density. This leads to the general rule that low frequencies are harder to isolate than higher frequencies, and if further isolation is needed at low frequencies, it often requires the use of higher surface densities to achieve the desired objective.

In practice, single-leaf partitions also exhibit structural wave effects. This causes the transmission loss to deviate from the mass law, due to the interaction of the stiffness, mass, and damping properties of the partition. The critical frequency corresponds to the frequency where the phase speed of bending waves in the partition (which is frequency dependent) matches the phase speed in the surrounding acoustic fluid. Above this critical frequency, the coincidence effect is observed, where waves incident from a particular angle pass through the partition with little attenuation, due to a matching of the phase speeds. This results in a coincidence dip that

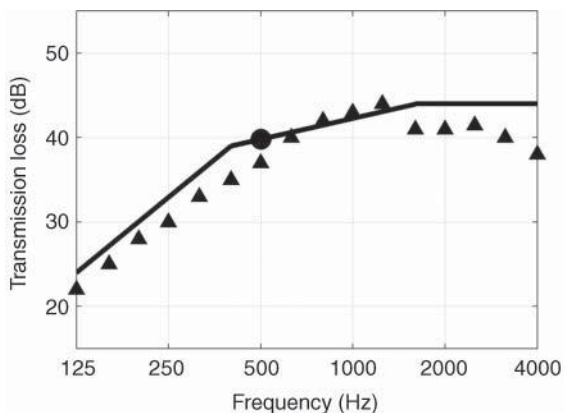
is observed as reduced transmission loss, typically from frequencies slightly below the critical frequency up to frequencies an octave or more above the critical frequency.

Double-leaf partitions are constructed using two single-leaf partitions with an acoustic cavity between them. The acoustic cavity may also be filled with an absorptive material. Double-leaf partitions have the ability to provide additional transmission loss. These designs offer the potential of increasing the transmission loss at most frequencies. However, they do introduce additional resonance effects, including the coincidence frequencies of both partitions and the mass–air–mass resonances that are established with the partitions providing mass effects and the cavity providing stiffness effects. At these resonances, the transmission loss is typically reduced to levels around that corresponding to the mass law.

## 5.5 Sound Transmission Class

The sound transmission class (STC) is a single-number rating system that attempts to characterize the sound isolation associated with an acoustic space. It represents the most common single-number metric used in North America for this purpose and is generally used to rate the sound insulation properties of windows, doors, and partitions. The STC is obtained using the transmission loss values associated with the one-third-octave bands from 125 to 4000 Hz. The STC is obtained as follows. The measured one-third-octave band values are compared with a reference contour that is obtained from three straight lines. The first line covers the range from 125 to 400 Hz and increases by 15 dB over this range. The second line covers the mid-frequency range from 400 to 1250 Hz and increases by 5 dB over this range from the value at 400 Hz. The third line for frequencies above 1250 Hz is a horizontal line matching the value of the second line at 1250 Hz. The following guidelines are used to match this reference contour to the measured one-third-octave band data.

1. No individual transmission loss value can be more than 8 dB below the reference contour after it is fitted to the data.
2. The total deficiency (obtained as the sum of all deviations below the reference contour) cannot exceed 32 dB. The STC reference contour is fitted to the data to be as high as possible while still meeting these two criteria. The STC value then corresponds to the transmission loss of the STC curve at 500 Hz. An example for determining STC is provided in Fig. 10, where the STC of this acoustical treatment is 40.



**Figure 10** An example of an STC measurement. Here, the STC = 40.

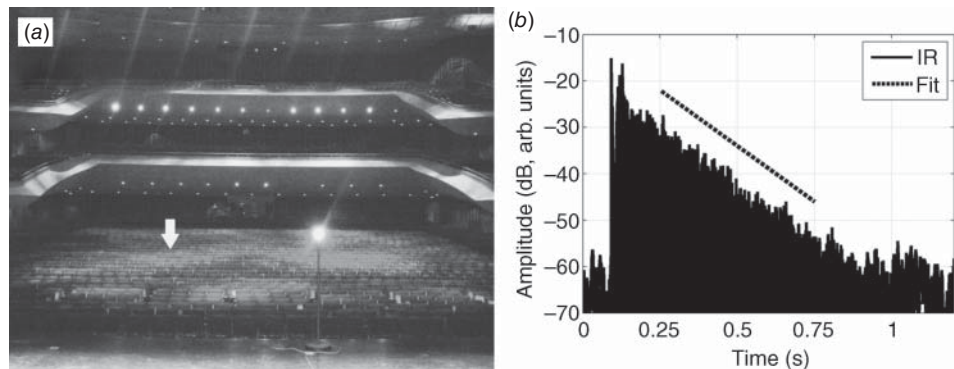
## 6 ROOM ACOUSTICS MEASUREMENTS

### 6.1 Reverberation

One of the first subjective characteristics that a person notices when entering any given room is whether the room is acoustically *live* or *dead*. The degree to which a room is live or dead greatly determines the ability of two people to hold a successfully understood conversation. If a room is too live, it may be difficult to understand speech except at short distances, whereas in a very dead room speech can generally be understood irrespective of distance. This perceptual characteristic is entirely dependent on the amount of reflections off of the walls in the room and the strength of those reflections, which we term room reverberation. For a given sized room, the degree to which the room is live or dead depends on the absorptive qualities of the materials placed on the surfaces of the walls, ceiling, and floor.

Reverberation is quantified through the measurement of an impulse response. An impulsive source, such as a starter pistol or a balloon pop, is used to excite the reverberation in the room and the response of the room due to this impulse may be measured at any selected microphone location. This impulse response may, in general, depend on both the locations of the source and the microphone. In a classroom, for example, one may place the impulsive source at the location where the instructor would teach from and then place the microphone at a given seat location.

Reverberation in a room is assumed to decay at a constant rate of decibels over time. The reverberation time, RT, is defined as the time it takes for the sound pressure level in a room to decay 60 dB. Figure 11a shows a voltage versus time impulse response as measured by a microphone in the Eisenhower Auditorium on the campus of The Pennsylvania State University (2500-seat capacity). The impulsive source was located on the stage while the microphone was placed at an audience seat location. Figure 11b shows the magnitude of the impulse response versus time on a decibel scale. The initial sound arrival occurs 91 ms into the recording. Note that from approximately the 200- to the 900-ms mark that the sound is decaying at a constant rate. After the 900-ms mark, the sound from the impulse is now into the noise floor (we know it is the noise floor because it matches the level before the initial sound arrival and because the sound level flattens out after that time). The initial arrivals of sound commonly do not follow the steady decay rate. To obtain the RT, we must select a portion of the impulse response with a constant decay. If we conservatively choose the time frame from 250 to 750 ms, we can avoid the initial sound arrivals and any influence of the noise floor. The dashed line in Fig. 11b displays a



**Figure 11** (a) Photograph of the Eisenhower Auditorium on the campus of The Pennsylvania State University. (b) Impulse response measurement with the source on stage and the microphone located at the seat location indicated by the arrow. The dotted line indicates the average slope of the impulse response's decay.

line that matches the slope of the decay rate. Over this 500-ms interval, the sound decays 24 dB. Thus, the RT is 1.25 s, since it will take that long for the impulsive sound to decay 60 dB.

The RT can be calculated (in metric units) for a given room if the room's volume,  $V$ , total surface area,  $S$ , and average absorption coefficient,  $\bar{\alpha}$ , of the room's surfaces are known:

$$RT = 0.161 \frac{V}{-S \ln(1 - \bar{\alpha})} \quad (22)$$

This formula is called the Norris–Eyring reverberation time (see Pierce,<sup>3</sup> pp. 263–265). The quantity  $\bar{\alpha}$  may be determined through an area-weighted average of the absorption coefficients of the room surfaces:

$$\bar{\alpha} = \sum_i \frac{S_i \alpha_i}{S} \quad (23)$$

where, for the  $i$ th surface,  $S_i$  is the surface area and  $\alpha_i$  is the absorption coefficient. Table 8 gives a listing of common room surface materials and their corresponding absorption coefficients. Table 9 gives a listing of absorption data for seating in terms of  $\alpha S$  in square feet per person or per seat. The absorption coefficients listed in these tables are broken down in terms of how absorbent a particular surface is, on average, over a given octave frequency band. These data represent collected and averaged values from the tables listed by Egan (Table 8 adapted from Egan,<sup>15</sup> pp. 32–34) and also Beranek (Table 9 adapted from Beranek,<sup>4</sup> pp. 300–301) and originally come from many sources. Beranek asserts that numerous inconsistencies in the data given by various authors make these values listed only approximate values.

The optimal RT for a given room depends on the primary intended use for that room. Perceptual studies were conducted to determine the optimal RT for various types of rooms. When the room is primarily used for speech, such as for a classroom, lower reverberation times are desired so that speech may be understood clearly above any reflections and echoes. On the contrary, when a room is used for musical performances, longer reverberation times are desired to give a sense of liveliness of the concert hall. Table 10 gives a listing of optimal reverberation times for various types of rooms. Thus if one measures an average RT for a given type of room, one may then use Eq. (22) and (23) to determine how they may change the room surfaces to increase or decrease the RT as needed.

**Table 8** List of Absorption Coefficients for Common Room Surface Materials

Material	Absorption Coefficients					
	125	250	500	1000	2000	4000
Acoustic tile (suspended, 2 cm thick)	0.76	0.93	0.83	0.99	0.99	0.94
Brick (unpainted)	0.03	0.03	0.03	0.04	0.05	0.07
Concrete (coarse)	0.36	0.44	0.31	0.29	0.39	0.25
Concrete (painted)	0.10	0.05	0.06	0.07	0.09	0.08
Drapery (heavy weight, half area)	0.14	0.35	0.55	0.72	0.70	0.65
Drapery (light weight, flat)	0.03	0.04	0.11	0.17	0.24	0.35
Glass (typical window)	0.35	0.25	0.18	0.12	0.07	0.04
Heavy carpet (on concrete)	0.02	0.06	0.14	0.37	0.66	0.65
Linoleum (on concrete)	0.02	0.03	0.03	0.03	0.03	0.02
Plaster (gypsum on brick)	0.01	0.02	0.02	0.03	0.04	0.05
Plaster (gypsum on concrete)	0.12	0.09	0.07	0.05	0.05	0.04
Plywood paneling (1 cm thick)	0.28	0.22	0.17	0.09	0.10	0.11

**Table 9** List of Absorption Coefficients for Various Seating Types and People (Data for Seating in Terms of  $\alpha S$  in Square Feet per Person or per Seat)

Material	Absorption					
	125	250	500	1000	2000	4000
Seats						
Upholstered back (leather)	2.0	2.5	3.0	3.0	3.0	2.5
Theater (heavily upholstered)	3.5	3.5	3.5	3.5	3.5	3.5
Wooden chairs	0.1	0.15	0.2	0.35	0.5	0.6
People in Seats (add to above values)						
Upholstered back (leather)	0.7	0.6	0.5	1.3	1.6	2.0
Theater (heavily upholstered)	0.7	0.6	0.6	1.0	1.0	1.0
Wooden chairs	4.0	7.5	11.0	13.0	13.5	11.0
Other Values (not added to above values)						
People standing	2.0	3.5	4.7	4.5	5.0	4.0
High school students (in chairs)	2.2	3.0	3.3	4.0	4.4	4.5
Elementary school students (in chairs)	1.8	2.3	2.8	3.2	3.5	4.0

**Table 10** List of Optimal Reverberation Times for Various Room Types

Room Type	Room Size (m <sup>3</sup> )			
	30	300	3,000	30,000
Office—speech	0.4	0.6	—	—
Classroom—speech	0.6	0.9	1.0	—
Workroom—speech	0.8	1.2	1.5	—
Rehearsal room—speech	0.8	0.9	1.0	—
Studio—music	0.4	0.6	1.0	—
Chamber music	—	1.0	1.2	—
Classical music	—	—	1.5	1.5
Modern music	—	—	1.5	1.5
Opera	—	—	1.4	1.7
Organ music	—	1.3	1.8	2.2
Romantic music	—	—	2.1	2.1
Room in home—speech	0.5	0.8	—	—
Room in home—music	0.7	1.2	—	—

Source: Data from Strong and Plitnik (2007), p. 197.

## 6.2 Room Resonances

The Fourier transform of a room's impulse response yields its frequency response. The frequency response of a room provides information about modal resonance frequencies of that room. For smaller rooms, the modes can cause undesirable coloration of the acoustic response at low frequencies (as is experienced when one sings in a typical shower). Thus, the frequency response may be used to identify problematic resonance frequencies. However, in order to reduce the strength of a given modal frequency, one must also know the spatial distribution of that mode.

The resonance frequencies of a rectangular room, of dimensions  $L_X \times L_Y \times L_Z$  are given by

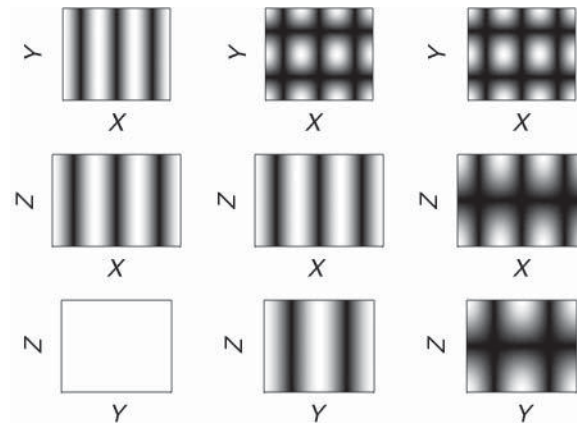
$$f_{l,m,n} = \frac{c}{2} \sqrt{\left(\frac{l}{L_X}\right)^2 + \left(\frac{m}{L_Y}\right)^2 + \left(\frac{n}{L_Z}\right)^2} \tag{24}$$

where  $l$ ,  $m$ , and  $n$  are integers (0, 1, 2, 3, ...). There are three types of room modes: axial, tangential, and oblique. Axial modes have amplitude dependence only along one of the axes, and they occur when two of the integers are equal to zero. Tangential modes have amplitude dependence in only two dimensions, and they occur when one of the integers is equal to zero. Finally, oblique modes have amplitude dependence in all three dimensions, and they occur when all integers are nonzero. Figure 12 gives an example of the spatial distribution of the sound pressure for each of these three types of modes. In the figure, note the lack of  $Y$  and  $Z$  dependence in the axial mode and the lack of  $Z$  dependence in the tangential mode. If one wishes to characterize a certain modal frequency in a room, both the microphone and the source used in this measurement must be placed away from nodal lines/planes (locations in the room where a mode does not respond).

Each resonance frequency has a finite-sized bandwidth associated with it, which depends on the absorption in the room. Increasing absorption decreases the room mode’s amplitude and makes the modal frequency response occur over a broader range of frequencies for that mode (so that it is not so apparent). For larger sized rooms, modal frequencies occur within a lower frequency range than for a smaller sized room. Above a frequency called the Schroeder frequency,  $f_s$ , modal frequencies overlap to the degree that no one mode dominates the acoustic response of the room. In general, above  $f_s$  one need not worry about undesirable coloration of the acoustic response due to a given room resonance. The  $f_s$ , valid for most rooms (except for very elongated rooms), is defined in terms of the RT and the volume of the room:

$$f_s = \sqrt{\frac{c^3}{4 \ln(10)}} \sqrt{\frac{RT}{V}} = 2090 \sqrt{\frac{RT}{V}} \tag{25}$$

where  $c$  is the speed of sound (343 m/s).



**Figure 12** Illustrations of the spatial variations in axial, tangential, and oblique room modes. Axial mode ( $l = 3, m = 0, n = 0$ ) is shown in the first column, tangential mode ( $l = 3, m = 2, n = 0$ ) is shown in the second column, and oblique mode ( $l = 3, m = 2, n = 1$ ) is shown in the third column.



### 6.3 Critical Distance

Above  $f_3$  a room is considered to be spatially uniform in its acoustic response, meaning that any reverberation in a room will be uniformly distributed. However, when two people are standing close enough to one another, successful communication can still take place. It turns out that there exists a distance at which the direct sound energy from a source equals the reverberant energy (whose energy is created by that source). This distance, for omnidirectional sources (sources without a preferred direction), is called the critical distance,  $r_C$ , and is defined as

$$r_C = \sqrt{\frac{\bar{\alpha}S}{16\pi(1-\bar{\alpha})}} \quad (26)$$

This distance increases for directional sources (see Pierce,<sup>3</sup> pp. 267–270).

#### *Echoes*

An echo is a delayed repetition of sound that results in a degradation of speech communication. It has been determined, through perceptual studies, that a reflection of sound that arrives 50 ms later than the direct sound arrival, or any other prominent reflection arrival, is perceived as an echo. This later arrival of sound must also be of sufficient amplitude above the usual constant decay of reverberant energy to be perceived as an echo. Further, this late reflection may only be perceived as an echo if there are no other prominent reflections that precede it by 50 ms. Thus, one way to mask a troublesome echo is to provide other prominent reflections within the 50 ms preceding the troublesome echo. Another way to reduce the echo is to locate the room surface providing the offending echo and treat it with highly sound-absorbent materials to reduce the amount of sound energy that is reflected.

#### *Noise Criteria*

In the absence of distinct tonal noise, one may define the noise criteria (NC) rating for a given room. The NC, given in decibels, for a room gives a measure of the perceived background noise since it depends on an overall, A-weighted, sound pressure level measurement,  $SPL_A$ :

$$NC = 1.24(SPL_A - 13) \quad (27)$$

This  $SPL_A$  measurement is made with only background noise present. Table 11 gives acceptable NC values for various types of rooms. In some cases, such as a library or a restaurant, spectrally uniform background noise may be desirable to mask the speech of others. An expansive treatment of additional background noise metrics is given by Blazier.<sup>17</sup>

**Table 11** List of Acceptable Noise Criteria Ratings for Various Room Types

Room Type	Noise Criteria Rating (dB)
Studio	15–20
Concert hall	15–20
Theater	20–25
Auditorium	25–30
Bedroom	25–30
Living room	30–35
Business offices	30–35
Restaurant	35–45

Source: Data from Ref. 16, p. 197.)



## 7 COMMUNITY AND ENVIRONMENTAL NOISE

Measurement and analysis of the impact of noise on individuals, communities, and the environment are major subfields within acoustics. These topics are inherently fraught with debate because of the subjectivity of human perception and in the challenge of defining acceptable limits. This section summarizes some of the measurements and calculations commonly carried out in community and environmental noise assessment.

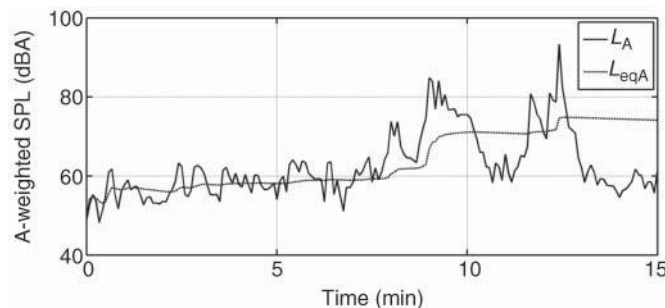
### 7.1 Representations of Community Noise Data

There are numerous ways of representing community noise. Because of the time scales involved, most involve level-based measurements and the tracking of events of significance, rather than detailed time waveform recordings. One possibility is to display the sound pressure level as a function of time, in addition to a calculation of the equivalent sound level [see Eq. (14)] over the sampling period. The running level measurements can be more helpful in identifying individual noise events than the equivalent level. As an example, the running A-weighted sound pressure level ( $L_A$ ) and the  $L_{A,eq}$  as a function of time is displayed in Fig. 13. The data, recorded using a Larson Davis 824 Sound Level Meter, include the working of several trash dumpsters during the early morning at an apartment complex in Provo, UT. Before the arrival of the garbage truck, major noise sources (>60 dBA) were due to intermittent traffic from the nearby street. After the arrival of the truck (around 8 min into the data shown), the most significant noise events were due to the dumpsters being shaken by the hydraulic arms on the truck before being noisily set back down.

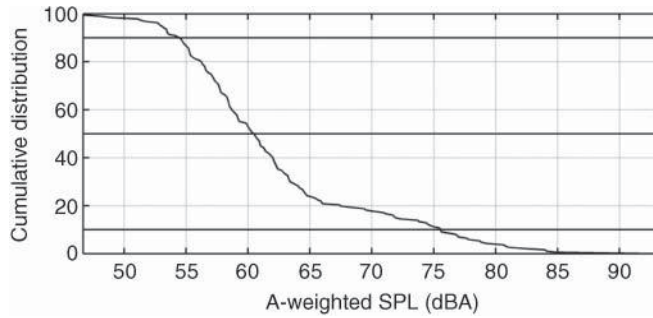
Other representations of community noise are statistical in nature. Using the same garbage truck example, a cumulative distribution function can be calculated. As shown in Fig. 14, this function shows the percentage of time that the recorded noise levels exceed a given value. From the cumulative distribution function,  $X$ -percentile-exceeded noise levels ( $L_X$ ) can be calculated. In Fig. 14, lines representing the  $L_{90}$ ,  $L_{50}$ , and  $L_{10}$  of 54.4, 60.4, and 75.3 dBA are shown.

There are various single-number metrics that are used to describe community noise. These metrics have been the result of attempts to correlate subjective response with objective, albeit empirical, measures. Some of the commonly used metrics are as follows:

- *Equivalent continuous sound level ( $L_{eq}$ )*. Although the  $L_{eq}$  was defined previously in Eqs. (14) and (15), further comments regarding common averaging times are merited. These include hourly levels, day levels (7 AM–10 PM), evening levels (7–10 PM), and night levels (10 PM–7 AM).



**Figure 13** A-weighted sound pressure level and  $L_{eq}$  as a function of time before, during, and after the garbage truck arrival.



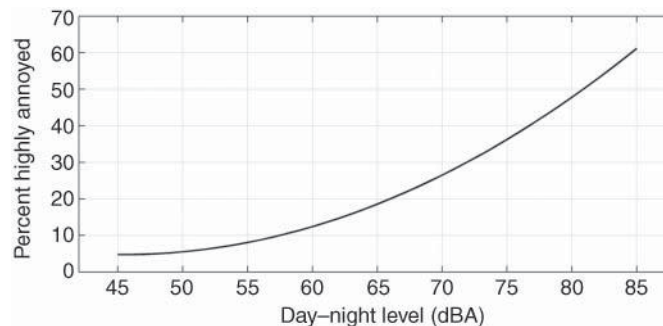
**Figure 14** Cumulative distribution of the time series in Fig. 13, showing what fraction of time the sound level exceeds a given sound pressure level.

- *Day–Night Level (DNL or  $L_{dn}$ )*. The  $L_{eq}$  obtained for a 24-h period after a 10-dBA penalty is added to the night levels (10 PM–7 AM). For individual  $L_{eq}$  calculations carried out over 1-h intervals ( $L_{1h}$ ),  $L_{dn}$  may be expressed as

$$L_{dn} = 10 \log_{10} \frac{1}{24} \left[ \sum_{i=0100}^{0700} 10^{0.1(L_{1h}(i)+10)} + \sum_{i=0800}^{2200} 10^{0.1L_{1h}(i)} + \sum_{i=2300}^{2400} 10^{0.1(L_{1h}(i)+10)} \right] \quad (28)$$

The DNL is important in, for example, land planning around airports and in predicting community annoyance due to transportation noise. The predicted community response in terms of percent of people highly annoyed (see Fidell et al.<sup>18</sup>) as a function of DNL is shown in Fig. 15.

- *Community Noise Equivalent Level (CNEL)*. CNEL is calculated using the  $L_{eq}$  obtained for a 24-h period after 5 dBA is added to the evening levels (7–10 PM) and 10 dBA is added to the night levels. It can be calculated similar to  $L_{dn}$ , with the appropriate penalty given during the evening (between 2000 and 2200 h).
- *Effective Perceived Noise Level (EPNL)*. This metric was designed for characterizing aircraft noise impact and is used by the Federal Aviation Administration (see FAR Part 36 Sec. A.36) in the certification of commercial aircraft. The metric accounts for (a) the nonuniform response of the human ear as a function of frequency (i.e., the perceived noise level), (b) the additional annoyance due to significant tonal components of the spectrum (the tone-corrected perceived noise level), and (c) the change in perceived



**Figure 15** Percentage of people highly annoyed for a given DNL.

noisiness due to the duration of the flyover event. Too involved to be repeated here, calculation procedures for EPNL may be found in FAR Part 36 Sec. A.36.4 or Raney and Cawthorn.<sup>19</sup>

## 7.2 Noise Surveys

In order to document existing community and environmental noise challenges and assist in, for example, land usage planning, properly conducted noise surveys are important. Adequacy of the noise survey parameters will change according to the specific issue and other legal or regulatory requirements. However, careful consideration of number of measurement locations, survey time and duration, appropriate measures, and other measurement parameters is important. In residential surveys, measurements are often made a prescribed distance from a property line. The survey may need to be made during different times of day or seasons and under different meteorological conditions, some of which favor sound propagation to the receiver. A log of individual noise events, such as aircraft flyovers, can form an important part of the survey.

Whatever the specifics of the measurements, an environmental survey report should include not only the data but also information essential to their interpretation. This includes (see Bies and Hansen,<sup>20</sup> p. 185):

- Reference to the appropriate regulatory document(s)
- Measurement dates, times, and measurement locations
- Local meteorology (wind, temperature, humidity, precipitation) during the survey
- Noise source descriptors
- Instrumentation (type and orientation of meter or microphone and acquisition system, presence of windscreen, etc.)
- Types of noise data recorded
- Impact of extraneous noise sources

## 8 SOUND INTENSITY MEASUREMENTS

### 8.1 Sound Intensity via the “ $p$ - $p$ ” Principle

Although sound pressure measurements are immensely useful in that they yield the sound field magnitude at the measurement location, they may not fully describe the sound energy transmission for many types of sound fields. The acoustic intensity can be a very important measure in that it is potentially a three-dimensional vector measurement of the net sound energy flux.

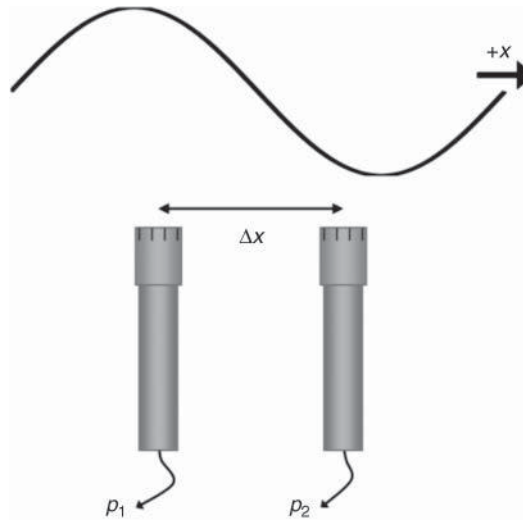
Acoustic intensity was defined previously in Eq. (3) as the sound power per unit area. The instantaneous intensity along direction  $x$ , with units of  $\text{W}/\text{m}^2$  may be written as

$$I_{i,x}(t) = p(t)u_x(t) \quad (29)$$

where  $p(t)$  and  $u_x(t)$  are the time-dependent pressure and particle velocity in the  $x$  direction. Of more practical measurement interest is the time-averaged intensity, which can be written as

$$I_x(t) = \frac{1}{T} \int_0^T p(t)u_x(t)dt \quad (30)$$

The measurement of  $p(t)$  is obtained in straightforward fashion with a microphone; however, direct particle velocity measurements are more difficult. Particle velocity measurements have been obtained using ultrasonic transducers or hot-wire techniques, and a commercial “ $p$ - $u$ ” probe exists (see Jacobsen and de Bree,<sup>21</sup>). However, the more common technique of obtaining  $u_x(t)$  involves processing the pressure signals from closely spaced, well-matched



**Figure 16** Layout of two microphones used to obtain particle velocity and pressure estimates needed for calculating acoustic intensity.

microphones, that is, the “ $p$ - $p$ ” principle (see Fahy,<sup>22</sup>). This is represented schematically in Fig. 16. The pressure at the center of the two microphones spaced  $\Delta x$  apart is obtained by averaging the pressure signals as

$$p(t) \approx \frac{p_1(t) + p_2(t)}{2} \quad (31)$$

and the particle velocity is estimated through Euler’s equation

$$\frac{\partial p}{\partial x} = -\rho_0 \frac{\partial u_x}{\partial t} \quad (32)$$

which results in

$$u_x(t) \approx \frac{1}{\rho \Delta x} \int_{-\infty}^t [p_2(\tau) - p_1(\tau)] d\tau \quad (33)$$

For the case of a time stationary signal, Fahy<sup>22</sup> shows that the mean intensity in the  $x$  direction may be written as

$$I_x = -\frac{1}{\rho \Delta x T} \int_0^T p_1(t) \int_{-\infty}^t p_2(\tau) d\tau dt \quad (34)$$

In other words, the average intensity in a time stationary field is obtained from averaging the product of one microphone’s signal and the integrated signal from a second, closely spaced microphone.

Given the prevalence of real-time spectral analyzers, it is helpful to define intensity in terms of the Fourier transforms of the pressure signals. In the frequency domain, the complex intensity is defined as

$$I_C(f) = I(f) + jJ(f) \quad (35)$$

In Eq. (35),  $I(f)$  is the mean active intensity and represents the in-phase components of the pressure and velocity signals, whereas  $J(f)$  is the amplitude of the “reactive” intensity and represents the in-quadrature portions of the signals (see Fahy<sup>22</sup>). The time average of the reactive intensity is zero; for additional information on its calculation and significance (see Fahy,<sup>22</sup>

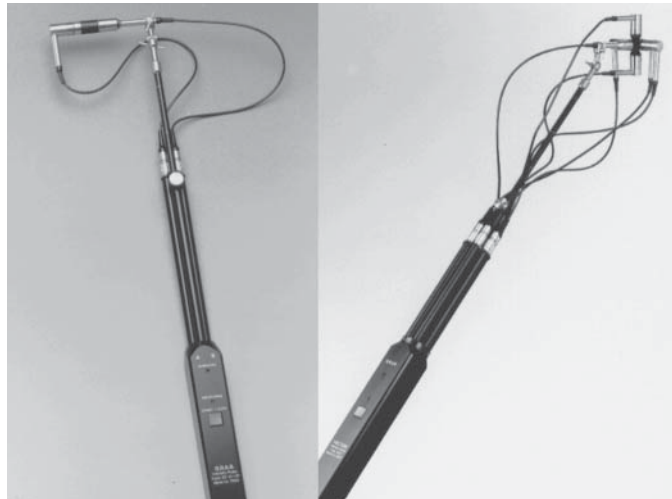
Jacobsen,<sup>23</sup> and Mann et al.<sup>24</sup>). For the two microphones in Fig 16, the active intensity spectrum [the spectral form of Eq. (34)] may be written as

$$I_x(f) = \frac{1}{2\pi f \rho \Delta x} \text{Im}\{G_{p_2 p_1}(f)\} \quad (36)$$

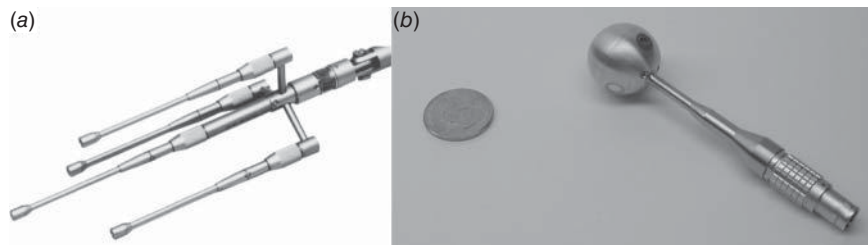
where  $G_{p_2 p_1}(f)$  is the single-sided time-averaged cross-spectral density between the two microphones. In the case of a multidimensional intensity probe, calculation of the intensity vector components is geometry specific but involves weighting cross-spectral components between various pairs. A method for deriving the calculation process that results in minimized least-square error has been proposed by Pascal and Li.<sup>25</sup>

## 8.2 Intensity Probes

There are several one- and multidimensional intensity probes available. These come in various configurations. One- and three-dimensional sound intensity probes are shown in Fig. 17. Alternate three-dimensional probes are displayed in Fig. 18, which use four microphones located



**Figure 17** One- (two microphones) and three-dimensional (three orthogonal pairs of microphones) sound intensity probes, with the microphones in the face-to-face configuration and employing a solid spacer.



**Figure 18** (a) Ono Sokki Tetra-phon, which uses four microphones in a side-by-side configuration and arranged in a regular tetrahedron. (b) Spherical intensity probe (along with a U.S. quarter for scale), developed by Brigham Young University and GRAS Sound and Vibration for rocket noise measurements. The microphones are arranged in a tetrahedral configuration on the surface of the sphere.

at the vertices of a regular tetrahedron. The probe at the left is the Ono Sokki Tetra-phone® and the probe at the right was developed for rocket noise measurements by Brigham Young University and GRAS Sound and Vibration (see Gee et al.<sup>26,27</sup>). Other possible configurations exist, such as those described by Pascal and Li.<sup>25</sup>

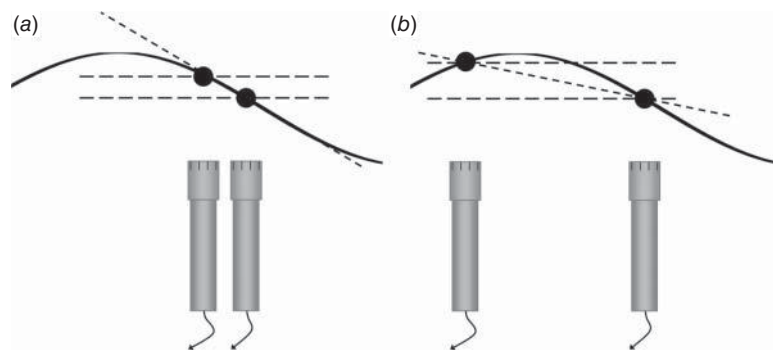
### 8.3 Systematic Measurement Errors

It is important to understand the possible sources of error in the intensity measurement technique. Some errors that arise include scattering from probe or holder surfaces and environmental effects, such as wind. These errors are field and measurement specific and are not treated further in this section. However, other systematic errors that arise are inherent in the finite-sum averaging and finite difference that takes place. When the microphone separation distance is small relative to a wavelength, the two microphones can be used to adequately represent the average pressure and the pressure gradient between the two microphones. However, as frequency and/or separation distance is increased such that the distance relative to a wavelength increases, errors result. Although there are errors associated with both the finite-differencing and summation, it is the latter that primarily causes the estimate of the intensity to be too low, as is illustrated in Fig. 19.

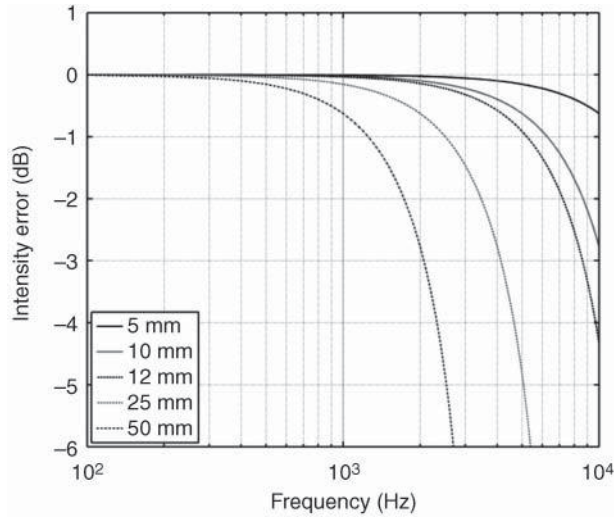
The error in intensity magnitude for different sensor spacings ( $\Delta x$ ) is shown in Fig. 20. The magnitude errors grow as a function of frequency and microphone spacing. Jacobsen et al.<sup>28</sup> have found that, in practice, probes that employ solid spacers with the microphones in the face-to-face configuration have a resonance phenomenon that partially counteracts the finite summation bias error and extends the probe's usable bandwidth. It is also worth noting that the phase errors introduced by the  $p$ - $p$  measurement principle are zero for the case of the plane progressive wave and planar interference fields, provided that the sensor separation distance is less than a half wavelength, at which point spatial aliasing begins to occur.

### 8.4 Transducer Mismatch

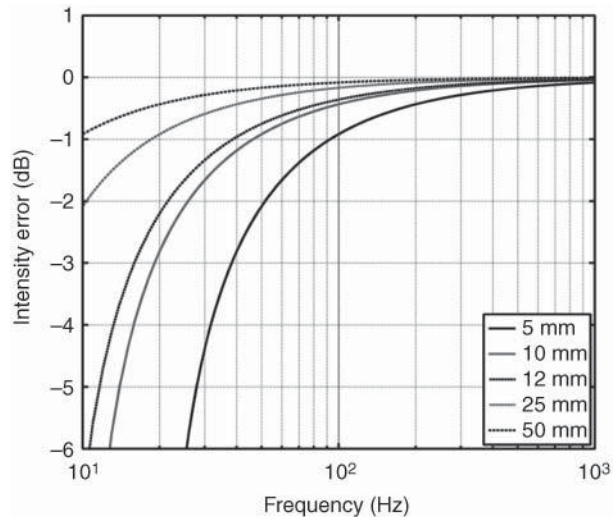
Another source of error is transducer or instrumentation system mismatch. Any amplitude or phase mismatch will result in errors in the estimation of  $p$  or  $u$ , which translate into intensity amplitude and/or direction errors. The intensity magnitude error for a progressive plane wave propagating along the probe axis with channel phase mismatch of  $0.1^\circ$  is shown in Fig. 21.



**Figure 19** Diagram showing the process of finite differencing and summation. (a) For small separation distance, the two pressure estimates (black dots) can be used to accurately represent the pressure at the midpoint between the microphones. (b) The separation distance has increased and although finite differencing results in a near-accurate slope estimate, the pressure average obtained will underestimate the true pressure.



**Figure 20** Error in intensity magnitude for ideal intensity probes with different microphone spacings. This underestimation of acoustic intensity at high frequencies is directly related to an underestimation in the acoustic pressure, based on the separation of the microphones.



**Figure 21** Intensity magnitude error for plane wave propagation along the probe axis with  $0.1^\circ$  phase error between channels and various sensor spacings.

The figure shows the increased error as frequency and sensor spacing decreases, as the acoustic phase difference between channels becomes progressively smaller and the phase error becomes relatively more important. In general, phase errors between measurement channels are frequency dependent and often grow as the low-frequency limit of the microphone is approached. For this reason, commercial intensity probes are sold with solid spacers of various lengths to provide accurate measurements at different frequency ranges.



In a field where both microphones are exposed to the same pressure, amplitude, and phase, the time-averaged intensity should be zero. This can be seen from the fact that the imaginary part of the cross spectrum between the two signals in Eq. (36) is zero. However, for a real probe with slightly mismatched microphones measuring a uniform sound field in a small cavity, the phase error between the microphones results in a residual or “false” intensity measurement. For a given pressure amplitude,  $p$ , phase error,  $\varphi_{\text{err}}$ , and separation distance relative to wavelength,  $k \Delta x$ , the residual intensity error,  $I_{\text{res}}$ , can be expressed as

$$\frac{I_{\text{res}}}{p^2 / (\rho c)} = \frac{\varphi_{\text{err}}}{k \Delta x} \quad (37)$$

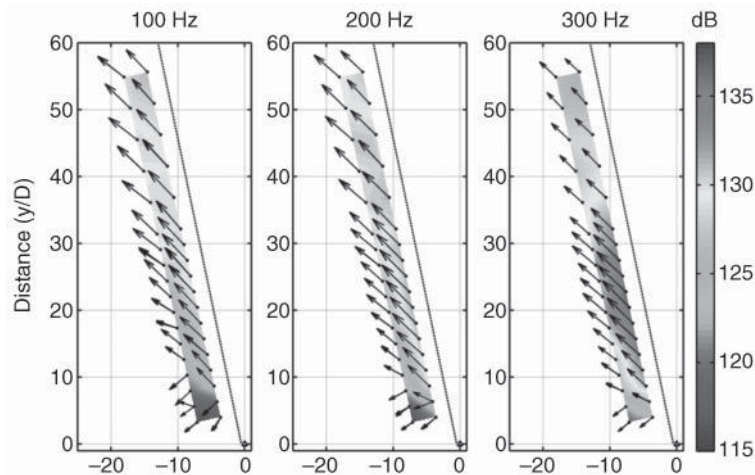
The pressure-residual intensity index, which is a convenient way of expressing the phase error, is calculated as

$$\delta_{pI_{\text{res}}} = 10 \log_{10} \left[ \frac{p^2 / (\rho c)}{I_{\text{res}}} \right] \quad (38)$$

For example, a  $0.1^\circ$  phase error at 100 Hz for a 25-mm microphone spacing results in an pressure-residual intensity index of 14.2 dB. For the 50-Hz one-third-octave band, ANSI standard S1.9-1996 calls for a minimum pressure-residual intensity index of 7.0 dB for a class 2 measurement system and 13.0 dB for a class 1 system. Other specifications for probe and calibration and classification are provided within the standard.

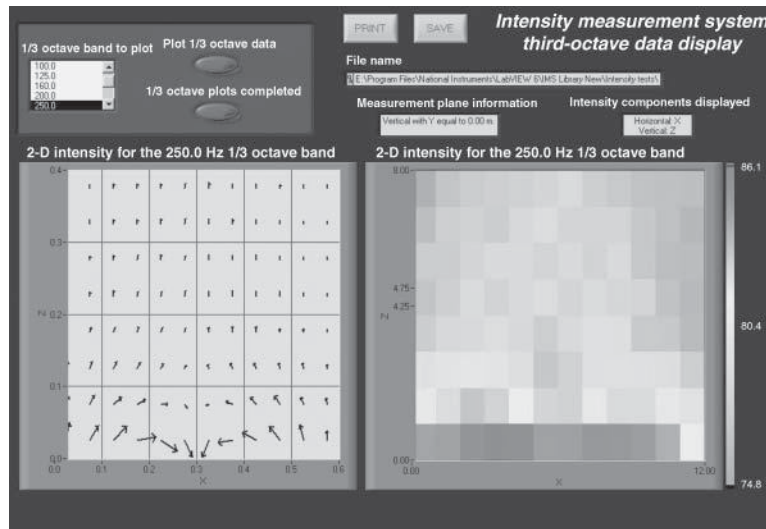
## 8.5 Sound Intensity Applications

As discussed below, one application of sound intensity measurements is the measurement of sound power. Other applications include sound source characterization and localization and examination of energy flow. Near-field intensity vectors for the radiated noise from a small solid rocket motor at three different frequencies are shown in Fig. 22 (see Gee et al.<sup>27</sup>). The intensity vectors reveal the directionality and magnitude of the sources. Another example is the graphical display of an intensity measurement system developed for NASA Glenn Research Center (see Dix et al.<sup>29</sup>). The system involves an intensity probe attached to a computer-controlled motion system that can be rapidly moved around to produce results such as those shown in Fig. 23.



**Figure 22** Measurement of vector sound intensity made near a rocket plume at three different frequencies. The vectors reveal the directionality and magnitude of the energy flow.





**Figure 23** Graphical display of an automated sound intensity measurement system developed for NASA Glenn Research Center.

The sources in this case comprise three loudspeakers receiving the same source signal but with the middle speaker out of phase with the other two. The intensity vectors clearly reveal the source/sink nature of the near-field energy flow, which the intensity magnitude alone (shown to the right) does not.

## 9 SOUND POWER MEASUREMENTS

When considering acoustic radiation from a source, sound power measurements are often preferable to sound pressure measurements. The sound power corresponds to the amount of acoustic energy radiated per unit time and can also be expressed as the integral of the acoustic intensity over the area through which the acoustic energy is radiated. It is expressed in units of watts (W). Unlike sound pressure, the measurement of sound power is independent of the distance from the source where the measurement is made. Furthermore, for many sources the sound power radiated is nearly independent of the physical location of the source. Thus, if the sound power is measured outdoors or inside a room, the value will be nearly identical; however, if the sound pressure radiated from that same source is measured in those two environments, significantly different results would be expected.

The magnitude of the sound power varies tremendously for normally encountered sources. For this reason, it is convenient to express the sound power on a logarithmic scale and is referred to as the sound power level. The sound power level,  $L_W$ , is given by

$$L_W = 10 \log_{10} \left( \frac{W}{W_{\text{ref}}} \right) \quad (39)$$

where  $W$  is the sound power of the source in watts and  $W_{\text{ref}}$  is the reference sound power. For airborne applications, the reference sound power is usually taken to be  $10^{-12}$  W.

Most sound power level measurements are obtained using pressure measurements, based on the relationship between the radiated power and the radiated pressure. For these measurements, the measurement can be categorized as a free field or a reverberant field condition.

## 9.1 Measurement of the Sound Power Level in a Free Field

The configuration corresponding to measurement of the sound power level in a free field is generally obtained in an anechoic chamber. An anechoic chamber has the property that there is no appreciable reflection from any of the walls of the chamber, generally obtained by constructing the walls with sound absorbing wedges. For a free field, the sound power can be obtained by integrating the sound intensity over an imaginary spherical surface of area  $S = 4\pi r^2$  enclosing the source. If the measurement is in the far field, the intensity is directly related to the acoustic pressure. Thus

$$\begin{aligned} W &= \int_S \mathbf{I} \times dS \\ &= \int_S \frac{p^2}{\rho c^2} dS \\ &= \frac{p_{\text{ave}}^2}{\rho c^2} S \end{aligned} \quad (40)$$

Using standard reference values (20  $\mu\text{Pa}$  for pressure and  $10^{-12}$  W for power) allows the sound power level to be obtained from the *average* sound pressure level as

$$L_W = \bar{L}_p + 10 \log_{10} \left( \frac{S}{S_0} \right) \quad (41)$$

where  $S_0$  is the reference area of  $1 \text{ m}^2$ . The average sound pressure level is obtained using

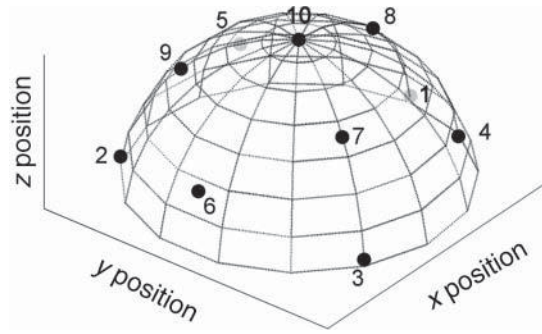
$$\bar{L}_p = 10 \log_{10} \left( \frac{1}{N} \sum_{i=1}^N 10^{0.1L_{pi}} \right) \quad (42)$$

Here,  $L_{pi}$  is the sound pressure level from the  $i$ th measurement location (in decibels), usually measured in third-octave or octave bands and typically A weighted, and  $N$  is the total number of measurement locations. The ISO standards outline the number of points that should be included in the measurement. There are also a number of standard measurement surfaces that are used.

For free-field measurements, the measurement surface is generally taken as an imaginary sphere. As the first step, an imaginary box (called the reference box) is constructed that is as small as possible but completely encloses the source of interest. The characteristic distance,  $d_0$ , associated with this box is taken as the distance from the projection of the center of this box on the floor to one of the upper corners of the box. The radius of the measurement sphere,  $R$ , should then be at least  $2d_0$ . If the size of the source is large, relative to the available measurement space, then the measurements can be made on the surface of a large imaginary box surface. The measurement locations are chosen to represent equal area on the sphere or box.

For many sources, it is more practical to measure the sound power in a hemianechoic room or outdoors. The procedure for this measurement parallels that described above for anechoic conditions, except that the measurement surface corresponds to either a hemisphere or a five-sided box. Several standards are available to guide the measurement of sound power for these conditions. Precision (or grade 1) methods yield reproducibility with a standard deviation of less than 1 dB, while engineering (or grade 2) methods and survey (or grade 3) methods yield reproducibility with a standard deviation of less than 1 dB or 3 dB, respectively.

Figure 24 shows the basic measurement positions that should be used for a hemispherical measurement surface. The engineering method described in ISO 3744 normally uses the 10 positions shown in this figure, while the survey method described in ISO 3746 only uses positions 4, 5, 6, and 10. The one restriction is that if the difference between any two sound



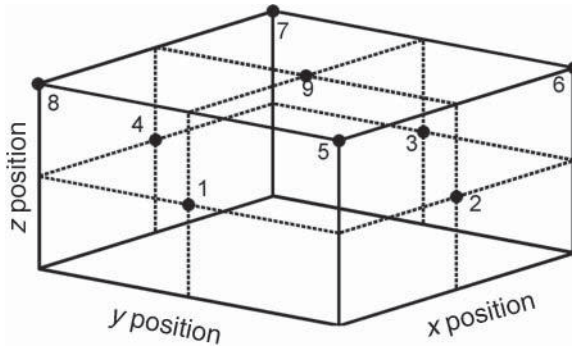
**Figure 24** Basic sound power measurement positions that should be used for a hemispherical measurement surface. The two measurement locations on the backside of the hemisphere are displayed here in gray.

**Table 12** Microphone Locations According to ISO 3745

No. <sup>a</sup>	$x/R$	$y/R$	$z/R$
1	-0.99	0	0.15
2	0.50	-0.86	0.15
3	0.50	0.86	0.15
4	-0.45	0.77	0.45
5	-0.45	-0.77	0.45
6	0.89	0	0.45
7	0.33	0.57	0.75
8	-0.66	0	0.75
9	0.33	-0.57	0.75
10	0	0	1.0
11	0.99	0	-0.15
12	-0.50	0.86	-0.15
13	-0.50	-0.86	-0.15
14	0.45	-0.77	-0.45
15	0.45	0.77	-0.45
16	-0.89	0	-0.75
17	-0.33	-0.57	-0.75
18	0.66	0	-0.75
19	-0.33	0.57	-0.75
20	0	0	-1.0

<sup>a</sup>Positions 1–10 are used for a hemispherical measurement surface of radius  $R$ , and positions 1–20 are used for a spherical measurement surface (the  $z$ -axis is the vertical axis).

pressure level measurements (in decibels) exceeds the number of measurement locations, the number of locations must be increased. If a fully anechoic condition exists, so that a spherical measurement surface is used, the measurements in the lower hemisphere correspond to those on the upper hemisphere. The coordinates for all 20-measurement positions are given in Table 12. Figure 25 shows the nine-measurement positions used if a box surface is implemented in a hemianechoic environment.



**Figure 25** The nine measurement positions used for sound power measurements if a box surface is implemented in a hemianechoic environment.

## 9.2 The Reverberation Method

The sound power of an unknown source can also be determined in a reverberant environment. The concept behind this measurement is that the acoustic power radiated in this environment must equal the power absorbed by the surfaces of the test room. If the test room is a reverberation chamber, the sound is considered to be diffuse. For such a field, the sound power can be obtained directly from the sound pressure level in the room if the absorption of the room is known, which can be determined through measuring the reverberation time in the room. Since the room is never truly diffuse, the sound pressure level is obtained through the use of multiple pressure measurements, as outlined in the ISO 3741 standard.

Since the room response is never truly diffuse, the measurement of the sound power is generally more problematic with a narrowband sound source than a broadband source using the reverberation method. Thus, the reverberation method is more accurate for use with broadband noise, with the sound power being measured in octave bands or one-third-octave bands.

In its simplest form, the sound power is obtained as

$$L_W = \bar{L}_p + 10 \log_{10} \left( \frac{A}{A_0} \right) - 6 \text{ dB} \quad (43)$$

where  $\bar{L}_p$  is the mean sound pressure level measured in the room (in decibels),  $A$  is the total absorption in the room (meters squared) obtained from measuring the reverberation time, and  $A_0$  is the reference absorption, taken as  $1 \text{ m}^2$ .

In practice, several corrections can lead to a more accurate measurement. Since the energy in the room is not truly diffuse, the standard requires the sound pressure measurements to be at least 1.0 m away from the boundary. However, the energy density is greatest near the walls, so it has been found that the term  $10 \log_{10} [1 + Sc/(8Vf)]$  can correct for this underestimate. To correct for air absorption in the room, the term  $4.34A/S$  is added. Corrections for meteorological conditions can also be added, resulting in the sound power being obtained as

$$L_W = \bar{L}_p + 10 \log_{10} \left( \frac{A}{A_0} \right) + 10 \log_{10} \left( 1 + \frac{Sc}{8Vf} \right) + 4.34 \frac{A}{S} - 6 + C_1 + C_2 \quad (44)$$

Here,  $S$  is the total surface area of the measurement room (meters squared),  $V$  is the volume of the measurement room (meters cubed),  $f$  is the center frequency of the frequency band of interest (Hertz),  $c$  is the speed of sound given by  $c = 20.05 \sqrt{273 + \theta} \text{ m/s}$  [where  $\theta$  is the temperature ( $^{\circ}\text{C}$ )],  $C_1 = -10 \log(B\sqrt{T_0}/B_0\sqrt{T})$  (where  $B$  is the static atmospheric

pressure,  $B_0 = 1.013 \times 10^5$  Pa,  $T$  is the temperature in kelvins, and  $T_0 = 313.15$  K), and  $C_2 = -15 \log(BT_1/B_0T)$  (where  $T_1 = 296.15$  K).

### 9.3 Comparison Method

The sound power can also be determined through the use of the comparison method. This method is simple and accurate but does require the use of a known reference power source. The reference power source, radiating reference sound power  $L_{W,\text{ref}}$ , is placed in the measurement volume, and the sound pressure level,  $L_{p,\text{ref}}$ , associated with the reference power source is measured. The unknown source is then operated and the sound pressure level,  $L_p$ , is measured. The unknown sound power is then obtained as

$$L_W = L_{W,\text{ref}} + L_p - L_{p,\text{ref}} \quad (45)$$

For accurate results, the test room should be hard walled with no major absorbing surfaces. The volume must exceed 40 times the volume of the reference box, a minimum of three microphones must be used (which remain in the same locations for both measurements), and the sound power should be processed in octave bands or one-third-octave bands. If the unknown source is not movable, the reference sound source is located on top of the unknown source.

## 10 SOUND EXPOSURE MEASUREMENTS

Two acoustical quantities that are important to determining hearing risk and appropriate conservation procedures are the sound exposure and noise dosage. Additional information on these measurements can be found in Kardous<sup>30</sup> and Marsh and Richings.<sup>31</sup>

### 10.1 Sound Exposure Level

The sound exposure, with  $W$ -type weighting filter applied, is defined for an event occurring over time  $T$  as

$$E_W = \int_0^T p_W^2(t) dt \quad (46)$$

where  $p_W(t)$  is the instantaneous weighted pressure. The most common weighting applied in this situation is A weighting. Without a weighting filter applied, this quantity is related to the total acoustic energy incident on a receiver. From the sound exposure in Eq. (46), the  $W$ -weighted sound exposure level (SEL) is calculated as

$$\text{SEL}_W = 10 \log_{10} \left( \frac{E_W}{E_{\text{ref}}} \right) \quad (47)$$

where  $E_{\text{ref}}$  is the reference sound exposure of  $400 \mu\text{Pa}^2 / s$ .

Relationships between sound exposure, the SEL and the  $L_{\text{eq}}$  defined previously in Eq. (14) can be stated. First, the SEL can be calculated from the  $L_{\text{eq}}$  of the same weighting as

$$\text{SEL} = L_{\text{eq}} + 10 \log_{10}(T) \quad (48)$$

Alternatively

$$\text{SEL} = p_{\text{ref}}^2 \times T \times 10^{0.1L_{\text{eq}}} \quad (49)$$

Although the international standard unit for sound exposure is the squared pascal second, a second unit, the squared pascal hour ( $\text{Pa}^2 / \text{h}$ ), is also used. This is a convenient unit for measuring workplace noise exposure, particularly since an A-weighted sound exposure of  $1 \text{ Pa}^2 / \text{h}$  is nearly equal to a constant level of 85 dB over an 8-h working day.

## 10.2 Noise Dosage

The noise dose is a metric used to quantify noise exposure in the workplace. According to ANSI S1.25, the noise dose for an 8-h workday and exchange rate,  $Q$ , is defined as

$$D_Q = \frac{100}{8} \int_0^T 10^{[(L_A(t) - L_C)/q]} dt \quad (50)$$

where  $t$  is measured in hours and  $T$  is the measurement duration. In Eq. (50),  $L_A(t)$  is the slow or fast A-weighted sound level in decibels, provided that the level is greater than a selected threshold level, or is  $-\infty$  if below the threshold. The level,  $L_C$ , is the criterion sound level that defines 100% noise dosage and  $q = Q/\log(2)$ , where  $Q$  is the exchange rate of 3, 4, or 5 dB. The exchange rate is the change in sound level that corresponds to a doubling or halving of the sound exposure duration while maintaining a constant percentage of criterion exposure. For Occupational Safety and Health Administration (OSHA) regulations, the threshold level is 80 dBA, the criterion level is 90 dBA, and the exchange rate is 5 dB. The exchange rate for the National Institute of Occupational Safety and Health (NIOSH) and most international standards is given as 3 dB.

An alternate method of calculating noise dosage is defined for a workday with noise exposure at different levels for discrete intervals. In this case

$$D = 100 \times \sum_i \frac{t_i}{T_i} \quad (51)$$

where  $t_i$  is the exposure time in hours and  $T_i$  is the allowable (100% dosage) duration for exposure at that level. Values for  $T_i$  can be calculated for an 8-h workday as

$$T = \frac{8}{2^{[(L - L_C)/Q]}} \quad (52)$$

(see Appendix A of OSHA 29CFR 1910.95 regulation).

## 10.3 Equipment

Personal sound exposure meters and noise dosimeters are used to assess noise exposure in the workplace. The essential elements of the dosimeter are shown in Fig. 26 and a typical class 2 dosimeter is displayed in Fig. 27. ANSI Standard S1.25 indicates that a dosimeter should allow for A or C weighting and fast and slow exponential averaging. It should also permit a criterion level of 95, 85, 84, 80, or variable dB, a threshold level of 90, 80, or variable dB, and an adjustable exchange rate of 3, 4, or 5 dB. The standard also specifies that the dosimeter should properly measure impulsive noises up to 140 dB, the maximum allowable peak sound

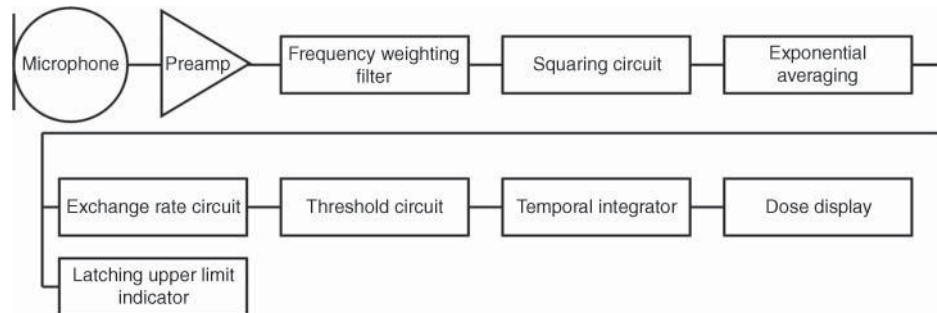
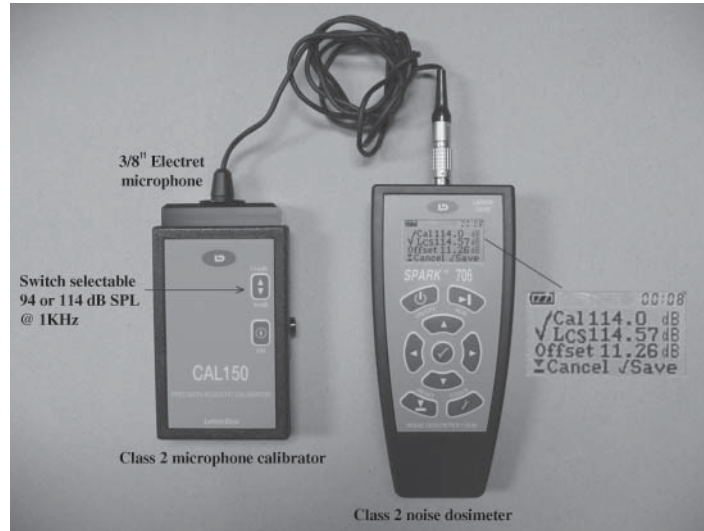


Figure 26 Elements of a noise dosimeter.



**Figure 27** A class 2 Larson Davis noise dosimeter with microphone inserted in a calibrator. (Photo courtesy of Chuck Kardous, NIOSH.)



**Figure 28** Noise dosimeter being worn. (Photo courtesy of Chuck Kardous, NIOSH.)



level without hearing protection. NIOSH has shown that many dosimeters have issues with these high-level measurements.<sup>32</sup>

The noise dosimeter may be used to monitor the noise environment in an area or worn as a personal dosimeter. In this case, the ANSI S12.19 standard specifies that the microphone should be located on the middle-top of a worker's shoulder and should be oriented approximately parallel to the shoulder's plane. This is shown in Fig. 28. The amount that the person affects the noise level measured depends on, for example, the noise spectrum, absorption due to clothing, angle of incidence, and microphone orientation. The increase may be as much as 5 dB, but an increase in level of around 1 dB is typical.

## REFERENCES

1. W. M. Lang, and M. A. Nobile, in C. M. Harris (Ed.), *Handbook of Acoustical Measurements and Noise Control*. 3rd ed., Acoustical Society of America, Melville, NY, 1998, Chapter 15.
2. F. V. Hunt, *Origins in Acoustics, The Science of Sound from Antiquity to the Age of Newton*, reprinted by the Acoustical Society of America, 1992.
3. A. D. Pierce, *Acoustics: An Introduction to Its Physical Principles and Applications*, reprinted by the Acoustical Society of America, 1989.
4. L. L. Beranek, 1993. "Acoustics," reprinted by the Acoustical Society of America.
5. L. E. Kinsler, A. R. Frey, A. B. Coppens, and J. V. Sanders, *Fundamentals of Acoustics*, 4th ed, Wiley, New York, 2000.
6. H. Fletcher and W. A. Munson, "Loudness, Its Definition, Measurement and Calculation," *J. Acoust. Soc. Am.* **5**(2), 82–108, 1933.
7. D. W. Robinson and R. S. Dadson, "Threshold of Hearing and Equal-Loudness Relations for Pure Tones, and the Loudness Function," *J. Acoust. Soc. Am.*, **29**(12), 1284–1288, 1957.
8. H. Davis and S. F. Silverman, *Hearing and Deafness*, 4th ed., Holt, Rinehart, & Winston, New York, 1978, Chapter 2.
9. ANSI S1.12-1967—R1977. Specifications for Laboratory Standard Microphones, New York, American National Standards Institute.
10. ANSI S1.10-1966—R1986 Method for the Calibration of Microphones, New York, American National Standards Institute.
11. E. D. Burnett and V. Nedzelnitsky, "Free-Field Reciprocity Calibration of Microphones," *J. Res. Nat. Bur. Stand.-A*, **92**(2), 129–151, 1987.
12. G. R. Torr and D. R. Jarvis, "A Comparison of National Standards of Sound Pressure," *Metrologia*, **26**, 253–256, 1989.
13. W. R. Maclean, "Absolute Measurement of Sound without a Primary Standard". *Jo. Acoust. Soc. Am. D*, **12**(13.1), 140–146, 1940.
14. R. Bobber, *Underwater Electroacoustic Measurements*, Peninsula Publishing, Newport Beach, CA 1990.
15. M. D. Egan, *Concepts in Architectural Acoustics*, McGraw-Hill, New York, 1972.
16. W. J. Strong and G. R. Plitnik, *Music Speech Audio*, 3rd ed., BYU Academic, Provo, UT, 2007.
17. W. E. Blazier, Jr., "Noise Control Criteria for Heating, Ventilating, and Air-Conditioning Systems," in *Handbook of Acoustical Measurements and Noise Control, Chapter 43*. 3rd ed., C. M. Harris (Ed., Acoustical Society of America, Melville, NY); 1998.
18. S. Fidell, D. S. Barber, and T. J. Schultz "Updating a Dosage Effect Relationship for the Prevalence of Annoyance Due to General Transportation Noise," *J. Acoust. Soc. Am.* **89**, 221–233, 1991.
19. J. P. Raney and J. M. Cawthorn, "Aircraft Noise," in C. M. Harris (Ed.) *Handbook of Acoustical Measurements and Noise Control*, 3rd ed., Acoustical Society of America, Woodbury NY, 1998.
20. D. A. Bies and C. H. Hansen, *Engineering Noise Control: Theory and Practice*, 4th ed., Spon Press, London, 2009.
21. F. Jacobsen and H.-E. Bree. "Comparison of Two Different Sound Intensity Measurement Principles," *J. Acoust. Soc. Am.* **118**, 1510–1517, 2005.



22. F. J. Fahy *Sound Intensity*, 2nd ed., E&FN Spon, London, 1995.
23. F. Jacobsen, "A Note on Instantaneous and Time-Averaged Active and Reactive Sound Intensity," *J. Sound Vibration*, **147**, 489–496, 1991.
24. J. A. Mann III, J. Tichy, and A. J. Romano, "Instantaneous and Time-Averaged Energy Transfer in Acoustic Fields," *J. Acoust. Soc. Am.*, **82**, 17–30, 1987.
25. J. Pascal and J. Li, "A Systematic Method to Obtain 3D Finite-Difference Formulations for Acoustic Intensity and Other Energy Quantities," *J. Sound Vib.*, **310**, 1093–1111, 2008.
26. K. L. Gee, J. H. Giraud, J. D. Blotter, and S. D. Sommerfeldt, Energy-Based Acoustical Measurements of Rocket Noise, *AIAA*, May, 2009–3165, 2009.
27. K. L. Gee, J. H. Giraud, J. D. Blotter, and S. D. Sommerfeldt, "Near-Field Acoust. Intensity Measurements of a Small Solid Rocket Motor," *J. Acoust. Soc. Am.*, **128**, EL69–EL74, 2010.
28. F. Jacobsen, V. Cutanda, and P. M. Juhl, "A Numerical and Experimental Investigation of the Performance of Sound Intensity Probes at High Frequencies," *J. Acoust. Soc. Am.*, **103**, 953–961, 1998.
29. G. Dix, K. L. Gee, and S. D. Sommerfeldt, "Design and Implementation of an Automated Intensity Scanning System at the Acoustical Testing Lab of NASA Glenn Research Center," in D. K. Holger and G. C. Maling, Jr. (Eds.), *Proceedings of Noise-Con 03*, New York, Noise Control Foundation, Poughkeepsie, 2003, Paper nc03\_202.
30. C. A. Kardous "Noise Dosimeters," in M. J. Crocker, (Ed.) *Handbook of Noise and Vibration Control*, Wiley, Hoboken, (NJ), 2007, Chapter 39.
31. A. H. Marsh and W. V. Richings, "Measurement of Sound Exposure and Noise Dose," in C. M. Harris (Ed), *Handbook of Acoustical Measurements and Noise Control*, 3rd ed., Acoustical Society of America, Melville NY, 1998, Chapter 12.
32. C. A. Kardous and R. D. Willson, "Limitation of Integrating Impulsive Noise When Using Dosimeters," *J. Occupat. Environ. Hyg.*, **1**, 456–462, 2004.

# Index

---

## A

- About.com, 527, 528
- ABS (American Bureau of Ships), 26
- Absolute viscosity, 810, 811
- Absorption:
  - of moisture, 483–484
  - of sound, 898–900
- Absorption coefficients, 898–900, 909, 976–977
- ABS polymers (acrylonitrile/butadiene/styrene) polymers, 363–365
- Accuracy, 648
  - of force transducers, 641
  - of microphones, 967
  - of viscometers, 835
- Acetals, 378–379
- Acoustics, 885–949
  - active noise control, 916–922
    - architectural, 922, 923
    - community noise in, 922–931
    - decibel scale, 889–890
    - defined, 886
    - equal loudness curves, 890–891
    - and hearing loss, 905–908
    - human auditory system, 942–946
    - impedance in, 893, 894
    - of loudspeakers, 948–949
    - of microphones, 946–949
    - nonlinear, 937–942
    - passive noise control in, 906–915
    - reflection and transmission of sound, 900–904
    - sound intensity, 887–888
    - sound power, 886–887
    - sound pressure, 888–889
    - sound quality analysis, 930, 932–937
    - and theory of sound, 894–900
    - weighting filters in, 891–893
  - Acoustical measurements, 953–995
    - of community and environmental noise, 980–982
    - decibel scale for, 958–959
    - frequency weightings, 959–962
    - fundamental, 954–962
    - with microphones, 962–969
    - of octave frequency bands, 962, 963
    - for rooms, 975–979
    - sound exposure, 992–995
    - sound intensity, 958, 982–988
    - sound isolation, 971–974
    - sound power, 957–958, 988–992
    - sound pressure, 955–957
    - sound pressure level, 969–971
    - standards for, 954, 955
- Acoustic filters, 910–913
  - bandstop filters, 910–912
  - high-pass filters, 913
  - low-pass filters, 911, 912
- Acoustic path, 907–908
- Acoustic radiation pressure, 940
- Acoustic source, 907–908
- Acoustic streaming, 940
- Acrylonitrile/butadiene/styrene (ABS) polymers, 363–365
- Acrylonitrile/styrene/acrylate (ASA) polymers, 365
- Active noise control, 916–922
  - applications of, 921–922
  - architectures for, 917–919
  - attenuation limits for, 919
  - filtered-*x* algorithm in, 919–920
  - identifying system for, 920
- Adhesives:
  - for electronic packaging, 498–499, 502
  - smart, 451
- Advanced thermal management materials, 430–432
- AED (auger electron spectroscopy), 855
- Aerospace applications, aluminum alloys for, 113
- Aerospace Materials Specifications (AMS), 26
- AFM (atomic force microscopy), 842–843
- Aircraft, aluminum alloys for, 113
- Alkyd resins, 395–396
- Allowable unit stress, 562

- Alloys:
- aluminum, *see* Aluminum alloys
  - copper, *see* Copper alloys
  - magnesium, *see* Magnesium alloys
  - nickel, *see* Nickel alloys
  - shape memory, 448–449
  - super-, *see* Superalloys
  - titanium, *see* Titanium alloys
- Alloy Center, 524–526
- Alloy elements, microstructure/properties of, 241
- Alloy steel(s), 28–36
- aluminum in, 23
  - boron in, 23
  - calcium in, 23–24
  - carbon in, 19–21
  - chromium in, 22
  - copper in, 22
  - dual-phase steels, 30
  - elements used in, 18–24
  - heat-resistant steels, 34–35
  - higher alloy steels, 31–36
  - high-performance steels, 30–31
  - hydrogen in, 24
  - lead in, 24
  - low-alloy steels, 29–31
  - manganese in, 20, 21
  - microalloyed steels, 30
  - molybdenum in, 22
  - nickel in, 22
  - niobium in, 23
  - nitrogen in, 24
  - phosphorus in, 21–22
  - rare earth elements in, 24
  - residual elements in, 24
  - selenium in, 24
  - silicon in, 21
  - stainless steels, 31–34
  - sulfur in, 22
  - tantalum in, 23
  - titanium in, 23
  - tool steels, 34
  - trip steels, 30
  - tungsten in, 23
  - ultrahigh-strength steels, 35–36
  - vanadium in, 22–23
  - wear-resistant steels, 35
  - zirconium in, 24
- Alpha alloys (titanium), 245
- Alpha-beta alloys (titanium), 245–247
- Alpha iron, 6
- Alternating stress amplitude, fatigue with, 572
- Alumina-based fibers (as composite reinforcement), 411
- Aluminum:
- in electronic packaging materials, 492–493
  - in steel, 23
  - surface finishes of, 487–488
- Aluminum alloys, 61–115
- advantages of, 62–65
  - by alloy class, 93–112
  - applications of, 93–114
  - cast alloys, 64–65, 80–87, 107–112
  - corrosion behavior of, 87–89
  - designation systems for, 65–73
  - in electronic packaging materials, 492–493
  - finishing of, 91–93
  - limitations of wrought/cast, 65
  - machining of, 89–91
  - market-area applications, 112–114
  - mechanical properties of, 73–87
  - nature of, 61–62
  - wrought alloys, 62–64, 73–79, 93–108
- Aluminum bronzes, 133, 147, 226
- American Bureau of Ships (ABS), 26
- American National Standards Institute (ANSI), 954, 955
- American Railway Engineering and Maintenance of Way Association (AREMA), 26
- American Society for Testing and Materials (ASTM) standards, 470, 832–833
- Amino resins, 396
- AMS (Aerospace Materials Specifications), 26
- Analogue outputs, 648
- Angle of twist, 598
- Annealing, 25, 26
- Anode, 46–47
- Anodic coatings, 296
- Anodized aluminum and aluminum alloys, 92, 487
- ANSI (American National Standards Institute), 954, 955
- Antimicrobial copper, 203
- Antimony, 24
- AOD, *see* Argon-oxygen decarburization
- aPP (atactic polypropylene), 359
- Apparent viscosity, 813
- Applied coatings, for aluminum alloys, 93
- Aramid fibers (as composite reinforcement), 411
- Architectural acoustics, 922, 923

- AREMA (American Railway Engineering and Maintenance of Way Association), 26
- Argon-oxygen decarburization (AOD), 4, 47–48, 332–334
- Armor, ceramic wear components, 462
- Aromatic polyamides, 377–378
- Aromatic polyketones, 389–391
- Arsenic, 24
- ASA (acrylonitrile/styrene/acrylate) polymers, 365
- Ashby's method (materials selection), 536, 537
- ASM International, 524–526
- ASTM E140, 16–17
- ASTM (American Society for Testing and Materials) standards, 470, 832–833
- Atactic polypropylene (aPP), 359
- Atmospheric absorption, 898–900
- Atomic force microscopy (AFM), 842–843
- Attenuation limits, 919
- Auditory system, 942–946
  - nervous system response to sound, 944
  - psychoacoustic effects of sound, 944–946
  - structure of ear, 942–944
- Auger electron spectroscopy (AED), 855
- Austenite, 18–19
- Austenitic alloys:
  - nickel, 40
  - stainless steels, 18–19, 31–32
  - welding of, 55–56
- Automotive engines, ceramic wear components, 461–462
- Automotive industry, aluminum alloys in, 112–113
- Average sound pressure level, 989
- A-weighted filters, 891, 960–961
- Axial strain, 648
- Axial stress, 557
- B**
- Bainite, 14, 15, 25
- Band pass filter, 648
- Bandstop filters, 910–912
- Bars, steel, 5
- Barks (unit), 933
- Basalt fibers (as composite reinforcement), 411
- Basic oxygen furnace (BOF), 4
- Beams of uniform strength, 586
- Beams, stresses on, 574–595
  - continuous beams, 586–588
  - curved beams, 588–591
  - and design, 584–586
  - flexure, 574–583
  - impact stresses, 591–595
  - vibratory stresses, steady/impulsive, 595
- Bearings, in ceramic wear applications, 460
- Bending, 601, 619
- Bending moment, 576, 579
- Bending springs, 619
- Beta alloys (titanium), 247
- Binary phase diagrams, 6
- Binaural quality index (BQI), 922
- Bioceramics, 463, 471
- Biological corrosion, 764–765
- Biomimetic structures, 440
- Biostatic properties of copper, 202
- Bisphenol A-based high-temperature sulfone (BisA-HTS) polymer, 385, 386
- Blades, stresses on rotating, 618
- Board-level interconnection, 503
- BOF (basic oxygen furnace), 4
- Boring (copper alloys), 207
- Boron, 23
- Boron fibers (as composite reinforcement), 410
- Boundary layer absorption, 899, 900
- BQI (binaural quality index), 922
- Bragg condition for interference, 638
- Brass(es), 43, 119, 128–130
  - envirobrasses, 144
  - free-cutting, 208
  - high-strength, 226
  - high strength yellow, 143
  - leaded, 128–129
  - leaded red, 141
  - leaded semired, 141
  - red, 141
  - semired, 141
  - silicon, 134, 143, 226
  - tin, 129–130
  - yellow, 128, 142–143
- Brazing, 211
- Brazing alloys, 132
- Breaking strength, 559
- Bridge resistance (load cell), 648
- Brinnelling failure, 706
- Brittle-coating method, 781
- Brittle fracture, 706
- Brittle materials, 458, 570
- Brittleness, 560
- Bronzes, 119
  - aluminum, 133, 147, 226
  - high-leaded tin, 146

- Bronzes (*continued*)
  - leaded phosphor, 132
  - leaded tin, 145–146
  - lead-free bearing, 226
  - nickel-tin, 147
  - phosphor, 131
  - silicon, 134, 143
  - tin, 145
- Bubble (tube) viscometers, 823–824, 834
- Buckling, 709
- Buckyballs, 450–451
- Building industry, aluminum alloys in, 112
- Bulk modulus, 562
- Bulk viscosity, 810
- B-weighted filters, 891–892, 961
  
- C**
- CA (cellulose acetate), 370
- CAB (cellulose acetate butyrate), 370
- Cadmium, 493
- Calibration:
  - defined, 648
  - of force transducers, 644–647
  - of microphones, 967–969
  - pistonphone, 967–968
  - reciprocity, 968
  - relative, 968
  - of resistance metal strain gauges, 665–666
  - switching, 968–969
- Calibration fluids, viscosity, 832
- Calibration transfer function, 969
- Cantilever beams, 574
- Capacity:
  - of force transducers, 641
  - of load cell, 648
- Capillary viscometers, 827–829, 834, 856
- Carbon fibers (as composite reinforcement), 409–410
- Carbon matrix composites:
  - applications of, 432–435
  - properties of, 429–432
- Carbon matrix materials, 414
- Carbon steels, 27–28, 53–55
- Cast alloys. *See also* Cast superalloys
  - aluminum, 64–65, 67, 69–72, 80–87, 107–112
  - copper, 140–149, 156–158
  - magnesium, 292, 293
  - manganese bronze, 143
  - special, 149
  - titanium, 252–254
- Casting(s):
  - AOD, 332–334
  - component production, 337–339
  - considerations, 336–337
  - continuous, 4–5
  - copper alloys, 209–210
  - ESR, 332–335
  - mechanical properties of, 292, 293
  - remelted ingot processing, 335–336
  - with superalloys, 332–337
  - titanium alloys, 258–259
  - VAR, 332, 333, 335
  - VIM, 332–334
- Cast leaded manganese bronze alloys, 143
- Cast superalloys:
  - applications of, 349–350
  - compositions of, 308
  - dynamic moduli of elasticity for, 324
  - effect of temperature on, 313–314, 317
  - physical properties of, 321–322
- Catalysts, smart, 448
- Cathode, 46–47
- Cauchy–Green strain, 683
- Cauchy stress tensor, 685
- Cavitation, 764
- CCCT (critical crevice corrosion temperature), 45
- Cellulose acetate (CA), 370
- Cellulose acetate butyrate (CAB), 370
- Cellulose propionate (CP), 370
- Cellulosic polymers, 370
- Cementite, 9, 14, 20, 25
- Ceramics:
  - in electronic packaging, 497
  - piezoelectric, 441, 443
- Ceramic failure, 789–807
  - delayed, 794–795
  - and design applying multiaxial Weibull statistics, 799–803
  - flaws, 791
  - fracture mechanics, 791–793
  - at high temperatures, 804–807
  - scatter, 795–799
  - strength, 791–793
  - thermal shock, 803–804
- Ceramic materials, 453–472
  - brittleness of, 455–458
  - for corrosion resistance, 465–466
  - future trends in, 471–472

- information sources about, 469–471
- in passive electronics, 466–467
- piezoceramics, 467–468
- processing of advanced, 454–455
- standards and test methods, 469–471
- thermostructural applications, 464–465
- transparent, 468
- in wear applications, 459–463
- Ceramic matrix composites (CMCs):
  - applications of, 435
  - properties of, 427–429
- Ceramic matrix materials, 414
- Cerium, 24
- Chemical changes, analysis of, 856
- Chemical composition of surface, 855
- Chemical conversion coatings, 296
- Chemical failure, 777
- Chemical finishes (aluminum alloys), 92
- Chemical industry, aluminum alloys in, 114
- Chemical inertness, 478–479
- Chemical method, 782, 783
- Chemical resistance, 355
- Chromium, 22, 40, 278–279, 493
- Circuit board design tools, 511–512
- Clear anodized aluminum alloys, 92
- CMCs, *see* Ceramic matrix composites
- CNEL (community noise equivalent level), 928, 981
- Cobble creep, 738
- Coffin-Manson equation, 730
- Coke, 4
- Cold cracking, 54
- Color anodized aluminum alloys, 92
- Columns:
  - defined, 601–602
  - eccentric loads on, 604
  - steel, 605, 607–608
  - stresses on, 601–608
  - with transverse/cross-bending loads, 604
  - wooden, 604–607
- Combined stresses, 566–570
- Combustibility, 482–483
- Community noise, 922–931, 980–982
  - criteria for, 929–931
  - and outdoor sound propagation, 923–926
  - representations of, 926–929, 980–981
  - response to, 930, 931
  - surveys of, 982
- Community noise equivalent level (CNEL), 928, 981
- Comparing/ranking (as method of materials selection), 517, 538–540
  - case study, 542–544
  - digital logic, 539
  - performance index, 539–540
  - weighted-properties, 538–540
- Comparison method for sound power measurement, 992
- Compensated temperature range, 654
- Compensation, strain gauge circuit, 630–631
- Component mounting (electronic), 499–500
  - of discrete components, 499
  - of printed circuit board components, 499–500
  - surface-mount technology, 500
- Composite materials (composites), 401–435
  - classes/characteristics of, 402–403
  - comparative properties of, 403–407
  - manufacturing considerations for, 407
  - matrix, 407–408, 411–414
  - properties of, 414–417, 427–429
  - reinforcement, 407–411
- Compression, 556, 557, 648
- Compressive strain, 558, 661
- Compressive stress, 556, 557
- Computerized materials databases, 549–550
- Computer modeling, of stresses, 620
- Concentric cylinder viscometers, 826
- Concert halls, listening quality in, 922, 923
- Condensation polymers, *see* Engineering thermoplastics
- Condenser microphones, 947, 948, 964–965
- Conduction, 508
- Cone and plate viscometers, 826
- Conformal geometry rigs, 846
- Connections, electronic equipment, 502–503
- Constant life diagrams (master diagrams), 728, 729
- Constitutive equations for sound, 895–896
- Constrained beam, 574
- Construction industry, aluminum alloys in, 112
- Contact stress(es), 616, 617
- Contact stress theory, 616
- Continuous beams, 574, 586–589
- Continuous casting, 4–5
- Continuous-cooling transformation (CT) diagram, 14, 16
- Continuous fiber-reinforced MMCs, 423–424
- Continuous sound level, 970–971

- Continuous vibratory systems:
  - of a bar, 874
  - of a beam, 875
  - free-vibration solution for, 875–877
  - of a shaft, 874–875
  - of a string, 873–874
- Control architectures, noise control, 917–919
- Convection, 508–509
- Conversion, principle of, 758
- Copper, 117–118
  - biostatic/antimicrobial properties of, 202–203
  - in electronic packaging materials, 493
  - physical properties of, 118, 119, 150–152
  - pure, 150–152, 159
  - safety and health issues with, 202, 214–215
  - in stainless steel, 41
  - in steel, 22, 24
- Copper alloys, 117–227
  - biostatic/antimicrobial properties of, 202–203
  - C10100-C19200, 163–167
  - C23000-C28000, 168–170
  - C36000-C52700, 171–173
  - C61300-C69400, 173–175
  - C70600-C77000, 175–179
  - C81100-C89550, 180–186
  - C90300-C93800, 187–192
  - C95200-C96400, 193–197
  - casting, 209–210
  - compositions of, 119–145
  - copper–beryllium, 226
  - copper–phosphorus, 132
  - copper–silicon, 134
  - copper–silver–phosphorus, 132
  - copper–silver–zinc, 132
  - copper–zinc, 135–136
  - corrosion behavior of, 199–202
  - designations of, 119
  - early history, 117–118
  - in electronic packaging materials, 493
  - fabrication of, 204–209
  - families of, 118–119
  - forging, 211
  - impact loading of, 198–199
  - machining, 204–209
  - mechanical properties of, 162–199
  - physical properties of, 150, 153–158
  - safety and health issues with, 214–215
  - sleeve bearings, 224–226
  - standards and specifications, 226–227
  - strengthening mechanisms for, 150, 152, 159
  - temperature of, 198
  - temper designations of, 159–162
  - temper of, 159–162
  - tube/pipe products, 215–224
  - welding of, 211–213
- Copper nickels, 119, 137–139, 148
- Corrosion:
  - of aluminum alloys, 87–89
  - biological, 764–765
  - ceramic materials, 465–466
  - of copper and copper alloys, 199–202
  - dry, 279
  - of electronic materials, 479–480
  - erosion, 201, 763–764
  - as failure, 706–707, 759–765
  - galvanic, 46–47, 89, 201, 761–762
  - hot-corrosion resistance, 346
  - intergranular, 46, 763
  - and magnesium and magnesium alloys, 296
  - of nickel and nickel alloys, 278–283
  - pitting, 40, 41, 44–45, 88–89, 281–282, 762–763
  - of stainless steels, 40, 43–47
  - stress, 43–44, 201, 709
  - of superalloys, 346–347
  - of titanium alloys, 231–232, 260–261
  - wet, 279
- Corrosion fatigue, 709
- Corrosion wear, 709
- Cost-benefit analysis (materials selection), 547–548
- Cost-per-unit-property method (materials selection), 535–536
- Cost requirements (materials selection), 534
- Couette flow model, 824
- CP (cellulose propionate), 370
- Cracking, in copper alloys, 214
- Creep, 35, 48, 708, 736–744
  - defined, 561, 648
  - deformation mechanism, 737–739
  - and electronic materials, 483
  - equations for calculating, 571, 572
  - for force transducers, 642
  - mechanism of, 571
  - mechanisms of creep-fatigue failure, 743–744
  - under multiaxial state of stress, 742–743
  - of polymer matrix composites, 423
  - prediction of long-term, 739–740
  - and stress analysis, 570–572

stress relaxation with, 571  
 under uniaxial state of stress, 740–742  
 Creep buckling, 709  
 Creep limit, 561  
 Creep rupture:  
   in ceramics, 806–807  
   failure due to, 736–744  
   of polymer matrix composites, 423  
 Creep strain, 805–806  
 Creep stress, 563, 570–571  
 Crevice corrosion, 45, 762  
 Critical angle, 902  
 Critical band rate, 933–934  
 Critical crevice corrosion temperature (CCCT),  
   45  
 Critical damping, 910  
 Critical distance, 979  
 Critical stress intensity, 716  
 Crystal lattice, 7  
 CT (continuous-cooling transformation)  
   diagram, 14, 16  
 Cup viscometers, 829–831, 834  
 Curved beams, 588–591  
 Cutting tool inserts, ceramic wear components,  
   461  
 C-weighted filters, 891–892, 961  
 C-weighted sound pressure level (LC), 928  
 Cylinders, stresses on, 608–610

## D

Damping capacity (hysteresis), 564–565  
 Dargies's method (materials selection),  
   536–538  
 Data, 515–528  
   for analytical comparisons, 517  
   for failure analysis, 520  
   for final design, 518  
   for maintenance, 519–520  
   for manufacturing, 519  
   for material specification, 518–519  
   for materials selection, 516–517  
   metadata, 521  
   for modeling material/product performance,  
     516  
   numeric databases as type of, 521  
   for preliminary design, 517–518  
   for quality assurance, 519  
   sources of, *see* Data sources  
   textual, 520–521  
 Databases, computerized materials, 549–550  
 Data sources, 522–528  
   Alloy Center, 524–526  
   ASM International, 524–526  
   categories of, 522, 523  
   Internet, 525, 527–528  
   knovel.com, 525, 527  
   platforms for, 524  
   quality/reliability of, 522–524  
   STN International, 524–526  
 Day–night level (DNL), 928, 981  
 Dealloying (“parting”), 201  
 Decibel scale, 889–890, 958–959  
 Deflection:  
   of curved beams, 589–581  
   defined, 649  
   elastic, 583  
 Deformation:  
   defined, 649  
   elastic, 706, 710–712  
   nickel alloys, 283  
   of a solid, 682–684  
 Degassing, 4, 24  
 Degree of enclosure, 506–507  
 Delta iron, 6  
 Dental restorations, 463  
 Design:  
   deterministic, 456  
   electronic packaging, 476–477, 506–509  
   final, 518  
   preliminary, 517–518  
   probabilistic, 456–458  
   stages of materials selection and, 533  
 Deterministic design, 456  
 Dezincification, 763  
 Diallyl phthalate, 396  
 DIC (digital image correlation), 659  
 Die castings, mechanical properties of, 292,  
   293  
 Diffuse fields, microphone selection for,  
   966–967  
 Diffuse reflection method, 840  
 Diffusion, 7  
 Diffusion creep, 738  
 Diffusive transport, 816  
 Digital image correlation (DIC), 659  
 Digital logic method (materials selection), 539  
 Dilatometer, 14, 16  
 Direct chemical attack, 706, 759–761  
 Discontinuities:  
   in reflection/transmission of sound, 904  
   and stress, 565–566



Discontinuous fiber-reinforced MMCs, 424–425  
 Discrete wiring, 502  
 Disks, stresses on rotating, 616  
 Dislocation creep, 739  
 Displacement, 649  
 Dissimilar-metal combinations, 212  
 Distortion control, welding, 213–214  
 Distortion-Energy Theory (Hencky–Von Mises Theory), 569, 570  
 Diversion, principle of, 758  
 DNL (day–night level), 928, 981  
 Double-leaf partitions, 914, 915, 974  
 Drag-type viscometers, 820–823  
 Drift, 649  
 Drilling (copper alloys), 206–207  
 Dry corrosion, 279  
 Dual-phase steels, 30  
 Ductile materials, static working stresses for, 569  
 Ductile rupture, 706  
 Ductility, 482, 560, 649  
 Ducts, HVAC, 913–914, 921  
 Duplex stainless steels, 33, 50–51, 56, 57  
 D-weighted filters, 891, 892, 961  
 D-weighted sound pressure level (LD), 929  
 Dynamic microphones, 948, 949, 965, 966  
 Dynamic stress, 563  
 Dynamic viscosity, 834  
 Dynamometers, 636–637

## E

Ear, structure of, 942–944  
 Early decay time (EDT), 922  
 Eccentricity, 649  
 Eccentric loads, 604  
 Echoes, 979  
 ECTFE (poly[ethylene chlorotrifluoroethylene]), 392, 393  
 EDT (early decay time), 922  
 EDX (energy dispersive x-ray analysis), 855  
 Effective perceived noise level (EPNL), 981, 982  
 Efflux viscometers, 857–858  
 EIC (environmentally assisted cracking), 201  
 Elastic deflection, 583  
 Elastic deformation, 706, 710–712  
 Elasticity, 558, 649  
 Elasticity limit, 854  
 Elastic limit, 558, 649

Elastomers, 396–398, 497  
 Elastorestrictive materials, 444  
 Electret condenser microphones, 947, 948, 965  
 Electrical conductivity, 477  
 Electrical contacts, 489  
 Electrical industry, aluminum alloys in, 112  
 Electrical steels, 28  
 Electrochemical finishes, for aluminum alloys, 92  
 Electrochromic smart windows, 447  
 Electrolytically deposited coloring, for aluminum alloys, 92  
 Electromagnetic shielding, 480–481  
 Electronic equipment:  
   attachment of, 484–485  
   interconnections of, 502–503  
   racks, frames, and mounting structures for, 485  
 Electronic materials:  
   chemical inertness of, 478–479  
   combustibility of, 482–483  
   corrosion of, 479–480  
   creep and, 483  
   density of, 480  
   ductility of, 482  
   electrical conductivity of, 477  
   electromagnetic shielding of, 480–481  
   electrostatic shielding of, 480–481  
   fatigue resistance of, 481  
   hardness of, 481  
   magnetic shielding of, 481  
   moisture absorption by, 483–484  
   properties of, 477–484  
   strength of, 480  
   sublimation by, 482  
   temperature range for, 480  
   thermal conductivity of, 477  
   thermal emissivity of, 478  
   thermal expansion of, 478  
   wear resistance of, 482  
 Electronic packaging, 475–512  
   applications of, 484–490  
   availability of information on, 477  
   component mounting in, 499–500  
   concerns in, 475–476  
   design techniques in, 476–477  
   fastening and joining in, 500–502  
   interconnections in, 502–503  
   materials selection process for, 476  
   physical design process for, 476

- prevention of shock/vibration failure, 503–506
  - properties of electronic materials, 477–484
  - protective, 509–510
  - scope of process, 475
  - software design aids for, 510–512
  - structural design in, 506–507
  - thermal design in, 507–509
  - types of candidate materials, 490–499
  - Electronic packaging applications, 484–490
    - electrical contacts, 489
    - encapsulation, 489–490
    - environmental endurance, 490
    - equipment and module enclosures, 485
    - equipment attachment, 484–485
    - equipment racks, frames, and mounting structures, 485
    - mechanical joints, 486–487
    - position-sensitive assemblies, 488
    - surface finishes, 487–488
    - temperature control, 485–486
  - Electronic packaging candidate materials, 490–499
    - adhesives, 498–499
    - ceramics and glasses, 497–498
    - metals, 491–494
    - plastics and elastomers, 494–497
  - Electron microscopes, 840–842
  - Electroplating, 93, 296, 488
  - Electrorheological materials, 445
  - Electroslag remelting (ESR), 332–335
  - Electrostatic shielding, 480–481
  - Electrostrictive materials, 443
  - Embrittlement, 22
  - Enameling steel, 28
  - Encapsulation, 489–490
  - Enclosure(s):
    - active noise control in, 921
    - degree of, 506–507
    - equipment and module, 485
    - for passive noise control, 915
  - Ends, of columns, 602
  - Endurance limit, 723, 724
  - Energy, 649
  - Energy dispersive x-ray analysis (EDX), 855
  - Engineering shear strains, 660
  - Engineering thermoplastics, 370–383
    - polyamides, 374–378
    - polyarylates, 381, 382
    - polycarbonate/ABS alloys, 379, 380
    - polycarbonates, 379, 380
    - polyester–carbonates, 380–381
    - polyphenylene ether, 381–383
    - thermoplastic polyesters, 371–374
  - Envirobrasses, 144
  - Environmental controls, for friction
    - measurements, 846
  - Environmental endurance, 490
  - Environmental failure, 777, 778
  - Environmentally assisted cracking (EIC), 201
  - Environmental noise, 980, 982. *See also* Community noise
  - EPNL (effective perceived noise level), 981, 982
  - Epoxy resins, 394
  - Epoxy-resin-based encapsulation materials, 490
  - Equal loudness curves, 890–891, 959–960
  - Equilibrium:
    - defined, 649
    - and finite-element method, 684–686
  - Equipment racks, 485
  - Equivalent continuous sound level, 927–928, 980
  - Erosion corrosion, 201, 763–764
  - Erosive wear, 847–849
  - Esawi's and Ashby's method (materials selection), 538
  - ESR (electroslag remelting), 332–335
  - Euler's formula, 602–603
  - Evaporation, 509
  - Expert systems, 550–551
  - Exponential-time-weighted sound pressure levels, 971
  - Extension, 649
  - Extensometer, 649
  - External work, 563–564
  - Extrinsic (term), 649
- F**
- Fabrication, *see* Manufacturing
  - Factor of safety, 562–563
  - Failure, 703–766. *See also* Ceramic failure; Plastic failure
    - analysis/restrospective design, 765–766
    - brinnelling, 706
    - brittle fracture, 706
    - chemical, 777
    - corrosion, 706–707, 759–765
    - creep/stress rupture, 736–744

- Failure (*continued*)
  - criteria of, 703–704
  - direct chemical attack, 706
  - ductile rupture, 706
  - elastic deformation, 706, 710–712
  - environmental, 777, 778
  - fatigue, 718–736
  - fracture mechanics/unstable crack growth, 711–717
  - fretting, 744–753
  - galling, 708–709, 754
  - impact, 707–708
  - mechanical, 776, 777
  - modes of, 573–574
  - spalling, 709
  - thermal, 777
  - types of, 704–709
  - wear, 744–745, 753–759
  - yielding, 706, 710–712
- Failure analysis, 777–786
  - brittle-coating method, 781
  - chemical method, 782, 783
  - fractography, 785, 786
  - heat reversion, 782, 783
  - identification analysis, 779–780
  - materials data for, 520
  - mechanical testing, 784–785
  - microtoming, 783–784
  - nondestructive testing techniques, 785
  - photoelastic method, 780–781
  - simulation testing, 785
  - strain gauge method, 781–782
  - stress analysis, 780–782
  - thermal analysis, 785
  - visual examination, 779
- Falling-needle viscometers, 822
- Falling-object viscometers, 820–823, 834
- Falling-sphere viscometers, 856, 857
- Faraday's law of induction, 965
- Fastening, of electronics, 500–501
- Fatigue, 706, 709, 718–736
  - fatigue crack propagation, 732–736
  - loading/laboratory testing of, 719–723
  - nonzero mean stress, 728–730
  - S-N-P* curves, 723–728
  - strain–life approach, 730–732
  - and stress analysis, 572–574
  - stress–life approach, 723–730
- Fatigue crack propagation, 732–736
- Fatigue limit (endurance limit), 723, 724
- Fatigue resistance, 481
- Fatigue stress, 563
- Feedback noise control systems, 918–919
- Feedforward noise control systems, 917, 918
- FEM, *see* Finite-element method
- FEP (fluorinated ethylene–propylene), 392, 393
- Ferrite, 9, 26
- Ferritic stainless steels, 3, 32–33, 49
- Ferrography, 859
- FFM (friction force microscopy), 843
- Fibers, as composite reinforcement, 408
- Fiber-optic connections (in electronic systems), 503
- Fiber-reinforced MMCs, 423–425
- Figure of merit, for materials, 540
- Filler metals, welding, 213
- Filters:
  - acoustic, 910–913
  - band pass, 648
  - weighting, 891–893, 960–961
- Filtered-*x* algorithm, 919–920
- Final design, materials data for, 518
- Finishing:
  - aluminum alloys, 91–93
  - magnesium alloys, 296
- Finite-element method (FEM), 681–702
  - and deformation of solid, 682–684
  - differential properties of shape functions, 693–695
  - differentiation in referential coordinates, 695–698
  - and equilibrium, 684–686
  - FEM approximation, 690–692
  - foundations of, 689–690
  - global/local transformations, 692–693
  - Hilbertian Sobolev spaces in, 690
  - and infinitesimal linearly elastic constitutive laws, 686–689
  - one-dimensional example of, 699–702
  - postprocessing, 698
  - in three dimensions, 690–692
- Finite strain theory, 660
- Fixed beam, 574
- Flexural vibration, 875
- Flexure, 574–583
  - bending moment, 576, 579
  - deflection due to shear, 583
  - elastic deflection of beams, 583
  - equilibrium conditions, 575–580
  - formula for, 580

- phenomenon, 575
- reactions at supports, 575
- Flow-type viscometers, 827–829
- Fluctuation strength, of sound, 935, 936
- Fluids:
  - behavior of solids vs., 809–810
  - calibration, 832
  - Newtonian, 812
  - pseudoplastic, 813
- Fluid layers, reflection/transmission of sound through, 902–904
- Fluorinated ethylene–propylene (FEP), 392, 393
- Fluorinated thermoplastics, 392–393
  - fluorinated ethylene–propylene, 392, 393
  - poly(chlorotrifluoroethylene), 392, 393
  - poly(ethylene chlorotrifluoroethylene), 392, 393
  - poly(tetrafluoroethylene), 392–393
  - poly(vinyl fluoride), 392, 393
  - polyvinylidene fluoride, 392, 393
- Foot-pound (lbf), 651
- Force, 624, 649. *See also* Force measurement
- Force balance transducers, 640, 641
- Forced convection, 509
- Forced-harmonic vibration, 867
- Forced-nonharmonic vibration, 868
- Forced vibration, 867, 868, 872–873
- Force-induced elastic deformation, 706
- Force measurement, 623–656
  - calibration of devices for, 642–648
  - with dynamometers, 636–637
  - with force balance transducers, 640, 641
  - with force transducers, 624–626
  - history of, 623–624
  - with magnetoelastic transducers, 640
  - with optical force transducers, 637–639
  - with resonant element transducers, 631–634
  - with surface acoustic wave transducers, 634–636
  - terms in, 648–656
  - uncertainty in, 644–645
  - universal testing machines for, 627–631
- Force transducers, 624–626
  - accuracy of, 642
  - calibration of, 642–648
  - capacity of, 641
  - creep for, 642
  - optical, 637–639
  - output of, 641
  - repeatability for, 642
  - temperature coefficient of, 642
  - uncertainty and temperature characteristics of, 625
- Forging:
  - of copper alloys, 211
  - of steel, 5
  - of superalloys, 340–341
  - of titanium alloys, 256–258
- Forming (magnesium alloys), 295
- Fractography, 785, 786
- Fracture, types of, 561, 562
- Fracture mechanics, 711–717, 791–793
- Fracture toughness, 714, 854
- Fragility, of electronic equipment, 503
- Free convection, 508
- Free-cutting brass, 208
- Free fields:
  - microphone selection for, 966
  - sound power measurements in, 989–991
- Free-field radiation, active noise control in, 921
- Free-machining steels, 22
- Free vibration, 866–867
  - in multi-degree-of-freedom systems, 872
  - normal-mode solution, 876–877
  - in single-degree-of-freedom systems, 866–867
  - wave solution, 875, 876
- Frequency, 649
- Frequency response, 649
- Frequency weightings, 959–962
- Fretting, 708, 744–753
- Friction, 650
- Friction force microscopy (FFM), 843
- Friction measurements, 844–847
  - with conformal vs. nonconformal geometry rigs, 846
  - environmental control for, 846
  - with inclined-plane rigs, 845
  - with pin-on-disc rigs, 845, 846
  - techniques for making, 846–847
- Frit, 28
- FSD (full scale), 650
- Fuel gas distribution systems, 217, 224
- Full annealing, steel, 25
- Fullerenes, 450–451
- Full scale (FSD), 650
- Functional requirements (materials selection), 532

**G**

Galling failure, 708–709, 754  
 Galvanic corrosion, 761–762  
   of aluminum alloys, 89  
   of copper alloys, 201  
   of stainless steels, 46–47  
 Gamma iron, 6  
 Gamma loop, 33  
 Gases:  
   low-density, 816–817, 819  
   pressure and viscosity of, 819  
   shielding, 212  
   temperature and viscosity of, 816–818  
 Gas–metal arc welding (GMAW), 213  
 Gas–tungsten arc welding (GTAW), 212, 213  
 Gauge factor, 650, 665–668  
 Gauge length, 650  
 Gauge resistance (strain gauge), 666, 667  
 Gels, smart, 447–448  
 Gerber's Law, 573  
 Gilmont-type falling-ball viscometers, 822, 823  
 Glass, in electronic packaging, 497–498  
 Glass fibers (as composite reinforcement), 408, 409  
 Global multiaxial fracture criterion (ceramics), 799–800  
 Glow discharge optical emission spectroscopy (GDOS), 855  
 GMAW (gas–metal arc welding), 213  
 Gold, 493  
 Goodman's Law, 573, 730  
 Grain boundary sliding, 739  
 Graphite fibers (as composite reinforcement), 409–410  
 Graphitization, 763  
 Grating, 650  
 Gravity, 645, 650  
 Grazing incidence, 902  
 Grips/fixtures, 650  
 GTAW (gas–tungsten arc welding), 212, 213  
 Guest Theory (Maximum-Shear Theory), 568–570  
 Guide to the Expression of Uncertainty in Measurement, 650

**H**

Haake-type falling-ball viscometers, 822, 823  
 Hadfield manganese steels, 21  
 Hard anodized aluminum alloys, 92

Hardenability (of steel), 16–18  
 Hardness, 481, 561, 852–854  
 Harper–Dorn creep, 738  
 HDPE (high-density polyethylene), 357, 358  
 Head hardening, 14  
 Health issues, *see* Safety and health issues  
 Hearing loss, 905–908  
 Hearing protection, 905–908  
 Heating, ventilation, and air-conditioning (HVAC) ducts, 913–914, 921  
 Heat-resistant steels, 34–35  
 Heat reversion, 782, 783  
 Heat transfer, 508–509  
 Heat treatment:  
   of nickel and nickel alloys, 285–286  
   of steel, 24–26  
 Helical compression springs, 619  
 Helmholtz resonator, 911, 912  
 Hencky–Von Mises Theory (Distortion-Energy Theory), 569, 570  
 High-copper alloys, 119  
   cast, 140  
   welding, 211  
   wrought, 124–127  
 High-cycle fatigue, 718  
 High-density polyethylene (HDPE), 357, 358  
 High-density polyethylene fibers (as composite reinforcement), 411  
 Higher alloy steels, 31–36  
   heat-resistant steels, 34–35  
   stainless steels, 31–34  
   tool steels, 34  
   ultrahigh-strength steel, 35–36  
   wear-resistant steels, 35  
 High-impact polystyrene (HIPS), 361, 362  
 High-leaded tin bronzes, 146  
 High-molybdenum alloys, 56–58  
 High-pass filters, 913  
 High-performance materials, 383–392  
   aromatic polyketones, 389–391  
   liquid crystalline polyesters, 386–387  
   poly(amide imides), 389, 390  
   poly(*p*-phenylene), 391–392  
   polyarylsulfones, 384–385  
   polybiphenyldisulfones, 385–386  
   polyetherimides, 387–389  
   polyimides, 387, 388  
   polyphenylene sulfide, 383–384  
 High-performance steels, 30–31  
 High-strength brasses, 226  
 High strength yellow brasses, 142

Hilbertian Sobolev spaces, 690  
 HIPS (high-impact polystyrene), 361, 362  
 Hooke's law, 558, 567, 650  
 Horizontal shear, 576, 585  
 Hot-corrosion resistance, 346  
 Hot cracking, 54, 55  
 Hot shortness, 20, 22  
 HQ-HTS (hydroquinone-based high-temperature sulfone) polymer, 385, 386  
 Humidity:  
   and calibration of force measurement devices, 644  
   measurement of, 851  
 HVAC (heating, ventilation, and air-conditioning) ducts, 913–914, 921  
 Hydrodynamic theory of lubrication, 838  
 Hydrogels, 447–448  
 Hydrogen:  
   in steel, 24  
   in titanium alloys, 243–244  
 Hydrogen damage, 764  
 Hydrogen flakes, 24  
 Hydroquinone-based high-temperature sulfone (HQ-HTS) polymer, 385, 386  
 Hypereutectoid steels, 9, 13  
 Hypoeutectoid steels, 9  
 Hysteresis, 564–565, 650

## I

Identification analysis, 779–780  
 IEC (International Electrotechnical Commission), 954, 955  
 IF (interstitial-free) steels, 3  
 IL, *see* Insertion loss  
 Impact failure, 707–708  
 Impact loading, 198–199  
 Impact polystyrene (IPS), 361, 362  
 Impact stresses, 563, 591–595  
   axial impacts, 592  
   for impacts on beams, 593  
   for impacts on structures, 593–595  
   live loads, 591–592  
   rupture from impact, 595  
   sudden loads, 591  
 Impedance:  
   in acoustics, 893, 894  
   mechanical, 506  
   and passive noise control, 909  
 Impulsive vibratory stress, 595  
 Inclined-plane rigs, 845  
 Induction, Faraday's law of, 965  
 Industrial tribology measurements, 859  
 Inertness, chemical, 478–479  
 Infinitesimal linearly elastic constitutive laws, 686–689  
 Infinitesimal strain theory, 660  
 Ingots:  
   melting/casting, 335–336  
   steel, 5  
 Initial screening (materials selection), 534–538  
   Ashby's method, 536, 537  
   case study, 541–542  
   cost-per-unit-property, 535–536  
   Dargies's method, 536–538  
   Esawi's and Ashby's method, 538  
   limits on material properties, 535  
 Initial time delay gap (ITDG), 922  
 Ink-on demand printing, 442  
 Insertion loss (IL), 908, 915, 973  
 Integral color anodized aluminum alloys, 92  
 Intensity, sound, 887–888, 958  
 Intensity probes, 984–985  
 Intensity reflection coefficient, 900  
 Intensity transmission coefficient, 900  
 Interequipment connections (electronics), 503  
 Interface, reflection/transmission of sound from a, 900–902  
 Interferometers, 638  
 Intergranular corrosion, 46, 763  
 Intermodule connections (electronics), 503  
 International Electrotechnical Commission (IEC), 954, 955  
 International Organization for Standardization (ISO), 954, 955  
 International prototype kilogram (IPK), 642–643  
 Internet, as data source, 525, 527–528  
 Interstitial-free (IF) steels, 3  
 Intramodule connections (electronics), 503  
 Intrinsic (term), 650  
 Intromission, angle of, 902  
 IPK (international prototype kilogram), 642–643  
 iPP (isotactic polypropylene), 359, 360  
 IPS (impact polystyrene), 361, 362  
 Iron, 6, 491  
 Iron alloys, 491  
 Iron–carbon equilibrium diagram (steel), 6–13

Ironmaking, 4  
 Iron sulfide, 20  
 IR spectroscopy, 855  
 ISO (International Organization for Standardization), 954, 955  
 Isotactic polypropylene (iPP), 359, 360  
 Isothermal transformation diagram (steel), 13–15  
 Isotropic bodies, 688  
 ITDG (initial time delay gap), 922

## J

Johnson's apparent elastic limit, 559  
 Joining:  
   magnesium and magnesium alloys, 293, 294  
   superalloys, 341–342  
   titanium alloys, 259–260  
 Joint preparation (welding), 213  
 Jominy test, 16  
 Joule, 650

## K

Kilogram force (kgf), 650–651  
 Kilopascal (kPa), 651  
 Kinematic viscosity, 810–812, 834  
 Knovel.com, 525, 527  
 Knowledge-based systems, 550–551

## L

Ladle, 4  
 Lagrangian strain tensor, 683  
 Lamellar, 9  
 Lamé relations, 688  
 Lanthanum, 24  
 Lateral force microscopy (LFM), 843  
 lbf (foot-pound), 651  
 LC (C-weighted sound pressure level), 928  
 LCPs (liquid crystalline polyesters), 386–387  
 LD (D-weighted sound pressure level), 929  
 LDPE (low-density polyethylene), 357, 358  
 Lead, 24, 493, 494  
 Leaded brasses, 128–129  
 Leaded coppers, 119, 148  
 Leaded phosphor bronzes, 132  
 Leaded red brasses, 141  
 Leaded semired brasses, 141

Leaded steels, 29  
 Leaded tin bronzes, 145–146  
 Lead-free bearing bronzes, 226  
 Lead-wire resistance, 676  
 LEDs (light-emitting diodes), 471  
 Length of a column, 602  
 LFM (lateral force microscopy), 843  
 Life-cycle assessment, of magnesium alloys, 297  
 Light-emitting diodes (LEDs), 471  
 Light-sectioning method, 840  
 Light-sensitive materials, 446–447  
 Limestone, 4  
 Limit of proportionality (LOP), 651  
 Linear low-density polyethylene (LLDPE), 357, 358  
 Linear variable differential transformer (LVDT), 651  
 Lined ducts, 913–914  
 Liquids:  
   pressure and viscosity of, 819  
   temperature and viscosity of, 818–819  
 Liquid crystals, temperature measurements with, 851  
 Liquid crystalline polyesters (LCPs), 386–387  
 Liquid metal strain gauges, 678  
 LLDPE (linear low-density polyethylene), 357, 358  
 Load, 651  
 Load at yield, 651  
 Load cell, 651  
 Local multiaxial fracture criterion (ceramics), 800–803  
 Longitudinal vibration, 874  
 LOP (limit of proportionality), 651  
 Loudness:  
   equal loudness curves, 890–891, 959–960  
   in sound quality analysis, 934–935  
 Loudspeakers, 948–949  
 Low-alloy steels, 29–31  
 Low-cycle fatigue, 718  
 Low-density gases, 816–817, 819  
 Low-density polyethylene (LDPE), 357, 358  
 Low-pass filters, 911, 912  
 Lubricants:  
   chemical analysis of particles in, 858  
   tribology measurements for, 855–858  
 Lubricant oxidation tests, 858  
 LVDT (linear variable differential transformer), 651  
 LX (X-percentile-exceeded sound level), 928



## M

- Machining:
  - of aluminum alloys, 90–91
  - of copper alloys, 204–209
  - of magnesium and magnesium alloys, 293
  - of nickel and nickel alloys, 287
- Magnesium, 289–291
  - in electronic packaging materials, 493
  - nonstructural applications of, 290
  - structural applications of, 290–291
- Magnesium alloys, 289–297
  - corrosion/finishing of, 296
  - fabrication of, 293–295
  - life-cycle assessment of, 297
  - properties of, 291–293
  - recycling of, 296
- Magnets, organic-based, 444, 450
- Magnetic shielding, 481
- Magnetoelastic transducers, 640
- Magnetostriction, 651
- Magnetorheological materials, 445–446
- Magnetostrictive materials, 443–444
- Maintenance, materials data for, 519–520
- Malleability, 560
- Manganese, 20, 21
- Manganese bronze, 143, 226
- Manufacturers, ceramic, 469
- Manufacturing:
  - of composites, 407
  - of copper alloys, 204–209
  - of magnesium alloys, 293–295
  - materials data for, 519
  - of nickel alloys, 282–285
- Maraging steel, 35–36
- Marine transportation, aluminum alloys in, 113
- Martensite, 14, 15, 24
- Martensitic stainless steels, 33–34, 50
- Mass, 651
- Master diagrams, 728, 729
- Material characteristics, measurement of, 852–855
- Materials data, *see* Data
- Materials databases, 549–550
- Material performance requirements, 532–534
  - in case study, 541
  - cost, 534
  - functional, 532
  - processability, 532, 533
  - reliability, 534
  - resistance to service conditions, 534
- Materials selection, *see* Selection of materials
- Matrix materials, 407–408, 411–414
  - carbon, 414
  - ceramic, 414
  - metal, 413–414
  - polymer, 412–413
  - properties of, 411
- Maximum-Shear Theory (Guest), 568–570
- Maximum-Strain Theory (Saint Venant), 568–570
- Maximum stress, 572
- Maximum-Stress Theory (Rankine's Theory), 568–570
- MDPE (medium-density polyethylene), 357
- Mean stress, 572
- Measuring Range, 651
- Mechanical design tools, 511
- Mechanical failure, 776, 777
- Mechanical fastening, of electronics, 500–501
- Mechanical finishes, for aluminum alloys, 91
- Mechanical impedance, 506
- Mechanical joints (in electronics), 486–487
- Mechanical testing, 784–785
- Median force, 651
- Medical gas piping systems, nonflammable, 217
- Medium-density polyethylene (MDPE), 357
- Megapascal (MPa), 651
- Melting:
  - of superalloys, 332–337
  - of titanium alloys, 255–256
- Merit, figure of, 540
- Metadata, 521
- Metals, in electronic packaging, 491–494
- Metallographic observation, 850
- Metal matrix, 413–414
- Metal matrix composites (MMCs):
  - applications of, 433–434
  - continuous fiber-reinforced, 423–424
  - discontinuous fiber-reinforced, 424–425
  - particle-reinforced, 425–427
  - properties of, 423–427
  - unidirectional, 424
- Microalloyed steels, 30
- Microcomputer-based design tools, 510–511
- Microphones, 946–949, 962–969
  - accuracy of, 967
  - calibration of, 967–969
  - condenser, 947, 948, 964–965
  - dynamic, 948, 949, 965, 966



- Microphones (*continued*)  
 electret condenser, 947, 948, 965  
 ribbon, 948  
 selection of, 965–967
- Microscopy, 840–844  
 atomic force, 842–843  
 friction force, 843  
 lateral force, 843  
 optical, 840  
 scanning electron, 840, 841  
 scanning tunneling electron, 841–842  
 transmission electron, 841
- Microstructure of titanium alloys, 236–254  
 alloy composition/general behavior,  
 237–240  
 alpha alloys, 245  
 alpha-beta alloys, 245–247  
 beta alloys, 247  
 cast alloys, 252–254  
 effects of alloy elements, 241  
 elastic constants/physical properties,  
 242–243  
 hydrogen in, 243–244  
 intermetallic compounds/transient secondary  
 phases, 241–242  
 mechanical properties, 244–254  
 oxygen/nitrogen in, 244  
 powder-formed alloys, 252, 254  
 processing effects, 243  
 strengthening, 238, 241  
 wrought/cast/powder metallurgy products,  
 254
- Microtoming, 783–784  
*MIL Handbook 17*, Vol 5, 471  
 Milling (copper alloys), 205, 206  
 Minimills, 4  
 Minimum load, 651  
 Minimum stress, 572  
 Mish metal, 24  
 Mixed-mode fatigue crack growth, 736  
 MMCs, *see* Metal matrix composites  
 Modulus, section, 580  
 Modulus of elasticity:  
 defined, 559, 561, 562, 651  
 of superalloys, 323–324  
 Modulus of rigidity, 559, 562  
 Modulus of rupture, 580  
 Mohr's Circle, 567, 568  
 Mohr's hypothesis, 799, 800  
 Moisture absorption, 483–484  
 Molecular theory, 815–816
- Molybdenum, 40–41, 44  
 in stainless steel, 40–41  
 in steel, 22
- Moment of inertia, 580, 596–597  
 Momentum diffusivity, 810  
 Motion, equations of, 865, 871  
 Mounting structures (for electronics), 485  
 MPa (megapascal), 651  
 Multiaxial Weibull statistics, 799–803  
 global multiaxial fracture criterion, 799–800  
 local multiaxial criterion, 800–803  
 strength under compression loading, 799
- Multi-degree-of-freedom systems, 862, 863,  
 870–873  
 equations of motion, 871  
 forced-vibration response, 872–873  
 free-vibration response, 872
- Multipoint tool machining, 90–91  
 Music wire, 36
- ## N
- Nabarro–Herring creep, 738  
 Nanomagnets, 445–446  
 National Institute of Standards and Technology  
 (NIST) database site, 527, 528  
 NC (noise criteria) ratings, 979  
 NDT (nondestructive testing techniques), 785  
 Nervous system response to auditory input, 944  
 Newton (unit), 651  
 Newtonian fluids, 812  
 Nickel, 267–268  
 in electronic packaging materials, 493  
 pure, 268  
 in stainless steel, 41  
 in steel, 22
- Nickel alloys, 267–287  
 and austenitic stainless steels, 51–52  
 classification of, 268–271  
 corrosion of, 278–283  
 fabrication of, 282–285  
 heat treatment of, 285–286  
 machining of, 287  
 mechanical properties of, 272  
 nickel alloys, 269, 270, 272  
 nickel–chromium–iron alloys, 270, 272–276  
 nickel–chromium–molybdenum alloys,  
 271–273, 277–278  
 nickel–copper alloys, 269, 270, 272–274,  
 279  
 nickel–iron alloys, 271, 272, 277

nickel–iron–chromium alloys, 270, 272, 273, 276–277  
 nominal chemical composition, 270–271  
 rupture stress, 273  
 trademarks of, 287  
 welding of, 287  
 Nickel–chromium–iron alloys, 270, 272–276  
 Nickel–chromium–molybdenum alloys, 271–273, 277–278  
 Nickel–copper alloys, 269, 270, 272–274, 279  
 Nickel–iron alloys, 271, 272, 277  
 Nickel–iron–chromium alloys, 270, 272, 273, 276–277  
 Nickel silvers, 119, 139–140, 148  
 Nickel–tin bronzes, 147  
 NIST (National Institute of Standards and Technology) database site, 527, 528  
 Nitinol, 449  
 Nitrogen:  
   in steel, 24  
   in titanium alloys, 244  
 Noise:  
   community, 922–931, 980–982  
   environmental, 980, 982. *See also* Community noise  
   Community noise  
 Noise control:  
   active, 916–922  
   passive, 906–915  
 Noise criteria (NC) ratings, 979  
 Noise dosage, 993  
 Noise dosimeters, 993–995  
 Noise reduction (NR), 973  
 Noise reduction coefficient, 909  
 Noise surveys, 982  
 Nonconformal geometry rigs, 846  
 Nondestructive testing techniques (NDT), 785  
 Nonflammable medical gas piping systems, 217  
 Nonlinear acoustics, 937–942  
   applications of ultrasound, 941–942  
   radiation pressure and streaming in, 940  
   sonic booms, 940  
   theory of, 938–940  
 Nonlinearity (term), 651–652  
 Nonrepeatability, 652  
 Nonzero mean stress, 728–730  
 Normalizing, of steel, 25  
 Normal stress, 557  
 Norris–Eyring reverberation time, 976  
 NR (noise reduction), 973  
 Numeric databases, 520  
 Nylons, *see* Polyamides

## O

Occupational Safety and Health Administration (OSHA), 905  
 Octave frequency bands, 892–894, 962, 963  
 Oil and gas industry, ceramics in, 471–472  
 One-third octave bands, 892, 893, 962, 963  
 Operating temperature range, 654  
 Operator inconsistency, in force measurement, 646–647  
 Optical force transducers, 637–639  
 Optical interference technique, 840  
 Optical microscopes, 840  
 Optimum solution (materials selection), 540–541, 543–545  
 Organic-based magnets, 444, 450  
 Orifice-type (cup) viscometers, 829–831, 834  
 Oscillating sphere viscometers, 832  
 OSHA (Occupational Safety and Health Administration), 905  
 Ostwald viscometer, 828  
 Outdoor sound propagation, 923–926  
 Overload, 652  
 Oxidation, of nickel alloys, 282, 283  
 Oxygen, 4, 244, 851

## P

PAs, *see* Polyamides  
 Packaging, aluminum alloys in, 114  
 Painted finishes, for magnesium alloys, 296  
 PAIs (poly[amide imides]), 389, 390  
 PARs (polyarylates), 381, 382  
 Parallel-plate viscometers, 826  
 Particle-reinforced MMCs, 425–427  
 “Parting” (dealloying), 201  
 Partitions:  
   passive noise control with, 914, 915  
   single- vs. double-leaf, 914, 915  
   sound isolation with, 973–974  
 PASCC (polythionic acid stress–corrosion cracking), 44  
 Passivation, 43  
 Passive electronics, 466–467  
 Passive noise control, 906–915  
   acoustic filters for, 910–913  
   enclosures for, 915  
   and impedance, 909  
   lined ducts for, 913–914  
   single- vs. double-leaf partitions for, 914–915

- Passive noise control (*continued*)
  - source, path, and receiver components of, 907–908
  - terminology used in, 908–909
  - vibration isolation mounts for, 909–910
- Patenting, 36
- PBT (poly[butylene terephthalate]), 371, 372
- PBT/PC alloy, 371–373
- PCs (polycarbonates), 379, 380
- PC/ABS (polycarbonate/ABS) alloys, 379, 380
- PCTFE (poly[chlorotrifluoroethylene]), 392, 393
- PE (polyethylene), 357–358
- Pearlite, 9, 14, 20, 24, 25
- PECs (polyestercarbonates), 380–381
- PEEK (polyetheretherketone), 389–391
- PEIs (polyetherimides), 387–389
- PEK (polyetherketone), 389–391
- Performance, modeling material/product, 516
- Performance index (materials selection), 539–540
- PES (polyethersulfone), 384–385
- PET (poly[ethylene terephthalate]), 372–374
- Petroleum industry, aluminum alloys in, 114
- Phenolic resins, 394
- Phon (unit), 890
- Phosphor bronzes, 131
- Photoelastic method, 780–781
- Photo etching, 652
- pH-sensitive materials, 446
- Piezoceramics, 467–468
- Piezoelectric effect, 652
- Piezoelectric force gauges, 846–847
- Piezoelectric materials, 440–443, 450
- Pin-on-disc rigs, 845, 846
- Pipes, reflection/transmission of sound in, 904
- Pistonphone calibration, 967–968
- Pitting corrosion:
  - aluminum alloys, 88–89
  - failure due to, 762–763
  - nickel alloys, 281–282
  - stainless steel, 40, 41, 44–45
- Plane waves, 897
- Plastics, 353–398
  - additives in, 355
  - chemical/solvent resistance of, 355
  - classification of, 354–355
  - elastomers, 396–398
  - in electronic packaging, 494–497
  - engineering thermoplastics, 370–383
  - fluorinated thermoplastics, 392–393
  - high-performance materials, 383–392
  - polyolefinic thermoplastics, 357–361
  - polyurethane/cellulosic resins, 369–370
  - properties of, 355–357
  - side-chain-substituted vinyl thermoplastics, 361–369
  - thermosets, 394–396
- Plastic failure, 771–785
  - chemical, 777
  - and design, 773–775
  - environmental, 777, 778
  - and material selection, 772–773
  - mechanical, 776, 777
  - and process, 775, 776
  - and service conditions, 775, 776
  - thermal, 777
- Plasticity, 558
- Plates, stresses on, 610–614
- Plate steels, 5
- Platforms, database, 524
- Pleasantness, of sound, 937
- Plumbing tube, copper-alloy, 215–225
  - type ACR, 216, 223–224
  - type DWV, 216, 222
  - type K, 216, 218–219
  - type L, 216, 219–220
  - type M, 216, 220–221
- PMCs, *see* Polymer matrix composites
- PMDA-ODA, 387, 388
- PMMA (poly[methyl methacrylate]), 366
- PMP (polymethylpentane), 361
- Poisson ratio, 558, 628
- Polar moment of inertia, 596–597
- Polar radius of gyration, 597
- Polymeric materials, *see* Plastics
- Poly(amide imides) (PAIs), 389, 390
- Poly(butylene terephthalate) (PBT), 371, 372
- Poly(ethylene chlorotrifluoroethylene) (ECTFE), 392, 393
- Poly(ethylene terephthalate) (PET), 372–374
- Poly(methyl methacrylate) (PMMA), 366
- Poly(*p*-phenylene), 391–392
- Poly(tetrafluoroethylene) (PTFE), 392–393
- Poly(trimethylene terephthalate) (PTT), 374
- Poly(vinyl fluoride) (PVF), 392, 393
- Poly(vinylidene chloride) (PVDC), 368–369
- Polyacetals, 378–379
- Polyamides (PAs, nylons), 374–378
  - acetals, 378–379
  - aromatic, 377–378

- PA 4/6, 376, 377
- PA 6 and PA 6/6, 374–376
- PA/PPE alloys, 375–376
  - semiaromatic polyamides, 376, 377
- Polyarylates (PARs), 381, 382
- Polyarylsulfones, 384–385
- Polybiphenyldisulfones, 385–386
- Polycarbonates (PCs), 379, 380
- Polycarbonate/ABS alloys (PC/ABS), 379, 380
- Polyesters:
  - liquid crystalline, 386–387
  - thermoplastic, 371–374
  - unsaturated, 395
- Polyestercarbonates (PECs), 380–381
- Polyetheretherketone (PEEK), 389–391
- Polyetherimides (PEIs), 387–389
- Polyetherketone (PEK), 389–391
- Polyethersulfone (PES), 384–385
- Polyethylene (PE), 357–358
- Polyethylene/poly(ethylene glycol) copolymers, 446
- Polyimides, 387, 388
- Polyketones, aromatic, 389–391
- Polymers, 447. *See also* Plastics
- Polymer matrix, 412–413
- Polymer matrix composites (PMCs):
  - applications of, 432–433
  - properties of, 417–423
- Polymethylpentane (PMP), 361
- Polyolefinic thermoplastics, 357–361
  - polyethylenes, 357–358
  - polymethylpentane, 361
  - polypropylene, 358–360
- Polyphenylene ether (PPE), 381–383
- Polyphenylene sulfide (PPS), 383–384
- Polyphenylsulfone (PPSU), 384, 385
- Polypropylene (PP), 358–360
- Polystyrene (PS), 361–362
- Polysulfone (PSU), 384, 385
- Polythionic acid stress–corrosion cracking (PASCC), 44
- Polyurethanes (PUs), 369, 370, 449
- Polyurethane-based encapsulation materials, 490
- Polyurethane resins (PURs), 369
- Polyvinyl chloride (PVC), 367–368
- Polyvinylidene fluoride (PVDF), 392, 393, 441–443
- Position-sensitive assemblies, 488
- Postprocessing (finite-element method), 698
- Postservice refurbishment, superalloy, 346–347
- Powder metallurgy:
  - superalloys, 340–341
  - titanium alloys, 252, 254
- Power reflection coefficient, 900
- Power transmission coefficient, 900, 911–913
- PP (polypropylene), 358–360
- PPE (polyphenylene ether), 381–383
- “*p–p*” principle, 982–984
- PPS (polyphenylene sulfide), 383–384
- PPSU (polyphenylsulfone), 384, 385
- Precipitation hardening stainless steels, 34
- Precision, 642, 652
- Preliminary design, materials data for, 517–518
- Prepared atmosphere, heat treatment in, 285–286
- Pressure:
  - radiation, 940
  - sound, 888–889, 955–957
  - and viscosity, 816–817, 819
- Pressure fields, microphone selection for, 967
- Pressure reflection coefficient, 900
- Pressure-residual intensity index, 987
- Pressure transmission coefficient, 900
- Principal strains, 663
- Principal strain coordinate system, 663
- Printed circuit board components, 499–500
- Probabilistic design, 456–458
- Processability requirements (materials selection), 532, 533
- Process annealing, 26
- Proeutectoid phase, 9
- Proportional limit, 558
- Protective electronic packaging, 509–510
- Proving ring, 636–637
- PS (polystyrene), 361–362
- Pseudoplastic fluids, 813
- psi (unit), 653
- PSU (polysulfone), 384, 385
- Psychoacoustic effects of sound, 944–946
- PTFE (poly[tetrafluorethylene]), 392–393
- PTT (Poly[trimethylene terephthalate]), 374
- PUs, *see* Polyurethanes
- Pugh method, 546–547
- PURs (polyurethane resins), 369
- PVC (polyvinyl chloride), 367–368
- PVDC (poly[vinylidene chloride]), 368–369
- PVDF, *see* Polyvinylidene fluoride
- PVF (poly[vinyl fluoride]), 392, 393

## Q

- Quality assurance, 519
- Quantitative methods of materials selection, 531–551
  - case study, 541–545
  - comparing/ranking, 538–540, 542–544
  - computerization of, 549–551
  - initial screening, 534–538, 541–542
  - optimum solution in, 540–541, 543–545
  - requirements for, 532–534, 541
  - stages of design and materials selection, 533
  - substitution, 545–548
  - and types of material information, 549
- Quasi-digital signals, 653
- Quenching, 24–26

## R

- Radiation (heat transfer), 509
- Radiation, free-field, 921
- Radiation damage, 709
- Radiation detectors, 850
- Radiation impedance, 893, 894
- Radiation pressure, 940
- Radius of gyration, 597, 602
- Rail transportation, aluminum alloys for, 113–114
- Random fields, microphone selection for, 966–967
- Range of stress, 572
- Rankine's Theory (Maximum-Stress Theory), 568–570
- Ranking, *see* Comparing/ranking
- RBS (Rutherford backscattering spectroscopy), 855
- Reaction injection molding (RIM), 369
- Reaming (copper alloys), 207, 208
- Receivers, passive noise control, 907–908
- Reciprocity calibration, 968
- Recrystallization annealing, 26
- Red brasses, 141
- Reducing atmosphere, heat treatment in, 285–286
- Referential coordinates, differentiation in, 695–698
- Reflection of sound, 900–904
  - at discontinuities in pipes, 904
  - at side branches of pipes, 904
  - from a single interface, 900–902

- from a solid surface, 902–904
  - through fluid layers, 902–904
- Refractive index, 653
- Relative calibration, 968
- Reliability, of materials data, 522–524
- Reliability requirements (materials selection), 534
- Remelted ingot processing, superalloy, 335–336
- Repeatability, 642, 653
- Rephosphorized steels, 22
- Reproducibility, 642, 653
- Residual stresses, 259, 854
- Resilience, 564, 565
- Resistance metal strain gauges, 664–676
  - alloys used in, 666–670
  - calibration parameters for, 666–670
  - description of, 664–665
  - sensitivity of, 665–666
  - strain gauge rosettes in, 670–673
- Resistance to service conditions, 534
- Resisting moment, 596
- Resisting shear, 576
- Resolution, 642
- Resonance, 653, 977–978
- Resonant element transducers, 631–634
- Resonant (vibrational) viscometers, 831–832, 834
- Restrained beams, 574, 585
- Reverberation, in rooms, 975–977
- Reverberation method, 991–992
- Reverberation time (RT), 975–976
- Reverse-flow viscometers, 828
- Rheology, 812–813
- Rhodium, 494
- Ribbon microphones, 948
- RIM (reaction injection molding), 369
- Ring dynamometer (proving ring), 636–637
- Rockwell hardness test, 853–854
- Rolling (steel), 5
- Room acoustical measurements, 975–979
  - critical distance, 979
  - and echoes, 979
  - noise criteria ratings, 979
  - resonance, 977–978
  - reverberation, 975–977
- Rosette equations (for strain gauges), 671–672
- Rotational viscometers, 824–826, 834, 856
- Roughness:
  - sound, 936
  - surface, *see* Surface roughness measurements
- Round shafts, torsional stresses in, 597

- RT (reverberation time), 975–976
- Rupture:
- creep, 423, 736–744, 806–807
  - ductile, 706
  - modulus of, 580
  - stress, 708, 736–744
  - work required for, 564
- Rupture strength, 559
- Rusting, 47
- Rutherford backscattering spectroscopy (RBS), 855
- S**
- Safety, factor of, 562–563
- Safety and health issues:
- with copper, 202, 214–215
  - with copper alloys, 214–215
- Saint Venant Theory (Maximum-Strain Theory), 568–570
- SAN (styrene/acrylonitrile) copolymer, 363, 364
- Sawing (copper alloys), 208, 210
- SAW (surface acoustic wave) transducers, 634–636
- Saybolt measurement system, 811, 812
- Scanning electron microscopes (SEM), 840, 841
- Scanning tunneling electron microscopy (STM), 841–842
- Scatter (ceramic failure), 795–798
- of lifetime, 798–799
  - of strength, 795–798
- SCC (stress corrosion cracking), 43–44, 765
- Scoring, 755
- Sea Water Reverse Osmosis (SWRO) process, 463
- Secant formula, 603
- Secondary ion mass spectroscopy (SIMS), 855
- Section modulus, 580
- Seizure (adhesive wear), 754
- SEL (sound exposure level), 992
- Selection of materials. *See also* Quantitative methods of materials selection
- for electronic packaging, 476
  - materials data for, 516–517
  - stages of design and, 533
  - for thermal shock conditions, 803–804
- Selective leaching, 763
- Selenium, 24
- Self-temperature compensation number (strain gauge), 668–670
- SEM (scanning electron microscopes), 840, 841
- Semiaromatic polyamides, 376, 377
- Semiconductor strain gauges, 676–678
- Semired brasses, 141
- Sensitivity, 653
- microphone, 968
  - strain, 665–666
  - transverse, 672–673
- Sensitization, 32
- Sensory pleasantness, of sound, 937
- Service conditions, resistance to, 534
- Shafts:
- stresses on rotating, 616
  - torsional stresses in, 597–600
- Shape functions, differential properties of, 693–695
- Shape memory alloys, 448–449
- Sharpness, sound, 935
- Shear:
- deflection due to, 583
  - horizontal, 576, 585
  - resisting, 576
  - vertical, 576
  - web, 584
- Shear center, 584
- Shear diagrams, 576
- Shear strain, 558, 660, 662
- Shear strain rate, 813
- Shear stress, 557, 597
- Shielding gases, 212
- Shipping, protective packaging for, 510
- Shock:
- electronic equipment failure due to, 503–504
  - isolation of, 880–881
  - sources of, 861–862
  - spectrum of, 868–870
  - thermal, 464–465, 708, 803–804
- Shock testing, 505
- Shore hardness test, 854
- Side branches, pipe, 904
- Side-chain-substituted vinyl thermoplastics, 361–369
- acrylonitrile/butadiene/styrene polymers, 363–365
  - acrylonitrile/styrene/acrylate polymers, 365
  - poly(methyl methacrylate), 366
  - poly(vinylidene chloride), 368–369
  - polystyrenes (PS, IPS, HIPS), 361–362
  - polyvinyl chloride, 367–368
  - styrene/acrylonitrile copolymer, 363, 364
  - styrene/maleic anhydride copolymer, 366

- Side-chain-substituted vinyl thermoplastics
  - (*continued*)
  - styrene/methyl methacrylate copolymer, 366, 367
  - syndiotactic polystyrene, 362–363
- Signa, 653
- Silicon-based encapsulation materials, 490
- Silicon brasses, 134, 143, 226
- Silicon bronzes, 134, 143
- Silicon-carbide based fibers (as composite reinforcement), 410–411
- Silver, 493
- Simple beams, 574, 585
- Simple stress, 557
- SIMS (secondary ion mass spectroscopy), 855
- Simulation testing, 785
- Single-degree-of-freedom systems, 862, 863, 865–868
  - equation of motion, 865
  - forced-harmonic vibration, 867
  - forced nonharmonic vibration, 868
  - free vibration, 866–867
- Single-leaf partitions, 914, 915, 973–974
- Single-point tool machining, 90, 204, 205
- SI units, 653
- Slenderness ratio, 602
- Sliding wear, 847, 848
- SLMs (sound level meters), 969–970
- SMA (styrene/maleic anhydride) copolymer, 366
- Small-scale yielding, 714
- Smart adhesives, 451
- Smart catalysts, 448
- Smart materials, 439–451
  - catalysts, 448
  - elastorestrictive materials, 444
  - electrorheological materials, 445
  - electrostrictive materials, 443
  - future considerations for, 450–451
  - hydrogels, 447–448
  - light-sensitive materials, 446–447
  - magnetorheological materials, 445–446
  - magnetostrictive materials, 443–444
  - pH-sensitive materials, 446
  - piezoelectric materials, 440–443, 450
  - polymers, 447, 450
  - shape memory alloys, 448–449
  - thermoreponsive materials, 446
  - unusual behaviors of, 449–450
  - versatility of, 450
- Smart polymers, 447, 450
- SMMA (styrene/methyl methacrylate) copolymer, 366, 367
- SMT (surface-mount technology), 500
- S–N–P* curves, 723–728
- SOAP (Spectroscopic Oil Analysis Program), 858
- Socket action, 615
- Soderberg's Law, 573
- Software, electronic packaging design, 510–512
- Soldering, 211, 502
- Solids:
  - behavior of fluids vs., 809–810
  - deformation of, 682–684
- Solid oxide fuel cells (SOFCs), 471
- Solid surfaces, reflection/transmission of sound
  - from, 902–904
- Solubility, 7
- Solvent resistance (of plastics), 355
- Sone, 892, 961
- Sonic booms, 940
- Sound(s). *See also* Noise control
  - and absorptive processes, 898–900
  - constitutive equations for, 895–896
  - fluctuation strength of, 935, 936
  - loudness of, 934–935
  - nervous system response to, 944
  - outdoor propagation of, 923–926
  - psychoacoustic effects of, 944–946
  - reflection and transmission of, 900–904
  - roughness of, 936
  - sensory pleasantness of, 937
  - sharpness of, 935
  - speed of, 896
  - theory of, 894–900
  - tonality of, 936–937
  - wave equation for, 896–898
- Sound exposure level (SEL), 992
- Sound exposure measurements, 992–995
  - equipment for making, 993–995
  - noise dosage, 993
  - sound exposure level, 992
- Sound intensity, 887–888, 958
- Sound intensity measurements, 982–988
  - applications of, 987–988
  - "*p–p*" principle for, 982–984
  - probes for, 984–985
  - systematic errors with, 985, 986
  - and transducer mismatch, 985–987
- Sound isolation measurements, 971–974
  - effect of partitions on, 973–974
  - insertion loss, 973



- noise reduction, 973
  - and sound transmission class, 974
  - transmission loss, 972
- Sound level meters (SLMs), 969–970
- Sound power, 886–887, 957–958
- Sound power level, 887, 957, 989–991
- Sound power measurements, 988–992
  - comparison method for making, 992
  - in free fields, 989–991
  - reverberation method for making, 991–992
- Sound pressure, 888–889, 955–957
- Sound pressure level (SPL), 955–957, 969–971
  - average, 989
  - meters for, 969–970
  - metrics for, 970–971
- Sound quality analysis, 930, 932–937
  - critical band rate in, 933–934
  - fluctuation strength in, 935, 936
  - limitations of, 937
  - loudness in, 934–935
  - procedures for, 932–933
  - roughness in, 936
  - sensory pleasantness in, 937
  - sharpness in, 935
  - tonality in, 936–937
- Sound transmission class (STC), 974
- Spalling failure, 709
- Special copper alloys, 119
- Specific acoustic impedance, 893
- Speckle pattern method, 840, 841
- Spectroscopic Oil Analysis Program (SOAP), 858
- Specular reflection method, 840
- Speed of sound, 896
- Spheres, stresses on, 608, 610
- Spherical waves, 898
- Spheroidizing, of steel, 25
- SPL, *see* Sound pressure level
- sPP (syndiotactic polypropylene), 359
- Springs:
  - bending, 619
  - helical compression, 619
  - stresses on, 618–619
  - tension, 619
  - torsional, under bending, 619
- SPS (syndiotactic polystyrene), 362–363
- Stainless steel(s), 31–35, 39–59
  - and AOD/dual certification/chemistry control, 47–48
  - austenitic, 18–19, 31–32
  - availability of, 49
  - chromium in, 40
  - copper in, 41
  - and corrosion, 40, 43–47
  - duplex, 33, 50–51, 56, 57
  - effect of alloying elements on, 40–42
  - ferritic, 3, 32–33, 49
  - martensitic, 33–34, 50
  - molybdenum in, 40–41
  - nickel alloy, 51–52
  - nickel in, 41
  - precipitation hardening, 34
  - Web sites related to, 58
  - welding of, 53–58
- Standard deviation, 653
- Standard uncertainty, 653
- State of strain, 660
- Static force, 653
- Static stress, 556–563, 569, 570
- STC (sound transmission class), 974
- Steady-stress component, fatigue with, 572
- Steady vibratory stress, 595
- Steel(s), 3–36
  - alloy, *see* Alloy steel[s]
  - carbon, 27–28
  - classification/specifications, 26
  - development of properties of, 5–18
  - electrical, 28
  - enameling, 28
  - free-machining, 22
  - heat treatment of, 24–26
  - hypereutectoid, 9
  - hypo-eutectoid, 9, 12
  - lead, 29
  - manufacture of, 4–5
  - maraging, 35–36
  - plate, 5
  - rephosphorized, 22
  - weathering, 22
- Steel columns, stresses on, 605, 607–608
- Steelmaking, 4
- Stiffness, 561
- STM (Scanning tunneling electron microscopy), 841–842
- STN International, 524–526
- Stokes law, 821
- Storage, protective packaging for, 510
- Strain, 654. *See also* Strain measurement
  - axial, 648
  - Cauchy–Green, 683
  - compressive, 558, 661
  - creep, 805–806



- Strain (*continued*)
  - definition of, 659–664
  - principal, 663
  - shear, 558, 660, 662
  - state of, 660
  - tensile, 558, 661
  - total, 558
  - true, 560, 655
  - unit, 558
- Strain-Energy Theory, 569, 570
- Strain gauges:
  - defined, 654
  - liquid metal, 678
  - measuring force with, 627–629
  - measuring friction force with, 846–847
  - resistance metal, 664–676
  - semiconductor, 676–678
- Strain gauge method of failure analysis, 781–782
- Strain gauge rosettes, 670–673
- Strain hardening (nickel alloys), 283–285
- Strain–life approach to fatigue, 730–732
- Strain measurement, 659–670
  - with liquid metal strain gauges, 678
  - practical challenges with, 664
  - with resistance metal strain gauges, 664–676
  - rosette equations for, 670–673
  - with semiconductor strain gauges, 676–678
  - and strain sensitivity, 665–666
  - Wheatstone bridge circuits in, 673–676
- Strain sensitivity, 665–666
- Strain theory, 660
- Strain transformation equations, 663
- Strand casting, 4–5
- Streaming, acoustic, 940
- Strength:
  - in architectural acoustics, 922
  - beams of uniform, 586
  - breaking, 559
  - and ceramic failure, 791–793
  - of electronic materials, 480
  - fluctuation, 935, 936
  - rupture, 559
  - tensile, 654
  - of titanium alloys, 231–232
  - ultimate, 559, 655
  - yield, 559, 655
- Stress(es), 555–621, 780–782
  - allowable unit, 562
  - axial, 557
  - on beams, 574–595
    - on columns, 601–608
    - combined, 566–570
    - compressive, 556, 557
    - computer modeling of, 620
    - concentration factors, 566
    - contact, 616, 617
    - creep, 563, 570–571
    - on cylinders/spheres, 608–610
    - defined, 556–563, 654
    - determination of principal, 566–567
    - discontinuities, 565–566
    - dynamic, 563
    - fatigue, 563, 572–574
    - impact, 563, 591–595
    - information sources about, 619–621
    - maximum, 572
    - mean, 572
    - minimum, 572
    - nonzero mean, 728–730
    - normal, 557
    - on plates, 610–614
    - range of, 572
    - relieving, in steel, 26
    - residual, 259, 854
    - on rotating elements, 616, 618
    - shafts/bending/torsion, 596–601
    - shear, 557, 597
    - simple, 557
    - socket action, 615
    - on springs, 618–619
    - static, 556–563, 569, 570
    - tensile, 556, 557
    - testing of, 621
    - thermal, 507
    - torsional, 596–601
    - total, 556
    - true, 559
    - on trunnions, 610, 614
    - unit, 556
    - and work/resilience, 563–565
- Stress corrosion, 709
  - of copper and copper alloys, 201
  - of stainless steels, 43–44
- Stress corrosion cracking (SCC), 43–44, 765
- Stress cycle, 572
- Stress–life approach to fatigue, 723–730
  - displaying data with  $S-N-P$  curves, 723–724
  - factors affecting  $S-N-P$  curves, 724–728
  - systems with nonzero mean stress, 728–730
- Stress ratio, 572
- Stress rupture, 708, 736–744

- Stress–strain curves, 625–626
  - Stress–strain relationship, 558–560, 567–568
  - Structural design of electronic packaging, 506–507
    - complexity and mechanical impedance in, 506
    - degree of enclosure in, 506–507
    - thermal expansion and stresses in, 507
  - Stylus profilometers, 839
  - Styrene/acrylonitrile (SAN) copolymer, 363, 364
  - Styrene/maleic anhydride (SMA) copolymer, 366
  - Styrene/methyl methacrylate (SMMA) copolymer, 366, 367
  - Sublimation, 482
  - Substitution (as method of materials selection):
    - case study, 548
    - cost-benefit analysis, 547–548
    - Pugh method, 546–547
  - Superalloys, 299–351
    - component production, 337–344
    - compositions of, 305–308
    - corrosion of and coatings for, 345–347
    - effect of temperature on, 310–317
    - evolution of, 330–333
    - for high-temperature applications, 349–350
    - improvements of, 331–333
    - for intermediate-temperature applications, 348–349
    - manufacture of articles using, 302, 303
    - melting/casting of, 332–337
    - modification of, 331
    - modulus of elasticity of, 323–324
    - obtaining information on, 303–304
    - properties of, 325–329
    - strengthening of, 300–302
    - trace-element concentrations for, 309
  - Suppliers, ceramics, 469
  - Surfaces, reflection/transmission of sound from, 902–904
  - Surface acoustic wave (SAW) transducers, 634–636
  - Surface finishes, for electronics, 487–488
  - Surface-mount technology (SMT), 500
  - Surface profilometers, 839
  - Surface roughness measurements, 839–844
    - with electron microscopes and AFM, 840–844
    - with optical microscopes, 840
    - with surface profilometers, 839
  - Surveys, noise, 982
  - Suspended-level viscometers, 828
  - Switching calibration technique, 968–969
  - SWRO (Sea Water Reverse Osmosis) process, 463
  - Syndiotactic polypropylene (sPP), 359
  - Syndiotactic polystyrene (SPS), 362–363
  - Systems, active noise control in, 920
  - Systematic errors, with sound intensity measurement, 985, 986
- T**
- Tandem mill, 5
  - Taper-sectioning method, 840
  - Tapping (copper alloys), 208, 209
  - Tare (term), 654
  - TBCs (thermal barrier coatings), 346
  - TEM (transmission electron microscopy), 841
  - Temperature(s):
    - and calibration of force measurement devices, 644
    - ceramic failure at high, 804–807
    - and copper, 198
    - effect of, on superalloys, 310–317
    - measurement of, 849–851
    - and viscometer selection, 835
    - and viscosity, 816–819
  - Temperature capability, titanium alloy, 230–232
  - Temperature coefficient, 642
  - Temperature control, for electronics, 485–486
  - Temperature-induced elastic deformation, 706
  - Temperature ranges:
    - compensated, 654
    - for electronic materials, 480
    - operating, 654
  - Tempered aluminum alloys, 70, 72–73
  - Tempering, 24–25
    - copper alloys, 159–162
    - steel, 26
  - Tensile strain, 558, 661
  - Tensile strength, 654
  - Tensile stress, 556, 557
  - Tensile test, 654
  - Tension, 556, 557, 654
  - Tension springs, 619
  - Tensorial shear strain, 662
  - Tertiary phase diagrams, 6

- Test environments, tribology, 849–852
- Textual data, 520–521
- Thermal analysis, 785
- Thermal barrier coatings (TBCs), 346
- Thermal conductivity, 477
- Thermal design in electronic packaging, 507–509
  - and modes of heat transfer, 508–509
  - objectives of, 507–508
- Thermal emissivity, 478
- Thermal expansion:
  - of electronic materials, 478
  - in structural design, 507
- Thermal failure, 777
- Thermal relaxation, 708
- Thermal shock, 464–465, 708, 803–804
- Thermal stress, 507
- Thermocouples, 849–851
- Thermoplastics:
  - electronic packaging with, 494–496
  - engineering, 370–383
  - fluorinated, 392–393
  - polyolefinic, 357–361
  - side-chain-substituted vinyl, 361–369
- Thermoplastic polyesters, 371–374
  - PBT/PC alloy, 371–373
  - poly(butylene terephthalate), 371, 372
  - poly(ethylene terephthalate), 372–374
  - poly(trimethylene terephthalate), 374
- Thermoplastic polyurethanes (TPUs), 369
- Thermoresponsive materials, 446
- Thermosets, 394–396
  - alkyd resins, 395–396
  - amino resins, 396
  - diallyl phthalate, 396
  - in electronic packaging materials, 496–497
  - epoxy resins, 394
  - phenolic resins, 394
  - unsaturated polyesters, 395
  - vinyl esters, 395
- Thin-film sensors, 850
- Threading (copper alloys), 208, 209
- Three-body wear, 755
- Three-lead-wire systems, 675–676
- Time–temperature transformation (TTT) diagrams, 12
- Tin, 24, 494
- Tin brasses, 129–130
- Tin bronzes, 145
- Titanium, 494
- Titanium alloys, 229–264
  - applications of, 261–263
  - biomedical applications of, 261
  - corrosion, 260–261
  - cryogenic applications of, 261
  - crystal structure behavior in, 234
  - high temperatures of, 234–236
  - information resources for, 264
  - manufacture of articles using, 232–233
  - manufacturing processes for, 254–260
  - mechanical behavior of, 235–236
  - melting, 255–256
  - metallurgy of, 233–236
  - microstructure/properties of, 236–254
  - new titanium products, 263
  - selection of, 263–264
  - strengthening mechanisms for, 232
  - temperature capability of, 230–232
  - wrought, 247–252
- TL, *see* Transmission loss
- Tonality, 936–937
- Tool steels, 34
- Torque, 654
- Torsional modulus, 655
- Torsional springs, 619
- Torsional stresses, 596–601
  - bending, 601
  - defined, 596
  - in shafts, 597–600
- Torsional vibration, 874–875
- Torsion test, 654
- Total strain, 558
- Total stress, 556
- Toughness, 560, 561, 714, 854
- TPUs (thermoplastic polyurethanes), 369
- Traceability, 655
- Traction, on a surface, 685
- Tramp elements, 24
- Transducers:
  - defined, 655
  - force, *see* Force transducers
  - magnetoelastic, 640
  - resonant element, 631–634
  - surface acoustic wave, 634–636
- Transducer mismatch, 985–987
- Transmission coefficient, 908
- Transmission electron microscopy (TEM), 841
- Transmission loss (TL):
  - active control of, 921
  - defined, 908
  - measuring, 972

passive control of, 915  
 for vibration isolation mounts, 909–910  
 Transmission of sound, 900–904  
   at discontinuities in pipes, 904  
   at side branches of pipes, 904  
   from a single interface, 900–902  
   from a solid surface, 902–904  
   through fluid layers, 902–904  
 Transparent ceramics, 468  
 Transverse sensitivity, 672–673  
 Transverse sensitivity coefficient (strain gauge),  
   667–668  
 Transverse vibration, 873–874  
 Tribology measurements, 837–860  
   friction, 844–847  
   for fundamental vs. applied research, 838  
   industrial context for, 859  
   of lubricant characteristics, 855–858  
   of material characteristics, 852–855  
   surface roughness, 839–844  
   test environments for, 849–852  
   wear, 847–849  
   and wear particle analysis, 858–859  
 Trip steels, 30  
 True strain, 560, 655  
 True stress, 559, 655  
 True stress–strain relationship, 560  
 Trunnions, stresses on, 610, 614  
 TTT (time–temperature transformation)  
   diagrams, 12  
 Tube/pipe products (copper and copper alloys),  
   215–224  
   fuel gas distribution systems, 217, 224  
   nonflammable medical gas piping systems,  
   217  
   plumbing tube, 215–225  
 Tube (bubble) viscometers, 823–824, 834  
 Tungsten, 23, 41  
 Tuning forks, 888, 889  
 Tuning fork sensors, 631–634  
 Tuning fork viscometers, 831, 832  
 Tuyeres, 4  
 Twist, angle of, 598  
 Twisting moment, 596  
 Two-body wear, 755

## U

Ultimate strength, 559, 655  
 Ultrahigh-molecular-weight polyethylene  
   (UHMWPE), 357, 358

Ultrahigh-strength steels, 35–36  
 Ultrasound, 941–942  
 Uncertainty:  
   in force measurement, 644–647  
   with force transducers, 625  
   in measurement, 650  
   standard, 653  
 Unidirectional MMCs, 424  
 Unified Numbering System (UNS), 26  
 Uniform strength, beams of, 586  
 Unit strain, 558  
 Unit stress, 556, 562  
 Universal force testing machines, 627–631  
 UNS (Unified Numbering System), 26  
 Unsaturated polyesters, 395

## V

Vacuum arc melting, 255  
 Vacuum arc remelting (VAR), 332, 333, 335  
 Vacuum induction melting (VIM), 332–334  
 Variable stress component, fatigue with, 572  
 Vertical deflection, 584  
 Vertical shear, 576  
 Very low-density polyethylene (VLDPE), 357  
 Vibration(s), 861–868, 870–883. *See also*  
   Shock  
   of beams, 595  
   of continuous vibratory systems, 873–877  
   and dynamics study, 861  
   electronic equipment failure due to,  
   504–505  
   flexural, 875  
   isolation of, 878–880  
   longitudinal, 874  
   modeling of, 862–864  
   in multi-degree-of-freedom systems,  
   870–873  
   nomenclature for, 882–883  
   in single-degree-of-freedom systems,  
   865–868  
   sources of, 861–862  
   standards for, 881–882  
   study of, 862  
   torsional, 874–875  
   transverse, 873–874  
 Vibrational viscometers, 831–832, 834  
 Vibration isolation mounts, 909–910  
   active noise control in, 921  
   and impedance, 909  
   transmission loss for, 909–910

- Vibration testing, 505–506
  - Vibratory stresses, 595
  - Vickers hardness test, 853
  - VIM (vacuum induction melting), 332–334
  - Vinyl esters, 395
  - Vinyl thermoplastics, side-chain substituted, *see* Side-chain-substituted vinyl thermoplastics
  - Viscometers, 819–832, 856–858
    - bubble (tube), 823–824, 834
    - capillary, 827–829, 834, 856
    - drag-type, 820–823
    - falling-object, 820–823, 834
    - flow-type, 827–829
    - orifice-type (cup), 829–831, 834
    - rotational, 824–826, 834, 856
    - selecting, 833–835
    - vibrational (resonant), 831–832, 834
  - Viscometry, *see* Viscosity measurement
  - Viscosity, 809–819
    - absolute, 810, 811
    - apparent, 813
    - and behavior of fluids vs. solids, 809–810
    - bulk, 810
    - defined, 810
    - dynamic, 834
    - of gases, 818
    - kinematic, 810–812, 834
    - of liquids, 818–819
    - mathematical formalism governing, 813–815
    - and molecular theory, 815–816
    - and pressure, 816–817, 819
    - and temperature, 816–819
    - units of, 811–812
  - Viscosity measurement (viscometry):
    - ASTM standards for, 832–833
    - calibration fluids for, 832
    - methods of, 819–832
    - rheology vs., 812–813
    - selecting a technique of, 833–835
    - in tribology experiments, 856–858
  - Visual examination, 779
  - VLDPE (very low-density polyethylene), 357
- W**
- Water purification, 463
  - Waves:
    - defined, 655
    - plane, 897
    - spherical, 898
  - Wave equations:
    - for plane waves, 897
    - for sound, 896–898
    - for spherical waves, 897
  - Wear:
    - defined, 707
    - failure due to, 744–745, 753–759
    - and fretting, 744–745
    - measurement of, 847–849
  - Wear particle analysis, 858–859
  - Wear resistance, electronic materials, 482
  - Wear-resistant steels, 35
  - Weathering steels, 22
  - Web shear, 584
  - Weibull distribution plots, 457–458
  - Weibull statistics, 799–803
    - compression loading, 799
    - global multiaxial fracture criterion, 799–800
    - local multiaxial fracture criterion, 800–803
  - Weighted-properties method (materials selection), 538–540
  - Weighting filters, 891–893
    - acoustic measurements for, 960–961
    - and octave bands in audio range, 892–894
    - types of, 891–892
  - Welds, properties of, 214
  - Welding:
    - carbon vs. stainless steel, 53–55
    - of copper and copper alloys, 211–213
    - in electronics, 502
    - gas–metal arc, 213
    - gas–tungsten arc, 212, 213
    - nickel and nickel alloys, 287
    - processes, 212, 213
    - of stainless steels, 53–58
  - Wet corrosion, 279
  - Wheatstone bridges, 629–630, 673–676
  - Windows, smart, 447
  - Wire, music, 36
  - Wooden columns, stresses on, 604–607
  - Work, 563–565
  - Wrought alloys:
    - aluminum, 93–108
    - copper, 120–132, 135–140, 153–155
    - magnesium, 292, 294
    - titanium, 247–252
  - Wrought superalloys:
    - applications of, 348–349
    - compositions of, 305–307

dynamic moduli of elasticity for,  
323–324  
effect of temperature on, 310–312,  
315–316  
physical properties of, 318–320  
processing of, 340–341

**X**

X-percentile-exceeded sound level (LX),  
928

**Y**

Yellow brasses, 128, 142–143  
Yielding failure, 706, 710–712  
Yield point, 559, 655  
Yield strength, 559, 655  
Young's modulus, 625, 655–656, 687, 854

**Z**

Zinc, 493

# **WILEY END USER LICENSE AGREEMENT**

Go to [www.wiley.com/go/eula](http://www.wiley.com/go/eula) to access Wiley's ebook EULA.